



IMPERIAL INSTITUTE  
OF  
AGRICULTURAL RESEARCH, PUSA.







PROCEEDINGS  
OF THE  
ROYAL SOCIETY OF LONDON

SERIES A

CONTAINING PAPERS OF A MATHEMATICAL AND  
PHYSICAL CHARACTER.

VOL. CXL.

LONDON:

PRINTED FOR THE ROYAL SOCIETY AND SOLD BY  
HARRISON AND SONS, LTD., ST. MARTIN'S LANE,  
PRINTERS IN ORDINARY TO HIS MAJESTY.

JUNE, 1933.

LONDON:  
HARRISON AND SONS, LTD., PRINTERS IN ORDINARY TO HIS MAJESTY,  
ST. MARTIN'S LANE.

# CONTENTS.

## SERIES A. VOL. CXL.

No. A 840.—April 1, 1933.

	PAGE
Chemical Equilibrium in Vapour of a Mixture of Hydrocarbons. By H. A. Wilson, F.R.S.....	1
The Energy Absorbed in the Cold Working of Metals. By W. Rosenhain, F.R.S., and V. H. Stott. (Plate 1).....	9
The Spectrum of H <sub>2</sub> —The Bands Ending on 2p <sup>3</sup> II Levels. Part II. By O. W. Richardson, F.R.S., and P. M. Davidson .....	25
The Effect of the Solvent on Reaction Velocity. III.—The Interaction of Persulphate Ions and Iodide Ions. By F. G. Soper and E. Williams. Communicated by J. L. Simonsen, F.R.S.....	59
The Effect of the Solvent on Reaction Velocity. IV.—The Rate and Critical Increments of some Chlorination Reactions. By R. E. Roberts and F. G. Soper. Communicated by J. L. Simonsen, F.R.S.....	71
The Crystalline Structure of Anthracene. A Quantitative X-Ray Investigation. By J. M. Robertson. Communicated by Sir William Bragg, O.M., F.R.S.....	79
The Photosynthesis of Hydrogen Chloride. I.—A New Experimental Method; The Inhibiting Effect of Hydrogen Chloride. By M. Ritchie and R. G. W. Norrish. Communicated by T. M. Lowry, F.R.S.....	99
The Photosynthesis of Hydrogen Chloride. II.—“Oxygen-Free” Mixtures. By M. Ritchie and R. G. W. Norrish. Communicated by T. M. Lowry, F.R.S.....	112
Gas Adsorption upon Electrically Conducting Films during their Condensation from Molecular Rays. By M. C. Johnson and T. V. Starkey. Communicated by S. W. J. Smith, F.R.S.....	126
The Moving Boundary Method for the Determination of Transport Numbers. By G. S. Hartley and J. L. Moilliet. Communicated by F. G. Donnan, F.R.S.....	141
The Scattering of Electrons in Thin Films. By G. O. Langstroth. Communicated by O. W. Richardson, F.R.S.....	159
The Relation between Mean Atomic Volume and Composition in Copper-Zinc Alloys. By E. A. Owen and L. Pickup. Communicated by Sir William Bragg, O.M., F.R.S.....	179
Variation of Mean Atomic Volume with Temperature in Copper-Zinc Alloys, with Observations on the $\beta$ -Transformation. By E. A. Owen and L. Pickup. Communicated by Sir William Bragg, O.M., F.R.S....	191
The Change of Resistance of a Semi-Conductor in a Magnetic Field. By J. W. Harding. Communicated by R. H. Fowler, F.R.S.....	205

	PAGE
The Structure of Surface Films. Part XVII.— $\gamma$ -Hydroxy-Stearic Acid and its Lactone. By N. K. Adam. Communicated by F. G. Donnan, F.R.S.....	223
Flow of Water through Fine Clearances with relative Motion of the Boundaries. By R. J. Cornish. Communicated by D. R. Hartree, F.R.S.....	227
No. A 841.—May 3, 1933.	
The Tides in Oceans on a Rotating Globe.—Part IV. By G. R. Goldsbrough, F.R.S.....	241
On the Rate of Oxidation of Monolayers of Unsaturated Fatty Acids. By A. H. Hughes and E. K. Rideal, F.R.S.....	253
On Eddington's Problem of the Expansion of the Universe by Condensation. By N. R. Sen. Communicated by Sir Arthur Eddington, F.R.S.....	269
The Excitation Potentials of Light Metals. II.—Beryllium. By H. W. B. Skinner. Communicated by A. P. Chattock, F.R.S.....	277
On the Reflection and Refraction of X-Rays by Perfect Crystals. By G. W. Brindley. Communicated by R. Whiddington, F.R.S.....	301
On a Penetrating Radiation from Thunderclouds. By B. F. J. Schonland and J. P. T. Viljoen. Communicated by C. T. R. Wilson, F.R.S.....	314
The Diffraction of Electrons in Mercury Vapour.—II. By F. L. Arnot. Communicated by H. S. Allen, F.R.S.....	334
The Relation Between Mean Atomic Volume and Composition in Silver-Zinc Alloys. By E. A. Owen and L. Pickup. Communicated by Sir William Bragg, O.M., F.R.S. (Plate 2).....	344
The Electrical Properties of Soil for Alternating Currents at Radio Frequencies. By R. L. Smith-Rose. Communicated by E. V. Appleton, F.R.S.....	359
The Luminous Reduction of Selenium Dioxide. By H. J. Emeléus and H. L. Riley. Communicated by J. C. Philip, F.R.S. (Plate 3).....	378
Investigations on the Spectrum of Selenium. Part II.—Se III. By J. S. Badami and K. R. Rao. Communicated by A. Fowler, F.R.S.....	387
The Theory of Metallic Corrosion in the Light of Quantitative Measurements. Part VI.—The Distribution of Corrosion. By G. D. Bengough and F. Wormwell. Communicated by Sir Harold Carpenter, F.R.S. (Plates 4-6).....	399
The Slow Combustion of Ethane at High Pressures. By D. M. Newitt and A. M. Bloch. Communicated by W. A. Bone, F.R.S.....	426
Acid Strength and its Dependence Upon the Nature of the Solvent. By W. F. K. Wynne-Jones. Communicated by Sir Harold Hartley, F.R.S.....	440
The Effect of Water Vapour on the Diffusion Coefficients of Ions in Nitrogen and Oxygen. By J. J. Nolan and A. C. Galvin. Communicated by A. W. Conway, F.R.S.....	452
An Electrical Calculating Machine. By R. R. M. Mallock. Communicated by C. G. Darwin, F.R.S.....	457

Phase Boundary Potentials of Adsorbed Films on Metals. Part I.—On the Behaviour of Oxygen on Gold. By H. K. Whalley and E. K. Rideal, F.R.S.....	484
Phase Boundary Potentials of Adsorbed Films on Metals. Part II.—On the Behaviour of Iodine on Platinum. By L. Jacobs and H. K. Whalley. Communicated by E. K. Rideal, F.R.S.....	489
Phase Boundary Potentials of Adsorbed Films on Metals. Part III.—The Examination of the Interaction of Copper and Iodine Vapour by the Method of Surface Potentials. By H. K. Whalley and E. K. Rideal, F.R.S.....	497
An Elementary Theory of Electronic Semi-Conductors, and Some of Their Possible Properties. By R. H. Fowler, F.R.S.....	505
Probability, Statistics, and the Theory of Errors. By H. Jeffreys, F.R.S.....	523
The Isotopic Constitution and Atomic Weight of Lead from Different Sources. By F. W. Aston, F.R.S.....	535
The Skin Friction of Flat Plates to Osborn's Approximation. By N. A. V. Piercy and H. F. Winny. Communicated by L. Bairstow, F.R.S.....	543
The Determination of the Angles between Covalencies, from Measurements of Electric Dipole Moment. By G. C. Hampson and L. E. Sutton. Communicated by N. V. Sidgwick, F.R.S.....	562
The Aerofoil in a Wind Tunnel of Elliptic Section. By L. Rosenhead. Communicated by H. Glauert, F.R.S.....	579
Investigations in the Infra-red Region of the Spectrum. Part VIII.—The Application of the Grating Spectrometer to Certain Bands in the Spectra of Triatomic Molecules (Sulphur Dioxide, and Carbon Disulphide). By C. R. Bailey and A. B. D. Cassie. Communicated by F. G. Donnan, F.R.S.....	605
The Collision of Slow Electrons with Atoms. III.—The Excitation and Ionization of Helium by Electrons of Moderate Velocity. By H. S. W. Massey and C. B. O. Mohr. Communicated by R. H. Fowler, F.R.S.....	613
Polish on Metals. By R. C. French. Communicated by G. P. Thomson, F.R.S. (Plates 7-9).....	627
Phenomena Occurring in the Melting of Metals. By W. L. Webster. Communicated by P. Kapitza, F.R.S.....	653
Dissociation of Excited Diatomic Molecules by External Perturbations. By C. Zener. Communicated by R. H. Fowler, F.R.S.....	660
A Contribution to the Theory of Film Lubrication. By A. M. Robb. Communicated by J. Proudman, F.R.S.....	668
The Principal Magnetic Susceptibilities of Some Paramagnetic Crystals at Low Temperatures. By L. C. Jackson. Communicated by A. P. Chattock, F.R.S.	695
The Photosynthesis of Hydrogen Chloride. III.—Mixtures Containing Oxygen. By R. G. W. Norrish and M. Ritchie. Communicated by T. M. Lowry, F.R.S.	713
Index.....	741



# PROCEEDINGS OF THE ROYAL SOCIETY.

## SECTION A.—MATHEMATICAL AND PHYSICAL SCIENCES.

### *Chemical Equilibrium in Vapour of a Mixture of Hydrocarbons.*

By H. A. WILSON, F.R.S., Rice Institute, Houston, Texas, U.S.A.

(Received December 2, 1932.)

In previous papers\* the writer has considered chemical equilibrium in mixtures of paraffins and unsaturated hydrocarbons. The theoretical equilibrium compositions at different pressures and temperatures were compared with results obtained in commercial cracking operations and it was concluded that the theory represented the main features of such cracking.

The hypothetical oils considered were supposed to contain only paraffins and unsaturated hydrocarbons and so differed from real oils which also contain naphthenes or cycloparaffins and aromatic hydrocarbons. The hypothetical oils therefore contained a higher percentage of hydrogen than real oils. For example a hypothetical oil of composition  $\text{CH}_{2.1}$  was found to correspond with heavy crude or fuel oil. The percentage of hydrogen in an oil of composition  $\text{CH}_{2.1}$  is 14.9 while heavy crude oils usually do not contain more than 12 or 13 per cent. of hydrogen. The percentage of hydrogen in naphthenes  $\text{C}_n\text{H}_{2n}$  is 14.3 so that hypothetical oils containing naphthenes will contain less hydrogen than paraffins but will still contain more hydrogen than actual oils.

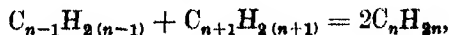
In the present paper naphthenes and aromatic hydrocarbons are considered in addition to paraffins and unsaturated bodies.

The equilibrium composition of a mixture is independent of the process by which equilibrium is reached so that any hypothetical reactions may be imagined to occur and the equilibrium composition calculated by means of them.

\* 'Proc. Roy. Soc.,' A, vol. 116, p. 502 (1927); vol. 120, p. 247 (1928); vol. 124, p. 16 (1929). These papers will be denoted by E I, E II and E III.



Chemical equilibrium in a gaseous mixture of naphthenes only will be discussed first. The equilibrium constant  $K_p$  of the reaction



is given approximately by the equation

$$\log K_p = \log q_n^2 / q_{n-1} q_{n+1} = 0,$$

where  $q_n$  denotes the partial pressure of  $C_nH_{2n}$ .  $\log K_p$  is nearly equal to zero, as in the case of similar reactions in any homologous series of hydrocarbons, because the properties of a hydrocarbon containing  $n$  carbon atoms are approximately the means of those of similar hydrocarbons containing  $n - 1$  and  $n + 1$  carbon atoms.

We have therefore  $q_n^2 / q_{n-1} q_{n+1} = 1$  so that  $q_n / q_{n-1} = q_{n+1} / q_n$ . The partial pressures therefore form a geometrical series and  $q_n = q_3 f^{n-3}$  where  $f$  is a proper fraction. The total pressure  $q$  is therefore given by the equation  $q = q_3 / (1 - f)$ . The equation  $q_n = q_3 f^{n-3}$  is the equilibrium condition in a mixture of naphthenes. If other hydrocarbons are also present this condition must still hold, but, of course,  $q_3 / (1 - f)$  will not be equal to the total pressure but only to the sum of the partial pressures of the naphthenes.

Now consider the reaction  $C_nH_{2n} = C_mH_{2m} + C_{n-m}H_{2(n-m)}$ . The equilibrium constant of this reaction is given approximately by the equation  $\log q_m q_{n-m} / q_n = \log T + D$  where  $T$  denotes the absolute temperature and  $D$  is a constant.\* The change of internal energy must be very small and so has been put equal to zero. Putting  $q_n = q_3 f^{n-3}$  we get  $\log q_3 f^{-3} = \log T + D$  or since  $q_3 = q(1 - f)$ ,  $\log q(1 - f) / f^3 = \log T + D$ . According to this the value of  $f$  and so the relative amounts of the different naphthenes in equilibrium is determined by the temperature and pressure of the vapour. The vapour has only one independent constituent and so according to the phase rule its composition is determined by the temperature and pressure as in the case, for example, of water vapour.

Now consider a mixture of paraffins and naphthenes. The equilibrium constant of the reaction  $C_nH_{2n+2} = C_mH_{2m} + C_{n-m}H_{2(n-m)+2}$  is given by the equation\*  $\log p_{n-m} q_m / p_n = \log T + C$ , where  $p$  denotes the partial

\* The equilibrium constant  $K_p$  of any gaseous reaction, when the change of heat capacity at constant volume is assumed to be small is given approximately by the equation  $\log K_p = -\Delta U / RT + (\Delta n) \log T + C$  where  $\Delta U$  denotes the change of internal energy and  $\Delta n$  the change in the number of mols. For a reaction in which one molecule dissociates into two  $\Delta n = 1$  so that  $\log K_p = -\Delta U / RT + \log T + C$ . When the numbers of chemical bonds between the carbon and hydrogen atoms are unchanged by the reaction  $\Delta U$  is very small so that  $\log K_p = \log T + C$  approximately.

pressure of the paraffin  $C_nH_{2n+2}$ . The partial pressures of the paraffins also form a geometrical series so that  $p_n = p_1 f'^{n-1}$ , where  $f'$  is a proper fraction. The above equation for  $\log p_{n-m}q_m/p_n$  therefore gives

$$\log q_3 f'^{-m} f^{m-3} = \log T + C.$$

Comparing this with  $\log q_3 f^{-3} = \log T + D$  we see that if  $f, f', C$  and  $D$  are all constants independent of  $n$  and  $m$ , which we are supposing is approximately the case, then we must have  $f' = f$  and  $C = D$ .

If  $p$  denotes the sum of the partial pressures of the paraffins and  $P$  the total pressure so that  $P = p + q$  we have, since

$$q = Tf^3 e^c / (1 - f), \quad P = p + Tf^3 a / (1 - f),$$

where  $a = e^c$ .

The mixture of paraffins and naphthenes has two independent constituents so that to fix the value of  $f$  in the vapour it is necessary to know the pressure, temperature and the relative numbers of carbon and hydrogen atoms present.

If vapour and liquid are supposed present then, since the physical properties of naphthenes are very similar to those of paraffins containing the same number of carbon atoms, the vapour pressure of a mixture of paraffins and naphthenes must be nearly the same as that of a mixture of paraffins provided the fraction  $f$  is the same for both.

The values of the fraction  $f$  given in E I for paraffins with vapour and liquid both present will therefore be approximately correct for a mixture of paraffins and naphthenes under the same conditions. The chart in E I gives the values of  $x = 4 - 2f$  at any temperature and pressure, so that the total pressure  $q$  of the naphthenes could be calculated by means of the equation  $q = Taf^3 / (1 - f)$  if the value of the constant  $a$  were known. The molecular fraction of naphthenes in the mixture is equal to  $q/P$  where  $P$  denotes the total pressure.

The ratio of paraffins to naphthenes in gasoline varies considerably but is frequently about 2, so to illustrate the variation of the naphthene fraction with pressure and temperature, indicated by the theory, we shall assume that at 30 atmospheres and 800° F. the naphthene fraction is 33.3 per cent.

The value of  $f$  at 30 atmospheres and 800° F. is 0.8 so that taking  $q = 10$  atmospheres and  $T = 700^\circ \text{ K.}$ , we get  $10 = 700a \cdot 0.8^3 / 0.2$ , which gives  $a = 1/179$ . Using this value of  $a$  the values of the naphthene molecular percentage given in Table I have been calculated. Since  $a = e^c$  the constant  $C$  is equal to  $-5.2$  if  $a = 1/179$ .

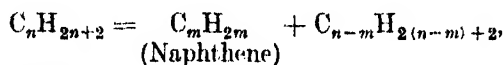
Table I.—Liquid and Vapour both present.

Temperature.	15 atmospheres.	30 atmospheres.	60 atmospheres.
°F.			
700	36	23	9
800	80	33	13
900	—	45	18
1000	—	—	24

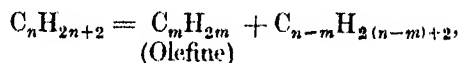
The equilibrium theory therefore indicates that with liquid and vapour both present the naphthene fraction increases with temperature, but falls with the pressure.

It is stated in Cross' handbook of petroleum that the yield of naphthenes increases with the pressure, but the writer does not know of any experimental results which support this statement. In commercial liquid phase cracking higher temperatures are usually used at higher pressures. It is shown below that with vapour only present the naphthene percentage indicated by the theory does increase with the pressure.

The equilibrium constants of the reaction



and the similar reaction



are given by the equations

$$\log p_{n-m}q_m/p_n = \log T + C$$

and

$$\log p_{n-m}p'_m/p_n = -7400/T + \log T + C',$$

which give  $\log q_m/p'_m = 7400/T + C - C'$  where  $p'_m$  is the partial pressure of the olefine  $C_mH_{2m}$ . This equation gives the equilibrium constant of the reaction  $\underset{\text{(Olefine)}}{C_mH_{2m}} = \underset{\text{(Naphthene)}}{C_mH_{2m}}$ . If we take  $C = -5.2$  and  $C' = 3$  we get

$\log q_m/p'_m = 7400/T - 8.2$ . At 900° F. or  $T = 756$  this gives  $\log q_m/p'_m = 1.6$  so that  $q_m/p'_m = 5$  approximately.

The naphthene percentages at 30 and 60 atmospheres and 900° F. calculated above are 45 and 18 respectively so that the percentages of olefines should be about 9 and 3.6. The percentage of unsaturated bodies, mostly olefines, obtained at 900° F. and 60 atmospheres is supposed to be about 5, and at

900° F. and 30 atmospheres it is said to be considerably greater than 5 but less than 20. Thus taking the constant  $C = -5.2$  appears to give unsaturated percentages of the right order of magnitude.

If unsaturated bodies are supposed present the paraffin and naphthene fractions will, of course, be reduced. The theory given in E II gives the ratio of unsaturated bodies to paraffins and the theory in the present paper gives the ratio of naphthenes to paraffins. If paraffins, naphthenes and unsaturated bodies are all supposed present then their percentages can be easily calculated from the theoretical ratios. Since, however, the percentage of unsaturated bodies is usually small in practice, in liquid phase cracking, and since there are no reliable results on naphthene fractions with which to compare the theory it does not seem worth while at present to make calculations of the fractions when all three sorts of hydrocarbons and both liquid and vapour are supposed present. The methods outlined in this and the previous papers can be used for such calculations whenever it seems desirable to make them.

When only vapour is supposed present the value of the fraction  $f$  for a mixture of paraffins, naphthenes and unsaturated bodies is determined by the temperature, pressure and composition of the vapour.

It is shown in E III that the number of mols. of carbon in vapour of a mixture of paraffins and unsaturated hydrocarbons, containing  $M$  mols. of  $\text{CH}_4$ , is equal to

$$\frac{M}{(1-f)^2(1-y)} + \frac{yM}{(1-f)(1-y)^2},$$

where  $y$  is the pressure of the unsaturated bodies divided by the total pressure and is given by  $y = \frac{1}{2} - \sqrt{\frac{1}{4} - Kf^2/p'(1-f)}$ ,  $p'$  is the total pressure and  $\log K = -7400/T + \log T + 3$ .

If the vapour also contains naphthenes of pressure  $q$ , and the total pressure is  $P$ , then  $p'$  in the expression for  $y$  must be replaced by  $P - q$  and  $q = Taf^2/(1-f)$ .

The number of mols. of carbon in the naphthenes in a volume  $V$  can easily be shown to be equal to  $kq(3-2f)/(1-f)$  where  $k = V/RT$ . The pressure of the paraffins is equal to  $P - q - y(P - q) = (P - q)(1 - y)$  so that the mols. of  $\text{CH}_4$  in the vapour is equal to  $k(P - q)(1 - y)(1 - f)$ .

The total mols. of carbon in the vapour is therefore equal to

$$k(P - q)/(1 - f) + ky(P - q)/(1 - y) + kq(3 - 2f)/(1 - f)$$

or

$$k\{P(1 - yf)/(1 - f)(1 - y) + q(2 - 3y)/(1 - y)\}.$$

The number of mols. of hydrogen in the paraffins and unsaturated bodies is shown in E III to be

$$\frac{2M}{1-y} \left\{ \frac{1}{1-f} + \frac{1}{(1-f)^2} \right\},$$

so that since the mols. of H in the naphthenes is twice the mols. of C we get for the total mols. of H

$$2k(P-q)(1-f) \left\{ \frac{1}{1-f} + \frac{1}{(1-f)^2} \right\} + \frac{2kq(3-2f)}{1-f},$$

or

$$2k \left\{ P \frac{2-f}{1-f} + q \right\}.$$

If  $x$  denotes the mols. of H in the vapour per mol. of carbon so that the composition of the vapour is  $\text{CH}_x$  then we have

$$x = 2 \left\{ P \frac{2-f}{1-f} + q \right\} / \left\{ \frac{P(1-yf)}{(1-f)(1-y)} + \frac{q(2-3y)}{1-y} \right\},$$

or

$$x = 2(1-y) \left\{ \frac{P(2-f) + q(1-f)}{P(1-yf) + q(2-3y)(1-f)} \right\}.$$

This equation together with  $y = \frac{1}{2} - \sqrt{\frac{1}{4} - Kf^2/(P-q)(1-f)}$ ,

$$\log K = -7400/T + \log T + 3 \quad \text{and} \quad q = Taf^3/(1-f),$$

are sufficient to determine  $f$  at any temperature  $T$  and total pressure  $P$  when  $x$  is supposed known.

Instead of trying to calculate  $f$  for a given value of  $x$  it is much easier to calculate  $x$  for a series of values of  $f$ . Table II gives some results obtained in this way. The naphthene fraction is equal to  $q/P$  and the unsaturated fraction

Table II (a).—Temperature 800° K. (981° F.). Vapour only present.

	Pressure in atmospheres.						
	15.	15.	15.	15.	30.	30.	30.
$x$ in $\text{CH}_x$ .....	2.79	2.49	2.33	2.00	2.38	2.24	2.00
H, per cent. ....	18.8	17.2	16.2	14.3	16.6	15.7	14.3
$f$ .....	0.50	0.60	0.65	0.70	0.70	0.75	0.80
Paraffins, per cent. ....	86.29	73.3	60.9	33.4	73.5	60.7	30.9
Naphthenes, per cent. ....	7.46	16.1	23.4	33.2	17.1	25.2	38.2
Unsaturated, per cent. ....	5.55	10.6	15.7	33.4	9.4	14.1	30.9

Table II (b).—Temperature 900° K. (1161° F.). Vapour only present.

	Pressure in atmospheres.								
	15.	15.	15.	30.	30.	60.	60.	120.	120.
$x$ in $\text{CH}_x$ .....	2.53	2.35	2.00	2.23	2.00	2.18	2.00	2.11	2.00
H, per cent. ....	17.4	16.4	14.3	15.7	14.3	15.4	14.3	15.0	14.3
$f$ .....	0.50	0.53	0.55	0.65	0.665	0.75	0.766	0.85	0.855
Paraffins, per cent. ....	70.9	60.9	43.8	56.8	42.7	59.6	42.0	51.2	41.1
Naphthenes, per cent. ....	8.4	10.6	12.4	13.2	14.7	14.2	16.1	17.2	17.8
Unsaturated, per cent. ....	20.7	28.5	43.8	30.0	42.6	26.2	41.9	31.6	41.1

to  $y(P - q)/P$ . These molecular fractions will not differ seriously from the percentages by weight.

The smallest possible value of  $x$  is 2 and the corresponding percentage of hydrogen in the vapour is 14.3. Oil vapour probably seldom contains much more than 14.3 per cent. of hydrogen so that the results for  $x = 2$  should be rather near those to be expected in practice. It appears that the percentage of naphthenes increases with the pressure although with liquid and vapour both present it decreases. The percentage of naphthenes is greater at 800° K. than at 900° K., although with liquid and vapour both present the naphthene percentage increases with the temperature.

The effect of temperature and pressure on the equilibrium amount of an aromatic hydrocarbon such as benzene  $\text{C}_6\text{H}_6$  can be estimated by means of a hypothetical reaction in which a molecule of an unsaturated hydrocarbon is supposed to change into the aromatic molecule.

Thus benzene may be supposed formed from the tetra-olefine  $\text{C}_6\text{H}_8$  so that  $\text{C}_6\text{H}_8$  (Olefine) =  $\text{C}_6\text{H}_6$  (Benzene). If  $p''''_6$  denotes the partial pressure of the olefine and  $a_6$  that of the benzene then we have  $\log a_6/p''''_6 = -30000/T + C$ . The heat of formation of benzene is about 60,000 calories greater than that of the tetra-olefine according to Thomsen's measurements and theory.

According to this equation  $a_6/p''''_6$  increases about 200 times for a rise of 100° C. from 700° K. to 800° K., 63 times from 800° K. to 900° K. and 28 times from 900° K. to 1000° K. Thus it is clear that the amount of benzene will increase very rapidly as the temperature is raised.

The partial pressure  $p''''_6$  of the olefine can be easily calculated at any temperature and pressure. If  $M$  denotes the mols. of  $\text{CH}_4$  in oil vapour, then it is shown in E III that the mols. of the olefine  $\text{C}_6\text{H}_8$  in the vapour is equal to  $M_2^2/f$ . It is shown above that  $M = (V/RT)(P - q)(1 - y)(1 - f)$ , so that we get  $p''''_6 = (P - q)(1 - y)(1 - f)fy^4$ .

In vapour, of composition  $\text{CH}_2$ , or containing 14.3 per cent. of hydrogen,  $y = \frac{1}{2}$  so that  $p''''_6 = (P - q)(1 - f)f/32$ . Using the values of  $q$  and  $f$  given above for the temperature  $900^\circ \text{K}$ , the values of  $p''''_6$  and of the tetra-olefine molecular fraction given in Table III were calculated.

Table III.

	Pressure in atmospheres.			
	15.	30.	60.	120.
$f$ .....	0.55	0.665	0.766	0.855
$p''''_6$ .....	0.104	0.178	0.282	0.382
Olefine $\text{C}_4\text{H}_6$ , per cent. ....	0.694	0.593	0.47	0.32

It appears that the amount of this olefine diminishes slowly as the pressure is increased. The equilibrium amount of benzene is proportional to  $p''''_6$ , at constant temperature, so that increasing the pressure must also reduce the amount of benzene.

The theory therefore indicates that to obtain a large yield of benzene it is necessary to use rather low pressures and high temperatures. This conclusion is in accordance with experience. The pressure should not be too low because at high temperatures very low pressures result in small values of the fraction  $f$  and so very large gas fractions.

The toluene  $\text{C}_7\text{H}_8$  fraction will be equal to the benzene fraction multiplied by  $f$ . Since  $f$  increases with the pressure it follows that a somewhat higher pressure should be used for toluene than for benzene.

### *Summary.*

In this paper the theory of chemical equilibrium in hydrocarbons developed in previous papers is applied to mixtures containing naphthenes or cyclo-paraffins as well as paraffins and unsaturated hydrocarbons. It is shown that the naphthene fraction increases with the temperature when liquid and vapour are both present but falls with the temperature when vapour only is present. It falls with the pressure when liquid and vapour are both present but rises when vapour only is present. The variation of the benzene  $\text{C}_6\text{H}_6$  fraction with the temperature and pressure is also considered.

*The Energy Absorbed in the Cold Working of Metals.*

By WALTER ROSENHAIN, D.Sc., F.R.S., and V. H. STOTT, M.Sc. (from the National Physical Laboratory\*).

(Received December 20, 1932.)

[PLATE I.]

It is well known that when ductile metals or alloys are subjected to plastic deformation at room temperature, *i.e.*, when they are subjected to "cold-working," considerable quantities of heat are liberated. It has further been suspected for a number of years, and has more recently been experimentally established by the work of Taylor and Farren, that the heat thus generated is less than the equivalent of the mechanical work expended upon the metal. A certain quantity of heat, therefore, is absorbed or becomes latent in the metal as the result of changes which it undergoes during the process of plastic deformation. The amount of heat thus absorbed is small, and is probably of little practical interest, but for theoretical reasons, an accurate determination of the amount of heat which becomes latent in this manner is of importance. One of the present authors became interested in this question some ten years ago on account of the important bearing which a knowledge of the amount of heat which becomes latent in this manner would have upon the theory, first put forward by Beilby, that a certain proportion of metal which undergoes plastic deformation becomes converted from the crystalline into an amorphous condition. Some unpublished results which came to his knowledge at that time suggested that the amount of such latent heat was considerable, and an experimental effort to determine this amount was, therefore, begun. In the earliest attempts a testing machine of the usual type used for engineering purposes was employed, and an endeavour was made to measure the heat generated in a small block of metal, of known dimensions and properties, when compressed by a definite amount. Subsequently, in view of the experimental difficulties encountered in working with small compression pieces, large bars of metals strained in tension were employed. It was found that reasonably satisfactory thermal measurements could be obtained, but with the appliances

\* The work described was completed in March, 1930, the senior author being at that time Superintendent of the Department of Metallurgy and Metallurgical Chemistry of the National Physical Laboratory. Circumstances prevented immediate publication of the results of the work.



then employed it was not possible to measure the amount of mechanical work applied to the test piece with sufficient accuracy. While this work was in progress, the results of the investigation of Taylor and Farren were published. These investigators had overcome most of the difficulties which had been encountered, and had succeeded in obtaining results of considerable accuracy. Further experimental work involving the use of tensile test pieces and testing machines was therefore abandoned, and another line of attack was adopted.

Although the results of Taylor and Farren are of the greatest interest, it was hoped that other methods of attacking the problem might make it possible to obtain still higher degrees of accuracy. It is obvious that in a tensile test piece the amount of mechanical work which can be done, and the degree of plastic deformation which can be applied to a piece of metal, are very much limited. For instance, even the most ductile sample of metal will usually break before it has been stretched plastically to twice its original length, whereas in such a process as rolling or wire drawing, very much larger amounts of plastic deformation can be applied. The application of a larger amount of plastic deformation also involves the expenditure of a much larger amount of power, and it was hoped that this would make it possible to measure the power used to a higher degree of accuracy. An investigation was therefore begun for the purpose of measuring the heat evolved in the process of wire drawing. This process appeared to be particularly promising for the purpose in question, since the work is applied in the form of a prolonged steady pull which should be capable of accurate measurement and control. Further, the process of plastic deformation takes place in a very small space within the die itself, and this can be immersed in the calorimeter by means of which the total amount of heat generated can be measured. Unfortunately the results obtained have not entirely justified these expectations. The measurement of the mechanical work done in wire drawing has proved to be a matter of much greater difficulty than was anticipated, mainly because it has been found that the resistance encountered by the wire in passing through the die is not sufficiently uniform to allow of the maintenance of a steady and easily measured tension. It will be seen below, however, that this difficulty has been to a large extent overcome by the experimental devices adopted. A more serious difficulty has been that, in such a process as wire drawing, although the amount of heat generated can be made as large as desired by the use of great lengths of wire, the rate at which this heat is generated is not very high. The result is that the rise of temperature in the calorimeter is very gradual, and that the numerous corrections which apply to calorimetric measurements of this sort become of

relatively very great importance owing to the long time over which an experiment has to be extended. It is this purely calorimetric difficulty which has served mainly to set a limit to the accuracy attainable by this method in its present form.

A complete experiment for the purpose described consists of a simultaneous measurement of the work required to draw a length of wire through the die, and the heat produced in the process. The excess of work over heat is equal to the increase of internal energy of the wire. In the usual notation,

$$U = Q - A,$$

where  $U$  is the increase in internal energy of the wire,  $Q$  the heat absorbed, and  $A$  the work done by the wire. In the actual experiment, both  $Q$  and  $A$  are negative,  $A$  being the greater numerically.

It should be noted that neither  $Q$  nor  $A$  are determined by the initial and final states of the metal, although, of course,  $U$  is so determined.  $A$  is made up of a part representing the internal work done on the metal, a part representing work done against superficial friction in the die, and a part representing friction elsewhere within the calorimeter.

The first measurements were made on annealed aluminium wire. The following description of the apparatus, and the consideration of errors and corrections, applies to this material. Later experiments have been made with copper wire, but since the various corrections are of smaller relative magnitude in the latter case, it is convenient to discuss the more difficult experiments in greater detail.

The calorimeter consists of a vacuum jacketed glass vessel containing oil (Price's Albaline A) with the die situated a little below the oil level. The wire, after passing downwards through the die, goes round a pulley near the bottom of the calorimeter, and thence passes out in a vertical direction, fig. 4, Plate 1. The mouth of the calorimeter is closed by a cork rendered oil proof by cellulose varnish, and provided with the necessary small apertures for the thermometer, stirrer, etc. Stirring is efficiently carried out by means of a thin ebonite shaft driven by a small electric motor carrying two propellers, working in a tube. The heat produced by the motor is carried away by a large cardboard chimney. The spokes of the pulley at the bottom of the calorimeter are set at an angle, and assist the stirring during wire drawing. Just above the die and inside the stirring tube is placed a small manganin heating coil with current and potential leads, with which the calorimeter may be calibrated. The resistance of the leads is negligible compared with that of the coil (about 16 ohms). The

temperature of the oil in the calorimeter is measured by means of one of three special mercury thermometers graduated in hundredths of a degree centigrade, and compared, at every half degree, with the laboratory standards. The room temperature is read on a calibrated thermometer graduated in tenths of a degree centigrade. The room temperatures in a number of positions close to the wire on the incoming side of the calorimeter were compared by means of sensitive thermometers, and differed by only two or three hundredths of a degree.

The wire to be drawn passes from the drum, shown on the right of fig. 4, over a spring-mounted, pivoted jockey pulley, followed by three guiding pulleys, to the 12-inch wheel hanging from a spring by means of which the tension of the wire is measured before it enters the die. Thence, the wire passes through the die, round a pulley near the bottom of the calorimeter, and up to the second large wheel where its tension is again measured. Since the wire tends to carry oil out of the calorimeter, a wiper is provided just above the oil level, which causes the bulk of the oil to run back. This wiper consists of two sets of light bristles directed downwards at an angle of  $45^\circ$  to the horizontal. The work done against friction in the wiper is less than a thousandth part of that done in the die. It is, of course, important not to have appreciable friction at the wiper, since, if heat were produced in the wire at this point, a considerable proportion would no doubt escape from the calorimeter.

After leaving the second tension measuring wheel, the wire passes over two guiding pulleys, and thence round approximately three-quarters of the circumference of the driving wheel, which is provided with a V-groove to grip the wire. Beyond the driving wheel is another guiding pulley in a pivoted mounting, and beyond that the wire passes between two vertical rollers, which move slowly backwards and forwards by means of gearing, so as to cause the wire to be wound evenly on the drum seen on the left of fig. 4. This drum is driven through a slipping clutch, and is so geared that, but for the slip in the clutch, its speed would always be too high. In this way the effect of the increased diameter of the drum, as the wire accumulates, has been counteracted.

To prevent vibration being transmitted from the main driving motor to other parts of the apparatus, an efficient flexible coupling is used to transmit the drive after the necessary reduction in speed has been obtained by a worm gear and a chain drive. The coupling consists of two parallel 9-in. discs, about 2 inches apart. Six short pegs on each disc project from points near the circumference towards similar pegs on the other disc. Opposite pegs are joined together by means of stout rubber pressure tubing firmly clamped on the pegs.

The length of wire entering and the greater length leaving the calorimeter are determined, in principle, by counting the revolutions of the tension measuring wheels, which are provided with small rectangular grooves in which the wire fits loosely. In order to avoid subjective counting, however, a mechanical counter is fitted on the driving wheel, and, by preliminary experiments with a given wire and die, the integral number of turns of the measuring wheel may be found from the readings of the counter. The fractions are read from the measuring wheels themselves. Actual measurement by means of a cathetometer, with the wire under the proper load, has shown that the readings thus obtained represent to less than one part in a thousand the correct lengths, although it was found that the wire leaving the second measuring wheel had stretched about 0.8 per cent. (The stretch is less for copper.) It follows, from this observation, that the first measuring wheel tends to rotate through a smaller angle than that corresponding with the length of wire which unwinds from it. Owing, however, to the relatively small tension of the wire before entering the die, the effect of such stretch has a negligible influence on the total work done. It is also probable that the stretch is considerably less in practice than the figure given above, which applies to a tension about fifteen times as great as that occurring during wire drawing.

If  $l_1$  and  $l_2$  are the lengths of wire entering and leaving the calorimeter in a given time, and  $T_1$  and  $T_2$  are the tensions before and after the calorimeter, at a given moment, the work done, in the time specified, is given by the expression

$$\int_0^{l_1} T_2 dy - \int_0^{l_1} T_1 dx,$$

where  $dx$  and  $dy$  represent small lengths of wire entering and leaving the calorimeter respectively.

Now

$$\frac{dx}{dy} = \frac{l_1}{l_2},$$

so that the work becomes

$$\begin{aligned} & \int_0^{l_1} T_2 dy - \int_0^{l_1} T_1 \left( \frac{l_1}{l_2} \right) dy \\ &= \int_0^{l_1} \left[ T_2 - T_1 \left( \frac{l_1}{l_2} \right) \right] dy. \end{aligned}$$

In the actual apparatus,  $T_2$  and  $T_1$  are measured in terms of the deflections of two springs, and these deflections are themselves measured electrically as voltages, in such a way that the final scale on a galvanometer may be adjusted

to any required size. It is also possible to apply the two voltages in mutual opposition to a single galvanometer. Hence, by making one voltage proportional to  $T_2$ , and the other proportional to  $T_1(l_1/l_2)$ , we obtain a reading equal to

$$k \left[ T_2 - T_1 \left( \frac{l_1}{l_2} \right) \right] = S,$$

where  $k$  is the constant of proportionality. If then, we take  $n$  readings of  $S$  at equal small intervals of length  $\delta y$ , the work done will be equal to

$$\begin{aligned} & \frac{1}{k} \sum_n S \delta y \\ &= \frac{1}{k} \frac{\sum_n S}{n} (n \delta y) \\ &= \left( \frac{1}{k} \right) \bar{S} l_2, \end{aligned}$$

where  $\bar{S}$  is the arithmetic mean of the whole set of readings of  $S$ .

In practice it is more convenient to measure the differences in  $S$  from an arbitrary point  $S_0$ . Denoting these differences by  $S'$ , the work becomes

$$\frac{1}{k} (S_0 + \bar{S}') l_2.$$

Turning again to the apparatus, each measuring spring is provided at its upper end with a vertical micrometer movement which permits adjustment of  $S_0$ . The hooks at the ends of the springs bear on knife edges which are located by grinding shallow V-shaped grooves on the hooks.

To the stirrup, carrying the measuring wheel which hangs from the lower end of each spring, is attached a phosphor-bronze spring carrying a horizontal iridio-platinum wire of  $1/3$  mm. diameter which makes sliding contact with a vertical rhodio-platinum wire of  $\frac{1}{2}$  mm. diameter. The spring carrying the iridio-platinum wire, fig. 1, is designed to be free from appreciable vertical movement whilst permitting slight horizontal movement. The rhodio-platinum wire forms one side of a Wheatstone bridge, the other side consisting of a similar wire set a little further back, so as to be out of contact with the iridio-platinum wire. The middle point of the second rhodio-platinum wire can be connected to one terminal of a galvanometer, the other terminal of which is connected to the iridio-platinum wire, which is otherwise insulated. On sending a current through the bridge in the usual way, the galvanometer will be deflected by an amount proportional to the current through the bridge,

and to the distance of the sliding contact from the null-point. The arrangement is shown diagrammatically in fig. 2. The arrangement of two bridges in opposition requires a separate battery for each bridge, and is shown in fig. 3. The adjustment of the galvanometer scale for each bridge is merely a

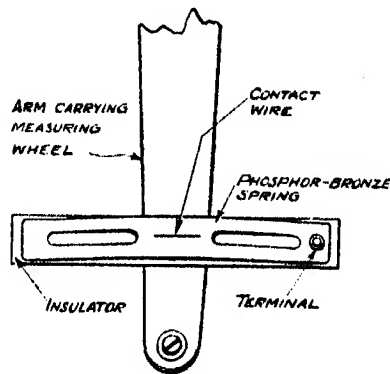


FIG. 1.

question of adjusting the current to a suitable value by means of a rheostat and ammeter. Switches are provided on the apparatus which enable the bridges to be used independently or in opposition. Before carrying out a determination, a preliminary trial permits the micrometers on each spring to be set so that each bridge separately will be nearly in equilibrium during

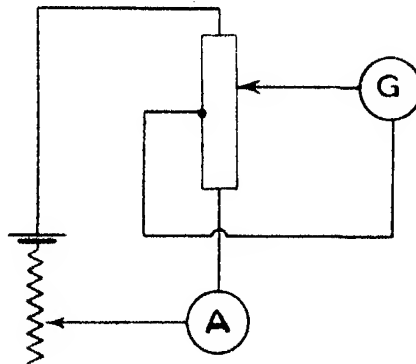


FIG. 2.

the actual determination, during which time, of course, the bridges will be combined in opposition. In this way, the error due to any possible imperfections in the contacts is reduced. The resistance of the galvanometer is 320 ohms. It has usually been convenient to add a series resistance of equal value.

The springs are calibrated by removing the calorimeter and replacing the wire over the measuring wheels by string. Weights are hung on the ends which normally lead to the calorimeter, the other ends passing over the usual guide pulleys and being anchored beyond. The micrometers are adjusted for different loads so that the Wheatstone bridges are in equilibrium. In order to perform this operation with precision very flexible string must be used ; the best kind is made of pure braided flax. The springs are allowed to oscillate before readings are taken, and then left loaded for 24 hours before the final readings are taken so as to minimize the slight hysteresis

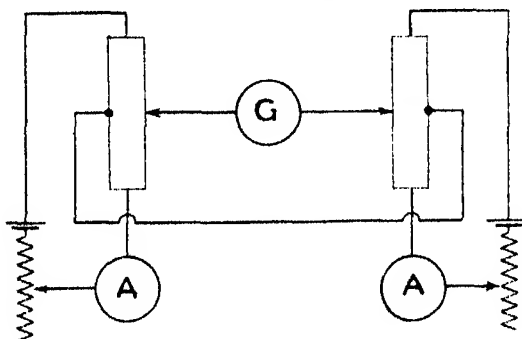


FIG. 3.

effects. When the apparatus is in normal use the springs are always under practically the working loads. The springs were calibrated before and after the first three determinations made on aluminium. The difference for the stronger spring was less than 0.04 lb., at the working load of 16 lb., and for the lighter spring zero. On working out the results of the first three determinations, the mean value of the above calibrations was used ; the second value was used for subsequent determinations. The difference of  $\frac{1}{8}$  per cent. is, however, of no importance. During the process of wire drawing, the conditions are substantially the same as during calibration, except for friction due to the motion, and the effects of the stiffness of the wire. It may be noted that the effect of static friction is not apparent during calibration, as the motion just before the oscillating spring comes to rest is sometimes in one direction, and sometimes in the other, and the variations disappear in the mean. The effect of backlash in the spring contacts of the bridges also tends to disappear in the same manner, both during calibration, and during wire drawing. The backlash amounts to about 0.04 lb. for the stronger spring, and is negligible for the other. A variation of 0.04 lb. is equivalent to about  $\frac{1}{4}$  per cent. of the work done. When using suitable string, the variation in

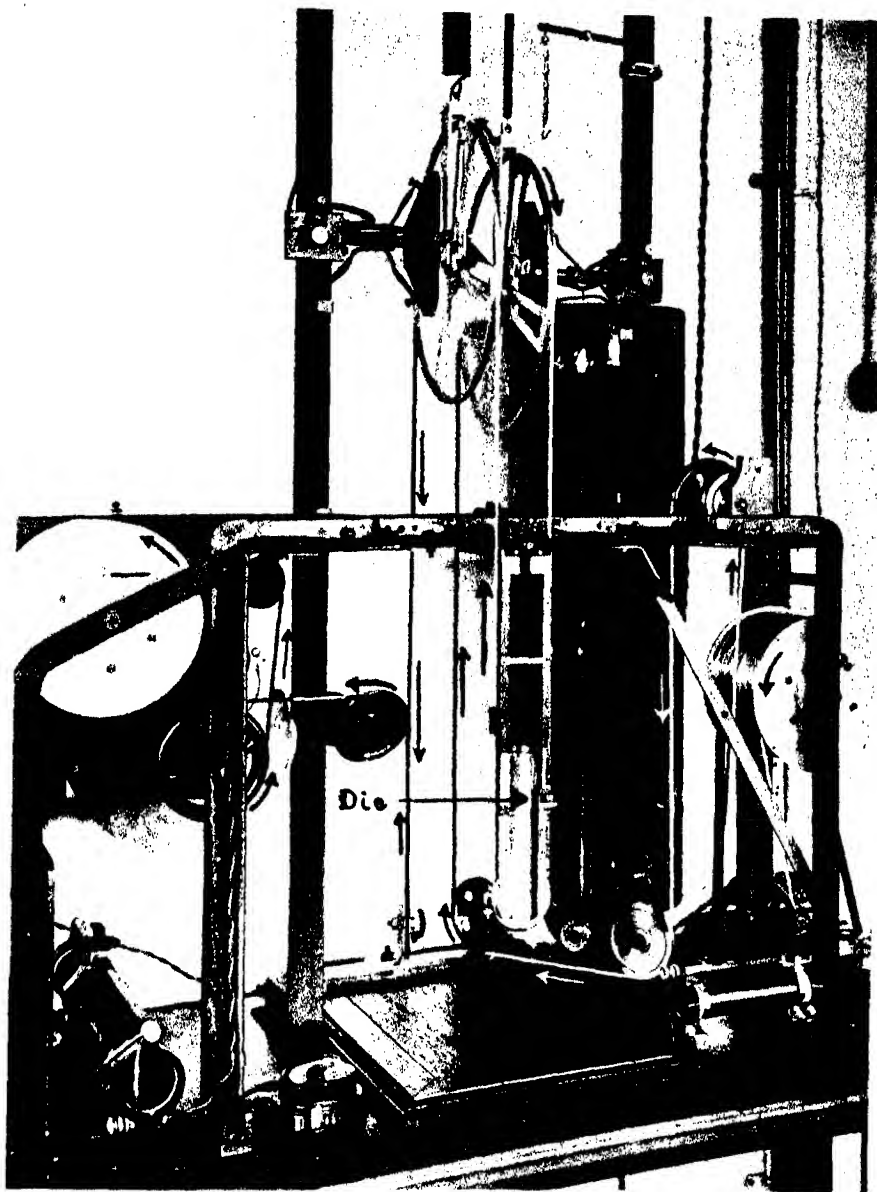


FIG. 4.—The thickness of the wire has been exaggerated for clearness.





successive equilibrium positions corresponds with a change of load of less than 0.01 lb., the working load being about 16 lb.

The corrections for friction and stiffness of the wire, are obtained by passing the wire round the measuring pulley, hanging equal weights on each end, and determining the least excess weight required on one side to maintain continuous rotation of the wheel. For annealed aluminium wire of the initial diameter (approximately 18 S.W.G., or 0.048 inch) the excess weight required for tensions between 1 and 14 lb. was 0.038 lb. (The friction due to the ball bearing under zero load amounts to about 0.0066 lb.) For wire which has passed through the die (approximately 20 S.W.G. or 0.036 inch) the excess weight required was 0.022 lb. These figures may vary slightly with the velocity. Ignoring such variation, a correction of 0.02 lb. must be added to the reading of the lighter spring and 0.01 lb. must be subtracted from the reading of the heavier spring. The total correction amounts to about  $1/5$  per cent. of the work done. It may be noted that work is done on the wire in bending it round the pulley before entering the calorimeter, and that some of the heat produced by this work may remain in the wire and enter the calorimeter. This work is less than 0.08 per cent. of the whole, and since the undissipated heat which may enter the calorimeter is still less, it may be disregarded. (The figure is obtained from the known stretch of the wire under a load fourteen times as great as that actually used.)

The calibration of the Wheatstone bridges is very simple. A known current is passed through one of the bridges with no load on the corresponding spring, and the galvanometer deflection noted for different values of the micrometer at the head of the spring. The very small backlash previously mentioned can be observed during this calibration. The currents through the bridges are measured with more than sufficient accuracy on Weston ammeters. The correct ratio of the currents in the two bridges, which enables a single galvanometer to be used for measuring changes in the power at any moment, is calculated from the various calibrations described, together with a knowledge of the extension of the wire given experimentally by  $l_1/l_2$ . The calibrations were repeated on many occasions during the progress of the work, and were never found to have changed. It was also found that the deflections of the galvanometer were strictly proportional to the applied voltage over the whole length of the scale. It should be mentioned that the readings of the quantity  $S'$  are taken some 10 times a minute during wire drawing at each revolution of the driving wheel, which is fitted with a signal bell. Equal lengths of wire are thus drawn through the machine between any two consecutive readings of

S'. These readings are divided into a set of even readings, and a set of odd readings, and averaged separately. The greatest difference between the two means for the experiments on aluminium corresponds with a difference of 1 part in 1500 of the work done.

The calorimetric determination is rather difficult, since the rate of heat production with aluminium is only about 5 watts, giving a rise of temperature of the calorimeter of about  $4\frac{1}{2}^{\circ}$  C. in half an hour. Measurements have not been made over longer periods than this owing to the uncertainty which would have been produced in the cooling corrections. The calorimeter is calibrated by the application of approximately the same power acting for the same length of time as that given out during wire drawing. Experiments have shown that considerable deviations from the standard times and power output are without measurable influence on the result. As a little oil is carried out of the calorimeter during wire drawing, calibration must be made before and after drawing, and the mean value taken to be the effective value during wire drawing. The change in the equivalent of the calorimeter due to loss of oil is about 1 per cent. for a run of half an hour. The electrical input to the calorimeter is measured potentiometrically with the aid of standard manganin resistances calibrated against the laboratory standards at  $20^{\circ}$  C. The temperature coefficient of such resistances is small enough to be neglected. The battery which feeds the calorimeter heating coil is allowed to discharge through a resistance equal to that of the heater for some time before an experiment. The voltage of the battery thereafter is very steady, which greatly facilitates the measurement of the power. The time during which the current flows is measured by means of a stop-watch which has been compared with the laboratory's standard clock. The combined effects of stirring and cooling are determined in the usual way, but, owing to the fact that the rate of supply of heat to the calorimeter during wire drawing, or during calibration, is constant, the calculation of the corrections is considerably simpler than usual. The calibration of the calorimeter can usually be repeated to within considerably less than 1 per cent. Greater accuracy was attained in the experiments on copper owing to the greater energy employed. The largest source of error probably arises from imperfect mixing of the oil. The rise of temperature of the calorimeter is usually about  $0.53^{\circ}$  C. per K-joule, the variations from this value being due to small changes in the quantity of oil employed. In calculating the results, it is assumed that wire enters the calorimeter at the temperature of the room and leaves it at the temperature of the oil. In order to determine whether the conductivity of the aluminium wire could affect the results, a cooling curve

of the calorimeter was determined with two thick wires leading out from it. After a considerable time had elapsed, the wires were removed. It was then easy to calculate that the cooling effect of two wires of the sizes used in wire drawing, if stationary, would be  $0.0002^{\circ}$  per minute per degree Centigrade difference of temperature between the room and the calorimeter. Now, during wire drawing, the temperature gradient along the wire leaving the calorimeter is greatly reduced. Also the incoming wire is supposed, for the purpose of calculation, to enter the calorimeter at room temperature. Both these causes result in the effective cooling of the calorimeter, during wire drawing, being slightly over-estimated, since the cooling is calculated from measurements made with the wire stationary. The error caused in this way cannot be greater than the total cooling effect of the wires, and, from the result above cannot therefore be greater than  $\frac{1}{4}$  per cent. The direction of the error is to reduce the discrepancy between the work done and the heat evolved. The thermal capacity of the aluminium wire leaving the calorimeter is taken as 1.616 joules per  $^{\circ}\text{C}$ . per metre and is based on Griffiths' value of 0.213 calories per gram at  $20^{\circ}\text{C}$ . The greatest value of the correction term involving this figure is about 10 per cent. of the heat imparted to the calorimeter. The final error due to an inaccurate knowledge of the specific heat of aluminium is not likely to be greater than one or two parts in a thousand. The error due to an incorrect value of the mean rise of temperature of the wire above that of the room is of the same order.

There is, however, a possible source of error which remains to be discussed, namely, the possibility of the wire leaving the oil at a temperature considerably higher than that of the latter. An attempt was made to investigate this question by determining the rise of temperature of a nickel wire, of the same diameter as the aluminium, when heated electrically in a current of oil flowing through a tube; the rise of temperature of the wire being measured by means of the change in its electrical resistance. Unfortunately, the distribution of velocity of the oil is not the same in the two experiments, and only approximate information can be obtained. It could be asserted with certainty from the results that the error which we are discussing is less than 10 per cent. This is otherwise obvious, since the difference between the work done and the heat produced is found to be little more than 1 per cent. There appears to be no way of obtaining a closer estimate of the error on the lines indicated above. But a rate of cooling of the wire equal to twice that corresponding with a 10 per cent. error would correspond with a 1 per cent. error, whilst three times the cooling rate would correspond with an error of 0.1 per cent. The

last value is by no means unlikely in view of the aids to cooling existing in the calorimeter which have been ignored because they are not susceptible to calculation, and in view of the inaccuracy of the various assumptions involved in the calculations.

The magnitude of the possible error due to the non-attainment of thermal equilibrium between the wire and the oil in the calorimeter could not be investigated by changing the conditions of the experiment, as, for example, by altering the dimensions of the calorimeter, varying the speed of wire drawing, etc. Any changes large enough for such a purpose, would have increased the errors from other causes, resulting in a loss of precision sufficiently serious to render inconclusive the results of experiments conducted under the changed conditions.

In calculating the final result, allowance must be made for the fact that the wire, after drawing, is in a state of tension, and that heat is evolved on its release. From the value of Young's modulus for drawn aluminium, it has been computed that a correction of 0.08 per cent. must be applied under the conditions of our experiments.

As has been mentioned, the technique described above is substantially the same for copper, but owing to its greater strength, the energy dealt with is considerably greater than with aluminium, and the various errors relatively less. The specific heat of copper was taken as 0.385 joules per gram at 20° C., a value obtained from the "International Critical Tables."

Two series of experiments were done on copper. In the first series, the same diamond die was used as for the aluminium. This die had a taper of 18° to the centre line. In the second series, the wire obtained from the first series was passed through a second die of 15° taper, giving to the wire the greatest extension possible without undue risk of rupture. In the first series of experiments on copper, the calibration of the springs before the determinations agreed very closely with the calibration performed afterwards, but in the second series, a discrepancy affecting the results to the extent of about 1 per cent. was found. This work was repeated, and again a discrepancy was found, although slightly smaller. Taking the mean calibration figures, however, the two sets of measurements agreed exactly. In view of the difficulty which is discussed later, of comparing the results on the hard and soft wires, it was decided not to repeat the measurements again.

The results of the various determinations are given below :—

**Aluminium (annealed)—**

Extension of wire .....	66 per cent.
Speed of wire leaving die .....	3·53 metres per min.
Tenacity before drawing .....	5·9 tons per sq. in.
Tenacity after drawing .....	8·15 „
(Work-heat)/Work—	
1st series .....	1·6 per cent.
	1·0 „
	1·9 „
	—
Mean .....	1·5 „
2nd series .....	0·6 „
	1·3 „
	1·0 „
	—
Mean .....	1·0 „
	—
Mean of both series .....	1·2 „

This is equivalent to 0·47 joules per gram.

Total work done (including friction in die).. 38 joules per gram.

**Copper (annealed)—**

Extension of wire .....	68·7 per cent.
Speed of wire leaving die .....	*4·37 metres per min.
Tenacity before drawing .....	16·1 tons per sq. in.
Tenacity after drawing .....	24·4 „
(Work-heat)/Work .....	3·3 per cent.
	3·0 „
	3·0 „
	—
Mean .....	3·1 „

This is equivalent to 0·96 joules per gram.

Total work done (including friction in die).. 31 joules per gram.

\* This speed is somewhat higher than that used for aluminium, as a new driving motor had to be used to provide the additional power.

Hard copper wire from previous experiments—

Extension of wire .....	28.5 per cent.
Tenacity before drawing .....	24.4 tons per sq. in.
Tenacity after drawing .....	25.5 „
(Work-heat)/work .....	0.2 per cent.
	0.2 „
	0.9 „
	—
Mean of more exact figures .....	0.5 „

This is equivalent to 0.12 joules per gram.

Total work done (including friction in die).. 24.5 joules per gram.

It is interesting to compare these results with those obtained by Farren and Taylor\* by direct extension of aluminium and copper rods. In this case, much smaller extensions were used than in the wire drawing method, in which stretching is assisted by lateral compression. We may reasonably suppose, however, that the change in internal energy of the metal when extended by either of the above methods will depend mainly on the percentage extension. The figures in Table I for aluminium are mean values taken from Farren and Taylor's paper; the percentage extension is represented by  $\epsilon$ , and  $T_1$  is the rise of temperature of the metal.

Table I.

$\epsilon$ .	$T_1/\epsilon$ .	$\log_{10} \epsilon$ .
10.23	0.211	1.010
16.50	0.241	1.217
22.30	0.258	1.348
66	0.314	1.820
	(extrapolated)	

The extrapolation is facilitated by the fact that the relation of  $T_1/\epsilon$  to  $\log \epsilon$  is almost linear.

Since

$$T_1/\epsilon = 0.314$$

when

$$\epsilon = 66$$

(the extension used in our experiments) we find  $T_1 = 20.7^\circ$  and since Farren and Taylor found that  $T_1/T_2$  has a constant value of 0.928 we have  $T_2 = 22.3^\circ$ ,

\* 'Proc. Roy. Soc.,' A, vol. 107, p. 422 (1925).

the change of internal energy of the metal resulting from 66 per cent. extension being equivalent to a rise of temperature of  $1.6^{\circ}$  C. or 1.4 joules per gram of metal.

For copper, the corresponding figures are shown in Table II.

Table II.

$\epsilon$ .	$T_1/\epsilon$ .	Log $\epsilon$ .
8.07	0.270	0.907
13.88	0.337	1.142
19.18	0.383	1.283
68.7	0.612	1.837
	(extrapolated)	

Hence we have

$$T_1/\epsilon = 0.612$$

$$\epsilon = 68.7,$$

therefore

$$T_1 = 42.04.$$

Now  $(T_2 - T_1)/T_1 = 9/91$  (Farren and Taylor, *loc. cit.*),

therefore

$$T_2 - T_1 = 4.16^{\circ} \text{ or } 1.6 \text{ joules per gram.}$$

It will be observed that these figures, both for copper and for aluminium are higher than our own. In this connection it must be remembered that if, in our experiments, the wire emerges from the calorimeter at an appreciably higher temperature than that of the oil, a point which we are unable to test, our values of the change of potential energy tend to be too large. There are therefore three possible reasons for the difference in the results. In the first place, the difference may be due to experimental error, and in the second place, the assumption of the equivalence of direct extension and wire drawing for equal extensions, may be too inaccurate. (Since writing the above, one of us has received a private communication from Professor Taylor suggesting that to make allowance for the difference between wire drawing and direct extension, for copper, the work calculated for direct extension should be raised by a fraction, of the order of 50 per cent., before comparing it with the results of wire drawing experiments.) Thirdly, the extrapolations of Farren and Taylor's results may be incorrect. Here it should be remarked that we have assumed that the constancy of the ratio  $T_1/T_2$  found by Farren and Taylor for extensions up to about 20 per cent. still holds for an extension of 68 per cent. in spite of the very considerable hardening of the metal.



Our work on copper seemed to suggest that the proportion of energy retained by the metal is a diminishing function of the work performed on it. Some uncertainty in the interpretation of our results is introduced by the lack of exact knowledge of the work expended against friction in the dies. Some measurements have fortunately been published by Sato,\* since the completion of our experiments, which confirm qualitatively our suggestion. As, however, his specimens were deformed by twisting, his data cannot be applied quantitatively to our results, since with torsion, the deformation is not uniformly distributed over the cross section of the specimen. It does not seem possible to compare our results with those of Smith† owing to the excessive extrapolation which would be required.

It appears, therefore, from the present work, that the order of magnitude of the energy differences found by Farren and Taylor is confirmed. The very large value of 70 per cent. for the proportion of latent energy found for steel by Giraud,‡ as compared with the value of  $13\frac{1}{2}$  per cent. found by Farren and Taylor, is presumably due to experimental error.

We wish, in conclusion, to express our thanks to Messrs. The General Electric Company, who kindly lent us the necessary diamond dies; to Messrs. The British Aluminium Company who supplied us with specially prepared wire; to Mr. H. P. Bloxam of the Metrology Department, who was responsible for the design and construction of the micrometers; and to Mr. G. H. Glaysher of the Metallurgy Department, who, with great skill, constructed the rest of the apparatus.

#### *Summary.*

It has been suspected for a number of years, and has more recently been established by Taylor and Farren, that the internal energy of a cold-worked metal is appreciably greater than that of the same metal in the annealed state. One of the authors became interested in this question some ten years ago on account of its connection with the phenomena of the plastic deformation of metals. Accordingly, attempts were made to measure the energy change in question by methods akin to that of Taylor and Farren. Considerable difficulties were encountered, and these methods were abandoned on the publication of Taylor and Farren's results.

The present paper deals with a new method of attacking the problem by means of measurements of the work done, and the heat produced, when a

\* Sci. Rep. Imp. Univ. Tôhoku, vol. 20, No. 1 (1931).

† 'Proc. Roy. Soc.,' A, vol. 125, p. 619 (1929).

‡ 'Rev. Métal.' vol. 25, p. 347 (1928).

considerable length of wire is drawn through a die which is enclosed in a calorimeter. This process has the advantage of being continuous in operation, and is associated with a much larger expenditure of energy per unit mass of metal, than are the previous processes. The accuracy attainable is limited, however, by the smallness of the total mass of metal which can be cold-worked during a period of time which is suitable for a calorimetric experiment.

An exact comparison of the results obtained, for aluminium and copper, with those of Fraren and Taylor, is not possible, owing to differences in the extent and manner of working the metals, but approximate confirmation of their results was obtained.

---

*The Spectrum of H<sub>2</sub>—The Bands Ending on 2p <sup>3</sup>Π Levels. Part II.*

By O. W. RICHARDSON, F.R.S., Yarrow Research Professor of the Royal Society, King's College, London, and P. M. DAVIDSON, Ph.D., Senior Lecturer in Physics, University College, Swansea.

(Received December 21, 1932.)

§ 1. *The Lines of the 3d <sup>3</sup>ΣΠ Δ → 2p <sup>3</sup>Π Complex.*

In a previous paper† we described what we believed to be the structure and properties of the bands which end on the important 2p <sup>3</sup>Π<sub>ab</sub> levels. In that paper we stated that "Although we believe these band systems to be correct in their main outlines some of the details cannot be fixed with the same degree of certainty as were the band systems described previously. We are doing further work which may modify them and make them more certain." This doubtfulness subsequently became intensified as a result of the theoretical investigations of one of us‡ on the distribution of intensity among the lines of the H<sub>2</sub> spectrum. These showed a satisfactory agreement with the intensities as measured by Kapuscinsky and Eymers§ for the other band systems for which calculations could be made, but some of the systems ending on 2p <sup>3</sup>Π appeared to be exceptional. Even when the correct final intervals,

† 'Proc. Roy. Soc.,' A, vol. 131, p. 658 (1931), referred to later as I.

‡ Davidson, 'Proc. Roy. Soc.,' A, vol. 138, p. 580 (1932).

§ 'Proc. Roy. Soc.,' A, vol. 122, p. 58 (1929).

and the groups of lines which satisfy them, have been discovered the task of correctly arranging them into bands is not an easy one. Owing to the way in which the bands are intermingled there are a number of alternative ways in which these groups can be put together. This difficulty is increased by the presence of numerous blends, by false combinations and, especially in these particular band systems, by the frequent absence of entire branches of bands and by the fact that there is no strength anywhere except in the diagonal bands.

Meanwhile a re-arrangement of some of these bands has been put forward by Sandeman.<sup>†</sup> This involves abandoning the weak lines (which arise from transitions between the symmetric<sup>‡</sup> states) in the  $3d^3\Pi_{ab} \rightarrow 2p^3\Pi$  and  $3d^3\Delta_{ab} \rightarrow 2p^3\Pi$  systems as they are described in I. In  $3d^3\Delta_a \rightarrow 2p^3\Pi$  ( $0 \rightarrow 0$ ) the first R'Q'P' set of symmetric lines are replaced by the corresponding set of anti-symmetric RQP lines of  $3d^3\Delta_b \rightarrow 2p^3\Pi$  while  $3d^3\Delta_b \rightarrow 2p^3\Pi$  itself is formed in the same way from the  $3d^3\Pi_b \rightarrow 2p^3\Pi$  and  $3d^3\Pi_a \rightarrow 2p^3\Pi$  bands of I. It thus puts all the strength of the original  $3d^3\Pi_{ab} \rightarrow 2p^3\Pi$  and  $3d^3\Delta_{ab} \rightarrow 2p^3\Pi$  systems into  $3d^3\Delta_{ab} \rightarrow 2p^3\Pi$ . In effect this abolishes the original  $3d^3\Pi_{ab} \rightarrow 2p^3\Pi$  bands although it makes little difference to the  $3d^3\Sigma \rightarrow 2p^3\Pi$  system. On this basis Sandeman has been able to extend the  $2p^3\Pi$  state to higher vibrational and rotational levels than we were able to do in I. None of our antisymmetric levels are altered in this state.

We believe that, apart from a few unimportant details, the arrangement of the  $3d^3\Delta_{ab} \rightarrow 2p^3\Pi$  systems proposed by Sandeman is correct. In fact, it is fully confirmed by our own work on the  $3d^3\Sigma \rightarrow 2p^3\Pi$ ,  $3d^3\Pi_{ab} \rightarrow 2p^3\Pi$ ,  $4d^3\Sigma \rightarrow 2p^3\Pi$ ,  $4d^3\Pi_{ab} \rightarrow 2p^3\Pi$  and  $4d^3\Delta_b \rightarrow 2p^3\Pi$  systems. We have been able to find each of these at the vibrational levels  $v' = 0, 1, 2, 3$  and  $v'' = 0, 1, 2, 3$ . There are also some other bands ending on  $2p^3\Pi$  which do not come from the 3,  $4d^3\Sigma\Pi\Delta$  complexes.

The general structure and properties of the bands are not altered in any fundamental way by these extensions and we shall employ the same notation and methods in dealing with the new material that we used in I.

The lines of the bands of the  $3d^3\Sigma \rightarrow 2p^3\Pi_{ab}$  system are set out in Table I. In this and similar tables of band lines the first column gives the rotational

<sup>†</sup> 'Proc. Roy. Soc.,' A, vol. 138, p. 395 (1932).

<sup>‡</sup> In the summary of Sandeman's paper the weak lines are referred to as antisymmetric and the strong as symmetric. This is probably an accident, though either notation may be defended, depending on which wave functions are alluded to. The notation we adopt is that which is in general use.

designation of the line. The number following the letter P, Q or R designating the branch of the band is the quantum number  $K$  of the final level. Thus R1 means a line involving a transition from an initial level with  $K = 2$  to a final level with  $K = 1$ , both levels being strong antisymmetric ( $a$ ) levels. Lines involving transitions between the alternate weak symmetric ( $s$ ) levels are indicated by dashes. Thus Q'2 means a line involving a transition between two  $s$  levels for each of which  $K = 2$ , and so on. The second column gives the wave number of the line. In general these are taken from the tables of Gale, Monk and Lee.<sup>†</sup> For lines not measured by them Finkelburg's<sup>‡</sup> and, in a few instances, Merton and Barratt's<sup>§</sup> measures have been used. Sometimes where both Gale, Monk and Lee's and Finkelburg's data are available Finkelburg's data have been used either because the lines are enhanced in his tables or else to give one investigator's measures for all the lines of a given band. As a rule the combinations are more consistent when the data of either table are adhered to than when they are mixed up, and in the region on the high frequency side of H $\beta$  Finkelburg's data are the more extensive.

The third column gives Kapuscinsky and Eymer's<sup>||</sup> measurements and the fourth the eye estimates of Gale, Monk and Lee. The fifth column gives the response of the lines to high (H) or low (L) pressure, the sixth to the condensed discharge (C) and the eleventh to helium (He). The data in these three columns are the observations of Merton and Barratt (*op. cit.*). The seventh column shows the effect of a magnetic field on the lines as recorded by Dufour<sup>¶</sup> or Croze,<sup>††</sup> the eighth and ninth under R.T. and L.A., the intensities at room temperature and with the tube immersed in liquid air as given by McLennan, Grayson-Smith and Collins,<sup>‡‡</sup> and the tenth column, under V, the excitation potential of the final level of the line as determined by Finkelburg, Lau and Reichenheim. An asterisk denotes interferometer measures of Gale, Monk and Lee.

The lines of the  $3d\ ^3\Pi_b \rightarrow 2p\ ^3\Pi_{ab}$  and  $3d\ ^3\Pi_a \rightarrow 2p\ ^3\Pi_{ab}$  systems are set out in the same way in Tables II and III respectively.

<sup>†</sup> 'Astrophys. J.,' vol. 67, p. 89 (1928).

<sup>‡</sup> 'Z. Physik,' vol. 52, p. 27 (1928).

<sup>§</sup> 'Phil. Trans.,' A, vol. 222, p. 369 (1922).

<sup>||</sup> 'Proc. Roy. Soc.,' A, vol. 122, p. 58 (1928).

<sup>¶</sup> 'Ann. Chim. Phys.,' vol. 9, p. 361 (1906); 'J. Phys. Rad.,' vol. 8, p. 259 (1909).

<sup>††</sup> 'Ann. Physique,' vol. 1, p. 58 (1914).

<sup>‡‡</sup> 'Proc. Roy. Soc.,' A, vol. 116, p. 277 (1927).

<sup>§§</sup> 'Z. Physik,' vol. 61, p. 782 (1930).

Table I.— $3d^2\Sigma \rightarrow 2p^3\Pi_{as}$ .

The 0 → 0 band.										The 1 → 0 band.									

The 2 → 2 band.			R.T. L.A. V.		The 1 → 2 band.	The 3 → 2 band.
R'1	16332.11	— 1			¶ 14373.46	0 18042.49 1
R2	16395.02	— 3				
R'3	16247.26	— 2				006
R4	16192.25	15.8 6		32 25	‡ 17937.03††	
Q1	16297.25	22.3 5	H++ C++ Z=0		14386.48	006 3
Q'2	16222.72	10.0 2	C++ Z=0			
Q3	16132.09	18.4 5	H++			
Q'4	16032.26	— 1a				
Q5	15926.52	— 3a	H+ C+		17879.60††	4 C++ 9 R.T. L.A.
P'1	16287.69	— 1	H+	13 10½a		
P2	16187.50	— 1			17920.33	3 C+
P'3, P4 and P6 are absent.					P4 is absent.	
R2 is also Q'6 of the 0 → 0 band.						
The 3 → 3 band.					The 2 → 3 band.	
† R'1	15976.14	— 0		2½a 3½a		
R2	15949.72	— 3	L+	9 8½	14202.3	0b
R'3	15910.77	— 0				
R4	15862.86	— 1a	C+			
Q1	15931.94	— 2			14199.2	1
† Q'2	15872.20	— 1				
Q3	15795.05	— 2			14047.6	1
Q'4	15706.57	— 1				
† Q5	15610.91	— 1				
P'1	15913.37	— 00				
P2	15827.48	— 1		2½a 2½		
† P'3 = [15716.4], P4 = [15589.01] and P6 are absent.					P4 absent.	
P2 might be absent and Q1 = 15932.26 19.8 3 H++ C+					21 20	
† Q5 is also Q3 of 0 → 5 3d'1I <sub>0</sub> → 2p'2.						

† Data for blends with lines of similar intensity.

‡ Most of this is 2 other lines.

§ This is 2 lines in the singlet systems which require most of the strength, the combination here is not good. The properties given for the lines in the 2 → 1 band may be influenced by blends with weaker lines.

|| This also is 2 lines in the singlet systems and the combination here also is poor (error about 0.1 wave-number).

¶ Coincident with 3d'1I<sub>0</sub> → 2p'1I<sub>0</sub>, 2 → 3, P3.

†† Coincident with lines of the singlet systems.

Table II.— $3d^3\Pi_0 \rightarrow 2p^3\Pi_{ab}$ .

<i>The 0 → 0 band.</i>										<i>The 1 → 0 band.</i>			
R1	17199.28*	44.0	10	H++ C++	Z?	77	52	11.89	He++	19317.37	—	0	
R'2	17202.51	14.3	4	C++	Z=0				He++				
R3	17199.28*	44.0	10	H++ C++	Z?	77	52	11.89	He++	19315.19	—	0a	
R'4	17191.46	—	1a						He++				
R5	17179.50	9.1	3	H++ C++		23	16		He++				
R'6	17162.25	—	0a										
Q'1	17125.07	—	2	C++					He++				
Q2	[17078.56]	—	ab	17079.1(-) T					He++	19196.60	—	0a	
Q'3	[17022.60]	—	ab										
Q4	16961.69†	—	0	C++		10	8		He0				
Q'5	[16897.79]	—	ab										
Q6	16831.97	—	0										
P'2	17004.40	14.9	3a										
P3	16898.48†	16.3	5	H++ C++	Z=0	42	31		He+	19010.55	—	0	
P'4	16784.66	—	1										
P5	16667.33	—	1	C++					He+				
P'6	[16549.38]	—	ab										
P7	16431.36	—	0	C+		10½a	10½a						
P'4 is also ? P'2 of the 1 → 1 band.													
<i>The 1 → 1 band.</i>										<i>The 2 → 1 band.</i>			
R1	16978.52*	28.0	10	H++ C+	Z	50	36	12.13		18947.44	—	1	
R'2	16988.72	22.7	8	C+	Z	42	32	12.15					
R3	16990.71	21.3	6	H++ C++									
R'4	16966.10	—	1a	C+						18956.39	—	1	
? R5	16977.18	—	0										
? Q'1	16899.76	—	0							ab			
Q2	16863.40§	—	1	C++									
Q'3	[16817.09]	—	ab										
Q4	[16753.80]	—	ab										
Q'5	[16705.70]	—	ab										
? Q6	[16645.39]	—	ab										
? P'2	16784.56§	—	1	C+	Z	14½	10½		He0				
P3	16692.00*	14.0	5	H++ C+	Z=0					18660.93	—	2	H+ C+
P'4	16590.90	8.0	1	C+									
P5	16484.00	—	1	C++						18449.78	—	0h	
P'6	[16375.—]	—	ab										
P7	[16265.0]	—	ab										

? Q'1 is also ? P'6 of 2 → 2  $3d^3A \rightarrow 2p^3\Pi$ .P5 is also in the position for Q2 of 3 → 1  $3d^3\Pi_0 \rightarrow 2p^3\Pi$ .







The 2 → 2 band.				The 1 → 2 band.				The 3 → 2 band.			
R' 1	16822.00	6.7	2	C + +	19½a	18½a					
R' 2	16897.19†	10.9	5	H + +	C + +	Z = 0	42	31	He +		
R' 3	16961.25††	—	0h	C + +			10	8	HeO		
R' 4	17013.50	—	1	C +			6½	5½a			
Q1	16684.88	—	1	C +	Z = 0						
Q' 2	[16712.59]	—	ab								
Q3	16734.20	11.0	4	C +					00		
Q' 4	16746.17	—	1								
Q5	16747.70‡	—	1								
P2	16575.12	24.5	5						14662.10	1	18376.62
P' 3	16548.90	11.1	3	H +	C +	Z = 0	17½a	14			
P4	16517.89	16.8	6	H + +	C +	Z = 0	3½	30			
P' 5	[16478.63]	—	ab								
P6	16431.36‡	—	0	C +			16½a	10½a			
R' 1 is also P' 3 of 0 → 0 Z → 2p <sup>3</sup> Π											
R4 is also Q1 of 0 → 0 Z → 2p <sup>3</sup> Π											
Q5 is also a doubtful line in the λ 4143 singlet progression. P6 is also P7 of 0 → 0 3d <sup>3</sup> Π <sub>b</sub> → 2p <sup>3</sup> Π. This P7 line depends on an interval which is not very certain. Alternatives are: Q5 = 16743.17 (3), P6 = 16426.79 (00).											
Q3 is also P2 of 0 → 0 3d <sup>3</sup> Σ → 2p <sup>3</sup> Π.											
18376.62 is also P4 of 0 → 0 4d <sup>3</sup> Π <sub>a</sub> → 2p <sup>3</sup> Π											
The 3 → 3 band.				The 2 → 3 band.							
R' 1	16511.46	—	1								
R2	16579.03	10.8	2	C +							
R' 3	16633.03	—	0	H +	C +						
R4	16678.57*	40.0	10	L + +	C =	Z = 0	38	40	HeO		
Q1	16388.32	—	1	C + +							
Q' 2	[16407.51]	—	ab								
Q3	16424.30	—	00								
Q' 4	16428.77	—	0	C + +			15½a	10½a	He + +		
Q5	16426.79	—	00								
P2	16283.83	8.6	2	C + +					14482.41	0	
P' 3	16261.79	12.0	4	C +			10½	10½a			
P4	16218.29	—	1h	C +			12½	12			
P' 5	[16175. —]††	—	ab								
P6	[16128. —]	—	ab								
R4 is concealed by R0 of 0 → 0 3p <sup>3</sup> Π → 2s <sup>3</sup> Σ.											
R2 is also P6 of 1 → 1 3s <sup>3</sup> Σ → 2p <sup>3</sup> Π.											
				P' 3 is also P3 of 4 → 1 3p <sup>3</sup> Σ → 2s <sup>3</sup> Σ.				R' 3 is also P' 5 of 1 → 1 3s <sup>3</sup> Σ → 2p <sup>3</sup> Π.			

† Data for a blend with an unclassified line of similar intensity.  
 .19134.07 is also R7 of 0 → 2 3d<sup>3</sup>Σ → 2p<sup>3</sup>Σ  
 ‡ Coincident with a weak line P3 of 2 → 7 3d<sup>3</sup>Π<sub>a</sub> → 2p<sup>3</sup>Σ.  
 § Properties are for a blend with P3 of 1 → 1 3d<sup>3</sup>Σ → 2p<sup>3</sup>Π.

‡ Probably a blend. It seems too strong and is a Z line.  
 § Properties are for a blend with P3 of 0 → 0 3d<sup>3</sup>Π<sub>b</sub> → 2p<sup>3</sup>Π.  
 †† Properties are for a blend with three other lines.  
 ‡‡ May be 16172.99 (0) M.B. He +.

The lines of the  $3d^3\Delta_{ab} \rightarrow 2p^3\Pi_{ab}$  systems are not tabulated, since these are the bands given by Sandeman (*loc. cit.*). Possible alterations or additions\* are:—

P7 of  $0 \rightarrow 0$   $3d^3\Delta_b \rightarrow 2p^3\Pi$  coincident with 17192·31 (6) = Q3 of  $2 \rightarrow 2$   $3d^3\Delta_a \rightarrow 2p^3\Pi$ .

P7 of  $2 \rightarrow 2$   $3d^3\Delta_b \rightarrow 2p^3\Pi$  coincident with 16863·40 (1) = Q2 of  $1 \rightarrow 1$   $3d^3\Pi_b \rightarrow 2p^3\Pi$ .

Q5 of  $3 \rightarrow 3$   $3d^3\Delta_a \rightarrow 2p^3\Pi$  may be coincident with 17030·88 (1) = P7 of  $1 \rightarrow 1$   $3d^3\Delta_b \rightarrow 2p^3\Pi$ .

R' 4 of  $3 \rightarrow 3$   $3d^3\Delta_b \rightarrow 2p^3\Pi$  may be coincident with 17287·27 (2) = P'3 of  $0 \rightarrow 0$   $3d^3\Delta_a \rightarrow 2p^3\Pi$ .

R4 of  $3 \rightarrow 3$   $3d^3\Delta_a \rightarrow 2p^3\Pi$  may be coincident with 17282·98 (1) = R3 of  $1 \rightarrow 1$   $3d^3\Pi_a \rightarrow 2p^3\Pi$ .

R1 of  $2 \rightarrow 1$   $3d^3\Delta_b \rightarrow 2p^3\Pi$  is 19495·90(1*h*), Q3 of  $2 \rightarrow 1$   $3d^3\Delta_a \rightarrow 2p^3\Pi$  is 19395·13(0), in  $3 \rightarrow 2$   $3d^3\Delta_b \rightarrow 2p^3\Pi$  R1 is 19227·90(1*h*), Q2 is 19117·98(1*h*) and P3 is 18955·30(0). R2 of  $3 \rightarrow 2$   $3d^3\Delta_a \rightarrow 2p^3\Pi$  is 19280·58(0) and Q3 and P4 of this band are 19117·98(1*h*) and 18901·60(1*a*) respectively. If R' 1 of  $3 \rightarrow 3$   $3d^3\Delta_a \rightarrow 2p^3\Pi$  is concealed by 17130·78(3*a*) = P4 of  $1 \rightarrow 1$   $3d^3\Delta_a \rightarrow 2p^3\Pi$  we make the error to be 0·5 wave number which seems prohibitive.

In all these systems the strength is practically confined to the diagonal bands. The  $0 \rightarrow 0$  and  $1 \rightarrow 1$  bands are the most intense with about equal strength,  $2 \rightarrow 2$  is weaker and  $3 \rightarrow 3$  weakest. Lines of the non-diagonal bands  $1 \rightarrow 0$ ,  $2 \rightarrow 1$ ,  $3 \rightarrow 2$ ,  $1 \rightarrow 2$  and  $2 \rightarrow 3$  have only been found with certainty for the  $a \rightarrow a$  (strong) transitions. In contrast with the diagonal bands having the same upper vibrational state  $v'$  there is a definite tendency for the non-diagonal bands to increase in intensity with increasing  $v'$ . Thus in  $3d^3\Pi_b \rightarrow 2p^3\Pi$  the strongest lines in the  $1 \rightarrow 0$  and  $1 \rightarrow 2$  bands are assigned intensity 0 by Gale, Monk and Lee, whereas in the  $3 \rightarrow 2$  band there are two lines to which they assign intensity 3. Another feature common to all these band systems is the pronounced tendency of the lines to be enhanced at high pressure and in the condensed discharge. This is in strong contrast to the bands which end on the other  $n = 2$  triplet state  $2s^3\Sigma_g$  where the lines, particularly those associated with low values of the quantum number  $K$ , have a marked tendency to be enhanced at low pressures and depressed in the condensed discharge. We can illustrate this by reference to the R4 line of

\* We feel rather sure that these new 3—2 bands are the correct ones.

the  $3 \rightarrow 3$  band of  $3d^3\Pi_u \rightarrow 2p^3\Pi$  in Table III. The properties assigned to this line in the table are those of the much stronger R0 of  $0 \rightarrow 0$   $3p^3\Pi \rightarrow 2s^3\Sigma$ , with which it is coincident. The only other low pressure line in Table III is P2 of the  $1 \rightarrow 1$  band. This is not a known blend but it has the appearance of being too strong in this band. There are no other lines described as depressed in the condensed discharge. In fact, all of the lines in Table III which are also in Merton and Barratt's tables are described as enhanced in the condensed discharge with the exception of four very weak lines which they may not have troubled to examine very carefully. The high pressure enhancement tends to diminish with increasing vibrational quantum number which seems rather strange. Thus in the  $3 \rightarrow 3$  bands in Tables I to III there is no  $H++$  line which is not a blend, there is only one  $H+$  line and there are two  $L+$  lines which are not known blends. In a given branch of a band the ratio of the numbers in the R.T. column to those in the L.A. column should increase with increasing quantum number  $K$ . This is so except occasionally where the data are probably unreliable mainly owing to overlapping lines. The value of the excitation potential  $V$  should increase by about 0.3 volt at each step in going from  $0''$  to  $1''$ ,  $1''$  to  $2''$  and  $2''$  to  $3''$ . The data are rather rough, but the mean value of the determinations for the  $0' \rightarrow 0''$  bands in Tables I to III is 11.83 and for the  $1' \rightarrow 1''$  bands is 12.21. The difference of these is 0.38 volt which is not unsatisfactory.

The effect of an admixture of an excess of helium on the lines of the bands of  $3d^3\Sigma \rightarrow 2p^3\Pi$ ,  $3d^3\Pi_b \rightarrow 2p^3\Pi$  and  $3d^3\Pi_u \rightarrow 2p^3\Pi$  is interesting. In each system the lines of the  $0 \rightarrow 0$  bands are strongly enhanced whereas the lines of all the other bands are practically unaffected. It is true that in Tables I to III there is in each  $0 \rightarrow 0$  band one line which is marked He0; but in each of these instances the properties are for a blend with another line which might cause confusion. Although many lines of the  $H_2$  spectrum are very responsive to helium we know of no other case in which the effect is of such a general character as this. The effects on the singlet bands with the corresponding upper level are quite different. For example, in the case of  $3d^1\Sigma \rightarrow 2p^1\Sigma$ , the response to helium as given by Merton and Barratt is, for the  $0 \rightarrow 0$  band, R0He0, R2He+, R4He+, R5He0, R1, R3, R6, P1, P2, P3, P4, P5 and P6 which include some very strong lines are not mentioned. In the  $0 \rightarrow 1$  band the only line mentioned is a rather weak line P2 described as He0. In the  $0 \rightarrow 2$  band R0 is He+, R1 He0, R2 He0, R3 He++, R4 He++, R5 He++, P4 He0 and in the  $0 \rightarrow 3$  band R4 is He+ and the others unmentioned. In the whole of the  $1'$  and  $2'$  progressions of  $3d^1\Sigma \rightarrow 2p^1\Sigma$  each of

which includes some of the strongest lines in the  $H_2$  spectrum there appears to be no reference to any response to helium. At any rate this singlet system seems to have this in common with the triplet  $\Pi$  systems under consideration, that if there is any helium response at all it is confined to the  $v' = 0$  level. It is not possible to say anything about the  $3d^1\Sigma\Pi_{ab} \rightarrow 2p^1\Pi$  systems, which correspond precisely in the singlet spectrum to the present bands in the triplet spectrum, since these lie in the infra-red and the reaction of the lines to helium is not known. We can, however, say something about the bands which come down to  $2p^1\Pi$  from the next higher electronic levels  $4d^1\Sigma$  and  $4d^1\Pi$ . In  $4d^1\Sigma \rightarrow 2p^1\Pi_{ab}$   $0' \rightarrow 0''$  there is definitely no response, the only line mentioned being R4. This is given as He0, although the properties are for a blend of this line with Q2 of  $3 \rightarrow 2$   $3p^3\Pi \rightarrow 2s^3\Sigma$ . In  $4d^1\Pi_a \rightarrow 2p^1\Pi_{ab}$  the helium response, if any, is confined to the R branch where He+ is found opposite a mixture of R2 and Q5 of  $2 \rightarrow 6$   $3d^1\Pi_b \rightarrow 2p^1\Sigma$ . In  $4d^1\Pi_b \rightarrow 2p^1\Pi_{ab}$  all the lines of the R branch are definitely enhanced. There is no evidence that the Q and P branches are affected, but the lines are very weak and may have been overlooked. In  $4d^1\Delta_{ab} \rightarrow 2p^1\Pi_{ab}$  the incidence of the helium response is uncertain owing to blends, but it looks to be rather irregular. All these  $4d^1\Sigma\Pi\Delta \rightarrow 2p^1\Pi$  systems are only known at the  $v' = 0$  vibrational level except  $4d^1\Pi_b \rightarrow 2p^1\Pi$  for which the P branch at  $1' \rightarrow 0''$  exists. This does not respond to helium, so far as can be ascertained from Merton and Barratt's data.

There is something analogous to this effect of helium on the  $3d^3\Sigma\Pi\Delta \rightarrow 2p^3\Pi$  systems in the case of the  $3p^3\Pi \rightarrow 2s^3\Sigma$  system. A detailed account of the effect on the lines of the Q branches of the diagonal bands of this system has been published by one of us.\* In that publication the  $0 \rightarrow 0$  band is called A, the  $1 \rightarrow 1$  band B, and so on. In general the effect of helium is to depress the lines of these bands, the degree of depression increasing as the magnitude of  $v' (= v'')$  for the bands increases. The effect is not the same on all the lines of a given band; those are most depressed which have the lowest K values. In the  $0 \rightarrow 0$  band, however, only the Q1 line is depressed and that slightly; the Q2 line is unaffected and the others are enhanced, the enhancement increasing progressively in going from Q3 to Q6. It appears, then, that we can make this rather general statement. For a considerable number of very diverse systems helium enhancement, if it occurs to any marked degree, is confined in its incidence to the  $v' = 0$  levels.

\* Richardson, 'Proc. Roy. Soc.,' A, vol. 111, p. 721 (1926).

The behaviour of the lines of these triplet  $\Pi$  bands in a magnetic field is also very characteristic.  $3d^3\Sigma \rightarrow 2p^3\Pi$  shows the strongest response in this respect. The Zeeman effect is most marked in the  $0 \rightarrow 0$  band, not quite so marked in the  $1 \rightarrow 1$  band and has definitely disappeared at the  $2 \rightarrow 2$  band. For the  $3 \rightarrow 3$  band there is no information. These properties are exactly parallel to those of the  $3d^1\Sigma \rightarrow 2p^1\Sigma$  system where the  $0'$  progression has a very large number of Z lines, the  $1'$  progression a small number, and in the  $2'$  progression none have been recorded. However, it is not certain that the strong lines of the  $2'$  progression (assuming it to be that originally assigned\* to  $3^1K \rightarrow 2p^1\Sigma$ ) have been examined for the Zeeman effect; so that the fact that no Z lines have been recorded may not mean much. In the original  $2'$  progression of  $3d^1\Sigma \rightarrow 2p^1\Sigma$ , now transferred to  $3^1K \rightarrow 2p^1\Sigma$ , there are no Z lines and there is one  $Z = 0$  line. Both possibilities are referred to, since it is not altogether certain that these two levels should be interchanged. In  $3d^3\Pi_b \rightarrow 2p^3\Pi$  there are only two certain Z lines and a considerable number of  $Z = 0$  lines. In  $3d^3\Pi_a \rightarrow 2p^3\Pi$  (Table III) there are a large number of  $Z = 0$  lines but only one Z line and this is coincident with one of the two Z lines in  $3d^3\Pi_b \rightarrow 2p^3\Pi$ . There is thus no evidence that  $3d^3\Pi_a$  shows any magnetic response at any level, vibrational or rotational. These properties of  $3d^3\Pi_b$  and  $3d^3\Pi_a$  are exactly parallel to those of  $3d^1\Pi_b$  ( $3^1B$ ) and  $3d^1\Pi_a$  ( $3^1A$ ).†

Of these triplet systems  $3d^3\Delta_b \rightarrow 2p^3\Pi$  is the strongest,  $3d^3\Sigma \rightarrow 2p^3\Pi$  next in intensity, then  $3d^3\Pi_b \rightarrow 2p^3\Pi$ , then  $3d^3\Pi_a \rightarrow 2p^3\Pi$  and  $3d^3\Delta_a \rightarrow 2p^3\Pi$  weakest with little to choose between the two of them. In both  $3d^3\Delta_b \rightarrow 2p^3\Pi$  and  $3d^3\Delta_a \rightarrow 2p^3\Pi$  all three branches P, Q and R are well developed with, on the whole, R and Q each stronger than P. In  $3d^3\Sigma \rightarrow 2p^3\Pi$  the R and Q branches are about equally strong, but the P branch very weak and only represented by the first two lines P' 1 and P2, of which the former is weak. In  $3d^3\Pi_b \rightarrow 2p^3\Pi$  the R branch is strongest, the P branch about half as strong, and the Q branch very weak, being represented as a rule only by faint Q' 1 and Q2 lines. In  $3d^3\Pi_a \rightarrow 2p^3\Pi$  there is some strength in all three branches, but the P branch dies out rapidly, being represented only by P2, P' 3 and P4.

The theoretical distributions of intensity between the branches will be given in a following paper. They are found to be in fair agreement with the experimental data.

\* Richardson and Davidson, 'Proc. Roy. Soc.,' A, vol. 124, p. 52 (1929).

† Richardson and Davidson, 'Proc. Roy. Soc.,' A, vol. 123, pp. 54, 466 (1929).

Similar intensity relations are found in the corresponding singlet bands  $3d^1\Sigma\Pi\Delta \rightarrow 2p^1\Pi$ . Of these systems\*  $3d^1\Delta_b \rightarrow 2p^1\Pi$  is the strongest, then  $3d^1\Sigma \rightarrow 2p^1\Pi$ , then  $3d^1\Pi_b \rightarrow 2p^1\Pi$ , with not much difference between these two, and finally  $3d^1\Pi_a \rightarrow 2p^1\Pi$  and  $3d^1\Delta_a \rightarrow 2p^1\Pi$  about equal and weakest. In  $3d^1\Delta_b \rightarrow 2p^1\Pi$ ,  $3d^1\Delta_a \rightarrow 2p^1\Pi$ , and  $3d^1\Pi_a \rightarrow 2p^1\Pi$  there is some strength in all branches, but P is usually the weakest. In  $3d^1\Sigma \rightarrow 2p^1\Pi$ , Q and R are strongest with P very weak or absent; while in  $3d^1\Pi_b \rightarrow 2p^1\Pi$  the Q lines are usually the weakest. All these singlet lines lie in the infra-red region between 12,000 and 14,000 wave-numbers.

It will be noticed that the bands in Tables I to III involve a considerable number of coincident lines or blends. There is, however, in nearly all these cases definite evidence of the presence of more than one line. Very often they are singled out in Gale, Monk and Lee's tables, being marked (*h*), meaning diffuse and possible double, or (*a*), (*b*) or (*c*), meaning that the wave-length measures from different plates show discrepancies beyond the average. In general the intensity of all these lines is thought to be adequate for all the positions claimed for them. As is to be expected, such lines often give rise to combination defects appreciably greater than those coming from single lines. The latter range up to about 0.05 wave-number whereas the former may be as much as three times this amount; further, the presence of such blends is often indicated by the properties of the lines as given in Merton and Barratt's tables.

## § 2. *The Final Levels.*

The relation of the band lines to the electronic and rotational structure will be evident from fig. 1. This is taken from I where the structure is fully described; so that it does not seem necessary to repeat the details here beyond what is required to make this paper intelligible. In fig. 1 which is merely diagrammatic and not drawn to scale the rotational levels are numbered according to the old *j* values. This *j* is equal to  $K + \frac{1}{2}$  where *K* is the quantum number used in the present paper.

The rotational combinations between strong (*a*) levels are collected in Table IV and those between weak (*s*) levels in Table V. There are no known inter-combinations between *a* and *s* levels. The designation in the first column on the left-hand side of Tables IV and V indicates the upper level of the band from

\* This statement is based on extensions of these systems which we discovered some time ago, but have not yet found time to publish. Some of them are used in the paper by Davidson, *loc. cit.*

which the data in the corresponding row are taken. In any band each alternate space in the corresponding row should be vacant, the corresponding lines, indicated by the heading at the top of the column, having no existence in that particular band. If there are more blank spaces than this it means that lines which are capable of occurring either do not exist or have not yet been discovered. For example, in  $3d\ ^3\Sigma \rightarrow 2p\ ^3\Pi$  the gaps under Q' 2 — P' 3, Q3 — P4, Q'4 — P' 5, and Q5 — P6 are due to the fact that the P branches are undeveloped and the extensive gaps in  $3d\ ^3\Pi_b \rightarrow 2p\ ^3\Pi$  are caused by the almost complete absence of the Q branches. In this and similar cases many of these

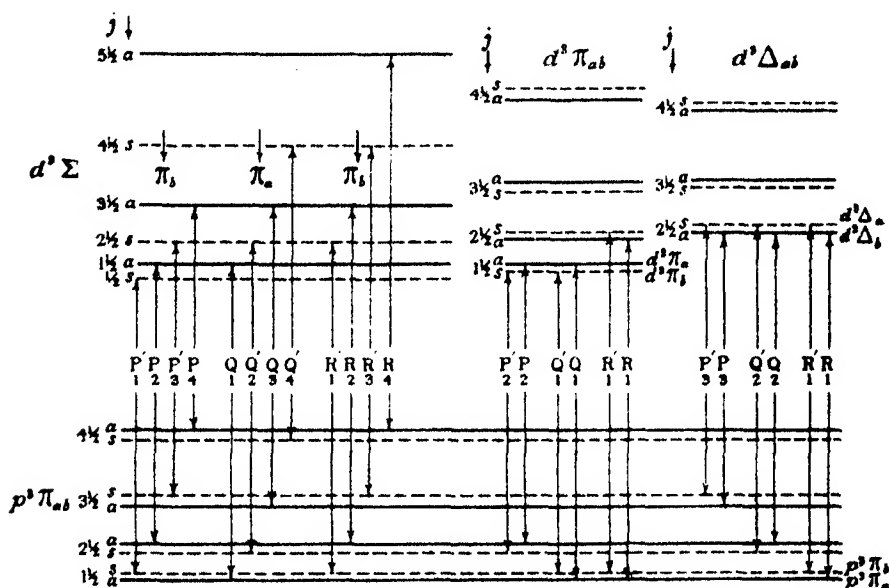


FIG. 1.—Structure and transitions of  $d^3\Sigma\Pi\Delta$  complex to  $p^3\Pi$ .

gaps could have been filled by subtracting from the experimental  $R(m) - P(m+2)$  interval the final mean values of one of the intervals  $R(m) - Q(m+1)$  or  $Q(m+1) - P(m+2)$ . Such indirect determinations have not been incorporated in these tables, although the agreement with the mean values of the data so obtained is of the same kind as that shown by the data actually included. The table thus includes only direct differences of the wave numbers of actually measured lines. In most of the cases where either of the lines used is believed to be a blend this is indicated by a dagger placed at that end of the interval at which the coincidence occurs. A few values which are accompanied by a question mark involve lines whose status is thought to be doubtful. In deducing the mean values of the single intervals, such as Q1 — P2,



Table IV.

	Q1-P2	R1-Q2	R2-Q3	Q2-P3	Q3-P4	R3-Q4	R4-Q5	Q4-P5	Q5-P6	R5-Q6	R6-Q7	Q6-P7
0 → 0												
3d <sup>2</sup> Σ	120.66		180.03									
3d <sup>2</sup> Π <sub>b</sub>						237.59	294.28	294.36		347.53		400.57?
3d <sup>2</sup> Π <sub>a</sub>	120.72		179.98	180.03	237.67	237.73	294.35	294.25		347.61		400.70?
3d <sup>2</sup> Δ <sub>b</sub>		120.72										
3d <sup>2</sup> Δ <sub>a</sub>			180.04		237.72		294.14					
4d <sup>2</sup> Σ	120.75		180.06	180.05		237.64	294.25		347.66			
4d <sup>2</sup> Π <sub>b</sub>	+120.83	120.71	180.04		237.69		294.21	294.10		+347.78		
4d <sup>2</sup> Π <sub>a</sub>		120.79		180.02								
4d <sup>2</sup> Δ <sub>b</sub>												
1 → 0												
3d <sup>2</sup> Σ	120.59		180.06				294.21					
3d <sup>2</sup> Π <sub>b</sub>		120.77		180.05								
3d <sup>2</sup> Π <sub>a</sub>	120.76											
3d <sup>2</sup> Δ <sub>b</sub>		120.76										
3d <sup>2</sup> Δ <sub>a</sub>	120.732	120.750	180.035	180.037	237.695	237.653	294.240	294.237	347.66	347.56		400.63?
Mean												
Final	120.74		180.036		237.674		294.239		347.60			400.63?
Mean	59.29 <sub>a</sub>		57.638		56.565		53.36		53.03?			
	1.66		1.07		3.20 <sub>a</sub>		0.33?					
1 → 1												
3d <sup>2</sup> Σ	115.05		171.35				279.76					380.45?
3d <sup>2</sup> Π <sub>b</sub>		115.12		171.40								
3d <sup>2</sup> Π <sub>a</sub>	+115.26		171.35		226.86	226.92	279.75	279.74		331.81		380.33?
3d <sup>2</sup> Δ <sub>b</sub>		115.17		171.31			279.78		331.79			
3d <sup>2</sup> Δ <sub>a</sub>			171.36		226.86				331.76			
3 <sup>2</sup> Σ	115.13		171.34		226.93		+279.81†	279.95		331.72		
4d <sup>2</sup> Σ			171.33			226.89	+279.67					
4d <sup>2</sup> Π <sub>b</sub>					+227.06							
4d <sup>2</sup> Π <sub>a</sub>		115.13		171.31								
4d <sup>2</sup> Δ <sub>b</sub>												
2 → 1												
3d <sup>2</sup> Σ	115.15		171.30		227.00		279.74		331.71†			
3d <sup>2</sup> Π <sub>b</sub>	115.11											
3d <sup>2</sup> Δ <sub>b</sub>		+115.36										
Mean	115.140	115.140	171.338	171.34	226.91 <sub>2</sub>	226.90 <sub>2</sub>	279.76 <sub>a</sub>	279.84 <sub>a</sub>	331.75 <sub>2</sub>	331.75 <sub>2</sub>		380.3 <sub>2</sub> ?
Final mean	115.140		171.339		226.90 <sub>2</sub>		279.770		331.75 <sub>2</sub>			
	56.20		55.57		52.86		51.98		48.60†			
	0.63		2.71		0.88		3.38?					

$2 \rightarrow 2$									
$3d^3\Sigma$ .....	109.75	†162.93					265.73		361.45 ?
$3d^3\Pi_b$ .....									
$3d^3\Pi_a$ .....	109.76	162.99†					265.80	316.34†	361.54 ?
$3d^3\Delta_b$ .....									
$3d^3\Delta_a$ .....	109.79	162.79	216.31	216.32			265.78	316.51	
$4d^3\Sigma$ .....	109.81	162.83	216.28				265.76		
$4d^3\Pi_b$ .....	109.83	162.71†							
$4d^3\Pi_a$ .....	109.88	162.81	216.42†					316.59	
$4d^3\Delta_b$ .....	109.59	162.73							
$1 \rightarrow 2$									
$3^3\Sigma$ .....	109.80								
$3 \rightarrow 2$									
$3d^3\Sigma$ .....	109.69+	162.89†							
$3d^3\Pi_b$ .....									
$3d^3\Pi_a$ .....	109.80	162.73†							
$3d^3\Delta_b$ .....	109.75	†162.68							
$3d^3\Delta_a$ .....	†109.92†								
Mean .....	109.775	162.85	216.29 <sub>a</sub>	216.3 <sub>2</sub>			265.76 <sub>2</sub>	316.5 <sub>2</sub>	361.50 ?
Final mean .....	109.770	162.8 <sub>2</sub>	216.30 <sub>2</sub>				265.76 <sub>2</sub>	316.5 <sub>2</sub>	361.5 <sub>2</sub> ?
		53.03	53.50	49.46	50.78		44.95 ?		
		-0.47	+4.04	-1.32	+5.83 ?				
$3 \rightarrow 3$									
$3d^3\Sigma$ .....	104.46	154.67					251.95		
$3d^3\Pi_b$ .....									
$3d^3\Pi_a$ .....	104.51	154.73	206.01				†251.78		
$3d^3\Delta_b$ .....	104.49								
$3d^3\Delta_a$ .....	104.48	154.71	206.07				252.10†		
$4d^3\Sigma$ .....		154.69							
$4d^3\Pi_b$ .....		154.66							
$4d^3\Pi_a$ .....	104.49	154.78	206.14†				251.95		
$4d^3\Delta_a$ .....	†104.35						252.06		
$4d^3\Delta_b$ .....	†104.60†	†154.75					252.00		
$2 \rightarrow 3$									
$3d^3\Sigma$ .....	104.473	154.7	206.040				252.005	251.975	
Mean .....	104.48 <sub>2</sub>	154.690	206.040				251.99		
Final mean .....	104.48 <sub>2</sub>	154.70 <sub>2</sub>	206.04	46.96					
		50.22	51.36	+5.41					
		-1.14							

Table V.

	0 → 0	Q'1-P'2	R'1-Q'2	R'2-Q'3	Q'2-P'3	Q'3-P'4	R'3-Q'4	R'4-Q'5	Q'4-P'5	Q'5-P'6	R'5-Q'6	R'6-Q'7	Q'6-P'7
3d <sup>2</sup> Σ <sup>+</sup> .....	120.82						+238.08				348.06†		
3d <sup>2</sup> Π <sub>g</sub> .....	120.67						237.96				348.23†		
3d <sup>2</sup> Π <sub>u</sub> .....	120.77			179.96		237.91		293.63	293.71	348.41			
3d <sup>2</sup> Δ <sub>g</sub> .....	+120.87			179.86			+238.07				348.40		
3d <sup>2</sup> Δ <sub>u</sub> .....	120.92†												
4d <sup>2</sup> Σ <sup>+</sup> .....	120.77			179.90			237.91†	293.86	+293.67†	348.39	348.50?		
4d <sup>2</sup> Π <sub>g</sub> .....	120.80						237.96	293.75	293.69	348.40	348.45		
4d <sup>2</sup> Π <sub>u</sub> .....	120.73			179.91	179.905	237.91							
Mean .....	120.79			179.90 <sub>4</sub>		237.93		293.72		348.42			
Final mean ..			59.12		58.02		55.79		54.70				
				1.10		2.23		1.09					
1 → 1													
3d <sup>2</sup> Σ <sup>+</sup> .....	115.02						226.39				331.14		
3d <sup>2</sup> Π <sub>g</sub> .....	+115.20						226.28						
3d <sup>2</sup> Π <sub>u</sub> .....	115.23†			171.60	+171.45	226.38		280.34	280.39	331.27	380.90		
3d <sup>2</sup> Δ <sub>g</sub> .....	115.01				171.63		226.37		280.45				
3d <sup>2</sup> Δ <sub>u</sub> .....	115.10				171.65		226.29						
3 <sup>2</sup> Σ <sup>+</sup> .....	115.01				171.71		226.17†						
4d <sup>2</sup> Σ <sup>+</sup> .....								280.51†	280.47†		380.83		380.82?
4d <sup>2</sup> Π <sub>g</sub> .....	+114.99†			171.60	171.663	226.38	226.333	280.34	280.420		380.865		380.82?
4d <sup>2</sup> Π <sub>u</sub> .....	115.03												
Mean .....	115.03			171.65		226.34 <sub>2</sub>		280.40 <sub>6</sub>		331.2 <sub>6</sub>	380.8 <sub>6</sub>		
Final mean ..			56.62		54.69		54.06		50.80		49.6 <sub>6</sub>		
				1.93		0.63		3.26		1.1 <sub>6</sub>			



and the final mean values of the pairs of equal intervals, such as Q1 — P2, and R1 — Q2, the values given by the blended lines have been ignored, except in a few cases where the data are very sparse. The staggering of these intervals, which is shown by the second differences of the final mean values, arises from the fact that they are not differences between successive rotational levels of either of the single electronic levels  $2p^3\Pi_a$  or  $2p^3\Pi_b$ ; but they are either the succession of intervals  $2p^3\Pi_b$  ( $K = 2$ ) —  $2p^3\Pi_a$  ( $K = 1$ ),  $2p^3\Pi_a$  ( $K = 3$ ) —  $2p^3\Pi_b$  ( $K = 2$ ), etc., or  $2p^3\Pi_a$  ( $K = 2$ ) —  $2p^3\Pi_b$  ( $K = 1$ ),  $2p^3\Pi_b$  ( $K = 3$ ) —  $2p^3\Pi_a$  ( $K = 2$ ), etc.

The structure of these final intervals is shown graphically in fig. 2. This is not drawn to scale and the doublet differences in particular are greatly

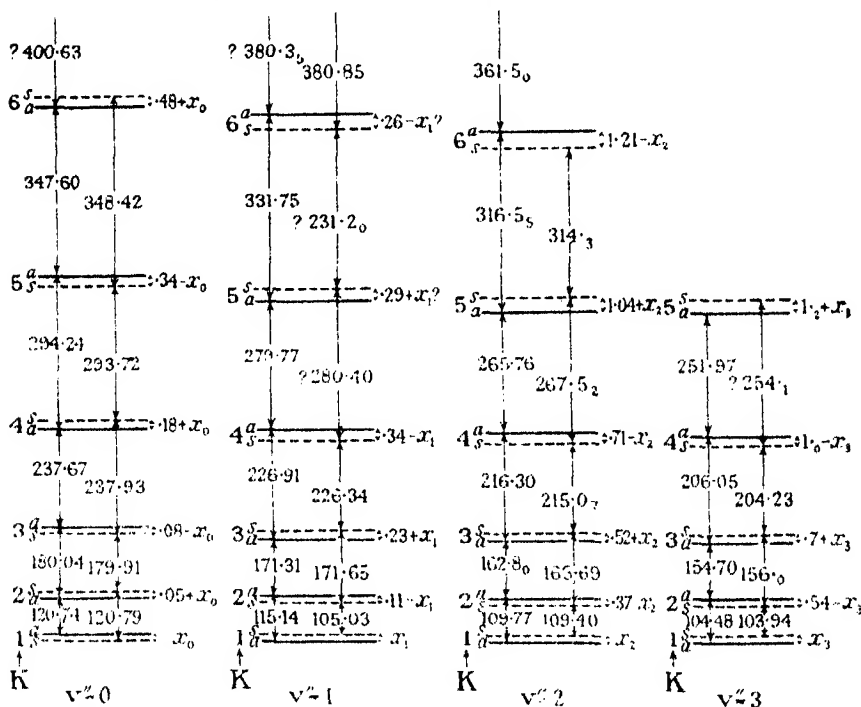


FIG. 2.

exaggerated. The measured mean differences, to 0.01 wave number, are inserted in the figure. It is not possible to determine the absolute values of the doublet differences. These can only be determined to within  $\pm x_0, x_1, x_2, x_3$ , where the suffix indicates the final vibrational level  $v'' = 0, 1, 2, 3$  and  $x_m$  is the height of the lowest  $s$  level above the lowest  $a$  level at the vibrational level  $v'' = m$ . Apart from doubtful elements it is clear that there is a general tendency both for these doublet differences to increase with increasing

K at each given vibrational level and also to increase with increasing  $v''$  at each given rotational level for which the data seem secure. This is probably true also for the values  $x_0$ ,  $x_1$ ,  $x_2$  and  $x_3$  at the lowest K = 1 level, although we can only guess it. Whether the apparent contraction at higher values of K shown at the  $v'' = 1$  level is real or not is very doubtful indeed, the two highest values at any rate being extremely uncertain. The values at  $v'' = 3$  for K > 2 are also not very sure. It will be noticed that at  $v'' = 0$  the relative position of the  $s$  and  $a$  levels is inverted compared with those at  $v'' = 1, 2$  and 3.

As has been stated the numbers in Tables IV and V are not successive rotational intervals of either of the electronic levels  $2p^3\Pi_b$  or  $2p^3\Pi_a$ . To obtain these we must evaluate the intervals, as they are shown in fig. 1, between  $s(j = 1\frac{1}{2}) a(j = 2\frac{1}{2}) s(j = 3\frac{1}{2}) a(j = 4\frac{1}{2})$ , etc., for  $2p^3\Pi_b$  and  $a(j = 1\frac{1}{2}) s(j = 2\frac{1}{2}) a(j = 3\frac{1}{2}) s(j = 4\frac{1}{2})$ , etc., for  $2p^3\Pi_a$ . These intervals can only be determined subject to  $\pm x_m (m = v'')$  the unknown doublet distance at the lowest rotational level. They are collected together in Table VI.

Table VI.—Rotational Differences of the Final Levels.

Rotational interval.	K (2) — K (1).	K (3) — K (2).	K (4) — K (3).	K (5) — K (4).	K (6) — K (5).	K (7) — K (6).
$2p^3\Pi_b$ $v'' = 0$	120.74 — $x_0$	179.96 + $x_0$	237.75 — $x_0$	293.90 + $x_0$	347.94 — $x_0$	
$v'' = 1$	115.14 — $x_1$	171.54 + $x_1$	226.68 — $x_1$	280.06 + $x_1$ ?	331.46 — $x_1$ ?	380.1 + $x_1$ ?
$v'' = 2$	109.77 — $x_2$	163.32 + $x_2$	215.7 <sub>8</sub> — $x_2$	266.8 <sub>0</sub> + $x_2$	315.5 <sub>0</sub> — $x_2$	
$v'' = 3$	104.48 — $x_3$	155.4 + $x_3$	205.3 <sub>0</sub> — $x_3$	253.2 + $x_3$		
$2p^3\Pi_a$ $v'' = 0$	120.79 + $x_0$	179.99 — $x_0$	237.85 + $x_0$	294.06 — $x_0$	348.08 + $x_0$	400.15 — $x_0$ ?
$v'' = 1$	115.03 + $x_1$	171.44 — $x_1$	226.57 + $x_1$	280.11 — $x_1$	331.5 <sub>0</sub> + $x_1$ ?	380.6 — $x_1$ ?
$v'' = 2$	109.40 + $x_2$	163.1 <sub>7</sub> — $x_2$	215.59 + $x_2$	266.47 — $x_2$	315.3 <sub>4</sub> + $x_2$	362.7 <sub>1</sub> — $x_2$
$v'' = 3$	103.94 + $x_3$	155.24 — $x_3$	204.9 <sub>3</sub> + $x_3$	253.0 — $x_3$		

### § 3. The Vibrational Intervals.

The material in Tables I to III permits a considerable extension of the vibrational intervals given in I. Up to the present only lines of the non-diagonal bands which involve transitions between the alternate strong ( $a$ ) levels have been found with certainty. As a result the final vibrational intervals for the successive values of K which relate to any given vibrational transition, such as  $1'' \rightarrow 0''$ , belong alternately to  $2p^3\Pi_a$  and  $2p^3\Pi_b$  levels. The mean values of these final intervals are given in the two columns under  $n = 2$  in Table VII. For comparison the corresponding intervals of the upper levels of the  $\alpha, \beta, \gamma$  bands ( $np^3\Pi \rightarrow 2s^3\Sigma$ ) are given in the columns under  $n = 2, 3, 4$  respectively. The data for  $n = 5$  have been computed from the lines of the  $\gamma$

bands as given by Richardson.\* It will be seen that for all values of  $K$  and  $\Delta''$ , the intervals drop by about 100 wave numbers in going from  $n = 2$  to  $n = 3$ , by about 30 from  $n = 3$  to  $n = 4$  and by about 16 from  $n = 4$  to  $n = 5$ . The values evidently tend to approach limits for  $n$  large which are not much below those for  $n = 5$ .

The values of  $w_0$  and  $xw_0$ , as defined in the old quantum mechanics, deduced from these intervals are shown under  $2p^3\Pi_a$  and  $2p^3\Pi_b$  at the bottom of Table IX. Their means are also given as they are probably identical, at any rate to the degree of accuracy of these determinations. These are followed by the values for the other triplet  $\Pi$  levels. Those for  $3p^3\Pi_a$ ,  $3p^3\Pi_b$  and  $4p^3\Pi_a$  are taken, or computed, from the data of Richardson and Das,† those for  $5p^3\Pi_a$  from "Molecular Hydrogen and its Spectrum," whilst that of  $w_0$  for  $H_2^+$  is the value for the molecular ion, the end of the series ( $\infty p^3\Pi_{ab}$ ), which we obtained by extrapolating the singlet states.‡ It is evident from these numbers that this value of  $w_0$  for  $H_2^+$  is slightly too high. Both this value and the limit towards which the series of triplet  $\Pi$  states are tending agree with Burrau's§ theoretical value of  $w_0$  for  $H_2^+$  to the accuracy (apart from a mistaken factor of 2) with which he states his result. It is remarkable that the computed  $w_0x$ , which should be less secure than the value of  $w_0$ , comes so near to the magnitude which the experimental values for  $np^3\Pi$  ( $n = 2, 3, 4, 5$ ) would lead one to expect. The value  $w_0x = 61$  is deduced from  $w_0 = 2280$  in combination with the ionization potential and heat of dissociation of  $H_2$  determined from data furnished by the singlet systems.|| It will be evident from the numbers at the bottom of Table VII that the allocation of the final levels to  $2p^3\Pi_{ab}$  is confirmed by the values of the vibrational constants of the levels. It will be shown in Part III that this allocation is equally well confirmed by the values of the rotational constants.

The mean values of the initial vibrational intervals  $\Delta V'K$  calculated from the final intervals in Table IX and equations of the type

$$\Delta V'K = \Delta V''(K+1) + P(K+1)(v+1 \rightarrow v+1) - P(K+1)(v \rightarrow v),$$

are set out in Table VIII. As only the values for the strong  $a$  levels are known the successive values of  $K$  jump by 2 in each band.

\* "Molecular Hydrogen and its Spectrum," Yale Univ. Press (*in the press*).

† 'Proc. Roy. Soc.,' A, vol. 122, p. 688 (1929).

‡ 'Proc. Roy. Soc.,' A, vol. 123, p. 466 (1929).

§ 'K. Danske Vid. Selsk., Math. Fys.,' vol. 7, No. 14 (1927).

|| "Molecular Hydrogen and its Spectrum," chap. VI. An earlier computation made by us using a similar method gave  $xw_0 = 60$  ('Proc. Roy. Soc.,' A, vol. 123, p. 466 (1929)).

Table VII.—Vibrational Intervals in  $np\ ^3\Pi_{ab}$  Levels.

$\Delta v''$ ↓	K ↓	$np\ ^3\Pi_a$ levels.				$np\ ^3\Pi_b$ levels.		
		$n = 2$ . Final levels of present band systems.	$n = 3$ . Upper levels of $\alpha$ bands Q branches.	$n = 4$ . Upper levels of $\beta$ bands Q branches.	$n = 5$ . Upper levels of $\gamma$ bands Q branches.	$n = 2$ . Final levels of present band systems.	$n = 3$ . Upper levels of $\alpha$ bands R'P' branches.	$n = 4$ . Upper levels of $\beta$ bands R'P' branches.
1'' - 0''	1	2338.85	2240.21	2209.60	2195.76		2239.45	
	2		2234.23	2203.55	2190.06	2333.27	2231.23	2204.8
	3	2324.55	2225.28	2194.57	2182.17		2216.28	2200.62
	4		2213.44	2182.57	2171.01	2313.61*	2196.79	2194.6
	5	2299.16*	2198.83					
2'' - 1''	1	2216.76	2114.84	2083.85	2069.97		2116.08	
	2		2109.09	2078.11	2063.06	2211.37	2113.34	2073.56
	3	2202.93	2100.38	2069.27	2051.97		2111.68	
	4		2089.00	2058.31	2037.31	2192.42	2108.50	
	5	2178.40	2074.79					
3'' - 2''	1	2098.05	1993.47	1962.12	1948.93		1994.47	
	2		1987.86	1956.48	1942.25	2092.77	1989.61	1948.30
	3	2084.56	1979.50	1948.05	1932.07		1981.13	
	4		1968.37	1937.08	1919.60	2074.17*	1970.8	
	5		1954.28					

\* These three values depend on a single pair of lines only. The rest are mean values of various numbers of concordant determinations.

Level→	$2p\ ^3\Pi_a$	Mean	$2p\ ^3\Pi_b$	$3p\ ^3\Pi_a$	$3p\ ^3\Pi_b$	$4p\ ^3\Pi_a$	$5p\ ^3\Pi_a$	H <sub>2</sub> +
$w_0$	2404.2	2404.0	2403.7	2307.5	2307.5	2276.5	2258.7	2280
$w_0x$	61.45	61.4	61.35	65.0		ca. 60	62.9	61

Table VIII.—Vibrational Intervals of  $3d\ ^3\Sigma$ ,  $3d\ ^3\Pi_{ab}$ ,  $3d\ ^3\Delta_{ab}$ .

Level ↓	$\Delta v$ ↓	K = 1	K = 2	K = 3	K = 4	K = 5	K = 6
$\Sigma$	From→	Q1 P2		R2 Q3		R4 Q5	
	1' - 0'	2087.19		2083.72		2072.94	
	2' - 1'	1910.77		1921.64		1914.74	
	3' - 2'	1732.75		1747.47		1744.78	
$\Pi_b$	From→		R1 P3		R3 P5		
	1' - 0'		2118.08		2115.93		
	2' - 1'		1968.94		1965.72		
	3' - 2'		1813.21				
$\Pi_a$	From→	Q1 P2		R2 Q3 P4			
	1' - 0'	2115.46		2110.40			
	2' - 1'	1912.98		1890.01			
	3' - 2'	1801.49		1774.6			
$\Delta_b$	From→		R1 P3		R3 P5		R5
	1' - 0'		2192.77		2150.53		2101.56
	2' - 1'		2069.52		2028.26		1976.83
	3' - 2'		1948.90		1907.75		
$\Delta_a$	From→			R2 Q3 P4		R4 Q5	
	1' - 0'			2145.17		2067.00	
	2' - 1'			2037.6		1951.81	
	3' - 2'			1925.48			



#### § 4. *The Initial Rotational Levels.*

Let us imagine for a moment that the  $x$ 's are zero. Then in the lower state the intervals between all the  $a$  and  $b$  levels at a given  $v$  are known completely (see fig. 2 for example). Hence the rotational intervals in any upper state can be immediately determined from the bands, in the usual way. This gives Table IX. It is to be remembered that  $x$  is not usually zero, and hence that in each diagram in Table IX the whole of the "dotted" levels are to be raised relative to the "solid" levels by the  $x$  of the corresponding lower vibrational state. Thus using  $F(K)$  for the true level, and considering, for instance,  $3d\ ^3\Sigma$   $v = 0$ , the number 30.06 is really  $F(2) - F(1) - x_0$ , while 70.09 is really  $F(3) - F(2) + x_0$ . The corresponding singlet levels are included in the table for comparison. One difference between the two sets of data should be mentioned. The singlet level differences do not involve any uncertainty corresponding to the small quantities  $x(v')$  which enter into the triplet data; because these levels have been measured (in our papers on the singlet systems), with reference to the  $2p\ ^1\Sigma$  state, where this duplicity does not occur and the intervals can be computed very accurately.

Unfortunately there is no evidence in the  $H_2$  spectrum that the corresponding triplet state  $2p\ ^3\Sigma$  exists, and, in fact, it has been concluded on theoretical grounds that it is unstable. The main hope of ever determining the small quantities  $x(v')$  lies in finding the transitions from  $4d\ ^3\Sigma\Pi\Delta$  down to  $3p\ ^3\Sigma$ . This last is a known state,\* but the bands, which should lie in the accessible part of the infra-red, have not yet been looked for.

The most striking feature of Table IX is the extraordinarily close similarity of the  $3d\ ^3\Pi_b$  and  $3d\ ^3\Delta_b$  levels with the  $3d\ ^1\Pi_b$  and  $3d\ ^1\Delta_b$  levels respectively. In fact, they are so much alike that the values of the second differences are in a great many instances interchangeable to the accuracy of the data, which for the most part is very high, and the small uncertainty  $x(v')$ . The only discrepancy is at the lowest level of  $v = 3$  in the  $\Pi_b$  levels. Here it is 82.31 for  $3d\ ^3\Pi_b$ , as against 77.30 for  $3d\ ^1\Pi_b$ . Even this divergence is not sure as there is an alternative possibility which would remove it. If instead of the  $Q' 1$  and  $P' 2$  lines given in Table II we use  $Q' 1 = 16367.90(1)$  which is coincident with  $P' 4$  of  $2 \rightarrow 2$ ,  $3d\ ^3\Pi_b \rightarrow 2p\ ^3\Pi$  and  $P' 2 = 16263.87(1)$  which is coincident with  $R4$  of  $2 \rightarrow 2$ ,  $3p\ ^3\Pi \rightarrow 2s\ ^3\Sigma$  the  $Q' 1 - P' 2$  final interval is 104.03 instead of the standard value 103.94. However, these alternative lines, according to

\* Richardson and Das,<sup>1</sup> 'Proc. Roy. Soc.,' A, vol. 122, p. 711 (1929); vol. 125, p. 309 (1929).

the measures of Kapuscinsky and Eymers, look a little too strong both as P' 4 of the 2 → 2 band and as R4 of the α band ; so it is quite possible that they also belong to the present band and the two lines in Table III are something else. We have therefore decided to insert both sets of values as alternatives in Table IX.

We now turn to the Σ levels. It will be noticed that the lowest interval of 3d<sup>3</sup>Σ is queried at each vibrational level. This is because this interval is determined at each level by a single P' 1 line which has no combinational confirmation. In fact, there is no possibility of such confirmation until either corresponding lines of the non-diagonal bands or lines coming from the same upper levels and going down to some other final level such as 3p<sup>1</sup>Σ can be found. This particular difficulty does not arise with the singlet levels which give rise to long progressions going down to 2p<sup>1</sup>Σ. There is no possible doubt that the singlet levels at K = 0 are upper levels of something which goes down to 2p<sup>1</sup>Σ at K = 1. The lines on which they are founded must be either (1) P1 lines, or (2) Q1 lines, or (3) R1 lines without any corresponding P3 lines. There is no reasonable doubt that the K = 0 level has been correctly assigned to 3d<sup>1</sup>Σ at v = 0 and v = 1. Whether the irregularly spaced level at K = 0 and v = 2 belongs to the other v = 2 levels is uncertain, and has therefore been queried. As a matter of fact, the P' 1 lines of 3d<sup>3</sup>Σ were selected in the following manner. It was observed that the intervals at v = 0 between K = 1 and K = 6, which are firmly established by the final combinations, are very similar to the corresponding intervals of 3d<sup>1</sup>Σ and that vacant line was chosen as P' 1 of 0 → 0 3d<sup>3</sup>Σ → 2p<sup>3</sup>Π which came nearest to making that similarity extend also to the lowest interval between K = 1 and K = 0. It was then noticed, without further reference to the properties of the singlet levels, that the levels of 3d<sup>3</sup>Σ above K = 1 at v = 1, 2 and 3, which also rest securely on the final combinations, are also very similar to those at v = 0 from which they change progressively and regularly as v changes to 1, 2 and 3. For the remaining P' 1 lines therefore those vacant lines were selected which would make this progressive and regular change with change in the vibrational quantum number extend also to the lowest rotational level. It is not possible to make any appreciable change in the lowest levels if it is assumed that the P' 1 lines really exist, if these similarities shown by the higher levels are to extend also to the lowest rotational level. In I we placed P' 1 of 0 → 0 3d<sup>3</sup>Σ → 2p<sup>3</sup>Π 13.79 wave numbers higher at 16870.70(1) but practically all the strength of this line is now required as P3 of 3 → 3 3d<sup>3</sup>Δ<sub>g</sub> → 2p<sup>3</sup>Π. It is true that the substituted line 16856.91(1h) is also R7 of 0 → 0 3p<sup>3</sup>Π → 2s<sup>3</sup>Σ,

Table IX.—Initial Rotational Levels of  $3d^3\Sigma$ ,  $3d^3\Pi_{ab}$ ,  $3d^3\Delta_{ab}$ , and  $3d^1\Pi_{ab}$  and  $3d^1\Delta_{ab}$ .

K	$3d^3\Sigma$	$v=0$	$3d^1\Sigma$	$v=0$	$3d^3\Sigma$	$v=1$	$3d^1\Sigma$	$v=1$	$3d^3\Sigma$	$v=2$	$3d^1\Sigma$	$v=2$	$3d^3\Sigma$	$v=3$	$3d^1\Sigma$	$v=3$
7																
6	278.30	52.15	270.97 or 253.33	53.52? or 36.08?	263.87	48.20	238.91	47.34			195.64	46.71				
5	226.15	52.61	217.45	53.07	215.68	49.26	189.57	51.24			148.93	29.90				
4	173.54	53.03	164.38	51.90	166.42	49.39	138.33	51.67	180.75	45.09	119.03	27.82	157.52	41.19	68.05	22.23
3	120.51	50.42	112.48	47.24	117.03	47.65	86.66	39.43	115.66	43.06	91.21	25.33	116.33	38.29	45.82	19.45
2	70.09	40.03	65.24	42.54	69.38	42.11	47.23	31.72	72.60	37.74	44.66	21.22	78.04	33.84	26.37	
1	30.06	32.13	22.70	30.23	27.27	29.96	15.51	20.25	34.86	25.29	44.66	105.91?	44.20	25.63?	Not known	
0	-2.05		-7.53		-2.69		-13.74		9.56		-61.25?		18.57?			
	$3d^3\Pi_b$	$v=0$	$3d^1\Pi_b$	$v=0$	$3d^3\Pi_b$	$v=1$	$3d^1\Pi_b$	$v=1$	$3d^3\Pi_b$	$v=2$	$3d^1\Pi_b$	$v=2$	$3d^3\Pi_b$	$v=3$	$3d^1\Pi_b$	$v=3$
7																
6	330.78	48.03	377.37	45.31	332.06	49.97	358.10	41.82			350.28	44.56			295.01	47.49
5	282.15	52.12	282.09	52.11	271.19	49.22	316.28	46.03	259.99	45.14	305.63	46.42			247.52	40.57
4	230.03	53.25	229.98	52.97	221.97	48.61	270.25	48.12	214.85	44.86	259.21	44.23			206.95	41.27
3	176.78	52.77	177.01	52.51	173.36	48.09	222.13	48.31	169.99	44.56	214.98	44.27	165.76	42.05	165.68	41.45
2	124.01	49.84	124.50	49.77	125.27	46.51	173.82	47.53	125.43	43.25	170.71	44.23	123.71	41.40	124.23	46.93
1	74.17		74.73		78.76		126.29	45.58	82.18		126.48	43.36	82.31	41.40	77.30	
							80.71				83.12		or 77.90	45.88		



but it is an  $h$  line and is too strong in the  $\alpha$  band. In fact, from every standpoint the new  $P' 1$  lines look definitely better than those used in I.

It will be seen that there is a very close resemblance between the levels of  $3d^3\Sigma$  and  $3d^1\Sigma$  at  $v = 0$ . As we have explained, this condition has been imposed on the lowest rotational level of  $3d^3\Sigma$  by the choice of the  $P' 1$  line. All the remaining levels, however, have been determined by considerations which have no similar interconnection. The  $K = 7$  level of  $3d^1\Sigma$  at  $v = 0$  is affected by a perturbation which we have discussed elsewhere.\* There are two possible sets of R6 lines to determine this level, but the one which leads to the abnormal differences 253.53 and 36.08 looks to be much the more convincing physically. In fact, the set which leads to the more normal differences 270.97 and 53.52 may well be merely the result of an accidental coincidence, since it consists only of three lines which have a wrong intensity distribution for a  $0'$  progression and two of them are now known to be coincident with lines of other bands.

$3d^3\Sigma$  and  $3d^1\Sigma$  are also very similar to each other at  $v = 1$ , but not so closely as at  $v = 0$ . At  $v = 2$  they differ quite markedly from each other and the dissimilarity is further intensified at  $v = 3$ . It is not absolutely certain, however, that the set of levels given in the table at  $v = 2$  really belongs to  $3d^1\Sigma$ . We† originally published them as the  $v = 2$  levels of  $3^1K$ . But if we replace them by the set of levels which we put originally in  $3d^1\Sigma$  at  $v = 2$ ‡ the difference between  $3d^1\Sigma$  and  $3d^3\Sigma$  at this vibrational level is increased rather than diminished; so that the difference is real whichever alternative we adopt and it cannot be regarded as an argument against the set of levels for  $3d^1\Sigma$  at  $v = 2$  which is given in Table IX. It should perhaps be added that the abnormally placed  $K = 0$  level of  $3d^1\Sigma$  at  $v = 2$  did not come out of  $3^1K$ . This comes from some lines which we first published§ as  $P1$  lines of the  $v' = 2$  progression of  $3d^1\Pi_a \rightarrow 2p^1\Sigma$ , before it was known that the upper level of this progression was a  $\Pi$  level. Whether they come from  $3d^1\Sigma$  or not they certainly cannot come from  $3d^1\Pi_a$  as this has no  $K = 0$  level.

The rotational levels of  $3d^3\Pi_a$  look very irregular; but then so do the rotational levels of  $3d^1\Pi_a$ . In fact, there is a good deal of resemblance between them which extends even to the details of the irregularities. As in the case of the  $\Sigma$  levels the similarity between  $3d^3\Pi_a$  and  $3d^1\Pi_a$  is closest at the  $v = 0$  level and falls off as  $v$  increases.

\* 'Proc. Roy. Soc.,' A, vol. 123, p. 74 (1929).

† 'Proc. Roy. Soc.,' A, vol. 124, p. 529 (1929).

‡ 'Proc. Roy. Soc.,' A, vol. 123, p. 73 (1929).

§ 'Proc. Roy. Soc.,' A, vol. 123, p. 468 (1929).

We have less information about the  $\Delta_a$  levels than the others. Their behaviour as  $v$  changes shows a good deal of resemblance to that of the  $\Pi_a$  levels. Thus the successive pairs of second differences 63·84, 59·36 : 63·85, 55·96 : 57·43, 39·55 : 50·05, 31·58 show a similar course to that of the two lowest second differences of  $3d^1\Pi_a$ , namely, 35·44, 34·61 : 44·68, 41·04 : 47·83, 42·45 : 48·92, 37·12. For  $3d^1\Delta_a$  the levels at  $v = 2$  and  $v = 3$  are unknown, at  $v = 1$  only one rotational level is known so that the intervals cannot be given. At  $v = 0$  the  $3d^1\Delta_a$  levels resemble all the other singlet levels in being very similar to the corresponding triplet levels, although the similarity is not so close as that shown by the  $\Pi_b$  and  $\Delta_b$  levels.

It will be noticed that the irregularity in the  $v' = 1$  level of  $3d^3\Sigma$  which was discussed in I, p. 679, has now disappeared. So have the other irregularities mentioned there. The bands in which these occurred have been entirely reconstructed.

#### § 5. The System $3s^3\Sigma \rightarrow 2p^3\Pi_{ab}$ .

This is a system ending on  $2p^3\Pi$  which does not come from the  $3d^3\Sigma\Pi\Delta$  complex, although the bands lie in the same region as those described already. Up to the present we have only found the  $v' = 1$  progression with certainty, so the description will be confined to that. In Tables IV and V, which were prepared before the properties of the system had been fully disclosed, the upper level of the system is called  $3^3Z$ ; but we now consider that there is no doubt that it is the hitherto undiscovered level  $3s^3\Sigma$ . However, those who disagree with this conclusion may still call it  $3^3Z$  if they wish.

The lines are set out in the usual way in Table X. The final rotational differences in Tables IV and V show that the main band has final vibration quantum number  $v'' = 1$ . The reason for assigning the initial quantum number  $v' = 1$  to the bands will be considered later. The strongest branch is the P branch and the weakest the R branch with Q intermediate. Most of the strength of R' 3 is required by the line of the  $\Delta$  band with which it is coincident and the R4 line is definitely absent. The lines of the non-diagonal bands are determined by the final vibration differences given in Table VII. The  $1 \rightarrow 2$  band is represented by the Q1 and P2 lines and the  $1 \rightarrow 0$  band by the P2 line. These Q1 and P2 lines give the rotational  $v'' = 2$  combination difference 109·80 as compared with the standard value 109·77<sub>0</sub>. In each of the three bands the strongest line is P2. Some of the properties of the lines as given by Merton and Barratt have not been put into Table X as they refer to blends and are merely confusing. Perhaps the He+ opposite P' 1 ought to be

Table X.— $3s^3\Sigma (= 3^3Z) \rightarrow 2p^3\Pi_{ab}$ .

	The $1 \rightarrow 1$ band.			The $1 \rightarrow 2$ band.		
R'1	17031.67	—	1a			
R2	17086.67	9.2	2	C—		
R'3	17139.77	17.6	5			
R4	[17190.56]		ab			
Q1	16917.50	10.9	3		14700.79	00
Q'2	16916.57	—	0			
Q3	16915.33	13.0	3	19	14½	
Q'4	16913.48	—	0			
Q5	16910.79	—	1½	C+		
						The $1 \rightarrow 0$ band.
P'1	16860.14	—	0a			
P2	16802.37*	52.0	10	L++		
P'3	16744.92	16.7	5	z = 0	60	55
P4	16688.40	19.0	4	H±	30	24
P'5	16633.03	—	0	z = 0		
P6	16579.03	10.8	2			
					14590.99	0c
						19135.64
						3.7
						2

R'3 is coincident with P3 of  $1 \rightarrow 1$   $3d^2\Delta \rightarrow 2p^3\Pi$  which requires most of the strength.  
P'1 is coincident with R6 of  $0 \rightarrow 0$   $3p^3\Pi \rightarrow 2s^2\Sigma$ .  
P'5 is coincident with R'3 of  $3 \rightarrow 3$   $3d^3\Pi \rightarrow 2p^3\Pi$ .  
P6 is coincident with R2 of  $3 \rightarrow 3$   $3d^3\Pi \rightarrow 2p^3\Pi$ .

omitted. We believe the other data in the table to be the properties actually representative of the lines of the present bands with the possible exception of the *h* line Q5. If these bands belong to  $3s\ ^3\Sigma \rightarrow 2p\ ^3\Pi$  we should expect them to have properties similar to the  $\alpha, \beta, \gamma \dots$  bands  $np\ ^3\Pi \rightarrow 2s\ ^3\Sigma$ ,  $n = 3, 4, 5 \dots$ . The characteristic features of the  $\alpha, \beta, \gamma$  bands are (1) depression in the condensed discharge of the lines with low *K*, frequently accompanied by enhancement of the lines with high *K* values; (2) low pressure enhancement of the low *K* lines changing over to high pressure enhancement at high *K*; (3) absence of the Zeeman effect. Examples of all these properties can often be found in a single branch of these bands; for instance, the P branch of  $0 \rightarrow 0\ 3p\ ^3\Pi \rightarrow 2s\ ^3\Sigma$ . These are just the properties shown, so far as data are available, in Table XIII. They are in strong contrast to the properties of  $3d\ ^3\Sigma \rightarrow 2p\ ^3\Pi$ , the other system ending on  $2p\ ^3\Pi$  and coming from an upper  $\Sigma$  level, set out in Table I. The excitation potential of the strong P2 line of the  $1 \rightarrow 1$  band has been measured as 12.39 volts by Finkelburg, Lau and Reichenheim. This is about right if the final level is  $v'' = 1$  of  $2p\ ^3\Pi$ . The band lines show evidence of the alternation of intensity in the ratio of 3 : 1 for the *a* : *s* lines which is characteristic of the H<sub>2</sub> spectrum.

If we extract the rotational term differences of the upper level by the same method as was used in the case of  $3d\ ^3\Sigma$ , we get the values given with their first and second differences in Table XI. These terms are very regular and do not

Table XI.

K	Term differences of $3s\ ^3\Sigma$ .
↓	↓
5	277.44
4	224.72 $\xrightarrow{52.72} 1.87$
3	170.13 $\xrightarrow{54.59} 1.37$
2	114.17 $\xrightarrow{55.96} 0.85$
1	57.36 $\xrightarrow{56.81} 0.55$
0	---

show the complicated uncoupling effects which are characteristic of the terms of the  $3d\ ^1\Sigma\Pi\Delta$  complexes. On the contrary, they are of the same type as the terms of the regular levels  $2s\ ^3\Sigma$  and  $2p\ ^1\Sigma$  and are given approximately by the expression

$$F(K) = B(K + \frac{1}{2})^2 + \beta(K + \frac{1}{2})^4. \quad (1)$$



Owing to the method of extraction the terms as set out in Table XI involve the unknown small doublet distance  $\pm x_1$  which is introduced when the lowest interval is measured by subtracting P' 1 from Q1. No doubt the effect of this is minute, but it is a disadvantage if we wish to determine the rotational constants of the level. We can avoid this uncertainty if we keep to the PR differences which depend solely on the upper levels. These are

$$R' 1 - P' 1 = f2 - f0 = 171.53, \quad R2 - P2 = F3 - F1 = 284.30,$$

$$R' 3 - P' 3 = f4 - f2 = 394.85, \quad R4 - P4 = F5 - F3 = 502.16.$$

By applying equation (1) to the two lowest of these differences we find for the constants of the upper level

$$2B_1 = 57.4_{35}, \quad \beta_1 = -0.019_{75}.$$

These compare with the values, shown in Table XII, of  $2B_1$  and  $-\beta$ , for a number of other hydrogen levels.

Table XII.

Level→	$2p^3\Pi_{ab}$	$3p^3\Pi_{ab}$	$4p^3\Pi_{ab}$	$5p^3\Pi_{ab}$	$2s^3\Sigma$	$3s^3\Sigma$	$2p^1\Sigma$	$H_2+$
$2B_1$ .....	57.8 <sub>6</sub>	56.7 <sub>6</sub>	55.7	56.3	63.50	57.4 <sub>35</sub>	36.98	55.4
$-\beta_1$ .....	0.019	0.019	0.017 <sub>8</sub>	0.03	0.021	0.019 <sub>8</sub>	0.0152	0.02

The values of  $2B_1$  for  $3p^3\Pi$  and  $4p^3\Pi$  are not very accurate. Owing to a perturbation at the  $v = 1$  level of  $3p^3\Pi$  the value of  $2B_1$  has been obtained by interpolation from the values of  $2B_0$ ,  $2B_2$  and  $2B_3$  (I, p. 674). The data for  $4p^3\Pi$  are very meagre. It is probable that the true values of  $2B_1$  for these  $np^3\Pi$  levels drop smoothly from the value at  $n = 2$  to that for  $H_2+$ , with most of the drop occurring between  $n = 2$  and  $n = 3$ ; just as do the values of  $2B_0$ , which are much more certain. At the first glance the value  $57.4_{35}$  looks too low for  $3s^3\Sigma$  in comparison with 63.50 for  $2s^3\Sigma$ . But we have to remember that the value for  $2s^3\Sigma$  is a long way from that for  $H_2+$ , which is also the end of the series  $ns^3\Sigma$ . If most of the drop in this series also takes place between  $n = 2$  and  $n = 3$  the value  $57.4_{35}$  for  $3s^3\Sigma$  is not unreasonable.

An alternative which may be considered is that the upper level of the progression is the  $v = 2$  level of  $3s^3\Sigma$ . This would make  $2B_2 = 57.4_{35}$  and  $2B_1$  would be about 60.5. This perhaps would not be an unreasonable value, although rather high. However, in a progression involving transitions between two levels of the type under consideration it is practically certain that the maximum strength will lie in the diagonal bands. In the strong band the upper and lower states have practically the same value of B, a fact

which is obvious without any analysis from the highly compressed Q branch, in which all five lines lie within a total range of 7 wave numbers. For the maximum strength to move from the  $1 \rightarrow 1$  band to the  $2 \rightarrow 1$  band we should require a value of B for the upper state a good deal different from that for the lower state. The discrepancy would have to be something comparable to that between the  $2B_1$  of  $2s^3\Sigma$  (63.5) and that of  $4p^3\Sigma$  (52.7). We think on these grounds that the possibility of the upper level of the progression being  $v' = 2$  can be safely disregarded.

We expect that the upper level is a  $\Sigma$  level because its transitions down to  $2p^3\Pi$  give rise to just those lines which should occur, in transitions from a  $\Sigma$  to a  $\Pi$  level. (The regularity of the structure of the upper level enables us to say that there is a line exactly where the  $P' 1$  line should occur, thus confirming the existence of the  $K' = 0$  level which occurs only in  $\Sigma$  levels.) It is not  $3d^3\Sigma$  because that level has already been described and, as we have seen, has quite different properties. It is a  $3\Sigma$  level (*i.e.*,  $n = 3$ ) because the denominator is quite close to 3 whatever value may be assumed, in reason, for the unknown initial vibrational intervals. It is not  $3p^3\Sigma$  because that level is already known\* and has a value of  $2B_1 = 49.16$ . In any event it could not be a  $np^3\Sigma$  level because those levels are odd and cannot go down to  $2p^3\Pi$  which is also an odd level. It cannot be a level of the type of the abnormal levels ( $^1K$ ,  $^1L$ ,  $^1M$ , etc.) which are so abundant at  $n = 3$  in the singlet spectrum. Its rotational structure is far too regular for this to be possible. It must be some regular even  $3\Sigma$  level and the only possible level it can be is  $3s^3\Sigma_g$ . Thus this argument by exclusion confirms the conclusion already arrived at by a study of the properties of the level. Except that the distribution of intensity between the branches does not agree very well with theory the whole of the evidence is entirely consistent with this conclusion.

#### § 6. Energy Levels, Intensities and Constants.

The present state of the wave-mechanics offers a quantitative explanation not only of the almost unperturbed states like  $2p^3\Pi$  but also of the strongly uncoupled upper  $d$  states. It yields the vibrational and rotational constants of the hypothetical unperturbed states associated with the actual states; and it enables the intensities in the bands to be calculated. When this is done the results are quite good, both in the  $3d^3$  and the  $4d^3$  systems. In fact, they are a strong argument for the correctness of the bands. In order not to prolong

\* Richardson and Das (*loc. cit.*).

the present communication, we shall give these results in Part III, confining the present paper mainly to the directly observed properties of the  $3d^3$  bands and of what we believe to be the  $3s^3\Sigma$  bands. Part III will include an account of the bands coming from the  $4d^3\Sigma^3\Pi^3\Delta$  complex and will also deal with the  $\nu_0$ 's and  $\nu_r$ 's of all the levels and with the other constants which can be derived from them. The values are not changed very radically from those given in I, § 9.

#### § 7. *Summary.*

This paper describes a reconstruction and extension of the band systems coming from  $3d^3\Sigma$ ,  $3d^3\Pi_{ab}$  and  $3d^3\Delta_{ab}$  and ending on  $2p^3\Pi_{ab}$  levels which were put forward in I. The new  $3d^3\Sigma \rightarrow 2p^3\Pi$  system is, in essentials, merely an extension of that described in Part I. The  $3d^3\Delta_{ab} \rightarrow 2p^3\Pi$  systems are, apart from unimportant details, the same as the re-arrangement and extension of the former  $3d^3\Pi_{ab} \rightarrow 2p^3\Pi$  and  $3d^3\Delta_{ab} \rightarrow 2p^3\Pi$  systems recently put forward by Sandeman. New bands have been found for the  $3d^3\Pi_{ab} \rightarrow 2p^3\Pi$  systems. Part of a band system ending on  $2p^3\Pi$  and coming from the hitherto undiscovered  $3s^3\Sigma$  level is also described. The properties of the levels are discussed and a few of the principal constants determined; but most of these are left over to a following paper which will also deal with the band systems coming down to  $2p^3\Pi$  from the  $4d^3\Sigma\Pi\Delta$  complex and with all the theoretical intensities.

---

*The Effect of the Solvent on Reaction Velocity. III.—The Interaction of Persulphate Ions and Iodide Ions.\**

By FREDERICK GEORGE SOPER and EMYLN WILLIAMS.

(Communicated by J. L. Simonsen, F.R.S.—Received October 14, 1932.)

Although in homogenous bimolecular gaseous reactions, the constants A and B of the empirical equation of Arrhenius,  $k = Be^{-A/RT}$ , have now a precise meaning, their exact significance for reactions occurring in solution is still doubtful. Inspection of the results obtained by various workers shows that changes of solvent may cause, for any one reaction, very marked changes in B so that, although in certain cases B is the same for the reaction in solution as for the reaction in the gaseous state,† it appears necessary to conclude that, in general, this constant embodies factors which are dependent on the solvent environment.

The considerable changes in B on change of solvent are shown for three reactions in Table I. Values of  $RT \ln B$  have been calculated for the interaction of dimethyl aniline and methyl iodide,‡ for bromoacetophenone and aniline,§ and for pyridine and allyl bromide.||

Table I.—Values of  $RT \ln B = RT \ln k + A$ .

Solvent.	$\text{PhNMe}_2 + \text{MeI}$ at 20°.	$\text{PhNH}_2 + \text{CH}_3\text{BrCOPh}$ at 37·8°.	$\text{C}_6\text{H}_5\text{N} + \text{C}_3\text{H}_7\text{Br}$ at 28·3°.
Benzene .....	—	3,830	9,570
Tetrachlorethane .....	13,843	—	10,700
Chloroform .....	—	6,860	—
Acetone .....	—	8,850	10,440
Nitrobenzene .....	15,010	10,820	—
Ethyl alcohol .....	—	12,200	11,525
Benzyl alcohol .....	16,650	12,370	—

\* Previous papers in this series have been published by Richardson and Soper ('J. Chem. Soc.,' p. 1873 (1929)) and Soper and Williams (*ibid.*, p. 2297 (1931)).

† Moelwyn-Hughes and Hinshelwood, 'Proc. Roy. Soc.,' A, vol. 131, p. 177 (1931).

‡ Essex and Gelormini, 'J. Amer. Chem. Soc.,' vol. 48, p. 882 (1926).

§ Cox, 'J. Chem. Soc.,' vol. 119, p. 142 (1921).

|| Hawkins, 'J. Chem. Soc.,' vol. 121, p. 1170 (1922).

The interrelation of the constants A and B observed for any single reaction carried out in a number of solvents is interesting and significant. In Table II, A is compared with  $RT\ln B$  and with  $RT\ln k$  for the interaction of aniline and bromoacetophenone (Cox, *loc. cit.*).

Table II.

Solvent.	A.	$RT\ln B$ .	$RT\ln k$
Benzene .....	8,090	3,830	4,260
Chloroform .....	10,760	6,860	3,900
Acetone .....	11,080	8,850	2,230
Nitrobenzene .....	13,470	10,820	2,650
Ethyl alcohol .....	13,900	12,200	1,700
Benzyl alcohol .....	14,290	12,370	1,920

Since  $k = Be^{-A/RT}$  or  $A = RT\ln B - RT\ln k$ , constancy of B would necessitate a reciprocal dependence of the velocity coefficient on the critical increment, whereas, in the present example, increase of A is attended by an increase in  $RT\ln k$ , instead of the decrease anticipated by analogy with gaseous reactions. The resulting concordance between changes in A and in  $RT\ln B$  on change of solvent cannot, in this case, be due to an artificial selection of data caused by the exclusion of excessively slow or excessively fast reaction velocities,\* which may result in some interrelation between these quantities when velocities of different reactions are compared. In the study of the effect of solvent on the rate of a particular reaction, very fast or slow rates are not excluded, but rather sought for, in illustration of the solvent influence.

An explanation of the interdependence of the constants A and B on change of solvent, follows from the suggestion made by Richardson and Soper† to account for the dependence of the solvent effect on the reaction type. It was observed that the effect of changing from a non-polar to a polar solvent is to increase the speed of reactions, where the products are polar relatively to the reagents, and to decrease the speed of reactions, where the reagent substances are the more polar. It was suggested that the solvent tends to disrupt the critical complex into those substances for which the solvent has the greater affinity. If, on these grounds, we formulate reaction velocity in solution by the equation,  $k = P \cdot Ze^{-E/RT}$ , where  $Ze^{-E/RT}$  represents, as in gas reactions, the collision frequency of molecules having the necessary energy

\* Lewis and Hudleston, 'J. Chem. Soc.', p. 1398 (1932).

† 'J. Chem. Soc.', p. 1873 (1929).

of activation, and  $P$  is a probability factor which is connected with the relative polar nature of reagents and products *and which varies with temperature*, then the Arrhenius constants  $A$  and  $B$  will acquire a modified significance. The relation of the constant  $A$  to  $E$ , the true energy of activation, will be obtained by separating  $P$  into temperature variable and non-variable parts, in order that comparison may be made with the equation  $\ln k = -A/RT + \ln B$ . Thus,

$$\ln k = - \left( \frac{E + RT^2 d \ln P / dT}{RT} \right) + (\ln Z + \ln P + T d \ln P / dT),$$

and, since the second part of the expression is independent of temperature (the variation of  $Z$  being neglected),

$$A = E + RT^2 d \ln P / dT$$

and

$$RT \ln B = RT \ln PZ + RT^2 d \ln P / dT.$$

The frequently observed parallelism between changes in  $A$  and  $RT \ln B$  on change of solvent thus finds explanation in the existence of the common term  $RT^2 d \ln P / dT$ , and, incidentally, variation in the observed critical increment, with temperature or solvent, may not necessarily imply appreciable alteration in the true energy of activation of the reaction.

An alternative interpretation of this temperature variable factor,  $P$ , is that, when reagent molecules of the requisite energy collide, the solvent may favour or may hinder their articulation into a critical complex. The solvent may, by its affinity for a particular type of molecule, tend to form that type, or, on the other hand, by its affinity for the reagent molecules tend to resist the formation of the new type. The critical complex when formed is then assumed to break down immediately to form the reaction products as in the theories of Scheffer,\* and of Brønsted.† The critical complex will have properties which are a mean of those of the products and reagents, and therefore, if the reaction is one where the products are relatively polar, the intermediate critical complex will also be polar in comparison with the reagents. Hence, as is observed, polar solvents, owing to their affinity for polar molecules, will favour the formation of such a critical complex, and will enhance the speed of reactions of this type. On this view the factor  $P$ , taking solubility as a measure of solvent affinity, may be written as  $s_x/s_1$  where  $s_x$  and  $s_1$  are the "solubilities" of the

\* Scheffer and Kohnstamm, 'Verslag. Akad. Wetensch. Amsterdam,' vol. 19, p. 878 (1911); Scheffer and Brandsma, 'Rec. Trav. Chim.,' vol. 45, p. 522 (1926).

† 'Z. phys. Chem.,' vol. 102, p. 169 (1922); *ibid.*, vol. 115, p. 337 (1925).

critical complex, and of the reagents, respectively in the solvent. Alternatively, since  $s$  is inversely proportional to the activity coefficient  $f$ ,

$$P = f_1/f_x$$

and

$$k = Ce^{-E/RT} \cdot f_1/f_x$$

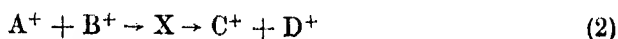
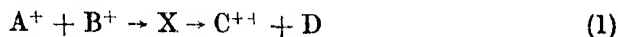
or

$$v = Cc_A c_B e^{-E/RT} \cdot f_A f_B / f_x,$$

which, omitting the exponential term, is the Bronsted equation.

The object of the present work was to differentiate between these alternative hypotheses. Both views are in accord with the equilibrium requirements of a reversible reaction, and with the general effect of  $x$  solvents on reactions of the two types, *i.e.*, those in which the products are more, and those in which the products are less polar than the reagents. Both suggestions would also account for the parallelism between  $A$  and  $RT \ln B$  for reactions examined in a series of solvents, since a probability factor has been introduced which may vary considerably with temperature. The first view, involving a variable break-up of the critical complex, associates the solvent effect with the relative properties of the reagents and products, whilst the second affirms that the effect will be determined solely by the properties of the reagents and of the critical complex. A study of a reaction between ions, in solutions of low ionic strength, should therefore provide evidence on this point.

If there is a tendency of the solvent to break up the critical complex after formation, in a manner which depends on the relative affinity of the solvent for the products and reagents, the effect of ionic strength of the solution on the speed of reactions of type 1 and 2



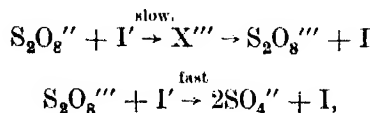
will not be exactly the same. Increase in ionic strength would tend to favour reaction 1 and hence to increase the slope of the  $\log k - \sqrt{\mu}$  curve above that of reaction 2.\*

A study of the persulphate-iodide reaction has therefore been made in order to compare the effect of ionic strength on the reaction with its corresponding effect on the thiosulphate-bromoacetate reaction, studied by La Mer† as a

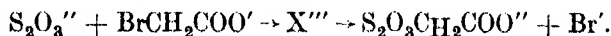
\* In both reactions, the velocity coefficient would be expected to increase since the specific collision frequency of ions of unlike sign increases with increase of ionic strength (Christiansen, 'Z. phys. Chem.', vol. 113, p. 35 (1924)).

† 'J. Amer. Chem. Soc.', vol. 51, p. 3341 (1929); 'Chem. Rev.', vol. 10, p. 179 (1932).

precision test of the Brønsted theory of reaction velocity. Since the persulphate-iodide reaction is bimolecular\* it proceeds in consecutive stages, necessitating an abnormal distribution of electrons in the product ions of the first stage, *e.g.*,



whilst the bromoacetate-thiosulphate reaction conforms to type 2, reagent and product ions being of similar valence.

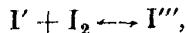


In both cases the critical complex has a charge of minus 3 and divergencies in the activity coefficient from the simple Debye-Hückel limiting law† may occur. However, over the same region of ionic strength, and in the presence of ions of similar valence, divergencies from this law should be common to both critical complexes and should affect the slope of the two  $\log k - \sqrt{\mu}$  curves to an equal extent.

### Experimental.

The persulphate-iodide reaction was first studied by Slater Price,‡ who found that the speed was independent of hydrogen ion concentration unless iron or some other catalyst was present. The effect of added salts on the velocity of the reaction has recently received much attention by von Kiss and his co-workers.§

The velocity of interaction is complicated to some extent by the fact that iodine formed removes iodide ions as tri-iodide,



and this reduces the concentration of one of the reagents, so that the bimolecular coefficient falls with time. According to von Kiss and von Zombory (*loc. cit.*), the tri-iodide ion does not react with persulphate, and when allowance is made for the tri-iodide equilibrium the reaction conforms to a bimolecular

\* Slater Price, 'Z. phys. Chem.,' vol. 27, p. 474 (1898).

† Gronwall, La Mer and Sandved, 'Phys. Z.,' vol. 29, p. 358 (1928).

‡ 'Z. phys. Chem.,' vol. 27, p. 474 (1898).

§ von Kiss and von Zombory, 'Rec. Trav. Chim.,' vol. 46, p. 225 (1927); von Kiss, 'Z. phys. Chem.,' vol. 134, p. 26 (1928); von Kiss and Bossanyi, 'Rec. Trav. Chim.,' vol. 47, p. 619 (1928); von Kiss, 'Rec. Trav. Chim.,' vol. 48, p. 508 (1929); von Kiss and Hatz, 'Rec. Trav. Chim.,' vol. 48, p. 7 (1929).



law. The reaction, they state, is sensitive to certain catalysts, *e.g.*, copper, ferrous salts and light.

Jette and King,\* however, consider that the tri-iodide ion can react appreciably with persulphate, and support their contention by fresh experimental data.

The method adopted in the present investigation avoids a decision as to the reactivity of the tri-iodide ion. The speed was examined only over the range of the first 25 per cent. change of the persulphate, so that the concentration of the tri-iodide ions, and therefore their effect, was always small, and further, the constants have been extrapolated to the commencement of the reaction.

While this work was in progress a paper was published by King and Jacobs† giving observations on the rate of interaction of persulphate and iodide ions over the range of ionic strength examined by us. These authors found that plotting  $\log k$  against  $\sqrt{\mu}$  gave a slope for the curve which agreed with the Brønsted equation up to  $\sqrt{\mu} = 0.06$ , but above this ionic strength there was an increasing negative deviation. Since a reaction in solutions containing only univalent ions would be expected to follow the theoretical expressions to much higher ionic strengths than if bivalent ions are present this particular reaction was regarded as a somewhat unsatisfactory test of the Brønsted equation and a further series of experiments was carried out, where the concentration of the bivalent persulphate ions was kept low, and the ionic strength increased by addition of iodide ions. Alternatively the concentration of both reactants was kept low and an inert salt added to keep up the ionic strength. Better agreement with theory was then obtained.

A comparison of our results with the results of King and Jacobs showed a serious discrepancy. At the higher concentrations the difference was not so great, but at the lower concentrations our values were some 30 per cent. lower. King and Jacobs' method of estimation involved the addition of small quantities of thiosulphate and starch to the reaction mixture and noting the time taken before the appearance of blue colour. From this time, which was determined by using a photoelectric cell, the velocity constants were calculated.

The large difference in the results of the two investigations, involving different methods of estimation, led us to examine the effect of light on the reaction. For this purpose solutions of M/2000 persulphate and M/1000 iodide were divided into two equal portions and mixed. The two resulting reaction mixtures, to which starch and 1 c.c. of thiosulphate (N/500) were

\* 'J. Amer. Chem. Soc.,' vol. 51, p. 1034 (1929).

† 'J. Amer. Chem. Soc.,' vol. 53, p. 1704 (1931).

added, were maintained at the same room temperature in a tank of water one being protected from light whilst the other was illuminated by a 100-watt (opal glass) lamp at 10 cm. distance. After  $2\frac{1}{2}$  hours the one which had been protected from light was a light blue colour, whilst the other was dark blue. The iodine produced in these two solutions during this time corresponded to 2.25 and 3.71 c.c. of N/500 thiosulphate respectively, showing that the reaction proceeds at a greater rate when illuminated.

This is not surprising when one considers the sensitivity of solutions of potassium persulphate to light, as shown by the work of Morgan and Crist.\* The photochemical decomposition was found to proceed according to a zero or linear order with a limited light intensity which might account for the greater divergency between our results and those of King and Jacobs in the more dilute solutions, where the photochemical reaction would have a greater effect.

In our experiments the reaction was carried out in standard 500 and 1000 c.c. flasks immersed in a thermostat at  $25.0^\circ \text{C.} \pm 0.02^\circ \text{C.}$ , the rate being followed by titration of the iodine formed. The potassium persulphate was purified by repeated crystallization until free from sulphate and was dissolved in water distilled first from chromic acid and then from baryta. To this solution was added the requisite quantity of a solution of B.D.H. "analytical reagent" potassium iodide, made up in water of similar high grade. Portions were pipetted out at intervals and titrated against standard thiosulphate in a long colourless glass cylinder with starch as indicator and in an atmosphere of nitrogen.† In this way end-points were obtained to 0.05 c.c. using N/500 thiosulphate. This represents a maximum error of 1 per cent. on a 5 c.c. titre, and causes the possibility of a 2 per cent. error in  $k_2$ .

The velocity coefficients were calculated from the formula

$$dx/dt = k[\text{S}_2\text{O}_8''][\text{I}'] = k(a-x)(b-2x)$$

which on integrating gives

$$\text{when } b > 2a \quad kt = \frac{1}{b-2a} \ln \frac{a(b-2x)}{b(a-x)}$$

$$,, \quad b < 2a \quad kt = \frac{1}{2a-b} \ln \frac{b(a-x)}{a(b-2x)}$$

$$,, \quad b = 2a \quad kt = \frac{1}{2a} \cdot \frac{x}{a-x}$$

\* 'J. Amer. Chem. Soc.', vol. 49, p. 16 (1927).

† Soper, 'J. Chem. Soc.', p. 1908 (1924).

The bimolecular nature of the reaction was confirmed by carrying out the reaction, at varying initial concentrations of the reagents, in the presence of 0.2 M potassium nitrate, which was added to keep the ionic strength approximately constant. The results shown in Table III were obtained.

Table III.—Velocity of Interaction of Persulphate Ions and Iodide Ions in presence of 0.2 M Potassium Nitrate.

Initial persulphate concentration.	Initial iodide concentration.	$k_2$ .
0.005 M	0.01 M	0.379
0.005 M	0.005 M	0.371
0.0025 M	0.005 M	0.371

The observed rate of production of iodine may not, however, give a true measure of the rate of interaction of persulphate ions and iodide ions. Persulphate, even in carefully purified water, shows a slight decomposition. The rate of this decomposition has been observed by Elbs and Neher,\* and by Levi and Migliorini,† and though, by careful purification and exclusion of light, the stability of the salt can be greatly increased, the decomposition in 10 days is still observable, viz., 3.6 per cent. for a M/200 solution.

The uncertainty in the observed velocity of interaction caused by the slight decomposition of persulphate depends on whether its spontaneous decomposition yields nascent oxygen which, with the iodide, slightly increases the rate of iodine production. The decrease in concentration of persulphate itself, owing to this decomposition, is not of importance since its effect on the velocity coefficient is eliminated by extrapolation to the time of starting the reaction. Examples of such extrapolations are shown in Table IV.

If the spontaneous decomposition of the persulphate results in an equivalent formation of iodine, correction may be made as follows. Representing the rate of formation of iodine as  $v$ ,

$$v = k_2[I'] [S_2O_8''] + k_1 [S_2O_8''],$$

where  $k_1$  is the velocity coefficient of decomposition of persulphate which is regarded as obeying a unimolecular law. If the uncorrected value for the velocity coefficient of interaction of persulphate ions and iodide ions be denoted

\* 'Chem. Z.', vol. 45, p. 1113 (1921).

† 'Gazzetta,' vol. 36, p. 599 (1906).

as  $k'_2$ 

$$k'_2[I][S_2O_8''] = k_2[I][S_2O_8''] + k_1[S_2O_8'']$$

and thus

$$k_2 = k'_2 - k_1/I'.$$

The effect of this correction would, therefore, be slightly to decrease the value of the velocity coefficient, the corrections increasing with fall of concentration of iodide, *i.e.*, the results at the *lower* ionic strengths would be subject to the greater decrease.

Table IV.

$[S_2O_8''] = 0.005 \text{ M}$ $[I'] = 0.01 \text{ M}$		$[S_2O_8''] = 0.008399 \text{ M}$ $[I'] = 0.0002 \text{ M}$		$[S_2O_8''] = 0.0002 \text{ M}$ $[I'] = 0.0004 \text{ M}$	
Time.	$k_1$ .	Time.	$k_2$ .	Time.	$k_1$ .
minutes		minutes		days	
30	0.121	126	0.0798	3	0.0607
60	0.119	269	0.0782	6	0.0594
90	0.118	329	0.0776	9	0.0574
120	0.115	384	0.0760	12	0.0549
150	0.114				
Extrapolated to time 0, $k_1 = 0.123$ .		Extrapolated to time 0, $k_2 = 0.0812$ .		Extrapolated to time 0 $k_1 = 0.0624$ .	

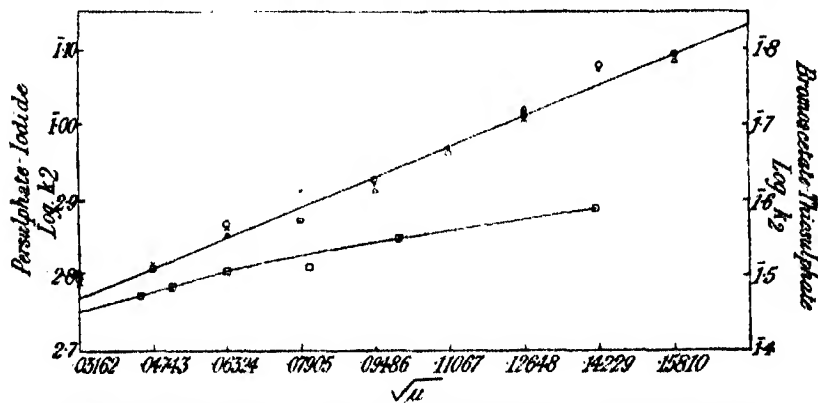
It was impossible to determine whether such formation of iodine from the persulphate decomposition actually resulted. Attempts at the direct estimation of the persulphate in dilute solution (N/200) using titanous salts, which would avoid the uncertainty, were not successful.

### Results and Discussion.

The value of the velocity coefficients obtained (without the above correction) are shown in Table V. In the first and second series of experiments the concentration of the iodide was always twice that of the persulphate. All these experiments were duplicated. In the third series of experiments, the persulphate concentration was kept low and the iodide concentration increased to change the ionic strength. This was done in order to eliminate any possible disturbing factor due to the divalent ions as suggested by King and Jacobs. The values of  $\log k$  have been plotted against  $\sqrt{\mu}$  in fig. 1, and the resulting points compared there with the corresponding ones for the bromoacetate-thiosulphate reaction.

Table V.

Molar concentration of iodide.	Molar concentration of persulphate.	$\mu$ .	$\sqrt{\mu}$ .	Series	$k_2$ .	$\log k_2$ .
0.01000	0.00500	0.02500	0.15810	1	0.1230	1.0899
0.01000	0.00500	0.02500	0.15810	2	0.1230	1.0899
0.02440	0.00020	0.02500	0.15810	3	0.1220	1.0864
0.00910	0.00405	0.02025	0.14229	1	0.1180	1.0719
0.00910	0.00405	0.02025	0.14229	2	0.1190	1.0755
0.00640	0.00320	0.01601	0.12648	1	0.1010	1.0043
0.00640	0.00320	0.01601	0.12648	2	0.1020	1.0086
0.01541	0.00020	0.01601	0.12648	3	0.1030	1.0128
0.00490	0.00245	0.01226	0.11067	1	0.0925	2.9661
0.00490	0.00245	0.01226	0.11067	2	0.0922	2.9647
0.00360	0.00180	0.00900	0.09486	1	0.0829	2.9186
0.00360	0.00180	0.00900	0.09486	2	0.0845	2.9269
0.00840	0.00020	0.00900	0.09486	3	0.0812	2.9096
0.00250	0.00125	0.00625	0.07905	1	0.0814	2.9106
0.00250	0.00125	0.00625	0.07905	2	0.0742	2.8704
0.00160	0.00180	0.00399	0.06324	1	0.0724	2.8597
0.00160	0.00180	0.00399	0.06324	2	0.0732	2.8645
0.00339	0.00020	0.00399	0.06324	3	0.0710	2.8513
0.00090	0.00045	0.00225	0.04743	1	0.0654	2.8156
0.00090	0.00045	0.00225	0.04743	2	0.0646	2.8102
0.00040	0.00020	0.00100	0.03162	1	0.0622	2.7938
0.00040	0.00020	0.00100	0.03162	2	0.0624	2.7952

FIG. 1.—1st series experiments  $\times$ . 2nd series experiments  $\circ$ . 3rd series experiments  $\Delta$ .

The slope of the  $\log k - \sqrt{\mu}$  curve obtained by La Mer\* for the latter reaction was found to be 2.0 at ionic strengths below 0.0025 in accordance with the requirements of the Brønsted theory. When corrected for an error in computing the ionic strengths the slope of the  $\log k - \sqrt{\mu}$  curve was reduced to 1.6. Later work by La Mer and Fessenden† shows that substitution of

\* 'J. Amer. Chem. Soc.,' vol. 51, p. 3341 (1929).

† 'Chem. Rev.,' vol. 10, p. 179 (1932).

potassium bromoacetate and thiosulphate for the corresponding sodium salts gives better agreement with theory.

In order to eliminate the uncertainty as to what constitutes the straight line of closest fit through a series of points, the slope of the  $\log k - \sqrt{\mu}$  curve for the persulphate has been determined by the Method of Least Squares. The evaluation of the slope by this method is considerably simplified if the points are equally spaced, i.e., if  $\sqrt{\mu}$  increases by the same amount over each interval.\*

The slope has been calculated for the three series of experiments, the values obtained being 2.422, 2.479 and 2.357 respectively, the latter value relating to those experiments where the persulphate concentration was kept low. The magnitude of these values prevents clear decision between the possible reaction processes which have been discussed, since the slopes are greater than were anticipated from either theory. The application of reaction velocity equations of the type  $\log k = C + m z_A z_B \sqrt{\mu} - n z_C z_D \sqrt{\mu}$  to a balanced reaction, coupled with the fact that, when  $z_A z_B = z_C z_D$ , the slope of the  $\log k - \sqrt{\mu}$  curve is between 0.7 and 1.0 (La Mer, *loc. cit.*, 0.8) limits, on the basis of the simple Debye-Hückel theory, the magnitude of the maximum slope obtainable. The enhanced slopes observed for the persulphate iodide reaction may perhaps be due partly to the high charge of the critical complex (Gronwall, La Mer and Sandved, *loc. cit.*), in which case it is significant that the slopes are greater than that observed in the bromoacetate-thiosulphate reaction,† where the charge of the critical complex is the same and similar deviations might be expected to occur. Such comparison is in agreement with the idea that some state of indecision exists in the critical complex causing it to resolve itself in a way partly dependent on the nature of the medium.

The work is now being extended to an investigation of the rate of interaction of univalent ions of unlike sign, where the products are neutral molecules. Here, since no ions will be present of higher charge than unity, the Debye-Hückel limiting law will be more precisely obeyed and a clearer decision possible.

\* Fisher, "Statistical Methods for Research Workers," London, p. 124 (1930).

† [Note added in Proof, December 6, 1932.—The bromoacetate-thiosulphate reaction has recently been reinvestigated by Kappana and Patwardhan ('J. Indian Chem. Soc.,' vol. 9, p. 379 (1932)), who find agreement with the requirements of the Brønsted equation for ionic strengths from 0.00125 to 0.012 $\mu$ . This would support the alternative view that the P factor is associated with the formation of the critical complex from the reagents, always assuming that the Debye-Hückel limiting law is obeyed for the activity coefficient of the trivalent bromoacetate-thiosulphate critical complex. The enhanced slopes for the persulphate iodide reaction would then have to be assigned to some other cause.]

*Summary.*

(1) For reaction velocity in solution the equation  $k = P \cdot Ze^{-E/RT}$  is proposed, where  $P$  is a probability factor which varies with temperature and is connected with the relative polar nature of reagents and products, and  $Ze^{-E/RT}$  is, as in homogeneous gas reactions, the collision frequency of molecules possessing the requisite energy of activation. Comparison with the Arrhenius equation,  $k = Be^{-A/RT}$ , shows that  $A = E + RT^2 d \ln P / dT$  and  $RT \ln B = RT \ln PZ + RT^2 d \ln P / dT$ . Changes in  $A$  and in  $RT \ln B$  for a particular reaction on change of solvent are frequently closely related, which is attributed to the major influence of the common term  $RT^2 d \ln P / dT$ .

(2) Alternative explanations of the physical nature of  $P$  are formulated: (a) the solvent exerts its effect on the breakdown of the intermediate critical complex causing it to resolve itself mainly into those substances, either products or reagents, for which it has the greater affinity; (b) the solvent exerts its effect in aiding or hindering the articulation of the reagent molecules to form the critical complex. In both cases the effect of polar as compared with non-polar solvents will be to favour the production of polar molecules and thus to accelerate or retard the reaction velocity, according as the reaction products or the reagent substances are the more polar.

(3) According to (b) the effect of ionic strength on the velocity coefficient of an ionic reaction should depend solely on the charges of the reagent ions and on that of the critical complex, whilst if (a) is correct, the relative charges of the reagent and product ions might also be expected to exert some influence, a medium of high ionic strength then tending to favour the production of high valence ions. The oxidation of iodide by persulphate ions, where the reagent and product ions are of dissimilar charge, has been studied over the range of ionic strength from  $\mu = 0.001$  to  $0.025$ . The  $\log k - \sqrt{\mu}$  curve obtained is compared with that plotted by La Mer (*loc. cit.*) for the bromoacetate-thiosulphate reaction, where the charges of the reagent and product ions are the same. The result favours alternative (a), but may be obscured by disturbances due to the high charge of the critical complex.

---

*The Effect of Solvent on Reaction Velocity. IV.—The Rate and Critical Increments of some Chlorination Reactions.*

By R. E. ROBERTS and F. G. SOPER.

(Communicated by J. L. SIMONSEN, F.R.S.—Received October 14, 1932.)

Moelwyn-Hughes\* has recently shown that the observed rates of a number of reactions in solution approximate to those calculated from the collision frequency of the reacting molecules and the critical increment of the reaction. At first sight, this fact brings reaction velocity in solution in line with reaction velocity in bimolecular homogeneous gas reactions, where a sufficient hypothesis to explain the observed reaction rates, is that reaction occurs whenever two molecules collide with a combined kinetic energy equal to, or greater than, the critical increment. There are, however, a number of reactions in solution, considered by Moelwyn-Hughes, which have a relatively low critical increment for which the calculated rate is several thousand times greater than that observed.† The conclusion drawn is that the observed critical increment of these reactions is false.

The reactions which show this anomalous behaviour are reactions of the type where quaternary ammonium salts are formed. In such reactions relatively nonpolar molecules are forming a salt. A reaction of the converse type where polar molecules are forming molecules of a less polar nature is the interaction of acetic anhydride and ethyl alcohol.‡ Here also it is found that the calculated rate is many thousand times greater than that observed.

The explanation advanced by Moelwyn-Hughes and Hinshelwood (*loc. cit.*) to account for these anomalous reactions is that ionization of one of the reagents is a precursor of reaction and that in consequence the observed critical increments involve the heats of ionization. This view is further examined by Moelwyn-Hughes and Rolfe§ for the interaction of acetic anhydride and ethyl alcohol, in which the actual reagents are assumed to be the anhydride molecule and the  $C_2H_5O^+$  ion. The calculated rate is then found to be approximately 500 times less than the observed rate whilst assumption of direct interaction

\* 'Chem. Rev.,' vol. 10, p. 241 (1932).

† Cf. Norrish and Smith, 'J. Chem. Soc.,' vol. 128, p. 129 (1928).

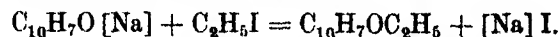
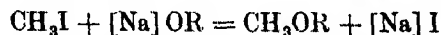
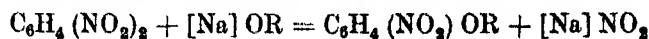
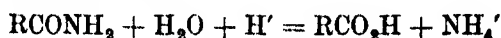
‡ Soper and Williams, 'J. Chem. Soc.,' p. 2297 (1931); Moelwyn-Hughes and Hinshelwood, *ibid.*, p. 230 (1932).

§ 'J. Chem. Soc.,' p. 241 (1932).



of the anhydride and alcohol molecules leads to a value too great by some  $10^8$  times. A fact that may be urged, however, against the view that reaction involves the ethoxide ion, is the effect of the solvent on the reaction velocity, the solvents arranged in order of their accelerating influence being: hexane > heptane > carbontetrachloride > chlorobenzene > benzene > anisole > chloroform > nitrobenzene, *i.e.*, the speed is less in polar than in nonpolar solvents, although the ionization of the ethyl alcohol and the concentration of the ethoxide ion will be greater in the former. It is possible that the increase in the concentration of the ethoxide ion in polar solvents is more than counterbalanced by an increase in the true critical increment, although on general principles, the reverse effect on the critical increment might be expected, since, in the formation of the critical complex, electronic displacements occur which will be facilitated, rather than rendered more difficult, by a polar environment.

The reactions considered by Moelwyn-Hughes, the speeds of which show agreement with the collision theory, are mainly of one type, namely, reactions in which ions, or molecules possessing electrovalency, appear on both sides of the reaction equation, *viz.*,



Only two reactions fail to conform to this type—a type where there is little change in the polar nature of the products and reagents—namely, (1) the formation of urea from ammonium cyanate, probably involving a transformation of unionized ammonium cyanate,  $\text{NH}_4 + \text{CNO}' = \text{NH}_4\text{CNO} = (\text{NH}_4)_2\text{CO}$  and (2) the formation of triethyl sulphonium bromide from ethyl bromide and diethyl sulphide. With the exception of the latter reaction, all the reactions which conform to the simple collision theory are reactions in which products and reagents are of similar polar nature. To this class of reaction may be added the decomposition of chlorine monoxide examined in carbon tetrachloride by Moelwyn-Hughes and Hinshelwood.\*

There appears to be evidence, therefore, for the view that reactions for which major discrepancies occur between calculated and observed rates are reactions in which the polar nature of the products differs appreciably from

\* 'Proc. Roy. Soc.,' A, vol. 131, p. 177 (1931).

that of the reacting substances. This would be in harmony with the reaction velocity equation put forward in the previous paper, where the rate of a reaction in solution is given by

$$k = PZe^{-E/RT}.$$

In this equation  $P$  is some probability factor which depends on the relative polar nature of products and reagents and modifies the rate calculated in terms of collision frequency  $Z$  and energy of activation  $E$ . Whether  $P$  affects the rate of formation of the critical complex or whether it modifies the breakdown of the critical complex into the products (by the relative affinity the solvent exerts for the products and reagents respectively) has been left open (*vide* previous paper). One of the general effects, which may be tested directly, of the introduction of the temperature variable  $P$  term, is to cause a similarity in the changes of the terms  $A$  and  $B$  of the Arrhenius equation  $k = Be^{-A/RT}$  with change of solvent. Thus it may be shown that

$$A = E + RT^2 d \ln P / dT$$

and

$$RT \ln B = RT \ln PZ + RT^2 d \ln P / dT,$$

so that if  $E$ , the true energy of activation, does not vary much with change of medium,  $A$  and  $RT \ln B$  should increase and decrease together since they both contain the same major term  $RT^2 d \ln P / dT$ .

To examine this point, the rates of chlorination of suitable phenols and anilides have been measured in a range of solvents. In such chlorinations,  $\geq \text{RH} + \text{Cl}_2 = \geq \text{RCl} + \text{HCl}$ , the reaction products are more polar than the reacting substances, as in the formation of quaternary ammonium salts; and, if divergences between calculated and observed reaction rates in the latter are due to this contrast in properties of products and reagents, rather than to special reaction mechanism, similar anomalies may be expected for the rates of chlorination.

#### Experimental.

The rates of chlorination of anilides and phenolic ethers have previously been studied in acetic acid or aqueous acetic acid as solvent,\* and in water.†

\* Orton and King, 'J. Chem. Soc.,' vol. 99, p. 1369 (1911); Orton and Bradfield, *ibid.*, p. 986 (1927); Bradfield and Jones, *ibid.*, pp. 1006, 3073 (1928), 2903 (1931); Bradfield, Jones and Spencer, *ibid.*, p. 2907 (1931).

† Soper, 'J. Phys. Chem.,' vol. 31, p. 1192 (1927).

The procedure followed in the present determinations was similar to that described by Orton, Soper and Williams,\* in which a solution of chlorine is added to the solution of the anilide and the residual chlorine estimated at suitable intervals by addition of portions to aqueous potassium iodide, and titration with standard thiosulphate in an atmosphere of nitrogen. The solvents selected were all shown to be stable to chlorine over periods greatly exceeding that of the time required for a velocity determination. The absence of rapidly chlorinated impurities was also demonstrated by dilution of a chlorine solution by the solvent, and examination of the titre after dilution. No disappearance of chlorine was experienced. The initial disappearance of chlorine during mixing with an anilide or ether solution was therefore regarded as equivalent to the anilide or ether chlorinated and the corrected initial concentrations,  $a$  and  $b$ , were employed in the bimolecular formula for the velocity coefficient,  $k = 1/t(a - b)$ ,  $\ln b(a - x)/a(b - x)$ ,  $a - x$  and  $b - x$  being the concentrations of ether and chlorine at time  $t$  minutes after the "arrest" of the first removed portion of the mixture. Details of a typical experiment are given in Table I.

Table I.—Chlorination of Acetylanthranilic Acid in Nitrobenzene. Temperature  $20.0 \pm 0.01^\circ$  C. Thiosulphate = 1.003 N/200. Initial [anthranilic acid] = 0.01183 M;  $[\text{Cl}_2]$  = 0.00689 M.

Time (minutes).....	0	6	10	15	20
Titre of 5 c.c. thiosulphate.....	11.05	8.46	6.95	5.47	4.39
$k_2$ .....	—	5.38	5.41	5.39	5.41

Experiments were carried out at  $20.0^\circ$  and  $30.0^\circ$  and in some cases also at  $0^\circ$ . Higher temperatures than  $30^\circ$  were not considered practicable owing to the increased volatility of chlorine and instability of the solvent to chlorine under these conditions. The acetic acid was purified by distillation from chromic acid according to the method of Orton and Bradfield,† and contained 1 per cent. of water by volume. The nitrobenzene, chloroform, tetrachloroethane and hexane were washed with appropriate acid or alkaline solutions and finally with water, thoroughly dried and distilled. With hexane the fraction boiling at  $67.8^\circ$  to  $68.4^\circ$  was used.

\* 'J. Chem. Soc.,' p. 998 (1928).

† 'J. Chem. Soc.,' p. 960 (1924), p. 983 (1927).

## Results and Discussion.

Velocity coefficients obtained at 20.0° are summarized in Table II, the values recorded being the mean of from two to four concordant experiments. The mean deviation from the mean for a series was found to be 2 per cent. or less, except for the rapid chlorination of *p*-cresyl methyl ether in acetic acid, the velocity coefficient of which is subject to an uncertainty of 8 per cent. owing to difficulties in accurately timing the arrest of the reaction in the portions removed for analysis. For purpose of comparison, the relative cohesions of the solvents calculated by two methods\* are included in this table. In general the rate is faster in solvents of high cohesion, as with quaternary ammonium salt formation. This behaviour is the opposite of that observed when the reaction products are less polar than the reacting substances.†

Table II.—Velocity Coefficients of Chlorination at 20.0°.

Solvent.	Cohesion.		Acetyl anthr- anilic acid.	<i>p</i> -Chlor- phenetole.	<i>p</i> -Cresyl- methyl ether.	<i>p</i> -Chlor- acet- anilide.	Methyl acet- anilide.
	$E\sigma/v^{\frac{1}{2}}$ .	$L/v$ .					
Hexane .....	9.45	243.2	—	—	0.0158	—	—
Chloroform .....	15.5	363.1	0.243	0.021	—	—	—
Tetrachlorethane .....	15.6	373.5	2.54	0.298	—	—	—
Nitrobenzene .....	17.2	400.3	5.40	0.175	—	0.242	0.0344
Acetic acid .....	14.7	424.7	0.985	1.90	1.940	0.355	4.55

Mean values of the velocity coefficients at 30.0° (except when otherwise indicated), together with the critical increments, evaluated from the formula,  $A = RT_1 T_2 / (T_2 - T_1) \cdot \ln k_2 / k_1$ , are given in Table III. On the basis of a possible error of 2 per cent. in a velocity coefficient at one temperature or of 4 per cent. in the ratio  $k_2 / k_1$ ,  $A$  is subject to an uncertainty of 700 cal. The zero critical increment in hexane is noteworthy. A similar zero critical increment was observed for the chlorination of diphenyl-ether in chloroform ( $k_{20} = k_{30} = 7.00$ ). It is immediately apparent from the small values of the critical increment observed that the discrepancies between calculated and observed reaction rates are very great, the former being several million times the latter. Chlorinations are thus anomalous reactions similar to those in which quaternary ammonium salts are formed.

\* Hildebrand, "Solubility," New York, p. 99 (1924).

† Richardson and Soper, 'J. Chem. Soc.,' p. 1878 (1929). Soper and Williams, *loc. cit.*

Table III.—Critical Increments of Chlorination.

Solvent.	Acetyl anthranilic acid.	<i>p</i> -Chlor- phenetole.	<i>p</i> -Cresyl- methyl ether.	<i>p</i> -Chlor- acetanilide.	Methyl acetanilide.
Hexane ....	—	—	0 ( $k_0 = 0.0158$ )	—	—
Chloroform .....	5,570 ( $k = 0.334$ )	—	—	—	—
Tetrachlorethane .....	3,240 ( $k = 3.05$ )	1,910 ( $k = 0.33$ )	—	—	—
Nitrobenzene .....	5,460 ( $k = 7.38$ )	6,940 ( $k = 0.26$ )	—	6,800 ( $k = 0.355$ )	6,750 ( $k = 0.0505$ )
Acetic acid .....	10,750 ( $k = 1.82$ )	10,640 ( $k = 3.48$ )	4,870 ( $k_{18} = 1,740$ $k_{20} = 2,300$ )	11,890 ( $k = 0.698$ )	13,350 ( $k = 9.72$ )

Comparison of the changes in  $RT\ln B$  and  $A$  with changes of solvent are made in Table IV for the chlorination of acetyl anthranilic acid and of *p*-chlor-phenetole. Except for the value enclosed by square brackets increases in  $A$  are paralleled by increases in  $RT\ln B$  as would be required by the presence of a probability factor,  $P$ , which is a strong function of temperature.

Table IV.

Solvent.	Acetyl anthranilic acid.		<i>p</i> -Chlorphenetole.	
	$A$ .	$RT\ln B$ .	$A$ .	$RT\ln B$ .
Chloroform .....	[5,570]	3,780	—	—
Tetrachlorethane .....	3,240	4,750	1,910	1,210
Nitrobenzene .....	5,460	6,440	6,940	5,930
Acetic acid .....	10,750	10,740	10,840	11,000

In effect, on alteration of solvent, large changes may occur in the observed critical increment, which are attended by relatively slight changes in the velocity coefficient. Where larger changes\* in the velocity coefficient were encountered as in the case of *p*-cresyl methyl ether in acetic acid and in hexane where  $k$  changes by 100,000 times, there is still no apparent reciprocity between the speed and the observed critical increment, for the critical increment alters in the wrong direction and becomes practically zero in the solvent where the speed is slower. At first sight the effect of medium on the velocity and critical increments of different chlorinations is haphazard, but a regularity emerges

\* Measured to avoid the artificial selection of velocity coefficients within a narrow range.

when the constants  $B$  of the Arrhenius equation are evaluated. According to Bradfield and Jones\* the changes in the velocity coefficient of chlorination of phenolic ethers can be accounted for in terms of alterations in the critical increment,  $A$ , which is identified with the sum of the energies required for activation of the chlorine and phenolic ether molecules. This fact may also be expressed by stating that the value of  $B$  is constant for the series of related chlorinations. Values of  $RT\ln B$  calculated at  $20^\circ$ , for the chlorinations carried out in acetic acid and in nitrobenzene are given in Table V.

Table V.—Values for  $RT\ln B$  for Chlorinations.

Solvent.	Acetyl anthranilic acid.	<i>p</i> -Chlor- phenetole.	<i>p</i> -Cresyl methyl ether.	<i>p</i> -Chlor- acetanilide.	Methyl acetanilide.
Acetic acid .....	10,740	11,000	9,280	11,290	11,400
Nitrobenzene .....	6,440	5,930	—	6,600	7,630

This approximate constancy of the quantity  $RT\ln B$  may be regarded as affording further support for the existence of the proposed  $P$  factor in the reaction velocity equation in solution. If  $P$  depends on the relative polar nature of the reagents and products (or on the relative affinity of the solvent for these substances) then it may be anticipated that in chlorinations, in which the reagent and product substances of contrasted physical properties are chlorine and hydrochloric acid, the factor  $P$  will be similar for all chlorinations in one solvent, since chlorine and hydrochloric acid are common to all the reactions. Since the Arrhenius  $B$  is related to  $P$  and  $Z$ , the collision frequency, by the equation

$$RT\ln B = RT\ln PZ + RT^2 d\ln P/dT,$$

and  $Z$  is sensibly constant since the substances chlorinated are of similar molecular weight, constancy of  $RT\ln B$  is required.

Replacement of acetic acid by nitrobenzene alters  $P$  and its temperature coefficient so that  $RT\ln B$  decreases by about 4000 cal. This decrease is attended by a similar decrease in the observed critical increment, due according to the present theory to the change in the value of  $RT^2 d\ln P/dT$ , rather than to an appreciable change in the actual energy required for activation. Certainly the zero values observed for the critical increment for *p*-cresyl methyl ether in hexane and for diphenyl ether in chloroform definitely negative the idea that

\* 'J. Chem. Soc.,' pp. 1006, 3073 (1928).

the observed critical increment can always be identified with the energy required for activation.

In conclusion, the authors wish to express their thanks to Dr. G. I. Davies for presenting the preparations of *p*-chlorphenetole and of *p*-cresyl methyl ether and to the Chemical Society for a grant which has defrayed the cost of the investigation. They also have pleasure in acknowledging the helpful interest of Professor J. L. Simonsen, D.Sc., F.R.S.

*Summary.*

(1) Major divergencies between observed reaction rates in solution and those calculated from the equation,  $k = Ze^{-E/RT}$ , are associated with reactions in which the polar nature of the reagents and products is sharply contrasted.

(2) The velocity coefficients and critical increments of the chlorination of some phenolic ethers and anilides have been measured in a series of solvents. In some cases zero critical increments are observed. As in quaternary ammonium salt formation the calculated reaction rates are anomalous. The alteration in the quantities  $A$  and  $RT\ln B$ , on change of solvent, are closely related; a fact which is interpreted in support of the reaction velocity equation,  $k = P \cdot Ze^{-E/RT}$  (*vide* previous paper).

(3) For phenolic ethers and anilides in one solvent,  $B$  is found to be approximately constant (*cf.* Bradfield and Jones, *loc. cit.*). Replacement of the solvent nitrobenzene, by acetic acid, raises  $B$  by approximately a constant amount. This constancy of  $B$  for chlorinations in a particular solvent, is discussed and is in agreement with the physical significance assigned to the factor  $P$ .

---

*The Crystalline Structure of Anthracene. A Quantitative X-Ray Investigation.*

By J. MONTEATH ROBERTSON, M.A., Ph.D.

(Communicated by Sir William Bragg, O.M., F.R.S.—Received October 17, 1932.)

The aromatic hydrocarbons naphthalene and anthracene were among the first organic compounds to be investigated by the X-ray method. The early work\* on these crystals afforded evidence that the long axes of the molecules lay along the *c* direction in the crystal, but less definite indication was obtained regarding the lateral disposition of the molecules. An attempt was made to settle this point by a study of the intensities of the principal X-ray reflections by visual estimate, and this led to a distorted "tetrahedral" structure being advanced.† Somewhat later it was shown by Sir William Bragg that this structure was untenable, the discrepancies between the calculated and the measured values of certain reflections being too great.‡ In this work absolute measurements of intensity were obtained for the more important planes, and the evaluation of the atomic positions carried out by Fourier analysis. This led to a structure consisting of molecules with flat or slightly distorted carbon rings, whose planes made an angle of about 25° with the *bc* plane, and with the long axis of the molecule tilted about 6° away from the direction of the *c* axis towards a more upright position. Almost at the same time Banerjee§ independently arrived at a structure, based upon the measurement of some intensities, together with the results of optical and magnetic measurements, which agreed very closely with Bragg's structure.

At the commencement of the present work, then, it could be taken that the structure of anthracene was approximately known. It was very important, however, to confirm these results by more accurate and more extensive intensity measurements, and also to attempt to work out the finer details of the structure. For example, it was not known if the carbon rings were quite flat like the graphite structure, or slightly puckered, perhaps intermediate between the diamond and graphite type: the evidence seemed to point to the

\* W. H. Bragg, 'Proc. Phys. Soc.,' vol. 34, p. 33 (1921); vol. 35, p. 167 (1923); "X-rays and Crystal Structure," p. 229 (1925); 'Z. Kristallog.,' vol. 66, p. 22 (1927); 'Nature,' vol. 121, p. 327 (1928).

† J. M. Robertson, 'Proc. Roy. Soc.,' A, vol. 125, p. 542 (1929).

‡ 'Nature,' vol. 125, p. 456 (1930).

§ 'Indian J. Phys.,' vol. 4, p. 557 (1930); 'Nature,' vol. 125, p. 456 (1930).



latter possibility. The carbon to carbon distance was not accurately known. The only estimate obtained was 1.48 Å., which is again intermediate between the diamond (1.54) and the graphite (1.42) distance.

As the anthracene structure involves 21 parameters without considering the hydrogen atoms, its complete determination is a very complicated task. With the results already obtained it was obviously desirable to apply the Fourier analysis, and this method has been extensively used in the present investigation. Briefly, the procedure has been as follows. First of all the parameters were determined as far as possible by trial and error, and then a preliminary Fourier analysis was carried out for two zones of reflections (about the *b* and *c* crystallographic axes). From the results of this analysis the values of the co-ordinates of the atoms were refined, and it was now found that a much better agreement was obtained between the observed and calculated values of the reflections. This was chiefly due to the presence of a hitherto unsuspected tilt in the axis of the molecule away from the *ac* plane. With the revised values of the co-ordinates it was now possible to make sure of the phase constants of some of the weaker reflections which had previously been doubtful. The intensity measurements were now checked and made as accurate as possible and a final double Fourier analysis carried out for the zones about the three crystallographic axes. The results of this final analysis are set out and discussed in this paper.

#### *Measurement of Intensities.*

Like most organic compounds, anthracene forms crystals which are usually small and friable, unsuitable for cutting or grinding into sections. The best method for measuring the integrated reflections from such crystals therefore appears to be that of completely immersing a small single crystal in the X-ray beam. As this method, although tested,\* has not been much used in quantitative work, Robinson in this laboratory has conducted a parallel investigation into the validity of the whole method, with special reference to anthracene, and has also determined the absolute values of some of the anthracene reflections. For the purposes of this paper, then, the writer has only required to measure the relative values of the integrated reflections from anthracene. These measurements were then calibrated with Robinson's absolute values, using one of his measured crystals for the purpose.

Two methods of measuring the intensities have been used, the ionization spectrometer and the integrating photometer devised by Robinson. The

\* Bragg, 'Proc. Phys. Soc.,' vol. 33, p. 304 (1921).

photographic method seems to be the most suitable for obtaining a complete survey of a large number of reflections, such as those required for making the two dimensional Fourier analyses. There is less chance of missing certain reflections, which may be comparatively weak, yet valuable for completing the detail in the analyses. But in general the more important reflections have been measured both by the ionization and photographic methods, and the following list is typical of the agreement obtained by the two methods. The figures give the integrated intensity in arbitrary units.

<i>hkl.</i>	Ionization spectrometer.	Robinson's photometer.
200	1000	982
201	652	645
202	253	258
001	711	667
002	192	194
003	52	59
004	81	72
005	32	31

The effect of extinction on the strong reflections is discussed by Robinson, but we believe that by using sufficiently small crystals, weighing about one-tenth of a milligram, the effect is largely eliminated. In making the relative measurements the smallest possible crystals were used in estimating the strong reflections, although slightly larger ones were occasionally used in measuring the weaker reflections, which do not appear to be affected by extinction.

Most of the measurements were made with copper radiation ( $\lambda = 1.54$ ). With this wave-length the absorption of the beam in the crystal is quite considerable, but again, with very small crystals, the effect is small. It did not seem practicable to apply a separate correction to each of the relative measurements to allow for the shape of the crystal, and the largest errors will probably be due to the varying thickness of crystal presented to the beam at each reflection. Several crystals of different shapes were usually measured, with good agreement except in extreme cases. In general, crystals with a nearly square section perpendicular to the rotation axis were sought, those in the form of thin flakes being avoided.

Table I gives the value of the structure factor for each reflection in absolute units, and it is compared with a value calculated from the co-ordinates found for the atoms (which are given on p. 93), and from an F-curve for carbon

Table I.—Measured and Calculated Values of the Structure Factor.

<i>hkl</i>	$\sin \theta$ Cu K $\alpha$	F calc.	F measured.	<i>hkl</i>	$\sin \theta$ Cu K $\alpha$	F calc.	F measured.
200	0.219	+60.5	59	205	0.658	+10.5	8.5
400	0.438	— 6.5	3	404	0.691	— 6	6
600	0.657	— 8.5	7	403	0.621	— 7	7
020	0.256	—19.5	24.5	402	0.553	+ 5	< 4
040	0.511	— 2	< 3	401	0.494	— 0.5	< 3
001	0.084	+34	30	401	0.395	+ 3	< 3
002	0.168	—20.5	22	402	0.368	— 4.5	6.5
003	0.252	+12	14.5	403	0.359	+ 4	6
004	0.336	— 20	22	404	0.368	— 0.5	< 3
005	0.420	—12	16	405	0.395	—13.5	11.5
006	0.504	+ 5	< 4	406	0.437	+ 6.5	< 4
007	0.588	— 1	< 4	406	0.620	+28.5	22
008	0.672	— 4.5	< 4	4010	0.690	+10.5	9
009	0.756	— 7	3	601	0.613	—15	12
011	0.152	— 9	9	602	0.576	— 3	< 4
012	0.209	— 3.5	3.5	603	0.550	+ 5	< 4
013	0.280	+ 2	4.5	604	0.538	— 3.5	< 4
014	0.358	+ 8.5	12.5	605	0.538	—19.5	18.5
015	0.435	+13.5	14	606	0.550	— 5.5	6
016	0.518	+ 0.5	< 4	605	0.658	+18	15.5
017	0.600	— 5	< 5	6010	0.709	+17.5	15
018	0.683	+ 9	6	804	0.735	— 1	< 4
019	0.767	+ 8.5	5.5	805	0.720	— 8.5	8.5
021	0.270	—17	17	806	0.715	— 8.5	7
022	0.305	+ 5.5	8.5	807	0.720	+ 2	< 4
023	0.359	— 0.5	5.5	110	0.167	+57	50.5
024	0.421	—13	15.5	210	0.253	+44.5	48.5
025	0.491	+ 3	< 4	310	0.352	+ 7	11.5
026	0.565	— 2	< 5	410	0.457	+21	24.5
027	0.640	— 0.5	< 5	510	0.563	— 6.5	4.5
028	0.719	+11.5	8	120	0.277	+21	19
031	0.393	+17	19	220	0.335	—10.5	13
032	0.418	0	< 3	320	0.416	+24	25.5
033	0.458	— 5.5	7.5	420	0.506	— 1.5	< 3
034	0.509	—13.5	14.5	520	0.604	+ 5.5	8
035	0.567	—16	14.5	130	0.397	—20	19.5
036	0.631	— 3	< 5	230	0.440	+ 2	< 3
041	0.520	— 3	< 4	330	0.504	— 6	7
042	0.540	+ 0.5	< 4	430	0.581	+ 2	< 4
043	0.571	— 1.5	< 5	140	0.521	— 1.5	< 3
044	0.612	— 0.5	< 5	240	0.556	— 2.5	< 4
045	0.661	+12.5	11.5	114	0.430	—15	14
051	0.046	+ 1	< 5	113	0.353	+ 5	6
052	0.062	— 1.5	< 5	112	0.278	0	< 3
053	0.088	+ 9.5	7	111	0.214	— 8.5	9.5
054	0.723	+ 5.5	< 6	111	0.158	+26	23.5
205	0.577	— 8.5	8	112	0.187	—12.5	12
204	0.495	—23.5	22.5	113	0.244	+11.5	12.5
203	0.418	— 4	4.5	114	0.310	—17	17.5
202	0.345	+ 4	4.5	115	0.388	—14	16.5
201	0.278	— 5	5	222	0.427	+ 5.5	6
201	0.184	+46	43	221	0.375	—13	13
202	0.184	—25.5	27	221	0.314	+ 6.5	5
203	0.220	+10.5	14.5	222	0.314	+ 2.5	< 3
204	0.275	+ 0.5	3	223	0.336	+ 1.5	< 3
205	0.342	— 7	5	224	0.372	—21.5	23.5
206	0.418	+ 8	5	225	0.427	—19.5	19.5
207	0.498	— 6.5	< 4				
208	0.576	+ 3.5	< 4				

based on the measured reflections from graphite.\* The value of the structure factor is obtained from the measured reflection by the usual formulæ for the "imperfect" crystal.

*Fourier Analysis of Experimental Results.*

From the preceding tables it will be seen that there is a fairly good average agreement between the measured and calculated values of  $F$ . The atomic  $f$ -curve derived from graphite, upon which the calculated values are based, cannot be expected to fit the anthracene results exactly. No allowance has been made for the hydrogen atoms; and it will be seen from the following analysis that slightly differing curves ought to be applied to the different atoms in the molecule. But the agreements obtained seem to be sufficient to determine the phase constant of each member beyond any reasonable doubt; that is, in this case, whether the sign of the structure factor is positive or negative. With this information it is then possible to proceed with the Fourier analysis, which has the great advantage of presenting the structure directly from the experimental measurements, only the sign of the terms being taken from the calculated results.

The method of the double Fourier series was first developed by W. L. Bragg† and the theory is described in his paper. The arrangement of the results adopted here is also similar to that employed by him. By this method the distribution of scattering matter in the unit cell as projected along any zone axis can be calculated. The density of scattering matter per unit area,  $\rho(y, z)$ , for the projection along the  $a$  axis is

$$\rho(y, z) = \frac{1}{A} \sum_{-\infty}^{+\infty} \sum_{-\infty}^{+\infty} F(0kl) \cos 2\pi(ky/b + lz/c),$$

$A$  being the area of the plane upon which the projection is made. Corresponding formulæ apply for the projections along the other zone axes, the coefficients in the Fourier series being the structure factors for the planes in the zone. For convenient reference these coefficients with their signs are collected below in Tables II, III and IV for the projections along the three crystallographic axes.

It will be seen that the values of the coefficients which terminate the series are mostly fairly small compared with the initial values. In a comparatively

\* Bernal, 'Proc. Roy. Soc.,' A, vol. 106, p. 749 (1924); Lonsdale, *ibid.*, vol. 123, p. 499 (1929).

† 'Proc. Roy. Soc.,' A, vol. 123, p. 537 (1929).

Table II.—Values and Signs of  $F(0kl)$ .When  $k$  is even,  $F(0kl) = F(0k\bar{l})$ .When  $k$  is odd,  $F(0kl) = -F(0k\bar{l})$ .

		$k$					
		0	1	2	3	4	5
9		- 3	+ 5.5	—	—	—	—
8		—	+ 6	+ 8	—	—	—
7		—	—	—	—	—	—
6		—	—	—	—	—	—
5		-16	+14	—	-14.5	+11.5	—
4		-22	+12.5	-15.5	-14.5	—	—
3		+14.5	+ 4.5	- 5.5	- 7.5	—	+7
2		-22	- 3.5	+ 8.5	—	—	—
1		+30	- 9	-17	+19	—	—
0		+188	—	-24.5	—	—	—
1	l	+30	+ 9	-17	-19	—	—
2		-22	+ 3.5	+ 8.5	—	—	—
3		+14.5	- 4.5	- 5.5	+ 7.5	—	-7
4		-22	-12.5	-15.5	+14.5	—	—
5		-16	-14	—	+14.5	+11.5	—
6		—	—	—	—	—	—
7		—	—	—	—	—	—
8		—	- 6	+ 8	—	—	—
9		- 3	- 5.5	—	—	—	—

Table III.—Values and Signs of  $F(h0l)$ . $h$  is always even.

		$h$				
		0	2	4	6	8
9		- 3	—	—	—	—
8		—	—	—	—	—
7		—	—	—	—	—
6		—	—	—	—	—
5		-16	- 8	—	—	—
4		-22	-22.5	- 6	—	—
3		+14.5	- 4.5	- 7	—	—
2		-22	+ 4.5	—	—	—
1		+30	- 5	—	—	—
0		+188	+59	- 3	- 7	—
1	l	+30	+43	—	-12	—
2		-22	-27	- 6.5	—	—
3		+14.5	+14.5	+ 6	—	—
4		-22	+ 3	—	—	—
5		-16	- 5	-11.5	-18.5	- 8.5
6		—	+ 5	—	- 6	- 7
7		—	—	—	—	—
8		—	—	—	—	—
9		- 3	+ 8.5	+22	+15.5	—
10		—	—	+ 9	+15	—

Table IV.—Values and Signs of  $F(hk0)$ .

When  $(h + k)$  is even,  $F(hk0) = F(\bar{h}k0)$ .

When  $(h + k)$  is odd,  $F(hk0) = -F(\bar{h}k0)$ .

		$k$			
		0	1	2	3
6	6	-7	—	—	—
5	5	—	-4.5	+8	—
4	4	-3	+24.5	—	—
3	3	—	+11.5	+25.5	-7
2	2	+59	+48.5	-13	—
1	1	—	+50.5	+19	-19.5
0	0	+188	—	-24.5	—
1	1	—	+60.5	-19	-19.5
2	2	+59	-48.5	-13	—
3	3	—	+11.5	-25.5	-7
4	4	-3	-24.5	—	—
5	5	—	-4.5	-8	—
6	6	-7	—	—	—

Table V.—Projection along the  $a$  axis.

$S(y, z) \times 10^{-1}$ .

	4	0	5	9	10	9	6	4	6	9	10	9	5	0	4
	5	5	5	7	8	9	7	5	4	5	7	9	5	1	3
	9	7	3	4	8	12	14	12	8	5	5	6	8	7	6
	8	7	5	9	18	26	30	26	19	12	8	10	12	14	16
	7	8	11	18	27	33	33	29	23	16	14	16	20	23	25
	15	18	24	28	29	27	22	18	17	17	21	27	31	35	36
	28	32	35	35	28	19	12	10	11	16	22	27	31	34	36
	31	33	36	34	26	17	10	8	9	12	15	18	22	28	32
	17	19	21	20	17	12	8	7	6	5	5	11	22	35	43
	5	7	11	14	15	15	14	9	4	2	4	14	31	50	63
	3	7	14	22	28	20	26	18	10	6	9	19	34	49	58
	9	14	21	29	35	37	33	24	19	18	22	28	34	37	38
	27	27	27	27	27	26	23	20	20	26	33	37	36	29	24
	54	47	36	25	17	13	10	10	15	22	29	32	28	21	15
	58	49	34	21	11	6	5	6	8	11	13	16	17	14	12
	33	28	20	13	7	6	6	6	6	6	7	13	20	28	33

$\xleftarrow{\quad b/4 \quad} \times \xrightarrow{\quad b/4 \quad}$   
 Centre of symmetry

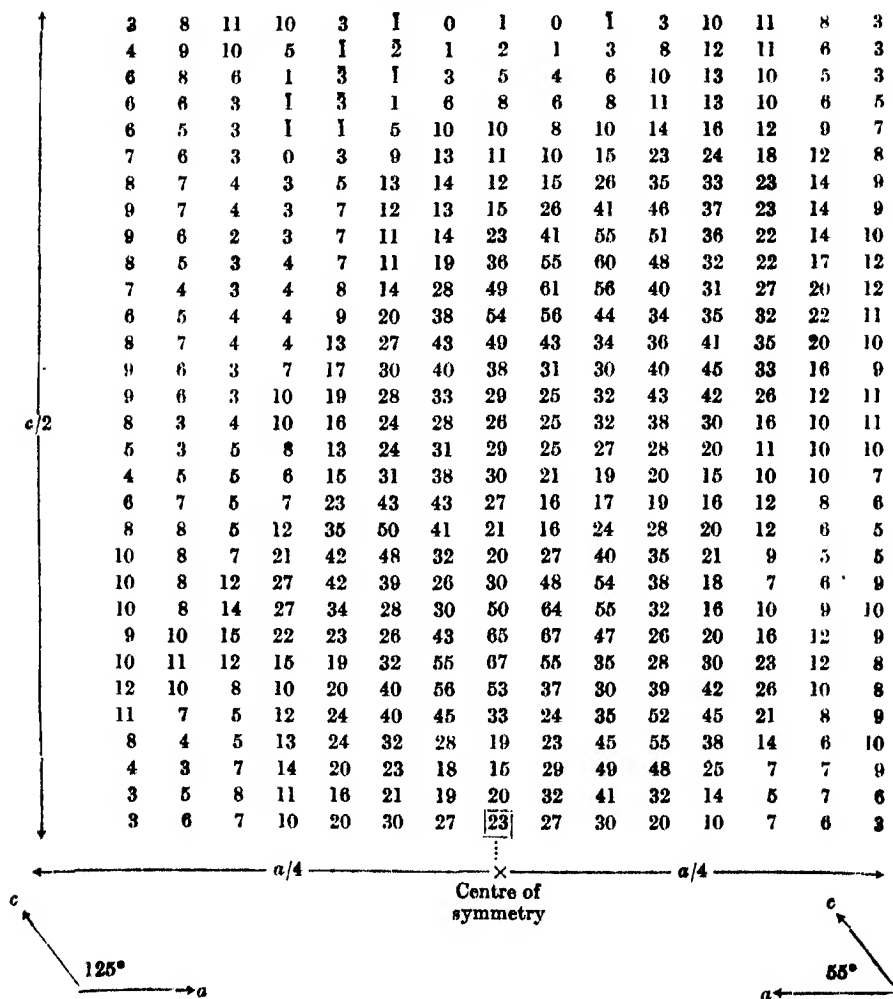
Table VI.—Projection along the  $b$  axis. $S(x, z) \times 10^{-1}$ .

Table VII.—Projection along the *c* axis.

$S(x, y) \times 10^{-1}$ .

	6	5	4	4	5	11	20	33	44	53	56	54	47	39	33
	6	5	3	3	8	16	30	45	61	72	77	74	66	53	42
	7	6	4	5	11	22	35	52	68	80	85	83	74	60	46
	7	5	6	6	13	22	35	48	60	70	75	73	65	54	41
	5	6	6	9	12	19	27	36	43	49	51	50	45	37	29
	6	6	7	8	10	13	17	20	24	26	27	26	24	21	17
	6	7	7	8	8	9	10	11	12	13	12	12	11	11	10
	8	8	8	7	8	7	7	7	8	8	8	8	8	8	9
$a/2$	8	8	7	7	7	7	7	7	8	8	8	8	8	8	8
	9	8	7	6	6	6	7	7	7	7	8	7	8	7	8
	12	10	8	6	6	5	5	6	5	5	5	6	6	6	5
	21	15	10	7	6	5	5	5	5	4	4	5	5	5	6
	28	19	12	10	9	8	7	7	6	5	4	5	6	7	7
	32	23	18	15	16	16	13	11	8	6	6	6	7	7	8
	32	27	27	28	31	33	31	27	20	13	8	6	5	6	7
	31	33	40	47	54	56	53	44	33	20	11	5	4	4	5

$\times$   $b/2$

Centre of symmetry

soft organic compound like anthracene (melting point  $217^{\circ}$  C.) the temperature factor is probably fairly large. This has the advantage of making the series fairly rapidly convergent without the necessity of applying an artificial temperature factor as has been suggested for certain inorganic compounds.\*

Tables V, VI and VII (above) give the summations for the projections along the three crystallographic axes, the figures corresponding to the series

$$S(y, z) = \sum \sum F(0kl) \cos 2\pi (ky/b + lz/c)$$

$$S(x, z) = \sum \sum F(h0l) \cos 2\pi (hx/a + lz/c)$$

$$S(x, y) = \sum \sum F(hk0) \cos 2\pi (hx/a + ky/b).$$

In the tables the figures have been divided by 10, so that the actual electron density per unit area is obtained from these figures by multiplying by 10 and dividing by the area of the plane upon which the projection is made.

The distribution of scattering matter in these projections is shown in figs. 1a to 4a. In each case the projection has been made on a plane perpendicular to the axis. The contour lines are drawn through points

\* Bragg and West, 'Phil. Mag.', vol. 10, p. 839 (1930).



of equal density at intervals of 100 in the values of  $S$ . Alongside each diagram is a drawing on the same scale showing the positions of the atoms and how they are linked together to form the anthracene molecules, figs. 1*b* to 4*b*.

The projection along the  $a$  axis, fig. 1, shows one complete unit cell and a small part of the next cell, which is added to show the extent of the gap between the ends of the molecules. In this projection

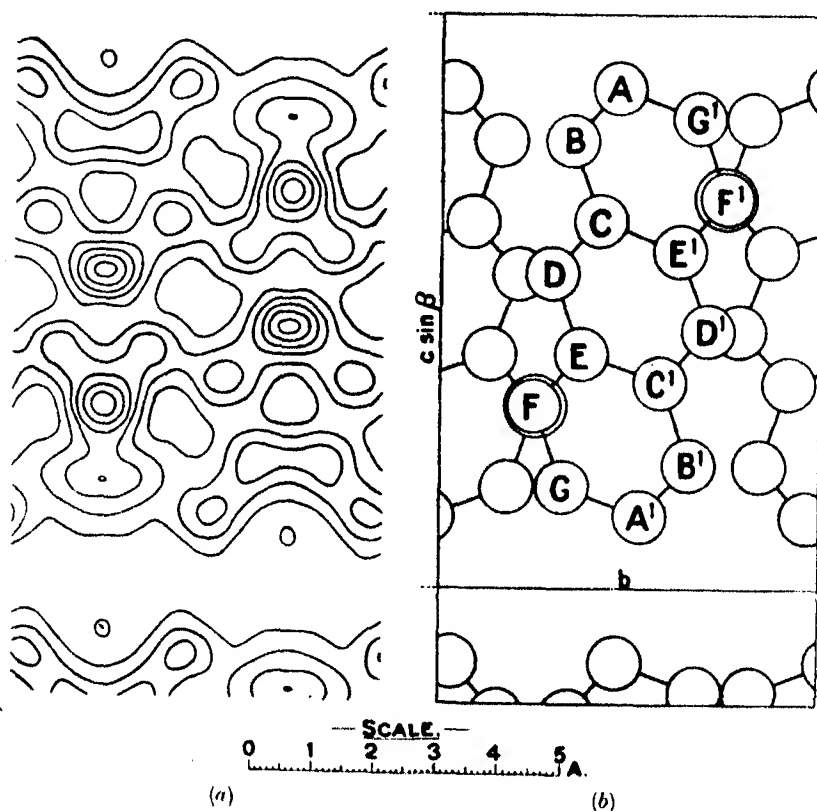


FIG. 1.—Projection along  $a$  axis.

the different molecules do not separate, because the centre one, which lies half a translation along the  $a$  axis in front of the others, overlaps them on either side. Some of the individual atoms, however, are quite clearly separated.

The projection along the  $b$  axis is the most striking, in that the individual molecules as well as many of the atoms are clearly separated.

Fig. 2 shows a single molecule on a large scale, occupying one-half of the unit cell. Fig. 3 shows on a smaller scale the mutual relations of six

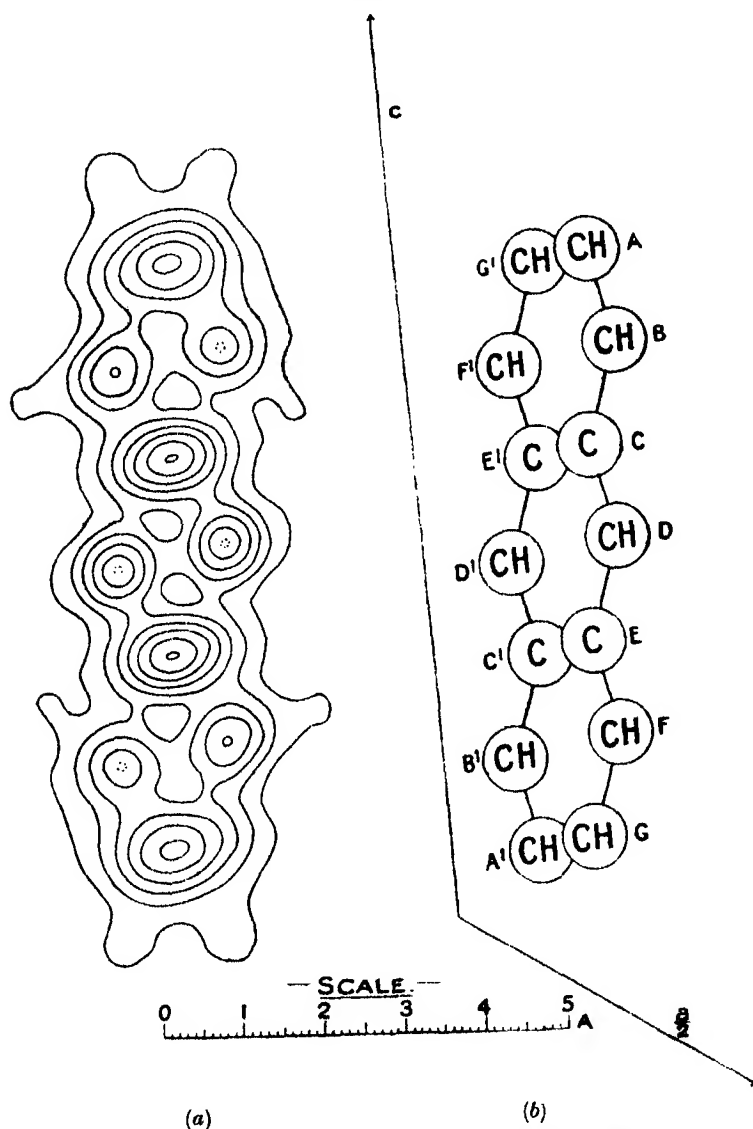


FIG. 2.—Projection along  $b$  axis. The dotted centres at atoms D and B mark densities of 560 and 460 respectively.

molecules. The centre ones, which are dotted, are identical with the others in this projection, but are actually removed half a translation along the  $b$  axis (perpendicular to the paper).

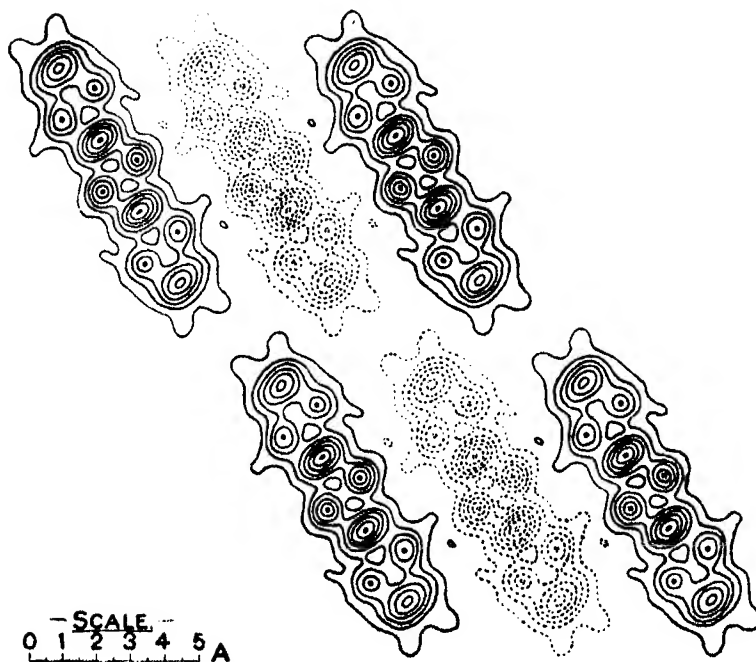


FIG. 3.—Projection along  $b$  axis showing mutual relation of molecules.

In the projection along the  $c$  axis, fig. 4, the molecules, seen end on, are very clearly separated, but not the individual atoms. The diagram shows the mutual relation of five molecules, the dotted line being the boundary of the unit cell.

#### *Crystal Data.*

Anthracene. Melting point  $217^{\circ}$  C. Monoclinic prismatic.  $a = 8.58$ ,  $b = 6.02$ ,  $c = 11.18$  Å.  $\beta = 125^{\circ}$ . Space group  $C_{2h}^2$  ( $P2_1/a$ ). 2 molecules of  $C_{14}H_{10}$  per unit cell. Total number of electrons per unit cell =  $F(000) = 188$ .

#### *The Structure Deduced from the Fourier Analysis.*

Several encouraging features are immediately evident from the contour diagrams. The carbon atoms which are sufficiently removed from their neighbours to separate clearly show a fairly high degree of spherical symmetry. Without such symmetry, of course, the analysis of organic compounds by atomic  $f$ -curves, which is a necessary preliminary to any Fourier analysis, would be very difficult. Again, in the projection along the  $b$  axis, the outlying atomic centres (B, D and F) are seen to lie quite accurately on a straight line,

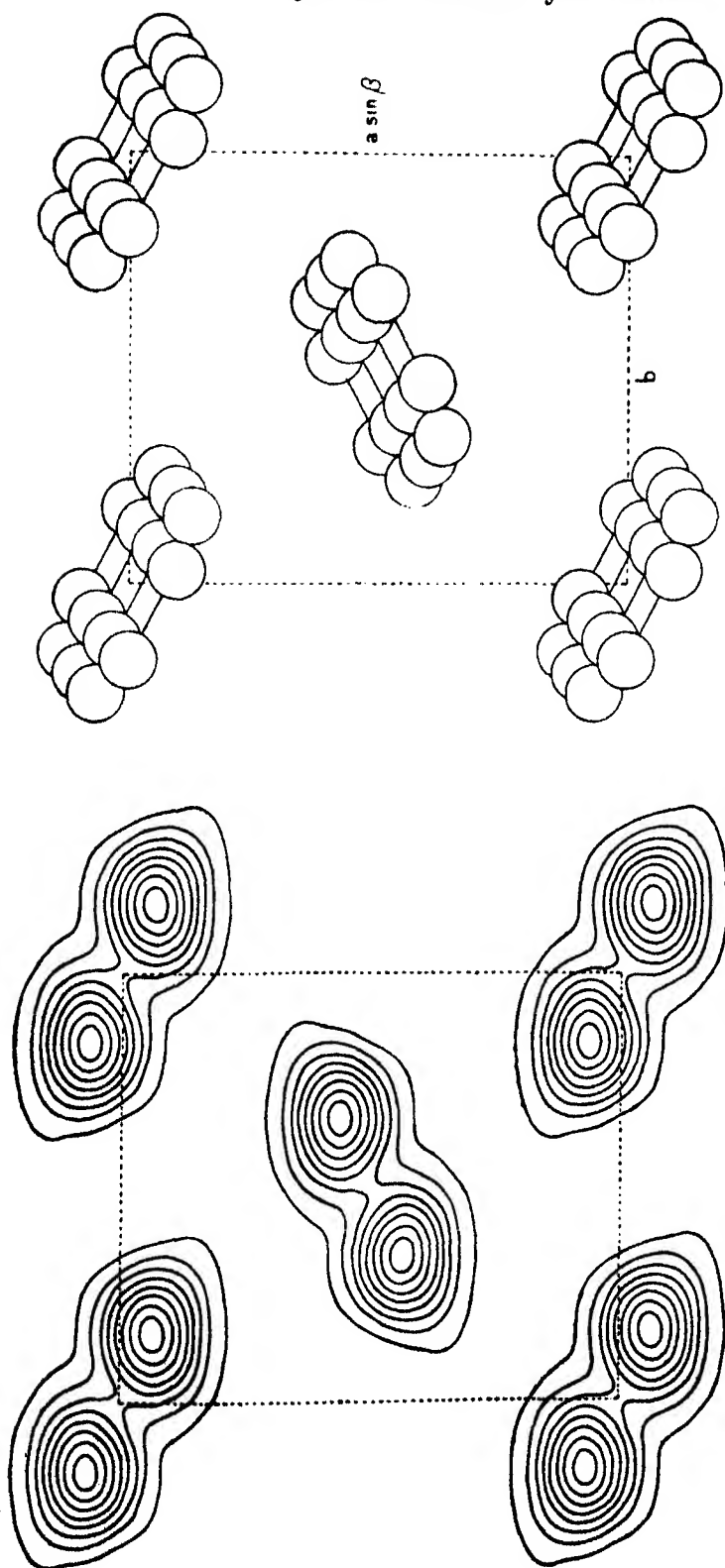


FIG. 4.—Projection along the  $c$  axis.

(b)

(a)

and this line is parallel to the line joining the peaks of the unresolved centres, AG', CE', etc. This regularity in the molecule is most striking, and is in harmony with our ideas of the chemical structure.

It will be noticed that in the projection along the *b* axis the outlying atoms, B, D and F, stand out clearly as isolated peaks, while in the *a* axis projection the inner atoms, A, C and E are quite clearly separated. Thus in one or other of the projections we get a clear picture of every atom in the molecule, with the exception of G, which is always somewhat obscured by its neighbours.

The molecule is inclined at varying angles to all the crystallographic axes; nevertheless, it is easy to apply a direct test of the form of the carbon rings. If these rings are regular plane hexagons, then the short cross lines AG', CE', EC' and GA' will be parallel to and one-half as long as the long cross lines BF', DD' and FB' in every projection. The test is rendered a little difficult because of the unresolved centres, but when the most reasonable positions are assigned to these centres it is found to hold to quite a high degree of accuracy.

It is now easy to obtain the actual orientation of the molecule in space. As the crystal is monoclinic it is convenient to use an axis, *c'*, perpendicular to the *a* and *b* axes. The apparent angle which the long axis of the molecule makes with this *c'* (vertical) direction in the projection along the *a* axis is 8.0°, and in the projection along the *b* axis, 30.1°. From these figures a simple calculation gives the actual angles,  $\chi$ ,  $\psi$  and  $\omega$  which the long axis of the molecule makes with the *a*, *b* and *c'* axes as

$$\begin{array}{ll} \chi = 119.7^\circ & \cos \chi = -0.495 \\ \psi = 96.9^\circ & \cos \psi = -0.121 \\ \omega = 30.7^\circ & \cos \omega = +0.860 \end{array}$$

(The angle with the *c* crystallographic axis is 8.5°.)

In the same way for the cross lines CE', DD', etc., the average apparent angle with the *c'* (vertical) direction measured on the *a* axis projection is 69.6° and on the *b* axis projection 46.9°. For the actual angles  $\chi'$ ,  $\psi'$  and  $\omega'$  with the *a*, *b* and *c'* axes these figures give

$$\begin{array}{ll} \chi' = 69.6^\circ & \cos \chi' = +0.349 \\ \psi' = 28.6^\circ & \cos \psi' = +0.878 \\ \omega' = 70.9^\circ & \cos \omega' = +0.327 \end{array}$$

The real angle between the long axis of the molecule and the cross lines DD', etc., is  $\arccos(\cos \chi \cos \chi' + \cos \psi \cos \psi' + \cos \omega \cos \omega')$  and with the above

figures this works out at  $89.9^\circ$ . This is a very satisfactory result, because it shows in a more precise way that the molecule is built from regular hexagon rings.

The radius of these hexagons, which is equal to the carbon to carbon distance, can readily be measured on the projections. In the projection along the *b* axis it is one-half of the distance between the outlying atoms BF', DD' and FB'. This is quite accurately constant, and is equal to 0.676 A. in this projection. Combined with the direction cosines given above, this gives a value of 1.41 A. for the real radius.

In the projection along the *a* axis the average distance between the inner atoms, CE', EC', etc., is 1.324 A., which combined with the direction cosines again gives a value of 1.41 A. for this interatomic distance.

The periodicity along the molecule, that is, the distance between the lines joining the centres AG', BF', CE', DD', etc., measured along the axis of the molecule, is quite reasonably constant. In the *a* projection it averages 1.07 A., and in the *b* projection 1.20 A. Combined with the direction cosines these figures give 1.23 and 1.21 A. for the real periodicities. The mean value, 1.22 A., is equal to  $(1.41 \times \sqrt{3}/2)$  A., the value required by a regular hexagon structure.

All the above information is, of course, contained in a statement of the co-ordinates of the atoms. But it has been given in the preceeding form because it is sometimes easier to measure the angle between certain lines in these diagrams than to locate the atomic centres accurately. The parameters as measured directly from the diagrams are now given in Table VIII. The figures in bold type refer to atoms which separate clearly as more or less circular masses in one or other of the diagrams. The remaining atoms are too near their neighbours and appear as unresolved ovals, but the probable

Table VIII.—Co-ordinates. Centre of Symmetry as Origin monoclinic axes.

Atom, cf. fig. 2.	<i>x</i> A.	$2\pi x/a$ .	<i>y</i> A.	$2\pi y/b$ .	From <i>a</i> projection <i>z</i> A.	From <i>b</i> projection <i>z</i> A.	$2\pi z/c$ (mean).
A.	0.81	33.8	0.19	11.4	4.17	4.10	133.0
B.	<b>1.06</b>	<b>44.6</b>	<b>0.94</b>	<b>56.5</b>	<b>3.14</b>	<b>3.11</b>	<b>100.5</b>
C.	0.54	22.6	0.49	29.5	1.57	1.55	50.3
D.	<b>0.81</b>	<b>34.1</b>	1.24	74.4	0.55	0.57	18.0
E.	0.28	11.9	0.78	46.8	-1.0	-0.98	-31.9
F.	0.56	23.5	1.53	91.4	-2.02	-1.98	-64.4
G.	0.02	0.6	1.06	63.6	-3.60	-3.54	-115.0

position of the centres can be estimated fairly well. It will be seen that only 14 of the 21 parameters can be directly measured from the diagrams. The  $z$  co-ordinates are estimated separately from the  $b$  and  $c$  axis projections, and the agreements obtained may be considered satisfactory, remembering that the two projections are based on different sets of experimental measurements.

#### *Intermolecular Distances.*

The distances between atoms on neighbouring molecules are in marked contrast to the distance of 1.41 Å. which has been found for the linked carbon atoms within the molecule. The molecule in the centre of the (001) face is derived from the corner molecule by a reflection in the (010) plane, or by a rotation about the  $b$  axis, and a shift of  $\frac{1}{2}a$ ,  $\frac{1}{2}b$ . Each molecule consists of two chains of seven carbon atoms, one chain being the inversion of the other. The co-ordinates of one such chain, forming an asymmetric unit, are given in Table VIII. The whole unit cell can be built up from these co-ordinates ( $x, y, z$ ) in the following way:—

$x$	,	$y$	,	$z$	....	(1) Standard unit	} Standard molecule.
$-x$	,	$-y$	,	$-z$	....	(2) Inversion of (1)	
$4.29 + x$	,	$3.01 - y$	,	$z$	....	(3) Reflection of (1)	} Reflected molecule.
$4.29 - x$	,	$3.01 + y$	,	$-z$	....	(4) Inversion of (3)	

It is then easy to calculate the distances between the centres of atoms in adjacent molecules. The distance between the standard and the reflected molecule varies from atom to atom owing to the inclination of the molecules, but the shortest distance found is about 3.77 Å. Between the molecules at the ends of the  $b$  axis, the closest distance of approach is 3.80 Å. Between those at the ends of the  $c$  axis the gap is somewhat greater, reaching a minimum of 4.06 Å. Owing to the molecules being inclined at about 30° to the vertical position, the distance between the ends of a standard molecule and a reflected molecule one translation along the  $c$  axis is less, reaching a minimum of about 3.67 Å. This is the closest distance of approach which has been found between the centres of atoms in adjacent molecules.

#### *Comparison with Other Structures.*

It is interesting to compare these distances with those determined in other structures involving the carbon atom. The carbon to carbon distance within the molecule of 1.41 Å. compares with a corresponding distance of 1.42 Å.

in graphite\* and hexamethylbenzene.† In the graphite structure there are two atoms on a vertical axis 3.41 Å. apart (the distance between the layers) and six symmetrically distributed about it at 3.70 Å. The (001) spacing in hexamethylbenzene is 3.70 Å. For the long chain hydrocarbon  $C_{29}H_{60}$  Müller‡ found the distance of nearest approach between two centres on two neighbouring molecules placed end to end to be approximately 4.0 Å., and for the same hydrocarbon the distance of nearest approach between two centres on two adjacent molecules placed sideways to lie between 3.6 and 3.9 Å.

#### *The Electron Distribution.*

The Fourier projections which have been made reveal some particularly interesting features, which are most noticeable in the projection along the *b* axis, fig. 2. On the central carbon atoms, D and D', which are the "meso-" positions in anthracene, the electron density reaches a height of 560 in the value of *S*. These atoms are very circular and rise to moderately sharp peaks. The atoms in the "benz-" positions, however, are somewhat flatter and more spread out, the electron density rising to a value of 500 on F, and only about 460 on B. The height of the peak is thus seen to fall away as we move farther out from the centre of the molecule. The same effect is noticeable for the unresolved centres, CE' being 700 and AG' only a little over 600 units at the maximum. Further, the form of the first contour line shows quite pronounced bulges around the atoms in the end benzene rings, which are absent from the atoms of the central ring.

Considerable caution, however, is necessary in accepting finer detail of this kind in the structure. The Fourier series is necessarily incomplete, the measurements being limited by the wave-length and the experimental conditions. This limitation is very liable to introduce false detail to the picture, similar to diffraction effects in the case of an optical instrument.§ In the present analysis the concluding coefficients are generally fairly small, but it is quite possible that if still more terms could be added they would have the effect of smoothing out some of the detail.

At the same time, the fall in the peak values of the electron density as we pass out from the centre of the molecule, combined as it is with a slight broadening of the structure, are rather pronounced experimental facts which it seems

\* Bernal, *loc. cit.*

† Lonsdale, *loc. cit.*

‡ Müller, 'Proc. Roy. Soc.,' A, vol. 120, p. 437 (1928).

§ Cf. Bragg and West, *loc. cit.*



somewhat difficult to explain in this way. Are they perhaps connected with the well-known chemical difference between the "meso-" and the "benz-" positions in anthracene? In most anthracene reactions the meso-positions are first attacked, and substituents only enter the end benzene rings at a later stage. It would seem that these chemical facts must ultimately be explained by some difference in the electron configuration.

Again, the effect might be explained by thermal agitation if we imagine the molecule oscillating slightly about its centre. The more outlying atoms would then have the largest amplitudes, with the consequent effects of broadening the picture and lowering the peak values of the electron density. In opposition to this view it may be considered that oscillations about any axis with such a high moment of inertia are improbable. It must be remembered, however, that the crystal molecule is far from being a free body in space. It is surrounded by other molecules, and in fact it appears to be somewhat more closely bound to its neighbours on either side than to those at either end of the *c* axis. Between the ends of the molecules, in the (001) plane, the electron density falls to very low values. It is only in this region that occasional small patches of negative density occur. The (001) plane, moreover, is the cleavage plane, and by far the most important natural face on the crystal. Hence the bonds between the ends of the molecules must be very weak. Between the sides of the molecules, on the other hand, the (100) and the (010) planes never appear as faces on the crystal. The (110) face is developed, but never to anything like the extent of the (001) face. It may be possible, then, that the relatively looser binding between the ends of the molecules will permit an oscillation about their centres capable of explaining the observed facts. The point could perhaps be decided by an investigation of the structure at different temperatures, especially near the melting point.

The form of the scattering centres given by the Fourier analysis is conveniently studied by making a relief model of the projections. When this is done for the projection along the *b* axis, the difference between the meso- and the benz-carbon atoms is very noticeable. On calculating the electron distribution in the carbon atom from the measured reflections of graphite, it is found that the graphite carbon atom is similar to the atoms in the end rings of the anthracene structure, but that in the anthracene middle rings the atoms are more sharply defined.

It is difficult to make an accurate electron count because even the centres which stand out most clearly actually overlap to a considerable extent in all

the projections. An estimate has been made, however, of the electron distribution along the molecule in the following way. The atoms appearing in the projection along the *b* axis, fig 2, were divided into groups of two by drawing parallel lines between the pairs AG', BF', CE', DD', etc., at a constant distance apart, equal to the mean distance between these groups. The procedure will be clear from fig. 5. The number of electrons in each section was then obtained by adding the appropriate figures in Table VI. These figures in Table VI can be taken as giving the mean value of  $S \times 10^{-1}$  in small cells each 1/1800th of the area of the unit cell. The actual number of electrons in a given area is thus obtained by adding up these figures and dividing by 180. Fig. 5 gives the result of this electron count. The figures in brackets are the number of electrons which we should expect to be associated with the centres from the chemical structural formula.

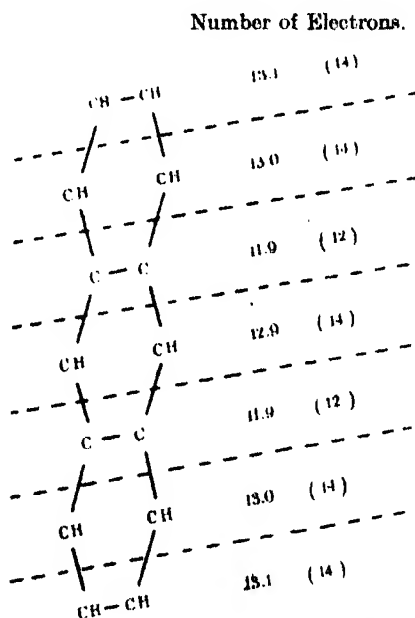


FIG. 5.—Electron count in anthracene.

It is interesting to observe that the tertiary carbon atoms give the lowest count of 11.9; at the same time it can hardly be said that the effect of the hydrogen atoms is fully evident. The bulges seen on the first contour line at the ends of the molecule are not included in the estimation. They account for a residue of about 2 electrons.

In conclusion, I wish to thank my wife for the help received in dealing with the large amount of numerical work involved in this analysis.

An investigation of this kind, which represents the X-ray method at its full power, is only possible after much gradual development of methods on the part of many people, and I am particularly indebted to Sir William Bragg, F.R.S., not only for his continual interest in the work, but for placing at my disposal many of his earlier, and often unpublished, results.

To the managers of the Royal Institution I am grateful for the facilities provided at the Davy Faraday Laboratory.

#### *Summary.*

The anthracene structure, which was already partly known, has been investigated in detail. The intensity measurements have been made as accurate and as complete as possible, and a double Fourier analysis carried out for the zones about the three crystallographic axes. From the results of this analysis the details of the structure are deduced. The carbon atoms are found to lie quite accurately at the corners of three regular plane hexagons, the distance from centre to centre being 1.41 Å. This molecule is, however, inclined at varying angles to all the crystallographic axes. These angles have been determined, and the structure is completely defined by a statement of the direction cosines of the long and the cross axes of the molecule which are given on p. 92. The 21 parameters of the structure have been determined from the analysis and are given on p. 93. All the carbon atoms in the molecule except one are resolved as circular masses in one or other of the projections.

The closest distance of approach between atoms in adjacent molecules is about 3.67 Å., in marked contrast to the distance of 1.41 Å. between the atoms within the molecule.

The peak values of the electron density are highest for the carbon atoms in the meso-positions, and fall off a little in the end benzene rings. This effect is accompanied by a slight broadening of the structure, and may be connected with the chemical difference between the meso- and benz-positions, or with thermal agitation. The electron count is in good agreement with the chemical structure, showing a minimum value at the tertiary carbon centres.

---

*The Photosynthesis of Hydrogen Chloride. I.—A New Experimental Method; The Inhibiting Effect of Hydrogen Chloride.*

By MOWBRAY RITCHIE\* and RONALD G. W. NORRISH, Department of Chemistry, University of Cambridge.

(Communicated by T. M. Lowry, F.R.S.—Received October 20, 1932.)

In spite of the many valuable investigations which have been carried out in recent years on the photochemical reaction between hydrogen and chlorine, no general agreement can be said to exist regarding the complete mechanism of the process. Examination of the various semi-empirical formulæ, which have been proposed to represent the rate of reaction, shows that the relative importance of all the experimental factors cannot have been fully realized; and while the divergence in the results of different workers has frequently been ascribed to the effects of small amounts of oxygen or other impurities in the gases used, or to various chain-breaking processes associated with the surfaces of the reaction vessels, yet a complete scheme has by no means been evolved to co-ordinate the results of all the experimental investigations. There are indeed major discrepancies in the published data of different workers which must be satisfactorily cleared up before such an attempt is made. For example, there is the question as to what extent the rate of the formation depends on the amount of light absorbed. Thus the reaction rate in oxygen-free systems has been given by Kornfeld and Müller† as directly proportional to the light intensity over a sixty-fold variation, a conclusion supported also by Marshall‡ for gas mixtures of low total pressures (less than 10 mm. Hg) and by Bodenstein and Unger§ for higher pressures; on the other hand, the results of Chapman and Gibbs|| indicate that the reaction rate is proportional to a power of the absorbed light which is definitely less than unity, the conclusion being that the limiting value of 0.5 would be reached in gas mixtures entirely free from oxygen. The role of hydrogen has also been the subject of considerable discussion. The data of Chapman and Underhill¶ indicate

\* Senior Student, 1851 Exhibition.

† 'Z. phys. Chem.,' vol. 117, p. 242 (1925).

‡ 'J. Phys. Chem.,' vol. 29, p. 1453 (1925).

§ 'Z. phys. Chem.,' B, vol. 11, p. 253 (1931).

|| 'Nature,' vol. 127, p. 854 (1931).

¶ 'J. Chem. Soc.,' vol. 103, p. 496 (1913).

a slight but distinct inhibiting effect at high hydrogen concentrations when a small but definite amount of oxygen was also present. Such an inhibiting effect was confirmed by M. C. C. Chapman,\* but is in disagreement with the findings of Bodenstein and Dux,† the discrepancy being ascribed by Thon‡ to the unsuspected presence of oxygen in the hydrogen used.

A similar state of uncertainty exists about the reaction kinetics in mixtures containing larger percentages of oxygen, various formulæ having been proposed from time to time by different workers. In addition no scheme of reaction which does not admit of the calculation of the absolute quantum efficiencies under all conditions can be said to be complete. The difficulties attendant on previous methods of investigation have, however, prevented any fruitful attempt being made in this direction.

The experimental method of attack on the problem is limited by the fact that no permanent pressure change accompanies the reaction between hydrogen and chlorine in a reaction vessel of constant volume, and while a small decrease in pressure is to be observed in those mixtures which contain oxygen, owing to the formation of water, yet the change is so small that for all practical purposes the concentration of oxygen can be regarded as constant. Chapman and his associates have largely made use of the water-actinometer, a method of investigation first employed by Bunsen and Roscoe, in which the addition of a sufficient quantity of liquid water to the reaction system removes the hydrogen chloride as it is formed, the consequent diminution in volume serving as a means of recording the rate of reaction. The method is of advantage only when the effect of hydrogen chloride itself on the rate of reaction can be neglected, and suffers from the disadvantages consequent on the addition of water to the reacting system; for example, the greater possibility of introduction of inhibiting impurities, the possible action of illuminated chlorine on water-vapour itself, and the practical complications involved by the saturation of the water by the chlorine. On the other hand, the method of experiment developed by Bodenstein and Dux (*loc. cit.*), which necessitates the freezing out of chlorine and hydrogen chloride, is open to the objection that at high pressures complete freezing out is not attained with certainty in the presence of an inert gas, while the original concentrations of the reactants may not be effectively regained before the experiment is resumed, owing to difficulties of mixing and slowness of diffusion.

\* 'J. Chem. Soc.,' vol. 123, p. 3002 (1923).

† 'Z. phys. Chem.,' vol. 85, p. 297 (1913).

‡ 'Fortschr. Chem. Phys.,' vol. 18, p. 11 (1926).

It is obvious that agreement cannot be expected between the results obtained by the two methods, if the hydrogen chloride produced has any effect on the rate of reaction; and though Bodenstein and Dux (*loc. cit.*) state that the rate of reaction is independent of the hydrogen chloride concentration, yet the results of our own experiments show definitely that their conclusion cannot be supported, and that hydrogen chloride does markedly retard the rate of reaction. Such an effect was first recognized from observations on the Draper effect\* following on sudden illumination of the reaction mixture, the Draper effect having been previously recognized as being intimately connected with the reaction velocity.†

In the light of this knowledge, the whole question of the rate of photochemical reaction between hydrogen and chlorine, both in "oxygen-free" and oxygen-containing mixtures, has been systematically re-examined by a method free from the objections previously noted, and which indeed involved no addition to, nor disturbance of, the reaction system. It consisted in determining the extent of reaction at any one time from the relative amount of light of a given wave-length which was transmitted by the residual chlorine. The wave-length suitable depended on the corresponding absorption coefficient, considered in conjunction with the range of chlorine pressure it was desired to investigate in any particular reaction vessel. The graphic relationship between chlorine pressure and  $\log_{10} I_0/I$ , where  $I_0$  represents transmitted light when the chlorine pressure is zero and  $I$  that transmitted by chlorine at any other pressure, is represented by a straight line passing through the origin. This graph was accordingly constructed from measurements with known chlorine pressures, and subsequently employed to determine the pressure of chlorine at any time during the course of the photochemical reaction. In the experiments here to be described, the wave-length chosen for this purpose was  $365 \mu\mu$ . With the thermopile-galvanometer system employed, concentrations of chlorine in the range of 0 to 100 mm. (for a given reaction vessel) were determined with an error of experiment normally not greater than 0.5 mm.

The experimental procedure falls into two divisions. When the reaction itself was carried out by light of wave-length  $365 \mu\mu$ , for a suitably slow reaction the chlorine concentration was continuously determined throughout the period of illumination, and the rate of reaction then calculated from the slope of the

\* Ritchie and Norrish, 'Nature,' vol. 129, p. 243 (1932).

† Cf. Bevan, 'Phil. Trans.,' A, vol. 202, p. 71 (1903); Ichikawa, 'Z. phys. Chem.,' B, vol. 10, p. 299 (1931).

resultant curve showing the relationship between pressure of chlorine and time of illumination. This method of procedure will be subsequently referred to as the "graphical method." On the other hand, when the reaction velocity was too high, or the intensity used was too low to permit of accurate measurement in this way, or when the reaction itself was carried out with light of wavelength other than  $365\text{ }\mu\mu$ , the concentration of chlorine after a given exposure was determined by  $365\text{ }\mu\mu$  light as before, an excess of oxygen being added to render the mixture insensitive. Calculation was then performed on the assumption that the changes in concentration of the reactants and in the intensity of absorbed light were linear over the range. This procedure will be subsequently referred to as the "method of averaging." Where the total change was not large, the error so introduced was negligible; comparative tests on similar reaction mixtures showed that for the range of pressures of chlorine involved in the experiments, practically identical results were afforded by the two methods.

The general results obtained in these ways, when the inhibitory effect of the hydrogen chloride is taken into account, are completely self-consistent for all gas mixtures with and without oxygen, and it is possible to obtain expressions which accurately reproduce the variation in quantum yield between limits as extreme as  $10^5$  and 10, obtainable experimentally by suitable variations of the reactants. In the present paper, the new technique and preliminary results are described; in the succeeding parts, accounts will be given of various aspects of the reaction.

## EXPERIMENTAL.

### *Apparatus.*

The apparatus is shown diagrammatically in fig. 1, and was similar to that used by Griffiths and Norrish.\* The quartz reaction vessel V, cylindrical in shape, with plane-end faces, was of  $25.4$  c.c. volume, the internal surface being approximately  $43$  sq. cm. Connection was made to the main apparatus by the ground joint J. The light beam from the quartz mercury vapour lamp, run at 150 volts and 4.0 amps. from a constant 220-volt battery system, was rendered parallel by a system of lenses and circular stops, and passed first through a  $2.5$  cm. layer of aqueous 6 per cent. copper sulphate solution F, and then through the appropriate wave-length filters before entering the

\* 'Proc. Roy. Soc.,' A, vol. 130, p. 591 (1931).

reaction vessel. The diameter of the beam was such that more than three-quarters of the total volume of the reaction vessel was illuminated. A quartz lens focussed accurately the emerging beam on the circular area comprising the elements of the Moll thermopile H, the system having been calibrated by means of a standard N.P.L. lamp. This focussing, as well as the general position of the light beam, was examined before and after every experiment. The thermopile itself was enclosed in a wooden box to screen it from external radiation. The Bourdon gauge, connected by capillary tubing to the reaction vessel, was normally used as a null instrument only, to introduce and measure the pressure of the reactant gases, though it was calibrated and used as a direct

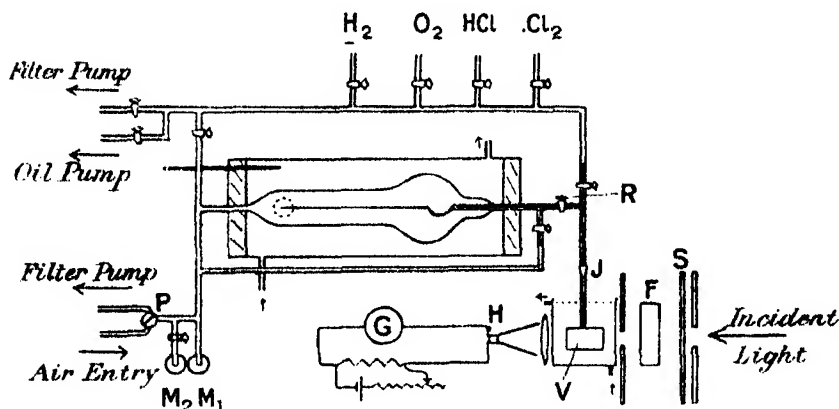


FIG. 1.

reading instrument when small amounts of oxygen ( $< 3$  mm.) were involved. The pressure of air in the outer jacket of the gauge was controlled by the two-way tap P, communicating with the filter pump or with the atmosphere (through guard-tubes of calcium chloride and phosphorus pentoxide), so that, except for very low pressures, the pressure inside the reaction vessel was obtained by means of the mercury manometer  $M_1$ , read in conjunction with the standard manometer  $M_2$ . The tap R, between gauge and vessel, was closed before the beginning of actual illumination in an experiment, the effective volume of the system being then that of the reaction vessel alone. The reaction vessel and gauge were shielded where necessary from external light. The system was evacuated through liquid air traps (not shown in the diagram) by means of a "Hyvac" oil pump.

The temperature of gauge and vessel was regulated to  $25 \pm 0.02^\circ \text{C}$ . by pumping water from an electrically controlled thermostat to a cistern with a



constant level device; from this the water flowed back to the thermostat in two streams, one through the outer jacket of the gauge, and the other through the tank which served as a bath for the reaction vessel.

The tap grease used throughout was Shell Apiezon Grease L, which is composed entirely of hydrocarbons of high boiling point. Very slight absorption of chlorine and hydrogen chloride took place normally when the pressure of either gas was high, and the grease stiffened after some time, but no abnormalities in reaction velocity could ever be ascribed to its use. No induction periods were ever observed, with the exception of the first one or two experiments after freshly cleaning the reaction vessel.

*Colour Filters.*—Monochromatic light was obtained by the following combinations of filters:—

- (1) 436  $\mu$ : a 3 cm. layer of 1 per cent. cuprammonium sulphate, combined with 0.5 cm. layer of 4 per cent. aqueous quinine hydrochloride solution and a 3 cm. layer of 6 per cent. aqueous copper sulphate solution.
- (2) 406  $\mu$ : a 3 cm. layer of 0.02 N iodine in carbon tetrachloride solution, combined with 0.5 cm. layer of 0.1 per cent. aqueous quinine hydrochloride solution and a 3 cm. layer of 6 per cent. aqueous copper sulphate solution.
- (3) 365  $\mu$ : Wratten filter No. 18a, in addition to a 3 cm. layer of 6 per cent. aqueous copper sulphate solution.

#### *Preparation of Reactants.*

*Chlorine* was generally prepared from pure hydrochloric acid, by the action on potassium permanganate, or occasionally obtained from a commercial cylinder of liquid chlorine. In either case, the gas was purified by washing with aqueous permanganate solution and then with water (in darkened vessels), passed slowly over phosphorus pentoxide, and collected by means of liquid air. This "crude" chlorine was then subjected to repeated fractional distillation following a long "boiling-off" under filter-pump suction. The number of distillations given was four or five, initial and final fractions being rejected. In each distillation, the receiving bulb was cooled in liquid air, and the distilling bulb surrounded by an empty vacuum vessel or by one containing solid carbon dioxide and ether mixture. When not in use, the final product was kept in the solid state by means of liquid air.

No difference could be recognized in the experimental results for the various samples of chlorine obtained and purified as above.

*Hydrogen* was prepared by electrolysis of potassium hydroxide solution containing a little baryta, it was passed over finely divided active copper heated electrically to 300° C. and then collected temporarily over air-free water. Immediately after preparation, it was passed very slowly over heated copper again, then over phosphorus pentoxide, and finally collected in glass bulbs of 2 to 3 litres' volume) attached to the main apparatus.

*Oxygen* was obtained by the catalytic action of manganese dioxide on hydrogen peroxide in presence of dilute sulphuric acid and passed through gas wash-bottles containing copper sulphate solution and over phosphorus pentoxide before being liquefied by means of liquid nitrogen. Two distillations were performed with rejection of initial and final fractions, and the product stored in glass reservoirs as before, the pressure being indicated by a mercury manometer. Further samples were later prepared by similar fractionation of oxygen obtained originally by electrolysis as well as from a commercial cylinder.

*Hydrogen chloride* was obtained by adding pure concentrated hydrochloric acid to concentrated sulphuric acid. After drying purification was carried out as before by fractional distillation, four or five distillations being carried through. A mercury manometer indicated the pressure in the glass reservoirs.

#### *Experimental Procedure.*

The apparatus was first completely evacuated by the Hyvac oil-pump for some considerable time, during which the focussing and general position of the light beam were verified. The intensity  $I_0$  was then measured (for  $\lambda = 365 \mu$ ) by alternately raising and lowering the shutter S, repeated observations being made. "Washing out" of connecting tubes and reaction vessel with pure chlorine followed. After complete re-evacuation (by oil pump and liquid air trap), chlorine was introduced to the required pressure, followed by oxygen and hydrogen chloride if desired, and the transmitted light again measured and compared with that given by calculation from the calibrating graph of  $\log I_0/I$  against chlorine pressure for the particular pressure involved. The system was further illuminated for several minutes before the introduction of hydrogen in order to destroy any inhibiting impurities introduced with the gases, although this precaution appeared unnecessary, since no difference in rate of reaction was observed when such pre-illumination was omitted. Hydrogen was then introduced to the required pressure, the tap R connecting the gauge and the reaction vessel being finally closed before the actual illumination was begun.

*Graphical Method.*

If the wave-length of the light used for the experiment was  $365\ \mu\mu$  and the reaction a suitably slow one, readings of the transmitted light were taken every 2 or 3 minutes by lowering and raising the shutter S, the time of non-illumination being noted. This period of non-illumination represents the time taken for the galvanometer light spot to come to rest, and was usually about 30 seconds. This general procedure of interrupted illumination seemed free from all objection, since an exposure of a given initial mixture for a given length of time under conditions of constant incident-intensity resulted in the same final concentration of chlorine being obtained whether the period of illumination was interrupted or not. When the "run" had proceeded for a suitable length of time, the vessel was evacuated and the intensity value  $I_0$  again measured. Fig. 2 shows the results obtained in a typical experiment. Curve I represents

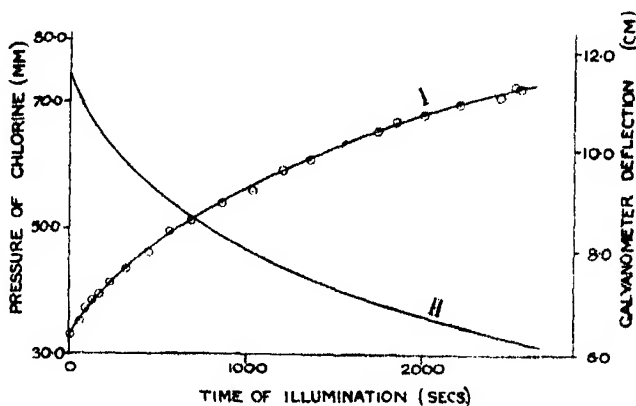


FIG. 2.

galvanometer deflection plotted against total time of illumination, and curve II concentration of chlorine plotted against time; the concentration of chlorine being calculated from various points on curve I by means of the calibration graph of pressure of chlorine against  $\log I_0/I$ . The tangent at any point in curve II gives the rate of decrease of concentration of chlorine (equal to one-half the rate of hydrogen chloride formation), the corresponding value for the amount of light then absorbed by the chlorine being easily calculated from the corresponding point on curve I.

*Method of Averaging.*

If, on the other hand, the reaction was carried out with a wave-length other than  $365\ \mu\mu$ , or the conditions with light of  $\lambda = 365\ \mu\mu$  were such as to render

observations taken in the above way inaccurate (*e.g.*, by reason of the speed of the reaction), illumination was continued without interruption for a suitable noted length of time. At the end of this period, the mixture was rendered insensitive by the addition of excess oxygen, the 365  $\mu\mu$  filter was replaced if necessary, and repeated observations of the transmitted light recorded. Re-evacuation of the system, followed by the redetermination of  $I_0$ , both for  $\lambda = 365 \mu\mu$  and for the wave-length used in the illumination, completed the experiment. In this way the initial and final concentrations of chlorine were determined for an illumination period of known duration under constant conditions of incident light-intensity. As indicated earlier, little error is introduced in the calculation of the rate and quantum efficiency of hydrogen chloride formation if the total change in concentration is not large.

#### *Calculation of Quantum Efficiency.*

Both the methods above described (the graphical method and the method of averaging) give values of the rate of formation of hydrogen chloride for known concentrations of reactants and under known conditions of incident intensity. The value of the amount of absorbed light under these conditions must be known before the corresponding quantum efficiency can be calculated.

The galvanometer deflection gives at once, from previous calibration, the number of light quanta falling per second on the elements of the thermopile. Owing to the character of the optical system by which the light was transmitted after leaving the reaction vessel, the number of quanta absorbed by the chlorine cannot be taken simply as the difference of the galvanometer readings when the reaction vessel is empty and when it contains chlorine at the required pressure. The necessary correction comes into two sections :—

(1) The light leaving the reaction mixture passed in turn through the fused quartz of the reaction vessel, the thermostating water, the quartz window of the thermostat and a layer of air before being focussed by the quartz lens on the circle of the thermopile elements. The transmission losses of this optical system were determined directly for the wave-lengths considered, and found to agree well with the values calculated in the ordinary way on the assumption of no absorption by the materials of the system. The light which is reflected back by the various surfaces of the optical system between the reaction vessel and the thermopile was partly reabsorbed, and must be allowed for. This correction is dependent on the ratio  $I/I_0$  and vanishes when the absorption of light by the chlorine is complete. The factors for transmission

and back reflection were combined and calculated\* by the expression

$$C = \frac{1}{abcdef} \left[ 1 + \frac{1}{I_0} \{ (1-a) + a^2 b^2 c^2 (1-d) + \frac{2}{3} a^2 b^2 c^2 d^2 (1-e) + a^2 b^2 c^2 d^2 e^2 (1-f) \} \right],$$

where *abc*, etc., represent the transmission coefficients for the various surfaces depicted in fig. 3. These were each calculated in the usual way as equal to

$$\left\{ 1 - \left( \frac{n_1 - n_2}{n_1 + n_2} \right)^2 \right\},$$

$n_1$  and  $n_2$  being the refractive indices for the particular wave-length in question of the materials on each side of the surface. The surfaces *a*, *d*, *e* and *f* only were regarded as contributing to the back reflection; the factor 2/3 was due to the convexity of the quartz lens and was only roughly estimated.

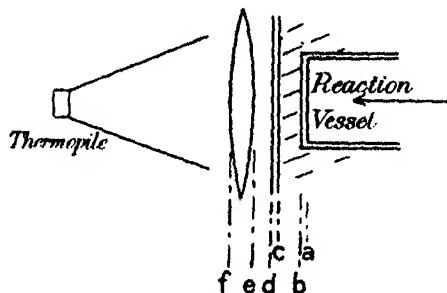


FIG. 3.

(2) Correction was also necessary (Griffiths and Norrish, *loc. cit.*) for the imperfect reflection of light by the metallic surface of the thermopile funnel in which a small amount of stray light unavoidably fell. This factor was never greater than 1.10 and remained very constant for any given "set up" and was frequently redetermined.

When an experiment was carried out by the graphical method for  $\lambda = 365 \mu\mu$  the absolute amount of absorbed light was given by

$$I_{\text{abs.}} = (I_0 - I) C,$$

where *C* is the combined correction factor and  $I_{\text{abs.}}$  is in galvanometer scale-division units. Where the method of averaging was employed, the average value of  $(I_0 - I)$  was calculated from calibration graphs of  $\log I_0/I$  against pressure of chlorine, for the particular wave-length in question.

\* Cf. Allmand and Spinks, 'J. Chem. Soc.,' p. 1658 (1931).

A deflection of 1 cm. of the light spot of the thermopile-galvanometer system was equivalent to a light intensity of 170 ergs. per second falling on the area of the elements of the thermopile.

The quantum efficiency of hydrogen chloride formation was then found by means of the formula

$$\gamma_{\text{HCl}} = \frac{0.377 \times 10^6}{\lambda I_{\text{abs.}}} \cdot V \cdot \frac{[\text{HCl}]}{t},$$

where

$V$  = volume of reaction vessel in cubic centimetres ;

$\frac{[\text{HCl}]}{t}$  = rate of formation of hydrogen chloride in millimetres Hg per second of illumination ;

$\lambda$  = wave-length of light employed in  $\mu\mu$  ; and

$I_{\text{abs.}}$  = total light absorbed in galvanometer scale divisions (centimetres), corrected as described.

It is obvious that in the above ways a systematic study can be made of the variation in quantum efficiency with change of concentration of any one constituent of the reaction mixture. In addition, for experiments of the type illustrated in fig. 2, the concentrations of all reactants and the amount of light absorbed vary to an extent sufficient to test thoroughly any empirical formula thus determined.

*Experimental Results—Variation of Quantum Efficiency with Pressure of Hydrogen Chloride.*

As an example of the working of the above methods of experimentation there are presented below the results which first established the inhibiting action of hydrogen chloride. In fig. 4, values of the quantum efficiency ( $\gamma_{\text{HCl}}$ )

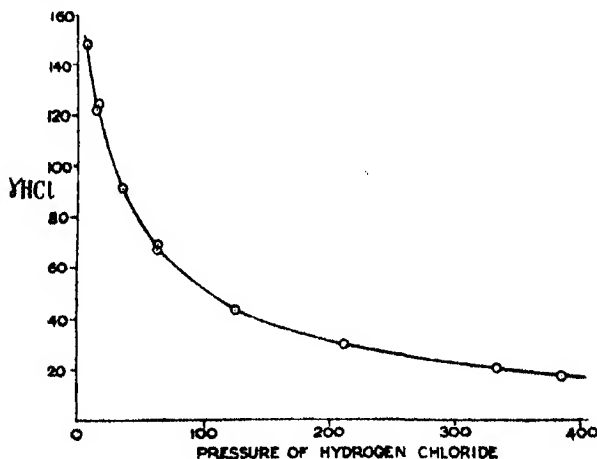


FIG. 4.

are plotted against pressure of hydrogen chloride where the pressure of oxygen was 50.0 mm. and those of chlorine and hydrogen were each equal to 43.0 mm. The wave-length of light employed was 365  $\mu$ . Where the concentration of hydrogen chloride is given as 16.0 mm., the initial mixture contained 51 mm. of chlorine, 51 mm. of hydrogen, but no hydrogen chloride, and the reaction was allowed to continue until the concentration of hydrogen chloride reached roughly 30 mm., the quantum efficiency being measured in the "graphical manner" at  $[\text{HCl}] = 16.0$  mm. In the same way, when  $[\text{HCl}]$  is given as equal to, say, 66 mm., 50 mm. HCl were originally present in the reaction mixture, illumination being then begun and the quantum efficiency measured at the total concentration of  $[\text{HCl}] = 66$  mm., i.e., when 16 mm. HCl had been produced by the illumination.

The hydrogen chloride used in the above experiments was prepared externally by the methods already described. It was therefore of the greatest importance to ascertain whether the same retarding effect was to be recognized with hydrogen chloride forming *in situ* as the result of illumination. Table I gives the quantum efficiencies recorded when the initial mixture contained 50.2 mm. oxygen, 74.7 mm.  $\text{Cl}_2$  and 74.6 mm.  $\text{H}_2$ , the course of the reaction being followed throughout by the graphical method as before. The values of  $I$ , the transmitted light, recorded in the second column of Table I, were obtained from the smoothed experimental curve of  $t$  against  $I$  (cf. fig. 2); the corresponding chlorine concentration was then calculated from the relationship  $\log I_0/I = p \cdot 0.00600$ , when  $p$  is the pressure of chlorine in millimetres, this expression having been experimentally determined for the reaction vessel in question. The fifth column of Table I gives the slope of the curve, where

Table I.

$$I_0 = 16.9 \text{ cm.}$$

$t$ sec.	$I$ cm.	$[\text{Cl}_2]$ mm.	$I_0 - I$ cm.	HCl mm./100 sec.	Quantum. efficiency $\gamma$
200	7.15	64.2	9.75	7.37	138
400	7.81	58.1	9.1	5.35	108
600	8.31	53.5	8.6	4.10	87.5
1000	9.13	46.7	7.8	2.92	69
1200	9.47	44.0	7.4	2.57	63.5
1400	9.81	41.6	7.1	2.37	61
1800	10.45	37.4	6.5	1.75	49.5
2000	10.6	35.8	6.3	1.60	46.5
2200	10.8	34.2	6.1	1.45	43.5

$[\text{Cl}_2]$  is plotted against time of illumination, and is expressed as millimetres of HCl produced per 100 seconds illumination. The quantum efficiency of HCl formation then follows from the expression

$$\gamma = \frac{0.377 \times 10^6 \times V}{\lambda C (I_0 - I)} \cdot \frac{[\text{HCl}]}{t},$$

where  $V = 25.4$ ,  $\lambda = 365$ , and  $C = 1.43$ .

These results can be tabulated to show the dependence of the quantum efficiency on the concentrations of the various reactants throughout the reaction as shown in Table II.

Table II.

$[\text{O}_2] = 50.2$  mm.

Initial  $[\text{Cl}_2] = 74.7$  mm.

„  $[\text{H}_2] = 74.6$  mm.

$[\text{Cl}_2]$	64.2	58.1	53.5	46.7	44.0	41.6	37.4	35.8	34.2
$[\text{H}_2]$	64.1	58.0	53.4	46.6	43.9	41.5	37.3	35.7	34.1
$[\text{HCl}]$	21.0	33.2	42.4	56.0	61.4	66.2	74.6	77.8	81.0
$\gamma$	138	108	87.5	69	63.5	61	49.5	46.5	43.5

From Table II, the quantum efficiency for  $\text{Cl}_2 = 43.0$  mm.  $\text{H}_2 = 43.0$  mm. and  $\text{HCl} = 63$  mm. is approximately 63 mols. per quantum; from fig. 4, the value for the same condition is 67.5. There is thus no doubt that the inhibiting action of hydrogen chloride, as exemplified by fig. 4, is one which is not owing to any unknown inhibitors introduced with the hydrogen chloride, but is a process which must be included in any scheme of reaction mechanism. The discussion of the bearing of these facts on the whole problem of the hydrogen-chlorine reaction is reserved for later papers in this series, in which the whole question of the kinetics of the reaction will be reinvestigated by the new technique.

The authors are indebted to the Government Grant Committee of the Royal Society for a research grant which has been applied in part to the prosecution of this work, and to the Commissioners of the Exhibition of 1851 for a senior award to one of them (M. R.)

#### Summary.

A description is given of a method of measurement of rates of reaction and quantum efficiencies of hydrogen chloride formation which depends



on measurement of light absorption by the chlorine of the reaction mixtures. The method has proved itself reliable and capable of yielding consistent results. In particular, results are given establishing a marked inhibiting effect of hydrogen chloride in hydrogen-chlorine mixtures containing oxygen.

---

*The Photosynthesis of Hydrogen Chloride. II.—“Oxygen Free” Mixtures.*

By MOWBRAY RITCHIE\* and RONALD G. W. NORRISH, Department of Chemistry, University of Cambridge.

(Communicated by T. M. Lowry, F.R.S.—Received October 20, 1932.)

The complete study of the photochemical hydrogen-chlorine reaction falls into four sections consequent upon the fact that the presence of oxygen in large or small quantity very materially alters the kinetics of the process. These may be classified as follows :—

- (1) The kinetics of pure hydrogen-chlorine mixtures.
- (2) The kinetics of oxygen-rich mixtures.
- (3) The transition region between (1) and (2).
- (4) The photosensitized formation of water associated with (2) and (3).

A mechanism proposed for any one of the above processes must be consistent with the other three, and a full and comparative study of all four should lead to a self-consistent mechanism by which all the above aspects of the problem can be unified in one explanation.

In the present paper we have applied the new method of experimentation described in Part I (p. 99) to the first of the above aspects—the reaction in the absence of oxygen. It is here that the reliable data are most scarce, undoubtedly owing chiefly to the difficulty of obtaining mixtures free from oxygen, but also partly to the intriguing interest of the other aspects of the problem. Bodenstein and Ungert† state that the reaction is uninhibited by either hydrogen or chlorine, and that its rate is proportional to the first power of the intensity of the absorbed light, and to the pressure of hydrogen, while it is independent

\* Senior Student, 1851 Exhibition.

† ‘Z. phys. Chem.,’ B, vol. 11, p. 253 (1930).

of the pressure of chlorine. Chapman and Gibbs, on the other hand,\* report that the rate of reaction is proportional to the square root of the intensity of absorbed light, though they give no further details of the kinetics of the reaction.

We have here a discrepancy of the gravest importance to the understanding of the mechanism of reaction. To account for their result Bodenstein and Unger were led to postulate the existence of a product derived from the silica of the reaction vessel under the influence of the illuminated chlorine which terminated the reaction chains, and was thus responsible for the dependence of the rate on the first power of the light intensity; Chapman and Gibbs, on the other hand, claimed that the mechanism of reaction is approximating to that of the analogous hydrogen-bromine combination, where reaction chains end by atomic recombination.

There is thus a clear cut issue to be decided. In addition, it is important to find if the inhibiting effect of hydrogen chloride (Part I, *loc. cit.*) extends to these oxygen-free mixtures and what bearing the other reactants have on the kinetics of the process.

It may be stated at once that the results of the present work make possible a definite choice between the several different kinetic possibilities and lead to a formula for the quantum efficiency which is consistent over a wide range. The expectation of Chapman and Gibbs has been found to be confirmed, in that the form of the kinetics approaches in a remarkably close manner that of the hydrogen-bromine reaction; the velocity is nearly proportional to the square root of the intensity of absorbed light, while the reaction is inhibited both by chlorine and by hydrogen chloride.

#### EXPERIMENTAL.

The results were obtained by the "method of averaging" (Part I, *loc. cit.*) involving the evaluation of the absorbed light from a knowledge of the average pressure of chlorine and its extinction coefficient. In no experiment was the total pressure of chlorine allowed to change by more than 30 per cent. during a run, while the total production of hydrogen chloride was kept constant at *ca.* 25 mm. The "graphical method" (Part I, *loc. cit.*) of plotting the course of reaction from point to point was found to be unsuitable in the present experiments in view of the high reaction velocities attained in the absence of oxygen. For the same reason violet light of wave-length  $406\ \mu\mu$  was used instead of ultra-violet light at  $365\ \mu\mu$ , which is much more strongly absorbed by the chlorine. The

\* 'Nature,' vol. 127, p. 584 (1931).

final concentration of chlorine was as before determined by means of its absorption of "365 light," after the introduction of sufficient oxygen to render the mixture insensitive. Full details of the apparatus, the method of procedure and the preparation and purification of the reactant gases will be given in Part III.

### Results.

(a) *Relation between Quantum Efficiency ( $\gamma$ ) and Light Absorbed ( $I_{\text{abs.}}$ ).*—The intensity of the incident light was varied by means of blue glass plates placed in the path of the beam. Results are given in Table I. The amount of light absorbed is given in galvanometer scale divisions (centimetres).

Table I.

$$\lambda = 406 \mu\mu. \quad [\text{H}_2] = 44.0 \text{ mm.} \quad [\text{HCl}] = 12.5 \text{ mm.}$$

$[\text{Cl}_2]$ mm.	Incident intensity $I_0$ cm.	$I_{\text{abs.}}$ calculated from $I_0$ cm.	$\gamma_{\text{expt.}}$	$\gamma (I_{\text{abs.}})^{0.4}$	$\gamma (I_{\text{abs.}})^{0.5}$
68.0	3.80	0.75	10600	9500	9200
67.0	11.95	2.30	6700	9350	10160
44.0	6.15	0.80	8770	8020	7840
43.7	13.45	1.75	7090	8860	9380
43.0	6.20	0.79	9210	8380	8200
44.0	8.55	1.11	7690	7870	8100
44.2	13.0	1.71	6830	8470	8932

It is obvious that the same concentrations of chlorine, hydrogen and hydrogen chloride do not give the same quantum efficiencies unless  $I_{\text{abs.}}$  is constant also; if, however, the rate of hydrogen chloride formation were proportional to the first power of  $I_{\text{abs.}}$ ,  $\gamma \left( = \frac{d[\text{HCl}]}{dt} / I_{\text{abs.}} \right)$ , would be independent of  $I_{\text{abs.}}$ . The numbers of the last two columns of the table show that for given concentrations of reactants the experimental results are in better agreement with the equation  $\gamma (I_{\text{abs.}})^{0.4} = \text{const.}$  rather than with the equation  $\gamma (I_{\text{abs.}})^{0.5} = \text{const.}$  It follows that the rate of formation of hydrogen chloride is given by the expression

$$\frac{d[\text{HCl}]}{dt} = k (I_{\text{abs.}})^{0.6}$$

in agreement with the result of Chapman and Gibbs (*loc. cit.*).

(b) *Relation between Quantum Efficiency ( $\gamma$ ) and Pressure of Chlorine [ $\text{Cl}_2$ ].*—In Table II,  $\gamma_{\text{expt.}}$  represents the experimental quantum efficiencies obtained for the conditions of chlorine concentration and absorbed light as given in the first and third columns respectively. The values of  $\gamma_{\text{calc.}}$  were obtained by calculation from the formula

$$\gamma_{\text{calc.}} = \frac{1.23 \times 10^4 [\text{Cl}_2]}{(22.0 + [\text{Cl}_2]) I_{\text{abs.}}^{0.4}}.$$

Table II.

$\lambda = 406 \mu\mu.$      $[\text{H}_2] = 44 \text{ mm.}$      $[\text{HCl}] = 12.5 \text{ mm.}$

$[\text{Cl}_2]$ mm.	Incident intensity $I_0$ cm.	$I_{\text{abs.}}$ calculated from $I_0$ cm.	$\gamma_{\text{expt.}}$	$\gamma_{\text{calc.}}$	$\gamma_{\text{calc.}}/\gamma_{\text{expt.}}$
12.0	12.50	0.46	5900	5930	1.00
23.0	12.00	0.84	6780	6740	1.00
44.0	6.15	0.80	8770	8900	1.02
44.2	13.0	1.71	6830	6620	0.97
67.0	11.95	2.30	6700	6640	0.99
68.0	3.80	0.75	10600	10400	0.98
90.3	5.85	1.47	8900	8500	0.96

The ratios of the final column show that the experimental results are well reproduced by a formula of the above kind and reveal the result of Bodenstein and Unger (velocity independent of pressure of chlorine, *loc. cit.*) as a limiting case, true only for large excess of chlorine.

(c) *Relation between Quantum Efficiency and Pressure of Hydrogen [ $\text{H}_2$ ].*—Table III gives the relevant data. The values of  $\gamma_{\text{calc.}}$  are derived from the expression

$$\gamma_{\text{calc.}} = \frac{2.8 \cdot 10^2 [\text{H}_2] [\text{Cl}_2]}{(22.0 + [\text{Cl}_2]) (I_{\text{abs.}})^{0.4}}$$

Table III.

$\lambda = 406 \mu\mu.$      $[\text{Cl}_2] = 44 \text{ mm.}$      $[\text{HCl}] = 12.5 \text{ mm.}$

$[\text{H}_2]$ mm.	Incident intensity $I_0$ cm.	$I_{\text{abs.}}$ calculated from $I_0$ cm.	$\gamma_{\text{expt.}}$	$\gamma_{\text{calc.}}$	$\gamma_{\text{calc.}}/\gamma_{\text{expt.}}$
44	6.15	0.800	8770	8960	1.02
92.4	5.48	0.715	18900	19600	1.03
168	5.02	0.643	37500	37400	1.00
217	4.90	0.637	46800	48500	1.04
293	6.04	0.785	55600	60000	1.08

which is obtained directly from that used in section (b), on the assumption that the quantum efficiency varies in a linear manner with the pressure of hydrogen. The agreement between the experimental and calculated values of  $\gamma$  shows that this is so, and that there is no inhibiting effect to be ascribed to the hydrogen when oxygen is absent from the system.

(d) *Relation between Quantum Efficiency and the Pressure of Hydrogen Chloride [HCl].*—In all the above experiments the average concentration of hydrogen chloride has been kept constant. When the effect of varying the latter was examined, an inhibiting effect similar to that already observed by us in mixtures containing oxygen was found to exist. This may be taken into account by suitably modifying the above formula, and under the heading of  $\gamma_{\text{calc.}}$  in Table IV are given the results calculated according to the expression

$$\gamma_{\text{calc.}} = \frac{2 \cdot 80 \cdot 10^2 [\text{H}_2] [\text{Cl}_2]}{([\text{Cl}_2] + 1 \cdot 70 [\text{HCl}]) (I_{\text{abs.}})^{0 \cdot 4}}.$$

Table IV.

$$\lambda = 406 \mu\mu.$$

[HCl] mm.	[H <sub>2</sub> ] mm.	[Cl <sub>2</sub> ] mm.	Incident intensity $I_0$ cm.	$I_{\text{abs.}}$ calculated from $I_0$ cm.	$\gamma_{\text{expt.}}$	$\gamma_{\text{calc.}}$	$\gamma_{\text{calc.}}/\gamma_{\text{expt.}}$
12.5	44.0	44.0	6.15	0.80	8770	8960	1.02
12.5	44.0	43.0	6.19	0.79	9220	9050	0.98
59.2	45.0	45.1	5.98	0.80	3960	4260	1.08
115	42.1	42.5	5.50	0.69	2420	2420	1.00
215	41.2	42.7	5.50	0.69	1360	1400	1.03
317	43.2	43.6	5.17	0.67	935	1060	1.13

It will be observed that with the above range of concentrations an increase of the pressure of hydrogen chloride from 12.5 to 317 mm. brings about roughly a ten-fold reduction in quantum efficiency.

*Maximum Value of Quantum Efficiency.*—The largest value of the quantum efficiency recorded in the above tables is  $5.6 \times 10^4$  (Table III). The formula deduced in section (d) suggests, however, that by increasing the concentration of hydrogen and chlorine and reducing the amount of light absorbed values greater than this should be obtainable. Accordingly using  $[\text{Cl}_2] = 62$  mm.,  $[\text{H}_2] = 430$  mm.,  $[\text{HCl}] = 12$  mm., and  $I_{\text{abs.}} = 0.24$  mm. ( $\lambda = 406 \mu\mu$ ), a value of  $1.2 \times 10^5$  was obtained for  $\gamma$ , in good agreement with those recorded

for the most sensitive mixtures by other workers.\* Upon the basis of the above formula, a value of  $1.57 \times 10^5$  is indicated, and it is probable that the somewhat low experimental result is to be ascribed to the presence of a small amount of oxygen in the hydrogen, which was too slight to be of any account until, as in the present instance, the pressure of hydrogen was very large.

#### THEORETICAL DISCUSSION.

The experimental results confirm the statement of Chapman and Gibbs (*loc. cit.*) and show that in the absence of oxygen the velocity is proportional to a power of the light intensity approaching  $\frac{1}{2}$  (actually 0.6). This makes it possible to conclude that the reaction chains are terminated principally by self-neutralization—i.e., by the recombination of atoms—rather than by any inhibitor such as the silicon oxychloride postulated by Bodenstein and Unger (*loc. cit.*), for in the latter case the velocity would become proportional to the first power of the light intensity, as it does in the presence of oxygen. The discrepancy between our results and those of Bodenstein and Unger would be removed if we could assume that in their apparatus there was some unknown source of oxygen or other inhibitor; we were, however, unable to obtain evidence of any attack on the silica by the chlorine in our case, and can only assume that our experiments, like those of Chapman and Gibbs† were free from such complications.

The form of our experimental equation is nearly identical with that obtained by Bodenstein and Lütkenmeyer‡ for the analogous reaction of hydrogen and bromine, and as is well known, can be derived kinetically as the direct consequence of the scheme of reaction proposed by Christiansen,§ Polanyi|| and Herzfeld.¶ It is given in Table V.

\* The following maximum values of  $\gamma$  have been recorded :—

Marshall ('J. Phys. Chem.,' vol. 29, p. 1453 (1925) )	$3 \times 10^4$
Kornfeld and Müller ('Z. phys. Chem.,' vol. 117, p. 242 (1925) )	$1 \times 10^5$
Porter, Bardwell and Lind ('J. Amer. Chem. Soc.,' vol. 48, p. 2003 (1926))	$7 \times 10^4$
Göhring ('Z. Electrochem.,' vol. 24, p. 235 (1918) )	$1 \times 10^5$

† In a private communication Mr. Chapman informs us that he has recently been unable to detect any effects which can be attributed to such an inhibitor as is postulated by Bodenstein and Unger.

‡ 'Z. phys. Chem.,' vol. 114, p. 208 (1924).

§ 'Dansk. Vid. Math. Phys. Medd.,' vol. 1, p. 14 (1919).

|| 'Z. Electrochem.,' vol. 26, p. 49 (1920).

¶ 'Z. Electrochem.,' vol. 25, p. 301 (1919).

Table V.

No.	Reaction	Heat effect*	Velocity coefficient.
(1)	$\text{Cl}_2 + h\nu = \text{Cl} + \text{Cl}$	—	$k_1$
(2)	$\text{Cl} + \text{H}_2 = \text{HCl} + \text{H}$	— 0.8 k cal.	$k_2$
(3)	$\text{H} + \text{Cl}_2 = \text{HCl} + \text{Cl}$	+ 44.8 k cal.	$k_3$
(4)	$\text{H} + \text{HCl} = \text{H}_2 + \text{Cl}$	+ 0.8 k cal.	$k_4$
(5)	$\text{Cl} + \text{Cl} = \text{Cl}_2$	+ 57.4 k cal.	$k_5$

Thus, we obtain upon the above basis

$$\frac{d[\text{HCl}]}{dt} = \frac{2k_2 k_3 \sqrt{\frac{k_1}{k_5}} [\text{H}_2] [\text{Cl}_2] (I_{\text{abs.}})^{0.5}}{(k_3 [\text{Cl}_2] + k_4 [\text{HCl}])} \quad (1)$$

whence

$$\gamma = \frac{2k_2 k_3 \sqrt{\frac{k_1}{k_5}} [\text{H}_2] [\text{Cl}_2]}{(k_3 [\text{Cl}_2] + k_4 [\text{HCl}]) (I_{\text{abs.}})^{0.5}} \quad (2)$$

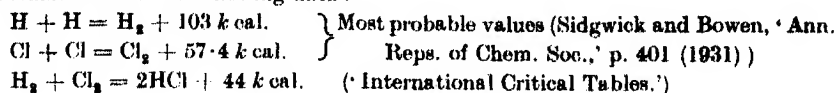
If reaction (4) did not occur, this expression would reduce to

$$\gamma = 2k_2 \sqrt{\frac{k_1}{k_5}} [\text{H}_2] (I_{\text{abs.}})^{-0.5} \quad (3)$$

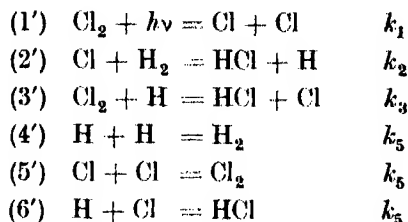
and the reaction would be uninhibited either by chlorine or hydrogen chloride. The fact that the experimental results are expressed by a relationship of the form of equation (2) rather than by equation (3) shows clearly that reaction (4) (*i.e.*, the reversibility of reaction (2)) must be taken into account here, as well as in the hydrogen-bromine reaction. This is in agreement with the fact that the heat of reaction (2) is very small.

We may, however, examine other possibilities. The scheme given above assumes that reaction (3) is very fast compared with reaction (2) so that the stationary concentration of chlorine atoms is large compared with that of hydrogen, and all chains virtually end by reaction (5). If, however, we go to the other extreme, and assume reactions (2) and (3) nearly equally probable and that (4) does not occur, the stationary concentrations of hydrogen and chlorine atoms become comparable. Reaction chains may then be terminated

\* Calculated from the following data :



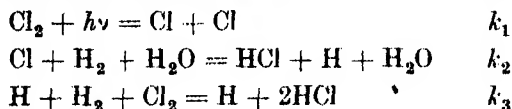
equally readily by any one of the three possible atomic recombinations. The scheme, formulated as follows,



then leads to the relationship

$$\gamma = \frac{2k_2 k_3 \sqrt{\frac{k_1}{k_6}} [\text{H}_2] [\text{Cl}_2]}{(k_2 [\text{H}_2] + k_3 [\text{Cl}_2]) (I_{\text{abs.}})^{0.5}}, \quad (4)$$

which differs from equation (3) by the term  $k_2[\text{H}_2]$ , which replaces the  $k_4[\text{HCl}]$  of the latter in the denominator. The experimental results easily distinguish between this and the former scheme and in favour of the former since marked inhibition by hydrogen chloride, but none by hydrogen, is observed. There remains the possibility for the starting of chains considered by Bodenstein\* in which chlorine atoms are to be considered only as the initiators and not as the propagators of chains, as follows :



the chains being propagated solely by hydrogen atoms. In the absence of oxygen the chains will be terminated by the recombination of hydrogen atoms



It is easy to show (assuming with Bodenstein that every chlorine atom reacts as above) that this mechanism leads to the result :

$$\gamma = k_3 \sqrt{\frac{k_1}{k_5}} [\text{H}_2] [\text{Cl}_2] (I_{\text{abs.}})^{-0.5} \quad (5)$$

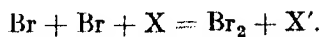
an expression which again is not confirmed by our results.

It is thus clear that while the experimental findings clearly conform to the "hydrogen-bromine" scheme of Christiansen, Polanyi and Herzfeld (*loc. cit.*) they are in disagreement with the other possibilities considered, and since these have been chosen to represent extreme cases as far as possible, we may with some confidence accept their mechanism as a working hypothesis.

\* 'Trans. Faraday Soc.,' vol. 27, p. 413 (1931).



There is, however, one point which must be further considered—the mechanism of recombination of chlorine atoms. According to the work of Jost and Jung\* the recombination of bromine atoms would appear to involve a third body in accordance with the well-known “dreierstoss theory” of Herzfeld.†



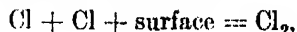
Their repetition of the work of Bodenstein and Lütke Meyer with special reference to this effect undoubtedly affords some evidence of a dependence of the velocity of hydrogen bromide formation on the total pressure ( $p$ ) according to the theoretical expression

$$\frac{d[\text{HBr}]}{dt} = \frac{k[\text{H}_2][\text{Br}_2]\sqrt{I_{\text{abs.}}}}{([\text{Br}_2] + k'[\text{HBr}])\sqrt{p}}$$

though their results with different inert gases appear to be extremely specific. Our own data, which extend over a wide variation of pressure, should be sufficient to show up such an effect if it existed in the hydrogen-chlorine reaction, and in view of the independence of the quantum efficiency on total pressure we can only assume that it is absent. In this respect our results are confirmed by the analogous results of Bodenstein and Lind‡ for the thermal combination of hydrogen and bromine which involves a similar scheme. Here, too, the velocity is apparently independent of the total pressure, and also of the presence of high concentrations of inert gas ( $\text{CCl}_4$ ,  $\text{H}_2\text{O}$  and air).

It remains to be considered how we are to explain this absence of the “third body effect” in our results; in this connection there exist the following possibilities none of which it must be admitted have as yet received adequate proof.

- (1) The atoms may recombine on the surface :



the adsorption of atoms by the surface being necessarily considered weak in order to account for the necessary kinetic relationship

$$k_1 I_{\text{abs.}} = k_2 [\text{Cl}]^2.$$

- (2) Alternatively recombination may occur by a mechanism visualized by Frenkel and Semenov,§ according to which a metastable  $^3\text{P}_1$  and a normal

\* ‘Z. phys. Chem.,’ B, vol. 3, p. 83 (1929).

† ‘Z. Physik,’ vol. 8, p. 132 (1922). See particularly Born and Franck, ‘Z. Physik,’ vol. 31, p. 411 (1925).

‡ ‘Z. phys. Chem.,’ vol. 57, p. 168 (1906).

§ ‘Z. Physik,’ vol. 48, p. 216 (1928).

$^2P_1$  halogen atom can recombine with light emission at the moment of collision without the intervention of a third body. Evidence for this in the case of halogens has been adduced by Kondratchew and Leipunsky\* from a study of the light emission of the flames of burning halogen hydrides. This activation to the  $^2P_1$  state for bromine would require 10,500 cal., but for chlorine only 2500 and should therefore occur much more readily in the latter case. It has, however, been pointed out that only one such activated collision in  $10^4$  is likely to be efficient,† and it is thus hardly probable that recombination by this process becomes more efficient than that by way of ternary collisions, except at very low total pressures.

(3) There is also the possibility that every chlorine atom which is liberated reacts to form  $Cl_3$ . Eyring and Rollefson in an extremely suggestive paper‡ have deduced from quantum mechanical considerations that the  $Cl_3$  molecule should be formed from Cl atoms and  $Cl_2$  molecules without the necessity of ternary collisions. If this is so, we might replace the Cl atoms in our scheme by  $Cl_3$  molecules without any alteration of the kinetic consequences.  $k_4$  would now refer to the reaction



for which triple collisions are unnecessary and the Christiansen-Herzberg-Polanyi formula follows unchanged.

The facts are at present insufficient to make decision possible as to the validity of any of these processes, and we shall not pursue the matter further for the present. It is hoped, however, to reopen the question from this point of view at a later date.

#### *Comparison of Photochemical Kinetics of the Hydrogen-Chlorine and Hydrogen-Bromine Reactions.*

(a) Let us refer back to the scheme of reaction in Table V, and to the experimental and theoretical formulæ :

$$\gamma = \frac{2 \cdot 8 \cdot 10^2 [H_2] [Cl_2]}{([Cl_2] + 1 \cdot 7 [HCl]) (I_{abs.})^{0.4}}$$

and

$$\gamma = \frac{2k_2 k_3 \sqrt{\frac{k_1}{k_5}} [H_2] [Cl_2]}{(k_3 [Cl_2] + k_4 [HCl]) (I_{abs.})^{0.5}}$$

\* 'Z. Physik,' vol. 50, p. 366 (1928).

† See Ruark and Urey, "Atoms, Molecules and Quanta," p. 403 (1930).

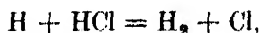
‡ 'J. Amer. Chem. Soc.,' vol. 54, p. 170 (1932).

Bodenstein\* has summarized and extended the reasoning of Bodenstein and Lutkemeyer (*loc. cit.*) and Jost (*loc. cit.*) and has arrived at the following values for the collision efficiencies of the reactions of the hydrogen-bromine and hydrogen-chlorine schemes :

Table VI. (Bodenstein).

Reaction.	Collision Efficiency.
$\text{H} + \text{Br}_2 = \text{HBr} + \text{Br}.$	$10^{-1}$
$\text{H} + \text{HBr} = \text{H}_2 + \text{Br}.$	$10^{-2}$
$\text{H} + \text{Cl}_2 = \text{HCl} + \text{Cl}.$	$10^{-2}$
$\text{H} + \text{HCl} = \text{H}_2 + \text{Cl}$	$10^{-4}$
$\text{Cl} + \text{H}_2 = \text{HCl} + \text{H}$	$10^{-4}$

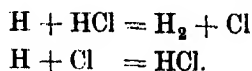
These conclusions are unaffected by the data of the present paper, except for reaction (4)



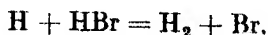
which it is now apparent must have a collision efficiency of the same order as reactions (3), for on comparing the experimental and theoretical expressions, we see that

$$k_4/k_3 = 1.7.$$

Accepting Bodenstein's estimate for reaction (3) we may thus assign an equal value of  $10^{-2}$  as the collision efficiency of reaction (4). This is a new aspect of the hydrogen-chlorine reaction, for, on the basis of the supposed absence of inhibition by hydrogen chloride it has always been assumed that  $k_4$  is negligibly small compared to  $k_3$  (*cf.* Bodenstein and Unger, *loc. cit.*). Thus the facts now presented bring the Nernst scheme into accord with the results of Bonhoeffer and Boehm† which hitherto seem to have been unjustifiably neglected; for it was shown by them that hydrogen atoms when passed into hydrogen chloride, react rapidly to give molecular hydrogen, a process which can only be satisfactorily explained on the basis of the reactions



Further, a comparison of the results which they obtained with hydrogen bromide under similar conditions indicates that the probability of the corresponding reaction



\* 'Trans. Faraday Soc.,' vol. 27, p. 413 (1931).

† 'Z. phys. Chem.,' vol. 119, p. 385 (1926).

is of the same order of magnitude, and gives us additional confirmation of the equality of the coefficients  $k_4$  in the two reactions. Thus the identity in order of magnitude of all four coefficients, for the two reactions is indicated and this can only be the case if the activations for the four reactions (3) and (4) are in each case zero.

(b) The temperature coefficient of the hydrogen-chlorine reaction determined by Padoa\* for ultra-violet light is given as 1.17, and by Porter, Bardwell and Lind† as about 1.10. Taking a mean of 1.14 we obtain an apparent activation for the reaction of 2300 cals. If we assume, that as in the hydrogen-bromine reaction this refers solely to reaction (2), the agreement with the slightly endothermic heat of reaction (2) (1000 cals.) is satisfactory. The temperature coefficient for the hydrogen-bromine reaction, determined by Bodenstein and Lütke Meyer (*loc. cit.*) is 1.5, giving an activation for reaction (2) of 17,000 cals. on the above assumption. Comparing then  $k_2$  for the two reactions, and remembering that the hydrogen-bromine reaction was measured at 500° Abs., while the hydrogen-chlorine reaction was measured at 300° Abs., we obtain

$$\frac{k_{2(\text{Cl})}}{k_{2(\text{Br})}} = \frac{e^{-\frac{2300}{R \cdot 300}}}{e^{-\frac{17000}{R \cdot 500}}} \therefore e^{13.2} \therefore 2 \cdot 10^6$$

If, however, as suggested on p. 119, the recombination of chlorine atoms according to reaction (5) requires an activation of *ca.* 2500 cals., then, to account for the observed activation of 2300 cals. for the hydrogen chlorine reaction, the activation of reaction (2) must be somewhat greater. Since the measured activation depends on the temperature coefficient of the ratio  $k_2/\sqrt{k_5}$  we may calculate as follows:

$$\frac{e^{-\frac{E_2}{R \cdot 300}}}{e^{-\frac{2500}{2R \cdot 500}}} = e^{-\frac{2300}{R \cdot 300}}$$

where  $E_2$  is the activation of reaction (2). From this,  $E_2 \therefore 3600$  cals.

Thus it follows (since the recombination of bromine atom, which depends according to Jost on ternary collisions, has no activation) that

$$\frac{k_{2(\text{Cl})}}{k_{2(\text{Br})}} \therefore \frac{e^{-\frac{3600}{R \cdot 300}}}{e^{-\frac{17000}{R \cdot 500}}} \therefore e^{11.0} \therefore 1.6 \cdot 10^5$$

\* Griffith and McKeown, "Photoprocesses," p. 656 (Longmans, 1929).

† 'J. Amer. Chem. Soc.,' vol. 48, p. 2603 (1926).

The value of  $k_2$  for the hydrogen-chlorine reaction therefore is, upon these reckonings, about  $10^6$  or  $10^5$  times as great as  $k_2$  for the hydrogen-bromine reaction; and since, as we have seen, the coefficients  $k_1$ ,  $k_3$ ,  $k_4$  and probably  $k_5$  are of similar orders of magnitude for the two reactions, the above ratio should also be the ratio of the corresponding quantum efficiencies. For the hydrogen-bromine reaction Lind\* reports a value of about unity at  $250^\circ \text{C.}$ , while an estimate has also been made from the data of Bodenstein and Lütke-meyer (*loc. cit.*) by Lewis and Rideal† which gives a maximum value of the same magnitude. Our own value for the maximum quantum efficiency of the hydrogen-chlorine reaction is of the order  $10^5$  and is thus in good agreement with the above considerations.

(c) If we take the activation of reaction (2) according to the above considerations to be between 2300 and 3600 cals., then the value of  $k_2$  is between  $2 \cdot 10^{-2}$  and  $2 \cdot 10^{-3}$  times the value of  $k_3$  and  $k_4$ , each reckoned as having zero activation. This is in agreement with the scheme of Christiansen, Polanyi and Herzfeld which we have adopted, for in order that self-neutralization of chains should occur solely through recombination of chlorine atoms (reaction 5) and not appreciably by recombination of hydrogen atoms, the stationary concentration of the former must be large as compared with the stationary concentration of the latter, and this demand is only fulfilled kinetically if  $k_2$  is small compared with  $k_3$  and  $k_4$ . In general accord with this, Kistiakowski‡ has calculated from entirely different considerations that  $k_2$  is some  $10^{-3}$  times smaller than  $k_3$ , while Bodenstein§ arrives in a different way at a similar result giving a factor of  $10^{-2}$ .

It may thus be claimed on the basis of the argument advanced above that the experimental results recorded here for the photochemical reaction of hydrogen and chlorine in the absence of oxygen, taken in conjunction with the thermal data, are in general dimensional accord with the corresponding reaction between hydrogen and bromine, and that their interpretation by an analogous mechanism leads to results which are in agreement with the thermal and other data recorded by previous workers.

The authors are indebted to the Government Grant Committee of the Royal Society for a research grant which has been applied in part to the prosecution

\* 'J. Phys. Chem.,' vol. 27, p. 55 (1924).

† 'J. Amer. Chem. Soc.,' vol. 48, p. 2553 (1926).

‡ 'J. Amer. Chem. Soc.,' vol. 52, p. 1872 (1930).

§ 'Trans. Faraday Soc.,' vol. 26, p. 415 (1931).

of this work, and to the Commissioners of the Exhibition of 1851 for a senior award to one of them (M. R.).

*Summary.*

The photochemical reaction between pure hydrogen and chlorine has been investigated by the photometric method described in Part I (*loc. cit.*).

The quantum efficiency can be expressed over a wide range by the formula :

$$\gamma = \frac{2.8 \times 10^3 [\text{H}_2] [\text{Cl}_2]}{([\text{Cl}_2] + 1.7 [\text{HCl}]) (\text{I}_{\text{abs.}})^{0.4}}$$

A maximum quantum yield of  $1.2 \times 10^5$  was obtained in good agreement with the results of earlier workers.

In agreement with Chapman and Gibbs the velocity of hydrogen chloride formation is proportional to a power of the intensity of absorbed light approaching 0.5 (actually 0.6). Reaction chains are thus terminated mainly by self-neutralization.

For such "oxygen-free" mixtures the atomic mechanism involves Nernst chains the atomic reactions of which are similar to those of the corresponding hydrogen-bromine reaction.

It is shown on the basis of the present data that the scheme of Christiansen, Polanyi and Herzfeld applied to the hydrogen chlorine reaction yields results in general dimensional agreement with the relevant thermal and statistical data of other workers.

---

*Gas Adsorption upon Electrically Conducting Films during their  
Condensation from Molecular Rays.*

By M. C. JOHNSON, M.A., D.Sc., and T. V. STARKEY, B.Sc., Physics Department,  
University of Birmingham.

(Communicated by S. W. J. Smith, F.R.S.—Received October 20, 1932.)

1. *Introduction.*

If two or more components in a gas mixture are simultaneously adsorbed upon a solid boundary, the resulting surface structure is not necessarily a simple mixture of the layers which each gas would contribute by itself. For instance, adsorbed molecules of each component may alter the rates of evaporation of the other components from the surface, and also their mobilities in migration along the surface, even if none of them react chemically while adsorbed. Hence the kinetics of interfacial layers on solids exposed to mixtures becomes prohibitively complex as a general problem. When, however, one component is a metallic vapour and the other is one of the gaseous impurities common in vacuum technique, the practical results of contamination of the former by the latter are often so important as to demand the empirical investigation of individual details in advance of any general treatment. The detail chosen in the present paper is the effect of certain gases on the electrical conduction of a metallic layer deposited from the vapour phase.

There is considerable evidence that a metallic vapour adheres differently to surfaces covered with various impurities, and such gas coverings may also be expected to have profound influence upon the lateral diffusion which has recently been proved to play an essential part in the building up of a crystalline solid. The electrical conductivity of such metallic deposits is known to be very small and uncertain compared with that of the bulk metal, and to vary discontinuously with several conditions; in particular it exhibits anomalies in ageing, in temperature dependence, etc.,\* many of which are commonly stated to be "probably due to occluded gas."

No attempt seems hitherto to have been made to approach more nearly the actual processes by which gas might enter and influence the electrical and structural properties of a metal film during its formation; it is desirable to know how much of the usual suggestion as to "occluded gas" can be made

\* Bartlett, 'Phil. Mag.', vol. 5, p. 848 (1928).

definite, and for this the experimental evidence must be repeatable, and quantitatively controllable, and such as to exhibit any gas effects at their maximum.

In fulfilment of these three requirements we measure the growth of conductivity in films of mercury deposited on a liquid-air cooled target from a unidirectional stream of atoms, among which any gas can be mixed to a known proportion of the molecules crossing unit area. Both the vapour and the gas are therefore directed at the target from an oven whose aperture obeys the condition for "atomstrahlen," and the surrounding vacuum is kept high enough to eliminate disturbing collisions in the gaseous phase.

It then becomes possible to connect the structure of the mixed adsorbate with its electrical conductivity, by varying the nature, duration and stream density of gases accompanying, preceding or succeeding a very faint stream of metal vapour. From a series of graphs showing the growth of conduction under the several controlled conditions we derive information as to the diffusion of one component through a loose adsorbed structure of the other, and throw light on the successive stages of growth which can be discriminated; the action of the gases may further be distinguished according as they alter the evaporation rate of the metal or alter the specific resistance of a given amount of the metal.

Such effects are unavoidably present in many researches with molecular rays, surface catalysts, thermionic and photoelectric surfaces; the information we obtain by experimentally magnifying the gas contamination may enable correct allowance to be made for its intrusion in cases where it cannot be eliminated.

## 2. Apparatus.

The source of mercury vapour was a liquid reservoir capable of precise thermostatic control (fig. 1) communicating with the adsorption vessel by a circular aperture of area,  $A$ ,  $0.0045 \text{ cm.}^2$ , cleanly bored in a platinum sheet; the latter was sealed by soft glass to the top of the reservoir tube, which thus constituted the usual "oven" of a molecular ray apparatus. The stream density at any

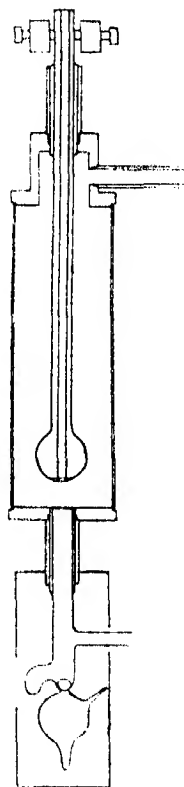


FIG. 1.



orientation situated at distance  $d$  from the aperture was then obtainable from vapour pressure data, temperature and dimensions by means of the well-known formula

$$v = \frac{p}{\sqrt{2\pi m k T}} \frac{A \cos^4 \theta}{\pi d^2}.$$

To avoid passing the mercury over any greased surface, such as a tap, a steel ball, fitting an accurately ground seating, could be moved to and from a side tube by external magnetic control. When the ball was in its seating any irregular annulus through which mercury vapour might still enter the oven was of very small area compared with the oven exit A; the stream density could thus be reduced to a negligible value before beginning an experiment. From a side tube a measured capillary connected with reservoirs and gas drying apparatus, etc., allowed admission of any gas at any required rate into the mercury stream. The oven pressures (mostly of the order of  $10^{-3}$  mm.) needed for any given number of molecules of any given gas to emerge from the aperture were calculated by an extension of the above formula to more than one component; care was taken that for each molecular weight this controlled admission did not exceed the maximum density for "molecular" flow. Using the laws of molecular flow through capillaries, the pressures in the reservoirs needed to maintain the desired pressures in the oven were also calculated for each gas.\*

The target was on the surface of a glass bulb whose neck was filled to a given level with liquid air; the temperatures both of inside and outside of the bulb were measured by thermocouples in control experiments, to determine the thermal sequence accompanying gradual change in composition of the liquid air, etc.

As deposition of mercury proceeded on the bulb, a conducting bridge was gradually formed, between electrodes which lead to a calibrated galvanometer system supplied with constant potential from a potentiometer. Previous writers on the resistance of films have emphasized the extreme difficulty of ensuring contact between electrodes and deposit; after preliminary work the plan was adopted of platinising two longitudinal bands along the whole length of the target bulb and tube, and then thickly copper plating to enable the portions which projected outside the adsorption chamber to be securely attached to leads. Regions in contact with other parts of the apparatus were protected by mica, and shellac protected the metal from amalgamation until very close

\* Dunoyer, "Vacuum Practice" (1926).

to the target. The target itself was a small rectangle on the bottom of the bulb, left bare both of platinum and of shellac, and bounded on two sides by the deposited platinum electrodes which were thus in the most intimate contact with the glass and with any mercury condensing. Repeatable results free from contact resistance were by this means obtained.

The space between aperture and target was continuously evacuated through a very wide trap and short, wide tubing by a three-stage diffusion pump, keeping the system below discharge pressure. Where lubrication was needed Shell-Mex grease of extremely low vapour pressure was used.

### 3. *Definition of Plane Resistance.*

It was found that by taking the known value of  $v$  and adopting in turn various hypothetical rates of re-evaporation, agreement could be obtained with any of the various high "specific resistances" mentioned by previous workers. This indicates the indefiniteness of a term which has been a source of ambiguity in many discussions of film resistance, owing to the impossibility of knowing accurately both the thickness and the mass of the metal, or even of defining precisely the cross-section offered to currents by material only a few atoms thick. Our experiments show that one reason for the abnormalities of film resistance is that density in such material is not a simple function of density in bulk; hence specific resistance, with its implication of a regular two-dimensional cross-section, loses its unique significance in these cases where the packing of the constituent particles is not constant. Accordingly, we confine all specification to the resistance offered by a strip of unit length and width to currents flowing in its plane. This is a quantity suitable for comparing the properties of sheets whose thickness is negligible compared with their area and whose two-dimensional cross-section would only be definable in terms of particular methods of estimation. The longitudinal resistance of the region bounded by the platinum on our target, corrected for lead resistance, is reduced to  $R$  ohms per cm.<sup>2</sup> from the measured dimensions, and  $1/R$  then forms the most convenient quantity in terms of which to discuss the results obtained.

From this definition of plane resistance,  $1/R$  would be a constant linear function of time during constant stream density if all impacts on the target contributed to the building up of a deposit of normal properties. The nature of gas-impregnated films is hence to be deduced from departures from such simple law.

4. *Curves of Growth of Conduction.*

The main features revealed by the experiments are exhibited in the form of graphs of  $1/R$  against  $t$ , of which figs. 2 to 7 typify many of similar character. The origin of time,  $t_0$ , was taken in each case at the opening of the ball valve when the target had reached thermal equilibrium. The beginning ( $\uparrow$ ) and the end ( $\downarrow$ ) of any gas admission into the beam of mercury atoms is indicated; the intensity of the latter becoming constant shortly after  $t_0$  and remaining so throughout each experiment. The time needed for establishment of the several pressure gradients was small compared with the length of any experiment. Comparison of one gas with another, *e.g.*, in fig. 4, was effected by admitting each at a given pressure below the maximum limit for molecular flow, for a length of time calculated to ensure the same total number of impacts on the target for each successive gas.

Characteristics of the several graphs are summarized as follows before their interpretation is discussed in the succeeding section.

Fig. 2. (a) *No Gas Admissions.*—It is probable that different physical mechanisms of resistance predominate at different times during growth at constant stream density; hence we distinguish within each curve three stages,  $\alpha$ ,  $\beta$ ,  $\gamma$ , in which, as to order of magnitude,  $R_\alpha > 50,000$  ohms per cm.<sup>2</sup>, and  $R_\gamma < 1000$  ohms per cm.<sup>2</sup>,  $\beta$  being a transition stage.

The rate of growth invariably increases through  $\alpha$ ,  $\beta$ , to a maximum in  $\gamma$ , where the growth is not only the fastest but approaches a constant rate not very different for all the experiments. But this characteristic  $\gamma$ -rate sets in earlier and at lower values of  $1/R$  in successive repetitions of the experiment, curves 1, 2, 3 being members of a typical sequence in which the liquid air bath was emptied between each. This process of successive shortening of the  $\alpha$ -stage can be made to begin again and repeat itself, starting from a duration as great as 4 hours and finally reaching a duration of only a minute or two; but each return to the longer  $\alpha$ -stage and the beginning of a fresh sequence only occurs (i) if the apparatus is left under vacuum for a week or so, or, alternatively, (ii) if any gas at atmospheric pressure and temperature is admitted for a moment. Thus, in the  $\alpha$ -stage at normal temperature, the deposit evaporates with extreme slowness spontaneously, but quickly under gas bombardment.

(b) *Gas Admission before  $t_0$  only.*—The dotted curves 4, 5, 6 also form part of a sequence with secularly shortening  $\alpha$ -stage, but before each member of this the target was exposed at its lowest temperature to  $H_2$  at low pressure,

admission of the gas then ceasing before each admission of mercury began. The lack of any apparent distinction between the sequences to which (a) and (b) belong indicates that the tenacious and slow-growing  $\alpha$ -stage is not itself

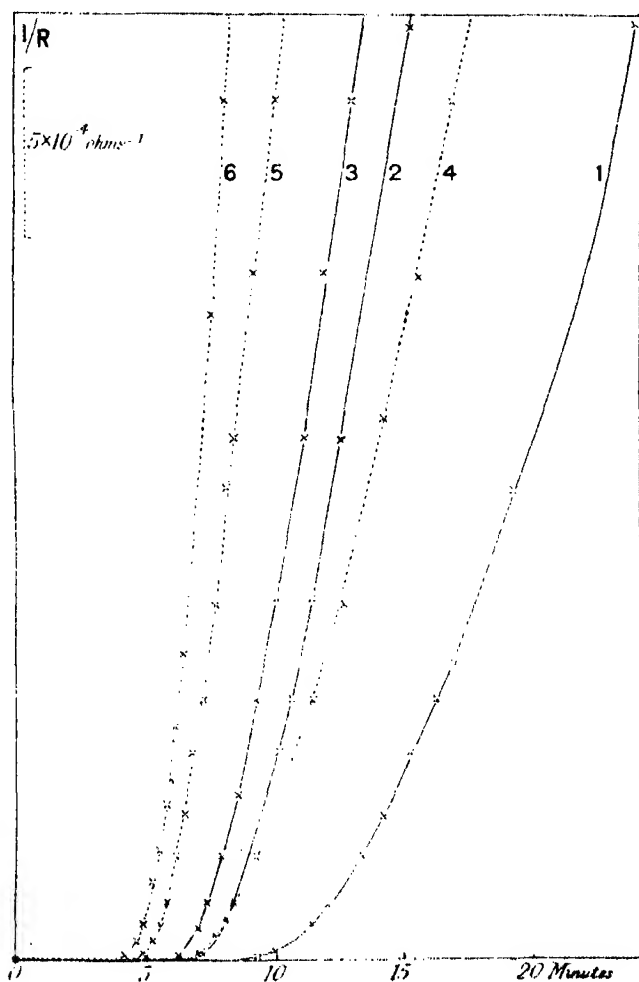


FIG. 2.

greatly affected by small amounts of gas to which layers may be exposed after the mercury stream has ceased.

(c) *Gas Admission throughout.*—If the smallest amount of  $H_2$  is mixed with the stream of mercury from  $t_0$  onwards, the initial stage is delayed much further, no detectable conductivity appearing after 7 hours. If admission of  $H_2$  is finally stopped, a slow rise of  $1/R$  then sets in.

Fig. 3.—If the liquid air is not renewed and the observations are continued a slight warming of the target occurs. Traceable in the thermocouple measurements shown. A very rapid evaporation of the outermost layers of deposit

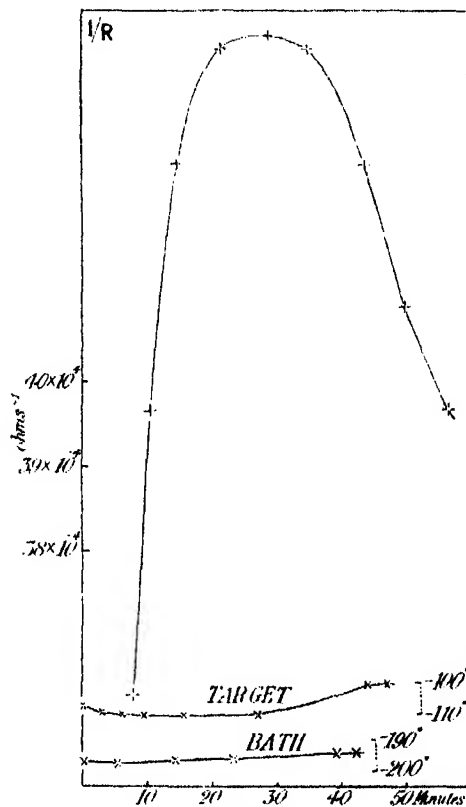


FIG. 3.

can under these circumstances be observed without the stimulus from gas bombardment. This loss occurs independently of whether any gas is then being admitted or not, but sets in later if much gas has previously been admitted (compare figs. 3 and 4) and often sets in earlier the larger the actual value of  $1/R$ .

Figs. 4 to 7. *Gas Admission after  $t_0$ .*—Fig. 4.—If gases are admitted after some interval beyond  $t_0$ , all to the same number of molecules and hence for different times, cessation of growth occurs almost instantaneously and continues until shortly after such admission ceases. The subsequent resumption of growth is slower, never regaining the  $\gamma$ -rate which had preceded gas admission.

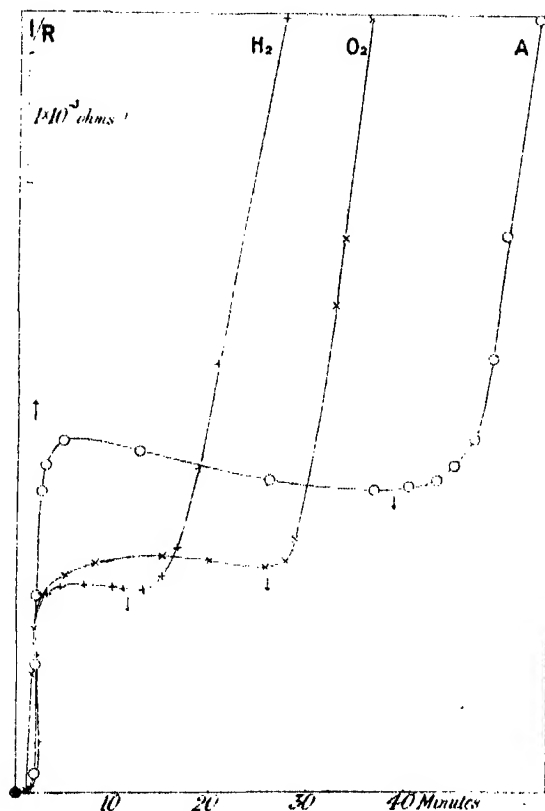


FIG. 4.

Fig. 5.—In the particular case of  $\text{CO}_2$  thus admitted, conductivity not only ceases to grow but falls to the  $\alpha$ -stage. This fall may be postponed in some cases until several minutes after the gas has ceased to be admitted, but it occurs at times which are clearly independent of any change of temperature, *e.g.*, the two curves exhibited fall at 15 and 50 minutes approximately.

Fig. 6.—The subsequent resumption of growth after  $\text{CO}_2$  admission is not only delayed for an hour or so, but finally sets in at a rate which is slow even in comparison with the rate of growth after equally long  $\alpha$ -stages in the gas-free sequences. On this graph is also shown the somewhat similar behaviour after exposure to the contents of an oxygen discharge tube.

Fig. 7.—If any of the gases pass through a discharge on their way to the oven (beginning at  $\uparrow$  and ending at  $\downarrow$ ) the fall takes place even with those gases which, in their ordinary state, merely caused cessation of growth, and

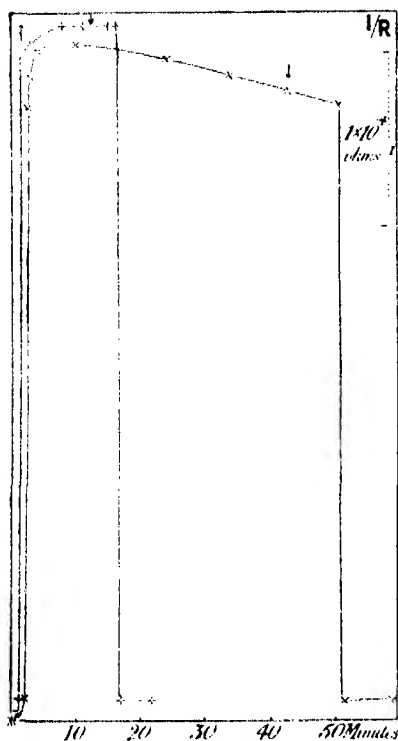


FIG. 5.

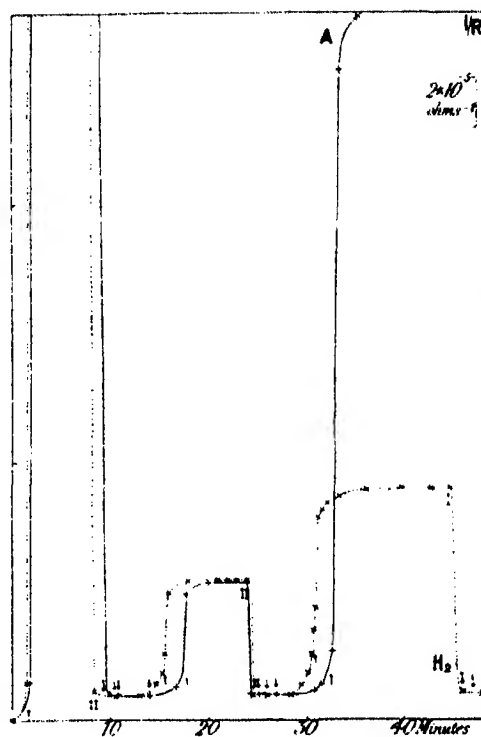


FIG. 7.

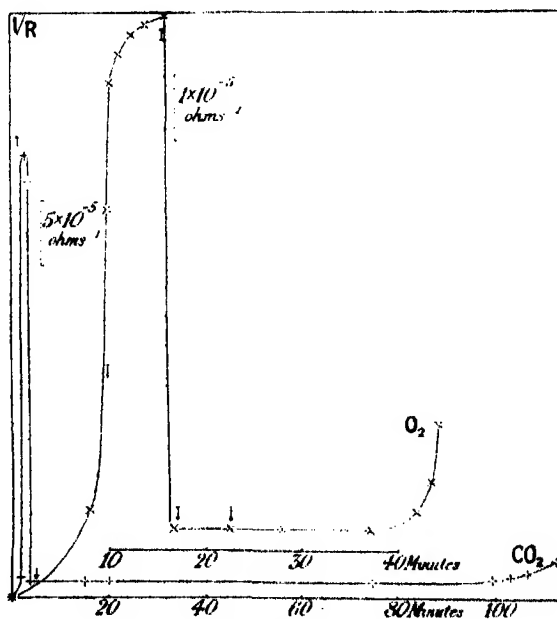


FIG. 6.

is again quite distinct from the fall due to temperature rise in fig. 3. The after-effects of discharge most resemble those of  $\text{CO}_2$  in the case of oxygen.

5. *Evidence from Conduction Curves as to Physical Properties of Mixed Deposit.*

By comparing the rates of growth before, during and after admission of certain quantities of gas with the rates obtained when no gas was added to the mercury stream some features in the physical state of the adsorbate become evident, which constitute the principal inference from these experiments.

But it is important to recognize that even in those instances where gas is not intentionally directed at the target the structure of the deposit should never be regarded as strictly gas-free, though for convenience of comparison we shall use that term. The surrounding residual gas even at  $10^{-6}$  mm. provides sufficient stray molecules to contaminate considerably any deposit from such an extremely weak vapour stream as is deliberately adopted here for revealing and intensifying the effects of gas. Thus the structure we investigate is similar to those met in most experiments at high vacuum, but must not be expected to resemble those which result from rapid deposition in denser vapour, where the closely packed mass approximates more nearly to a stratified model. The present results are obtained by adding at will to a contamination which, as in most condensations at the lowest pressures, cannot be entirely eliminated.

(i) *Rates of Evaporation.*—Deposits from mercury vapour so dense as to be comparatively gas-free do not readily re-evaporate as the surface is raised even to room temperature; their ultimate coalescence into globules is familiar, a common experience with boiling mercury, and liquefaction *in situ* was even shown by Egerton to occur in atomic ray experiments under different conditions to ours.\* This is to be expected for a *pure* substance of melting point  $-39^\circ \text{C.}$  and boiling point  $360^\circ \text{C.}$  But in the present experiments stream density is low enough for gas impacts often to intervene between those of the metal atoms; now, many metals are known to be more weakly adsorbed upon a gas-covered metal than upon the bare surface of their own or other kind; for instance, in the so-called "critical" or "transition" phenomena,† intervention of gas layers preventing full exercise of the normal energy of sublimation or of adsorption. Hence it is of interest to examine the present results for any signs of a weakened average adhesion, or readier escape by thermal agitation, than for the pure material in bulk.

\* 'Phil. Mag.,' vol. 33, p. 33 (1917).

† Fraser, "Molecular Rays" (London. 1931).



This abnormal evaporation is shown in fig. 3. That genuine re-evaporation occurs both here and between the separate curves of fig. 2, not merely liquefaction into drops or other loss of conduction without loss of material, is shown by the fact that no secular accumulation occurs beyond the  $\alpha$ -stage, however often the experiments are repeated, and that even the cumulative effects at the  $\alpha$ -stage are swept away by momentary exposure to atmospheric temperature and pressure.

Ease of re-evaporation of metal from gas-covered metal may next be exhibited in intensified form by introducing more gas in addition to the unavoidable contamination. The result, fig. 4, appears as a further increase in rate of evaporation until rate of condensation is balanced and the net amount of conducting material on the target ceases to grow.

Since strong adhesion of a gas atom to a metal surface is not incompatible with weak adhesion of the metal vapour atom to the gas-covered surface, the evaporation rate of the mixture may be a very complex phenomenon, and we do not pursue at present the above simple general explanation into its minor complications, such as the delay in purely thermal desorption recorded in the note on fig. 3.

(ii) *Structure at the  $\alpha$ -stage.*—The excessive ease of re-evaporation is not constant through all depths of the deposit, and is much less marked at the initial  $\alpha$ -stages, where lack of cumulative effects at normal temperature and pressure again proves the phenomena to be not merely due to liquefaction. This tenacity at the  $\alpha$ -stage becomes intelligible when the nature of the target is considered, and very probably represents the period at which some of the original surface is still, here and there, exposed. An unbaked glass surface does not offer a plane target, since it is known to support vapours supplied to it from its own interior structure, to a depth of many molecules and in scattered patches. The initial deposition of mercury must for some time be occupied in filling up these irregularities. The identification of stage  $\alpha$  with this process is supported by the following considerations :—

(a) On such a surface the normal adhesion to a plane, controlling the interval between arrival and departure of an impinging atom, is supplemented or even greatly magnified by mechanical trapping; this depends on the large probability of recapture by adjacent surfaces at all orientations before the evaporating particles can escape irrevocably into the gas phase. We recorded (p. 130) the prolongation of normal evaporation time *in vacuo* from a few minutes at stage  $\gamma$  to several days at stage  $\alpha$ , and this must be greatly contributed to by such trapping, resulting in a progressive filling up of the irregularities each

time an experiment is repeated without complete desorption. The secular decrease in space available for this peculiar mode of growth may be considered to underlie the observed secular shortening of the  $\alpha$ -stage which continues until steps are taken to stimulate complete evaporation by bombardment at higher gas pressure.

(b) Since the lateral migration, now known to play an essential part in crystal growth, must be impeded by the obstructions belonging to the original target until all such irregularities are filled up, the rate of growth of conduction in the  $\alpha$ -stage should be slow, as it is actually found to be.

(c) This immobilization of mercury in interstices should also result in the deposit at this stage offering a less penetrable target for subsequently impinging gases; that this is so is shown by the comparative insensitivity to rarefied gas applied to residual layers left in the  $\gamma$ -stage, as noted in connection with fig. 2 (A).

(iii) *Diffusion through a Loose Structure at the  $\gamma$ -Stage.*—An important indication as to this is afforded by the "after-effects" characterizing figs. 4 to 7. In all the "gas-free" curves, fig. 2, the rate of increase rose throughout any curve towards a limit, approaching it more rapidly the shorter the  $\alpha$ -stage. But in fig. 4 the attainment of maximum rate had been reached early, and gas was then applied at the  $\gamma$ -stage; after cessation of gas admission an interval, clearly visible on each curve, is needed for re-establishment of flow equilibrium, but after that the interrupted growth is resumed but at a slower rate. The repetition of this phenomenon at widely differing time intervals shows that it is not an incipient temperature effect. The after-effect of temporarily admitting gas is thus to prevent return to the maximum  $\gamma$ -rate, allowing subsequently deposited mercury atoms to contribute only a comparatively slow growth of conductivity.

If the applied gases did no more than form stratified layers upon the surface, weakening the adhesion of the next arriving mercury atom, this after-effect could not outlast the very short time needed for a single layer of the latter to accumulate, i.e., for a very small increase in conductivity to appear; but actually it prevents return to the  $\gamma$ -rate throughout a rise of conductivity of over 100 per cent., indicating that the gas permeates the whole *subsequently* deposited structure. It becomes necessary to suppose it can diffuse upwards from the reservoir that it forms upon, and within, the previously deposited mass.

That the gas also permeates the *previously* formed structure is shown in figs. 5, 6 and 7; here  $\text{CO}_2$  and all ionized gases not only produce cessation of

growth, as did  $H_2$ ,  $O_2$  and A, but an almost total loss of previous conductivity down to the  $\alpha$ -stage, the effect making itself felt to a depth corresponding to over 90 per cent. of the conducting structure.

A lower limit to the rate of this diffusion from surface into volume is indicated roughly in fig. 5, where the full effect of admitting gas is sometimes not apparent until 5 to 8 minutes after the supply of gas has been cut off, which is of the same order as the time needed to attain a fresh flow equilibrium. This rate of diffusion represents, at this temperature and pressure, a very rapid transport compared with the spread of a gas into a normally packed solid, either by lattice diffusion, or by grain-boundary diffusion.

This evidence that gas applied to the surface spreads almost at once through the whole deposit affects any model by which such metal films may be pictured; the structure must resemble a sponge, rather than any lattice, in the extreme looseness of its packing.

This conclusion is in accord with some microscopic studies of mercury deposited in the presence of gas by Volmer and Estermann,\* in which the first approach to solidification appeared to be a foliated growth with random orientation of its edges.

(iv) *Distinctions between Gas Effects on Conduction and Gas Effects on Evaporation.*—Any apparent modification of the growth in conduction by gases may include not only the promotion of re-evaporation of mercury, *i.e.*, a decrease in the net mass deposited from a constant stream, but also changes in the resistance offered to electric currents by any given mass.

It is *a priori* likely that both occur in all the instances here discussed, but so far only the former has been proved; the data must be examined for evidence for or against the latter, in view of the "gap" theory which gives a plausible explanation of the high resistivity shown by thin films. This theory has recently been given more precise form by Frenkel,† who considered the normal lattice impedance to electron flow as supplanted, in these films, by large potential barriers, or gaps between separated conducting aggregates. The existence of such aggregates is an obvious inference from any model based on the diffusion processes we have described, and gases in such structures will modify this non-metallic gap resistance, both (a) by altering the quantum-mechanical transmission coefficient for each gap, and (b) by inhibiting the migrations by which the gaps become closed, in such crystal-growing processes as sintering.

\* 'Z. Physik,' vol. 7, p. 13 (1921).

† 'Phys. Rev.,' vol. 36, p. 1604 (1930).

It is in the observations involving  $\text{CO}_2$ , fig. 6, that such effects appear as a necessary implication of the experiments, not to be explained simply by the facilitated re-evaporation. If, in these cases, the apparent loss of conductivity represented solely a loss of material through evaporation stimulated by impinging gas, the latter would itself be lost together with the impregnated metal; the completeness of such loss would follow from the inability of the gas to permeate the underlying  $\alpha$ -layers when these are already deposited (p. 137). In such an event any subsequent recovery after withdrawal of gas would be expected to obey the same laws of growth as in the "gas-free" experiments, *i.e.*, to repeat some part of the sequence represented in fig. 2, where re-evaporation above the  $\alpha$ -layers is invariably followed by a faster, not a slower, rise. This is not the case; the final growth after treatment by  $\text{CO}_2$  is very slow, even compared with that which followed equally long delays imposed by more normal means. The curves for ionized oxygen also shows a less marked but definite dissimilarity from the way in which conduction rises after removal of the whole upper structure.

Hence after almost total loss of conductivity the subsequent new growth still exhibits after-effects from the gas, indicating that more of the latter remains than can be occluded at the  $\alpha$ -stage. Hence the loss of conduction in these experiments cannot be entirely a loss of material, but must include the other alternative, the formation of obstructing layers acting by (a) or (b) in the gaps between material which still persists on the surface.

The "gap" theory of resistance requires for (a) no physical hypothesis beyond the well-known alteration of electron transmission across a potential barrier effected by monomolecular layers on thermionic and photoelectric emitters; hence there is no need to postulate any insulating compound of known chemical type for these obstructing layers in the gas-impregnated metal deposit. Saturated monomolecular layers of gases adsorbed upon the enormous accessible area presented by structures of the type studied by Volmer and Estermann are sufficient to account for the increase of resistance and for the increase of evaporation. That the gas deposition is fully saturated is shown by further experiments, in which reduction of the pressure of the intruding gases did not weaken perceptibly their effect upon conduction.

It is a pleasure to acknowledge gratefully the kindness of Professor S. W. J. Smith, F.R.S., in making possible these experiments.

6. *Summary.*

Experiments are described in which a beam of molecular rays condenses into an electrically conducting film on a liquid air cooled target; the beam consists of (a) a constant stream of mercury vapour, with (b) controlled additions of  $H_2$ ,  $O_2$ , A,  $CO_2$ , and various ionized gases, in turn.

Analysis of curves showing the rate of growth of conductivity reveals certain repeatable effects which persist after cessation of gas admission. By comparing slopes of the curves before, during and after the introduction of definite amounts of a given gas the following features of the mixed deposit are illustrated.

(1) The first mercury atoms are trapped and prevented from free lateral migration in the irregularities of a vapour covered target, and constitute the stage of growth characterized by (a) slowest rise of conductivity, (b) least penetrability to subsequently applied gas, (c) an evaporation rate measurable in days instead of minutes.

(2) Subsequent mercury atoms build up an outer structure loose enough for gases to diffuse in and out of it at velocities high compared with penetration into an ordinary lattice or crystal aggregate.

(3) The action of  $H_2$ ,  $O_2$  and A can be explained as the formation of saturated monomolecular layers upon the enormous accessible area of loose metallic deposit. Mercury atoms striking these adsorb so weakly that evaporation of a large proportion of the deposit can occur immediately on rise in temperature of a few degrees at  $-110^\circ C$ .

(4) With  $CO_2$  and ionized oxygen there is further evidence that non-conducting barriers are formed in the interstices, causing fall of conductivity, and not merely facilitating re-evaporation of mercury.

These results are in accord with what is known from microscopical data concerning the growth of loosely aggregated structures from mercury vapour in the presence of gas. They also confirm, and illustrate some of the processes assumed by, the "gap" theory of the mechanism of thin film resistance.

---

*The Moving Boundary Method for the Determination of Transport Numbers.*

By G. S. HARTLEY and JOHN L. MOILLIET, The Sir William Ramsay Laboratories of Inorganic and Physical Chemistry, University College, London.

(Communicated by F. G. Donnan, F.R.S.—Received October 27, 1932.

Revised December 8, 1932.)

*I. Introduction and Definitions.*

The lack of a simple and fairly complete theoretical treatment of the moving boundary method has been felt in this laboratory in the course of transport number measurements in dye solutions. The results of these measurements are shortly to be published by Dr. C. Robinson and one of us (J. L. M.). In the present paper we shall attempt to develop a theory of the method, of necessity including some previous work, and to explain experimental results in the literature and the aforementioned work on dye solutions. Doubts have been expressed as to the validity of the method, in spite of the convincing experimental work of MacInnes, Smith, Longworth, and co-workers, to whom we shall frequently have occasion to refer. These attacks on the method, we believe, have arisen from a misunderstanding of the fundamental principles involved, and we shall endeavour to answer them in this paper. In order to avoid confusion, we shall first explain the terminology to be used, which we hope will be adhered to in future communications from ourselves and co-workers.\*

In this paper we confine ourselves to electrolytes (including colloidal electrolytes). The application of the method to colloids will be the subject of a future communication from this laboratory.

An electrolyte in solution will be considered as composed of an electro-positive and an electronegative radical. It will be important to distinguish between quantities pertaining to a radical, which are experimentally determinable, and quantities pertaining to the ionised part of the radical, which are dependent on a knowledge of the degree and manner of dissociation of the

\* The nomenclature here described is not that used by one of us (G. S. H.) in two previous communications: 'Phil. Mag.,' vol. 12, p. 473 (1931), and with C. Robinson, 'Proc. Roy. Soc.,' A, vol. 134, p. 20 (1931).

electrolyte. This distinction has been made by MacInnes, Longworth, and co-workers, and by Miller,\* who use the term "ion constituent."

We shall define the transport number  $T$  of an electropositive radical, for example, as the number of gram-equivalents of it which, as a result of electrical conductance alone, cross a section in the interior of the solution, fixed with respect to the solvent, in the direction of positive electricity, when  $F$  (one faraday) coulombs of positive electricity flow. Since this quantity is determined experimentally for the radical itself, and not for that fraction of it which exists as free ions, we prefer to speak, for example, of the transport number of chlorine or chloride radical in a sodium chloride solution, rather than of the transport number of chloride ion. This is the quantity measured directly in the usual Hittorf experiment when a weighed amount of solution is analysed. In the moving boundary method a small correction† for volume changes is necessary. As this correction has already been fully treated, it will not be taken into consideration in this paper, *i.e.*, a section fixed with respect to the apparatus will be assumed fixed with respect to the solvent.

The mobility of a radical will be defined as its rate of transfer (in gram-equivalents per second) across a section of unit area normal to the potential gradient, divided by the concentration and by the potential gradient. The rate of transfer is assumed proportional to the potential gradient, *i.e.*, Ohm's law is assumed valid. This quantity will be identical with the mean velocity of any radical under unit potential gradient if the time interval considered be sufficiently great, and the equilibrium among the various states of combination in which the radical may occur is sufficiently rapid. It is assumed in this paper that this equilibrium is too rapid to have any disturbing effect.

The mobilities of electropositive and electronegative radicals we shall denote by  $U$  and  $V$ , respectively. These quantities are frequently called "ionic" mobilities. We shall confine this latter term to the mean velocity under unit potential gradient of an ion species  $i$  while it exists as the free ion, and denote this quantity by  $L_i$ . The relation between our  $U$   $V$  system and an  $L$  system will be dealt with in a future paper by one of us (G. S. H.).‡ When

\* 'Z. phys. Chem.,' vol. 69, p. 436 (1909).

† Lewis, 'J. Amer. Chem. Soc.,' vol. 32, p. 863 (1910). Cf. Longworth, *ibid.*, vol. 54, p. 2753 (1932).

‡ It is interesting to note that Faraday's original meaning of the word "ion" was that of our electropositive or electronegative radical. This meaning is now no longer in general use, particularly since the word was introduced into gaseous physics, and a return to it is neither possible nor desirable. In phrases like "anion transport number" Faraday's meaning persists and gives rise to considerable confusion.

the degree of dissociation is small,  $U$  or  $V$  may be small, even if  $L$  is large. Thus the mobility of lithium radical in decinormal lithium acetate is greater than that of hydrogen radical in decinormal acetic acid, although the mobility of hydrogen ion is much greater than that of lithium ion.

The quantities  $u = UF$  and  $v = VF$ , or  $L_i = L_i F$ , we shall call the "equivalent conductivities" of the radicals or ions concerned. These quantities are often called "mobilities," but we prefer the term used above, since the word "mobility" implies dimensions more consistent with those of our quantities  $U$ ,  $V$ , or  $L_i$ .

Since we confine ourselves to the radical quantities ( $u$ ,  $U$  and  $v$ ,  $V$ ), the conclusions we draw will be independent of assumptions as to the microscopic state of our solutions.

## II. Fundamental Relationships.

Consider a column of cross-sectional area  $Q$  of an electrolyte solution containing positive radicals  $A$ ,  $B$ , etc., whose concentrations in gram-equivalents per cubic centimetre are  $c_A$ ,  $c_B$ , etc., and negative radicals  $R$ ,  $S$ , etc. Let the specific conductivity be  $\kappa$ , and let a current  $I$  flow. Then from Ohm's law the potential gradient must be given by

$$\frac{dE}{dh} = \frac{I}{Q\kappa}. \quad (1)$$

By definition, the rate of transfer of the radical  $A$  is equal to  $\frac{I}{F} T_A$  gram-equivalents per second.

The mean velocity of the  $A$  radical is  $\frac{dE}{dh} U_A$  cm./second, hence the rate of transfer is equal to  $\frac{dE}{dh} U_A c_A Q = \frac{I}{\kappa} c_A U_A$ . Equating these values for rate of transfer, we obtain

$$T_A \kappa = c_A F U_A = c_A u_A. \quad (2)$$

In the case of a pure electrolyte, where  $\kappa/c$  is defined as  $\lambda$ , the equivalent conductivity, (2) simplifies to

$$T_A = \frac{u_A}{\lambda}. \quad (2A)$$

The total excess of positive over negative radicals transferred per second in the direction of positive current is  $\frac{I}{F} [\Sigma T_{A, B \dots} + \Sigma T_{R, S \dots}]$  gram-equivalents.



But an excess of positive radicals cannot be transferred without the transference of  $F$  coulombs of positive electricity per gram-equivalent, hence the product of this amount by  $F$  is equal to the current  $I$ , hence

$$\Sigma T_{A, B \dots} + \Sigma T_{R, S \dots} = 1 \quad (3)$$

Combining this with equation (2), we obtain

$$\kappa = \Sigma u_{A, B \dots} + \Sigma v_{R, S \dots} \quad (4)$$

and for a pure electrolyte this becomes

$$\kappa = uc + vc \quad \text{or} \quad \lambda = u + v. \quad (4A)$$

### III. The Rate of Displacement of Concentration in a Conducting Solution.

The theory of this subject has been treated by Kohlrausch,\* Weber,† and von Laue.‡ We present here a simpler treatment.

Let  $R$  be any negative radical in an electrolyte solution, pure or mixed, and let  $T_R$  and  $c_R$  be its transport number and concentration respectively. Consider a column of unit cross-sectional area, through which a current  $I$  is flowing, and where  $c_R$  is a function of the distance  $h$  along the column, as shown in fig. 1. Let the negative current be in the direction of increasing  $h$ .

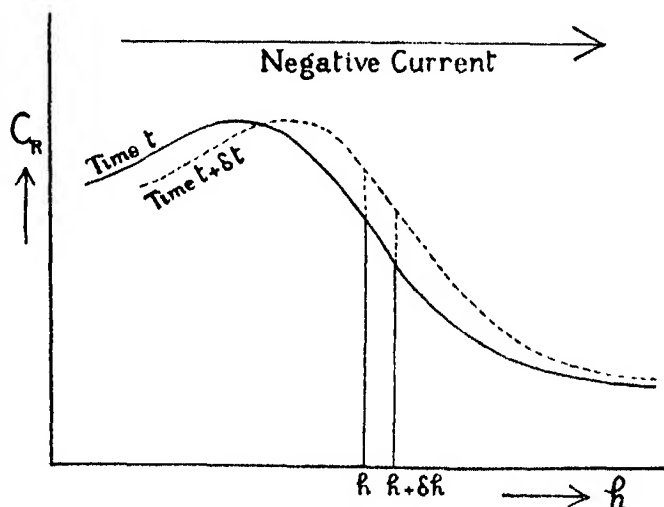


FIG. 1.

\* 'Ann. Physik,' vol. 62, p. 209 (1897).

† 'SitzBer. preuss. Akad. Wiss.,' p. 936 (1897).

‡ 'Z. anorg. Chem.,' vol. 93, p. 329 (1915).

During  $\delta t$  seconds there will pass a section at  $h$  in the direction of negative current  $I\delta t$  coulombs, and therefore, by definition,  $\frac{1}{F} T_R \delta t$  gram-equivalents of R. Similarly,  $\frac{1}{F} (T_R + \delta T_R) \delta t$  gram-equivalents will pass the section at  $(h + \delta h)$ , and consequently the elementary volume  $\delta h$  between them will lose  $\frac{1}{F} \delta T_R \delta t$  gram-equivalents of R, and the mean concentration in the volume will decrease by  $\frac{1}{F} \frac{\delta T_R}{\delta h} \delta t$ , which, in the limit where  $\delta h = 0$ , is equal to  $\frac{1}{F} \frac{dT_R}{dh} \delta t$ .

After a time  $\delta t$ , therefore, the initial concentration  $c_R$  in  $\delta h$  will assume a value  $\left( c_R - \frac{1}{F} \frac{dT_R}{dc_R} \frac{dc_R}{dh} \delta t \right)$ , which is the concentration initially obtaining at a distance  $-\frac{1}{F} \frac{dT_R}{dc_R} \delta t$  from the given section. This concentration has, therefore, advanced through a distance  $\frac{1}{F} \frac{dT_R}{dc_R} \delta t$  in time  $\delta t$ , i.e., it advances in the direction of negative current with a velocity

$$\frac{1}{F} \frac{dT_R}{dc_R}. \quad (5)$$

The function  $dT_R/dc_R$  will be a complicated one in the general case, because  $T_R$  is not a function of  $c_R$  alone, but also of the concentrations and mobilities of the other radicals present, which may be largely independent of  $c_R$ .

For a pure electrolyte, however,  $dT_R/dc_R$  is a unique function of  $c_R (= c_A)$  at any one temperature, and is, by (3) equal to  $-dT_A/dc_A$ .

A concentration in a pure electrolyte is therefore propagated or displaced in the direction of negative current with a velocity equal to  $\frac{1}{F} \frac{dT}{dc}$ .

Another special case of (5) is of interest. If we have a radical Y (say negative) present in small quantity in the presence of a large excess of other radicals at constant concentration,  $v_Y$  will be constant and  $d\kappa/dc_Y$  negligible.

$\frac{dT_Y}{dc_Y} = \frac{d}{dc_Y} \left( \frac{c_Y v_Y}{\kappa} \right)$  will therefore become  $v_Y/\kappa$ . The rate of displacement of the concentration of Y,  $\frac{1}{F} \frac{dT_Y}{dc_Y}$ , will therefore be

$$\frac{1}{F} \frac{v_Y}{\kappa} = \frac{dE}{dh} V_Y, \quad (6)$$

i.e., the concentration will advance with the velocity of the Y radicals.

In deriving (5), diffusion has been ignored. Its effect will, of course, be to flatten out any variations in concentration that may exist.

#### IV. *The Boundary between two Pure Electrolytes.*

A. *The Existence of the Boundary.*—Let a solution of AX lie above one of AR, as shown in fig. 2, and let us suppose that a certain amount of intermixing has occurred. The solutions are chosen so that the heavier of the two is below, and so that  $V_R$  is greater than  $V_X$  in any solution which may occur. Let us suppose the negative current to flow downwards.

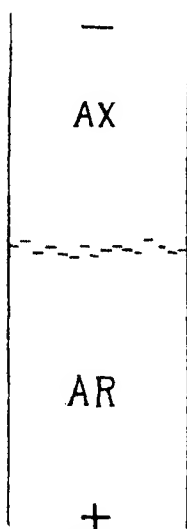


FIG. 2.

The motion of the R and X radicals can be arbitrarily split up into three simultaneous motions: (1) a uniform velocity of all the individual radicals in the direction of potential gradient; (2) additional velocities, depending on the instantaneous state of dissociation or aggregation, also in the direction of potential gradient, but positive or negative, having an average value of zero; and (3) the entirely random thermal motion, also with an average value of zero. We will first consider the effect of (1) alone, the others being assumed non-existent.

Since  $V_R$  is always greater than  $V_X$ , the R radicals will be moving faster than the X radicals in every part of the system. Wherever R and X radicals exist together, R radicals will always be overtaking X radicals, but X can never be overtaking R. Further, the velocity of the X radicals at any place will be equal, and hence the foremost of these radicals will remain the foremost throughout. If we start with a finite number of R radicals above this foremost X radical, it follows that after a finite time interval all the R radicals will have passed this X radical, i.e., complete separation of the two electrolytes will have occurred.

The effect of the other two component motions will clearly be to cause interdiffusion of the two electrolytes. The three components together will therefore give rise to an equilibrium condition giving a boundary of limited diffuseness. The theoretical calculation of the depth of the boundary is a matter of considerable difficulty,\* but it is found experimentally that with

\* Since this paper was communicated, a successful computation of the depth of the boundary between KCl and LiCl has been published by MacInnes and Longworth in a general review of the method ('Chem. Rev.', vol. 11, p. 171 (1932)).

suitable electrolytes and apparatus a boundary is obtained which appears as sharp as the interface between two immiscible liquids.

B. *The Velocity of the Boundary.*—Consider the system in fig. 2, in which the speed of the boundary is that of the R radicals immediately below it. AR is called the leading electrolyte and AX the indicator.

The rate of transfer of R in gram-equivalents per second across any section in AR is given by  $\frac{1}{F} T_R$ , where  $T_R$  is the transport number of R in the immediate neighbourhood of the section. Since the boundary remains sharp, then if the concentration of AR remains the same throughout the volume which will be swept out by the boundary during a determination, the volume velocity of the boundary is given by the equation

$$\frac{d\phi}{dt} = \frac{1}{F} \frac{T_R}{c_R}. \quad (7)$$

Within the boundary, diffusion and diffusion potential will invalidate the ordinary fundamental relationships of Section II. However, the only conditions that need be satisfied in order for the method to be valid are that the boundary should be sharp enough for its position to be accurately determined, and that the concentration of the solution into which it is advancing should remain constant.\*

C. *The Constancy of Concentration of the Leading Radical R.*—As Kohlrausch† has pointed out, it is impossible for concentration changes to develop spontaneously in the interior of a homogeneous solution as a result of electrolysis alone, hence regions of changed concentration can develop only at the boundary. Such regions can, however, be shown to disappear for all known cases.

Suppose that in some way the concentration has changed just below the boundary. This new concentration will advance with a velocity given by  $\frac{1}{F} \frac{dT_R}{dc_R}$ , assuming the column to be of unit cross-sectional area. The boundary will be moving with a velocity given by  $\frac{1}{F} \frac{T'_R}{c'_R}$ , where primed quantities are

values, not necessarily constant, in the region of changed concentration. If the region of change is moving upwards, it will meet the boundary and disappear; if it is moving downwards, it will be overtaken by the boundary and

\* The fact that in a satisfactory moving boundary system the velocity of the boundary remains constant, provided the current flowing is kept constant, is experimental proof that the boundary moves with the same velocity as the mean resultant velocity of the leading radicals, and that conditions in the boundary itself are unimportant.

† 'Ann. Physik,' vol. 62, p. 209 (1897).

disappear, provided that  $T_R/c_R$  is always greater than  $dT_R/dc_R$ . So far as we know, this is always true.\*

D. *The Concentration of the Indicator Radical X.*—Let us consider AR to remain homogeneous, and suppose the boundary to sweep through a small volume  $\delta\phi$  during the passage of a current  $I$  for a short time interval  $\delta t$ . From (7) it is evident that  $\delta\phi = \frac{1}{F} \frac{T_R}{c_R} \delta t$ . If  $T_X$  is the transport number of the X radical in AX, then  $\frac{1}{F} T_X \delta t$  gram-equivalents of X will have crossed the original position of the boundary into  $\delta\phi$ , and the mean concentration of X in this new region of indicator will be  $\frac{T_X}{T_R} c_R$ . If there are to be no regions of changed concentration developed in the indicator, this new concentration must be the same as the old, or  $\frac{T_X}{c_X} = \frac{T_R}{c_R}$ , which is the well-known relation of Kohl-

rausch. Where this relation is satisfied,  $\kappa_{AR} > \kappa_{AX}$ , or  $\left(\frac{dE}{dh}\right)_{AX} > \left(\frac{dE}{dh}\right)_{AR}$ .

The concentration and transport number of an indicator solution which satisfy Kohlrausch's relation will be denoted by the index K, and the relation will be written

$$\frac{T_X^K}{c_X^K} = \frac{T_R}{c_R}. \quad (8)$$

Suppose a boundary to be formed between AR and a solution of AX of concentration  $c'_X$ , differing from the Kohlrausch concentration. Consider a plane section above the initial boundary position at such a distance that a small volume  $\delta\phi$  lies between the two. Let a small time interval  $\delta t$  elapse, during which the boundary sweeps through an equal volume  $\delta\phi$ , which is equal to  $\frac{1}{F} \frac{T_R}{c_R} \delta t = \frac{1}{F} \frac{T_X^K}{c_X^K} \delta t$ . The amount of X crossing the section above the boundary is given by  $\frac{1}{F} T'_X \delta t$ , hence the mean concentration between this

section and the final position of the boundary is  $\frac{\delta\phi c'_X + \frac{1}{F} T'_X \delta t}{2 \delta\phi}$ , and substituting for  $\delta\phi$ , this is equal to  $\frac{1}{2} \left[ c'_X + c_X^K \frac{T'_X}{T_X^K} \right]$ .

\* Even in the rather extreme example of a 0.1-0.2 N cadmium iodide solution, an increased concentration would be propagated downwards with a velocity of about  $1.6 I/F$ , while the boundary between the region of change and some suitable indicator would move downwards with a velocity of at least  $4.2 I/F$ .

If the Kohlrausch concentration  $c_x^K$  differs by a finite amount from  $c'_x$ , then the mean concentration differs by a finite amount from  $c'_x$ , although  $\delta t$  and  $\delta\phi$  may be made indefinitely small. Hence any concentration change occurs abruptly. During this time interval the concentration change itself will have moved through a volume  $\frac{I}{F} \frac{dT_x}{dc_x} \delta t$ . This will, in all cases we know, be less than  $\frac{I}{F} \frac{T_x^K}{c_x^K} \delta t$ , i.e., less than the volume considered on either side of the original boundary position. Consequently there must exist a uniform concentration on either side of the abrupt change, which on the boundary side can only be the Kohlrausch concentration  $c_x^K$ .

E. *Mobility from the Velocity of the Boundary.*—If the cross-sectional area  $Q$  of the tube in which the boundary moves and the specific conductivity  $\kappa_{AR}$  of the AR solution are measured, the potential gradient in the latter can be calculated from (1).<sup>\*</sup> The mobility of R may then be obtained directly from the linear velocity of the boundary. This procedure is not essentially different from substituting the value of  $T$  obtained from equation (7) in equation (2). We use the quantities  $T$  and  $I$  rather than  $dE/dh$  and  $U$  or  $V$ , since  $I$  and not  $dE/dh$  is necessarily constant throughout the apparatus.

F. *The Movement of the Common Radical across the Boundary.*—Mukherjee† has claimed to show that there will always be a deficiency in the amount of the common ion behind a moving boundary, except when both the leading and the indicator ions (or radicals, to use our terminology) have the same transport numbers in their respective solutions. This deficiency would destroy electrical neutrality and seriously affect the motion of the boundary. This conclusion results from Mukherjee's having assumed that if the time interval considered be indefinitely small, the motion of the boundary can be neglected. Since, however, these infinitesimals are of the same order, this assumption is incorrect. As has been pointed out by MacInnes and Dole,‡ when the appropriate transport numbers are used and the movement of the boundary considered, transport of the common ion involves no violation of electrical neutrality.

<sup>\*</sup> Calculation of this quantity  $dE/dh$  from the total external potential difference applied, which is not infrequently done, is quite erroneous, since the value of  $\kappa$  cannot remain the same for both solutions.

† 'J. Indian Chem. Soc.,' vol. 5, p. 593 (1928).

‡ 'J. Amer. Chem. Soc.,' vol. 53, p. 1364 (1931).

*V. The Boundary between Two Pure Electrolytes—Experimental.*

In the preceding sections it has been shown theoretically that the velocity of a moving boundary is independent of the initial concentration of the following (indicator) solution, since in all realizable cases the leading solution remains of constant concentration, and the indicator solution adjusts its concentration to a final constant value. However, disturbing effects such as concentration and temperature convection have been ignored, and it will be shown that experimentally they limit the independence of the boundary velocity from the initial concentration of the indicator solution.

A. *Falling Boundaries.*—Early workers\* with moving boundaries, with the exception of Denison and Steele, did not obtain results of much quantitative significance. Denison and Steele assumed complete automatic adjustment of the indicator to the Kohlrausch concentration.

MacInnes, Smith, and co-workers,† in a series of investigations on solutions of uni-univalent electrolytes, found that the value obtained for the transport number of a radical varied with the concentration of the indicator radical, except in a fairly limited region about the Kohlrausch concentration. The general type of their curves is shown in fig. 3. The range in which transport number was independent of indicator concentration, was greater the more dilute the solutions and the smaller the bore of the tube in which the boundary moved. Within the adjustment range, the value of  $T$  was independent of the potential gradient used; outside it, higher potential gradients gave higher apparent transport numbers. Outside the adjustment range the variation in observed transport number was least when the difference in the mobilities of the leading and indicator radicals was greatest. The earlier measurements of these investigators are precise to at least 0.2 per cent.; in later work to 0.02 per cent.

\* Whetham, 'Z. phys. Chem.,' vol. 11, p. 220 (1893); Nernst, 'Z. Elektrochem.,' vol. 3, p. 308 (1897); Masson, 'Phil. Trans.,' A, vol. 192, p. 331 (1899); 'Z. phys. Chem.,' vol. 29, p. 501 (1899); Abegg and Gaus, *ibid.*, vol. 40, p. 737 (1902); Steele, *ibid.*, vol. 40, p. 689 (1902); Denison, 'Trans. Faraday Soc.,' vol. 5, p. 165, (1909); 'Z. phys. Chem.,' vol. 44, p. 575 (1903); Denison and Steele, *ibid.*, vol. 57, p. 110 (1906); 'Phil. Trans.,' A, vol. 205, p. 449 (1906).

† 'J. Amer. Chem. Soc.,' vol. 45, p. 2246 (1923), vol. 46, p. 1398 (1924); MacInnes and Brighton, *ibid.*, vol. 47, p. 994 (1925); Smith and MacInnes, *ibid.*, vol. 47, p. 1009 (1925); MacInnes, Cowperthwaite and Blanchard, *ibid.*, vol. 48, p. 1909 (1926); MacInnes, Cowperthwaite, and Huang, *ibid.*, vol. 49, p. 1710 (1927); MacInnes, Cowperthwaite and Shedlovsky, *ibid.*, vol. 51, p. 2671 (1929).

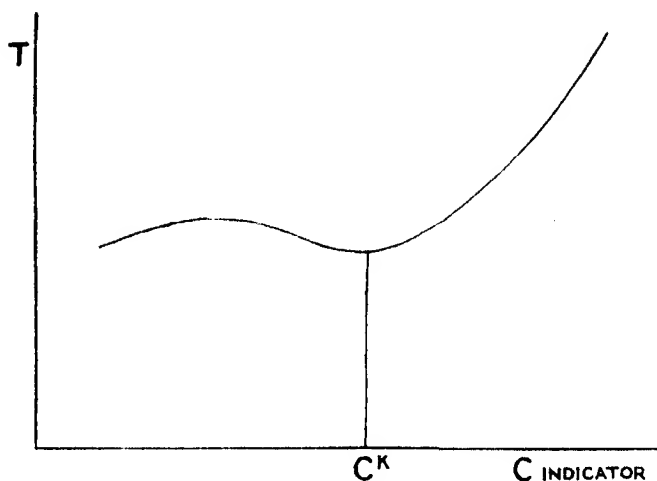


FIG. 3.

In the work done in this laboratory on dye solutions, the investigators obtained curves of the general type shown by fig. 4. To the left of the Kohlrausch concentration the transport number of the negative radical in the dye was independent, within the precision of the measurements (0.3 per cent.) of the indicator concentration. To the right the curve rose quite steeply.

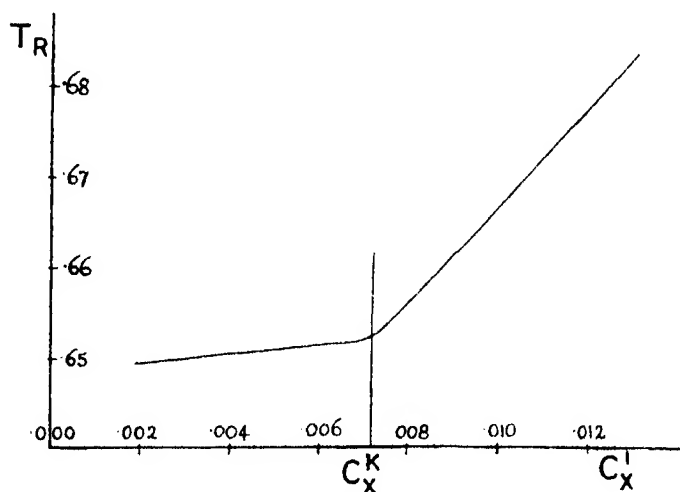


FIG. 4.

The increase in  $T$  to the right of the Kohlrausch concentration can be explained by convection effects. As Longworth\* has pointed out, convection currents will be set up by the original indicator solution above being heavier

\* 'J. Amer. Chem. Soc.,' vol. 52, p. 1904 (1930).



than the new indicator solution below, because the former is more concentrated,\* and, being a better conductor, cooler. The currents thus set up not only undo the automatic adjustment of the indicator, but sweep up a part of the leading solution. With dye solutions, fine red streamers are plainly visible running up into an indicator that was initially too concentrated, and the latter soon becomes coloured. The boundary remains sharp and the velocity fairly constant. Since a part of the leading solution has been carried up into the indicator, the value of  $d\phi/dt$ , and hence of  $T$ , is evidently too large.

These disturbing effects will be less, and therefore the adjustment range greater, with dilute solutions, for the density differences encountered will be less. The heat convection effect will be less in a small bored tube, for the heat developed is carried away more quickly. In an indicator solution near the adjusted value, the concentration remains fairly uniform along the column of indicator, hence temperature differences are not great, and the heat convection effect may be negligible, even with large potential gradients. The sharpening effect will act to return leading radicals, which have been swept up into the indicator, back to the leading solution; therefore the effect of convection currents will be partly neutralized when the difference in the mobilities of the leading and following radicals is very great.

**B. Rising Boundaries.**—Boundaries in which the indicator solution is heavier, and placed below the solution to be investigated, can be used only when the indicator radical is much slower and its solution much heavier than that of the leading radical, as Longworth (*loc. cit.*, 1930) has pointed out. Otherwise the heat convection set up by the warmer solution being below will seriously affect the shape and velocity of the boundary.† With a rising boundary the region of new indicator is above the old, hence concentration and temperature convection will affect the boundary if the original indicator was too dilute, but much less, if at all, when the indicator was originally too concentrated (Longworth, *loc. cit.*, 1930).

Cady and Longworth,‡ observing rising boundaries between solutions of alkali halides and indicator solutions of the corresponding cadmium salt formed electrolytically, estimated the concentration of the indicator near the boundary (a) from the change in the total resistance of their apparatus when a known length of leading solution had been displaced by indicator, and (b) by measuring

\* If the density of the indicator decreases with increasing concentration, the steep rise in  $T_R$  will be to the left of  $c_X^K$ .

† MacInnes, Cowperthwaite and Huang, 'J. Amer. Chem. Soc.', vol. 49, p. 1710 (1927).

‡ 'J. Amer. Chem. Soc.', vol. 51, p. 1656 (1929).

the conductivity just behind the boundary with two platinized points. Both measurements indicated, within the experimental error, that the indicator near the boundary was at the Kohlrausch concentration.

C. *The Sharpening Effect*.—The strength of the sharpening effect has been shown by MacInnes and Cowperthwaite,\* who stopped a boundary after noting its velocity, allowed the indicator and leading solutions to interdiffuse for periods up to half an hour, and then restarted the current; the boundary reformed and became perfectly sharp. After a given length of time, it had reached the point at which it would have been, subtracting the time that the current was off, if it had never been allowed to become diffuse; thence the boundary moved with its initial velocity. In the work on dyes previously mentioned, the same effect was observed.

These results are to be expected from theoretical considerations. The leading radicals, in the region unaffected by interdiffusion, proceed with their original velocity. Leading and indicator radicals are separated by the sharpening effect, and any regions of changed concentration in the leading solution near the boundary disappear. The indicator readjusts its concentration to the Kohlrausch value. Since the leading solution is again at its initial concentration, and since the same amount of current has been flowing as before the interruption, the boundary must be at the place at which it would have been if interdiffusion had not occurred.

D. *Erroneous Moving Boundary Measurements*.—Even in fairly recent literature, some authors have assumed that the slower, following ion (radical) determines the velocity of a boundary. This is a theoretical misconception, for it is the leading radical which remains of constant concentration, while the following radical changes its concentration to the Kohlrausch value. This assumption is also not in agreement with experiment. If the following radical did determine the velocity of the boundary, the velocity would depend on the initial concentration of the following radical. There would have been no flat places in the curves shown in paragraph (A) of this section, the slopes would have been much steeper, and the value of transport number obtained would have fallen with increasing concentration of the following radical, given the same current, instead of rising.

Engel and Pauli,† as a preliminary to measurements on colloids, used potassium chloride, sulphate, and acetate solutions as "indicators" for

\* 'Proc. Nat. Acad. Sci., Wash.,' vol. 15, p. 18 (1929).

† 'Z. phys. Chem.,' vol. 126, p. 247 (1927). See also Pauli and Valkó, "Die Elektrochemie der Kolloide," p. 151 (1929).

potassium permanganate, the permanganate always following. The boundary velocity, from which they attempted to calculate the mobility of permanganate, varied greatly and was larger the larger the mobility of the "indicator" radical. They therefore attack the method on the grounds that the velocity of a moving boundary is not independent of the nature of the "indicator," and quote Denison and Steele\* as having observed the same effect. The latter workers, however, had their indicators following the solutions to be measured, and observed that sometimes the values obtained for transport numbers varied with the nature of the indicator ion.† These variations were never so great as those found by Engel and Pauli, the largest being slightly over 1 per cent. Denison and Steele were also quite possibly outside the range of indicator concentration within which heat and concentration convection are negligible, for in the case cited they were working with a normal solution.

Lorenz and Neu‡ made a number of measurements, in at least some of which their "indicator" appears to have been leading the slower radical whose mobility was to be measured, for they state (p. 55) that the boundary always gives the velocity of the following ion. The method which they used for calculating mobilities from boundary velocities is not clear.

E. *The Moving Boundary Method and the Hittorf Method.*—Theoretically, the moving boundary method and the Hittorf method measure the same quantity by a direct and an indirect method, respectively, if the volume corrections previously mentioned are made in the moving boundary method. This was clearly pointed out by Miller.§

Discrepancies between older determinations by the two methods gave rise to misgivings, empirically justified at the time, as to the validity of the moving boundary method. Recent Hittorf measurements,|| however, with considerably improved technique, have shown striking agreement with the results of MacInnes, Longworth, and co-workers with moving boundaries. The latter workers have attained a higher degree of precision than is possible

\* 'Z. phys. Chem.,' vol. 57, p. 110 (1906).

† Recently Longworth has shown the velocity of a boundary to be independent of the nature of the following radical. ('J. Amer. Chem. Soc.,' vol. 54, p. 2752 (1932), especially Table VI.)

‡ 'Z. anorg. Chem.,' vol. 116, p. 45 (1921).

§ 'Z. phys. Chem.,' vol. 69, p. 436 (1909).

|| MacInnes and Dole, 'J. Amer. Chem. Soc.,' vol. 53, p. 1357 (1931) on KCl solutions; Jones and Bradshaw, *ibid.*, vol. 54, p. 138 (1932), and Longworth, *ibid.*, vol. 54, p. 2753 (1932) on LiCl.

with the Hittorf method, especially in very dilute solutions, and, as they point out, with far less effort.

#### VI. The Boundary between a Mixed Leading Electrolyte and a Pure Indicator.

If we have an electrolyte AS as indicator for a mixture of AR and AX, fig. 5, the mobilities always being in the order  $V_R > V_X > V_S$ , two boundaries will result: one between the original mixture and AX, and one between AX and AS. The system  $AR + AX$  followed by AX will be considered here, but it is impossible to use the same argument as before with regard to the sharpness of the boundary, and the treatment of the latter involves the previous assumption of the velocity of the boundary and is therefore logically incomplete.

A. *The Indicator Concentration and the Permanence of the Boundary.*—It can be shown by the reasoning of Section IV, D that, if a sharp boundary exists, the concentration of the indicator which is consistent with constancy of composition on either side of the boundary is given by

$$\frac{T_X^I - T_X^{II}}{c_X^I - c_X^{II}} = \frac{T_R^{II}}{c_R^{II}}, \quad (9)$$

where the index I refers to quantities in AX, and II refers to quantities in  $AR + AX$ .\*

A will usually be some univalent radical, and the R radical is the only one likely to be of high valence type. Consequently  $U_A$  will not be greatly different in the two solutions, or definitely less in solution (II), since mobility is lowered by the presence of a high valence radical of opposite sign. Further, the electrolytes are chosen so that  $V_R$  is greater in all solutions than  $V_X$ , hence  $T_A^{II}$  will usually be definitely less than  $T_A^I$ . Making use of equation (3), we obtain that

$$T_X^{II} + T_R^{II} > T_X^I,$$

and combining this with (9), we have that

$$c_X^{II} + c_R^{II} > c_X^I.$$

Since solution (II) will therefore be more concentrated than (I) and will also

\* On the assumption that the mobility ratio  $V_X/U_A + V_X$  is the same in both solutions, Longworth derives a special case of (9) and experimentally verifies it ('J. Amer. Chem. Soc.', vol. 52, p. 1897 (1930)).

—	
AS	
AX	I
AR AX	II
+	

FIG. 5.

contain a more mobile radical, it follows from (4) that  $\kappa_I$  will usually be less than  $\kappa_{II}$ , and hence

$$\left(\frac{dE}{dh}\right)_I > \left(\frac{dE}{dh}\right)_{II}.$$

From this last relation it follows that any R radicals diffusing into the region above the boundary will be accelerated and caused to overtake it. Below, the advancing boundary will largely suppress diffusion. The boundary will therefore remain sharp.

B. *Automatic Adjustment.*—If the boundary remains sharp, instantaneous accommodation in an indicator not satisfying (9), and being lighter than that which would satisfy (9), can be demonstrated exactly as before. Below the boundary, concentration changes cannot occur if  $dT_R/dc_R$  and  $dT_X/dc_X$  are both less than  $T_R^{II}/c_R^{II}$ . In the mixed solution  $dT_R/dc_R$  is not a function of  $c_R$  alone, but also of the change of  $c_X$  with  $c_R$

$$\frac{dT_R}{dc_R} = \left(\frac{\partial T_R}{\partial c_R}\right)_{c_X} + \left(\frac{\partial T_R}{\partial c_X}\right)_{c_R} \frac{dc_X}{dc_R}.$$

It is empirically true that  $(\partial T_R/\partial c_R)c_X$  will be less than  $T_R/c_R$  in all ordinary cases, and therefore an inequality in the concentration of R can advance at a greater velocity than the boundary only if  $dc_X/dc_R$  has some special value. Further, if the velocity of this region of change is to be maintained, this appropriate change of  $c_X$  with  $c_R$  must advance with it, i.e.,  $dT_X/dc_X$  and  $dT_R/dc_R$  must be equal, a condition that seems unlikely to be fulfilled. Accommodation in the leading solution is thus rendered improbable. It can be shown as in the case of pure AR leading pure AX that, if  $(dT_X/dc_X)^I$  is always less than  $T_X^I/c_X^I$ , the AX concentration in solution (I) will adjust its concentration automatically to that satisfying (9).

C. *Hydrolysis.*—Let us consider the case of a solution of AR where HR is a weak acid.  $OH^-$  ions will be present, and, if a non-hydrolysed electrolyte containing no added hydroxide be used as indicator, these  $OH^-$  ions will be removed from the region of AR immediately below the boundary, since  $L_{OH^-} > V_R$ . The AR in this region will therefore be further hydrolysed, more undissociated HR will therefore be formed, and the mobility of the R radicals thereby reduced until the equilibrium  $OH^-$  concentration is sufficiently low for the loss to be made up by the transfer from the indicator of  $OH^-$  formed by the dissociation of water. This may not occur before  $V_R$  has been reduced to less than  $V_X$ , in which case the boundary will be destroyed. At all events, the gradient of  $OH^-$  concentration built up in AR will produce a gradient of R concentration.

If free hydroxide were added to the indicator, this removal of  $\text{OH}^-$  from the AR region below the boundary might be compensated. The necessary concentration must satisfy the equation

$$\frac{T_R^{\text{II}}}{c_R^{\text{II}}} = \frac{T_{\text{OH}^-}^{\text{I}} - T_{\text{OH}^-}^{\text{II}}}{c_{\text{OH}^-}^{\text{I}} - c_{\text{OH}^-}^{\text{II}}} \quad (10)$$

The AX concentration must simultaneously satisfy the Kohlrausch relation (8), but there seems no reason why the concentrations could not be so chosen as to satisfy both (8) and (10), at least initially. The system, however, will not be stable. If a small quantity of OH diffuse from (I) to (II), the new  $\text{OH}^-$  concentration just below the boundary will advance with a linear velocity equal to  $\left(\frac{dE}{dh}\right)_{\text{II}} L_{\text{OH}^-}^{\text{II}}$ , from equation (6), since the  $\text{OH}^-$  concentration is small.

But the linear velocity of the boundary is  $\left(\frac{dE}{dh}\right)_{\text{II}} V_R^{\text{II}}$ , and since  $L_{\text{OH}^-}^{\text{II}}$  will be greater than  $V_R^{\text{II}}$ , the new concentration will advance into the leading solution, and the initial conformity to equation (10) will be destroyed. The moving boundary method is therefore inapplicable to an electrolyte which is appreciably hydrolysed. The reasoning of this section can, of course, be used to show that appreciable degree of hydrolysis of the indicator will also invalidate the method.

In conclusion, we should like to thank Professor F. G. Donnan, C.B.E., F.R.S., for the kindly interest he has shown in this investigation, and Mr. B. Topley, Mr. H. Terrey, and Dr. O. J. Walker for textual criticisms. We are also particularly indebted to Dr. Conmar Robinson, with whom this paper has been discussed at considerable length.

### Summary.

I. The quantities used in this paper: transport number, mobility, and equivalent conductivity of a radical, are defined in terms independent of assumptions as to the state of dissociation or aggregation of the electrolytes considered.

II. The fundamental relations among these quantities are worked out.

III. The equations governing the displacement of concentrations in conducting solutions are derived.

IV. If there be a moving boundary between two pure electrolyte solutions having a common radical, and if the leading non-common radical be faster than the following non-common radical, it is shown theoretically that :—

- A. The two solutions become separated up to a limit determined by diffusion.
- B. The expression giving transport number of the leading radical from the boundary velocity can be derived on the assumption that the leading radical remains at constant concentration.
- C. For all known electrolytes, the leading radical remains at constant concentration.
- D. There is a concentration of the following (or indicator) solution at which inequalities in it cannot develop. The indicator automatically attains this concentration.

V. Experimental work on both rising and falling boundaries, and particularly the effect of temperature and concentration convection, is discussed. Apparent deviations from theory are shown to be due to these effects. Erroneous moving boundary measurements in the literature are criticized, and the theoretical and experimental connection with the Hittorf method is pointed out.

VI. It is also shown, though less rigidly than in the case of two pure electrolytes, that a sharp boundary will usually exist under similar conditions between a mixture of two electrolytes with a common radical and a pure solution of the one which has the slower non-common radical. The equation relating the three concentrations concerned, and that governing the velocity of the boundary, are derived. The case of a hydrolysed electrolyte is briefly discussed.

---

*The Scattering of Electrons in Thin Films.*

By G. O. LANGSTROTH, Ph.D., 1851 Exhibition Scholar, King's College,  
London.

(Communicated by O. W. Richardson, F.R.S.—Received November 2, 1932.)

*Introduction.*

The laws governing the single elastic scattering of electrons by atoms have been fully investigated from the theoretical side. The more general problem which includes inelastic scattering has also been investigated,\* but the results are not readily applicable to experimental data.

The nature of the results of experimental investigations varies considerably; for the most part electron energies of at least 40 kilovolts and comparatively thick foils have been used. The results of these experiments,† which are not wholly in accord for different investigators, indicate that the variation of scattering with voltage and with angle follows the Rutherford law. The absolute intensity is in all cases too large, and it appears to vary with the atomic number of the scattering atom more rapidly than predicted.

On the other hand, with films of the order of  $10^{-6}$  cm. thick and with lower voltages there appears to be no consistent agreement with any theory of elastic scattering.‡ In general, the angle distribution curves are found to be very much flatter than the theoretical. Moreover, the intensity relations between the coherent and general scattering in electron diffraction experiments with thin films exhibits anomalous characteristics.§ Not even the background, near the centre of the pattern at least, is scattered in accordance with the classical theory of multiple scattering.||

In the present experiment the scattering of electrons of from 8 to 25 kilovolts energy by films of various thicknesses was studied, with the object of ascertaining whether the observed behaviour is due to a serious modification of the elastic scattering laws in this region or to some other factor.

\* Elsasser, 'Z. Physik,' vol. 45, p. 522 (1927).

† Schonland, 'Proc. Roy. Soc.,' A, vol. 113, p. 87 (1926); Neher, 'Phys. Rev.,' vol. 38, p. 1321 (1931).

‡ Klemperer, 'Ann. Physik,' vol. 3, p. 849 (1929).

§ Thomson, 'Proc. Roy. Soc.,' A, vol. 125, p. 352 (1929).

|| White, 'Phil. Mag.,' vol. 9, p. 641 (1930).



The following measurements were made : (1) The angle distribution of the scattered electrons between  $65^\circ$  and  $160^\circ$  for various thicknesses of celluloid and aluminium film, and its variation with voltage ; (2) the total number of electrons scattered back (between  $60^\circ$  and  $170^\circ$ ) from various thicknesses of aluminium film, and its variation with voltage ; (3) a few determinations of the probability of transmission for a thick aluminium leaf ( $7 \times 10^{-5}$  cm.), and its variation with voltage. Electrons of less than 3.5 kilovolts energy, and a large fraction of those of considerably higher energy, were prevented from entering the measurements by the use of a retarding foil. In the total intensity and transmission measurements a retarding potential of lower value was used.

The angle distribution curves for celluloid under single scattering conditions were found to be in all cases flatter than the theoretical. They showed a systematic variation with voltage and with film thickness which was not due to multiple scattering. The scattered intensity was of the predicted order of magnitude.

The angle distribution curves for aluminium showed little variation in form over the wide range of conditions employed, although with the thinnest films used single scattering conditions prevailed. The absolute intensity of scattering was several times that predicted for elastic scattering.

The manner in which variations with film thickness and with voltage occur indicates that in most cases the scattered quantity contains a considerable number of secondary electrons, which have at least one-half the primary energy, and which come for the most part from within small distances from the film surface. This is not at variance with the results of scattering experiments with higher voltages and thicker foils, for under these conditions their effect must be comparatively small. That they do occur is known from the experiments of Neher (*loc. cit.*).

The results also lead to the following conclusions : (a) The angle distribution curves for elastic scattering in this voltage region do not differ from those predicted by the Rutherford or Wentzel formula by more than 10 per cent. at intervals of  $20^\circ$ . There is reason to believe that the discrepancy is less than this ; (b) the probability of the production and escape of high speed secondary electrons is considerably greater for aluminium than for celluloid ; (c) experiments carried out on the scattering of electrons in this region of voltage and film thickness are capable of yielding an accurate determination of the elastic scattering laws only if very high retarding potentials are used.

If the presence of high-speed secondary electrons, which have the characteristics indicated by these experiments, is general, it furnishes an explanation of the anomalous intensity characteristics observed in diffraction experiments with thin films. In particular it does so for aluminium and celluloid.

### 1. Applications of Theory.

The results of this experiment in the single scattering region have been compared with the Wentzel wave mechanics formula for elastic scattering by an atom.\* The distribution is given by

$$\rho = \frac{nt}{16} \left( \frac{eZ}{V} \right)^2 \frac{1}{(\sin^2 \theta/2 + \alpha^2)^2}, \quad \alpha^2 = \frac{13 \cdot 4 Z^2}{V (\text{volts})},$$

where  $n$  is the number of atoms per cubic centimetre of the scatterer,  $t$  is the thickness of the scattering film,  $Z$  is the atomic number of the scattering atoms, and  $V$  is the voltage through which the primary electrons fall. It differs from the Rutherford, or from the non-relativistic wave mechanics formula† for nuclear scattering in the constant  $\alpha^2$ , which takes account of the screening effect of the atomic charge cloud. With 12 kilovolt electrons the screening effect lowers the ratio of the intensity scattered at  $100^\circ$  to that at  $160^\circ$  by about 0.4 per cent. for celluloid, and by about 18 per cent. for aluminium. The wave mechanics expression for nuclear scattering with relativity and electron spin taken into account,‡ gives the ratio  $100^\circ/160^\circ$  at 12 kilovolts to be about 2 per cent. higher than the Rutherford value.

There seems no reason to believe that appreciable modification of these laws is necessary for the voltages used in this experiment. Mott§ has estimated that the influence of radiative forces on the scattering is never more than 2 or 3 per cent. On the relativistic classical theory,|| there was some doubt concerning the behaviour of electrons which had traversed "spiral" orbits,¶ but these are not predicted by the wave mechanics for the magnetic electron.\*\*

It is highly improbable also, that scattering of incident electrons by orbital electrons can appreciably affect the measurements. On the assumption that

\* 'Z. Physik,' vol. 40, p. 590 (1927).

† Gordon, 'Z. Physik,' vol. 48, p. 180 (1928).

‡ Mott, 'Proc. Roy. Soc.,' A, vol. 135, p. 429 (1932).

§ 'Proc. Camb. Phil. Soc.,' vol. 27, p. 255 (1931).

|| Darwin, 'Phil. Mag.,' vol. 25, p. 201 (1913).

¶ Schonland, 'Proc. Roy. Soc.,' A, vol. 119, p. 673 (1928).

\*\* Mott, 'Proc. Roy. Soc.,' A, vol. 124, p. 425 (1929).

the latter behave as an electron gas, no electrons are scattered through more than  $90^\circ$ .<sup>\*</sup> This assumption neglects the binding energy of the orbital electrons which with aluminium is an appreciable fraction (about 0.06 for the K shell) of the primary energy at 20 kilovolts. A high upper limit can be calculated if the electrons be assumed to be fixed scattering centres of atomic number one. Their contribution is then  $Z/(Z^2 + Z)$  of the total intensity. Scattering by conduction electrons cannot be effective, since their number, as indicated by theories of thermal and electrical conductivity, is of the same order of magnitude as that of the atoms, and they approximate more nearly to the ideal of an electron gas.

Single scattering conditions were estimated with the aid of Wentzel's criterion.<sup>†</sup> This depends on the experimental evaluation of the ratio  $\theta/4\omega$  which has been found to increase considerably with the primary voltage.<sup>‡</sup> The value 3.0§ was used in all cases, but final estimates were made from examination of the observed curves and their variation with voltage.

## 2. Apparatus.

*Angle Distribution Measurements.*—The tube for the determination of angle distribution is shown diagrammatically in fig. 1. The Faraday cylinder C and earthed surrounding cylinder were mounted on a crank, and could be rotated about the target F as shown by means of a ground glass joint. An

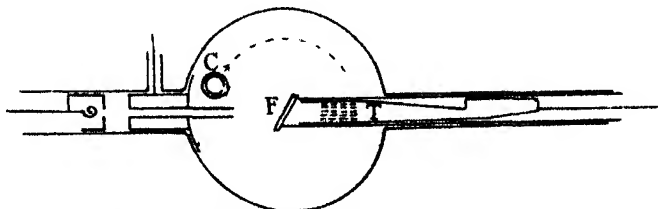


FIG. 1.—Experimental tube for angle distribution measurements.

angle reading device was attached to the crank outside the shielding. The diameter of the circular openings in the cylinders subtended an angle of about

<sup>\*</sup> Darwin, 'Phil. Mag.,' vol. 27, p. 499 (1914); see also Mott, 'Proc. Roy. Soc.,' A, vol. 126, p. 259 (1930).

<sup>†</sup> 'Ann. Physik,' vol. 69, p. 335 (1922).

<sup>‡</sup> Neher, *loc. cit.*

<sup>§</sup> Cf. Rutherford, Chadwick and Ellis, "Radiations from Radioactive Substances" (1930).

4° at the film. The opening of the protecting cylinder was covered with a carefully chosen aluminium foil, whose transmission characteristics are contained in the data. The Faraday cylinder was connected to one set of quadrants of a Dolezalek electrometer.

The scattering film was mounted on a metal ring about 1 cm. in internal diameter, which was fastened to the electron trap T by a small screw. The angle between the normal to the foil surface and the direction of incidence of the electrons was 30°.

The electron trap was designed in accordance with the fact observed by Rupp, that electrons striking a surface at an angle near grazing undergo almost complete specular reflection. It contained "baffle plates" of thin metal foil placed edgewise to the direction of incidence of the electrons. A ground glass joint enabled it to be easily removed to change a film, and to be replaced in exact position. It was connected to earth through a sensitive galvanometer.

The electron source was a thoriated tungsten filament. The diameter of the circular openings in the electron gun was 1.5 mm. and the length of the anode passage was 45 mm. The electron beam did not spread appreciably as shown by discoloration on films which had been used a great deal. The anode was always earthed.

The containing tube was made of pyrex. The interior surface of the main bulb was silvered and kept at earth potential; the outside was covered with metal foil also earthed. The seals with the exception of the greased crank joint were made with sealing wax.

The pumping system consisted of a two-stage mercury diffusion pump backed by a Hyvac oil pump, liquid air and charcoal being used to condense residual vapours. In general a pressure of less than  $10^{-6}$  mm. of mercury was maintained.

The high potential was obtained from the terminals of two oil immersed glass plate condensers, each of capacity 0.033 microfarads, kept charged through a rectifying tube by a large induction coil operated by a mercury break.

*Total Scattering Measurements.*—The tube is shown diagrammatically in fig. 2. Because of the insulation I, electrons scattered by more than 170° were not included in the measurements. The aluminium cylinder C and the trap T were connected to earth through sensitive galvanometers. The grid R was kept at the required negative potential, usually 186 volts.

*Transmission Measurements.*—In order to determine the fraction of the incident electrons transmitted by a foil, the tube for total scattering was used with slight modifications. The foil was mounted on a holder which fitted into

cylinder C and made good contact with it. The electron trap with the foil-holder removed to give it a 90° end, was placed very close behind the foil and

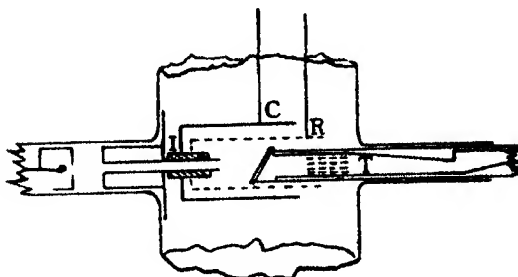


FIG. 2.—Experimental tube for total scattering measurements.

served as a Faraday cylinder. When required a retarding field could be applied between the trap and the foil. Each was connected to earth through a sensitive galvanometer.

### 3. Procedure.

*Angle Distribution Measurements.*—The following were the important measurements :—

(a) The angle of scattering was measured by a 5 cm. pointer fixed to the Faraday cylinder crank and a semi-circular scale. This device was frequently calibrated. Single angle readings were correct to 2°.

(b) Absolute measurement of primary voltage was made by means of a spark gap of 4 cm. balls.\* In order to detect variations in voltage during the measurements, an electrostatic voltmeter with a long light needle, and a long focus telescope were used. The latter was placed alongside the electrometer scale. The cross hair of the telescope was set on the voltmeter needle at the instant of sparking and the spark gap was then widened. The deflection was watched during drift measurements, and any variation was corrected by altering the primary current of the induction coil. The controls were placed so that this could be done while observing the deflection. The error in absolute voltage at 15 kilovolts was less than 2.3 per cent. and the variation during a run did not exceed 2 per cent.

(c) The scattered current was determined by reading the rate of drift of the electrometer. The sensitivities corresponding to various needle voltages varied from 7.20 to  $1.87 \times 10^{-13}$  amperes per millimetre per second.

\* Kaye and Laby, "Physical and Chemical Constants," 6th ed., p. 97.

(d) The transmitted and absorbed current was proportional to the deflection of the galvanometer connected to the electron trap. The sensitivity,  $2.32 \times 10^{-10}$  amperes per millimetre, was decreased when necessary by shunting. The spot of light was thrown on the electrometer scale.

A single determination of a distribution curve consisted in taking readings at intervals of  $10^\circ$  from  $60^\circ$  to  $160^\circ$ , and then back from  $160^\circ$  to  $60^\circ$ . In the region where the intensity change was rapid the interval was reduced to  $5^\circ$ .

In making a series of measurements both large and small incident currents were used in order to detect if possible any constant error. No variation of the ratios was observed when this was done.

In order to determine the effect of stray scattering in the apparatus, and of X-rays, measurements were made without a scattering film. The curves so obtained were subtracted from those obtained with a film in calculating the results. The magnitude of the correction was about 4 per cent. for a celluloid film  $5 \times 10^{-5}$  cm. thick, and considerably less for the aluminium films.

A series of tests showed that inductive effects were absent.

*Total Scattering and Transmission Measurements.*—The ratio of the scattered to the incident current was given by the ratio of the current through the galvanometer connected to cylinder C, to the sum of both galvanometer currents. The transmission measurements were similar. The sensitivities of the galvanometers without external shunts were 2.86 and  $4.76 \times 10^{-10}$  amperes per millimetre.

Two sets of readings, one with a large and one with a small incident current, were always taken at each voltage. No variation in ratio was observed. The correction for stray scattering was less than 2 per cent. Inductive effects were absent.

#### 4. *The Scattering Films.*

*Celluloid Films.*—These were prepared by evaporating a solution of celluloid in amyl acetate (concentration 0.00200 gm. per cubic centimetre) on a water surface. After mounting, the films were dried in an oven at about  $40^\circ$  C. for a day or two. This seemed to increase their strength. They were easily punctured in the tube and for this reason very small incident currents had to be used.

The thickness was determined from the amount of solution used to produce a film of known area, and it is believed that the error introduced in this way is

less than 20 per cent. For the following reason, however, the films were thinner than calculated: it was found that the scattering power of a film decreased slowly with use, and that the spot where the electrons impinged differed in appearance from the rest of the film. This is no doubt due to partial volatilization of the constituents with a consequent decrease in thickness. Such volatilization does take place rapidly with celluloid at about 130° C. The ease with which films were punctured if too high incident currents were used supports this view.

In order to make theoretical estimates of absolute intensity and single scattering conditions it is necessary to know  $n$  the number of atoms per cubic centimetre, and  $\bar{Z}$  the effective atomic number. The composition of celluloid may vary in the degree of nitration of the cellulose, and in the proportion and nature of the solvent. The calculations were based on a composition of 75 parts  $C_{24}H_{32}N_8O_{36}$  to 25 parts  $C_{10}H_{16}O$ , suggested by analyses of this substance. The uncertainty in the constants was estimated by considering the effect on them of varying the proportion and composition of the constituents. While  $n$  and  $\bar{Z}$  may reasonably be changed by as much as 18 and 6 per cent., the change is in opposite directions so that the change in  $n\bar{Z}^2$  is never more than 10 per cent. The spacing of the planes\* and a probable structure† is known from the results of electron diffraction experiments.

The effective atomic number (5.4) was calculated from  $\bar{Z}^2 = \frac{\sum_K Z_K^2 n_K}{\sum_K n_K}$ , where the subscripts refer to the various elements involved. The value of  $n$  ( $9.6 \times 10^{22}$  atoms per cubic centimetre) was determined from the density in the usual way.

*Aluminium Films.*—The large films required for this work were made by an electrolytic method. A piece of aluminium leaf was floated on a 0.4 per cent. aqueous solution of hydrochloric acid. This was made an anode by touching it with a fine wire, and an aluminium rod inserted vertically in the solution served as a cathode; the aluminium was then electrolysed away from the foil until the desired thickness was obtained. The optimum current was found by trial.

The method is extremely flexible; beaten leaf is very irregular in thickness and only small areas, here and there, are suitable for films. The foil was viewed by transmitted light while it was being electrolysed, and one could

\* Thomson, 'Proc. Roy. Soc.,' A, vol. 119, p. 651 (1928); Reid, *ibid.*, vol. 119, p. 663 (1928).

† Jones, 'Phil. Mag.,' vol. 12, p. 641 (1931).

judge in about a minute whether any areas were suitable; in this way a very large area of foil could be examined in a short time. The ratio of the suitable to the unsuitable area was about 1 : 600 for the leaf used.

Satisfactory films could be made in this way whereas etching by hydrochloric acid (or caustic soda solution) was entirely unsuccessful. In the latter case the films were always broken by bubbles of gas if high concentrations were used, or were irregular and had many small holes with low concentrations. This is probably due to the solution penetrating crevices in the foil and enlarging them as etching proceeds. On the other hand, thinning electrolytically tends to reduce, rather than to increase, existing irregularities.

The films were mounted in the following way. After washing, enough methylated alcohol was introduced on to the surface of the water to form a thick layer in which the film floated. A metal ring was manoeuvred under the film and it was removed vertically. The advantage of the method is obvious when one considers that the surface tension of water and alcohol are approximately 73 and 23 dynes per centimetre. It was possible to mount easily films which would break on an attempt to remove them from a water surface.

The films were standardized by determining their absorption of white light at normal incidence, and their thicknesses were estimated from these measurements. When the thickness is very small the equation  $\log_{10} \frac{i_0}{i_t} = at$ , holds approximately, where  $i_t$ ,  $i_0$  are the transmitted and incident intensities,  $t$  is the thickness in  $\mu$ , and  $a$  is a constant which can be calculated from metal reflection data. The value 25 has been used, but optical constants for thin metal films appear to vary to some extent with the method of preparation of the film.\*

Small regions existed in all aluminium films which visual examination showed to be thicker than the surrounding parts. In order to obtain an estimate of the thickness of these, contact photographs were taken of several films in which a part had been overlapped in mounting to form a double thickness. In a series of positives made with varying exposure times, the dark spots due to the irregularities disappeared before the general blackening of the double thickness. For this reason it is believed that the thickness of the irregular regions does not exceed, and is probably less than, twice the film thickness. This, as well as the increased effective thickness due to film tilt, has been taken into account in the theoretical calculations.

\* 'Int. Crit. Tables,' vol. 5, p. 255 *et seq.*



## 5. Results.

*Angle Distribution Measurements.*—For this apparatus, the ratio ( $\rho_0$ ) of the Rutherford scattering at any angle ( $\theta$ ), to the incident current is given by

$$\rho_0 = \frac{\pi nt}{448} \left( \frac{eZ}{V} \right)^2 \left[ \cot^2 \frac{\theta_2}{2} - \cot^2 \frac{\theta_1}{2} \right] \frac{1}{\sin \theta}$$

where  $(\theta_1 - \theta_2) = 4.1^\circ$  and  $\theta = \frac{1}{2}(\theta_1 + \theta_2)$ . The Wentzel values, which are given in the tables, can be easily obtained from the known ratio of the Wentzel to the Rutherford scattering.

The experimental values for absolute intensity have been calculated for elastic scattering. Upper limits for aluminium have been estimated by assuming that the scattered electrons have the same energy distribution as those from solid aluminium.\*

A correction must be made to the absorbed and transmitted current as given by galvanometer readings, if an appreciable portion of the incident current is scattered. Such a correction is essential for aluminium and has been made from the total scattering data. Corrections for stray scattering were also made.

Because of the large number of angles involved it is not convenient to tabulate experimental readings directly. The values in the tables have been taken from the experimental curves.

For purposes of comparison the theoretical and experimental curves for celluloid have been fitted together at  $80^\circ$ . This does not involve a change greater than the uncertainty in the values. The estimated absolute intensity scattered at  $120^\circ$  is, however, given in Table I.

Table I.—Celluloid : absolute intensity scattered at  $120^\circ$ .

Film thickness ( $10^{-5}$ cm.) .....	5			1	
	8	12	16	8	12
Energy (kv.) .....					
Theory ( $\times 10^{-6}$ ) .....	20.5	9.35	5.41	4.11	1.87
Experiment ( $\times 10^{-6}$ ) .....	19	9.3	7.4	2.7	1.8

\* Wagner, 'Phys. Rev.', vol. 35, p. 98 (1930).

Table II.—Celluloid : relative intensity scattered at various angles. Measurements were also made with a film  $1.3 \times 10^{-4}$  cm. thick (see fig. 4).

Film thickness	$5 \times 10^{-5}$ cm.						$1 \times 10^{-5}$ cm.			
	8 kv.		12 kv.		16 kv.		8 kv.		12 kv.	
Energy	Theory.	Exp.	Theory.	Exp.	Theory.	Exp.	Theory.	Exp.	Theory.	Exp.
Angle.	Theory.	Exp.	Theory.	Exp.	Theory.	Exp.	Theory.	Exp.	Theory.	Exp.
70	—	36.0	—	19.0	—	15.6	—	12.3	—	65°=3.36
75	—	—	—	—	—	17.2	—	14.1	—	6.38
80	60.4	60.4	29.0	29.0	16.9	16.9	12.2	12.2	5.78	5.78
85	50.2	65.1	24.5	27.6	14.3	15.3	9.90	9.04	4.96	—
90	43.0	61.0	20.6	25.1	12.0	14.0	8.40	7.87	4.20	4.78
100	32.2	50.2	15.0	21.1	8.75	11.6	6.42	6.15	3.03	4.48
110	25.3	39.9	11.6	17.4	6.60	10.1	5.02	5.28	2.32	4.48
120	20.4	29.5	9.38	14.6	5.41	9.16	4.11	4.90	1.87	4.48
130	17.2	25.6	8.00	12.8	4.60	8.67	3.51	4.85	1.60	4.48
140	15.0	23.3	6.90	11.7	4.01	8.43	3.01	4.90	1.38	4.48
150	13.5	21.7	6.20	11.0	3.59	8.40	2.73	4.95	1.23	4.71
160	12.5	21.4	5.70	11.0	3.28	8.30	2.50	5.02	1.15	5.00

Table III.—Aluminium : absolute intensity scattered from a film transmitting 25 per cent. of the incident light (maximum thickness  $7 \times 10^{-6}$  cm.).

Energy	20 kv.		16 kv.	12 kv.	8 kv.
Angle	Theory ( $\times 10^{-6}$ ).	Experiment ( $\times 10^{-6}$ ).	Experiment ( $\times 10^{-6}$ ).	Experiment ( $\times 10^{-6}$ ).	Experiment ( $\times 10^{-6}$ ).
70	—	8.61	9.79	18.7	16.4
80	3.31	18.5	18.6	35.0	32.1
90	—	23.7	24.5	41.2*	38.4
100	1.86	25.8	26.7	42.2	38.4
110	—	24.3	26.5	41.2	34.0
120	1.24	20.7	23.3	36.7	30.1
130	—	17.3	20.5	31.2	25.7
140	0.92	14.7	17.9	27.4	21.7*
150	—	13.7	15.4	23.9	18.5
160	0.78	12.9	13.7	21.5	13.6
160†	—	13.9	15.2	27.8	27.5

\* The single scattering angle limit is marked by an asterisk.

† These values were estimated on the assumption that the energy distribution of the scattered electrons was similar to that of electrons scattered from solid aluminium.

Distribution curves were also obtained at 24, 20, 16, 12 and 8 kilovolts with a film of maximum thickness  $1 \times 10^{-5}$  cm., and at 25, 20 and 14 kilovolts with a film  $7 \times 10^{-5}$  cm. thick. The distributions were similar to those above

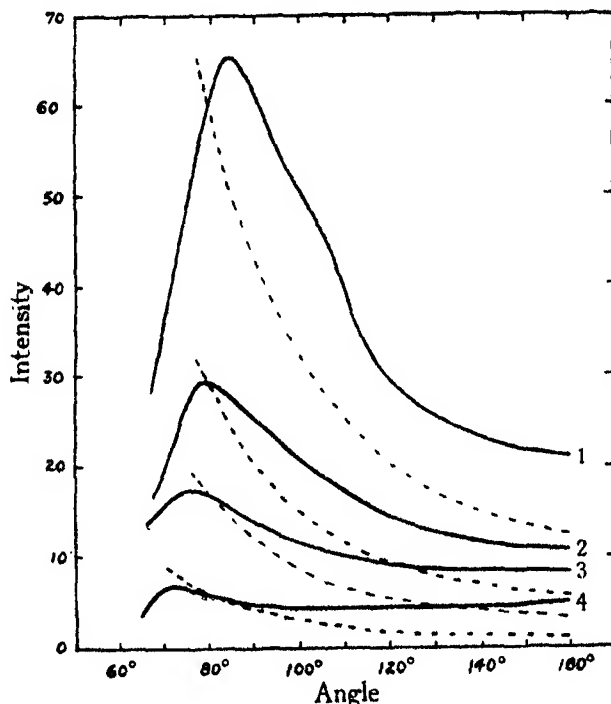


FIG. 3.—Some angle distribution curves for celluloid. Curves (1), (2) and (3) are for 8, 12 and 16 kilovolt electrons, with a film  $5 \times 10^{-5}$  cm. thick. Curve (4) is for 12 kilovolt electrons, with a film  $1 \times 10^{-5}$  cm. thick. The Wentzel distributions are indicated by dotted lines.

The sharp intensity decrease in these curves below  $75^\circ$  or  $80^\circ$  is due to the fact that as the angle of scattering approaches that of the film plane, the electrons traverse increasingly longer distances within the film before escaping, and hence are more and more strongly absorbed. For example, an 8 kilovolt electron scattered through  $150^\circ$  at a point  $2.5 \times 10^{-5}$  cm. from the film surface, stands about a 1000 times better chance of escaping without a further collision of  $10^\circ$  or more, than one scattered through  $75^\circ$ .

given and there was no change in the position of the maximum. The curve for 14 kilovolts and  $7 \times 10^{-5}$  cm. thickness has been included in fig. 4.

*Total Scattering Measurements.*—The total number of electrons scattered back from the film is, for Rutherford scattering,

$$R = \frac{\pi n t}{4} \left( \frac{eZ}{V} \right)^2 \left\{ 0.325 + \frac{1}{\pi} \int_{60}^{120} -\cos^{-1}(1.73 \cot \theta) \cot \theta/2 \operatorname{cosec}^2 \theta/2 d\theta \right\}.$$

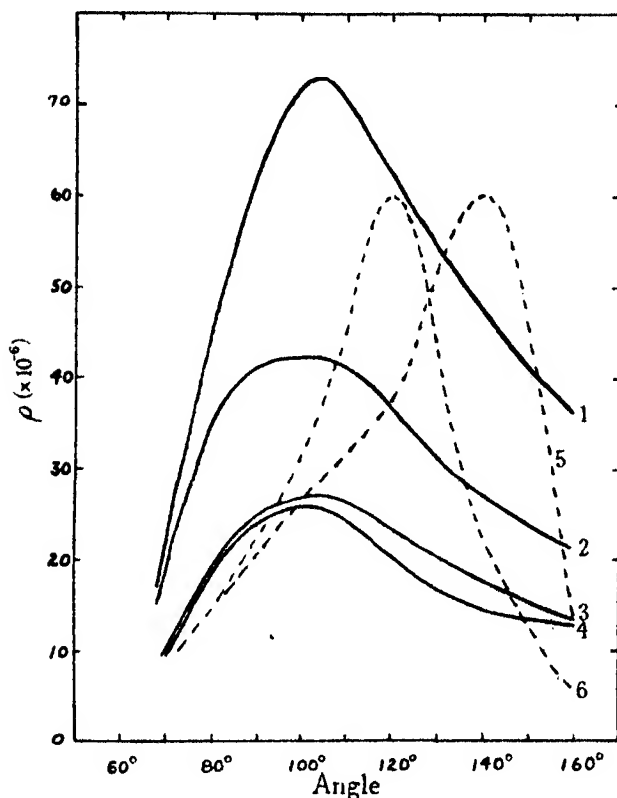


FIG. 4.—Absolute scattering curves for aluminium. Curves (2), (3) and (4) are for a film  $7 \times 10^{-6}$  cm. maximum thickness at 12, 16 and 20 kilovolts. (1) is for a film  $7 \times 10^{-6}$  cm. thick at 14 kilovolts. The dotted lines (5) and (6) are curves for a celluloid film  $1.3 \times 10^{-4}$  cm. thick at 8 and 16 kilovolts. The ordinates for (5) and for (6) are in arbitrary units.

Table IV.—Fraction of the incident electrons scattered back from aluminium films with more than 186 volts energy.

Light transmission (per cent.) .....	30	29	23	15	5	0
Maximum thickness ( $\times 10^{-6}$ cm.) ....	6.0	6.0	7.2	9.0	30	70
kv.						
4	0.106	0.113	0.111	0.144	0.169	0.190
8	0.0940	0.0985	0.114	0.141	0.166	0.194
12	0.0795	0.0888	0.104	0.125	0.147	0.181
16	0.0681*	0.0743*	0.0940	0.117	0.137	0.171
20	0.0578	0.0644	—	0.105*	0.122	0.148
24	0.0450	0.0534	—	0.093	0.111	0.134

\* Single scattering should prevail under these conditions. The predicted scattering for columns 1, 2 and 4 at 20 kilovolts is 0.00322, 0.00322 and 0.00482.

Energy distribution determinations with low retarding potentials indicate that relatively few scattered electrons have energies between 40 and 186 volts.

*Transmission Measurements.*—Table V contains the data for the retarding foil.

Table V.—Fraction of the incident beam transmitted by an aluminium film  $7 \times 10^{-6}$  cm. thick.

Energy (kv.) .....	4	6	8	10	12	16	20
No retld. pot. ....	0.0053	0.0560	0.267	0.453	0.590	0.720	0.770
186 v. retld. pot. ....	0.000	0.0017	0.0693	0.190	0.319	0.478	0.560

#### 6. Discussion.

(a) *Celluloid.*—The greatest discrepancy from theory of the absolute magnitude of the observed scattering (Table I) is 37 per cent. Owing to the uncertainty in  $n$ ,  $Z$ ,  $t$ ,  $V$ , and the error introduced in determining apparatus dimensions, the theoretical calculations are good to only 40 per cent. The observed values should be good to 10 per cent. Theory and experiment therefore agree within these limits.

The theoretical estimates are probably too high, because partial volatilisation of the film takes place, and also because a straightforward application of the theory yields too high results if inelastic scattering is appreciable. This follows from the fact that all electrons passing a nucleus within a distance  $\rho_s$  are considered as being scattered by more than  $\theta$ , and the total scattering is calculated by comparing the sum of all areas  $\pi\rho_s^2$  with the total area under consideration.

The ratios expressing the variation of the scattered intensity with voltage should be good to less than 13 per cent. Two points in their behaviour are significant: (a) while the intensity ratio for 12 : 8 kilovolts is only 6 per cent. too large for the thick film, it is 41 per cent. too large when a thin film is used; (b) the discrepancy of the observed ratio from the theoretical increases with the voltage, being about 46 per cent. too large for 16 : 8 kilovolts with a thick film.

The observed angle distributions are in all cases flatter than the theoretical. The closest approach to the Wentzel distribution gives the ratio  $120^\circ/150^\circ$  to be about 10 per cent. low. Observational errors should not account for more than a 5 per cent. variation. The curves show systematic variations of two

types, (a) a decrease in slope with increasing voltage and (b) a decrease in slope at large angles with decreasing film thickness.

As previously stated the variations from theory cannot be due to extraneous effects such as stray scattering, or X-ray effects. If they were due to electronic scattering or radiation, one might expect to find the curves steeper than theory, since electrons scattered at large angles should have lost a greater fraction of their energy. This is not the case, neither can they be attributed to multiple scattering. The curve for the thick film at 8 kilovolts shows a distortion below about  $110^\circ$  which is due to multiple or plural scattering. This disappears with increased voltage and the general form of the curve remains unchanged with further increase. It is believed that the highest single scattering angle limit for the data is about  $120^\circ$ . The Wentzel criterion value for 12 kilovolts and  $5 \times 10^{-5}$  cm. thickness is  $117^\circ$ , but owing to the uncertainty in the calculations this may be as low as  $106^\circ$ . Moreover, the calculated values should be too high for reasons similar to those which cause the intensity calculations to be too high. The presence of multiple scattering in this experiment would produce angle distributions steeper than the theoretical, and a variation with voltage more rapid than predicted. The observed behaviour is just the reverse.

The character of the results is believed to be due to the presence of secondary electrons of at least half the primary energy which are emitted most strongly at small angles to the normal to the film surface. On this basis both the variation with voltage and with film thickness receive a satisfactory explanation as follows.

The experimental ratios for variation of intensity with voltage for the thick film are 1 : 0.49 : 0.39 at 8, 12 and 16 kilovolts. The theoretical values are 1 : 46 : 0.266. If the total number of secondary electrons produced at 12 and 16 kilovolts does not differ greatly one can estimate from the absorbing characteristics of the retarding foil what percentage contribution they should make at 12 kilovolts, if at 16 kilovolts they are 46 per cent. of the total. The result is about 5 per cent., which is in accord with the observations. Moreover, the decreasing slope of the angle distribution curves with increasing voltage is explained, since a greater number of secondary electrons have sufficient energy to penetrate the retarding foil and thus impose their distribution on that for elastic scattering.

The variations with film thickness\* are accounted for if secondary electrons formed deep within a film lose an appreciable fraction of their energy by

\* Neher (*loc. cit.*) has observed a similar effect with much higher voltages and thicker films.

multiple scattering and further inelastic collision before escaping. A rough calculation shows that the greatest probability of escape without passing through an entire K shell is 250 times larger for a secondary electron formed  $1 \times 10^{-5}$  cm. from the surface, than for one formed at  $5 \times 10^{-5}$  cm. The frequency of inelastic collision must be comparatively high for these low voltages. Moreover, the probability of escape without undergoing a nuclear deflection of more than  $10^\circ$ , is about 40 times greater for an electron formed at  $1 \times 10^{-5}$  cm., than for one formed at  $5 \times 10^{-5}$  cm. These values will be considerably increased by the fact that the electrons do not travel in straight lines within the film.

It seems reasonable to suppose that the number of secondary electrons escaping with sufficient energy to enter the measurements is not very much greater for a  $5 \times 10^{-5}$  cm. film than for one  $1 \times 10^{-5}$  cm. thick at these low voltages. On this basis, a discrepancy from the theory of 41 per cent. for the latter would lead one to expect one of about 8 per cent. for the former because of the increase in elastic scattering. The observed ratio of the intensity scattered at 8 kilovolts to that at 12 kilovolts is 1:0.65 for the thin, and 1:0.49 for the thick film. The theoretical ratio is 1:0.46, so that this explanation gives results in accord with the observed facts. This method of comparison is permissible, since the number of secondary electrons penetrating the retarding foil at 8 kilovolts primary energy must be relatively small.

In addition, the decrease in slope of the observed curves with decreasing film thickness is well explained, since with the thin film the secondary electron distribution is imposed relatively about five times as strongly.

This explanation is sufficient to account for all aspects of the scattering, which greatly increases the probability of its being the correct one. Since the observed distribution curves approach the curve for elastic scattering as secondary electrons are eliminated, the true curves cannot differ from the predicted curves by more than the least discrepancy noted in this experiment. This is less than 10 per cent. for the ratio  $120^\circ/150^\circ$ . An experiment carried out with much higher retarding potentials should yield accurate curves for elastic scattering.

(b) *Aluminium*.—The results for aluminium contain the following significant features.

(1) The absolute intensity of all electrons scattered back from a film with energy greater than 186 volts is roughly 18 times greater than expected for single elastic scattering. Calculations from the angle distribution measurements, of the absolute intensity scattered at  $140^\circ$  with

more than 3.5 kilovolts energy give values about 16 times greater than expected.

(2) The observed variation with voltage of the intensity of all electrons scattered back from a film with energy greater than 186 volts, is given by  $\rho = A - 0.0029 V$ , where  $A$  is a constant depending on the foil thickness. This is true both for regions where Wentzel's criterion is fulfilled, and for those in which multiple scattering should predominate. The intensity variation with voltage for secondary electrons of more than 3.5 kilovolts energy, as calculated from the angle distribution measurements, takes place more rapidly, but still considerably more slowly than the theory.

(3) The angle distribution does not vary in form for those conditions under which single scattering should exist and for those under which multiple scattering predominates.

(4) The variation with voltage of the fraction of the incident electrons transmitted by a foil  $7 \times 10^{-5}$  cm. thick is best expressed by the relation  $T = e^{-K/V^2} - AV^2$ , where  $K$  and  $A$  are constants.

The results are entirely different from those expected for single scattering. As previously stated extraneous effects cannot be the cause. It is believed that they are not due to multiple scattering. The aluminium films, however, contained regions of unequal thickness. The photographic examination described, indicated an upper limit of twice the thickness as calculated from light absorption measurements, and this value has been used in all the theoretical calculations. In order to account for multiple scattering at  $150^\circ$  with 20 kilovolt electrons, the film would have to contain areas  $6 \times 10^{-5}$  cm. thick. These would be quite opaque, and it is difficult to see how they could have escaped detection in a film transmitting 30 per cent. of the incident light. Moreover, if the scattering were simply multiple, there should have been a change in the form of the angle distribution curve as single scattering conditions were approached. No appreciable variation was observed.

The character of the results is believed to be due to the presence of high speed secondary electrons. As in the case of celluloid these probably come from within small distances from the film surface.\* If the great majority come from within  $7 \times 10^{-6}$  cm. from the surface for a primary energy of 20 kilovolts,

\* The probability that a secondary electron, formed  $6 \times 10^{-6}$  cm. below the surface and travelling normally to it, should escape without passing through the M and L shells of an atom is less than 1 in 10,000. The radius of the L shell was taken from the charge distribution calculations of James, Brindley and Wood, 'Proc. Roy. Soc.,' A, vol. 125, p. 401 (1929).



the intensity of single scattering at  $140^\circ$  for a film  $7 \times 10^{-5}$  cm. thick should be about 2.3 times the predicted value. That the discrepancies noted by Schonland (*loc. cit.*) in the region of 40 kilovolts were not so large as this may be due to a decrease in the probability of production of secondary electrons with increasing voltage. This is to be expected since the time of stay of an electron in an atomic field is less and since the energy of the primary electrons is farther from the ionization energy (1200 volts). That these electrons do exist with primary voltages as high as 128 kilovolts, and that they exhibit similar characteristics to those found in this experiment, is known from Neher's work (*loc. cit.*).

The fact that the "excess" scattering is greater for aluminium than for celluloid indicates that the probability of production and escape of high speed secondary electrons is much greater for the former.

A masking effect of the secondary electrons from aluminium probably accounts for the difference in the character of the angle distribution curves for thick films shown in fig. 4. While the form of the curve for a film  $7 \times 10^{-5}$  cm. thick did not change from that for the thinnest film of aluminium, the curve for a celluloid film  $1.34 \times 10^{-4}$  cm. thick showed a decided movement of the maximum toward larger angles, as conditions receded from single scattering conditions. The aluminium film was equivalent to a celluloid film  $2.6 \times 10^{-4}$  cm. thick as estimated by Wentzel's criterion, so that multiple scattering should have been farther advanced for it.

(c) It is of interest to examine the results of other experiments to see if the presence of high-speed secondary electrons, such as are indicated by this experiment, makes itself felt. Klemperer and Neher both found evidence of high speed electrons other than those elastically scattered. A group of experiments which should show their presence strongly are those on coherent scattering, for conditions are favourable for them appreciably to affect the results, *i.e.*, very thin films and comparatively low voltages.

In this respect Thomson (*loc. cit.*) has made the following observations. (1) The increase in critical voltage (*i.e.*, that at which the rings become indistinguishable from the background) with increased film thickness is surprisingly small. (2) The critical voltage seems to be considerably lower for non-conducting films than for films of pure metal. (3) There appears to be a lower limit at about 10 kilovolts beyond which rings cannot be obtained. They appear again at about 300 volts as shown by Rupp's\* work.

\* 'Ann. Physik,' vol. 1, p. 773 (1929).

This behaviour may be accounted for in the following way, if slow electrons are not very effective in producing photographic blackening.

(1) Two lead films of approximate relative thickness 1 : 9 had respective critical voltages of 15·5 and 27 kilovolts. If the background is due entirely to multiple scattering, one should expect a much higher value for the latter voltage (about 45 kilovolts). If, however, there is a considerable proportion of high speed secondary electrons in the scattered quantity at 15·5 kilovolts, a considerably lower value than 45 is to be expected. This is so since the percentage effect of fast secondary electrons will be several times less with the thick film, and since the number produced at the higher voltage will be somewhat less.

(2) Thomson's lead foils had a limiting critical voltage of about 15·5 kilovolts, but a compound of lead gave rings with voltages as low as 5·8 kilovolts. Photographs with metallic oxides have been obtained with very low primary voltages\* and celluloid shows rings at least as low as 6·5 kilovolts.† The present experiment indicates that the probability of production and escape of fast secondary electrons is considerably greater for aluminium than for celluloid. This fact accounts for the lower critical voltage limit found for celluloid and suggests that other cases may be due to the same cause.

Finally some curves of White's (*loc. cit.*) indicate that the variation of the intensity of the background with angle is not so marked as might be expected if it were due entirely to multiple scattering. This is in accord with the presence of high speed secondary electrons.

In conclusion I wish to express my thanks to Professor O. W. Richardson for helpful criticism, to the engineering department of King's College for the loan of apparatus, and to the Royal Commission for the Exhibition of 1851 whose award made this work possible.

#### *Summary.*

(1) The angle distribution of electrons scattered between 65° and 160° by celluloid and aluminium films of various thickness has been determined for various primary voltages between 8 and 25 kilovolts. No electrons of less than 3·5 kilovolts energy entered the measurements, and single scattering conditions were fulfilled for the thinnest films.

\* Ponte, 'C. R. Acad. Sci. Paris,' vol. 188, p. 244 (1929); 'Ann. Physique,' vol. 13, p. 395 (1930).

† Jones, 'Phil. Mag.,' vol. 12, p. 641 (1931).

(2) The total number of electrons scattered back from various thicknesses of aluminium film with more than 186 volts energy was determined for primary voltages of from 8 to 24 kilovolts.

(3) The fraction of the incident electrons transmitted by a thick aluminium foil ( $7 \times 10^{-5}$  cm.) was determined for primary voltages of from 4 to 20 kilovolts.

(4) The results show systematic variations from the predicted results for elastic scattering.

(5) The variations are believed to be due to the presence of a considerable number of high speed secondary electrons. These must possess at least half the primary energy, and must come for the most part from within small distances from the film surface. Their effect in experiments with thicker foils and higher voltages should be comparatively small.

(6) The probability of production and escape of fast secondary electrons is believed to be considerably smaller for celluloid than for aluminium, at these voltages.

(7) The presence of secondary electrons of the characteristics indicated by these experiments is sufficient to explain the anomalous intensity relations observed in electron diffraction experiments with thin films.

(8) The departure from the Wentzel law for single elastic scattering under these conditions is not more than 10 per cent. at intervals of  $20^\circ$ . There is reason to believe that it is much less than this.

---

*The Relation between Mean Atomic Volume and Composition in  
Copper-Zinc Alloys.*

By Professor E. A. OWEN, M.A., D.Sc., and LLEWELYN PICKUP, M.Sc.(Lond.),  
Ph.D.(Wales), University College of North Wales, Bangor.

(Communicated by Sir William Bragg, O.M., F.R.S.—Received October 11, 1932.)

A great deal of work has been done by X-ray methods on the relation between atomic volume and composition in alloy systems, but a large portion of the data so far recorded has not been determined with the high precision attainable by present methods of analysis. This paper contains the results of precision measurements on copper-zinc alloys covering the whole range of composition from one end of the equilibrium diagram to the other.

Previous work in this field covers several binary systems. Vegard and his co-workers examined the alkali halides,\* the copper-nickel and other alloys,† and found that generally the lattice dimensions change linearly with the composition. The gold-copper system did not follow this rule; this was confirmed later by van Arkel and Basart,‡ who deduced from their observations that the fifth exponent of the atomic "diameter" was more suitable than the first as an additive quantity. Westgren and his collaborators§ also measured the lattice dimensions of a number of binary alloy systems. They found that a marked contraction takes place in all cases where chemically unrelated metals are alloyed with each other, the contraction being too pronounced to make the linear dimensions additive. In a paper on the silver-cadmium alloy systems, by Astrand and Westgren,|| the change in atomic volume with composition is traced through all the pure phases  $\alpha$ ,  $\beta$ ,  $\gamma$ ,  $\epsilon$  and  $\eta$  of that system. The discontinuities between the phases are but slightly marked; this is taken to indicate that in this system the atoms occupy approximately the same space, whatever their grouping may be. Owen and Preston,¶ in a study of the copper-zinc system, tentatively took a smooth curve through the determined

\* Vegard and Schjelderup, 'Phys. Z.', vol. 18, p. 1 (1917).

† Vegard, 'Skr. VidenskSelsk. Christ.', vol. 14 (1927); Vegard and H. Dale, 'Z. Kristallog.', vol. 67, p. 148 (1928).

‡ 'Z. Kristallog.', vol. 68, p. 475 (1928).

§ Westgren and Phragmen, 'Trans. Faraday Soc.', vol. 25, p. 379 (1929).

|| 'Z. anorg. Chem.', vol. 175, p. 90 (1928).

¶ 'Proc. Phys. Soc. Lond.', vol. 36, p. 49 (1923).

atomic volumes for various compositions. They found a marked contraction in atomic volume.

#### *Experimental Procedure.*

The experimental technique was the same as that adopted in the determination of phase boundaries in the copper-zinc equilibrium diagram.\* The X-ray photographs were taken by the aid of precision cameras, with which lattice parameters could be determined to an accuracy of at least 1 in 4000. Since the reflection lines in the photographs could be readily identified, the atomic volumes of both phases in the mixed regions, in addition to those in the pure regions, could be separately determined and accurately studied.

The alloys were subjected to prolonged heat treatments at suitable temperatures in lump form to produce homogeneity, and before mounting on the precision camera, each specimen was further annealed in the form of filings to remove the effect of cold work. Previous investigation had shown that it was only by paying close attention to the heat treatment that reliable results could be obtained. The filings used for each photograph were analysed after the photograph was taken. It was considered more satisfactory to adopt this procedure than to conduct the analysis on a portion of the specimen which had not actually been used to produce the photograph.

Since much work had already been done on filings annealed at 500° C., it was decided to keep to this temperature as far as possible. Below about 30 per cent. copper, annealing was carried out at 380° C., since the alloys became partially liquid slightly above this temperature. The specimens were annealed in evacuated thin-walled tubes of ordinary glass or pyrex, and all samples were rapidly air-cooled from the annealing temperature, since it had been found in a separate investigation that the quenching operation into iced-water, which entailed more time and labour, gave, within experimental error the same parameter values.

Unless otherwise stated, the X-ray tube was fitted with a copper target.

#### *General Survey of the Different Phases.*

In Tables I to V are set out the parameters, mean atomic volumes and compositions of the alloys examined in the various phases. The  $\alpha$ -phase has a face-centred cubic structure, the  $\beta$ -phase a body-centred cubic structure, and the  $\gamma$ -phase a body-centred cubic structure containing 52 atoms in the unit cube. The  $\epsilon$ - and  $\eta$ -phases have close-packed hexagonal structures.

\* Owen and Pickup, 'Proc. Roy. Soc.,' A, vol. 137, p. 397 (1932).

Table I.

 $\alpha$ -phase ; annealing temperature 500° C.

Copper per cent.		Parameter A.	Mean atomic volume $\times 10^{24}$ cm. <sup>3</sup>
By weight.	Atomic.		
100	100	3.607 <sub>0</sub>	11.741
90.6	90.9	3.627 <sub>7</sub>	11.935
89.3	89.6	3.629 <sub>1</sub>	11.949
76.8	77.3	3.657 <sub>6</sub>	12.233
74.8	75.4	3.662 <sub>0</sub>	12.286
70.3	70.9	3.673 <sub>2</sub>	12.390
67.3	67.9	3.679 <sub>7</sub>	12.456
62.7	63.4	3.692 <sub>0</sub>	12.591
61.7	62.3	3.693 <sub>0</sub>	12.601
59.5	60.2	3.696 <sub>0</sub>	12.625
58.1	58.8	3.695 <sub>1</sub>	12.614
57.6	58.3	3.695 <sub>5</sub>	12.617

Table II.

 $\beta$ -phase ; annealed at 500° C.

Copper per cent.		Parameter A.	Mean atomic volume $\times 10^{24}$ cm. <sup>3</sup>
By weight.	Atomic.		
59.8	60.5	2.942 <sub>7</sub>	12.748
58.1	58.8	2.942 <sub>4</sub>	12.740
57.6	58.3	2.942 <sub>0</sub>	12.748
52.9	53.6	2.945 <sub>1</sub>	12.779
49.4	50.1	2.949 <sub>1</sub>	12.824
43.4	44.1	2.949 <sub>2</sub>	12.826
42.2	42.0	2.949 <sub>1</sub>	12.824

Table III.

 $\gamma$ -phase ; annealed at 500° C.

Copper per cent.		Parameter A.	Mean atomic volume $\times 10^{24}$ cm. <sup>3</sup>
By weight.	Atomic.		
42.2	42.9	8.819 <sub>0</sub>	13.192
41.2	41.8	8.828 <sub>2</sub>	13.231
39.6	40.3	8.837 <sub>1</sub>	13.274
35.5	36.2	8.855 <sub>0</sub>	13.353
31.1	31.7	8.874 <sub>0</sub>	13.440

Table III.—(continued).  
 $\gamma$ -phase ; annealed at 380° C.

Copper per cent.		Parameter A.	Mean atomic volume $\times 10^{24}$ cm. <sup>3</sup> .
By weight.	Atomic.		
45.3	46.0	8.829 <sub>8</sub>	13.239
41.4	42.1	8.830 <sub>7</sub>	13.243
38.7	39.4	8.837 <sub>6</sub>	13.273
35.3	36.0	8.854 <sub>1</sub>	13.348
30.4	31.0	8.874 <sub>6</sub>	13.441
24.6	25.1	8.873 <sub>7</sub>	13.437

Table IV.  
 $\epsilon$ -phase ; annealed at 380° C.

Copper per cent.		Parameters.		Mean atomic volume $\times 10^{24}$ cm. <sup>3</sup> .
By weight.	Atomic.	a in A.	c.	
23.5	24.0	2.730 <sub>3</sub>	1.570	13.835
20.2	20.7	2.732 <sub>3</sub>	1.568 <sub>8</sub>	13.854
16.8	17.2	2.745 <sub>6</sub>	1.561	13.904
13.2	13.5	2.759 <sub>6</sub>	1.554 <sub>2</sub>	14.137
11.7	12.0	2.760 <sub>6</sub>	1.554	14.156
9.0	9.2	2.760 <sub>2</sub>	1.554	14.155

Table V.  
 $\eta$ -phase ; annealed at 380° C.

Copper per cent.		Parameters.		Mean atomic volume $\times 10^{24}$ cm. <sup>3</sup> .
By weight.	Atomic.	a in A.	c.	
4.2	4.30	2.673 <sub>8</sub>	1.804	14.932
1.8	1.85	2.688 <sub>9</sub>	1.817 <sub>6</sub>	14.965
1.0	1.02	2.664 <sub>6</sub>	1.836	15.041
0	0	2.659 <sub>1</sub>	1.856	15.108

These results are shown graphically in fig. 1. The boundaries of the  $\beta$ -phase at 500° C. are taken from our previous paper. The atomic volume of each phase in a mixed region remains constant in this series of alloys, but the constant atomic volume of one phase depends on the other phase with it. For example, the atomic volume of the  $\beta$ -phase is smaller in the presence of the  $\alpha$ -phase than it is in the presence of the  $\gamma$ -phase. Similar changes in the constant atomic volumes of  $\gamma$ -,  $\epsilon$ -, and  $\eta$ -phases are noted after annealing at 380° C.

The fall in atomic volume in the  $\gamma$ -phase alloys annealed at 500° C. persists beyond 40 atomic per cent. copper and is consistent with the position of the  $(\beta + \gamma) - (\gamma)$  boundary already recorded. At 380° C., the phase boundary assumes approximately the value given to it in the accepted equilibrium diagram of the system.

From the slopes of the nearly-linear curves of fig. 1 the change in the mean atomic volume which takes place in the pure regions when a zinc atom replaces

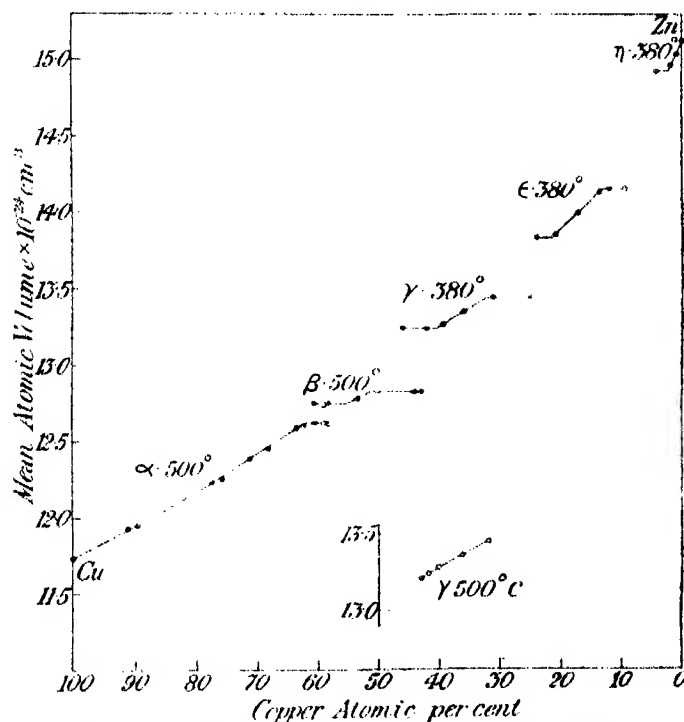


FIG. 1.—Cu-Zn alloys. Mean atomic volume of phases.

a copper atom can be approximately calculated. The figures obtained are given in Table VI.

Table VI.

Phase.	Increase in mean atomic volume when a zinc atom replaces a copper atom.
$\alpha$	$0.022 \times 10^{-24} \text{ cm.}^3$
$\beta$	0.025
$\gamma$	0.022
$\epsilon$	0.043
$\eta$	0.070



The increase in mean atomic volume produced by the substitution of a zinc atom for a copper atom is nearly the same in each of the phases  $\alpha$ ,  $\beta$  and  $\gamma$ . The zinc atom, therefore, occupies approximately the same volume in these three phases. The increase in the  $\alpha$ -,  $\beta$ - or  $\gamma$ -phase is about half that in the  $\epsilon$ -phase, and about a third that in the  $\eta$ -phase. Hence assuming a "spherical" copper atom and a "non-spherical" zinc atom, the latter occupies different volumes according to the phase in which it is found, and this appears only possible by a change of orientation in packing.

The next point considered was whether information regarding the relation between the different phases could be obtained from the mean distances between the atoms when new phases appeared. Accordingly, the mean distance of the closest approach of atoms was calculated for the minimum lattice of each phase. It was found that in pure copper and in the minimum lattice of the  $\beta$ -phase, the closest distance of approach was 2.55 Å. The same value was obtained from the minimum lattice of the  $\gamma$ -phase if it were assumed that seven atoms arrange themselves along the diagonal of the cube. When the distance of closest approach was calculated for the two hexagonal lattices ( $\epsilon$  and  $\eta$ ), it was found that in the  $\epsilon$ -phase the values ranged from 2.661 to 2.672 Å. and in the  $\eta$ -phase from 2.863 to 2.906 Å. These figures do not appear to bear any relation to the values calculated for the  $\alpha$ -,  $\beta$ - and  $\gamma$ -phases. From the examination of other alloy series forming similar phase fields to those appearing in the copper-zinc series, it was concluded that the identity of the value of the distance of the nearest approach of atoms in pure copper, the minimum lattice of the  $\beta$ -phase and the minimum lattice of the  $\gamma$ -phase was only characteristic of the copper-zinc alloys and was not found in the other series examined.

From the curves in fig. 1 showing the relation between mean atomic volume and composition, the values given in Table VII are obtained for the phase boundaries.

Table VII.

Phase boundary.	Temperature.	Composition in per cent. copper.	
		Atomic.	By weight.
	° C.		
( $\alpha$ ) - ( $\alpha + \beta$ )	500	62.2	61.5
( $\alpha + \beta$ ) - ( $\beta$ )*	500	55.3	54.6
( $\beta$ ) - ( $\beta + \gamma$ )*	500	51.4	50.7
( $\beta + \gamma$ ) - ( $\gamma$ )	380	40.5	39.8
( $\gamma$ ) - ( $\gamma + \epsilon$ )	380	32.3	31.7
( $\gamma + \epsilon$ ) - ( $\epsilon$ )	380	21.5	21.0
( $\epsilon$ ) - ( $\epsilon + \eta$ )	380	13.0	12.7
( $\epsilon + \eta$ ) - ( $\eta$ )	380	2.0	1.9

\* The values of these boundaries were obtained from previous work.

*Detailed Analysis of the  $\varepsilon$ - and  $\eta$ -Phases.*

The photographs of the hexagonal phases revealed some interesting features which called for further investigation. To derive the two parameters of the hexagonal lattice—the base side  $a$  and the axial ratio  $c$ , the following formula was employed :—

$$a = \lambda \sqrt{\frac{4(h^2 + hk + k^2)/3 + l^2/c^2}{2 \cos(s/8r)}}, \quad (1)$$

where  $s$  is the measured arc between corresponding lines in the photographs,  $r$  the radius of the camera, and  $h$ ,  $k$  and  $l$  the Miller indices for the reflecting planes. Reflections from at least two sets of planes, with different Miller indices, are required to determine the two parameters. But if the planes giving reflection lines have indices of the form  $(hko)$ , the value of  $a$  can be determined from only one set of reflecting planes, since then  $l^2/c^2$  disappears from the formula.

The camera used in the investigation was circular over its whole range to a high degree of accuracy, since the parameters, calculated from reflection lines situated at different points along the film, agree closely, as will be seen from Table VIII where  $\theta$  denotes the Bragg glancing angle and  $\lambda$  the wave-lengths characteristic of copper radiation of the K series. The values for the copper

Table VIII.—Copper-zinc alloy containing 38.7 per cent. copper by weight, in the pure  $\gamma$ -phase region. Filings annealed at 500° C. for 10 minutes and air-cooled. Face-centred cubic structure containing 52 atoms per unit cell.

Reflecting planes.	$\lambda$ .	$\frac{\pi}{2} - \theta$ .	Parameter (A.).
		$^{\circ}$ $'$	
(871)	$a_1$	21 50	8.841 <sub>7</sub>
	$a_2$	21 27	8.840 <sub>6</sub>
(961)	$a_1$	19 8	8.838 <sub>5</sub>
	$a_2$	18 45	8.840 <sub>6</sub>
(10.42)	$a_1$	17 41	8.838 <sub>5</sub>
	$a_2$	17 14	8.838 <sub>5</sub>
(11.10)	$a_1$	16 8	8.838 <sub>5</sub>
	$a_2$	15 40	8.840 <sub>6</sub>
(11.21)	$a_1$	12 33	8.839 <sub>5</sub>
	$a_2$	11 52	8.838 <sub>5</sub>
(880)	$a_1$	10 14	8.837 <sub>4</sub>
	$a_2$	9 26	8.837 <sub>4</sub>
(11.30)	$a_1$	7 26	8.838 <sub>5</sub>
	$a_2$	6 17	8.839 <sub>5</sub>

Mean value = 8.839<sub>1</sub> A.

wave-lengths were taken from the International Critical Tables:  $\alpha_1 = 1.53739$ ;  $\alpha_2 = 1.54126$ ;  $\beta = 1.38927$  A.

In order to determine the indices of the reflecting planes for hexagonal structures, the approximate values of  $a$  and  $c$  obtained from ordinary powder X-ray spectra were taken together with the values for  $\theta$  obtained by measuring the arc between corresponding reflection lines in the photographs taken with the precision camera. Assuming this camera to be circular, a value for  $c$  is sought such that the values for  $a$ , calculated from the values of  $\theta$  for all the lines recorded, agree with one another as closely as possible. The determination of the parameters of the  $\eta$ -phase alloys is an example of this method of procedure. Two are recorded here, namely, pure zinc, and an alloy containing 1.8 per cent. copper by weight. It was found necessary to use a cobalt target for this work, since a copper target only gave one measurable doublet of a large arc. The reflections obtained with the cobalt target are given in Table IX.

Table IX.

(1) Pure zinc; filings annealed at 410° C. for 6 hours.

Reflecting planes.	$\lambda$ .	$\frac{\pi}{2} - \theta$ .	Value of $a$ when $c = 1.856$ .
		° ' "	A.
2131	$\beta$	19 22	2.659 <sub>2</sub>
2023	$\alpha_1$	18 53	2.659 <sub>1</sub>
	$\alpha_2$	18 31	2.659 <sub>1</sub>
1015	$\alpha_1$	10 16	2.658 <sub>3</sub>
1124	$\alpha_2$	8 23	2.658 <sub>2</sub>

Mean value of  $a = 2.659_1$  A.

(2) Cu-Zn alloy containing approximately 1.8 per cent. copper by weight; filings annealed at 380° C. for 12 hours.

Reflecting planes.	$\lambda$ .	$\frac{\pi}{2} - \theta$ .	Value of $a$ when $c = 1.8175$ .
		° ' "	A.
2131	$\beta$	19 51	2.669 <sub>3</sub>
2023	$\alpha_1$	18 20	2.669 <sub>2</sub>
	$\alpha_2$	17 57	2.668 <sub>1</sub>
1124	$\alpha_1$	6 1	2.669 <sub>2</sub>
	$\alpha_2$	4 22	2.668 <sub>1</sub>

Mean value of  $a = 2.668_2$  A.

There is close agreement between the values calculated for zinc and for the 1.8 per cent. alloy. The mean value in each case is correct to well within 1 in 4000.

According to previously published results\* the  $\epsilon$ -phase of the copper-zinc alloys has a close-packed hexagonal lattice, with  $a = 2.718$  A. and axial ratio  $c = 1.6$  approximately. Taking these approximate values, it was found that the three doublets registered on the film by this phase with copper radiation were reflections from the planes (30 $\bar{3}$ 0), (20 $\bar{2}$ 4) and (10 $\bar{1}$ 5). The values of the parameters  $a$  and  $c$  were calculated as follows. Since the planes (30 $\bar{3}$ 0) are of the form ( $hko$ ) and gave a small arc, an accurate value of  $a$  was calculated directly. This value of  $a$  was substituted in equation (1) and ascertaining from the photograph the value of the arc ( $s$ ) corresponding to the reflection lines of the planes (10 $\bar{1}$ 5), a value for  $c$  was found. Using this value of  $c$ , together with the reflections from the third doublet (20 $\bar{2}$ 4), a second value of  $a$  was calculated. From each photograph, both values of  $a$  obtained in this manner were almost identical. Table X contains the results obtained with an alloy containing 23.5 per cent. copper by weight and is cited as an example of the agreement found between the two values of  $a$ .

Table X.—Copper-zinc alloy containing 23.5 per cent. Cu. filings annealed at 300° C. for 12 hours.

Reflecting planes.	$\lambda$ .	$\frac{\pi}{2} - \theta$ .	Parameters.		Remarks.
			$a$ .	$c$ .	
30 $\bar{3}$ 0	$a_1$	12 47	2.730 <sub>6</sub>	—	Calculated directly since $l = 0$ .
	$a_2$	12 6	2.730 <sub>2</sub>	—	
10 $\bar{1}$ 5	$a_1$	17 30	—	1.570 <sub>0</sub>	Calculated using $a$ from (30 $\bar{3}$ 0).
	$a_2$	17 2	—	1.570 <sub>0</sub>	
20 $\bar{2}$ 4	$a_1$	14 30	2.730 <sub>4</sub>	—	Calculated using $c$ from (10 $\bar{1}$ 5).
	$a_2$	13 53	2.730 <sub>5</sub>	—	

Mean values :  $a = 2.730_3$ ;  $c = 1.570_0$ .

By the above procedure accurate data were obtained for alloys in the  $\epsilon$ - and  $\eta$ -phases. These data not only enabled the relation between mean atomic volume and composition to be established, but also the relation between the

\* See Elam, 'J. Inst. Met.', vol. 41, p. 1 (1929).

base side  $a$  and the axial ratio  $c$ , or the relation between the height  $ac$  and the base side  $a$  of the elementary hexagonal prisms in alloys of different compositions. Tables XI and XII give details of the various quantities concerned in these relations for the two phases.

Table XI.— $\epsilon$ -phase.

Composition, atomic per cent. Cu.	Base side $a$ .	Axial ratio $c$ .	Height $ac$ .
24.0	2.730 <sub>3</sub>	1.570	4.286 <sub>3</sub>
20.7	2.732 <sub>3</sub>	1.568 <sub>3</sub>	4.285 <sub>3</sub>
17.2	2.745 <sub>3</sub>	1.561	4.285 <sub>3</sub>
13.5	2.759 <sub>3</sub>	1.554 <sub>3</sub>	4.288 <sub>3</sub>
12.0	2.760 <sub>3</sub>	1.554	4.289 <sub>3</sub>
9.2	2.760 <sub>3</sub>	1.554	4.289 <sub>3</sub>

Table XII.— $\eta$ -phase.

Composition, atomic per cent. Cu.	Base side $a$ .	Axial ratio $c$ .	Height $ac$ .
4.3	2.673 <sub>3</sub>	1.804	4.823 <sub>3</sub>
1.85	2.669 <sub>3</sub>	1.817 <sub>3</sub>	4.852 <sub>3</sub>
1.02	2.664 <sub>3</sub>	1.836	4.892 <sub>3</sub>
0.0	2.659 <sub>3</sub>	1.856	4.934 <sub>3</sub>

The graphs, figs. 2 and 3, show the relations between base side and composition, and between axial ratio and composition. Fig. 2 shows that the base side  $a$  varies linearly with composition, but whereas in the  $\epsilon$ -phase, the base side increases, in the  $\eta$ -phase it decreases with decreasing copper content. On the other hand, the axial ratio, fig. 3, decreases in the  $\epsilon$ -phase and increases in the  $\eta$ -phase with decreasing copper content, the reverse effect to that found with the base side. The change in the dimensions of the elementary cell in the  $\epsilon$ -phase alloys is almost entirely due to the change which takes place in the base side, the height remaining practically constant over the whole range. In the  $\eta$ -phase alloys, on the other hand, the height changes far more rapidly than the base side, the height increasing as the base side decreases.

To account for these experimental results, it must be assumed that the orientation of the zinc atoms in the one phase is different from that in the other—a conclusion already arrived at by studying the mean atomic volume of these two phases.

In the mixed regions both  $a$  and  $c$  remain constant throughout the range of composition. It is therefore possible from these graphs to derive the boundary limits of the  $\epsilon$ - and  $\eta$ -phases. The boundaries so obtained are those at 380° C.

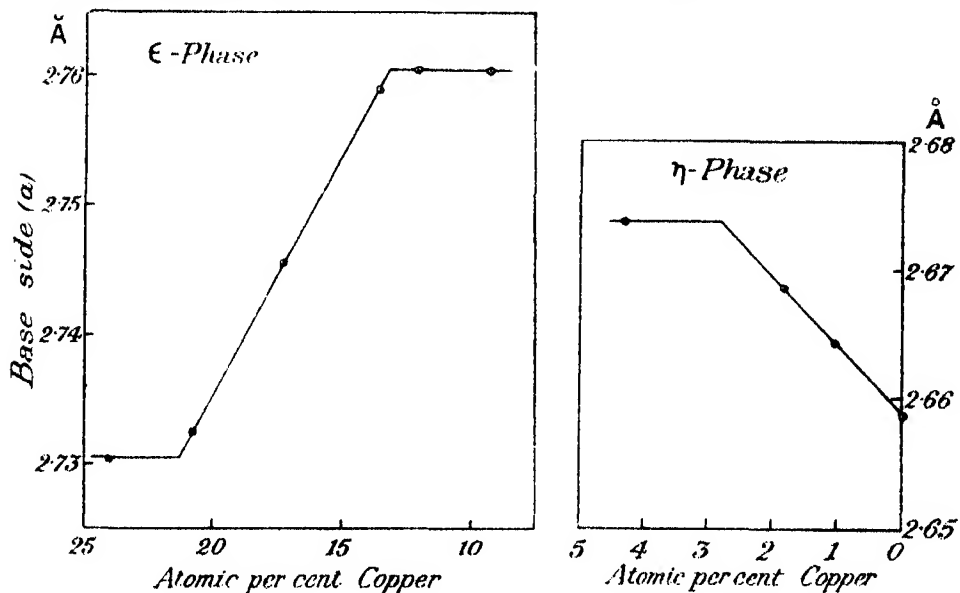


FIG. 2.

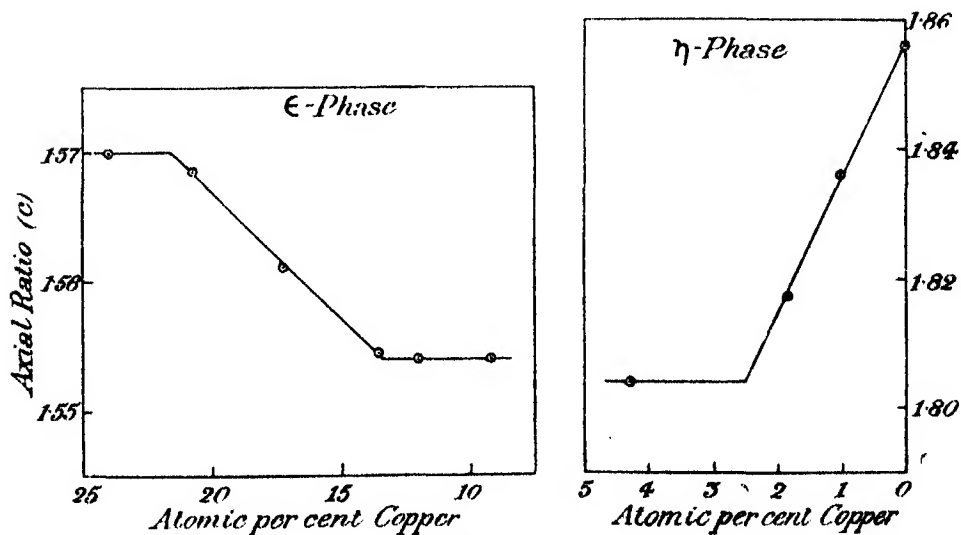


FIG. 3.

in the equilibrium diagram, since filings of all these alloys were annealed at that temperature. Reading the boundaries off the graphs, the results, given

in Table XIII, are obtained, which are in close agreement with those deduced from the atomic volume-composition curves.

Table XIII. Boundaries of phases at 380° C. in atomic per cent. copper.

Boundary.	From fig. 2.	From fig. 3.	Mean.	I.C.T.
$(\gamma + \epsilon) - (\epsilon)$	21.3	21.5	21.4	18.2
$(\epsilon) - (\epsilon + \eta)$	13.0	13.4	13.2	12.2
$(\epsilon + \eta) - (\eta)$	2.85	2.5	2.7	1.5

In the last column (I.C.T.), the approximate readings of the boundaries read from the copper-zinc diagram in the International Critical Tables are given for a temperature of 380° C.

Although the agreement for each boundary in the second and third columns relating to  $a$  and  $c$  respectively is fairly close, the agreement between the mean values of these and the last column (I.C.T.) is not very satisfactory. These differences, probably, are partly owing to inaccurate chemical analysis of the alloys—such small percentages of copper require elaborate methods for their determination—and partly to inaccuracy in the I.C.T. diagram. From a consideration of the curves in figs. 2 and 3, it is thought that any error in the determination of the copper content of the alloys is small enough to conclude that the boundaries determined by the X-ray method are a close approximation to the true values.

We wish to express our indebtedness and thanks to the Royal Society for a grant which enabled us to carry out the work.

### *Summary.*

(1) In the copper-zinc series the mean atomic volume of both phases present in mixed regions remains constant.

(2) There is approximately a linear increase of mean atomic volume with increasing atomic per cent. composition in all the pure phases. The rate of increase is practically the same for the  $\alpha$ -,  $\beta$ - and  $\gamma$ -phases, but that of the  $\epsilon$ - and  $\eta$ -phases is greater, the rate of increase of mean atomic volume being greater for the  $\eta$ - than for the  $\epsilon$ -phase.

(3) The change in atomic volume when one copper atom is replaced by one zinc atom may be explained on the assumption that the zinc atom is not "spherical" and that it packs differently in the various phases.

(4) The analysis does not reveal any relation between the distance of closest approach of atoms from phase to phase.

(5) The  $(\beta + \gamma) - (\gamma)$  boundary is not at the same composition for all temperatures, as is given in the equilibrium diagram reproduced in the International Critical Tables. This corroborates the results on this phase boundary previously recorded.

(6) A detailed study of the  $\epsilon$ - and  $\eta$ -phases of the copper-zinc series shows that the base side of the hexagonal unit varies linearly with composition, but whereas in the  $\epsilon$ -phase the base side increases, in the  $\eta$ -phase it decreases with decreasing copper content. The axial ratio, on the other hand, decreases in the  $\epsilon$ -phase and increases in the  $\eta$ -phase as the copper content decreases. In the mixed regions both the base side and the axial ratio remain constant.

(7) The positions of the phase boundaries at the temperatures at which the alloys were annealed are derived from these results.

(8) Pure zinc is found to have the following parameter values at ordinary room temperature :— $a = 2.659$ , A. ;  $c = 1.856$ .

---

*Variation of Mean Atomic Volume with Temperature in Copper-Zinc Alloys, with Observations on the  $\beta$ -Transformation.*

By PROFESSOR E. A. OWEN, M.A., D.Sc., and LLEWELYN PICKUP, M.Sc.(London),  
Ph.D.(Wales), University College of North Wales, Bangor.

(Communicated by Sir William Bragg, O.M., F.R.S.—Received November 3, 1932.)

It has been shown in previous papers\* how X-ray analysis may be applied to determine phase boundaries in equilibrium diagrams. In the present paper an account is given of the application of the same experimental technique to study the change in mean atomic volume with temperature in certain alloys of the copper-zinc system. In the first part of the paper an account is given of the experimental determination of the change in mean atomic volume in alloys quenched from different temperatures ; in the second part the  $\beta$ -transformation is discussed.

\* Owen and Pickup, 'Proc. Roy. Soc.,' A, vol. 137, p. 397 (1932) ; vol. 139, p. 526 (1933).



I. *Variation of Mean Atomic Volume with Temperature.*

A description of the general method of procedure will be found in the papers referred to above.

In a preliminary investigation of the variation of mean atomic volume with temperature, an alloy was chosen from the ( $\beta + \gamma$ ) region of the copper-zinc system, which after being thoroughly lump-annealed, contained 42.7 per cent. copper by weight. Filings taken from it were annealed at temperatures ranging from 350° C. to 800° C., and were either rapidly air-cooled or quenched in iced water. The results obtained by X-ray analysis of this alloy are set out in Table I.

Table I.

$\beta$ -phase.			$\gamma$ -phase.	
Temperature.	Parameter.	Calculated mean atomic volume $\times 10^{24}$ .	Parameter.	Calculated mean atomic volume $\times 10^{24}$ .
°C.	A.	cm. <sup>3</sup>	A.	cm. <sup>3</sup>
350	2.950 <sub>3</sub>	12.84 <sub>2</sub>	8.834 <sub>4</sub>	13.26 <sub>3</sub>
380	2.949 <sub>9</sub>	12.83 <sub>3</sub>	8.829 <sub>9</sub>	13.23 <sub>3</sub>
410	2.949 <sub>2</sub>	12.82 <sub>7</sub>	8.823 <sub>9</sub>	13.21 <sub>2</sub>
450	2.949 <sub>1</sub>	12.82 <sub>4</sub>	8.820 <sub>9</sub>	13.19 <sub>3</sub>
500	2.949 <sub>1</sub>	12.82 <sub>4</sub>	8.819 <sub>9</sub>	13.19 <sub>4</sub>
600	2.948 <sub>9</sub>	12.82 <sub>9</sub>	8.820 <sub>9</sub>	13.19 <sub>3</sub>
650	2.949 <sub>3</sub>	12.82 <sub>7</sub>	8.821 <sub>9</sub>	13.20 <sub>3</sub>
710	2.949 <sub>1</sub>	12.83 <sub>2</sub>	8.824 <sub>9</sub>	13.21 <sub>7</sub>
800	2.950 <sub>1</sub>	12.83 <sub>3</sub>	8.830 <sub>7</sub>	13.24 <sub>3</sub>

In fig. 5, the mean atomic volumes are plotted against the temperature for both phases. Loss of zinc was reduced by giving the minimum annealing time at each temperature to produce good reflection lines and to establish equilibrium. Loss of zinc within the range of the ( $\beta + \gamma$ ) region would, however, produce no change in the parameters of the lattices at a fixed temperature. All photographs showed reflection lines from the  $\beta$ - and  $\gamma$ -phases, and therefore the composition of all the samples must have been in the ( $\beta + \gamma$ ) region.

A marked feature of the  $\gamma$ -phase curve, fig. 5, is the definite change in its slope at about 500° C., while a similar but smaller change is shown in the  $\beta$ -phase curve. As the temperature at which these changes occur is almost identical with that assigned to the so-called  $\beta - \beta'$  transformation, it was decided to study in more detail the change of mean atomic volume with temperature in other alloys.

Alloys were chosen such that the  $\alpha$ -,  $\beta$ - and  $\gamma$ -phases could be studied as single phases and as mixtures. These alloys and the phase or phases they represented are shown in Table II. All these alloys had received a prolonged lump-annealing heat treatment (500 hours at about 500° C.).

Table II.

Alloy marked.	Phase or phases present.	Alloy marked.	Phase or phases present.
673 Z	$\alpha$	453 Z	$\beta + \gamma$
589 Z	$\alpha + \beta$	432 Z	$\beta + \gamma$
561 Z	$\beta$	414 Z	$\gamma$
523 Z	$\beta$	387 Z	$\gamma$

Filings from all these samples were annealed at different temperatures; only those annealed at 600° C. and above were quenched in water, as it had been found that there was no measurable difference in the parameters whether the filings were air-cooled\* or water-quenched below this temperature. The actual sample worked upon weighed about 0.3 to 0.4 gm. and was enclosed in an evacuated glass (or silica for 600° C. and above) container. The mean atomic volumes given in Tables III to IX were calculated from the parameter values by using the following formulæ: (1) for the face-centred cubic  $\alpha$ -phase,  $a^3/4$ ; (2) for the body-centred cubic  $\beta$ -phase,  $a^3/2$ ; (3) for the body-centred cubic  $\gamma$ -phase,  $a^3/52$ ; where  $a$  is the parameter value.

Table III.—Alloy marked, 673 Z. Composition in the  $\alpha$ -region.

Temperature.	Parameter.	Calculated mean atomic volume $\times 10^{24}$ .	Temperature.	Parameter.	Calculated mean atomic volume $\times 10^{24}$ .
°C.	A.	cm. <sup>3</sup>	°C.	A.	cm. <sup>3</sup>
800	3.679 <sub>1</sub>	12.45 <sub>0</sub>	450	3.681 <sub>5</sub>	12.47 <sub>3</sub>
600	3.680 <sub>2</sub>	12.46 <sub>4</sub>	400	3.681 <sub>6</sub>	12.46 <sub>8</sub>
500	3.679 <sub>7</sub>	12.46 <sub>4</sub>	350	3.680 <sub>4</sub>	12.46 <sub>3</sub>

\* The glass tubes containing the filings were thin-walled (0.5 mm. thick), about 2 cm. long and 0.5 cm. diameter, and therefore cooled rapidly in air when removed from the furnace.

**Table IV.**—Alloy marked 589 Z. Composition in the ( $\alpha + \beta$ ) region below about 700° C.

$\alpha$ -phase.			$\beta$ -phase.	
Temperature.	Parameter.	Calculated mean atomic volume $\times 10^{24}$ .	Parameter.	Calculated mean atomic volume $\times 10^{24}$ .
°C.	A.	cm. <sup>3</sup>	A.	cm. <sup>3</sup>
800	—	—	2.934 <sub>7</sub>	12.63 <sub>8</sub>
700	3.690 <sub>5</sub>	12.56 <sub>8</sub>	2.936 <sub>1</sub>	12.65 <sub>8</sub>
650	3.691 <sub>5</sub>	12.57 <sub>8</sub>	2.938 <sub>7</sub>	12.68 <sub>8</sub>
600	3.694 <sub>2</sub>	12.60 <sub>8</sub>	2.941 <sub>3</sub>	12.72 <sub>8</sub>
550	3.694 <sub>7</sub>	12.60 <sub>8</sub>	2.942 <sub>3</sub>	12.73 <sub>8</sub>
500	3.696 <sub>3</sub>	12.62 <sub>8</sub>	2.943 <sub>6</sub>	12.74 <sub>8</sub>
450	3.696 <sub>5</sub>	12.62 <sub>7</sub>	2.943 <sub>6</sub>	12.75 <sub>7</sub>
400	3.695 <sub>7</sub>	12.61 <sub>7</sub>	2.944 <sub>5</sub>	12.76 <sub>8</sub>
350	3.694 <sub>2</sub>	12.60 <sub>4</sub>	2.944 <sub>5</sub>	12.77 <sub>8</sub>

**Table V.**—Alloy marked 561 Z. Composition in the ( $\alpha + \beta$ ) region below 600° C.

Temperature.	$\beta$ -phase parameter.	Calculated mean atomic volume $\times 10^{24}$ .
°C.	A.	cm. <sup>3</sup>
800	2.939 <sub>3</sub>	12.69 <sub>8</sub>
700	2.939 <sub>5</sub>	12.69 <sub>8</sub>
650	2.939 <sub>6</sub>	12.69 <sub>8</sub>
600	2.939 <sub>8</sub>	12.70 <sub>2</sub>
500	2.942 <sub>7</sub>	12.74 <sub>1</sub>
400	2.943 <sub>5</sub>	12.75 <sub>7</sub>
350	2.944 <sub>5</sub>	12.76 <sub>8</sub>

**Table VI.**—Alloy marked 523 Z. Composition in the  $\beta$ -region.

Temperature.	$\beta$ -phase parameter.	Calculated mean atomic volume $\times 10^{24}$ .
°C.	A.	cm. <sup>3</sup>
800	2.946 <sub>1</sub>	12.78 <sub>8</sub>
700	2.946 <sub>7</sub>	12.79 <sub>8</sub>
600	2.946 <sub>8</sub>	12.78 <sub>7</sub>
500	2.946 <sub>8</sub>	12.78 <sub>7</sub>
450	2.946 <sub>8</sub>	12.79 <sub>8</sub>
400	2.946 <sub>8</sub>	12.79 <sub>1</sub>
350	2.946 <sub>8</sub>	12.79 <sub>8</sub>

**Table VII.**—Alloy marked 453 Z. Composition in the ( $\beta + \gamma$ ) region.

$\beta$ -phase.			$\gamma$ -phase.	
Temperature.	Parameter.	Calculated mean atomic volume $\times 10^{24}$ .	Parameter.	Calculated mean atomic volume $\times 10^{24}$ .
°C.	A.	cm. <sup>3</sup>	A.	cm. <sup>3</sup>
700	2.949 <sub>8</sub>	12.83 <sub>8</sub>	8.824 <sub>8</sub>	13.21 <sub>7</sub>
600	2.949 <sub>3</sub>	12.82 <sub>7</sub>	8.819 <sub>8</sub>	12.19 <sub>4</sub>
500	2.949 <sub>3</sub>	12.82 <sub>7</sub>	8.819 <sub>8</sub>	13.19 <sub>8</sub>
450	2.949 <sub>7</sub>	12.83 <sub>8</sub>	8.819 <sub>8</sub>	13.19 <sub>8</sub>
400	2.950 <sub>1</sub>	12.83 <sub>8</sub>	8.823 <sub>4</sub>	13.21 <sub>8</sub>
350	2.951 <sub>1</sub>	12.85 <sub>0</sub>	8.828 <sub>0</sub>	13.23 <sub>1</sub>

Table VIII.—Alloy marked 414 Z. Composition in the  $\gamma$ -region.

Temperature.	Parameter.	Calculated mean atomic volume $\times 10^{24}$ .	Temperature.	Parameter.	Calculated mean atomic volume $\times 10^{24}$ .
°C.	A.	cm. <sup>3</sup>	°C.	A.	cm. <sup>3</sup>
800	8·830 <sub>6</sub>	13·24 <sub>4</sub>	450	8·829 <sub>5</sub>	13·23 <sub>7</sub>
700	8·831 <sub>1</sub>	13·24 <sub>6</sub>	400	8·829 <sub>7</sub>	13·23 <sub>8</sub>
600	8·831 <sub>6</sub>	13·24 <sub>5</sub>	380	8·830 <sub>7</sub>	13·24 <sub>8</sub>
500	8·829 <sub>4</sub>	13·23 <sub>7</sub>	350	8·832 <sub>8</sub>	13·25 <sub>1</sub>

Table IX.—Alloy marked 387 Z. Composition in the  $\gamma$ -region.

Temperature.	Parameter.	Calculated mean atomic volume $\times 10^{24}$ .	Temperature.	Parameter.	Calculated mean atomic volume $\times 10^{24}$ .
°C.	A.	cm. <sup>3</sup>	°C.	A.	cm. <sup>3</sup>
800	8·838 <sub>8</sub>	13·27 <sub>8</sub>	450	8·840 <sub>6</sub>	13·28 <sub>8</sub>
600	8·839 <sub>6</sub>	13·28 <sub>0</sub>	400	8·840 <sub>5</sub>	13·28 <sub>8</sub>
500	8·838 <sub>3</sub>	13·27 <sub>7</sub>	350	8·840 <sub>1</sub>	13·28 <sub>8</sub>

The parameter values in Table III show erratic variations between 3·679<sub>1</sub> and 3·681<sub>5</sub> A., which are greater than the experimental error. Chemical analysis showed that these variations could be attributed to variations of composition. The actual values of the mean atomic volumes after correction for change in composition are shown by the crosses in fig. 1. These indicate that the mean atomic volume does not change appreciably with temperature. The parameter was therefore taken to be constant in the pure  $\alpha$ -region throughout the temperature range; it is constant also in the  $\beta$ - and  $\gamma$ -phases.

The mean atomic volume of the  $\alpha$ -phase in alloy 589 Z when plotted against temperature, fig. 2, shows a marked change over the temperature range. Unlike alloy 673 Z, this alloy is in the ( $\alpha + \beta$ ) region. Provided the temperature be constant, the parameter of the  $\alpha$ -phase is independent of the composition in the ( $\alpha + \beta$ ) region, since the phase is then saturated. The marked diminution of the mean atomic volume at the higher temperatures could arise from the composition moving from the mixed ( $\alpha + \beta$ ) region into the pure  $\alpha$ -region, if enough zinc volatilized. It was therefore necessary to ascertain whether all the samples of this alloy after annealing remained in the ( $\alpha + \beta$ ) region, since variations of composition *within* this region would not affect

the value of the parameter, or mean atomic volume. The results of chemical analysis carried out on the samples photographed are given in Table X.

Table X.

Annealing temperature of sample.	Composition (per cent. copper by chemical analysis).	Annealing temperature of sample.	Composition (per cent. copper by chemical analysis).
°C.		°C.	
700	60.0	500	59.5
650	59.9	450	59.2
600	59.2	400	59.4
550	59.5	350	59.8

These compositions show little variation, and all are in the  $(\alpha + \beta)$  region. The relation representing the mean atomic volume of the  $\alpha$ -phase in this alloy with different temperatures, fig. 2, cannot therefore be accounted for by assuming that the composition moves out of the  $(\alpha + \beta)$  region. In view of the small changes in compositions after annealing revealed by chemical analysis of alloys 673 Z and 589 Z, all the experimental data given in Tables I and III to IX are shown in figs. 1 to 8. The forms of the curves are not due to any radical change in composition brought about by annealing.

The chief conclusion arrived at from the curves is that as the temperature changes, a change in mean atomic volume takes place in both the constituents in a mixed region, whereas the mean atomic volume in the pure phases remains constant for all temperatures.

There appear at least three possible ways of changing the mean atomic volume with temperature, namely, (1) by change of type of lattice; (2) by a change in the orientation of the zinc atom; (3) by the substitution of atoms of one kind for those of another, a pure solution effect.

Since the  $\alpha$ -,  $\beta$ - and  $\gamma$ -phases do not show a change of lattice type with change of temperature, the first explanation is untenable.

Should there be a change in the orientation of the zinc atoms at high temperature, causing an increase in the lattice parameter, and the effect arises solely from this change in orientation, the zinc atom would have to change its orientation, as the temperature is lowered, in such a manner as to occupy minimum volume at about 500° C., at which temperature the lattice, for example, the  $\beta$ -lattice in the  $(\beta + \gamma)$  region, would change from a contracting to an expanding one. Although this may be a possible explanation of the change in mean atomic volume with temperature, experimental data so far

obtained do not lend it much support. For it has been shown (p. 179) that the change in mean atomic volume when a zinc atom replaces a copper atom, is very approximately the same in the  $\alpha$ -,  $\beta$ - and  $\gamma$ - phases, which all have cubic structures, from which we would conclude that the orientation of the zinc atom in

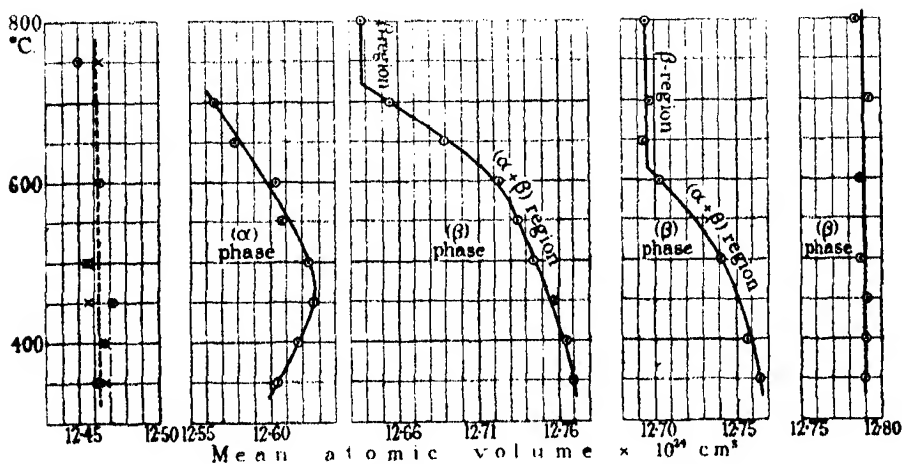


FIG. 1.

FIG. 2.

FIG. 3.

FIG. 4.

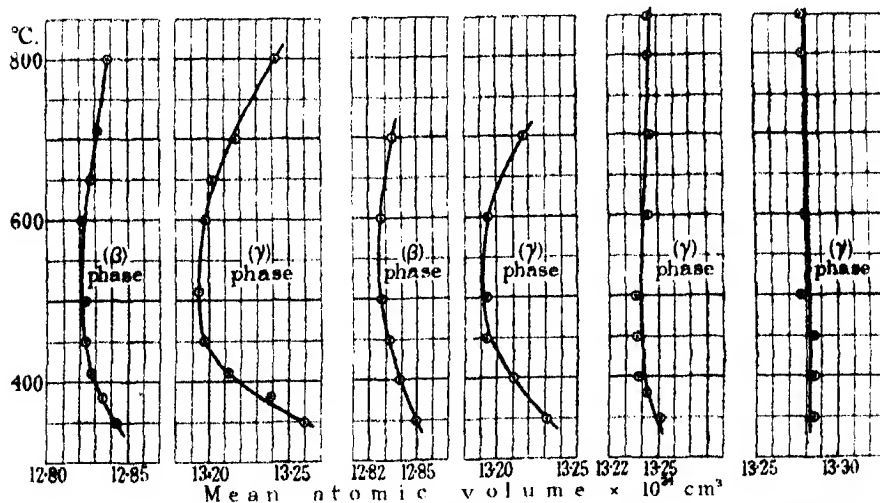


FIG. 5.

FIG. 6.

FIG. 7.

FIG. 8.

packing is the same in the three phases. There exists, on the other hand, indirect experimental evidence (p. 179) that a change in orientation of the zinc atom takes place in the hexagonal structures at the zinc end of the system, the change in volume when a zinc atom replaces a copper atom being much greater

in the  $\epsilon$ - and  $\eta$ -phases than in the  $\alpha$ -,  $\beta$ - and  $\gamma$ -phases. The change in volume appears to be a minimum in the cubic lattices. If the form of the mean atomic volume-temperature curves now obtained is to be explained by change in orientation of the zinc atoms, then the zinc atom in alloys in the  $(\beta + \gamma)$  region must occupy a volume at about 500° C., somewhat less than that which it occupies in the three cubic lattices at the other temperatures. Without further data, however, it is impossible to decide definitely against this explanation of the effect.

The third, and the one which appears to us the most probable, explanation is that of change in solid solubility—atoms go in and come out of solution in the different constituents of a duplex alloy as the temperature changes. Now since the lattice type is the same throughout the temperature range, and also since the parameter value of each phase at a constant temperature is the same irrespective of alloy composition, provided this remains in the mixed region, it is possible to test the curves obtained here, figs. 1 to 8, by superimposing the curves of alloys of different compositions in the same mixed region. Fig. 9 shows the superimposed curves, the curve (a) being added for comparison with the  $\alpha - (\alpha + \beta)$  boundary previously recorded.

The coincidence of curves from two alloys in the same region for a phase is exactly that to be expected on the grounds of change in solubility, for the three examples given. Further, the  $\beta$ -phase curves of alloys 589 Z and 561 Z, fig. 9 (b), do not coincide over the entire range of temperature. In alloy 589 Z the mean atomic volume becomes constant from about 720°–730° C. to 800° C., and in alloy 561 Z it becomes constant from about 640° C. to 800° C. Since a constant mean atomic volume with change of temperature is associated with a pure phase region, the composition of these two alloys must, in these temperature ranges, be in the pure  $\beta$ -phase region. We deduce from the curves that the  $\beta$ -phase boundary for alloys of these two compositions occurs at about 725° C. and 640° C.—values in fairly good agreement with those obtained from the positions of the boundary as previously determined\* by X-ray analysis, namely, 720° C. and 620° C. respectively.

It is clear, from the coincidence of the mean atomic volume curves, that the general form of these curves for a phase in a mixed region must be the same as the form of the boundary in the equilibrium diagram between the mixed region and the pure phase region. There is a marked similarity between these curves and the curves determined by X-ray analysis showing the positions of the phase boundaries.\*

\* Owen and Pickup, *loc. cit.*, p. 416.

On this view, when an alloy in the  $(\beta + \gamma)$  region cools slowly, zinc comes out of solution from both the  $\beta$ - and the  $\gamma$ -constituents for temperatures down to about  $500^\circ \text{C}$ ., and is taken into solution again below this temperature; in the  $(\alpha + \beta)$  region, copper comes out of solution from both the  $\alpha$ - and the

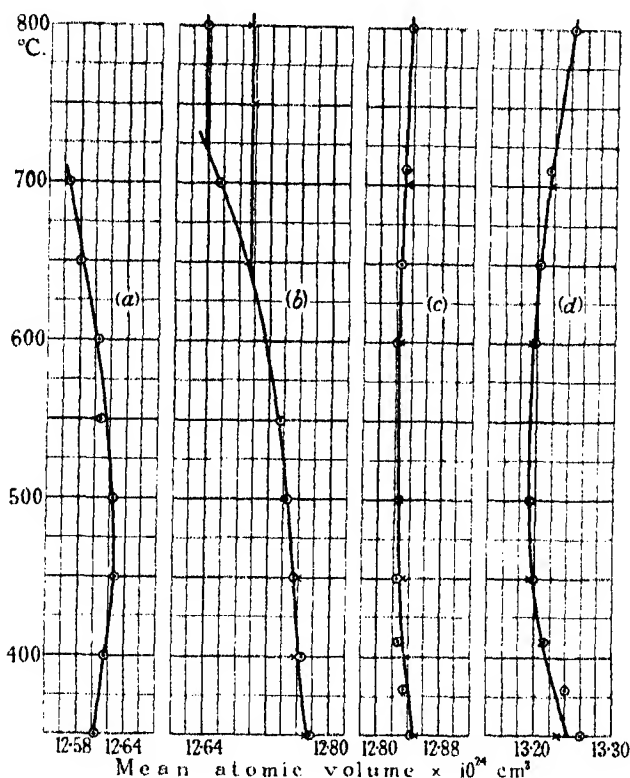


FIG. 9.

- (a)  $\alpha$ -phase in the  $(\alpha + \beta)$  region;  $\odot$  ... alloy 589 Z.  
 (b)  $\beta$ -phase in the  $(\alpha + \beta)$  region;  $\odot$  ... alloy 589 Z,  $\times$  ... alloy 561 Z.  
 (c)  $\beta$ -phase in the  $(\beta + \gamma)$  region;  $\odot$  ... alloy 453 Z,  $\times$  ... alloy 432 Z.  
 (d)  $\gamma$ -phase in the  $(\beta + \gamma)$  region;  $\odot$  ... alloy 453 Z,  $\times$  ... alloy 432 Z.

$\beta$ -constituents for temperatures down to about  $500^\circ \text{C}$ ., but whereas it continues to come out of the  $\beta$ -constituent, it is taken into solution at about the same rate by the  $\alpha$ -constituent below this temperature. As the temperature is altered, the lattices continuously change in dimensions, owing to solubility effects. In each case, the same type of lattice is maintained but a continuous rearrangement of atoms takes place.



II. *The  $\beta$ -transformation.*

The transformation which occurs at about 470° C. in the  $\beta$ -region of this alloy system has received much attention by metallurgists.

Roberts-Austen,\* in 1897, was the first to observe the effect; later, although Shepherd† had doubted its existence, Carpenter and Edwards‡ concluded that it was present, and interpreted it as being caused by the breaking up of the  $\beta$ -phase into  $\alpha$ - and  $\gamma$ -phases. Matsuda§ from studies of thermal analysis, thermal expansion, electrical resistance, thermo-electric and mechanical properties, concluded that the transformation was a progressive change of the same nature as the  $A_2$  transformation in iron. It was, therefore, not a change in phase but a change in atomic energy, which is a function of temperature only, and independent of time. Imai,|| chiefly from measurements of electric resistance, found that the transformation began below 300° C. and continued till it terminated at 480° C., and that the  $\gamma$ -phase also showed transformations of the same nature at 480° C. and 260° C. Gayler¶ found a slight but definite change in the direction of the boundary,  $(\alpha + \beta) - (\beta)$ , at the transformation temperature; Haughton and Griffiths,\*\* by means of electric resistance measurements of alloys ranging from 62.6 to 45.7 per cent. copper, also showed distinct changes in the direction of the boundaries  $(\alpha + \beta) - (\beta)$  and  $(\beta) - (\beta + \gamma)$  at the transformation temperature. The work of Saldau and Schmidt†† on the microscopical examination of well-annealed alloys suggests a definite displacement of the  $\beta$ -phase boundaries towards the zinc end, at and below the transformation temperature. Owen and Preston‡‡ found the  $\beta$ -constituent above and below the transformation temperature to have the same type of lattice and practically the same parameter value. Phillips and Thelin,§§ by taking diffraction patterns at room temperature and at 520° C., found the  $\beta$ -phase to be body-centred cubic at each temperature, but with an increase of 1.7 per cent. in the parameter value at 520° C. Von Goler and

\* 'Fourth Rep. Alloy Res. Ctee. Inst. Mech. Eng.,' p. 31 (1897).

† 'J. Phys. Chem.,' vol. 8, p. 421 (1904).

‡ 'J. Inst. Met.,' vol. 5, p. 127 (1911).

§ 'Sci. Rep. Tôhoku Univ.,' vol. 1, p. 11 (1922).

|| 'Sci. Rep. Tôhoku Univ.,' vol. 11 (5) (1922).

¶ 'J. Inst. Met.,' vol. 34, p. 235 (1925).

\*\* 'J. Inst. Met.,' vol. 34, p. 245 (1925).

†† 'J. Inst. Met.,' vol. 34, p. 258 (discussion) (1925).

‡‡ 'Proc. Phys. Soc.,' Lond., vol. 36, p. 49 (1924).

§§ 'J. Franklin Inst.,' p. 204 (1927).

Sachs,\* from Laue photographs of single crystals of  $\beta$ -brass at various temperatures, failed to find any change in the lattice structure between 400° C. and 500° C. that could be ascribed to the so-called transformation at 465°–470° C.

Very little evidence, therefore, appears to have been put forward to suggest the nature of this apparently abnormal effect, except that it is probably not a ( $\beta$ ) to ( $\alpha + \gamma$ ) transformation, although experimental evidence published by Masing,† Heike and Ledebur,‡ and Andrew and Hay§ seems to support such a eutectoid change.

If a transformation takes place in the pure  $\beta$ -phase, and if the change in mean atomic volume with temperature has any connection with the transformation, we should expect to find the most marked effect with alloy 523 Z, representing the pure  $\beta$ -region throughout the temperature range. Since this alloy shows a constant parameter value at all temperatures, then either (1) the quenching has failed to retain the  $\beta$ -modification which is stable above the transformation temperature, or (2) the so-called  $\beta$ -transformation is really a solubility effect.

As the  $\beta$ -transformation in the copper-zinc alloys has been considered by some to be analogous to the  $A_2$  transformation in iron, experiments were made on samples of very pure iron (total impurities 0.018 per cent. + traces, not estimated), quenched drastically to retain, if possible, the  $\beta$ - and  $\gamma$ -modifications.

All samples showed reflections of the  $\alpha$ -modification only, with a parameter value of 2.860 Å. The  $\gamma$ -iron is a definitely established modification of iron, since it has a face-centred cubic structure as compared to the body-centred cubic structure of  $\alpha$ -iron.|| It is evident that exceedingly rapid quenching is required to retain the  $\gamma$ -structure in pure iron, or that it can only be retained when the iron holds a certain amount of impurity (for example, carbon). It is well known that when carbon or other elements are present it is much easier to retain the  $\gamma$ -modification of iron by quenching.

If the change in mean atomic volume with temperature, observed in the mixed regions ( $\alpha + \beta$ ) or ( $\beta + \gamma$ ) of the copper-zinc alloys, should arise from the  $\beta$ -transformation, it must be assumed that the other phase present ( $\alpha$  or  $\gamma$ ) acts in the same way as carbon in steel, in assisting to retain, by quenching, the modification which is stable above the transition temperature in the pure  $\beta$ -phase.

\* 'Naturwiss,' vol. 16, p. 412 (1928).

† 'Z. Metallk.,' vol. 16, p. 96 (1924).

‡ 'Z. Metallk.,' vol. 16, p. 380 (1924).

§ 'J. Roy. Tech. Coll.,' Glasgow, vol. 1, p. 1 (1924).

|| Westgren and Phragmen, 'J. Iron Steel Inst.,' vol. 105, p. 241 (1922).

If the second alternative suggested here be assumed, namely, that the phenomenon is due to change in solubility, the change in mean atomic volume with temperature can be explained, and further the constant values in the pure regions are to be expected, since the lattices in these regions are unsaturated. The evolution of heat shown in cooling curves is then the heat of solution. From the consideration of the form of the mean atomic volume-temperature curves we conclude that a certain amount of zinc or copper (according to the region considered) comes out of solution as the alloy cools. This amount, though small, reaches a maximum at a temperature of about  $500^{\circ}\text{C}$ ., approximately the temperature at which the  $\beta$ -transformation occurs. As the temperature is lowered, the zinc or copper is again taken into solution.

This explanation is in accord with the facts that (1) the  $\alpha$ - and  $\gamma$ -phases show a similar transformation to that of the  $\beta$ -phase, and (2) the transformation temperature is really a range of temperature rather than a "transition point."

Matsuda found a transformation in the  $\alpha$ -phase at about  $280^{\circ}\text{C}$ ., while Imai confirms Matsuda in that the  $\gamma$ -phase also has a transformation at about  $480^{\circ}\text{C}$ .

Saldau and Schmidt, using alloys which had been annealed for 84 days at about  $440^{\circ}\text{C}$ ., also found a change in both the  $(\alpha + \beta) \rightarrow (\beta)$  and the  $(\beta) \rightarrow (\beta + \gamma)$  boundaries, towards the zinc end, similar to that indicated by our atomic volume-temperature curves. These authors state: "the modification  $\beta$  simultaneously with the setting down of phase  $\alpha$ , dissolves corresponding quantities of phase  $\gamma$ . Thus, on one side, corresponding to richer copper concentrations, a destructive reaction of solid solution was going on, and on the other side, corresponding to poorer copper concentrations, a formation of solid solution took place."

#### *Conclusions.*

In view of the X-ray data in the first part of this paper, there appears little doubt that the form of the mean atomic volume curves in the mixed regions is that of the phase boundaries, and the marked change in their direction at about  $500^{\circ}\text{C}$  is probably associated with the  $\beta$ -transformation. If this is so, no transformation in lattice form is tenable, but there is a "transformation" in solubility. Also the pure  $\beta$ -phase would then show no transformation since it is unsaturated, which is consistent with the X-ray data obtained. Also such a change in solubility need not be confined to the  $\beta$ -phase alone (in the mixed region) as it is equally likely to occur in the  $\alpha$ -,  $\gamma$ - or any other phase; this is consistent with the data cited by Matsuda and Imai. The range of temperature attributed to these transformations is more compatible with the

solubility theory than any other theory based on atomic rearrangement such as, for example, a change in orientation or an allotropic change involving a change of lattice type. Further, an allotropic modification is associated with a transition "point" rather than a transition "range."

The explanation of these transformations which is based on solubility is of very general application; there are other alloy systems, some of which we have already investigated, in which changes similar to those described above are to be found.

The only apparent failure in the solubility theory discussed here is its inability to account for the heat exchanges recorded on the thermal curves of pure  $\beta$ -phase alloys by some workers. As comparatively large masses are required for these thermal curves, there may be some difficulty in attaining the true equilibrium state throughout the entire mass. If there should be any  $\alpha$ - or  $\gamma$ -phase present, this could give the heat exchange recorded. It should, however, be possible to check this point by repeated heating, followed each time by a determination of the thermal curve, and noting whether the heat exchange becomes less. In this connection, microscopical evidence of the absence of a "foreign" phase cannot be considered reliable or accurate enough.

In regard to the attainment of true thermal equilibrium, this is obtained more expeditiously by annealing filings than by annealing a small solid sample; though the best method of attaining equilibrium in filings is first to anneal a small sample, about 1 c.c., for a prolonged time (for copper-zinc alloys about 500 hours at 500° C.), and then to anneal the filings for a comparatively short time at the required temperature for experiment.\* While it is recognized that samples in the form of filings are not applicable to most methods of investigation, it is only this form which is found to be most suitable for X-ray analysis as applied in our investigations. Although objections may be raised to the use of filings, in our opinion they are the form in which copper-zinc samples are most readily brought into thermal equilibrium. As this is a vital point in every investigation on alloy systems, it may be possible to devise methods of investigation, other than X-ray analysis, where annealed filings could be used with advantage.

As the tendency of metallurgical research is to modify phase boundaries to a greater or less extent in most alloy systems, the boundaries accepted at present, especially at low temperatures, can only be regarded as approximate, owing to the difficulty of obtaining true equilibrium. Since equilibrium at

\* The comparative effects of lump annealing and powder annealing are dealt with in another paper, Owen and Pickup, 'Proc. Roy. Soc.,' A, vol. 139, p. 526 (1933).

low temperatures is obtained more readily in samples in the form of filings, such as have been used in our investigations, than in samples of the usual lump form, the forms of the boundaries deduced from X-ray analysis of filings are probably more reliable than those obtained by the usual metallurgical methods.

While sufficient data may not have been obtained to establish satisfactorily the solubility theory suggested here as an explanation of the  $\beta$ -transformation in copper-zinc alloys the results of this investigation may be of sufficient interest to stimulate further researches with the object of critically testing the theory, which is applicable to all the so-called transformations detected in the copper-zinc and other alloy systems.

We wish to express our indebtedness and thanks to the Royal Society for a grant which enabled us to carry out the work.

#### *Summary.*

(1) The changes in mean atomic volume which take place in the  $\alpha$ -,  $\beta$ - and  $\gamma$ -phases of the copper-zinc alloy system, with change in temperature, have been investigated by X-ray precision analysis. Alloys in both the pure and the mixed (duplex) regions were examined over a temperature range from 350° C. to 800° C.

(2) In all the pure phases, a constant mean atomic volume was found at all temperatures.

(3) Both the  $\beta$ - and the  $\gamma$ -phases in the ( $\beta + \gamma$ ) region showed a definite *minimum* mean atomic volume at about 500° C.; the  $\alpha$ -phase in the ( $\alpha + \beta$ ) region showed a *maximum* value at about the same temperature.

(4) The changes in mean atomic volume are shown not to be due to changes in composition.

(5) By superimposing the mean atomic volume-temperature curves of the same phase obtained from alloys in the same mixed region, they are found to coincide almost exactly for alloys of different compositions *within* the region. They give the general form of the phase boundaries in the thermal diagram.

(6) To account for the changes in mean atomic volume with temperature three possible explanations are put forward. Of these, the one based upon a change in solubility appears to fit the experimental facts most *satisfactorily*.

(7) The  $\beta$ -transformation which occurs in this system at about 470° C. is discussed in the light of the experimental results obtained.

---

*The Change of Resistance of a Semi-Conductor in a Magnetic Field.*

By J. W. HARDING, M.Sc., Research Student, Emmanuel College, Cambridge  
Post-Graduate Scholar of the University of New Zealand.

(Communicated by R. H. Fowler, F.R.S.—Received November 9, 1932.)

*Introduction.*

One may say that prior to the introduction of the Fermi-Dirac statistics into the theory of metallic conduction and allied phenomena a general mathematical method of attack on the various problems had been developed which necessarily still forms the basis of the modern treatment; but nevertheless in most cases the older theory had little success in predicting the order of magnitude, and in some cases, even the qualitative features of the various effects. However, the ground had been well prepared, so that as soon as it was realized that the electrons in a metal did not really obey the Maxwell but the Fermi-Dirac statistics, the mere introduction of the latter distribution function in the place of the former in the classical equations proved sufficient to clear away many of the old difficulties. Since the appearance of Sommerfeld's paper\* in 1928 the first order effects have received on the whole a satisfactory explanation. In the case of the second order effects, however—and it is with one of these that the present paper deals—there are still very considerable difficulties to be faced.

The problem of the change of resistance of a metal in a magnetic field has been treated by Sommerfeld,† making use of a method which was originally developed by Gans.‡ The calculations follow closely the classical treatment of Lorentz in that the mean free path of an electron is introduced phenomenologically as a parameter to be determined from the known experimental value of the conductivity. In the classical theory one pictures the process as follows. The metal is regarded as having a regular three-dimensional lattice structure with the metallic ions situated at the lattice points. It is further supposed that there are a certain number of conduction electrons, which might well correspond with the valency electrons, and that the assembly of conduction electrons obeys the classical distribution law. When an electric

\* 'Z. Physik,' vol. 47, p. 50 (1928).

† *Loc. cit.*

‡ 'Ann. Physik,' vol. 20, p. 293 (1906).

field is applied in a given direction the electrons are accelerated and experience elastic collisions with the metallic ions. Finally an equilibrium state is reached in which the number of electrons entering a given velocity range in unit time is just equal to the number ejected by collisions, and the mathematical expression of this state takes the form of an integral equation which must be solved to find the change in the original distribution function due to the applied field. From the change in the distribution function the conductivity is calculated. In the semi-classical calculations of Sommerfeld the model is the same except that the Fermi-Dirac statistics are used instead of the Maxwellian. If one compares the value of the conductivity, thus obtained, with the experimental value, one obtains a mean free path which is about a hundred times greater than the lattice spacing. This large value is not very plausible on classical ideas ; but is readily understandable on wave mechanical principles.

If now a magnetic field is applied at right angles to the electric field, the electrons are acted upon by a force which would, if the field were strong enough, make them describe circular paths. As it is, the electrons suffer collisions with the lattice and the path becomes a zig-zag made up of arcs of circles, the net result of which is to increase greatly the distance through which the electron has to travel to pass from one end of the conductor to the other, and consequently the chances of a collision, and hence the resistance to its motion. It is further seen that there is a transfer of electrons transversely to the applied electric field, which proceeds until an electromotive force is built up which is sufficient to counterbalance this effect. This is, of course, the origin of the Hall effect. Mathematically the treatment is similar to that already used when the magnetic field is absent. One has to set up an integral equation expressing that the distribution is steady under the applied electric field, the magnetic field, and also, it must be remembered, the transverse Hall field.

Sommerfeld found that for moderate field strengths the change of resistance follows a square law

$$\Delta\rho/\rho_0 = BH^2. \quad (1)$$

If the coefficient B is calculated for silver, for example, it comes out as  $1.2 \times 10^{-17}$ , which is about ten thousand times smaller than the observed value. Further, if we assume the result obtained by Bloch that the mean free path is inversely proportional to the absolute temperature, the above law gives a change of resistance which is independent of the temperature, whereas experimentally it is known to decrease as the temperature rises. The fact

that the theory does not give the qualitative features of the effect correctly is perhaps even more serious than that the coefficient is too small.

Frank\* has extended these calculations to make them applicable to strong fields, and finds that the change of resistance may be expressed in the form

$$\frac{\Delta\rho}{\rho_0} = \frac{BH^2}{1 + CH^2}. \quad (2)$$

B is the same as the constant in Sommerfeld's formula ; but since it is not of the correct order of magnitude, Frank chooses the constant B so as to give the correct curve for small values of H, and then determines C with the help of formula (2) so as to fit one point on the experimental curve. When this is done it is found that the correct form of Kapitza's curves is given by the function (2), and that C, which decreases with the temperature, is of the right order of magnitude to express the departure from the quadratic law for high fields.

We are, however, still faced with the primary difficulty that the theory gives far too small a value for the change of resistance, and the temperature dependence is wrong. Peierls† has discussed in some detail the relative importance of the various effects which might account for the change of resistance, and finally comes to the conclusion that to obtain the right order of magnitude for the effect one must take into account the fact that the electrons in a metal are not moving freely, but are strongly influenced by the potential field due to the metallic ions ; in other words, one must go a stage further than the usual calculation and consider variations of the electron energy function from spherical symmetry, when that energy function is expressed in terms of wave numbers or of the electron velocities. If one imagines the energy expanded as a power series in  $u, v, w$ , where  $u, v, w$  are quantities analogous to the three components of velocity on the classical theory, or more precisely where  $u = 2\pi k/G$ ,  $v = 2\pi l/G$ , and  $w = 2\pi m/G$ ,  $k, l$  and  $m$  being the electronic quantum numbers and  $G$  a large integer, so that  $u, v$  and  $w$  may be treated as continuous variables, it takes the form

$$E(uvw) = A + B(u^2 + v^2 + w^2) + C(u^2v^2 + v^2w^2 + w^2u^2) \\ + D(u^4 + v^4 + w^4) + \text{terms of higher order}, \quad (3)$$

when we remember that the function must have cubic symmetry, and that terms involving odd powers of the variables must vanish. Now on the Bloch

\* 'Z. Physik,' vol. 64, p. 650 (1930); 'Rev. Mod. Phys.,' vol. 3, p. 16 (1931).

† 'Leipziger Vorträge,' p. 75 (1930).



model\* of a metal the levels derived from the  $s$  terms have energies given by

$$E(uvw) = W - 2\beta(\cos u + \cos v + \cos w).$$

For small values of  $u, v, w$  this expression takes the form

$$E(uvw) = W' + \beta(u^2 + v^2 + w^2), \quad (4)$$

and this is the form in which the energy function is generally used in applications of the theory. We have stopped at the first two terms of the expansion (3), and this is equivalent to the assumption of free electrons. One hopes to be able to explain the effects by including only these lower order terms; but when one remembers that the number of electrons in a metal is very large and that the Pauli Exclusion Principle applies, so that the electrons cannot all have low velocities, one is no longer surprised when one finds that the procedure gives the wrong result and it is found necessary to include higher order terms. If one attempts to carry through the calculations including these higher order terms, one finds that the departure from spherical symmetry complicates the problem enormously, so that the calculations for such a case have not yet been carried out. Peierls† makes some general deductions as to the form of the solution in its dependence on the field and the temperature, and shows that a saturation effect is to be expected for very strong fields; but does not, of course, evaluate the numerical constants involved. Peierls shows, in fact, that with Fermi statistics the solution of the integral equation must be a function of  $H/T$ , and Bethe‡ has pointed out that as a consequence of this, if the theory gave the correct order of magnitude for the coefficient  $B$ , one would also automatically obtain the right kind of temperature dependence.

There is a class of substances, however, which proves to be more amenable to mathematical treatment; these are the semi-conductors, typical examples of which are germanium, tellurium and molecular graphite. In the theory of semi-conductors recently developed by A. H. Wilson,§ it is shown that the number of electrons taking part in the conduction process is very small, and that these electrons may be considered as obeying Maxwellian statistics. Under these circumstances one should be able to explain the resistance change without having to take into account the higher order terms; in fact, if it

\* 'Z. Physik,' vol. 52, p. 555 (1928); referred to as *loc. cit.*

† 'Ann. Physik,' vol. 10, p. 100 (1931).

‡ 'Nature,' vol. 127, p. 336 (1931).

§ 'Proc. Roy. Soc.,' A, vol. 133, p. 458 (1931); referred to as W I. 'Proc. Roy. Soc.,' A, vol. 134, p. 277 (1931); referred to as W II.

should prove necessary to include the higher order terms, one would be forced to the conclusion that the successes of the present theory of conduction are mostly fortuitous.

In the calculations it was thought preferable to follow the Bloch treatment with its explicit evaluation of the mean free path rather than the equivalent classical calculation. The final results, however, should agree, provided the correct value of the mean free path is inserted into the classical formulæ. It was found that the theory gives the correct form of the curve required to explain the experimental results both for low and for high fields, and also that the order of magnitude of the resistance change is correct, although the actual numerical values are rather lower than those found by Kapitza.\*

The variation of the change of resistance with the temperature given by the theory is in the right direction, *i.e.*, the change of resistance decreases with increasing temperature, and the bend in the curve is shifted to lower field strengths.

#### *Discussion of the Model.*

In order to understand the further development of the theory it becomes necessary to examine a more accurate model of a metal (Bloch, *loc. cit.*), and we therefore give a résumé of some well-known results. In a wave mechanical treatment we can approach the problem from two different standpoints, depending on whether we wish to obtain a picture of the motion of a loosely bound, or of a tightly bound electron in a metallic lattice. In the first case we regard the electron as moving in a smeared triply-periodic field due to all the other electrons and to the ions of the lattice. The wave equation for the one-dimensional problem, which is of the type known as Hill's equation,† may be discussed exactly, and the three-dimensional case may be treated by approximate methods. One finds that the energy levels of the electron in the lattice are split up into bands of allowed and disallowed energies. In the case of tightly bound electrons, we proceed by building up the metal out of a large number of individual atoms, each of which has, of course, a number of discrete energy levels. If we now put them all together in lattice array and first of all disregard the interactions between neighbouring atoms, each of the states of the total system consisting of all the atoms will have a degeneracy equal to the number of atoms, or twice this if we take into account the two

\* 'Proc. Roy. Soc.,' A, vol. 123, p. 318 (1929).

† L. Brillouin, "Die Quantenstatistik" (Springer) (1931), may be consulted for general information and references on this and other parts of the subject.

directions of electron spin. If the interactions are then introduced as a perturbation, the degenerate levels will be spread into bands each consisting of a large number of discrete levels; and in a metal, where the number of constituent atoms is large, the bands are practically continuous. We are thus again led to the conclusion that there are bands of allowed and disallowed energies in the spectrum of an electron in a periodic lattice field, and since this is so in the two limiting cases, we may safely conclude that this is a general feature for electrons of all degrees of binding.

Bloch has carried the theory a stage further, and shows that if the lattice field is perfectly periodic the electron can travel through it quite freely, and the conductivity for such a lattice is infinite. Actually, of course, the perfect periodicity of the lattice field is destroyed by the thermal motions of the ions, which may be considered as a perturbation causing transitions of an electron from a given state to one of greater or less energy, the difference in energy being taken up by the ions of the lattice regarded as quantized harmonic oscillators: the whole assembly is subject to the laws of statistical equilibrium. It is only by taking into account this transfer of electronic energy into thermal motion that one can obtain a finite value of the conductivity.

It has already been seen that the energy spectrum of an electron in the lattice field is split up into bands of allowed and disallowed energies. In metals successive bands overlap in the three-dimensional model, a fact which is sometimes overlooked in one-dimensional treatments of conduction problems; but if we assume that there is no overlapping of the bands, and that a certain number of the lower bands are completely filled up, there will be no conduction at ordinary temperatures, since the thermal energy of the lattice vibrations is insufficient to remove one of the electrons from one of the full bands to a higher empty band, and the Pauli Exclusion Principle prevents transitions within the band itself. These are the conditions existing for an insulator. If now an impurity is present, and if one of its energy levels is occupied by an electron and happens to fall between one of the full bands and the next higher empty band, it is quite possible that, if the energy difference between the discrete level and the bottom of the higher band is small enough, the thermal vibrations may cause the electron to leave its atom and pass over into the next higher band, in which it is free to contribute towards the conduction. The atom itself is, of course, ionized, and acts as a scatterer of electrons and so contributes towards the residual resistance. Since the number of electrons in the upper band is small, the electron gas is no longer degenerate, and Maxwellian statistics may be applied. This is the model (Wilson, *loc.*

*cit.*) which we shall use in the subsequent calculations. It must be remembered that, on this theory, there is a sharp distinction between semi-conductors and ordinary conductors, and that the difference is not merely one of degree. A semi-conductor is characterized by a negative temperature coefficient, and by the fact that its conductivity depends entirely on the impurities present, becoming a much worse conductor when the amount of impurity is reduced.

### The Integral Equation.

Following Wilson (W II, p. 280) we take as our model of a semi-conductor a simple cubic lattice containing  $G^3$  atoms of which  $N_0$  are foreign atoms. It is further assumed that each atom of impurity possesses a single electron in a discrete state of energy  $W_1$ . The next band of allowed energies is given by

$$E_{uvw} = W_2 + 6\beta - 2\beta (\cos u + \cos v + \cos w),$$

where  $u, v, w$  may assume the values  $2\pi/G$  ( $0, \pm 1, \pm 2, \dots$ ). For small values of  $u, v, w$  this expression takes the form

$$E_{uvw} = W_2 + \beta (u^2 + v^2 + w^2) = W_2 + \beta \rho^2.$$

We now have to set up the Boltzmann equation expressing the condition that the distribution of electrons must be steady under the combined influence of the electric and magnetic fields and the collisions with the lattice.

The alteration of the distribution function  $n(uvw)$  due to the electric field  $F$  is given by

$$- \frac{2\pi e F}{h} \frac{\partial n}{\partial u},$$

and that due to the magnetic field at right angles to the applied electric field by

$$\frac{eH}{mc} \left( u \frac{\partial}{\partial v} - v \frac{\partial}{\partial u} \right) n.$$

The alteration due to collisions with the lattice has been worked out by Bloch\* and is given by

$$\begin{aligned} n_a = & \frac{\partial}{\partial t} \frac{G^3}{8\pi^3} \sum_{f, g, h} \frac{2\pi^2 C^2 h\nu}{\mu^2 v^2 8\pi^2 M} [\{n(uvw) [1 - n(u'v'w')] N_{fgh} - n(u'v'w') \\ & \times [1 - n(uvw)] (N_{fgh} + 1)\} \Omega(E_{uvw} - E_{u'v'w'} + h\nu) \\ & + \{n(uvw) [1 - n(u'v'w')] (N_{fgh} + 1) - n(u'v'w') \\ & \times [1 - n(uvw)] N_{fgh}\} \Omega(E_{uvw} - E_{u'v'w'} - h\nu)]. \quad (5) \end{aligned}$$

\* Cf. *loc. cit.*, p. 587 et seq.

The meaning of the various quantities is as follows.  $C$  is a quantity of the order of the square of the reciprocal of the atomic radius,  $M$  is the mass of the crystal cube of volume  $(Ga)^3$ ,  $v$  is the velocity of propagation of sound, and  $\mu = 8\pi^2 m/h^2$ .

$$\Omega (E_{uvw} - E_{u'v'w'} \pm h\nu) = \frac{1 - \cos 2\pi t [E_{uvw} - E_{u'v'w'} \pm h\nu]/h}{(E_{uvw} - E_{u'v'w'} \pm h\nu)^2} = \Omega^\pm,$$

and if we assume that the lattice vibrations are always in thermal equilibrium,

$$N_{fgh} = \frac{1}{e^{h\nu/kT} - 1},$$

where

$$v = \frac{v}{2\pi a} \sqrt{f^2 + g^2 + h^2} = \frac{v}{2\pi a} R. \quad (6)$$

Further, the three conditions

$$u - u' = \pm f, \quad v - v' = \pm g, \quad w - w' = \pm h,$$

must be satisfied.

If we take into account the fact that, in the case we are treating, there are few electrons in the upper band, we may omit those factors in equation (5) which give expression to the Pauli Principle. It is, of course, understood that the Pauli Principle still applies to those electrons in the full lower bands. Making this change, and substituting integrations for the triple summations in the usual way, since, when  $G$  is large,  $u'$ ,  $v'$ ,  $w'$  are practically continuous variables, equation (5) takes the form

$$n_a = \frac{\partial}{\partial t} \cdot \frac{G^3}{8\pi^3} \iiint_{-\infty}^{\infty} \frac{2\pi^2 C^2 h \nu}{\mu^2 v^2 8\pi^2 M} [\{n(uvw) N_{fgh} - n(u'v'w') (N_{fgh} + 1)\} \Omega^+ \\ + \{n(uvw) (N_{fgh} + 1) - n(u'v'w') N_{fgh}\} \Omega^-] du' dv' dw'.$$

In carrying out the integrations, we first of all use polar co-ordinates  $\rho$ ,  $\theta$ ,  $\phi$  and  $\rho'$ ,  $\theta'$ ,  $\phi'$ , so that we have  $u^2 + v^2 + w^2 = \rho^2$  and  $u'^2 + v'^2 + w'^2 = \rho'^2$ , the axis of  $u$  being  $\theta = 0$ . Then instead of  $\rho'$ ,  $\theta'$ ,  $\phi'$  we use polar co-ordinates  $R$ ,  $\vartheta$ ,  $\varpi$  in the  $f$ ,  $g$ ,  $h$  space, and finally, instead of  $R$  we use the equivalent variable  $v$  given by (6). The line joining  $(u, v, w)$  to the origin is taken as  $\vartheta = 0$ , and  $\vartheta$  is therefore the angle between the direction of propagation of the incident electronic wave and that of the elastic vibration, the direction cosines being proportional to  $(u, v, w)$  and to  $(f, g, h)$  respectively.

On making these changes of co-ordinates the equation becomes

$$n_a = \frac{G^3 2\pi^2 C^2 h}{8\pi^3 \mu^2 v^2 8\pi^2 M} \left( \frac{2\pi a}{v} \right)^3 \frac{\partial}{\partial t} \iiint v^3 dv \sin \vartheta d\vartheta d\varpi [\{n(uvw) N_v - n(v\vartheta\varpi) (N_v + 1)\} \Omega^+ \\ + \{n(uvw) (N_v + 1) - n(v\vartheta\varpi) N_v\} \Omega^-].$$

We first consider briefly the integration involving the time factor, as it has been considered by several writers.\* It acts as a sort of  $\delta$ -function, contributing a factor  $\pi \mathbf{v}/2\hbar a \beta v \rho$  when  $v$  lies in the range  $v = 0$  to  $v = v\rho/\pi a$ ; otherwise zero. This is true for the range of electron velocities which is of practical importance, namely, those for which  $\rho \gg \Theta/T_0$ , where  $T_0 = \beta/k$ .

We now have

$$n_a = \frac{(aG)^3 \pi C^2}{8M\rho a \beta \mathbf{v}^4 \mu^2} \int_0^{2\pi} \int_0^{v\rho/\pi a} v^2 dv d\varpi [\{n(uvw) N_v - n(v\vartheta\varpi) (N_v + 1)\}_{E' = E + \hbar v} + \{n(uvw) (N_v + 1) - n(v\vartheta\varpi) N_v\}_{E' = E - \hbar v}],$$

so that the complete Boltzmann equation may now be written

$$\begin{aligned} \frac{eH}{mc} \left( u \frac{\partial}{\partial v} - v \frac{\partial}{\partial u} \right) n - \frac{2\pi a e}{h} \left[ F_u \frac{\partial n}{\partial u} + F_v \frac{\partial n}{\partial v} \right] \\ = \frac{(aG)^3 \pi C^2}{8M\rho a \beta \mathbf{v}^4 \mu^2} \int_0^{2\pi} \int_0^{v\rho/\pi a} v^2 dv d\varpi [\{n(uvw) N_v - n(v\vartheta\varpi) (N_v + 1)\}_{E' = E + \hbar v} \\ + \{n(uvw) (N_v + 1) - n(v\vartheta\varpi) N_v\}_{E' = E - \hbar v}]. \quad (7) \end{aligned}$$

When a magnetic field is applied a current begins to flow transversely to the direction of the applied electric field. This causes a transverse potential difference to be set up which finally stops the flow of current transverse to the applied electric field. This potential is represented by the term  $F_v$  in the equation.

We attempt to solve this integral equation for the perturbed distribution function by assuming that

$$n = n_0 + uX_1 + vX_2, \quad (8)$$

where  $X_1$  and  $X_2$  are functions of the energy alone, and the initial distribution

$$n_0 = 4\pi^3 \frac{N}{G^3} \left( \frac{\beta}{\pi k T} \right)^{3/2} e^{-\beta \rho^2/kT}.$$

Introducing the expression for  $n$  given by equation (8) into the right-hand side of equation (7), we have

$$\begin{aligned} n_a = \frac{(aG)^3 \pi C^2}{8M\rho a \beta \mathbf{v}^4 \mu^2} \int_0^{2\pi} \int_0^{v\rho/\pi a} v^2 dv d\varpi [\{n_0(E) + uX_1(E) + vX_2(E)\} \\ - \{n_0(E + \hbar v) + u'X_1(E + \hbar v) + v'X_2(E + \hbar v)\} e^{\hbar v/kT} \\ + \{n_0(E) + uX_1(E) + vX_2(E)\} e^{\hbar v/kT} \\ - \{n_0(E - \hbar v) + u'X_1(E - \hbar v) + v'X_2(E - \hbar v)\}] \frac{1}{e^{\hbar v/kT} - 1}. \end{aligned}$$

\* W I, p. 483; W II, p. 283; Brillouin, "Die Quantenstatistik," p. 343, or "Les Statistiques Quantiques," vol. 2, p. 287.

The terms independent of  $X$  vanish on account of the equilibrium conditions. We now introduce  $x = h\nu/kT$  as a new integration variable, and assume that  $T \ll T_0$ , so that we may write

$$\left. \begin{aligned} n_0(E + kTx) &= n_0(E - kTx) = n_0(E), \\ X_1(E + kTx) &= X_1(E - kTx) = X_1(E), \\ X_2(E + kTx) &= X_2(E - kTx) = X_2(E). \end{aligned} \right\}$$

By this process we reduce the integral equation to an ordinary equation in  $X_1$  and  $X_2$ , and we have

$$n_a = \frac{G^3 \pi C^2}{8M\rho a \beta \nu \mu^2} \left( \frac{ak\Theta}{h\nu} \right)^3 \left( \frac{T}{\Theta} \right)^3 \int_0^{2\pi} \int_0^{\kappa\rho\Theta/T} \frac{x^2 dx d\pi}{e^x - 1} [\{uX_1(E) + vX_2(E)\} \\ - \{u'X_1(E) + v'X_2(E)\} e^x + \{uX_1(E) + vX_2(E)\} e^x - \{u'X_1(E) + v'X_2(E)\}] \quad (9)$$

where  $\kappa = h\nu/\pi ak\Theta$ , and  $\Theta$  is the Debye characteristic temperature.

On substituting

$$u' = u + f, \quad v' = v + g$$

equation (9) becomes

$$n_a = - \frac{G^3 \pi C^2}{8M\rho a \beta \nu \mu^2} \left( \frac{ak\Theta}{h\nu} \right)^3 \left( \frac{T}{\Theta} \right)^3 \int_0^{2\pi} \int_0^{\kappa\rho\Theta/T} \frac{x^2 dx d\pi}{e^x - 1} \{f_{\vartheta_1} X_1(E) + g_{\vartheta_1} X_2(E)\} \\ + \{f_{\vartheta_2} X_1(E) + g_{\vartheta_2} X_2(E)\} e^x. \quad (10)$$

A little consideration shows that

$$\left. \begin{aligned} f &= \frac{2\pi akTx}{h\nu} \left[ \cos \vartheta \cdot \frac{u}{\rho} + \cos \varpi \sin \vartheta \sin \theta_1 \right] \\ g &= \frac{2\pi akTx}{h\nu} \left[ \cos \vartheta \cdot \frac{v}{\rho} + \cos (\varpi + \alpha) \sin \vartheta \sin \theta_1' \right] \end{aligned} \right\} \quad (11)$$

where  $\theta_1$  and  $\theta_1'$  are the angles between the direction of  $\rho$  and the  $u$  and  $v$  axes respectively, and  $\alpha$  is an arbitrary fixed angle. The subscripts  $\vartheta_1$  and  $\vartheta_2$  in (10) mean that in the expressions for  $f$  and  $g$  those values of  $\vartheta$  should be taken which correspond to the appropriate resonance terms  $E_{uvv} - E_{u'v'v'} \pm h\nu = 0$ . This gives us

$$\left. \begin{aligned} \cos \vartheta_1 &= \frac{h\nu}{4\pi a \beta \rho} - \frac{\pi akT}{h\nu \rho} x \\ \cos \vartheta_2 &= - \frac{h\nu}{4\pi a \beta \rho} - \frac{\pi akT}{h\nu \rho} x \end{aligned} \right\} \quad (12)$$

When we have inserted the values for  $f$  and  $g$  as given by equations (11) into

(10), have integrated over  $\varpi$ , and made use of equations (12), we are left with

$$n_a = -\frac{G^3 2\pi^2 C^2}{8\pi\rho^2 a\beta v\mu^2} \left(\frac{ak\Theta}{h\nu}\right)^3 \left(\frac{T}{\Theta}\right)^3 \frac{2\pi akT}{h\nu} (uX_1 + vX_2) \int_0^{\kappa\rho\Theta/T} \frac{x^3}{e^x - 1} \left\{ \frac{h\nu}{4\pi a\beta\rho} \right. \\ \left. - \frac{\pi akT}{h\nu\rho} x - \frac{h\nu}{4\pi a\beta\rho} e^x - \frac{\pi akT}{h\nu\rho} x e^x \right\} dx.$$

Since  $x$  is supposed small, we may put  $e^x = 1$  in the numerator of the integrand, and  $e^x - 1 = x$  in the denominator, and hence obtain after a simple integration

$$n_a = \frac{VC^2 k^5 a T \Theta^4 \kappa^4 \rho}{256 M \beta v^6 m^2 h} (uX_1 + vX_2).$$

The Boltzmann equation now finally takes the simple form

$$\frac{eH}{mc} \left( u \frac{\partial}{\partial v} - v \frac{\partial}{\partial u} \right) [n_0 + uX_1 + vX_2] - \frac{2\pi ae}{h} \left[ F_x \frac{\partial n_0}{\partial u} + F_y \frac{\partial n_0}{\partial v} \right] \\ = \frac{VC^2 k^5 a T \Theta^4 \kappa^4 \rho}{256 M \beta v^6 m^2 h} (uX_1 + vX_2),$$

yielding the following two equations to determine  $X_1$  and  $X_2$ ,

$$\left. \begin{aligned} \frac{eH}{mc} X_2 - \frac{4\pi ae\beta}{h} \frac{\partial n_0}{\partial E} F_x - T\rho\gamma X_1 &= 0 \\ T\rho\gamma X_2 + \frac{4\pi ae\beta}{h} \frac{\partial n_0}{\partial E} F_y + \frac{eH}{mc} X_1 &= 0 \end{aligned} \right\}$$

where

$$\gamma = \frac{VC^2 k^5 a \Theta^4 \kappa^4}{256 M \beta v^6 m^2 h}.$$

If we further put

$$\frac{eH}{m\gamma T} = \alpha,$$

we obtain

$$X_1 = -\frac{4\pi ae\beta}{hT\gamma} \frac{\alpha F_y + \rho F_x}{\alpha^2 + \rho^2} \frac{\partial n_0}{\partial E}, \quad (13A)$$

$$X_2 = \frac{4\pi ae\beta}{hT\gamma} \frac{\alpha F_x - \rho F_y}{\alpha^2 + \rho^2} \frac{\partial n_0}{\partial E}. \quad (13B)$$

The total currents in the  $x$ - and  $y$ -directions are given by

$$J_x = \frac{4\pi ae\beta}{h} \int \frac{G^3}{4\pi^3} u^2 X_1 du dv dw, \quad (14A)$$

$$J_y = \frac{4\pi ae\beta}{h} \int \frac{G^3}{4\pi^3} v^2 X_2 du dv dw. \quad (14B)$$



Since  $J_y$  must be zero under experimental conditions, we have the following equation expressing  $F_y$  in terms of  $F_x$ ,

$$F_y \int \frac{v^2 \rho}{\alpha^2 + \rho^2} \frac{\partial n_0}{\partial E} du dv dw = \alpha \cdot F_x \int \frac{v^2}{\alpha^2 + \rho^2} \frac{\partial n_0}{\partial E} du dv dw,$$

and, on substituting for  $\partial n_0 / \partial E$ , we obtain

$$F_y = \alpha \cdot F_x \frac{\int_0^\infty \frac{\rho^4}{\alpha^2 + \rho^2} e^{-\beta \rho^2 / kT} d\rho}{\int_0^\infty \frac{\rho^6}{\alpha^2 + \rho^2} e^{-\beta \rho^2 / kT} d\rho} \quad (15)$$

### *Resistance for Moderate Fields.*

Considering first the case of moderate field strengths, we may expand the denominators in the integrands of equation (15), and integrate term by term. To a close approximation we find

$$F_y = \alpha \Gamma(\frac{3}{2}) \cdot (\beta/kT)^{\frac{1}{2}} F_x.$$

Hence

$$X_1 = - \frac{4\pi a e \beta}{h T \gamma} \frac{\alpha^2 \Gamma(\frac{3}{2}) (\beta/kT)^{\frac{1}{2}} + \rho}{\alpha^2 + \rho^2} \cdot \frac{\partial n_0}{\partial E} \cdot F_x,$$

and the conductivity

$$\sigma = \frac{J_x}{F(Ga)^3} = - \left( \frac{4\pi a e \beta}{h} \right)^2 \frac{G^3}{T \gamma 4\pi^3} \int \left[ \frac{\alpha^2 \Gamma(\frac{3}{2}) (\beta/kT)^{\frac{1}{2}}}{\alpha^2 + \rho^2} + \frac{\rho^5}{\alpha^2 + \rho^2} \right] \frac{\partial n_0}{\partial E} \sin^2 \phi \cdot \cos^2 \theta \sin \theta d\rho d\theta d\phi. \quad (16)$$

Retaining only quadratic terms in  $H$ , this reduces to

$$\begin{aligned} \sigma &= \frac{32\pi^{3/2} e^2 a^3 \beta^{7/2} N}{3(Ga)^3 h^2 \gamma k^{5/2} T^{7/2}} \int_0^\infty \left[ \rho^3 - \alpha^2 \left\{ \frac{\rho^3}{\alpha^2 + \rho^2} - \Gamma(\frac{3}{2}) (\beta/kT)^{\frac{1}{2}} \rho^2 \right\} \right] e^{-\beta \rho^2 / kT} d\rho \\ &= \frac{16\pi^{3/2} e^2 a^3 \beta^{3/2} N}{3(Ga)^3 h^2 \gamma k^{1/2} T^{3/2}} \left[ 1 - 0.22 \alpha^2 \frac{\beta}{kT} \right], \end{aligned}$$

so that\*

$$\frac{\sigma}{\sigma_0} = \frac{\rho_0}{\rho} = \left[ 1 - 0.22 \left( \frac{e}{mc\gamma} \right)^2 \frac{\beta}{kT^3} H^2 \right].$$

where  $\sigma_0$  is the conductivity in the absence of the magnetic field.

On substituting for  $\gamma$ , and  $\kappa = h\nu/\pi a k \Theta$ , we find that the change of resistance is

$$\frac{\Delta \rho}{\rho_0} = 0.22 \left( \frac{256 e M \nu^2 m \beta^{3/2} \pi^4 a^3}{V C^2 k^{3/2} h^3 c T^{3/2}} \right)^2 H^2. \quad (17)$$

\*  $\rho$  in this equation will not, of course, be confused with the integration variable above.

*The Change of Resistance in Strong Fields.*

The approximate evaluation of the integrals by a series expansion is not valid for strong fields. It is, however, quite easy to carry out all the integrations exactly. It is found that all the integrals involved can be reduced to the following three types,

$$\int_0^\infty \rho^n e^{-\beta\rho^2/kT} d\rho = \frac{1}{2} \Gamma\left(\frac{n+1}{2}\right) (kT/\beta)^{\frac{n+1}{2}},$$

$$\int_0^\infty \frac{\rho}{\alpha^2 + \rho^2} e^{-\beta\rho^2/kT} d\rho = \frac{1}{2} e^{\alpha^2\beta/kT} \int_{\alpha^2\beta/kT}^\infty \frac{e^{-t}}{t} dt = -\frac{1}{2} e^{\alpha^2\beta/kT} \text{Ei}(-\alpha^2\beta/kT),$$

and

$$\int_0^\infty \frac{e^{-\beta\rho^2/kT}}{\alpha^2 + \rho^2} d\rho = J.$$

This latter integral is transformed by a differential equation method,\* and one finds

$$J = e^{\alpha^2\beta/kT} \frac{\sqrt{\pi}}{\alpha} \int_{\alpha(\beta/kT)^{\frac{1}{2}}}^c e^{-t^2} dt, \quad (18)$$

where  $c$  is a constant which is determined by the fact that the integral  $J$  must be zero when  $\beta/kT$  becomes infinite.

For positive values of  $\alpha$  we then have†

$$\int_0^\infty \frac{e^{-\beta\rho^2/kT}}{\alpha^2 + \rho^2} d\rho = e^{\alpha^2\beta/kT} \frac{\sqrt{\pi}}{\alpha} \int_{\alpha(\beta/kT)^{\frac{1}{2}}}^\infty e^{-t^2} dt = \frac{\pi}{2\alpha} e^{\alpha^2\beta/kT} [1 - \Phi[\alpha(\beta/kT)^{\frac{1}{2}}]]. \quad (19)$$

Using these values of the integrals, we find from equation (15) of the previous section

$$F_v = w \cdot \frac{\Gamma(\frac{3}{2}) - \sqrt{\pi} \cdot w^2 + \pi w^3 e^{w^2} [1 - \Phi(w)]}{1 - w^2 - w^4 e^{w^2} \text{Ei}(-w^2)} F_e.$$

Substituting this value of  $F_v$  in equation (13A), and making use of (14A), we find

$$\frac{\Delta\rho}{\rho_0} = \frac{1 - w^2 - w^4 e^{w^2} \text{Ei}(-w^2)}{[1 - w^2 - w^4 e^{w^2} \text{Ei}(-w^2)]^2 + w^2 \pi [0.5 - w^2 + w^3 e^{w^2} \sqrt{\pi} [1 - \Phi(w)]]^2} - 1, \quad (20)$$

where

$$w^2 = \alpha^2 \beta / kT.$$

\* Gans, *loc. cit.*, p. 326 (Appendix).

† For tables of the functions  $\text{Ei}$  and  $\Phi$ , see Jahnke and Emde, 'Funktionentafeln,' pp. 19 and 31 (1909).

*The Hall Effect.*

The Hall coefficient  $R$  is defined by the equation

$$R = \frac{F_y}{J_x \cdot H} = \frac{1}{H\sigma_0} \cdot \frac{F_y}{F_x} \frac{\rho}{\rho_0}.$$

On substituting the values of  $F_y/F_x$  and  $\rho/\rho_0$  we find

$$R = \frac{w}{H\sigma_0} \frac{\sqrt{\pi}}{2} \cdot \frac{1 - 2w^2 + 2w^3 e^{w^2} \sqrt{\pi} [1 - \Phi(w)]}{1 - w^2 - w^4 e^{w^2} \text{Ei}(-w^2)} \frac{\rho}{\rho_0}.$$

For vanishing magnetic field we have

$$R_0 = \frac{w}{H\sigma_0} \frac{\sqrt{\pi}}{2} = \frac{\sqrt{\pi} \cdot e \left( \frac{\beta}{kT} \right)^{\frac{1}{2}}}{2mc\gamma T} \cdot \frac{1}{\sigma_0},$$

so that the result may be expressed in the convenient form

$$R/R_0 = \frac{1 - 2w^2 + 2w^3 e^{w^2} \sqrt{\pi} [1 - \Phi(w)]}{1 - w^2 - w^4 e^{w^2} \text{Ei}(-w^2)} \frac{\rho}{\rho_0}. \quad (21)$$

*Comparison with the Classical Formulæ.*

It has been remarked already in the introduction that although the Bloch method has been followed in these calculations, the final formulæ should be identical with those given by the classical treatment, provided that the correct expression for the mean free path is substituted in the latter formulæ.

However, a comparison of formula (20) of a preceding section with formula (35) of Gans' paper shows that there is a difference, and a closer investigation reveals that the difference is due to a slip in Gans' derivation of his equation (28) for the  $y$ -component of the current by interchanging certain terms in the expression (27) for the  $x$ -component. The  $x$ -component equation involves the integral (19), which, in Gans' notation, is written

$$e^{a^2\beta/kT} \frac{\sqrt{\pi}}{\alpha} \Theta [\alpha (\beta/kT)^{\frac{1}{2}}]. \quad (22)$$

Gans effectively substitutes  $-\alpha$  for  $\alpha$  in this function (22), forgetting that (19) or (22) is the value of the integral (18) only for positive values of  $\alpha$ . If  $\alpha$  is to have negative values, the constant of integration  $c$  in equation (18) must be put equal to  $-\infty$ , so that the integral  $J$  still vanishes when  $\beta/kT \rightarrow \infty$ .

When this change is made in Gans' formula (35) for  $\sigma/\sigma_0$ , it becomes identical with that obtained in this paper, provided the value of  $w$  is the same in the two

cases. The formula (34) of the same paper for the Hall effect is likewise wrong; the correct form is given in equation (21) of the preceding section.

This correction completely alters the character of Gans' solution for high fields. For example, if his function is plotted, one finds that  $\Delta\rho/\rho_0$  increases steadily and becomes infinite at about 250 kilo-gauss (at 300° K.), changes discontinuously to minus infinity, and then increases again. Similarly, the experimentally determined variation of the Hall coefficient with the magnetic field is quite different from that given by his equation (35').

### Numerical Results.

1. *The Change of Resistance for Moderate Fields.*—Taking the values for the various constants as given in the following table, we may make an estimate of the order of magnitude of the change for small to moderate field strengths.

From equation (17) we find

Germanium.

$$\Delta\rho/\rho_0 = 1.57 \times 10^{-12} H^2.$$

M/V	(density) 5.47
<i>e</i>	$4.77 \times 10^{-10}$ e.s.u.
<i>v</i>	$4 \times 10^5$ cm./sec.
<i>m</i>	$8.98 \times 10^{-28}$ gram
$\beta$	$1.59 \times 10^{-12}$ erg. (1 volt)
<i>a</i>	$10^{-8}$ cm.
C	$10^{16}$ .
<i>k</i>	$1.37 \times 10^{-16}$ erg./degree
<i>h</i>	$6.547 \times 10^{-27}$ erg. secs.
<i>c</i>	$3 \times 10^{10}$ cm./sec.
T	300° K.

This is in very reasonable agreement with the observed magnitude of the change for small fields. It is some ten thousand times as great as the value obtained by Sommerfeld in the case of pure metals, using Fermi statistics.

If the value is calculated for another temperature, the variation with temperature given by equation (17) is seen to be in the right direction.

2. *The Change of Resistance for Strong Fields.*—The function representing  $\Delta\rho/\rho_0$  has been plotted in curve I of fig. 1, with

$\Delta\rho/\rho_0$  as ordinate and *w* as abscissa, where *w* is given by

$$w = \frac{256eMv^2m\beta^{3/2}\pi^4a^3H}{VC^2k^{3/2}h^3cT^{3/2}} = 1.39 \times 10^{-2} H/T^{3/2},$$

from which the point corresponding to any pair of simultaneous values of *H* and *T* may be found. The points corresponding to  $10^5$ ,  $2 \times 10^5$ , and  $3 \times 10^5$  gauss for two different values of *T*, namely, at 193° K. (the temperature of a mixture of solid CO<sub>2</sub> and ether in Kapitza's experiments), and at 300° K.

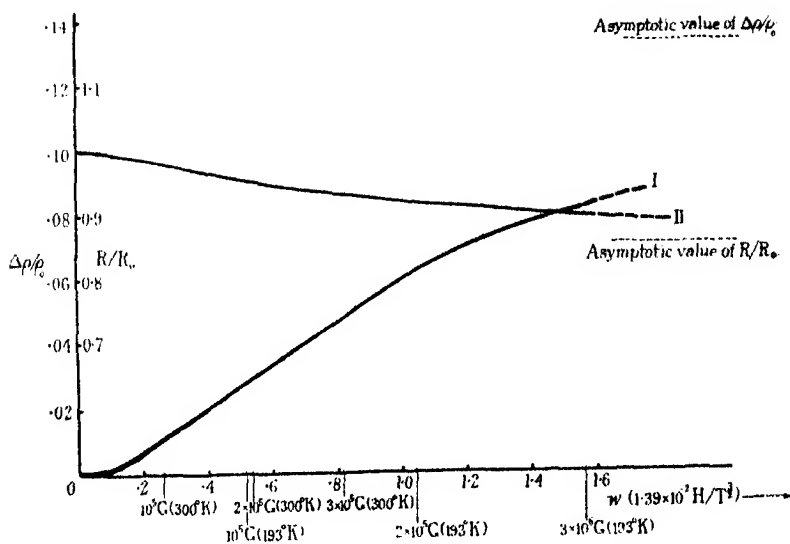


FIG. 1.

(approximately room temperature), have been marked on the graph for comparison. In fig. 2 the function  $\Delta\rho/\rho_0$  is shown for larger values of the argument  $w$ . The lower portion of the full line curve has been plotted by the use of

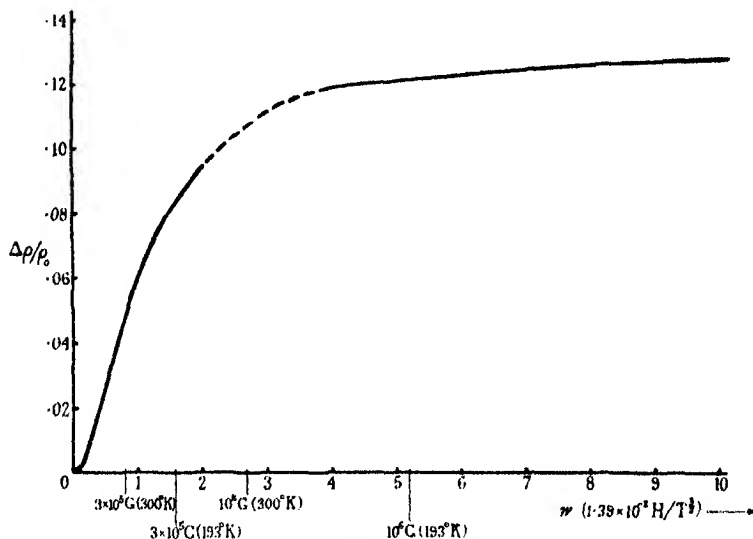


FIG. 2.

tables, and the upper portion by the aid of asymptotic series. The usual tables are rather inadequate for the accurate plotting of the intermediate section (shown dotted in the graph).

We may find the limiting value of  $\Delta\rho/\rho_0$  for very large  $H$  by making use of the asymptotic expansions,\*

$$\text{Ei}(-w^2) = e^{-w^2} \left( -\frac{1}{w^2} + \frac{1}{w^4} - \frac{2}{w^6} + \frac{6}{w^8} - \frac{24}{w^{10}} + \dots \right),$$

$$\sqrt{\pi} [1 - \Phi(w)] = e^{-w^2} \left( \frac{1}{w} - \frac{1}{2w^3} + \frac{3}{4w^5} - \frac{15}{8w^7} + \frac{105}{16w^9} - \dots \right).$$

Substituting these series in formula (20) we find

$$\lim_{H \rightarrow \infty} \Delta\rho/\rho_0 = \lim_{w \rightarrow \infty} \frac{\left[ 2 - \frac{6}{w^2} \right] - \frac{1}{w^2} \left[ 2 - \frac{6}{w^2} \right]^2 - \frac{\pi}{4} \left[ \frac{3}{2} - \frac{15}{4w^2} \right]^2}{\frac{1}{w^2} \left[ 2 - \frac{6}{w^2} \right]^2 + \frac{\pi}{4} \left[ 2 - \frac{15}{4w^2} \right]^2} = 0.132.$$

It is seen that the curve is of the typical form of the resistance curve obtained in measurements with polycrystalline rods. The theory gives rather lower values than one obtains experimentally; but considering the assumptions it has been necessary to make in solving the integral equation, the agreement is quite reasonable. One may hope that a more accurate treatment of the integral equation will lead to higher values for the resistance change, and so improve the agreement with experiment.

The temperature change is again in the right direction, *i.e.*, the bend is shifted towards lower field strengths as the temperature is decreased, and a crude classical calculation shows that the bend in the curve sets in at a point in the graph where the radius of the electronic orbit becomes comparable with the mean free path.

3. *The Hall Coefficient.*—It may be noted that the expression (21) is not identical with the corresponding equation (35') of Gans' paper, for a reason which has already been fully discussed in a preceding section. The function (21) has been plotted in curve II of fig. 1. For very high fields we use the asymptotic expressions for the functions  $\Phi$  and  $\text{Ei}$ , and obtain

$$\lim_{H \rightarrow \infty} R/R_0 = 1.132 \lim_{w \rightarrow \infty} \left[ \frac{\frac{3}{2} - \frac{15}{4w^2}}{2 - \frac{6}{w^2}} \right] \sim 0.849.$$

Unfortunately there appear to be no available data for the variation of the Hall effect with the magnetic field with which the results of this paper may be compared. Most of the experimental work relating to this question has been

\* Jahnke and Emde, *loc. cit.*

done on bismuth, which is not, of course, a semi-conductor, although it does exhibit some semi-conducting properties in addition to those of a metal. In the absence of data on semi-conductors, it may be interesting just to note that for bismuth the variation of the Hall effect with the magnetic field\* is similar to that which the present theory predicts for semi-conductors.

Finally, we find that the classical formula of Gans, as corrected by us, becomes identical with formula (20) of this paper, provided

$$\frac{e\hbar H}{mc} = \alpha (2\beta/m)^{\frac{1}{2}}.$$

Substituting for the values of the various constants, one obtains

$$l = 1.44 \times 10^{-6} \text{ cm.},$$

which is about a hundred times the lattice spacing, and agrees well with the value of the mean free path which one would expect to obtain in a wave mechanical treatment.

In conclusion the writer wishes to thank Professor R. H. Fowler for his encouragement and criticism throughout the course of the work, and Mr. A. H. Wilson for kindly suggesting the problem and for many helpful discussions.

#### *Summary.*

Wilson's theory of semi-conductors has been applied to the problem of the change of resistance of a semi-conductor in a magnetic field. The theory gives the right form of curve required to explain the experimental results both for low and high fields, and yields the correct order of magnitude for the effect. The variation of the change of resistance with the temperature is also in the right direction.

\* Heaps, 'Phys. Rev.', vol. 29, p. 332 (1927).

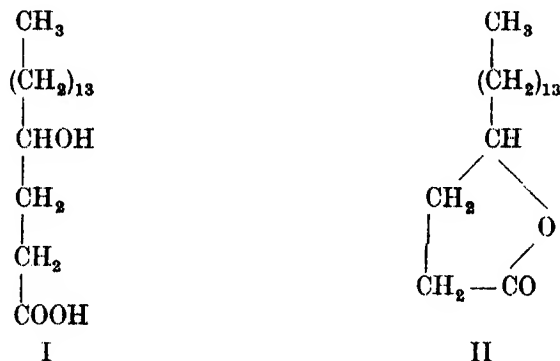
---

*The Structure of Surface Films. Part XVII.— $\gamma$  Hydroxy-Stearic Acid and its Lactone.*

By N. K. ADAM, from the Sir William Ramsay Laboratories of Inorganic and Physical Chemistry, University College, London, W.C.1, and Imperial Chemical Industries, Ltd.

(Communicated by F. G. Donnan, F.R.S.—Received November 9, 1932.)

This paper describes observations, mostly made in 1924 and not hitherto published in detail,\* on the surface pressure of  $\gamma$  hydroxy-stearic acid (I) and its lactone (II) spread as monomolecular films on aqueous solutions.



Most of the measurements were made with the modification of Langmuir's apparatus described in Parts I and II of this series of papers,† in which jets of air prevent the film passing the ends of the float. A few confirmatory observations have been made since, with the apparatus of Adam and Jessop, in which thin metallic ribbons block these gaps. The acid and lactone were kindly given me by Dr. P. W. Clutterbuck, of Manchester University.

The principal results are shown in fig. 1. Curve I is the compression curve of the lactone on distilled water, from 6° to 20°. Similar curves were obtained on hydrochloric acid (up to normal strength), on N/10 sodium carbonate and on N/10 caustic soda. On warming, the films (on water) expanded to a curve closely resembling the well-known liquid expanded curve of films of fatty acids.

\* A note of the principal result, that the lactone is hydrolysed to the acid in the films on moderately strong soda solutions, has been published ('Chem. Rev.,' vol. 3, p. 134 (1926); "The Physics and Chemistry of Surfaces," p. 83 (1930)).

† 'Proc. Roy. Soc.,' A, vol. 99, p. 336 (1921); vol. 101, p. 452 (1922).



The area, extrapolated from 4 dynes per centimetre to no compression, was  $29 \pm 1$  sq. A. for the condensed film; the expanded film tended to an area at low compressions of about 48 sq. A.; the expansion was half completed at a temperature within a few degrees of  $27^\circ$ , under 1.4 dynes per centimetre compression.

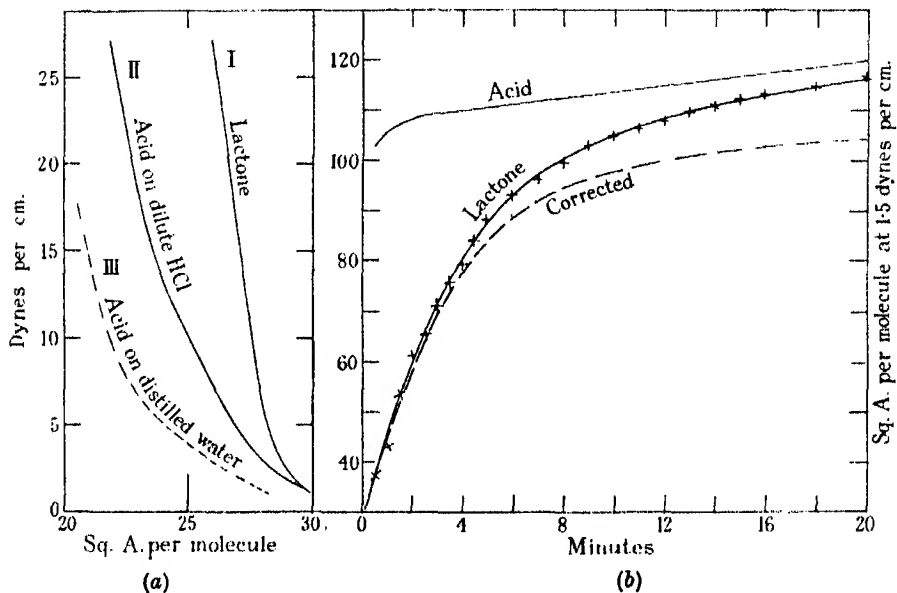


FIG. 1.—(b) Hydrolysis of lactone on N NaOH at  $17.5^\circ$ .

The acid, on N/50 hydrochloric acid, gave curve II at and below  $4^\circ$ . At higher temperatures it gave an expanded film, probably liquid expanded, with an area at low compressions in the neighbourhood of 52 sq. A. The estimates of the area of the expanded films are not of great accuracy in these cases. The temperature of half expansion under 1.4 dynes per centimetre was  $10.5^\circ$ . Similar films were obtained on normal hydrochloric acid. On N/10 and normal caustic soda, the films were gaseous, with moderately large corrections to the simple equation for a perfect gaseous film. On distilled water, reproducible results were difficult to obtain with the acid. As a rule, a transient surface pressure of 1 or 2 dynes per centimetre was observed at areas up to 35 sq. A. This usually diminished to about 0.3 dynes in a minute or less. On further rapid compression, a curve similar to the dotted curve III was obtained. The area usually diminished by 1 or 2 sq. A. on further waiting. In a few cases, however, after waiting about an hour, curves

resembling those of fatty acids with "close-packed chains," with an area about 21 sq. A. and very incompressible, were obtained.

*Hydrolysis of the Lactone on Normal Caustic Soda.*

On normal caustic soda solutions, the films of the lactone underwent rapid expansion, obviously a hydrolysis to the acid. The middle curve, fig. 1, *b* shows the area of the lactone under 1.5 dynes per centimetre compression at various times after the film was put on; the upper curve is a control curve done with the acid. There is a rapid increase of area in the case of the lactone for about 10 minutes, passing gradually into a very slow increase, which is also shown with the film of the acid. This slow final increase of area is probably due to the accumulation of contamination from the caustic soda solutions, which are very difficult to obtain with clean surfaces. The lower dotted curve represents an attempt at correcting the area of the lactone for the probable rate of accumulation of contamination, as follows. The straight part of the curve for the acid was extrapolated to zero time, and the increase in area of the acid over the initial area (neglecting the first more rapid increase), at each time, was subtracted from the observed area of the lactone. This curve is of approximately the form to be expected for a monomolecular reaction, assuming the area to be the mean of the areas of the lactone and acid present at any moment. The reaction is half completed in about 2.4 minutes at 17.5°, and in about 1 minute at 32°. The small initial rise in the case of the acid may be due to its containing a trace of lactone.

After the films of acid and lactone had been on the soda for some time, they were compressed. The compression curves were identical (gaseous films) within experimental error, as is to be expected if the lactone is hydrolysed to the acid.

*Discussion.*

The lactone has a saturated ring of five atoms at its lower end. The area found, 29 sq. A., is slightly smaller than the area of 30 recently found for the *p* alkyl cyclohexanols by Danielli.\* Models indicate that the lactone ring would probably be smaller than the cyclohexanol ring. The observed difference in the films is only about 1 sq. A. at low compressions, but increases at higher compressions, the lactone film being much more compressible than the cyclohexanol film.

\* Adam, Danielli, Haslewood and Marrian, 'Biochem. J.,' vol. 26, p. 1235 (1932).

The condensed film of the acid reaches about the same area as the lactone at low compressions, but is much more compressible. It appears that the hydroxyl group has a tendency to approach the carboxyl group, in which it is possibly aided by the attraction of the water molecules underlying the film. Compression tends to squeeze the chains out straight, but apparently does not succeed in doing so completely, owing to the tendency of the  $\gamma$  hydroxyl group to approach the carboxyl group and the underlying water.

The expansion temperature of the acid, on dilute hydrochloric acid, is some  $36^\circ$  lower than that of stearic acid, containing a chain of equal length without a hydroxyl group. This is no doubt owing to the tendency of the hydroxyl to approach the water. The "gaseous" state of the films on alkaline solutions is due to ionization of the end group decreasing the lateral adhesion between the molecules. Stearic acid also gives a gaseous film on alkaline solutions.

#### *Summary.*

$\gamma$  hydroxystearolactone forms a condensed film of area about 29 sq. A. at zero compression on water, dilute acid, and dilute alkali.

$\gamma$  hydroxystearic acid forms a liquid expanded film at and above room temperature, on slightly acid solutions, and a condensed film near  $0^\circ$ . There is some tendency for the hydroxyl group to approach the water, in films of the hydroxyl acid; but this group can be forced away from the surface by lateral compression of the film.  $\gamma$  hydroxystearic acid forms a "gaseous" film on alkaline solutions, like other fatty acids.

On normal caustic soda, the films of the lactone are rapidly hydrolysed to the acid, the change being detected by the increase in area which occurs, since the acid is a gaseous film and the lactone a condensed film.

---

*Flow of Water through Fine Clearances with relative Motion of the Boundaries.*

By R. J. CORNISH, M.Sc., A.M.I.Mech.E.

(Communicated by D. R. Hartree, F.R.S.—Received November 14, 1932.)

1. *Introduction.*

In practice in many cases of flow through fine annular clearances, the inner boundary consists of a bush keyed to a rotating shaft, and in the investigation about to be described, it was found that up to a certain critical speed of rotation the resistance to flow is unaffected, but above this speed the resistance increases as the speed increases. Curves are given by means of which the critical angular velocity and the resistance at higher angular velocities can be ascertained for the range of clearances investigated.

2. *Apparatus.*

Two apparatuses, Nos. I and II, were used, each consisting in principle of a brass cylinder mounted on a shaft and capable of rotating inside a hollow cylinder, also of brass. The surfaces were finished as smooth as possible by grinding.

Apparatus II is illustrated in fig. 1. The shaft was supported in ball-bearings, which are not shown in the figure. The revolving bush was approximately 20 cm. in diameter by 28 cm. in length. By means of set-screws it could be placed centrally within the hollow bush, the concentricity being tested by means of feeler-gauges. Water was supplied at one end under pressure from a tank giving a constant static head, and the quantity was measured at exit by taking the time required to fill one of a series of flasks and cans. The temperature was measured by calibrated thermometers at entrance and exit, and the average used to get the viscosity. The viscosity-temperature curve was drawn from data given in the International Critical Tables (1926). There was no means of controlling the inlet temperature, but it varied from about 6° C. to 21° C. according to the season. The corresponding range of kinematic viscosity is about 0.015 to 0.010 C.G.S. units, and as far as possible curves were checked at different viscosities.

Pressures could be measured at points A, B, C, D, E, F, G, and H, fig. 1. A gauge hole was also drilled in each end-cover to check the readings at A and H. Water or mercury manometers were used, according to the pressure.

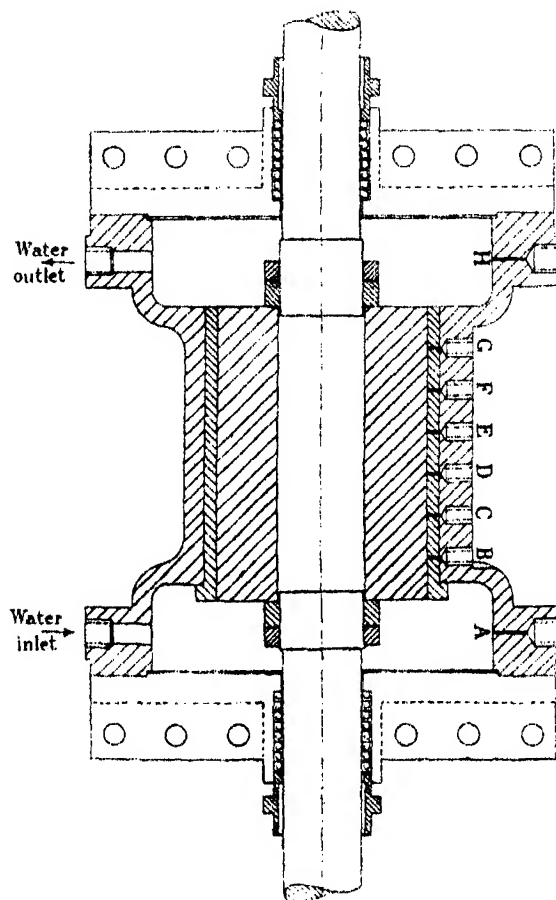


FIG. 1.—Sectional plan of apparatus II, with top half of end-covers removed.

The shaft was direct coupled to a D.C. motor, giving a range of speeds from 0 to 2000 r.p.m. The speed of rotation was obtained by a revolution-counter which was engaged just before starting to measure the quantity of water, and disengaged immediately on completing that measurement; the time was taken with a stop watch, and a direct reading tachometer was used as a check.

Apparatus I was similar in principle, but the construction only allowed for checking the concentricity at one end. However, long feelers were used and very fair results obtained. The diameter of the annular clearance was 12 cm. and the length 15 cm.; the outer bush was slightly shorter than the inner.

Pressure water was supplied from a centrifugal pump, and the temperature was taken at the outlet of the delivery pipe. As very small values of  $mS/v^*$  were not investigated with this apparatus, the temperature rise in the clearance cannot have been enough to introduce any serious errors through not measuring the temperature at both entrance and exit.

In each case the diameters of the bushes were measured by micrometer gauges reading to a hundredth of a millimetre. Owing to slight machining errors the diameters were not perfectly uniform, and the average clearance was taken as the cube root of the average of the sum of the cubes of the clearances at equally spaced distances. The cube average was used because with laminar flow the flow for a given pressure difference varies as the cube of the clearance. Finally, the clearance was calculated from the experimental results with the rotor stationary, by assuming the correctness of the theoretical formula for laminar flow (§ 4, *a*). This value, which was used in all subsequent calculations, was found to agree with the measured value within the possible errors of measurement. It should be mentioned that in all cases the clearance was a few per cent. greater at the ends, and this "bell-mouthing" is referred to later in the estimate of entrance and exit losses.

Table I.

Apparatus.	<i>r</i> cm.	<i>l</i> cm.	<i>m</i> cm.	<i>r/m</i> .
Ia .....	6.00	15.0	0.0107	560
Ib .....	6.00	15.0	0.0139	432
Ic .....	6.00	15.0	0.0174	345
Id .....	6.00	15.0	0.0176	341
II .....	10.00	28.0	0.0233	429
Suzuki <i>a</i> .....	8.88	3.81	0.01425	624
.. <i>b</i> .....	8.88	3.81	0.033	269
.. <i>c</i> .....	8.88	3.81	0.0645	138
.. <i>d</i> .....	8.88	3.81	0.0235	378

Table I gives the leading dimensions of the various annular clearances on which experiments were made. In assessing the results, reference is made to the work of Suzuki,<sup>†</sup> and for convenience the details of his clearances are given in the table.

### 3. Limitations of the Apparatus.

(*a*) The heat generated by the friction of the rotating surface could only escape from the rotor along the shaft or through the water. With small

\* See index to symbols, p. 239.

† 'J. Fac. Eng., Imp. Univ., Tokyo,' vol. 18, p. 88 (1929).

quantities of water flowing, the rise in temperature at high speeds of rotation was very rapid, and the inner bush became much warmer than the outer, thus causing a reduction in the clearance. The results for high speeds of rotation at low Reynolds numbers must therefore be accepted with caution.

(b) Owing to the slight variations-in diameter, and the fact that the only method of centring the rotor was with feelers, exact concentricity could not be guaranteed. However, in the case of apparatus II the rotor was several times removed for cleaning, and the general agreement of the results at different times shows that the errors introduced by faulty centring cannot have been large. At very low pressures, appreciable errors were introduced owing to small pressure differences generated by the rotation of the rotor, presumably due to its not being exactly co-axial with the stator. The pressure difference indicated by the manometers was therefore made up of that due to friction and that generated by the rotor. Changing the direction of rotation did not necessarily alter the sign of the latter value, whereas it usually altered the magnitude, so the true pressure drop could not be obtained by averaging the results obtained with both rotations. Attempts were made to estimate the allowance for this effect by rotating the bush with no water flowing, but the rapid heating of the water by friction made it difficult to get reliable readings. The author has therefore not reported the results for values of  $mS/v$  less than 10, except in the case of the critical angular velocity. Apart from the effect above noted, the direction of rotation did not affect the resistance.

(c) The effect of rotation on the gauges connected to the pressure openings within the clearance was very complicated, and the author was unable to interpret or to systematize the readings. The pressures used to calculate the resistance were those of the manometers connected to the high pressure and low pressure chambers. In practice this point is unimportant, except that the effect of rotation on the entrance and exit losses could not be estimated. From the experiments without rotation, the sum of these losses was found to be approximately  $S^3/2g$ ; the slight "bell-mouthing" of the entrance doubtless explains why this value is rather less than would be expected. The same value has been taken for these losses in the experiments with rotation. That this is permissible is indicated by the work of Yendo,\* who used rotors of two different lengths, and therefore the losses could be ascertained by difference methods. It was found that the speed of rotation had very little effect on the entrance and exit losses. In any case, with the length of clearance space used by the

\* 'Rep. Yokohama Tech. Coll.,' No. 1, p. 23 (1930).

author these losses were small compared with the pressure-drop owing to skin friction. Unfortunately, Yendo does not give the water temperatures, so his work could not be used to check the friction losses.

#### 4. Theoretical Investigation.

(a) *Rotor Stationary.*—As the clearance is small compared with the radius, the formula for laminar flow between a pair of parallel plates can be used, i.e.,

$$\frac{R}{\rho S^2} = 3 \left( \frac{mS}{\nu} \right)^{-1}, \quad (1)$$

or

$$\frac{Rm}{\mu S} = 3. \quad (2)$$

From figs. 3 and 4 it will be seen that the author's curve for  $\omega = 0$  departed from this line at about  $mS/\nu = 100$ . This is because the pressures were measured outside the clearance, and the effect was the same as that often observed in pipe flow when gauge holes are placed too near the entrance, before the flow has become steady.\* The amount of deviation from the theoretical line was not large, and, as it is doubtful to what extent a similar effect occurred when the rotor was revolving, no correction was made.

For turbulent flow in any form of pipe with smooth boundaries, Davies and White† give a general formula which reduces to

$$\frac{Rm}{\mu S} = 0.0283 \left( \frac{mS}{\nu} \right)^{3/4}. \quad (3)$$

The same formula is obtained by putting  $\omega = 0$  in Suzuki's expression (see equation (5)).

The experiments of Davies and White‡ on flow between parallel plates, and those of the author on flow through annular clearances with the rotor stationary, only extend up to  $mS/\nu = 2000$ . Up to that point they are better represented by the expression

$$\frac{Rm}{\mu S} = 0.0197 \left( \frac{mS}{\nu} \right)^{4/5}. \quad (4)$$

Within the range considered the curves corresponding to (3) and (4) practically coincide, and it seems probable that as  $mS/\nu$  increases, equation (3) would best represent the correct curve.

\* For a full discussion see Davies and White, 'Proc. Roy. Soc.,' A, vol. 119, p. 95 (1928).

† 'Engineering,' vol. 128, p. 71 (1929).

‡ 'Proc. Roy. Soc.,' A, vol. 119, p. 92 (1926).



(b) *Rotor Revolving*.—The first published work on this subject known to the author is that of G. I. Taylor,\* who investigated the case where there is no flow parallel to the axis. Above a critical angular velocity an eddy system is produced, and it is possible that, when there is flow parallel to the axis, eddies are formed which are immediately swept away.

Goldstein† is examining mathematically the critical angular velocity conditions in the case of axial flow, but his final results have not yet been published.

Suzuki (*loc. cit.*) investigated theoretically the increase in resistance due to rotation, working from Karman's law of velocity distribution, which is applicable only in the turbulent flow region. His formula reduces to

$$\frac{Rm}{\mu S} = 0.0283 \left( \frac{mS}{\nu} \right)^{3/4} \left[ \frac{1}{2} \left\{ \left( 1 + 0.629 \frac{r^2 \omega^2}{S^2} \right)^{3/8} + \left( 1 + 0.629 \frac{\beta^2 r^2 \omega^2}{S^2} \right)^{3/8} \right\} \right]. \quad (5)$$

He does not give any indication of the value of  $\beta$ , which seems to vary with different clearances.

The principle of dynamical similarity may be applied to the problems of the resistance and of the critical angular velocity at which the type of motion changes. On the assumptions that  $R$  depends on  $m$ ,  $r$ ,  $S$ ,  $\mu$ ,  $\rho$  and  $\omega$ , and that  $\omega_c$  depends on  $m$ ,  $r$ ,  $S$ ,  $\mu$ , and  $\rho$ , the following expressions are obtained :—

$$\frac{Rm}{\mu S} = f_1 \left( \frac{mS}{\nu}, \frac{r}{m}, \frac{m\omega}{S} \right) \quad (6)$$

$$\frac{m\omega_c}{S} = f_2 \left( \frac{mS}{\nu}, \frac{r}{m} \right). \quad (7)$$

## 5. Results.

(a) *Resistance to Flow*.—Equation (6) suggests that  $Rm/\mu S$  should be plotted against  $m\omega/S$  for constant values of  $mS/\nu$  and  $r/m$ , but it was found that by using  $r\omega/S$  as abscissa instead of  $m\omega/S$  a series of curves was obtained which was identical for all the clearances used by the author, and two of those of Suzuki. This is shown in fig. 2, from which it appears that the curves there given apply to all values of  $r/m$  between 341 and 624. Within this range the only points showing serious disagreement are some of those for Suzuki's apparatus *d*. To avoid confusing the figure, the points from this apparatus, for high values of  $mS/\nu$ , have not been included; they all fall below the curves of fig. 2. This apparatus was peculiar in that at entrance and exit the boundaries

\* 'Phil. Trans.' A, vol. 223, p. 289 (1923).

† 'Rep. Brit. Ass.' p. 347 (1931).



were rounded off to minimize losses; this may have had the effect of reducing the tendency to turbulence.

In the author's experiments, it was found to be impossible to keep  $mS/\nu$  absolutely constant, so fig. 2 could not be plotted directly. For experimental purposes with any given apparatus, the most convenient method was to find the relationship between  $Rm/\mu S$  and  $mS/\nu$  for a number of values of  $\omega/\nu$ , which could easily be kept approximately constant. Fig. 3 shows the results obtained from apparatus II. Curves of this type were drawn for each apparatus and from them fig. 2 was plotted, using the relationship

$$\frac{r\omega}{S} = \frac{\omega}{\nu} \cdot \frac{\nu}{mS} \cdot rm.$$

In fig. 4,  $Rm/\mu S$  is plotted against  $mS/\nu$  for a series of constant values of  $r\omega/S$  (i.e.,  $\frac{\text{peripheral velocity of rotor}}{\text{average velocity of axial flow}}$ ). For values of  $mS/\nu$  from 1000

upwards these curves agree closely with equation (5), if  $\beta$  is taken as 0.8.

Suzuki's experiments with larger clearances show that the resistance corresponding to a given value of the ratio  $r\omega/S$  diminishes as  $r/m$  diminishes; that is, when the clearance is larger relative to the diameter, the effect of rotation is less. In view of the shortness of his rotor, the entrance and exit losses rather tended to "swamp" the frictional resistance with these larger clearances, so the present writer has not felt justified in using this work to extend his own.

(b) *Critical Angular Velocity.*—In fig. 2 it is seen that, for values of  $mS/\nu$  less than 300, the curves may be divided into two parts. When  $r\omega/S$  is below a critical value,  $Rm/\mu S$  is constant and approximately equal to 3. (The actual experimental points in support of this statement have been omitted to avoid confusion.) Above the critical value ( $r\omega_c/S$ )  $Rm/\mu S$  increases, at first rapidly and then more slowly, as  $r\omega/S$  increases. The curves for  $mS/\nu = 400, 500$  and 600, show an additional complication, due probably to the abnormal entry conditions causing an early onset of turbulence of the type usually associated with high Reynolds numbers; the point of change to the special type of disturbance associated with rotation is fairly clear, however. For still higher values of  $mS/\nu$  no such definite point can be detected.

The relationship between  $r\omega_c/S$  and  $mS/\nu$  was specifically investigated only with apparatus II, but it may be deduced from fig. 2 that the results are valid at least from  $r/m = 341$  to  $r/m = 624$ . For the reason explained in the second paragraph of § 5 (a), the method employed was first to find  $Rm/\mu S$  for a

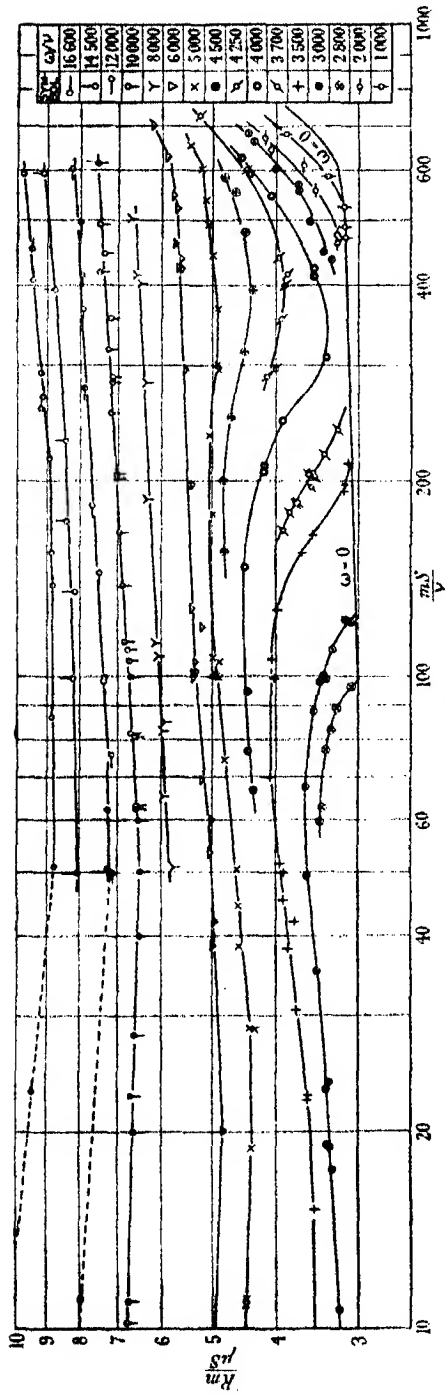


FIG. 3.

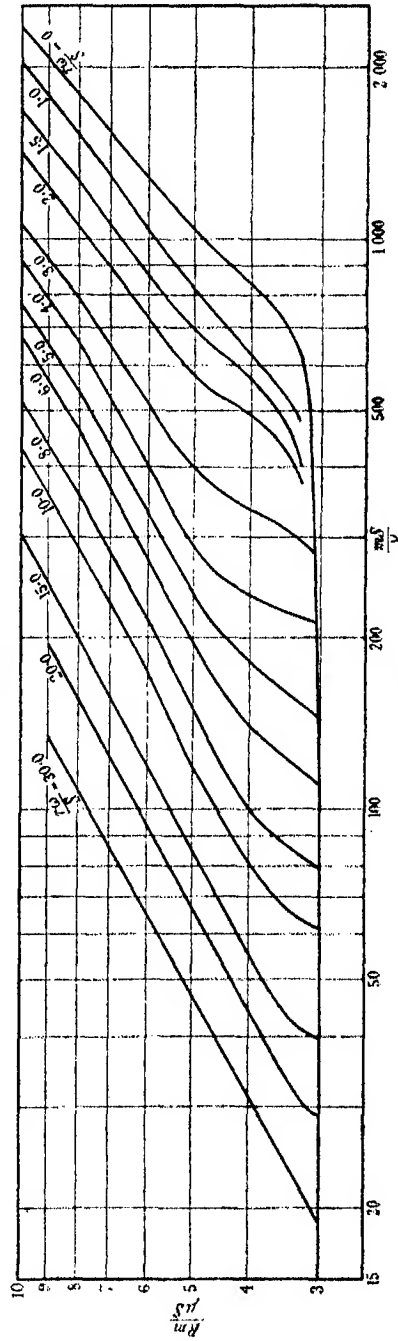


FIG. 4.

number of values of  $\omega/\nu$  near the critical, keeping  $mS/\nu$  as nearly constant as possible. An example of the curves obtained is given in fig. 5. The results of these experiments were used to draw fig. 6, where  $r\omega_c/S$  is plotted against  $mS/\nu$ .

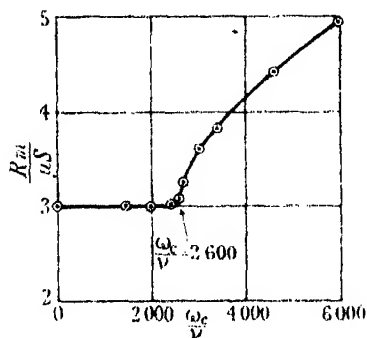


FIG. 5.

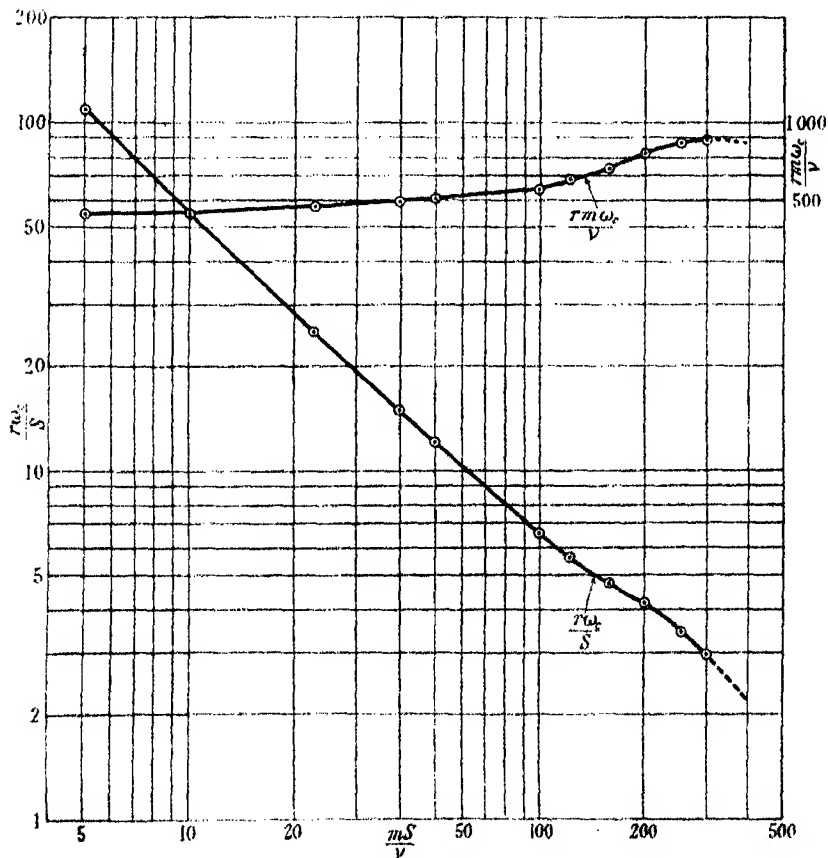


FIG. 6.

In connection with the arrangement adopted in fig. 7,  $rm\omega_0/v$  also has been plotted against  $mS/v$  in fig. 6.

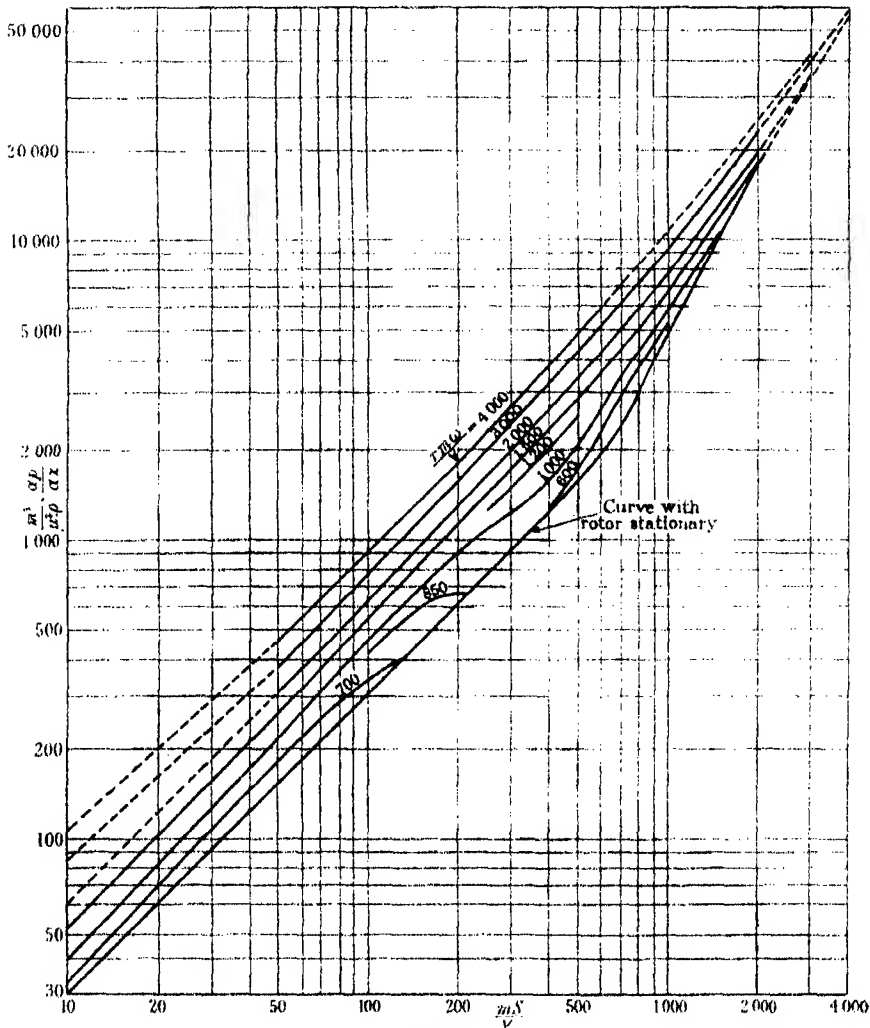


FIG. 7.

### 6. Practical Application.

For use in practice, none of the forms of curve drawn is as convenient as those of fig. 7. Here the ordinate has been taken as  $\frac{m^3}{\mu^2\rho} \cdot \frac{dp}{dz}$ , obtained by multiplying  $Rm/\mu S$  by  $mS/v$ . Thus  $S$ , which is the usual unknown, only

occurs in the abscissa,  $mS/\nu$ . To generalize the effect of rotation, curves have been plotted for a series of values of  $rm\omega/\nu$ ; these will be valid over the same range as fig. 2, since  $\frac{rm\omega}{\nu} = \frac{r\omega}{S} \cdot \frac{mS}{\nu}$ . Fig. 7 may therefore be applied for all values of  $r/m$  from 341 to 624; a large number of practical cases falls within this range. The portions shown dotted are estimated from rather less reliable evidence than those shown full. To enable fig. 7 to be easily reproduced for use in practice, sufficient numerical information has been given in Table II.

Table II.  
Values of  $\frac{m^3}{\mu^2 \rho} \cdot \frac{dp}{dz}$  for plotting fig. 7.

$\frac{rm\omega}{\nu}$	$mS/\nu$																
	10	30	50	70	100	150	200	250	300	400	500	600	800	1000	1500	2000	3000
0	30.0	90	150	210	300	455	608	765	921	1240	1575	1930	3060	4850	10270	17600	34500
300											1600	2110	3440	5040			
600										1280	1725	2320	3720	5300			
700	32.8	103	180	252	341												
750					375	476											
800	36.0	111	193	278	400	532											
850					416	589	664										
900					432	631	780	850	984	1380	1890	2580	4070				
950						852	992	1075									
1000	39.3	123	215	313	460	687	900	1090	1230	1585	2080	2700	4230	5800	10650		
1050								1175	1350	1740	2230	2810					
1200	43.5	135	231	336	500	750	1000	1250	1510	2020	2540	3120	4520	6160	11100		
1500	50.5	152	257	371	548	840	1125	1420	1725	2320	2940	3600	5040	6720	12000	18000	
2000	61.0	179	297	423	625	960	1290	1640	1980	2700	3430	4200	5900	7700	13100	19600	35100
2500	72.0	206	337	476	695	1060	1440	1815	2200	3000	3830	4690	6550	8500	14300	21000	37500
3000	84.0	231	377	525	760	1170	1580	2000	2420	3300	4230	5160	7200	9300	15450	23000	39900
4000	106.0	285	455	630	900	1350	1820	2300	2790	3800	4900	5970	8200	10600	17250	24400	41400

In this table particulars are also given of curves for a number of additional values of  $rm\omega/\nu$ , which were omitted from fig. 7 to avoid confusing the figure when reproduced to a small scale. An important feature from the designer's standpoint is the rapid convergence of the curves in the turbulent flow region, showing that with high values of  $mS/\nu$  the friction is practically unaffected by ordinary speeds of rotation. That this is also true for values of  $r/m$  less than those covered by fig. 7, is evident from Suzuki's experiments with larger clearances.

The application of the curves needs considerable care owing to the heating effect dealt with in § 3, *a*. Where a small axial flow is accompanied by high

speeds of rotation, the clearance will be reduced by the rise in temperature of the inner bush, while the average viscosity of the liquid will also be reduced.

A possible complication might arise from the expansion of the rotor owing to centrifugal force. Exact calculation is made impossible by the difficulty of estimating the initial stresses in the rotor, but an approximate investigation showed that the reduction in the clearance by centrifugal action is negligible with the clearances and speeds of rotation dealt with in this paper.

Moreover, the accuracy of centring of the rotor will also have to be considered; in the stream line region eccentricity may increase the quantity for a given pressure difference by an amount up to 150 per cent. of that with concentricity.\* In the turbulent flow region the effect is much less, the increase being not more than 30 per cent. for maximum eccentricity. These figures have only been obtained for the case when the rotor is stationary; no work has been published on the effect of rotation with an eccentric rotor.

The author wishes to record his thanks to Professors A. H. Gibson and D. R. Hartree, F.R.S., of Manchester University, and to Mr. T. Y. Sherwell and members of the staff of Messrs. Mather & Platt, Ltd., at whose works part of the research was carried out.

#### *List of Symbols.*

- $r_1$  = radius of inner cylinder.
- $r_2$  = radius of outer cylinder.
- $r$  = mean radius of annulus =  $\frac{1}{2} (r_1 + r_2)$ .
- $m$  = hydraulic mean depth =  $\frac{1}{2} (r_2 - r_1)$ .
- $l$  = axial length of clearance space.
- $dp/dz$  = pressure gradient parallel to the axis.
- $R$  = resistance per unit area of wall surface =  $m \cdot dp/dz$ .
- $S$  = mean velocity of flow parallel to the axis.
- $\rho$  = density of fluid.
- $\mu$  = absolute viscosity of fluid.
- $\nu$  = kinematic viscosity of fluid.
- $\omega$  = angular velocity of inner cylinder (radians per second).
- $\omega_c$  = critical angular velocity.

#### *Summary.*

The paper describes the author's experiments on the resistance to flow of water through a series of fine annular clearances, in which the cylindrical

\* Schneckenburg, 'Z. ang. math.', vol. 11, p. 40 (1931).



bush forming the inner boundary could be rotated. In the laminar flow region the resistance is unaffected by rotation at low speeds, but is increased when the angular velocity rises above a critical value. In the region of turbulent flow the effect of a given speed of rotation diminishes as the Reynolds number increases; this part of the work was correlated with that of Suzuki.

It is shown that dynamical similarity depends on the ratio of radius to hydraulic mean depth. For values of this ratio from 341 to 624 curves are given by means of which the critical angular velocity and the resistance at higher angular velocities can be calculated.

---

*The Tides in Oceans on a Rotating Globe.—Part IV.*

By G. R. GOLDSBROUGH, F.R.S.

(Received January 20, 1933.)

§ 1. *Introductory.*

In previous papers\* of this series approximate solutions of the tidal equations have been given which represent the semi-diurnal tide in an ocean bounded by two meridians of longitude  $60^\circ$  apart. The present investigation is to find the nature and periods of the free oscillations in such an ocean, particularly of that mode which has a period near to the period of the semi-diurnal tide.

The principal conclusion is that in an ocean of uniform depth 12,880 feet and bounded by two meridians of longitude  $60^\circ$  apart there is a normal mode of vibration having a period of 12 hours 33 minutes of mean solar time. In the course of the work it is shown that the normal frequencies appear in groups of three: one giving a wave travelling in a positive direction, the second giving a wave travelling in a negative direction, and both of them remaining finite as the speed of rotation diminishes. The third is an oscillation of "the second class," corresponding to a wave travelling in the positive direction and reducing to a steady motion as the speed of rotation diminishes.

§ 2. *The Equations and the Method of Solution.*

The equations to be solved for the case of uniform depth  $h$  are, in the usual notation

$$\left. \begin{aligned} \frac{\partial u}{\partial t} - 2\omega v \cos \theta &= -\frac{g}{a} \frac{\partial \zeta'}{\partial \theta}, \\ \frac{\partial v}{\partial t} + 2\omega u \cos \theta &= -\frac{g}{a \sin \theta} \frac{\partial \zeta'}{\partial \phi}, \\ -\frac{\partial \zeta}{\partial t} &= \frac{h}{a \sin \theta} \left\{ \frac{\partial}{\partial \theta} (u \sin \theta) + \frac{\partial v}{\partial \phi} \right\}, \\ \zeta' &= \zeta - \bar{\zeta}. \end{aligned} \right\} \quad (1)$$

\* Part I, 'Proc. Roy. Soc.,' A, vol. 117, p. 694 (1928); Part III, *ibid.*, vol. 126, p. 1 (1929). These will be referred to as I and III respectively.

On taking out the time factor  $e^{i\sigma t}$  and putting  $\mu = \cos \theta$  the equation (1) reduces to

$$\left. \begin{aligned} i\sigma u - 2\omega\mu v &= g \frac{\sqrt{(1-\mu^2)}}{a} \frac{\partial \zeta'}{\partial \mu}, \\ i\sigma v + 2\omega\mu u &= -\frac{g}{a\sqrt{(1-\mu^2)}} \frac{\partial \zeta'}{\partial \phi}, \\ \frac{i\sigma a \zeta}{h} &= \frac{\partial}{\partial \mu} \{u \sqrt{(1-\mu^2)}\} - \frac{1}{\sqrt{(1-\mu^2)}} \frac{\partial v}{\partial \phi}. \end{aligned} \right\} \quad (2)$$

Apply Love's transformation, which is given by

$$\left. \begin{aligned} u &= \sigma \left\{ \sqrt{(1-\mu^2)} \frac{\partial p}{\partial \mu} + \frac{1}{\sqrt{(1-\mu^2)}} \frac{\partial q}{\partial \phi} \right\}, \\ v &= -\sigma \left\{ \frac{1}{\sqrt{(1-\mu^2)}} \frac{\partial p}{\partial \phi} - \sqrt{(1-\mu^2)} \frac{\partial q}{\partial \mu} \right\}, \end{aligned} \right\} \quad (3)$$

and write

$$\Delta \equiv \frac{\partial}{\partial \mu} (1-\mu^2) \frac{\partial}{\partial \mu} + \frac{1}{1-\mu^2} \frac{\partial^2}{\partial \phi^2}.$$

Then, from the equation of continuity,

$$\begin{aligned} i\sigma \zeta a/h &= \frac{\partial}{\partial \mu} \{u \sqrt{(1-\mu^2)}\} - \frac{1}{\sqrt{(1-\mu^2)}} \frac{\partial v}{\partial \phi} \\ &= \sigma \left\{ \frac{\partial}{\partial \mu} (1-\mu^2) \frac{\partial p}{\partial \mu} + \frac{1}{1-\mu^2} \frac{\partial^2 p}{\partial \phi^2} \right\} \\ &= \sigma \Delta(p). \end{aligned}$$

Therefore

$$\zeta = (h/a) \Delta(p). \quad (4)$$

On substituting (3) in the first and second of equations (2) we have

$$\begin{aligned} -\sigma^2 \left\{ \sqrt{(1-\mu^2)} \frac{\partial p}{\partial \mu} + \frac{1}{\sqrt{(1-\mu^2)}} \frac{\partial q}{\partial \phi} \right\} + 2\omega i \sigma \mu \left\{ \frac{1}{\sqrt{(1-\mu^2)}} \frac{\partial p}{\partial \phi} - \sqrt{(1-\mu^2)} \frac{\partial q}{\partial \mu} \right\} \\ = (g/a) \sqrt{(1-\mu^2)} \frac{\partial \zeta'}{\partial \mu}, \end{aligned} \quad (5)$$

and

$$\begin{aligned} \sigma^2 \left\{ \frac{1}{\sqrt{(1-\mu^2)}} \frac{\partial p}{\partial \phi} - \sqrt{(1-\mu^2)} \frac{\partial q}{\partial \mu} \right\} + 2\omega i \sigma \mu \left\{ \sqrt{(1-\mu^2)} \frac{\partial p}{\partial \mu} + \frac{1}{\sqrt{(1-\mu^2)}} \frac{\partial q}{\partial \phi} \right\} \\ = -\frac{g}{a\sqrt{(1-\mu^2)}} \frac{\partial \zeta'}{\partial \phi}. \end{aligned} \quad (6)$$

Divide equation (5) by  $\sqrt{1 - \mu^2}$  and differentiate the quotient with regard to  $\phi$ ; multiply equation (6) by  $\sqrt{1 - \mu^2}$  and differentiate the product with regard to  $\mu$ ; and add the results. We have then

$$\begin{aligned} & -\sigma^2 \Delta(q) + 2\omega i \sigma \mu \Delta(p) + 2\omega i \sigma (1 - \mu^2) \frac{\partial p}{\partial \mu} \\ & + 2\omega i \sigma \frac{\partial q}{\partial \phi} = 0. \end{aligned} \quad (7)$$

Again, multiply equation (5) by  $\sqrt{1 - \mu^2}$  and differentiate the product with regard to  $\mu$ ; divide equation (6) by  $\sqrt{1 - \mu^2}$  and differentiate the quotient with regard to  $\phi$ ; subtract the results and we find

$$\begin{aligned} & -\sigma^2 \Delta(p) + 2\omega i \sigma \frac{\partial q}{\partial \phi} - 2\omega i \sigma (1 - \mu^2) \frac{\partial q}{\partial \mu} - 2\omega i \sigma \mu \Delta(q) \\ & = (gh/a^2) \Delta^2(p) - (g/a) \Delta(\bar{\zeta}). \end{aligned} \quad (8)$$

In (7) and (8) substitute  $f = \sigma/2\omega$ ,  $\beta = gh/4\omega^2 a^2$ , and they reduce to the suitable forms

$$\left. \begin{aligned} & -f \Delta(q) + i \mu \Delta(p) + i(1 - \mu^2) \frac{\partial p}{\partial \mu} + i \frac{\partial q}{\partial \phi} = 0, \\ & -f^2 \Delta(p) + i f \frac{\partial p}{\partial \phi} - i f \mu \Delta(q) - i f (1 - \mu^2) \frac{\partial q}{\partial \mu} \\ & - \beta \Delta^2(p) = - (g/4\omega^2 a^2) \Delta(\bar{\zeta}). \end{aligned} \right\} \quad (9)$$

If the boundaries of the ocean are two meridians  $0, \phi_1$ , the conditions to be fulfilled in addition are that the solutions must be finite at the poles  $\mu = \pm 1$ , and that  $v = 0$  when  $\phi = 0, \phi_1$ . For convenience we put  $\alpha = \pi/\phi_1$ . Then appropriate forms for the solution of equation (9) are\*

$$\left. \begin{aligned} p &= \sum_s \sum_n A_{sa+n}^{\alpha} P_{sa+n}^{\alpha}(\mu) \cos s\alpha\phi \\ q &= \sum_s \sum_n B_{sa+n}^{\alpha} P_{sa+n}^{\alpha}(\mu) \sin s\alpha\phi \end{aligned} \right\} \quad (10)$$

where  $s, n$  are integral. These forms satisfy the required boundary conditions term by term.

Now in the range  $0$  to  $\pi/\alpha$  we have the following valid expansions,  $r$  and  $s$  being integers :

$$\sin s\alpha\phi = \sum_r a_r^s \cos r\alpha\phi, \quad (r - s) \text{ odd},$$

\*  $P_{sa+n}^{\alpha}(\mu)$  is defined as in Lamb, "Hydrodynamics," 6th ed., p. 117.

where

$$a_r^s = \frac{4s}{(s^2 - r^2)\pi}, \quad r \neq 0,$$

and

$$a_0^s = \frac{2}{s\pi};$$

$$\cos s\alpha\phi = \sum_r b_r^s \sin r\alpha\phi, \quad (r-s) \text{ odd},$$

where

$$b_r^s = \frac{4r}{(r^2 - s^2)\pi}.$$

Also in the range  $(-1, 1)$  we have the following expansion\* when  $\alpha$  is an integer,

$$P_{sa+n}^{sa} = \sum_m g_{ra+m}^{ra} (s\alpha, s\alpha + n) P_{ra+m}^{ra} (\mu),$$

where

$$g_{ra+m}^{ra} (s\alpha, s\alpha + n) = \frac{1}{2} (2r\alpha + 2m + 1) \frac{m!}{(2r\alpha + m)!} \int_{-1}^1 P_{sa+n}^{sa} P_{ra+m}^{ra} d\mu.$$

Then on substituting from (10) in the left-hand member of the first of equations (9) we have

$$\begin{aligned} & -f\Delta(q) + i\mu\Delta(p) + i(1 - \mu^2) \frac{\partial p}{\partial \mu} + i \frac{\partial q}{\partial \phi} \\ &= \sum_s \sum_n \left[ fB_{sa+n}^{sa} (s\alpha + n)(s\alpha + n + 1) P_{sa+n}^{sa} \sin s\alpha\phi \right. \\ & \quad + iB_{sa+n}^{sa} s\alpha P_{sa+n}^{sa} \cos s\alpha\phi \\ & \quad - i\mu(s\alpha + n)(s\alpha + n - 1) A_{sa+n}^{sa} P_{sa+n}^{sa} \cos s\alpha\phi \\ & \quad \left. + i(1 - \mu^2) A_{sa+n}^{sa} \frac{d}{d\mu} P_{sa+n}^{sa} \cos s\alpha\phi \right] \\ &= \sum_s \sum_n \left[ fB_{sa+n}^{sa} (s\alpha + n)(s\alpha + n + 1) P_{sa+n}^{sa} \sin s\alpha\phi \right. \\ & \quad + iB_{sa+n}^{sa} s\alpha \sum_r \sum_m g_{ra+m}^{ra} (s\alpha, s\alpha + n) b_r^s P_{ra+m}^{ra} \sin r\alpha\phi \\ & \quad - i \frac{(s\alpha + n)(s\alpha + n + 2)(n + 1)}{2(s\alpha + n) + 1} A_{sa+n}^{sa} \sum_r \sum_m g_{ra+m}^{ra} (s\alpha, s\alpha + n + 1) b_r^s P_{ra+m}^{ra} \sin r\alpha\phi \\ & \quad \left. - i \frac{(s\alpha + n + 1)(s\alpha + n - 1)(2s\alpha + n)}{2(s\alpha + n) + 1} A_{sa+n}^{sa} \sum_r \sum_m g_{ra+m}^{ra} (s\alpha, s\alpha + n - 1) b_r^s P_{ra+m}^{ra} \sin r\alpha\phi \right] \end{aligned}$$

where  $(r - s)$  must be odd.

\* See MacRobert, 'Proc. Edin. Math. Soc.', vol. 42, p. 88 (1926). On the methods of calculating the coefficients  $g_m^{ra}(s, n)$ , see I, pp. 703-704.

This expression may be made to vanish, and the conditions under which the first equation of (9) may be satisfied thus found, by equating to zero the coefficients of  $P_{ra+m}^{ra} \sin r\alpha\phi$ . We then find

$$\begin{aligned} & fB_{ra+m}^{ra} (r\alpha + m)(r\alpha + m + 1) \\ & + i \sum_s \sum_n \left[ B_{sa+n}^{sa} s\alpha g_{ra+m}^{ra} (s\alpha, s\alpha + n) b_r^s \right. \\ & \quad - A_{sa+n}^{sa} \frac{(s\alpha + n)(s\alpha + n + 2)(n + 1)}{2(s\alpha + n) + 1} g_{ra+m}^{ra} (s\alpha, s\alpha + n + 1) b_r^s \\ & \quad \left. - A_{sa+n}^{sa} \frac{(s\alpha + n + 1)(s\alpha + n - 1)(2s\alpha + n)}{2(s\alpha + n) + 1} g_{ra+m}^{ra} (s\alpha, s\alpha + n - 1) b_r^s \right] \\ & = 0. \quad (11) \end{aligned}$$

In similar fashion the second of equations (9) produces the result (for the case of the free oscillations in which  $\bar{\zeta} = 0$ )

$$\begin{aligned} & (r\alpha + m)(r\alpha + m + 1) \{f^2 - \beta(r\alpha + m)(r\alpha + m + 1)\} A_{ra+m}^{ra} \\ & - if \sum_s \sum_n \left[ s\alpha A_{sa+n}^{sa} \alpha_r^s g_{ra+m}^{ra} (s\alpha, s\alpha + n) \right. \\ & \quad - B_{sa+n}^{sa} \alpha_r^s \left\{ \frac{(s\alpha + n)(s\alpha + n + 2)(n + 1)}{2(s\alpha + n) + 1} g_{ra+m}^{ra} (s\alpha, s\alpha + n + 1) \right. \\ & \quad \left. + \frac{(s\alpha + n + 1)(s\alpha + n - 1)(2s\alpha + n)}{2(s\alpha + n) + 1} g_{ra+m}^{ra} (s\alpha, s\alpha + n - 1) \right\} \left. \right] \\ & = 0. \quad (12) \end{aligned}$$

In these equations  $r, m, s, n$  may take any integral values subject to the condition that  $r - s$  is always odd. There is consequently a double infinity of pairs of linear equations to determine the coefficients  $A_{ra+m}^{ra}, B_{ra+m}^{ra}$ .

It is to be noticed that since  $g_{ra+m}^{ra}(s\alpha, s\alpha + n)$  involves the integral  $\int_{-1}^1 P_{sa+m}^{sa} P_{ra+n}^{ra} d\mu$ , this quantity is zero except when  $m, n$  are both even or both odd. This places a further restriction upon the terms that may appear in equations (11) and (12).

An analogous result may be found when  $\bar{\zeta} \neq 0$  and applied to the case of the forced oscillations.

### § 3. Simple Properties of the Equations.

Examination of equations (11) and (12) shows at once the following simple properties :—

(a) The term  $A_0^0$  does not appear in either equation.

(β) Since  $r - s$  is always odd (and we assume  $f$  to be real) the coefficients  $A^r_s$  and  $B^r_s$  may be divided into two sets. Taking those with  $r$  even to be real, it is clear that those with  $r$  odd will be pure imaginaries. On making up the final results therefore we shall have  $A^r_s$  and  $B^r_s$  with even  $r$  associated with  $\cos \sigma t$  and  $A^r_s$ ,  $B^r_s$  with odd  $r$  associated with  $\sin \sigma t$ .

(γ) If, leaving  $A^r_s$ ,  $B^r_s$  with even  $r$  unchanged, we change the signs of  $f$  and those  $A^r_s$ ,  $B^r_s$  with odd  $r$ , the equations remain unchanged. Or conversely, a change in the sign of  $f$  is accompanied by a change in the signs of  $A^r_s$ ,  $B^r_s$  with odd  $r$ . This result is important, as in what follows it will appear that the values of  $f$  occur in pairs with equal values and opposite signs.

If we write  $u = P \cos \sigma t + Q \sin \sigma t$ , where  $P$  is the sum of certain terms with even values of  $r$ , and  $Q$  is the sum of other terms with odd values of  $r$ , then, since a change in the sign of  $f$  (or  $\sigma$ ) produces a change in the sign of  $Q$ , it follows that the motions represented by  $\pm f$  are the same, and only one sign of  $f$  need be considered.

(δ) The values of  $r$  and  $s$  permissible are restricted by the condition that  $r - s$  is to be odd. A further restriction on the integers also occurs. Since the coefficient  $g^r_m(s\alpha, n)$  involves the integral  $\int_{-1}^1 P^r_m P^s_n d\mu$  which vanishes except when  $m - r\alpha$ ,  $n - s\alpha$  are both odd or both even, certain further terms become zero.

(ε) Bearing in mind that  $f = \sigma/2\omega$  and  $\beta = gh/4\omega^2 a^2$ , it is evident that as  $\omega \rightarrow 0$  the equations reduce to the results:—

$$B^r_n = 0 \text{ for all values of } r \text{ and } n,$$

$$A^r_n \text{ is arbitrary, and}$$

$$\sigma^2 = gh n(n+1)/a^2.$$

This is the well-known solution for the case of no rotation.

(ζ) From the property of the coefficients in (δ) it follows that in any equation if the difference of the suffixes of  $A^r_m$  is even, that of the suffixes of any  $B^r_n$  must be odd, and conversely.

#### § 4. *Approximate Solutions of the Equations.*

It will be assumed that a finite number of terms in the series (10) will give an approximation to the solution of equations (1). Since  $\zeta = (h/a)\Delta(p)$ , the smallest number of terms in the expansion of  $p$  that may be taken in order to

give an adequate idea of the motion is two—one real and one imaginary. From the work of Hough\* it may be concluded that these two terms will predominate, and that the other terms in  $p$  will form a double series receding from these predominant terms. Further, it would appear that *any* two terms in  $p$  may be chosen as the predominant terms and corresponding results evaluated.

Two terms must also be chosen in the expansion for  $q$ . It is not clear how they should be chosen, for they cannot be entirely arbitrary.

In working out the lowest mode it is natural to select the two lowest terms in A and the same in B, provided we have one real and one imaginary in each case. But with higher modes, corresponding to  $A_n^a$  it is best to take  $B_{n-1}^{a+}$  or  $B_{n+1}^{a+}$ , though this may have to be modified by judgment in special cases.

We proceed to take numerical values and solve the equations approximately in order to obtain an idea of the nature of the free oscillations. For simplicity and also because it corresponds roughly to the Atlantic Ocean, we choose the meridians  $60^\circ$  apart, making  $\alpha = 3$ . As the depth we take  $h = 12,880$  feet which gives  $\beta = gh/4\omega^2 a^2 = 1/22 \cdot 54$ .

I. *Lowest Symmetrical Oscillation.*—Restrict the terms to  $A_2^0, A_3^0, B_4^0, B_7^0$ .

The equations to be solved are then :—

$$\begin{aligned} 6(f^2 - 6\beta)A_2^0 - if \left[ 3A_3^0 a_6^1 g_2^0(3, 3) - B_3^0 a_0^1 \left\{ \frac{4 \cdot 6 \cdot 2}{9} g_2^0(3, 5) \right. \right. \\ \left. \left. + \frac{5 \cdot 3 \cdot 7}{9} g_2^0(3, 3) \right\} \right] &= 0, \\ 12(f^2 - 12\beta)A_3^0 - if \left[ -B_7^0 a_1^2 \left\{ \frac{7 \cdot 9 \cdot 2}{15} g_3^0(6, 8) \right. \right. \\ \left. \left. + \frac{8 \cdot 6 \cdot 13}{15} g_3^0(6, 6) \right\} \right] &= 0, \\ 20fB_4^0 + i \left[ 6B_4^0 g_4^0(6, 7) b_1^2 - A_2^0 b_1^0 \left\{ \frac{2 \cdot 4 \cdot 3}{5} g_4^0(0, 3) \right. \right. \\ \left. \left. + \frac{3 \cdot 1 \cdot 2}{5} g_4^0(0, 1) \right\} \right] &= 0, \\ 56fB_7^0 + i \left[ 3B_4^0 g_7^0(3, 4) b_2^1 - A_3^0 b_2^1 \frac{3 \cdot 5 \cdot 1}{7} g_7^0(3, 4) \right] &= 0. \quad (13) \end{aligned}$$

\* 'Phil. Trans.,' A, vol. 191, p. 166 (1898).



The coefficients work out as follows, logarithms being indicated :—

$$6g_4^3(6, 7) b_1^2 = n [3.31178]; \quad 3g_7^6(3, 4) b_2^1 = [3.45860];$$

$$\frac{15}{7} g_7^6(3, 4) b_2^1 = [3.31249]; \quad 3a_6^1 g_2^0(3, 3) = n [1.32415];$$

$$\left\{ \frac{24}{5} g_4^3(0, 3) + \frac{6}{5} g_4^3(0, 1) \right\} b_1^0 = n [2.14857];$$

$$\left\{ \frac{16}{3} g_3^0(3, 5) + \frac{35}{3} g_2^0(3, 3) \right\} a_0^1 = [1.99282];$$

$$\left\{ \frac{42}{5} g_3^3(6, 8) + \frac{208}{5} g_3^3(6, 6) \right\} a_1^2 = [4.43876].$$

The form of equations (13) indicates that the eliminant of the constants A, B, will be a cubic in  $f^3$ . For the given numerical values the cubic is

$$f^6 - 0.876f^4 + 0.161f^2 - 0.000746 = 0,$$

the solutions of which are  $f^3 = 0.617, 0.254, 0.00475$ . Of this triad of roots the first two correspond to those given by  $\sigma^2 = 12gh/a^2, 6gh/a^2$  for no rotation. The third belongs to the oscillations of "the second class"\* which become steady motions in the limiting case of no rotation. On completing the calculation we have the following results which approximately represent the motion.

(i)  $f^3 = 0.254, f = 0.504$ , period = 23.8 sidereal hours.

$$A_2^0 = 1, A_3^3 = -0.00044i.$$

$\zeta = h/a \Delta(p)$ , therefore omitting an arbitrary constant we have

$$\zeta = 6P_2 \cos \sigma t + 0.00528 P_3^3 \cos 3\phi \sin \sigma t.$$

There is an amphidromic point at  $\phi = 30^\circ, \mu = 1/\sqrt{3}$ , and the direction of rotation of the nodal lines is positive.

(ii)  $f^3 = 0.617, f = 0.785$ , period = 15.3 sidereal hours.

$$\zeta = 6P_2 \cos \sigma t - 1.59 P_3^3 \cos 3\phi \sin \sigma t.$$

There is an amphidromic point at  $\phi = 30^\circ, \mu = 1/\sqrt{3}$ , and the direction of rotation of the nodal lines is negative.

(iii)  $f^3 = 0.00475, f = 0.0689$ , period = 7.2 sidereal days.

$$\zeta = 6P_2 \cos \sigma t + 0.512 P_3^3 \cos 3\phi \sin \sigma t.$$

\* Hough, *loc. cit.*, p. 159.

The direction of rotation of the nodal lines is positive.

These directions of rotation correspond exactly to those found by Lamb for a flat rotating circular basin.\*

II.—It has been shown that for a similar ocean there would seem to be a free oscillation with a period not far from those of the semi-diurnal tides. We proceed to find this period in the present case.

Take as principal coefficients the set  $A_4^0, A_5^0, B_4^3, B_7^6$ .

The equations to be solved are :

$$20(f^2 - 20\beta) A_4^0 - if \left[ 3A_5^0 a_0^1 g_4^0(3, 5) - B_4^3 a_0^1 \left\{ \frac{4 \cdot 6 \cdot 2}{9} g_4^0(3, 5) + \frac{5 \cdot 3 \cdot 7}{9} g_4^0(3, 3) \right\} \right] = 0,$$

$$30(f^2 - 30\beta) A_5^0 - if \left[ -B_7^6 a_1^2 \left\{ \frac{7 \cdot 9 \cdot 2}{15} g_5^3(6, 8) + \frac{8 \cdot 6 \cdot 18}{15} g_5^3(6, 6) \right\} \right] = 0,$$

$$20f B_4^3 + i \left[ 6B_7^6 g_4^3(6, 7) b_1^2 - A_4^0 \left\{ \frac{4 \cdot 6 \cdot 5}{9} g_4^3(0, 5) + \frac{5 \cdot 3 \cdot 4}{9} g_4^3(0, 3) \right\} b_1^0 \right] = 0,$$

$$56f B_7^6 + i \left[ 3B_4^3 g_7^6(3, 4) b_2^1 - A_5^0 \left\{ \frac{5 \cdot 7 \cdot 3}{11} g_7^6(3, 6) + \frac{6 \cdot 4 \cdot 8}{11} g_7^6(3, 4) \right\} b_2^1 \right] = 0.$$

We have also :

$$6g_4^3(6, 7) b_1^2 = n[3 \cdot 31178]; \quad 3g_7^6(3, 4) b_2^1 = [3 \cdot 45860];$$

$$\left\{ \frac{40}{3} g_4^3(0, 5) + \frac{20}{3} g_4^3(0, 3) \right\} b_1^0 = n[2 \cdot 81823];$$

$$\left\{ \frac{105}{11} g_7^6(3, 6) + \frac{192}{11} g_7^6(3, 4) \right\} b_2^1 = [3 \cdot 91058];$$

$$\left\{ \frac{16}{3} g_4^0(3, 5) + \frac{35}{3} g_4^0(3, 3) \right\} a_0^1 = n[2 \cdot 48756];$$

$$\left\{ \frac{42}{5} g_5^3(6, 8) + \frac{208}{5} g_5^3(6, 6) \right\} a_1^2 = [3 \cdot 81313];$$

$$3g_4^0(3, 5) a_0^1 = n[2 \cdot 25683].$$

\* "Hydrodynamics," 6 ed., p. 327.

On taking these values in equations (14) and eliminating the coefficients  $A_4^0$ ,  $A_5^3$ ,  $B_4^3$ ,  $B_7^0$ , the following equation results :

$$f^6 - 2.307f^4 + 1.238f^2 - 0.0062 = 0. \quad (15)$$

The positive roots are  $f^2 = 1.37, 0.931, 0.0049$ . The general character of these roots is as before. We take the complete solutions in detail.

(i)  $f^2 = 1.37, f = 1.17$ , period = 10.8 sidereal hours.

$$\zeta = 20P_4 \cos \sigma t - 0.59 P_5^3 \cos 3\phi \sin \sigma t.$$

The equation of the nodal lines is

$$\begin{aligned} \tan \sigma t &= - \frac{0.59 P_5^3 \cos 3\phi}{20 P_4} \\ &= - \frac{0.59 \cdot 52.5 (1 - \mu^2)^{3/2} (9\mu^2 - 1) \cos 3\phi}{\frac{5}{2} (35\mu^4 - 30\mu^2 + 3)}. \end{aligned}$$

The amphidromic points as given by this approximation occur at

$$\phi = 30^\circ, \quad \mu = 0.35, 0.86. \quad (16)$$

The direction of motion of the nodal lines is negative.

(ii)  $f^2 = 0.931, f = 0.965$ , period = 12.4 sidereal hours.

$$\zeta = 20 P_4 \cos \sigma t + 0.00224 P_5^3 \cos 3\phi \sin \sigma t.$$

The amphidromic points are as in case (i), but the direction of motion is positive.

(iii)  $f^2 = 0.00488, f = 0.070$ , period = 7.1 sidereal days.

$$\zeta = 20 P_4 \cos \sigma t + 2.04 P_5^3 \cos 3\phi \sin \sigma t.$$

The direction of rotation of the nodal lines is positive. This is an oscillation of "the second class."

In view of the importance of case (ii) of this set it is desirable to proceed to a further approximation. This will also have the advantage of exhibiting to some extent the degree of accuracy obtained in the preceding approximations.

Starting with the values already obtained viz.,

$$\begin{aligned} f^2 &= 0.931, & A_4^0 &= 1, & A_5^3 &= ni[5.87342], \\ B_4^3 &= ni[3.47870], & B_7^0 &= n[7.17299], \end{aligned}$$

we proceed to find approximate values of the adjacent coefficients by substituting the stated values in equations (11) and (12). The following are the results :

$$\begin{aligned} A_3^3 &= i[4.18808], & A_7^3 &= ni[7.87354], \\ A_6^6 &= [\cdot 607634], & A_8^6 &= [8.25827], \\ A_2^0 &= [1.57963], & A_6^0 &= n[2.57305], \\ B_6^3 &= i[4.86681], & B_9^6 &= n[9.64308], \\ B_{10}^9 &= ni[11.83713]. \end{aligned} \tag{17}$$

The equations (14) are now made more exact by the inclusion of the nine constants of (17) with the approximate values just derived. The left-hand numbers of equations (14) are now found to be equal to small numerical quantities instead of zero. These numerical quantities may be transferred to the left-hand side as additional coefficients of  $A_4$  (which has the value unity). The eliminant of this new set of equations gives

$$f^6 - 2.307 f^4 + 1.288 f^2 - 0.0154 = 0$$

instead of equation (15). The relevant root of this equation is 0.911, or  $f = 0.954$ .

The value of 0.911 is just over 2 per cent. different from the first approximation 0.931. Hence we may regard the former value as fairly reliable and may also regard the values of the periods of the various modes as given by the first approximations as probably correct within about 5 per cent.

The period therefore of one of the symmetrical modes of free oscillation of an ocean bounded by two meridians  $60^\circ$  apart and of depth 12,880 feet is 12.5 sidereal hours, or 12 hours 33 minutes of mean solar time.

The value of  $f$ , 0.954, which has just been obtained, is extremely close to the value, 0.9625, for the lunar semi-diurnal tide  $M_2$ . This indicates that the  $M_2$  tide will be largely magnified by resonance in such a basin as we have considered in this investigation. This result confirms the theory already put forward by the writer in previous papers, *loc. cit.*, I, p. 717 ; III, p. 15.

In the third of the previous papers the  $M_2$  tide was worked out for an ocean similar to the ocean now considered and the co-tidal lines were drawn. It is interesting to note that the approximate positions of the amphidromic centres found for the free oscillations of the appropriate mode in this paper are not far from two of those found for the  $M_2$  tide. From result (16) the

amphidromic points are at  $\phi = 30^\circ$ ,  $\theta = 20.5^\circ$ ,  $59.2^\circ$ . For the  $M_2$  tide the positions were found to be  $\phi = 30^\circ$ ,  $\theta = 28.5^\circ$ ,  $46^\circ$ .

The inclusion of higher terms in the series would doubtless improve the first set of results.

Also, for the  $M_2$  tide two further amphidromic points appear which have no corresponding existence in the approximations of the present paper. But it is equally obvious that the inclusion of higher terms would allow for the appearance of these also.

One arithmetical point remains to be noted. The series for  $p$ ,  $q$  converge, arithmetically, fairly rapidly as the approximate values (17) show. When, however, we form the series for  $\zeta$  by the relation  $\zeta = (h/a)\Delta(p)$  the convergence is not so good. This explains why a few terms of  $p$  and  $q$  may give an accurate value of  $f$ , but more are needed to show the characters of the tide height  $\zeta$  and the nodal lines.

#### § 5. *Extensions of the Process.*

The solutions of the equations worked out in the preceding paragraphs have been arrived at only in the cases where the associated Legendre functions have integral orders and degrees. If it may be assumed that the expansions for  $p$  and  $q$  are valid in the more general cases and that the further operations are also permissible, then the methods given would apply to *any* width of ocean. For example, an ocean between two meridians  $120^\circ$  apart, corresponding roughly to the Pacific Ocean, would require  $\alpha = 3/2$ , and the associated Legendre functions involved would be of the form  $P_{\frac{3}{2}}^s \tau^{\frac{s}{2}+m}$ . The chief manipulative difficulty in such a case would be the calculation of the integrals

$$\int_{-1}^1 P_{\frac{3}{2}}^s \tau^{\frac{s}{2}+m} P_{\frac{3}{2}}^s \tau^{\frac{s}{2}+n} d\tau, \text{ though the methods used for the simpler forms}$$

occurring in this paper could doubtless be applied.

#### *Summary.*

In this paper the periods of the normal modes of free tidal oscillation of an ocean of uniform depth bounded by two meridians are investigated.

Solutions of the general dynamical equations of the tides are assumed in the form of doubly infinite series of spherical harmonics with undetermined coefficients. The relations between these coefficients are deduced as linear simultaneous algebraic equations.

The algebraic equations can be solved to a first approximation without much difficulty, and in one case have been solved to a second degree of approximation.

The results show that free waves exist which travel respectively in positive and negative directions about the amphidromic points. There are also oscillations of "the second class."

An important free period of symmetrical oscillation is found, for a depth of 12,880 feet, to be 12 hours 33 minutes of mean solar time. This mode is important in connection with the theory of the semi-diurnal tide.

---

### *On the Rate of Oxidation of Monolayers of Unsaturated Fatty Acids.*

By ARTHUR HENRY HUGHES and ERIC KEIGHTLEY RIDEAL, F.R.S.

(Received February 2, 1933.)

#### *Introduction.*

In previous communications\* the results of examination of the surface potentials of monolayers under different states of compression and on different substrates were presented. It was shown, *inter alia*, that not only could information as to the orientation of the surface phase be obtained even in such complex cases as monolayers of proteins, but the effects of alteration of inclination as well as of adhesion of the polar groups to the substrate were capable of quantitative measurement. Marked changes in the surface potentials are obtained when the polar group undergoes chemical reaction such as in the formation of oxonium compounds by a ketonic oxygen or on ionization of a carboxyl group, whilst changes of minor character are associated with a variation in the electrokinetic potentials of the film forming material. It is evident that it should be possible to follow the alteration of surface potential with time in cases where a chemical reaction involving a change in the summation of the vertical components of the groups forming the effective double layer is proceeding in a monolayer. Reactions in monolayers at air-

\* Schulman and Rideal, 'Proc. Roy. Soc.,' A, vol. 130, p. 259 (1931); Hughes and Rideal, *Ibid.*, vol. 137, p. 62 (1932); Schulman and Hughes, *Ibid.*, vol. 138, p. 430 (1932).

liquid and liquid-liquid interfaces present, apart from their importance in biological processes, certain unusual aspects of interest in the sphere of reaction kinetics. In order to visualize these aspects in more detail we will consider a simple case, a monolayer of oleic acid distended at an air-liquid interface undergoing oxidation by means of a dilute solution of an oxidizing agent such as acid permanganate present in the substrate. The oxidation proceeds in bulk phase quite smoothly, the double bond undergoing progressive oxidation to a dihydroxy and ketonic acid respectively before rupture of the chain ensues. In a highly expanded film of oleic acid the double bond is extended on the substrate and the molecular orientation of the reactant is such that the double bond in every molecule is equally accessible to the oxidizing agent, the  $\text{MnO}_4^-$  ion. On compression of the film the surface density of molecules increases and eventually when the molecular area attains some  $30 \text{ \AA}^2$  the limit of film stability is reached and the film collapses. Corresponding to the increase in the number of molecules of oleic acid per square centimetre one should anticipate an increase in the velocity of oxidation of the film, provided that we ensure the constancy of the active mass of the other reactant, the  $\text{MnO}_4^-$  ion. The velocity constant should also vary exponentially with the temperature providing a measure of the apparent energy of activation in the usual manner. A closer consideration of the system, however, reveals the fact that at some point during the process of compression the reactive group, in this case the double bond, will be removed from the water surface by the compression of the molecules constituting the monolayer. If it were not for the fact that the molecules were in thermal agitation, once this critical point had been reached all the double bonds in the surface would be rendered inaccessible to the oxidant, and reaction would cease. On further compression the hydrocarbon barrier now erected between the layer of double bonds and the oxidant in the substrate increases in thickness until either the molecules in the film become vertically orientated or, as generally happens, the film collapses. Owing to thermal agitation, however, the surface molecules are not at rest, and double bonds can penetrate the hydrocarbon barrier and attain access to the oxidant. The ease of penetration will depend both on the thickness of the barrier and on the mobility of the molecules, which will be influenced both by the temperature and their cohesion. We have under these conditions a reaction, the velocity of which is determined not only by the usual factors such as the collision frequency, and the probability, and magnitude of the energy transfer involved in activation, but in addition by what may be defined as an accessibility factor, the accessibility coefficient being unity in highly distended films but zero in highly compressed rigid films.

It may not be without biological significance that in the systems examined in this communication a very large change occurs in the accessibility coefficient, and thus in the magnitude of the reaction velocity coefficient as a result of a relatively small change in the compression or surface tension of the interface. We may note that this molecular orientation as an important factor in reaction kinetics must often be present in heterogenous catalysis at solid surfaces, *e.g.*, in the dependence on the pressure of the rates of hydrogenation of unsaturated hydrocarbons examined especially by Schuster,\* but as yet we have no exact knowledge of the actual configuration and change in orientation or alteration in the surface density of the adsorbate in such systems.

Similar considerations are clearly applicable to reactions in bulk phases where only specific portions of large and complex molecules are involved, as examples of which may be cited the polymerization of unsaturated hydrocarbons or in the combination between the dextro and laevo forms of complex organic reactants discussed in detail by Mills.†

In the following pages are described the results obtained on the examination of the rate of change of surface potential observed with monolayers of four unsaturated fatty acids: oleic, petroselinic,  $\Delta\alpha\beta$  iso-oleic, and chaulmoogric acids; a series possessing the unsaturated double bond in various positions relative to the polar carboxyl group. The structures and melting points of the specimens used are set out in Table I

Table I

Acid.	Structure.	Melting point.
Oleic .....	$\text{CH}_3(\text{CH}_2)_7 \text{CH}=\text{CH}(\text{CH}_2)_7\text{COOH}$ .....	°C. 11
<i>cis</i> -petroselinic .....	$\text{CH}_3(\text{CH}_2)_{10}\text{CH}=\text{CH}(\text{CH}_2)_4\text{COOH}$ .....	30
$\Delta\alpha\beta$ iso-oleic .....	$\text{CH}_3(\text{CH}_2)_{16}\text{CH}=\text{CH} \cdot \text{COOH}$ .....	59
Chaulmoogric .....	$\begin{array}{c} \text{CH}=\text{CH} \\   \\ \text{CH}_2-\text{CH}_2 > \text{CH} \cdot (\text{CH}_2)_{12} \cdot \text{COOH} \end{array}$	68

### Experimental

The change in the air-liquid potential difference caused by the deposition of a unimolecular film on an aqueous surface was measured by the method described by Schulman and Rideal (*loc cit.*). In working with an underlying solution containing potassium permanganate a modification was necessary

\* 'Z. Elektrochem.,' vol. 38, p. 617 (1932).

† 'Presidential Address, B.A.' (1932).



in the electrode in contact with the solution. Satisfactory results are obtained with a bridge as follows :  $\text{Ag/N/100 H}_2\text{SO}_4\text{/N/100 H}_2\text{SO}_4 + \text{K MnO}_4\text{/air}$ , the potential of such a system remaining constant to 1 mv. for several hours.

Measurements of the two dimensional surface pressure of the films were made on a Langmuir-Adam trough sensitive to 0.2 dyne/cm.

The films were spread for oleic, petroselinic and  $\alpha\beta$  iso-oleic acids from dilute solutions in 60°–80° petrol ether, and for chaulmoogric acid from benzene solution. The volume of solution expelled on to the surface was measured by a micrometer syringe.

We are indebted to Professor T. P. Hilditch for a specimen of *cis*-petroselinic acid, to Dr. N. K. Adam for a specimen of  $\alpha\beta$  iso-oleic acid and to Mr. H. Eyde for a specimen of chaulmoogric acid.

#### EXPERIMENTAL RESULTS.

##### *Oleic and cis-petroselinic Acids.*

It was shown by Adam\* from a study of force/area characteristics that a film of oleic acid underwent a profound change on an acid solution of potassium permanganate at a concentration of about 1 per cent. The film on dilute acid alone is a liquid expanded film of normal type with a limiting area of about 55 A.<sup>2</sup> per molecule at room temperature, but in presence of the  $\text{KMnO}_4$  is converted into a vapour expanded film with a limiting area certainly greater than 100 A.<sup>2</sup> per molecule. The suggested interpretation was that the double bond in the centre of the molecule was anchored to the surface much more strongly under the influence of the potassium permanganate.

In the experiments to be described the behaviour of the film was examined on a solution containing a very much smaller concentration of  $\text{KMnO}_4$ , in an attempt to regulate the conditions so that the kinetics of any chemical change occurring in the film might be followed.

In fig. 1 is shown the relation between the surface potential ( $\Delta V$ ) for the film and the number of molecules ( $n$ ) per square centimetre for a film of oleic acid on N/100  $\text{H}_2\text{SO}_4$  (or HCl). The general form of curve is that of an expanded film as obtained for myristic acid under the same conditions (included for comparison in fig. 1). Film collapse occurs at a larger area (30 A.<sup>2</sup>) for oleic acid than for myristic acid.

It is important that addition of 1 per cent.  $\text{KMnO}_4$  to the N/100  $\text{H}_2\text{SO}_4$  has no effect on the myristic acid film. With the oleic acid, however, the

\* Adam and Jessop, 'Proc. Roy. Soc.,' A, vol. 112, p. 362 (1926).

instantaneous surface potential of the film placed on the surface at, say, 50 sq. A. per molecule is about 270 mv., i.e., some 100 mv. higher than in the absence of the  $\text{KMnO}_4$ . This potential rapidly falls, about 100 mv. in the first 10 minutes at 20° C., and in 90 minutes the film has almost completely disappeared.

Under these conditions it appears, therefore, that a rapid oxidation of the oleic acid has taken place resulting in an initial increase of potential, but that

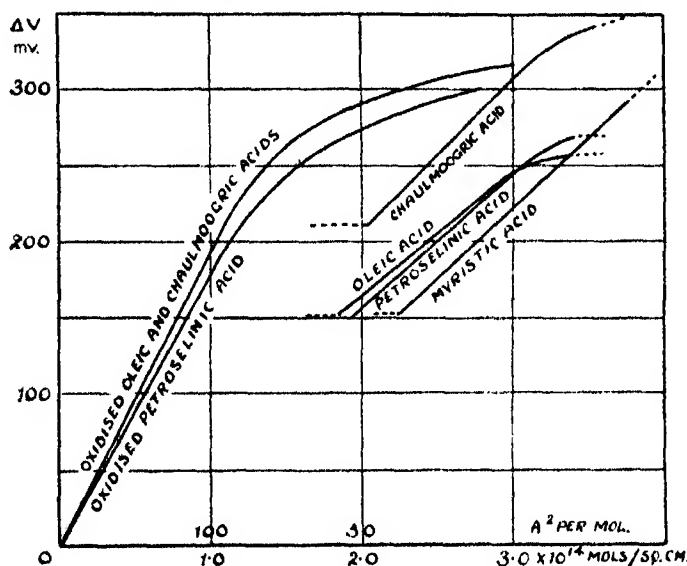


FIG. 1.

the ultimate products of oxidation are sufficiently soluble to diffuse away into the underlying solution.

By greatly reducing the concentration of the permanganate it was found that the first process could be conveniently studied with time.

With a concentration of 0.0015 or 0.0030 per cent.  $\text{KMnO}_4$  the value of  $\Delta V$ , initially that of oleic acid on  $\text{N}/100 \text{ H}_2\text{SO}_4$  alone, rises rapidly at first and then more slowly to a maximum value in 10 to 20 minutes according to the conditions of experiment.

The maximum value of  $\Delta V$  attained varies with the initial value of the area per molecule and a smooth curve may be drawn corresponding to a fairly stable film of "oxidized oleic acid" and coincides with the graph of  $\Delta V/a$  obtained on compression of a film which has been deposited at a large area per molecule, say, 200 sq. A., and left until it has reached a steady potential.

The curve is shown in fig. 1, the oxidized film being uniform down to the largest areas investigated, about 500 sq. A. per molecule. After reaching the maximum value corresponding to the oxidized film the potential begins to decrease slowly owing to solution of the film. The oxidation has continued presumably to the stage of fracture at the double bond, and a fragment with only nine carbon atoms will not form a stable unimolecular film.

A further point of importance is that a film of oleic acid deposited at an area per molecule of say 70 sq. A. is not uniform initially, but is composed of patches of the expanded film in equilibrium with the vapour. The latter has a much smaller surface potential, about 10 mv. as against 150 mv. for the expanded film. When such a film is spread on the dilute  $\text{KMnO}_4$  solution a preliminary process of anchoring of the film is observed. The potential remains nearly constant until the whole surface is uniform in potential at about 160 mv. it then rises to its maximum "oxidized film" value.

For petroselinic acid the general behaviour of the film on dilute acid alone and in the presence of potassium permanganate is very similar to that of oleic (fig. 1). It forms an expanded film with limiting area of 52 sq. A. per molecule, and is oxidized with increase of surface potential to a vapour expanded film which slowly goes into solution. The striking difference between the two acids in relation to the velocity of oxidation, is discussed in the following paragraph.

#### *Kinetics of the Reaction.*

In fig. 2 is plotted a family of curves of the change of surface potential with time for a unimolecular film of oleic acid on 0.0015 per cent.  $\text{KMnO}_4$  in  $\text{N}/100 \text{H}_2\text{SO}_4$ , at varying number of molecules per square centimetre.

The course of such a curve is dependent on a number of factors. In the first place it appears that two reactions are taking place: (1) a preliminary oxidation of the central double bond presumably to a dihydroxy compound  $\text{CH}_3(\text{CH}_2)_7-\text{CH}(\text{OH})\cdot\text{CH}(\text{OH})\cdot(\text{CH}_2)_7\text{COOH}$ , which tends to lie flat on the surface (i.e., to vaporize the film) followed by a splitting of the molecule in the centre to a carboxy and a dicarboxy acid of nine carbon atoms, which latter are slowly soluble in the underlying solution. The rate of diffusion will thus be influenced by the rate at which the final products diffuse away from the surface, and also by the rate of replenishment of the oxidizing agent in the surface layer.

As an approximation we may suppose for the preliminary reaction that if the total number of molecules per square centimetre be " $n$ ," and that at time

" $t$ " there are present  $n_1$  with resolved vertical dipole moment  $\mu_1$ ,  $n_2$  with resolved vertical component  $\mu_2$  for the reactant and product respectively, then

$$\Delta V = 4\pi(n_1\mu_1 + n_2\mu_2) \quad \text{and} \quad n_1 + n_2 = n.$$

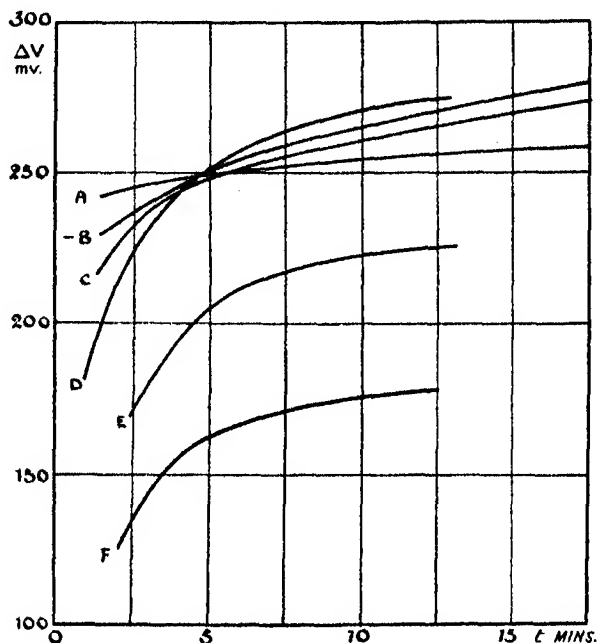


FIG. 2.—Oxidation of oleic acid  $\Delta V$ /time by 0.003 per cent.  $\text{KMnO}_4 + \text{N}/100 \text{ H}_2\text{SO}_4$ ,  $14^\circ \text{C}$ ., varying number of mols./sq. cm. ( $n$ ).

Curve.	$n$ .	Curve.	$n$ .
A	$2.84 \times 10^{14}$	D	$1.68 \times 10^{14}$
B	$2.55 \times 10^{14}$	E	$1.09 \times 10^{14}$
C	$2.22 \times 10^{14}$	F	$0.83 \times 10^{14}$

Assuming the unimolecular law

$$\frac{dn_1}{dt} = -Kn_1 \quad (1)$$

$$\frac{d\Delta V}{dt} = 4\pi(\mu_1 - \mu_2) \frac{dn_1}{dt} = -4\pi K(\mu_1 - \mu_2)n_1,$$

while

$$\begin{aligned} \Delta V &= 4\pi n_1(\mu_1 - \mu_2) + 4\pi n\mu_2 \\ &= 4\pi n_1(\mu_1 - \mu_2) + \Delta V_\infty, \end{aligned}$$

where  $\Delta V_\infty$  = maximum potential attained =  $4\pi n \mu_2$ ,

$$\text{or } n_1 = \frac{\Delta V - \Delta V_\infty}{4\pi(\mu_1 - \mu_2)}$$

therefore

$$\frac{d\Delta V}{dt} = -K(\Delta V - \Delta V_\infty). \quad (2)$$

The values of  $K$  evaluated by applying equation (2) are found to be constant over a range of about 5 minutes during the early part of the reaction. It is of interest to plot  $K$  against  $n$ , the initial number of molecules per square centimetre in the film, and to compare the results for oleic acid with those obtained for petroselinic acid, the latter acid having the  $-\text{CH}=\text{CH}-$  bond three carbon atoms closer to the terminal  $-\text{COOH}$  group than has oleic acid, fig. 3.

The main feature of the graph is the rapid decrease in reaction velocity as the area per molecule in the film is decreased below about 55 sq. A. for oleic acid, but only below about 40 sq. A. for petroselinic acid ( $K = 2.303 k$ ).

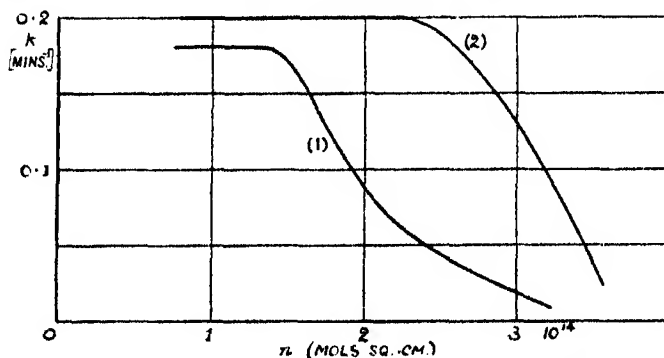


FIG. 3.—Velocity constants  $[k]$  oxidation of (1) oleic acid, (2) petroselinic acid, 0.003 per cent.  $\text{KMnO}_4 + \text{N}/100 \text{ H}_2\text{SO}_4$ ,  $15^\circ \text{C}$ .

It is impossible completely to inhibit reaction in either case, but at the highest compressions the rate of oxidation is reduced certainly tenfold; an accurate value of  $K$  cannot be obtained in this region owing to the very small changes in  $\Delta V$  concerned.

While there is no absolutely sharp point during compression at which the reaction velocity falls off from its maximum value, owing to the thermal agitation of the molecules in the film, yet it is of great significance that the difference between the approximate areas per molecule for the two acids when this decrease is observed corresponds to the area of three  $\text{CH}_2$  groups lying in the surface, namely,  $\frac{2}{3} \times 2.5 \times 4.5 \text{ sq. A.} \doteq 17 \text{ sq. A.}$  Since in petroselinic

acid the  $\text{CH}=\text{CH}$  bond is three carbon atoms nearer to the terminal  $\text{COOH}$  group than in oleic acid it seems justifiable to conclude that the observed difference between the two acids is in reality due to the double bond being removed from the vicinity of the oxidizing agent at an earlier stage of compression for oleic acid than for petroselinic acid.

A further point of interest is noticed in regard to the change in two dimensional surface pressure ( $F$ ) concomitant with the reduction in reaction velocity.

For oleic acid an increase in  $F$  of only 1 dyne per centimetre will halve the reaction velocity, and for petroselinic acid a change of about 9 dynes per centimetre is required to effect a similar reduction.

The surface pressure curves are included for reference, fig. 4.

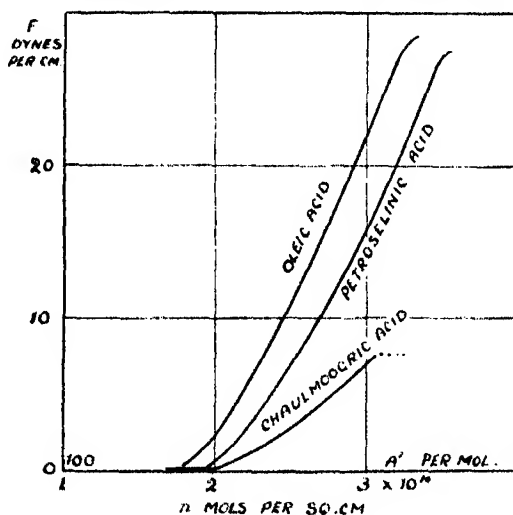


FIG. 4.—Force/ $\pi$  curves;  $\text{N}/100 \text{ H}_2\text{SO}_4$ ,  $15^\circ \text{C}$ .

#### $\Delta\alpha\beta$ iso-oleic Acid.

The general behaviour of  $\alpha\beta$  iso-oleic acid as a unimolecular film presents some striking contrasts to that of oleic or petroselinic acids under the same conditions, i.e., on  $\text{N}/100 \text{ HCl}$  at  $20^\circ \text{C}$ .

As shown by Adam\* the force/area characteristics of this acid under these conditions are those of a liquid condensed film with a large limiting area ( $28.7 \text{ sq. A.}$ ). The limiting area here found is rather smaller, namely,  $26.4 \text{ sq. A.}$  per molecule, as shown by the surface pressure curve, fig. 5 (A). This is probably a more accurate value, owing to improvement in the method of spreading the film.

\* 'Proc. Roy. Soc.,' A, vol. 101, p. 452 (1922).

The values obtained for the surface potentials are plotted in fig. 5 (C). The film is uniform in potential at areas below  $26.4 \text{ A.}^2$  and a potential of 610 mv. ; the  $\Delta V/n$  curve is linear from  $26.4$ – $23 \text{ A.}^2$  per molecule but shows a slight break at  $23 \text{ A.}^2$ ; film collapse taking place at about  $19.5 \text{ A.}^2$  per molecule at 756 mv.

These values of the surface potential provide interesting evidence as to the properties of the  $-\text{CH}=\text{CH}-$  bond in the  $\alpha\beta$  position as distinct from its

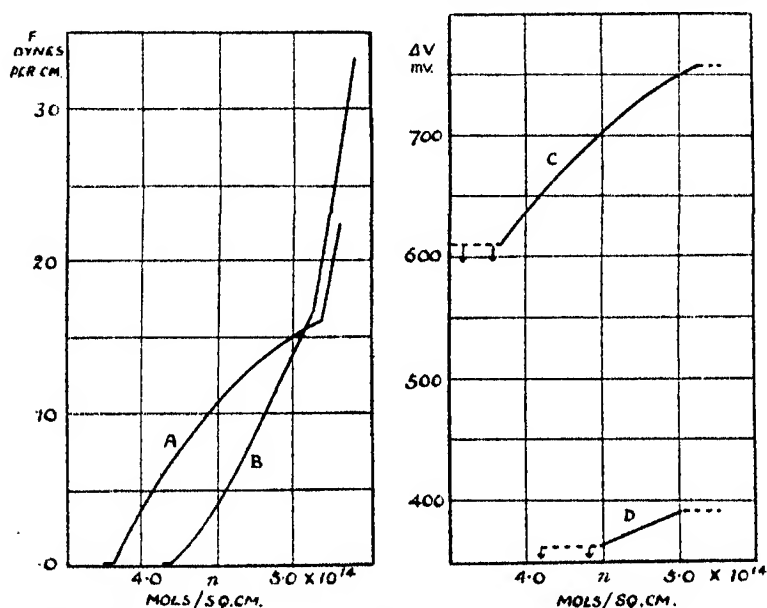


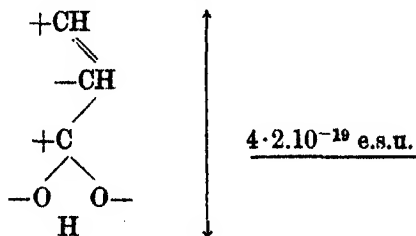
FIG. 5.—Surface pressures and potentials,  $N/100 \text{ H}_2\text{SO}_4$ ,  $15^\circ \text{C}$ . A, oleic acid ; B, palmitic acid, oxidized iso-oleic acid ; C, iso-oleic acid ; D, palmitic acid, oxidized iso-oleic acid.

properties when removed some distance from the terminal  $-\text{COOH}$  group. Thus the vertical component of the electric moment per molecule ( $\mu$ ) calculated from the Helmholtz equation  $\Delta V = 4\pi n\mu$  is very much larger for the  $\alpha\beta$  iso-oleic acid than for oleic or petroselinic acids as is seen from the values given in Table II ; the value for the  $\alpha\beta$ -acid being about double that for the other two acids.

Table II.

Acid.	State of film.	$\text{A.}^2$	$\mu$
Oleic acid .....	Liquid expanded .....	55	$2.1 \cdot 10^{-19}$ e.s.u. per mol.
Petroselinic acid .....	" " .....	55	$2.1 \cdot 10^{-19}$ "
$\alpha\beta$ iso-oleic acid .....	" condensed .....	26	$4.2 \cdot 10^{-19}$ "
Chaulmoogric acid .....	" expanded .....	50	$2.5 \cdot 10^{-19}$ "
Myristic acid .....	" " .....	45	$1.8 \cdot 10^{-19}$ "

The close proximity of the  $-\text{CH}=\text{CH}-$  bond to the dipole system of the carboxyl head clearly causes a marked distortion of the former, resulting in an increased dipole moment in the sense indicated :—



The double bond would appear to have only a small dipole moment when removed by at least four carbon atoms from the carboxyl group; the values of  $\mu$  for oleic and for petroselinic acid being identical within experimental error. Whether this small effect is that of the  $-\text{CH}=\text{CH}-$  group *per se*, or an induced effect along the hydrocarbon chain is impossible as yet to decide.

The oxidation of  $\alpha\beta$  iso-oleic acid has been examined on very dilute potassium permanganate solutions, in N/100  $\text{H}_2\text{SO}_4$ .

With a concentration of 0.003 per cent.  $\text{KMnO}_4$  an immediate rapid decrease in surface potential takes place, and is complete in about 20 minutes. The resulting film on examination by compression proves to be a liquid condensed film having a surface potential and a surface pressure curve identical with that of palmitic acid, fig. 5 (B) and (D). The area per molecule at any given potential for the oxidized  $\alpha\beta$  iso-oleic acid on dilute  $\text{KMnO}_4$  solutions is, however, about 5 per cent. smaller than for palmitic acid, indicating the formation of a second product which is not remaining in the unimolecular film. Le Sueur\* obtained by graduated oxidation of  $\alpha\beta$  iso-oleic acid, first the  $\alpha\beta$  dihydroxy stearic acid and finally palmitic acid. The dihydroxy acid is much more soluble in water than palmitic acid and would dissolve rapidly from a unimolecular film, thus accounting for the apparent decrease in area per molecule of the stable film of palmitic acid. On 1 per cent.  $\text{KMnO}_4$  the oxidation of  $\alpha\beta$  iso-oleic acid is complete in 2 minutes at  $15^\circ \text{C}$ ., and the oxidized film coincides in molecular area and surface potential with that of palmitic acid.

The behaviour of a film of palmitic acid was found to be the same on N/100  $\text{H}_2\text{SO}_4$  whether potassium permanganate was present in the solution or not.

One curious point was noticed, namely that the oxidized film of  $\alpha\beta$  iso-oleic acid became solid at high compressions, below about 20 sq. A. per molecule

\* 'J. Chem. Soc.,' vol. 85, p. 1708 (1904).



while palmitic acid itself does not give a solid condensed film under these conditions. This rigidity of the film obtained by oxidation may be due to the presence of some precipitated oxide of manganese beneath the film.

It will be noticed that with oleic and petroselinic acids the oxidation is accompanied by an increase of surface potential with a subsequent slow decrease owing to solution of the products of oxidation. For  $\alpha\beta$  iso-oleic acid no increase is observed, but only a continuous decrease. If the first step in the oxidation is, as supposed, the formation of  $\alpha\beta$  dihydroxy stearic acid, the surface potential of this acid must be equal to or less than that of  $\alpha\beta$  iso-oleic acid. The second step, involving the disruption of the  $\alpha\beta$  linkage must, further, be proceeding much more rapidly than for oleic or petroselinic acids under the same conditions.

#### *Chaulmoogric Acid.*

On dilute acid solutions (N/100 HCl or  $\text{H}_2\text{SO}_4$ ), chaulmoogric acid forms an expanded film with a limiting area of transition to a vapour film at 50 sq. A. per molecule. The  $\Delta V/n$  and  $F/n$  curves are shown in figs. 1 and 4.

The film is very unstable on compression and collapses at about 33 sq. A. per molecule at 7 dynes per centimetre, a much lower pressure than that for oleic or petroselinic acids, *cf.* fig. 4. Examination of the surface potentials shows that the film is uniform over the range 50–33 sq. A. per molecule. The corresponding value of the vertical component of the electric moment per molecule ( $\mu$ ) is  $2.5 \cdot 10^{-19}$  e.s.u. This value is considerably larger than that for oleic or petroselinic acids under the same conditions and indicates that the double bond, here present in a five ring, is definitely more polar than that in a straight chain, *cf.* Table II.

Examination of the behaviour of chaulmoogric acid on 0.003 per cent.  $\text{KMnO}_4$  shows that there is an immediate rise in surface potential followed by a slow decrease, the film disappearing almost completely in 3 hours. The maximum values of the surface potential correspond to a vapour expanded film, fig. 1. The same process of expansion can be traced when a film of chaulmoogric acid is deposited on the surface at an area equivalent to, say, 500 sq. A. per molecule, as was observed for oleic or petroselinic acids.

In order to follow the kinetics of the initial process of oxidation it was necessary to use a more dilute solution of potassium permanganate. With 0.0003 per cent.  $\text{KMnO}_4$  the initial rise of potential was complete in about 10 minutes, and again followed an approximately unimolecular relation. With the more dilute solution, however, the velocity constant derived in the same

manner as for oleic or petroselinic acids remains constant at  $k = 1.3 \text{ mins.}^{-1}$  over the whole range of compression of the film.

The question as to the position of the double bond in the film of chaulmoogric acid is difficult to decide. From the rate of oxidation of the film it is clear that the double bond in the five ring has ready access to the surface layer.

It has been shown that a film of oleic acid oxidizes only very slowly at an area per molecule of 30 sq. Å., the double bond being removed by seven carbon atoms from the carboxyl group. In chaulmoogric acid the double bond is removed by thirteen carbon atoms from the carboxyl group. If, therefore, the double bonds are out of the surface the rate of oxidation at the same area per molecule would be expected to be much smaller for chaulmoogric acid than for oleic acid; which is not so. The range of area 50–33 sq. Å. would preclude the possibility of the double bonds of all the molecules being in the surface, since the double bond entails also the presence of a five ring, the area of which is at least 20 sq. Å. It is probable, however, that a large proportion of the double bonds are actually in the surface and react very rapidly with the oxidizing agent.

#### *Chemical Reactivity and Dipole Moment.*

It is of interest to compare the rate of oxidation of the four acids under discussion in relation to the values of  $\mu$ , the vertical component of the electric moment per molecule, given in Table II.

For oleic and petroselinic acids, where  $\mu$  is almost exactly the same, the reaction velocities at areas where the double bonds are equally available are also approximately the same ( $k = 0.2 \text{ mins.}^{-1}$ ), with a concentration of 0.003 per cent.  $\text{KMnO}_4$ .

For chaulmoogric acid with the same concentration of  $\text{KMnO}_4$ , the reaction velocity is too great to be measured, but at one-tenth this concentration the reaction velocity is of the same order,  $k = 1.3 \text{ mins.}^{-1}$ . The value of  $\mu$  is correspondingly larger, presumably owing to the deformation of the double bond by virtue of its presence in a five ring instead of a straight chain.

Turning to  $\alpha\beta$  iso-oleic acid the deformation of the double bond is very marked, as indicated by the high value of  $\mu = 4.2 \cdot 10^{-19} \text{ e.s.u.}$ , and the reaction velocity is too great to be measured even on very dilute  $\text{KMnO}_4$  at 0.0003 per cent.

It is not possible at this stage to assert a definite relation between reaction velocity and dipole moment, yet since it is probable that reaction velocity is dependent on the deformability of the reactive group, here the double bond,

the suggestion may be made that the values of the electric moment ( $\mu$ ) may indeed provide a measure of the deformability.

### *Products of Oxidation.*

The course of the oxidation of a double bond by potassium permanganate is known to take place through the medium of a dihydroxy compound with the ultimate formation of two carboxyl groups.

Fig. 1 shows the  $\Delta V/n$  curves for the initial oxidation products of oleic, petroselinic and chaulmoogric acids. The films are vapour expanded, as would be expected for a molecule with two polar groups near the centre of the molecule in addition to the terminal COOH group. The value of  $\mu$  is  $5.0 \cdot 10^{-19}$  e.s.u. per molecule in this vapour expanded film for chaulmoogric and oleic acids, and only slightly smaller for petroselinic acid.

Allowing as a rough approximation  $2.0 \cdot 10^{-19}$  e.s.u. per molecule for the carboxyl group, and assuming the various dipole moments to be additive, we arrive at a value of  $\mu = 3.0 \cdot 10^{-19}$  e.s.u. for the initial oxidation product of one double bond. This is certainly larger than the value for one OH group, which is  $2.0 \cdot 10^{-19}$  e.s.u. as found for the expanded film of a long chain aliphatic alcohol (Schulman and Hughes, *loc. cit.*), and is probably the value corresponding to two adjacent OH groups lying flat in the surface.

Further, oxidation of these three acids involves a splitting of the molecule into short chain fragments, and as has been observed, the film slowly dissolves. It is only with  $\alpha\beta$  iso-oleic acid that the final oxidation product can be traced and identified, rupture of the double bond splitting off two carbon atoms and leaving a stable film of palmitic acid.

### *Autoxidation in Surface Films.*

A study of the properties of unimolecular films of  $\alpha$  and  $\beta$  elæostearic acids reveals some features of interest in relation to autoxidation.

The  $\alpha$ - and  $\beta$ -acids are respectively the *cis* and *trans* modifications of the doubly conjugated system:—



(Morrell and Samuels).\*

We are indebted to Dr. Morrell for the gift of specimens of these acids; the melting points were:— $\alpha$ -acid  $48^\circ$  C.,  $\beta$ -acid  $71^\circ$  C. Benzene was used as solvent in spreading the films.

\* 'J. Chem. Soc.', p. 2251 (1932).

On dilute acid solutions both the  $\alpha$  and  $\beta$  acids spread to a unimolecular film which undergoes spontaneous oxidation, complete in 15 minutes at 20° C. The product forms a stable film with a limiting area of about 125 sq. A. per molecule in each case. At larger areas the film is non-uniform, showing fluctuations in surface potential of about 50 mv. This limiting area indicates that the molecules are lying flat in the surface, having increased adhesion in the centre of the molecule due to oxidation of the double bond system.

Fig. 6, A, shows the  $\Delta V/n$  curve for the final oxidized film of  $\alpha$ - or  $\beta$ -elæostearic acids, the same curve being obtained for both acids.

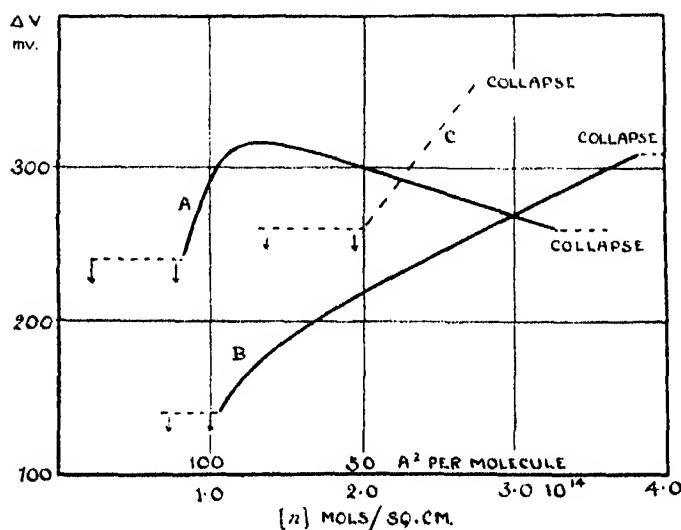


FIG. 6.— $\alpha$ - and  $\beta$ -elæostearic acids, 20° C. A, N/100 HCl or  $H_2SO_4$  "oxidized"; B,  $\alpha$ -acid N/100 HCl + O, 12 per cent. hydroquinone; C,  $\beta$ -acid, ditto.

The electric moment per molecule of the oxidized acid is  $8.0 \cdot 10^{-19}$  e.s.u. per molecule in its most expanded state, i.e., when the whole molecule is lying flat in the surface. Again assuming as an approximation that  $2.0 \cdot 10^{-19}$  e.s.u. is the value for the terminal COOH group, there remains an electric moment of  $6.0 \cdot 10^{-19}$  e.s.u. per molecule for the oxidation product of the doubly conjugated system. Now in dealing above with the oxidation of one double bond, the value  $3.0 \cdot 10^{-19}$  e.s.u. has been ascribed to two adjacent OH groups. It seems probable, therefore, that the autoxidation involves the oxidation of two of the three double bonds in the elæostearic acid molecule. Further, on compression of the oxidized film it will be noticed from fig. 6 that a very sharp decrease in the vertical component of the electric moment per molecule takes place below 100 sq. A. per molecule. This must be due to the removal from

the surface of some polar portion of the molecule. The area of 100 sq. A. corresponds to approximately  $(100/125) \times 18$ , *i.e.*, 14 carbon atoms lying flat in the surface. Thus the oxidation process concerns at any rate the double bond in the molecule remote from the terminal carboxyl group, and either of the following structures may be tentatively assigned to the oxidation product :

- (1)  $\text{CH}_3(\text{CH}_2)_3\text{CHOH} \cdot \text{CHOH} \cdot \text{CHOH} \cdot \text{CH}=\text{CH}(\text{CH}_2)_7\text{COOH}$ .
- (2)  $\text{CH}_3(\text{CH}_2)_3\text{CHOH} \cdot \text{CH} : \text{CH} \cdot \text{CHOH} \cdot \text{CHOH}(\text{CH}_2)_7\text{COOH}$ .

For either acid, the atmospheric oxidation as observed by the increase of surface potential with time, is completely inhibited by the presence of 0.12 per cent. hydroquinone in the underlying solution, (N/100 HCl). The values of the surface potential under these conditions are perfectly steady with time, but whereas for the  $\alpha$ -acid, fig. 6, B, the film thus obtained has the characteristics to be expected for the unoxidized unsaturated acid, and is comparable to that of oleic acid; the  $\beta$ -acid, fig. 6, C, the film in the presence of hydroquinone has a higher surface potential than has the  $\alpha$ -acid, and only approximates to uniformity in potential ( $\pm 15$  mv.) over the range 50–35 sq. A. per molecule. This is the only point of difference so far observable between the unimolecular films of the *cis* and *trans* forms of elæostearic acid. The behaviour of the  $\beta$ -acid may be due to the formation of an unstable addition product with the hydroquinone, which cannot be formed with the  $\alpha$ -acid.

The antioxygenetic action of the hydroquinone varies markedly with its concentration in the underlying solution. At a concentration of 0.0001 per cent. hydroquinone autoxidation proceeds unchanged. At ten times this concentration the rate of oxidation is approximately halved, while at 0.12 per cent. hydroquinone, the autoxidation is completely inhibited.

On N/100  $\text{H}_2\text{SO}_4$  containing 0.0015 per cent.  $\text{KMnO}_4$  both the  $\alpha$ - and  $\beta$ -acids undergo rapid oxidation involving a splitting of the molecule into short chain fragments which dissolve in the underlying solution, the reaction being too rapid to follow.

#### Summary.

(1) The method of surface potentials has been employed to study chemical reactions occurring in a unimolecular film; the reactions examined being the oxidation by acidified potassium permanganate of long chain unsaturated aliphatic acids such as oleic acid.

(2) With a concentration of 0.003 per cent.  $\text{KMnO}_4$  in N/100  $\text{H}_2\text{SO}_4$  oxidation of a fully expanded film of oleic acid is complete in 15 minutes at

room temperature. The reaction velocity is shown to depend on the accessibility of the double bond to the oxidizing agent, and decreases markedly on compression of the film. Reaction velocity has been studied as influenced by the position of the double bond in relation to the polar carboxyl headgroup.

(3) Autoxidation in a unimolecular film has been observed for the elæostearic acids, and the effect of hydroquinone as an antioxygen to this reaction has been examined.

---

*On Eddington's Problem of the Expansion of the Universe by  
Condensation.*

By N. R. SEN.

(Communicated by Sir Arthur Eddington, F.R.S.—Received June 20, 1932.—

Revised January 10, 1933).

1. The discovery of the general receding motion of the spiral nebulae by Hubble lent importance to the Friedmann-Lemaître solution of Einstein's field equations and it was promptly suggested that our present universe started from a static condition, and owing to certain unknown causes began expanding and has since been doing so continuously. Eddington\* pointed out that the static Einstein universe was unstable and so "exploded" (as Eddington put it) in some past age. Eddington suggested that the reason for explosion was the condensation of matter into stellar bodies out of the nebular mass uniformly filling up the Einstein universe. McCrea† and McVittie, working on this idea, proposed a proof showing that for a single condensation the universe would start contracting, but for more condensations start expanding from the equilibrium state. This proof they have recently withdrawn as being erroneous.‡ Meanwhile, Lemaître§ himself enunciated a theorem stating that condensation itself could not cause expansion or contraction, but it was the stagnation of energy (ultimately amounting to condensation) which disturbed the equilibrium and caused the universe to swell up, but McCrea and McVittie||

\* 'Mon. Not. R. Astr. Soc.,' vol. 90, p. 668 (1930).

† *Ibid.*, vol. 91, p. 128 (1930); vol. 91, p. 274 (1931).

‡ *Ibid.*, vol. 92, p. 7 (1931).

§ *Ibid.*, vol. 91, p. 490 (1931).

|| *Ibid.*, vol. 92, p. 7 (1931).

showed that his proof was incorrect. Eddington's problem thus remains where it was when first proposed.

In this note we give a proof which shows that condensations, no matter whatever be their number, would start expansion of the Einstein universe.

2. Before proceeding further it is necessary to state the limitation under which the whole discussion is to be carried on. In the exact treatment of the problem, factors other than merely gravitational such as contraction, radiation, etc., play a part. Here we examine only one aspect, if a rearrangement of matter alone in the Einstein universe, apart from other considerations, is in itself a cause of expansion; counteracting effects which may probably be produced by other factors are beyond the scope of our enquiry here. We shall thus confine ourselves to a consideration of gravitation alone and examine the effect of a suitable rearrangement of matter, which as we shall see presently, we can easily imagine to take place infinitely slowly.

The method of handling the problem can be briefly sketched thus. We first take the Einstein universe and imagine, as suggested by Eddington,\* that round some irregularity (in the way of greater density) at a certain region,

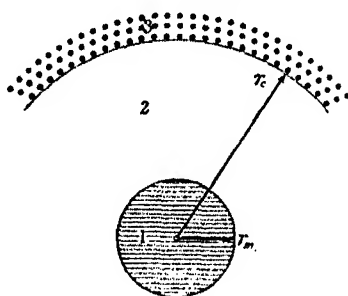


FIG. 1.

condensation of matter takes place owing to increased local gravitational pull. This condensation we take as a spherical mass which ultimately detaches itself from the thinly diffused material of the Einstein universe and is separated from it by a vacuum. Next we fit in three gravitational fields: (1) of the inner condensation for which we take Schwarzschild's inner field of a spherical mass with constant energy density bounded by the spherical surface  $r = r_m$ ;

\* I am greatly indebted to Sir Arthur Eddington for this suggestion in a private letter as well as for his criticism which has been very helpful to me. I have also used a suggestion from him to put the argument at the end of paragraph 2 in its present form. For all this and the interest taken by him in this present paper I desire cordially to thank Sir Arthur Eddington.

(2) of the region from  $r_m$  up to another spherical surface of radius  $r_0$  ( $r_0 > r_m$ ) in which there is Schwarzschild's external field in empty space ; (3) of the undisturbed Einstein universe from  $r_0$  outwards. Suppose we succeed in establishing the continuity of metric and pressure at the bounding surfaces  $r_m$  and  $r_0$  of (1) and (2), and (2) and (3) respectively. Next we shall calculate the total amount of matter (energy) in the condensed sphere (1) and the amount which was originally present in the Einstein universe within the spherical surface  $r_0$ . To the first approximation, they will be found to be equal. Hence, if the material within the sphere  $r_0$  of the Einstein universe be condensed into a spherical mass, the outside Einstein universe, will, to the first approximation, remain unaffected. A closer approximation, however, gives the total matter in (1) greater than the total matter within the sphere  $r_0$  of the original Einstein universe. The formation of a condensation within  $r_0$ , leaving the outside Einstein universe unaffected, would require the presence of a greater amount of matter than was originally present in the Einstein universe within  $r_0$ .

Now consider two equilibrium configurations, (1) the Einstein universe in which we particularly confine our attention to the total matter within a sphere of radius  $r_0$ , and (2) another hypothetical equilibrium configuration with a condensation within  $r_0$  and the undisturbed Einstein universe outside  $r_0$ . The latter, according to our previous argument, contains slightly more mass than the former. In the actual universe this extra mass is not available. Hence the gravitational effect of a condensation of matter within  $r_0$  of the Einstein universe and with no change outside  $r_0$  is the same as that of the equilibrium configuration (2), less that of the gravitational field of a small missing mass in the condensation within  $r_0$ . The equilibrium configuration implies no force but the deficit gravitational field of the missing mass in  $r_0$  has repulsive effect and is responsible for the expansion. In exactly the same manner we can construct other condensations in other places of the Einstein universe, as we shall see later. The total gravitational field in the Einstein universe with these condensations will be that of an equilibrium configuration (2) less the gravitational fields of the missing masses in the condensations. These missing gravitational fields produce repulsion causing the Einstein universe to expand.

3. To fit in the three gravitational fields as stated in the previous section we first take the following metric for the spherical condensation (1)

$$ds^2 = \left[ 1 - \left( \frac{r}{A} \right)^2 \right]^{-1} dr^2 + r^2 (d\theta^2 + \sin^2 \theta d\phi^2) - V^2 dt^2 \quad (0 \leq r \leq r_m), \quad (1)$$



where

$$A^2 = \frac{3}{\lambda + kc^2\mu} \quad (2)$$

$\mu$  being the density of energy and  $k$  the gravitational constant,  $r_m$  the outer boundary of the sphere where the pressure vanishes, and

$$V = \frac{c}{2} [(3 - \lambda A^2) \cos \Theta_m - (1 - \lambda A^2) \cos \Theta].$$

$$\sin \Theta = \frac{r}{A}. \quad (3)$$

On

$$r = r_m, \quad \Theta = \Theta_m, \quad V = c \cos \Theta_m.$$

Outside this sphere and between  $r_m$  and  $r_0$  we have Schwarzschild's outer field

$$ds^2 = \frac{dr^2}{1 - \frac{1}{3}\lambda r^2 - \frac{\alpha}{r}} + r^2(d\theta^2 + \sin^2\theta d\phi^2) - c^2\left(1 - \frac{1}{3}\lambda r^2 - \frac{\alpha}{r}\right)dt^2 \quad (r_m \leq r \leq r_0). \quad (4)$$

Beyond  $r_0$  we have the metric of the Einstein universe

$$ds^2 = \frac{dr^2}{1 - \lambda r^2} + r^2(d\theta^2 + \sin^2\theta d\phi^2) - c^2 dt^2 \quad (r \geq r_0). \quad (5)$$

It is assumed that both  $r_m$  and  $r_0$  are very small compared to  $1/\sqrt{\lambda}$ , the radius of the Einstein universe.

The metrics (4) and (5) can be made continuous on the boundary  $r = r_0$  if we put\*

$$\alpha = \frac{2}{3}\lambda r_0^3, \quad (6)$$

as the gravitational field (4) is then equivalent to

$$ds^2 = \frac{dr^2}{1 - \frac{1}{3}\frac{\lambda}{r}(r^3 + 2r_0^3)} + r^2(d\theta^2 + \sin^2\theta d\phi^2) - c^2 \frac{1 - \frac{1}{3}\frac{\lambda}{r}(r^3 + 2r_0^3)}{1 - \lambda r_0^2} dt^2 \quad (r_m \leq r \leq r_0). \quad (4')$$

the time variable only differing by a constant factor  $(1 - \lambda r_0^2)$ . Also since the pressure in the Einstein universe vanishes the continuity of pressure at  $r = r_0$  is also ensured. We have next to satisfy ourselves that on the surface of separation  $r_0$  of the two gravitational fields (5) and (4') there is no surface

\* This fit was suggested by M. v. Laue, "Die Relativitätstheorie," II, p. 246.

density of matter. The conditions that a surface, at any point of which the unit normal vector has components  $v_s$ , and on which the metric is continuous, should be free from surface density are\*

$$\left\{ \begin{matrix} km \\ m \end{matrix} \right\}_2^1 v_l - \left\{ \begin{matrix} kl \\ s \end{matrix} \right\}_2^1 v_s = 0 \quad (k, l = 1, 2, 3, 4),$$

where  $\{ \}_2^1$  is the discontinuity in the value of Christoffel's bracket at a point of the surface. When the right-hand side of the above equation is different from zero a surface distribution of matter (material tensor) is to be expected. In the present case all the first derivatives of  $g_{\mu\nu}$  are continuous except  $\partial g_{11}/\partial r$  on  $r_0$ . But it can easily be verified from the above equations that a surface layer of matter is absent.†

Secondly, we write down the conditions that the pressure and the metrics (1) and (4) are continuous on  $r = r_m$ . The pressure is evidently continuous as it vanishes on  $r_m$  for both the fields.

The continuity of  $g_{11}$  gives

$$1 - \left( \frac{r_m}{A} \right)^2 = 1 - \frac{1}{3} \lambda r_m^2 - \frac{\alpha}{r_m},$$

which by (2) is equivalent to the relation

$$\alpha = \frac{1}{3} k c^2 \mu r_m^3, \quad (7)$$

$\mu$  being the density of inner condensation supposed uniform. Since the density  $\rho$  of the Einstein universe is given by

$$\lambda = \frac{1}{2} k c^2 \rho, \quad (8)$$

we have from (6), (7) and (8)

$$\rho r_0^3 = \mu r_m^3, \quad (9)$$

which we rewrite as

$$s = \frac{r_m}{r_0} = \left( \frac{\rho}{\mu} \right)^{\frac{1}{3}}. \quad (9')$$

Substituting from (2) and (9') we have further

$$\left( \frac{r_m}{A} \right)^2 = \frac{1}{3} \lambda \left( 1 + \frac{2}{s^3} \right) s^2 r_0^2. \quad (10)$$

With the above conditions the continuity of  $g_{44}$  is automatically adjusted on  $r = r_m$  with a trivial transformation of the time variable.

\* The general conditions from which these are derived by equating the right-hand side to zero were established by me in a paper published in 'Ann. Physik,' vol. 73, p. 365 (1924).

† Sen, *loc. cit.* A similar case is worked out here.

Now the volume of the condensed sphere is

$$2\pi\Lambda^3 (\Theta_m - \tfrac{1}{2} \sin 2\Theta_m),$$

so that by (3) the total mass (energy) of this sphere is

$$\frac{4\pi}{3} r_m^3 \mu \left[ 1 + r_0^3 \left( \frac{r_m}{A} \right)^2 + \dots \right]. \quad (11)$$

The total mass of the sphere  $r_0$  of the Einstein universe is given by

$$4\pi\rho \int_0^{r_0} \frac{r^2 dr}{\sqrt{1 - \lambda r^2}}. \quad (12)$$

Next we have to decide which of these two masses is greater. For our purpose it will be sufficient if we expand the denominator of the above integral and keep only the first power of  $\lambda$ . This gives the value of the integral as

$$\frac{4\pi}{3} \rho r_0^3 \left[ 1 + \frac{3\lambda}{10} r_0^2 + \dots \right], \quad (13)$$

whereas by (10) and (11) the mass of the condensed sphere is

$$\frac{4\pi}{3} \mu r_m^3 \left[ 1 + \frac{\lambda}{10} \left( 1 + \frac{2}{s^3} \right) s^2 r_0^2 + \dots \right]. \quad (14)$$

Owing to relation (9) the first terms of these two expressions are equal so that if only Euclidean geometry is admitted the mass of the condensed sphere is equal to the total mass within the sphere  $r_0$  of the Einstein universe. To this order, the condensation has no influence on the Einstein universe. But taking the second term into consideration, we find that the mass of condensation is *greater* than the total mass originally present within  $r = r_0$  of the Einstein universe. For this we should have

$$\frac{\lambda}{10} \left( 1 + \frac{2}{s^3} \right) s^2 r_0^2 > \frac{3\lambda}{10} r_0^2.$$

or

$$s^2 + \frac{2}{s} > 3,$$

or

$$(s - 1)^2 (s + 2) > 0.$$

Since  $s$  is a fraction ( $s < 1$ ) this inequality is satisfied, for all values of  $s$ , which establishes the above statement. At this stage we can apply the arguments in the previous section which enable us to conclude that, when there is rearrangement of matter in the Einstein universe in the form of some condensation

(this we may imagine to take place infinitely slowly), which ultimately detaches itself from the thin material of the surrounding Einstein universe, the result is expansion of the whole.\*

4. We may try to fix the condensed sphere within the Einstein universe itself without any intervening vacuum. This would require a continuous transition of metric (1) to metric (5) on  $r = r_m$ . We should then have the line element (1) for  $0 \leq r \leq r_m$  and (5) for  $r \geq r_m$ . This gives

$$1 - \left(\frac{r_m}{A}\right)^2 = 1 - \lambda r_m^2,$$

whence we have by (2) and (8)

$$\mu = \frac{2\lambda}{kc^2} = \rho. \quad (15)$$

This does not give the requisite fit as it implies zero pressure for the condensation and makes the sphere  $r_m$  only a portion of the Einstein universe. This is really to be expected. A fit may probably be obtained by taking a heterogeneous sphere of which the density gradually decreases outwards and is equal to that of the Einstein universe on the surface. The calculations can be made only for a few special cases for which solutions are known. But the analysis given in the last article clearly indicates how the formation of condensation and the consequent thinning of the material of the Einstein universe along a spherical boundary would lead to the expansion of this universe.

5. The manner in which the gravitational fields have been fitted together in article 3 has got the special advantage that the adjustment has been made by leaving the Einstein universe outside  $r = r_0$  entirely unaltered. We can evidently take other condensations in other parts of the Einstein universe

\* It may be not without interest to enquire how the equilibrium of configuration (2) in § 2 above, is disturbed by taking a deficit mass in the condensation. Formula (13) suggests that this deficit mass can be provided for by slightly diminishing  $\mu$ , the density of the condensation and by (7) this means an effective diminution in  $\alpha$ . Now consider the motion of a particle on  $r_0$  the boundary of the outside Einstein universe. Since it starts from rest we can put the velocities  $\dot{x}_k$  all equal to zero. The equation of the geodesic then gives the initial motion of the particle

$$\left(\frac{d^2r}{dt^2}\right)_{r_0} = -\frac{c^2}{2} \left(\frac{\partial g_{44}}{\partial r}\right)_{r_0} = -\frac{c^2}{2} \left(\frac{\alpha}{r_0^2} - \frac{3}{2}\lambda r_0\right).$$

For the value of  $\alpha$  given by (6), that is for equilibrium, the acceleration vanishes meaning that there is a balance between the attractions of the condensation and the Einstein universe on  $r_0$ . But if the value of  $\alpha$  be slightly diminished, thereby causing an effective deficit in mass in the condensation the acceleration is positive. The particle will move into the Einstein universe and the sphere  $r_0$  will expand.

and similar fits may be obtained provided their gravitational fields do not overlap.\* The arguments of the previous section are now applicable and exactly identical conclusions can be drawn. Hence we can say generally that formation of condensations and their tendency to separate themselves ultimately from the parent nebular material of the Einstein universe would cause expansion of the latter. Eddington's suggestion of condensation being a cause of expansion of the Einstein universe is entirely correct.

*Summary.*

Since the discovery of the general receding motion of the spiral nebulae by Hubble attempts are being made to identify our present universe with an expanding universe of Friedmann-Lemaître type, given by a dynamic solution of Einstein's field equations. Eddington has suggested that our universe was probably initially a static Einstein universe, more or less uniformly filled with nebulous matter, and that sometime in the past age condensation of this nebulous matter into stellar bodies disturbed the static universe, which then started on its career of expansion. A proof of this statement presented difficulties, specially as there was the equal probability of contraction of the static universe, which view was to some extent supported by the works of McCrea and McVittie, who for a time maintained that a single condensation would cause contraction, but a larger number of condensations would produce the opposite effect. These proofs have recently been withdrawn by the authors, and further their criticism shows that another proof of expansion given by Lemaître is also unacceptable. In the present paper it is proved that if round some irregularities in the way of greater density, in the nebulous mass of the static Einstein universe, condensation takes place and these comparatively more dense nebulous masses detach themselves from the parent body, the static Einstein universe starts expanding. The proof also clearly shows that the number of condensations is immaterial and there is expansion in every case.

\* Laue, *loc. cit.*

---

*The Excitation Potentials of Light Metals. II.—Beryllium.*

By H. W. B. SKINNER, Wills Physical Laboratory, Bristol.

(Communicated by A. P. Chattock, F.R.S.—Received September 24, 1932.—

Revised December 9, 1932.)

§ 1. *Introduction.*

In a recent paper,\* an account was given of new measurements on the excitation potentials of lithium metal. Here we shall describe the corresponding results for the next element, beryllium, attention being again mainly focussed on the excitation of the K-radiation.

The purpose of these investigations may be defined as an attempt to determine the effect of the metallic binding on the atomic constants of these light elements. Thus, in Paper I, it was shown that the minimum energy needed for the excitation of the K-radiation of lithium metal is considerably less than the K-ionization potential of the free atom. This low value seemed at first sight inconsistent with the facts of the excitation of X-rays in heavier elements. But, if we adopt a more direct comparison, it is easy to see that the observation that this minimum excitation potential agrees numerically with the energy required for a  $K \rightarrow L$  switch in the free atom implies simply that the effect of the binding here is small. We shall show that for beryllium the effect of the binding is definitely observable; its magnitude, about 20 volts, is considerable compared with the absolute K-excitation energy, about 100 volts. In the attempt to correlate these observations, it became apparent that the theory of Paper I is incomplete. We shall therefore give a corrected treatment in its application to lithium and beryllium metals, and it will be seen that, on certain assumptions, the new theory seems capable of accounting in detail for the observed break-potentials. It has also been found that there is an appreciable difference between the minimum K-excitation potentials of beryllium in the form of a metal and of a polar compound. These problems are closely related to work done on the influence of chemical binding on the absorption-edges and lines in the region of harder X-rays. Thus Bäcklin† studied the  $K_{\alpha}$  line of sulphur, and other elements when used in the form of various compounds, and found shifts of the order of 10 volts. Such investigations open up the question of how far the spectroscopic data of X-rays from solid targets are representative of atomic constants.

\* 'Proc. Roy. Soc.,' A, vol. 135, p. 84 (1932), quoted as Paper I.

† 'Z. Physik,' vol. 33, p. 547 (1925).

When the experiments were begun, there were no recent measurements on the soft X-ray excitation curve of beryllium metal. During its course, a preliminary note was published by Christensen\* on the subject. Our investigation was already at a fairly advanced stage and his results were in serious disagreement with those obtained. It was necessary therefore to clear up the discrepancy, and it may perhaps be claimed that this has been done; we shall show that the curve is very sensitive to the purity of the metallic surface. Work has also been published on a closely related problem; the K-radiation from beryllium has been analysed by Söderman†, Prins‡, and Faust§, using a grating. Unfortunately their results do not agree in all particulars; though neither is definitely irreconcilable, those of Faust fit better with what would be expected from our measurements.

## § 2. *Experimental Method.*

The principle of the method of obtaining the excitation curve for a metal is shown in fig. 1. The radiation emitted from the metallic anode A under the

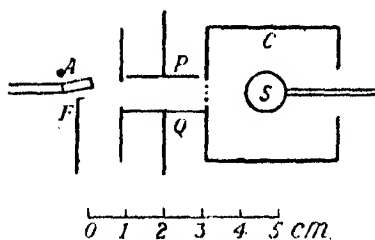


FIG. 1.—Diagram of apparatus.

impact of electrons of a defined voltage  $V$  from the filament  $F$ , passes through the ion-filtering condenser plates  $P$ ,  $Q$  and falls on to the metal sphere  $S$ . The photoelectric current  $i$  from  $S$  to the surrounding cylinder  $C$  is measured for a constant primary electron current and is plotted against  $V$ , which is varied in small steps.  $i$  is used as a measure of the intensity of the radiation emitted from  $A$ . The resulting curve in general shows breaks and these are characteristic of the metal of  $A$ .

The measurements of the photoelectric current were carried out exactly as before, namely, by using a Compton electrometer with a high resistance leak as a null instrument in conjunction with an accurate potentiometer. A primary current of 2 m.a. was invariably used, and the photoelectric currents were of the same order of magnitude for beryllium as those observed when using a lithium anode.

The apparatus used in the first instance for beryllium was identical with that

\* 'Phys. Rev.', vol. 39, p. 549 (1932).

† 'Z. Physik,' vol. 65, p. 656 (1930).

‡ 'Z. Physik,' vol. 69, p. 618 (1931).

§ 'Phys. Rev.', vol. 36, p. 161 (1930).

used for lithium and so need not be described again in detail. It was pumped continuously, with liquid air always kept on the trap; the pressure was less than  $10^{-7}$  mm., and probably considerably less. The anode A and the photoelectric sphere, which were of copper as before, were freed from gas by a preliminary strong heating after the bake-out. The primary electron-current was supplied by a dull-emitter filament with a volt-drop of 0.5 volt. The beryllium, 98 per cent. pure, was evaporated on to the anode A by heating with electron bombardment to about  $1200^{\circ}$  C. from an open cup of molybdenum supported by a tungsten wire. The anode could then be slid into its place 2 or 3 mm. from the filament.

When beryllium is evaporated, it is found that at first it does not form a clean surface. Only after a considerable quantity has been distilled off is the metal sufficiently gas-free for oxidation to be avoided. But after a time the beryllium can be so thoroughly outgassed that the actual distillation on to the anode can be carried out at a pressure of the order of  $10^{-6}$  mm. Then the metal films produced are clean; that is to say they appear brightly metallic when evaporated slowly or form a silver matt surface when evaporated quickly to form a thicker layer. As will be shown, the preparation of a beryllium surface as perfect as possible is crucial for the experiments.

The apparatus thus described worked perfectly; but because of the results obtained compared with those of Christensen, it was necessary to make certain that the experiments were not affected by any peculiarity of the apparatus. It seemed conceivable that the results might depend on the nature of the filament and on the metal chosen for the photoelectric cell, and it was essential to eliminate both these possibilities.

The danger with the dull-emitter filament was that it might continuously distil a small quantity of barium metal on to the beryllium anode, though this was, from the first, unlikely, since no breaks in the relevant voltage region were found when using a lithium anode. But nevertheless a definite test with a change of filament seemed worth while. A tungsten strip-filament, with a volt drop of 1.0 volt was therefore substituted for the dull-emitter. But the disputed characteristics of the curves, namely a set of variations of the photoelectric current when the voltage of the primary electron beam is varied between 90 and 120 volts, were unaffected by this change.

The metal of the photocell was therefore changed from copper to nickel. It was thought possible that the results might be influenced by some selective light-absorption, for wave-lengths comprised in the band emitted by the beryllium metal, on the part of the metal of the photoelectric sphere. Except



that the nickel photocell seemed only about half as sensitive as the copper one, no changes of the curve in the region mentioned were observed which lay outside the limits of error. A molybdenum plate was afterwards substituted for the nickel sphere; because copper and nickel are adjacent elements in the periodic table and there was a faint chance that any difference in their absorption peculiarities might be too small to measure. But, although the sensitivity of the photocell was about halved again, the characteristics of the curve were once more reproduced. Finally, by heating the molybdenum plate very strongly after the distillation of the beryllium on to the anode, it was shown that the results do not depend on the presence of a thin film of beryllium which might incidentally be deposited on to the photoelectric plate. These experiments seem to prove conclusively that the soft X-ray curves are, except in absolute magnitude, independent of the material of the photocell.

Actually, when the material of the photoelectric sphere was changed from copper to nickel, it was decided to banish copper completely from the apparatus. It was noticed that under certain conditions copper in the form of a compound has a tendency to be distilled about the apparatus during the bake-out. The copper anode A was therefore replaced by one of nickel. This had a beryllium plate let into the nickel holder, because it seemed desirable to investigate the behaviour of beryllium metal without distillation; the holder was so shaped that no appreciable amount of radiation could reach the photocell from the nickel parts.

Most of the more accurate experiments were carried out with the apparatus with a tungsten filament, a nickel photoelectric cell, and the remaining parts entirely of nickel, tungsten and molybdenum. The anode was not externally heated as in the experiments with lithium; it was allowed to take up its equilibrium temperature in the neighbourhood of the filament. With the tungsten filament and nickel anode, the working temperature of the anode was possibly  $200^{\circ}$  or  $300^{\circ}$  C. With the dull-emitter and copper anode, the temperature was very little above that of the room. No investigation was carried out to determine whether this temperature change had any effect on the soft X-ray curves; but it is certain that the main characteristics of the curves are uninfluenced by it.

When using the dull-emitter filament, it was found that the pressure in the apparatus was so low that the ion-trap, P, Q, fig. 1, was almost unnecessary. When using the tungsten filament, however, a large number of positive ions were produced, even when the anode A was removed away from the filament. This consisted of a tungsten strip about 1 mm. wide and 1 cm. long, welded by

the use of platinum as a solder on to tungsten leads (this method was used as being the least likely to deposit impurities on to the beryllium surface). The effect of the light from the filament was negligible; but it seemed impossible to prevent a copious emission of ions—presumably mainly of sodium—which built itself up slowly when the current was switched on and therefore almost certainly came from the tips of the filament leads. This current was easily dealt with by applying a potential difference of about 100 volts between P and Q, and is mentioned mainly to prove the efficiency of the ion-trap which has sometimes been doubted. The actual results are therefore genuinely the effect of radiation emitted from the beryllium surface.

### 3. Experimental Results.

As already stated, the purpose of the experiments is to determine the variation of the photoelectric current  $i$  with the voltage  $V$  accelerating the electrons which excite the radiation in the beryllium metal, when the primary electron current is maintained constant.

In Paper I, the method of presenting the experimental results was to plot as a function of  $V$ , not  $i$ , but  $\Delta i/\Delta V$  measured for small increments of  $V$  of  $\frac{1}{2}$  volt, 1 volt, or 2 volts. This method has the great advantage that over most of the range of  $V$ ,  $\Delta i/\Delta V$  varies only very slowly with  $V$ . In the neighbourhood of the excitation voltages, on the other hand,  $\Delta i/\Delta V$  changes abruptly by a considerable amount. It was further shown (*loc. cit.*, § 8) that  $\Delta i/\Delta V$  gives a closer representation of the true excitation function than  $i$  itself does. This is owing to the fact that when one fires an electron of defined velocity on to a metal surface, the electron suffers small losses of energy which determine a range in the metal and which have nothing to do with the actual excitation of radiation. Thus the excitation process caused by an electron with an initial voltage  $V$  may occur when the electron has any velocity less than  $V$ . From this follows the advantage of using  $\Delta i/\Delta V$  instead of  $i$  as a measure of the excitation.

The values of  $V$  for which abrupt changes in  $\Delta i/\Delta V$  occur may be called the measured *break-potentials*. To correct these values in order to obtain the true break-potentials, we must take into account (1) the contact potential difference between the filament and the anode, and (2) the acceleration of the electrons in passing into the metal of the anode. As Richardson and Chalkin\* have shown, these two corrections amount together simply to the addition of the

\* 'Proc. Roy. Soc.,' A, vol. 110, p. 247 (1926).

work-function of the filament. So far as I am aware, this correction has not so far received any experimental confirmation. In fact, in a recent paper,\* a failure to observe any change in the excitation point on changing from a thoriated filament with an effective work function of 2.6 volts to a tungsten filament with an effective work-function of 4.9 volts was reported. It is therefore of great interest that in these experiments on beryllium, a shift of all the measured excitation points of about 2.5 volts was observed when the tungsten filament was substituted for a dull-emitter. This can be seen in fig. 2, which shows the small section of the excitation curves for beryllium in

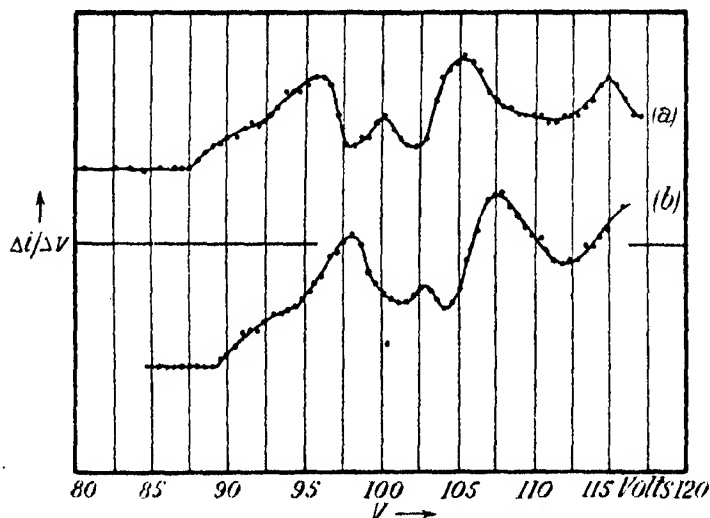


FIG. 2.—Uncorrected differential excitation curves of beryllium showing shift caused by change of filament. (a) tungsten filament; (b) dull emitter.

which the changes of  $\Delta i/\Delta V$  are most violent. The curves are direct plots of  $\Delta i/\Delta V$  in arbitrary units against  $V$ , measured from the centre of the filament, (a) for a tungsten filament and (b) for a dull-emitter.† It is seen that the two curves are almost alike except for the shift due to the change of filament. The theoretical shift, assuming the work function of the dull-emitter to be about 2 volts, should be 2.9 volts. Thus the values for the break potentials, corrected as described above, are within the limits of error independent of the nature of the filament.

\* Davies, Horton and Blundell, 'Proc. Roy. Soc.,' A, vol. 126, p. 668 (1930).

† It happened that curve (a) was taken with a copper photocell and curve (b) with a nickel photocell. We have seen that the results are unaffected by this change, but to allow comparable variations in the ordinates of the two curves, we have divided those of curve (a) by a factor of two relative to those of curve (b).

We now pass on to the description of the actual experimental results. Figs. 3 and 4 show two plots of the same experimental material obtained with a clean beryllium surface, and a nickel photocell. Fig. 3 is a straight plot of

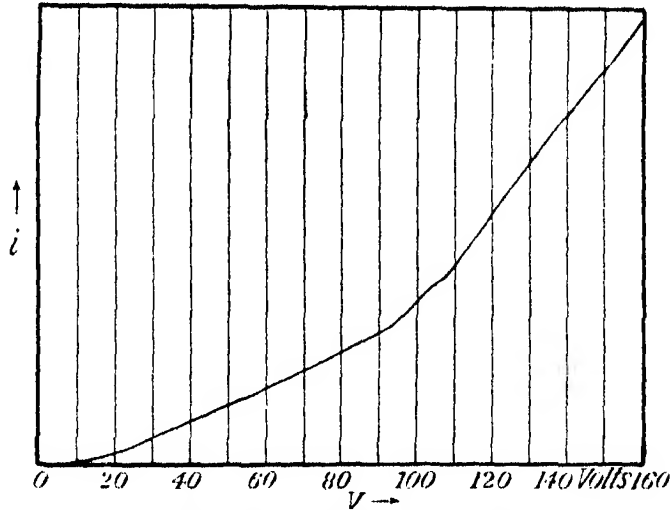


FIG. 3.—Corrected excitation curve of beryllium.

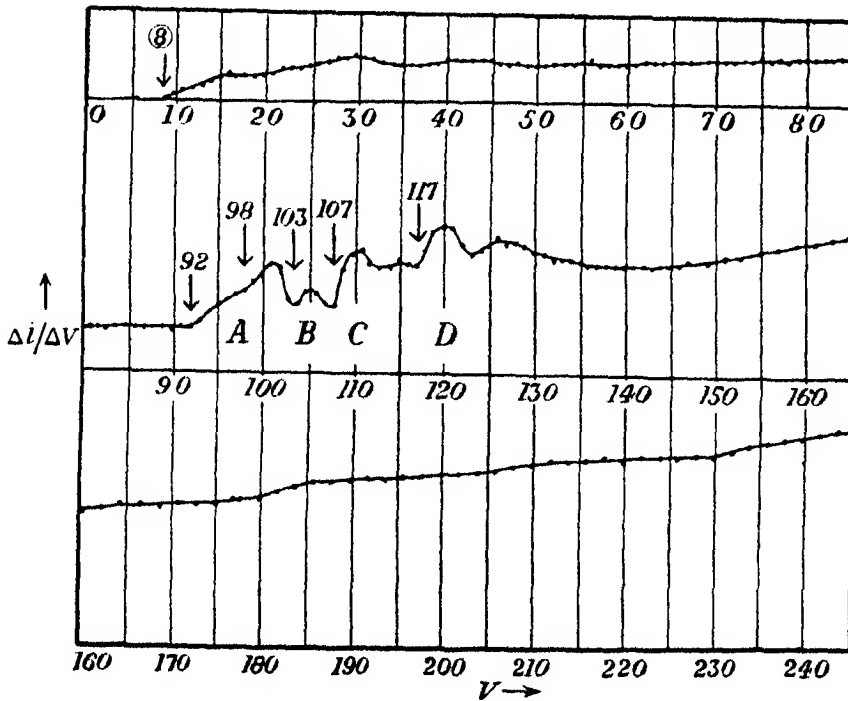


FIG. 4.—Corrected differential curve of beryllium.

$i$  against  $V$ , in which the accuracy of the points exceeds that of drawing the curve; fig. 4 is a differential plot of  $\Delta i/\Delta V$  against  $V$ , and the advantage of the latter is at once apparent. The correction of 5 volts for the work function of the filament has already been made. The excitation is found to start at 8.5 volts. It rises almost continuously till we reach the value 92 volts when large and abrupt changes in  $\Delta i/\Delta V$  begin to occur and persist until we come to 125 volts. After this, in the range investigated there are only comparatively slow variations of  $\Delta i/\Delta V$ .

The most interesting voltage region for beryllium is therefore that between 90 and 125 volts. For lithium it was shown that the K-excitation breaks of the metal lie in a region some 10 volts below the value of the K-excitation potential of the free atom. The K-excitation potential of the free beryllium atom is at about 115 volts. It is therefore clear that the breaks in the region between 90 and 125 volts correspond to the excitation of K-radiation in the beryllium metal. At first sight, it is very surprising that the region of the K-excitation potentials of beryllium is so much greater than for lithium, 30 volts instead of 10. This point will be discussed later; but it is quite clear that if we can establish that a clean beryllium surface actually gives this type of excitation curve, then the minimum K-excitation point for beryllium metal must be taken at 92 volts.

During the course of the present experiments, this K-excitation curve, with only minor differences, has been obtained more than 20 times, using both dull-emitter and tungsten filaments, and using the apparatus with copper anode and photoelectric sphere, and that made entirely of nickel. All these curves are alike in that the three peaks A, B, C are always observed, and the shape of the peaks is, within the experimental error, always the same. The peak D is also always observed but the subsequent progress of the excitation curves are not always quite identical. In fig. 2 two typical examples have already been given on a large scale.

In no experiment with a beryllium metal surface have these peaks A, B and C been completely missed, but twice they were found weak compared with the general excitation, when, however, the cleanness of the beryllium was not free from suspicion. In these cases the rise near D is marked.

Now in the brief note of Christensen (*loc. cit.*) it is claimed that the K-excitation only begins at 113 volts; there is a further break at 124 volts. Therefore the peaks A, B, C are almost if not completely missing; we say "almost" because he speaks of rather unrepeatable weak breaks. It was very necessary to ascertain the cause of this disagreement. As already stated,

radical changes were made in the apparatus without any result on the curves.

The only remaining possibility seemed to be in the beryllium surface itself. This metal does not appear to be easily oxidized; but actually, like aluminium, it is covered with an invisible oxide skin. At high temperatures it oxidizes very easily, and the difficulty in preparing an uncontaminated surface is owing to the fact that the distillation temperature is relatively high. A set of experiments was therefore carried out with surfaces prepared in various ways. In the first experiment a beryllium plate, already thoroughly outgassed,

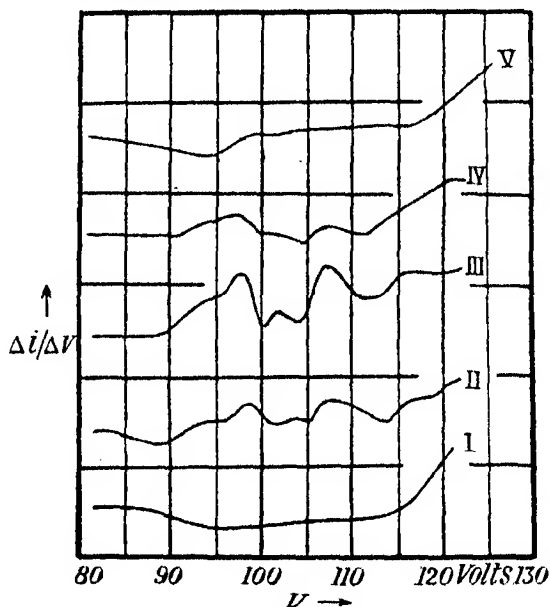


FIG. 5.—Uncorrected curves for surfaces with various degrees of oxidation. I. Oxidized; II, thin Be distilled layer; III, thick Be layer; IV, slightly re-oxidized; V, more heavily oxidized.

was used without distillation on to it. The apparatus was baked out in the usual way; then the anode was heated bright red-hot in a good vacuum. At this temperature beryllium oxidizes readily in the gas given off by itself and it was found that, after heating, the plate, which was originally polished, was covered with a faint yellowish film. The excitation curve was taken and it was found that, for the first time, no trace of the peaks A, B or C was visible. The curve is given in fig. 5, curve I. A very thin film of beryllium was then evaporated on to the plate and the result, curve II, shows the peaks rather weakly. With a thicker layer of beryllium, curve III, the peaks had resumed

their normal magnitude. The anode was now heated red-hot in the vacuum; the surface still looked perfect, but as curve IV shows the peaks are considerably reduced in strength. Finally the beryllium plate was heated with a small pressure of air in the apparatus (pressure about  $5 \cdot 10^{-5}$  mm.). The surface now showed considerable signs of oxidation. Curve V was very similar to curve I in that the peaks had gone.

It may probably be fairly claimed that these experiments establish the fact that the peaks A, B, C are due to clean metallic beryllium. We also have come to the interesting conclusion that the K-excitation curve for metallic beryllium is quite different from that of beryllium in the form of the oxide. It is true that curves I and V, fig. 5, are not quite alike; but one must remember that the oxide is a good insulator and so it may be hard to obtain reproducible results. Also it is difficult to say what the true break-potential is as one does not know what correction to apply for contact voltages, etc. It seems therefore best to leave the experimental value uncorrected. From curve I we obtain the value 115 volts, from curve V the value 117 volts.

In Table I, the values of the corrected break voltages are given. The values are taken as the best fit for a number of the most accurately taken curves. The breaks of columns (a) and (b) are easy to pick up on all the curves. Those of column (c) have not been so carefully investigated but, except for those

Table I.—Corrected Break-Voltages for Beryllium Metal below 240 Volts.

Type of excitation.	Results of present paper.			Results of Christensen.
	(a)	(b)	(c)	
Valence electron .....	$8.5 \pm 1$		(?) $12 \pm 1$	12
			$19 \pm 1$	19
			$35 \pm 2$	26
			$50 \pm 2$	34
				46
K-electron .....	$92 \pm 0.5$	$97.5 \pm 1$	(?) $113 \pm 1$	113
		$103 \pm 1$		
		$107.5 \pm 0.5$		
		$116 \pm 1$		124
			$122 \pm 2$	
			$141 \pm 3$	
			$177 \pm 3$	
			$230 \pm 3$	

(a) Minimum excitation potentials; (b) strong breaks; (c) weak breaks.

marked doubtful, none have been missed on any reliable run. A few other faint breaks were observed in individual runs, and the actual shape of the curves, especially around D, fig. 4, has been found to vary somewhat. But it must be remembered that the results represented by fig. 5 show that any slight surface contamination would show itself mainly here; the microcrystalline structure of the beryllium surface may also affect the shape of the curves. The division of the breaks into the types (a), (b) and (c) is somewhat arbitrary; but, as will appear, a weak break is not necessarily a genuine excitation potential in the sense that it corresponds to the starting point of a new mechanism for the excitation which could not occur at a lower voltage. The results of Christensen (*loc. cit.*) are added for comparison. It is a curious fact that, although he has missed all our strong K-excitation breaks, the low-voltage breaks in the two sets of experiments appear to agree well.

As shown in Paper I, there is a second type of experiment possible with the apparatus used.\* So far, the results described have been obtained by varying the accelerating voltage  $V$  of the primary electron beam incident on to the metal surface. If, however, we keep  $V$  fixed and apply a variable retarding voltage  $W$  between S and C, fig. 1, by measuring the photoelectric current for successive values of  $W$  and plotting  $\Delta i/\Delta W$  against  $W$ , we obtain a velocity analysis of the photoelectrons. Some conclusions may be drawn about the actual nature of the radiation emitted, but the limitations of the method are serious. Velocity analysis curves for the photoelectrons ejected from nickel by the beryllium radiation are shown in fig. 6 for two values of  $V$ , 180 and 300 volts. These have a greater dispersion than those obtained by Rudberg† by a magnetic analysis of the photoelectrons ejected by the beryllium K-radiation. Taking the value 4 volts as the work function of nickel, we may conclude that the short wave-length end of the beryllium K-radiation band is at about 111 volts. Owing to "loss of velocity" effects, arising from the finite depth from which the photoelectrons come, it is not possible to come to any definite conclusion with regard to the structure of the band except that there are indications that its extent on the long wave-length side is considerable. Our upper limit agrees well with that found by Söderman and Faust (*loc. cit.*), who

\* We must state here that the analysis of the *low-velocity* photoelectrons ejected by Li radiation, Paper I, fig. 7, was incorrect. It was thought that certain abrupt breaks were real; but it now seems that these were mainly due to the errors of a certain voltmeter. The results represented by Paper I, fig. 6, are correct. The low-velocity distribution curve of the photoelectrons ejected by beryllium radiation is similar to that for lithium, and quite smooth.

† 'K. Svenska. VetenskAkad. Handl.,' vol. 7, p. 1 (1929).



used the more promising method of a grating-analysis of the radiation. They agree in finding a main band between about 100 and 112 volts. Söderman found it smooth within these limits; but Faust found maxima in the band, and also traces of radiation outside it especially on the high-energy side. This discrepancy may possibly arise from the different beryllium surfaces used; Faust employed a metal plate, while Söderman, as far as one can gather,\* "rubbed" the beryllium into an anode of another metal. The results of

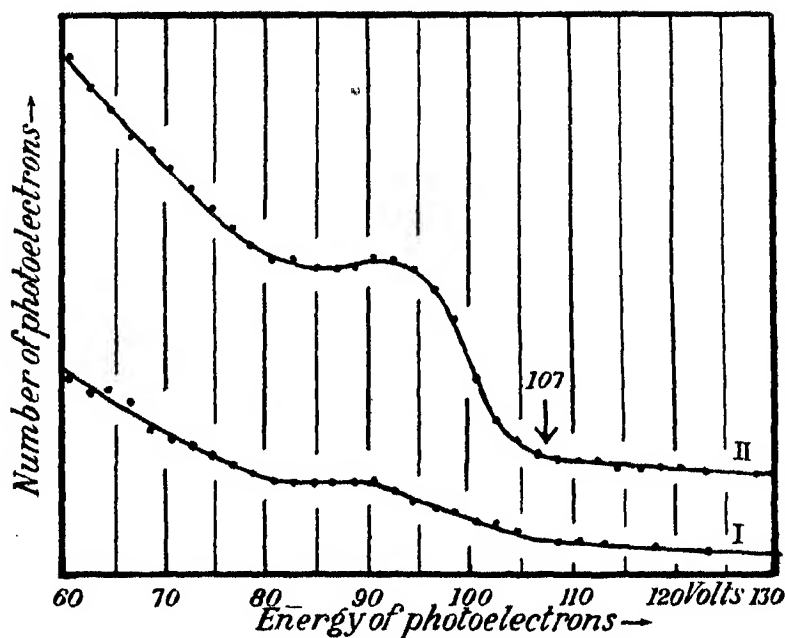


FIG. 6.—Velocity analysis curves for photoelectrons.

Faust are more in accord with what might be expected for the K-radiation from beryllium *metal*; on account of the number of break-potentials in the range between 90 and 110 volts, a smooth band of radiation is hardly to be anticipated. It is evident that the existence of the 92-volt break carries with it the implication that radiation of this energy or less can be emitted. Such radiation is weak, even according to Faust's results; but it must be remembered that the experiments were performed using a bombarding potential of several thousand volts, and that it is quite likely that the intensity-distribution in the radiation band may vary markedly with the exciting voltage.

\* 'Z. Physik,' vol. 52, p. 795 (1929).

§ 4. *The Excitation of K-radiation in Light Metals.*

The experiments of Paper I and of this paper have shown that for lithium metal there are three break-potentials associated with the emission of K-radiation, and that for beryllium there are at least five. These may clearly be taken as representing discrete K-excited states of the metals. In order to interpret them, we now proceed to attempt an approximate calculation of the energies of the possible K-excited metallic states. The primary data consist of the atomic energy-constants and the problem is to consider how these are altered by the lattice-binding.

For simplicity, let us first confine attention to the *minimum* K-excitation potentials. The theory put forward in Paper I, although mainly correct in outline, was not sufficiently developed to explain the low value of this quantity which is found for beryllium metal. Hence it is necessary to start again from the beginning.

At the outset, we may form the most elementary picture possible of the process of K-excitation of a metal; this is a level-system analogous to that used in the classification of the data obtained from the ordinary X-ray spectrum of a heavy element. In our case, we have only the K-level and the L-levels, which are the metallic valence- or conduction-electron levels. In fig. 7, the depth of the levels gives the work done in taking a K-electron, or a valence-electron, to a state at rest outside the surface of the metal. In the excitation process, a K-electron must be taken right through the lower valence-electron levels since these are filled by electrons. It may be placed in the lowest *empty* level; this corresponds to the minimum K-excitation voltage, which is represented by the shortest upward arrow.

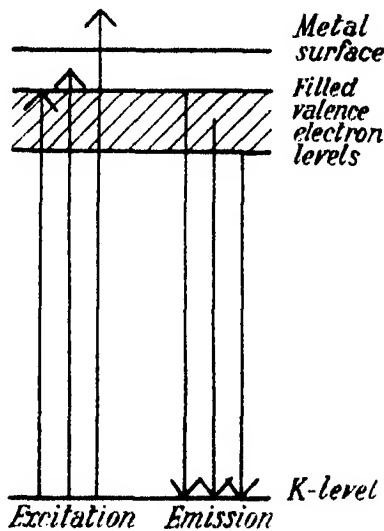


FIG. 7.—Excitation and emission of K-radiation.

Fig. 7 also gives the radiation quanta which may be emitted after the excitation process. Any valence-electron may fall back into the K-level, as shown by the downward arrows. Thus the radiation will consist of a band running up to a high energy head at a value equal to the

minimum energy of excitation. Calculations on the intensity-distribution in this band have been made by Houston.\* But we shall see that the actual radiation emitted from a metal is almost certainly too complex for representation by a single diagram of this type. We can use the experimental results for the minimum K-excitation potentials of lithium and beryllium to construct diagrams like fig. 7, but we propose to go deeper into the problem. We shall begin by attempting to calculate these minimum K-excitation potentials in order to compare the results with the experimental data. To do this we must go beyond any representation like that of fig. 7; we must form a model of the transient excited state of the metal which exists when a K-electron is missing from one of the atoms, i.e., the K-excited state from which the radiation will be emitted in a lapse of time long compared with that taken in the excitation process.

It is clear that the minimum K-excitation potential of a metal may be expected to be of the order of magnitude of the K-ionization potential of the free atom. It is actually appreciably smaller. The values of these two quantities for lithium are 53.7 and 62.5 volts\* respectively; while for beryllium there is a still larger gap, the values being 92 and 118 volts.† A closer approximation is given by calculating the energy required for a  $K \rightarrow L$  atomic transition; the values for lithium and beryllium are about 53 and 110 volts. It will be seen that the correspondence for lithium is close, as has previously been emphasized. For beryllium, on the other hand, there is no such agreement; and this distinction between the results for the two metals is the primary fact which we have to explain.

It is instructive first to consider the case of a lattice which is so stretched out that the interaction of the atoms may be neglected. It is clear that the transition of an electron  $K \rightarrow L$  is possible just as for the free atom. This may be regarded as the basis of the numerical agreement for lithium, the interaction in this case having small effect.

When we pass to the ordinary unstretched metallic lattice, we have to consider in what way the binding of the original valence-electrons will be affected by the circumstance that there is a K-electron missing from one of the atoms. It is evident that, in fig. 7, this re-adjustment of the electrons is implicit in the energy-value representing the work done in removing a K-electron to the metal surface. We have now to consider what types of orbit are possible for electrons moving in a lattice which has one of its atoms K-ionized. Clearly,

\* 'Phys. Rev.', vol. 38, p. 1791 (1931).

† The method of obtaining these figures will be given later.

this particular atom will exert forces on the electrons very different from those caused by the other unexcited atoms. In fact the sudden removal of a K-electron will make the K-ionized atom in lithium metal behave momentarily as a charge of about two units, instead of about one unit for the normal metallic atom. *Thus, in the transient excited state of the metal, the K-ionized atom can be compared with an impurity atom which happens to be present in the unexcited metal; in that local conditions around each are quite different from those at other points.* On the other hand, apart from the formation of this special atom, the rest of the metal may be taken as approximately unaffected by the K-excitation process; the same levels will continue to exist among the  $(N - 1)$  similar atoms of the excited lattice as in the original lattice of  $N$  atoms. The readjustment of the lattice to the K-excitation, roughly stated, may be said to consist of some of the original metallic valence-electrons being dragged by the increased core-charge into the L-shell of the K-ionized atom, the remainder retaining about the same mean energy as before.

The behaviour of an impurity atom in a metal has been considered by Wilson.\* Consider a lattice of  $N$  atoms, one of which is different from the rest; if the interaction is negligible, we have  $(N - 1)$  states of equal energy in which an electron is removed from one of the like atoms, and just one state of a different energy in which an electron is removed from the impurity. It is evident that, when one allows for interaction, the  $(N - 1)$  states will split up into a band with a definite energy-range (the band of the valence- or conduction-electrons) the one state, though it may be perturbed, will remain sharp. It follows that, if the interaction is not too great, an impurity may be regarded as existing in the metal as a discrete entity, atom or ion, and forming a "hole" into which the metallic valence-electrons cannot penetrate. Its actual state depends on how many electrons it can profitably "capture" from the metal, if we imagine it to be introduced in a heavily ionized condition. Thus it will go on taking electrons until the binding-energy of the next captured electron would be less than the binding-energy to the metal as a whole. Consider the K-ionized lithium and beryllium atoms as "impurities" which do not take part in the chemical binding of the lattice. Since the ionization potentials of both as free atoms in a K-excited neutral condition are about 8 volts, each must exist, in the state of lowest energy of the whole system, as a *neutral atom in a "hole" in the metal*, having thus L-shells of two and three electrons respectively. It is also clear that there must be a number of discrete states of the

\* 'Proc. Roy. Soc.,' A, vol. 134, p. 277 (1931).

metal corresponding to the excited, ionized, and ionized and excited states of the "impurity" atom. These will be found experimentally as a number of discrete K-excitation potentials of the metal,  $V_K^2, V_K^3, \dots$  of higher voltage than the minimum K-excitation potential,  $V_K^1$ . As we have seen, these are actually observed.

We shall now proceed to a more quantitative use of the model, at first disregarding the higher excitation potentials and confining attention to the calculation of the minimum K-excitation potential  $V_K^1$ . We begin by determining the energy required for the corresponding process in the free atom, namely,  $v_{KL}$ , the work done in a  $K \rightarrow L$  transition. This is not only instructive from the theoretical point of view, but also useful since the numerical values are required. If  $n$  is the valency, we first remove  $n$  valence electrons successively from the atom. The work done in this step is  $\sum_n i_r$ , where  $i_r$  is the  $r$ th successive ionization potential of the element. Next, we remove a K-electron, doing work  $i_{n+1}$ . Finally we replace  $(n+1)$  electrons into their lowest state in the L-shell of the K-ionized atom, thus regaining energy  $\sum_{n+1} i'_r$ , where  $i'_r$  is the  $r$ th successive ionization potential of the atom with a K-electron missing. Therefore

$$v_{KL} = \sum_{n+1} (i_r - i'_r). \quad (1)$$

The numerical data for the quantities  $i_r$  are known for lithium and beryllium; those for the quantities  $i'_r$  can only be estimated. We shall assume that the value of  $i'_r$  is the same as that of  $i_r$  for the next element in the periodic table, thus imagining for example a nucleus of charge 3 screened by one K-electron to be equivalent in its effect on the L-electrons to a nucleus of charge 4 screened by two (more tightly bound) K-electrons. Calculating for the  $(1s, 2s^2)$  state of lithium, we get the value 53 volts.\* This may be compared with a rough experimental value of  $54 \pm 2$  volts, obtained by Mohler† for the K-radiation from lithium vapour. For the lowest K-excited state of beryllium,  $(1s, 2s^2, 2p)$ , a corresponding calculation gives the result 110 volts. These calculated values may be expected to be too small by possibly about 2 volts for lithium, and rather more for beryllium.

Now returning to the metal, we shall build up the K-excited state previously

\* We use for the ionization potentials of lithium the values 5.3, 75.3; of beryllium the values 9.3, 18.0, 153; of boron the values 8.3, 24.4, 37.8 volts.

† 'Bull. Bur. Stand.,' vol. 20, p. 167 (1923).

defined from the normal state by means of a set of operations as nearly as possible analogous to those performed on the free atom.

- (a) We remove  $n$  valence-electrons from the metal in such a way as to "clear a space" around a single atom.
- (b) We remove a K-electron from this atom, imagining the metallic valence-electrons to be held fixed in energy.
- (c) Still holding the valence-electrons, we replace  $(n + 1)$  electrons into the L-level of the K-ionized atom.
- (d) We finally release the metallic valence-electrons.

After the step (a) has been accomplished, we have an ion consisting of a nucleus and K-electrons only and this may be regarded as existing in a small "hole" in the metal. The next step is the removal of a K-electron; fig. 8 represents the potential energy of this electron in its passage out of the metal

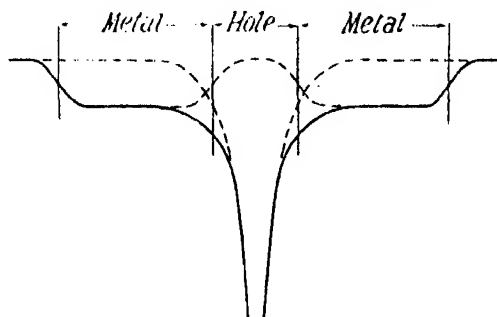


FIG. 8.—Potential curve about the K-ionized atom in metal.

The dotted curves give the potential arising from the ion and the metal separately (for simplicity a Sommerfeld model of the metal is used); the full curve gives the combined effect. The same diagram is also applicable to the replacement of the first L-electron; but for the other  $n$ , the shape of the atomic curve must be altered successively to include the shielding of the L-electrons already replaced. The conception of the "hole" is still legitimate since we suppose the K-excited atom not to be subject to the forces of chemical binding. The hole is about 3 Å in diameter; the  $(n + 1)^{th}$  electron to be replaced in the L-shell is bound to the free atom with about 8 volts, and thus has a potential energy of about -16 volts, and the L-orbits have a diameter of about 1.0 Å. We must consider what errors can occur in using the ionization potentials of the free atom in estimating the energy involved in steps (b) and (c). Two effects are to be taken into account; (1) the weakening of the binding-force of the electrons owing to the presence of the surrounding metal, and (2) the

actual alteration of the potential energy of an electron in the hole. A rough calculation shows that (1) is almost certainly negligible for all the electrons. The magnitude of (2) depends on how the inner potential of the metal falls off within a distance of about 1 Å., from the edges of the hole; but this is a relatively large distance for forces due to incomplete shielding, and it seems unlikely that there will be any serious error. We shall see subsequently that this conclusion receives some empirical support. To sum up, it seems improbable that, in using the atomic ionization potentials to represent the work done in steps (b) and (c), we commit an overestimate of more than a few volts.

In evaluating the energy involved in stages (a) and (d), it is simpler first to consider lithium, with only one valence-electron per atom. In removing an electron from the metal, we are undoubtedly freeing a certain atom of the valence-electron which may be said to "belong" to it, and we are thus clearing this atom for the stages (b) and (c). Consider the hole in the metal; the potential energy of the metallic valence-electrons per atom is slightly raised in the formation of the new surface of the empty hole, but it is lowered again by the residual field of the K-excited atom with its two L-electrons. The first effect will probably predominate; but only a small error is to be expected if we take the mean binding-energy of a metallic valence-electron after stage (d) to be the same as in the original metal. This error is in the opposite sense to the error involved in steps (b) and (c). In performing stage (a), we may remove an electron from the metal in applying any energy between two limits, the smaller of which is the work-function. But to retain the mean energy of the electrons in the metal the same as before, we must apply an energy  $\bar{\phi}$  equal to the mean energy of these electrons. Then no readjustment energy need be taken into account in stage (d).

Thus in comparing the energy necessary for the K-excitation of lithium metal step by step with that required for the free atom, the only difference to be accounted for is the use of  $\bar{\phi}$  instead of  $i_1$  in stage (a). But  $i_1$  is only 5 volts, and  $\bar{\phi}$  can differ but slightly from this value. Thus the approximate relation

$$V_K^1 = v_{KL}, \quad (2)$$

must be expected to hold with a tolerance of not more than a few volts, as we have already shown to be the case.

When we return to the general case, the energy  $U_n$  involved in stages (a) and (d) cannot be estimated so unambiguously. It is true that by applying an energy  $n\bar{\phi}$  we can remove  $n$  electrons from the metal, but these are not

necessarily from the same atom. We have to distinguish between two models of the metal in which (A) *the metallic valence-electrons are treated as firmly bound to the individual atoms and thus only able to travel about by exchange, and (B) they are treated as free to attach themselves to any atom.* With model (A), the work done in stage (a) must approximate to the corresponding amount for the free atom, namely,  $\sum_n i_r$ , and so equation (2) would again follow.

For beryllium, we have seen that there exists a marked discrepancy of almost 20 volts; it seems impossible, especially in view of the good agreement for lithium, that an error of this order of magnitude can have crept in. It is evident that the assumption underlying the supposed equality of  $U_n$  and  $\sum_n i_r$  is that the interaction of the  $n$  electrons which can be said to "belong" to a certain atom at a given instant is of paramount importance compared with the interaction of these  $n$  electrons with others in the metal. If this is not so, we come effectively to model (B), in which the electrons can scarcely be said to "belong" to the atoms, but are bound to the lattice as a whole. The work done in stage (a) can now be taken as  $n\bar{\phi}$ , and in place of (2), we obtain the approximate relation :

$$V_K^1 = v_{KL} - \sum_n i_r + n\bar{\phi}. \quad (3)$$

Use of the numerical values leads to a value of  $\bar{\phi}$  of about 5 volts, both for lithium and for beryllium. On account of the fact that the values of  $v_{KL}$ , calculated from equation (1), are slightly too low, this would have to be diminished; but the other approximations probably tend towards an increase. On the whole, the value of  $\bar{\phi}$  may be considered as of a reasonable order of magnitude.

It therefore seems that, although the result for lithium would be consistent with either model, that for beryllium definitely demands nearly free metallic valence-electrons. This conclusion could probably have been anticipated, since in a conductor an electron must be free to pass from atom to atom without any appreciable increase in the energy of the system being involved. The distinction between the results for lithium and for beryllium appears as a consequence of their respective monovalence and divalence.

We shall next show that a reasonable numerical agreement may be obtained between the calculated and observed values of the higher K-excitation potentials  $V_K^2, V_K^3, \dots$ , which, as we have seen, correspond to excited and ionized states of the "impurity" atom. Accepting the experimental value of  $V_K^1$ , the higher states can be built up successively from the lowest K-excited



state by removing an electron and replacing it into a higher level of the K-excited atom, or into a level of the lattice. In this way, some of the chief uncertainties of the previous absolute calculation of  $V_K^1$  are avoided. On the other hand, we still have to assume that the ionization potentials of the K-excited atom in the metal are those of the free atom. The assumptions underlying this approximation have already been discussed; it is perhaps rather surprising that it appears to be almost unnecessary within the accuracy of the measurements to take into account any such perturbation. Similarly we neglect any changes in the energy of the lattice which may result from alterations of the residual field of the K-excited atom. We may point out that this is easier to justify since the metallic valence-electrons are free and so able to travel considerable distances in the lattice; also that an error from this cause would tend to compensate any error of the previous type.

For beryllium, we may be sure that the minimum K-excitation potential,  $V_K^1$ , corresponds to the lowest atomic state ( $1s \cdot 2s^2 \cdot 2p$ ) in which a K-electron is missing; for lithium also, we shall assume that it corresponds to the lowest state ( $1s \cdot 2s^2$ ).\* Unfortunately, we again have to rely on the numerical data for beryllium and boron† as approximations for K-excited lithium and beryllium atoms; similar approximations are also made for the energies of the ionized atomic states. For instance, the two sufficiently separated states of  $Be^+$  ( $1s \cdot 2s \cdot 2p$ ) are taken as the same as those of  $B^+$  ( $1s^2 \cdot 2s \cdot 2p$ ); corresponding to the singlet and triplet of the latter, we have a doublet and doublet-quartet, but certainly we need not take into account the actual multiplet-splitting nor that introduced by the incompleteness of the K-shell. The method of procedure will be clear from the following example: to pass from the lowest K-excited state  $Be$  ( $1s \cdot 2s^2 \cdot 2p$ ) to the state  $Be^+$  ( $1s \cdot 2s^2$ ), we remove the  $2p$  electron doing work of 8.3 volts (numerically the first ionization potential of boron). We replace the electron into the lowest empty valence-electron level of the metal, thus regaining energy equal to the work-function (taken as 3.0 volts). We therefore get a value for the corresponding excitation potential of the metal equal to  $(92 + 5.3)$  or 97.3 volts. It will be seen that, at any rate for the states fairly near to the

\* There may be a slight uncertainty in this choice, since the state  $Li$  ( $1s \cdot 2s^2$ ) can only radiate by a double electron-jump to a state like  $Li$  ( $1s^3 \cdot 2p$ ) and this might be improbable even in the metal.

† Data for the spectra of  $Be$  and  $B$  in normal and ionized condition were obtained from the "International Critical Tables" (vol. 5, p. 395); some additional values for  $Be$  were from Paschen and Kruger ('Ann. Physik,' vol. 8, p. 1005 (1931)). The work-functions of  $Li$  and  $Be$ , also required, were simply guessed by analogy with other metals to be 2.5 and 3.0 volts.

lowest K-excited state, the approximation used for the energy levels of the free atom is adequate since the numbers involved are quite small.

The results are given in Table II, together with the experimental material extracted from Table I of Paper I and Table I of this paper. There is nothing arbitrary in the choice of atomic types; all states are included which are separated by more than about 2 volts and it is estimated that this is the minimum that could have been resolved. Since all the observational material is included, the agreement appears to be very satisfactory; but, of course, owing to the many approximations made, we cannot overlook the possibility that it is partly accidental. However, there seems to be a strong case for this general method of interpreting the observed break-potentials as corresponding to the existence of definite states of the K-excited atom in the metal.

Table II.—Calculated and Observed Excitation-Voltages.

Lithium.			Beryllium.		
Atom type.	Calculated.	Observed.	Atom type.	Calculated.	Observed.
Li (1s. 2s <sup>2</sup> ) .....	53.7*	53.7	Be (1s. 2s <sup>2</sup> . 2p) .....	92.0*	92
Li (1s. 2s. 2p) .....	$\begin{Bmatrix} 56.4 \\ 59.0 \\ 60.5 \end{Bmatrix}$	56.2	Be <sup>+</sup> (1s. 2s <sup>2</sup> ) .....	97.3	97.5
Li <sup>+</sup> (1s. 2s) .....	60.5	60.1	Be <sup>+</sup> (1s. 2s. 2p) .....	$\begin{Bmatrix} 100.9 \\ 106.5 \end{Bmatrix}$	103
Li <sup>+</sup> (1s. 2p) .....	64.3	—	Be <sup>+</sup> (1s. 2s. 3s) .....	112.3	113 (?)
Li <sup>+</sup> (1s. 3s) .....	71.3	—	Be <sup>+</sup> (1s. 2s. 3p) .....	113.1	
Li <sup>+</sup> (1s. 3p) .....	72.3	—	Be <sup>++</sup> (1s. 2s) .....	118.4	116
Li <sup>++</sup> (1s) .....	76.0	—	Be <sup>++</sup> (1s. 2p) .....	124.5	122
			Be <sup>++</sup> (1s. 3s) .....	140.7	141
			Be <sup>++</sup> (1s. 3p) .....	142.7	
			Be <sup>++</sup> (1s) .....	153.2	—

\* Assumed values.

It will be understood that, for each of the K-excitation potentials  $V_K^2$ ,  $V_K^3$  ..., the diagram of fig. 7 must be redrawn, just as it must for the ordinary, "spark" X-ray spectra. A further technical similarity is that apparently the corresponding excited states can only be reached by multiple electron-jumps. But it is doubtful whether in our complex many-electron problem this is of any real physical significance.†

We have now dealt with the case when the K-excited atom in the metal is left, after the excitation, in its lowest state or in a state of higher energy,

† One can only distinguish between the terms "electron-jump" and "rearrangement due to altered screening" if the energy involved in the former is considerably the greater.

and we have shown that a set of discrete excitation potentials  $V_K^1, V_K^2 \dots$ , is obtained. The further possibility arises that, after the excitation, the metallic valence-electron system may not be left in its lowest state. Fig. 7 takes account of this possibility; evidently the K-electron need not be transferred into the lowest metallic state, but can go into a higher state or it may even be given enough energy for it to be ejected from the metal. Since there are excited states of the metal corresponding to any arbitrary energy, it follows that, for each of the excitation potentials  $V_K^1, V_K^2 \dots$ , there exists a continuous band of metallic states of greater energy. Thus each value  $V_K$  represents only the minimum energy with which a metallic state of a given type can be excited; and excited states of the different types will overlap.

In the special case of excitation by electron-bombardment, we must also bear in mind that, after the impact, the impinging electron forms part of the metal. This electron also may lie in the lowest empty valence-electron state or in a higher state. Strictly every energy of the impinging electron defines a state of the metal belonging to each group of states corresponding to one of the excitation potentials  $V_K$ . But it is possible to speak of the probability of excitation of a *state of given type* for a defined energy of the exciting electron. The variation of this probability is the *excitation-function* for the type of metallic states. This function cannot be a smooth curve like an atomic excitation- or ionization-function. For, as is well known, the excited states of *one* electron in a metal form a set of bands extending over an energy range of some hundreds of volts, with zones of more or less allowed or forbidden energy; in a three-dimensional lattice, these are not spaced in any simple way.\* Since the excess energy of the excited metal is not necessarily taken up as the excitation of a *single* electron (including the impinging electron), the zone-structure may not show itself in a straightforward manner. But the excitation-function must be expected to exhibit oscillations which die out only slowly with increasing energy; and the observed curve,† being built up of the various excitation-functions, will to a certain extent reproduce these oscillations.

In the experiments on lithium, it was pointed out in Paper I that the temperature of the metal was sufficiently near to the melting point for the zone-structure to be largely evened out by the heat-motion of the nuclei. The observed curve is therefore smooth away from the regions of actual

\* Kronig, 'Z. Physik,' vol. 75, p. 191 (1932).

† For a note on the relation between the excitation-function and the observed curve, see Paper I, § 8.

excitation. But with beryllium the temperature was well below the melting point and it is probable that the zone-structure shows itself as oscillations of the observed curve outside the region of the K-excitation potentials.

A further characteristic difference may be noted between the curves obtained for lithium and beryllium. The rise to a maximum just above the minimum K-excitation potential for lithium (see Paper I, fig. 5) occupies only about 1 volt, whereas the corresponding rise for beryllium occupies some 5 volts. This indicates that the number of excited states of the metal which lie very near to the lowest K-excited state is considerably greater in lithium than in beryllium, and probably demonstrates different peculiarities of the excited lattice-electron systems of the two metals.

We come next to the consideration of the type of radiation which may be expected from the K-excited metallic state. From any one of the continuous set of states corresponding to a given atomic excitation, the return to the normal metal may occur either by a radiationless process (such as the ejection of a photoelectron) or by the emission of radiation in the form of one or more quanta. Thus theoretically we can always get radiation up to the limit of the energy of the impinging electron, and there is no rigid distinction between "continuous" and "characteristic" radiation. But experiment shows that most of the energy is degenerated into the immediate region of the K-excitation voltages. If we could observe the radiation emitted by beryllium under bombardment by electrons with energy little above 92 volts, it is evident that we should expect a band of radiation running up to that energy as a maximum, fig. 7. But experiment is only possible with a high bombarding voltage, and then the excitation is complex, a number of distinct types being possible of which fig. 7 represents only one. One must also bear in mind that, with high-voltage excitation, the lattice-electron system may be carrying considerable energy; the radiation emitted may therefore consist of a band which extends on the high-energy side of the corresponding minimum excitation potential as well as on the low-energy side. The radiation observed, being built up of the overlapping of a number of such bands, might not show any very marked structure corresponding to the actual excitation potentials. Until the experimental question of the radiation emitted is cleared up, it is useless to discuss this problem further.

A few remarks may be added relating to the observed K-excitation potential of beryllium in the form of oxide. It may be recalled that the value found, about 116 volts, is some 24 volts higher than for the metal. The oxide ( $\text{BeO}$ ) is a *polar* compound and very stable. In considering the K-excited state of

the molecule, it is significant that the radius of the L-orbit of the  $\text{Be}^{++}$  ion is only about half the normal radius of the hydrogen atom; and thus it is plausible to suppose that the binding-energy of the electrons belonging to the negative oxygen atom is but slightly affected by a  $\text{K} \rightarrow \text{L}$  transition in the beryllium ion. Also the alteration of the potential energy due to the oxygen ion of a beryllium electron in its passage from the K-level to the L-level must be small. Thus the K-excitation potential of beryllium in the oxide should be almost equal to the energy required for a  $\text{K} \rightarrow \text{L}$  transition in the atomic ion  $\text{Be}^{++}$ , namely 115 volts (using our previous method of calculation). In any case, it is easy to see that, especially for an element with valency greater than one, a very different result may be obtained for the compound than for the metal.

So far, the discussion has been confined to the excitation of K-radiation. On the other hand, the experiments both with lithium and beryllium have shown that radiation begins to get excited at a very low bombarding voltage (about 8 volts in each case). Although it is possible that the effects of surface contamination have not been entirely avoided for excitation by such slow electrons, it seems fairly safe to assume that the low-voltage radiation is due to the excitation of lattice-electron states. The oscillations of the observed curve, which follow the low-voltage breaks, are probably connected with the zone-structure of these excited states. The radiation may be expected to be continuous in character. Mohler and Boeckner,\* in recent notes, have reported the observation of continuous spectra from electrodes of various metals subjected to heavy electron-bombardment in low-voltage arcs. The radiation runs throughout the visible and ultra-violet regions.

In conclusion, I wish to express my thanks to Dr. R. Peierls for a valuable criticism of the theoretical section of this paper. It was completed during the tenure of a Rockefeller Fellowship at the Massachusetts Institute of Technology, and I am indebted to Professor J. C. Slater and other members of the staff for helpful discussion.

#### § 5. *Summary.*

(1) When a metal is bombarded by electrons of a defined voltage, the variation of the intensity of the radiation emitted with the value of this voltage is called the excitation curve of the metal. New measurements of this curve for beryllium are described and the characteristic break-potentials

\* 'Bur. Stand. J. Res.,' vol. 6, p. 673; vol. 7, p. 751 (1931); vol. 9, p. 413 (1932).

are tabulated. Both tungsten and dull-emitter filaments have been used, and it is shown that the breaks are displaced corresponding to the change of filament. When a correction for the work-function of the filament is applied the break-potentials obtained are consistent.

(2) Radiation begins when the energy of the exciting electrons exceeds 8.5 volts. The minimum K-excitation potential is found to be 92 volts. At this point the curve starts a set of violent fluctuations which persist up to about 125 volts. Thereafter the fluctuations are comparatively mild.

(3) With a slightly oxidized surface, the set of fluctuations starting at 92 volts does not occur. A break at about 116 volts is found.

(4) A discussion of the process of excitation of K-radiation in light metals is attempted. An approximate model for the excited state of the metal, based on the state for the corresponding atomic system, is proposed. It seems possible to account for the magnitudes of the minimum K-excitation potentials of lithium and beryllium metals; and calculation indicates that all the stronger breaks in the observed curves may be correlated with the higher energy states of the free atoms or ions. Different results may also be expected for the pure metal and for the oxide.

---

### *On the Reflection and Refraction of X-Rays by Perfect Crystals.*

By G. W. BRINDLEY, M.Sc., University of Leeds.

(Communicated by R. Whiddington, F.R.S.—Received November 8, 1932.)

#### 1. *Introduction.*

It is now well established that from the point of view of the theory of X-ray reflection, the majority of crystals can be divided into those which are relatively perfect and those which are relatively imperfect or mosaic. The intensity of reflection of X-rays by the former has been much less extensively studied than by the latter and hitherto no really satisfactory agreement appears to have been found between the observed intensities of reflection from highly perfect crystals such as diamond and the results predicted by the theoretical treatment of the subject. It will be shown in what follows that this lack of agreement is very largely removed when the atomic scattering factor,  $f$ , which plays such an important part in the theory of reflection by mosaic crystals, is taken into account for perfect crystals.

2. *The Theoretical Treatment of X-ray Reflection by Darwin and Ewald.*

A brief account will first be given of the theory of X-ray reflection as developed by Darwin\* in which a formula for the intensity of reflection is derived by considering the phase relations between waves manifoldly reflected inside a crystal; Darwin showed that for an ideal crystal, reflection should be perfect over a small angular range  $\Delta\theta$  and outside this range should fall abruptly to zero in the manner indicated in fig. 1. The reflected intensity is proportional to the magnitude of the range  $\Delta\theta$ , the centre of which,  $\theta_0$ ,

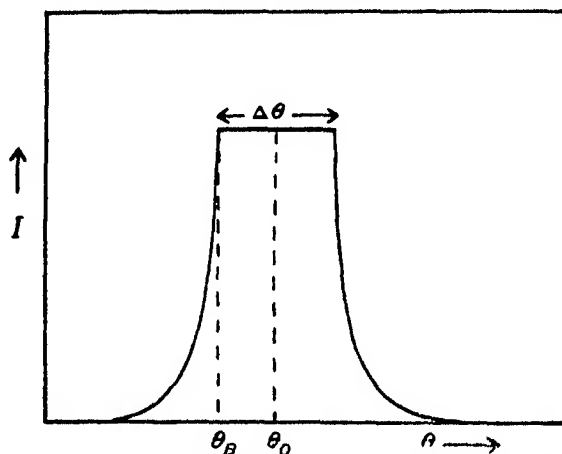


FIG. 1.—Theoretical reflection curve for a perfect crystal.

coincides approximately with  $\theta_B$ , the angle given by the simple Bragg law, but not exactly owing to the appreciable refraction of X-rays by crystals. It follows from Darwin's treatment that

$$\Delta\theta = q\lambda/\pi d \cos \theta_0, \quad (1)$$

where  $d$  is the spacing of the lattice planes taking part in the reflection and  $q$  is the fractional amplitude scattered by a single plane of atoms in the direction of the reflected beam;  $q$  is given by

$$q = \frac{n\lambda}{\sin \theta_0} \cdot \left( \frac{e^2}{mc^2} \right) \cdot f, \quad (2)$$

where  $n$  is the number of atoms per unit area of the plane,  $f$  is the atomic scattering factor, and  $e$ ,  $m$ , and  $c$  have their usual significance. Actually

\* 'Phil. Mag.' vol. 27, pp. 315, 675 (1914); vol. 43, p. 800 (1922).

Darwin uses  $f$  in the same sense that  $fe^2/mc^2$  is used here. If  $N$  is the number of atoms per unit volume, then  $n = Nd$ , whence it follows from (1) and (2) that

$$\Delta\theta = \frac{2N\lambda^2}{\pi} \left( \frac{e^2}{mc^2} \right) \frac{f}{\sin 2\theta_0}. \quad (3)$$

This formula applies only when the incident radiation is plane polarized with the electric vector normal to the plane of incidence and to crystals containing atoms of one kind only at the points of a simple lattice. If the incident radiation is unpolarized, an additional factor must be included of the form\*

$$\left( \frac{1 \pm \cos 2\theta_0}{2} \right),$$

the positive sign applying when  $2\theta_0 < 90^\circ$  and the negative sign when  $2\theta_0 > 90^\circ$ . For lattices which are not simple and which contain atoms of more than one kind,  $f$  must be replaced by  $|F|$ ;  $F$  is the structure factor for the unit cell and is given by

$$F = \sum_n f_n e^{i\phi_n},$$

where  $\phi_n$  is the phase of the waves scattered by the  $n$ th atom and the summation is over the whole cell.

Then, in the general case, the average breadth  $\overline{\Delta\theta}$  of the region of perfect reflection for unpolarized radiation is given by

$$\begin{aligned} \overline{\Delta\theta} &= \frac{2N\lambda^2}{\pi} \left( \frac{e^2}{mc^2} \right) |F| \frac{1 \pm \cos 2\theta_0}{2 \sin 2\theta_0} \\ &= \frac{N\lambda^2}{\pi} \left( \frac{e^2}{mc^2} \right) |F| \cot \theta_0 \quad \text{for } \theta_0 < 45^\circ \\ \text{and} \quad &= \frac{N\lambda^2}{\pi} \left( \frac{e^2}{mc^2} \right) |F| \tan \theta_0 \quad \text{for } \theta_0 > 45^\circ \end{aligned} \quad (4)$$

It follows from these equations that the intensity of reflection by a perfect crystal should be proportional to  $|F| \cot \theta_0$  for  $\theta_0 < 45^\circ$  and to  $|F| \tan \theta_0$  for  $\theta_0 > 45^\circ$ .

X-ray reflection by perfect crystals has been considered by Ewald† from a different point of view, namely, under what conditions the waves scattered by the induced dipoles in a crystal give rise to a strong reflected beam of the

\* Ewald, 'Phys. Z.', vol. 27, p. 182 (1926).

† 'Ann. Physik,' vol. 49, p. 1 (1916); vol. 54, p. 519 (1918); 'Phys. Z.', vol. 26, p. 29 (1925); vol. 27, p. 182 (1926).



Bragg type. Owing to the interaction between the scattered waves and the direct wave, the radiation is transmitted with a slightly different velocity and direction inside a crystal; as in optics, this may be represented empirically by a refractive index  $\mu$ . Ewald shows that for an ideal crystal, reflection is perfect over a narrow range of angles from

$$\xi = 0 \quad \text{to} \quad \xi = 4/\Omega,$$

where

$$\xi = \sin 2\theta \cdot (\theta - \theta_0) \quad \text{and} \quad 1/\Omega = (\mu - 1).$$

$\theta_0$  is the glancing angle of reflection given by the simple Bragg law. If the classical expression for refraction is assumed to hold in the X-ray region,

$$(\mu - 1) = \frac{e^2}{2\pi m} \sum_k \frac{N_k}{v_k^2 - v^2}, \quad (5)$$

and if  $v$  is not too near a critical absorption frequency so that  $v_k^2$  can be neglected, then the range of perfect reflection is given by

$$\Delta\theta = \frac{2N\lambda^2}{\pi} \left( \frac{e^2}{mc^2} \right) \cdot \frac{1}{\sin 2\theta}. \quad (6)$$

This equation is valid for a simple lattice containing dipoles of only one kind. For a lattice which is not simple or which contains dipoles of several kinds, Ewald shows that

$$\Delta\theta = \frac{2N\lambda^2}{\pi} \left( \frac{e^2}{mc^2} \right) \cdot \frac{|S|}{\sin 2\theta} \quad (7)$$

where  $S$  is the structure factor of the lattice.  $S$  is similar to  $F$ , but omits the scattering factor  $f$ . For unpolarized radiation,

$$\left. \begin{aligned} \overline{\Delta\theta} &= \frac{N\lambda^2}{\pi} \cdot \left( \frac{e^2}{mc^2} \right) |S| \cot \theta \quad \text{for } \theta < 45^\circ \\ &= \frac{N\lambda^2}{\pi} \left( \frac{e^2}{mc^2} \right) |S| \tan \theta \quad \text{for } \theta > 45^\circ \end{aligned} \right\} \quad (8)$$

These equations are very similar to the corresponding equations given by Darwin's treatment, the only difference being that they do not incorporate the atomic scattering factor.

### 3. Comparison with Experimental Results.

The main difficulty which has arisen in testing these conclusions has been the lack of sufficiently perfect crystals, diamond and calcite crystals being

almost the only crystals which have so far been found suitable. Ehrenberg, Ewald, and Mark,\* in particular, have made an extensive series of experiments on the intensity of reflection of X-rays from single crystals of diamond as perfect as could be obtained and their results will now be considered in relation to equations (4) and (8). As only relative intensity measurements were obtained, it is unnecessary to consider the constant factors in these equations and they may therefore be written more briefly as follows:—

$$\text{From equation (4), } I \propto \overline{\Delta\theta} \propto \begin{cases} |F| \cot \theta & (\theta < 45^\circ) \\ |F| \tan \theta & (\theta > 45^\circ) \end{cases} \quad (4')$$

$$\text{From equation (8), } I \propto \overline{\Delta\theta} \propto \begin{cases} |S| \cot \theta & (\theta < 45^\circ) \\ |S| \tan \theta & (\theta > 45^\circ) \end{cases} \quad (8')$$

The structure factor for the diamond lattice is easily calculated if the atoms are assumed to be spherically symmetrical. There are 8 atoms in the unit cell of the lattice. For spectra of type  $(h, k, l)$ , the structure factor is  $S = 4\sqrt{2}$  if  $h, k$ , and  $l$  are all odd numbers. If two indices are odd and one even, or two even and one odd,  $S = 0$ . If all three indices are even,  $S = 8$  unless  $h/2, k/2$ , and  $l/2$  are odd, when  $S = 0$ . Actually a weak  $(2, 2, 2)$  reflection is observed which suggests that the atoms are not exactly spherically symmetrical.

In fig. 2, the experimental results of Ehrenberg, Ewald, and Mark are represented for a diamond crystal of ellipsoidal shape. The intensities are in arbitrary units and are plotted against  $\cot \theta$  for  $\theta < 45^\circ$  and against  $\tan \theta$  for  $\theta > 45^\circ$ . The circles are for reflections with three odd indices,  $S = 4\sqrt{2}$ , and the triangles for reflections, with three even indices,  $S = 8$ ; the crosses are obtained by multiplying the intensities of the former by  $\sqrt{2}$  and they obviously lie close to a mean line drawn through the triangles. Results of a similar character were obtained for a second diamond crystal, but as these were considered to be less reliable than the results for the first crystal, they will not be considered here.

Now according to equation (8'), the intensities of reflection should be proportional to  $\cot \theta$  for  $\theta < 45^\circ$  and to  $\tan \theta$  for  $\theta > 45^\circ$  for spectra of a given type. This is illustrated in fig. 2 where  $I$  in arbitrary units is plotted against  $\cot \theta$  and  $\tan \theta$  for different values of the proportionality constant. It is seen at once that the theoretical line might be made to fit the experimental results approximately for  $\theta < 45^\circ$ , but there would be no agreement whatever for  $\theta > 45^\circ$ .

\* 'Z. Kristallog.,' vol. 66, p. 547 (1928).

Possible explanations for this lack of agreement between the experimental and theoretical results for large values of  $\theta$  are discussed by Ehrenberg, Ewald, and Mark\* in an important passage. They observe that the discrepancies may be attributable to the effect of the atomic scattering factor of carbon, but that this conclusion would only be valid if it could be proved that the discrepancies do not arise from small imperfections in the crystal lattices of

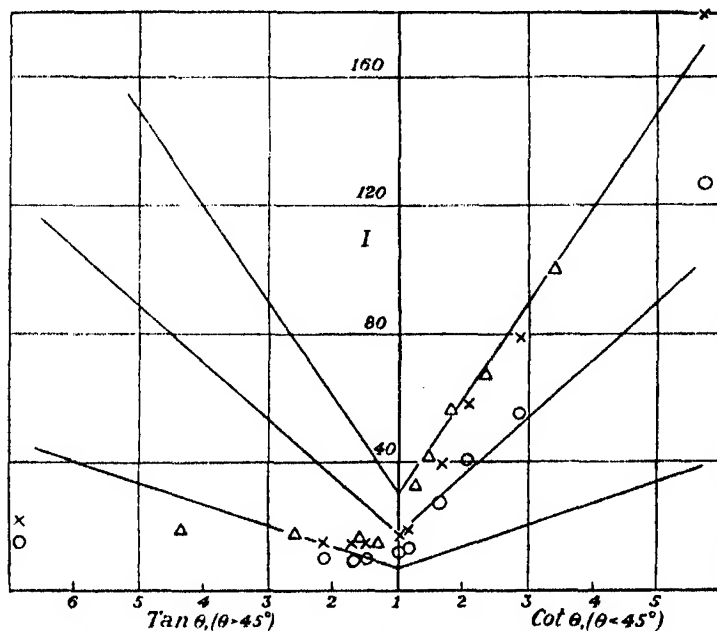


FIG. 2.—Comparison of the observed intensities of reflection from diamond with the theoretical value, the atomic structure factor being omitted.

the diamonds used. On general grounds it is obvious that any lattice imperfection would have a far greater effect on high order than on low order reflections, just as with an optical grating with badly ruled lines. The heat motion of the lattice, if appreciable, would similarly reduce the intensities of the high order reflections; Ehrenberg, Ewald, and Mark show, however, by direct experiment that the heat motion of the diamond lattice has no appreciable effect on the reflected intensities.

It will be shown in the following sections that when a correction is made for

\* 'Z. Kristallog.', vol. 66, p. 580 (1928). "Es liegt nahe, diese Benachteiligung durch den Atomfaktor zu deuten. Aber dieser Schluss wäre erst dann eindeutig, wenn streng erwiesen wäre, dass nicht doch Unvollkommenheiten des Kristallgitters in den hohen Ordnungen sich störend machen, die bei den niederen Ordnungen noch keine wesentliche Rolle spielen."

the atomic scattering factor, the discrepancies between the experimental and theoretical results largely disappear.

#### 4. The Atomic Scattering Factor for Carbon.

Values of the atomic scattering factor  $f$  for carbon have recently been given by James and the writer.\* These values were calculated on the assumption that the carbon atom is spherically symmetrical, an assumption which is probably only approximately true for diamond as is shown by the existence of the (2, 2, 2) reflection. Any lack of spherical symmetry, however, will be confined mainly to the L electrons which contribute appreciably to  $f$  only at small angles; this is shown by James and the writer in their fig. 3. For  $(\sin \theta)/\lambda > 0.4$ , the L electrons do not contribute appreciably to  $f$ . It will be shown in what follows that, with only one exception, all the experimental results are for values of  $(\sin \theta)/\lambda > 0.4$  so that any uncertainty in  $f$  arising from the L electrons will not affect the conclusions of this paper. The  $f$  values previously calculated for carbon have been extended to larger values of  $\theta$  and are tabulated in column 5 of Table II. They refer to the scattering by a carbon atom *at rest* and if there is any appreciable lattice vibration in diamond (thermal vibration and zero point energy) a correction has to be made of the form† :—

$$f_t = f \cdot e^{-M}$$

where

$$M = \frac{6h^2}{mk\Theta} \left\{ \frac{\Phi(x)}{x} + \frac{1}{4} \right\} \left( \frac{\sin \theta}{\lambda} \right)^2. \quad (9)$$

In this expression for  $M$ ,  $\Phi(x)/x$  is a function given by Debye which depends on thermal vibration and the additional  $1/4$  takes into account the zero point energy of the lattice. Experiment and theory both show that for diamond at ordinary temperatures, the temperature factor is negligible; experiments at high temperatures and at the temperature of liquid air have failed to show any variation of the intensity of reflection with temperature.

The zero point energy factor, however, does not depend on the temperature and its presence or absence would not be revealed directly by carrying out experiments at different temperatures. It has been pointed out to the writer by James in a private communication that for large angle scattering, the effect of zero point energy is appreciable, for although the characteristic temperature  $\Theta$  of diamond,  $1860^\circ$ , is high compared with the characteristic temperatures

\* 'Phil. Mag.,' vol. 12, p. 81 (1931).

† See James and Brindley, *loc. cit.*

of other crystals, the mass  $m$  of the carbon atom is relatively small. For zero point energy alone,

$$M = \frac{6h^2}{mk\Theta} \cdot \frac{1}{4} \cdot \left( \frac{\sin \theta}{\lambda} \right)^2.$$

In this expression,  $h$  is Planck's constant ( $6.547 \times 10^{-27}$ ),  $k$  is Boltzmann's constant ( $1.371 \times 10^{-16}$ ),  $m$  is the mass of the carbon atom ( $12.00 \times 1.662 \times 10^{-24}$ ), and  $\Theta$  is  $1860^\circ$ . If  $\lambda$  is in A., then

$$M = 0.128 \left( \frac{\sin \theta}{\lambda} \right)^2.$$

This leads to the values for  $e^M$  given in Table I.

Table I.—Correction Factor for Zero Point Energy in Diamond.

$(\sin \theta)/\lambda$ .	$e^M$ .	$(\sin \theta)/\lambda$ .	$e^M$ .
0	1.0	0.8	1.085
0.1	1.001	0.9	1.109
0.2	1.005	1.0	1.136
0.3	1.012	1.1	1.166
0.4	1.021	1.2	1.202
0.5	1.032	1.3	1.241
0.6	1.047	1.4	1.286
0.7	1.064		

Using these values of  $e^M$ , the corrected scattering factor  $f_t$  has been calculated; values of  $f_t$  are given in Table II, column 6. It is seen that the correction for zero point energy becomes appreciable only beyond  $(\sin \theta)/\lambda = 1.0$ .

The atomic scattering factor is usually represented as a function of  $\sin \theta$  or of  $(\sin \theta)/\lambda$  and it then shows a rapid fall at small values of  $\sin \theta$  owing to the outer electrons contributing appreciably only at small angles, followed by a much less rapid fall caused by the inner electrons scattering appreciably even at large angles. For perfect crystals, it is the variation of  $f$  with  $\cot \theta$  and  $\tan \theta$  which is important; this is shown in fig. 3. For  $\theta < 45^\circ$ ,  $f$  varies almost linearly with  $\cot \theta$  (except for very large values of  $\cot \theta$ ), and for  $\theta > 45^\circ$ ,  $f$  is almost constant with respect to  $\tan \theta$ .

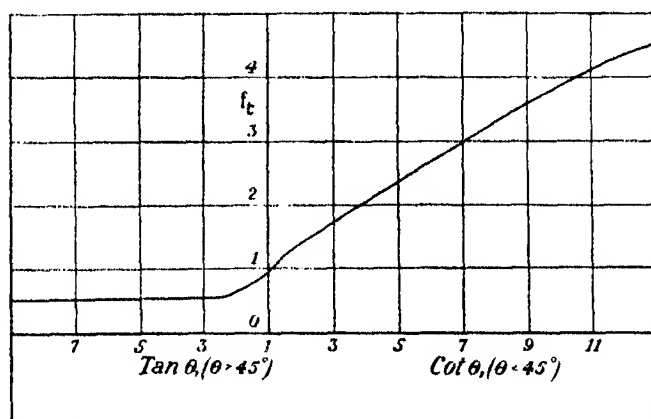
##### 5. Comparison of Experimental and Theoretical Results taking into Account the Atomic Scattering Factor.

With the data given above, the variation of the reflected intensity with angle can be calculated according to expression (4'); neglecting constant factors, we have

$$\left. \begin{aligned} I &\propto f_t \cot \theta & \text{for } \theta < 45^\circ \\ I &\propto f_t \tan \theta & \text{for } \theta > 45^\circ \end{aligned} \right\}$$

Table II.— $f$  Values for Carbon.

$(\sin \theta)/\lambda$ .	$\sin \theta$ for $\lambda = 0.708 \text{ \AA.}$	$\theta^\circ$ .	$\cot \theta, \theta < 45^\circ$ . $\tan \theta, \theta > 45^\circ$ .	$f$ (carbon).	$f_t = f \cdot e^{-u}$ .
0	0	0	$\infty$	6.00	6.00
0.05	0.035	2.0	28.6	5.5	5.5
0.10	0.071	4.2	13.6	4.6	4.6
0.15	0.106	6.1	9.36	3.65	3.65
0.20	0.142	8.2	6.94	3.0	3.0
0.25	0.177	10.2	5.56	2.52	2.52
0.30	0.212	12.2	4.62	2.23	2.23
0.40	0.283	16.4	3.40	1.86	1.86
0.50	0.354	20.7	2.65	1.65	1.65
0.60	0.425	25.2	2.12	1.48	1.48
0.70	0.496	29.7	1.75	1.33	1.33
0.80	0.566	34.5	1.46	1.20	1.20
0.90	0.637	39.6	1.21	1.07	1.07
1.00	0.708	45.1	1.00	0.96	0.96
1.10	0.779	51.2	1.24	0.83	0.83
1.20	0.850	58.3	1.62	0.73	0.73
1.25	0.885	62.2	1.90	0.68	0.68
1.30	0.921	67.1	2.37	0.63	0.63
1.35	0.956	73.0	3.27	0.58	0.58
1.40	0.992	82.8	7.92	0.53	0.53

Fig. 3.—Atomic structure factor,  $f_t$ , for carbon.

The results are shown in fig. 4 for different values of the proportionality factor. There is seen to be a close similarity between the curves and the experimental results particularly at values of  $\theta$  greater than  $45^\circ$ . The agreement between experiment and theory is still not exact, but is obviously very much better as a result of taking into account the atomic scattering factor.

Several possible reasons may be found for the lack of exact agreement between the observed and the calculated values, but one which it is important to mention is the influence of the actual shape of the diamond crystal on the

reflected intensities. This is because the intensity of reflection by perfect crystals, according to Ewald's treatment of the theory, is different for the Laue and Bragg arrangements, the maximum reflected intensity in the latter case being twice that in the former. Although the experimental results used in this paper were obtained for a crystal of ellipsoidal shape, it is not certain whether the "crystal form factor" is quite negligible. The differences observed between the experimental results for this crystal and the results for a crystal of octahedral shape may arise possibly from this cause. However, although it would certainly be necessary in any exact comparison of experiment

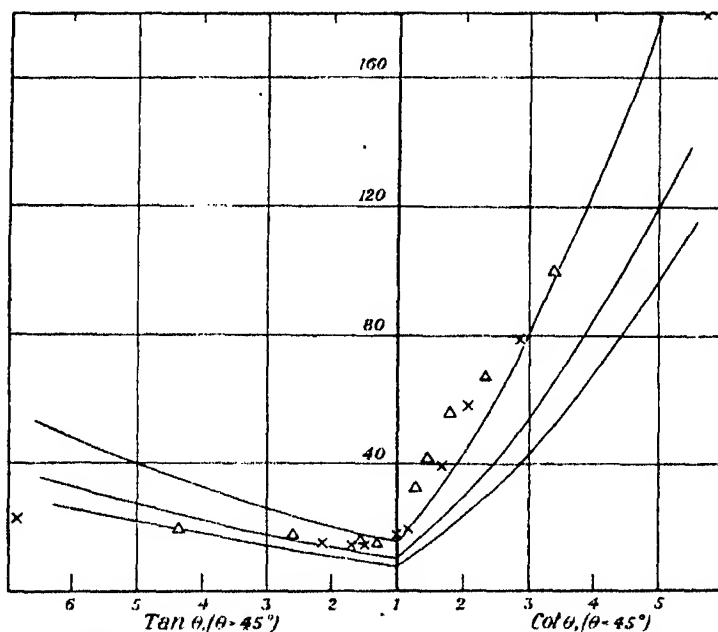


FIG. 4.—Comparison of observed results with theory with the atomic structure factor taken into account.

and theory to take into account considerations of this kind, it is satisfactory for the present to find that when the atomic scattering factor is included in the calculations, there is a very much better general agreement between experiment and theory.

#### 6. On the Refraction of X-rays by Perfect Crystals.

The results discussed in the previous sections have an important bearing on a method suggested by Ehrenberg and Mark\* for the determination of the

\* 'Z. Physik,' vol. 38, p. 129 (1926).

refractive indices of perfect crystals for X-rays. In fig. 1,  $\theta_B$  is the glancing angle of reflection given by the simple Bragg reflection law,  $n\lambda = 2d \cdot \sin \theta_B$ , and  $\theta_0$ , the centre of the reflected beam, is the angle measured experimentally. The difference between  $\theta_B$  and  $\theta_0$  depends on the refractive index of the crystal for the radiation employed. Ehrenberg and Mark have pointed out that all methods of determining refractive indices based on the measurement of deviations from the Bragg law depend on only half the width of the reflected beam and that it should be possible with perfect crystals to determine their refractive indices directly from measurements of the total width of the reflected beam. The question therefore arises whether the atomic scattering factor must be taken into account when the width of the reflected beam is considered. Darwin indicates that the scattering factor  $f$  reduces the intensity of reflection by reducing the width of the region of total reflection and the results given in the previous sections support Darwin's conclusions. There is also direct evidence; Davis and Purks,\* for example, have measured the angular widths of reflections from highly perfect calcite crystals. Their results for  $\lambda = 0.708$  A. and  $\lambda = 1.537$  A. are compared with  $\overline{\Delta\theta}$  calculated from equation (4) in Table III.

Table III.

$\lambda$ in A.	Order of reflection.	F .	Angular widths.	
			Observed.	Calculated.
0.708	1	25.1	3.2	3.2
0.708	2	11.0	0.9	0.7
1.537	1	25.1	5.4	6.4
1.537	2	11.0	1.7	2.0

The agreement between the observed and calculated values is very close. If  $Z$ , the atomic number, which for calcite is 50, is used in place of  $|F|$  the agreement between the observed and calculated widths completely disappears, particularly for the second order reflections.

It follows from Ewald's treatment of the theory of reflection that the range of perfect reflection is

$$\Delta\theta = \frac{4(1-\mu)}{\sin 2\theta}$$

or, if the incident radiation is unpolarized,

$$\overline{\Delta\theta} = \frac{4(1-\mu)}{\sin 2\theta} \left( \frac{1 \pm \cos 2\theta}{2} \right). \quad (10)$$

\* 'Phys. Rev.,' vol. 34, p. 181 (1929).



Darwin's treatment leads to the following equation

$$\overline{\Delta\theta} = \frac{4(1-\mu)}{\sin 2\theta} \cdot \frac{f}{Z} \cdot \left( \frac{1 \pm \cos 2\theta}{2} \right) \quad (11)$$

for a simple lattice composed of atoms of one kind; in the general case,  $f$  must be replaced by  $\sum_n (f_n e^{i\phi_n})$ .

Ehrenberg and Mark carried out experiments on the angular widths of reflections of a number of tungsten L lines from a very fine zinc blende crystal. The wave-lengths employed varied from 1.2419 Å. to 1.4845 Å., all of which are in the region of the K-absorption edge of zinc. These data are not very suitable for testing equations (10) and (11) because it is now well established that for wave-lengths in the neighbourhood of an absorption band the scattering factor  $f$  is not a function solely of  $(\sin \theta)/\lambda$  but has values which are definitely smaller. The uncertainty in  $f$  for Zn for the wave-lengths used by Ehrenberg and Mark makes their data unsuitable for the present calculations. The results obtained by Davis and Purks are more suitable; their results for the first order reflections are probably more reliable than for the second order reflections, the first order reflections being wider and therefore more easily measured. Their data for the first order reflections lead to the results given in Table IV.

Table IV.

Calculated Values of $(1 - \mu)$ for Calcite.		
	From (10).	From (11).
$\lambda = 0.708$ Å. ....	$3.6 \times 10^{-6}$	$1.8 \times 10^{-6}$
$\lambda = 1.537$ Å. ....	$13.6 \times 10^{-6}$	$6.8 \times 10^{-6}$
Values from other Sources.		
$\lambda = 0.708$ Å. ....	$(1 - \mu) = 2.0 \times 10^{-6}$ (Davis and Hatley).	
$\lambda = 0.708$ Å. ....	$(1 - \mu) = 2.03 \times 10^{-6}$ (Hatley).	
$\lambda = 1.537$ Å. ....	$(1 - \mu) = 8.48 \times 10^{-6}$ (Linnik and Laschkarew).	

The data given in Table IV show that the values of  $(1 - \mu)$  calculated from equation (11) agree very much better with the values from other sources than the values calculated from equation (10). The results given by Davis and Hatley\* were obtained by a method involving the measurement of deviations

\* Davis and Hatley, 'Phys. Rev.', vol. 23, p. 290 (1924); Hatley, 'Phys. Rev.', vol. 24, p. 486 (1924).

from the Bragg law, while the result given by Linnik and Laschkarew\* was obtained by measuring the critical angle of reflection.

Finally I would like to express my indebtedness to Dr. W. T. Astbury and to Professor Dr. P. P. Ewald for reading the manuscript of this paper.

#### 7. *Summary.*

It is pointed out that no really satisfactory agreement appears so far to have been found between the observed intensities of X-ray reflections from perfect crystals and values calculated theoretically. Such comparisons have not previously taken into consideration the atomic scattering factor  $f$ , which is so important in the theory of X-ray reflection by imperfect or mosaic crystals. Experimental results for diamond by Ehrenberg, Ewald, and Mark are considered in relation to the theoretical results of Ewald and Darwin, and it is shown that when the scattering factor for carbon is taken into account, there is a reasonably close agreement between the experimental results and the calculated values.

The foregoing results are considered briefly in relation to a method suggested by Ehrenberg and Mark for obtaining the refractive indices of perfect crystals for X-rays by measuring the angular widths of the reflected beams. It is shown that if the atomic scattering factor is taken into account when the widths of the beams are considered, results can be obtained in satisfactory agreement with values obtained by independent methods.

---

\* Linnik and Laschkarew. 'Z. Physik,' vol. 38, p. 659 (1926).

*On a Penetrating Radiation from Thunderclouds.*

By B. F. J. SCHONLAND, M.A., Ph.D., Senior Lecturer and Fellow in Physics,  
and J. P. T. VILJOEN, M.Sc., The University of Cape Town.

(Communicated by C. T. R. Wilson, F.R.S.—Received November 15, 1932.)

The possibility of the production of fast  $\beta$ -rays by a charged thundercloud has been discussed by Professor C. T. R. Wilson,\* who has shown that such a cloud should spray upwards a stream of "runaway electrons" of energy as high as  $5 \times 10^9$  electron-volts. The action of the earth's magnetic field upon this stream should cause it to return to the earth at considerable distances from the cloud, supposing that the energy of the particles was not converted into  $\gamma$ -radiation by nuclear encounters on the way.

A search for such particles in the region below a thundercloud has already been made by one of us,† but without success. The fact that they are not produced in this region can be ascribed either to the field being too small and limited in extent or to the effect of nuclear stoppage. Although their presence would have strengthened the original suggestion, their absence does not invalidate Wilson's view that upward-moving particles generated in the strong field within the cloud do exist. To test this suggestion directly, however, is a more difficult problem, for the supposed electron spray as it returned to earth would be spread out over a wide region and its intensity at any particular point would not be large.

An account is given in the present paper of some experiments made upon distant thunderclouds in the summer of 1931–1932. The instrument used was a Geiger-Müller tube counter, which registered the ionizing particles entering it. The observations to be described show that such a counter exhibits two effects caused by distant thunderstorms. The first of these is a pronounced tendency towards registration of an impulse at the moment a distant lightning flash occurs. The second is the registration of more impulses during a time-interval of a few seconds before a lightning flash than during the corresponding interval after a flash.

These effects appear to us to arise from the Wilson process mentioned above, but further observations are necessary before we can be certain that the

\* 'Proc. Camb. Phil. Soc.,' vol. 22, p. 534 (1925); 'J. Franklin Inst.,' vol. 208, p. 1 (1929).

† Schonland, 'Proc. Roy. Soc.,' A, vol. 130, p. 37 (1930).

location of the thunderstorms is in accord with that to be anticipated if magnetic bending of  $\beta$ -particles were the manner in which they are transmitted.

§ 1. *Apparatus.*

A Geiger-Müller tube counter was arranged to give an automatic record of the passage of ionizing particles through it. The impulses were conveyed after amplification to a relay which operated the pen of an electric chronograph. A second pen marked upon the same tape the moments at which lightning flashes took place, the sudden field changes being picked up by an aerial connected to a two-valve amplifier with a relay in its output circuit. A third pen, operated by a chronometer with electrical contacts, marked half-seconds on the tape.

The counter, which is shown in fig. 1, was a sealed portable type devised by us and constructed in Cape Town. The brass tube was 15.6 cm. long, 3.8 cm. in diameter, and 1.5 mm. thick. It was mounted inside a glass tube to which a flat brass base-plate B was joined with sealing-wax. Connection to the central wire was made through a platinum seal and spring S, and the base-plate was joined to the counter-tube by means of a spring contact. The two tubes were filled with argon at a pressure of about 3 cm. A circular drying tube T, filled with silica gel, was found to improve the action of the counter and to prevent a rise of working voltage after filling. The potential difference required to operate the counter, about 700 volts, was supplied by a battery of dry cells. It was measured and kept under control with the aid of an electrostatic voltmeter with a sensitivity of 1.5 scale divisions per volt. This instrument, shown at V in fig. 2, was a modification of the mica mirror electrometer described by one of us.\*

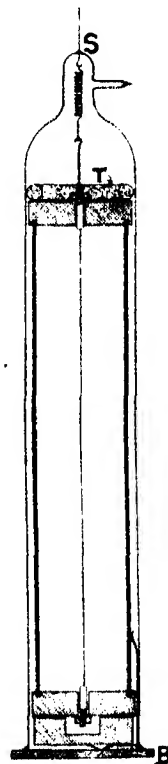


FIG. 1.

The counter impulses passed through a two-valve resistance-capacity coupled amplifier, fig. 2, to a polarized relay of standard Post Office pattern. The tongue T of the relay operated a chronograph pen by breaking the current through the pen-magnet M. On returning to its position of rest, the tongue earthed the grid of the first valve and so placed the arrangement in a position

\* Schonland, 'Proc. Camb. Phil. Soc.,' vol. 25, p. 340 (1929).

to record the next impulse.\* By bringing a few milligrams of radium near the counter, the fastest rate at which the pen could be worked was found to be 170 impulses per minute. The maximum rate used in the actual experiments was 126 impulses per minute. The flat portion of the characteristic curve relating the number of impulses recorded per minute to the applied voltage extended over a range of only 10 volts. In these experiments, however,

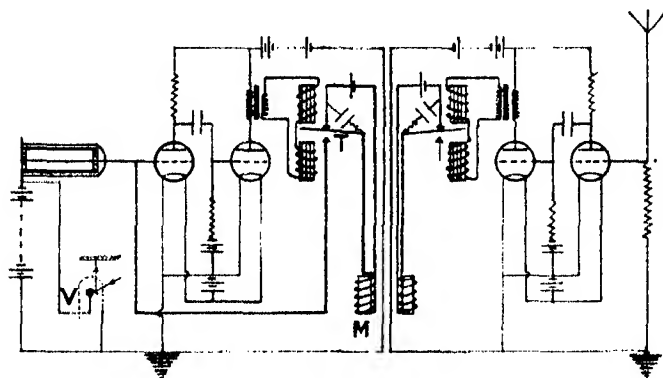


FIG. 2.

as will be seen, the operating efficiency of the counter was of secondary importance.

The counter with its amplifier and relay was mounted in a zinc-lined box (connected to earth) to screen it from disturbances due to electromagnetic waves. As a further precaution, adopted at a later stage of the experiments (after Storm 22), all the additional equipment, including high and low tension batteries, meters and switches, was placed in another large zinc-lined case and the leads carried inside an earthed pipe.

The counter, whose axis was horizontal, had an iron plate 10 cm. thick below it and was surrounded by an iron rampart of the same thickness. This left open a cone of semi-vertical angle  $45^\circ$  which could be covered in when required by iron slabs. In certain experiments the shielding was increased to 20 cm. of iron all round the counter. The instrument was set up in an upper room in the Physics Department of the University of the Witwatersrand, Johannesburg. The data concerning the walls and roof have been given in a previous paper (Schonland, *loc. cit.*).

The instrument used to detect the effects of lightning flashes was placed in another room and at a distance of 30 metres from the counter. An aerial

\* Jacobsen, 'Nature,' vol. 128, p. 674 (1931).

30 metres long, at an average height of 5 metres, was connected to earth through a resistance of 1 megohm. The terminals of this resistance led a resistance-capacity coupled two-valve amplifier, fig. 2. As in the case of the counter amplifier, the plate current of the second valve passed through the primary of a step-down transformer whose secondary was connected to a polarized P.O. relay. The tongue of this relay operated the circuit of the second chronograph pen. The two amplifiers and their relays were 30 metres apart.

It was found that the lightning recorder was able to pick up the effects of flashes judged to be about 70 kilometres away. By making visual observations of the lightning at night we satisfied ourselves that the arrangement responded only to actual flashes. The single click of the pen, however, which was characteristic of the more distant discharges became multiple as a storm came nearer. It was found that the separate clicks from nearer discharges corresponded to the separate strokes composing the main flash itself, for the sound of the pen clicks accurately reproduced the visible flicker of the discharge.

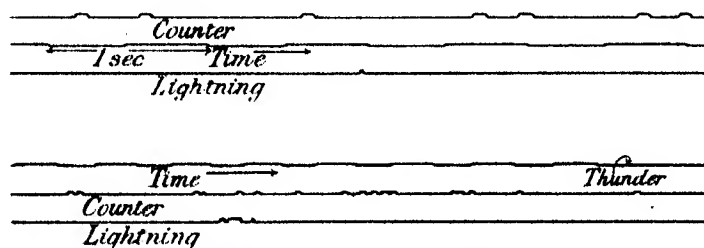


FIG. 3.—(a) Distant lightning flash ; (b) flash at 1.5 km.

An example of a typical distant lightning record is shown in fig. 3 (a) and of a near discharge 1.5 km. away in fig. 3 (b). When the thunder following a discharge was audible it was marked upon the tape by interrupting the time-marking for half a second, as in fig. 3 (b). The distances of the nearer discharges could then be determined from the lightning-thunder interval. The present paper deals mainly with observations on distant storms, the discharges from which did not give audible thunder. Where distances are given they are generally estimates based on the heights of the clouds or the lengths of the flashes.

The chronograph, made by the Cambridge Scientific Instrument Company, was placed in the same room as the counter and about three metres from it. The tape was driven through at rates ranging from 2 to 6 cm. per second. The movement of the pens was due to springs which operated as soon as the relays cut off the currents from the pen-magnets. Sparking at break on the

relay-points was prevented by shunting the gaps with condensers and series resistances, fig. 2.

### § 2. *Tests and Methods of Measurement.*

The results to be described deal with the time relations between lightning strokes and counter impulses and the methods of examining these relations fall into two categories. In the second and simplest are those observations where all that is required is a knowledge of the number of counter impulses occurring either 1, 2 or 5 seconds before or after any given lightning discharge. This information is easily obtained from the tape records without any special aids to measurement.

The first set of measurements we shall discuss is also concerned with the distribution of counter impulses in time around lightning flashes, but in this case in the shortest time intervals which can be safely determined on the tapes. These measurements were made by enlarging the records eleven times with an epidiascope. The positions of the beginnings of the pen movements due to counter impulses and to lightning discharges and the time scale were marked on large sheets of paper and then measured up with a pair of dividers.

By comparing the results of measurements made by two observers it was found that the position of the beginning of a pen-marking could be located without error to within  $1/200$  second in all cases where the speed of the tape through the machine exceeded 2 cm./sec. The speed, and so the resolving power, was generally greater and never less than this.

A possible inaccuracy in the setting of the pens and a possible difference in their times of response to simultaneous counter impulses and lightning discharges was tested for as follows: a Wimshurst machine was set up within a metre of the Geiger counter, with one side of its spark-gap joined to a short aerial a few metres high, while the other side was connected to the earth lead of the counter amplifier. Each spark of the machine thus gave practically simultaneous impulses to the input circuits of the chronograph pens. Test records were made in this way at frequent intervals during the experiments. An example which shows that the joint effects of differences in pen-setting and time lag amounted to less than the limit of measurement 0.005 second is given in Table I.

Table I.—Test for Lag and Pen-setting.

Discharge number.....	1	2	3	4	5	6	7	8
Counter leading by (sec.)	—	—	—	0.004	0.003	—	—	—
Lightning leading by (sec.)	<0.001	<0.001	0.005	—	—	0.001	0.003	<0.001

Very early in the experiments it appeared that the records showed some evidence of the occurrence of systematic coincidences between the lightning and the counter impulses, and a series of tests was made to find out if these were of instrumental origin. It was possible, with two sensitive amplifiers in use, that the act of breaking the current in one relay circuit would involve the other by the emission of a feeble electromagnetic wave, in spite of precautions such as shielding and the provision of condensers across the relay points.

To test whether the counter relay could set off the amplifier of the lightning recorder in this way, both instruments were adjusted to their most sensitive condition at a time when no lightning was taking place. The early morning was usually chosen. No movement of the lightning pen when the counter was set going could be detected. This test was made on several occasions for 30 minutes at a time.

The reverse effect, the operation of the counter amplifier by the lightning recorder, was examined by utilizing times when a great deal of lightning was taking place. The potential on the outer case of the counter was removed, but the counter amplifier left in action. Here again no mutual effect could be observed, the counter pen remaining silent while the lightning pen was in continual movement. A variation of this test in which the counter voltage was not removed but reduced, so that it only gave occasional impulses, was also negative in its results.

Finally, a test was made with an artificial thunderstorm. The Wimshurst machine, with a small aerial attached, was set up some 30 metres away from the counter, which it then was unable to affect directly. Counter and lightning recorder were set going and a record made as in an actual storm, the sparks from the machine providing flashes at irregular intervals. The record was analysed by the method described in § 3 (Storm 0), and the analysis showed that in this case there was no evidence for systematic coincidences between counter impulses and the kicks of the lightning recorder.

These and other tests, to exclude such sources of trouble as the motor driving the tape-machine, seem to make it quite certain that any systematic coincidences between counter impulses and lightning flashes must arise from the thunderstorm itself.

### *§ 3. Evidence for Systematic Coincidences.*

If the counter impulses and the lightning discharges were two quite independent sets of events whose sequence and whose occasional coincidences



were governed by pure chance, the number of such coincidences would be subject to well-known laws. If  $n$  is the number of counter impulses per second,  $N$  the total number of lightning flashes on a particular record, and  $t$  seconds the limit of resolution on the tape, the expectation of chance coincidences on the record is  $2Nnt$ .

Inspection of the records showed that the number of coincidences sometimes considerably exceeded this chance expectation; in certain cases the ratio of the number observed to the number expected was of the order of 10 : 1. To get definite information on this point the records were measured up by the magnification method already described. Each record of a storm or set of storms was examined for impulses which lay within 1/10th second of a lightning

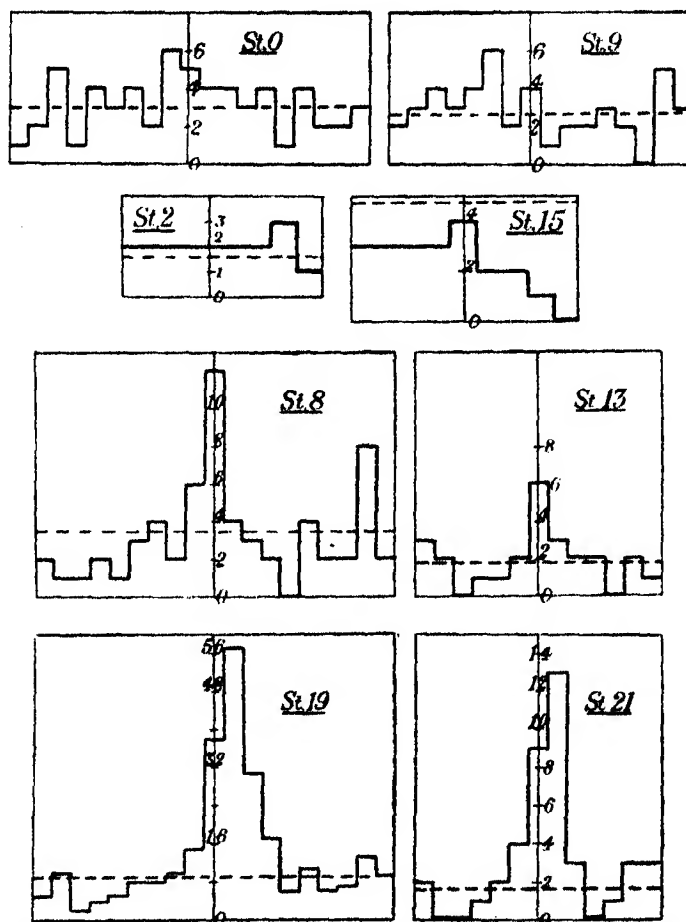


FIG. 4.—Distribution of counter-impulses in time with respect to lightning discharges. (Horizontal time-intervals each 0.001 second.)

flash, and for these impulses the exact time-interval was determined to within 0·005 second. In this way the numbers of impulses occurring in intervals between  $t$  and  $-t$ ,  $t$  and  $3t$ ,  $-t$  and  $-3t$ , and so on, were found. The results were then plotted on distribution curves which showed the number of impulses in each interval  $2t$  seconds wide. This interval width was taken as 0·01 second. The results of an examination of some 11 records are shown in figs. 4 and 5. The dotted line in each case represents the number,  $2N\mu$ , of impulses which should have been present in each interval from pure chance.

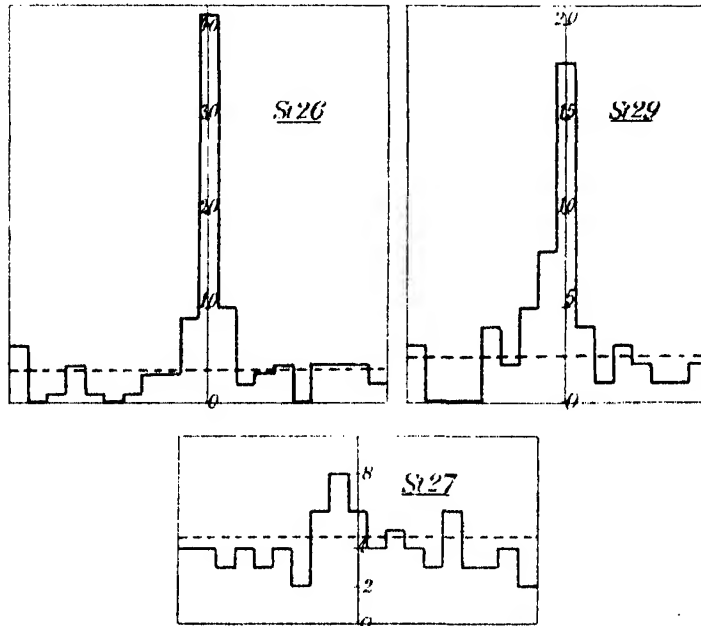


FIG. 5.—Distribution of counter-impulses in time with respect to lightning discharges. (Horizontal time-intervals each 0·001 second.)

Fig. 4 begins with some storm records which do not show any evidence or systematic coincidences. The first, storm 0, is the artificial storm referred to in § 3, in which lightning effects were produced by a Wimshurst machine. The next three storms, 9, 2 and 15, are real storms which failed to show any effects other than those due to chance. There follow the distribution curves for storms 8, 13, 19, 21, 26 and 29, in each of which a pronounced peak occurs in the interval centred on the moments of occurrence of lightning flashes. The last curve of fig. 5 (storm 27) is referred to later on.

That peaks of this nature are not due to chance can be shown as follows: If the average number of counter impulses occurring in any one interval is  $x$ ,

the probability that  $\nu$  impulses occur is  $\frac{x^\nu}{\nu!} e^{-x}$ . Thus the probability of the appearance of an interval with  $\nu$  or more impulses in it is given by

$$p = \sum_{m=\nu}^{m=\infty} \frac{x^m e^{-x}}{m!}$$

and the chances against the appearance of a peak of height  $\nu$  in any particular interval are  $1/p:1$ . Taking from fig. 3 the least prominent peak, that of storm 13, the chances are 60.7:1 against its appearance at the centre of the distribution curve. The chances against the appearance of the most prominent peak, that of storm 26, fig. 4, are  $1.4 \times 10^{28}$  to 1.

All the available information about the storms in these figures, and about others which have not been analysed by the magnification method, is summarized in Tables II and III. The records taken during a particular period of thunderstorm activity are given a serial number in column 1 and referred to for convenience as belonging to a "storm" with this number. Actually, however, as the second and third columns show, there was always more than one storm in action during a run. The fourth column gives the time occupied in the taking of a record, and the fifth the number of flashes recorded in this time. The next three columns show the number of coincidences observed, the number of chance coincidences expected, and the ratio of these two quantities. The method of studying coincidences by magnifying the record and plotting a distribution curve proved very laborious and was only used in a certain number of cases, indicated in the tables. In other cases the number of coincidences was determined directly from the records, using 0.01 second as the resolving power and 0.02 second as the interval width. A comparison of the results obtained by the two methods in three cases, storms 2, 9 and 15, showed that for obtaining the approximate number of coincidences the simple direct method was quite reliable.

In column 9 is given the average number of impulses recorded by the counter per second. The variation of the entries under this head is due mainly to variations in the potentials applied to the counter on different days. These are of no consequence in the present work, for the potential was kept constant during a particular run. The last column gives the thickness of iron placed over the top of the counter. The remaining portions of the tables refer to questions discussed in the following section.

It will be seen that Table II is devoted to those distant storms which showed systematic coincidences, and Table III to those which did not. No storms

Table II.

1	2	3	4	5	6	7	8	9	10	11	12	13										
Storm record No.	Distances (km).	Directions.	Duration (min.)	No. of flashes on record.	Coincidences.			Counter Rate flashes/sec.	1-second intervals.			2-second intervals.			5-second intervals.			Iron shield on top (cm.)				
					Observed.	Expected.	Obs./ Expd.		Flashes examined.	"before."	"after."	Forward excess.	Flashes examined.	"before."	"after."	Forward excess.	Flashes examined.		"before."	"after."	Forward excess.	
8 { a { b {	22 50	N.E., E., W.	13	65	9*	2.3	3.9	1.77	51	84	89	5	51	179	172	7	237	222	+15	0		
	35 50	E., W., N.E.	23	234	12	3.5	3.4	1.50	123	196	190	6	123	402	370	32	41	345	298	+47	0	
13	20-50	S., S.W., W.	27	180	6	1.8	3.3	1.60	27	37	50	7	27	73	60	13	20	130	120	+10	6	
10 {	60 50 30	S.E., S., N.E.	35	460	57	8.8	6.5	1.90	46	103	87	16	46	225	198	27	24	274	264	+10	6	
21	50-70	N.N.W., N., N.E.	18	98	13	1.6	8.1	1.64	44	76	82	6	44	147	151	4	24	193	197	-4	20	
26	30-40	S.W., S.E.	13	300	41	3.6	11.4	1.50	15	19	15	4	18	48	42	6	10	63	72	-9	0	
29 {	30 40 60	N.E., S.S.E., E.	16	400	18	2.4	7.5	0.60	42	30	24	6	48	68	53	15	13	42	41	+1	6	
Totals .....					1737	156	24.0	6.5		348	545	517	+28	357	1142	1046	+96	159	1284	1214	+70	
Total forward excess .....									+28 ± 32.6			+96 ± 49.7			+70 ± 50.6							

\* Determined by direct inspection method; others by magnification method.

Table III.

1	2	3	4	5	6	7	8	9	11	12	13						
Storm record No.	Distances (km.).	Directions.	Duration (min.).	No. of flashes on record.	Coincidences		Counter rate klicks sec.	2-second intervals.				3-second intervals.				Iron shield on top (cm.).	
					Obs.	Exptd.		Obs. Exptd.	Flashes exmd.	$\Sigma$ before	$\Sigma$ after	Fwd. excess.	Flashes exmd.	$\Sigma$ before	$\Sigma$ after		Fwd. excess.
2	45	E. & S.	63	127	2*	1.6	1.3	1.26	109	244	259	-15	57	544	-10	0	
4	20-45	?	42	293	6	7.5	0.8	1.30	131	326	335	-9	89	541	-6	0	
6	40-60	N.E.	13	167	7.0	7.0	1.0	2.10	73	299	308	-9	11	135	-4	0	
7 { <sup>a</sup> b	25	E.	9	25	6	4.0	1.5	2.00	18	66	69	-3	9	90	-3	0	
	35, 20	E., W.	8.5	78					46	176	181	-5	16	84	-6		
8c {	50 25	N.W. W.	29	213	10	6.8	1.5	1.50	123	301	389	+2	44	337	-2	0	
9	?	?	25	220	4*	2.5*	1.6	1.14	97	246	221	-25	75	484	0	0	
12	50	S., S.E.	40	183	1	4.4	0.23	1.20	125	297	296	+1	83	492	+4	0	
14 {	20 35	S.W. "all round"	20	23	1	0.6	1.7	1.20	14	28	27	-1	7	35	-1	6	
	35	S., W., E.	30	247	4*	4.9	0.8	2.00	52	207	228	-21	23	225	-9	6	
16 { <sup>a</sup> b	30, 40	S.W., S.	21	100	4	3.8	1.1	2.05	38	140	145	-5	1	7	-3	6	
	40, 20	S.E., S.W.	14	216	21	9.7	2.2	2.20	80	369	359	+10	22	198	-20		
Totals					66	52.8	1.25		897	2789	2817	-28	467	3172	-32		
Total forward excess										-28 $\pm$ 74.9				-32 $\pm$ 70.9			

\* Determined by magnification method; others by direct inspection.

nearer to the station than 25 km. are included in these tables, for none of our records of storms within 25 km. show any evidence of systematic coincidences. Storm 11, for example, which passed close overhead gave a record lasting 54 minutes from the time it was 25 km. away to the south-west to the time when it had receded some 20 km. to the north-east. 1000 lightning flashes were recorded, of which 24 were coincident with counter impulses, while the chance expectation was 17. In fig. 5, storm 27, is shown the distribution curve obtained from the record of a violent overhead thunderstorm, many of whose flashes occurred within less than 2 km. from the station. The slight peak shown in the curve cannot be considered significant. To follow up this point we have abstracted from all the records of overhead storms those close discharges whose distance is determinable from the lightning-thunder interval, and examined them for coincidences. The results are shown in Table IV below, the two halves of which refer to observations made with the top of the counter open and with the top closed by either 7 or 20 cm. of iron.

Table IV.—Coincidences from Overhead Storms.

Top open.				Top closed.		
Distance (secs.).	No. of discharges.	Coincidences.		No. of discharges.	Coincidences.	
		Observed.	Expected.		Observed.	Expected.
0-9	26	1	0.39	52	0	0.78
9-12	49	0	0.74	33	0	0.50
12-15	15	0	0.23	22	0	0.33
15-25	16	1	0.24	12	0	0.18
0-25	106	2	$1.6 \pm 1.3$	119	0	$1.8 \pm 1.3$

The table shows that there is no evidence for systematic coincidences from these 225 very close discharges. It may be compared with the results from storm 26 (Table II) whose 300 discharges at a distance of about 30 km. gave 41 coincidences, 11.4 times as many as should have arisen by chance.

The multiplicity of the lightning discharge caused the pen markings in the case of these near flashes to be spread over a considerable time, the separate strokes occupying sometimes a total interval of a second. Since the separate kicks of the pen were not always clearly defined we have, in Table II, considered only those coincidences which occurred at the beginning of a discharge.

The absence of any systematic coincidences from close discharges disposes

of the possibility that such coincidences can be due to the response of the counter amplifier to Hertzian waves. Three of the 78 discharges in the first line of Table IV took place, according to the lightning-thunder interval, within less than 300 metres of the counter, and 11 within less than 1 km., yet none of these were simultaneous with counter impulses. It follows from this argument that the radiation from the distant thundercloud which gives rise to coinciding counter impulses is not ordinary long-wave electromagnetic radiation.

#### § 4. *Evidence for other Counter Impulses of Thunderstorm Origin.*

In this section we describe the results of an examination of the tape records to determine whether a thundercloud is able to affect a Geiger-Müller counter at times other than the moment of discharge. The examination was based on the possibility that a cloud might give rise to such counter impulses when approaching the fully-charged state, before a flash takes place. Such a thunderstorm effect should show itself as a difference between the number of impulses recorded by the counter in two equal intervals of time respectively just before and just after a discharge.

A lightning discharge more or less completely removes the electrification of a thundercloud, which thereupon begins to recover. This recovery or regeneration of the cloud charges follows a curve which is approximately exponential, being very rapid at first and slowing down as the cloud approaches the fully-charged condition. The study of South African storms has shown that in general they attain 90 per cent. or more of their full electrification 5 seconds before a flash occurs and have recovered less than 25 per cent. 5 seconds afterwards. We have therefore chosen three sets of time intervals for investigation, 1, 2 and 5 seconds before and after the flash takes place.

Since the number of counter impulses in an interval is subject to statistical fluctuations, a considerable number of flashes must be examined in this way before one can hope to establish any forward excess, and certain precautions must be observed in making the measurements. Consider a portion of the record on which there are two flashes, A and B, following one another at an interval of 5 seconds, fig. 6, and suppose that these are produced by two different storms, only one of which, B, is effective in producing this type of counter impulse. The effect of storm B will be greater during the interval AB, 5 seconds before it discharges, than during the interval cA from 10 to 5 seconds before. Measurements made of the intervals cA and AB, 5 seconds before and after the ineffective flash A, should therefore show a backward excess due

to the presence of the later flash B. This effect will be reversed on measuring the corresponding intervals AB and Bd for flash B. Thus in a summation the two flash measurements may annul each other, though an effect is present from one of them.

To avoid this difficulty the measurements were restricted to those flashes which were clear of others behind by more than a certain time. For the measurement of the 5-second intervals the clearance was set at 10 seconds, and for the 1- and 2-second intervals at 4 seconds. Flashes occurring in the forward intervals were allowed. Thus if, in fig. 6, A and B were 3 seconds apart, B would alone be measured up. Even if the B storm were ineffective, the presence of an effective A storm flash 3 seconds before might cause B to show a slight forward excess.

A second precaution was to exclude from the measurements all flashes which gave rise to coincident counter-impulses, accidental or systematic.

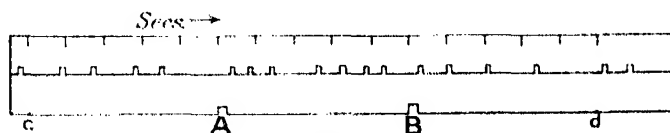


FIG. 6.

Flashes for which another flash in the forward interval gave a coincidence were also rejected. The measurements thus stand by themselves and are independent of any possible flaw in the interpretation of systematic coincidences. In the case of a discharge sufficiently near to give a multiple marking, measurements for the forward interval were made from the beginning of the discharge and for the backward interval from the end.

The results of an examination of the records of the distant storms discussed in the preceding section are shown in Tables II and III. The measurements for each of the three intervals of time occupy four columns. The first column gives the number of flashes on the record which were sufficiently clear behind to satisfy the above-mentioned criterion, the second gives the total number of counter impulses in the intervals before flashes occurred, and the third the total number in the intervals after the flashes. The fourth column shows the "forward excess." Table II gives the data for those storms which showed systematic coincidences, Table III for those which did not.\* The storms of Table II show a definite tendency towards an excess of the forward over the

\* The 1-second intervals were not used for the storms shown in Table III.



backward counts, particularly marked in the case of storms 8 and 19. The totals given at the bottom of the table show that this forward excess in the case of the 2- and 5-second intervals exceeds the probable error in the measurement by a factor of 2.1 and 1.4 respectively. For the 1-second intervals it is 0.86 times the probable error.

These figures are, perhaps, not sufficiently high to establish the reality of the effect looked for, but a graphical analysis of the data seems to bring it out quite strongly. This is shown in figs. 7 and 8, for the 2- and 5-second

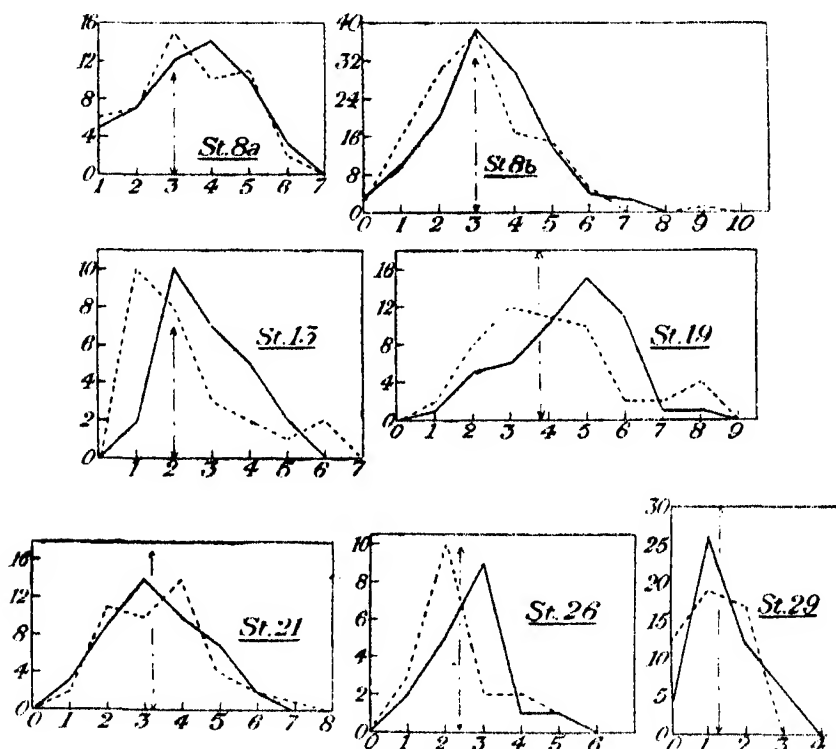


FIG. 7.—Distribution of counter-impulses in 2-second intervals — before flash; ---- after flash. Abcissae = number of impulses in an interval; ordinates = number of intervals.  $\longleftrightarrow$  = average number of impulses in 2 seconds.

intervals respectively. Each set of curves in these figures relates to a particular storm record, and the ordinate gives the total number of cases in which a forward (or backward) interval contains the number of counter impulses represented by the abscissa. The results for the forward intervals are shown as continuous curves, while those for the backward intervals are shown dotted. The vertical line in each curve shows the average number of counter impulses

in the interval. This is determined from a count made on the whole tape record.

All the curves shown, with the exception of the last one (storm 2), relate to storms from Table II which showed systematic coincidences. This last curve is typical of the ineffective storms in showing no significant difference between the forward and the backward counts. The rest of the storms in these figures show with one exception a definite shift forward of the curves for the forward intervals. The exception is storm 21, and may arise from the fact that in the

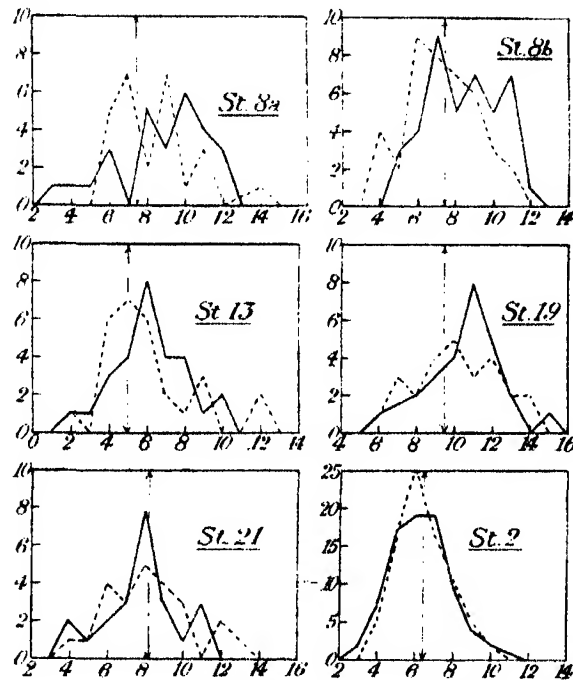


FIG. 8.—Distribution of counter-impulses in 5-second intervals. — before flash. Abscissæ = number of impulses in an interval. - - - after flash. Ordinates = number of intervals.  $\longleftrightarrow$  = Average number of impulses in 5 seconds.

case of this measurement the counter was shielded on all sides with 20 cm. of iron.

The examination of the records in the case of overhead and near thunderstorms shows that close lightning flashes give rise to a significant forward defect. This result confirms the conclusion of one of us that no runaway electrons are emitted downwards from a thundercloud.\* The action of an overhead thunderstorm in cutting off some of the ionizing particles due to the

\* Schonland, 'Proc. Roy. Soc.,' A, vol. 130, p. 37 (1930).

fine-weather penetrating radiation has already been observed.\* The further observations we have made on this question will be discussed in another paper.

§ 5. *The Location of the Effective Storms.*

In the preceding sections we have brought forward evidence for the production of counter impulses by a distant thunderstorm (a) at the moment the cloud discharges, and (b) during the few seconds before a discharge when the cloud is practically fully charged. It is convenient to distinguish between these two effects by calling the impulses of case (a) flash impulses and those of case (b) forward impulses.

Since neither flash nor forward impulses are found when the storm is near or overhead the effects observed cannot be due to ordinary Hertzian waves and further the radiation which causes them cannot be emitted in a downward direction by the cloud. The simplest view to take is to suppose them to be due to electrified particles projected upwards by the cloud and subsequently bent downwards by the action of the earth's magnetic field. The runaway electron theory of Wilson provides a mechanism for the production of upward-moving electrons and of energy initially as high as  $5 \times 10^9$  volts. The subsequent history of this electron spray in the earth's field presents, however, a complicated problem, the main features of which have been given by Hulburt.\* In equatorial regions, where the field is approximately horizontal, an electron shot upwards in a nearly vertical direction would descend to earth to the east\* of the cloud. The dimensions of the region sprayed would be about 1000 km. for electrons of initial energy  $5 \times 10^9$  e-volts. In higher magnetic latitudes, where the field is considerably inclined to the horizontal, Hulburt finds the spray to be more spread out, and exact calculation is difficult, though here also the tendency is for the down-coming particles to swing to the east. He finds also that for clouds in the Southern Hemisphere the spray will be mainly directed to the north and east of the parent thundercloud.

To test this explanation of the effects observed, it would be necessary to show that thunderstorms only produced them when at a sufficient distance for fast-moving particles to be bent down and when lying to the west of the counter itself. Since observations on distant thunderclouds always involve picking up the effects of two or more storms, means would have to be provided for distinguishing the flashes from different storms from one another. These were

\* 'Phys. Rev.', vol. 37, p. 1 (1931); we have quoted this paper with "east" substituted for "west" as it appears to us that a slip has been made.

not available in the present experiments, and all that could be done was to note the directions and distances of storms likely to affect the lightning recorder. This information is given in Tables II and III, columns 3 and 2. The preponderance of storms to the east of the station shown in Table II is perhaps due to the fact that we had a much better view in that direction than to the west. The only storm about which we have definite information with regard to location is No. 13, concerning which it was noted that no thunderclouds whatever could be seen to the east, north-east, or south-east of the station. Since this record gave both flash and forward impulses from westerly thunderstorms, it supports the electron-spray explanation. In a repetition of the experiments we intend to examine this question with the aid of the wireless direction-finder. It may be, however, that the effects observed are owing to secondary products of the Wilson particles generated by the thunderclouds, such as  $\gamma$ -rays or neutrons. Until further observations have been made it is not profitable to discuss such possibilities.

#### § 6. *The Penetrating Power of the Radiation.*

The radiation responsible for the effects described was able to penetrate considerable thicknesses of iron. Storm No. 21 of Table II gave rise to flash impulses, though the counter was shielded with 20 cm. of iron all round. Three others, Nos. 13, 19 and 29, produced both flash and forward impulses through a shield of iron 6 cm. thick.

It has been shown that the ionizing particles associated with the penetrating radiation, which are presumably in most cases fast electrons or protons, produce about 36 ion-pairs per centimetre of path in ordinary air.\* This would entail an expenditure of less than  $10^9$  e-volts in traversing the whole atmosphere in a vertical direction once. Since the thunderstorm electron spray suggested by Wilson would have initial energy up to a maximum of  $5 \times 10^9$  e-volts it could traverse the atmosphere twice and still have sufficient energy on reaching the earth to penetrate considerable thicknesses of iron.

#### § 7. *The Effect of the Charge Distribution in the Cloud upon the Emission of Fast Electrons.*

The evidence we have put forward in § 3 shows that while some thunderstorms give rise to flash impulses, others do not. The results of § 4 show that the same holds for forward impulses. Apart from the question of the location

\* Locher, 'Phys. Rev.', vol. 39, p. 883 (1932).

of the storm with respect to the counter, there are other reasons why a thundercloud may sometimes not be able to produce forward impulses at all, and why in some cases even flash impulses may be absent.

As regards forward impulses, it is possible that the strong fields required within the cloud may not extend over any considerable region except at the moment at which a discharge occurs. Further, it is possible that the potential difference between the upper positive pole of the cloud and the conducting regions of the upper air may be very considerable during the time that the cloud charges are being built up. If it was of the same order as that between the poles of the cloud, upward moving runaway electrons would be stopped by a retarding field after they had left the cloud. Under these conditions the electrons responsible for forward impulses could not be produced at all.\*

The same argument would appear to discount the appearance of flash impulses as well. If, however, the first stage in a lightning discharge was a discharge between the upper pole and the upper air, the condition within the cloud would momentarily be that contemplated by Wilson's theory, while the retarding field would be destroyed. The impulses from runaway electrons would thus occur only at the moment at which such a composite discharge took place. It would seem possible, therefore, that the presence of forward and of flash impulses may depend upon the distribution of electric charge in the thundercloud considered.

#### § 8. *Possible Effects in an Ionization chamber.*

We may attempt to estimate the additional ionization to be expected in an ionization chamber from the action of distant storms by using the information given by these counter experiments. The effect due to flash impulses will be considered first. The storm record (No. 26), on which these were most frequent, showed one systematic coincidence for every eight lightning discharges. Since two separate thunderstorms were involved in this record, we may assume as an optimum estimate that a single suitably placed thundercloud gives rise to one flash impulse for every four flashes, in a counter of the size used by us. A very active storm discharging four times per minute would thus produce one flash impulse per minute. This agrees with the fact that the storm records of Table II, with a duration of 145 minutes in all, were found to give a total of 132 systematic coincidences.

In fine weather the counter recorded about 100 impulses per minute, so flash impulses from a suitably placed storm should give an increase in the

\* We are indebted to Professor C. T. R. Wilson for this suggestion.

counter rate of the order of 1 per cent. It would be very difficult to determine this effect by an ionization method during the comparatively short time available for observations. It is, of course, possible that the flash impulse corresponds to the entry of more than one particle into the counter. On the other hand it is well known that the fine-weather impulses represent to some extent the arrival of proton-electron groups travelling together.

The figures for the forward impulses, though less certain, suggest that these might have a greater effect. The average rates of production of forward impulses for the storms of Table II (obtained by dividing the total forward excess by the total number of flashes examined and the time interval) are 0.08, 0.13 and 0.09 per second for the 1-, 2- and 5-second intervals before a flash. If we suppose that in general three storms were in action, of which only one was effective, these rates become 0.24, 0.39 and 0.27 forward impulses per second. The production of such impulses can only occur during the time that the cloud charges are building up to their maximum, a time of the order of 10 seconds. We may thus take 0.30 impulses per second as a reasonable upper limit for the average rate of production during this period, and the total number of forward impulses before each flash as 3.0. An active and suitably placed storm might therefore produce 12 forward impulses, from four flashes, per minute, and these would increase the ionization in a closed vessel by 12 per cent. This is, of course, an optimum estimate, but it suggests that an increase of the order of 5 per cent. might be found from a storm in the correct position.

We wish to express our thanks to Professor H. H. Paine of the University of the Witwatersrand for the hospitality of his laboratory and the loan of the chronograph, to Professor A. Ogg of the University of Cape Town for his generous assistance and interest, and to Mr. J. Linton for much help. We wish also gratefully to acknowledge a financial grant from the Research Grant Board of the Union of South Africa.

#### *Summary.*

An arrangement for the study of the time relations between the impulses of a Geiger-Müller counter and the discharges of distant thunderclouds is described. The observations show that some of the counter impulses are systematically coincident with lightning flashes. These impulses and others occurring a few seconds before discharges take place are ascribed to a penetrating radiation emitted by the thunderclouds. The effects are not observed from storms distant less than 30 km. from the counter.

---

*The Diffraction of Electrons in Mercury Vapour.—II.*

By F. L. ARNOT, Ph.D., Lecturer in Natural Philosophy, The University,  
St. Andrews.

(Communicated by H. S. Allen, F.R.S.—Received November 16, 1932.)

*Introduction.*

The interference of electrons is now a well established fact. It has been shown\* that when a homogeneous beam of electrons falls upon a regular arrangement of scattering centres, such as a crystal, a ruled grating, or a complex gaseous molecule, the angular distribution of the scattered electrons shows interference maxima and minima.

The analagous, though distinct, phenomenon of the *diffraction* of electrons has, however, only recently been demonstrated. Evidence of the diffraction of electrons was first obtained about two years ago by Bullard and Massey,† and the author.‡ While investigating the angular distribution of elastically scattered electrons in mercury vapour I found well-marked maxima and minima. In this case the scattering was produced, not by an ordered arrangement of scattering centres, but by a random distribution of atoms. It has been shown§ theoretically that the results obtained can be satisfactorily explained on the assumption of scattering by a single centre, and consequently they represent a true diffraction effect.

The results obtained by Arnot and by Bullard and Massey have subsequently been confirmed and extended by Pearson and Arnquist,|| Ramsauer and Kollath,¶ Hughes and McMillen and Webb,\*\* Tate and Palmer,†† and by Mohr and Nicoll.‡‡

\* Cf. G. P. Thomson, "The Wave Mechanics of Free Electrons."

† 'Proc. Roy. Soc.,' A, vol. 130, p. 579; vol. 133, p. 637 (1931).

‡ 'Proc. Roy. Soc.,' A, vol. 130, p. 655; vol. 133, p. 615 (1931).

§ Arnot, 'Proc. Roy. Soc.,' A, vol. 133, p. 615 (1931); Henneberg, 'Naturwiss.,' vol. 30, p. 561 (1932); Massey and Mohr, 'Proc. Roy. Soc.,' A, vol. 136, p. 289 (1932) and previous papers.

|| 'Phys. Rev.,' vol. 37, p. 970 (1931).

¶ 'Ann. Physik,' vol. 12, p. 837 (1932).

\*\* Hughes and McMillen, 'Phys. Rev.,' vol. 39, p. 585; vol. 41, p. 39 (1932); Hughes, McMillen and Webb, 'Phys. Rev.,' vol. 41, p. 154 (1932).

†† 'Phys. Rev.,' vol. 40, p. 731 (1932).

‡‡ 'Proc. Roy. Soc.,' A, vol. 138, pp. 229, 469 (1932).

In my original work on mercury vapour, results were obtained over an angular range of  $18^\circ$  to  $126^\circ$ , and for electrons of various energies between 8 and 800 volts. The present paper deals with an extension of this work to larger scattering angles, and to lower energies.\*

### Apparatus.

The apparatus employed in this work, with the exception of the electron gun, was the one which I used at the Cavendish Laboratory, Cambridge, and with which the original results for mercury vapour and other gases were obtained. This apparatus has been fully described in previous papers,† and the reader is referred to them for details and for an account of the experimental procedure.

In order to obtain results at larger angles than was previously possible, an electron gun, shown in fig. 1, of a different type, had to be designed and built.‡

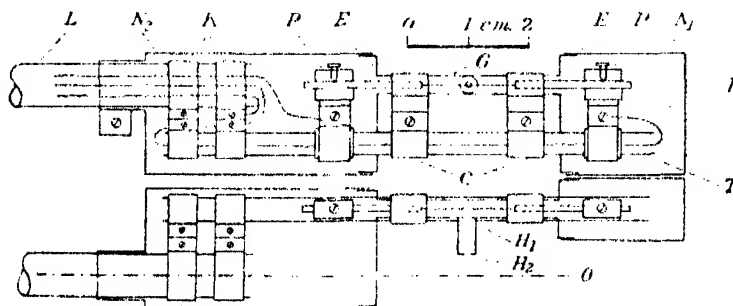


FIG. 1.—Electron gun.

All the parts including screws and nuts were made of copper, permanent joints and connections being silver-soldered. The tube *G* of 3 mm. diameter, at the centre of which was fixed a small T-piece containing the holes  $H_1$  and  $H_2$ , was supported by two clamps *C* on the copper tube *T*. The holes  $H_1$  and  $H_2$ , which served to define the electron beam, were each 1 mm. in diameter, and were spaced 6 mm. apart. Two small copper posts *P*, with drilled heads and set-screws, were clamped to the tube *T*, but were insulated from it by the split cylinders of sindanyo *I*. These posts served to support the filament rigidly in the centre of the tube *G*. The filament, which was about 15 mm. of tungsten

\* A preliminary report of this work appeared in 'Nature,' vol. 130, p. 438 (1932).

† Arnot, 'Proc. Roy. Soc.,' A, vol. 129, p. 361 (1930); vol. 130, p. 655 (1931); vol. 133, p. 615 (1931).

‡ This was constructed by Mr. G. H. Ross in the laboratory workshops.



wire of 200 microns diameter, was spot welded to short lengths of nickel wire. These nickel ends were then slipped into the drilled heads of the posts P and secured by the set-screws. It was thus quite a simple matter to renew the filament.

The tube T was supported by the clamps K from the pyrex glass tube L. This tube could be rotated about the axis O by a small ground glass joint, and the gun therefore set at different angles to the receiving system, fig. 2. The entire gun could be removed from the apparatus by means of a larger ground glass joint. The filament leads and the lead to the anode of the gun passed down the centre of the glass tube L, through the ground glass joint, to seals outside the main body of the apparatus. In order to ensure that the scattering took place in a field-free space it was necessary to shield the posts P, and the leads to them. This was effected by attaching to the tube G end plates E, over which the detachable copper covers N<sub>1</sub> and N<sub>2</sub> could be slipped.

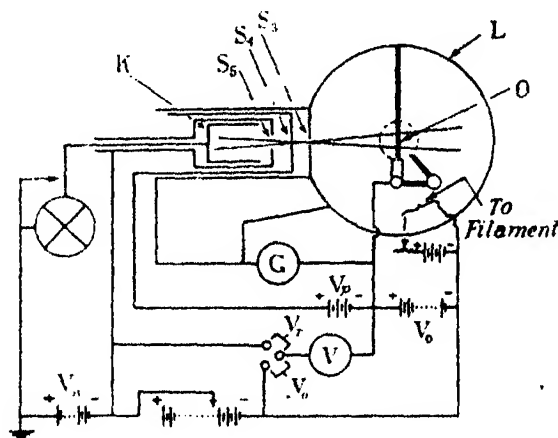


FIG. 2.—Diagram of apparatus.

A diagram of the essential parts of the apparatus is given in fig. 2. The receiving system consisted of three concentric cylinders containing the slits S<sub>3</sub>, S<sub>4</sub>, S<sub>5</sub>, and the concentric Faraday cylinder K within the inner shielding cylinder. The dimensions of these slits were the same as before (see previous papers, *loc. cit.*); but in order to allow the electron gun to revolve through the full angular range of 360° the whole system was moved back, so that the distance of S<sub>3</sub> from the scattering point O was now 25 mm. instead of 12 mm. as before. The inside of the collision chamber was lined with the large nickel cylinder L.

A difference of potential  $V_p$  of 9 volts was applied between the first two slits  $S_3$  and  $S_4$  to stop positive ions from entering the Faraday cylinder. An *effective* potential of  $V_r = (V_o + V_p - 3)$  volts, where  $V_o$  is the energy of the primary electron beam, was applied between the next two slits,  $S_4$  and  $S_5$ , so as to stop all but the elastically scattered electrons from being received. And finally a potential  $V_H$  of 20 volts was applied between the slit  $S_5$  and the Faraday cylinder, to prevent secondary electron emission from the latter.

Both in this work and in my previous work with this apparatus it was noticed that the accelerating field between K and  $S_5$  penetrated slightly into the region between  $S_5$  and  $S_4$ , across which the retarding field  $V_r$  was placed. This penetration of the accelerating field into the retarding field causes part of the retarding field to be ineffective in stopping inelastically scattered electrons. The *effective* value of  $V_r$  is therefore always less than the actual value of  $V_r$  as read on a voltmeter connected between  $S_4$  and  $S_5$ . It would not therefore be sufficient to set the actual value of  $V_r$  equal to  $(V_o + V_p - 3)$  volts, for in this case some inelastically scattered electrons might be received. To insure that only the elastically scattered electrons were received the following procedure was adopted, not only in this work, but also in my previous work with this apparatus. At each energy  $V_o$  of the primary electron beam a velocity distribution curve of the scattered electrons was taken. From an examination of this curve the retarding potential could then be set so as to exclude from the Faraday cylinder all inelastically scattered electrons. This procedure was not made sufficiently clear in my previous papers, and has led Tate and Palmer\* to suggest that my previous results contained large numbers of inelastically scattered electrons.

The glass work was of pyrex, and the whole apparatus up to within a few centimetres of the ground glass joints was baked out at a temperature of  $360^\circ \text{C.}$ , the joints being kept below room temperature by means of water coolers. The apparatus was connected through a liquid air trap to a diffusion pump backed by a Hyvac pump, and a good "sticking vacuum" was obtained on a sensitive McLeod gauge. During a run the pumps were kept going with no liquid air on the trap. The earth's magnetic field was neutralized by a single large coil set at right angles to the direction of the earth's field.

The current in the electron beam was measured by the galvanometer G. Beams of from 0.1 to 1.0 microamps were employed. Retarding potential curves showed that the homogeneity of the primary electron beam was good,

\* 'Phys. Rev.,' vol. 40, p. 731 (1932). This criticism has been answered by a recent letter, see Arnot, 'Phys. Rev.,' vol. 41, p. 838 (1932).

[illegible]

The results obtained over an angular range of from  $20^\circ$  to  $175^\circ$  for electrons having various energies between 2 volts and 200 volts are shown in figs. 3 and 4. The number at the side of each curve is the energy of the primary electron beam in volts.\* The curves have all been reduced to a common pressure and a common value for the intensity of the electron beam. The ordinates of both figures represent  $I_\theta$  in arbitrary units, where  $I_\theta$  is defined thus. If a beam of electrons passes through a gas containing  $N$  atoms per unit volume, then  $NI_\theta$  is the proportion of the beam elastically scattered in the direction  $\theta$  per unit solid angle and per unit length of the beam. The experimental points from which these curves have been drawn are given in Tables I to III.

Table II.

11.		12.		14.		16.		18.		20.	
$\theta^\circ$	$I_\theta$	$\theta^\circ$	$I_\theta$	$\theta^\circ$	$I_\theta$	$\theta^\circ$	$I_\theta$	$\theta^\circ$	$I_\theta$	$\theta^\circ$	$I_\theta$
24	340	19	263	21	230	21	217	21	182	21	152
29	201	24	151	26	117	26	93.5	26	72.5	26	60.0
34	99.0	29	83.0	31	54.1	31	42.7	31	30.0	31	23.6
39	58.0	34	47.0	36	31.3	36	24.6	36	18.8	36	14.8
44	37.0	39	29.2	41	21.0	41	17.6	41	14.8	41	14.1
49	21.5	44	21.2	46	15.0	46	15.1	46	15.2	46	16.0
54	17.8	49	15.4	51	11.6	51	12.0	51	14.1	51	16.1
59	15.8	54	12.7	56	9.60	56	11.7	56	13.6	56	15.7
64	14.7	59	12.1	61	9.80	61	11.4	61	12.9	61	14.9
69	13.9	64	11.4	66	8.95	66	10.2	66	11.4	66	13.6
74	12.9	69	10.7	71	8.70	71	8.70	71	9.35	71	10.1
79	12.3	79	10.4	81	7.37	81	6.87	81	6.55	81	5.78
89	12.4	89	10.5	91	7.50	91	6.87	91	6.20	91	5.60
99	12.2	99	10.0	99	7.04	101	7.48	101	7.28	101	7.00
109	10.6	109	9.00	109	6.73	111	6.58	111	6.95	111	7.08
119	10.0	119	8.08	119	5.95	123	5.30	118	5.62	121	5.90
129	9.7	129	7.41	129	6.38	133	6.12	128	5.02	128	4.95
139	11.0	139	8.80	139	9.22	143	12.0	138	7.48	138	7.50
149	15.8	149	12.8	149	16.2	153	21.4	148	14.80	148	15.8
159	39.5	159	18.8	159	26.1	163	28.5	158	26.0	158	28.9
164	66.5	164	24.8	169	28.7	168	27.9	168	30.3	168	33.8
169	34.7	169	50.0	174	62.8	173	79.5	173	34.2	173	42.5
174	12.7	174	35.4								

With the exception of the three upper curves for electrons of 10 volts, 11 volts and 12 volts, all the curves in fig. 3 have been displaced in a vertical direction to lessen overlapping. The base line for each curve is marked at the side of the figure. The three upper curves have the same baseline. In fig. 4 the curves have not been displaced at all.

\* The curves in fig. 3, reading from the top to the bottom of the figure, are in ascending order of electron energies.

Table III.

25.		30.		42.		82.		200.	
$\theta^\circ$ .	$I_\theta$ .	$\theta^\circ$ .	$I_\theta$ .	$\theta^\circ$ .	$I_\theta$ .	$\theta^\circ$ .	$I_\theta$ .	$\theta^\circ$ .	$I_\theta$ .
22	123	22	131	24	130	25	140	20	116
27	46.0	27	45.0	29	74.8	30	87.0	25	69.2
32	16.6	32	19.5	34	43.1	35	52.3	30	30.1
37	13.2	37	18.2	39	37.0	40	38.5	35	12.0
42	16.6	42	22.8	44	37.5	50	17.5	40	7.90
47	21.4	47	28.1	49	38.0	60	9.75	50	21.3
52	22.8	52	30.5	54	32.4	70	9.15	60	25.0
57	22.5	57	29.6	59	24.0	80	10.2	70	12.0
62	20.2	62	26.2	69	11.1	90	11.1	80	2.08
67	16.6	67	20.6	79	4.24	100	10.2	90	0.82
72	12.0	72	14.4	89	7.50	110	7.40	100	1.67
82	5.20	82	5.10	99	16.9	120	5.15	110	2.05
92	4.82	92	5.30	109	24.0	130	2.60	120	3.54
102	8.22	102	10.9	119	21.6	140	1.91	130	4.55
108	10.0	113	15.2	129	13.1	150	3.55	140	3.31
118	8.2	123	12.0	139	6.45	160	5.00	150	1.06
128	5.68	133	6.20	149	8.73	170	5.95	160	1.93
138	6.30	143	7.75	159	16.8	175	6.38	165	2.38
148	15.8	163	20.0	169	22.5			170	4.31
158	30.0	163	39.2	174	41.2			175	0.53
163	33.4	173	80.7						
168	40.7								
173	61.0								

The agreement between these results and the earlier results\* obtained over the angular range of  $18^\circ$  to  $126^\circ$  is quite satisfactory. The points shown as crosses on the 30-volt curve in fig. 3 are the experimental points for 30-volt electrons obtained in this earlier work. The most interesting feature of the new results is the strong backward scattering observed at angles near  $180^\circ$  for electrons having energies between about 50 volts and 10 volts. As the energy of the electrons is increased from 10 volts the maximum at  $140^\circ$  in the 10-volt curve moves out to larger angles, at first becoming higher and sharper, and then decreasing in height as it merges into the strong backward scattering at  $180^\circ$ . The two rudimentary maxima, which appear at about  $65^\circ$  and  $90^\circ$  in the 11-volt curve, gradually become more fully developed as the energy of the electrons is increased. Whereas the maximum at  $65^\circ$  moves in steadily to smaller angles, the peak at  $90^\circ$  at first moves out to larger angles until the electrons reach an energy of about 40 volts, after which it changes its direction and moves in steadily to smaller angles until it finally merges into the main

\* Arnot, 'Proc. Roy. Soc.,' A, vol. 130, p. 655 (1931).

peak at  $0^\circ$ . The change in the direction of movement of this peak at about 40 volts was observed and reported in my earlier work on mercury vapour.\*

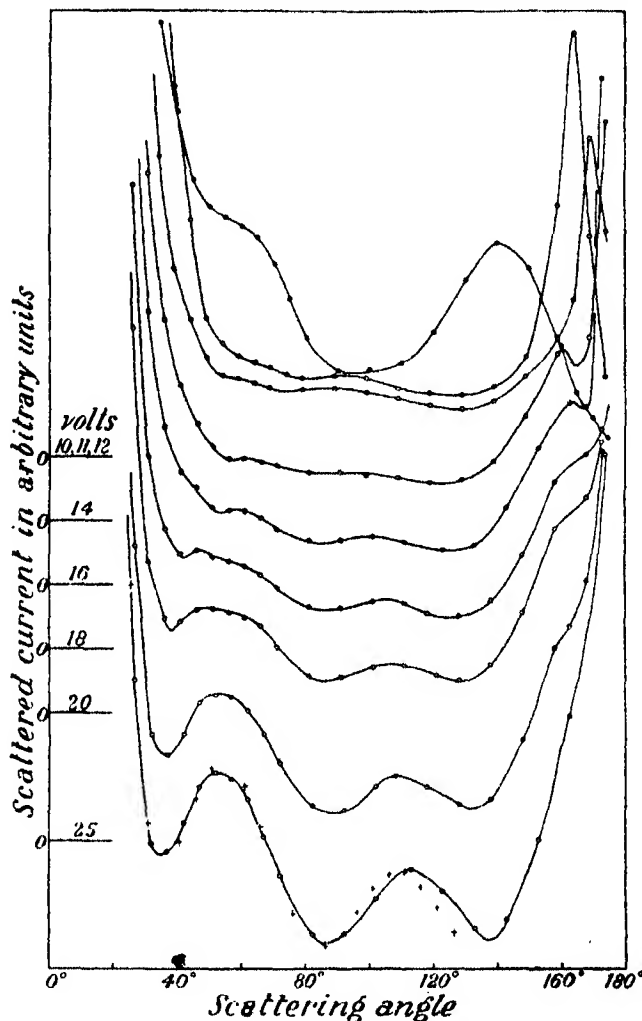


FIG. 3.—Angular distribution of elastically scattered electrons. Curves for 10, 11, 12, 14, 16, 18, 20, 25 and 30-volt electrons.

The 82-volt and 200-volt curves both show relatively little backward scattering. Henneberg† has recently calculated a scattering curve for electrons of

\* In the earlier work it was thought that this peak at first moved in to smaller angles, but this is not confirmed by the present, more detailed, work over this region of electron energies.

† Private communication. I am indebted to Dr. Henneberg for permission to mention these results.

203 volts. The general agreement between his theoretical curve and my experimental curve for 200-volt electrons is very satisfactory. The theoretical curve shows the three maxima found in the experimental curve, but in the

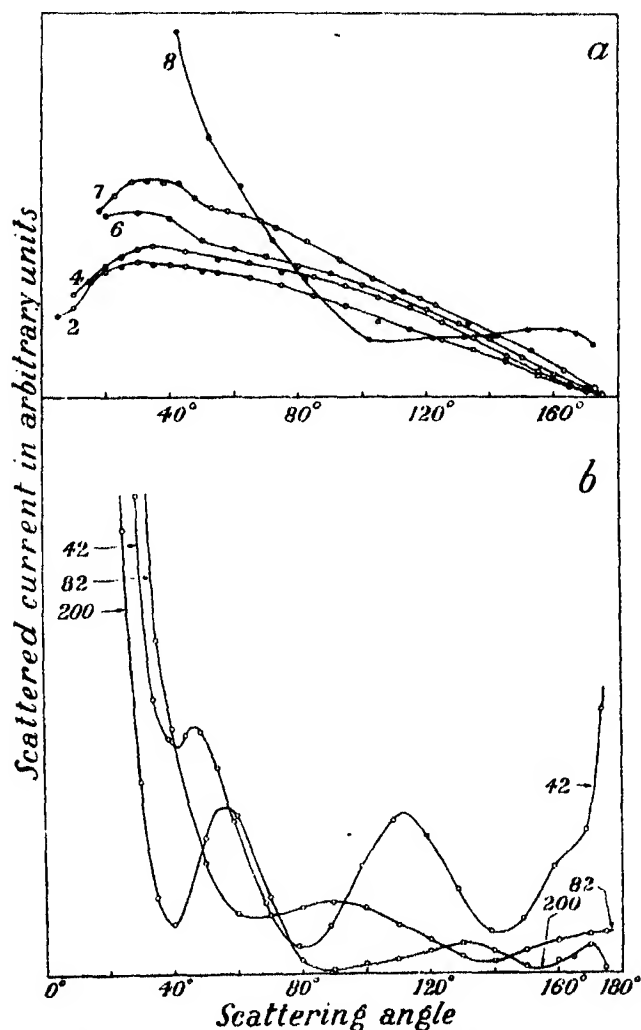


FIG. 4.—Angular distribution of elastically scattered electrons. (a) curves for 2, 4, 6, 7 and 8-volt electrons; (b) curves for 42, 82 and 200-volt electrons.

theoretical curve the maxima and minima are displaced towards smaller angles with respect to those of the experimental curve. Henneberg suggests that this effect may be caused either by neglecting the atomic shells in using the Thomas-Fermi field, or by neglecting the effect of polarization.

Considerable difficulty was experienced in getting the apparatus to work below the ionization potential. Although the intensity of the electron beam showed no appreciable diminution as the gun potential was changed from 11 volts to 8 volts, the intensity of the scattered current often fell off considerably. What was more serious, however, was that the scattered current at small angles appeared to decrease exponentially with time. It could always be brought back to its initial value by raising the gun potential above the ionization potential for a few seconds. This effect seems to indicate a charging up of a layer of grease, gas, or oxide on the slits of the receiving system, the charge being removed by the presence of positive ions. This explanation is supported by the fact that the scattered current was much larger, and did not vary with time, when the apparatus was heated to above 350° C. by the baking-out furnace. Unfortunately it was not possible to work the apparatus satisfactorily with the furnace on owing to the fact that the quartz insulation of the Faraday cylinder was not good when hot.

In view of these difficulties the results obtained for electrons of energy less than 10 volts are doubtful. They have, however, been included in fig. 4, as it is believed that they show in a general way the trend of the correct curves. It should be emphasized that the difficulties experienced with the working of the apparatus mentioned above only occurred below the ionization potential. Above 10 volts the apparatus gave no trouble at all.

The absorption curve for electrons in mercury vapour\* shows that the total effective cross-section of the mercury atom increases rapidly as the energy of the electrons is reduced below the ionization potential. It will be seen from the curves in fig. 4, however, that in spite of the increased scattering power of the atom, the total scattered current is less for 2-volt electrons than for 7-volt electrons. This apparent decrease in the total scattered current as the energy of the electrons is decreased from 7 volts to 2 volts is probably due to the rapid decrease in the effective area of the slits of the receiving system as the velocity of the electrons is reduced. It is notoriously more difficult to make slow electrons pass through slits than fast ones.

In conclusion, I should like to thank Professor H. S. Allen who, in spite of difficulties caused by a recent fire, has provided every facility for the carrying out of this work.

\* Brode, 'Proc. Roy. Soc.,' A, vol. 125, p. 134 (1929).



*Summary.*

The author's earlier work on the angular distribution of elastically scattered electrons in mercury vapour has been extended to larger angles and to lower electron energies. Results are given over an angular range of  $20^\circ$  to  $175^\circ$  for seventeen different values of the energy of the primary electron beam between 2 volts and 200 volts.

The results obtained above the ionization potential show several diffraction maxima and minima. The scattering curves for electrons having energies between the ionization potential and about 50 volts rise steeply at angles near  $180^\circ$ , showing that there is considerable backward scattering for electrons of these energies. Investigations are at present in progress with other gases and vapours.

---

*The Relation between Mean Atomic Volume and Composition in  
Silver-Zinc Alloys.*

By Professor E. A. OWEN, M.A., D.Sc., and LLEWELYN PICKUP, M.Sc.(London),  
Ph.D.(Wales), University College of North Wales, Bangor.

(Communicated by Sir William Bragg, O.M., F.R.S.—Received November 17,  
1932.)

[PLATE 2.]

The silver-zinc system is similar in many respects to the copper-zinc system. The latter has already been investigated in detail by X-ray precision methods, and it is desirable that similar data should be obtained concerning the silver-zinc system, so that a closer comparison, than has hitherto been possible, may be made between the two systems. In the present paper an account is given of a detailed study of the relation between the mean atomic volume and the composition of alloys in this system. Although the X-ray technique was in general the same as that employed in our previous investigations,\* an interesting experimental difficulty in connection with the preparation of the alloys was encountered at the outset of the work. When the alloys were prepared in the usual way by melting the one component in the other, it was impossible to obtain reflection lines on the photographic film, however carefully the alloys

\* 'Proc. Roy. Soc.,' A, vol. 137, p. 397 (1932); vol. 139, p. 526 (1933).

were annealed. To overcome the difficulty, it was found necessary to prepare the alloys by the process of inter-diffusion, a method hitherto but little used for the preparation of alloys for X-ray analysis. By this method we were able to investigate alloys in the silver-zinc system over the whole composition range. It is probable that the method may be of service in other connections and that the results recorded here may assist in suggesting its more general use.

### 1. Preparation of Alloys.

Five alloys, three in the pure  $\alpha$ -region and two in the  $(\alpha + \beta)$  region were prepared by adding a basis alloy (containing about 50 per cent. silver) to molten silver. Filings off these "as cast" ingots were annealed at 300° C. and 600° C. Only the alloy containing about 94 per cent. silver gave reflection lines, which showed practically identical parameter values, 4.039<sub>5</sub> Å. at 300° C., and 4.039<sub>5</sub> Å. at 600° C.; as compared with 4.077<sub>3</sub> Å. obtained for pure silver. The absence of reflection lines with the other four alloys was thought at first to be due possibly to non-homogeneity caused by insufficient annealing. The ingots were therefore annealed in lump form (about 1 c.c.) at 500°–550° C. for about 500 hours. Filings taken off two of these alloys (94 and 86 per cent. silver) were further annealed *in vacuo* at 600° C. for 1½ hours. Again no reflection lines were registered by the latter alloy. The absence of reflection lines after this annealing treatment could only be explained by the presence of lattice distortion, which was not eliminated by the annealing given. These observations inclined us to the view that there exists a certain type of distortion which is very difficult to remove by simple annealing, and which is different from that produced by cold work, such as filing. Westgren and Phragmen\* make the following statement concerning the silver-zinc and the gold-zinc alloys: "it was considered useless to take precision photograms of the  $\alpha$  Ag-Zn and  $\alpha$  Au-Zn alloys, as their interferences were found to be very cloudy. The real cause of this diffuseness of the lines still remains to be unravelled." We have not seen any attempt to explain this difficulty in subsequent papers.

The introduction of zinc atoms into the copper lattice increases the parameter, while their introduction into the silver lattice decreases the parameter, as shown by the data from Debye-Scherrer powder photographs. The thermal contraction of the lattice over a long range of temperature when cooling from the molten state, intensified by the contraction due to the entry of zinc into the

\* 'Phil. Mag.', vol. 50, p. 320 (1925).

silver lattice, was considered as a possible cause of the distortion which is not removable by simple annealing. To test this, attempts were made to diffuse the zinc into silver at a temperature much below the latter's melting point (*ca.* 963° C.). After some preliminary experiments it was found that by heating a mixture of filings of silver and of zinc (25 per cent. zinc) at 430°–440° C. for 20 hours in evacuated glass tubes, distinct changes in the appearance of the mixture were noted. The mass "coked" slightly, but was easily broken up. After being thoroughly crushed and mixed in an agate mortar, it was re-annealed at 300°–320° C. for 46 hours. Precision photographs showed a resolved doublet, which gave a parameter value of 4.012 Å., compared with 4.077<sub>3</sub> Å. for pure silver. Direct proof was therefore obtained of the diffusion of zinc into silver at a comparatively low temperature. A mixture of copper and zinc filings was similarly prepared and treated, when their inter-diffusion also was observed. From such experiments two conclusions were possible:—

- (1) The diffusion of zinc into silver and into copper takes place, at least in reasonable time, when the temperature of diffusion is above that of the melting point of zinc, but much below the melting point of silver or of copper.
- (2) In the diffusing process, the phases are produced in order from the zinc-rich end. Therefore shells of highly concentrated zinc alloys are at first produced locally around nuclei of copper, but although these shells become solid, an even distribution of zinc throughout the whole mass takes place by solid interdiffusion after sufficient time. The final phase or phases produced depend on the composition of the initial mixture.

For the present purposes, it was necessary to determine the treatment for complete interdiffusion in the samples. At this stage, the relation between the composition and parameter value of the silver-zinc alloys was unknown, so that "pilot" mixtures of copper-zinc filings were treated, since the parameter values of these latter alloys and their corresponding composition were available.\* It was assumed, and afterwards confirmed, that the copper-zinc pilot mixtures were satisfactory criteria of complete interdiffusion. Table I gives a set of results obtained by heating a 70 per cent. copper-zinc mixture at 450°–470° C. for different times. The composition given in the last column is derived from the parameter value by means of the known relation between the  $\alpha$ -phase composition and its parameter value.

\* Owen and Pickup, 'Proc. Roy. Soc.,' A, vol. 137, p. 397 (1932).

Table I.

	Temperature.	Time of diffusion hours.	Parameter.	Composition per cent. copper.
Composition of mixture by chemical analysis, 69.5 per cent. Cu.	° C. 450-470 450-470 450-470	18 36 42	A. 3.692 <sub>3</sub> 3.678 <sub>4</sub> 3.676 <sub>1</sub>	62.1 68.6 69.4

About 42 hours' heating at 450°-470° C. was therefore considered sufficient to produce almost complete diffusion in a 70 per cent. mixture; about 20 hours at this temperature were found to be sufficient for a 30 per cent. mixture. Further, it was not found necessary to anneal the mixtures at a low temperature after breaking them up, after diffusion, to remove any cold work, provided the breaking up was carried out gently.

A range of silver-zinc mixtures was next prepared from 100 down to about 30 per cent. silver, and these were heated to effect complete diffusion at about 470° C. for times varying from 50 to 20 hours, according to the data obtained from the pilot mixtures of copper-zinc filings. Good reflection lines were registered by these mixtures, which were now silver-zinc alloys, so that the large contraction of the silver lattice, due to both the thermal and the solubility effects, is most probably the cause of the lattice distortion observed in these alloys when prepared by the usual melting process. With a 50 per cent. silver alloy, both the "diffusion" alloy and the "melted" alloy gave identical  $\gamma$ -phase parameter values. It was therefore possible to prepare by diffusion alloys of a predetermined composition with accuracy. Below about 20 per cent. silver, the presence of so much zinc caused the diffused mass to become too hard to break up, so that the alloys below this composition were made by the ordinary melting method and no difficulty was encountered in obtaining satisfactory reflection lines with these alloys. A more complete investigation of the interdiffusion of metals, on the lines indicated here, has been made,\* and an account of this is now being prepared for publication.

## II. The Determination of Mean Atomic Volumes.

It was decided to study the relation of mean atomic volume to composition at 380° C., since at this temperature no semi-liquid regions are encountered

\* 'Nature,' vol. 130, p. 201 (1932).

across the whole system. All alloys were therefore broken up gently after diffusion, annealed at 380° C. in evacuated glass tubes, and air-cooled.

For brevity, alloys are referred to by their silver content in per cent. by weight, for example, alloy (66). For reference purposes, a reproduction of the Ag-Zn thermal diagram from the "International Critical Tables" is given in fig. 1.

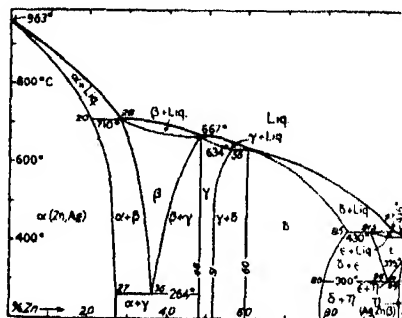


FIG. 1.

In Table II the experimental results obtained for the  $\alpha$ -phase are given for different compositions. Fig. 2, Plate 2, is a reproduction of the photographs obtained.

Table II.— $\alpha$ -phase.

Face-centred cubic. Mean atomic volume =  $a^3/4$ . Annealing temperature, 380° C.

Per cent. silver.		Para-meter.	Mean atomic volume $\times 10^{24}$ .	Per cent. silver.		Para-meter.	Mean atomic volume $\times 10^{24}$ .
By weight.	Atomic.			By weight.	Atomic.		
100	100	A.	cm. <sup>3</sup>	75	64.5	A.	cm. <sup>3</sup>
95	92.1	4.077 <sub>3</sub>	16.946	70	58.6	4.003 <sub>9</sub>	16.047
85	77.5	4.062 <sub>3</sub>	16.758	66	54.1	4.003 <sub>3</sub>	16.040
		4.035 <sub>3</sub>	16.431				

Cu radiation-reflecting planes, (422) and (511).

The  $\alpha$ -phase lines in alloy (66) were very faint, owing to the nearness of the pure  $\beta$ -region. Whereas both this and alloy (70) are in the  $(\alpha + \beta)$  region, and should therefore contain a considerable amount of the  $\beta$ -phase, no  $\beta$ -phase reflection lines were shown.

A further series of alloys were then prepared by diffusion having the compositions 64, 62, 60, 58, 55, and 52 per cent. silver by weight. All these were annealed at 380° C. The first of these gave reflection lines too faint for

measurement. The absence of good reflection lines from the  $\beta$ -phase was attributed to the change of  $\beta$  into  $(\alpha + \gamma)$  at about  $264^\circ \text{C.}$ , see fig. 1, and to the possibility that the cooling down from  $380^\circ \text{C.}$  was not drastic enough to retain the  $(\alpha + \beta)$  structure. Alloy (60) was heated to  $500^\circ \text{C.}$  for 1 hour in an evacuated silica tube and quenched in iced-water. Again no reflection lines were obtained suitable for measurement. That the absence of lines was owing to the change of  $\beta$  into  $(\alpha + \gamma)$ , and not to the diffusion method itself, was shown by alloy (52), in the pure  $\gamma$ -region which gave satisfactory reflection lines. It was therefore concluded that to obtain the necessary precision photographs of the  $\beta$ -phase at  $380^\circ \text{C.}$ , the sample must be maintained at this temperature during the actual exposure. For Debye-Scherrer powder photographs, quenched samples probably do contain sufficient  $\beta$ -phase to give reflection lines of small glancing angles, but the accuracy of parameter measurements from such samples is too low for the present requirements. For these reasons, the  $\beta$ -phase could not be studied satisfactorily at this stage, and the work was resumed on the other phases.

Six alloys in the  $\gamma$ -region were made by diffusion, with silver contents of 55, 52, 49, 46 and 42 per cent. by weight. This phase has a body-centred cubic lattice containing 52 atoms to the unit cell. The experimental data from these six alloys are contained in Table III.

Table III.— $\gamma$ -phase. Body-centred cubic. Mean atomic volume =  $a^3/52$ .  
Annealing temperature,  $380^\circ \text{C.}$

Per cent. silver.		Para- meter.	Mean atomic volume. $\times 10^{24}$ .	Per cent. silver.		Para- meter.	Mean atomic volume $\times 10^{24}$ .
By weight.	Atomic.			By weight.	Atomic.		
55	42.5	A. 9.348 <sub>1</sub>	cm. <sup>3</sup> 15.710	49	36.7	A. 9.318 <sub>6</sub>	cm. <sup>3</sup> 15.558
52	39.7	9.333 <sub>9</sub>	15.643	46	34.1	9.316 <sub>7</sub>	15.552
50	37.6	9.322 <sub>3</sub>	15.580	42	30.5	—	—

Cu radiation-reflecting planes, (965), (11.32) and (11.50).

The reflections registered by alloy (55) were very faint and only those from the (11.50) planes were found to be measurable. This was considered to be caused by the presence of the  $\beta$ -phase. The accuracy of the parameter value was therefore in some doubt, especially as the value obtained did not conform to that expected from the  $(\beta + \gamma) - (\gamma)$  boundary of the thermal diagram, fig. 1. Further diffusion alloys were therefore made containing 56 and 53.4

per cent. silver by weight, so as to obtain, if possible, better reflection lines, and hence a more accurate parameter value. Of these two alloys, the former gave no measurable reflection lines, while those of the latter were very faint and could not be measured with great accuracy. They gave, however, a mean parameter value of  $9.345\text{\AA}$ . (mean atomic volume,  $15.697 \times 10^{-24} \text{ cm.}^3$ ), which being slightly greater than that of alloy (55), shows that both these alloys are in the pure  $\gamma$ -region. Consequently the  $(\beta + \gamma) - (\gamma)$  boundary in fig. 1 requires some modification. The alloy (42) gave no  $\gamma$ -phase reflections but a strong doublet from the  $\delta$ -phase.

To study the  $\delta$ -phase, six alloys were made by diffusion, containing 40, 30, 20, 17, 15 and 12 per cent. silver by weight. Of these, the last three could not be used as they were too hard to break up after diffusion owing to their high zinc content. Alloys representing these compositions were therefore made by the usual melting method, using a 50 per cent. basis alloy and adding zinc. It was also found better to prepare the alloys containing 40 and 30 per cent. silver, by diffusing the mixtures at a lower temperature, about  $440^\circ \text{ C.}$ , for similar reasons.

The  $\delta$ -phase registered, in general, three doublets, but these were towards the outside of the film, and in a poor position for accurate measurement. Taking approximate values\* for the base side  $a$  and the axial ratio  $c$  of the close-packed hexagonal lattice of this phase, these doublets were found to be from the  $(21\bar{3}3)$ ,  $(30\bar{3}0)$  and  $(20\bar{2}4)$  planes. In order to register, if possible, reflections in more favourable positions on the film, a cobalt anticathode was tried. While its use did not produce the desired result, reflection lines from other planes were registered, fig. 3, Plate 2. By combining the data from both anticathodes (Cu and Co) for each alloy, accurate values for  $a$  and  $c$  were obtained. These data are collected in Table IV for comparison.

Considering that the positions of the reflection lines were not in the positions for the highest accuracy possible, the agreement was considered satisfactory, and the values of the mean atomic volume obtained from the means of  $a$  and  $c$  in each case, are probably very near the true values.

To calculate these hexagonal parameter values the usual formula

$$a = \lambda \frac{\sqrt{\frac{4}{3}(h^2 + hk + k^2) + \frac{l^2}{c^2}}}{2 \sin \theta} \quad (1)$$

was used. The values of  $a$  and  $c$  were derived in the following manner:—

\* See Elam, 'J. Inst. Met.', vol. 41, p. 329 (1929).

- (i) With copper radiation, the (30 $\bar{5}$ 0) planes were used to obtain a value for  $a$  directly, and this value was substituted in the formula to calculate  $c$  from the (21 $\bar{5}$ 3) planes ;
- (ii) With cobalt radiation, the (21 $\bar{5}$ 0) planes were used to obtain a value for  $a$  directly, and this value was substituted in the formula to calculate  $c$  from the (21 $\bar{5}$ 1) planes.

Table IV.— $\delta$ -phase. Close-packed hexagonal. Mean atomic volume =  $\sqrt{3} \cdot a^2 c / 4$ . Annealing temperature, 380° C.

Per cent. silver.		Radiation used.	Parameter.		Mean Atomic volume $\times 10^{24}$ .
By weight.	Atomic.		$a$ in Å.	$c$ .	
46	34.1	Cu	2.819 <sub>2</sub>	1.587	cm. <sup>3</sup> 15.403
		Co	2.819 <sub>2</sub>	1.588	
42	30.5	Cu	2.819 <sub>0</sub>	1.582	15.348
		Co	2.818 <sub>5</sub>	1.583	
40	28.8	Cu	2.819 <sub>1</sub>	1.579	15.312
		Co	2.818 <sub>2</sub>	1.578	
30	20.6	Cu	2.816 <sub>5</sub>	1.564	15.112
		Co	2.815 <sub>7</sub>	1.561	
20	13.2	Cu	2.811 <sub>8</sub>	1.556	14.948
		Co	2.811 <sub>6</sub>	1.549	

To obtain data of the phases in alloys below 20 per cent. silver, it was necessary to prepare these alloys by the usual melting process as already mentioned. The three alloys made, gave by chemical analysis\* the compositions 15.6, 9.7, and 5.2 per cent. silver by weight. Although copper radiation gave reflection lines of the  $\delta$ -phase from the first two alloys, nickel radiation was used to investigate these alloys, since it had previously been found to give good reflection lines from pure zinc in favourable positions on the film. It was found satisfactory for reflections from the  $\delta$ -,  $\epsilon$ - and  $\eta$ -phases, which are present at these compositions.

It will be seen in fig. 1 that the  $\epsilon$ -phase changes into ( $\delta + \eta$ ) on cooling through 300° C., so that there were ( $\delta + \eta$ ) and ( $\eta$ ) regions below, and ( $\delta + \epsilon$ )

\* Our thanks are due to Dr. P. J. Durrant for a private communication giving the working details of a "Tartrazine Indicator" method (Berry and Durrant, 'The Analyst,' vol. 55, p. 613 (1930)), which was modified slightly for our particular purposes.



and ( $\epsilon$ ) above, this temperature. The parameter values of the  $\delta$ - and  $\epsilon$ -phases found when the alloys were annealed at 380° C. are given in Table V.

Table V.— $\delta$ - and  $\epsilon$ -phases. Close-packed hexagonal. Mean atomic volume =  $\sqrt{3} a^2 c/4$ . Annealing temperature, 380° C.

Per cent. silver.		$\delta$ -phase.			$\epsilon$ -phase.		
By weight.	Atomic.	$a$ .	$c$ .	Mean atomic volume.	$a$ .	$c$ .	Mean atomic volume.
15.6	10.2	2.804 <sub>7</sub>	1.566	$\times 10^{24}$ cm. <sup>3</sup> 14.959	—	—	—
9.7	6.3	2.805 <sub>8</sub>	1.564	14.959	2.699 <sub>8</sub>	1.765	15.039
5.7	3.2	—	—	—	2.688 <sub>5</sub>	1.791	15.067
Pure zinc	—	—	—	—	2.659 <sub>2</sub>	1.856	15.111

Ni radiation,  $\delta$ -phase, (11 $\bar{2}$ 4), (21 $\bar{3}$ 2) doublets, (21 $\bar{3}$ 3)  $\beta$ .  
 $\epsilon$ -phase, (21 $\bar{3}$ 1), (20 $\bar{2}$ 4) doublets, (21 $\bar{3}$ 3)  $\beta$ .

Since none of the reflecting planes were of the form ( $hki0$ ) a value for  $a$  could not be calculated directly. By substituting in turn a set of values of  $h$ ,  $k$ ,  $l$  and  $\theta$  for each of two reflection lines from the same photograph in equation (1) and equating the right-hand side, a value for  $c$  was obtained. In this way each pair of reflections gave a value for  $c$ ; whence a mean value for  $c$  was found to give the most consistent values for  $a$  from all the reflection lines registered by one phase on the same photograph. The consistency of  $a$  attainable with a suitably chosen value of  $c$  for each of the  $\delta$ - and  $\epsilon$ -phases is shown in Table VI for one alloy.

The  $\eta$ -phase being present only below 300° C., was obtained by heating filings from these last three alloys first to 380°–400° C. for 3 hours and, after allowing them to cool down slowly to about 275° C., the heating was maintained at this lower temperature for 48 hours. After a series of precision photographs had been taken, these samples were again heated at 275° C. for a further 24 hours, and rephotographed. No further change had taken place after the second 24 hours' annealing, while the distribution of lines was different from that given by these alloys after annealing at 380° C. It was therefore assumed that annealing at 275° C. had produced the  $\delta$ - and  $\eta$ -phases stable at this temperature.

The method of analysis of these photographs was the same as that described for the photographs representing the 380° C. treatment. The results are contained in Table VII.

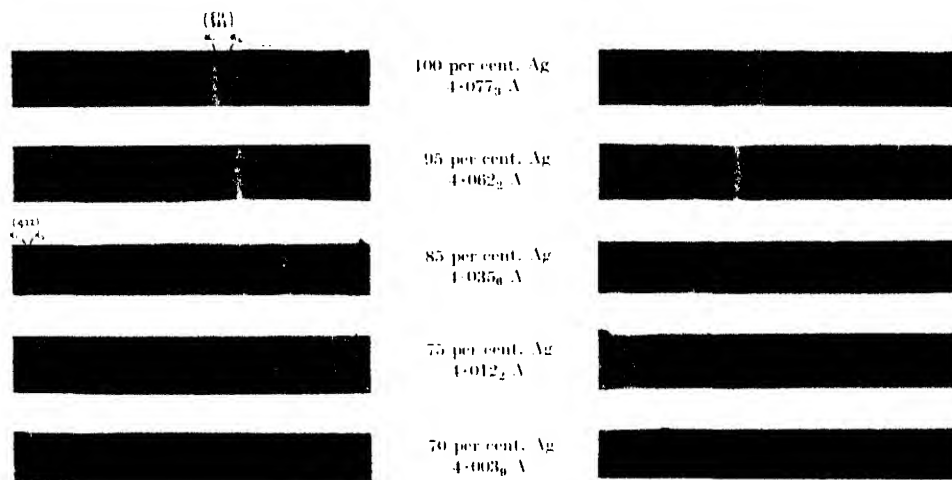


FIG. 2.—Showing change in  $\alpha$ -phase parameter (copper radiation).

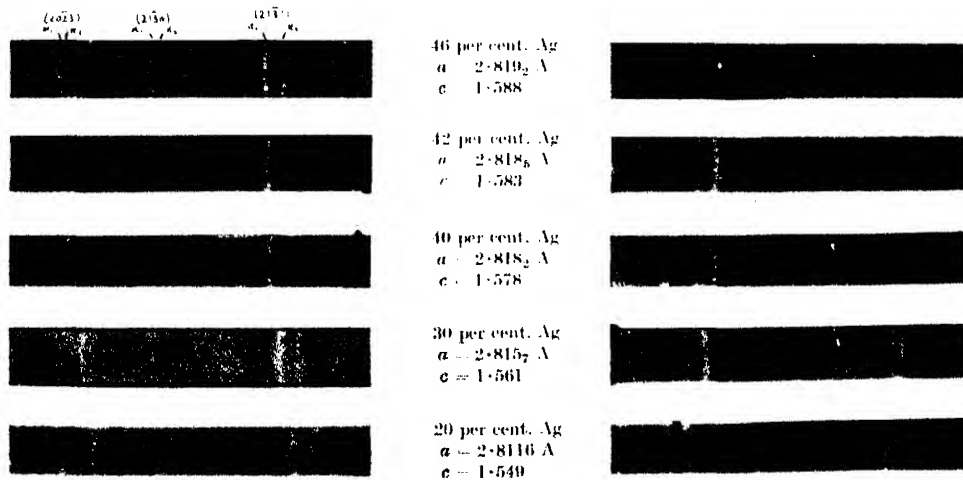


FIG. 3. Showing change in  $\delta$ -phase parameter (cobalt radiation).



Table VI.—Ag-Zn alloy, 9.7 per cent. silver by weight. Sample annealed at 380° C. for 5 hours. Nickel radiation.

$\pi/2 - \theta$ ( $\theta$ = Bragg glancing angle).	Phase.	Reflection planes.	$\lambda$ .	Base side $a$ in Å.	
				$\delta$ -phase $c = 1.564_0$ .	$\epsilon$ -phase $c = 1.765_3$ .
17 47 17 24	$\epsilon$	21 $\bar{1}$ 1	$a_1$ $a_2$		2.699, 2.699,
16 47 16 21	$\delta$	11 $\bar{2}$ 4	$a_1$ $a_2$	2.805, 2.805,	
15 43	$\delta$	21 $\bar{3}$ 3	$\beta$	2.805,	
14 13	$\epsilon$	21 $\bar{3}$ 3	$\beta$		2.699,
12 25 11 51	$\delta$	21 $\bar{3}$ 2	$a_1$ $a_2$	2.805, 2.806,	
7 28 6 30	$\epsilon$	20 $\bar{2}$ 4	$a_1$ $a_2$		2.699, 2.699,

## Mean Values.

	$\delta$ -phase.	$\epsilon$ -phase.
$a$	2.805, Å°	2.699, Å°
$c$	1.564	1.765
Atomic volume .....	$14.959 \times 10^{-24}$ cm. <sup>3</sup>	$15.039 \times 10^{-24}$ cm. <sup>3</sup>

Table VII.— $\delta$ - and  $\eta$ -phases. Close-packed hexagonal. Mean atomic volume =  $\sqrt{3} a^2 c / 4$ . Annealing temperature, 275° C.

Per cent. silver.		$\delta$ -phase.			$\eta$ -phase.		
By weight.	Atomic.	$a$ .	$c$ .	Mean atomic volume.	$a$ .	$c$ .	Mean atomic volume.
15.6	10.2	2.808,	1.560	$\times 10^{24}$ cm. <sup>3</sup> 14.973	—	—	$\times 10^{24}$ cm. <sup>3</sup> —
9.7	6.3	2.808,	1.561	14.977	2.685,	1.798	15.070
5.7	3.2	—	—	—	2.685,	1.795	15.063
Pure zinc	—	—	—	—	2.659,	1.856	15.111

The data which have been given in the preceding tables are plotted in fig. 4. The mean atomic volume of both phases in all the mixed regions are shown to be constant. In the pure phase regions,  $\alpha$ ,  $\gamma$  and  $\delta$ , it becomes less as the zinc content increases. Only in the  $\epsilon$ -phase (stable above 300° C.) does the mean atomic volume show an increase with increasing zinc content.

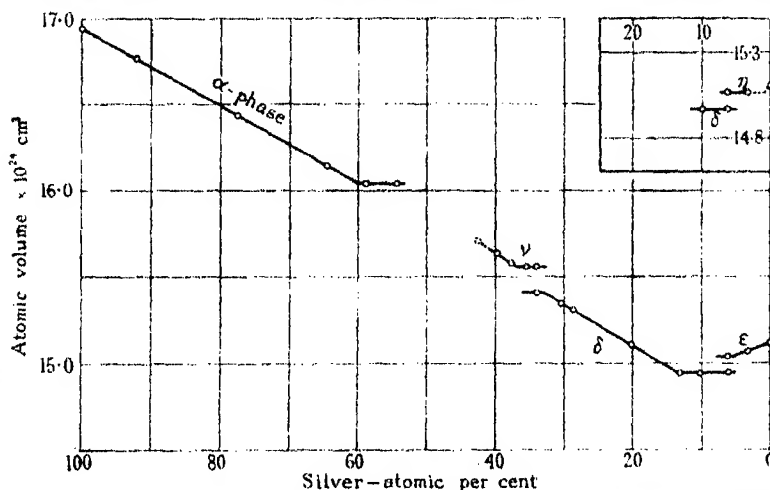


FIG. 4.—Annealing temperature, 380° C.; inset annealing temperature, 275° C.

From fig. 4 the phase boundaries at 380° C. can be obtained approximately and their values are given in Table VIII, together with readings taken from the thermal diagram in fig. 1.

Table VIII.—Approximate phase boundaries at 380° C.

Boundary.	Per cent. silver.		Reading (per cent. by weight) I.C.T. diagram, fig. 1.
	By weight.	Atomic.	
$\alpha - (\alpha + \beta)$	71.2	60.0	78.5
$(\gamma) - (\gamma + \delta)$	49.1	38.9	49.0
$(\gamma + \delta) - (\delta)$	44.7	32.9	40.0
$(\delta) - (\delta + \epsilon)$	20.4	13.4	17.4
$(\delta + \epsilon) - (\epsilon)$	8.8	5.5	7.2

Although the boundary readings given by the X-ray data are only taken to be approximate, it is considered that these values are probably as near the true values as those read off from fig. 1.

For each of the three pure phases,  $\alpha$ ,  $\gamma$  and  $\delta$ , the rate of decrease of atomic volume with atomic composition is practically the same, suggesting the same

form of packing. Assuming the linear relation shown, the decrease in the mean atomic volume when a zinc atom replaces a silver atom is almost identical with the increase when a zinc atom replaces a copper atom in the  $\alpha$ -,  $\beta$ - and  $\gamma$ -phases of the copper zinc alloy system. See Table IX.

Table IX.

Silver-Zinc Alloys.		Copper-Zinc Alloys.	
Phase.	Decrease in mean atomic volume when a zinc atom replaces a silver atom.	Phase.	*Increase in mean atomic volume when a zinc atom replaces a copper atom.
$\alpha$	$0.022 \times 10^{-24} \text{ cm.}^3$	$\alpha$	$0.022 \times 10^{-24} \text{ cm.}^3$
$\gamma$	0.02	$\beta$	0.025
$\delta$	0.024	$\gamma$	0.022

\* See Owen and Pickup, 'Proc. Roy. Soc.,' A, vol. 140, p. 179 (1933).

If the packing of the zinc atom in all these phases is the same, then approximately the mean space occupied by the silver atom is as much greater than that occupied by the zinc atom, as the space occupied by the copper atom is less.

Taking the mean atomic volumes of copper and silver to be  $11.741$  and  $16.946 \times 10^{-24} \text{ cm.}^3$  respectively, then the mean of these two values, namely,  $14.344 \times 10^{-24} \text{ cm.}^3$ , is roughly the space occupied by the zinc atom in all these phases. As the mean atomic volume found from pure zinc is  $15.111 \times 10^{-24} \text{ cm.}^3$ , the zinc atom appears to occupy less space by about 5 per cent. when alloyed in these phases than it does in the pure metal.

The constant mean atomic volume of the  $\delta$ -phase is slightly greater at  $275^\circ \text{ C.}$  in the  $(\delta + \eta)$  region than it is at  $380^\circ \text{ C.}$  in the  $(\delta + \epsilon)$  region. This is consistent with the general form of the boundary between the pure  $\delta$ -region and these two mixed regions, as shown in fig. 1. From the data in fig. 4 it is found that the  $(\delta) - (\delta + \epsilon)$  boundary at  $380^\circ \text{ C.}$  is at 20.4 and that the  $(\delta) - (\delta + \eta)$  boundary at  $275^\circ \text{ C.}$  is at 22.5 per cent. by weight.

In Table X the changes in the base side  $a$  and in the height  $ac$  with composition, are shown for the hexagonal lattices of the  $\delta$ -,  $\epsilon$ - and  $\eta$ -phases.

The change in the dimensions of the elementary cell in the  $\delta$ -phase at  $380^\circ \text{ C.}$  is mostly due to the change which takes place in the height; also the height of the  $\epsilon$ -phase cell changes more than the base side at this temperature. At  $275^\circ \text{ C.}$  the change in the dimensions of the  $\eta$ -phase cell is due chiefly to the change in height, though this is not as marked as in the  $\delta$ -phase at  $380^\circ \text{ C.}$

Table X.

Temperature.	Phase.	Per cent. silver.		Base a. (A.)	Axial ratio c.	Height ac. (A.)
		By weight.	Atomic.			
°C  380	δ	46	34.1	2.819 <sub>2</sub>	1.588	4.477
		42	30.5	2.818 <sub>2</sub>	1.583	4.462
		40	28.8	2.818 <sub>7</sub>	1.579	4.451
		30	20.6	2.816 <sub>1</sub>	1.563	4.402
		20	13.2	2.811 <sub>7</sub>	1.553	4.367
		15.6	10.2	2.804 <sub>7</sub>	1.566	4.392
		9.7	6.3	2.805 <sub>2</sub>	1.564	4.388
	ε	9.7	6.3	2.699 <sub>2</sub>	1.765	4.765
		5.2	3.2	2.688 <sub>5</sub>	1.791	4.815
		0.0	0.0	2.659 <sub>2</sub>	1.856	4.935
275	δ	15.6	10.2	2.808 <sub>2</sub>	1.560	4.382
		9.7	6.3	2.808 <sub>1</sub>	1.561	4.381
	η	9.7	6.3	2.685 <sub>1</sub>	1.798	4.828
		5.2	3.2	2.685 <sub>2</sub>	1.795	4.821
		0.0	0.0	2.659 <sub>2</sub>	1.856	4.935

In Table XI a comparison is made of the change in the dimensions of the hexagonal lattices present in the copper-zinc and silver-zinc alloy systems.

Table XI.

System.	Phase.*	Change in height with increasing base side.
Cu-Zn	ε	Increases in (ε + η), decreases in (γ + ε).
Ag-Zn	δ	Increases in (δ + γ), decreases in (δ + ε).
Cu-Zn	η	Decreases in the pure η-region.
Ag-Zn	ε	Decreases in the pure ε-region.
Cu-Zn	ε	Increases in the pure ε-region.
Ag-Zn	δ	Increases in the pure δ-region.

\* This is the nomenclature adopted in the International Critical Tables.

The packing of atoms in the hexagonal units appears to be different in the different phase units of one alloy system; and there appears to be analogous packing in the other alloy system. In comparing the observations, the "size" of the zinc atom is taken to be less than that of the silver and greater than that of copper. From these observations it would appear that a more detailed X-ray investigation on the present lines would help considerably the study of the different forms of packing, and also the orientation of the "polar" zinc atom in these hexagonal lattice units.

*Conclusions.*

When samples of alloys are required in a powder form, these can, for certain alloy systems, be prepared accurately by the interdiffusion of the two metals by heating mixtures of them, at a comparatively low temperature. The interdiffusion of copper and zinc, and silver and zinc, can be brought about by heating mixtures to 450°–470° C. for about 50 hours *in vacuo*. This temperature is just above the melting point of zinc.

Since the zinc atom occupies less space than the silver atom, the contraction of the silver lattice produced by the solution of zinc in it, causes lattice distortion, in addition to the thermal contraction on cooling. This distortion is such that the usual annealing is not sufficient to remove it from the planes having small spacing, which give the reflection lines in the precision camera. It is concluded therefore that this distortion is somewhat different from that produced by cold work, such as filing, as this can be eliminated by simple annealing.

The change from  $\beta$  to  $(\alpha + \gamma)$  at 264° C., or the distortion brought about by it, could not be sufficiently prevented by rapid quenching from above this temperature, to enable reflection lines to be registered by the  $\beta$ -phase.

The mean atomic volume of the pure phases,  $\alpha$ ,  $\gamma$  and  $\delta$ , becomes less with increasing zinc content, indicating a closer packing than that calculated by simple substitution. The effective packing space of the zinc atom is therefore less when alloyed with silver ( $\alpha$ -,  $\gamma$ - and  $\delta$ -phases) and with copper ( $\alpha$ -,  $\beta$ - and  $\gamma$ -phases) than that in the pure state.

Only in the  $\epsilon$ -phase (stable above 300° C.) was the mean atomic volume found to increase with increasing zinc content.

As in the copper-zinc system, the mean atomic volume at a constant temperature changes with composition in the pure regions whilst that of both phases in the mixed regions remains constant. These results form the basis of the determination of the positions of phase boundaries by the X-ray precision method. At 380° C. the boundaries in fig. 1 are roughly confirmed by the data in fig. 4, while the form of the pure  $\delta$ -boundary adjoining the  $(\delta + \eta)$  region at 275° C. and the  $(\delta + \epsilon)$  region at 380° C. is corroborated by the X-ray data.

The analogy between the silver-zinc and copper-zinc systems is perhaps best brought out by the comparison of the changes in the dimensions of the hexagonal lattice units of these two systems. Further investigation on these units would probably yield more specific data about the way in which zinc atoms pack with reference to their orientation.



We again express our thanks to the Royal Society for a grant which enabled us to carry out this work.

*Summary.*

(1) A study has been made of the mean atomic volumes of the different phases in the silver-zinc alloy system by means of the X-ray precision camera, for a temperature of 380° C.

(2) To make alloys in the  $\alpha$ -phase region it was necessary to make diffusing mixtures of silver and zinc particles at about 450° C. The "as cast" alloys in this region gave no reflection lines owing to lattice distortion. As a result of the  $\beta$ -phase transforming into  $(\alpha + \gamma)$  at 264° C., no reflection lines of the  $\beta$ -phase could be obtained by quenching alloys from above this temperature.

(3) The mean atomic volume in pure phases, at a constant temperature, changes almost linearly with composition, becoming less in the  $\alpha$ -,  $\gamma$ - and  $\delta$ -regions with increasing zinc content. In the mixed regions, it remains constant for both phases.

(4) Phase boundaries have been determined approximately; they are in general agreement with those at present accepted for the silver zinc system at 380° C.

(5) From a preliminary study of the hexagonal lattice units ( $\delta$ ,  $\epsilon$  and  $\eta$ ) and a comparison of these with the hexagonal lattices of the Cu-Zn system, the analogy between the two systems is shown.

---

*The Electrical Properties of Soil for Alternating Currents at Radio Frequencies.*

By R. L. SMITH-ROSE, D.Sc., Ph.D., A.M.I.E.E. (The National Physical Laboratory).

(Communicated by E. V. Appleton, F.R.S.—Received November 22, 1932.)

1. *Importance of Knowledge of Electrical Properties of Soil in Physics and Electrical Engineering.*

A knowledge of the electrical properties of the ground is of importance in connection with several branches of physics and engineering. A complete study of soil physics, for example, should take account of the electrical, as well as of the other physical properties. In geodetic survey work, particularly when prospecting for oil and minerals, increasing use has been made during recent years of electrical methods, which depend for their success upon a detailed knowledge of the electrical conductivity of the materials of the earth. For the protection of electrical generating plant and distribution networks, it is necessary to provide adequate earth connections at specific points and to ensure that these connections are made in such a manner that their electrical resistance is very small. Similar considerations apply to radio transmitting and receiving stations using earthed aerial arrangements, where it is desirable to make the resistance of the earth connections as low as possible.

Apart from these matters, an accurate and detailed knowledge of the electrical properties of the earth's surface has become necessary in connection with the recent growth of radio communication. Until a few years ago, the main object was to obtain communication over comparatively great distances and on long wave-lengths, when the effect of the earth was not of major importance, but the progress during the past ten years has been such that the effect of the earth is now more obvious. In the majority of broadcasting systems, for example, the service area is generally that covered by radiation transmitted directly along the ground, and the decrease of field intensity with distance is controlled by the electrical properties of the earth. Furthermore, with the widespread use of short wave-lengths for communication, the design of both transmitting and receiving antenna systems is seriously affected by the electrical properties of the ground above which they are erected.

## 2. Theoretical Relations between Dielectric Constant and Conductivity.

The classical electromagnetic equations express the mode of propagation of electrical energy through a non-conducting medium having assigned values of dielectric constant and permeability, the velocity of propagation being calculable in terms of these quantities. If the medium has a finite conductivity, the modifications required in these equations will be made clear by the following simple considerations:—

Consider a centimetre cube of the medium through which the wave is passing, and let  $X$  be the intensity of the uniform linear electric field parallel to one face of the cube; then the displacement current is  $\frac{\kappa}{4\pi} \frac{dX}{dt}$  and the conduction current,  $X\sigma$ , where  $\sigma$  and  $\kappa$  are the conductivity and dielectric constant of the material respectively.

The total current  $i$  flowing in the direction of the electric force is thus:

$$\frac{\kappa}{4\pi} \frac{dX}{dt} + X\sigma.$$

For a pure sine wave alternating current of frequency  $\omega/2\pi$ , we have

$$\frac{\partial X}{\partial t} = j\omega X,$$

where

$$j = \sqrt{-1}.$$

Therefore

$$\begin{aligned} i &= \left( \frac{\kappa}{4\pi} - \frac{j\sigma}{\omega} \right) \frac{dX}{dt} \\ &= \frac{1}{4\pi} \left( \kappa - j \frac{2\sigma}{f} \right) \frac{dX}{dt} \\ &= \frac{\kappa'}{4\pi} \frac{dX}{dt}, \end{aligned}$$

where

$$\kappa' = \left( \kappa - j \frac{2\sigma}{f} \right).$$

For a perfect dielectric, i.e.,  $\sigma = 0$

$$i = \frac{\kappa}{4\pi} \frac{dX}{dt}.$$

It is thus apparent that the electromagnetic equations applicable to a pure

dielectric will hold for a conductor if the quantity  $\kappa'$  is used throughout in place of the dielectric constant  $\kappa$ , where

$$\kappa' = \kappa \left( 1 - j \frac{2\sigma}{\kappa f} \right).$$

It may be noted that in the extreme case in which  $2\sigma/\kappa f$  is very small compared with unity, the conductivity has a negligible effect. Similarly, when  $\frac{2\sigma}{\kappa f} \gg 1$ , the effect of the dielectric constant is unimportant.

It will be evident from such considerations that in order to ascertain the effect of a material, such as soil, for alternating currents flowing therein, whether applied direct or whether resulting from the passage of electric waves through or over it, it will be necessary to have a knowledge of the two quantities  $\kappa$  and  $\sigma$  at the frequency of the currents in question.

*Note on Units.*—In the publications of previous writers, there is some divergence of opinion as to whether the conductivity is more conveniently expressed in electrostatic or electromagnetic units, or as the reciprocal of a resistivity in ohm-cm. (i.e. ohms per centimetre cube). In the author's opinion the procedure to adopt is that of expressing  $\sigma$  in electrostatic units, when the quantity may be substituted directly into any equations, such as those given above, involving  $\kappa$  or  $\kappa'$  which are almost invariably expressed in electrostatic units. If electromagnetic units are employed for  $\sigma$ , it is necessary to use a conversion factor for the ratio of the units ( $c^2$ ) which introduces an unnecessary quantity into all the formulæ involved. In order to facilitate the conversion of the quantities in the mind of the reader, the following relations are given, taking the velocity of light,  $c = 3 \times 10^{10}$  cm. per second

$$\sigma_{e.s.u.} = \sigma_{e.m.u.} \times 9.10^{20}$$

$$\sigma_{e.s.u.} = \frac{1}{\rho} \times 9.10^{11},$$

where " $\rho$ " is the resistivity in ohms per centimetre cube.

### 3. *The Measurement of Soil Constants by a Laboratory Method.*

A review of previous work on this subject shows that in certain rather scattered frequency ranges and for various localities, measurements of the electrical properties of the soil have been made, chiefly by field methods depending upon wave propagation phenomena, and in a few cases only, by laboratory methods. It was considered desirable to obtain more complete and detailed

information on this subject in a systematic manner under controlled conditions. This investigation was prompted by the availability of a method of measuring resistance and reactance at radio frequencies which has been described in a previous paper by Colebrook and Wilmotte.\*

The principle of this method depends for its application upon the change in reactance of a valve-maintained oscillating circuit when it is coupled to another or measuring circuit, which contains the component under investigation. This latter circuit comprises an inductance coil and one or more variable condensers of good quality suitable for precision measurements. The coil of the valve oscillator is coupled to that of the measuring circuit, and as the condenser of the latter is adjusted the reactance of the oscillating circuit, and so the frequency generated, is varied in a characteristic manner. When the measuring circuit is exactly in tune with the oscillator the change in reactance is zero, and the condenser reading thus gives the value of capacity ( $C_0$ ) required to tune the coil to the working frequency; on either side of this setting the reactance change passes through a maximum, the two changes being of opposite sign.

If the condenser readings (capacities  $C_1$  and  $C_2$ ) of the measuring circuit are noted for the two conditions of maximum reactance change, the resistance of this circuit is given by the formula

$$R_1 = \frac{1}{2\omega} \left( \frac{1}{C_1} - \frac{1}{C_2} \right), \quad (1)$$

where  $\omega = 2\pi \times \text{frequency}$ .

Having thus obtained the value of the resistance of the measuring circuit alone, the component to be measured is connected either in series or parallel with the measuring circuit. The new values of the three critical condenser readings  $C_0'$ ,  $C_1'$  and  $C_2'$  are then determined in the manner just described. It is then clear that the equivalent capacity of the component introduced in the measuring circuit is given by the difference  $C_0' - C_0$ , while the resistance of the circuit has been increased by an amount  $R_2 - R_1$ , where

$$R_2 = \frac{1}{2\omega} \left( \frac{1}{C_1'} - \frac{1}{C_2'} \right). \quad (2)$$

The actual values of the resistance and reactance of the component introduced into the measuring circuit can then easily be computed from the usual circuit formulæ.

From this brief discussion it will be clear that the measurements of resistance

\* 'J. Inst. Elect. Eng. Lond.,' vol. 69, p. 497 (1931).

and reactance involve a knowledge of the frequency in use and of the capacity introduced into the measuring circuit. With high-class variable condensers in this circuit the method is capable of a fairly high degree of accuracy at radio frequencies. For further details of the operation of the method reference may be made to the original paper by Colebrook and Wilmotte (*loc. cit.*).

In order to apply this method to the study of the electrical properties of soils, the material under test is placed in a suitable container, made in the form of a fixed condenser. If  $C_a$  is the capacity of this condenser in air, while  $C_s$  and  $R_s$  are the capacity and shunt resistance of the condenser when it is filled with soil, then the apparent dielectric constant or permittivity " $\kappa$ " of the soil is given by

$$\kappa = \frac{C_s}{C_a}, \quad (3)$$

while the conductivity " $\sigma$ " or resistivity " $\rho$ " can be found from the relationship

$$\sigma = \frac{1}{\rho} = \frac{1}{4\pi C_a R_s}. \quad (4)$$

For the simple ratio of capacities, equation (3) gives the dielectric constant in electrostatic units; in equation (4)  $R_s$  will usually be measured in ohms, and then if  $C_a$  is measured in centimetres,  $\rho$  will be given in the unit ohms per centimetre cube, or more briefly ohm-cm. To obtain the conductivity  $\sigma$  in electrostatic units, the relationship  $\sigma_{e.s.u.} = \frac{9 \times 10^{11}}{\rho}$  may be employed.

Preliminary experiments were carried out with containers of various sizes and shapes. These experiments served to show the very large order of variation with moisture content of the apparent dielectric constant and conductivity of the soil, and also to demonstrate the effect of packing the soil in the container. In the latter connection it was found that as the soil was packed more and more tightly the conductivity increased to a maximum which was obtainable with a cylindrical container. Consistent results to an order of 10 per cent. or less were finally obtained for tightly rammed soil in cylindrical containers of various dimensions, with either flat circular electrodes at the ends or with concentric electrodes, the outer of which formed the container. It was therefore assumed that this was the desirable condition simulating soil in a well rolled field or unploughed meadow. The open cylindrical containers were made of ebonite with brass plate electrodes, while the concentric cylinder was made of brass, with keramot insulation. There has been no reason to

suppose that the material of the electrodes has affected the results, but the final container employed was made of copper. The capacity of the type of container finally used was about  $2.36 \mu\mu\text{F}$ . This capacity was calculated from the geometry of the system, and was also measured by using distilled water, the dielectric constant of which is accurately known at frequencies up to at least 150 megacycles per second.\* The use of water as the dielectric in this manner considerably increased the accuracy of the capacity measurement, by reducing the stray capacity effects of leads, etc. The measurements were made throughout with a potential difference of about 0.5 volt across the condenser.

#### 4. *Results obtained on Soil at the National Physical Laboratory.*

It was realized at the outset that a systematic study of the electrical properties of the earth must take account of the moisture content of the soil under examination. Accordingly whenever a sample of soil was taken out for electrical measurement, a portion of this soil was placed in an electric oven and maintained at a temperature of just over  $100^{\circ}\text{C}$ . for 24 hours to determine the loss of weight by evaporation. Furthermore, in order to get a definite idea of the fluctuation of the value of moisture content of surface soil from day to day, a measurement was made daily over a period of 12 months of the moisture content only of a sample of soil taken from one site. In all cases in this paper the moisture content is given as the percentage of moisture to dry soil by weight.

The majority of the measurements were made on samples of soil taken from a selected site approximately in the centre of a flat, open field, which has been used to a considerable extent for various ultra-short wave field experiments.† These samples were measured in one or other of the cylindrical containers at six frequencies between 100 and 10,000 kilocycles per second.

(a) *Conductivity at Radio Frequencies.*—The results of an extended series of measurements of the electrical conductivity on samples of soil from the selected site (No. I) just referred to, over a range of frequencies from 100 to 10,000 kilocycles per second are shown in fig. 1. The various curves refer to samples having the different moisture contents indicated. The majority of moisture contents over about 15 per cent. were obtained on samples of surface soil taken direct from the site. The lower values were obtained by partially

\* 'Int. Crit. Tables,' vol. 6, p. 77 (1929).

† Smith-Rose and McPetrie, 'Proc. Phys. Soc.,' vol. 43, p. 592 (1931); vol. 44, p. 500 (1932).

drying out the soil in a warm atmosphere, while for the values shown for a moisture content of 39 per cent., the soil was artificially moistened with distilled water, for the moisture content of surface soil at this site rarely exceeds 30 per cent. even in times of prolonged heavy rain.

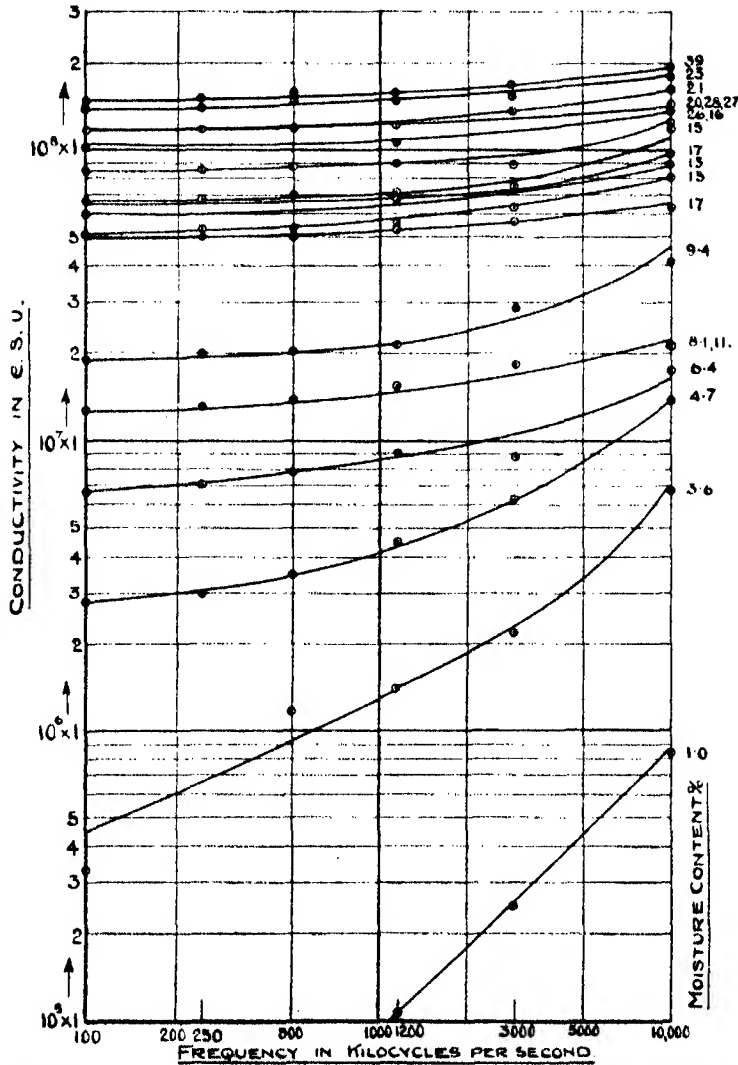


FIG. 1.—Relation of conductivity to frequency and moisture content for soil from Site I (N.P.L.).

Several characteristic features may be observed from the curves given in fig. 1. In the first place, at a typical frequency of, say, 3,000 kc./s. the conductivity increases from about  $3 \times 10^5$  to about  $1.5 \times 10^8$  e.s.u. as the



moisture content is increased from less than 1 per cent. to about 20 per cent. or more. Secondly, at the lower moisture contents the conductivity rises appreciably with increasing frequency; whereas at the higher values of moisture content the change of conductivity with frequency is slight, although there remains a definite tendency for the conductivity to rise at the highest frequencies. Further, while at low moisture contents the change in con-

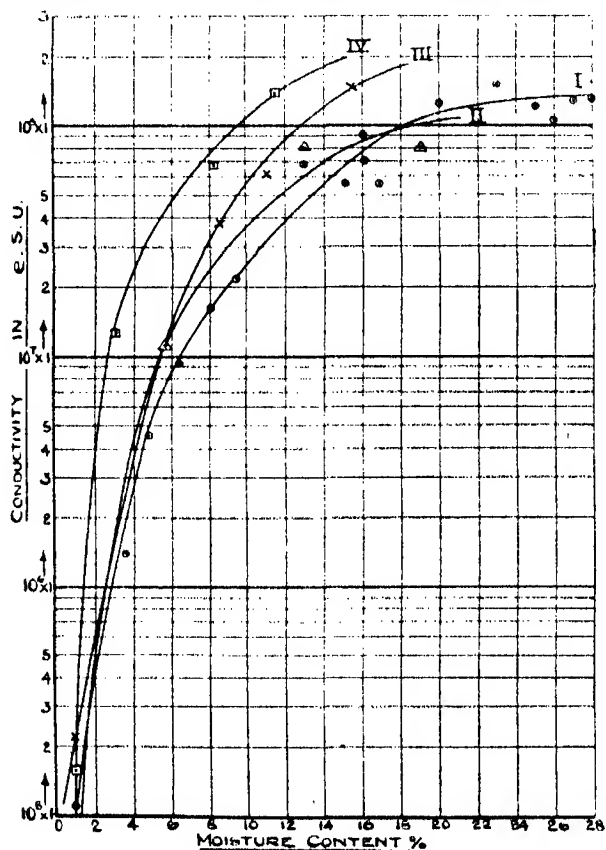


FIG. 2.—Relation between conductivity and moisture content for soils from Sites I-IV (N.P.L.) at a frequency of 1,200 kilocycles per second.

ductivity with moisture is fairly rapid, the rate of change decreases considerably at moisture contents of about 15 per cent., and for values between 15 per cent. and 39 per cent. there is no definite correlation, the conductivity values in this region varying somewhat erratically for the different samples from about  $0.5 \times 10^8$  to  $2 \times 10^8$  e.s.u. The variation of conductivity with moisture content at a single frequency of 1,200 kc./s. for the same soil is shown by curve I in fig. 2. This curve illustrates clearly how the conductivity tends

to a maximum value for moisture contents of 20 per cent. and over. As will be seen later, it is such moisture contents which normally prevail throughout the year for soil taken from this site at a depth of less than 2 feet. The remaining curves shown in fig. 2 refer to soil taken from three other sites near the National Physical Laboratory. It will be seen that the maximum value of conductivity reached is in the same region, lying between limits of 0·8 and  $1·5 \times 10^8$  e.s.u. This value is, however, attained for lower moisture contents, of from 12 per cent. to 19 per cent., which were found to be normal values for the surface soil taken at random from these sites. A relatively small part of the variation in the results obtained on different samples may have been due to the effect of temperature, which was not controlled during the measurements. In view of the large order of variations in conductivity obtained on samples from different sites (*see also* Section 5 below), it was not considered expedient at the present stage to make accurate measurements of the temperature coefficient, which, as Higgs\* has shown, is of the order of 3 per cent. per degree Centigrade at a frequency of 50 cycles per second.

Within a small range, the effect of the depth at which the sample of soil was taken is shown by the results given in Table I, as obtained on samples taken from the top and bottom of a trench which was cut along the edge of the field forming Site I. The three tests refer to three positions along the trench, about 200 yards apart, and were made on different days.

**Table I.**—Results of Measurements on Samples of Soil taken from the Top and Bottom of a Trench near Site I.

Date.	Depth from surface in feet.	Moisture content per cent.	Conductivity in e.s.u. $\times 10^{-8}$ at frequencies in kilocycles per second of—		
			100.	1,200.	10,000.
10.3.32	0	23	0·79	0·83	1·0
	1·5	19	1·05	1·1	1·2
11.3.32	0	15	1·2	1·3	1·3
	1·5	15	1·9	1·9	1·9
14.3.32	0	28	1·6	1·6	1·9
	1·5	17	1·1	1·3	1·4

It will be seen from this table that the difference in conductivity at the surface and at a depth of 1 foot 6 inches is not greater than the variation obtained at the different sites. It was not considered worth while investigating

\* 'J. Inst. Elect. Eng. Lond.,' vol. 68, p. 736 (1930).

samples from greater depths on this site, since an opportunity was being provided of carrying this out at one or two Post Office stations where the data obtained would have a direct practical application.

(b) *Variation of Moisture Content of Surface Soil.*—In order to obtain a definite idea as to the magnitude of the seasonal variation of moisture content of the soil, this quantity was measured for a sample of soil taken every day from Site I over a period of 12 months. The results showed that during the greater part of the year the moisture content of the soil was between 16 per cent. and 30 per cent. It was only during periods of heavy rain that the upper limit was exceeded, and the samples, having the maximum moisture content experienced of about 39 per cent., were taken actually while it was raining. As soon as the rain stopped the normal drainage of the soil soon reduced the value to 30 per cent. or less.

In the other direction, the moisture in the surface soil decreased steadily during the dry summer season, but it was only after several weeks of hot, dry weather that the moisture content reached its lower limit of 4 per cent. This condition, however, prevailed for only a few inches below the surface. Measurements made during this period on samples taken from a depth of 1 foot showed that the moisture content did not fall below a minimum value of 16 per cent.

The results given in section (a) above show that when the moisture content falls below its normal range of from 16 per cent. to 30 per cent., the conductivity decreases considerably. This means that for the case of radio wave propagation the depth of penetration of the waves into the earth will increase slightly into the more moist, and thus better conducting, subsoil, and this factor will serve to counteract appreciably any departure of the moisture content of the soil from its normal value, so far as its effect on the attenuation of the waves is concerned. Furthermore, it has been seen from the results given above that an increase in the moisture content above its normal value does not materially change the conductivity.

(c) *Dielectric Constant at Radio Frequencies.*—As explained in Section 3, the ratio of the capacity of the specimen condenser filled with soil to its capacity in air gives the value of the apparent dielectric constant or permittivity of the soil under the prevailing conditions. The results of measurements made on samples of soil from Site I under the same conditions as those described for the conductivity measurements are given in fig. 3. For dry soil the dielectric constant varies from 2.8 to 2.6 as the frequency is raised from 100 to 10,000 kilocycles per second; with a moisture content of 3.6 per cent., the dielectric constant varies from 5.6 to 2.9 for the same range of frequencies. As the

moisture content is increased, both the actual value of the dielectric constant and its variation with frequency increase considerably, as shown by the curves in fig. 3. Since the dielectric constant at low radio frequencies appears to exceed 80, which is approximately the value obtained for pure water at all frequencies, it is evident that the measurements are affected by polarization effects resulting from the electrolytic conduction taking place in the soil. Such phenomena are well known in the investigation of dielectrics and electrolytes at audio and radio frequencies, and the effects are sometimes interpreted as being caused by the formation of a film of molecular thickness

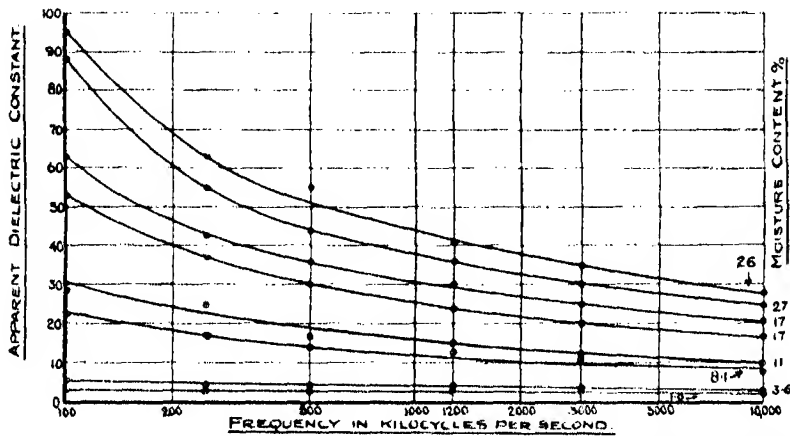


Fig. 3. Relation of apparent dielectric constant to frequency and moisture content for soil from Site I (N.P.L.).

over the surfaces of the electrodes. These films act as leakage condensers of very high capacity, in series with the body of the material under investigation. At very low frequencies and with material of reasonably high conductivity, the total capacity approaches that of the two films in series. As the frequency is increased the resistance of the films and the capacity of the material come into play to an increasing extent, and at infinitely high frequencies the effect of the films should become negligible. On this hypothesis the true values of the dielectric constant of the soil are those to which the curves in fig. 3 approach asymptotically at high radio frequencies. Thus for normal moisture contents between 16 per cent. and 30 per cent., the dielectric constant of the soil from Site I lies between 18 and 30, and this is probably the value that is effective for the propagation of waves along the earth. It will be shown later, however, that even the higher "apparent" values, recorded in fig. 3, play a negligible part in comparison with the corresponding conductivity values given in fig. 1.

The graphs in fig. 4 illustrate the mode of variation of the apparent dielectric constant with moisture content at a frequency of 1,200 kc./s. for each of the four sites at Teddington. It will be seen that although, as previously pointed out, the normal moisture content differs considerably for these four sites, the limiting values of the dielectric constant are of the same order.

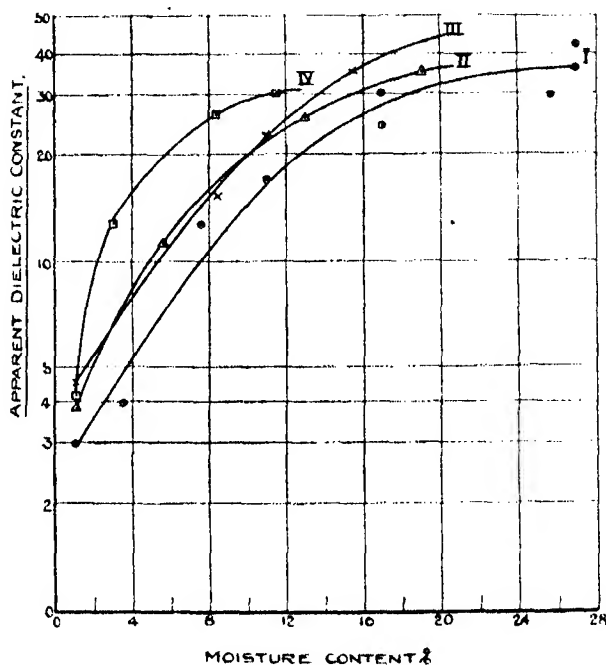


FIG. 4.—Relation between apparent dielectric constant and moisture content for soils from Sites I-IV (N.P.L.) at a frequency of 1,200 kilocycles per second.

(d) *Extension of the Frequency Range.*—As the necessary apparatus was available the opportunity was taken to obtain measurements in the audio-frequency range. The radio-frequency range was extended to 50 kc./s., while an audio-frequency range of from 0.5 to 4 kc./s. was also available. Preliminary measurements showed that while, at audio frequencies, the conductivity value was similar to that obtained at low radio frequencies, the apparent dielectric constant had increased considerably in value, as would be expected from the polarization effects described above. The results of a complete series of measurements carried out on a typical sample of soil taken from Site I (N.P.L.) at frequencies from 0.5 to 10,000 kc./s. are given in fig. 5. Here it is seen that for soil with a moisture content of 26 per cent., the conductivity of about  $10^8$  e.s.u. is maintained down to 500 cycles per second.

At the lower end of the frequency range the conductivity curve has been extended to include the corresponding value given by Higgs\* for a frequency of 50 c.p.s. in previous measurements made at the N.P.L. At the upper end of the frequency range the conductivity curve has also been extended to cover the experimental values obtained in field measurements† on the same site at frequencies from 30 to 190 megacycles per second (wave-lengths 10 to 1.6 m.). The diagram, fig. 5, also shows the conductivity values obtained in field measurements in this country at various frequencies.

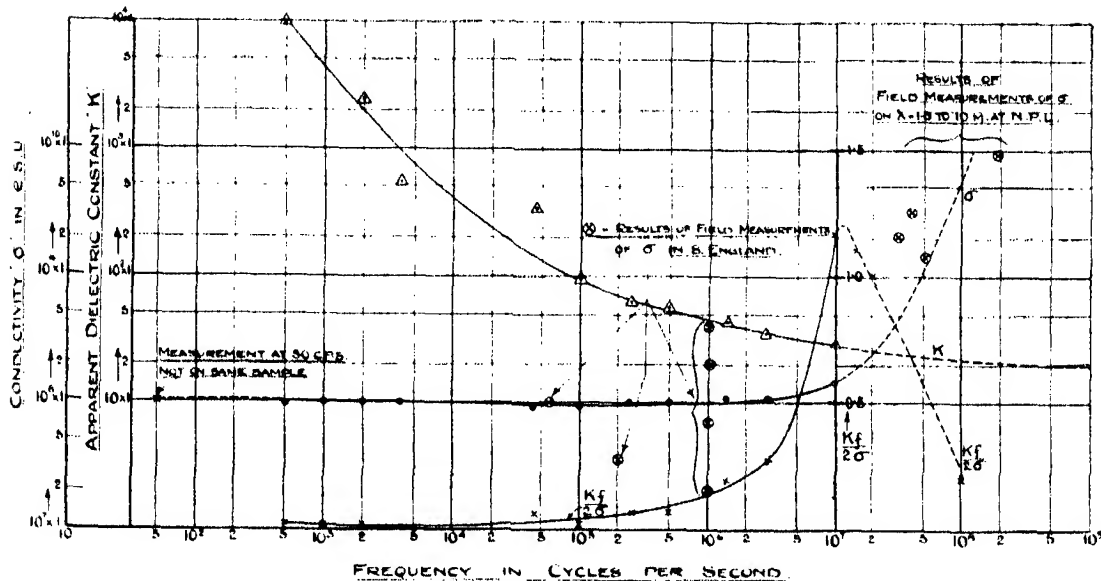


FIG. 5.—Results of laboratory measurements of electrical properties of surface soil from Site 1 (N.P.L.), at frequencies between 500 and  $10^9$  cycles per second. 25.5.32. Moisture content = 26 per cent.

Concerning the apparent dielectric constant, it is seen that the measured values of this quantity rise to as much as 10,000 at the lowest audible frequency employed. The curve connecting this quantity with frequency is quite smooth and is seen to be asymptotic to a value of about 20 at very high frequencies, and it is reasonable therefore to assume that this is the true dielectric constant of the soil, at any rate for the radio frequencies.

The lowest curve in fig. 5 shows the relationship between frequency and the quantity  $\kappa f/2\sigma$ , where  $\kappa$  is the apparent dielectric constant as measured. It is seen that even with the high apparent value, the above quantity is less than

\* *Loc. cit.*

† Smith-Rose and McPetrie, *loc. cit.*

about 0.1 for frequencies below 1,000 kc./s. From the reasoning given in Section 2, it is thus evident that for frequencies below this the dielectric constant of the soil plays a negligible part in the propagation of waves along the earth. As the frequency is increased from 1,000 to 10,000 kc./s. the value of  $\kappa f/2\sigma$  increases considerably and exceeds a value of unity. The broken-line extension of this curve is calculated from the limiting value of  $\kappa = 20$  and from the extension of the conductivity curve to include the field measurements with ultra-short waves. It is apparent from the shape of this curve that in a band of frequencies around 10,000 kc./s., the dielectric constant of the earth may play an important part in the propagation of waves, and in view of the almost complete lack of data upon this subject, it is desirable that both this quantity and the conductivity should be investigated further by both laboratory and field methods.

#### 5. Results obtained on Surface Soil from other Sites.

In Table II are given the results of conductivity measurements at three radio frequencies on samples of soil taken at random from several different sites, together with corresponding results for different samples taken from the same site, I, at Teddington. All the samples were taken from within a few inches of the surface.

Table II.—Results of Conductivity Measurements on Samples of Surface Soil taken at Random from Different Sites.

Date.	Site.	Moisture content per cent.	Conductivity in e.s.u. $\times 10^{-9}$ at frequencies in kilocycles per second of—		
			100.	1200.	10,000.
21.3.32	Banstead (1) ....	15	1.2	1.2	1.4
23.3.32	„ (2) ....	23	2.8	3.1	3.3
19.4.32	Pulham .....	25	2.6	2.7	4.1
27.4.32	Slough (W.P.) .....	37	3.0	3.0	4.2
27.4.32	„ (N.P.) ....	29	1.5	1.7	2.2
29.8.32	Rugby (1) .....	60	3.4	3.9	6.0
8.9.32	„ (2) .....	22	0.61	0.67	1.0
6.9.32	Baldock .....	21	0.88	0.93	1.3
11.3.32	Teddington (1) ....	15	1.2	1.2	1.3
14.3.32	„ .....	28	1.6	1.6	1.9
21.3.32	„ .....	22	1.4	1.4	1.7
18.5.32	„ .....	25	1.2	1.2	1.9
25.5.32	„ .....	26	1.1	1.1	1.4
1.9.32	„ .....	13	0.6	0.7	0.9
5.9.32	„ .....	21	1.2	1.3	1.6

This Table II shows first of all that at some of the places appreciably higher conductivity values are obtained than those experienced at Teddington even for approximately the same moisture content. At the typical site selected at Teddington the conductivity does not exceed  $2 \times 10^8$  e.s.u., whereas at Pulham, at the Radio Research Station, Slough (West Park), and at Rugby, values exceeding  $4 \times 10^8$  e.s.u. have been measured. The values of moisture content of the first sample obtained from Rugby and the two samples taken at Slough are worthy of note as being considerably higher than those normally found at the other sites.

It is thus evident that the conductivity of the soil varies considerably for different sites, and that this variation is only partly accounted for by the variation in the moisture content of the surface soil under normal weather conditions.

#### *6. Measurements on Subsoils and the Penetration of Electric Waves.*

When an electric wave is transmitted over the surface of the earth, the resulting electric currents set up penetrate to a depth which is dependent upon the wave-frequency and the conductivity of the earth. A complete study of this subject must, therefore, take account of the electrical constants not only of the surface soil, but also of the subsoil to such a depth as is involved in wave propagation. To make the laboratory investigation complete, therefore, it is necessary to extend the measurements to samples of subsoil taken at various depths. With the co-operation of the Post Office this has been done for sites at the Rugby and Baldock stations, where the results are likely to prove directly applicable to some of the problems involved in radio communication.

The necessary samples of soil were taken from two sites at the Rugby station about 60 feet apart, and one at Baldock at depths limited to 10 feet from the surface. Care was taken that the subsoil was not exposed to the air for longer than was absolutely necessary, and as a sample was taken out it was immediately sealed and sent to the National Physical Laboratory for measurement. Determinations of the moisture content were made on all samples in accordance with the practice adopted throughout this investigation. A summary of the results obtained and a brief description of the nature of each sample of soil, is given in Table III.

At Rugby the conductivity of the subsoil, which consists of blue clay, is from five to ten times the corresponding value at Baldock, where the subsoil is practically pure chalk. For the first site at Rugby, abnormally high values of moisture content, with correspondingly high values of conductivity, were



Table III.—Measurement on Samples of Soil taken at Various Depths.

Site.	Depth.		Type of soil.	Moisture content per cent.	Conductivity, $\sigma_e$ a.u. $\times 10^{-9}$ at frequencies in kilocycles per second of—		Apparent dielectric constant at 10,000 kilocycles/sec.	Amplitude of current at 10,000 kilocycles/sec.
	Feet.	Metres.			100	1,200		
Rugby (1)	0	0	Dark fibrous loam	60	3.4	3.9	6.0	1.0
	1	0.30	Loam and clay	33	7.1	7.2	8.8	0.63
	2	0.61	Clay and sand	26	8.7	9.0	13.0	0.35
	3	0.91	Blue clay	25	9.9	10.0	13.0	0.18
	10	3.03	"	23	6.2	6.9	8.3	0.003
Rugby (2)	0	0	Loam	22	0.61	0.67	1.0	1.0
	1	0.30	Loam and clay	13	0.95	1.3	1.5	0.86
	3	0.91	Blue clay	27	8.2	8.5	14.0	0.34
	5	1.61	Clay and sand	21	6.0	7.0	9.8	0.10
	10	3.03	Blue clay	25	6.9	7.5	11.0	0.006
Baldock	0	0	Fibrous loam	21	0.88	0.93	1.3	1.0
	1	0.30	Chalky loam	21	0.65	0.81	0.90	0.88
	2	0.61	Chalk	24	0.27	0.40	0.64	0.80
	3	0.91	"	27	0.80	0.87	1.1	0.72
	5	1.61	"	26	1.4	1.7	2.1	0.52
	10	3.03	"	27	1.4	1.6	2.0	0.19

obtained on the samples taken from the first foot of soil. This high moisture content was considered to be due to the fact that the clay was somewhat nearer the surface, while the top soil was of a very fibrous nature, with good moisture retaining properties. The samples taken at depths of from 3 to 10 feet were very similar in appearance for both sites at Rugby, and the results given in Table III show that the average conductivity is of the order  $10 \times 10^8$  e.s.u. and the apparent dielectric constant about 45.

The results obtained on the samples from Baldock show that their electrical properties are similar to those from Teddington, the measured values of both conductivity and dielectric constant tending to increase with depth, probably owing to the increased moisture content of the chalk subsoil.

The last column of Table III indicates the amplitude of the current that would be found at any depth at a frequency of 10,000 kc./s., assuming unit amplitude at the surface. These current values have been calculated from the relation

$$\frac{I_x}{I_0} = e^{-\frac{2\pi r}{\lambda} \alpha}$$

where

$I_0$  = amplitude of current at surface,

$I_x$  = amplitude of current at depth " $x$ ,"

$\lambda$  = wave-length employed,

$$\alpha^2 = \frac{\sigma}{f} \sqrt{\frac{\kappa^2 f^2}{4\sigma^2} + 1} - \frac{\kappa}{2}.$$

When  $\frac{\kappa f}{2\sigma} \ll 1$ , the formula for  $\alpha$  reduces to

$$\alpha = \sqrt{\frac{\sigma}{f} - \frac{\kappa}{2}}.$$

In making the calculation the average value of conductivity and dielectric constant given in Table III was used for each layer of soil for which measurements were available. From these results it is seen that at Rugby, over 90 per cent. of the current is carried in the first 1.5 metres (5 feet) of soil, while for Baldock a little less than half the current flows in this depth of soil; an extrapolation of the results shows that a depth of about 4 metres (13 feet) is required to carry 90 per cent. of the current. These results refer only to a frequency of 10,000 kilocycles per second. The depth of penetration for a given current amplitude will vary with the frequency to a considerable extent. For example,

for soil of conductivity  $10^8$  and dielectric constant 20, which are approximately the values of the soil at Teddington and Baldock, the current will have decreased to one-tenth of its amplitude at the surface, at depths of about 5, 12 and 25 metres for frequencies of 10,000, 1,000 and 200 kilocycles per second (wavelengths 30, 300 and 1,500 m.) respectively.

#### *7. Conclusions and Acknowledgments.*

This paper contains a description of the results of the application of a laboratory method of determining the electrical conductivity and dielectric constant of the soil. The results of a preliminary survey of the behaviour of these constants for a few representative samples of soil under conditions of varying moisture content and applied frequency, are discussed in some detail. It is shown that the results obtained by this laboratory method are in fair agreement with such data as are available from field measurements, which have usually been carried out by means of some characteristic feature of the propagation of waves along the earth's surface.

It is considered that the results of this brief investigation justify the inclusion of the laboratory method as a useful tool in radio communication technique. The method possesses advantages of ease and rapidity of operation over any field method, and these may be offset against the fact that the results are limited to one small portion of the soil at a time. The latter possible disadvantage may be overcome, as shown above, by making a rapid survey of samples from different sites and at different depths below the surface. For the exploration of a large area it will suffice to measure a range of samples at a single frequency, which may, if desired, be in the audible range. After a first selection of sites in this manner, a more detailed examination may be carried out over the desired range of radio frequencies, and at the requisite depth which may be estimated with fair accuracy from the results obtained on a few samples of subsoil.

It is outside the scope of this paper to discuss further the effect of the electrical properties of the soil on the propagation of waves in radio communication. This matter, in its relation to broadcasting and the efficiency in transmission and reception by means of antenna arrays, has already received considerable attention from other investigators.\* It is not only the waves

\* Eekersley, T. L., 'J. Inst. Elect. Eng. Lond.,' vol. 67, p. 992 (1929). Eekersley, P. P. Eekersley, T. L., and Kirke, H. L., 'J. Inst. Elect. Eng. Lond.,' vol. 67, p. 507 (1929).. Eekersley, P. P., 'Proc. Inst. Radio Eng.,' vol. 18, p. 1160 (1930). Walmsley, T., 'J. Inst. Elect. Eng. Lond.,' vol. 69, p. 299 (1931). McPetre, J. S., 'J. Inst. Elect. Eng. Lond.,' vol. 70, p. 382 (1932).

transmitted along the surface which are affected, but the resultant field owing to waves incident on the earth's surface from the upper atmosphere is largely determined by the properties of the ground. A comparatively recent paper by Potter and Friis\* illustrates very clearly the magnitude of the improvement in reception which may result from correctly locating an antenna array on the ground so that its optimum angle of reception is the direction of arrival of the incoming waves, making due allowance for reflection from the ground.

This investigation was carried out as part of the programme of the Radio Research Board and is published by the permission of the Department of Scientific and Industrial Research. The author desires to acknowledge his appreciation of the assistance rendered by Mr. A. C. Gordon-Smith in making the electrical measurements and to Mr. W. H. H. Brookes for determining the moisture contents of the various samples of soil used.

#### *Summary.*

The application of a laboratory method for measuring the conductivity and dielectric constant of samples of soil taken from selected sites at the National Physical Laboratory, Teddington, is described. These measurements were made over a range of frequencies of from 1000 cycles per second to 10 million cycles per second, and for various moisture contents ranging from practically zero up to a value exceeding that normally experienced for surface soil taken direct from the ground. The results of these measurements show that the conductivity varies from less than  $10^5$  e.s.u. for dry soil, up to a value of approximately  $10^8$  e.s.u. for normal moisture content. Corresponding values for the dielectric constant range from 2 or 3 for dry soil up to about 20 for moist soil at high radio frequencies. The results of measurements made on a number of samples of soil taken at random from several other sites are included in the paper, and show that both the normal moisture content and the conductivity can have values which are appreciably higher than those experienced at Teddington.

The paper concludes with a brief discussion of the penetration of radio-frequency currents in the earth, and the effective depth of penetration has been calculated in some instances with the aid of the experimental values of conductivity and dielectric constant determined above.

\* 'Proc. Inst. Radio Eng. Lond.,' vol. 20, p. 699 (1932).

---

*The Luminous Reduction of Selenium Dioxide.*

By H. J. EMELÉUS, Imperial College of Science and Technology, London, and  
H. L. RILEY, Armstrong College, Newcastle.

(Communicated by J. C. Philip, F.R.S.—Received November 22, 1932).

[PLATE 3.]

*Introduction.*

In the course of some recent investigations\* on the oxidizing action of selenium dioxide on organic compounds it was found that, if the temperature was raised above the point required for the specific oxidizing reaction, the reduction of the dioxide was accompanied by a characteristic moonlight-like flame. This was first observed in the reaction of ethylene with selenium dioxide at a temperature of *circa* 400° C, but subsequently a number of other substances were found to behave similarly, the following having been studied in some detail: ethylene, acetylene, methyl-, ethyl-, and propyl-alcohols, acetaldehyde, acetone, benzene, toluene, ether, carbon disulphide, and ammonia.

When the oxidation takes place at lower temperatures, *i.e.*, at temperatures which are not sufficiently high for the luminous reaction, intermediate products are formed from all of the carbon compounds. Acetaldehyde, for example, is oxidized quantitatively to glyoxal, the dioxide being reduced to elementary selenium, whilst ethylene also yields glyoxal. The present investigation was undertaken in the hope that the nature of the light emitted when the reactions are carried out at higher temperatures might possibly explain the highly selective nature of the oxidations at the lower temperatures.

*Experimental.*

The conditions used for producing the flames in selenium dioxide vapour were as follows. Powdered resublimed oxide (15–20 gm.) was heaped near the closed end of a clear silica tube, 2.0 cm. in diameter, 20 cm. long, with a side inlet tube at 0.5 cm. from the closed end; this served as a window in photographing the spectra. The open end of the tube was attached to a con-

\* Riley, Morley and Friend, 'J. Chem. Soc.,' p. 1875 (1932); Riley and Friend, *ibid.*, p. 2342 (1932); Imperial Chemical Industries and Riley, 'B.P.,' 354, 798 (1931) and 376, 306 (1932); I. G. Farb. A.G., 'B.P.,' 347, 743 (1931); Schwenk and Borgwardt, 'Ber. deuts. chem. Ges.,' vol. 65, p. 1601 (1932).

denser for removing liquid products of reaction and reactants, any uncondensed gases being led into an efficient draught cupboard. A fairly rapid stream of gas from a cylinder, or, with liquids, a stream of vapour from a distilling flask containing the gently boiling liquid, was passed over the oxide to displace air from the apparatus. The tube was then heated rapidly, either electrically or with a Bunsen burner. Reduction started at below  $100^{\circ}\text{C}$ . in every case, and at  $350^{\circ}$ – $400^{\circ}\text{C}$ . a blue flame suddenly appeared. With the aliphatic compounds, carbon disulphide, and ammonia the flames were fairly persistent, occasional heating being sufficient to maintain them continuously. With the aromatic compounds—particularly benzene—strong and continuous heating was necessary. One charge of selenium dioxide gave a flame of 10–25 minutes duration, after which a new tube had to be set up.

The rate of passage of gas or vapour could be varied within wide limits, provided the oxide was sufficiently heated. The only effect of altering this factor was to change the size of the flame, which took the form of a tongue of light 5–20 cm. long, stretching down the tube from the heated oxide. The flame spectra were photographed end-on through the closed end of the silica tube, which was placed directly in front of the spectrograph slit. It was necessary to withdraw the tube and heat its end with a free flame every few minutes during an exposure, in order to remove a film of condensed material from the window.

Ethylene, from a cylinder of the compressed gas, was used in the first series of experiments. The approximate ignition temperature, measured with a thermocouple in contact with the heap of selenium dioxide, was  $350^{\circ}$ – $400^{\circ}\text{C}$ . and the reading then rose rapidly to *circa*  $600^{\circ}\text{C}$ . The flame was definitely in the gas phase, and not at the surface of the oxide. The vapour pressure of selenium dioxide at  $320^{\circ}\text{C}$ . = 849 mm. (Landolt-Bornstein Tables), so that a plentiful supply of vapour would be available. The light intensity was sufficient to render small print visible at 1 metre from the tube. When the temperature was allowed to fall until the flame was just extinguished there was a very short temperature interval in which a faint white chemiluminescence was visible.

Acetylene, prepared by the action of water on calcium carbide, behaved in the same way as ethylene, as also did methyl-, ethyl-, and propyl-alcohols, acetaldehyde, acetone, ether, and carbon disulphide. These latter substances were all obtained from the ordinary commercial samples, but highly purified ethyl alcohol gave results identical with those from "rectified spirit." During the reaction with acetylene the end of the tube rapidly became covered with a

deposit of carbon, for which reason the flame spectrum could not be photographed. Hydrogen sulphide was also found to give a flame with selenium dioxide, but the deposition of sulphur prevented photographs being taken. Benzene and toluene inflamed in selenium dioxide vapour at temperatures above 450° C., benzene being more difficult to ignite than toluene, whilst both substances burned with a smoky flame.

The reaction between selenium dioxide and ammonia started at room temperature if the oxide were at all damp, or at about 40° C. if the sample were dry. The white oxide rapidly blackened, owing to the separation of selenium, and minute flashes of pale blue light were visible in a dark room. On warming the tube to 80°–100° C. a steady bluish chemiluminescence could be observed. As the temperature was raised the luminescence increased in volume and became brighter, a rose pink tinge appearing at *circa* 350° C. The normal flame, resembling those obtained with the organic substances, made its appearance at 400°–430° C. On cooling, these phenomena could be observed in the reverse order.

#### *The Chemical Reactions.*

It is already known that when selenium dioxide reacts with ketones, aldehydes, ethylene, and acetylene below 230° C. the principal products are glyoxals (Riley and co-workers, *loc. cit.*). The reaction with alcohols is more complex, and is the subject of a separate paper, in course of publication. When the reaction temperature is allowed to rise so that the flame appears, the yield of the particular glyoxal falls off, and the amount of carbon monoxide, carbon dioxide, and water formed increases. These three substances are the principal products from the flames of all of the organic compounds examined. At 400° C. intermediate products would probably be unstable, and the oxides of carbon and water might come from their decomposition, or, alternatively, from a direct oxidation process, differing in mechanism from the non-luminous oxidation. The lack of control of the flame conditions would make it difficult to carry out complete analyses of the reaction products, which would serve to decide this point.

In the experiments with carbon disulphide large amounts of sulphur dioxide and carbon dioxide were detected among the products. The reaction with ammonia gave almost exclusively nitrogen and water, a little nitric acid also being detected. Indications of the formation of a detonating substance (possibly a selenium-nitrogen compound) were also obtained in the course of the reaction, very slight explosive cracks occurring from time to time in the cooler parts of the apparatus.

According to Klages\* the reduction of selenium dioxide with hydrogen is accompanied by luminous phenomena. The authors failed to verify this observation with hydrogen from a cylinder. The oxide could, in fact, be sublimed quite freely in a stream of hydrogen with only slight reduction. It is possible that the hydrogen used by Klages was contaminated with hydrocarbons. It is also of interest that sulphur dioxide had only a slight reaction with selenium dioxide under the above conditions, no luminous phenomena being observed.

#### *The Flame Spectra.*

Photographs of the flame spectra were taken on (a) a glass grating spectrograph, with a linear dispersion of 35 Å. per millimetre; (b) a Hilger small quartz spectrograph; (c) a quartz spectrograph with lenses working at an aperture of f. 4.5. The bright flames needed exposures of 5-30 minutes on the grating instrument. Since band heads in the flame spectra were always partly obscured by a continuous radiation, and were difficult to see when using a comparator, measurements were made with an accurate scale on enlargements of the negatives printed on contrast paper, and with a copper arc reference spectrum. An additional check on the identity of band systems was obtained by superposing plates taken on the same instrument.

The hot flames supported by selenium dioxide gave bands and continuous radiation in the visible spectrum, and no light in the ultra-violet. There were 12 broad bands between 5620-4600 Å., of which six between 5620-5100 Å. were very diffuse and had a breadth of 50-70 Å. The remainder were somewhat sharper and were definitely degraded towards the red, some of the bands showing evidence of fine structure and having double heads, of which, however, only the more intense were measured. The continuous radiation extended over the whole of the visible spectrum, and had a maximum intensity at 4400-4600 Å. Between 4500-4200 Å. there were further bands, almost obscured by the continuous background, but apparently belonging to the same series as above. Between 4100-3800 Å. was a series of closely spaced and very diffuse bands, considerably less intense than the above, and extending to 3600 Å. when photographed with a quartz spectrograph.

Plates showing all of these characteristics were obtained from the flames of selenium dioxide with methyl-, ethyl-, and propyl-alcohols, acetone, ether, ethylene, and toluene. Only the stronger bands between 4700-4400 Å. were observed in the case of the flames with acetaldehyde, benzene, ammonia,

\* 'Chem. Z.', vol. 45, p. 450 (1898).



and carbon disulphide, though there is little doubt that longer exposures would show the remainder. All of the plates taken with the grating instrument were compared by direct superposition with that from the selenium dioxide-methyl alcohol flame, and the spectra were found to be identical in all cases for bands above 4600 Å. Where bands at shorter wave-lengths were sufficiently well defined for comparison to be made there was again a complete correspondence between the different negatives. Reproductions of the flame spectra of methyl and propyl alcohols are shown in Plate 3. (a) is the spectrum of the methyl alcohol-selenium dioxide flame, photographed on the grating instrument with an exposure of 30 minutes, and with a copper arc comparison spectrum. It shows the broad diffuse bands particularly well. (b) is the spectrum of the propyl alcohol-selenium dioxide flame, photographed on the same instrument with an exposure of 15 minutes. The continuous background is less intense, and a number of the sharper bands are visible. Both plates show the sodium lines, partly resolved. They were always present in the flame spectra, and probably represent impurity in the selenium dioxide. These two reproductions are typical of all of the spectra so far described.

In Table I is given average wave-length measurements for the violet edges of the bands. The error of measurement is probably less than  $\pm 5$  Å.

In the second column of the table the positions of the band heads in the spectrum of the selenium flame in oxygen are recorded. The bracketed values indicate bands found to correspond with those measured in the selenium dioxide flames, but not measured directly. To produce this flame the selenium was heated strongly in oxygen in a quartz tube, when it ignited readily. The flame was distinctly more blue in appearance than when combustion occurred in the vapour of the dioxide. The spectrum was photographed on the grating instrument and on the small quartz spectrograph; in the latter case no ultra-violet spectrum was observed. The visible spectrum consisted of broad diffuse bands between 5700–4600 Å., identical with those observed in the selenium dioxide flames. Below 4300 Å. there was a well-developed series of closely spaced bands, degraded to the red. The positions of their heads are recorded in the second column of Table I. They were sharper than the corresponding bands in the selenium dioxide flames, and relatively more intense, whilst the two sets of wave-length measurements show very definite differences, so that the two groups of bands are not definitely identical. The closely spaced bands in the selenium-oxygen flame agree well with a series of absorption bands observed with selenium dioxide at 350° C. by Evans and Antonoff.\*

\* 'Astrophys. J.,' vol. 34, p. 277 (1911).

Table I.

Flames burning in $\text{SeO}_2$ .	Flame of Se in $\text{O}_2$ .	Absorption of $\text{SeO}_2$ .	Se in Geissler tube and flame (Salet).
A.	A.	A.	A.
5620	—	—	5650
5530	—	—	5550
5410	—	—	—
5370	(5370)	—	5370
5245	(5245)	—	5270
5140	(5140)	—	5160
5025	(5025)	—	5050
4930	(4930)	—	4950
4850	(4850)	—	4840
4750	(4750)	—	4750
4685	(4685)	—	4670
4600	(4600)	—	4610
4435	—	4437	—
4405	—	4395	4400
4375	—	4365	—
4340	—	4330	—
4310	4295	4290	—
4270	4260	4256	—
4240	4225	4220	—
4200	4190	4185	—
4165	4160	4157	—
4130	4125	4117	—
4100	4095	4083	—
4060	4060	4055	—
4030	4030	4020	—
4000	4000	3990	—
—	3965	3960	—

The measurements of these authors are given in column 3, Table I, and a comparison of the two sets of values shows fairly definitely that the band system in the selenium-oxygen flame must be the emission spectrum of selenium oxide. In Plate 3 (c) is a photograph of the selenium-oxygen flame spectrum, taken on the grating spectrograph with an exposure of 30 minutes. A strong continuous background masked the broad diffuse bands at longer wave-length, but the bands attributed to  $\text{SeO}_2$  (or  $\text{SeO}$ ) are visible.

Special tests were made with the large aperture spectrograph to verify that no ultra-violet bands were given by the flames burning in selenium dioxide vapour, and, in particular, that the water bands, commonly observed in the spectra of burning hydrogen compounds, were not excited. The large aperture spectrograph recorded them in the spectrum of a Bunsen flame placed at 10 cm. from the slit with an exposure of 1 minute. With a 90-minute exposure of the selenium dioxide-methyl alcohol flame no trace of the (OH) bands was observed, nor did similar tests with the flames of selenium dioxide and propyl alcohol, acetone, ammonia, or carbon disulphide give any indication of ultra-violet

bands or continuum (below 3600 Å.). Unless, therefore, the transparency of the quartz had been impaired, it was clear that any ultra-violet emission from these flames must have been of very low intensity compared with that in the visible spectrum. During the exposures the end of the quartz tube was heated every few minutes to remove any film of condensed material, and the transparency of the quartz in the ultra-violet was specially tested. Evans and Antonoff (*loc. cit.*) found that absorption by selenium dioxide vapour was continuous below 4000 Å., but with the method used in producing the flames absorption by the vapour of the dioxide is unlikely to have masked short wave-length emission bands, as the reacting vapour or gas always approached the selenium dioxide from the direction of the window, and combustion took place in a definite flame front.

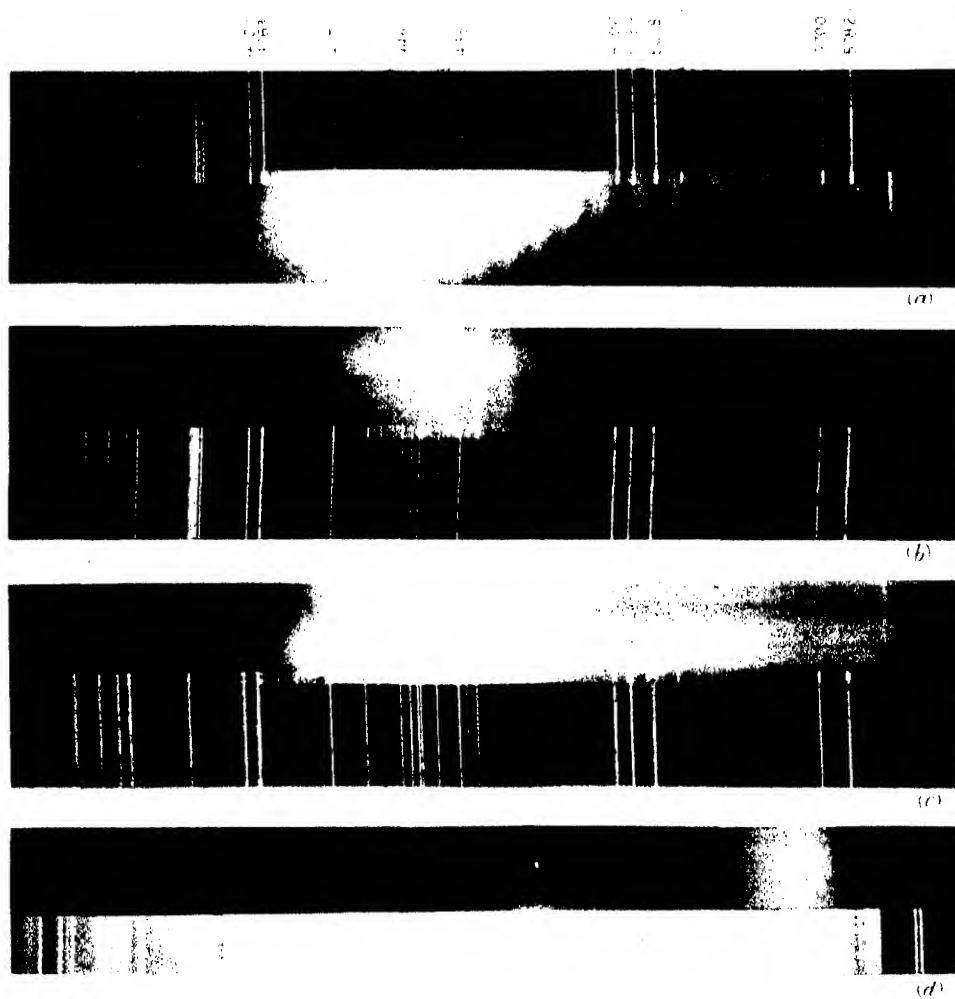
In order to determine if the intensity of the water bands in a hydrogen flame burning at a silica jet was influenced by the admixture of selenium vapour, the image of a flame 1.5 cm. high was focussed on the slit of the small quartz spectrograph, and an exposure of 30 minutes was made. Next an equal exposure was made with sufficient selenium volatilized into the hydrogen stream to colour the whole flame an intense blue. In this case, although bands in the visible due to selenium were observed, the intensity of the water bands was the same as in the simple hydrogen flame.

The normal flame of ammonia burning in the vapour of selenium dioxide, as already described, gave the same spectrum as the flames of the organic compounds and carbon disulphide. The reaction with ammonia was, however, unique in giving a well-marked phosphorescent flame. The spectrum of this was photographed on the large aperture spectrograph with rapid plates, the same type of tube being used as for the hot flames, but the temperature being controlled to about 300° C. With an exposure of 5½ hours seven band heads between 5200-4600 Å. common to the spectrum of the hot selenium dioxide-ammonia flame, were recorded. Very much longer exposures would be needed to verify all of the detail, but it is very probable that the low temperature flame has the same spectrum as that at higher temperatures. A reproduction of this photograph on the quartz spectrograph is shown in (d), Plate 3. Owing to the low dispersion of the instrument in the visible the bands can scarcely be distinguished.

#### Discussion.

The emission spectra of selenium in the Geissler tube and flame has been studied by Salet\* using a low dispersion (this being necessary, if the results

\* 'Ann. chim. phys.,' vol. 28, p. 5 (1873).





are to be of use for comparison with those given here), it was found to consist of a series of bands between 5650–4610 Å. These values are included for comparison in the last column of Table I. They agree approximately with the diffuse emission bands in the spectra of the flames in selenium dioxide vapour, and the latter are therefore probably to be attributed to the selenium molecule. The same bands occur in the flame of selenium burning in oxygen. It is of interest that a similar series of bands in the visible spectrum, attributed to  $S_2$ , was observed in the flame spectrum of sulphur or carbon disulphide in oxygen by Fowler and Vaidya.\*

In the selenium flames there is also some evidence that the  $Se_2$  molecule is responsible for emission, for Rosen† has recorded a series of broad diffuse bands at the red end of the selenium fluorescence spectrum, his measurements agreeing approximately with the values for the selenium dioxide flames. Paternò and Mazzucchelli‡ observed a continuous emission with diffuse bands on heating selenium in a quartz tube to 1400° C., and Rosen (*loc. cit.*) has identified these bands with the diffuse system in the fluorescence spectrum. At 800°–1000° C., when the thermal emission first becomes visible, the dissociation of selenium into  $Se_2$  molecules is almost complete. Probably, therefore, the emission of these broad diffuse bands is to be attributed to the simple molecule. The origin of the faint group of closely spaced bands in the region 4400–4000 Å. cannot be regarded as settled; there is partial agreement with the absorption spectrum of  $SeO_2$ , however, and there are indications of the bands in all of the flames burning in selenium dioxide, so that they are probably associated with selenium.

These results prove definitely that the chief emission from the flames of very diverse substances burning in selenium dioxide vapour is characteristic of selenium, and perhaps also of its oxide, but not of the substance undergoing oxidation. This is surprising, because all carbon-hydrogen and carbon-hydrogen-oxygen compounds when burnt in oxygen give very characteristic flame spectra. The chief emission bands are due to (CH),  $(C_2)$ , and (OH), or in the case of the phosphorescent combustion of some of the carbon compounds, a series of bands of unknown origin is observed in the blue.§ With the possible exception of a band at 4310 Å., which might be due to (CH), there is no indication of the above band systems in the flame spectra which we have examined

\* 'Proc. Roy. Soc.,' A, vol. 132, p. 310 (1931).

† 'Z. Physik,' vol. 43, p. 95 (1927).

‡ Cf. Kayser, "Handbuch d. Spectroscopie," vol. 6, p. 461 (1912).

§ Emeléus, 'J. Chem. Soc.,' p. 1733 (1929).

Bands in the visible might be blotted out by strong selenium emission and continuum, but there should have been no difficulty in observing the ultra-violet OH bands. The same is true of the flame of ammonia in oxygen, which normally gives systems due to NH and OH,\* and of the normal carbon disulphide flame, which gives bands attributed to S<sub>2</sub>, SO, SO<sub>2</sub>, and CS, and has a considerable emission in the ultra-violet.†

The reason why all of these characteristics of the normal flames are missing when the oxygen needed for combustion is supplied by selenium dioxide is not clear. The experiment described, in which selenium was burnt with hydrogen, shows that it does not interfere with the emission of the (OH) bands under such conditions.

In the present state of the problem there is too little evidence for the possible reaction mechanism to be discussed in detail. The spectroscopic results do, however, show that selenium dioxide does not simply furnish oxygen for the combustion by dissociation. If this were so, then the emission bands of selenium might be superposed on the normal flame spectra, but the latter would not be suppressed. The alternative is that the SeO<sub>2</sub> molecule forms a definite intermediate compound with the substance undergoing oxidation—this might be the counterpart of the peroxides postulated in combustion in oxygen. From such a complex selenium must be eliminated, leaving intermediate oxidation products which may be isolated at lower temperatures, but which undergo a non-luminous thermal decomposition if the temperature is sufficiently high. The radiation from the selenium molecule is evidently a process which occurs readily, for selenium is capable of giving a thermal emission, and the energy of the oxidation reaction would be sufficient for its excitation at the higher temperatures at which the transition from the dark to the luminous reaction is observed.

The authors are indebted to Dr. L. C. Martin for the loan of the grating spectrograph used.

#### *Summary.*

(1) Selenium dioxide vapour will react with methyl-, ethyl-, and propyl-alcohols, acetone, acetaldehyde, ether, ethylene, acetylene, benzene, toluene, ammonia, hydrogen sulphide, and carbon disulphide at *circa* 400° C., giving a bright blue flame.

(2) The principal oxidation products are oxides of carbon, carbon, and

\* Fowler and Badami, 'Proc. Roy. Soc.,' A, vol. 133, p. 325 (1931).

† Fowler and Vaidya, *loc. cit.*

water, from the carbon compounds; nitrogen and water from ammonia; and sulphur dioxide, sulphur, and oxides of carbon from carbon disulphide.

(3) All of the flames have the same spectrum, consisting of bands and continuous radiation between 5700–3600 Å.; the band systems being attributed to the  $\text{Se}_2$  molecule, and possibly also to the oxide of selenium. The same bands occur in the flame of selenium in oxygen, which also shows emission bands attributed to  $\text{SeO}_2$ . None of the flames has an ultra-violet spectrum.

(4) These flame spectra are totally different from those of the corresponding flames in oxygen.

(5) A phosphorescent flame has been obtained by heating selenium dioxide in an ammonia stream at 100°–300° C. Its spectrum has been photographed, and is the same as that of the hot flame of ammonia burning in selenium dioxide.

---

*Investigations on the Spectrum of Selenium.—Part II, Se III.*

By J. S. BADAMI, Ph.D., Physikalisch-Technische Reichsanstalt, Berlin, and  
K. R. RAO, D.Sc., Science College, Andhra University, Waltair, India.

(Communicated by A. Fowler, F.R.S.—Received November 25, 1932.)

*Introductory.*

The present paper is a continuation of the work on the spectra of selenium, carried out by the authors partly in Professor Fowler's Laboratory at the Imperial College and partly in Professor Siegbahn's Laboratory at Uppsala. A detailed account of the experimental part of the investigation together with the analysis of Se IV and Se V has been given in a previous communication.\* As already reported in 'Nature'† the experimental data there described have led to the identification of the system of energy levels characteristic of the spectrum of doubly-ionized selenium. It is the purpose of the present paper to give an account of the structure of this spectrum so far as it is revealed by a study of the spectrograms of selenium under different conditions of excitation.

\* 'Proc. Roy. Soc.,' A, vol. 131, p. 154 (1931).

† 'Nature,' vol. 128, p. 496 (1931).



*Observational.*

The lines of the spectrum in question appear when discharges, even of moderate intensity, are passed through selenium vapour contained in a capillary tube. In the ordinary spark in air, the spectrum is represented only by a very few of the stronger lines which could be ascribed to Se III, but with strong discharges through capillary tubes, the lines are considerably enhanced and the complete spectrum is easily photographed. In the region of very short wave-lengths, below  $\lambda 1500$ , the source found suitable for the excitation of the spectrum was the spark in vacuum between aluminium poles tipped with metallic selenium. With this source, excited by a 50 K.V. transformer, it was found necessary to include an inductance of about 0.5 m.h. to elicit lines of Se III and Se II. At the same time, a study of the spectra excited with and without inductance in series in the secondary circuit has greatly facilitated the assignment of the lines to the various stages of ionization of the element. Reference may be made to a reproduction of the spectra in the previous paper by the authors (*loc. cit.*), where the method of measurement and the instruments employed for photographing the various regions of the spectrum have also been described.

*Predicted Terms.*

The term structure of Se III, predicted by the Heisenberg-Hund theory, is similar to that of Ge I and As II; it is shown in Table I, in which the terms are based on the normal  $s^2p$  configuration of the next higher ion, Se IV. The last row gives the terms involving an inner electron transition, based on the configuration  $sp^2$  of the core. The discovery of such terms has been made in only a few spectra and is a special feature of the analysis of Se III suggested in this paper. The notation is the same as that adopted in the preceding paper, to which reference has already been made.

Table I.—Predicted Terms of Se III.

3, 3, 3,	4, 4, 4, 4,	5, 5, 5,	Term prefix.	Terms.
2 6 10	2 2		4p	<sup>3</sup> P <sup>1</sup> D <sup>1</sup> S
2 6 10	2 1	1	5s	<sup>3</sup> P <sup>1</sup> P
2 6 10	2     1		4d	<sup>3</sup> F <sup>3</sup> D <sup>3</sup> P <sup>1</sup> F <sup>1</sup> D <sup>1</sup> P
2 6 10	2	1	5p	<sup>3</sup> D <sup>3</sup> P <sup>3</sup> S <sup>1</sup> D <sup>1</sup> P <sup>1</sup> S
2 6 10	1 8		sp <sup>2</sup>	<sup>3</sup> S <sup>3</sup> S <sup>1</sup> D <sup>1</sup> D <sup>3</sup> P <sup>1</sup> P

*Analysis.*

The analysis of the spectrum presented considerable difficulty owing to the largeness of the characteristic intervals involved and the consequent superposition of different multiplets. Further, on account of the very large number of close lines occurring in the spectrum, particularly in the extreme ultra-violet, a headway could not be made with the analysis until plates were taken with a high dispersion vacuum spectrograph, such as that used at Uppsala, which gave a dispersion of about 2.8 Å. per millimetre at  $\lambda$  900. By a careful scrutiny of many of these plates taken with and without series inductance, it has been possible to classify almost all the important lines in this region, and with the aid of this classification to extend the scheme into the region of longer wave-lengths. The first clue to the discovery of regularities in the spectrum was afforded by our knowledge of the identifications of the important multiplets of the iso-electronic spectrum of As II, arising from the transition of the electron from the  $5s$  to the  $4p$  state. The triplet  $4p\ ^3P-5s\ ^3P$  thus identified is one of the strongest groups in the region  $\lambda$  800, although in the corresponding spectrum of doubly-ionized sulphur, of the same chemical group as selenium, Ingram\* noticed that this group presented very abnormal features. The intensity of this group in S III is much less than what might be expected of a resonance group, and the intervals of the  $5s\ ^3P$  term are abnormally small. When an " $s$ " electron is added to an ion in a  $^3P$  state, we derive the four levels  $^3P_{0,1,2}$  and  $^1P_1$  and according to the theory of multiplet separations developed by Goudsmit,† the separation of the " $s$ " levels with  $j = 2$  and  $j = 0$  is constant through the whole series of levels and equal to the  $p$  doublet of the ion. This rule generally holds good with remarkable accuracy, as shown in Table II, which was started previously by Rao.‡ In S III, however,  $4s\ ^3P_0-4s\ ^3P_2$  is as low as  $450\text{ cm.}^{-1}$ , while the limiting difference  $^3P_1-^3P_2$  is about  $950\text{ cm.}^{-1}$ . In the spectrum of Se III, now under consideration, the relation is found true and it is indeed peculiar that it should break down only in a single instance.§

The abnormality in the interval ratio of  $4s\ ^3P_1-4s\ ^3P_2$  to  $4s\ ^3P_0-4s\ ^3P_1$ , observed by Ingram in S III, is seen to be a characteristic feature of all the

\* 'Phys. Rev.,' vol. 33, p. 907 (1929).

† 'Phys. Rev.,' vol. 31, p. 946 (1928).

‡ 'Proc. Roy. Soc.,' A, vol. 124, p. 472 (1929).

§ The case of N I, in which also the first  $s\ ^3P$  term interval is abnormally small, is different from that under consideration (cf. 'Phys. Rev.,' vol. 33, p. 912 (1929)).

Table II.—Term Intervals in Spectra of  $s^2 p^2$  Electronic Configuration.

	C I.	N II.	O III.	F IV.	Si I.	P II.	S III.	Cl IV.	Ge I.	As II*.	Se III.	Br IV*.
$m s (^2P_0-^2P_1)$	60.1	167.96	375.3	618	271.93	528.1	449.7	1446	1666.1	2778	4114.1	5970
$m + 1 s (^2P_0-^2P_2)$	—	170.70	373	—	282.9	546.8	924.2	—	1740.2	—	—	—
$m + 3 s (^2P_0-^2P_2)$	—	173.4	—	—	284.4	—	—	—	1764.9	—	—	—
	C II.	N III.	O IV.	F V.	Si II.	P III.	S IV.	Cl V.	Ge II.	As III.	Se IV.	Br V.
Limit: $^2P_1-^2P_2$	64.0	174.4	387	—	287	566	950	1500	1768	2940	4376	6085

\* As II: A. S. Rao, 'Proc. Phys. Soc.', vol. 44 p. 343 (1932). Br IV: From unpublished results of A. S. Rao.

similar spectra of the next row of the periodic table, i.e., of Ge I, As II, Se III, as is evident from Table III.

Table III.—Interval Ratios.

Spectrum.	$\frac{(5s^3P_1 - 5s^3P_2)}{(5s^3P_2 - 5s^3P_1)}$
Ge I .....	5.65
As II .....	6.00
Se III .....	7.16

All the classifications obtained in the present work are collected in multiplet form in Table IV and a catalogue of these lines is given in Table V. The tables are self-explanatory.

#### Discussion.

The group of  $5p$  terms was identified chiefly with the aid of the differences of the  $5s^3P$  terms. It is interesting to observe that the line  $\nu 24704.4$  is stronger than any of the three lines  $\nu 25969.3$ ,  $29578.9$  or  $30083.0$  and this feature has led the authors to designate the level  $118563.6$  as  $5p^1P_1$  instead of  $5p^3P_1$ . This assignment, however, has left  $5p^3P_1$  unidentified, and it is considered possible that the  $5p^3P$  term may present some anomalous feature, either in the relative magnitude of the intervals of its components or the absence or faintness of one line of the group, say,  $5s^3P_2 - 5p^3P_1$  as in S III. The same difficulty has presented itself in the case of the  $5p^3P$  term of As II, which has been under investigation by A. S. Rao.\* Effective comparison of the spectra could not be made with either P II or S III, as in neither of these have singlets or inter-combination lines been identified. However, when the spectra of As II and Se III are correlated, the difficulty is overcome if it is supposed that, in both these spectra, the intensity of the inter-combination line  $5s^1P_1 - 5p^3P_1$  is abnormally large. The magnitude of the intervals of the component levels of  $5p^3P$ , as well as their ratio, are then mutually consistent with each other. The levels  $5p^3D$  and  $^1D$  as well as  $5p^3S$  could afterwards be easily located, but the level  $5p^1P_1$  is yet undiscovered.

The group of  $4d$  terms may next be considered. All the levels  $^3F^3D^3P$  and  $^1F^1D^1P$  have been identified.  $4d^3F_2$  and  $4d^3F_3$  give fairly strong combination lines with  $4p^3P_1$  and  $4p^3P_2$  respectively and the identification is confirmed by the detection of the complete and characteristic multiplet

\* *Loc. cit.*, and also 'Current Science' (in the press).

Table IV.—Multiplets in Se III.

$4p$	$^3P_0$ 274924	$^3P_1$ 273183	$^3P_2$ 270987	$^1D_2$ 261892
$5s\ ^3P_0 = 148647.1$ 504.5		124532 (6)		
$^3P_1 = 148142.6$ 3609.6	126780 (6)	125040 (4)	122844 (6)	113746 (4)
$^3P_2 = 144533.0$		128649 (8)	126454 (7)	117357 (3)
$^1P_1 = 143268.1$	131659 (2)	129914 (1)	127720 (2)	118623 (9)
$4d\ ^3F_3 = 135863.7$ 1257.9		122309 (4)	—	111014 (1)
$^3F_2 = 134405.8$ 2009.7			121372 (6)	112274 (3)
$^3F_4 = 132306.1$				
$^1F_2 = 126249$			—	135643 (7)
$^3D_1 = 134284.3$ —1230.0	140639 (6)	138895 (6)	136698 (3)	127606 (3)
$^3D_2 = 135514.3$ 2604.9		137661 (8)	135468 (3)	126376 (0)
$^3D_3 = 132909.4$			138070 (9)	128981 (0)
$D_1 = 135720.3$		137455 (1)	135261 (3)	126170 (5)
$P_0 = 132608.2$ 442.4		140572 (6)		
$^3P_1 = 132165.8$ —52.1	[142753]	141012 (7)	138816 (6)	129720 (6)
$^3P_2 = 132217.9$		140964 (7)	138764 (7)	—
$^1P_1 = 137977.5$	136939 (2)	135201 (5)	133007 (6)	123910 (5)
$sp\ ^3D_1 = 183833$ 1632	91090 (6)	89352 (10)	[87156]	—
$^3D_2 = 182201$ 3825		90984 (9)	88788 (3)	—
$^3D_3 = 178376$			92613 (8)	
$^3P_0 = 168442$ 109		104741 (7)		
$^3P_1 = 168333$ —76	106592 (6)	104850 (8)	102658 (6)	93557 (1)
$^3P_2 = 168409$		104774 (7)	102581 (9)	93482 (1)
$^1X = 127105$		146079 (1)	143881 (2)	134787 (7)

Table IV—(continued).

$6p$	$^3D_1$ 209.5 12712.6	$^3D_2$ 3172.0 121403.1	$^3D_3$ 3172.0 118231.1	$^3P_0$ 1577.4 120141.0	$^3P_1$ 3413.4 118663.6	$^3P_2$ 3413.4 117049.8	$^3S_1$ 115621.1	$^1D_2$ 113753.8
$5s^3P_0 = 148677.1$ $504.5$	26934.3 (9)				30083.0 (5)		33026.0 (2)	
$^3P_1 = 149142.6$ $3699.6$	26429.9 (2)	26739.5 (10)		28001.5 (8)	28678.9 (8)	31092.5 (5)	32521.2 (4)	34389.0 (3)
$^3P_2 = 144533.0$	22820.5 (0)	23129.8 (4)	26301.8 (10)		25869.3 (5)	27483.2 (10)	28912.0 (10)	30778.8 (4)
$^1P_1 = 143268.1$	21555.4 (7)	21864.8 (3)		23126.9 (3)	24704.4 (9)	26218.3 (2)	27646.9 (3)	28614.2 (10)
$4d^3P_2 = 136663.7$ $2257.9$	29159.9 (8)	29469.1 (6)	32641.1 (3)		32308.4 (4)	33822.7 (2)	—	37119.3 (0)
$^3F_2 = 134406.8$ $2999.7$		28211.7 (9)	31383.1 (5)			32564.6 (5)	—	35861.2 (1)
$^3F_4 = 132306.1$			29283.4 (10)					
$^3D_1 = 134284.3$ $-1230.0$	[12571.7]	[12881.2]		[14143.3]	15720.2 (1)	—	—	20530.9 (2)
$^3D_2 = 135514.3$	[13801.7]	[14111.2]	17282.3 (2)		16950.2 (5)	—	—	21759.0 (1)
$^3D_3 = 132909.4$ $2604.9$		[11506.3]	[14678.3]			15859.1 (8)		
$^1D_2 = 135720.3$					17156.9 (1)		20099.1 (2)	21966.4 (3)
$^3P_0 = 132608.2$ $442.4$	[10895.6]				[14045.2]		16987.1 (2)	
$^3P_1 = 132165.8$	[10453.2]	[10762.7]			[12025.4]	15116.6 (2)	16544.7 (5)	—
$^3P_2 = 132217.9$ $-52.1$	[10505.3]	[10814.8]	[13986.8]		[13653.3]	15167.1 (3)	16586.8 (6)	—
$^1P_1 = 137977.5$		16574.2 (1)				20927.5 (1)		24223.8 (9)

Table V.—List of Classified Lines in Se III.

$\lambda$ I.A. (int.).	$\nu$ .	Classification.	$\lambda$ I.A. (int.).	$\nu$ .	Classification.
9563.83	10458.2	$4d^1P_1-5p^1D_1$	3027.04 (2)	33026.0	$5s^1P_1-5p^1S_1$
9516.39	10505.3	$^3P_2-^3D_2$	2955.73 (2)	33822.7	$4d^1F_3-^3P_3$
9288.80	10762.7	$^3P_1-^3D_2$	2907.06 (3)	34389.0	$5s^1P_1-^1D_2$
9243.99	10814.8	$^3P_2-^3D_2$	2787.71 (1)	35861.2	$4d^1F_3-^1D_2$
9175.50	10895.6	$^3P_0-^3D_1$	2693.22 (0)	37119.3	$^3F_4-^1D_2$
8688.50	11506.3	$^1D_2-^3D_2$			
8313.45	12025.4	$^3P_1-^3P_0$	$\lambda$ vac.		
8001	12495	$^1F_3-^1D_2$	1126.28 (3)	88788	$4p^1P_1-^3p^1D_2$
7952.19	12571.7	$^1D_2-^3D_1$	1119.17 (10)	89352	$^3P_1-^3D_1$
7761.12	12881.2	$^1D_1-^3D_2$	1099.10 (9)	90984	$^3P_1-^1D_2$
7349.40	13602.8	$^3P_1-^3P_1$	1097.82 (6)	91090	$^3P_1-^1D_2$
7322.22	13653.3	$^3P_2-^3P_1$	1079.78 (8)	92613	$^3P_1-^1D_2$
7243.49	13801.7	$^1D_1-^3D_1$	1069.72 (1)	93482	$^1D_1-^3P_2$
7147.63	13986.8	$^3P_2-^3D_2$	1068.87 (1)	93557	$^1D_1-^3P_1$
7117.91	14046.2	$^3P_0-^3P_1$	974.84 (9)	102581	$^3P_1-^3P_1$
7084.62	14111.2	$^1D_2-^3D_1$	974.11 (6)	102658	$^3P_1-^3P_1$
7068.54	14143.3	$^1D_1-^3P_0$	954.74 (7)	104741	$^3P_1-^3P_1$
6810.90	14678.3	$^1D_2-^3D_2$	954.44 (7)	104774	$^3P_1-^3P_1$
6613.40 (2)	15116.6	$^3P_1-^3P_2$	953.74 (8)	104850	$^3P_1-^3P_1$
6591.40 (3)	15167.1	$^3P_2-^3P_2$	938.16 (6)	106592	$^3P_1-^3P_1$
6359.51 (1)	15720.2	$^1D_1-^3P_1$	900.79 (1)	111014	$^1D_1-4d^1F_3$
6303.80 (6)	15859.1	$^1D_1-^3P_2$	890.68 (3)	112274	$^1D_1-^3F_3$
6042.55 (5)	16544.7	$^3P_1-^3S_1$	879.15 (7)	113746	$^1D_1-5s^1P_1$
6031.80 (1)	16574.2	$^1P_1-^3D_2$	852.10 (3)	117357	$^1D_1-^3P_1$
6023.58 (6)	16596.8	$^3P_1-^3S_1$	843.01 (9)	118623	$^1D_1-^3P_1$
5898.11 (5)	16950.2	$^1D_2-^3P_1$	823.91 (6)	121372	$^1D_1-4d^1F_3$
5885.18 (2)	16987.1	$^3P_0-^3S_1$	817.60 (4)	122309	$^3P_1-^3F_3$
5826.06 (1)	17156.9	$^1D_1-^3P_1$	814.04 (6)	122844	$^3P_1-5s^1P_1$
5784.68 (2)	17282.3	$^1D_2-^3D_2$	807.04 (5)	123910	$^1D_1-4d^1P_1$
4973.96 (2)	20099.1	$^1D_1-^3S_1$	803.01 (6)	124532	$^3P_1-5s^1P_1$
4869.36 (2)	20530.9	$^1D_1-^1D_2$	799.76 (4)	125040	$^3P_1-^3P_1$
4777.07 (1)	20927.5	$^1P_1-^3P_2$	792.58 (5)	126170	$^1D_1-4d^1D_2$
4637.91 (7)	21555.4	$5s^1P_1-^3D_1$	791.29 (0)	126378	$^1D_1-^3D_2$
4594.52 (1)	21759.0	$4d^1D_2-^1D_2$	790.80 (7)	126454	$^3P_1-5s^1P_1$
4572.29 (3)	21864.8	$5s^1P_1-^3D_2$	788.77 (6)	126780	$^3P_1-^3P_1$
4551.13 (3)	21966.4	$4d^1D_2-^1D_2$	783.66 (3)	127606	$^1D_1-4d^1D_1$
4380.80 (0)	22820.5	$5s^1P_1-^1D_1$	782.96 (2)	127720	$^3P_1-5s^1P_1$
4322.75 (3)	23126.9	$^1P_1-^3P_0$	777.81 (8)	128649	$^3P_1-^3P_1$
4322.22 (4)	23129.8	$^3P_2-^3D_2$	775.81 (0)	128981	$^1D_1-4d^1D_2$
4127.01 (9)	24223.8	$4d^1P_1-^1D_2$	770.89 (6)	129720	$^1D_1-^3P_1$
4046.72 (9)	24704.4	$5s^1P_1-^3P_1$	769.74 (1)	129914	$^3P_1-5s^1P_1$
3849.62 (5)	25960.3	$^3P_2-^3P_1$	759.54 (2)	131659	$^3P_1-^3P_1$
3813.05 (2)	26218.3	$^1P_1-^3P_2$	751.84 (6)	133007	$^3P_1-4d^1P_1$
3800.94 (10)	26301.8	$^3P_2-^3D_2$	741.94 (7)	134787	$^1D_1-^1X$
3752.53 (2)	26429.9	$^3P_1-^1D_1$	739.64 (5)	135201	$^3P_1-^3P_1$
3738.73 (10)	26739.5	$^3P_1-^3D_2$	739.31 (3)	135261	$^3P_1-^1D_2$
3711.68 (9)	26934.3	$^3P_0-^3D_2$	738.18 (3)	135468	$^3P_1-^3D_2$
3687.56 (10)	27483.2	$^3P_2-^3P_2$	737.23 (7)	135643	$^1D_1-^3F_3$
3616.02 (3)	27646.9	$^1P_1-^3S_1$	731.54 (3)	136698	$^3P_1-^3D_2$
3570.22 (8)	28001.5	$^3P_2-^3P_0$	730.25 (2)	136939	$^3P_1-^3P_1$
3543.62 (9)	28211.7	$4d^1F_3-^1D_2$	727.51 (1)	137455	$^3P_1-^1D_2$
3457.79 (10)	28912.0	$5s^1P_1-^3S_1$	726.42 (8)	137661	$^3P_1-^3D_2$
3428.39 (8)	29159.9	$4d^1F_3-^1D_1$	724.27 (9)	138070	$^3P_1-^3D_2$
3413.93 (10)	29283.4	$^3F_4-^1D_2$	720.65 (7)	138764	$^3P_1-^3P_1$
3392.41 (6)	29469.1	$^3F_3-^1D_2$	720.38 (6)	138816	$^3P_1-^3D_2$
3387.23 (10)	29514.2	$5s^1P_1-^1D_1$	719.97 (6)	138895	$^3P_1-^3D_2$
3379.83 (8)	29578.9	$^3P_1-^3P_1$	711.38 (6)	140572	$^3P_1-^3P_0$
3323.18 (5)	30083.0	$^3P_2-^3P_1$	711.04 (6)	140639	$^3P_1-^3D_2$
3248.06 (4)	30777.8	$^3P_2-^1D_2$	709.40 (7)	140964	$^3P_1-^3P_1$
3215.28 (5)	31092.5	$^3P_1-^3P_2$	709.16 (7)	141012	$^3P_1-^3P_1$
3185.51 (5)	31383.1	$4d^1F_3-^3D_2$	700.51	[142753]	$^3P_1-^3P_1$
3094.27 (4)	32308.4	$^3F_3-^3P_1$	695.02 (2)	143881	$^3P_1-^1X$
3074.03 (4)	32521.2	$5s^1P_1-^3S_1$	684.56 (1)	146079	$^3P_1-^1X$
3069.93 (5)	32546.6	$4d^1F_3-^3F_3$			
3062.55 (3)	32641.1	$^3F_3-^3D_2$			

Note.—Lines of  $\lambda$  between 9563.83 and 6610.90 are calculated.

$4d^3F-5p^3D$  in the quartz region. The reality of the levels receives further support from their combinations with  $5p^3P_{1,2}$  and  $5p^1D_2$ . The term  $4d^3D$  is found to be partially inverted and, in this feature, is analogous to the iso-electronic spectra of Ge I and As II.\* One line of the multiplet  $4p^3P-4d^3P$  is missing, which might throw some doubt on this classification, but the detection of  $4d^3P-5p^3S$  supports the assignment. A further test of the correctness of the levels  $4d^3P$  and  $4d^3D$  is the existence, though partially, of their combinations with the terms of the  $5p$  state. Some of these lines lie in the far infra-red, which has not yet been satisfactorily investigated. The frequencies of such lines are merely calculated values and are enclosed in brackets in Table IV.

The relative values of the intensities, perhaps, suggest that the levels  $4d^1P_1$  and  $4d^3P_1$  should be interchanged but this would lead to abnormally large intervals of the  $4d^3P$  terms, and the adopted assignment is supported by other combinations with the higher  $5p$  term. The identification of  $4d^1F_3$  rests on a single line  $\nu$  135643, which has been selected from among two or three lines, in the proper region, which have not otherwise entered into the scheme.

As already remarked, a special feature of the analysis is the discovery of multiplets involving a transition of one of the inner electrons. All the lines entering into these two groups behave very similarly under the action of different intensities of excitation in the discharge tube as well as in the vacuum spark. An examination of the plates unmistakably indicated that they should form the characteristic multiplets suggested in this scheme. In spite of the anomalous intensity of the line  $^3D_1-^3P_1$  of the group  $sp^3D-4p^3D$ , it is believed that the group is correctly identified. It has been difficult, however, to detect with certainty, the levels  $^5s$  or  $^3s$  or the singlets, belonging to this configuration. Besides the levels included in the above tables, many more have been identified, from among lines which could be definitely assigned to the doubly-ionized atom of selenium in the region of short-wave-lengths. The definite classification of these and the analysis of the spectrum of singly-ionized selenium will form the subject of future communications.

Attention may here be drawn to a very interesting sequence† of the interval ratios of the components of the  $mp^3P$  terms in the spectra of the type under consideration. It will be seen from the following table, which exhibits these ratios, that there is a regular departure from the theoretical ratio 2 : 1, indicating a gradual and progressive change from the normal Russell-Saunders type of

\* Cf. 'Proc. Phys. Soc.,' vol. 44, p. 345 (1932), alternative choice.

† This has been kindly pointed out to the authors by A. S. Rao.



Table VI.—Interval Ratios of  $mp\ ^3P$  Terms.

Spectrum.	$mp \frac{{}^3P_1 - {}^3P_2}{{}^3P_0 - {}^3P_1}$	$m + 1p \frac{{}^3P_1 - {}^3P_2}{{}^3P_0 - {}^3P_1}$
Cl I .....	1.86	1.63
N II .....	1.68	1.66
O III .....	1.66	1.59
F IV .....	1.75	—
Si I .....	1.90	—
P II .....	1.84	3.17
S III .....	1.78	2.63
Cl IV .....	1.76	—
Ge I .....	1.53	—
As II .....	1.39	1.15
Se III .....	1.26	0.96
Br IV .....	0.92	0.95
Sn I .....	1.03	—
Sb II* .....	0.85	—

\* R. J. Lang (private communication).

coupling. Obviously, the ratio diminishes with increasing nuclear charge in the case of  $mp$  as well as in  $(m + 1)p$  terms.\*

Also the ratio in certain cases becomes even less than unity, so that the difference  ${}^3P_0 - {}^3P_1$  is greater than  ${}^3P_1 - {}^3P_2$ . This feature begins to happen at the second stage of ionization (*i.e.*, in Se III) in the  $5p$  terms and in Br IV even in the  $4p$  terms; while, in the spectra of the next row of the periodic table it is exhibited at the first stage of ionization and, in the last row, in the arc spectrum itself.

#### Term Values.

For the evaluation of the absolute values of the terms, the two members of the series  $5s\ ^3P - mp\ ^3P$  and of  $5s\ ^1P_1 - mp\ ^1D_2$  have been used. The terms are based on the mean value  $4p\ ^3P_0 = 274924\text{ cm.}^{-1}$  thus obtained. The error in such an evaluation may, doubtless, be as large as some thousands. The degree of accuracy of the absolute values must therefore be taken to be limited by this consideration. The largest term  $4p\ ^3P_0$  leads to a value of 33.9 volts for the third ionization potential of selenium. The terms obtained, together with those of As II† and Ge I‡ for purposes of comparison, are given in Table VII.

It is seen from Table VII that the value of the terms of the  $sp^3$  configuration,

\* The value 1.75 in the case of F IV appears to be anomalous; but the measurements of the differences are subject to large errors.

† The term values here given are partly from unpublished results of A. S. Rao.

‡ K. R. Rao, 'Proc. Roy. Soc.,' A, vol. 124, p. 465 (1929).

Table VII.—Term Values.

Term.	Se III.		As II.		Ge I.		Term.	Se III.		As II.		Ge I.	
	v.	$\Delta v.$	v.	$\Delta v.$	v.	$\Delta v.$		v.	$\Delta v.$	v.	$\Delta v.$	v.	$\Delta v.$
$4p^3\ ^3P_0$	274924	1741	162788	1063	65558.0	537.11	$4d^3\ ^3D_1$	134284.3	-1230.0	63723	483	16585.7	-80.4
$\ ^3P_1$	273183	2196	161725	1477	65000.89	832.50	$\ ^3D_2$	135514.3	2604.9	63240	562	16676.1	262.2
$\ ^3P_2$	270987		160248		64148.09		$\ ^3D_3$	132909.4		62398		16413.9	
$\ ^1D_2$	261892		152893		58432.78		$\ ^1D_2$	135730.3		60305		17078.3	
$3p^3\ ^3D_1$	183833	1633	89041	114	5833.3	-36.6	$\ ^3P_0$	132608.2	442.4	59547	30	13578.2	-278.2
$\ ^3D_2$	182201	3325	88927	332	5869.9	-33.0	$\ ^3P_1$	132165.8	-52.1	50467	-47.5	13853.4	-267.2
$\ ^3D_3$	178376		88545		5902.9		$\ ^3P_2$	132217.9		50942		14120.6	
$\ ^3P_0$	168442	109	78340	154			$\ ^1P_1$	137977.5		61302		12711.0	
$\ ^3P_1$	168333	-76	78156	470			$3p^3\ ^3D_1$	121712.6	309.5	65876	260		
$\ ^3P_2$	168409		77686				$\ ^3D_2$	121403.1	3172.0	65676	2084		
$\ ^3P_0$	148047.1	504.5	84059	397	28106.43	250.59	$\ ^3D_3$	118231.1		63592			
$\ ^3P_1$	148142.6	3609.6	83662	2381	27855.84	1415.51	$\ ^1D_2$	113753.8		60399			
$\ ^3P_2$	144533.0		81281		26440.33		$\ ^3P_0$	120141.0	1577.4	64553	943		
$\ ^1P_1$	143268.1		79972		25537.65		$\ ^3P_1$	118563.6	1513.5	63810	1080		
$4d^3\ ^3P_2$	135663.7	1287.9	73962	722	15489.3	254.1	$\ ^3P_2$	117049.8		62530			
$\ ^3P_0$	134405.8	2699.7	73240		15235.2		$\ ^3S_1$	115621.1		61702			
$\ ^3P_1$	132306.1		—		—								
$\ ^3P_2$	126249		53916		13906.0								

relative to those of  $5s$  or  $4d$  state, is increasing with increasing ionization, so that, as is evident from the spectra themselves, the multiplets  $4p\ ^3P-sp\ ^3P$  and  $4p\ ^3P-sp\ ^3D$  are observed more predominantly in Se III than in either As II or Ge I. As already remarked in a previous paper,\* this feature might throw some light on the relative importance of the inner electron transition when we pass from the arc to the successively higher spark spectra of the various elements. In a "normal" spectrum, it is expected that, of terms arising from a given electronic configuration, the separations between the sub-levels are small compared with those between the different terms themselves. A departure from this general rule is observed in the spectrum of As II, as well as in that of Se III. The intervals of the  $5p\ ^3P$  term are larger than usual so that the level penetrates partially into that designated as  $5p\ ^3D$ . A similar interpenetration of the sub-levels of different terms is evident also among those arising from the  $4d$  configuration. Increase of nuclear charge, as might generally be expected, seems to favour the occurrence of this feature. Further, an examination of the term values of all the spectra that are iso-electronic with C I, Si I and Ge I, which have hitherto been investigated, shows that this feature appears only in the case of As II and Se III indicating, for the first time, a definite departure from the characteristics of a "normal spectrum," even in the relatively simple case of an  $s^2p^2$  electron system.

It is a pleasure to express our deep sense of gratitude to Professor A. Fowler, F.R.S., for his very stimulating and continued interest in our work.

#### *Summary.*

Following the publication of the analysis of the spectra of Se IV and Se V, the spectrum of doubly-ionized Se has been investigated with the aid of the experimental data available in the previous work. The triplet and singlet systems of Se III due to the configurations  $4p^2$ ,  $4p5s$ ,  $4p5p$ ,  $4p4d$  and  $4s4p^2$  have been discovered, an important feature being the identification of the terms of the last-mentioned state. About 110 lines have entered into the scheme; besides these, lines belonging to a few triplet groups, expected to lie in the far infra-red, have been calculated. The absolute values of the terms have been determined from two members of a triplet and a singlet series. The largest term,  $4p\ ^3P_0 = 274924\text{ cm.}^{-1}$ , leads to a value of 33.9 volts for the third ionization potential of selenium. An examination of these term values has shown that there is an interpenetration of the sub-levels of terms belonging to the  $4d$  state as well as of those of the  $5p$  state, indicating a definite departure from normality even in the relatively simple case of an  $s^2p^2$  electronic system.

\* K. R. Rao, 'Proc. Roy. Soc.,' A, vol. 125, p. 238 (1929).

*The Theory of Metallic Corrosion in the Light of Quantitative Measurements. Part VI.—The Distribution of Corrosion.*

By G. D. BENGOUGH and F. WORMWELL.

Communicated by Sir Harold Carpenter, F.R.S.—Received November 25, 1932.)

[PLATES 4–6.]

In previous parts of this research it has been shown that the rate of oxygen supply to the whole metal surface is the factor which generally controls the rates of corrosion of zinc and mild steel in the conditions studied, though other factors may affect them appreciably in special conditions. Such factors are the evolution of hydrogen and the formation of protective films or masses of corrosion products which may result from increased alkalinity, or other causes. Neither the basic potential of the metal nor the conductivity of the electrolyte exercised control over a wide range of salt concentration. Corrosion distribution was at first sporadic but was soon concentrated at a few large irregularly shaped areas.

For many purposes distribution is more important than the total amount of corrosion, especially when it is so localized as to be called pitting. The irregular distribution of corrosion was formerly believed to be caused by chemical and physical heterogeneity of the metal, but differential aeration is now usually believed to be a more frequent cause of local corrosion and this view was accepted in Parts I to III of this research.

The matter was first studied in detail by J. Aston,\* who showed that areas on the surface of iron and steel which were covered with wet rust were anodic to the surrounding metal. McKay† followed up Aston's ideas, and U. R. Evans and his associates‡ have studied the differential aeration produced by partial immersion of metals in stagnant solutions. Most of their experiments have been carried out for short times, such as a few days, and only give information about the initial stages of corrosion.

\* 'Trans. Amer. Electrochem. Soc.,' vol. 29, p. 449 (1916).

† 'Ind. & Eng. Chem.,' vol. 17, p. 23 (1925).

‡ 'J. Inst. Met.,' vol. 30, p. 261 (1923), and many other papers, the most recent of which are by Evans, Bannister and Britton, 'Proc. Roy. Soc.,' A, vol. 131, p. 355 (1931), and Evans and Hoar, *ibid.*, vol. 137, p. 343 (1932).

Herzog and Chaudron,\* using an extreme method of differential aeration, associate themselves with Evans' views; Bengough, Stuart and Lee† at first accepted the idea that zinc corrosion products would act as oxygen screens and so build up potential differences that would localize corrosion, but in later papers this view was rejected.‡

It is generally agreed that the unattacked, or less corroded, areas of zinc and iron specimens in alkaline chlorides are wholly or partially protected by a film; this was originally thought to be formed by direct oxidation, but most authors now regard it as maintained by precipitation of hydroxide or hydrated oxide or carbonate. Evans explains its formation, on differentially aerated specimens, as due to the larger local oxygen supply which reacts with the hydrogen displaced by metal corroding elsewhere, and so causes a relatively high concentration of alkali; consequently any metal entering solution through the pores in an air-formed oxide film formed by direct oxidation is instantly precipitated.

On totally immersed specimens a starting point of the differential aeration process of corrosion is often considered to be the relative absence of oxygen from the inside of pits, pores, cracks or crevices in or between metals. Speller§ says "the variation in the concentration of dissolved oxygen on the surface of the corroding metal is perhaps the most active cause of pitting."

The "differential aeration principle" has been freely used to explain corrosion in industry.|| Montgomerie and Lewis,¶ in a paper on corrosion in the hulls of merchant vessels, say "intensity of corrosion occurs in those parts where a patch of rust prevents access of oxygen to the material beneath. Such a part becomes anodic to the surrounding structure and wastage goes on with increasing rapidity as the area of the part is circumscribed, resulting in the pitting so frequently observed. The paradoxical fact has, therefore, to be accepted that, while a free access of oxygen is necessary for the continuance of the corrosive action, the most intense corrosion occurs on those parts of the metal where access of oxygen to the surface is least."

The present paper is an attempt to estimate the limits, if any, within which

\* 'C. R. Acad. Sci. Paris,' vol. 192, p. 837 (1931); Chaudron, 'Chim. et Ind.,' vol. 26, p. 273 (1931).

† 'Proc. Roy. Soc.,' A, vol. 116, pp. 429, 458 (1927); vol. 121, p. 116 (1928).

‡ Bengough, Lee and Wormwell, 'Proc. Roy. Soc.,' A, vol. 131, pp. 515-517 (1931); vol. 134, p. 321 (1931).

§ "Corrosion, Causes and Prevention" (1926), p. 364, McGraw Hill Book Co.

|| Evans, 'J. Inst. Metals,' vol. 46, p. 22 (1931).

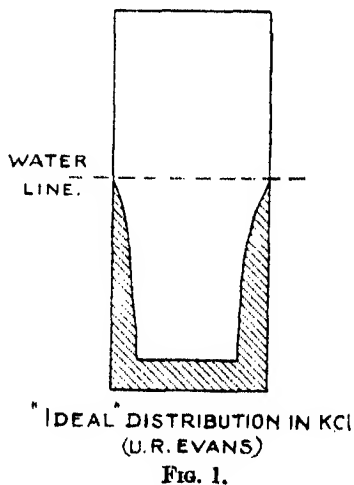
¶ Institution of Engineers and Shipbuilders in Scotland, 1932.

the differential aeration principle holds.\* Three of the supposed most important methods of producing differential aeration sufficient to affect corrosion distribution have been used, namely, partial immersion, deposits of corrosion products and neutral bodies, and crevices.

### I. Effect of Partial Immersion.

Evans and Hoar† have shown that almost the whole of the hydrogen depolarization at a partially immersed steel surface takes place over a band 2 mm. in depth at the water-line (in 4 cm. diameter vessels) and could find no oxygen in the solution below; this puts Cobb's early observation‡ on a definitely quantitative basis. Evidently a very high degree of differential aeration occurs and conclusions based on partial immersion experiments should be applied with caution when the degree of differential aeration is either unknown or probably small.

A typical experiment used by Evans to demonstrate the effect of differential aeration was partially to immerse thin sheet iron or steel (ground on No. 1 emery paper) in KCl solution in a vessel of 4 cm. diameter. Corrosion normally began on the three immersed edges and spread upwards and inwards as shown in fig. 1. The upward spreading was explained by the gradual exhaustion of oxygen from below upwards, and the screening effect of the rust formed by corrosion. In the short experimental periods studied a considerable area remained uncorroded.



Evans and Hoar showed that in constant temperature conditions the current passing between the attacked and unattacked areas corresponded reasonably closely with the amount of anodic corrosion that occurred during two days.

Experiments have been made by us to ascertain the persistence and downward extension of the protected areas of half-immersed specimens. Emery

\* See Monypenny, "Stainless Iron and Steel," p. 255, 2nd ed. (1931) (Chapman & Hall), for a statement from the point of view of a metallurgist.

† 'Proc. Roy. Soc.,' A, vol. 137, p. 343 (1932).

‡ 'J. Iron Steel Inst.,' vol. 83, p. 174 (1911).

polished sheets of rolled copper-free mild steel and "Anaconda" zinc\* were cut into strips 15 cm.  $\times$  2 cm.; one piece of the steel was marked on one side with a series of deep horizontal scratches and all four were degreased in carbon tetrachloride and weighed. They were then hung vertically on glass hooks in N/2 NaCl in the authors' simple type of closed vessel† containing oxygen, and maintained at 25° C.; a length of about 12.5 cm. of each specimen was immersed. The pressure in the vessel fell owing to absorption of oxygen but was brought back to 760 mm. every 3 or 4 days.

Corrosion started along the cut edges of both steel strips, and at the end of a few hours was observable right round the three immersed edges. At the end of 28 and 139 days the specimens were removed and photographed, figs. 2 to 4, Plate 4. Protection was apparently complete near the centre of the specimens down to a depth of at least 10 cm. Corrosion had spread nearly to the centre of one face of each of the specimens, while elsewhere it had formed a narrow irregular band 3 or 4 mm. wide, extending right up to the water-line where a pit occurred, fig. 4. In many places abrupt changes in the amount of corrosion occurred where there was no corresponding change of accessibility to oxygen.

The length of liquid path between the most deeply immersed corroded area and the cathode (strip along water-line) was at least 10 cm., whereas it was only 1 or 2 cm. for other equally corroded areas; hence electrolytic resistance is not a factor which controls distribution in the conditions obtaining; moreover, the total corrosion was similar to that on a specimen of the same width but with only 3.5 cm. immersed.

The two zinc strips were tested for 25 and 72 days and photographed, figs. 5 and 6, Plate 4. Almost unattacked areas occurred on both sides of the strip tested for 25 days, the two largest areas being situated just below the water-line, fig. 5, but most of each surface was attacked and specially heavily near the top of the specimen. No unattacked areas existed on the specimen tested for 72 days, fig. 6, and the most intense attack occurred at the water-line, along which the specimen had been punctured; there were several pitted areas scattered about the surface. It was evident that the distribution of corrosion had been controlled partly by the oxygen supply (in the sense that there was most corrosion where most oxygen reached the metal), partly by films of corrosion products which had given varying degrees of protection, and partly by preferential attack on the edges; clearly the "differential aeration principle" must be strained to breaking point to interpret these facts.

\* Analyses and other details of the metals used in the research are given in the Appendix.

† 'Proc. Roy. Soc.,' A, vol. 131, p. 496 (1931).

On the thin strips of emery-ground metal used by Evans and by ourselves, corrosion normally begins at the edges which cannot be made physically exactly like the faces. Thicker specimens, either turned or milled, can be made more nearly alike on all surfaces, and there is then less tendency for corrosion to begin at the edges. Fig. 7, Plate 4, shows the distribution on a vertical specimen of mild steel, 0.4 cm. thick, 2.0 cm. wide and 5.0 cm. long, prepared on a milling machine, with 3.0 cm. immersed in N/2 NaCl in our standard vessel at 25° C., beneath an atmosphere of purified air; corrosion began along one edge only and gradually spread downwards and inwards till, at the end of 206 days, it covered the area shown; part of the bottom edge of the specimen was protected. Evidently differential aeration had again not been the sole deciding factor, since a part only and not the whole of the bottom edge of the specimen had been attacked. Fig. 8, Plate 4, shows a specimen from a similar experiment, but in a vessel with a diameter of 12.5 cm. Corrosion started on one side near the centre of the specimen and spread outwards and downwards and reached the bottom edge; on the other side corrosion was confined to a very narrow strip near the bottom. Fig. 9, Plate 4, shows that part of even the bottom edge of another specimen was protected for the whole period of an experiment, *i.e.*, 50 days in N/2 NaCl and oxygen. Fig. 10, Plate 4, shows an emery-ground specimen wholly immersed in N/10 KCl with the top edge 1.5 cm. below the liquid surface. A bright unattacked area stretched from the top to the bottom of both sides of the specimen, the rest of which was attacked; a second experiment showed a similar result. Thus differential aeration has ceased to decide the distribution of corrosion even at this shallow depth.

N/2 calcium and magnesium chloride solutions tend to creep up the surfaces of partially immersed steel specimens even in constant temperature conditions, and the most severe corrosion in oxygen often takes place at the wetted areas well above the obvious water-line, that is, at the most aerated part, as shown (for magnesium chloride) in fig. 11, Plate 5. With magnesium chloride there is a narrow protected band, a millimetre or two in width, at the top of the visible meniscus, but below this the attack is general over the whole surface of the specimen. The probable reason for this is that the low solubility of magnesium hydroxide only allows sufficient alkalinity to afford protection quite close to the water-line. The distribution on the immersed surface in calcium chloride more nearly resembles that in sodium chloride, evidently because of the higher solubility of the hydroxide.

The distribution in sea-water beneath oxygen or purified air, fig. 12, Plate 5, somewhat resembles that in magnesium chloride. A mass of hard dense black



and white product forms at the water-line and adheres strongly to the metal, spreading along the liquid surface similarly to fig. 22, Plate 6. Underneath this there is a narrow protected area 1 or 2 mm. wide. The whole of the rest of the metal surface is attacked. It is possible that the well-known buffering action of sea-water prevents rise of alkalinity to a value sufficient to give protection except at the very narrow zone mentioned. If this zone be the main cathode

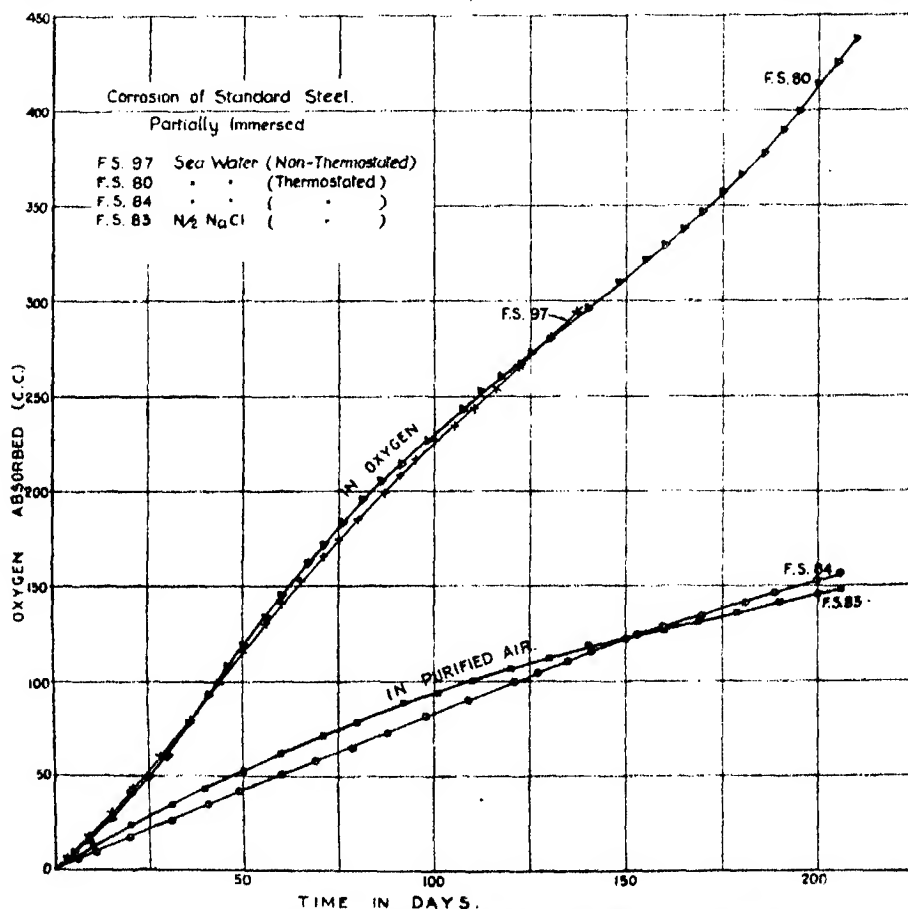


FIG. 13.—Corrosion of standard steel; partially immersed.

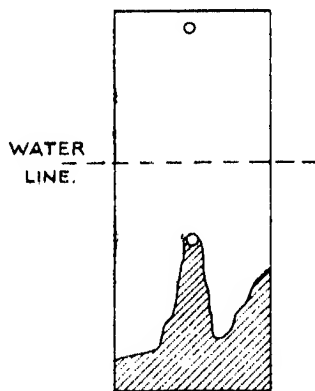
of the specimen it follows that the heavy deposit of corrosion product has but a very slight screening effect against oxygen, for the oxygen/time curve of this specimen was nearly linear as shown in fig. 13 (F.S.80). This is also true for a specimen exposed to convection currents obtained by repeating the last experiment on a laboratory bench (see F.S.97, fig. 13). In ordinary "service" conditions even these narrow protected zones are usually obliterated owing to

the destruction of the protective film by alternate wetting and drying, and heavy "water-line" corrosion occurs at the most highly aerated region of the metal.

Experiments were carried out with milled mild steel specimens partially immersed in  $N/2$  NaCl, or tap-water for 66 days, and exposed on a laboratory bench. Corrosion occurred all over the immersed surfaces in  $N/2$  NaCl right up to the water-line, fig. 32, Plate 6; in tap-water the result was similar except that a band about 2 mm. in depth was protected at the water-line. A specimen of sheet zinc partially immersed in  $N/2$  NaCl for 55 days was attacked most in the neighbourhood of the water-line with one or two protected areas much lower down.

It is now clear that the simple distribution of corrosion shown in fig. 1 cannot be regarded as typical even of half immersed conditions; moreover, it is easily upset by movement of solution and by other physical means. A hole was bored through a steel specimen in such a position that it would normally be in the protected area of a partially immersed specimen; corrosion began round the hole and spread downwards as shown in fig. 14; after a time, however, corrosion spread upwards to areas of *high* oxygen supply at and above the water-line as shown in fig. 14A, Plate 5. A similar result is sometimes due to a short deep scratch, or to some other physical or chemical peculiarity of the metal itself, which causes it to be locally reactive and to pass into solution preferentially. The downward

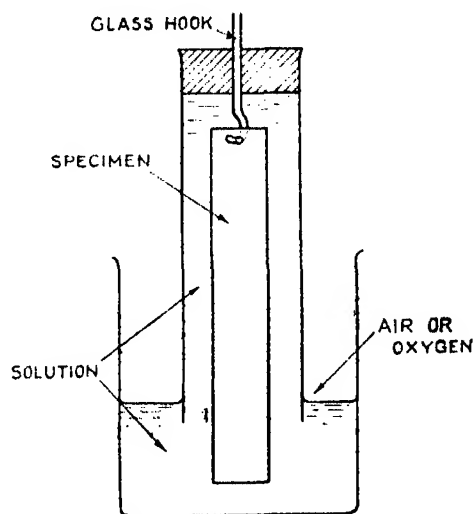
spread of corrosion appears to be a gravity effect. Concentrated metallic chloride solution formed at a reactive area tends to fall and neutralize the alkali beneath it; since protection is due to alkalinity, corrosion would tend to occur below the active area owing to the continual neutralization of alkali by the downward streaming metallic chloride. No doubt some alkali also falls, but a thin film of it can be shown by indicators to spread over, and cling obstinately to, metal surfaces, probably owing to surface tension factors. Distribution of corrosion may therefore be considered on the basis of a general tendency for metallic chloride to sink and alkali to spread over the whole surface of the metal, but at and below corroding areas it may be considered to be neutralized by reaction with metal ions. Any slight upward spreading from a starting



EFFECT OF HOLE.  
FIG. 14.

point is probably due to diffusion and convection acting against gravity. If this be a correct explanation, differential aeration will sometimes apparently be the deciding factor, because the distribution of greatest aeration and greatest alkalinity happen to coincide.

The two factors can easily be separated by inverting the oxygen supply so that it takes place from below upwards as shown in fig. 15. The maximum aeration will now occur at or near the bottom of the specimen which should



PRINCIPLE OF INVERTED EXPERIMENT.

FIG. 15.

be protected on the differential aeration theory, but attacked on the view suggested above.

Fig. 16, Plate 5, shows that the aerated bottom of a steel specimen tested in  $N/2$  NaCl for 10 days at  $25^{\circ}C$  is attacked and the less aerated top protected (compare with fig. 14). Several other specimens tested for periods up to 35 days showed similar results, i.e., the attack started at the hole bored to take the glass suspension hook, and as usual, spread downwards, notwithstanding that this is the direction of greater oxygen supply.

Other experiments were carried out under the ordinary conditions of a laboratory shelf; results are shown in fig. 17, Plate 5, which gives photos of portions of a specimen immersed for 130 days in  $N/2$  NaCl, and fig. 18, Plate 5, of a specimen in sea-water for 101 days; the less aerated top portions are almost completely protected.

In  $N/2$  NaCl and "equilibrium" water the amount of corrosion decreased

steadily from the bottom to the top. In the sea-water the whole of the top three-quarters of the specimen was well protected, together with a small area round the bottom edge of the specimen. Tap-water showed a similar result, but the corrosion was rather more widely disseminated.

If the distribution of alkali, and not necessarily of oxygen, be the controlling factor in the distribution of corrosion on zinc and mild steel, then a solution buffered so as to prevent local rise of alkalinity should cause corrosion to spread over the whole metal surface, provided that the electrolyte resistance is insufficient to affect the result. Tests were made with N/2 NaCl saturated with boric acid as a buffer and the whole brought to  $p_H$  7 with a little NaOH. Standard steel specimens wholly immersed in this solution were attacked all over their surfaces, and partially immersed milled strips over the whole of the immersed surface.

The above explanation seems to account satisfactorily for the spreading of corrosion over the surfaces of partially immersed specimens of zinc and mild steel without having recourse to the hypothesis adopted by Evans\* and many others that precipitated corrosion products act as oxygen screens.

The conclusions to be drawn from the partial immersion experiments in chloride solutions and from previous work, seem to be:—

- (1) Zinc and mild steel of the types used in this research tend to pass into solution slowly and sporadically over the general surface, but more quickly at reactive places such as edges, bored holes, tears and burrs, crystal boundaries or chemically specialized areas.
- (2) The intense aeration which characterizes a water-line produces, in some solution, a relatively large local supply of alkali which tends to spread over the whole surface of the metal and, where concentrated, to stop corrosion.
- (3) This alkali is neutralized by soluble metallic salts at and below reactive places, and corrosion continues in their neighbourhood because the alkali concentration is kept sufficiently low. The downward spreading of corrosion from any starting point comes about through the tendency of heavy metallic salts to fall and so depress alkalinity, which can only be reinforced from above.
- (4) Since the alkali is specially produced near a water-line, protection will tend to be greatest there, but the relatively slow initial sporadic cor-

\* Britton and Evans, 'Trans. Electrochem. Soc.,' vol. 61, p. 445 (1932).

rosion will often be stopped far below the water-line, even where there is little or no oxygen in solution.

- (5) The protection afforded near the water-line by alkali is most definite in constant temperature conditions, but even in these is only temporary with zinc, though prolonged with mild steel; even with the latter it is often confined to a narrow band a millimetre or two in width. The distribution of corrosion shown in fig. 1 is exceptional and favoured by constant temperature, the method of preparing the metal, stagnancy and a narrow vessel. The nature and concentration of the electrolyte and the nature of the atmosphere may affect the distribution.
- (6) In ordinary conditions of exposure to the atmosphere, active corrosion often occurs at and about the water-line; this is due to the breakdown of the protective film by wetting and drying and by the action of  $\text{CO}_2$  and other acid gases in the atmosphere.
- (7) Protection near a water-line or elsewhere may fail locally after a time owing to surface tension or other factors. The rate of local corrosion will then be enhanced by the rate of oxygen supply to the surrounding film-covered metal. If the failure remains localized, intense pitting may result, but local failure may spread towards both more and less aerated regions, even in strongly alkaline conditions.
- (8) If alkali concentration be kept low and nearly uniform, corrosion is widely spread and intense pitting is unlikely to occur; the distribution of oxygen does not appreciably affect the distribution of corrosion on small or moderately sized specimens in  $\text{N}/2$   $\text{NaCl}$ , because the electrolyte resistance between different parts of such specimens is not a controlling factor.
- (9) Factors which affect the distribution of alkali and the adhesion of the film formed in it will decide the distribution of corrosion. Differential aeration is only one of several of these factors.

## II. *Effect of Accumulation of Corrosion Products and Foreign Bodies.*

It has generally been assumed that differential aeration sufficient to affect corrosion distribution can be produced by local accumulations of corrosion products such as magnetic and ferric oxides and zinc hydroxide. The physical condition of such substances is often different at attacked and protected areas.

*Effect of Corrosion Products at Protected Areas.*—It is generally believed that the clearly defined protected areas of mild steel and zinc, such as occur in the

early stages of experiments on both half-immersed and fully-immersed specimens in  $N/2$  NaCl, owe their protection to films which consist mainly of a special form of hydrated ferric oxide or zinc oxide. With steel the films are often invisible but sometimes of a blue or brownish colour, and the protection holds good for long periods; with zinc the films soon become obvious, thicken, change colour and finally lose adhesion and protective properties.

The fact that the films prevent or lessen corrosion in the presence of oxygen, which may be used for corrosion elsewhere, suggests that protection is due to the waterproofing properties of the films, that is, metallic ions cannot penetrate them at all, or only slowly, and dissolved oxygen cannot reach the metal beneath. Actually there is no "aeration" of the metal in these protected areas; oxygen only reaches the outside of the protective film. The corrosion paradox, which is so often cited in expositions of the differential aeration theory, does not exist; the fact is that metal enters solution where there is no protective film, *irrespective of whether the oxygen supply reaches that particular area or only the outside of a neighbouring film* which allows the passage of electrons but not of ions. An isolated film failure at a spot in a highly aerated region may give rise to intense local corrosion, provided the new precipitated corrosion product is of a suitably porous type. The presence of the film—not differential aeration *per se*—is actually the cause of the intense action since *oxygen over it cannot be used by the metal beneath it*, and is therefore available to reinforce any that actually reaches the unprotected spot. The total amount of corrosion is determined by the total oxygen supply, and is not affected by the distribution of oxygen. Fig. 19 shows curves for two standard steel specimens, F.S.99 wholly immersed in  $(3N/50 \text{ KOH} + 2N/50 \text{ KCl})$ , and F.S.5 in  $N/10 \text{ KCl}$ . They are quite similar, though the steel in the former is only attacked at a few places (the attack generally originated at glass contacts) as shown in fig. 20, Plate 6, while in the latter the attack gradually spreads over the whole surface of the metal. Fig. 21, Plate 6, shows the accumulation of corrosion products round the supporting glass points; also that they are hard enough to lift the specimen off a point, though in the absence of excess alkali they remain quite soft for long periods.

The greatest depth of penetration into specimen F.S.99 in the alkaline solution was 3.2 mm., at other parts 2.9, 2.0, and 0.9 mm. The deepest penetration on a specimen in  $N/10 \text{ KCl}$  for a similar time (120 days) was only 0.11 mm.

It sometimes happens that the cathodic product in partially immersed specimens is not exclusively in the form of a film, but massive and non-pro-

tective. A machined specimen of standard steel was partially immersed in sea-water in an oxygen atmosphere for 210 days at 25° C. It was then roughly dried and photographed, fig. 22, Plate 6. The whole of the immersed surface was attacked, except a narrow band about 2 mm. wide which was either at, or just above, the obviously wetted part of the specimen. This band became covered with a hard "collar" of corrosion product containing iron oxides

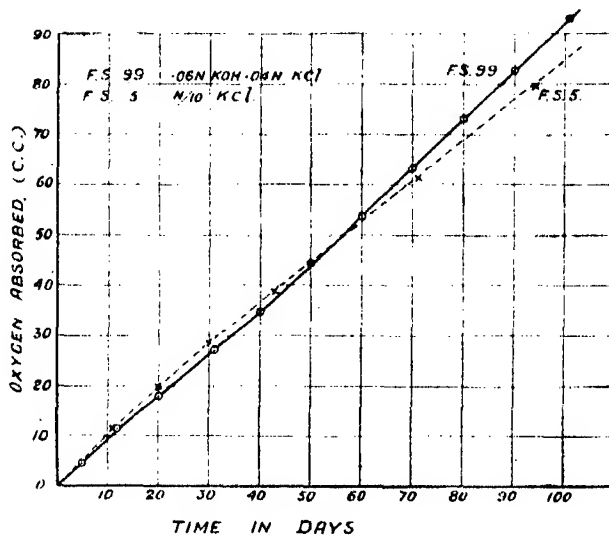


FIG. 19. — Curves for F.S.99 and F.S.5.

and white magnesium and, possibly, calcium compounds. The corrosion rate fluctuated somewhat as usual with sea-water, as shown in fig. 13 (F.S.80), but at the end of 200 days corresponded to 2.5 c.c. of oxygen per day as compared with 2.4 c.c. for the first 40 days; evidently the screening effect produced by the building of this great mass of corrosion product was negligible.

*Effect at Attacked Areas.*—In chloride solutions the corrosion products at or near attacked areas occur generally as opaque loose masses, which may coagulate and harden in time. They permit the passage of metallic ions, otherwise corrosion would cease, but the question arises whether they screen off oxygen from the metal beneath. Aston, Evans and most writers who attach importance to differential aeration assume that they do so, but this assumption requires a very delicate selective property of the screen. Our own tests with zinc and steel often point in the opposite direction, and our evidence is provided by the form of the oxygen absorption/time curves in immersed conditions, such as those given in fig. 23 for mild steel and zinc in N/10 KCl.

The high corrosion rate during the first few hours, when the curve was parabolic, was probably owing mainly to the fact that the solution was initially saturated with oxygen, the concentration of which must steadily have fallen owing to corrosion and only slow replacement by diffusion and convection from the surface. An equilibrium value for the oxygen supply was reached at the end of about 3 days and maintained for 17. Except during the first few

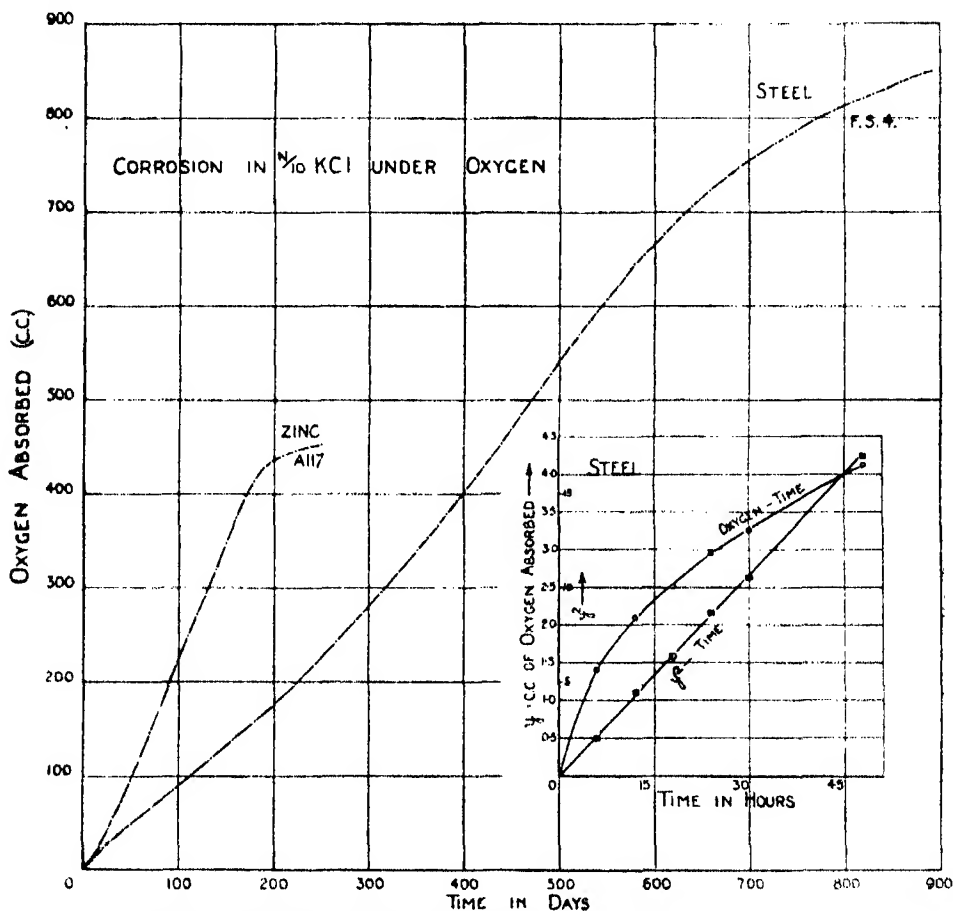


FIG. 23.—Corrosion in N/10 KCl under oxygen : zinc and mild steel.

hours it never reached the value of 1.5 c.c. per day, characteristic of zinc in precisely similar conditions, and it might be thought that this difference was due to the oxygen-screening action of the accumulations of black magnetic and brown ferric oxides. These gradually covered the specimen and in less than 200 days both corroded and uncorroded areas were completely hidden. In spite of the building up of thick masses of oxides the oxygen absorption curve



either remained linear or actually increased in slope as shown in fig. 23 ; only after about 600 days did the slope begin to decrease.

It has been found that the black magnetic and ferric oxides can be removed from the metal surface fairly completely by shaking in the early stages of the experiment ; the slopes of the curves were not altered for more than a day by this procedure ; the temporary alteration was, of course, due to induced convection currents.

A curve for purified iron showed similar results, though the increase of slope after about 200 days was not quite so great as with steel. Other specimens in stronger solutions gave either constant or increasing slopes after the specimens had become completely covered with ferric and magnetic oxides.

It seems clear, therefore, that for about 600 days oxygen can readily penetrate thick masses of the two oxides, and that their effect on the rate of oxygen supply to the metal must be negligibly small when this rate is of the order that commonly occurs in corrosion experiments in stagnant solution. Moreover, the settling of oxides on protected areas does not set up corrosion by differential aeration or otherwise. Similar results have already been recorded for zinc.\*

The criticism has been made that the conditions in our experiments at constant temperature are characterized by very slow but uniform supplies of oxygen to the metal, and that though the oxides mentioned do not form effective screens in our conditions they would do so with more irregular and rapid supplies. Since our specimens are suspended horizontally we do not agree that the oxygen supply is uniform over the whole metal surface, but the two points raised were tested directly by placing standard corrosion vessels on the laboratory bench where they were affected by temperature and pressure fluctuations and slight draughts. In such conditions convection currents are set up which increase the rates of oxygen supply and absorption. The daily oxygen readings fluctuated rather widely and the average readings for corrosion in N/2 KCl and N/10 KCl for each period of 10 days are plotted in fig. 24. It will be seen that the curves are approximately linear and there is no sign of any gradual fall in corrosion rate as the magnetic and ferric oxides accumulate on the metal surfaces. Chappell has obtained similar linear results with vertical steel specimens in sea-water, and Heyn and Bauer in distilled water, both authors using loosely covered beakers exposed on a laboratory bench.

It should be noted that the corrosion products in our experiments (mainly

\* 'Proc. Roy. Soc.,' A, vol. 131, p. 494 (1931).

ferric and magnetic oxides) are similar to those usually found in ordinary experiments in open beakers and in many conditions in which corrosion occurs in practice, except for the presence of  $\text{CO}_2$ . Since such precipitated corrosion products are sometimes unable to act as oxygen screens, the opposite assumption should not be made in the absence of direct evidence, particularly since the assumption is not essential for an explanation of corrosion distribution.

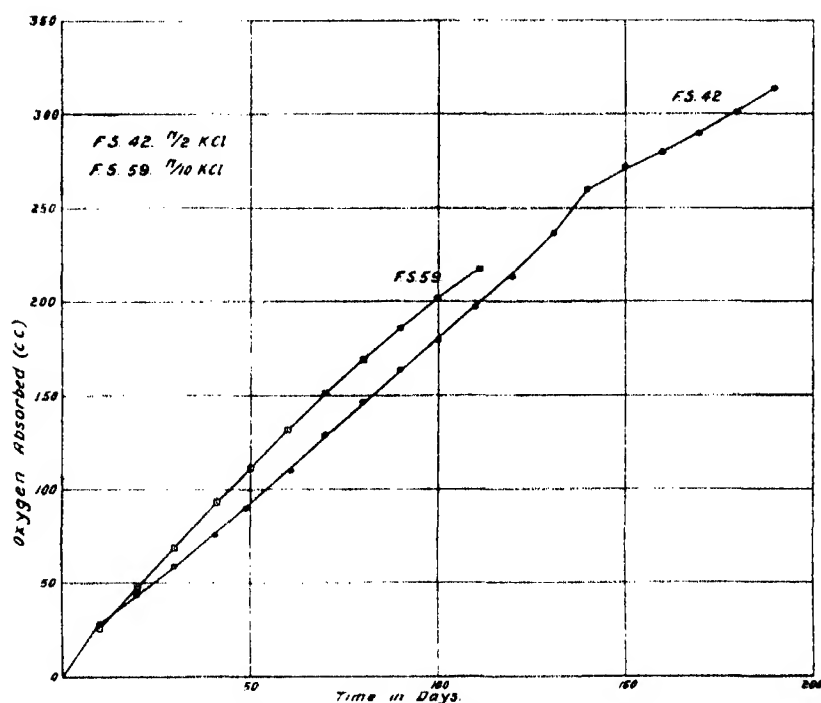


FIG. 24.—Curves for F.S.42 and F.S.59.

A striking illustration of the ease of penetration of oxygen through oxide masses is afforded by the behaviour of a specimen tested at  $25^{\circ}\text{C}$ . in  $\text{N}/10$   $\text{KCl}$  in a vessel 14.4 cm. in diameter beneath an atmosphere of oxygen. The specimen soon became completely covered with mixed oxides so that it could not be seen, yet the rate of oxygen absorption which was at first rather less than 3 c.c. per day, rose gradually to 6 c.c. per day at the end of 134 days, that is, more than seven times the usual rate in a standard vessel at a similar period; the curve is given in fig. 25 (F.S. 88).

Aston in his original paper on differential aeration found that filter paper appeared to cause corrosion of the underlying metal and he assumed that both

it and iron oxides screened oxygen from the metal. To test this we have completely wrapped a standard specimen of steel in at least one thickness of filter paper which was tied on with cotton; an oxygen absorption/time curve in N/10 KCl was then taken in a standard apparatus. The curve and that of a freely exposed specimen are shown in fig. 26 and are closely similar for the first 50 days, so that the oxygen screening effect of the paper must have been negligible. Much corrosion product found its way through the paper and completely covered it. After 50 days the oxygen absorption rate actually increased, probably owing to the steadily increasing rate of hydrogen evolution causing a stirring of the liquid; this is an interesting instance of a "neutral"

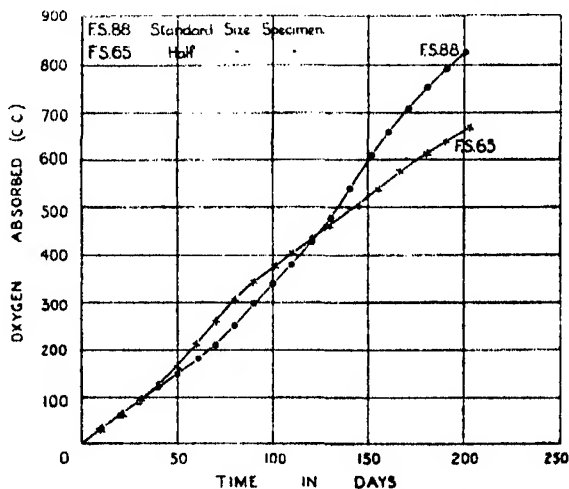


Fig. 25.—Curves for F.S.88 and F.S.65.

foreign body greatly increasing the corrosion rate in a hitherto unsuspected manner. The experiment was repeated with a similar result.

Fine washed silver sand has a somewhat different effect from filter paper. If a standard steel specimen be embedded in it to a depth of 1.5 cm. and immersed at the usual depth in N/10 KCl at 25°, it will corrode much more slowly than in the absence of sand, though the rate of hydrogen evolution is notably increased (*cf.* curves in fig. 27 with F.S.5 of fig. 26). The slower rate of corrosion is probably due to interference with convection and the diffusion of oxygen and ions to and from the metal. If a piece of steel of the dimensions 5 cm. × 2 cm. × 0.4 cm. be half embedded vertically in the sand so that its top be 1.5 cm. below the surface of N/10 KCl, contained in a standard sized vessel exposed to the laboratory air, the general expectation would be that differential aeration would cause the embedded part to corrode fast relatively

to the top part, which should be protected. Actually corrosion occurred on both parts for a day or two, after which it almost ceased on the embedded

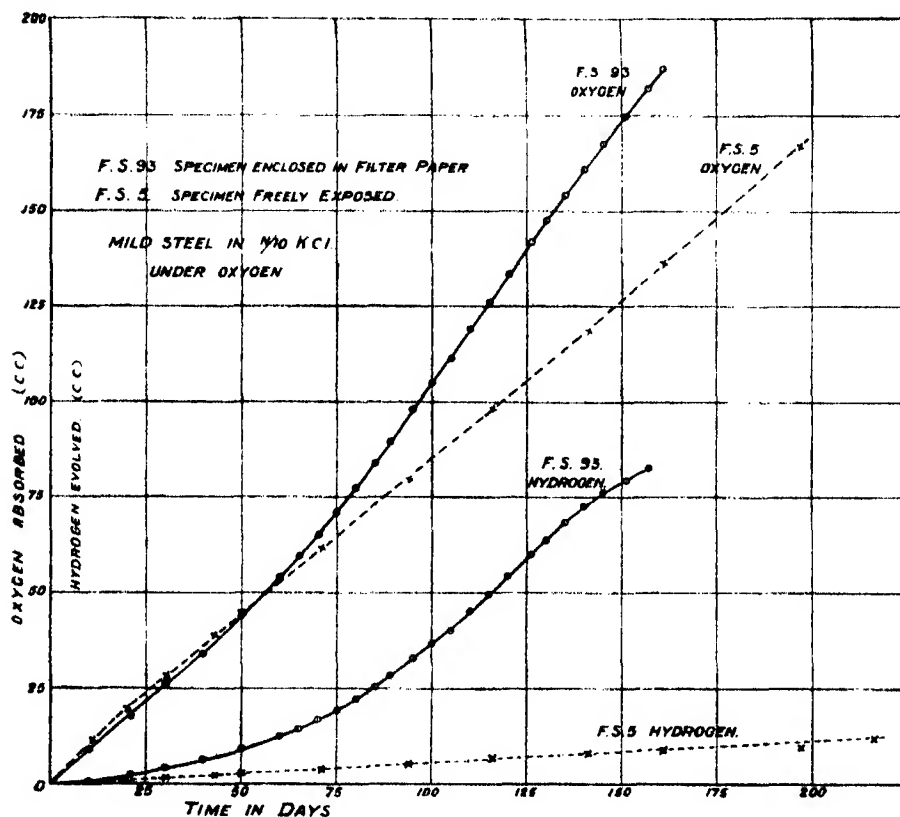


FIG. 26.—Curves for F.S.93 and F.S.5.

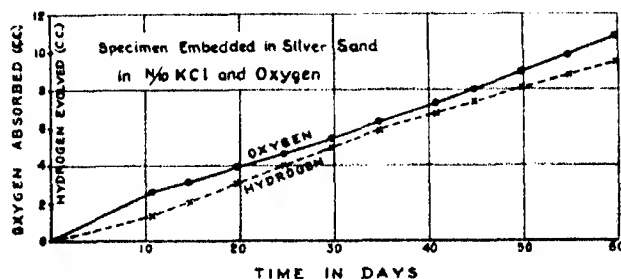


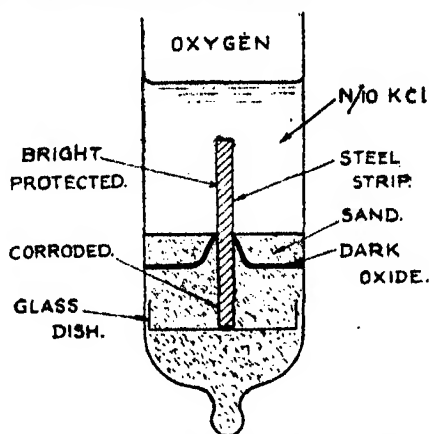
FIG. 27.—Curves for specimens in silver sand.

part but was quite active on the exposed part of the specimen. At the end of 50 days the attack on the embedded part was scarcely noticeable, but elsewhere relatively severe, as shown in fig. 28, Plate 6. The experiment was

repeated with a similar result. The specimens used had holes bored through them near the top and it was thought that these might have caused the corrosion in the neighbourhood, consequently a third experiment was made on an un bored specimen, but the result was again similar.

The initial apparent differential aeration effect which occurred in all the experiments was probably owing to the sand preventing the formation of a protective film on the embedded surface. Sand has been observed to act in this way even in fairly strongly alkaline chloride solutions which are usually protective.

Two more experiments were carried out with standard steel discs arranged horizontally; one of them was embedded in silver sand up to one-third of the thickness, the other was arranged just clear of the sand, which would thus cut out any convection currents which would otherwise reach the bottom surface. The specimens were then covered with N/10 KCl to the standard depth and exposed to laboratory air and temperature fluctuations. At the end of 109 days an examination of the specimens showed that little or no corrosion had occurred on the bottom (partially shielded) surfaces and far more on the top and sides which were freely exposed to oxygen.



SPECIMEN HALF-EMBEDDED IN SAND

FIG. 29.

A vertical specimen half embedded in sand was tested at 25° C. in standard conditions in an oxygen atmosphere. At the end of 34 days most corrosion had occurred on the embedded part (fig. 29); a similar result was obtained with air freed from acid gases, but the reverse effect was obtained with ordinary air. Evidently the balance is somewhat delicate but biased in one direction in ordinary air, and in the other by purified air and oxygen.



FIG. 2. 28 days. FIG. 3. 139 days. FIG. 4. 139 days. FIG. 5. 25 days. FIG. 6. 72 days.  
Reduced to  $\frac{1}{2}$ . Reduced to  $\frac{1}{2}$ . Reduced to  $\frac{1}{2}$ . Reduced to  $\frac{1}{2}$ . Reduced to  $\frac{1}{2}$ .  
The short black lines denote the water line.

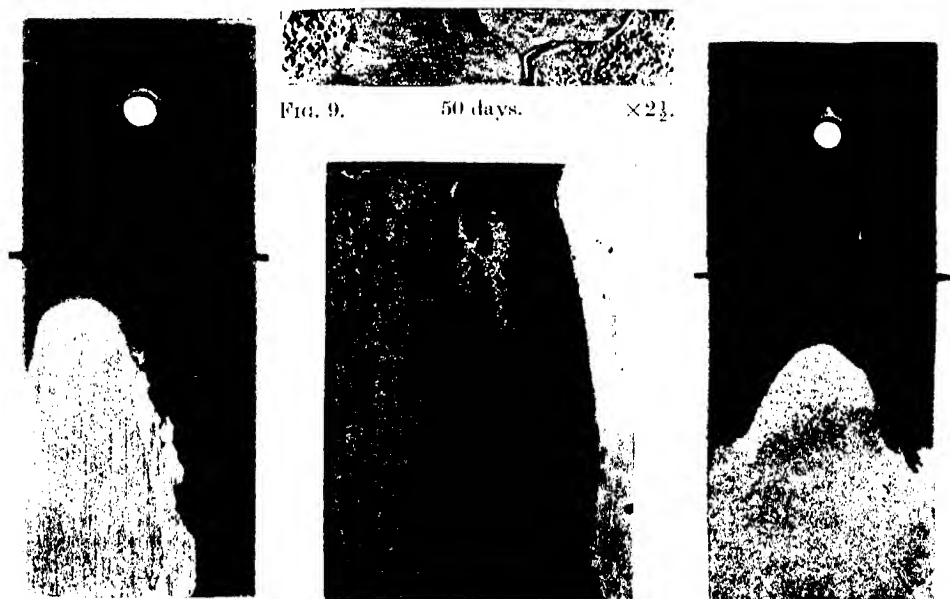


FIG. 7. 206 days.  $\times 1.5$ .

FIG. 10. 150 days.  $\times 2$ .

FIG. 8. 140 days.  $\times 1.5$ .

(Facing p. 417)

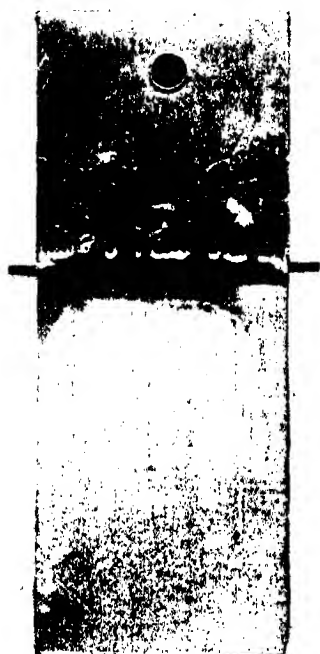


FIG. 11. 50 days.  $\times 1.7$ .



FIG. 12. 206 days.  $\times 1.5$ .

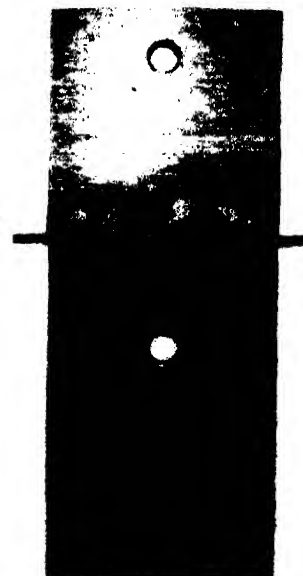


FIG. 14A. 60 days.  $\times 1.5$ .



FIG. 16. 10 days.  $\times 1.6$ .



TOP.



CENTRE.



BOTTOM.

FIG. 17. 130 days.  $\times 30$ .



TOP.



CENTRE.



BOTTOM.

FIG. 18. 101 days.  $\times 30$ .



FIG. 20. 120 days.  $\times 2\frac{1}{2}$ .



FIG. 21. 50 days  $\times 2$ .



Part above sand.



Embedded part.

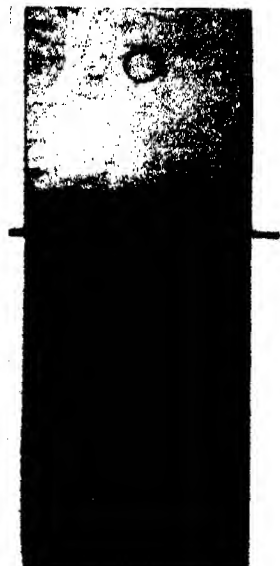
FIG. 28. 50 days.



FIG. 22. 210 days.  
Natural Size.



FIG. 30. 61 days.



$\times 2\frac{1}{2}$ . FIG. 32. 66 days.  $\times 1.5$ .





Further experiments conducted under non-constant temperature conditions showed that a mixture of purified air and  $\text{CO}_2$  behaved like atmospheric air. Purified air mixed with a trace of  $\text{SO}_2$  (6 parts in 10 millions) gave results which seemed to be determined mainly by factors connected with the metal surface; thus a thin emery-ground specimen, with cut edges, gave most corrosion on the exposed parts, but a standard milled specimen was corroded only on the embedded surfaces. The explanation of these results seems to be that the distribution of corrosion is determined by the greatest difference of potential that can be set up between any two parts of the specimen. Sometimes this will be between two parts of the exposed surface, and sometimes between the embedded part as a whole and the exposed surface. The presence of  $\text{CO}_2$  tends to destroy protection on the part exposed to oxygen, which therefore becomes the most corroded.

An experiment was carried out in pure oxygen with only the top of a horizontal steel disc exposed at a depth of 0.3 cm. below the surface of N/10 KCl in a standard apparatus at  $25^\circ$ . The bottom and sides were protected with wax. The corrosion rate corresponded at first with about 4.5 c.c. of oxygen per day, but steadily fell off till after 61 days it was only 2 c.c. per day. Much of the surface of the specimen was protected, but pitting, fig. 30, Plate 6, occurred beneath hard mounds of corrosion product. These somewhat resembled those formed in very dilute solutions in presence of oxygen (but not of air). The fall in corrosion rate is evidently due to changes affecting the corroded areas, since the protected (cathodic) areas remained bright and freely exposed to oxygen; nearly all the ferric oxide either attached itself to the glass stand or fell to the bottom of the vessel. Probably the hard mounds of oxide which formed over the attacked areas acted as oxygen and ion screens, and so caused anodic polarization which steadily cut down the corrosion rate. Thus the concentration of the solution and the purity and amount of oxygen supply may determine whether or not the corrosion product will form oxygen screens. Since the distribution of the pits was related to the position of the central capillary and glass uprights, it may be that surface tension factors also affect the corrosion products. In crevices left by the wax only slight corrosion occurred.

Reference has been made above to the depression of the slopes of the iron curves in N/10 KCl below those of zinc; if, as we assert, this be not owing to accumulation of magnetic and ferric oxides, it is still possible that it is owing to a precipitated film of ferrous material formed right at the anode. Such a layer might act as a mechanical obstructant to iron ions entering the solution

and so depress the corresponding rate of oxygen absorption. The corrosion process would then be under anodic oxygen control, which might be exerted through the rate of oxidation of the layer.

This view receives support from the fact that the rate in N/10 KCl, though much higher initially than that in N/10,000 KCl, falls off much more rapidly, and after 48 hours is less than the rate in the dilute solution, fig. 31. This suggests that in N/10 KCl the rapid initial corrosion builds up a film of corrosion products which produces some form of anodic polarization. This layer may

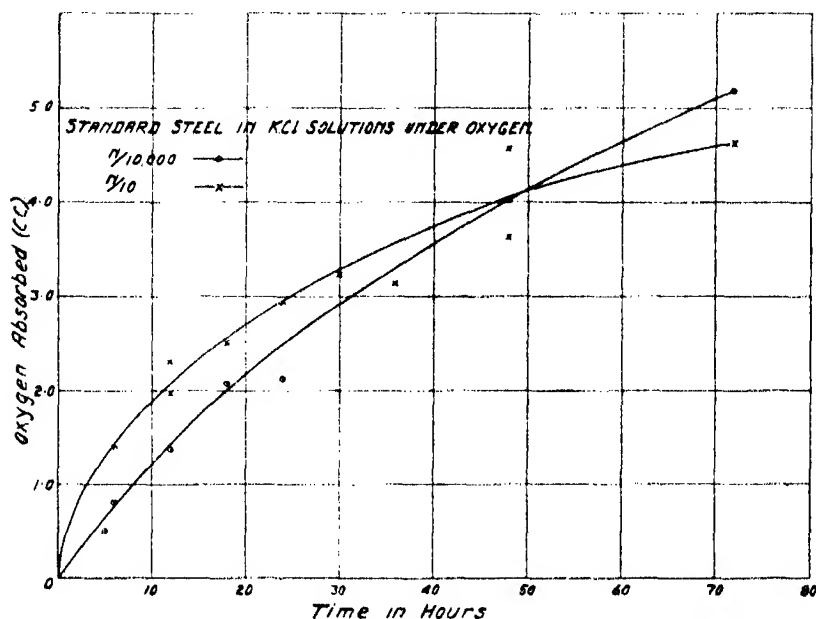


FIG. 31.—Curves in N/10,000 and N/10 KCl for 72 hours.

only allow the entrance of iron ions into solution at a rate determined by its own rate of oxidation to higher oxides of a non-protective type. The main effect, therefore, of the ferrous film would be to depress the local corrosion rate, and not to maintain it owing to an oxygen screening effect.

Experiments were tried in which specimens, which had been corroded in a standard corrosion apparatus for 70 and 76 days, were heavily brushed with a hard brush on the top surfaces and sides. The apparatus was resealed and the experiment continued. No important increases in corrosion rates were observed except for the first day or two and these were perhaps caused by the disturbance of the temperature conditions. Other specimens were

removed from the thermostat and shaken so as to remove corrosion products at the end of various periods up to 473 days ; the results were similar.

The experiments show that if a film exists it must be formed completely in a day or two, after which its rate of formation is balanced by its rate of destruction by oxidation, which in turn is dependent upon the rates of oxygen supply and reaction with the ferrous film.

The fall in the rate of oxygen absorption after about 600 days, as shown in fig. 23, was investigated by opening the corrosion vessel and removing the corrosion products by means of a glass rod. It was found that a brittle crust had been formed since an observation at about 473 days, when the corrosion products were still loose and easily shaken off the metal. After removal of the crust, the rate of oxygen absorption, previously about 0.3 c.c. per day, rose to 1.4 c.c. per day, a value rather higher than that corresponding to the post-parabolic portion of the curve. Possibly the slightly increased value was due to roughening of the anode, which may reduce the polarizing effect of the film discussed above.

This research has shown that four physically different types of corrosion products may be formed in chloride solutions on mild steel specimens in presence of oxygen, and that they have widely different effects on the rate of corrosion of the underlying metal. The four types of product are :—

- (1) A thin transparent film, probably of ferric oxide, which is usually highly protective ;
- (2) a loose stratified layer consisting of magnetic and ferric oxides which are freely pervious to oxygen and ions ;
- (3) hard “ sponges ” which form in alkaline solutions and are also pervious to ions and probably, therefore, to dissolved oxygen ;
- (4) hard crusts, consisting of ferric and magnetic oxides, which resist the passage of oxygen and ions.

In addition, there is probably a film of ferrous oxide in contact with the corroding metal. When types (1) and (2) occur together, corrosion will gradually spread and penetration will be slight. With types (1) and (3) corrosion will be severely localized, and penetration will be greatest since the rate of corrosion is maintained. With (1) and (4) corrosion will also be localized but the rate of corrosion and of penetration will gradually fall as the crust closes over the corroded area.

It will be seen that this discussion postulates that whenever metal ions can penetrate the anodic corrosion products dissolved oxygen can also do so ;

this seems more likely than the assumption that though ions can freely penetrate dissolved oxygen cannot, as required by the differential aeration principle.

The conclusion that an obstructive film of ferrous hydroxide is formed over the corroding surface of pure iron and mild steel suggests an explanation of the fact that they do not corrode in the absence of oxygen. The usual explanation is that a polarizing film of hydrogen is formed, but since it has been shown that hydrogen gas can be evolved in all the solutions tested this explanation is rendered less likely.

### III. *Effect of Crevices.*

A common view is expressed by Hedges\* as follows: "In the ordinary way even a chemically pure metal free from strain has not a perfectly continuous surface, but contains scratches and crevices due to grinding or other causes. Even when subsequently polished these crevices are not completely eliminated, but are often imperfectly bridged over by a film of worked metal leaving perhaps minute perforations. Cavities formed in the metal in this way are particularly inaccessible to oxygen and therefore become anodic to the surrounding metal, to which atmospheric oxygen can diffuse. The corrosion then becomes concentrated at such spots, with the result that the cavity becomes deeper and deeper and the phenomenon of 'pitting' occurs."

The view is at variance with many known facts about the initiation and subsequent changes of corrosion distribution and intensity in alkali chloride solutions. Corrosion of cast zinc or rolled mild steel normally begins at very numerous sporadically distributed centres; it soon ceases at those situated in certain well-defined areas but continues at others in different areas.† It is impossible to suppose that crevices are confined to the latter since the distribution of the areas is largely a matter of the arrangement of the specimen in the liquid. Consequently, crevices cannot be normally an important factor in the distribution of corrosion. A further objection is that pitting only occurs exceptionally and can then be explained on quite different lines, whereas, according to the statement quoted, it should be an ordinary feature of corrosion experiments and metals should be quickly perforated.

Doubt about the accepted explanation of the effect of crevices was aroused by observations which showed that if a piece of zinc were corroded in N/10,000  $K_2SO_4$  till definite and easily visible pits formed, and were then removed, stripped of corrosion products by dilute acetic acid, thoroughly washed and

\* "Protective Films on Metals," p. 466 (Chapman & Hall) (1932).

† 'Proc. Roy. Soc.,' A, vol. 131, p. 506 (1931); vol. 134, p. 334 (1931).

replaced in the original solution, corrosion did not begin at the original pits but at new centres which gave rise to an entirely new set of pits.\*

The conclusion that small differences of level do not cause sufficient differential aeration to localize corrosion was supported by a study of the distribution of initial corrosion centres on zinc and mild steel specimens turned with a fine cut on a precision lathe. A nearly sporadic distribution occurs, but the most active centres in dilute solutions of sodium and potassium chlorides and sulphates are often at tears and burrs situated at the crests of the marks and not in the trough. Scratches sometimes seem to localize corrosion, often at the burr rather than at the bottom of the scratch, but the effect is usually ephemeral.

In our experiments on zinc, chemical composition has had a more important influence on localization of attack than invisible crevices; on very highly purified zinc etch pits were formed on crystal faces, but on less pure zinc the deepest attack was usually along crystal boundaries.

A deep crevice in a specimen can be represented by placing a turned circular disc in a solution and then another disc eccentrically on top of it. A film of liquid will be enclosed between the two and will be in contact with the outside solution owing to eccentric arrangement of the turning grooves, even if the ridges of the grooves actually touch. An experiment was tried by placing the specimens horizontally in N/10 KCl for 13 days. The normal amount of corrosion took place on the aerated top of the specimen; the surfaces that formed the crevices were less attacked than the aerated surfaces.

An experiment was carried out with a steel disc definitely separated by glass rods 0.1 mm. in diameter from a plane glass surface. The result was similar; the usual amounts of corrosion occurred on the top and sides of the disc and a relatively trifling amount in the "crevice."

It was thought possible that the reason why indifferent substances such as glass, wax, filter papers, etc., seem to cause corrosion in their neighbourhood might be that they affect the distribution of protective films. A solution 9/100 N with respect to KOH and N/100 with respect to KCl does not attack totally immersed mild steel owing to the formation of a protective film, but if a disc be placed in this solution in a vessel with a plane glass bottom and be separated from the bottom by glass rods, 0.1 mm. in diameter, the bottom of the disc is corroded though the top and sides are still protected. With thicker rods no corrosion occurs on the bottom except at contacts with the glass; evidently the protective film is pulled off by sufficiently close proximity of the

\* 'Proc. Roy. Soc.,' A, vol. 131, p. 509 (1931).

glass plate, probably owing to surface tension factors. If the mixed solution be replaced by  $N/10$  KOH no corrosion occurs; evidently the film can be re-formed more quickly than it can be removed if sufficient KOH be present. Similar effects were obtained with zinc using a solution of  $N/20$  KOH +  $N/20$  KCl, which is normally protective to zinc for more than 200 days.

Filter paper has an effect similar to, but less powerful than, glass in localizing corrosion. In the mixed solution used for steel no corrosion occurred in four days when a disc was placed on four thicknesses of filter paper, but if a solution  $3/40$  N KOH +  $1/40$  N KCl were used the disc was only corroded on the bottom where it was in contact with the filter papers, at the end of 2 days.

Whether or not corrosion in a crevice becomes severe depends partly on the presence or absence of a protective film on the metal outside the crevice. Such a film will encourage attack in the crevice, but the amount of corrosion may not be great owing to electrolytic resistance and slow rate of diffusion in a narrow crevice; in the absence of a film most of the available oxygen will be used for corrosion outside the crevice.

Corrosion sometimes occurs at cracks in metals but it has been found in all the specimens examined by us that it is located not at the bottom of the cracks, as would be expected on the differential aeration principle, but at the edges of the mouth of the crack.

The general conclusion of this section of the paper is that many cases of corrosion localized at crevices, crannies and near "indifferent" substances such as glass, wax and filter paper, are not due to differential aeration, but to the fact that the local conditions are unsuitable for the formation of protective films, even if sufficient alkali be present to afford protection in normal conditions; in some conditions the attack is probably due to the fact that the spreading of alkali to the affected spot has been hindered in some way.

#### *Summary of Conclusions.*

The general conclusion reached in this research is that corrosion, on zinc and mild steel in stagnant conditions, is often most active at places where it would not be expected according to the differential aeration principle.

Apparent agreement with the principle sometimes occurs because precipitated protective films are quickly formed over the metal in presence of relatively great oxygen supplies; dissolved oxygen, however, is not really an inhibitor of corrosion, as frequently assumed, but a stimulator. Its occasional apparent action as a local inhibitor is owing to the intervention of secondary products which prevent access of oxygen to the metal beneath and entrance of ions into

solution, but corrosion is proportionately increased elsewhere. Since the distribution of protective films, and not necessarily of oxygen supplies, is the main influence in deciding the distribution of corrosion, it seems desirable that a complete restatement should be made of the factors which control distribution in apparently stagnant conditions. This is attempted below for metals such as the mild steel and zinc used in this research on which the distribution is not markedly influenced by localized chemical peculiarities or phase arrangement.

*The Film Distribution View of Corrosion.*—Corrosion distribution is determined mainly by the distribution of protective films which cause the metal to be locally cathodic to bare, or less completely protected, metal. Such films are usually quickly formed, mainly by electrochemical reactions, on zinc, iron and mild steel, in all the conditions studied.

When the films are widespread, corrosion may be sufficiently localized to be called pitting; when the films are restricted corrosion is spread out over areas the sizes of which vary with the experimental conditions and with time, and may finally cover the whole surface of the metal.

Factors which influence the character, distribution and continued adherence of films in the solutions and conditions studied in this research are :—

1. Alkali distribution.
2. Surface tension factors.
3. Presence of specially reactive areas at the metal surface.
4. Gravity.
5. Movement of liquid.
6. Alternate wet and dry conditions.
7. The presence of certain foreign bodies.
8. Nature of the solution.

No doubt other factors remain yet to be discovered.

The precise effect of a given factor may vary with the metal.

Alkali distribution is affected by :—

- 1 (a) Sites of depolarization by oxygen.
- 1 (b) Creep tendency.
- 1 (c) Neutralization by metallic salts or atmospheric gases.

Surface tension factors may be important, for instance, in :—

- 2 (a) Water-line conditions.
- 2 (b) Presence of certain foreign bodies.



Specially reactive areas may be due to physical differences in the metal, which may act either directly or, according to Evans, through the medium of air-formed films.

The average rate of corrosion is often determined by the total rate of oxygen supply to the total surface of both protected and attacked areas, but the intensity of corrosion at any given part is determined by the film distribution. Occasionally the rate and intensity of corrosion are determined by the concentration of anions.

The authors wish to acknowledge the help they have received in the experimental work from Mr. T. J. Nurse. The research was carried out for the Corrosion of Metals Research Committee of the Department of Scientific and Industrial Research, and the thanks of the authors are due to the Chairman, Professor Sir Harold Carpenter, F.R.S., and to Professor G. T. Morgan, F.R.S., for many facilities afforded and for permission to publish.

#### *Summary.*

Previous parts have dealt mainly with total corrosion rates found for the whole surfaces of metal specimens; the present part deals mainly with the distribution of corrosion, which is usually not uniform.

It is widely believed that distribution is controlled mainly by differential aeration such as may occur over the surfaces of metals either partially or wholly immersed in salt solutions; most corrosion is thought to occur at the least aerated parts.

Causes of differential aeration sufficient to affect distribution are usually considered to be partial immersion, deposits of corrosion products, and foreign bodies, and crevices.

Experiments have now indicated that there is no close correlation between rate of oxygen supply to a given area and the intensity of corrosion at that area; intensity is actually controlled by the distribution of protective films which are not necessarily confined to highly aerated regions, nor absent in less aerated regions. The spread of alkali, the presence of reactive areas in the metal, gravity and other factors affect film distribution which often undergoes important changes with time, although the nature of the oxygen supply has not been altered. Certain deposits of corrosion products usually assumed to act as oxygen screens do not actually so behave; others which do so have been found to cut down corrosion locally instead of stimulating it. Certain types of crevice have been shown not to stimulate corrosion by differential

aeration, as supposed ; others to stimulate it by interference with the formation of protective films. An explanation of certain types of " pitting " is given.

A convenient way of expressing the facts at present known, is outlined as a " film distribution view " of corrosion.

APPENDIX.

*Analyses of Metals Used.*

<i>Standard Steel.</i>		<i>Zinc.</i>	
	per cent.		per cent.
Carbon .....	0·13	Lead .....	0·042
Silicon .....	0·15	Iron .....	0·003
Sulphur.....	0·034	Copper .....	0·0008
Phosphorus .....	0·034	Cadmium .....	0·0078
Manganese .....	0·46	Arsenic .....	0·0008
Nickel .....	0·20		
Chromium .....	0·04		
Copper .....	0·05		
Oxygen .....	0·02		

The steel was in the form of rolled bars to which the following final treatment was applied : gradual heating from 500° to 910° C., during 2½ hours ; maintenance of temperature between 905° and 915° C. for 1½ hours ; subsequent cooling to atmospheric temperature in absence of draughts. The zinc was in the form of rolled sheet about 1 mm. thick.



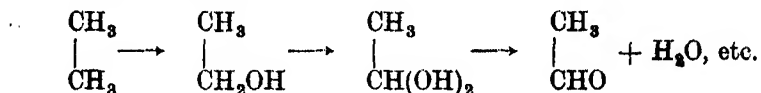
*The Slow Combustion of Ethane at High Pressures.*

By D. M. NEWITT, D.Sc., and A. M. BLOCH, B.Sc.

(Communicated by W. A. Bone, F.R.S.—Received November 30, 1932.)

In 1904 the slow combustion of ethane at atmospheric pressure was shown by Bone and Stockings\* to proceed smoothly without any separation of carbon or liberation of hydrogen, via acetaldehyde, formaldehyde, formic and carbonic acids to the ultimate production of oxides of carbon and steam, as though the process really involved a series of successive hydroxylations. A more recent study of the same reaction by Bone and Hill† shows it to be preceded by an "induction period" during which practically no oxidation occurs. Moreover, although ethyl alcohol was not identified among the products of oxidation, there was strong indirect evidence that  $C_2H_5O$  (or possibly even some less oxygenated-ethane) had been initially formed.

At the temperature at which ethane and oxygen interact with measurable velocity at atmospheric pressure ethyl alcohol oxidizes so very rapidly that the chances of its surviving in the products are remote. For this reason upholders of the hydroxylation theory have always postulated a "non-stop" run through the mono-hydroxy to the di-hydroxy stage, the first identifiable intermediate product being acetaldehyde, thus:



On employing ozonized oxygen, however, the temperature of interaction is considerably lowered, and Drugman showed that at 100° C. ethyl alcohol, acetaldehyde and acetic acid are successively formed.

High pressure is particularly favourable to the survival of intermediate products in such reactions, because not only does it allow of comparatively low temperatures being used, but also where the change involves a diminution in the number of molecules in the system it assists by increasing the thermal stability of the products. Thus in previous work from these laboratories on the oxidation of methane at pressures between 50 and 100 atmospheres and temperatures between 330° and 400° C. all the intermediate products (i.e.,

\* 'J. Chem. Soc.,' vol. 85, p. 693 (1904).

† 'Proc. Roy. Soc.,' A, vol. 129, p. 434 (1930).

methyl alcohol, formaldehyde, formic acid, etc.) arising from successive "hydroxylations" were identified and isolated.\*

In the present paper experiments upon the slow oxidation of ethane in a static system at pressures up to 100 atmospheres are described, and it is shown that in favourable circumstances upwards of 60 per cent. of the ethane burnt may appear in the products as alcohols, aldehydes and acids.

### *Experimental.*

*Apparatus and Method.*—The apparatus used consisted of an electrically heated steel reaction vessel of 500 c.c. capacity connected through an inlet valve with (a) a storage cylinder containing the initial ethane-oxygen mixture previously compressed to the requisite high pressure, (b) a standard Bourdon tube pressure gauge, and (c) a train of cooling coils surrounded by an ice-salt mixture, followed by scrubbers containing distilled water, for the removal at atmospheric pressure of condensable and water-soluble reaction products. The general lay-out of the apparatus has been described in a previous communication.†

The experimental method consisted in bringing the reaction vessel to the required temperature, evacuating and then rapidly filling it to the desired pressure with the compressed ethane-oxygen mixture the composition of which was varied in different experiments between the limits 85 to 90 C<sub>2</sub>H<sub>6</sub>/15 to 10 O<sub>2</sub>. The inlet valve was closed and the progress of the reaction followed by observing the change in temperature of the gaseous media as indicated by a platinum-rhodium couple situated in a tube traversing axially the reaction chamber.

On completion of the reaction, the products were released through the outlet valve and passed successively through the cooling coils and scrubbers, the contents of which were subsequently mixed, diluted with distilled water and aliquot parts used for the quantitative estimation of the various constituents so removed. The remaining gaseous products were analysed.

*Preparation of Gases.*—Ethane not being available commercially in sufficiently large quantities for the experiments, a method was developed for its preparation by (i) the catalytic hydrogenation of ethylene, over a reduced nickel catalyst at 80° C. and 50 atmospheres pressure, followed by (ii) liquefaction of the product (after removal therefrom of any unchanged ethylene by means of bromine), and subsequent fractionation of the liquid. This finally resulted in

\* 'Proc. Roy. Soc.,' A, vol. 134, p. 591 (1932).

† *Loc. cit.*, p. 593.

a product containing 97.3 per cent. of ethane (C/A on explosion analysis = 1.250) and 2.7 per cent. of nitrogen.

The oxygen employed was purchased in cylinders from the British Oxygen Company, and after its composition had been checked by analysis, was used without further purification.

Ethane-oxygen mixtures of the desired composition were made up in 10 cubic foot gas holders and were compressed into cylinders to 150 atmospheres by means of a 2-stage water-lubricated compressor. It was found necessary to keep the cylinder in a thermostat at 40° C. as otherwise there was a tendency for the constituents to separate. As a precaution, samples were taken and their compositions checked by analysis immediately before each experiment.

*Identification and Estimation of the Products.*—A qualitative analysis of the condensed products from a few preliminary experiments with a 90 C<sub>2</sub>H<sub>6</sub>/10 O<sub>2</sub> medium at 270° C. and 100 atmospheres pressure revealed the presence of ethyl and methyl alcohols, aldehydes and acids in considerable quantities. The identification and quantitative estimation of all the components of such a complex mixture proved a matter of considerable difficulty and numerous comparative tests had to be made before reliable methods could be evolved. Finally the following methods were adopted.

*Ethyl Alcohol.*—After removal of any acetaldehyde and acetic acid present, this was identified by oxidizing it to acetic acid and preparing the corresponding anilide, which was identified by its melting point (112° C.). The quantitative estimation was similarly based on its conversion to acetic acid. The condensate was first refluxed for 2 hours with aniline and phosphoric acid and was then distilled, the distillate so obtained being entirely free from aldehyde. Whereupon the alcohol was oxidized by refluxing with acid dichromate, the resultant acetic acid separated by steam distillation, and estimated by titration with N/10 caustic potash. From the total so obtained, the amount of free acetic acid originally present in the condensate, if any, was deducted.

*Methyl Alcohol* was identified by means of its *p*-nitrobenzoyl derivative, and by conversion into methyl salicylate. It was estimated (together with any formaldehyde present) by a modification of the Deniges method.\* Measured quantities of the condensate were oxidized with potassium permanganate under standard conditions, excess of the oxidizing agent being removed by oxalic acid. Sufficient concentrated sulphuric acid was then added to prevent the development of any colour caused by acetaldehyde produced from ethyl alcohol, and finally the total formaldehyde was estimated colorimetrically

\* 'C. R. Acad. Sci. Paris,' vol. 150, p. 832 (1910).

with Schiff's reagent against standard solutions of methyl alcohol oxidized in the same way.

*Aldehydes* were detected by Schiff's reagent, and acetaldehyde by the instant precipitation of amorphous iodoform when treated in the cold with a solution of iodine followed by caustic potash. The total aldehydes present were estimated by Ripper's bisulphite method, and formaldehyde by Romijn's potassium cyanide method, the difference between the two results giving the acetaldehyde present.

*Acids*.—The total acidity was determined by N/10 alkali. Formic acid was estimated separately by neutralizing the condensate, evaporating to dryness twice and oxidizing the residue by permanganate, according to a method of Fauchet.\*

*Peroxides and Glyoxal* were always tested for but never found.

*Gases*.—The gaseous products after removal of aldehyde vapour by exposure to solid zinc chloride were analyzed in the usual way. Finally, after the foregoing estimation and analyses, "balances" were drawn up showing how the carbon of the ethane actually burnt was distributed among the various products.

*Isolation of Alcohols, Aldehydes and Acids from the Products of Combustion of a*  
*90 C<sub>2</sub>H<sub>6</sub>/10 O<sub>2</sub> Mixture.*

In this preliminary series of experiments an initial mixture containing a large excess (90 C<sub>2</sub>H<sub>6</sub>/10 O<sub>2</sub>) of the combustible gas was employed at an initial pressure of 100 atmospheres, the reaction being carried out in a copper-lined vessel, the temperature of which was varied from one experiment to another so as to include both slow and rapid rates of combustion.

The general character of the oxidation was found to be similar to that previously found by one of us and A. E. Haffner for corresponding methane-oxygen mixtures. For example, at the lowest initial temperature employed (260° C.) there was an induction period of 81·5 minutes, during which neither heat evolution nor any appreciable oxidation occurred; this was followed by a reaction period of 14 minutes, during which the temperature rose 3° C., and the whole of the free oxygen was used up. With increase of the initial temperature, both the "induction" and the "reaction" periods were shortened, until at 278° C. the induction period became inappreciable and the reaction was completed in 1 minute, the temperature rise being 21° C.

\* 'Chem. Soc. Abs.,' vol. 2, p. 499 (1912).

A complete quantitative analysis of the condensable intermediate products was made with results as summarized in Table I.

It will be seen that ethyl alcohol was always the predominant condensable product, the maximum yield of it being at  $272.5^{\circ}\text{C}$ ., when it represented no less than 36.5 per cent. of the ethane burnt. Also, methyl alcohol, acetaldehyde and acetic acid were all present in comparatively large quantities, together with smaller amounts of formaldehyde and formic acid; indeed the total carbon appearing in the combined alcohols, aldehydes, and acids varied between 43.6 and 71.7 per cent. of the ethane burnt in the different experiments, but peroxides were never found at all. Steam was always found in these and all subsequent experiments.

The isolation, for the first time, of ethyl alcohol from the products of the interaction of ethane and oxygen is of special interest in that it substantiates much previous indirect evidence all pointing to its initial formation. Moreover, the formations of methyl alcohol and acetic acid, in addition to the previously observed acetaldehyde and formaldehyde, have also an important bearing on the mechanism of the combustion, which will be discussed later on.

*Second Series.—A Comparison between the Reaction Products of an  $88.2\text{ C}_2\text{H}_6/11.8\text{ O}_2$  Medium at Pressures of 50 and 100 Atmospheres and Temperatures between circa  $270^{\circ}$  and  $310^{\circ}\text{C}$ .*

Owing to the presence of acetic acid among the oxidation products it was decided to replace the copper-lined reaction vessel used hitherto by one of the same design and dimensions made of a highly resistant alloy steel.

In comparing the results of oxidation experiments at two different pressures regard must be had to both the maximum reaction temperature and the reaction velocity; for the most favourable condition for the isolation of condensable intermediate products are those in which the reaction takes place comparatively slowly and with only a small temperature rise.

Two groups of experiments were therefore carried out with a mixture of initial composition  $88.2\text{ C}_2\text{H}_6/11.8\text{ O}_2$  at 50 and 100 atmospheres, respectively, in which the initial temperature was varied over a wide range so as to obtain both slow and rapid reaction.

From the results, which (with the exception of the steam formation) are detailed in Table II, it will be seen that (i) at each reaction pressure there was always a well-defined "induction" and "reaction" period, the duration of which so rapidly diminished with rising temperature that at  $310^{\circ}$  both had

Table I.—Reaction Products of a 90 C<sub>2</sub>H<sub>6</sub>/10 O<sub>2</sub> Medium at 100 Atmospheres and Temperatures between 260° C. and 278° C.

Initial temperature. ° C.	Duration of		Percentage of the carbon of the ethane burnt surviving as							Ratio CO/CO <sub>2</sub> in gaseous products.
	Induction.	Reaction.	C <sub>2</sub> H <sub>5</sub> OH.	CH <sub>3</sub> OH.	CH <sub>3</sub> CHO.	H . CHO.	CH <sub>3</sub> COOH.	H . COOH.	Total in condensable products.	
260.0	mins. 81.5	mins. 14.0	29.5	9.3	4.5	0.06	19.5	0.4	61.26	0.54
268.5	10.25	7.0	27.5	9.5	5.0	0.06	13.5	0.3	55.86	0.53
272.0	5.5	3.25	36.5	20.0	8.0	0.30	6.5	0.4	71.70	1.08
272.2	1.5	5.0	33.5	19.1	7.0	0.20	6.5	0.4	66.70	0.69
278.0	Nil	1.0	22.3	11.4	7.7	2.20	Nil	Nil	43.60	5.19



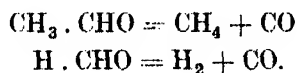
Table II.—Reaction Products of an  $88.2\text{C}_2\text{H}_6/11.8\text{O}_2$  Medium at Pressures of 50 and 100 Atmospheres and Temperatures between  $262.2^\circ$  and  $294.0^\circ\text{C}$ .

Initial temperature, ° C.	Duration of		Maximum reaction temperature, ° C.	Percentage of the carbon of the ethane burnt surviving as—										Total carbon so accounted for per cent.	Ratio CO/CO <sub>2</sub> in gaseous products.	
	Induction, mins.	Reaction, mins.		C <sub>2</sub> H <sub>5</sub> OH	CH <sub>3</sub> OH	CH <sub>3</sub> CHO	H · CHO	CH <sub>3</sub> COOH	H · COOH	CO	CO <sub>2</sub>	CH <sub>4</sub>	Total liquid products.			Total gaseous products.
50 Atmospheres.																
279.2	18.0	100.0	281.2	14.8	10.8	4.7	0.2	15.2	0.3	19.3	32.5	Nil	46.0	51.8	97.8	0.59
286.0	7.0	3.75	295.5	24.4	14.1	8.3	2.0	1.7	0.9	34.8	10.0	Nil	51.4	44.8	96.2	3.48
288.0	6.5	3.75	296.0	20.5	11.3	7.3	1.2	2.3	0.7	31.6	7.1	13.7	43.2	52.4	95.7	4.45
289.0	4.25	2.75	295.0	16.0	14.4	4.9	2.0	2.4	0.4	36.0	4.6	20.7	40.1	61.3	101.4	7.80
294.0	2.0	3.25	307.5	17.2	14.1	5.2	1.9	Nil	0.7	40.8	7.8	8.1	39.1	56.1	95.2	5.22
100 Atmospheres.																
262.2	25.0	15.0	271.2	22.6	10.5	6.2	0.04	27.2	0.8	8.9	19.2	2.0	67.34	30.1	97.44	0.46
265.0	21.0	13.0	277.0	21.8	12.5	6.6	0.08	22.4	0.7	18.8	15.9	1.1	64.08	35.8	99.98	1.18
266.5	23.5	11.0	277.5	23.7	11.2	6.0	0.05	23.8	0.6	9.3	14.2	8.6	65.35	32.1	97.45	0.65
270.5	12.0	4.5	283.5	23.6	14.0	9.7	0.05	12.5	0.5	22.4	8.7	8.6	60.35	39.7	100.05	2.58
275.0	5.75	2.75	305.0	16.5	13.1	6.8	0.10	4.9	0.3	37.2	5.1	16.1	41.70	58.4	100.10	7.30
278.0	4.0	1.25	312.0	14.6	15.4	11.1	0.60	2.2	0.3	37.6	2.8	14.3	44.20	54.7	98.90	13.40

become exceedingly short; and (ii) increasing the "reaction pressure" so favoured the survival of alcohols, aldehydes, and acids that in several of the experiments at 100 atmospheres as much as about two-thirds of the carbon of the ethane burnt so survived, as compared with between about 40 and 50 per cent. only at 50 atmospheres.

At both pressures ethyl alcohol and/or acetic acid always predominated among the surviving condensable products, there being apparent in each case a fairly low "optimum" temperature for their separate or joint survival. The proportion of ethane burnt surviving as methyl alcohol was not nearly so much affected by variations in temperature and pressure. Moreover, in most of the experiments there was a fairly constant ratio between the survival of ethyl alcohol and acetaldehyde, namely, about 3.0 at 50 atmospheres and between 3.3 and 4.0 at 100 atmospheres. Formaldehyde and formic acid were found in relatively small quantities only and "peroxides" not at all.

As regards the gaseous products with slow reaction speeds they consisted entirely, or almost so, of oxides of carbon, but as reaction quickened both methane and traces of hydrogen appeared, doubtless as the result of secondary thermal decomposition of acetaldehyde and formaldehyde, respectively, thus



It will be seen that in each experiment the whole of the carbon of the ethane burnt was substantially accounted for among the foregoing products showing how complete had been the analyses involved.

*Third Series.—Influence of Pressure upon the Survival of Products from Equal Reaction Rates.*

In this series of experiments, while the reaction-pressure was raised in steps from 15 up to 100 atmospheres care was taken simultaneously to lower the temperature so as to maintain an approximately equal reaction speed and temperature rise throughout, thus enabling data to be obtained for what seems a true comparison of the yield of condensable products obtained at the different pressures.

The results, which are detailed in Table III, showed that whereas an increase in pressure favoured the survival of ethyl alcohol, acetaldehyde, and acetic acid (i.e., of products not involving any rupture of the ethane molecule) it seemed to have an opposite effect upon the survival of methyl alcohol and formaldehyde.

Table III.—The Effect of Initial Pressure on the Survival of Intermediate Products from the reaction of an  $88.4 \text{ C}_2\text{H}_6/11.6 \text{ O}_2$  Medium.

Initial pressure.	Initial temperature.	Duration of reaction.	Percentage of the carbon of the ethane burnt surviving as—						
			$\text{C}_2\text{H}_5\text{OH.}$	$\text{CH}_3\text{OH.}$	$\text{CH}_3\text{CHO.}$	$\text{H. CHO.}$	$\text{CH}_3\text{COOH.}$	$\text{H. 'COOH.}$	Total in condensable products.
atmos.	$^{\circ}\text{C.}$	mins.	16.0	19.4	1.9	4.5	Nil	Nil	41.8
15	315	3.0	17.2	14.1	5.2	1.9	Nil	0.7	39.1
50	294	3.25	18.0	16.6	6.8	0.4	3.6	0.6	46.0
75	279	2.5	23.6	14.0	9.7	0.1	12.5	0.5	50.4
100	270.5	4.5							

*Fourth Series.—The Influence of Oxygen Concentration upon the Survival of Intermediate Products.*

So far we had not worked with  $C_2H_6-O_2$  mixtures containing more than 11.8 per cent. of oxygen, because of the difficulty of controlling the temperature in the reaction chamber with higher oxygen content. Later on, however, we succeeded in carrying out two comparative experiments, the results of which are detailed in Table IV, with mixtures of composition  $89 C_2H_6/11 O_2$  and  $84.5 C_2H_6/15.5 O_2$ , respectively, each at a pressure of 100 atmospheres and the same initial temperature of about  $270^\circ C$ .

In comparing the results it should be remembered that whereas with the first mixture the reaction temperature rose to  $283.5^\circ$  only, with the second it rose to  $315.8^\circ$  owing to the greater oxygen content. It was therefore not surprising in the latter experiment that there was a much smaller survival of condensable products, and especially of ethyl alcohol, acetaldehyde, and acetic acid, although that of methyl alcohol was not so much affected. In the second experiment there was much more methane formed than in the first, a circumstance also associated with a slight carbon deposition and some liberation of hydrogen, neither of which had been observed in the first; these features are attributable to more secondary decomposition of acetaldehyde and formaldehyde at the higher reaction temperature reached in the second experiment.

*Fifth Series.—Progressive Pressure Oxidation.*

In the following series of three experiments starting with an  $88 C_2H_6/12 O_2$  mixture, so as to avoid any large rise in reaction temperature, a progressive oxidation was effected in the following manner: (1) In the first instance as soon as all the original oxygen had disappeared, the resulting products were withdrawn and analysed, but (2) on repeating the experiment, a second charge of oxygen was introduced into the reaction chamber as soon as the first had disappeared, and the products were not withdrawn for analysis until this additional oxygen had disappeared, whilst (3) in the third experiment two such additional charges of oxygen were successively introduced and were allowed to be used up before the products were finally withdrawn.

We were thus enabled to follow the course of oxidation much further than before, while keeping the oxygen concentration low and preventing any undue rise in reaction temperature. The results, which are detailed in Table V (where the various products therein are expressed as cubic centimetres of gas or vapour per litre of the original mixture taken) showed that, as the oxidation

Table IV.—The Effect of Oxygen Concentration on the relative proportions of Intermediate Products Surviving at 100 Atmospheres.

Composition of initial gases per cent.		Initial temperature. ° C.	Maximum reaction temperature. ° C.	Percentage of the Carbon of the ethane burnt surviving as—											Total carbon so accounted for per cent.
				C <sub>2</sub> H <sub>5</sub> OH.	CH <sub>3</sub> OH.	CH <sub>3</sub> CHO.	H . CHO.	CH <sub>3</sub> COOH.	H . COOH.	CO.	CO <sub>2</sub> .	CH <sub>4</sub> .	Total in condensable products.	Total in gaseous products.	
89.0	11.0	270.5	283.5	23.6	14.0	9.7	0.05	12.5	0.5	22.4	8.7	8.6	60.35	39.7	100.05
84.5	15.5	271.8	315.8	7.4	10.0	4.8	0.90	2.4	0.15	31.2	3.7	33.4	25.65	68.3	93.95*

\* There was some carbon deposited in this experiment.

Table V.—The Effect of Progressive Oxidation on the Relative Proportions of the Products at 289° C. and 50 Atmospheres.

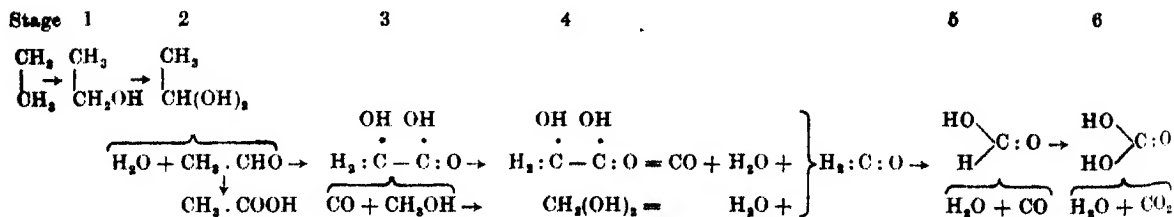
Reacting medium.	Products from reacting media (1), (2), and (3) as cubic centimetres of vapour or gas per litre of initial mixture (1) at N.T.P.								Ratio CO/CO <sub>2</sub>
	C <sub>2</sub> H <sub>5</sub> OH.	CH <sub>3</sub> OH.	CH <sub>3</sub> CHO.	H . CHO.	CH <sub>3</sub> COOH.	H . COOH.	CO.	CO <sub>2</sub> .	
(1) 88 C <sub>2</sub> H <sub>6</sub> /12 O <sub>2</sub> .....	14.4	25.9	4.5	3.6	2.1	0.7	70.0	13.4	5.2
(2) Products from (1) + an additional 12 O <sub>2</sub> .....	13.5	38.9	4.7	3.2	2.3	0.7	158.8	30.7	5.2
(3) Products from (2) + an additional 12 O <sub>2</sub> .....	13.1	42.9	5.7	3.1	1.9	1.0	206.4	35.1	5.9

proceeded, while there was a small progressive falling off in the concentrations of the ethane, ethyl alcohol and formaldehyde, those of methyl alcohol, acetaldehyde and both oxides of carbon materially increased; the  $\text{CO}/\text{CO}_2$  ratio remaining fairly constant throughout. The concentration of acetic and formic acids (always relatively small) were, however, not much affected. Also the products contained about 5 per cent. of methane and less than 2 per cent. of hydrogen. Obviously, the further the oxidation proceeded, the more of the hydrocarbon was burnt to oxides of carbon and steam.

### Discussion.

The prominence, and in some experiments the predominance, of ethyl alcohol among the surviving condensable and water-soluble intermediate oxidation products—which taken together accounted in many experiments for upwards of 60 (and in one case for more than 70) per cent. of the carbon in the ethane burnt—*without any trace of peroxide ever being detected*, adds greatly to the already overwhelming weight of evidence in favour of the “hydroxylation” as against the “peroxidation” theory of hydrocarbon combustion.

In one experiment no less than 36.5 per cent. of the total carbon of the ethane burnt was found in the products as ethyl alcohol, another 20 per cent. as methyl alcohol, 8 per cent. more as acetaldehyde, 6.5 per cent. as acetic acid, besides smaller proportions as formaldehyde and formic acid, together substantiating almost quantitatively the following “hydroxylation” scheme. In this (be it noted) each one of the six possible “hydroxylation” steps is represented by one or more of the products actually isolated, thus making the proof complete.



There was neither any liberation of carbon nor hydrogen except when the reaction temperature had risen so rapidly as to cause an inflammation of the reacting medium; usually, though not invariably, some methane appeared in the products as the result of the thermal decomposition of some of the acetaldehyde vapour. Otherwise the only thermal decompositions accompanying the

main course of the oxidation were those of the less stable of the successively formed hydroxylated molecules, as shown in the scheme.

The general influence of an increase in the reaction pressure was favourable to the survival of those products (*i.e.*, ethyl alcohol, acetaldehyde and acetic acid) whose formation did not involve any disruption of the bond between the two carbon atoms of the ethane burnt; conversely a lowering of the pressure tended to promote such disruption and to favour the formation, or survival, of methyl alcohol, formaldehyde, and formic acid.

Carbon monoxide was, or might be, formed as the result of thermal decomposition (i) simultaneously with methyl alcohol at the *third* hydroxylation stage, (ii) simultaneously with steam and formaldehyde at the *fourth* stage, and (iii) simultaneously with steam at the *fifth* stage; while in all experiments carbon dioxide was certainly formed by the thermal decomposition of carbonic acid at the *sixth* stage and possibly also to a small extent in some experiments by the independent oxidation of the monoxide.

In conclusion we desire to thank Professor Bone for his interest in the work and Radiation Limited for their Research Fellowship which has enabled one of us (A.M.B.) to devote his whole time to it.

#### *Summary.*

In the slow combustion of ethane-oxygen mixtures of composition 85 to 90  $C_2H_6/15$  to 10  $O_2$ , at high pressures, intermediate products, representing the six possible "hydroxylation" steps whereby the ethane molecule is oxidized, have been isolated.

At 100 atmospheres pressure upwards of 60 (and in one case more than 70) per cent. of the carbon of the ethane burnt survived as condensable and water soluble intermediate products. Ethyl alcohol and/or acetic acid predominated among the surviving intermediate products but, in addition, considerable quantities of methyl alcohol, acetaldehyde and steam were always present together with smaller amounts of formaldehyde and formic acid.

The effect of increasing the initial pressure of the reacting medium was in general to favour the survival of ethyl alcohol, acetaldehyde and acetic acid (*i.e.*, of products formed without any rupture of the ethane molecule).

---



*Acid Strength and its Dependence Upon the Nature of the Solvent.*

By W. F. KENRICK WYNNE-JONES, The University, Reading.

(Communicated by Sir Harold Hartley, F.R.S.—Received December 1, 1932.)

The development of our views concerning the nature of acids and bases and, in particular, the precision given to these views by the definitions proposed by Brönsted and Lowry\* of an acid as a substance which splits off protons, and of a base as a substance which takes up protons, have led to a much clearer understanding of the behaviour of acids and bases in different solvents. The essential dependence of the ionization of acids and bases upon the basicity or acidity of the solvent has been emphasized in a number of papers,† and many authors have shown how by suitable choice of solvent a much greater range of acidity is available than when water alone is employed.

Despite the very notable advances that have been made, there is a further problem, that of the relative strengths of different acids, to which a satisfactory solution has not yet been found. So far as any single solvent is concerned, it is usual to regard the dissociation constant of an acid as a measure of its strength, and on this basis numerous attempts have been made to correlate acid strength and constitution.‡ Many of these attempts have been expressed quantitatively, and that the opinion is widely held that some such relation can be formulated is evidenced by the innumerable "proofs of structure," which are advanced on the basis of measurements of dissociation constants. However, an examination of the data for different solvents shows that the fundamental assumption that the intrinsic strength of an acid is measured by its dissociation constant in a particular solvent is invalid, since an acid which is stronger than another in one solvent is often weaker in a second solvent; thus in water *o*-nitrobenzoic acid has a dissociation constant of  $6.2 \times 10^{-3}$  compared with

\* Brönsted, 'Rec. Trav. Chim.,' vol. 42, p. 718 (1923); Lowry, 'J. Soc. Chem. Ind.,' vol. 42, p. 43 (1923).

† Brönsted, 'Ber. deuts. chem. Ges.,' vol. 61, p. 2049 (1928); Hall and Conant, 'J. Amer. Chem. Soc.,' vol. 49, p. 3047 (1927); Schwarzenbach, 'Helv. Chim. Acta,' vol. 13, p. 870 (1930); Hammett and Dietz, 'J. Amer. Chem. Soc.,' vol. 52, p. 4795 (1930); Wynne-Jones, 'J. Chem. Soc.,' p. 1064 (1930).

‡ Ostwald, 'Z. phys. Chem.,' vol. 3, p. 177 (1889); Wegscheider, 'Mhft. Chem.,' vol. 23, p. 289 (1902); Flürscheim, 'J. Chem. Soc.,' vol. 95, p. 718 (1909) and vol. 97, p. 84 (1910); Derick, 'J. Amer. Chem. Soc.,' vol. 33, p. 1152 (1911); MacInnes, 'J. Amer. Chem. Soc.,' vol. 50, p. 2587 (1928).

$1.6 \times 10^{-3}$  for 3.5 dinitrobenzoic acid, while in ethyl alcohol the respective constants are  $2.42 \times 10^{-9}$  and  $8.16 \times 10^{-9}$ . This fact, which emerges very clearly from the extensive work of Goldschmidt on solutions in methyl and ethyl alcohols and is confirmed by the work of Larsson and of Halford,\* means that it is impossible to transfer a scale of acidity from one solvent to another, and renders of doubtful significance the rules previously formulated on the basis of results in water.

Since the ionization of an acid, A, in a solvent, S, is due to a reaction of the type

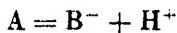
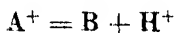


it appears at first that a change of solvent will affect all acids similarly; there are, however, two factors that will complicate the relations—

- (1) the electrostatic action between  $SH^+ + B$  will depend upon the solvent;
- (2) the chemical potentials of A and B may vary differently with change of solvent.

The second factor is difficult to estimate, and it has been proposed by Bjerrum and Larsson† that, since B differs from A only by a proton, we may consider variations in their chemical potentials to be the same.

The influence of the first factor may be shown in outline by comparing the ionization of two different types of acid



The equilibrium for an acid of the first type will be relatively insensitive to changes in the dielectric constant whereas, for an acid of the second type, a decrease in the dielectric constant will shift the equilibrium from right to left. The quantitative expression of this dependence of the equilibrium upon the dielectric constant has already been worked out by Bjerrum and Larsson, and by Brönsted.‡

\* Larsson, 'Dissertation,' Lund (1924); Halford, 'J. Amer. Chem. Soc.,' vol. 53, p. 2944 (1931).

† 'Z. phys. Chem.,' vol. 127, p. 358 (1927).

‡ Bjerrum and Larsson, 'Z. phys. Chem.,' vol. 127, p. 358 (1927); Brönsted, 'Chem. Rev.,' vol. 5, p. 231 (1928).

If " $\psi$ " is the electrostatic potential of an isolated ion of radius " $r$ " and charge " $\epsilon$ " in a solvent of dielectric constant " $D$ ," then

$$\psi = \frac{\epsilon}{Dr}$$

and the electrical work done by the ion on transfer to a second solvent is

$$A = \frac{\epsilon^2}{2r} \left( \frac{1}{D_1} - \frac{1}{D_2} \right).$$

For an acid of the first type the change in dissociation constant will therefore be

$$\Delta \ln K = - \frac{\epsilon^2}{2kT} \left( \frac{1}{r_{H^+}} - \frac{1}{r_A} \right) \Delta \left( \frac{1}{D} \right), \quad (1)$$

where  $r_{H^+}$  is the radius of the hydrogen ion and  $r_A$  is the radius of the acid ion.

For an acid of the second type the corresponding relation will be

$$\Delta \ln K = - \frac{\epsilon^2}{2kT} \left( \frac{1}{r_{H^+}} + \frac{1}{r_B} \right) \Delta \left( \frac{1}{D} \right), \quad (2)$$

where  $r_B$  is the radius of the anion of the acid.

These equations take into account only the electrostatic effects, and consequently cannot reproduce the actual changes in the dissociation constants; nevertheless they show that, so far as the electrical effect is determined by the ionic radius, specific variations are to be expected even for acids of the same type.

Bjerrum and Larsson and also Brönsted have attempted to evaluate the electrical part of the dissociation constants and to apply the above equations, but both these treatments depend upon a knowledge of the partition coefficient of the hydrogen ion between the solvents employed, and consequently they are open to grave objection since, on the experimental side, this quantity eludes measurement, while theoretically, as shown by Guggenheim\* the concept of individual ion partition coefficient is incapable of precise definition. We may, however, avoid these uncertainties and at the same time eliminate the chemical effect of varying solvation of the proton by considering not the changes in the actual dissociation constants but changes in the relative constants taking some acid as a standard.

\* 'J. Phys. Chem.,' vol. 33, p. 842 (1929).

Since the dissociation of an acid may be regarded as occurring in two steps



the observed dissociation constant is the product of the separate constants for the two steps

$$K = k_1 \cdot k_2.$$

Hence if we take as standard an acid,  $A_0$ , and consider its dissociation in two solvents  $S'$  and  $S''$ , we may write

$$\begin{aligned} K'_0 &= k'_0 \cdot k'_2 \\ K''_0 &= k''_0 \cdot k''_2 \end{aligned}$$

where  $k'_0$  and  $k''_0$  refer to the primary ionization of the acid in the two solvents and  $k'_2, k''_2$  refer to the solvation of the proton. In the same way for any other acid,  $A$ , we have

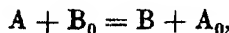
$$\begin{aligned} K' &= k' \cdot k'_2 \\ K'' &= k'' \cdot k''_2 \end{aligned}$$

and hence for the relative constants of this second acid we have

$$\begin{aligned} K'_r &= \frac{K'}{K'_0} = \frac{k'}{k'_0} \\ K''_r &= \frac{K''}{K''_0} = \frac{k''}{k''_0} \end{aligned}$$

in which the terms involving the basicity of the solvent no longer appear.

The relative dissociation constant of an acid,  $A$ , compared with a standard acid,  $A_0$ , is actually the constant for the equilibrium



where  $B$  and  $B_0$  are the conjugate bases of the two acids  $A$  and  $A_0$ . If the charges carried by these basic molecules are  $z\epsilon$  and  $z_0\epsilon$  then the change in the relative dissociation constant when the dielectric constant is altered is given by

$$\Delta \ln K_r = -\frac{\epsilon^2}{2kT} \left( \frac{z^2}{r_B} + \frac{(z_0+1)^2}{r_A} - \frac{(z+1)^2}{r_A} - \frac{z_0^2}{r_{B_0}} \right) \Delta \left( \frac{1}{D} \right)$$

the ionic radii being assumed to be independent of the solvent. If either the

acid or basic molecules are uncharged, two of the terms within the bracket disappear, but the terms may be similarly reduced if we make the approximation

$$r_A = r_B = r$$

$$r_{A_0} = r_{B_0} = r_0$$

and we thus obtain the relation

$$\Delta \ln K_r = \frac{\epsilon^2}{2kT} \left( \frac{2z+1}{r} - \frac{2z_0+1}{r_0} \right) \Delta \left( \frac{1}{D} \right).$$

If both the acids are uncharged, this equation becomes

$$\Delta \ln K_r = \frac{\epsilon^2}{2kT} \left( \frac{1}{r_0} - \frac{1}{r} \right) \Delta \left( \frac{1}{D} \right) \quad (3)^*$$

and, if both carry single positive charges,

$$\Delta \ln K_r = \frac{\epsilon^2}{2kT} \left( \frac{1}{r} - \frac{1}{r_0} \right) \Delta \left( \frac{1}{D} \right) \quad (4)^*$$

while, if the standard acid is uncharged and the other acid carries a single positive charge, we have

$$\Delta \ln K_r = \frac{\epsilon^2}{2kT} \left( \frac{1}{r} + \frac{1}{r_0} \right) \Delta \left( \frac{1}{D} \right) \quad (5)^*$$

These equations involve the assumptions that the solvent is a continuous dielectric and that the ions are spherical, and consequently it is improbable that they can be applied quantitatively to the ions of organic acids in which the charge is often located at one end of the ion. Nevertheless we may expect that the equations will give a qualitative explanation of the variations in relative strength of acids, and in particular the dependence of  $\log K_r$  upon the dielectric constant should be of the form required by the equations; that is to say, if values of  $\log K_r$  are plotted against the reciprocal of the dielectric constants a straight line should be obtained for each acid.

#### *Test of the Relationship.*

Although many measurements of the strengths of acids have been made in different solvents, few of these can be employed for an exact test of the relation-

\* In my original derivation of these equations, I started from equations (1) and (2) which I assumed to represent the electrical effects. I am indebted to Mr. E. A. Guggenheim for pointing out to me that those equations become meaningless when applied to the hydrogen ion which is a different entity in each solvent. The modified deduction given above is due to Mr. Guggenheim.

ship suggested above. Most of the data are unsuitable either because they were determined by methods which do not lead unambiguously to the true dissociation constant (*e.g.*, indicator methods or e.m.f. measurements in solvents of low dielectric constant) or because of considerable experimental errors due frequently to inadequate purification of the solvents; a few apparently reliable data cannot be employed because they consist of isolated measurements and so do not allow of the calculation of  $K_r$ .

A careful examination of the data shows that we are virtually restricted to the results for water, and those of Goldschmidt and his collaborators for methyl and ethyl alcohols.\* Fortunately these results cover a wide range of substances and include acids which are positively charged (type I) as well as acids which are uncharged (type II). Benzoic acid has been chosen as standard for the uncharged acids since its dissociation constants are accurately known in these three solvents and it serves as a useful basis of comparison for other aromatic acids; the ease with which it can be obtained pure, and its solubility in a variety of solvents, also make it a convenient standard. For positively charged acids the pyridinium ion has been adopted as standard.

In fig. 1 are shown the data for uncharged acids. For the majority of these acids the slopes of the lines are small, but for picric acid and trinitrocresol quite steep curves are obtained. Applying equation (3) the radii of the picrate and trinitrocresolate ions may be calculated if a value is assumed for the radius of the benzoate ion, and taking this arbitrarily to be 0.8 Å the radii of the other two ions are found to be 2.7 Å.† As already indicated such a calculation is without quantitative significance. Nevertheless the relatively large radius of the picrate ion is in agreement with the conclusions drawn by Ulich‡ from his investigation into the mobilities of organic ions. Ulich has pointed out that the localization of the charge on a carboxylate ion makes such an ion behave as though it had a very small radius, while the picrate ion presumably possesses a greater symmetry and hence behaves as a large ion. As showing the great variations in  $K_r$  that may occur, it is interesting to com-

\* Goldschmidt, 'Z. phys. Chem.,' vol. 91, p. 46 (1916); Goldschmidt and Aas, *ibid.*, vol. 112, p. 423 (1924); Goldschmidt and Aarflot, *ibid.*, vol. 117, p. 312 (1925); Goldschmidt and Mathiesen, *ibid.*, vol. 119, p. 453 (1926); Goldschmidt, Marum and Thomas, *ibid.*, vol. 129, p. 223 (1927) and vol. 132, p. 257 (1928).

† According to equation (3), an upper limit to the radius of the benzoate ion is fixed by the condition  $r_{\text{picrate}} = \infty$ ; substitution in the equation gives a value of 1.15 Å for the radius of the benzoate ion. These values are of course to be interpreted as "effective" radii and not the actual radii which may be deduced from X-ray analysis.

‡ 'Fortsehr. Chem. Phys.,' vol. 18, No. 10 (1926).

pare the strengths of picric and nitric acids in the three solvents; the curves show that whereas in ethyl alcohol their strengths are almost identical, nitric acid is about five times as strong as picric acid in methyl alcohol, and in water nitric acid would appear to be about 100 times as strong as picric acid. The actual strength of nitric acid in water is unknown, but the constant calculated by extrapolation of the curve in fig. 1 is about 40, a value quite compatible with the known behaviour of this acid as a strong or completely ionized electrolyte. The curves for the three nitrobenzoic acids show that the *o*-acid behaves

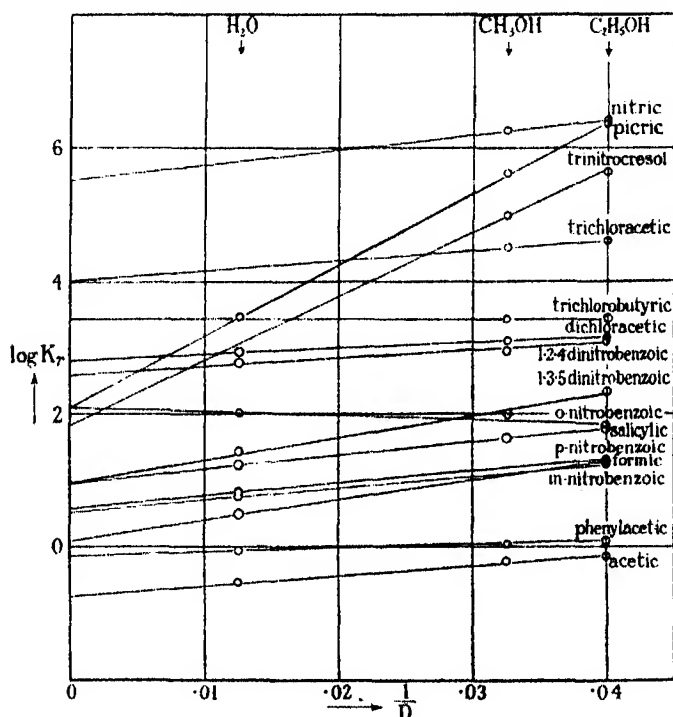


FIG. 1.—Nitric acid values from Murray-Rust and Hartley, 'Proc. Roy. Soc.,' A, vol. 126, p. 84 (1929); acetic acid value in  $\text{CH}_3\text{OH}$  from Bjerrum, Unmack and Zechmeister, 'K. Dansk. Vidensk. Selsk. Mathfys. Medd.,' vol. 5, p. 11 (1924); acetic acid value in  $\text{C}_2\text{H}_5\text{OH}$  from Larsson, "Dissertation," Lund (1924).

very differently from the other two, and it is evident that even with such very similar substances the relative strengths may vary considerably with the solvent.

Fig. 2 shows the results for positively charged acids, for which the most noticeable effect is the grouping of the curves according to the type of ammonium ion. Thus the curves for the primary ammonium ions are steeper than those for the secondary, which in turn are steeper than those for the tertiary ions.

In fig. 3 are given for comparison some results for acids of the two types mentioned above and also for negatively charged acids. Benzoic acid has been used as standard for all the acids, hence equations (3) and (5) are applicable. For negatively charged acids the effect of the separation of the electrical charges in the basic molecule plays an important part in determining the dissociation constant, but since this effect has been shown by Bjerrum\* to depend upon the dielectric constant in a similar way to the other electrical effect we may still expect the variations in  $\log K_r$  to be proportional to  $1/D$ .

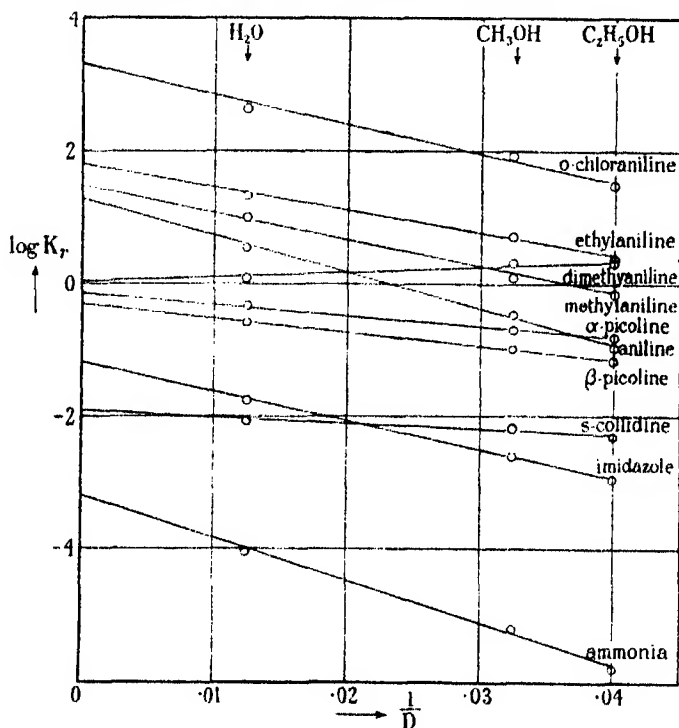


FIG. 2.

The results summarized above show clearly that variations in the relative strengths of acids in different solvents are determined by electrical forces which may be related to the dielectric constants of the solvents. It is therefore possible to split up the relative strength of an acid into two terms (1) that due to electrical forces, (2) the intrinsic strength. The latter is independent of the solvent and affords a true measure of relative acid strength. The intrinsic strength of an acid may be obtained by employing the fact that it is the relative

\* 'Z. phys. Chem.' vol. 106, p. 219 (1923).



strength of the acid when electrical forces are inoperative, that is to say, in a solvent of infinite dielectric constant. Such a solvent is, of course, non-existent, but in view of the linearity of the curves shown in the figures it is proposed to derive values of the intrinsic strength by extrapolation of the curves to  $1/D = 0$ , an extrapolation which is fortunately comparatively short.

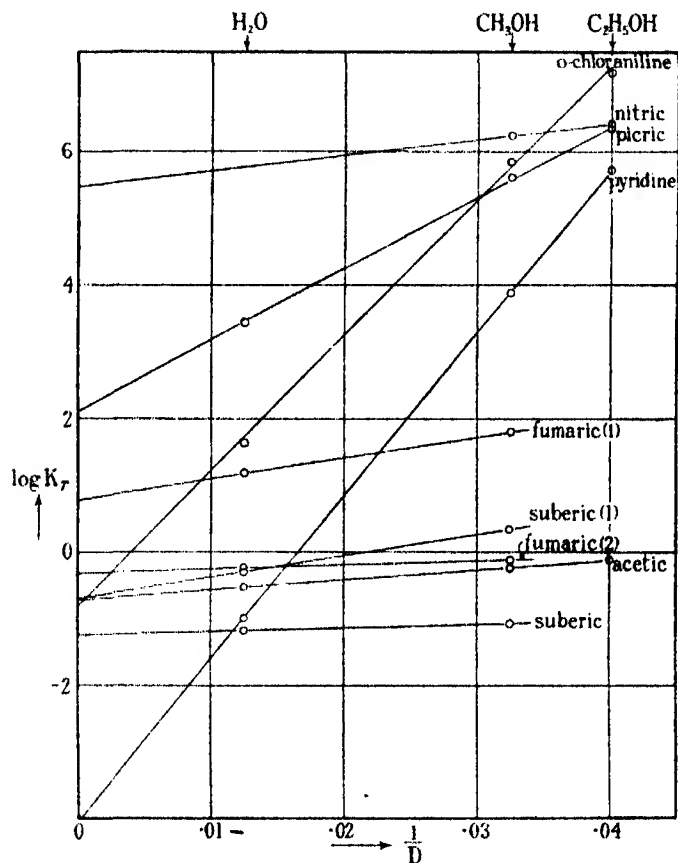


FIG. 3.

In Table I are given values of the logarithms of the intrinsic strengths of the uncharged acids already considered.

The data are inevitably scanty, and as the lines are determined only by 3 points the extrapolated values are not very reliable, nevertheless certain interesting facts emerge. Thus, compared with results for water, picric acid has become much weaker, whereas *o*-nitrobenzoic acid has become stronger; 1.3.5 dinitrobenzoic acid is seen to have the same intrinsic strength as

Table I.—Intrinsic Strengths of Acids.

Acid.	log A.	Acid.	log A.
Nitric .....	5.5	Salicylic .....	1.0
Trichloroacetic .....	4.0	<i>p</i> -nitrobenzoic .....	0.55
Trichlorobutyric .....	3.4	<i>m</i> -nitrobenzoic .....	0.5
Dichloroacetic .....	2.8	Formic .....	0.1
1. 2. 4 dinitrobenzoic .....	2.6	Benzoic .....	0.00
Floric .....	2.1	Phenylacetic .....	-0.1
<i>o</i> -nitrobenzoic .....	2.1	Acetic .....	-0.7
Trinitroresol .....	1.7		
1. 3. 5 dinitrobenzoic .....	1.0		

salicylic acid, while 1. 2. 4 dinitrobenzoic acid is much stronger. The difference in strength between *o*-nitrobenzoic acid and the *m*- and *p*- acids is very marked, and it will be interesting to obtain data for other substituted benzoic acids.

The values for the positively charged acids are not tabulated, since the steepness of the curves, in fig. 3, renders extrapolation rather uncertain and considerably magnifies the effect of small errors in the data. It can, however, be shown that the intrinsic strengths are of real significance for the comparison of structure and acid strength. It is well known that the introduction of an alkyl group into the ammonia molecule increases the basicity of the molecule but this effect is not regular. The order of basic strengths (deduced from the dissociation constants in water) is  $\text{NH}_3 < \text{primary amine} < \text{secondary amine} > \text{tertiary amine}$ . Now we have seen that the variation in the relative acid strengths of the ammonium ions depends upon the degree of substitution, and that the relative strengths of the primary ammonium ions decrease more rapidly with decrease in dielectric constant than do the relative strengths of the secondary ammonium ions, and in turn these decrease more rapidly than the relative strengths of the tertiary ammonium ions. It therefore seems quite probable that the order obtaining in aqueous solution is accidental and not the true order of the intrinsic strengths.

Unfortunately no data are available for the strengths of the aliphatic amines in the alcohols, but if we assume that the variation of  $\log K_a$  with dielectric constant is the same for the alkylammonium ions as for the anilinium ion, for the dialkylammonium ions as for the methylanilinium ion, and for the trialkylammonium ions as for the dimethylanilinium ion, it is possible to obtain the intrinsic strengths of the various acids from the values of  $K_a$  in water. It is obvious that values obtained in this way are liable to considerable

error, but they may still be expected to possess a semi-quantitative significance. In Table II are collected the values of  $-\log K_r$  (the relative strengths in water taking the pyridinium ion as standard) and of  $-\log A$  (the intrinsic strengths for  $D = \infty$ ) for certain alkylammonium ions.

Table II.—Intrinsic Strengths of Substituted Ammonium Ions.

	Methyl.		Ethyl.		Propyl.		Isobutyl.	
	$-\log K_r$	$-\log A$	$-\log K_r$	$-\log A$	$-\log K_r$	$-\log A$	$-\log K_r$	$-\log A$
$\text{NH}_4^+$ ....	4.05	3.20	4.05	3.20	4.05	3.20	4.05	3.20
Mono- .....	5.16	4.35	5.55	4.75	5.43	4.65	5.25	4.45
Di- .....	5.46	4.90	5.85	5.40	5.78	5.30	5.44	4.90
Tri- .....	4.57	4.75	5.65	5.85	5.50	5.70	5.17	5.35

Except for the methylammonium ions the anomaly observed in aqueous solution disappears when the values of the intrinsic strengths are adopted and the order of acid strength is seen to be tri < di < mono <  $\text{NH}_4^+$ .

For a study of the effect of substitution upon the strengths of the acids we must also take into account the fact that the various ions have different numbers of ionizable hydrogen atoms attached to them and in consequence the value of  $\log K_r$  for the  $\text{NH}_4^+$  ion must be decreased by 0.6 (log 4), the values for the primary ammonium ions by 0.48 (log 3), and those of the secondary ammonium ions by 0.3 (log 2). Without further data, however, no exact study can be made.

We may consider finally the intrinsic strengths of negatively charged acids. According to Bjerrum's theory the second dissociation constant of a dibasic acid will be a quarter of the first dissociation constant due simply to the statistical effect of differing numbers of protons attached to the acid and basic molecules. In addition Bjerrum has shown that if the distance apart of the two carboxyl groups is  $r$  A.

$$\ln \frac{K_1}{K_2} = \frac{e^2}{kDT r}.$$

This expression is clearly of the same form as the equations already employed and the electrical effect should be zero when  $D = \infty$ , hence the intrinsic strengths corresponding to the first and second stages in the dissociation of a dibasic acid should differ only by the statistical factor of 4. This is actually found to be true for suberic acid, but for fumaric acid the difference is greater

owing undoubtedly to a direct influence through the molecule of one carboxy group upon the other.

Ebert\* who made the determinations of the dissociation constants of the dibasic acids in methyl alcohol came to the conclusion that for both suberic and fumaric acids there was another non-electrical term in addition to the statistical factor, but the values he adopted for the dissociation constants of suberic acid in water seem to be unreliable.

*Summary.*

It has been shown that, although the relative strengths of acids vary considerably with the solvent, the variations depend upon the dielectric constant, and the data for acids in water, methyl and ethyl alcohols are all in accord with the relation

$$\Delta \log K_r \propto \Delta (1/D).$$

It is suggested that the intrinsic (relative) strength of an acid is the value of its relative strength in a medium of infinite dielectric constant, and on this basis values of the intrinsic strength of some acids are derived by extrapolation.

\* 'Ber. deuts. chem. Ges.,' vol. 58, p. 175 (1925).

*The Effect of Water Vapour on the Diffusion Coefficients of Ions in Nitrogen and Oxygen.*

By J. J. NOLAN and A. C. GALVIN, University College, Dublin.

(Communicated by A. W. Conway, F.R.S.—Received December 12, 1932.)

In a previous paper\* an account has been given of an investigation of the effect of water vapour on the diffusion coefficients and mobilities of ions in air. It was found that as the concentration of water vapour in the air varied, the values of the diffusion coefficients for positive and negative ions showed rather wide oscillations. These oscillations appeared to be of an irregular character, but a long series of experiments showed that the values of the coefficients found for any vapour pressure could be reproduced with a considerable degree of accuracy. In a subsidiary investigation, it was found that the mean mobilities of the ions varied in the same way with vapour pressure, if the fields to which the ions were exposed were less than about 1.4 volts per centimetre. In stronger fields the oscillations were suppressed, the mobility values plotted against vapour pressure lying on a smooth curve.

The method used for the determination of the diffusion coefficients was practically the same as that originally used by Townsend. The chief difference was the employment of only one long and one short tube for the capture of the diffusing ions, instead of the sets of 24 tubes in parallel used in Townsend's apparatus. The ionization was produced by  $\alpha$ -particles from polonium. A rather small volume of air, enclosed and kept at a definite humidity, was passed alternately through the long and the short tube, after exposure to the  $\alpha$ -radiation, and the diffusion coefficient was calculated from the ratio of the concentrations of the ions in the issuing air by the use of Townsend's formula.

With this method of working, there will be an accumulation in the air of ozone and oxides of nitrogen formed by the action of the  $\alpha$ -particles.† Since the influence of these bodies on the ionization has been established,‡ it seemed possible that the periodic variation in the diffusion coefficients might be caused by their presence. The examination of nitrogen and oxygen separately was

\* J. J. Nolan and T. E. Nevin, 'Proc. Roy. Soc.,' A, vol. 127, p. 155 (1930); hereafter cited as I.

† Lind, "The Chemical Effects of Alpha Particles and Electrons," 2nd ed. (1928), *passim*.

‡ Tyndall, Grindley and Sheppard, 'Proc. Roy. Soc.,' A, vol. 121, p. 185 (1928).

therefore undertaken. The apparatus was, in the main, similar to that already used for air, and the few modifications introduced will appear in the following description.

### Nitrogen.

The nitrogen was generated by heating a solution containing equal parts of sodium nitrite and ammonium sulphate. It was purified by slow passage through a train of towers containing, first, broken glass and dilute sulphuric acid, then broken glass and a concentrated solution of potassium bichromate and sulphuric acid. It was then dried by bubbling through strong sulphuric acid and passage over phosphorus pentoxide. In the process of filling, the apparatus was evacuated and the nitrogen was allowed to pass slowly in until atmospheric pressure was reached. This process was made easy because the generation of the nitrogen, once it had begun, proceeded very quietly without further application of heat, the reaction being exothermic. The evacuation and filling were repeated ten times and the generating and purifying train was then cut off from the rest of the apparatus. Humidity control was obtained by circulating the nitrogen for several hours through the apparatus, part of the circuit including a long horizontal vessel containing a sulphuric acid solution of a known strength. This circulation was achieved by a mercury oscillating pump.\* For each value of the humidity the apparatus was refilled, in order to make sure that the purity of the gas was not being affected by small leakages.

The details of the determination of the diffusion coefficients are given very fully in the previous paper I, and need not be repeated here. The values found, adjusted to 15° C. and 760 mm. mercury pressure, are plotted in fig. 1 and a few sample readings are given below.

### Nitrogen.

Water vapour pressure mm. Hg.	Diffusion coefficients.	
	D <sub>+</sub> .	D <sub>-</sub> .
0.28	0.0404	0.0510
5.37	0.0320	—
5.44	—	0.0488
14.00	0.0435	0.0455

\* Donnelly *et al.*, 'J. Soc. Chem. Ind. Trans.', vol. 46, p. 437 (1927).

The corresponding mean mobilities, calculated from  $K/D = 40.3$  can be read off on the scale on the right of the figure. It is at once clear that the type of oscillation found with air has disappeared. The values obtained for the negative ions are specially steady, diminishing only slowly with increasing water vapour pressure. Over the range covered, only two of the values found lie outside the limits 0.051 and 0.048. The corresponding limits for mean mobility are 2.05 and 1.93 cm./sec./volt/cm. The values obtained for the positive ions, on the other hand, diminish fairly rapidly at first, with increasing

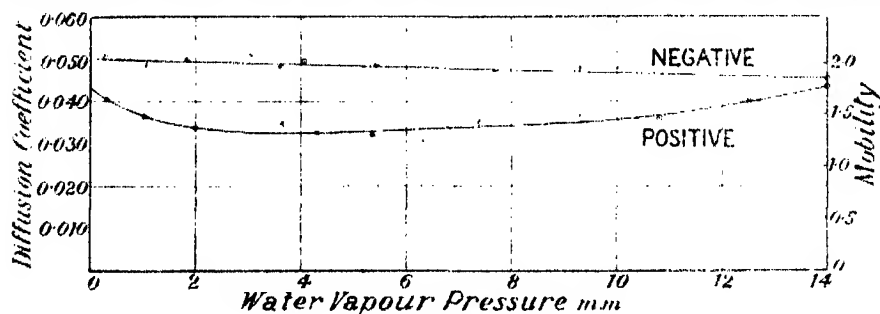


FIG. 1.

concentration of water vapour, and then slowly increase. The final value obtained at a pressure of 14 mm. Hg is higher than that found with the driest gas used. The limits in this experiment are, on the high side, about 0.040 with the dry gas and 0.043 with the wet gas, and on the low side, 0.032, at a vapour pressure between 4 and 5 mm. The corresponding values for mean mobilities are 1.61, 1.73 and 1.29.

The values for diffusion coefficients are all higher than those found by Salles in the only previous work on nitrogen\* with which we are acquainted. For nitrogen supplied commercially, guaranteed 99.5 per cent. pure and dried by caustic potash, calcium chloride and phosphorous pentoxide, Salles found  $D_+ = 0.0295$  and  $D_- = 0.0414$ . When these figures are converted into mean mobilities, the resulting values, 1.19 and 1.67, appear very low for dry nitrogen and suggest that some impurity was present in sufficient quantity to load up the ions. We do not, of course, claim that a very high degree of purity was reached in our own measurements. They are, however, satisfactory in showing that the oscillations found with air are absent when nitrogen alone is used.

In comparing our absolute values with those found by Tyndall and Powell† and Zeleny‡ it must be remembered that our mobilities are mean values, and

\* Salles, 'Ann. Physique,' vol. 2, p. 273 (1914).

† 'Proc. Roy. Soc.,' A, vol. 129, p. 162 (1930).

‡ 'Phys. Rev.,' vol. 38, p. 969 (1931).

that they refer to ions of age about 0.2 second. The high values found for the negative ions and their small variation with varying humidity suggest that, for these ions, we are dealing with something relatively simple. It may not be without significance that the value which we find for the dry gas (2.05) is practically identical with what one would obtain by extending Powell and Brata's\* mass-mobility curve for nitrogen to the condition where the mass of the ion is large compared with that of the gas-molecule.

#### Oxygen.

This gas was obtained commercially and was stated to be 98 per cent. pure, the remaining 2 per cent. being nitrogen. No attempt was made to remove the nitrogen. The processes of filling and humidity control were practically the same as those described for nitrogen.

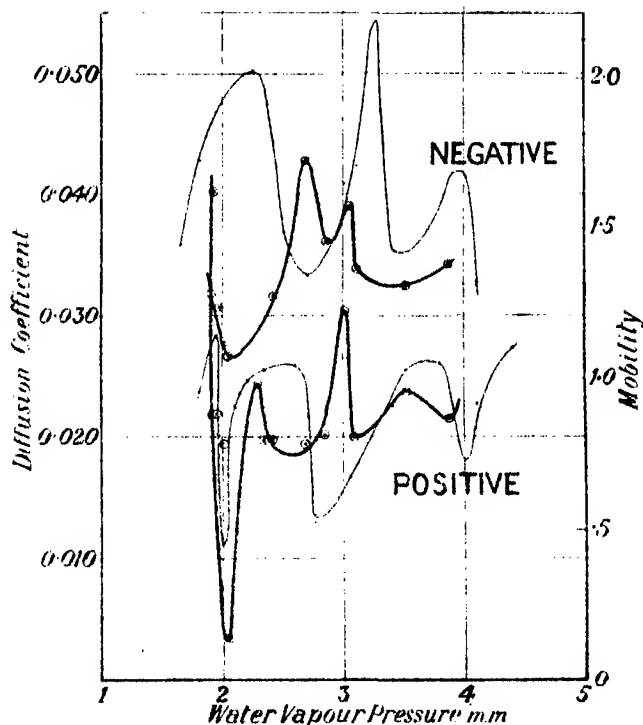


FIG. 2.

It was at once found that the diffusion coefficients for this gas showed very wide variations for small changes in water vapour pressure. It was decided therefore to work over a restricted range of vapour pressures. The results obtained are shown graphically in fig. 2. The lighter curves in the figure are

\* 'Proc. Roy. Soc.,' A, vol. 138, p. 117 (1932).



taken from the previous paper and refer to measurements made on air. As will be seen, the oscillations previously found with air reappear. While there is no general parallelism between the two sets of curves, there are a few points of resemblance, the most notable of which is the set of values obtained for positive ions at about 2 mm. pressure. The very sudden rise and fall in the case of air coincides exactly with a similar variation of still wider amplitude in the case of oxygen.

In view of the character of these variations, it has not been thought profitable at present to extend the observations on oxygen to a wider range of humidity values. The results obtained support the view that the oscillations previously found with air are caused by the formation of such bodies as ozone and oxides of nitrogen by the action of the  $\alpha$ -particles. How these bodies affect the ions so as to cause the mobility values to rise and fall with variations in water vapour pressure is, of course, not yet clear. In the general study of mobility problems, these bodies and the effects they give rise to introduce an undesirable complication and are therefore to be avoided. But their existence must be recognized in the study of atmospheric ionization. About half of the ionization of the lower atmosphere is due to  $\alpha$ -particles.\* The products of the so-called chemical action of the radiation may not accumulate in the atmosphere to the same extent as they do in a closed vessel, but they are certainly present in sufficient proportion to affect the mobilities of the ions. The results of the previous work show that, except where the atmospheric field is greater than 1.4 volts/cm. there will be a loading and unloading of the ions, as the atmospheric humidity varies. And it is to be expected that, not merely in the matter of variations of this type, but in other respects, will the actual behaviour of ions in atmospheric air differ from their behaviour in a highly purified and dried gas.

#### *Summary.*

- (1) The diffusion coefficients of ions have been measured in nitrogen, containing water vapour at different concentrations. Oscillations previously found with air were not observed.
- (2) When observations were made in oxygen the oscillations reappeared.
- (3) The effects in air and oxygen are attributed to the formation of oxides of nitrogen and ozone by the action of  $\alpha$ -particles.

\* V. F. Hess, "The Electrical Conductivity of the Atmosphere," English ed., p. 168 (1928).

---

*An Electrical Calculating Machine.*

By R. R. M. MALLOCK, M.A.

(Communicated C. G. Darwin, F.R.S. Received March 31, 1933).

*Introduction.*

1. In connection with many problems of engineering and physics it is necessary to solve sets of linear algebraic simultaneous equations involving a large number of unknowns; for instance in the determination of secondary stresses in bridges and other structures sets of equations involving from ten to twenty, or even more, unknowns may occur and the labour involved in the solution when the number of unknowns is more than about six is very great.

Various attempts have been made to design a machine which will solve such equations automatically and quickly, but, as far as the author knows, none of them has been really successful.

From time to time the author tried to design an electrical machine operating with direct current, but met with no success; however the reasons that caused the failure of any direct current arrangement led him to consider the use of alternating current, and immediately it appeared that it would be possible to make a machine in which a fair degree of accuracy might be expected. Shortly, such a machine consists of a set of alternating current transformers each with a number of windings, the unknowns being proportional to the fluxes in the transformers and the coefficients to the numbers of turns in the windings, and can be operated from any ordinary alternating current mains. It was recognized that owing to the resistance in the windings considerable errors would occur and various schemes for reducing these errors were considered: two of these, of which one necessitates a series of approximations being made by the operator and the other applies the corrections automatically, have been developed and have proved successful.

An experimental machine for the solution of six equations was made by the author and tested early in 1931, and the tests proved conclusively that results quite accurate enough for most purposes could be obtained. By using the first of the methods mentioned above it was found that the errors in the roots, after a few approximations had been made, were usually less than 0.4 per cent. Later the automatic correcting devices mentioned were added to part of the machine and it was found that sets of four equations could be solved

directly with an accuracy at least as good as the above ; with this arrangement the solution is immediate and the whole time taken is that required to set up the coefficients and to read off the roots.

A machine which can deal with ten equations has now been built by the Cambridge Instrument Co., Ltd., and, owing to improved design and to the use of better materials, the errors in the roots have been reduced, in favourable cases, to less than 0·1 per cent. of the largest root.

With certain small additions the machine can be used for the direct solution, by the method of least squares, of a set of equations of condition without forming the normal equations.

2. To explain the principle on which the machine operates we will consider the system shown diagrammatically in fig. 1, where  $X, Y, Z, U$  are four small alternating current transformers and  $a_1, b_1, c_1, \dots$  are coils having respectively  $a_1, b_1, c_1, \dots$  turns, assuming for the present that in any transformer the flux through each turn is the same, *i.e.*, that there is no stray flux, and that the voltage drops in the coils, due to resistance, are negligible.

Each of the three sets of coils  $a_1, b_1, c_1, d_1$ ;  $a_2, b_2, c_2, d_2$ ;  $a_3, b_3, c_3, d_3$  is connected in series and short circuited as shown in the diagram ; the direction in which a coil is connected corresponding to the sign of the symbol representing the number of turns.

If an alternating voltage is applied to an independent coil  $E_x$ , on the transformer  $X$ , a current will flow in the coil and will induce a flux in the core of  $X$ , this flux will induce e.m.f.'s and consequently currents, in the circuits  $a_1b_1c_1d_1, \dots$  and these currents will induce fluxes in the other cores. After a short time a steady state will be attained.

Under the conditions postulated the e.m.f. induced in any coil of a given transformer is proportional to the number of turns in the coil, and the p.d. of the coil is equal to the induced e.m.f. ; if, therefore,  $x, y, z, u$ , are the e.m.f.'s induced in single turns of the four transformers, the p.d. of a coil  $a_1$  will be  $a_1x$ , and the p.d. of the four coils in series will be  $a_1x + b_1y + c_1z + d_1u$  : since the circuit is shorted this must be zero, so that we have

$$\text{and similarly} \quad \left. \begin{aligned} a_1x + b_1y + c_1z + d_1u &= 0 \\ a_2x + b_2y + c_2z + d_2u &= 0 \\ a_3x + b_3y + c_3z + d_3u &= 0 \end{aligned} \right\} . \quad (2.1)$$

That is, the currents in the circuits  $a_1b_1c_1d_1, \dots$ , and the fluxes in the transformer cores will attain such values that the equations (2.1) will be satisfied.

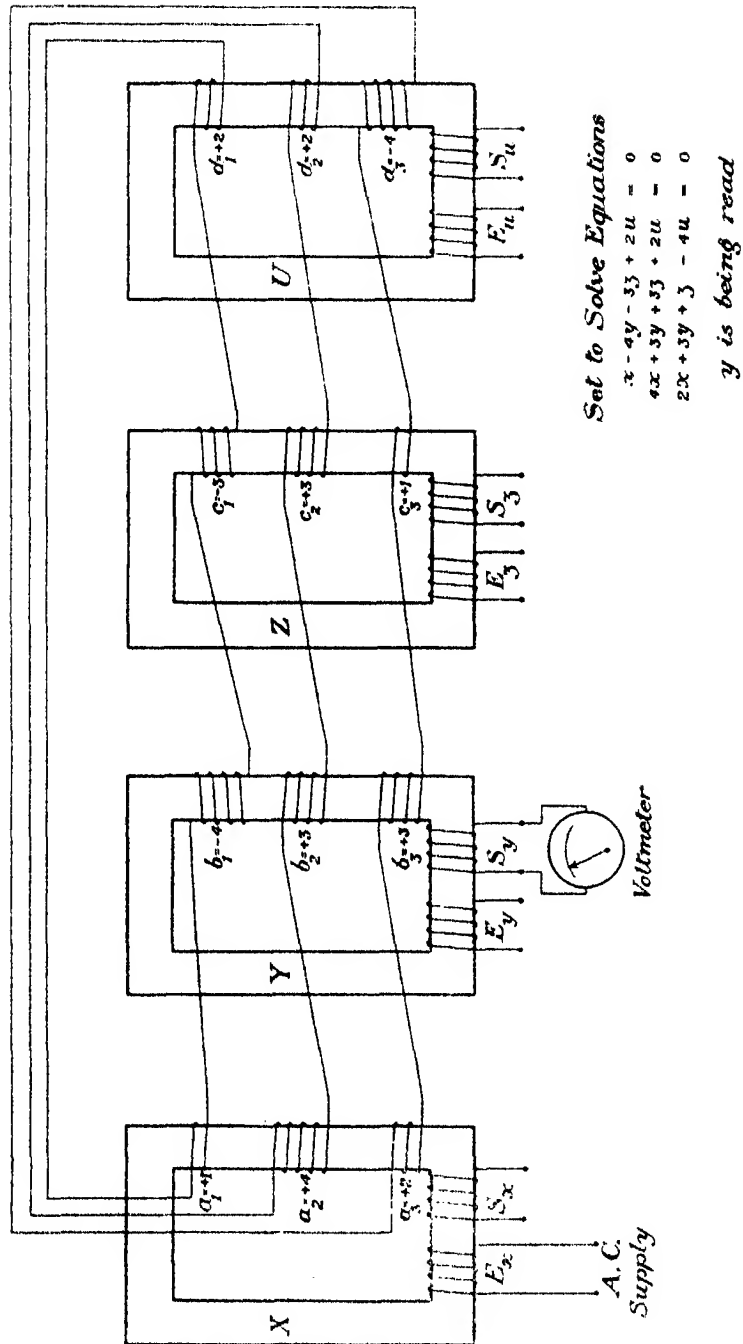


FIG. 1.—Showing diagrammatically the principle of the machine.

It should be noticed that  $x, y, z, u$  may be taken as instantaneous values, so that the equations (2.1) are satisfied at every instant whatever may be the wave-form of the applied e.m.f. and even if the e.m.f. is not periodic. Further, the wave-forms of the e.m.f.'s  $x, y, z, u$ , and the applied e.m.f. will all be the same, and the equations will still be satisfied if we take  $x, y, z, u$  to represent the magnitudes of any specified harmonic.

If we now measure the e.m.f.'s induced in an additional coil  $S_x$  on  $X$  and corresponding coils  $S_y, S_z, S_u$  on  $Y, Z, U$ , each of these coils having the same number of turns, we can find the ratios  $x/u, y/u, z/u$  and these will be the roots  $x, y, z$  of the equations

$$\left. \begin{aligned} a_1x + b_1y + c_1z + d_1 &= 0 \\ a_2x + b_2y + c_2z + d_2 &= 0 \\ a_3x + b_3y + c_3z + d_3 &= 0 \end{aligned} \right\}. \quad (2.2)$$

From this we see that an arrangement such as that shown in fig. 1 provides a method of obtaining directly the roots of a set of simultaneous equations. By increasing the number of transformers and the number of coils on each transformer the system can be extended so as to deal with any number of equations.

In addition to the circuits  $a_1b_1c_1d_1, \dots$ , one or more circuits, such as  $a_0b_0c_0d_0$ , which are left open instead of being short circuited, may be formed. As no currents can flow in these circuits they will not affect the fluxes in the transformers and so will not affect the values of  $x, y, z, u$ , due to the existing circuits.

The e.m.f. induced in such a circuit is

$$a_0x + b_0y + c_0z + d_0u. \quad (2.3)$$

This can be measured, and from this  $a_0x + b_0y + c_0z + d_0$  can be deduced, or, if the measuring instrument is arranged so as to give  $u = 1$ , the value of the latter expression can be read off directly.

We see, therefore, that, by means of the arrangement described, a number of expressions such as  $a_0x + b_0y + c_0z + \dots$ , can be evaluated, when  $x, y, z, \dots$ , are defined by a set of linear simultaneous equations.

In this way many types of mathematical expression, which do not at first sight appear to have any connection with simultaneous equations, can be evaluated.

For example, a set of expressions such as

$$a_0A + b_0B + c_0C + d_0D,$$

where  $A, B, C, D$ , are fixed and  $a_0, b_0, c_0, d_0$ , have various values, can be evaluated. For, if the values of  $a_1, a_2, a_3, \dots$ , in (2.1) are chosen so that  $x, y, z, u$  are connected by the equations

$$\left. \begin{aligned} Dx - Au &= 0 \\ Dy - Bu &= 0 \\ Dz - Cu &= 0 \end{aligned} \right\}, \quad (2.4)$$

it is easily seen that

$$a_0x + b_0y + c_0z + d_0u = u \{a_0A + b_0B + c_0C + d_0D\}/D.$$

Hence, if the measuring instrument is adjusted so as to give  $u = D$ , the value of  $a_0A + b_0B + c_0C + d_0D$ , or of several such expressions with different values for  $a_0, b_0, c_0, d_0$ , can be read off directly.

This provides a quick method of checking a set of roots determined by the machine,  $A/D, B/D, C/D$ , being made equal to these roots and  $a_0, b_0, c_0, d_0$  being taken to be  $a_1, b_1, \dots, a_2, b_2, \dots$ , etc., the coefficients of the original equations, in succession.

The results—the *equation errors*—so obtained can, if they are large, be used to enable the machine to obtain a second approximation to the roots. This process is valuable as, owing to various causes, there will be errors in the roots found by the machine and, if the equations are ill-conditioned, these errors may be serious, but the fact that the original equations were ill-conditioned will not affect the accuracy of the checking process.

For the reason just given it is quite impossible to give any definite figure for the errors to be expected in the roots, but when the new machine is used to evaluate a sum of products, such as

$$a_1A_1 + a_2A_2 + \dots + a_nA_n,$$

where  $a_1, a_2, \dots, A_1, A_2, \dots$ , all lie between  $+1$  and  $-1$ , it is found that when the result is not greater than 1 the average error is less than 0.0002, and that with larger results it is slightly but not proportionately greater.

The errors are due principally to the fact that both the resistance drops in the equation circuits and the effect of stray flux are appreciable, although the latter is very much the smaller of the two. The methods adopted to minimize these errors will be discussed later and it will be shown that the former can be greatly reduced by means of certain correcting devices, called *compensators*.

3. The machine that has been built by the Cambridge Instrument Co., Ltd., is designed to deal with ten equations.

It contains 11 main transformers,\*—one for each unknown and one for the constant member; on each transformer there are 11 coefficient coils—one for each equation—corresponding to the coils  $a_1, a_2, a_3$ , in fig. 1, and the eleventh for a purpose to be explained in § 14.

The number of turns in circuit in each of these coils can be adjusted by means of a set of three 10-way switches, the ratio of this number to the maximum number being shown in figures near the corresponding set of switches. The sense in which the coil is connected is controlled by a reversing switch and is indicated by a + or — sign. By this means the number of turns in circuit can be adjusted in steps of 0·001 from — 0·999 to + 0·999 of the maximum, and one extra step of 0·001 in either direction can be added by means of the reversing switch, which has two extra positions, so that settings of + 1·000 and — 1·000 can also be obtained.

On each transformer there are also an *exciting coil* and a *search coil*, corresponding respectively to  $E_x$  and  $S_x$  in fig. 1, the latter being a *unit coil*, that is having a number of turns equal to the maximum number in a coefficient coil. There are other coils for use in connection with the compensator.

Each transformer is provided with a compensator, which includes an amplifier and other transformers.

There is also one transformer called the *supply transformer* which is used to supply the exciting current to one of the main transformers, its primary is connected to the mains and its secondary consists of a coil with an adjustable number of turns, the number being adjusted by a three-figure switch in the same way as in the coefficient coils.

There are two measuring instruments—the first giving the results directly by the deflection of a pointer, so that the accuracy is limited to about  $\pm 1$  per cent., and the second consisting of a zero indicating instrument and a special transformer, called the *measuring transformer*, provided with a coil of which the number of turns in circuit can be adjusted by switches similar to those used for the coefficient coils. The turns in this coil are adjusted until the instrument indicates that its voltage is equal to that to be measured and the result is then shown to four figures.

By means of selector switches the voltage in any search coil, or any other voltage, can be applied to and measured by either of these instruments.

A rough indication of the magnitudes of the roots is also given by the relative brightness of a set of flash lamps; as these can all be seen at the same time they provide a quick method of picking out the largest root.

\* The arrangement of a machine for two equations is shown diagrammatically in fig. 2.

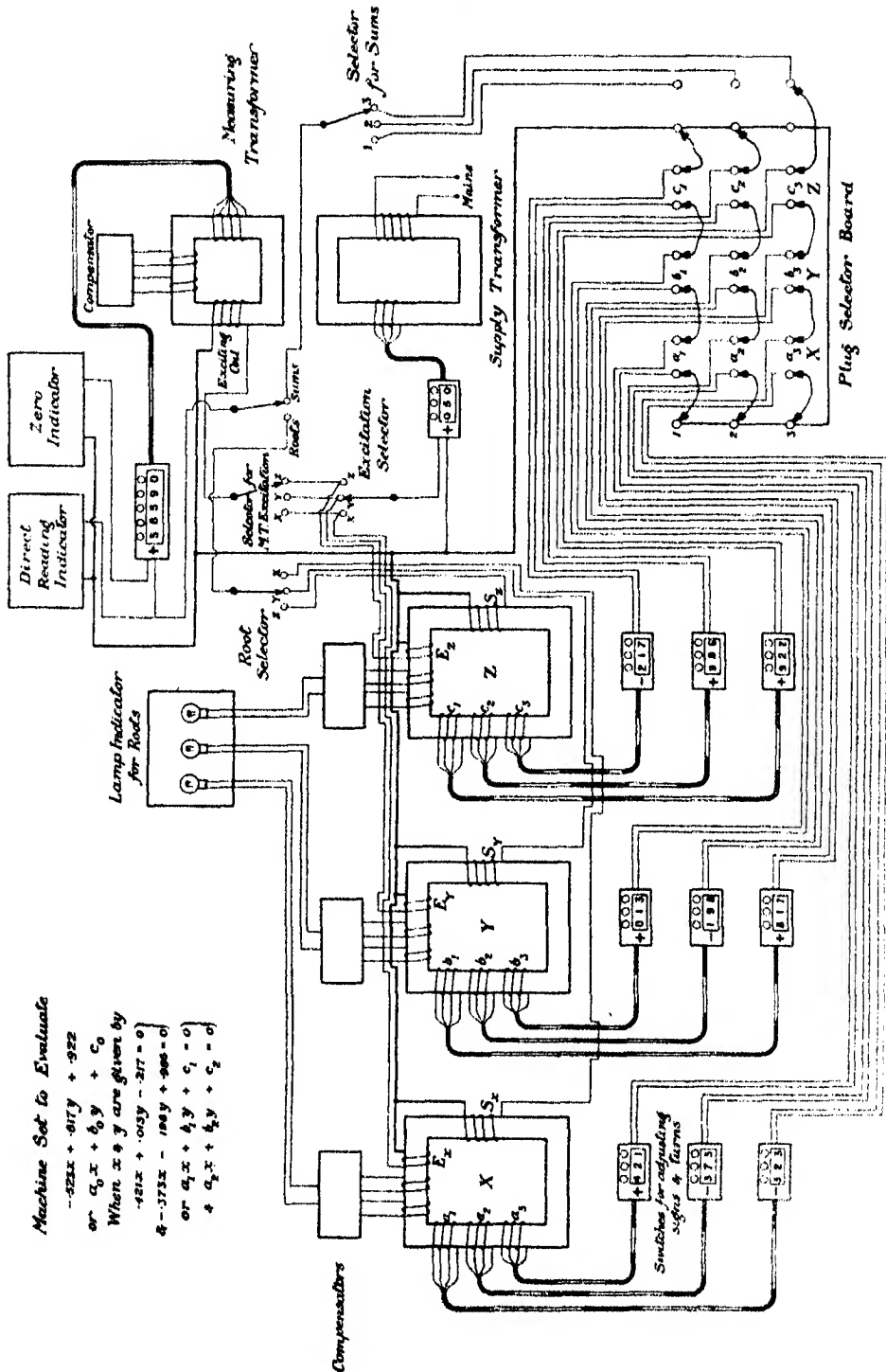


FIG. 2.—Arrangement of a machine for solving two equations.



4. To use the machine for solving a set of equations such as (2.2) we first adjust the coefficients so that none is greater than 1 and all are given to three places of decimals, at the same time ensuring that as many as possible are reasonably large; this involves multiplying some or all of the equations by simple factors, and substituting for some or all of the original unknowns new unknowns bearing simple ratios to them.

One transformer is assigned to each unknown and one to the constant member, the coefficient coils are adjusted so as to correspond to the coefficients, and, by means of a system of plugs and sockets they are connected in series, forming circuits, called *equation circuits*, such as  $a_1, b_1, c_1, \dots, a_2, b_2, c_2, \dots$ , in fig. 1.

A small alternating voltage is then applied to one of the exciting coils by means of the supply transformer, this is increased until the brightest flash lamp can be easily picked out, the excitation is then transferred to the transformer corresponding to this lamp, and is set to a certain standard value; this is desirable because with this arrangement the errors are reduced to a minimum.

The roots can now be read off in succession either, for rough results, on the direct reading instrument or, for accurate results, by means of the measuring transformer.

To check the roots so found by the method described in § 3, coefficient coils on another transformer are set to the values of the roots, certain additional plug connections are made and a special switch is moved from "Solve" to "Check"; the equation errors are then read off directly, and if these are large they can be used to enable the machine to determine corrections to the roots already found.

If the coefficients are given to more than three figures and the roots are required to a corresponding degree of accuracy, the first three figures of the coefficients are set up and approximate values of the roots are found as described above; the equation errors are now determined, by other means, to three significant figures, and from these results corrections to the previous roots can be found by means of the machine, this process may be repeated until the roots are determined to the required degree of accuracy—usually about three figures will be found each time.

#### *Causes and Elimination of Errors.*

5. So far we have considered an ideal machine in which there is no stray flux and in which the resistance drops due to the currents in the coils are zero;

actually the resistance drops are large enough to cause appreciable errors, and we will now consider in detail the factors which determine the magnitude of these drops and the methods adopted to minimize them. The much smaller effects of stray flux are considered in § 15.

In § 2 and § 3  $x, y, \dots$  represent the voltages per turn, while  $a, b, \dots$  represent the number of turns in circuit. We will now take  $x, y, \dots$  to represent the voltage induced in a unit coil, i.e., a coefficient coil with the maximum number of turns in circuit, while  $a, b, \dots$  will represent the ratio of the number of turns in circuit to the maximum number, so that  $a, b, \dots$  will never be greater than 1; all the equations of § 2 and § 3 will then hold without alteration.

We will take  $x, y, \dots, i, \dots$  to represent instantaneous values,  $\mathbf{x}, \mathbf{y}, \dots, \mathbf{i}, \dots$  to be complex quantities representing the fundamental, or any harmonic, of the voltages and currents, the components in phase and in quadrature (leading  $90^\circ$ ) with the supply voltage being distinguished by the suffixes  $p, q$ , so that, for instance,  $\mathbf{x} = \mathbf{x}_p + j\mathbf{x}_q$ . Further, we will take  $I, H, \dots$  to be the magnitudes of the fundamentals of currents  $\mathbf{i}, \mathbf{h}, \dots$  and  $X, Y, \dots$  to be the voltages indicated by the measuring instrument; the latter will be, very nearly, but owing to the effects of harmonics and phase displacements not exactly, equal to the magnitudes of the corresponding fundamentals. The unknowns in the equations to be solved will, as before, be denoted by  $x, y, z$ .

The flux in the core of a transformer depends on the total ampere-turns in the coils and we define the *magnetizing current*,  $i_m$ , as being the current in a unit coil required to produce a given alternating flux, so that the magnetizing current depends on the e.m.f. induced in a unit coil. We will assume that the e.m.f. is sinusoidal, in which case the magnetizing current will not be sinusoidal, but we shall, for the present, consider the fundamental,  $i_m$ , only.

The flux leads on the induced e.m.f. by  $90^\circ$  while  $i_m$  leads on the flux by an angle which depends on the material of the core and the flux density at which it is being worked.

The magnitudes of the components  $i_{mp}, i_{mq}$ ,\* respectively in phase and in quadrature with  $\mathbf{x}$ , depend on the frequency and on the dimensions, magnetic properties and resistivity of the core. For cores of given dimensions, working at a given frequency and flux density,  $I_{mp}$  is proportional to the loss due to hysteresis and eddy currents in the core, while  $I_{mq}$  is, roughly, inversely proportional to the permeability of the material.

As it is necessary to make  $i_m$  as small as possible we must use a material

\* If  $\mathbf{x}$  is taken as real and positive  $i_{mp}$  is negative and  $i_{mq}$  is positive.

with a high permeability and must ensure that the losses are kept as low as possible.

With the silicon iron alloys normally used for transformer cores the maximum permeability is about 5000, and the eddy current loss, with plates 0.02 inch thick, is a small fraction of that due to hysteresis; with a nickel iron alloy, such as mumetal, the maximum permeability is about 50,000, and the hysteresis loss is about one-tenth that in the silicon iron alloys, but the eddy current loss is about the same, consequently the latter is now of greater importance than the former, and it is therefore necessary to use plates as thin as possible in order to make full use of the higher permeability.

With mumetal, the material used,  $I_{mp}$  is about 40 per cent. greater than  $I_{mq}$  at the maximum flux density normally used in the machine, this flux density corresponding, roughly, to the maximum permeability of the material.

Typical curves connecting  $I_{mp}$ ,  $I_{mq}$  with  $X$  are shown in fig. 3.

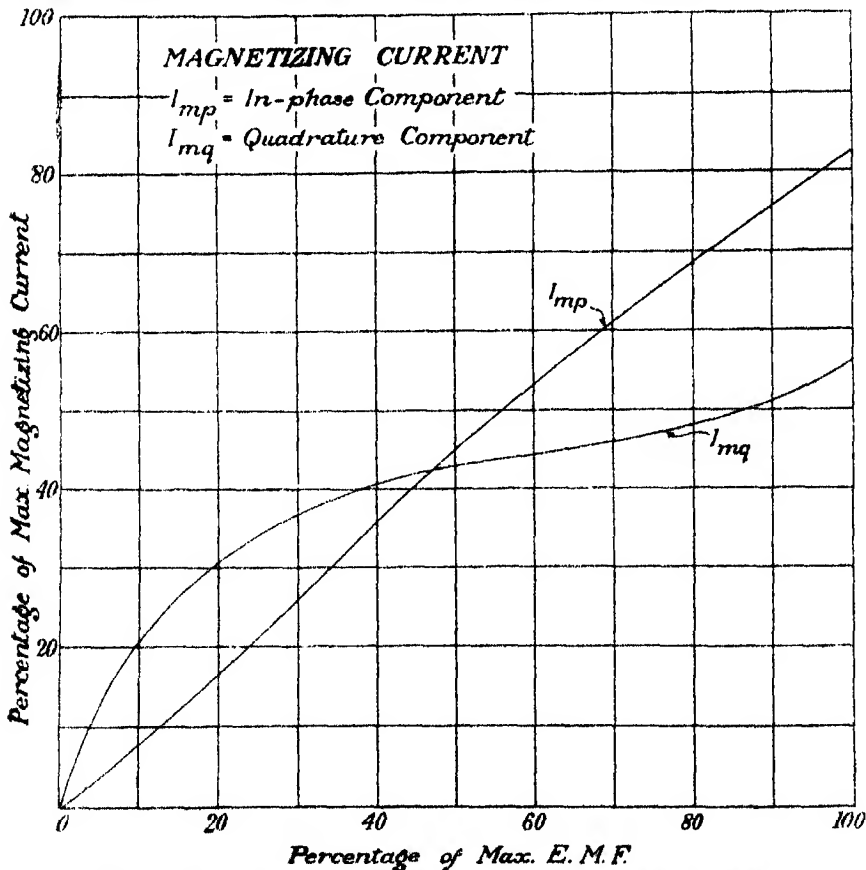


FIG. 3.—Typical relation between magnetizing current and voltage.

6. We have seen, in § 2, that the function of the equation currents is to induce the necessary flux in the un-excited transformers, so that, on each of these, the total ampere-turns due to the equation currents must be equal to those due to the required magnetizing current.

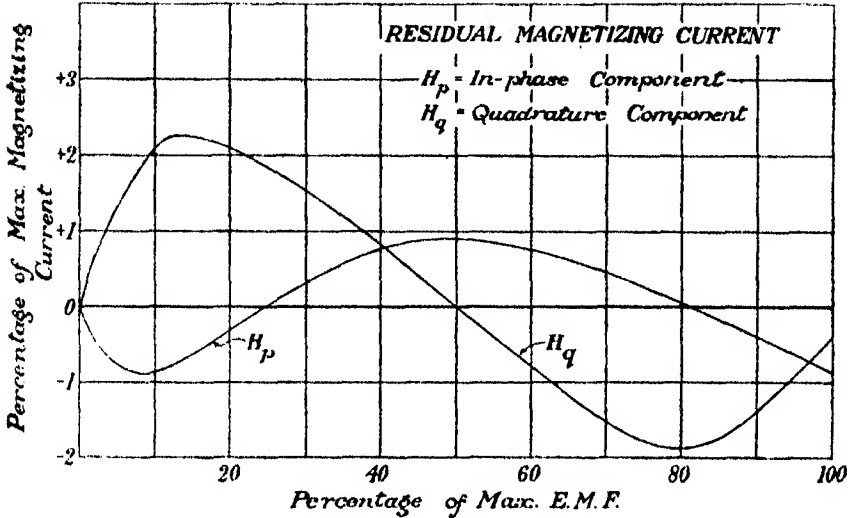


FIG. 4.—Typical relation between residual magnetizing current and voltage.

That is, taking  $X$  to be the excited transformer, the equation currents  $i_1$ ,  $i_2$ ,  $i_3$  and the magnetizing currents  $i_{mx}$ ,  $i_{my}$ , ... are related by the equations

$$\left. \begin{aligned} b_1 i_1 + b_2 i_2 + b_3 i_3 &= i_{my} \\ c_1 i_1 + c_2 i_2 + c_3 i_3 &= i_{mx} \\ d_1 i_1 + d_2 i_2 + d_3 i_3 &= i_{mu} \end{aligned} \right\} \quad (6.1)$$

and if we take into account the resistance drops in the equation circuits, but still ignore the effects of stray flux which, as we shall see later, are considerably smaller, the equations (2.1) must be replaced by

$$\left. \begin{aligned} a_1 x + b_1 y + c_1 z + d_1 u &= r_1 i_1 \\ a_2 x + b_2 y + c_2 z + d_2 u &= r_2 i_2 \\ a_3 x + b_3 y + c_3 z + d_3 u &= r_3 i_3 \end{aligned} \right\}, \quad (6.2)$$

where  $r_1$ ,  $r_2$ ,  $r_3$ , are the resistances of the three equation circuits.

Further the exciting current  $i_e$  from the external source and the external voltage  $E$  satisfy the equations

$$\left. \begin{aligned} a_1 i_1 + a_2 i_2 + a_3 i_3 + i_e &= i_{mz} \\ x &= -E + r_e i_e \end{aligned} \right\} \quad (6.3)$$

In practice  $E$  is not measured but is adjusted so as to bring the largest of  $X, Y, Z, U$  to a certain standard value, so that, as we are not concerned with the value of  $i_e$ , we can ignore the last two equations and take either  $X, Y, Z$  or  $U$  to be known.

The equations (6.1), (6.2) and (6.3) all apply to the instantaneous values of the currents and voltages involved, and they will therefore also apply if we replace  $i, x, y, \dots$  by  $i, x, y, \dots$  representing the complex values corresponding to the fundamental or to any harmonic.

If we consider only the equations corresponding to the fundamental we can assume that  $i_{mx}, i_{my}, i_{mz}, i_{mu}$  depend respectively on  $x, y, z, u$ , as explained in § 5, so that the six equations (6.1) and (6.2) involve six unknowns—three of the voltages  $x, y, z, u$  and the three equation currents  $i_1, i_2, i_3$ ; the values of all the unknowns are therefore determinate.

7. The equations (6.2) differ from (2.1) owing to the presence in each of a term  $r_e i_e$ , so that if (2.1) are to be satisfied as nearly as possible the resistance drops,  $r_e i_e$ , must be made as small as possible. As these resistances are made up of the resistances of the coefficient coils, while the equation currents are related to the magnetizing currents by (6.1), the transformers must be designed so that the average, and therefore the maximum, values of these resistances and currents are as small as possible; more exactly, if  $R_{(max.)}$  is the resistance of a coefficient coil set to the maximum number of turns, the ratio

$$R_{(max.)} I_{m(max.)} / X_{(max.)}$$

should be as small as possible, and it can be shown that for similar transformers this is roughly proportional to  $n/\mu W^{2/3}$ , where  $n$  is the maximum number of equations that can be dealt with,  $\mu$  is the effective a.c. permeability and  $W$  is the weight of the core. Hence, as mentioned in § 5, it is necessary to use for the cores a material with the highest possible permeability, but it is impracticable to obtain much reduction of the above ratio by increasing the size of the transformers.

As the method of measurement used only takes account of the in-phase component of the voltage it is  $I_{mp}$ , the in-phase component of  $i_m$ , corresponding

to the energy loss in the core, that must be made as small as possible, although it is, for various reasons, necessary to keep the quadrature component reasonably small as well. In the experimental machine  $R_{(\max.)} I_{mp(\max.)}/X_{(\max.)}$  is about 0.015, and in the new machine it is about 0.0021.

It can be shown that when the equations are ill-conditioned the errors in the roots may be much larger than this quantity, so that it is desirable to find some means of reducing it still further.

Two general methods of doing this suggest themselves—first the introduction into each equation circuit of an additional e.m.f.  $e_s$ , which is forced to be as nearly as possible equal to  $r_s i_s$ , so that (6.2) become

$$a_s x + b_s y + c_s z + d_s u = r_s i_s - e_s, \quad (s = 1, 2, 3),$$

where  $r_s i_s - e_s$  is much smaller than  $r_s i_s$ , or, secondly, the addition to each transformer of a unit coil carrying a current  $i_e$ , which is forced to be as nearly as possible equal to  $i_m$ , so that (6.1) becomes

$$b_1 i_1 + b_2 i_2 + b_3 i_3 = i_{mv} - i_{ev}, \text{ etc.}, \quad (7.1)$$

where  $i_{mv} - i_{ev}$ , etc., are much smaller than  $i_{mv}$ , etc.

Methods of obtaining both these results by means of amplifiers were considered and as the second proved to be very much the simpler it was adopted and has proved successful; with a device operating in this way it has been found possible automatically to make  $i_e$  so nearly equal to  $i_m$  that, as  $X$  varies between 0 and  $X_{(\max.)}$ , the in-phase component of the residual magnetizing current,  $h_{mp} = i_{mp} - i_{ep}$ , is never greater than 0.015  $I_{mp(\max.)}$ , while the maximum value of the quadrature component may be three or four times as great. The value of  $R_{(\max.)} H_{p(\max.)}/X_{(\max.)}$ , which now replaces  $R_{(\max.)} I_{mp(\max.)}/X_{(\max.)}$  is therefore about  $3 \times 10^{-5}$ .

With this device, called a *compensator*, in operation in connection with each transformer we must substitute for (6.1) and (6.3) the equations

$$\left. \begin{aligned} b_1 i_1 + b_2 i_2 + b_3 i_3 &= h_v \\ c_1 i_1 + c_2 i_2 + c_3 i_3 &= h_s \\ d_1 i_1 + d_2 i_2 + d_3 i_3 &= h_u \end{aligned} \right\}, \quad (7.2)$$

and

$$\left. \begin{aligned} a_1 i_1 + a_2 i_2 + a_3 i_3 + i_e &= h_x \\ x &= -E + r_e i_e \end{aligned} \right\}, \quad (7.3)$$

while (6.2) hold without alteration.

Comparing (6.1) and (7.2) we see that, on the average,  $r_1 i_1, r_2 i_2, \dots$  will be reduced to a small fraction of their previous values by the introduction of the compensators so that the equations (6.2) will be much more nearly equivalent to (2.1) than they were before, and the errors in the roots will be much reduced.

From (7.2) we see that  $i_1, i_2, i_3$ , and therefore the errors in the roots, will be the same whether a compensator is used in connection with the excited transformer or not, but, from (6.3) and (7.3), that if a compensator is used  $i_e$  will be reduced from approximately  $i_{ms}$  to a value of the same order as  $i_1, i_2, i_3$ .

The automatic method of compensation mentioned above is described in § 12 and § 13, and a method of compensation, in which the correct adjustment is obtained by a series of trials, in § 14.

#### *Method of Least Squares.*

8. So far we have assumed that the number of equations is equal to the number of unknowns; we will now consider what results will be given when this condition is not satisfied. We will, as before, assume that there are three unknowns, but that there are  $n$  equations where  $n$  may be either less than or greater than 3.

If  $U$  is excited and all the transformers are provided with compensators (6.2), (7.2) and (7.3) become:—

$$a_s x + b_s y + c_s z + d_s u = r_s i_s \quad (s = 1, 2, \dots, n) \quad (8.1)$$

$$\left. \begin{aligned} a_1 i_1 + a_2 i_2 + \dots + a_n i_n &= h_x \\ b_1 i_1 + b_2 i_2 + \dots + b_n i_n &= h_y \\ c_1 i_1 + c_2 i_2 + \dots + c_n i_n &= h_z \end{aligned} \right\} \quad (8.2)$$

and

$$\left. \begin{aligned} d_1 i_1 + d_2 i_2 + \dots + d_n i_n + i_e &= h_u \\ u &= -E + r_e i_e \end{aligned} \right\} \quad (8.3)$$

We will consider first the case where the number of equations is greater than the number of unknowns.

We saw in § 7 that the residual magnetizing currents  $h_x, h_y, h_z, h_u$  are very small and we will therefore neglect them, considering later under what conditions this is justifiable.

Consider now the expression

$$S = \left[ \frac{1}{r} (ax + by + cz + du)^2 \right].^*$$

The conditions that  $S$  shall be a minimum when  $u$  is fixed and  $x, y, z$  vary are

$$\left[ \frac{a}{r} (ax + by + cz + du) \right] = 0, \text{ etc.}$$

or from (8.1):—

$$[ai] = 0, \quad [bi] = 0, \quad [ci] = 0.$$

These, however, since we are taking  $h_x, h_y, h_z, h_u$  to be zero, are the equations (8.2) satisfied by the equation currents.

Hence (8.1) and (8.2) show that the roots given by the machine will be such that

$$\left[ \frac{1}{r} (ax + by + cz + du)^2 \right],$$

$u$  being fixed, is a minimum.

That is  $X/U, Y/U, Z/U$  are the roots, as given by the method of least squares, of the equations of condition

$$a_s x + b_s y + c_s z + d_s u = 0 \quad (s = 1, 2, 3, \dots, n) \quad (8.4)$$

the weights,  $w_s$ , being such that  $w_s \propto 1/r_s$ .

We see therefore that the machine can be used to solve a set of equations of condition directly, the method of setting up the equations being the same as in the solution of ordinary simultaneous equations, except that it is now necessary to adjust the resistances of the equation circuits.

If we take the values of the weights to be fixed so that the average of the reciprocals is 1 we can put  $r_s = r_m/w_s$ , where  $r_m$  is the average resistance of all the equation circuits, and the results we have found above will hold whatever  $r_m$  may be; however, there are certain limits between which  $r_m$  should lie.

If  $v_1, v_2, \dots, v_n$  are the residuals of the equations of condition (8.4) we see from (8.1) that  $v_s = r_s i_s / u$  and hence that, as  $r_m$  is varied,  $i_s \propto 1/r_m$ ; since we are neglecting the residual magnetizing currents  $h_x, h_y, h_z, h_u$  in (8.2) it is essential that  $i_1, i_2, \dots, i_n$  should be large compared with them, so that  $r_m$  must

\*  $\left[ \frac{1}{r} (ax + by + cz + du)^2 \right]$  represents, as usual,  $\sum_{s=1}^n \left\{ \frac{1}{r_s} (a_s x + b_s y + c_s z + d_s u)^2 \right\}$ .



not be too large. On the other hand it can be shown that if  $i_1, i_2, \dots, i_n$  are large the effects of stray flux, which we have neglected may become important.

It appears therefore that the best value to choose for  $r_m$  will depend on the average value of the residuals, so that if the residuals are very small the resistances should be as small as possible, while if they are large it may be necessary to increase the resistances of the equation circuits to many times their normal values. However, a considerable latitude in the choice of  $r_m$  will be possible without causing a serious increase in the errors due to the machine.

9. The individual residuals, the sum of the weighted squares of the residuals and the quadratic mean errors to be feared in the roots can all be determined directly by means of the machine.

We have seen that the residuals are given by  $v_s = r_s i_s / u$ , and hence if  $e_s$  is the voltage drop in a resistance  $r_0$  forming part of an equation circuit,  $e_s = r_0 i_s = u (r_0 / r_m) w_s v_s$ , so that we can, by measuring  $e_s$ , find the value of  $w_s v_s$  for each equation. The measuring instrument would usually be adjusted so as to give  $U = 1$ , and  $r_0 / r_m$  could be chosen to be some simple ratio, say 1/10 or 1/100, so that the value of  $w_s v_s$  would, practically, be read off directly.

The sum of the weighted squares of the residuals, can be determined by measuring the drop in a known resistance due to the external current  $i_s$ , for since  $v_s = r_s i_s / u$ , we have  $[wv^2] = \frac{1}{u^2} [ur^2 i^2]$ , and if we multiply the three equations (8.2) and the first of (8.3) by  $x, y, z, u$ , respectively and add, we have, neglecting  $h_x, h_y, h_z, h_u$ :

$$[i(ax + by + cz + du)] + i_s u = 0,$$

that is, from (14.1)

$$[ri^2] = -i_s u,$$

and hence

$$\begin{aligned} [wv^2] &= \frac{1}{u^2} [ur^2 i^2] \\ &= \frac{r_m}{u^2} [ri^2], \text{ since } r_m = w_s r_s \\ &= -r_m i_s. \end{aligned}$$

If therefore the external current is passed through a known resistance  $r_0$  and the drop,  $e$ , in this resistance is measured,  $u$  being as before taken to be 1, we have

$$[wv^2] = -\frac{r_m}{r_0} e. \quad (9.1)$$

Now it can be shown\* that the sum of the weighted squares of the residuals,  $[wv^2]$  is equal to

$$\frac{\begin{vmatrix} [waa] & [wab] & [wac] & [wad] \\ [wba] & [wbb] & [wbc] & [wbd] \\ [wca] & [wcb] & [wcc] & [wcd] \\ [wda] & [wdb] & [wdc] & [wdd] \end{vmatrix}}{\begin{vmatrix} [waa] & [wab] & [wac] \\ [wba] & [wbb] & [wbc] \\ [wca] & [wcb] & [wcc] \end{vmatrix}}, \quad (9.2)$$

and that, if  $\epsilon_x$  is the quadratic mean error to be feared in the determination of  $x$

$$\frac{[wv^2]}{(n-3)\epsilon_x^2} = \frac{\begin{vmatrix} [waa] & [wab] & [wac] \\ [wba] & [wbb] & [wbc] \\ [wca] & [wcb] & [wcc] \end{vmatrix}}{\begin{vmatrix} [wbb] & [wbc] \\ [wbc] & [wcc] \end{vmatrix}}. \quad (9.3)$$

Comparing (9.2) and (9.3) we see that the latter represents the value of  $[wv^2]$  corresponding to a set of equations obtained from the actual equations (8.4) by omitting the constant terms,  $d_s$ , and treating  $x$  as being unity, i.e., to the equations

$$b_s y + c_s z + a_s = 0 \quad (s = 1, 2, \dots, n). \quad (9.4)$$

If therefore, we have the original equations set up on the machine we can determine the new  $[wv^2]$  by reducing the coefficients of  $U$  to zero, transferring the excitation to the transformer  $X$  and measuring  $[wv^2]$  by the method already explained, (9.1).

Calling this quantity  $[wv^2]_x$  we have

$$\epsilon_x^2 = \frac{1}{n-3} \frac{[wv^2]}{[wv^2]_x}.$$

To determine  $\epsilon_y^2$ ,  $\epsilon_z^2$  we merely have to transfer the excitation to  $Y$  and  $Z$  in turn and make the corresponding measurement in each case.

As the resistances of the equation circuits will be altered when the  $U$ -coefficients are cut out it will be necessary to re-adjust them to their original values.

It can be shown that the errors in the roots—that is, the errors due to the

\* Whittaker and Robinson "The Calculus of Observations." pp. 246, 247.

machine—will tend to be large when the normal equations are ill-conditioned, further, since it is necessary for the transformer corresponding to the constant member to be excited, large errors may be introduced if any of the roots are much greater than 1. For ordinary simultaneous equations, as in § 3, errors due to this latter cause can be minimized by exciting the transformer corresponding to the largest root, but for equations of condition this is not possible.

When the roots of a set of equations of condition have been found the corresponding residuals can be found, more accurately than by the method described above, by that described at the end of § 4. The residuals found thus may be used to enable a second approximation to the roots to be obtained.

When the number of equations of condition exceeds the number of coefficient coils available on a transformer two transformers can be used for any unknown. For instance if  $x$  occurs in 20 equations and there are only 11 coefficient coils on a transformer two transformers are assigned to  $x$ ,  $-X$  and  $X'$ , say, and 10 coefficients are set up on each. The eleventh coefficient coil on each is then set to its maximum and the two are connected to form a circuit corresponding to the equation  $x - x' = 0$ .

As the roots will not satisfy any of the equations exactly,  $x$  will not be exactly equal to  $x'$ ; however, as the resistance of this circuit can be made very low, so that the weight of the corresponding equation will be very large compared to the weights of the original equations, it is not likely that any serious error will be introduced. If necessary means could be provided to reduce any difference that there might be between  $x$  and  $x'$ .

10. When the number of equations is less than the number of unknowns (8.1), (8.2) and (8.3) all hold, but in considering these equations we cannot neglect  $h_x$ ,  $h_y$ ,  $h_z$ , even though they are very small, as it is now the ratios of these quantities to one another rather than their actual magnitudes that affect the values of  $x$ ,  $y$ ,  $z$ . As there is no simple relation between the voltages  $x$ ,  $y$ ,  $z$  and the corresponding residual magnetizing currents  $h_x$ ,  $h_y$ ,  $h_z$ —the relation, in fact, may vary greatly from one transformer to another—it is impossible to determine what results will be given: it is sometimes found that no steady condition is attained but that the voltages continually change.

These conditions also exist when the number of equations is equal to the number of unknowns but the equations are not independent—the state that is approached when the equations are very ill-conditioned.

*Methods of Measurement.*

11. In the ideal machine considered in § 2 the values of  $x, y, z, u$  satisfy the equations (2.1) at every instant, so that the wave forms of all of them will be the same. We might therefore measure these voltages in any one of various ways. We might, for instance measure the r.m.s. values, or the rectified values, or the components in phase with some specified voltage. The first two of these methods do not give the signs directly and the non-uniformity of the scales would be inconvenient, with the last method, however, the sign is given by the sense of the deflection and the deflection is nearly proportional to the voltage; further, certain errors, due to the imperfections of the machine, are eliminated if this method is used. For these reasons the last method is used.

Two methods of measurement, which can be used simultaneously, are provided; in the first results are given directly by the deflection of the instrument and can be determined to within about  $\pm 1$  per cent., and in the second a null method is used, the balance being obtained by adjusting switches similar to those used for the coefficient coils and the results being given to four figures.

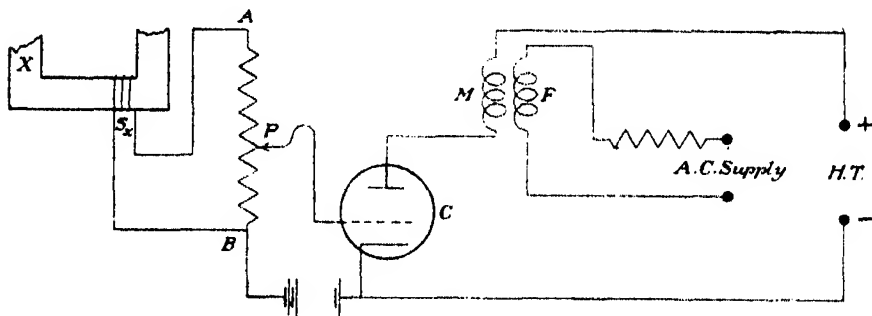


FIG. 5.—Arrangement of direct reading measuring instrument.

Fig. 5 shows an arrangement for direct measurement. Here  $M$  and  $F$  are the moving and fixed coils of a wattmeter, the latter being connected through a high resistance to the external voltage so that the flux due to the current in them is nearly in phase with the external voltage.  $AB$  is a potential divider of at least  $1\text{ M}\Omega$  arranged so that any required proportion,  $PB$ , of the voltage  $AB$  can be applied to the grid of a valve  $C$ . The current in  $M$ , which is in the anode circuit, will then be proportional to and nearly in phase with the voltage  $AB$ , and the deflection will be proportional to the component of  $AB$  that is in phase with the flux due to  $F$ .

To find the values of  $X/U, Y/U, Z/U$ , which are equal to the roots  $x, y, z$  of

the equations (2.2),  $AB$  is first connected by means of a selector switch to the search coil  $S_u$  and  $P$  is adjusted so that the deflection of the wattmeter is 1;  $AB$  is then connected in succession to  $S_x$ ,  $S_y$ ,  $S_z$ , and the corresponding deflections are equal to the roots.

The voltage in any other circuit, such as the open equation circuit (2.3) is measured in a similar way.

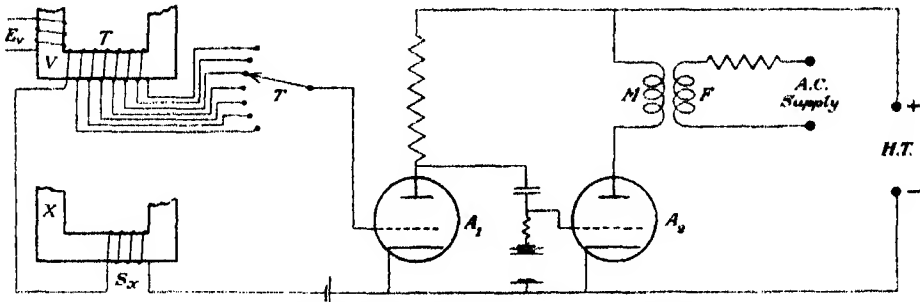


FIG. 6.—Arrangement of zero indicating instrument.

Fig. 6 shows an arrangement for obtaining accurate values. Here  $V$  is the measuring transformer, on which is wound an adjustable coil  $T$ , the ratio of the turns in circuit to those in a unit coil being denoted by  $T$ .

The exciting coil,  $E_v$ , of this transformer may be connected either to the supply transformer, in parallel with the exciting coil of the excited main transformer  $X$ , say, so that  $v = x$ , or to  $U$ , the transformer corresponding to the constant member, so that  $v = u$ .

An amplifier,  $A_1, A_2$ , and a wattmeter,  $M, F$ , are arranged as above, except that in this case a two-stage amplifier will usually be required.

The coil  $T$  is connected, by means of a selector switch, in opposition to  $S_u$  and the resultant voltage,  $Tv - x$ , is applied to the grid of the first valve, so that a current proportional to and nearly in phase with  $Tv - x$  flows in the moving coil  $M$  of the wattmeter.

$T$  is then adjusted, by means of a set of switches similar to those used in connection with the coefficient coils, until the deflection of the wattmeter is zero, so that the mean value of  $Tv - x$  is zero; in the ideal case  $x/v$  is constant, so that  $Tv - x = 0$  at every instant and  $T = x/v$ .

If the measuring transformer is excited so that  $v = x$  the values of  $T$  corresponding to the voltages in  $S_x, S_y, S_z, S_u$  will be 1,  $y/x, z/x, u/x$ , and the roots  $x, y, z$  will be the ratios of the first three to the last, but if it is excited so that  $v = u$  the values of  $T$  will give the roots directly.

It can easily be shown that any phase displacement or distortion due to the amplifier will not affect the result, provided, as we have seen happens in the ideal machine, the voltages are all in phase with one another.

When the effects of resistance, etc., are taken into account the voltages are not all in phase with one another and their wave forms will not all be the same. However, it can be shown that the errors introduced by the measuring instrument will be no larger than those already existing in the voltages to be measured.

The results given by the null method will not be affected by variations in the voltage of the mains, but results given by the direct reading method described above will be affected by variations taking place while series of readings is being taken.

### Compensation.

12. Fig. 7 shows diagrammatically the arrangement of a compensator.  $X$  represents one of the main transformers as in fig. 1,  $E_x$ ,  $a_1$ ,  $a_2$ , ... are the exciting and coefficient coils, while  $F$  and  $S'$  are additional coils for use in connection with the compensator.

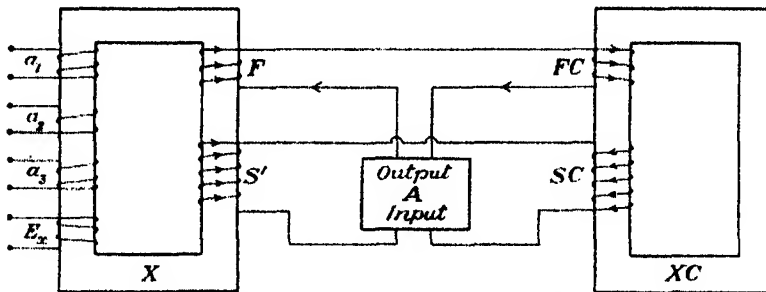


FIG. 7.—The principle of the compensator.

As explained in § 7 the object of the compensator is to force a current  $i_c$  to flow in a unit coil,  $F$ , called the *compensating coil*,  $i_c$  being equal to  $i_m$ , the magnetizing current, so that the total ampere-turns due to  $E_x$ ,  $a_1$ ,  $a_2$ , ... must be zero. For instance, if, when there is no compensator and the coils  $a_1$ ,  $a_2$ , ..., are open, so that no current flows in them, a voltage  $x$  from an external source is applied to  $E_x$ , a current  $i_m$ , the magnetizing current corresponding to  $x$ , will flow in  $E_x$ ; if now the compensator, assumed to be perfect, is put into operation the current in  $E_x$  is to be reduced to zero by forcing a current  $i_m$  to flow in  $F$ .

In fig. 7  $A$  is an amplifier and  $XC$  a transformer, the compensating transformer, which has the same dimensions as and is made of similar material

to  $X$ , so that when the fluxes are the same in both the magnetizing currents are the same.

The coils  $F$  on  $X$ , and  $FC$  on  $XC$  are unit coils in series with one another and with the output circuit of the amplifier  $A$ .  $S'$  and  $SC$  are equal search coils opposing one another and connected between the grid and cathode of the valve.

If current is flowing in some or all of  $E_x, a_1, a_2, \dots$ , there will be a flux in  $X$  and a voltage will be induced in  $S'$ , this will produce a larger voltage in the output circuit  $F, FC$  and a flux will be induced in  $XC$ ; a voltage will then be induced in  $SC$ , opposing that in  $S'$ , so that the grid voltage, and therefore the output voltage and the current in  $F, FC$  will depend on the difference between the fluxes in  $X, XC$ . If the amplification is large the difference between the voltages in  $S'$  and  $SC$  will be small compared with that in  $F$ , i.e., with that in  $S'$ , so that the fluxes in  $X$  and  $XC$  will be nearly equal. The current  $i_c$  flowing in  $F, FC$ , is the magnetizing current corresponding to the flux in  $XC$ , so that it must be nearly equal to  $i_m$ , the magnetizing current corresponding to the flux in  $X$ . That is, the object of the compensator is nearly attained.

$XC$  need not be of the same size as  $X$ , provided the relative numbers of turns in the various coils are correctly adjusted; if  $XC$  is made smaller than  $X$  there is a saving in weight, and in the amount of power that has to be supplied by the amplifier.

13. We will now consider in greater detail the operation of the compensator.

There are several possible arrangements of the amplifier but, whatever arrangement is adopted, it is essential that there shall be no direct current in the windings of the main or the compensating transformer, as any such current would greatly reduce the effective permeability of the cores; this is most easily effected by using an output transformer in the anode circuit.

One possible arrangement is shown in fig. 8: here  $X$  and  $XC$  are, as before, the  $X$ -transformer and its compensating transformer, while  $XO$  is the output transformer of the amplifier. The instantaneous values of the currents and potentials at various points are indicated in the figure,  $v_a, v_g$  denoting the changes of the anode and grid potentials from their steady values. The filament circuit of the valve is not shown; a valve with an indirectly heated cathode would normally be used.

$B$  is a unit coil representing one or more coils (such as  $E_x, a_1, a_2, \dots$ , in fig. 7) connected to the external source or to other parts of the machine, so that if

$i_b$  is the current in this coil it is the object of the compensator to reduce  $i_b$  to zero under all circumstances.

$T$ ,  $t$ , etc., refer to the various coils on the transformers,  $R_0$  is the resistance of the coil  $t_0$ ,  $R$  is an adjustable resistance and  $R + R_1$  is the resistance of the whole circuit  $RTT_0T_0$ . The impedance and amplification factor of the valve are  $S$  and  $\mu$  respectively.

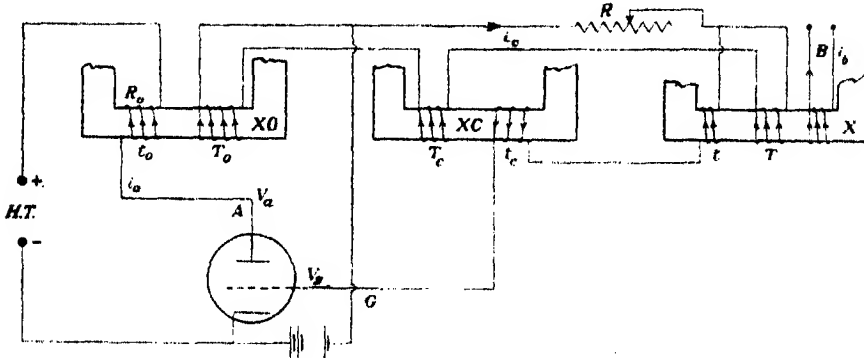


FIG. 8.—Detailed arrangement of compensator.

By considering the circuits  $t_0A$ ,  $t_0G$  and  $TT_0T_0$  we obtain the equations:—

$$\begin{aligned} v_a &= t_0x_0 - R_0i_a \\ v_g &= tx - t_0x_0 - Ri_c \\ 0 &= Tx + T_0x_0 + T_0x_0 - (R + R_1)i_c. \end{aligned}$$

If  $i_{m0}$  is the magnetizing current, in a unit coil, of  $XO$  we have

$$i_{m0} = t_0i_a + T_0i_c.$$

and lastly,  $v_a$ ,  $v_g$  and  $i_a$  are connected by the equation

$$v_a + \mu v_g = Si_a.$$

Eliminating  $i_a$ ,  $v_a$ ,  $v_g$  and  $x_0$  from these equations we obtain the relation

$$x = \frac{\mu t_0 + \rho T_0}{\mu t - \rho T} \cdot x_0 - \frac{1}{\mu t - \rho T} \left\{ \left( \rho R_1 + \frac{S'}{\rho} - (\mu - \rho) R \right) i_c - \frac{S'}{t_0} i_{m0} \right\} \quad (13.1)$$

where  $S' = S + R_0$  and  $\rho = t_0/T_0$ .

For convenience we will put  $i_{m0} = -mi$  and will write the above equation in the form

$$x = \lambda x_0 - \beta i_c. \quad (13.2)$$



We will suppose that the plates of which the cores of  $X$  and  $XC$  are built are of similar material and of the same shape, the linear dimensions of the  $XC$  plates being  $a$  times those of the  $X$  plates, that all the plates are of the same thickness and that the total thickness of the core of  $XC$  is  $b$  times that of  $X$ .

Under these conditions, when the flux density is the same in both cores, the loss per unit volume and the permeability will be the same in both, the total flux in  $XC$  will be  $ab$  times that in  $X$  and the ampere-turns on  $XC$  will be  $a$  times those on  $X$ .

If this compensator is to operate correctly the flux densities in the two cores must always be equal and must correspond to the current  $i_0$ , hence we must make  $T_0 = aT$ , and  $x_0$  must be equal to  $abx$ . If we assume that  $\beta i_0$  may be neglected in comparison with  $x_0$  the latter condition will be satisfied if we make  $\lambda = 1/ab$ .

Putting  $\lambda = 1/ab$  we find that

$$t_0 = \frac{1}{ab} \cdot t - \frac{\rho Ta}{\mu} \left( 1 + \frac{1}{a^2 b} \right). \quad (13.3)$$

If  $\mu$  is assumed to be constant this gives a definite value for  $t_0$ .

Hence, if  $t_0$  has this value and  $T_0 = aT$  the compensator will ensure that  $x_0 = abx$ ; for the reasons given above the total ampere-turns on  $XC$  will be  $a$  times those on  $X$  so that  $T_0 i_0 = a(T i_0 + i_0)$ , and therefore  $i_0$  is zero and the object of the compensator is attained.

In § 12 it was assumed that the two cores were the same size, i.e., that  $ab = 1$ , and that  $t_0 = t$ ; this is the value of  $t_0$  given by (13.3) when  $\mu$  is infinite, but from (13.3) we also see that, if  $\beta i_0$  is negligible, the same results can be obtained when the value of  $\mu$  is finite by slightly reducing  $t_0$ .

So far we have neglected the term  $\beta i_0$ , however this will not necessarily be very small so that we must take it into consideration. From (13.1) and (13.2) we have

$$\beta i_0 = \frac{1}{\mu t - \rho T} \left\{ \left( \rho R_1 + \frac{S'}{\rho} - (\mu - \rho) R + \frac{m S'}{t_0} \right) \right\} i_0.$$

Hence, if we make

$$R = \frac{1}{\mu - \rho} \left\{ \rho R_1 + \frac{S'}{\rho} + \frac{m S'}{t_0} \right\}, \quad (13.4)$$

$i_0$  will be reduced to zero.

As neither  $S'$ ,  $m$  nor  $\mu$  is exactly constant this does not give quite a definite value for  $R$ ; however, we shall see that the maximum possible value of  $R$  is fixed by other considerations.

If certain simplifying assumptions are made, of which the most important are that  $\beta$  is constant and that the instantaneous value of the flux is proportional to that of the magnetizing current, it can be shown that, if each transformer in the machine is provided with a compensator, the system will be unstable if  $\beta$  is negative, and that, if  $\beta$  is positive but  $t_0$  less than the value given by (13.3), the system may become unstable if the equations are very ill-conditioned. Of the above assumptions the former is probably fairly correct, but the latter, which is equivalent to neglecting hysteresis effects and to assuming that the permeability is constant, is, of course, far from being correct; however the results so found suggest the conditions under which instability may be expected, and both results have been roughly verified experimentally.

It is found that there is a value of  $R$  for which the system is stable and the residual magnetizing current,  $h = i_m - i_n$ , is small for all values of  $X$  up to the normal maximum, the in-phase component,  $H_p$ , varying between  $\pm 0.015 I_{mp(max.)}$  and the quadrature component between  $\pm 0.06 I_{mq(max.)}$ .

It should be noticed that (13.1) refers to the instantaneous values of the currents and voltages, so that the harmonics of  $i_m$  (of which the third may be 30 per cent. of the fundamental even when  $x$  is sinusoidal) will be reduced in the same proportion as the fundamental.

Typical curves showing the relation between the fundamentals of  $h_p$ ,  $h_q$ , and that of  $x$  are shown in fig. 4.

14. As an alternative to the method of automatic compensation described in § 12 and § 13 a method which does not require any valves or extra transformers may be used: the results obtained, however, are less accurate and, as several trials usually have to be made, the time taken to obtain the final solution is considerably longer.

In this method compensation is effected by forming an exciting circuit consisting of one coefficient coil (the eleventh coil mentioned in § 3) on each transformer, all connected in series, and passing a definite current through this circuit. The number of turns in each coil is so adjusted that the resultant ampere-turns correspond to the voltage per unit coil that is expected in the corresponding transformer, the relation between voltage and turns being given by a table based on the known relation between magnetizing current and voltage.

For the first trial any values may be taken for the expected voltages—usually one would be taken as  $X_{(max.)}$  and the others as zero; the roots, that is the voltages of the transformers, are then determined in the usual way, the turns

in the coils forming the exciting circuit are adjusted so as to correspond to these voltages and a new set of roots is found. As the first set of roots will be roughly correct the ampere-turns on each transformer, due to the exciting current, will now correspond roughly to the magnetizing current so that the equation currents will be comparatively small and the new set of roots will be more nearly correct than the previous set. The turns in the coils of the exciting circuit are now readjusted and the process is repeated until the fact that consecutive sets of roots are equal shows that no better results can be obtained.

*Note on Stray Flux and Capacity Effects.*

15. We have throughout assumed that the flux through every turn on a transformer is the same: actually this cannot be exactly true however the currents may be distributed in the windings.

When current is flowing in the compensating coil only a certain stray field is produced, and when currents are also flowing in the coefficient coils there will be an additional stray field; the latter will induce e.m.f.'s in the coefficient coils, but it is found that these e.m.f.'s will be only a small fraction of the resistance drops. Except when the machine is being used for the solution of equations of condition the resistance drops in the coefficient coils are the direct cause of the errors in the results, so that the latter stray field will merely cause small changes in existing errors and may therefore be neglected. We need therefore consider only the stray field due to the magnetizing current flowing in the compensating coil. It is found that the effect of this field is to induce in a coefficient coil an e.m.f. which is never greater than  $2 \times 10^{-5} X_{(\max.)}$ , where  $X_{(\max.)}$  is the standard maximum value of  $X$ .

When this is taken into account each equation of (6.2) will have to be modified by the addition of a term not greater than (and, on the average, considerably smaller than)  $2(n+1) \times 10^{-5}$ ,  $n$  being the number of unknowns in the original equations.

When compensators are not used the effect of the whole stray field is much less than that of the resistance drops.

With a set of equations of condition it can be shown that the effect of stray flux is much the same as above, except that, owing to the fact that large in-phase currents are flowing in the coefficient coils, considerable errors may be introduced unless the measuring instrument is accurately adjusted so as to ignore the quadrature components of the e.m.f.'s, whereas with an ordinary

set of equations a considerable change of phase would not cause any appreciable errors.

Errors somewhat smaller than those due to the stray field of a transformer may be caused by the stray fields of neighbouring transformers.

16. We have throughout ignored the effects of any currents that there may be due to capacity between the various coils on the transformers. Such currents would cause resistance drops in the coils, but, as the currents and consequent drops would be approximately in quadrature with the supply voltage, they would not affect the accuracy of the results unless they were very large. These currents have been observed, but they appear to be too small to cause any appreciable errors.

---

*Phase Boundary Potentials of Adsorbed Films on Metals.—Part I.—  
On the Behaviour of Oxygen on Gold.*

By HAROLD KENNETH WHALLEY and ERIC KEIGHTLEY RIDEAL, F.R.S.

(Received February 2, 1933.)

Whilst changes in interfacial potential differences owing to surface absorption can be measured both by thermionic and by photoelectric methods, these are not generally applicable to systems containing gases at relatively high pressures. That changes in metal gas potential differences occur when adsorption or surface reaction occurs was first demonstrated by Volta in measurements of contact potentials by a condenser method. His principle, with various modifications, has been employed by numerous subsequent workers, notably Fabroni,\* De la Rive,† Pellat‡, Hughes,§ Henning,|| and especially Dubois.¶ Ionization of the gap between two surfaces by means of the emission from radioactive materials was first employed by McLennan and Burton,\*\* and by Lord Blythswood and Allen,†† but their results are discordant, the cause indubitably lying, as Greimacher‡‡ pointed out, in their use of radium salts. Reliable measurements of interfacial potential differences at liquid-gas interfaces were obtained by Guyot,§§ Frumkin,||| Rideal and Schulman,¶¶ when the relatively short range  $\alpha$ -particles emitted by polonium were used as the source of ionization. This method has been extended to the examination of metal surfaces by Andauer and by Joffé and Lukirsky.\*\*\*

On examination of the results obtained either by the various modifications of Volta's method, or by that of Guyot for changes in the metal-gas potential differences as a result of oxidation of the surface, one is impressed by the smallness of the changes recorded. Andauer observed changes in the order of 0.1 volts when metal surfaces are reduced and oxidized, whilst the more recent publications of Dubois include the following values :—

\* 'J. Phys. de l'abbé Rozier,' vol. 49, p. 348 (1799).

† "Traité d'Electricité," vol. 2, p. 776.

‡ 'Ann. Chim. Phys.,' vol. 193 (1881).

§ 'Phil. Mag.,' vol. 28, p. 337 (1914).

|| 'Phys. Rev.,' vol. 4, p. 228 (1914).

¶ 'Ann. Physique,' vol. 14, p. 627 (1930).

\*\* 'Phil. Mag.,' vol. 6, p. 343 (1903).

†† 'Phil. Mag.,' vol. 6, p. 751 (1903).

‡‡ 'Ann. Physique,' vol. 16, p. 708 (1906).

§§ 'Ann. Physique,' vol. 2, p. 516 (1924).

||| 'Z. phys. Chem.,' vol. 115, p. 485 (1925).

¶¶ 'Proc. Roy. Soc.,' A, vol. 130, p. 259 (1931).

\*\*\* 'J. Phys. Radium,' vol. 1, p. 405 (1930).

Metal.	Treatment.	P.D. change
Pt .....	O <sub>2</sub> cold	volts.
	O <sub>2</sub> heated	0.04
		0.54 decaying to 0.30 in 33 minutes.
Au .....	O <sub>2</sub> cold	0.14
	O <sub>2</sub> heated	0.32 decaying to 0.30 in 15 minutes.

These changes on oxidation should be comparable to those obtained by thermionic means. We may note that for the surface of nickel, conversion to nickel oxide effects a rise of 1.42 volts in the thermionic work function. It seems probable that the low values recorded by the investigations employing the method of surface potentials are caused by a lack of appreciation of the extreme tenacity with which oxygen is held even by platinum and gold. Langmuir\* indeed records the observation that oxygen cannot be removed from platinum at 360° C. in the best vacuum obtainable. Furthermore, since the method of surface potentials involves the presence of a gas, and since measurements are usually made at relatively low temperatures, unless complete removal of the oxygen from both the gas and the containing vessel is effected, irreversible adsorption will proceed relatively quickly.

By the method of surface potentials an attempt has been made to evaluate the difference in contact potential between gold and oxidized gold.

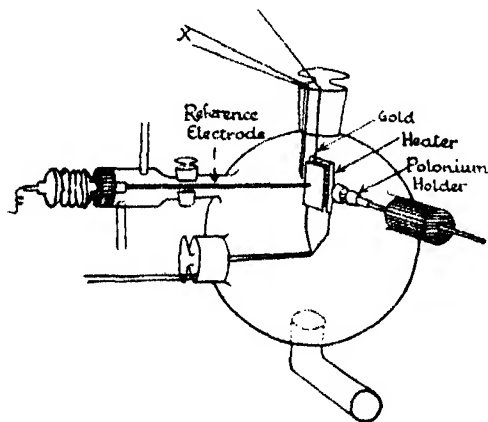


FIG. 1.

#### Gold and Oxygen.

*Apparatus.*—In fig. 1 is a diagram of the apparatus constructed for measuring alterations in the interfacial potential differences over the gold surface. The

\* 'J. Amer. Chem. Soc.,' vol. 40, p. 1390 (1918).

gold itself was suspended within a Pyrex bulb, and could be heated by the furnace which when not in use was rotated into a position well outside the ionized gas zone around the gold foil.

The platinum-platiniridium thermocouple (X) enabled the temperature to be measured, which, though not necessarily the temperature of the gold served the double purpose of indicating the approximate extent of heating, and allowing the adjustment of the heating filament current to such a value that the gold in successive experiments was treated in the same manner. The polonium deposited on a nickel disc was shielded from direct radiation by a brass sheath, and the conduction of heat along this sheath to the polonium was greatly restricted by employing only thin strip connections. The reference electrode was introduced through a wide bored tap, and was insulated therefrom by quartz attached to the electrode. The bulb could be evacuated by a mercury vapour pump backed by a Hyvac oil pump, the order of the pressure so attained being indicated by the appearance of a discharge tube. Before evacuation of the bulb, the electrode was withdrawn into the sidearm, a stout rubber sheath allowing this movement to be made without opening the apparatus to the air.

Cleaning of the gold was attempted by preliminary evacuation, followed by the admission of pure ethyl alcohol vapour at a pressure of about 3 cm. In this vapour the gold was heated to approximately 250° C. to burn off the oxygen and evacuation restarted, the heating being continued until a hard vacuum was obtained. Purified nitrogen was then admitted and necessary measurements taken.

The ethyl alcohol employed for the reduction of the oxidized gold was previously purified by repeated distillation from freshly prepared lime, and finally from aluminium-mercury couple. The purification of cylinder nitrogen consisted in forcing the gas through a porous pot immersed at the foot of a column of alkaline sodium hydrosulphite about 60 cm. long; this ensured the formation of bubbles less than 1 mm. in diameter. The reagent employed is superior to pyrogallol in that it introduces no difficultly removable impurities—like carbon monoxide—whilst its speed of removal of oxygen is of the same order. This portion of the purification train was so designed that fresh hydrosulphite solution could be introduced without interfering with its action or allowing leakage of air into the gas stream. The nitrogen then passed over 50 cm. red hot reduced copper, and was stored over water. From the reservoir the gas passed over calcium chloride, 150 cm. hot copper, through concentrated soda solution, over 40 cm. solid soda, 80 cm. phosphorus pent-

oxide, filtered through 40 cm. glass wool, through 20 cm. sodium vapour at 400° C. (with a vapour pressure at this temperature of 0.3 cm. Hg) and finally through a liquid air trap.

The bulb containing the gold was supported upon ebonite pillars, and the whole was enclosed within an earthed cage. On a support inside the cage was placed a Lindemann electrometer, the shadow of the needle cast by the aid of a small lamp and mirror system being observed on an etched glass scale within a periscope. The gold was one electrode, the reference electrode being a calomel half element, the tip of which was closed by a gel made up of agar-agar in 0.1 N KCl, the concentration being the same as that used in the calomel half element. Adequate insulation of this reference electrode from the bulb was effected by an amber plug in the side arm of the bulb. Wires from the reference electrode and the Lindemann electrometer needle were brought to a mercury cup supported by quartz, and by a small electromagnet operating an earthed copper rod, connection between the electrometer needle and either the reference electrode or the earth could be established. The gold plate was connected through to earth by way of a potentiometer box, which enabled measurable potentials to be applied exactly to balance the algebraic sum of the interfacial potential differences, the electrometer being used as a null instrument.

The ionization of the gas between the two electrodes should be great to ensure a steady current. This condition was satisfied over a range of about 1 cm., the separation normally being 2 to 3 mm.

### *Experimental.*

If the reference electrode and its intrinsic interfacial potential difference remains unchanged during a particular series of experiments, then any difference of potential applied to the plate by means of the potentiometer box in order to maintain the unearthed electrometer needle at zero charge is equal and opposite to the change in potential of the metal-gas interface.

Preliminary experiments revealed the rapidity on admission of the nitrogen of the adsorption of traces of oxygen present in the nitrogen which has passed through all the purification train except the sodium vapour column.

That these elevations of the gas-gold potential difference were not caused by an alteration in the nature of the metal itself after heating was demonstrated by leaving the heated gold *in vacuo* (overnight), and admitting nitrogen on the following day; the usual rise from a low value (—690 mv.) to a steady



value ( $-410$  mv.) was observed. Nor is the rise due to contamination of the reduced gold surface by moisture or any other impurity from the reference electrode, for replacement of the calomel half-element by an outgassed carbon electrode did not alter the trend of the potential difference changes. Further proof of this effect was demonstrated with an earlier apparatus in which the purification of the gas was less rigorous, by heating the gold in hydrogen; partial reduction of the surface occurred, as the following records illustrate:—

In nitrogen.	In hydrogen.	
	Before heating.	After heating.
mv. 72 185	mv. 42 154	mv. —50 —114

Later experiments using nitrogen purified by the complete train as described in the previous section still showed this initial rise of potential difference owing to traces of oxygen, which must be of the order of one part in tens of millions, the final value being naturally dependent on the uncontrollable amount of oxygen admitted to the gold. The lowest value obtained of the surface potential of reduced gold was  $-1110$  mv. Incidentally, during the admission of nitrogen this adsorption was followed by using the polonium holder as temporary reference electrode. Readings from such a system are approximate at best, disturbing factors being the unfavourable relative positions of the gold and the polonium holder, the disturbance of the ionized zone by turbulence caused by admitting the gas, and the long range of the  $\alpha$ -particles at low pressures. Nevertheless, a rising of the potential difference throughout the period of admission was clearly marked, proving that the continued later effect was due to traces of oxygen.

The surface potential of gold cleaned with chromic acid, washed with distilled water, pure alcohol, and redistilled petrol ether, and subsequently heated gently and allowed to cool was  $+450$  mv., this value remaining constant over an hour. Hence, a minimum value of the potential difference between clean and oxidized gold is  $1.56$  volts, a value comparable with those obtained from measurements of the thermionic work function.

The method thus appears to be capable of providing information on the effects of adsorbed films, though it was found impossible to retain gold in the reduced state at ordinary temperatures in an atmosphere of nitrogen for any

period of time, in spite of the most rigorous precautions against contamination by oxygen. This difficulty finds its parallels in previous attempts of a similar nature, and particularly in the observation of Roberts\* that the rate of contamination of a tungsten surface in helium purified by a circulation process was such that the accommodation coefficient increased from 0.025 to 0.11 within half-an-hour of admission of the gas to the metal. We have found, however, that with due precautions gold, platinum and copper surfaces can be obtained in reproducible stable states (as typified by their surface potentials) in the presence of air and that such surfaces act as invariant substrates for certain supra-depositions. An account of the use of the observation to investigate adsorption and evaporation of surface films is given below.

---

*Phase Boundary Potentials of Adsorbed Films on Metals.—Part II.—  
On the Behaviour of Iodine on Platinum.*

By LEWIS JACOBS and HAROLD KENNETH WHALLEY.

(Communicated by E. K. Rideal, F.R.S.—Received February 2, 1933.)

We have noted that both gold and platinum on exposure to air are immediately covered with a film of chemi-adsorbed oxygen. On treatment of a platinum surface with an oxidizing agent such as hot chromic acid or on heating in air to a high temperature, and subsequent rapid washing with distilled water, ethyl alcohol and petrol ether, the platinum is found to have acquired a high air-metal potential difference, the magnitude of which is dependent on the mode and intensity of the oxidation. Furthermore, these high values are found to be transitory in character and decay with time. The rate of decay is found to be accurately exponential in character, and a few of the unimolecular velocity constants derived from the equation

$$\frac{d(\Delta V)}{dt} = -k\Delta V \quad \text{or} \quad k = \frac{1}{t} \log \frac{\Delta V_t}{\Delta V_0}$$

are given in Table I.

Table I.—Temperature ca. 15° C.

Experiment No. ....	1	2	3	4	5	6	7
$K \times 10^{-4}$ .....	5.98	11.67	5.85	8.05	6.12	1.00	3.45

\* 'Proc. Roy. Soc.' A, vol. 135, p. 192 (1932).

It appears probable that we are dealing with the slow unimolecular decay of an unstable oxide of platinum. Indeed with strong oxidizing agents the initial rate of change in phase boundary potential is relatively rapid and the complete curve can be separated into two exponential curves suggesting the existence of another but very unstable higher oxide of platinum. The values of  $k$  are, however, quite irreproducible, as shown by Table I, and the complete study of this decay and the determination of a heat or heats of activation, as for iodine on platinum, was not undertaken.

It was sufficient for our present purpose to know, from the unimolecular character of the curves, that the oxide slowly decomposes leaving the surface of platinum supporting only a very stable chemi-adsorbed film of oxygen, the surface potential correspondingly falling to values between 0 and 200 mv. against a reference electrode of platinum carrying a deposit of polonium of 400 to 600 mv. against a similarly coated reference electrode of copper. The results quoted by Dubois (*loc. cit.*) are comparable both in form and magnitude with our observations, but the implication of Dubois that after the completion of the decay the platinum surface is free from oxygen does not appear to be warranted. The surface in this condition was found to serve as a nearly invariant substrate upon which films of iodine could be deposited and their rate of evaporation followed. This substrate probably consists of two layers; a chemi-adsorbed layer of oxygen adhering most tenaciously to the surface as observed with a gold surface (Part I) and a layer more readily removable held by the operation of Van der Waals forces, the evidence for this latter layer being given below.

#### *Evaporation of Iodine.*

The platinum electrode consisted of a square piece of foil 6 sq. cm. in area which rested during the experiments on a glass plate on a glass tripod fixed in a wax block inside the Faraday cage, the polonium holder being about 3 mm. from the foil.

When the platinum plate was flooded with 0.1 to 0.2 c.c. of a solution of iodine in redistilled petrol ether containing  $8.66 \times 10^{-4}$  gm./c.c.—about 25 to 50 times the amount necessary for a monolayer on the assumption that the specific surface of the foil is unity—a sudden rise of potential of the order of 300 mv. is observed, this is followed after a short interval by an accurately exponential fall of the air metal potential difference until within some 5 per cent. of completion. As the simplest explanation we may suggest that the adsorbed iodine exalts the potential difference, and that the subsequent

evaporation of the iodine obeys the unimolecular law,\* until over 90 per cent. has been evaporated.

The curves in figs. 1 (a) and 1 (b) are typical of the results obtained.

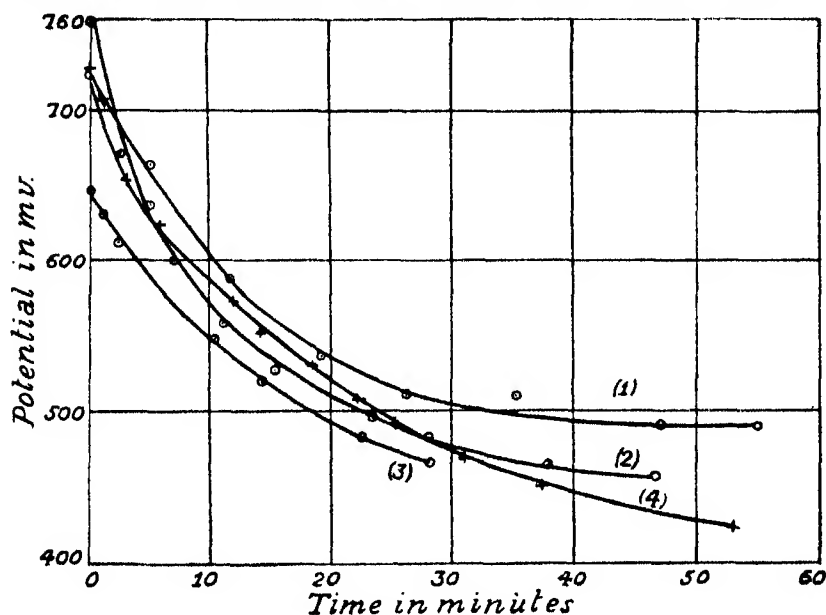


FIG. 1 (a).—Evaporation of iodine at 298.67° K. V against T.

Curve.....	1	2	3	4
Zero .....	490	442	419	399

The evaluation of the exponential constant

$$\left( k = \frac{1}{t} \log \frac{\Delta V_t}{\Delta V_0} = \frac{1}{t} \log \frac{V_t - Z}{V_0 - Z} \right)$$

involves the estimation of a zero value Z from the form of the surface potential-time curves. In most experiments this was calculated from the mean of a series of points at constant time intervals inserted in the equation :

$$kt = \log \frac{V_t - Z}{V_0 - Z} = \log \frac{V'_t - Z}{V'_0 - Z}$$

i.e.,

$$\frac{V_t - Z}{V_0 - Z} = \frac{V'_t - Z}{V'_0 - Z} = \frac{V_t - V'_t}{V_0 - V'_0}.$$

\* Petrol ether alone caused small fluctuations of the p.d., but values were rapidly restored to normality. The petrol ether and excess iodine of the iodine solution caused slight irregularities only in the initial part of the exponential, this part not being shown in the curves in fig. 1.

In other experiments where the exponential was followed nearly to its end the zero was estimated by extrapolation. Table II shows the fairly close agreement between the estimated zeros after the evaporation of the iodine, and the initial surface potentials before addition of the iodine, demonstrating the nearly invariable nature of the substrate during an experiment.

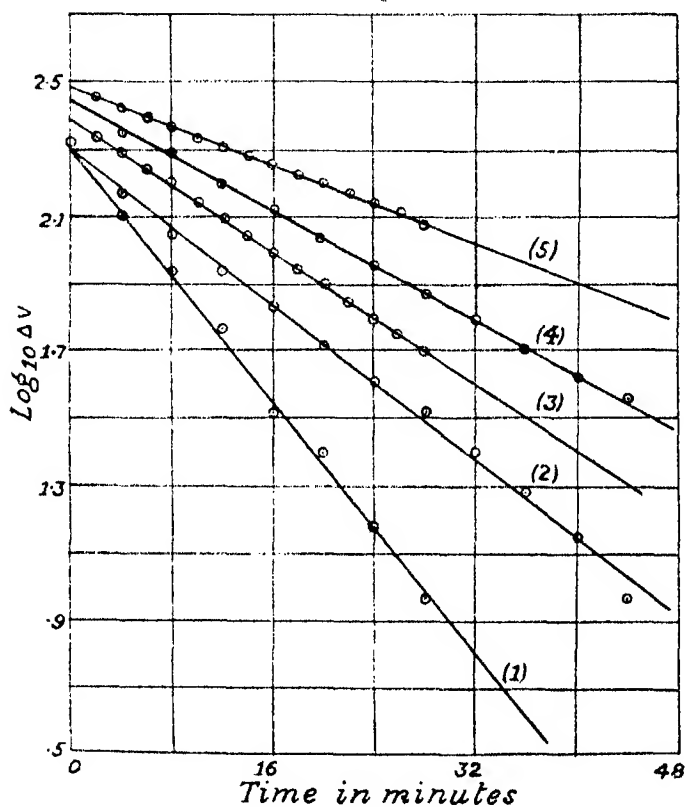


FIG. 1 (b).— $\text{Log}_{10} \Delta V$  against  $T$ .

Curve.....	1	2	3	4	5
Zero .....	490	442	419	399	302

Table II.

(1) Pt. wire holder.

(2) Cu. wire holder.

Experiment .....	10	11	12	13	14	15	1	2	3	4	5	6
Initial surface potential (mv.) .....	0	80	72	165	208	198	585	520	513	469	448	363
Estimated zero (mv.)....	0	70	60	170	183	183	605	521	509	480	419	369

The first few curves obtained by this method showed that although the iodine evaporation was of a strictly exponential character, the value of the unimolecular constant  $k$  varied from one experiment to another. The following investigation was undertaken to see whether the variation of  $k$  could be represented sufficiently well by the two variables,  $Z$  the platinum potential and  $T$  the absolute temperature, permitting the determination of  $\lambda$  the gram molecular heat of desorption and its dependence on  $Z$ .

*Experimental.*

The air-metal potential of the platinum plate with the iodine on it was measured, as previously described using a copper wire, coated at its end with polonium, as the air electrode.

The evaporation was studied at the five different temperatures  $11.20^\circ$ ,  $17.17^\circ$ ,  $21.5^\circ$ ,  $25.67^\circ$ ,  $30.24^\circ$  C. During the course of an experiment the temperature was maintained constant to within  $0.5^\circ$  C. with the aid of a rheostat controlled heating lamp, and frequently read to a  $1/10^\circ$  C., the time mean of the results being taken as the required average temperature. At each constant temperature a range of velocity constants for different values of  $Z$  was desired. This range of about 200 mv. for  $Z$  was found to be obtained sufficiently well if the platinum was thoroughly washed with distilled water, ethyl alcohol and petrol ether.

It was found that at any one temperature  $k$  was given by the expression

$$k = Be^{\alpha Z}, \quad (1)$$

where  $\alpha$ ,  $B$  are constants which vary with the temperature.

The values of  $\log_{10} k$  were plotted against  $Z$ , and from these isothermals the values of  $\log_{10} k$  for various values of the phase boundary potential of the air-metal interface,  $Z = 100, 200, 250, 300, \dots 650$  were read off, and a series of curves  $\log_{10} k$  against  $1/T$  at a constant value of  $Z$  plotted. These latter curves are shown for values of  $Z$  400  $\dots$  550 in fig. 2.

The points on these lines are rather widely scattered about the lines, owing to the fact that even with careful cleaning of the platinum other foreign substances may settle on it, causing appreciable changes in the phase boundary potential, and this investigation is concerned only with the amount of adsorbed oxygen on the surface.

These curves, which represent the process of evaporation of iodine on a

constant substrate at various temperatures, are straight lines, conforming to the usual equation for an evaporative process.

$$k = Ae^{-\frac{\lambda}{RT}}, \quad (2)$$

where  $A$  = constant,  $\lambda$  = gram molecular heat of desorption,  $R$  = gas constant. From equation (2) the equation of each straight line is :

$$\log_{10} k = \log_{10} A - \frac{\lambda}{2.303 RT} \quad (3)$$

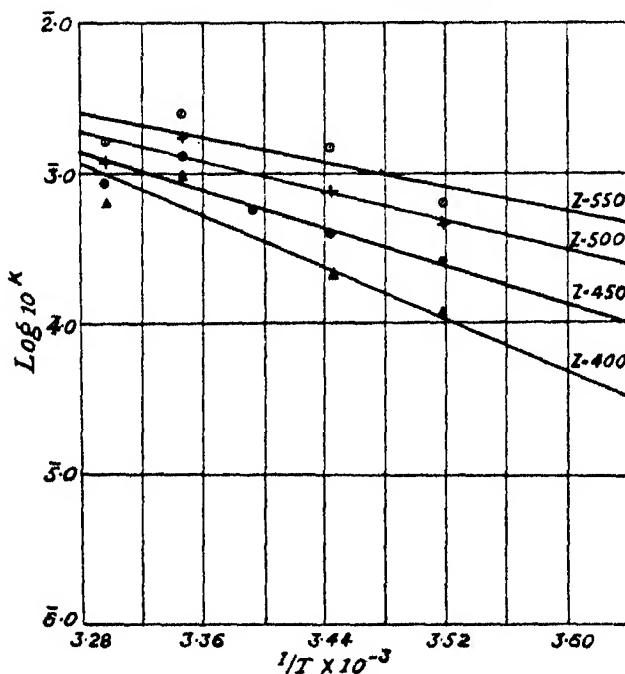


FIG. 2.— $\log_{10} k$  against  $1/T$  for a series of constant platinum potentials.

The experimentally determined straight lines permit of the determination of  $A$  and  $\lambda$  from equation (3) for each value of  $Z$ . Both  $\log_{10} A$  and  $\lambda$  prove to be linear functions of  $Z$  as shown by figs. 3 and 4 respectively. Thus

$$\log_{10} A = 20.96 - 3.03 \times 10^{-2} Z \quad (4)$$

$$\lambda = 34,990 - 46.17 Z. \quad (5)$$

From (2) and (5) the value of the unimolecular velocity constant  $k$  is found to be

$$k = Ae^{-\frac{34,990 - 46.17Z}{RT}}. \quad (6)$$

This equation is identical with (1) when  $T$  is constant.

The dependence of the latent heat of evaporation on  $Z$  as revealed by (5) is most readily interpreted on the assumption that there is a variable layer of

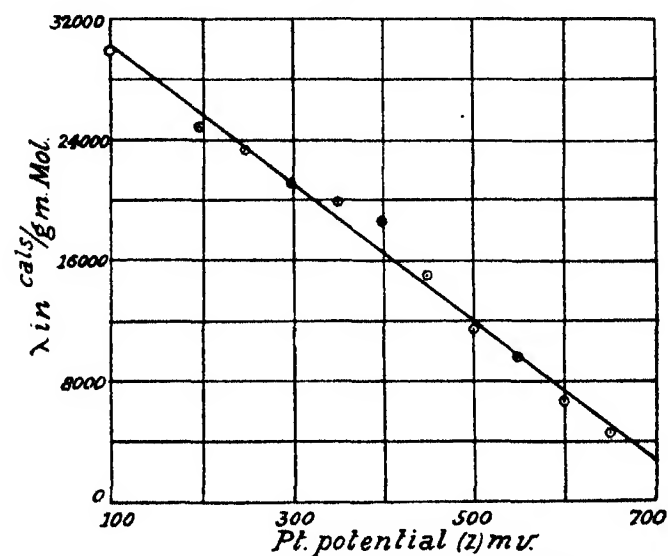


FIG. 3.— $\lambda$  in cal./gm. molecule against  $Z$ . Equation is  $\lambda = 34,990 - 46.17 Z$ .  $\lambda = 0$   $Z = 758$ .

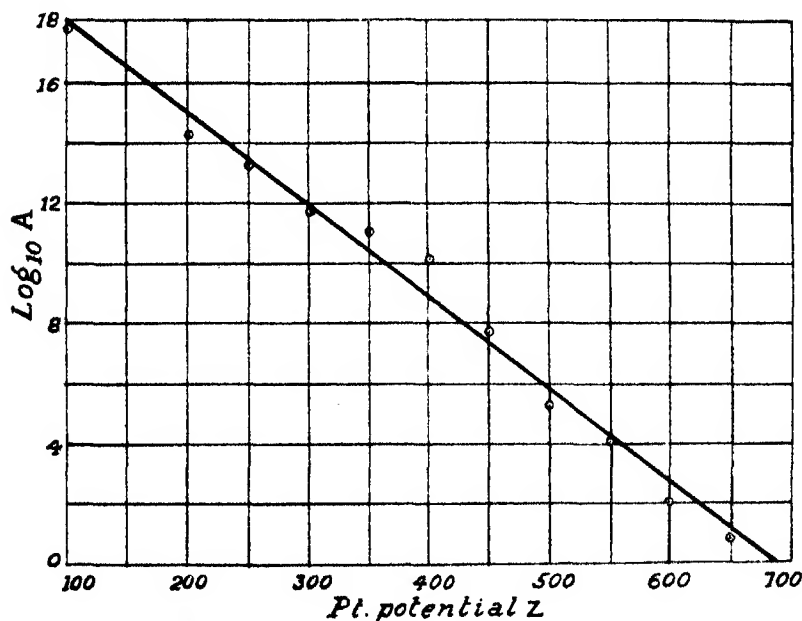


FIG. 4.— $\log_{10} A$  against  $Z$ . Equation of line is  $\log_{10} A = 20.96 - 3.03 \times 10^{-3} Z$



496 *Phase Boundary Potentials of Adsorbed Films on Metals.*

oxygen or oxide on the surface and that the variation in  $Z$  may be represented by

$$Z = A_0 + A_1 \theta$$

where  $\theta$  is dependent on the adsorbed oxygen,  $A_0$ ,  $A_1$  being constants.

Equation (5) is thus

$$\lambda = (34,990 - 46 \cdot 17 A_0) - 46 \cdot 17 A_1 \theta$$

exhibiting an analogy with the usual thermionic equation showing the linear dependence of the work function on the fraction of the surface covered.

$\lambda$  vanishes entirely when  $Z = 758$  mv. (from (5)), *i.e.*, at a saturation value for  $\theta$ . However, the surface is not found to be stable for values of  $Z > 650$  mv. so that direct observation at this point is not possible.

From equation (4) we note that for small values of  $Z$ ,  $A$  is of the order of  $10^{17}$ , falls with increasing  $Z$ , and becomes 10 when  $Z = 690$  mv. This suggests that the frequency of transfer of energy by oscillation of the substrate molecules to the adsorbed iodine, which is undergoing the unimolecular reaction of evaporation, is dependent on the strength of the field.

The rate of evaporation of iodine from gold, which had been cleaned in oxidizing acids or by heating and allowing to attain a stable state as typified by a steady surface potential over hours, was determined in a few cases. Agreement with the previously discussed data for platinum surfaces was obtained in that an exponential rate of decay of elevation of potential difference was observed, the velocity constant rising with increasing oxygen content of the gold (at a constant temperature). A summary of some of the results is given in Table III.

Table III.—Pt. Wire Holder.

Experiment.	Temperature. ° C.	Observed zero.	Calculated zero.	$k$ .
16	27	120	108	$9 \cdot 594 \times 10^{-5}$
17	20	201	201	$1 \cdot 242 \times 10^{-4}$
18	20	245	235	$2 \cdot 50 \times 10^{-4}$

*Phase Boundary Potentials of Adsorbed Films on Metals.—Part III.—  
The Examination of the Interaction of Copper and Iodine Vapour by  
the Method of Surface Potentials.*

By HAROLD KENNETH WHALLEY and ERIC KEIGHTLEY RIDEAL, F.R.S.

(Received February 2, 1933.)

With both platinum and gold, measurements by the method of surface potentials revealed the fact that at low temperatures iodine is reversibly adsorbed on the surface of these metals on which a film of chemi-adsorbed oxygen was present, and does not penetrate into or undergo chemical reaction with the metal substrate. With less noble metals it is known from the work of Kohlschütter and Krähenbühl,\* of Tammann and especially Evans, that in spite of the presence of a thin layer of oxide which is invariably present, iodine readily attacks the metal, forming an iodide. The rate of attack is governed by a diffusion process through an ever-increasing thickness of solid, and the process is of the type designated as activated, in that the temperature coefficient of the diffusion process is exponential in character.

After the exposure of a sheet of copper to the vapour of iodine we might anticipate that the phase boundary potential would be modified both by an adsorbed film of iodine on cuprous iodide, which adsorbed film should be readily volatile, as well as by a layer of cuprous iodide on the metal substrate. Further, the cuprous iodide is unstable (pseudomorphous form), and should in course of time become converted into a true cuprous iodide lattice (idiomorphous form), which later may undergo a process of sintering or crystallization. Since the iodide of copper is a semi-conductor it might be anticipated, from analogy with cuprous oxide and from the theory of formation of rectifying contacts suggested by Schottky† and by Wilson‡ that the full contact potential between the iodide and metal would not come into existence until the layer of pure insulating iodide attains a sufficient and critical thickness. Finally, if the idiomorphous as well as the pseudomorphous iodide form rectifying contacts with copper the conversion of the one into the other will affect the contact potential as well as the critical thickness required. It was thought desirable to examine the possibility of following the growth of a semi-conductor, formed

\* 'Z. Elektrochem.,' vol. 29, p. 570 (1923).

† 'Z. Physik,' vol. 14, p. 87 (1923).

‡ 'Proc. Roy. Soc.,' A, vol. 136, p. 487 (1932).

by chemical attack at a metal surface, by the measurement of the phase boundary potentials.

*Experimental.*

The method adopted for determining the surface potential was identical with that previously described. A freshly polished copper disc after careful washing with petrol ether was exposed to a stream of iodine vapour at a pressure of 0.025 mm. in air and after different periods of time the disc was removed and surface potential measurements commenced.

It was found in common with the behaviour of gold and platinum that a marked change in the surface potential occurred on treatment of the surface with iodine. The surface potential commenced to fall on removal of the plate from exposure to iodine vapour. Examination of a large number of potential time curves revealed the fact that whilst their form was in general much more complicated than that for gold or platinum where a simple process of evaporation of iodine took place, it was not difficult to identify and isolate three separate phenomena as follows. (1) An exponential fall of the potential difference with the time similar to that obtained with the noble metals; (2) an autocatalytic type of fall of potential attributable to the conversion of the unstable form of cuprous iodide to the stable cuprous iodide; the usual type of reaction associated with the conversion of one solid phase into another by a process involving the formation and growth of nuclei; (3) finally, there was an irregular fall, which could be initiated or accelerated by mechanical shock or treatment with water vapour, attributed to the sintering or fracture of cuprous iodide crystals.

*The Evaporation of Iodine from the Iodide Layer.*

The rate of evaporation of iodine from the iodide layer on the surface of the copper could readily be followed, both in experiments where the autocatalytic change referred to above is delayed, and from surfaces of iodide which had already undergone the process of conversion to the idiomorphous form of cuprous iodide and of sintering, and were thus quite stable. The unimolecular velocity constants  $k$  were evaluated in the same manner as that previously described, whilst the thickness of the underlying layer of iodide was computed from the Newtonian colour of the film on the assumption that the refractive index was  $\mu = 2.09$ . The data in Tables I and II are typical of the results obtained.

Table I.—Experiments on Unsintered Films.

Experiment.	Nature of film.	Temperature of evaporation.	$k \times 10^4 \text{ sec.}^{-1}$ .
I	Freshly formed film 600 Å. thick (brown)	° C. 22	5.57
II	Freshly formed film 650 Å. thick (reddish violet)	22	5.50

Mean  $k$  for unsintered film =  $5.54 \cdot 10^{-4} \text{ sec.}^{-1}$ .

Table II.—Experiments on Sintered Films.

In experiments III–VI a sintered film 1030 Å. thick was exposed to iodine vapour for 47, 23, 35, 47 seconds respectively.

Experiment.	Temperature of evaporation.	$k \times 10^4 \text{ sec.}^{-1}$ .
	° C.	
III	21.8	5.69
IV	22.4	5.69
V	22.4	5.69
VI	22.4	5.33

Mean  $k$  for sintered film =  $5.60 \cdot 10^{-4} \text{ sec.}^{-1}$ .

It will be noted that the value for the unimolecular constants of evaporation of iodine, obtained for the surface of freshly formed cuprous iodide is almost identical with that obtained from the stable cuprous iodide so that  $K$  (mean) =  $5.57 \times 10^{-4}$ , a value of the same order as those obtained for the rates of evaporation of iodine from oxidized gold or platinum surfaces.

*The Autocatalytic Conversion of Cuprous Iodide into the Crystalline Form.*

On prolonged exposure of the copper plate to iodine it is found that the decrease of potential with the time although initially of the unimolecular type proceeds after a variable period of time more rapidly, revealing a point of inflexion of the curve. A typical curve is shown in fig. 1.

During this period the iodine is evaporating and some species of change is taking place in the cuprous iodide layer, which may be identified with the conversion of the pseudomorphous form of the iodide freshly prepared by direct attack into the true idiomorphous crystalline variety. From the

previous values obtained for the process of unimolecular evaporation which, as we have seen, is identical for both forms of cuprous iodide, it is possible to separate the experimental curve (E) into its two constituent curves A and B. A represents the course of the evaporation of the iodine from the iodide substrate, and B the conversion of the iodide into the idiomorphous form, a process

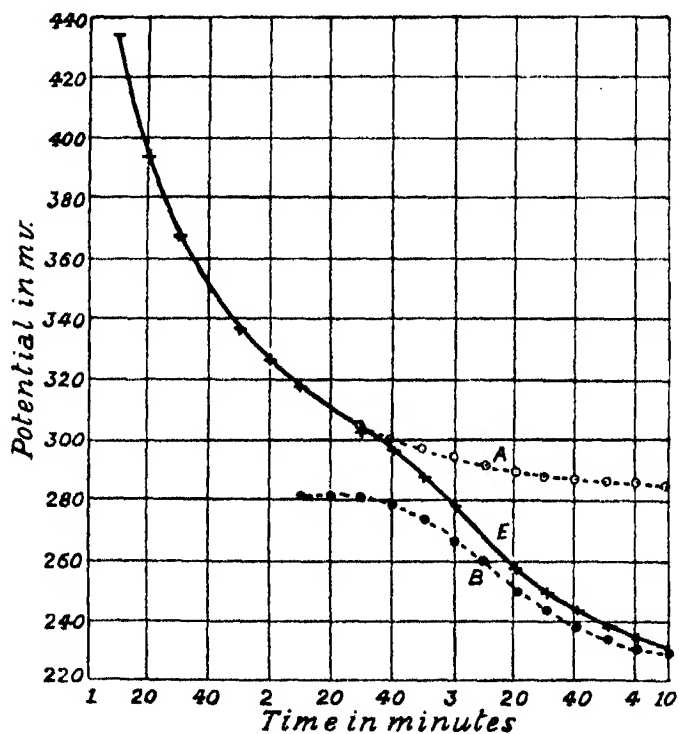


FIG. 1.—E —+— experimental; A --- ○ --- } separated curves.  
B --- • --- }

which evidently alters the magnitude of the contact potential of one or both of the interfaces presented by the layer. The conversion of one solid phase into another when dependent on nucleus formation and growth from nuclei is an autocatalytic process, and curve B is found to be autocatalytic in that it obeys the form :

$$\frac{d \Delta V}{dt} = -K_2 \Delta V (\Delta V_0 - \Delta V),$$

or

$$K_2 = \frac{1}{\Delta V_0 t} \log_e \frac{\Delta V}{\Delta V_0 - \Delta V}.$$

In fig. 2 are plotted a number of derived curves confirming the autocatalytic behaviour of the reaction, a typical series of values obtained is given in Table III

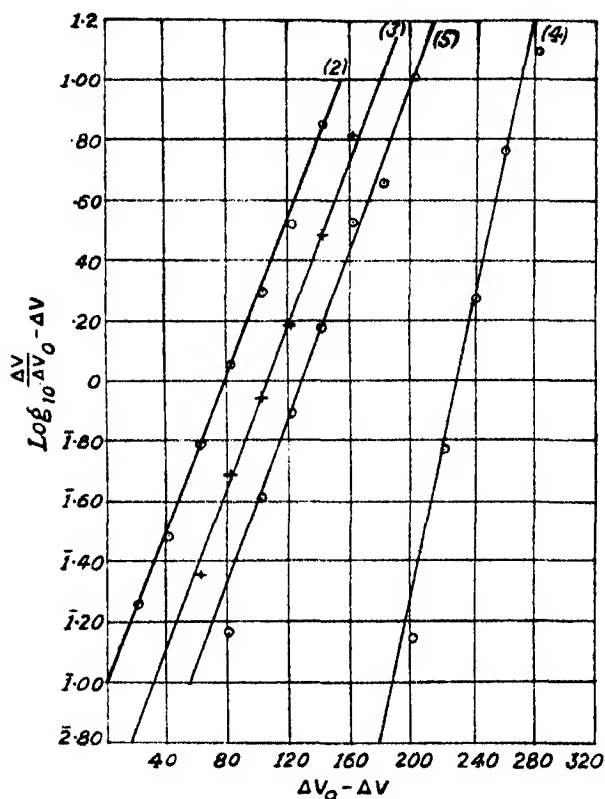


FIG. 2.—Crystallization of Cu I.  $\text{Log}_{10} \frac{\Delta V}{\Delta V_0 - \Delta V}$  against  $\Delta V_0 - \Delta V$ .

$\Delta V_0 = 251$  mv. Readings at 20-minute intervals.

$\Delta V_\alpha = 195$  mv. from the autocatalytic curve.

Table III.

$\Delta V$ .	$\Delta V_0 - \Delta V$ .	$\text{Log}_{10} \frac{\Delta V}{\Delta V_0 - \Delta V}$ .	$\Delta V$ .	$\Delta V_0 - \Delta V$ .	$\text{Log}_{10} \frac{\Delta V}{\Delta V_0 - \Delta V}$ .
mv.			mv.		
240	7	1.2549	214	37	0.2894
238	13	1.4804	208	43	0.5196
230	21	1.7881	202	49	0.8451
222	29	0.0510			

A number of reaction velocity constants derived from the equation

$$K_2 = \frac{1}{\Delta V_0 t \text{ (min.)}} \log_{10} \frac{\Delta V}{\Delta V_0 - \Delta V}$$

are summarized in Table IV.

Table IV.

Experiment No.	$\Delta V_0$ .	Thickness in A.	Temperature.	$K_2 \times 10^4$ .
	mv.		°C.	
2	195	500	23	2.30
3	205	600	23	1.96
4	224	600	25	4.23
5	310	640	20.9	0.65
6	315	680	20	0.23
7	340	1300	22.3	2.53

The autocatalytic nature of the curves depicted in fig. 2 was found to obtain up to a thickness of *ca.* 600 A., and above a thickness of about 1100 A. in regions where, as will be noted, the surface potential of the iodide film varies with the thickness in approximately a linear manner.

As an example of the influence of mechanical shock on the surface potential of a thick iodide film, a phenomenon probably associated with the fracture of crystals, the data in Table V may be cited.

Table V.

Hours after formation of the film.	Surface potential in millivolts.
14	177
15	173
Mechanical shock 16	145
Shock 16.3	133
„ 17	100

*The Variation of the Surface Potential with the Thickness of the Iodide Layer.*

The maximum value of the rectifying contact potential copper/cuprous oxide is not developed until the oxide layer attains a certain minimum thickness. Schottky and Deutschmann\* obtained a capacity equivalent to a thickness of 1300 A. for the layer.

\* 'Phys. Z.,' vol. 30, p. 839 (1929).

In the following curves are shown the alteration in the sum of the contact potentials of the system air/cuprous iodide/copper with increasing thickness of iodide as determined by means of the Newtonian interference colours.

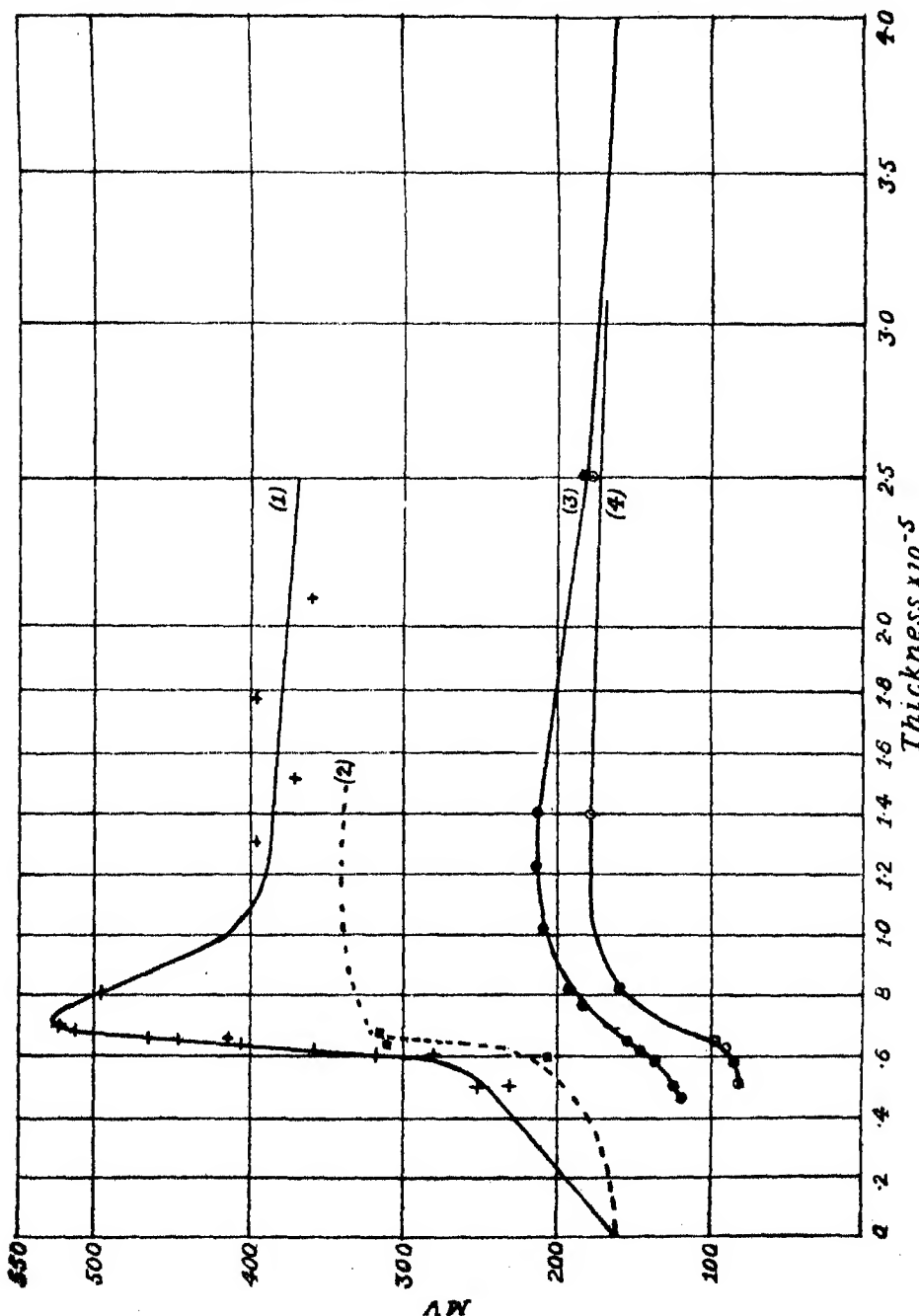


FIG. 3.—(1) Non-crystalline Cu I; (2) crystalline Cu I; (3) crystalline and sintered after 24 hours; (4) crystalline and sintered after 48 hours.



## 504 *Phase Boundary Potentials of Adsorbed Films on Metals.*

It will be observed that the contact potential is much higher for the initial pseudomorphous form than for the crystalline or idiomorphous form and that progressive decrease takes place as the crystals undergo growth owing to sintering. The change may be associated with the elimination of impurities such as traces of cupric iodide yielding cuprous iodide and iodine which latter in time diffuses away from the layer.

The contact potential rises very rapidly with increasing thickness from 600 to 800 Å., a region associated with great instability of the film, as we have noted from the irregularity in the "constants" of the autocatalytic process of recrystallization. It seems possible indeed that the film becomes increasingly susceptible to spontaneous crystallization as the thickness attains 700 Å., and that with thicknesses greater than this the pseudomorphic form is not realizable at the temperatures employed in this investigation.

Our thanks are due to Pembroke College, Cambridge, The Goldsmiths Company, and The Department of Scientific and Industrial Research for a Scholarship, an Exhibition and Research Grant respectively to one of us (H.K.W.), to Trinity College, Cambridge, the Lord Kitchener National Fund and the Mitchell Educational Foundation of the City of London for Scholarships, Exhibitions and Grants (L.J.) and to the Imperial Chemical Industries for assistance in purchase of the necessary apparatus.

### *Summary.*

A method for the investigation of phase boundary potentials at a metal gas interface is described. It is shown that the surface potential of gold is modified by as much as 1.46 volts when a film of oxygen is present on the surface, a value comparable to the alteration caused by an oxygen layer in the thermionic work function. The rate of evaporation of iodine from the surface of platinum on which a film of oxygen is present is found to be unimolecular in character and the latent heat of evaporation is shown to be dependent on the phase boundary potential which can be altered by oxygen.

The evaporation of monolayers of iodine from cuprous iodide is similarly unimolecular in character, but the phase boundary potential between copper and iodine is altered by the presence of a layer of cuprous iodide. The magnitude of the phase boundary potential is a function both of the thickness and crystalline state of the cuprous iodide layer which bears certain analogies to a layer of cuprous oxide in rectifying contact.

---

*An Elementary Theory of Electronic Semi-Conductors, and Some of Their Possible Properties.*

By R. H. FOWLER, F.R.S.

(Received February 22, 1933.)

§ 1. *Introduction.*

The formal theory of electronic semi-conductors was started by A. H. Wilson.† It has recently been carried further by Bronstein,‡ and has, of course, been applied (for example to the theory of rectifying contacts) and discussed in a number of other places. There is, however, I think, still room for a more general but quite elementary discussion of a number of possible models, all of which represent possible varieties of semi-conductors; it is to be understood throughout that only electronic conduction is in question. Granted certain general quantum mechanical theorems, the elementary theory can be made both simple and exact. After presenting such a version of the theory here, it is my purpose to show how the proposed model semi-conductors can account for the positive or negative or zero Hall coefficients which are observed, and also for the large positive or negative thermoelectric power of a semi-conductor-metal thermocouple and for the sign relationships of the two effects. The possibility of the explanation of an abnormal sign for the Hall coefficient is, of course, no new thing; it was first contemplated in the work of Peierls§ on metals and at his suggestion taken over (but not elaborated) by Bronstein (*loc. cit.*) for semi-conductors. But a satisfactory (even elementary) theory requires us to consider the conduction in a solid as a mixed phenomenon due to two almost independent families of electrons. This has not been undertaken by Bronstein or by Peierls and such a theory is given here. It may prove of importance in further study of semi-conductors, beyond the phenomena on which attention is concentrated here.

The scope of this paper then is as follows. We give an elementary theory of the effective number of "conduction" electrons in model semi-conductors of various types. We take account both of the few ordinary electrons in otherwise empty levels, and of the few holes or vacancies in otherwise completely full electron levels which function as positive electrons. We work out for semi-

† 'Proc. Roy. Soc.,' A, vol. 133, p. 458; vol. 134, p. 277 (1931).

‡ 'Phys. Z. Sowjetunion,' vol. 2, p. 28 (1932).

§ 'Z. Physik,' vol. 53, p. 265 (1929).

conductors, conducting partly by electrons and partly by holes, the isothermal Hall coefficient and the thermo-electric power of the thermocouple formed by the semi-conductor and an ideal metal. We thus show in detail how abnormal signs of the Hall effect and the thermo-electric power can be fitted into the theory.

It is not the purpose of this paper to attempt to account in detail for the properties of any actual specimen of a semi-conductor, but rather to explore the possibilities of the models used. These are rather varied, and it seems worth while to put them on record in this way, in the hope that someone, who really knows the facts, will feel interested to examine whether the theoretical predictions and correlations, based on these models, are satisfied in practice, or if not, where they break down.

## § 2. *The Elementary Theory of a Semi-conductor.*

The work of Bloch, of Peierls, and of other authors, and especially A. H. Wilson,<sup>†</sup> has shown that to a sufficient approximation a semi-conductor and its important electrons can be considered in the following way. The possible electron levels of the crystalline lattice of the semi-conductor in question, are broken up into bands of which we are interested in only two:—a lower band of states (suffix 2) exactly full of electrons at the absolute zero, and an upper band of states (suffix 1) entirely empty at the absolute zero. At the temperatures at which we are interested, there will be a few electrons in band 1 and a few empty states in band 2, effectively confined to the lowest states of band 1 and the highest states of band 2. One of these empty states we may speak of as an *occupied hole* or a *positive electron*. The negative electron of an upper occupied state or the positive electron of a lower occupied hole, have energies and momenta which are sufficiently closely equivalent to those of a *free* particle of effective mass  $m_1$ ,  $m_2$  respectively, contained in a volume  $V$ , the volume of the lattice considered. The states have weights  $\omega_1$ ,  $\omega_2$  respectively. The weights  $\omega_1$ ,  $\omega_2$  include the factor 2 for the spin of the electron (negative or positive!) and are exactly 2 for bands of lattice states formed out of atomic or molecular S-states. For lattice states formed out of atomic P-states and so on,  $\omega_1$ ,  $\omega_2$  may contain extra factors (*e.g.*, for *cubic* lattice states formed out of atomic P-states  $\omega = 6$ ). Strictly speaking, the effective masses  $m_1$ ,  $m_2$  are not scalar, but symmetrical tensors of the second rank. Bronstein has shown how this refinement can be simply introduced, but we shall neglect it here.

<sup>†</sup> Whom see for other references.

The few electrons in band 1 are classically "free" because they are not restricted from any natural transition by Pauli's principle. The few holes in band 2 are similarly classically free. Since they are surrounded by full states, any natural transition is possible to them, such a transition being more usually regarded as the reverse transition by an electron. Both obey Maxwellian statistics, the electrons being distributed with kinetic energies increasing upwards from zero at the bottom of band 1, and the holes with kinetic energies increasing downwards from zero at the top of band 2. Both electrons and holes move quasi-classically through the lattice, the holes as if they were positive electrons, with free paths which must be calculated by quantum mechanical theory, but which for our purposes can be represented symbolically by  $l_1$ ,  $l_2$  respectively. All these statements have been fully substantiated by more exact theory. Accepting them, the special applications that we wish to make can be made very simply.

In addition to the lattice levels we shall have sometimes to suppose that a limited number of impurities are present in the lattice which, as described by Wilson, provide distinct isolated levels for electrons, *which at low temperatures may normally be either full or empty*, depending on the type of impurity which is supplied. Semi-conductors without impurities owe their conductivity and other electrical properties to thermal excitation of electrons from band 2 to band 1. These we shall refer to as *intrinsic semi-conductors*. Semi-conductors with impurity levels full of electrons at low temperatures owe their conductivity to the excitation of electrons to band 1 both from the impurity levels and from band 2, the former predominating at ordinary temperatures. These we shall refer to as *normal extrinsic semi-conductors*. Semi-conductors with impurity levels empty at low temperatures owe their conductivity to the excitation of electrons from band 2 both to the impurity levels and to band 1, the former again predominating at ordinary temperatures. These we shall refer to as *abnormal extrinsic semi-conductors*. We use the words normal and abnormal because the corresponding models "normally" possess Hall coefficients of normal and abnormal sign respectively.

The essential first step, which may now be carried out quite simply, is the calculation of the numbers of free electrons and free holes. The simplification is naturally really only superficial, since we have made use already of the more complicated considerations in laying down our rules of procedure. But these rules are of more general scope than the coming applications, and the applications are, in a different way, of more general scope than the rules, so it is well to separate them.

§ 3. *The Free Electrons, as a Problem in Dissociative Equilibrium.*

(i) *Intrinsic Semi-conductors.*—The equilibrium concentration of free electrons and free holes for an intrinsic semi-conductor can be simply determined as a classical dissociative equilibrium.



Suppose there are  $N^*$  electrons in volume  $V$  in the band 2 when full, and let  $N_1$  of these be excited to band 1. Then by the classical laws of dissociative equilibrium†

$$\frac{N_1 \times N_1}{N^* - N_1} = \frac{f_1(T)f_2(T)}{g(T)}. \quad (1)$$

Here  $f_1(T)$  is the partition function for a classical particle of mass  $m_1$  with states of weight  $\omega_1$  in a volume  $V$ , and  $f_2(T)$  the same for a mass  $m_2$  and weight  $\omega_2$  in the lower band:  $g(T)$  is the partition function for a bound electron in band 2 which is practically full. We can therefore assimilate the exact problem to the classical one by treating all the  $N^*$  states of the band as equivalent and taking  $g(T) = N^*$ . Since  $N_1 \ll N^*$  we have therefore

$$N_1^2 = f_1(T)f_2(T). \quad (2)$$

Take the energy zero for definiteness in the top of band 2. Then‡

$$f_1(T) = \omega_1 \frac{(2\pi m_1 kT)^{3/2}}{h^3} V e^{-\Delta W_1/kT}, \quad (3)$$

$$f_2(T) = \omega_2 \frac{(2\pi m_2 kT)^{3/2}}{h^3} V, \quad (4)$$

where  $\Delta W_1$  is the width of the energy gap separating bands 1 and 2. Thus

$$\frac{N_1}{V} = (\omega_1 \omega_2)^{1/2} \frac{\{2\pi (m_1 m_2)^{1/2} kT\}^{3/2}}{h^3} e^{-1/2 \Delta W_1/kT}, \quad (5)$$

which is Wilson's result.

(ii) *Normal Extrinsic Semi-conductors.*—When the energy levels are arranged as in fig. 1, the energy levels of the impurities lying  $\Delta W_2$  above band 2, then at sufficiently low temperatures band 2 can be neglected, and the dissociative equilibrium is



† Cf. Fowler, "Statistical Mechanics," § 5.3.

‡ Fowler, *loc. cit.*, equation (97).

Thus if the energy zero is taken in the impurity levels

$$\frac{N_1 \times N_1}{N_0 - N_1} = \frac{f_1(T) N_0}{N_0}, \quad (6)$$

where  $N_0$  is the number of impurity levels in volume  $V$ . Thus when  $N_1 \ll N_0$ ,

$$\frac{N_1}{V} = \left(\frac{N_0}{V}\right)^{\frac{1}{2}} \omega_1^{\frac{1}{2}} \frac{(2\pi m_e kT)^{\frac{3}{2}}}{h^3} e^{-\frac{1}{2}\Delta W'/kT}, \quad (7)$$

again agreeing with Wilson. Similar results can be obtained for the abnormal type.

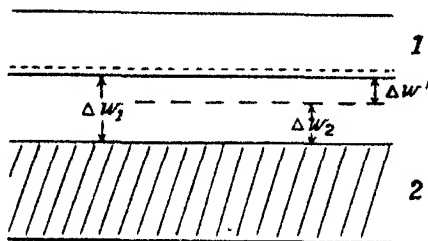


FIG. 1.

#### § 4. General Formulæ for the Free Electrons.

It will be convenient to dispose of more general formulæ than (7) and its analogues, and these are best obtained, as in Wilson's papers, as follows. The average number  $\bar{M}_g$  of electrons in any group of levels whatever is given by the well-known formula of Fermi and Dirac

$$\bar{M}_g = \sum_{(g)} \frac{1}{1 + \lambda e^{\epsilon_r/kT}}. \quad (8)$$

$\epsilon_r$  is the energy of any level,  $\sum_{(g)}$  denotes summation over all the levels of the group, degenerate levels being represented by the proper repetition of terms in (8):  $\lambda$  (equivalent to the partial potential of the electrons) has to be fixed so that the total number of electrons is correct, or by equality with its value for electrons in another phase or group in common equilibrium.

(i) *Intrinsic Semi-conductors*.—Energy zero at the top of band 2.

Conditions are classical in band 1, so that throughout that band  $\lambda e^{\epsilon_r/kT} \gg 1$ .

Thus

$$\begin{aligned} N_1 &= \sum_{(b1)} \frac{1}{\lambda} e^{-\epsilon_r/kT} = \frac{1}{\lambda} f_1(T), \\ &= \frac{\omega_1}{\lambda} \frac{(2\pi m_e kT)^{\frac{3}{2}}}{h^3} V e^{-\Delta W_1/kT}. \end{aligned} \quad (9)$$

Band 2 is practically full, so that throughout that band  $\lambda e^{*}/kT \ll 1$ . Thus

$$\begin{aligned} N^* - N_1 &= \sum_{(b2)} (1 - \lambda e^{*}/kT) = N^* - \lambda \sum_{(b2)} e^{*}/kT, \\ &= N^* - \lambda f_2(T). \end{aligned}$$

Thus

$$N_1 = \lambda \varpi_2 \frac{(2\pi m_2 kT)^{3/2}}{h^3} V, \quad (10)$$

$$\lambda = \left(\frac{\varpi_1}{\varpi_2}\right)^{3/2} \left(\frac{m_1}{m_2}\right)^{3/2} e^{-\frac{1}{2}\Delta W_1/kT}. \quad (11)$$

Combination of (11) and (9) reproduces (5).

(ii) *Normal Extrinsic Semi-conductors*.—Energy zero at the top of band 2. Electrons in band 1 from both band 2 and impurities. Denote now the number of electrons and holes in bands 1 and 2 by  $N_1$ ,  $N_2$  respectively. Then  $N_1$  is still given by (9) and  $N_2$  by (10). The number of electrons on the impurities is  $N_0 - N_1 + N_2$ . Therefore

$$N_0 - N_1 + N_2 = N_0 \frac{1}{1 + \lambda e^{\Delta W_1/kT}},$$

it being assumed that the impurity levels lie  $\Delta W_2$  above the top of band 2. (If these levels are not all at the same height we should have to replace this by

$$N_0 - N_1 + N_2 = \sum_r \frac{N_0^{(r)}}{1 + \lambda e^{\Delta W_1^{(r)}/kT}}.$$

In the simple case it follows that

$$N_1 - N_2 = \frac{N_0}{e^{-\Delta W_1/kT}/\lambda + 1}. \quad (12)$$

Combining (9), (11) and (12) the equation for  $\lambda$  is

$$\frac{\varpi_1}{\lambda} \frac{(2\pi m_1 kT)^{3/2}}{h^3} V e^{-\Delta W_1/kT} = \frac{N_0}{e^{-\Delta W_1/kT}/\lambda + 1} + \lambda \varpi_2 \frac{(2\pi m_2 kT)^{3/2}}{h^3} V. \quad (13)$$

For any given values of the lattice and impurity constants  $\Delta W_1$ ,  $\Delta W_2$ ,  $N_0$ ,  $m_1$ ,  $m_2$ ,  $\varpi_1$  and  $\varpi_2$  the values of  $\lambda$  as a function of  $T$  can be easily computed from the formula. For small values of  $T$  the lower band states are unimportant,  $N_2 \cong 0$ ,  $N_1 \ll N_0$  and  $e^{-\Delta W_1/kT}/\lambda \gg 1$ . Thus

$$\begin{aligned} \frac{\varpi_1}{\lambda^2} \frac{(2\pi m_1 kT)^{3/2}}{h^3} e^{-(\Delta W_1 + \Delta W_2)/kT} &= \frac{N_0}{V}, \\ \lambda &= \left(\frac{V}{N_0}\right)^{1/2} \varpi_1^{1/2} \frac{(2\pi m_1 kT)^{3/4}}{h^{3/2}} e^{-\frac{1}{2}(\Delta W_1 + \Delta W_2)/kT} \end{aligned} \quad (14)$$

Equations (14) and (9) combined reproduce (7). For larger values of  $T$ , the impurity contribution is swamped by the electrons of the lower band, and we recover (11) and (5).

(iii) *Abnormal Extrinsic Semi-Conductors*.—Energy zero at the top of band 2. Holes in band 2 produced by electrons being supplied to the impurities and to band 1.

This case differs only from (ii) in that the number of electrons on the impurities is  $N_2 - N_1$ , so that

$$N_2 - N_1 = \frac{N_0}{1 + \lambda e^{\Delta W_2/kT}}. \quad (15)$$

Combining (9), (11) and (15) the equation for  $\lambda$  is

$$\frac{\varpi_1}{\lambda} \frac{(2\pi m_1 kT)^{3/2}}{h^3} V e^{-\Delta W_1/kT} + \frac{N_0}{1 + \lambda e^{\Delta W_2/kT}} = \lambda \varpi_2 \frac{(2\pi m_2 kT)^{3/2}}{h^3} V. \quad (16)$$

For small values of  $T$  the upper band states are unimportant,  $N_1 \cong 0$ ,  $N_2 \ll N_0$  and  $\lambda e^{\Delta W_2/kT} \gg 1$ . Thus

$$\lambda = \left(\frac{N_0}{V}\right)^{1/2} \frac{1}{\varpi_2^{1/2}} \frac{h^3}{(2\pi m_2 kT)^{3/2}} e^{-1/2 \Delta W_2/kT}. \quad (17)$$

Equations (17) and (10) give

$$\frac{N_2}{V} = \left(\frac{N_0}{V}\right)^{1/2} \varpi_2^{1/2} \frac{(2\pi m_2 kT)^{3/2}}{h^3} e^{-1/2 \Delta W_2/kT}. \quad (18)$$

For larger values of  $T$  the upper band states take charge and we recover (11) and (5).

#### § 5. Thermionic and Photoelectric Work Functions, and Volta Contact Potentials for Semi-conductors.

Before passing to our main subject which requires a formal introduction of "free path phenomena" we can study work functions and contact potentials on the basis of these equilibrium formulæ. For this purpose it is wisest to define an energy zero independent of the level system of any particular conductor, and we take the zero as the energy of an electron at rest at infinity. The levels of a semi-conductor are then as shown in fig. 2. The energy of every level of electrons or holes in the semi-conductor is now reduced by  $\Delta W_*$  from its previous value. To obtain all the necessary results we have only to introduce the additional standard formulæ

$$\frac{N_x}{V} = \frac{2}{\lambda} \frac{(2\pi m_x kT)^{3/2}}{h^3}, \quad (19)$$



for the equilibrium concentration  $N_0/V$  of classical electrons outside the metal, and

$$I = \frac{1}{4} \frac{N_0}{V} e \bar{v} (1 - r) \quad (20)$$

for the saturated thermionic current per cm.<sup>2</sup>. In these formulæ  $m_0$  is the ordinary rest mass of the electron,  $\bar{v}$  its classical mean velocity at temperature  $T$  in free space, and  $r$  the fraction of electrons reflected when incident on the

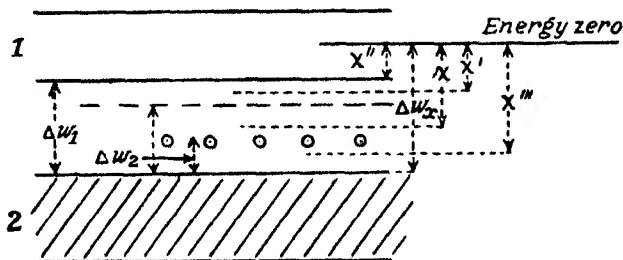


FIG. 2.

semi-conductor from outside. It is assumed that the energy zero falls within band 1, and more strictly in a region of band 1 within which the quasi-classical approximations of the preceding sections are valid. Combining (19) and (20) we have

$$I = (1 - r) AT^2/\lambda, \quad (21)$$

where  $A = 120$  amperes/cm.<sup>2</sup>, the standard thermionic constant. We have merely to substitute the various values of  $\lambda$ . The change of energy zero multiplies every expression for  $\lambda$  by  $e^{\Delta W_0/kT}$ .

(i) *Intrinsic Semi-conductor*.—With the new energy zero

$$\lambda = \left(\frac{w_1}{w_2}\right)^{\frac{1}{2}} \left(\frac{m_1}{m_2}\right)^{\frac{1}{2}} e^{(\Delta W_0 - \frac{1}{2}\Delta W_1)/kT}, \quad (22)$$

$$I = (1 - r) A \left(\frac{w_2}{w_1}\right)^{\frac{1}{2}} \left(\frac{m_2}{m_1}\right)^{\frac{1}{2}} T^2 e^{-\chi/kT}, \quad (23)$$

with  $\chi = \Delta W_0 - \frac{1}{2}\Delta W_1$ . The effective work function is the same as that for an ideal metal with the top of the Fermi-Dirac electron cloud level with the centre of the forbidden band in the semi-conductor. This equivalence has already been discussed by Wilson† and we need not comment on it again here. It is, however, perhaps reasonable to allow oneself a wild speculation concerning the extra factor in  $A$ . It appears to be agreed (experimentally) that

† 'Proc. Roy. Soc.,' A, vol. 136, p. 487 (1932).

for a metal  $r \cong 0$ , that for clean tungsten  $A \cong 60$  and that  $A = 120$  is an impossible value. Accepting this experimental conclusion the theory of metals has recently been in something of a difficulty. It seems possible that something of the same sort is affecting the metallic  $\lambda$  as affects it here for the intrinsic semi-conductor, owing to the different effective properties of loosely and tightly bound metallic electrons.

(ii) *Normal Extrinsic Semi-conductor.*—(a) Low  $T$ ,  $N_1 \gg N_2$ . Equation (14) gives  $\lambda$  when corrected by the factor  $e^{\Delta W_2/kT}$ . Then (see fig. 2 for  $\chi'$ )

$$I = (1 - r) T^{\frac{1}{2}} e^{-\chi'/kT} \cdot A \varpi_1^{-\frac{1}{2}} \frac{h^3}{(2\pi m_1 k)^{\frac{1}{2}}} \left( \frac{N_0}{V} \right)^{\frac{1}{2}} \quad (24)$$

(ii)—(b) Medium  $T$ ,  $N_1 \cong N_0$ . From (13)  $\lambda$  in such a range (corrected for the change of energy zero) is given by

$$\frac{1}{\lambda} = \frac{N_0}{V} \frac{1}{\varpi_1} e^{(\Delta W_1 - \Delta W_2)/kT} \frac{h^3}{(2\pi m_1 kT)^{\frac{1}{2}}}, \quad (25)$$

so that

$$I = (1 - r) A T^{\frac{1}{2}} e^{-\chi''/kT} \cdot \frac{N_0}{V} \frac{1}{\varpi_1} \frac{h^3}{(2\pi m_1 k)^{\frac{1}{2}}}. \quad (26)$$

Equation (26) is actually the classical emission formula for a conductor containing a fixed number  $N_0$  of electrons in a volume  $V$ .

At higher temperatures we pass over, of course, to the forms of case (i).

(iii) *Abnormal Intrinsic Semi-conductor.*—Low  $T$ ,  $N_1 \cong 0$ . Equation (17) gives  $\lambda$  when the right-hand side is multiplied by  $e^{\Delta W_2/kT}$ . The resulting emission formula is

$$I = (1 - r) A T^{\frac{1}{2}} e^{-\chi'''/kT} \cdot \left( \frac{V}{N_0} \right)^{\frac{1}{2}} \varpi_2^{\frac{1}{2}} \frac{(2\pi m_2 k)^{\frac{1}{2}}}{h^{\frac{1}{2}}}. \quad (27)$$

This queer formula, of course, holds only in a limited temperature range.

The possibility of distinguishing experimentally between the  $\frac{1}{2}\Delta W$  of the formulæ for  $N$  or  $\chi$  (or for the conductivity) and the width of the forbidden band has been discussed in general terms by Wilson, on the basis of comparing the  $\frac{1}{2}\Delta W$  of the conductivity with the threshold of the inner photoconductivity effect. While such an experimental test of the theory is not impossible, it has not yet been effected and may well be very difficult. The foregoing formulæ for the thermionic emission suggest the bare possibility of another test, namely, the test of comparing the thermionic work function with the threshold for the *outer photoelectric effect*. At low temperatures the effective threshold of the

outer photoelectric effect will be for all models  $\Delta W_x$  and should therefore differ from  $\chi$  (for example for the intrinsic semi-conductor

$$\Delta W_x = \chi_{ph} = \chi + \frac{1}{2} \Delta W_1).$$

The reason for this value of the photoelectric threshold is that the excited electrons in the upper band will be too few to affect the photoelectric yield curve, which will therefore be determined by the electrons near the top of band 2.

*Volta contact potentials* are determined in all cases by equating the  $\lambda$ 's for the electrons in the two substances. As a standard of comparison we shall take an ideal metal with a simple Fermi-Dirac distribution of electrons, and shall neglect for this ideal metal all terms but those of the highest order. This is perfectly general and legitimate, since all we require is some *definite* standard. We shall therefore take the metal to be an enclosure in which the potential energy of an electron is  $-W_e$  relative to our chosen zero. It is well-known that for such an assembly to the specified approximation

$$\lambda = e^{(W_e - W_a)/kT} \quad \left( W_a = \frac{h^2}{8m_0} \left( \frac{3N_0}{\pi V} \right)^{2/3} \right), \quad (28)$$

$$= e^{\chi_m/kT}, \quad (29)$$

where  $\chi_m$  is the thermionic photoelectric threshold for the metal.

We shall define the contact potential  $V_m^x$  of any substance  $x$  against our standard metal as the amount by which the potential of  $x$  must exceed that of  $m$  when in equilibrium together. Let the *algebraic* charge on the electron be  $e$ . Then all the energy levels of electrons and holes alike, in substance  $x$ , have been raised by  $eV_m^x$  relative to those of the metal. Expressions for  $\lambda$  for substance  $x$  must therefore be multiplied by

$$e^{-eV_m^x/kT}.$$

The formulæ for  $\lambda$  have already been given and it will suffice to record the results for  $V_m^x$ , all for low temperatures.

(i) *Intrinsic Semi-conductor*—

$$eV_m^x = \chi_x - \chi_m - kT \log \left\{ \left( \frac{w_2}{w_1} \right)^{1/2} \left( \frac{m_2}{m_1} \right)^{1/4} \right\}. \quad (30)$$

(ii) *Normal Extrinsic Semi-conductor*—

$$eV_m^x = \chi_x - \chi_m - kT \log \left\{ \left( \frac{N_0}{V} \right)^{1/2} \frac{1}{w_1^{1/2}} \frac{h^3}{(2\pi m_1 kT)^{3/2}} \right\}. \quad (31)$$

(iii) *Abnormal Extrinsic Semi-conductor*—

$$\varepsilon V_m^s = \chi_s - \chi_m + kT \log \left\{ \left( \frac{N_0}{V} \right)^{\frac{1}{2}} \frac{1}{\omega_s^{\frac{1}{2}}} \frac{h^{\frac{1}{2}}}{(2\pi m_s kT)^{\frac{1}{2}}} \right\}. \quad (32)$$

These formulæ show that the contact potentials against a metal will be more or less of normal type, not highly temperature-sensitive over the low temperature range, but one can have important temperature variations of the contact potential as  $\lambda$ , for an extrinsic semi-conductor changes over from one type of formula to another. The changes will be of the order of the change in the effective thermionic work function.

It is perhaps worth recording that if we have two examples of the same normal extrinsic semi-conductor with different amounts of impurity then

$$\begin{aligned} \varepsilon V_x^v &= \varepsilon (V_m^v - V_m^s), \\ &= -\frac{1}{2} kT \log \frac{N_v}{N_x}. \end{aligned} \quad (33)$$

This is entirely of classical form and strictly non-metallic in type. It might amount to as much as 0.1 volt.

#### § 6. *Steady States in Conductors Containing both Free Electrons and Free Holes.*

In order to proceed further with any discussion of steady states of flow it is necessary to generalize the usual discussion of such states to include states of flow in which two more or less independent groups of particles are both conveying the current. We shall base our generalization substantially on Brillouin's account of the metallic case,<sup>†</sup> but it is here really simplified to the classical theory of Lorentz and Bohr, extended to two sets of carriers. The whole discussion will be purely formal, expressed in terms of a free path  $l$  which we shall not attempt to calculate, but for which we shall take over known results of the quantum theory of metals.

In equilibrium let the number of free electrons (or holes) in one group per unit volume with velocity components in the range

$$\xi, \xi + d\xi; \quad \eta, \eta + d\eta; \quad \zeta, \zeta + d\zeta \quad (\xi^2 + \eta^2 + \zeta^2 = v^2)$$

be

$$dn = \varpi \left( \frac{m}{h} \right)^3 f^0(v) d\xi d\eta d\zeta = f^0 d\omega, \quad (34)$$

<sup>†</sup> "Die Quantenstatistik," chap. 7.

in which  $m$  is the *effective* mass of the electron. Strictly

$$f^0 = \frac{1}{1 + \lambda e^{(W + \frac{1}{2}mv^2)/kT}}, \quad (35)$$

where  $W$  is the energy of the state of zero kinetic energy in the group, referred to the chosen energy zero. Actually for our classical groups  $dn$  reduces to

$$\begin{aligned} dn &= \omega \left( \frac{m}{h} \right)^3 \frac{1}{\lambda} e^{-(W + \frac{1}{2}mv^2)/kT} d\xi d\eta d\zeta, \\ &= n \left( \frac{m}{2\pi kT} \right)^3 e^{-mv^2/2kT} d\xi d\eta d\zeta. \end{aligned} \quad (36)$$

Here  $n$  is the total number of electrons in the group *per unit volume*. We shall throughout the rest of this paper replace the previous  $N/V$ 's by the corresponding  $n$ 's, whenever convenient. To preserve usual forms it is wise to use (34) and replace it by (36) in the final formulæ.

Suppose the electrons (or holes) of a single group, of algebraic charge  $\epsilon$ , are subjected to electric fields  $F_x, F_y$ , and a magnetic field  $H_z$  (for short  $H$ ) referred to right-handed axes. Then the electrons or holes move as if subject to forces  $\epsilon(F_x + \eta H)$ ,  $\epsilon(F_y - \xi H)$ . The distribution function becomes

$$f = f^0 + \xi \phi(v) + \eta \psi(v); \quad (37)$$

the currents flowing are

$$I_x = \frac{1}{2} \epsilon \int v^2 \phi(v) d\omega, \quad I_y = \frac{1}{2} \epsilon \int v^2 \psi(v) d\omega, \quad (38)$$

and to the first order in  $H$

$$\phi(v) = -\frac{l}{v} \left[ \left( \frac{\epsilon F_x}{m} \frac{1}{v} \frac{\partial f^0}{\partial v} + \frac{\partial f^0}{\partial x} \right) + \frac{l}{v} \frac{\epsilon H}{m} \left( \frac{\epsilon F_y}{m} \frac{1}{v} \frac{\partial f^0}{\partial v} + \frac{\partial f^0}{\partial y} \right) \right], \quad (39)$$

$$\psi(v) = -\frac{l}{v} \left[ \left( \frac{\epsilon F_y}{m} \frac{1}{v} \frac{\partial f^0}{\partial v} + \frac{\partial f^0}{\partial y} \right) - \frac{l}{v} \frac{\epsilon H}{m} \left( \frac{\epsilon F_x}{m} \frac{1}{v} \frac{\partial f^0}{\partial v} + \frac{\partial f^0}{\partial x} \right) \right]. \quad (40)$$

Equations (39) and (40) are approximations obtained from Boltzmann's equation by making  $\partial f / \partial t = 0$ , taking account of collisions with the lattice.

Now suppose we have two sets of such carriers distinguished by suffices 1 and 2, and can (at first) treat them as independent. Then equations (39) and (40) apply to both types with the addition of the proper suffix to  $\phi, \psi, l, \epsilon, m, f^0$ , and  $d\omega$ , and

$$I_x = \frac{1}{2} \epsilon_1 \int v^2 \phi_1(v) d\omega_1 + \frac{1}{2} \epsilon_2 \int v^2 \phi_2(v) d\omega_2, \quad (41)$$

$$I_y = \frac{1}{2} \epsilon_1 \int v^2 \psi_1(v) d\omega_1 + \frac{1}{2} \epsilon_2 \int v^2 \psi_2(v) d\omega_2. \quad (42)$$

All this is sufficiently obvious. The points requiring attention are to decide on the proper equations of condition in any given problem, and what correction if any to apply for the interaction of the groups.

### § 7. The Thermoelectric Power in a Mixed Semi-conductor.

We wish to calculate the e.m.f. round the circuit shown in fig. 3. The circuit may be assumed to be of high resistance so that we may calculate the e.m.f. for zero current. For our ideal metal all properties are assumed to be independent of temperature so that the problem is to calculate the change of electrostatic potential along the semi-conductor for zero current when there is a temperature gradient. This gradient is assumed to be so small that the

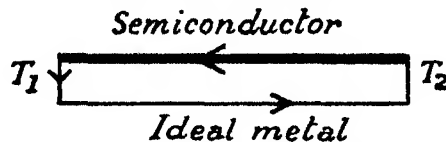


FIG. 3.—The arrows show normal direction of positive current when  $T_1 > T_2$ .

equilibrium values of  $n_1$  and  $n_2$  are everywhere established; the gradient may be taken along the  $x$ -axis so that all variations in  $y$  vanish, and there is no magnetic field. The primary equation is therefore

$$0 = \epsilon_1 \int l_1 v \left\{ \frac{\epsilon_1 F_x}{n_1} \frac{1}{v} \frac{\partial f_1^0}{\partial v} + \frac{\partial f_1^0}{\partial x} \right\} d\omega_1 + \epsilon_2 \int l_2 v \left\{ \frac{\epsilon_2 F_x}{n_2} \frac{1}{v} \frac{\partial f_2^0}{\partial v} + \frac{\partial f_2^0}{\partial x} \right\} d\omega_2. \quad (43)$$

The problem is now determinate since  $\partial f_1^0/\partial x$  and  $\partial f_2^0/\partial x$  are fixed by the given temperature gradient. There is one small internal inconsistency. The assumption of equilibrium values of  $n$  everywhere implies that no charges have shifted so that no space charge has built up. This implies that  $\partial F_x/\partial x = 0$ , which will not necessarily be correct. But the changes of the  $n$ 's required to build up the necessary space charge are excessively small and have been rightly neglected.

Equation (43) can now be simply treated, ignoring variations of the  $l$ 's with  $v$ †. Thus it gives

$$\left\{ -\frac{\epsilon_1 l_1 F_x}{kT} n_1 \bar{v}_1 + \epsilon_1 l_1 \frac{\partial}{\partial x} (n_1 \bar{v}_1) \right\} + \left\{ -\frac{\epsilon_2 l_2 F_x}{kT} n_2 \bar{v}_2 + \epsilon_2 l_2 \frac{\partial}{\partial x} (n_2 \bar{v}_2) \right\} = 0.$$

† Though it is in general necessary for us to make this approximation it is in fact not necessary in this section. The integrals in which  $l_1$  (or  $l_2$ ) enters are effectively the same and require the use of the same mean value in (44) which is thus an exact consequence of (43).

Remembering that  $F_x$  is derived from a potential ( $F_x = -\partial\Phi/\partial x$ ) and that  $\partial/\partial x$  may be replaced by  $\partial/\partial T$  we find that

$$-\frac{\partial\Phi}{\partial T} \{ \varepsilon_1^2 l_1 n_1 \bar{v}_1 + \varepsilon_2^2 l_2 n_2 \bar{v}_2 \} = kT \left\{ \varepsilon_1 l_1 \frac{\partial}{\partial T} (n_1 \bar{v}_1) + \varepsilon_2 l_2 \frac{\partial}{\partial T} (n_2 \bar{v}_2) \right\}. \quad (44)$$

We now introduce in (44) explicit formulæ for  $n_1$  and  $n_2$ .

(i) *Intrinsic Semi-conductor*.— $n_1 = n_2$  given by (5);  $-\varepsilon_1 = \varepsilon_2 > 0$ .

$$-\frac{\partial\Phi}{\partial T} [\varepsilon_1^2 l_1 n_1 \bar{v}_1 + \varepsilon_2^2 l_2 n_2 \bar{v}_2] = [\varepsilon_1 l_1 n_1 \bar{v}_1 + \varepsilon_2 l_2 n_2 \bar{v}_2] \left( 2k + \frac{\frac{1}{2}\Delta W_1}{T} \right). \quad (45)$$

If we could ignore the contribution of the holes (suffix 2) this would reduce to

$$-\frac{\partial\Phi}{\partial T} = \frac{1}{\varepsilon_1} \left( 2k + \frac{\frac{1}{2}\Delta W_1}{T} \right), \quad (46)$$

$$\Phi(T_1) - \Phi(T_2) = -\frac{1}{\varepsilon_1} \left( 2k \{T_1 - T_2\} + \frac{1}{2}\Delta W_1 \log \frac{T_1}{T_2} \right). \quad (47)$$

Thus  $\Phi(T_1) > \Phi(T_2)$  when  $T_1 > T_2$ , and the current would flow in the direction shown in fig. 3 for the normal direction of the positive current. The magnitude of the thermo-electric e.m.f. is large. For example, if  $\frac{1}{2}\Delta W_1/\varepsilon = 0.8$  volts, the e.m.f. for  $T_2 = 273^\circ$  K. is approximately  $0.8 \delta T/T_2$  or nearly 3 millivolts per degree. The e.m.f. for such a thermocouple whose junctions are at  $273^\circ$  K. and  $373^\circ$  K. respectively would be as large as 0.25 volts.

From the nature of the electronic lattice states we are forced to conclude that

$$l_1 \bar{v}_1 > l_2 \bar{v}_2. \quad (48)$$

It follows from (45) that *an intrinsic semi-conductor and a metal must always form a thermocouple with an e.m.f. of normal sign, i.e., that shown in fig. 3*. When the holes are taken into account the e.m.f. will not, however, be quite so large as that calculated above.

(ii) *Normal Extrinsic Semi-conductor*.—Low  $T$ ,  $n_2 = 0$ . Here  $n_1$  is given by (7), and (44) gives

$$\Phi(T_1) - \Phi(T_2) = -\frac{1}{\varepsilon_1} \left\{ \frac{5}{4} k (T_1 - T_2) + \frac{1}{2} \Delta W_1 \log \frac{T_1}{T_2} \right\}. \quad (49)$$

This is always normal and again can be of the order of 0.1 volt for the  $273^\circ$ – $373^\circ$  K. interval.

If we go to higher temperatures we must take  $n_1$  and  $n_2$  to be given by (9) and (10), and  $\lambda$  by (13). Then (44) gives

$$-\frac{\partial \Phi}{\partial T} \left[ \epsilon_1 n_1 \bar{v}_1 + \epsilon_2 n_2 \bar{v}_2 \right] = \left[ \epsilon_1 l_1 n_1 \bar{v}_1 \left( 2k + \frac{\Delta W_1}{T} - \frac{kT}{\lambda} \frac{\partial \lambda}{\partial T} \right) + \epsilon_2 l_2 n_2 \bar{v}_2 \left( 2k + \frac{kT}{\lambda} \frac{\partial \lambda}{\partial T} \right) \right]. \quad (50)$$

In spite of the inequality  $l_1 n_1 \bar{v}_1 > l_2 n_2 \bar{v}_2$  we might be tempted to think that  $\partial \Phi / \partial T$  might have an abnormal sign. But on examining (44) more closely we see that such an event requires

$$\frac{\partial n_2}{\partial T} > \frac{\partial n_1}{\partial T}$$

by an appreciable margin. But for our normal extrinsic semi-conductor

$$\partial n_1 / \partial T > \partial n_2 / \partial T,$$

since  $n_1$  grows with  $T$  not only by absorbing all the  $n_2$  electrons from band 2 but also by taking a further positive supply from the impurity levels. Thus the sign is always normal.

(iii) *Abnormal Extrinsic Semi-conductor*.—Low  $T$ ,  $n_1 = 0$ . Here  $n_2$  is given by (18), and (44) then gives

$$\Phi(T_1) - \Phi(T_2) = -\frac{1}{\epsilon_2} \left\{ \frac{5}{4} k (T_1 - T_2) + \frac{1}{2} \Delta W_2 \log \frac{T_1}{T_2} \right\}. \quad (51)$$

Since  $\epsilon_2 > 0$  this has the abnormal sign opposite to that shown in fig. 3. In the general case at higher temperatures we still have  $\partial n_2 / \partial T > \partial n_1 / \partial T$ , tending to an equality as the temperature rises. But since  $n_2 > n_1$  and  $l_1 \bar{v}_1 > l_2 \bar{v}_2$  we no longer have a definite inequality between  $n_1 l_1 \bar{v}_1$  and  $n_2 l_2 \bar{v}_2$ . The thermoelectric power of a thermocouple formed of such a semi-conductor and a standard metal will vanish and change sign to normal as the temperature rises. We shall return to this case again after discussing the Hall effect. The general formula is still (50),  $\lambda$  being given by (16).

It will be observed that equation (43) does not, in general, make both partial currents vanish. In the equilibrium case, which we have set up, there is therefore actually a flow of electrons in one direction in the conductor and an equal flow of holes in the same direction. At any particular place therefore,  $n_1$  and  $n_2$  will be increasing at equal rates. They will increase or diminish until the increased or diminished rate of recombination exactly balances the contribution made by the flow. The assumption of a normal  $n_1$  and  $n_2$  is



therefore not exactly correct and a more exact theory is, strictly speaking, necessary and in fact, possible. It will not, however, alter the form of our result and we shall therefore not stay to develop it here.

§ 8. *The Isothermal Hall Effect in a Mixed Semi-conductor.*

The isothermal Hall coefficient  $R$  is defined by the relation

$$F_y = RH I_x, \quad (52)$$

subject to the equations of condition  $I_y = 0$ ,  $T = \text{const.}$  If  $\sigma$  is the conductivity defined by  $I_x = \sigma F_x$  then

$$R\sigma = F_y/HF_x. \quad (53)$$

We shall ignore changes of  $\sigma$  due to  $H$ .

We start by recalling the formulæ for one set of carriers only. Then

$$I_x = \sigma F_x = - \int l v \left[ \frac{\epsilon F_x}{m} \frac{1}{v} \frac{\partial f^0}{\partial v} + \frac{\partial f^0}{\partial x} \right] d\omega,$$

$$0 = \int l v \left\{ \left[ \frac{\epsilon F_x}{m} \frac{1}{v} \frac{\partial f^0}{\partial v} + \frac{\partial f^0}{\partial y} \right] - \frac{l}{v} \frac{\epsilon H}{m} \left[ \frac{\epsilon F_x}{m} \frac{1}{v} \frac{\partial f^0}{\partial v} + \frac{\partial f^0}{\partial x} \right] \right\} d\omega.$$

The equations are obviously insoluble without two more equations of condition. These are always taken to be  $\partial f^0/\partial x = 0$ ,  $\partial f^0/\partial y = 0$  for the isothermal case. They may be regarded as the conditions of no space charge. The condition  $\partial f^0/\partial x = 0$ , however, lies deeper even than this. It is a condition of uniformity of the conductor along the direction of the current. The conductor could well be a closed circuit, when a value of  $\partial f^0/\partial x \neq 0$  is unthinkable. Solving the last equations under these conditions we find

$$\sigma = \frac{8}{3\pi} \frac{\epsilon^2 l n}{m v} = \frac{1}{3} \frac{\epsilon^2 l n \bar{v}}{kT}, \quad (54)$$

$$R\sigma = \frac{\epsilon}{m} \frac{l}{v}, \quad (55)$$

$$R\epsilon = \frac{3\pi}{8} \frac{1}{n}. \quad (56)$$

For two sets of carriers, the uniformity condition still requires us to impose *both* the conditions

$$\frac{\partial f_1^0}{\partial x} = 0, \quad \frac{\partial f_2^0}{\partial x} = 0.$$

Neglecting  $H$  we then obtain, of course,

$$\sigma = \sigma_1 + \sigma_2 \quad \left( \sigma_1 = \frac{1}{2} \frac{\epsilon_1^2 l_1 n_1 \bar{v}_1}{kT}, \quad \sigma_2 = \frac{1}{2} \frac{\epsilon_2^2 l_2 n_2 \bar{v}_2}{kT} \right). \quad (57)$$

The conditions across the flow are less simple. The uniformity condition is essentially inapplicable. The condition of no space charge requires

$$\frac{\partial n_1}{\partial y} = \frac{\partial n_2}{\partial y}, \quad (58)$$

assuming that no change with  $y$  occurs in the number of bound electrons, but one more condition is still required. This condition is strictly that the equal rates of increase of electrons and holes by transport to any neighbourhood must be exactly balanced by the increased rate of recombination owing to the slight excess of electrons and holes present there. If the extra rate of recombination is slow we must have  $(I_v)_1 = (I_v)_2 = 0$  separately. One can see that the exact relations must be of the form

$$(I_v)_1 = (I_v)_2 = K' \frac{\partial n_1}{\partial y} = K' \frac{\partial n_2}{\partial y}, \quad (59)$$

which we shall use without more detailed enquiry for the present discussion. Thus the  $y$ -equations are

$$-\frac{l_1 \epsilon_1 n_1 \bar{v}_1}{kT} F_v + l_1 \bar{v}_1 \frac{\partial n_1}{\partial y} + \frac{l_1^2 \epsilon_1^2 n_1 H F_e}{m_1 kT} = K \frac{\partial n_1}{\partial y}, \quad (60)$$

$$-\frac{l_2 \epsilon_2 n_2 \bar{v}_2}{kT} F_v + l_2 \bar{v}_2 \frac{\partial n_2}{\partial y} + \frac{l_2^2 \epsilon_2^2 n_2 H F_e}{m_2 kT} = K \frac{\partial n_2}{\partial y}. \quad (61)$$

The elimination in the general case is not very illuminating. We record only the two limiting cases

(a)  $K \ll l\bar{v}$ . Then

$$R\sigma = \left( \frac{l_1 \epsilon_1^2 n_1}{m_1 \bar{v}_1} - \frac{l_2 \epsilon_2^2 n_2}{m_2 \bar{v}_2} \right) / (\epsilon_1 n_1 - \epsilon_2 n_2).$$

This reduces easily to

$$R\sigma = \frac{3\pi}{8} \frac{\sigma_1 - \sigma_2}{\epsilon_1 (n_1 + n_2)}. \quad (62)$$

(b)  $K \gg l\bar{v}$ . Then

$$R\sigma = \epsilon_1 \left( \frac{l_1^2 n_1}{m_1} - \frac{l_2^2 n_2}{m_2} \right) / (l_1 \bar{v}_1 n_1 + l_2 \bar{v}_2 n_2). \quad (63)$$

The correct formula will be somewhere in between. The important factors in (62) and (63) can also be put in the respective forms

$$\left. \begin{aligned} l_1 \bar{v}_1 n_1 - l_2 \bar{v}_2 n_2 \\ l_1^2 \bar{v}_1^2 n_1 - l_2^2 \bar{v}_2^2 n_2 \end{aligned} \right\}. \quad (64)$$

These results can now be applied very simply to the various models. We see at once that an intrinsic semi-conductor and a normal extrinsic semi-conductor will both have a normal sign for the Hall coefficient at all temperatures. The abnormal extrinsic semi-conductor will have an abnormal sign for the Hall coefficient at low temperatures which will vanish and then become normal as the temperature rises. On comparing this with the thermo-electric power of the same semi-conductor we see at once that there is in general no reason why the signs of the two effects should change at the same temperature, but that either could change first, so that over a limited temperature range one could have either combination of signs, one normal and one abnormal, for the Hall coefficient and the thermo-electric power. But for the models examined here, the theory suggests that for any substance for which either sign is abnormal both will become abnormal at sufficiently low temperatures. For any substance which does not conform a still more complicated model must be used.

As we have said before, we do not propose to attempt a detailed comparison with the properties of an actual substance. It is sufficient to record in concluding this paper that normal and abnormal signs have been recorded for both the effects here discussed, usually both normal or both abnormal though I believe exceptions are known. Substances of the type proposed probably therefore exist. But whether the necessary correlations of the effects over wider temperature ranges conform to the theory awaits further investigation.

#### *Summary.*

Wilson's theory of semi-conductors is presented in a simple form and applied to three different models of semi-conductors. These models represent (1) pure substances of very small conductivity, (2) substances with impurities supplying excitable electrons, (3) substances with impurities absorbing excited electrons. The equilibrium state, thermionic and photoelectric work functions, contact potential, conductivity, Hall coefficients, and thermoelectric power are worked out for all these models, using where necessary as a standard of comparison, a model representing an ideal metal. The signs of the Hall coefficient and the thermoelectric power are specially examined and the possible appearance of abnormal signs in either or both of these effects accounted for.

---

*Probability, Statistics, and the Theory of Errors.*

By HAROLD JEFFREYS, M.A., D.Sc., F.R.S.

(Received February 9, 1933.)

Dr. Fisher and I seem to agree on the formal correctness of each other's mathematical development, when once the initial assumptions are given. But in the data and in the interpretation of the conclusions I can find no basis of agreement to use as the starting-point in a reply to his criticisms.\* It seems to be necessary therefore for me to begin at an earlier stage and explain why a theory of probability is necessary, and what is the scope of such a theory. By "probability" I mean probability and not frequency, as Fisher seems to think, seeing that he introduces the latter word in restating my argument. If in the process I have to repeat a certain amount of matter previously published, but with which Fisher shows no acquaintance, I must ask the reader's indulgence.

It is a commonplace of logic that if two propositions  $p$  and  $q$  are so related that  $p$  implies  $q$ , then  $q$  does not necessarily imply  $p$ . Yet in scientific work, as in ordinary life, we habitually argue in a way that resembles in form the inference that  $q$  does imply  $p$ . We state a theory and develop its consequences to the point where they yield deductions verifiable by observation. If these are found to be true, we say that the theory is "verified"; further, we proceed to draw other inferences from the theory and to expect them to be verified in the future. So far as scientific and philosophical writers have considered this dilemma, or so far as it is possible to infer their beliefs from their methods of presentation, there seem to be three main attitudes.

1. Frank belief that scientific inference is invalid. Thus Bertrand Russell† states two alternatives: "induction appears to me to be either disguised deduction or a mere method of making plausible guesses."

From discussion with a number of philosophers I have found that the latter view is widely held; though these philosophers show by their actions that they often accept inductive inferences as a basis for action, and can, if pressed, be brought to admit that, for some reason they do not claim to understand,

\* 'Proc. Roy. Soc.,' A, vol. 130, pp. 343-348 (1933).

† "Principles of Mathematics," p. 11.

this invalid process does in fact usually lead to correct predictions of events that can be observed. Most of us have indeed met the man who disposes of an inference from a large number of observed instances by saying that we have not examined *all* instances.

2. Acceptance of Russell's first alternative. The straightforward inference of " $q$  implies  $p$ " from " $p$  implies  $q$ " is impossible, but " $q$  implies  $p$ " may be inferred from " $p$  implies  $q$ " together with some other proposition or propositions. The problem then becomes to examine the nature of this further proposition. Thus Russell\* says in a later publication: "If induction remains at all, which is a difficult proposition, it will remain merely as one of the principles according to which deductions are effected." There are at least three attempts at solution: the law of contradiction, the doctrine of causality, and the theory of probability. It may happen that besides " $p$  implies  $q$ " we have " $\text{not-}p$  implies  $\text{not-}q$ "; then the verification of  $q$  establishes  $p$ . But it would do so equally well if we had " $\text{not-}p$  implies  $\text{not-}q$ " without " $p$  implies  $q$ ." For our purposes, however, this circumstance never seems to arise. An infinite number of laws will usually fit any set of observed data, and we are rarely, if ever, in a position to say that no law other than one would fit the data.

The alleged "law of causality" has been discussed elsewhere†; but so far as I am aware nobody has succeeded in stating it in a form that helps us in the least to say *what* laws are causal; and without providing such a criterion it remains irrefutable, but useless.

I believe that the correct solution is in terms of probability; that our laws themselves, and further observational results obtainable from them, are never proved, what is proved being that they have definite degrees of reliability on the knowledge available.

We must notice at once that any solution on the lines of providing a means of generalization must involve an *a priori* postulate. By an *a priori* proposition I mean, as in logic, one believed independently of experience. We cannot prove the legitimacy of generalization by logic; nor can we prove it from logic and experience together. The only type of experience that we could utilize in making such an inference would be the success of previous inferences by methods of generalization. But we cannot infer from this at any moment that such methods will lead to correct inferences in the future without a

\* "Our Knowledge of the External World," p. 34.

† Jeffreys, "Scientific Inference," p. 209.

postulate\* entitling us to generalize our previous experience of the successes of generalization, and we are no further forward.

*There is therefore no possibility of drawing any inductive inference without an a priori assumption, and if any method appears to avoid such an assumption it must be either erroneous in principle or involve some a priori assumption that the author has not stated and possibly has not noticed.*

This point needs emphasis, because many critics of the theory of probability think that they can dispose of it by pointing out that it makes assumptions that cannot be proved either logically or experimentally. Any theory capable of justifying generalization must necessarily make some assumptions of this character, and the issue is whether such assumptions shall be made or generalization entirely abandoned; and, of course, science with it. I see no reason, however, when the hypotheses are clearly stated, why the rest of the process should not be deductive.

3. Belief that the whole of science is *a priori*. This is an extreme form of Russell's first alternative. It seems to be the view of most writers on the theory of relativity, and in particular of Sir Arthur Eddington. The usual process is to start with a limited number of purely *a priori* postulates, and from them to develop deductively the consequences in the form of a number of physical laws. I have no wish to decry the method, which has certainly led to valuable results. My comment is that it is only a part of scientific method, whereas the authors seem to think that it is the whole. I feel no *a priori* certainty in the correctness of the initial assumptions (and this would be too weak a description of the feelings of many other scientific workers) but they have a finite probability in terms of the simplicity postulate originally stated by Dr. Wrinch and myself,† and restated in my "Scientific Inference"; and

\* It might appear that such a postulate would be the principle of generalization itself, and that the argument would be a vicious circle of the type understood in ordinary speech, namely, an inference of the form "*p* implies *p*, therefore *p*." But whatever such a postulate would be it could not be this one. Let *p* denote a proposition describing facts of observation, and  $\phi$  a propositional function such that  $\phi(p)$  means "the facts included in *p* may be generalized." Then  $\phi$  is a principle of generalization, and its possible arguments are a certain range of propositions. The statement that  $\phi$  has been verified in all known cases of its arguments is then  $(p = p_1, p_2 \dots p_n) \phi(p)$ , or  $\phi(p_1), \phi(p_2) \dots \phi(p_n)$ . But if  $\phi$  was the principle needed to generalize this we should be considering the proposition  $\phi \{(p = p_1, p_2, \dots p_n) \cdot \phi(p)\}$ , and the propositional function  $\phi$  appears in its own argument. Such a proposition is meaningless by the theory of types. It appears therefore that a postulate needed to generalize a principle of generalization could not be the same as the principle itself, so that the argument would not be circular in the popular sense; but it remains true that we are no further forward.

† 'Phil. Mag.', vol. 42, p. 386 (1921).

with repeated experimental verification of the conclusions the posterior probability may approach (but not reach) certainty. But so far as can be judged from the writings of official\* relativists the experimental verification has nothing to do with the reasons for accepting the postulates. Otherwise I should have expected them to mention some lines of argument that, in fact, they never do mention. It is frequently asked whether the observed facts explained by the theory of relativity and not by Newton's theory are capable of any other explanation; whether the eclipse displacement of star images and the excess motion of the perihelion of Mercury are explicable by means of the refraction and gravitation of matter near the sun; and whether there is any other form of the law of gravitation that would explain them as well as Einstein's. I have discussed elsewhere† the possible amount of matter near the sun and shown that its effects on the two phenomena would be negligible. We cannot perhaps disregard the possibility that official relativists see some error in my discussion, but in that case, if their attitude on more fundamental issues was the same as mine, they might have been expected to produce a better one. I have also shown that there is no law of gravitation of simplicity comparable with Einstein's (and therefore, according to our theory, with any appreciable prior probability) that will explain the facts; but this result, which seems to be of interest to many, to judge by their questions, has not been thought worthy of mention by official relativists. I can only conclude that they are so fully convinced by the *a priori* argument that experimental evidence is unnecessary. To holders of such a view experiments become merely a game that some people (occasionally even the holders themselves) find amusing, and sometimes a means of enabling them to detect mistakes in the mathematics. But then the failure of a prediction must lead to one of two results: either denial of the experimental facts, or discovery that the original hypotheses, at first believed on *a priori* grounds with certainty, are now on *a priori* grounds impossible, and must be replaced by new hypotheses, also believed with certainty on *a priori* grounds. My own attitude would be, of course, that apart from purely logical (including mathematical, but not empirical) inconsistencies, both sets of hypotheses had a finite probability independent of the experiments, but that the experiments show the one to be impossible on the new data, and give the other a high posterior probability.

\* Perhaps I should apologize for the word "official"; but I consider myself a believer in the principle of relativity, and some means is needed to distinguish me from those who believe it for different reasons from those that make it acceptable to me.

† 'Mon. Not. R. Astr. Soc.,' vol. 80, pp. 138-154 (1919).

It may be remarked that whether we believe them or not, the first and third of these attitudes cannot be logically disproved. Taking the first, if a man restricts his data to the bare facts of logic and the immediate data of sensation, and refuses to admit any further hypothesis, he can never get further than the development of pure mathematics and the description of sensation ; and the further hypothesis needed for generalization is certainly incapable of proof on these data alone. But psychologically this attitude seems to be impossible ; everybody does in fact make inferences by generalization, and in particular accepts testimony, which needs this principle to establish that different people mean, at least approximately, the same thing by the same words. As Russell\* has remarked, complete scepticism is barren, but irrefutable.

The third belief also is incapable of disproof. However many hypotheses have been investigated and abandoned, the fact on this view affords no ground for disbelieving the one advocated at any given moment. For if we inferred its falsity from previous instances we should be using a principle of generalizing from observation, which a holder of this belief would not admit. So long as such a hypothesis is undisproved, we are not in a position to say flatly that it is false, and its author can maintain that it is certain. The real objection to this view, apart from personal beliefs, is its limited range of applicability. If it is correct, it may be possible some day to infer the ratio of the velocity of elastic waves at the centre of the earth to the velocity of light from purely *a priori* considerations ; but it seems likely that it will take some time, and at present I prefer to use quicker if more pedestrian methods.

Coming to the hypotheses of Group 2, we see that they admit the force both of observation and of some *a priori* consideration not derivable from the postulates of pure logic. It seems that anyone accepting the possibility of generalizing from experience must adopt some hypothesis of this group. But at the start we come up against the difficulty already mentioned under the law of contradiction. Given the finite number of observations available on any occasion, there is usually more than one law that will fit them. If we have to decide on the observations alone we are no further forward, because these laws will in general give different predictions of future events. The observations do not establish a unique inference, but a range of inferences. By pure logic we have no means of deciding between these, and therefore it is at this point that our new principle must enter. We introduce the idea of a relation between one proposition *p* and another proposition (or aggregate of propositions)

\* " Our Knowledge of the External World," p. 67.



$q$ , expressing the *degree* of knowledge concerning  $p$  provided by  $q$ . This may amount to implication ( $q$  implies  $p$ ) or inconsistency ( $q$  implies not- $p$ ), as extreme cases. This relation is called "the probability of  $p$  given  $q$ ." The fundamental assumption of the theory is that probabilities are comparable in terms of the relations "more probable than" and "less probable than," which are transitive. With this assumption we can proceed, by a series of conventions, involving no further hypothesis, to the measurement of probabilities by numbers from 0 to 1 and to the fundamental laws connecting probabilities.\* From these the formal development follows deductively. The principle of Inverse Probability, which Fisher and others habitually mention as an unwarranted hypothesis, becomes on this view a theorem.

The existence of a numerical theory of probability, however, is not enough for practical application without some rules for deciding what numbers are to be put into it. The fundamental rule is the Principle of Non-sufficient Reason, according to which propositions mutually exclusive on the same data must receive equal probabilities if there is nothing to enable us to choose between them. This principle, considering our fundamental notion, seems to me so obvious as hardly to require statement; but it is at this point that many writers, having proceeded correctly so far, refuse to take the necessary further step and render the theory sterile or confused. I have already considered the point at some length,† and will here only give an example. Keynes‡ writes as follows: "Let us suppose that there is no positive evidence relating to the subjects of the propositions under examination that would lead us to discriminate in any way between certain alternative predicates. If, to take an example, we have no information whatever as to the area or population of the countries of the world, a man is as likely to be an inhabitant of Great Britain as of France, there being no reason to prefer one alternative to the other. He is also as likely to be an inhabitant of Ireland as of France. And on the same principle he is as likely to be an inhabitant of the British Isles as

\* In my treatment it is proved that the product formula

$$P(pq|h) = P(p|h)P(q|ph)$$

holds when the propositions are disjunctions of exclusive and equally probable alternatives, but I do not give a general proof. One has, however, been given by F. P. Ramsey ("Foundations of Mathematics," pp. 177-182). It may be remarked that many writers state the law verbally in a way equivalent to suppressing the  $p$  in the last factor. From this they have no difficulty in deducing absurd results, the absurdity of which they attribute to the theory of probability.

† "Scientific Inference," pp. 20, 29; 'Proc. Camb. Phil. Soc.,' vol. 29, pp. 83-87 (1933).

‡ "Treatise on Probability," p. 44 (1921).

of France. And yet these conclusions are plainly inconsistent. For our first two propositions together yield the conclusion that he is twice as likely to be an inhabitant of the British Isles as of France.

"Unless we argue, as I do not think we can, that the knowledge that the British Isles are composed of Great Britain and Ireland is a ground for supposing that a man is more likely to inhabit them than France, there is no way out of the contradiction. It is not plausible to maintain, when we are considering the relative populations of different areas, that the number of names of subdivisions which are within our knowledge, is, in the absence of any evidence as to their size, a piece of relevant evidence."

Keynes here commits the fallacy, against which he argues effectively elsewhere, of supposing that the probability of a proposition is a function of that proposition and nothing else, instead of an expression of our state of knowledge of the proposition relative to particular data. Suppose, to make the issue a little more precise, that a man in Buenos Aires receives a message to the effect that a European of unspecified nationality is coming to visit him. He must then assess the probability of the various possible nationalities with respect to his available knowledge. If his data are that Great Britain, Ireland, and France are three different countries, and he has no further information as to the number and mobility of their inhabitants, he must assess their probabilities equally, and the probability that the visitor comes from Great Britain or Ireland is twice the probability that he comes from France. If, on the other hand, he considers that the British Isles are one country, of which Great Britain and Ireland are divisions, he must assign to the British Isles and France the same probability, dividing that assigned to the British Isles equally between Great Britain and Ireland. Keynes's dilemma does not exist, and is merely an indication of incomplete analysis of the nature of the data.

Keynes agrees with Fisher in the belief that a probability cannot be assessed on our *a priori* knowledge alone, though, I think, in nothing else. But it may be remarked that if we can assign a meaning to a probability on experience, we can certainly assign one without it. Consider two propositions  $p$  and  $q$ , and denote our *a priori* knowledge by  $h$ . Then

$$\begin{aligned} P(p|qh) P(q|h) &= P(pq|h) = P(p|h) P(q|ph) \\ P(\sim p|qh) P(q|h) &= P(\sim p|h) P(q|\sim p \cdot h) \end{aligned}$$

and by division

$$\frac{P(p|h)}{P(\sim p|h)} = \frac{P(p|qh)/P(q|ph)}{P(\sim p|qh)/P(q|\sim p \cdot h)}$$

But the sum of the numerator and denominator in the expression on the left is unity. Hence if  $P(p|qh)$  and  $P(\sim p|qh)$ , the posterior probabilities of the proposition  $p$  and its contradictory on the data are known, as Keynes would admit, and those of  $q$  on the hypotheses  $p$  and not  $p$  are also known, as I think even Fisher would admit,  $P(p|h)$  is perfectly definite. This proposition is capable of generalization by replacing  $h$  by  $rh$ , where  $r$  may be any other set of observational data. It follows that if we can assess the probability of a proposition  $p$  on data  $qrh$ , we can also assess it on data  $rh$ , and then on data  $h$ . It is essential to the theory that a true *a priori* distribution of probability exists, that is, a probability assignable on our *a priori* data alone. This is to be distinguished from the prior probability, which is the probability before some particular test, and may rest on a certain amount of previous observational evidence.

Such an *a priori* distribution of probability must satisfy certain conditions, and can be tested in two ways. We may consider it as such, examining what distribution describes our *a priori* knowledge; or we may investigate what distribution is consistent with facts otherwise known about the posterior probability on certain types of data. Both methods have been applied to the problem discussed in the paper\* attacked by Fisher, and lead to the same result. My postulates for the case under discussion are (1) that the quantity to be measured has a true value  $x$ , about which the probability of various measures is distributed according to the normal law with precision constant  $h$ †; (2) that the prior probability that  $x$  and  $h$  lie in particular ranges  $dx$ ,  $dh$  is  $f(h)dx dh$ ; (3) that, apart from the measures, we have no knowledge relevant to the values of  $x$  and  $h$ . My reason for discussing these hypotheses is that they appear to be satisfied, with one trifling caution, stated in the paper, in the majority of actual methods of measurement. Fisher considers that it is an objection to my theory that with different assumptions I should have got a different answer, and thereby misses the entire point of the theory. Had I begun with different assumptions I should have been discussing a different problem. If, as he suggests, I might have begun with the form

$$f(h) = ae^{-ah}$$

that would imply previous knowledge that the probability is  $e^{-1}$  that  $h$  exceeds

\* 'Proc. Roy. Soc.,' A, vol. 138, pp. 48-55 (1932).

† It is, of course, a fallacy to say that the *observations* are distributed according to the normal law. The normal law is a continuous distribution, and the observations are in all cases a finite set.

the known value  $1/a$ , and is inconsistent with the hypothesis that we have no previous knowledge about the value of  $h$ .\* With such previous knowledge there would, of course, be no need for any further discussion of the form of  $f(h)$ ; if it is already known, it is known, and there is no more to be said. As a matter of general principle, I must point out again at this stage that in problems of inference the introduction of an *a priori* assumption is not a defect; on the contrary, no correct theory can be developed without one, and the important thing is that the assumption should be correct.

Fisher says that it would be remarkable that on *a priori* grounds such a distribution of probability could be determined; still, remarkable or not, it has been obtained. I think that in this statement he is confusing the existence of the probability distribution with the possibility of making inferences from it. *The fact is that my distribution is the only distribution of prior probability that is consistent with complete previous ignorance of the value of  $h$ .* It is clear that with such ignorance  $f(h)$  cannot involve any quantity other than  $h$ ; for if it involved some known quantity  $a$  of the same dimensions as  $h$ , we could determine the prior probability that  $h$  is less than  $a$ , namely,

$$\int_0^a f(h) dh / \int_0^\infty f(h) dh. \quad (1)$$

Since  $h$  is a measured quantity, not a pure number, the only significant functions of  $h$  not involving other quantities of its own dimensions are powers of  $h$ ; e.g.,  $e^{-h}$  means nothing if  $1/h$  is a length. Then the ratio of the probabilities that  $h$  is less and greater than  $h_0$  is

$$\int_0^{h_0} h^n dh / \int_{h_0}^\infty h^n dh. \quad (2)$$

If  $n > -1$ , this is zero for all values of  $h_0$  and it is certain that  $h$  is infinite. If  $n < -1$ , it is infinite for all values of  $h_0$  and it is certain that  $h$  is zero. But with  $n = -1$ , the integrals diverge at both limits and their ratio is indeterminate. It is in this case, and only in this, that the distribution of probability tells us nothing as to the probability that  $h$  will exceed any definite value; and for this reason alone it must be the correct distribution when we have no previous knowledge relevant to the value of  $h$ .

\* We are familiar with the fallacy that if  $p$  implies  $q$ ,  $q$  implies  $p$ . Fisher's argument here is of the form "if  $p$  implies not  $q$ , and  $q$  implies not  $p$ , then  $p$  is false." It would follow that when a necessary and sufficient condition is known for the truth of a proposition, that proposition is always false. The argument is therefore of great power.

If we have one observation, say  $a$ , the posterior probability of  $x$  and  $h$  is given by the law

$$I(x, h) dx dh \propto f(h) \frac{h}{\sqrt{\pi}} e^{-h^2(x-a)^2} dx dh, \quad (3)$$

and the contribution from each value of  $h$  is greatest for  $x = a$ , which is therefore the most probable value, as we should expect. But suppose we take  $f(h) \propto 1/h$ , and attempt to determine the posterior probability of values of  $h$ . The probability that  $h$  lies in a particular range  $dh$  is proportional to

$$dh \int_{-\infty}^{\infty} I(x, h) dx \propto dh \int_{-\infty}^{\infty} e^{-h^2(x-a)^2} dx \propto \frac{dh}{h}, \quad (4)$$

so that a single observation does not affect the distribution of the probability of  $h$ . This is what we should expect, since a single observation can tell us nothing about its own precision. It is only when we have two observations that a definite standard of precision, given by their separation, is introduced; and it is precisely then that the theory for the first time leads to definite results as to the probability that  $h$  exceeds a certain value, the integrals corresponding to (2) converging at both limits. At all points the theory gives results in accordance with expectation.

Fisher proceeds to reduce my theory to absurdity by integrating with respect to all values of the observed measures. This procedure involves a fundamental confusion, which pervades the whole of his statistical work, and deprives it of all meaning. The essential distinction in the problem of inference is the distinction between what we know and what we are trying to find out: between the data and the proposition whose probability on the data we are trying to assess. If we have made two observations,  $\pm a$  in my notation,  $u \pm v$  in Fisher's, those are our observations, and there is no more to be said. To integrate with respect to them and average a function of them over the range of integration is an absolutely meaningless process. Yet in Fisher's constructive, as well as in his destructive work, this process is carried out again and again.

Fisher, in trying to construct a theory of statistical inference without the use of probability, naturally has to adopt a number of *a priori* hypotheses, of the existence of which he seems to be unaware. I should point out therefore, first, that his fundamental definition of frequency is meaningless.\* He says: "When we say that the probability of throwing a five with a die is one sixth,

\* 'Phil. Trans.,' A, vol. 222, p. 312 (1922).

we must not be taken to mean that of any six throws with that die one and one only will necessarily be a five; or that of any six million throws, exactly one million will be fives; but that of a hypothetical population of an infinite number of throws, with the die in its original condition, exactly one sixth will be fives." That a mathematician of Dr. Fisher's ability should commit himself to the statement that the ratio of two infinite numbers has an exact value can only be regarded as astonishing. The difficulty had, of course, been evaded by Venn and others previously by introducing the idea of a limit when the number of tests becomes large, but at the cost of making it impossible ever to determine a probability or to prove any inference\*; further, it avoids no assumption, for the existence of the limit can be proved, if at all, only by using probability as a primitive idea, which the aim of the definition is to avoid. But the simple answer to Fisher's theory is that the hypothetical infinite population does not exist, that if it did its properties would have to be inferred from the finite facts of experience, and not conversely, and that all statements with respect to ratios in it are meaningless. As an analysis of the form taken by the probability of the observations given the hypothesis Fisher's treatment may in certain cases have some value, but as a theory of the converse process involved in the testing of a hypothesis it has no status whatever.

The second part of Fisher's paper illustrates this point very clearly. He starts with a "normal population with standard deviation  $\sigma$ " and infers a differential  $df$  for the distribution of the variation of the standard deviation  $s$  in a sample drawn in the usual way. This form can be made significant if we abandon the idea of a normal population with an infinite number of members and state the result in terms of the probability of the composition of a sample, given the true value and the standard error.† But Fisher, having got his distribution (which of course, becomes on my view the distribution of the *probability* of the standard deviation in the sample) proceeds to say that the distribution of the ratio  $s/\sigma$  is calculable solely from the number of observations in the sample. But the determination of the probability of  $s$ , given  $\sigma$ , is not the same thing as the determination of the probability of  $\sigma$  given  $s$ ; to compare them the prior probability of  $\sigma$  must be introduced. It is of no use to say, as

\* Wrinch and Jeffreys, 'Phil. Mag.,' vol. 38, pp. 715-731 (1919); Jeffreys, "Scientific Inference," pp. 218-222; Keynes, *loc. cit.*, chapt. VIII.

† Fisher's use of "standard deviation" differs from mine; I use "error" to denote any difference from the true value, and "deviation" to denote any difference from the mean of the actual sample, which will in general differ somewhat from the true value.

Fisher does, that the prior probability of  $\sigma$  is unknown ; partly because this is often untrue, and partly because, if the prior probability is in fact unknown, it introduces an element of uncertainty into all possible inferences beyond the observed data, and Fisher's estimates of the uncertainty are in all cases too low. Further, Fisher's "fiducial probability" refers to a mean taken over all possible random samples, and it may be asked why this should be thought to have much relevance to any particular sample. To take an illustration from the hackneyed but useful problem of balls in a bag, suppose we have drawn five white balls in succession. Our inferences would differ in the following cases, according to our previous knowledge : (1) total ignorance of the composition of the collection in the bag ; (2) knowledge that the bag contained 100 balls, a white one having been inserted every time a coin came down heads, and a black one every time it came down tails ; (3) knowledge that it contained originally precisely five white balls. In the first case we should infer that considerably more than half the balls are probably white ; in the second we should infer that by a coincidence we have happened to pick five white balls in succession out of a collection that probably contains about 50, and almost certainly between 30 and 70 black ones ; and in the third that there are no white balls left in the bag. Fisher's method would include all these in his mean ; and such a mean is useless for purposes of inference to a particular case.

The theory of probability, on the other hand, allows us to take such previous knowledge into account completely.

#### *Summary.*

(1) The process of generalizing from observational data is necessary to the greater part of scientific method. A theory of this process cannot be constructed from logic and observation alone, but requires an *a priori* postulate incapable of proof from logic and observation. It is necessary to have such a postulate or to reject scientific inference altogether.

(2) It is impossible to disprove the possibility of deriving the whole of science from *a priori* considerations without reference to observation ; but there seems to be no convincing reason for believing it, and the domain of such a method is in any case too restricted for general application.

(3) The theory of probability provides a primitive postulate capable of serving as a foundation for an adequate theory of generalization from experience. Objections to the theory all seem to arise from failure to apply its rules

correctly. In particular the objection to the assessment of a probability without previous observational knowledge amounts to the statement that ignorance cannot be described, which seems clearly untrue.

(4) Fisher's theory rests on incorrect premises and his fundamental definition is mathematically meaningless. The later development confuses the known and the unknown, and makes it impossible to allow for previous relevant knowledge.

---

*The Isotopic Constitution and Atomic Weight of Lead from Different Sources.*

By F. W. ASTON, F.R.S.

(Received March 14, 1933.)

In continuation of the previous communications\* on the isotopic constitution of the elements determined by photometry of their mass-spectra this paper contains an account of experiments made on lead. Much of the work was done over a year ago and, on account of their great importance in geological problems, some of the numerical results were published.† It seemed desirable that the complete account should include, if possible, results of at least one of those abnormal samples reported to have an atomic weight less than 206. These have now been obtained and as the mass-spectrograph is now being partially reconstructed and may not be available for further work of the same kind for some time further delay is unnecessary.

Lead is unique among the elements in that it is formed in workable amounts by different processes of radioactive disintegration and so does not have a constant isotopic constitution. The first mass-spectra showing its lines were obtained with the second mass-spectrograph by a discharge in the tetramethyl made from ordinary lead‡ and indicated isotopes 206, 207, 208 roughly in proportions 4, 3, 7 with possibly others. Two years later a specimen of the methyl compound of lead from Norwegian Broggerite was prepared and analysed. The mass-spectra obtained were poor but enabled the three lines 206, 207, 208 to be identified and their relative intensities roughly estimated

\* 'Proc. Roy. Soc.,' A, vol. 134, p. 571 (1932).

† 'Nature,' vol. 129, p. 649 (1932).

‡ 'Nature,' vol. 120, p. 224 (1927).



at 100, 10.7, and 4.5. At the time there was no reason to suppose that the intensities could be affected by the presence of a hydride, so the percentages were worked out at 86.8, 9.3, 3.9. The presence of line 207 was of the greatest interest for, as was pointed out, there was excellent reason for identifying this with the final product of the actinium series, which would settle the atomic weights of the members of the series, that of protactinium being 231.\* Assuming the ratio 100 : 7 for the number of atoms of uranium lead to actinium lead Lord Rutherford† was able to work out the period of actino-uranium, the parent of the actinium series and an isotope of uranium, to be  $4.2 \times 10^8$  years, and deduce other important cosmical conclusions.

These results were criticized by Holmes‡ who maintained that the percentages of 207 found by the mass-spectrograph and used in the calculations were much too high. His own estimate from chemical atomic weights was about 3 which makes the period of actino-uranium much the same as that of uranium I.

Accurate knowledge of the isotopic constitution of the radiogenic leads is of the first importance in the problems of geologic time and of the origin of actinium. Mass-spectrum analysis appears to be the only possible source of this. Dr. A. v. Grosse who is particularly interested in the actinium problem kindly offered to prepare for me specimens of methyls of leads from ores whose geological and chemical data were well established. Such leads were fortunately made available owing to the generous action of the scientists who owned them and as soon as a few rare samples had been prepared I started the work of analysis. This was in November, 1931, immediately after the analysis of uranium fluoride which, as reported,§ gave the definite information that uranium was essentially a simple element and contained no isotope other than 238 to the extent of 3 per cent., a result which itself had a definite bearing on the general problem.

Since the analysis of the Broggerite lead several things had occurred affecting the outlook on the work. The most hopeful one was the improvement in the vacuum technique of the instrument. Lead tetramethyl decomposes during the discharge and the hydrogen formed during the long exposures was known to be the cause of the feeble and ill-defined results previously obtained, for it was not removed efficiently by the cooled charcoal used for evacuation.

\* F. W. Aston, 'Nature,' vol. 123, p. 313 (1929).

† *Ibid.*

‡ 'Nature,' vol. 126, p. 348 (1930).

§ F. W. Aston, 'Nature,' vol. 128, p. 725 (1931).

This difficulty had now been removed by the use of a high-speed diffusion pump on the slit system.\* On the other hand the work of Bainbridge† had made it clear that lines 65 and 69 in the mass-spectrum obtained from zinc methyl were due to hydrides and not, as I had assumed,‡ to true isotopes. His later work§ has shown that three isotopes of germanium 71, 75, 77|| are also under suspicion for the same reason. The sequence of relative intensities of mass-spectra derived from tin tetramethyl make it reasonably certain that with that element, at least, little or no hydride is present, but it was clear that results obtained from lead tetramethyl could no longer be assumed free from hydride effect and that this must be looked for and if possible measured.

Other difficulties in the way of accurate analysis of leads are raised by the fact that the mass numbers are high, which means that the magnetic deflecting fields must be correspondingly great with consequent difficulties in maintaining them constant. The photographic efficiency of lead rays will be small and the curve relating blackening with intensity will be of the unfavourable type shown by mercury. The lines will be too close together for the method of intermittent exposures, but in some compensation for this it so happens in practice that lead methyl, if perfectly pure, gives an extraordinarily smooth and steady discharge so that reliable results can be obtained simply by exposures of different periods taken in sequence.

The first methyl analysed was that of a sample of very pure uranium lead called Katanga I. The discharge ran well, which is evidence of the high purity of the compound, and thanks to the improved vacuum clean sharp spectra were produced. Three lines 206, 207, 208, were visible and their intensities were determined to be 100, 9.51, 0.19 respectively, the accuracy being at least five times as great as for the Broggerite lead already noted. Of course, every effort was made to eliminate mercury and its mass-spectrum was reduced so far that comparison between its lines 202 and 204 could be used to show that no appreciable quantity of Pb 204 was present.

Using the same discharge tube, which was in an unusually good setting, an attempt was made to analyse a sample of methyl from lead derived from Swedish Kolm, one of those with an abnormally low atomic weight. This was found to be very impure. The discharge behaved unsteadily and no results

\* 'Proc. Roy. Soc.,' A, vol. 134 p. 572 (1932).

† 'Phys. Rev.,' vol. 39, p. 847 (1932).

‡ 'Proc. Roy. Soc.,' A, vol. 130, p. 305 (1931).

§ Privately communicated.

|| 'Proc. Roy. Soc.,' A, vol. 132, p. 495 (1931).

could be obtained. A third sample Katanga II was now admitted and the discharge again ran perfectly as with Katanga I. The bulb was run for a long time under normal conditions, by which it is certain that much the greater part of the lead left in the walls from the previous samples must have been removed. Again good spectra were obtained and the ratios when measured were indistinguishable from those of Katanga I.

The inlet apparatus was carefully washed as before and sample Wilberforce admitted. As before good spectra resulted, but a careful scrutiny of line 206 suggested that the discharge was still contaminated with lead from the earlier samples. In order to make quite certain of this very important point the methyl of ordinary lead was admitted with all the usual precautions. Even after exhaustive running the spectra showed line 206 stronger than line 208. This made it perfectly certain that the bulb was still contaminated with lead 206 from the previous samples and that no reasonable period of running would eliminate it. This unfortunate residual effect would, of course, not be serious in samples so nearly identical as Katanga I and II, but for general analysis it was very evident that a fresh discharge bulb would be necessary for each lead.

This is a much more serious difficulty than would appear at first sight, for the setting of a new discharge tube is an uncertain operation at best. During investigations on isotopes in the past, once a favourable one had been obtained weeks of useful work with a great variety of compounds could be expected. In addition the hope of comparing the mass-spectra of different radiogenic leads under identical experimental conditions vanished, and one would have to be content with the nearest approximation practicable.

The difficulty had to be faced, and as no further work of a sufficient urgency could be found for it I regretfully dismantled a bulb still working extremely well and after a tedious series of trials replaced it with another which was moderately satisfactory. As ordinary lead was now in the apparatus this was now analysed with results which will be detailed later.

So far no information on the vital question of the presence or absence of hydride effect had been possible, but when, after further delay, another fresh tube was got into working order and Thorite lead admitted, highly satisfactory and definite evidence was obtained. Lines 206, 207, 208, 209 appeared with relative intensities finally established at 4.9, 1.5, 100, 2.3. Now Pb 209 is known to exist only to a small extent in ordinary lead so it is at once obvious from the intensities of lines 206 and 207 that any effect of 209 caused by the presence of traces of ordinary lead in the sample can be neglected. On purely theoretical grounds the presence of Pb 209 in so pure a thorium lead is extremely

improbable, and this conclusion is fortunately supported by evidence from the mass-spectrum itself. There is, corresponding to the line 208, another very strong line 223 due to  $\text{PbCH}_3$ , but no trace of an effect at 224 could be detected. This is negative evidence which in the case of isotopes is always the most conclusive. It is therefore quite safe to conclude that under the particular experimental conditions the discharge in lead methyl gives rise to a monohydride only, and this to the extent of 2.3 per cent.

It is admittedly unfortunate that any hydride at all is formed, but so long as every effort is made to ensure the closest agreement of experimental conditions it is possible to use this figure as a correction with considerable confidence. When it is applied to the lines given by Katanga I, which happens to be one of the leads upon which the criticisms of Holmes were based, the effect at 208 practically vanishes and the 206:207 ratio reduces to 100:7.2 showing a remarkably close agreement with Lord Rutherford's estimate as opposed to that of Holmes.

A definite conclusion on the hydride correction having been obtained the Wilberforce sample, which was regarded as the most important geologically, was again taken in hand and a fresh bulb fitted. This was not so good as the previous ones but moderately dependable values for the relative intensities of the lines were obtained. As no other samples of first-class importance were immediately available it was decided to publish the numerical results already obtained and to use the mass-spectrograph for other work until further material arrived.

In June, 1932, another sample made of lead from Kolm was received. This was very small in quantity and though apparently rather purer than the earlier one was quite unsuitable for quantitative photometry. Before it was quite exhausted one mass-spectrum was obtained which showed that 206 and 207 were present and that the proportion of the latter was in no way abnormal for a uranium lead. After this failure the apparatus was used for other work during which the simplicity of niobium and tantalum was demonstrated and two new and very rare isotopes of mercury discovered.\*

In February of this year I received from Dr. v. Grosse the methyl of a lead from Great Bear Lake which was reported to have an atomic weight even lower than that of Kolm lead. An entirely satisfactory analysis was carried out and the quantities of 207 and 208 were both found greater than in Katanga I. By good fortune the discharge was exceptionally free from mercury so

\* F. W. Aston, 'Nature,' vol. 130, pp. 130, 847 (1932).

that the presence of any lighter isotopes sufficient to account for the abnormal chemical atomic weight could be disproved quite definitely. This result confirmed the opinion, which had been suggested by the work with Kolm lead, that an abnormally low atomic weight was not of necessity associated with peculiarly interesting isotopic constitution. Further experiments with a view to increasing resolving power now required the apparatus to be dismantled so it was decided to analyse one more sample only. This was a uranium lead from Morogoro which gave results much the same as Katanga I.

#### *Measurements on Packing Fraction.*

The first attempts to determine the masses of the lead isotope had shown that these were integral with those of mercury to within one or two parts in 10,000. The much improved definition now obtained held out hopes that much better comparisons could be made. Increased accuracy has been obtained, but full advantage cannot be taken of it until higher resolution is available on account of the inevitable error involved in measuring the distance between lines not of the same intensity. The two unit mass intervals between 202, 204 and 204, 206 and also the three unit intervals 201, 204 and 204, 207 were measured on several plates, and in each case appeared integral within one-hundredth of a unit (1 in 20,000), but the line 204 cannot possibly be similar in intensity to 201, still less to 202, and too little is known of their exact mass differences, or indeed of their packing fractions, to enable the masses of 206 and 207 to be fixed. All that can be said at present is that the isotopes of lead probably have packing fractions between 0 and +1. This positive value will tend to balance the correction, still by no means certain, between the physical and chemical scales so that the mean mass numbers should not differ much from the chemical atomic weights, which is found to be so in most of the samples.

#### *Results obtained with Ordinary Lead.*

The same sample of methyl was used as had been employed in the first analysis. This had been kindly supplied by C. S. Piggot.\* No less than five new isotopes were visible on spectra taken with long exposures. The most abundant of these 204 was estimated by measuring the increase in intensity in line 204 relative to the other lines in the mercury group, which could not be eliminated entirely but was reduced as far as possible. These measurements

\* 'J. Acad. Sci., Wash.,' vol. 18, p. 269 (1928).

were made in December, 1931, but before they were published the isotope Pb 204 had already been announced by Schüler and Jones\* from their work on hyperfine structure.

The photometric intensities of the lines were compared by taking a very large number of exposures of many different periods. After correcting these for the presence of 2·3 per cent. of hydride the following figures were obtained for percentage abundance :—

Mass numbers . .	203	204	205	206	207	208	209	210
Abundance . . . .	0·04	1·50	0·03	27·75	20·20	49·55	0·85	0·08

These correspond to a mean mass number 207·190. The present international atomic weight is 207·22. The quantities of the rarer isotopes are only to be regarded as rough estimates.

*Results obtained with Radiogenic Leads.*

The following seven specimens were investigated. For all except the Kolm lead the methylys were prepared by Dr. v. Grosse.

*Katanga I.*—Lead from pitchblende, Katanga, Belgian Congo. Methyl prepared from a sample of the chloride, supplied by Hönigschmid, which had actually been used for his atomic weight determination. Atomic weight 206·048.†

*Katanga II.*—Extracted by v. Grosse and Kurbatow from Katanga pitchblende supplied by Mme. Pierre Curie and Mme. Irene Joliot-Curie. Atomic weight 206·05.

*Thorite.*—Lead from thorite from Langesundfjord, Norway, supplied by Fajans. Part of sample used by Hönigschmid who obtained the highest recorded figure  $207·90 \pm 0·013$  for its atomic weight.‡

*Wilberforce.*—Origin pitchblende from Wilberforce, Ontario. Methyl prepared from chloride used by Baxter and Bliss who found atomic weight 206·195.§

*Bear Lake.*—Uranium lead from Great Bear Lake, Canada. Supplied through Professor A. C. Lane. Reported to have atomic weight about 205·95.

\* 'Naturwiss.,' vol. 10, p. 171 (1932).

† Hönigschmid and Birkenbach, 'Ber. deuts. chem. Ges.,' vol. 56, p. 1837 (1923).

‡ Fajans, 'SitzBer. Heidelberg. Akad. Wiss.,' vol. 3, p. 2 (1918); 'Electrochem.,' vol. 25, p. 91 (1919).

§ Baxter and Bliss, 'J. Amer. Chem. Soc.,' vol. 52, p. 4951 (1930).

## 542 *The Isotopic Constitution and Atomic Weight of Lead.*

*Morogoro.*—Lead from pitchblende from Morogoro, East Africa, obtained from F. Kranz, Bonn.

*Kolm.*—Methyl supplied by G. P. Baxter. Made with material used in determination of atomic weight 206·013.\*

No isotopes other than 206, 207, 208 were found in these leads. The intensities of the lines were compared by giving exposures of periods suitable to give approximately the same blackening, for example, 10 minutes and 1 minute, for 207 and 206 in Katanga I.

The following tables shows the values obtained for percentage abundance after correcting for hydride :—

Lead.	206.	207.	208.	Mean mass number.
Katanga I and II .....	93·3	6·7	(0·02)	206·067
Thorite .....	4·6	1·3	94·1	207·895
Wilberforce .....	85·9	8·3	5·8	206·199
Bear Lake .....	89·8	7·9	2·3	206·102
Morogoro .....	93·1	6·9	0	206·069

Some of these results have already been discussed by v. Grosse.† in connection with the actinium problem. The three sources of error in fixing the atomic weight from mass-spectrum data, namely, the uncertainties of packing fraction, relative abundance and change of scale, happen, with lead, to be all of the same order, about 1 in 10,000. It is very desirable that some source of intense lead rays should be devised which would give mass-spectra free from hydrides for as long as they are present no absolute certainty of composition can be arrived at. But even with this uncertainty the direct results of the mass-spectrograph appear preferable to any indirect calculation from the chemical atomic weight.

In conclusion I should like to express my cordial thanks to all the chemists who have so generously placed rare materials at my disposal, and particularly to Dr. A. v. Grosse for preparing the methyl compounds which made the research possible.

### *Summary.*

Ordinary lead and a variety of radiogenic leads have been analysed with the mass-spectrograph by means of their volatile methyls and the abundance of their isotopes estimated by means of photometry.

\* Baxter and Bliss, 'J. Amer. Chem. Soc.', vol. 52, p. 4848 (1930).

† 'Phys. Rev.', vol. 42, p. 565 (1932).

The presence of a small quantity of hydride has been detected. This has been measured and corrected for.

Measurements of the packing fractions have been made, but with somewhat inconclusive results.

The atomic weights are found to agree fairly well with those found chemically, but the abnormally low value reported for lead from Great Bear Lake is not supported.

---

*The Skin Friction of Flat Plates to Oseen's Approximation.*

By N. A. V. PIERCY, D.Sc., and H. F. WINNY, Ph.D.

(Communicated by L. Bairstow, F.R.S.—Received November 2, 1932.)

Recent observation that flow past tangential flat plates may remain steady up to Reynolds' numbers so great as  $5 \times 10^5$  has renewed interest in the problem of calculating the motion. For large motions, such as are characterized by Prandtl's thin boundary layer of viscous effects, there has long existed the well-known theory of Blasius which recent experiments by Hansen tend to confirm. Approaching the problem from the opposite extreme, Bairstow and Misses Cave and Lang have obtained a solution according to Oseen's approximation to the equations of viscous flow. Their result is given in the form of an integral equation for the distribution of doublets along the plate which will exactly satisfy Oseen's suggestion and the boundary conditions for an infinite fluid. But the solution of the equation has depended so far upon constructing a group of simultaneous equations with numerical coefficients determined by graphical means. The process is cumbersome and only two evaluations have been attempted, viz., at Reynolds' numbers 4 and  $4 \times 10^4$ .

Exact treatment of Bairstow and Misses Cave and Lang's integral equation presents difficulties, but it is possible to find an analytical solution of the equation whose errors throughout the experimental range are probably less than those involved in graphical manipulation. This enquiry is the subject of Section I of the present paper. Section II gives the streamlines and other details of the flow.

In pursuance of the plan adopted in the original investigation, no essential approximations are introduced further to those implied by Oseen's neglect of



certain inertia terms in the complete equations of motion. The physical significance of the results obtained must be decided, except in the case of small motions, by experiment, and unfortunately observations have only been made at large Reynolds' numbers. Even under these conditions, however, divergence from experiment is not so great as might be anticipated. This will appear in Section III, where the present results are also compared with those of the Prandtl-Blasius theory.

### Section I—Analytical Solutions.

The motion is assumed to be two-dimensional and the length  $d$  of the plate is given for convenience the value 2. The plate moves in its own plane through an infinite expanse of fluid at a velocity  $U$ , the ratio of which to  $\nu$ , the kinematic coefficient of viscosity of the fluid is denoted by  $2k$ , so that

$$R = \text{Reynolds' number} = Ud/\nu = 4k. \quad (1)$$

Taking the origin at the nose of the plate and  $Ox$  in the direction of  $-U$ , let us denote by  $E$  and  $M$  two points which may occupy any positions on the boundary and write  $\xi_E, \xi_M$  for  $kx_E, kx_M$ , respectively, and  $w$  for the difference  $\xi_M - \xi_E$ . The equation (E (13), *loc. cit.*) obtained by Bairstow and Misses Cave and Lang for the distribution  $\chi_E$  of doublets along the plate appropriate to the problem is

$$\frac{\pi U}{2} = \int_0^{2k} \left\{ e^w K_0(w) - \frac{1}{2} \frac{\partial}{\partial w} [e^w K_0(w) + \frac{1}{2} \log w^2] \right\} \chi'_E(\xi_E) d\xi_E, \quad (2)$$

where

$$\chi'_E(\xi_E) = \frac{\partial}{\partial \xi_E} \chi_E$$

and  $K_0$  is the Bessel function defined\* generally by

$$K_n(\xi) = \int_0^\infty e^{-\xi \cosh t} \cosh nt \, dt. \quad (3)$$

The doublets satisfy the equations of viscous motion to Oseen's approximation, viz.,

$$\nu \nabla^4 \psi = U \nabla^2 (\partial \psi / \partial x), \quad (4)$$

and  $\chi_E$  as obtained from (2) satisfies the boundary conditions. A solution for

\* The Bessel functions are reckoned as for positive arguments throughout the paper.

$\chi_E$  gives immediately the resistance  $D$  of unit span of the plate by the relation (F (8), *loc. cit.*)

$$D = 4\mu \int_{x_E=0}^{x_E=\frac{1}{2}} d\chi_E \quad (5)$$

where  $\mu = \rho v$ .

*Small Motions, First Approximation.*—With the origin changed to midway along the plate (2) may be written

$$\pi U = \int_{-k}^k \left\{ e^w [K_0(w) - \frac{\partial}{\partial w} K_0(w)] - \frac{1}{w} \right\} \chi'(\xi_E) d\xi_E. \quad (6)$$

Assuming  $w$  small and expanding the kernel, we find, retaining only first terms of the expansions,

$$\pi U = \int_{-k}^k \left( 1 - \gamma - \log \frac{w}{2} \right) \chi'(\xi_E) d\xi_E, \quad (7)$$

where  $\gamma$  is Euler's constant = 0.5772... If the solution is assumed to be of the form

$$\chi'(\xi_E) = A/(k^2 - \xi_E^2)^{\frac{1}{2}}, \quad (8)$$

substitution gives

$$U = A \left[ -\log \frac{k}{2} - \gamma + 1 + \log 2 \right].$$

Hence (8) is a solution of (7) if

$$A = U / \left( 1 - \gamma - \log \frac{k}{4} \right). \quad (9)$$

The distribution of doublets along the plate is given by

$$\chi_E = \int_{-k}^{\xi_E} \chi'(\xi_E) d\xi_E = \frac{U}{1 - \gamma - \log \frac{k}{4}} (\pi - \cos^{-1} x_E). \quad (10)$$

The resistance  $D$ , given by

$$D = 4\mu (\chi_1 - \chi_{-1}),$$

is conveniently specified by a "coefficient of drag"  $k_D$  defined and evaluated as follows:—

$$k_D \equiv \frac{D \cdot d}{\rho U^2 \cdot d^2} = \frac{\pi}{k} \cdot \frac{1}{1 - \gamma - \log \frac{k}{4}}. \quad (11)$$

The result (11) may alternatively be deduced from a generalization by Birstow and Misses Cave and Lang\* of Lamb's† solution for the small motion according to Oseen's approximation of circular cylinders.

*Small Motions, Second Approximation.*—The smallest Reynolds' number at which there is available a graphical solution is  $R = 4$ , the coefficient of drag found being 1.527. Since the formula (11) then gives  $k_D = 1.727$ , it is of interest in the present investigation to form a closer analytical estimate.

Expanding the kernel of (6) as before but retaining squares of small quantities leads to

$$\pi U = \int_{-k}^k \left\{ -\left(\gamma + \log \frac{w}{2}\right) \left(1 + \frac{w}{2} + \frac{w^2}{4}\right) + \left(1 + \frac{w}{4} + \frac{w^2}{6}\right) \right\} \chi'(\xi_E) d\xi_E. \quad (12)$$

It is now assumed for the form of the solution that

$$\chi'(\xi_E) = \frac{A + B\xi_E + C\xi_E^2}{\sqrt{(k^2 - \xi_E^2)}}. \quad (13)$$

After substitution and reduction we find:—

on equating the coefficients of  $\xi$

$$B = \frac{A}{2} \left( \frac{1}{2} + \gamma + \log \frac{k}{4} \right),$$

on equating those of  $\xi^2$

$$C = \frac{A}{4} \left( \frac{7}{6} + \gamma + \log \frac{k}{4} \right),$$

and on equating constant coefficients

$$U = A \left\{ -\left(\gamma + \log \frac{k}{4}\right) \left(1 + \frac{7}{48} k^2\right) + 1 + \frac{3}{32} k^2 \right\}.$$

These values of  $A$ ,  $B$ ,  $C$  make (13) satisfy (6) to the order of the squares of small quantities, and to this order

$$\chi_E = A(\pi - \cos^{-1} x_E) - Bk \sqrt{(1 - x_E^2)} + \frac{Ck^2}{2} \{ \pi - \cos^{-1} x_E - x_E \sqrt{(1 - x_E^2)} \}. \quad (14)$$

The drag coefficient now becomes

$$\begin{aligned} k_D &= \frac{1}{k} \cdot \frac{\chi_1 - \chi_{-1}}{U} = \frac{\pi}{kU} \left( A + \frac{Ck^2}{2} \right) \\ &= \frac{\pi}{k} \cdot \frac{1 + \frac{k^2}{8} \left( \frac{7}{6} + \gamma + \log \frac{k}{4} \right)}{1 + \frac{3}{32} k^2 - \left( 1 + \frac{7}{48} k^2 \right) \left( \gamma + \log \frac{k}{4} \right)} \end{aligned} \quad (15)$$

\* *Loc. cit.*, p. 428. Cf. also Berry and Swain, 'Proc. Roy. Soc.,' A, vol. 102, p. 766 (1922).

† "Hydrodynamics," p. 606.

At  $R = 4$  this expression gives  $k_D = 1.624$ , a value only 6.5 per cent. in excess of the graphical result. But it is evident from the form of (15) that as the Reynolds' number approaches 4 the analytical estimate involves appreciable errors which are rapidly increasing. This straining of the small motions solution is again reflected in the doublet distribution  $\chi_E$  given by (14), which is shown in fig. 1 as a chain-line and may there be compared with the corresponding graphical result indicated by the circular points. Although the

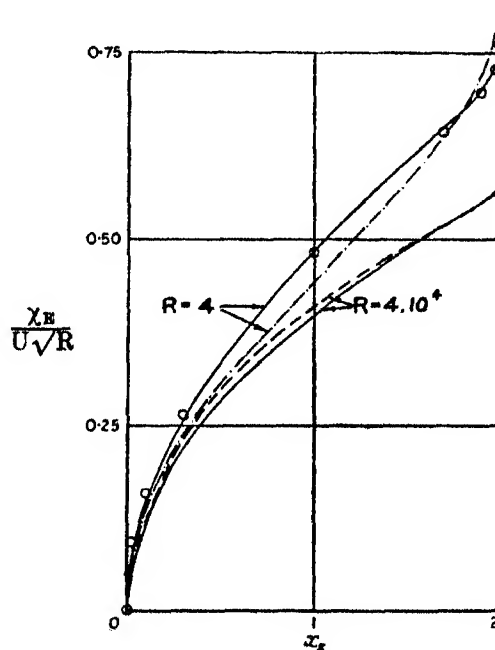


FIG. 1. — present solution (40); - · - present small motion solution (14); — — graphical solution  $R = 4 \times 10^4$ ; o o graphical  $R = 4$ , Bairstow and Misses Cave and Lang.

second approximation gives appreciably less difference from the graphical result than the first, this remains considerable. Errors of this order are to be expected in (14) and the graphical work may be anticipated to provide the closer solution at  $R = 4$ . At smaller Reynolds' numbers, of course, (14) and (15) rapidly become reliable.

*Asymptotic Solution.*—A satisfactory analytical solution is readily obtained for motions which are large though not necessarily approaching the limit for steadiness. We suppose  $R$  to be so great that a small contribution to the integral of (2), arising when the point  $E$  passes through the point  $M$ , may be

neglected, so that it may be assumed that only large values of  $w$  are effective in contributing to the integral.

Introducing the asymptotic expansion of  $K_0(w)$ :

$$K_0(w) = e^{-w} \sqrt{\left(\frac{\pi}{2w}\right)} \left\{ 1 - \frac{1^2}{8w} + \frac{1^2 \cdot 3^2}{2} \cdot \frac{1}{(8w)^2} - \dots \right\} \quad (16)$$

and substituting in (6) (with the origin changed to the nose of the plate as in (2)), we see that the kernel of the equation is of order  $k^{-\frac{1}{2}}$  when  $w$  is large and positive, and of order  $k^{-1}$  when it is large and negative. Thus only positive values need be considered. On retaining the first terms only of the expansions, the expression for  $\chi'(\xi_E)$  reduces to

$$U \sqrt{\left(\frac{\pi}{2}\right)} = \int_0^{\xi_M} \frac{\chi'(\xi_E) d\xi_E}{\sqrt{(\xi_M - \xi_E)}} \quad (17)$$

where the integration is to extend from 0, the nose of the plate, now only to  $\xi_M$ .

The solution of (17) follows from Abel's work\* and is

$$\chi'(\xi_E) = \frac{U}{\sqrt{(2\pi\xi_E)}} \quad (18)$$

Hence

$$\chi_E = U \sqrt{\left(\frac{2\xi_E}{\pi}\right)} \quad (19)$$

and

$$k_D = 2/\sqrt{(\pi k)} = 2 \cdot 257/\sqrt{R}. \quad (20)$$

At  $R = 4 \times 10^4$  the expression (20) gives  $k_D = 0.011284$ , 3.1 per cent. less than the corresponding result obtained by graphical means, viz.,  $k_D = 0.01164$ . In fig. 1 the distribution of  $\chi_E$  according to (19) is shown as a marked full-line curve and may be compared with the graphical distribution which is plotted as a broken-line. Fair agreement exists, and it will appear later that for so large a Reynolds' number the asymptotic solution gives a close approximation except for a failure to reproduce an infinite value of  $\partial\chi/\partial x$  occurring at the back edge of the plate.

Errors in (20) become appreciable for  $R < 10^3$  and for mathematical and physical reasons it is desirable to investigate whether the range of application of the simple asymptotic solution may be extended without introducing serious complication. The following development was undertaken in the first place

\* Abel, "Collected Works," p. 11 (1823). Cf. also Bôcher, 'Camb. Math. Tracts,' No. 10, p. 6 (1914).

with this aim, but the conclusions reached were found to be of wider interpretation.

*Extended Solution.*—While  $k$  remains large a second approximation is suggested by (18) in the form

$$\chi'(\xi_E) = \frac{U}{\sqrt{(2\pi\xi_E)}} + f'(\xi_E) \quad (21)$$

where the added term is assumed to be of order  $k^{-1}$ . Substituting in (6), modified to locate the origin at the nose of the plate, we have

$$\pi U = \int_0^{2k} \left\{ e^w \left[ K_0(w) - \frac{\partial}{\partial w} K_0(w) \right] - \frac{1}{w} \right\} \left\{ \frac{U}{\sqrt{(2\pi\xi_E)}} + f'(\xi_E) \right\} d\xi_E. \quad (22)$$

Approximation of the kernel of this integral equation for  $f'(\xi_E)$  by a use of the same method as employed to obtain (17) gives

$$U \sqrt{\left(\frac{\pi}{2}\right)} - \frac{U}{2\pi} \int_0^{2k} \left\{ e^w \left[ K_0(w) - \frac{\partial}{\partial w} K_0(w) \right] - \frac{1}{w} \right\} \frac{\partial \xi_E}{\sqrt{\xi_E}} = \int_0^{\xi_M} \frac{f'(\xi_E) d\xi_E}{\sqrt{w}}. \quad (23)$$

To order unity the first term only of the asymptotic expansion of  $K_0$  is sufficient, and the left-hand side of (23) becomes

$$U \sqrt{\frac{\pi}{2}} - \frac{U}{\sqrt{(2\pi)}} \int_0^{\xi_M} \sqrt{\left(\frac{1}{w\xi_E}\right)} d\xi_E. \quad (24)$$

On making the substitution:  $Z = \xi_E/\xi_M$  the integration is readily effected and the whole expression is seen to vanish, as would be expected from the significance of the first approximation (18).

The order of smallness assumed for  $f'(\xi_E)$  requires evaluation, however, of terms of order  $k^{-1}$  on the left-hand side of (23). It is convenient to investigate in the first place the term of this order arising from the difference between the second term of (24) and

$$- \frac{U}{2\pi} \int_0^{2k} e^w \left[ K_0(w) - \frac{\partial}{\partial w} K_0(w) \right] \frac{d\xi_E}{\sqrt{\xi_E}}. \quad (25)$$

Since,  $k$  remaining large, the asymptotic expansions cease to hold only close to  $M$ , the difference under consideration may be supposed to arise at the point  $M$ . The term to be added to (24) is

$$- \frac{UA}{2\pi\sqrt{\xi_M}}, \quad (26)$$

where  $A$  is obtained from

$$A = \int_{-h}^h e^w \left[ K_0(w) - \frac{\partial}{\partial w} K_0(w) \right] dw - \sqrt{(2\pi)} \int_0^h \frac{1}{\sqrt{w}} dw, \quad (27)$$

where  $h$  may be supposed large and for convenience to approach  $\infty$ .

The expression for  $A$  may be rewritten

$$A = \int_0^h \left\{ e^w K_0(w) + e^{-w} K_0(w) + e^w K_1(w) - e^{-w} K_1(w) - \sqrt{\left(\frac{2\pi}{w}\right)} \right\} dw. \quad (28)$$

It is known that when  $h$  is large the first of these integrals

$$\int_0^h e^w K_0(w) dw = \sqrt{(2\pi h)} - 1. \quad (29)$$

Evaluating the second,

$$\begin{aligned} \int_0^h e^{-w} K_0(w) dw &= \int_0^\infty \left\{ \int_0^h e^{-w(1+\cosh t)} dw \right\} dt \\ &= \int_0^\infty \frac{dt}{1+\cosh t} - \int_0^\infty \frac{e^{-h(1+\cosh t)} dt}{1+\cosh t} \\ &= 1 \end{aligned} \quad (30)$$

as  $h$  approaches  $\infty$ . The sum of these two integrals vanishes with one-half of the fifth integral of (28), leaving

$$A = \int_0^h \left\{ e^w K_1(w) - e^{-w} K_1(w) - \sqrt{\left(\frac{\pi}{2w}\right)} \right\} dw \quad (31)$$

$$= \int_0^h \{ e^w K_1(w) - e^{-w} K_1(w) - e^w K_0(w) \} dw - 1 \quad (32)$$

from (29). Making use of (3), integrating with regard to  $w$  and collecting terms,

$$A = - \int_0^\infty \frac{e^{-h(\cosh t - 1)} \{ (1 - e^{-2h}) \cosh t + 1 \} dt}{\cosh t + 1} + \int_0^\infty \frac{dt}{\cosh t + 1} - 1, \quad (33)$$

vanishing as  $h$  approaches  $\infty$ .

Thus the additive term (26) is zero to the order considered and (23) becomes

$$\int_0^{\xi_M} \frac{f'(\xi_E) d\xi_E}{\sqrt{w}} = \frac{U}{2\pi} \int_0^{2k} \frac{d\xi_E}{w\sqrt{\xi_E}} \quad (34)$$

$$= \frac{U}{2\pi\sqrt{\xi_M}} \log \frac{\sqrt{(2k)} + \sqrt{\xi_M}}{\sqrt{(2k)} - \sqrt{\xi_M}} \quad (35)$$

the integration being readily performed.

We are now in a position to evaluate  $f'(\xi_E)$  by a further use of Abel's solution, by which we obtain from (35)

$$f'(\xi_E) = \frac{U}{2\pi^2} \cdot \frac{d}{d\xi_E} \int_0^{\xi_E} \frac{1}{\sqrt{\{\xi_M(\xi_E - \xi_M)\}}} \log \frac{\sqrt{(2k)} + \sqrt{\xi_M}}{\sqrt{(2k)} - \sqrt{\xi_M}} d\xi_M. \quad (36)$$

Integrate with regard to  $\xi_E$  and define  $f(\xi_E)$  such that it vanishes when  $\xi_E = 0$ . On making the substitutions:  $\cos^2 \theta = \xi_M/\xi_E$  and  $\sin^2 \alpha = \xi_E/2k$ , the following convenient expression is found for  $f(\xi_E)$ :

$$f(\xi_E) = \frac{U}{\pi^2} \int_0^{\frac{\pi}{2}} \log \frac{1 + \sin \alpha \cos \theta}{1 - \sin \alpha \cos \theta} d\theta. \quad (37)$$

This may be simplified. For regarding  $f(\xi_E)$  as a function of  $\alpha$  and differentiating,

$$\begin{aligned} \frac{d}{d\alpha} f(\xi_E) &= \frac{U}{\pi^2} \int_0^{\frac{\pi}{2}} \frac{2 \cos \alpha \cos \theta}{1 - \sin^2 \alpha \cos^2 \theta} d\theta \\ &= \frac{U}{\pi^2} \cdot \frac{2\alpha}{\sin \alpha}. \end{aligned} \quad (38)$$

Hence

$$f(\xi_E) = \frac{2U}{\pi^2} \int_0^{\alpha} \frac{\alpha_1}{\sin \alpha_1} d\alpha_1. \quad (39)$$

Combining with (19) we obtain a final expression for  $\chi_E$ , viz.,

$$\frac{\chi_E}{U} = \sqrt{\left(\frac{2\xi_E}{\pi}\right)} + \frac{2}{\pi^2} \int_0^{\alpha} \frac{\alpha_1}{\sin \alpha_1} d\alpha_1 \quad (40)$$

where

$$\sin \alpha = \sqrt{(\xi_E/2k)} = \sqrt{(x_E/2)}. \quad (41)$$

Apparently, the remaining integral cannot be evaluated exactly, but its form is very suitable for quadrature, by which we have determined the approximate values:—

$\alpha \div \frac{1}{2}\pi:$	0.2	0.3	0.4	0.5	0.6	0.7	0.8	0.9	1.0
$\frac{2}{\pi^2} \int_0^{\alpha} \frac{\alpha_1}{\sin \alpha_1} d\alpha_1:$	0.064	0.097	0.130	0.165	0.201	0.239	0.280	0.323	0.371

For the resistance coefficient

$$k_D = \frac{2}{\sqrt{(\pi k)}} + \frac{2}{\pi^2 k} \int_0^{\alpha} \frac{\alpha_1}{\sin \alpha_1} d\alpha_1. \quad (42)$$



The definite integral may be expanded in various ways, but that which we have found most convenient is

$$\int_0^{\frac{\pi}{2}} \frac{\alpha_1}{\sin \alpha_1} d\alpha_1 = \frac{\pi}{2} + \pi \log \frac{3^3 \cdot 7^7 \dots (4n-1)^{4n-1}}{1 \cdot 5^5 \dots (4n-3)^{4n-3} (4n+1)^{2n}} \quad (43)$$

where  $n$  approaches  $\infty$ . This expansion rapidly yields the value 1.83077... Hence (42) reduces to

$$k_D = \frac{4}{\sqrt{(\pi R)}} + \frac{1.4839 \dots}{R}. \quad (44)$$

For large motions (44) adds little to the asymptotic expression (20) but at smaller Reynolds' numbers the correction becomes important; at  $R = 10^3$  it is 2 per cent.; if the comparison were made at  $R = 1$ , it would be 66 per cent. We have not investigated analytically the restriction with regard to Reynolds' number finally implied in (44), and there appear difficulties in the way of doing so. But this step is seen to be unnecessary on tentatively comparing the estimate of resistance which the formula provides with the graphical solution at  $R = 4$  and, at still smaller Reynolds' numbers, with the small motions solutions. Various results are collected for comparison in the following table:—

Reynolds' number.	Estimations of $k_D$ by:—			Graphical methods.
	(11).	(15).	(44).	
$4 \times 10^4$	—	—	0.01132	0.01164
4	—	—	1.4994	1.527
1	—	3.870	3.741	—
$4 \times 10^{-2}$	—	48.97	48.38	—
$10^{-2}$	161.10	—	170.96	—
$4 \times 10^{-3}$	360.38	—	406.67	—

The solution (44) differs from the graphical results by only 2.8 per cent. at the large Reynolds' number and by 1.8 per cent. at  $R = 4$ . At  $R = 1$  it differs from (15) by 3.3 per cent. and exactly agrees with the small motions solution at a Reynolds' number slightly less than  $4 \times 10^{-2}$ . The various solutions of (2) are plotted in fig. 2, together with Blasius' solution to Prandtl's approximation which will be referred to in Section III. Thus (44) gives the resistance of flat plates according to Oseen's approximation with unimportant errors throughout the experimental range. It would appear probable that an

explanation of its success at very small Reynolds' numbers must be sought in a comparison of the quantities that are neglected on the two sides of (23).

This success makes of interest a tentative comparison of the distribution  $\chi_E$  of the sources as given by (40) with the corresponding graphical solution at  $R=4$ . The result is exhibited in fig. 1, where the full-line is analytical and is seen to agree closely with the graphically obtained points shown as circles. The analytical solution for  $\chi_E$  at  $R = 4 \times 10^4$  is changed from the asymptotic result only imperceptibly except for a very rapid increase to an infinite value of

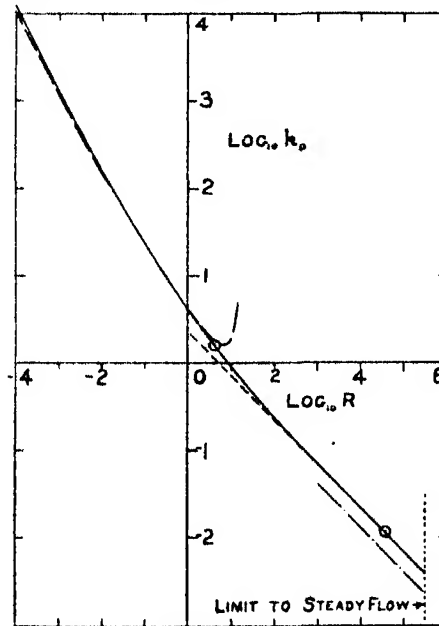


FIG. 2.—Present solutions: — — — asymptotic (20); — — — extended (44); — — — small motion 2nd (15). Graphical:  $\odot \odot$  Bairstow and Misses Cave and Lang. Prandtl's boundary layer theory: — · — Blasius' solution.

$\partial\chi/\partial x$  at the back edge of the plate, a characteristic that was also found in the graphical investigation and will be inferred in Section II to have a peculiar interest in connection with the flow.

## Section II.—Illustrations of the Flow.

*The Streamlines for  $R = 4$ .*—The streamlines at large Reynolds' numbers can be obtained approximately by very simple means as will appear in Section III, but with small motions their delineation calls for graphical work. Let the point E still be restricted to the surface of the plate, but now let M occupy

any position on the plate or in the fluid. Denote the vector EM by  $r$  and the angle which it makes with  $Ox$  by  $\theta$ . In the original paper the stream function is expressed in terms of the distribution of doublets and a function  $L$  of  $r$  and  $\theta$ :

$$\psi_M = \int L_{EM} d\chi_E. \quad (45)$$

A sufficient range of values for present purposes of  $L$  and its derivatives, viz.,

$$\frac{\partial L}{\partial x} = \frac{1}{\pi k} \cdot \frac{\partial}{\partial y} \{e^{ks} K_0(kr) + \log kr\} \quad (46)$$

$$\frac{\partial L}{\partial y} = \frac{2}{\pi} \cdot e^{ks} K_0(kr) - \frac{1}{\pi k} \cdot \frac{\partial}{\partial x} \{e^{ks} K_0(kr) + \log kr\}, \quad (47)$$

has been worked out by Zahra of the Imperial College and the tables are available. The following values were chosen for  $y_M$ : 0.04, 0.1, 0.2, 0.4, 0.7, 1.0, 2.0, and a curve of  $L_{EM}$  to base  $w$  was plotted for each. Graphical integrations were carried out for  $x_M = -0.5, -0.2, -0.05, 0, 0.05, 0.1, 0.2, 0.3, 0.5, 1.0, 1.7, 1.8, 1.9, 1.95, 2.0, 2.05, 2.2$  and 2.5, remembering that the length of the plate has been given the value 2. Hence from a series of curves on a  $y_M$ -base tables were constructed leading to figs. 3 and 4, where  $O$

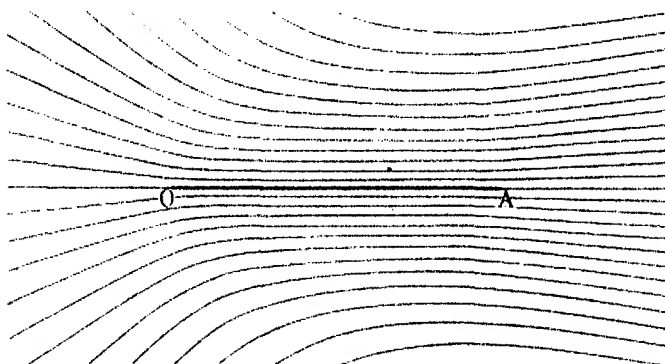


FIG. 3.—Streamlines relative to infinity,  $R = 4$ .

is the nose and A the back edge of the plate. The former figure shows the stream function relative to the fluid at infinity, the latter shows it relative to the plate.

*The Molecular Rotation.*—Various expressions for the molecular rotation  $\zeta$  are given in the original paper. From (46) and (47),

$$\zeta_M \equiv \nabla^2 \psi_M = \int \nabla^2 L_{EM} d\chi_E \quad (48)$$

$$= \frac{2}{\pi} \int \frac{\partial}{\partial y_M} e^{k y_M} K_0(kr) d\chi_E \quad (49)$$

or again, making use of (46),

$$\zeta_M = 2k \int \frac{\partial L_{EM}}{\partial x_M} d\chi_E - \frac{2}{\pi} \int \frac{\partial}{\partial y_M} \log kr d\chi_E \quad (50)$$

while on the boundary

$$\zeta_M = -2\partial\chi_M/\partial x_M. \quad (51)$$

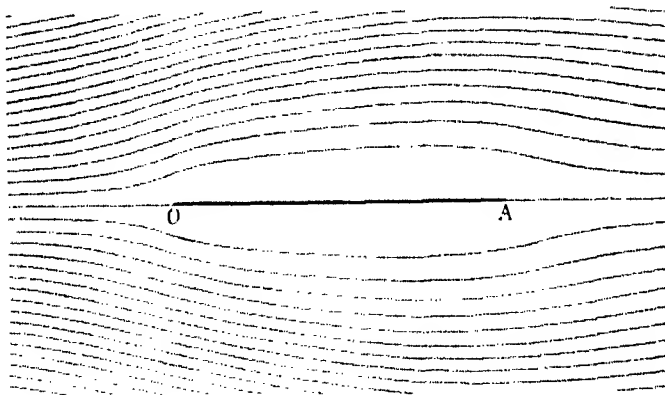


FIG. 4.—Streamlines relative to plate,  $R = 4$ .

A graphical solution was first obtained for  $R = 4$  by use of the available tables. To introduce  $r$  and  $\theta$  for this purpose (50) may be written

$$\zeta_M = 2k \int \left\{ \frac{\partial L_{EM}}{\partial x_M} - \frac{1}{\pi k} \cdot \frac{\sin \theta}{r} \right\} d\chi_E. \quad (52)$$

The first term contains the second to opposite sign so that evaluation is most conveniently effected as a single integration. A series of lines at right angles to the plate were chosen at  $x_M = -0.5, -0.2, -0.05, 0, 0.05, 0.2, 0.3, 0.4, 0.5, 1.0, 1.4, 1.8, 1.95, 2.0, 2.05, 2.2, 2.5, 3.5$ , and along each of these  $\zeta_M$  was obtained graphically at  $y_M = 0.04, 0.1, 0.2, 0.4, 0.7, 1.0, 2.0$  and  $4.0$ . Fig. 5 was then constructed from curves of  $\zeta_M$  set out on a  $y_M$ -base.

For large Reynolds' numbers it is possible to obtain an approximate solution

for the distribution of  $\zeta_M$  from the asymptotic expression (19) for  $\chi_E$ , but the distribution of vorticity for  $R = 4 \times 10^4$  has been found graphically from the graphical solution for  $\chi_E$ .

Substituting from (16) in (49) since  $kr$  remains large and retaining only the first term of the expansion,

$$\zeta_M = - \sqrt{\left(\frac{2k}{\pi}\right)} \int \frac{\sin \theta}{\sqrt{r}} \cdot e^{-kr(1-\cos \theta)} d\chi_E. \quad (53)$$

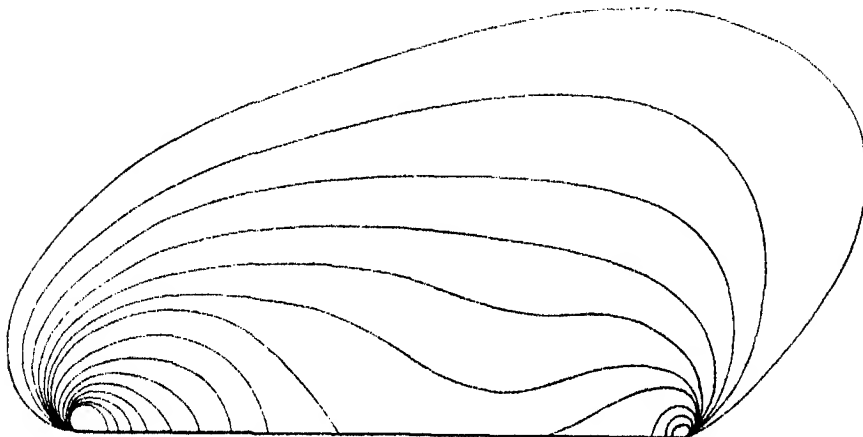


FIG. 5.—Molecular rotation for  $R = 4$ .

The intervals chosen for  $x_M$  were practically the same as with the smaller Reynolds' number, but it was found unnecessary to go more deeply into the fluid than  $y_M = 0.04$ . The actual values chosen for  $y_M$  were: 0.001, 0.004, 0.01, 0.015, 0.02, 0.025, 0.04. Using the system of calculation already described fig. 6 was constructed, where the linear scale perpendicular to the plate has been expanded ten times to make the details discernible.

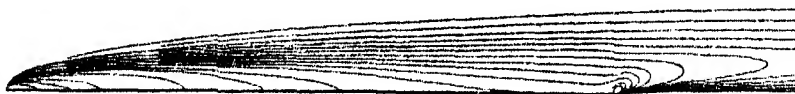


FIG. 6.—Molecular rotation for  $R = 4 \times 10^4$ . Linear scale perpendicular to plate  $\times 10$ .

The peculiar distribution of rotation close to the back edge of the plate follows from the rapid increase in  $\partial\chi/\partial x$  occurring before that edge is reached. This feature has already been noted in (40), but in the analytical solution it is more localized than in the graphical one. In either case the final increase in

$\chi_E$  recedes to the back edge as  $R$  increases and may possibly be associated with the production of an eddy in this region at large Reynolds' numbers.

*Section III.—Comparison with the Prandtl-Blasius Theory and with Experiment.*

Prandtl's approximate form of the equations of motion depends, as is well known, upon the layer of fluid appreciably affected by viscosity remaining thin until the wake is reached and so the theory is restricted to large Reynolds' numbers. Blasius' solution on this assumption for flat plates gives for the drag coefficient :

$$k_D = 1.327/\sqrt{R}. \quad (54)$$

This is plotted as a chain-line in fig. 2 for comparison with the present solution to Oseen's approximation. The asymptotic solution (20) is seen to be of the same form as (54) but to indicate a resistance that is greater by 70 per cent.

To carry the comparison further, and before introducing experiment, it is desirable to obtain a general expression for  $u_M$  according to Oseen's equation. It will be appreciated on account both of the nature of the Prandtl-Blasius solution and of the restricted range of existing experimental observations that attention in the present section is of necessity confined to large Reynolds' numbers such that errors in the asymptotic solution may be neglected.

From (45) of Bairstow and Misses Cave and Lang's original paper,

$$u_M = - \int \frac{\partial L_{EM}}{\partial y_M} \cdot \frac{d\chi_E}{dx_E} dx_E. \quad (55)$$

The expression (47) may be rewritten

$$\frac{\partial L_{EM}}{\partial y_M} = \frac{1}{\pi} \left\{ e^w [K_0(kr) + \cos \theta \cdot K_1(kr)] - \frac{\cos \theta}{kr} \right\}, \quad (56)$$

while from (18)

$$\frac{\partial \chi_E}{\partial x_E} = U \sqrt{\left( \frac{k}{2\pi x_E} \right)}. \quad (57)$$

On substituting (56) and (57) in (55) it is seen that the last term of (56) will result in an increment of  $u_M$  of order  $k^{-1}$  and when  $\theta$  is small this is negligible because, from the asymptotic expansions of  $K_0$ ,  $K_1$ , it is evident that the remaining term of (56) will contribute a quantity of order unity. Only large and positive values of  $w$  ( $= kx_M - kx_E$ ) need be considered, for when  $w$  is large and negative the integral is obviously negligible. Also  $kr$  may be considered to

be large, for when this is not so the integral will augment  $u_M$  by a term again of order  $k^{-1}$ . Hence, while  $\theta$  may be considered sufficiently small to neglect the difference between  $\cos \theta$  and unity, retaining only the first terms of the asymptotic expansions, we find (55) reduces for  $k$  large to

$$u_M = -\frac{U}{\pi} \int_0^{\infty} \frac{e^{w\tau} \sqrt{(k^2 y^2 + w^2)}}{\sqrt{[x_E (x_M - x_E)]}} dx_E, \quad (58)$$

where  $x_E$  may be supposed to have an upper limit which approaches  $x_M$  as closely as is consistent with  $\theta$  remaining small. On expanding by the binomial theorem with this assumption:

$$w = \sqrt{(k^2 y^2 + w^2)} = -\frac{k^2 y^2}{2w}, \quad (59)$$

reducing (58) to

$$u_M = -\frac{U}{\pi} \int \frac{e^{-\frac{k^2 y^2}{2w}}}{\sqrt{[x_E (x_M - x_E)]}} dx_E. \quad (60)$$

Making the substitution:

$$\frac{k^2 y^2}{2w} = z^2,$$

we obtain

$$u_M = -\frac{Uy}{\pi} \sqrt{\left(\frac{2k}{x_M}\right)} \int \frac{e^{-z^2} dz}{\sqrt{\left(\frac{ky^2}{2x_M}\right)} z \sqrt{\left(z^2 - \frac{y^2 k}{2x_M}\right)}} \quad (61)$$

where the integration may now be regarded as extending to  $\infty$ .

This integral may be evaluated. For considering the integral:

$$I \equiv \int_a^\infty \frac{ae^{-z^2} dz}{z \sqrt{(z^2 - a^2)}} = \int_0^\infty \frac{e^{-a^2 \cosh^2 t} dt}{\cosh t},$$

$$\frac{dI}{da} = -2a \int_0^\infty \cosh t \cdot e^{-a^2 \cosh^2 t} dt = -e^{-a^2} \sqrt{\pi},$$

therefore

$$I = -\sqrt{\pi} \int_0^a e^{-a_1^2} da_1 + \text{a constant},$$

and when  $a = 0$ ,

$$I = \int_0^\infty \frac{dt}{\cosh t} = \frac{\pi}{2},$$

so that

$$I = -\sqrt{\pi} \int_0^a e^{-a_1^2} da_1 + \frac{\pi}{2} = \sqrt{\pi} \int_a^\infty e^{-a_1^2} da_1.$$

Hence (61) is expressible in the form

$$u_M = -\frac{2U}{\sqrt{\pi}} \int_{\sqrt{\left(\frac{ky^2}{2x_M}\right)}}^{\infty} e^{-a_1^2} da_1 \quad (62)$$

and its values may be written down from tables of the probability integral.

At large Reynolds' numbers the expression (62) gives  $u_M$  correctly through the entire boundary layer, becoming  $-U$  on the boundary  $y = 0$ . Thus the expression is readily checked by re-calculating the drag coefficient  $k_D$  from the velocity gradient it gives on the boundary.

Again, it will be noted from (62) that the velocity distribution at the large Reynolds' numbers considered is a function of  $y/\sqrt{(vx/U)}$  only. This is well known also to be characteristic of Blasius' solution to Prandtl's approximation. The assumptions made in deriving (62) are tantamount to supposing a thin boundary layer to exist. Agreeing, as is usual, to mark the edge of the boundary layer by a small change of the velocity of the fluid from the undisturbed value, and accepting 1 per cent. of the relative velocity of the plate for this purpose, we find, from tables of the probability integral, for  $\Delta$  the thickness of the boundary layer on either side of the plate at the position  $x$  along it

$$\Delta_e = 2.58 \sqrt{x/k} = 3.64 \sqrt{(vx/U)}. \quad (63)$$

At the back edge of the plate this gives

$$\Delta/d = 3.64/\sqrt{R}, \quad (64)$$

while the corresponding thickness found by Blasius is given by

$$\Delta/d = 5.5/\sqrt{R}. \quad (65)$$

Thus the two boundary layers are of the same parabolic form, but the boundary layer according to Oseen's equation is one-third thinner than that resulting from Prandtl's approximation.

At large Reynolds' numbers observations have been made by Burgers and Zijnen\* and by Hansen† of the distribution of velocity through steady boundary layers attached to flat plates. The two sets of experiments are not in agreement, but Hansen has investigated the difference and has shown reason why his results apply more reliably to flat plates moving through an infinite fluid.

\* 'Verh. Akad. Wet. Amst.,' vol. 13, p. 32 (1924).

† 'Z. Math. Phys.,' vol. 8, p. 185 (1928).



Accordingly, Hansen's observations, although they show the greater divergence from the present analytical solution, will alone be considered. They were made with plates of length 50 cm. in an airstream whose velocity ranged from 400 cm. per second to 3600 cm. per second, fine pitot tubes being traversed close to the surface at various distances  $x$ , from 1 cm. to 25 cm., behind the nose or front edge. During the course of the experiments effects of varying the shape of the nose and the roughness of the surface were investigated but were found not to be important in the present connection.

The observations given in the original paper are replotted in fig. 7 against the non-dimensional quantity  $y/\sqrt{(vx/U)}$ , together with the present solution, which is shown as a full-line, and Blasius' solution, shown as a broken-line.

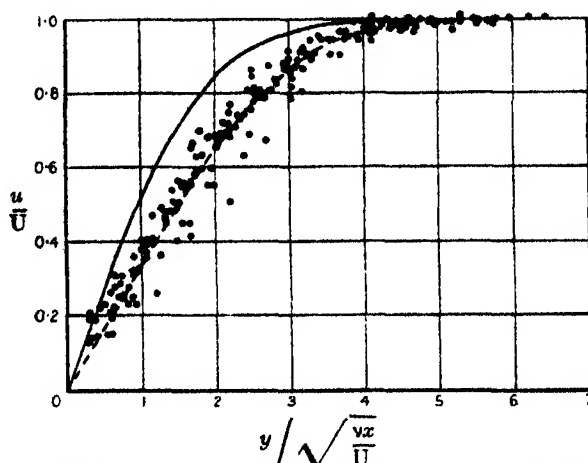


FIG. 7. — Oseen's approximation ( $R$  large); - - - Prandtl's approximation (Blasius); . . Experiment (Hansen) ( $R$  large).

As will be seen from the figure, the experimental points lie close to the Blasius solution, with which, however, they are not completely in accord, but show a displacement towards the present solution. At the high Reynolds' numbers at which the experiments were carried out this result would be expected. But with much smaller motions experiment would be anticipated to agree more closely with the results of Oseen's approximation; it would be of interest to conduct experiments at much smaller Reynolds' numbers to verify this deduction.

The authors acknowledge with pleasure the valuable help and suggestions received from Professor Bairstow, F.R.S., and they are indebted for a grant to the Department of Scientific and Industrial Research.

*Summary.*

In 1923 Professor Bairstow and Misses Cave and Lang obtained an integral equation for the distribution of doublets satisfying exactly the equation, of viscous motion to Oseen's approximation, and the boundary conditions for a flat plate moving in its own plane through an infinite expanse of fluid. Hitherto, the equation has yielded, however, only to cumbersome methods of evaluation at chosen Reynolds' numbers. In the present paper Abel's work is applied to obtain an approximate analytical solution in the form of a simple continuous function of Reynolds' number. The method is proved only for motions of appreciable magnitude, but comparison with a second order solution for small motions, which is also obtained, and with existing graphical evaluations shows that it applies with unimportant errors throughout the experimental range.

Streamlines and other details of the flow are illustrated. A feature of large motions is a concentration of vorticity at the back edge of the plate, suggesting the eventual formation of an eddy there.

At the large Reynolds' numbers considered in the well-known Prandtl-Blasius theory the present solution reduces to the same form. Asymptotically, the resistance is found to be 70 per cent. greater and the viscous boundary layer one-third thinner than calculated by Blasius from Prandtl's approximate equations. This indicates the ultimate importance of the inertia terms neglected by Oseen. Examination of careful experiments recently carried out by Hansen, however, suggests that the present theory may diverge somewhat less from observation than from Blasius' solution even near the limiting Reynolds' number for steadiness, viz.,  $5 \times 10^5$ . There appears need for further experiments at intermediate Reynolds' numbers, when closer agreement between observation and the present solution might be expected.

---

*The Determination of the Angles between Covalencies, from  
Measurements of Electric Dipole Moment.*

By G. C. HAMPSON and L. E. SUTTON.

(Communicated by N. V. Sidgwick, F.R.S.—Received December 6, 1932.)

*Introduction.*

Of the methods which have been devised for the measurement of angles between covalencies, the one based on measurements of electric dipole moments is among the most valuable.

Descriptions of considerable experimental work on the subject have been published by several authors, but the discussions of the basis of the method, its further possible applications, the possible errors and their probable importance, are not only scattered, but incomplete. It therefore appeared desirable that a more complete, general treatment of these matters should be given, and the present communication is an attempt to do this.

In the discussion that follows, all electric dipole moments are given in terms of  $10^{-18}$  e.s.u.

*Basis of Method.*

Covalencies may be regarded as characterized by electric dipole moments, the axes of which lie along the lengths of the valencies, and the moment of a particular link is approximately constant in magnitude in similar types of compound.\*

Since electric dipole moments are vectors, it is possible to apply the methods of vector analysis in suitable cases to determine the angles between them, from a knowledge of their individual magnitudes and that of their resultant, and therefore we may sometimes evaluate the angles between covalencies from such measurements.†

\* Thompson, 'Phil. Mag.,' vol. 46, p. 497 (1923); Højendahl, "Studies of Dipole Moment," Diss., Copenhagen (1928); Eucken and Meyer, 'Phys. Z.,' vol. 30, p. 398 (1929); Debye, "Polare Molekeln," Leipzig, p. 59, *et seq.* (1929); Smyth, "Dielectric Constant and Molecular Structure," New York, pp. 63, 88, 99, 101 (1931); Wolf and Fuchs, "Stereochemie" (Freudenberg), Leipzig and Vienna, p. 235 (1932); Sutton, 'Proc. Roy. Soc.,' A, vol. 133, p. 668 (1931).

† Smyth and Morgan, 'J. Amer. Chem. Soc.,' vol. 49, p. 1030 (1927); Bergmann and Engel, 'Z. Phys. Chem.,' B, vol. 8, p. 117 (1930), *cf. later.*

These determinations are often only qualitative, thus in particular it is frequently possible to decide whether or not the covalencies in a molecule are collinear, or coplanar, but sometimes angles may be determined comparatively accurately and it is with this latter, quantitative type of determination, that we are concerned in this communication.\*

### Simple Quantitative Applications.

In the case, a very common one, wherein there are two covalency moments of known, but not necessarily equal, magnitude  $\mu_1$ ,  $\mu_2$ , the angle between them,  $\theta$ , may be calculated, if the magnitude of their resultant  $\mu_R$  also be known, from the equation

$$\theta = \cos^{-1} \frac{\mu_R^2 - \mu_1^2 - \mu_2^2}{2\mu_1 \mu_2}. \quad (1)$$

Similarly, if there are three vectors of known, *equal* magnitude  $\mu_1$ , equally inclined to each other, it is possible, knowing the magnitude of the resultant  $\mu_R$ , to calculate the angle  $\theta$  between each pair, from the equation

$$\theta = 2 \cos^{-1} \frac{1}{2} \sqrt{\frac{3\mu_1^2 + \mu_R^2}{3\mu_1^2}}. \quad (2)$$

When the covalency moments under consideration are the only ones in the molecule (as are the O—H moments in the water molecule) or when any others are so small that they may be neglected by comparison, the resultant moment of these components is the total moment of the molecule. This resultant has, however, more often to be determined from the change in moment which occurs when the components are introduced into a molecule which already has an appreciable moment. Certain restrictions apply to this latter method, since the change in moment is a function not merely of the magnitude of the resultant of these vectors so introduced, but also of the angle between it and the moment of the original molecule. The practical consequences of this will appear subsequently.

An example of the application of the former of these methods is the calculation of the angles between the C—halogen valencies in methylene chloride, bromide, and iodide, and in chloroform, bromoform, and iodoform. We may assume that in these compounds the moments of the C—H valencies may be

\* For qualitative applications see Williams, 'Fortschr. Chem. Phys.,' vol. 20, p. 280 *et seq.*; Smyth, *loc. cit.*, p. 66 *et seq.*; Sidgwick and Bowen, 'Chem. Soc. Ann. Rep.,' p. 387 *et seq.* (1931); Wolf and Fuchs, *loc. cit.*, p. 252 *et seq.*

neglected in comparison with those of the C—halogen links, and that the magnitude of the latter may be taken as equal to those of the corresponding methyl halides. The errors introduced by these two assumptions tend to cancel out each other.\*

The values obtained are given in Table I and compared with those calculated, for the chloro compounds, by Bewilogua† from the distances between the atoms as determined by X-ray diffraction experiments on the vapours.

(Dipole moment values are from Debye, *loc. cit.*, including supplements.)

Table I.

Substance.	$\mu_1$ .	$\mu_R$ .	$\theta$ Dipole.	$\theta$ X-Ray.
$\text{CH}_2\text{Cl}_2$ .....	$1.88 \pm 0.05$	$1.56 \pm 0.05$	$131^\circ \pm 3^\circ$	$124^\circ \pm 6^\circ$
$\text{CHCl}_3$ .....	$1.88 \pm 0.05$	$1.11 \pm 0.05$	$116^\circ 16' \pm 10'$	$116^\circ \pm 3^\circ$
$\text{CH}_2\text{Br}_2$ .....	1.80	1.40	$134^\circ 0'$	—
$\text{CHBr}_3$ .....	1.80	0.99	$116^\circ 44'$	—
$\text{CH}_2\text{I}_2$ .....	1.63	1.10	$140^\circ 34'$	—
$\text{CHI}_3$ .....	1.63	0.90	$116^\circ 40'$	—

#### Interaction between Dipoles.

The agreement of the two sets of data is within the limits of experimental error. In some other cases wherein the components are close together there is, however, sufficient interaction between them to vitiate the calculation. For example, the angles between the C—halogen valencies in the ortho di-halogenated benzenes calculated by Smyth and Morgan (*loc. cit.*) and by Bergmann, Engel, and Sandor‡ are improbably large, though there are no X-ray measurements in the vapour by which they may be checked. For *cis*-dichloroethylene, however, such measurements have been made,§ and Bergmann and Engel|| compared the results obtained by the two methods.

\* Bergmann, Engel, and Wolff, 'Z. phys. Chem.,' B, vol. 17, p. 81 (1932), have performed a similar calculation, allowing a value of 0.4 for the moment of the C—H link. There appears to be no experimental justification for so high a value being taken.

† 'Phys. Z.,' vol. 32, p. 265 (1931). Bewilogua used his observed angles to calculate dipole moments for comparison with those reported.

‡ 'Z. phys. Chem.,' B, vol. 10, p. 106 (1930).

§ Debye and Ehrhardt, 'Phys. Z.,' vol. 31, p. 142 (1930), for revised values see Bewilogua, 'Physikalisch-Chemisches Taschenbuch' (Drucker), Leipzig (1932).

|| 'Z. phys. Chem.,' B, vol. 8, p. 111 (1930).

Taking the moment of chlorbenzene (1.55) to give the moment of the C—Cl link in this case and taking the mean of Errera's value\* and Müller and Sack's value,† 1.80, for the moment of *cis*-dichloroethylene, he calculated the angle to be 106°.‡

The value given by the X-ray data, now recalculated taking the Cl—Cl distance as 3.6 Å., the C = C distance as 1.33 Å.§ and the C—Cl distance as 1.8 Å.,|| is, however, 78° which agrees quite well with the value 70.5° calculated from the Van't Hoff model for the molecule. Here, therefore, there is marked interaction, though the vectors are farther apart than in methylene chloride. This has been treated by Smallwood and Herzfeld¶ as a simple polarization, but in view of the comparatively normal behaviour of the chlorinated methanes it is probable that some other effect, connected with the presence of the double bond, is more important.\*\*

#### *Substitution Methods.*

If the components between which the angle is being measured are covalencies formed by monovalent atoms with some polyvalent linking atom or group, as in the cases cited, or in water or ammonia, then this angle must necessarily be calculated from their resultant, and, as we have seen, if they are close together errors are apt to arise from interaction. If, however, at least one of the covalencies is formed by a carbon atom, which is part of a benzene ring, with such a linking atom or group, the angle between this and another may be determined as the angle between the latter and the covalency of the benzene ring, which is in the *para* position to the former, assuming these *para* covalencies to be collinear.†† Risk of interaction is then greatly reduced, owing to the greater separation of the polar groups used. Thus, there becomes available

\* 'Phys. Z.', vol. 27, p. 764 (1926).

† 'Phys. Z.', vol. 31, p. 815 (1930).

‡ The moment of vinyl chloride has not been measured, but from the similarity of the moments of vinyl bromide (1.4) and brombenzene (1.52) it appears probable that it would be approximately equal to that of chlorbenzene.

§ 'Chem. Soc. Ann. Rep.', p. 384 (1931).

|| Bewilogua, 'Phys. Z.', vol. 32, p. 265 (1931).

¶ 'J. Amer. Chem. Soc.', vol. 52, p. 1919 (1930).

\*\* Cf. Hückel, "Dipole Moment and Chemical Structure," p. 90 (Debye), London (1931); Bennett, 'Chem. Soc., Ann. Rep.', p. 132 (1929); Sutton, *loc. cit.*

†† Williams, 'Phys. Z.', vol. 29, p. 683 (1928); Errera, *loc. cit.*; Weissberger and Sängewald, 'Phys. Z.', vol. 30, p. 792 (1929); Smyth, Morgan and Boyce, 'J. Amer. Chem. Soc.', vol. 50, p. 1536 (1928); Smyth and Morgan, *loc. cit.*; Walden and Werner, 'Z. Phys. Chem., B, vol. 2, p. 10 (1929).

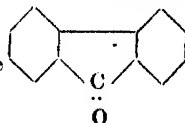
a series of methods for determining angles which we may classify as the "substitution methods." Not only do these offer the possibility of obtaining more accurate values but, even more important, they frequently provide the only possible means of measuring the angles between the covalencies of certain atoms, as for example oxygen or nitrogen, where, since it is impossible to determine the moment of any oxygen or nitrogen valency independently of a previous knowledge of the angle, the first group of methods, not using substitution, is inapplicable.

The first to be considered are the methods in which mono-substitution is employed. Suppose that it is desired to find the angle between the covalencies Ph—A and A—B and that there is a group X\* substituted in the *para* position to AB, that it has a moment  $\mu_{PhX}$  which acts along the axis of the benzene ring, and that the total moment of the molecule is  $\mu_0$ .† If, now, a second group Y,‡ which has a moment  $\mu_{PhY}$  also acting along the axis of the benzene ring, be substituted for the first, this will cause a change of moment of  $\mu_{PhY} - \mu_{PhX}$ , which will be denoted by  $\mu_s$ ,‡ along the same axis, and the total moment will change to  $\mu_T$ .‡

If X is, for example, hydrogen, and Y is chlorine, then  $\mu_s$  is the observed moment of chlorobenzene, provided that neither  $\mu_{PhX}$  nor  $\mu_{PhY}$  is altered by the presence of the group A—B in the *para* position. In general,  $\mu_s$  is the moment of  $p\text{-C}_6\text{H}_4\text{XY}$ . From these data the vector triangle PQR can be solved, by applying equation (1), and the angle  $180 - \phi$ , between the vector  $\mu_{PhX}$  or  $\mu_{PhY}$  (and therefore the covalency Ph—A) and  $\mu_0$  thus obtained.§

\* Such as H, Cl, Br, I, CN, CH<sub>3</sub>, NO<sub>2</sub> and NC.

† If the group AB is attached rigidly to the benzene ring, so that the two cannot rotate

relative to each other, as in fluorenone , the angle between its moment and

the *meta* covalency may be determined (Bergmann, Engel and Hoffmann, 'Z. phys. Chem.', B, vol. 17, p. 92 (1932)); if the group is not rigidly attached, this angle changes as the group rotates, and the measurements cannot be interpreted. Provided that the only axis of rotation is the line through the two *para* covalencies, the angle between the group moment and the *para* covalency is constant, and can therefore be determined.

‡ These terms,  $\mu_0$ ,  $\mu_s$ , and  $\mu_T$ , are employed in preference to the  $\xi$ ,  $\eta$ , and  $\mu$ , employed by Bergmann, or the  $\mu_1$ ,  $\mu_2$ ,  $\mu$ , employed by Smyth, as they are more self-explanatory.

§ It is also possible, in principle, to determine  $\phi$  from the moment of a compound, in which there are two of the groups AB at opposite ends of the molecule, which can rotate freely relative to one another about a common axis, viz., the line of the valencies joining them to the molecule (e.g., hydroquinone di-methyl ether).  $\phi$  is now the angle between



(a) the angle  $\psi$  between the covalency A—B and the moment  $\mu_0$  is known ;  
(b)  $\theta$  is a known function of  $\phi$ .

(c) the magnitude of the moment  $\mu_{\text{PhA}} - \mu_{\text{PhX}}$  or  
(d) the moment  $\mu_{\text{AB}}$  of the covalency A—B is known,

If the linking atom or group is attached to two or more benzene rings, another, quite independent method of measuring the angle between these becomes available. By introducing groups into the *para* positions in each

the moment of each group and this axis, so the component of each perpendicular to it is  $\mu_0 \sin \phi$ , and therefore the observed moment is  $2\mu_0 \sin \phi$  (Williams, 'Z. phys. Chem.,' A, vol. 138, p. 75 (1928)) whence  $\phi$  can be evaluated. Actually, this method is not very useful, because of the uncertainty that the rotation is completely free, because it is very insensitive if  $\phi$  is between  $65^\circ$  and  $90^\circ$ , and because it cannot distinguish between an acute and an obtuse angle.



ring, so as to cause known changes of moment  $\mu_s$  along the axis of each, and determining their resultant from the change in the moment of the molecule when they are introduced, the angle between them may obviously be obtained. This resultant may be determined from two measurements, of the moment of the molecule before and after substitution, and  $\theta$  can be calculated either from the equation :—

$$\theta = 2 \cdot \cos^{-1} \mu_R / 2\mu_s = 2 \cdot \cos^{-1} (\mu_T - \mu_0) / 2\mu_s^* \quad (3)$$

applicable to the di-phenyl compounds, or from the equation :—

$$\theta = 2 \cdot \cos^{-1} \frac{1}{2} \sqrt{\frac{3\mu_s^2 + \mu_R^2}{3\mu_s^2}} = 2 \cdot \cos^{-1} \frac{1}{2} \sqrt{\frac{3\mu_s^2 + (\mu_T - \mu_0)^2}{3\mu_s^2}} \quad (4)$$

applicable to the tri-phenyl compounds, only if  $\mu_T$  or  $\mu_R$  and  $\mu_0$  are collinear, which in practice means that they must lie along the axis of symmetry of the molecule. Thus, when this condition holds, there are two independent methods of determining the angle between the given covalencies, namely the method just described, and also the previous one using mono-substitution, the condition (b), that  $\theta$  is a known function of  $\phi$  then being satisfied. For compounds with two phenyl groups, *e.g.*, di-phenyl-methane, di-phenyl ether, di-phenyl sulphide, or benzophenone

$$\theta = 360^\circ - 2\phi, \quad (5)$$

and for those with three, *e.g.*, tri-phenyl-methane, or tri-phenyl-amine

$$\theta = 2 \cdot \cos^{-1} \frac{1}{2} \sqrt{3 \cos^2 \phi + 1}. \quad (6)$$

For the latter compounds yet a third, independent determination of the angle may be made, from the change of moment, following substitution into the *para* positions of two of the three benzene rings, when

$$\cos \theta = \frac{3\mu_T^2 + 5\mu_0^2 - 6\mu_s^2 \pm 4\mu_0 \sqrt{\mu_0^2 + 3\mu_T^2 - 3\mu_s^2}}{6\mu_s^2} \quad (7)$$

Thus in general, for compounds satisfying the symmetry condition, that  $\mu_0$  should be collinear with the axis of symmetry of the molecule, there are as many independent ways of determining  $\theta$  as there are benzene rings attached to the central atom.

\* Unless the sense of the moment  $\mu_T$ , relative to  $\mu_0$ , can be deduced independently, these equations give ambiguous results, for  $\mu_R$  can be taken as the numerical sum or difference of  $\mu_T$  and  $\mu_0$ . The mono- and poly-substitution methods are then not entirely independent (*cf.* p. 572).

The next most complex case is that where the moment  $\mu_0$  of an unsubstituted di-phenyl compound is not collinear with the bisector of the angle between the axes of the benzene rings, but is equally inclined to both of these, e.g., di-phenyl-amine, di-phenyl sulphoxide. In order to evaluate  $\theta$  it is then necessary to make three determinations of moment, those of the unsubstituted, the mono-*p*-substituted, and the di-*p*-substituted compounds,  $\mu_0$ ,  $\mu_T$ ,  $\mu_T'$  respectively, when the following equation may be applied

$$\theta = \cos^{-1} \frac{\mu_T'^2 + \mu_0^2 - 2\mu_T^2}{2\mu_0^2} \quad (8)$$

The angle  $\omega$ , between the resultant QP, fig. 2, of the unsubstituted molecule,  $\mu_0$ , and the perpendicular to the plane containing the axes of the two benzene rings,  $Q_Z$ , may also be calculated, from the equation:—

$$\omega = \sin^{-1} \frac{\mu_T^2 - \mu_0^2 - \mu_0^2}{2\mu_0 \cdot \mu_0 \cdot \cos \theta/2} \quad (9)^*$$

If QP, i.e.,  $\mu_0$ , is the resultant of two equal moments, QM, QN, acting along the axes of the two benzene rings, and of another, QS, which, to satisfy the symmetry condition for the type of molecule under consideration, is not coplanar with but is equally inclined to these, then if the resultant, QT, of MQ and NQ alone, be known the angle  $90^\circ - \sigma$ , between the third valency QS and the plane containing the first two may be calculated, using equation (2), and then, since  $\tau$ , the angle between QS and QM, is given by the equation

$$\cos \tau = \sin \sigma \cdot \cos 2\theta, \quad (10)$$

\* The general equations, of which these are simplified forms, were derived by Mr. A. F. Walker, of Brasenose College, to whom we are greatly indebted. The proof is the following, using the nomenclature of fig. 2. The vectors MM', NN', QP ( $a, b, c$ ) are known; the angles  $\theta$  and  $\omega$  are unknown.

MM' has components  $(-a \cdot \sin \theta/2, a \cdot \cos \theta/2, 0)$ ;

NN' has components  $(b \cdot \sin \theta/2, b \cdot \cos \theta/2, 0)$ ;

QP has components  $(0, c \cdot \sin \omega, c \cdot \cos \omega)$ .

The resultant of NN' and QP,  $\alpha$  say, is known, thus

$$\begin{aligned} \alpha^2 &= b^2 \cdot \sin^2 \theta/2 + (b \cdot \cos \theta/2 + c \cdot \sin \omega)^2 + c^2 \cdot \cos^2 \omega \\ &= b^2 + c^2 + 2bc \cdot \cos \theta/2 \cdot \sin \omega. \end{aligned} \quad (i)$$

Resultant of MM', NN', and QP, R say, is known, thus

$$\begin{aligned} R^2 &= (a-b)^2 \cdot \sin^2 \theta/2 + \{(a+b) \cdot \cos \theta/2 + c \cdot \sin \omega\}^2 + c^2 \cdot \cos^2 \omega \\ &= a^2 + b^2 + 2ab \cdot \cos \theta + 2(a+b) \cdot c \cdot \cos \theta/2 \cdot \sin \omega + c^2 \\ (R^2 - a^2 - b^2 - c^2 - 2ab \cdot \cos \theta) b &= (a+b) (\alpha^2 - b^2 - c^2) \\ 2ab^2 \cdot \cos \theta &= (R^2 - a^2 - b^2 - c^2) b - (a+b) (\alpha^2 - b^2 - c^2) \\ &= (R^2 - a^2) b + a(b^2 + c^2) - (a+b) \alpha^2. \end{aligned} \quad (ii)$$

We thus have  $\theta/2$  and (i) then gives  $\omega$ .

the angles between all the valencies of the central atom may be determined. If only QS and not QT be known an ambiguous solution results.

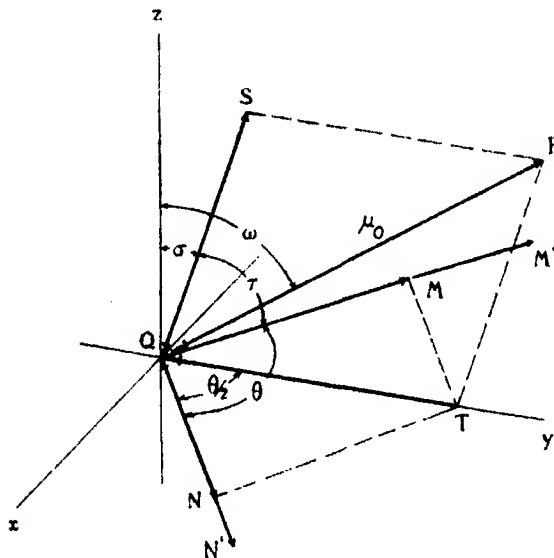


FIG. 2.

An alternative method of determining  $\theta$  and  $\omega$  in this type of molecule is to measure the moments of two derivatives each with two identical groups substituted into the *para* positions, these groups being, of course, unlike in the two derivatives, and differing as widely as possible in the substitution moments,  $\mu_s$ , and  $\mu'_s$ , which each sets up when introduced. If the total moments are  $\mu'_T$  and  $\mu''_T$  respectively, then\*

$$\theta = \cos^{-1} \frac{\mu'_s(\mu_0 - \mu'_T)(\mu_0 + \mu'_T) - \mu_s(\mu_0 - \mu''_T)(\mu_0 + \mu''_T) - 2\mu_s\mu'_s(\mu'_s - \mu_s)}{2\mu_s\mu'_s(\mu'_s - \mu_s)} \quad (11)$$

\* From the above data it will be seen that

$$\begin{aligned} \mu'^2_T &= \mu_0^2 + 4\mu_s^2 \cdot \cos^2 \theta/2 - 4\mu_0\mu_s \cdot \cos \theta/2 \cdot \sin \omega \\ \mu''^2_T &= \mu_0^2 + 4\mu'^2_s \cdot \cos^2 \theta/2 - 4\mu_0\mu'_s \cdot \cos \theta/2 \cdot \sin \omega \\ \sin \omega &= \frac{\mu'^2_T - \mu_0^2 - 4\mu_s^2 \cdot \cos^2 \theta/2}{4\mu_0\mu_s \cdot \cos \theta/2} = \frac{\mu''^2_T - \mu_0^2 - 4\mu'^2_s \cdot \cos^2 \theta/2}{4\mu_0\mu'_s \cdot \cos \theta/2} \\ \cos^2 \theta/2 &= \frac{\mu'_s(\mu_0 - \mu'_T)(\mu_0 + \mu'_T) - \mu_s(\mu_0 - \mu''_T)(\mu_0 + \mu''_T)}{4\mu_s\mu'_s(\mu'_s - \mu_s)} \\ \cos \theta &= \frac{\mu'_s(\mu_0 - \mu'_T)(\mu_0 + \mu'_T) - \mu_s(\mu_0 - \mu''_T)(\mu_0 + \mu''_T) - 2\mu_s\mu'_s(\mu'_s - \mu_s)}{2\mu_s\mu'_s(\mu'_s - \mu_s)}. \end{aligned}$$

$\omega$  can then be evaluated by substitution into the equations for  $\mu'^2_T$  and  $\mu''^2_T$ .

The angle  $\theta$  cannot be determined from the moments of two differently mono-*para*-substituted compounds, since functions of  $\theta$  and  $\omega$  do not then appear as independent variables in the equations.

One still more complex system which deserves attention is that in which the linking group is attached to two benzene rings but where the moment of the unsubstituted molecule,  $\mu_0$ , though coplanar with the axes of these rings, is not collinear with the bisector of the angle  $\theta$  between them. Examples of this type are molecules with the group  $\text{Ph}_2\text{C} =$  doubly bound to another which is unsymmetrical about the plane of the double bond, such as the N-methyl ether of benzophenone oxime, or an anil of benzophenone. Fig. 3 represents such a system, OX, OY are the actual axes of the benzene rings 1 and 2, OZ

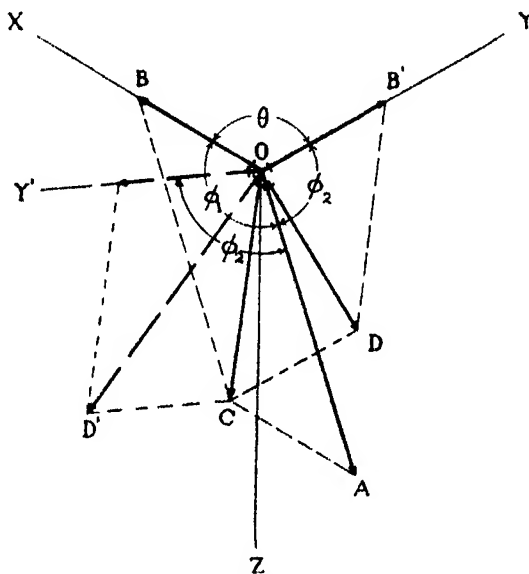


FIG. 3.

is the bisector of the actual angle  $\theta$  between them (and therefore is the direction of the double bond), OA represents  $\mu_0$ .

By introducing a substituent into ring 1, so as to set up a change of moment  $\mu_s$ , OB, along OX, and measuring the total moment  $\mu_T$ , OC, of the product, the parallelogram OBCA can be solved, and the angle  $\phi_1$  thus obtained. Similarly, by substitution into ring 2,  $\phi_2$  can be determined. Since, however, these angles are specified only relatively to OA,  $\theta$  is not uniquely determined, for it could be either the sum or the difference of  $\phi_1$  and  $\phi_2$  (corresponding to XOY and XOY'). To decide between these values, the moment  $\mu'_T$ , OD, of the di-substituted derivative must be measured and compared with the possible values it could have for these values of  $\theta$ , OD and OD', when the correct angle may be distinguished. Thus it is necessary to know the moments

of four different substances. If a single mono-substituted compound and the di-substituted one were used, a similar ambiguity would arise, though in practice it would usually be possible from other considerations (*cf.* footnote p. 568) to choose the correct value in such pairs.

The angles between other covalencies and OX, OY may be calculated by methods similar to those described on p. 567 if the necessary data, *e.g.*, the magnitude of the component of  $\mu_0$  along OZ, are obtainable. If, however, there is a third benzene ring attached to the linking group, as in the anil of benzophenone  $\text{Ph}_2\text{C}:\text{N}.\text{Ph}$ , the angle between any pair of benzene ring axes may be determined by the above described method, and the complete spatial arrangement of the molecule thus derived.

More complex systems than this can be devised, but their analysis is at present of no practical value.

#### *Discussion of Errors.*

In view of the anomalies in the moments of the *ortho*-di-substituted benzenes, which have already been mentioned on p. 564 it appears possible that the groups in the *para*-position to each other may also interact and thus cause the angles calculated by the above described methods to be in error. Various authors have examined this subject\* and in particular Smyth and Wall† have discussed its bearing on this special problem. From comparisons of the observed and calculated moments of *para* di-substituted compounds, they concluded that the interaction was negligible. The range of compounds which they considered was, however, limited and several more relevant values are now available, and are included in Table II, which is an expansion of that given by the above authors.

The dipole moment values quoted are taken from Debye, *loc. cit.*, including supplements 1 and 2, or from Wolf and Fuchs, *loc. cit.*, when they are the only reported values; when several values have been reported the arithmetic mean is given, and the number of values from which it is derived indicated by a bracketted figure.

In general, the observed and calculated values agree to within 0.2 except—

(a) Where the smallness of the moment renders its value peculiarly liable

\* Hojendahl, *loc. cit.*, p. 114; Smallwood and Herzfeld, *loc. cit.*; Tiganik, 'Z. phys. Chem.,' B, vol. 18, p. 425; Wolf and Fuchs, *loc. cit.*.

† 'J. Amer. Chem. Soc.,' vol. 54, p. 1854 (1932).

- to error owing to increased experimental difficulties and the greater effect of uncertainty in the atom polarization (see p. 576),\* and
- (b) Where the two groups cause large and opposed electrometric effects in the benzene ring† as in *p*-nitrophenyl azide and the *p*-cyano-phenyl-halides.

Table II.

Para substituents.		Observed.	Calculated.
CH <sub>3</sub>	NO <sub>2</sub>	4.40 (2)	4.38
	Cl	1.84 (2)	2.01
	Br	1.97	1.97
	NC	3.98	3.94
	N <sub>3</sub>	1.96	2.00
NO <sub>2</sub>	F	2.63	2.48
	Cl	2.42 (3)	2.37
	Br	2.49 (2)	2.41
	I	2.63	2.66
	CN	0.69	0.03
	N <sub>3</sub>	2.8	2.38
CN	Cl	2.61	2.34
	Br	2.64	2.38
	I	2.80	2.63
Cl	NC	2.07	1.93
	N <sub>3</sub>	(0.35)	0.00

Basic Values of  $\mu_s$ .

Ph. . CH <sub>3</sub>	0.45 (3)	Ph. . Cl	1.56 (13)	Ph. . F	1.45
Ph. . NO <sub>2</sub>	3.93 (6)	Ph. . Br	1.52 (5)	Ph. . NC	3.49
Ph. . CN	3.90 (8)	Ph. . I	1.27 (2)	Ph. . N <sub>3</sub>	1.55 (2)

A test which gives a clearer idea of the effect of such possible interactions on the angles as calculated by these methods is the comparison of the values obtained for  $\phi$ , the angle between the moment of the unsubstituted molecule and the axis of the benzene ring, in anisole and aniline, from various *para*-substituted derivatives.‡ Most of the data are those quoted by Bergmann and

\* Errera, "Polarisation Dielectrique," Paris, Press. Univ. (1928); Hojendahl, *loc. cit.*, p. 37; Smyth, *loc. cit.*, p. 163; Wolf and Fuchs, *loc. cit.*, pp. 195, 213.

† See Sutton, *loc. cit.*, and references therein, also Hammick, New and Sutton, 'J. Chem. Soc.', p. 742 (1932).

‡ A few data exist for substituted phenols but the values of  $\phi$  which they give are so discordant that it appears probable that the measurements are in error (Sutton, *loc. cit.* p. 693): the extrapolation of the  $P_s/f_s$  curve for these substances would be especially difficult, owing to their marked association (Sidgwick, "Electronic Theory of Valency," p. 132, Oxford (1928); Sidgwick and Bayliss, 'J. Chem. Soc.', p. 2027 (1930)).

Tschudnowsky,<sup>†</sup> but the values of the angles have been recalculated, both graphically and arithmetically, and in some cases differ appreciably from those given by these authors.

Table III.— $\phi$  in Anisole.

Para-substituent.	Moment of para-substituted derivative. $\mu_T$ .	$\phi$ .	$\mu_R$ .
F	2.09	76	1.45
Cl	2.24	71.5	1.56
Br	2.12	78*	1.52
I	2.27	48	1.3
NO <sub>2</sub>	4.36	77	3.93
CH <sub>3</sub>	1.20	80	0.45

$\mu_0$  (anisole) 1.19 (2).

\* [Note added 13 January, 1933.—A more recent value of 2.24 for *p*-bromoanisole obtained by Smyth and Walls ('J. Amer. Chem. Soc.', vol. 54, p. 3230 (1932)) makes  $\phi$  69°.]

Table IV.— $\phi$  in Aniline.

Para-substituent.	Moment of para-substituted derivative. $\mu_T$ .	$\phi$ .	$\mu_R$ .
F	2.75	47	1.45
Cl	2.97	35	1.56
	2.93	39.5	—
	2.90	43	—
Br	2.87	42	1.52
I	2.82	17	1.3
CH <sub>3</sub>	1.31	50.5	0.45
NO <sub>2</sub>	6.4	(0)	3.93

$\mu_0$  (aniline) 1.55.

The angles calculated from all except the iodo compounds and *p*-nitraniline are concordant to within about 8°, being 71.5–80° for the anisoles, and 40°–47° for the anilines, and this corresponds to an uncertainty of about 0.15 in

<sup>†</sup> 'Z. phys. Chem.', B, vol. 17, p. 100 (1932); *ibid.*, p. 107.

the moments along the benzene axis,\* which is roughly equal to the average discrepancy between observed and calculated moments in Table I.

The anomalies shown by the iodo compounds may be due to inaccuracies in the observed moments,† but that of *p*-nitraniline is very probably due to pronounced interaction between the *para* groups.‡ In this compound, again, the groups set up large and opposed electromeric effects in the ring: a further example of the mutual effect of such pairs of groups is the abnormality of the moments of the *p*-nitroso-di-alkylanilines§ wherein the nitroso group sets up a large electromeric effect|| and the di-alkyl-anilino groups almost certainly set up positive ones. It is, indeed, surprising that the value of  $\phi$  from *p*-nitroanisole is normal. In general, therefore, it appears that provided the compounds used are not of this type the "interaction moment" along any benzene ring axis will not be more than about 0.15 and, to give a rough generalization, angles should be determined within  $\pm 5^\circ$  of their true value.¶ Obviously it is desirable to use as many different substituents as possible, and take a mean value.

In some cases it is possible to minimize the effect of possible interaction by choosing the most suitable of the alternative substitution methods, if more than one is available, according to the following considerations. As we have seen, the angle in a di-phenyl compound which has its moment and axis of symmetry collinear may be determined by either a mono- or a di-substitution method, and it may be shown that, in general, the value obtained from one will be more prone to error caused by interaction than will the other. Suppose that in the mono-substituted compound there is an interaction through the ring which causes a small change of moment  $\delta_1\mu_a$  along the direction of  $\mu_a$ , then by differentiating the Thomson equation (1), calling the angle between the vectors  $\rho$ ,\*\* we find

$$\frac{\delta_1\rho}{\delta_1\mu_a} = \left( \frac{1}{\mu_a \tan \rho} + \frac{1}{\mu_0 \sin \rho} \right).$$

If in the di-substituted derivative similar small changes  $\delta_2\mu_a$  arise in each

\* Determined graphically as the difference of the projections of the anisole or aniline moment vector on the benzene ring axis at the extremes of the observed range of angle.

† Cf. Bergmann and Tschudnowsky, *loc. cit.*

‡ Højendahl, *loc. cit.*, p. 113; Bennett, *loc. cit.*; Hückel, *loc. cit.*

§ Le Fèvre and Smith, 'J. Chem. Soc.', p. 2239 (1932).

|| Hammick, New and Sutton, *loc. cit.*

¶ Cf. K. L. Wolf, 'Z. phys. Chem.', B, vol. 17, p. 465 (1932).

\*\*  $\rho$  will be  $\theta/2$  or  $180 - \theta/2$ , according to the direction relative to the benzene ring, or "sense," of  $\mu_a$ .



ring, then from the differentiation of the equation  $\mu_T = \mu_0 + 2\mu_s \cdot \cos \rho$ , on which equation (3) is based, it follows that

$$\frac{\delta_2 \rho}{\delta_2 \mu_s} = \frac{1}{\mu_s \tan \rho}.$$

If  $\delta_1 \mu_s = n \cdot \delta_2 \mu_s$ , then

$$\frac{\delta_1 \rho}{\delta_2 \rho} = n \left( 1 + \frac{\mu_s}{\mu_0 \cdot \cos \rho} \right), \quad (12)$$

and the first method is more or less accurate than the second as this term is a proper or improper fraction, which may be positive or negative. In the di-substituted compound the total amount of interaction is likely to be greater than that in the mono-substituted one but, since the central, linking atom or group may tend to a state of saturation, or exhaustion, towards these effects, the amount in *each* ring in the former is probably less, i.e.,  $n$  is at least unity but is probably not more than 2. Whatever the value of  $n$ , if  $\rho < 90^\circ$ , so that  $\cos \rho$  is positive, the error in  $\rho$ , and therefore in  $\theta$ , is greater in the first value, while if  $\rho > 90^\circ$  the reverse holds true unless

$$\frac{\mu_s}{\mu_0 \cdot \cos \rho} < -\frac{(n-1)}{n},$$

when again the di-substituted compound gives the more accurate result. This criterion may be applied to decide how best to use various possible substituent groups.

Another matter to be considered is the error in determining the moments. This decreases rapidly as the magnitude of the moment increases because the polarization, which is the term calculated directly from the dielectric data, is a function of the square of the dipole moment. Errors in measurement, therefore, become very much less important when the compound has a considerable moment, and so too do those due to atom polarization, which are liable to be present when the approximate solution method is used\* (for reference see p. 573).

\* [Note added in proof January 13, 1933.—Smallwood in a recent paper ('Z. phys. Chem.', B, vol. 19, p. 242 (1932)), has pointed out that the possible importance of the effect of the solvent in affecting the magnitude of moments determined in solution is often overlooked and suggests that errors may frequently arise from this cause. On examining the available data (e.g., Smyth and Walls, 'J. Amer. Chem. Soc.', vol. 54, p. 3230 (1932), for values in benzene and heptane) it appears, however, that cases where there is marked interaction are exceptional and fall into two main classes, viz., compounds whose moments are functions of the freedom of rotation of the groups in

For this reason the moments of the compounds, both before and after substitution, and of the substituents themselves should be as large as possible, since it is on the accurate determination of these that the evaluation of the angle depends. As a first approximation, taking the absolute errors in polarization due to observation, or neglected atom polarization, as constant, the absolute error in the moment is inversely proportional to the magnitude of the moment. It may be shown that the error in the angle of a triangle, calculated from a knowledge of the lengths of the sides, which are independently variable and each liable to the above type of error, is a minimum when the triangle is equilateral. In practice, one side, QP ( $\mu_0$ ), of the vector triangle is necessarily fixed, and the practical conclusion then is that PR ( $\mu_s$ ) and QR ( $\mu_T$ ) should be at least as great as QP: the possible error in  $\phi$  decreases as they increase relative to QP.

#### Experimental Applications.

Many of the substitution methods described above have already been applied. Of those involving mono-substitution (see p. 566) the first has been used by Hassel and Naeshagen\* to determine the angle between the C = O and Ph — C links in acetophenone, and by Smyth and Walls (*loc. cit.*) to determine that between the C — Cl or C — C  $\equiv$  N and Ph — C valencies in benzyl chloride or cyanide, it being assumed that the moments of the unsubstituted compounds are collinear with the C = O, C — Cl, and C — C  $\equiv$  N valencies, i.e., that the angle  $\psi$  is zero.

The second of these methods has been employed to measure the angles in di-phenyl-methane, di-phenyl ether, di-phenyl sulphide, benzophenone, di-phenyl ethylenic compounds, and di-phenyl sulphone,† the relation  $\theta = 360 - 2\phi$  holding for all these compounds. It has also been used to measure the angle in tri-phenyl-methane,‡ wherein  $\theta = 2 \cdot \cos^{-1} \frac{1}{2} \sqrt{3 \cdot \cos^2 \phi + 1}$ .

them relative to one another, and compounds liable to undergo chemical association. It may be remarked that the agreement between the observed and calculated values in Table I could hardly be fortuitous. It is possible that some of the smaller moments, particularly those of substances with highly polar groups in them, e.g., *p*-nitrobenzonitrile, measured in benzene may be liable to an appreciable error of this sort.]

\* 'Z. phys. Chem.,' B, vol. 15, p. 417 (1932).

† Bergmann, Engel and Wolff, 'Z. phys. Chem.,' B, vol. 17, p. 81 (1932); Bergmann, Engel and Sandor, 'Z. phys. Chem.,' B, vol. 10, p. 397 (1930); Bergmann and Tschudnowsky, 'Z. phys. Chem.,' B, vol. 17, p. 107 (1932); Bergmann, Engel and Meyer, 'Ber. deuts. chem. Ges.,' vol. 65, p. 446 (1932); Bergmann and Tschudnowsky, 'Ber. deuts. chem. Ges.,' vol. 65, p. 457 (1932); Smyth and Walls, 'J. Amer. Chem. Soc.,' vol. 54, p. 3230 (1932).

‡ Bergmann, Engel and Wolff, *loc. cit.*

The third method has been used by Smyth and Walls (*loc. cit.*) to evaluate the angles in anisole and phenetole, taking a value of the moment of the Ph — O valency calculated from the moment of di-phenyl ether, of which the angle had already been determined independently.

The fourth method does not appear to have been applied.

Of the di-substitution methods only that for compounds having two benzene rings and a moment collinear with the axis of symmetry has been used. By means of it, the angles in di-phenylmethane, di-phenyl ether, di-phenyl sulphide, benzophenone, and some di-phenyl ethylenic compounds have been measured (see previous references to these substances).

The tri-substitution method has been used only for tri-phenyl-methane (see previous reference).

The methods in which the moments of mono- and di-substituted derivatives, or of two di-substituted ones, are used simultaneously (see p. 569) have not been previously described. We attempted to use the data for di-phenyl sulphoxide, and the mono- and di-chloro derivatives given by Bergmann and Tschudnowsky\* but obtained a value of about  $-2$  for  $\cos \theta$ . On closer examination it appeared that the values of  $P_{A+O}$  (atom polarization plus orientation polarization), at infinite dilution, used by these authors in calculating the moments of the mono- and the di-chloro compounds were not the most probable extrapolations from their points, and we have therefore recalculated these moments taking values of 270 and 144 (*vice* 323 and 157) for  $P_{A+O}$ , thereby obtaining moments of 3.60 and 2.62 (*vice* 3.94 and 2.7). Using our values,  $\theta$ , from equation (8) is  $119^\circ 36'$ , and  $\omega$  from equation (9) is  $-73^\circ 1'$ . Now, taking the angle between the Ph — S covalencies in di-phenyl sulphide to be  $140^\circ$  (see references above), it follows that, from the moment of the substance (1.47), the moment along each of these valencies is 2.2. If we assume that the moment along each of these is the same in di-phenyl sulphoxide as in di-phenyl sulphide, their resultant in the former compound will be  $2 \times 2.2 \times \cos 59^\circ 48' = 2.21$ . On solving the vector triangle formed by this resultant, the total moment of the molecule, and the moment of the S  $\rightarrow$  O link, the angle  $\sigma$  is found to be  $-37^\circ 30'$ , and therefore  $\tau$  is  $107^\circ 47'$ . The moment of the S  $\rightarrow$  O link, which is evaluated incidentally, appears to be 2.35.

Further discussion of the experimental results will be given in a later paper, in which the results of further measurements on some of the types of substance enumerated will be described.

\* 'Ber. deuts. chem. Ges.,' vol. 65, p. 457 (1932).

In conclusion, the authors wish to express their gratitude to Dr. N. V. Sidgwick for his helpful advice and criticism, and to the Department of Scientific and Industrial Research for grants which have enabled them to conduct this research.

*Summary.*

(1) The principles of the methods of determining angles between covalencies from measurements of electric dipole moment have been explained, and the various methods have been classified.

(2) Some extensions of these methods to more complicated molecules have been described and one has been applied, using existing data for the di-phenyl sulphoxides.

(3) The causes and importance of possible errors have been discussed, and a method of minimizing their effect has been described.

(4) A brief survey has been given of the applications of these methods which have been made up to the present.

---

*The Aerofoil in a Wind Tunnel of Elliptic Section.*

By L. ROSENHEAD, Ph.D., Fellow of St. John's College, Cambridge.

(Communicated by H. Glauert, F.R.S.—Received December 12, 1932.)

*1. Introduction.*

The lift and drag experienced by an aerofoil in a wind tunnel differ from the lift and drag experienced by the same aerofoil under free air conditions. These differences, which are the induced effects due to the walls of the enclosure, can be determined by the aid of general considerations laid down by Prandtl.\* In a closed tunnel, that is, a tunnel with rigid walls, the necessary boundary condition is that the velocity normal to the walls shall be zero. In an open tunnel, or free jet, the condition is that the pressure is constant over the boundary. Assuming that trailing vortices spring from the aerofoil and extend downstream without distortion, Prandtl has shown that the problem can be converted into one dealing with the flow in a section of the wake far behind the aerofoil, the necessary boundary condition being that the velocity potential is

\* 'Nachr. Ges. Wiss. Göttingen,' p. 107 (1919).

constant over the trace of the open tunnel. Prandtl (*loc. cit.*) himself has investigated the interference experienced by an aerofoil in a tunnel of circular section for an elliptic distribution of lift across the span. Glauert,\* to whom a considerable extension of the theory is due, found approximate values of the induced drag in a rectangular tunnel when the span of the aerofoil is indefinitely small. Terazawa† modified Glauert's method and obtained the exact solution for an aerofoil with uniform distribution of circulation in a rectangular channel. Rosenhead‡ obtained exact results for uniform and elliptic distributions both in circular and rectangular tunnels.

More recently, in connection with the building of a wind tunnel of elliptic section, Glauert was led to reconsider the general problem of wind tunnel interference, and his conclusions are embodied in three valuable papers. In the first of these§ he pointed out that the problem discussed by previous investigators is that in which the lift distribution is prescribed to be the same as that in free air, and the aerofoil is twisted in the tunnel to a position in which this distribution is maintained. In general, if the aerofoil is not twisted in this way, there is a change in the distribution of circulation. If this change is taken into account, Glauert has shown for a tunnel of circular section "that the formulæ derived from the assumption of elliptic distribution of lift are sufficiently accurate for all conventional shapes of aerofoil, but that those derived from the assumption of a uniform distribution over-estimate the effect of increasing span of the aerofoil."

He has also shown that, with elliptic distribution of lift, if  $\eta$  and  $\delta$  are defined by the equations|| :—

$$\frac{v}{V} = \eta \frac{S}{C} k_L,$$

$$\delta = \frac{1}{L} \int \eta dL,$$

the necessary corrections  $\Delta\alpha$ ,  $\Delta k_D$  to be added to the angle of incidence and to the drag coefficient, are given by the equations

$$\Delta\alpha = \frac{\Delta k_D}{k_L} = \delta \frac{S}{C} k_L.$$

\* Glauert, "Aerofoil and Airscrew Theory," p. 189 (1930), or 'Aero. Res. Ctte. Rep. and Mem.,' No. 867 (1923).

† Terazawa, 'Rep. Aer. Res. Inst. Tokyo Imp. Univ.,' vol. 4, p. 89 (1928).

‡ Rosenhead, 'Proc. Roy. Soc.,' A, vol. 129, p. 135 (1930).

§ Glauert, 'Aero. Res. Ctte. Rep. and Mem.,' No. 1453 (1931).

|| See list of symbols on p. 603.

In his second paper,\* Glauert reduced Rosenhead's results for the elliptic distribution in the rectangular tunnel to forms suitable for computation and applied the results to the square and Duplex wind tunnels. And in the third paper† he obtained some general theorems on wind tunnel interference. He proved that :—

- (1) The interference on a very small aerofoil in an open tunnel of any shape is of the same magnitude, but opposite in sign, as that on the same aerofoil, rotated through a right angle in a closed tunnel of the same shape.
- (2) The interference velocity is uniform across the span of an aerofoil in any elliptic tunnel having the tips of aerofoil as foci.

The first theorem is strictly true only for very small aerofoils, but will be approximately true for aerofoils of moderate size, and is true for any size of aerofoil in a circular tunnel. As a verification of the theorem, the magnitude of the correction for a small aerofoil in an elliptic tunnel has been calculated.

During the course of some correspondence, Mr. Glauert suggested that as his analysis only dealt with the cases  $s \rightarrow 0$  and  $s = \sqrt{a^2 - b^2}$  it would be very useful if intermediate values could be obtained. This necessitated an exact solution of the problem which is embodied in the following paper. In view of Mr. Glauert's conclusions, the analysis is restricted to the case of elliptic distribution of lift, and all his results for the elliptic tunnel emerge as particular cases of the general solution. In particular, theorem (1) is verified and the divergence from it with increasing span is noted. Further, theorem (2) is verified; the interference velocity is constant across the span of an aerofoil in any elliptic tunnel (closed or open) having the tips of the aerofoil as foci—the respective values being

$$\frac{b}{2(a+b)} \frac{SV}{C} k_L \quad \text{and} \quad -\frac{a}{2(a+b)} \frac{SV}{C} k_L,$$

which are identical with the results obtained by the original investigator. I should like to place on record my indebtedness to Mr. Glauert for many helpful suggestions dealing with the following investigations.

## 2. *To Summarize.*

The complex potentials which have their real or imaginary parts constant over the boundary of an ellipse and also possess logarithmic singularity

\* 'Aero. Res. Ctte. Rep. and Mem.,' No. 1459 (1932).

† Glauert, 'Aero. Res. Ctte. Rep. and Mem.,' No. 1470 (1932).

at an arbitrary internal point are obtained by the use of doubly periodic functions.

The results are extended to obtain the corrections to the lift and angle of incidence induced on an aerofoil either by the rigid walls of an elliptic tunnel or by an open jet of elliptic section, when there is an elliptic distribution of lift over the aerofoil. The results are embodied in various graphs and tables.

If the aerofoil lies symmetrically along the major axis, the correction factor decreases as the aerofoil becomes larger, and *vice versa* if it lies along the minor axis.

In agreement with Glauert, the interference or induced velocity over an aerofoil whose span is equal to the focal distance is found to be constant when there is an elliptic distribution of circulation. Further, Glauert's theorem on wind tunnel interference on small aerofoils is verified in the particular cases discussed, and the variations from it with increasing span are noted.

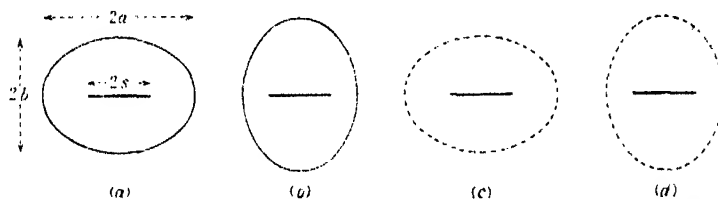


FIG. 1.—(a) Correction factor  $\delta_1$  (closed tunnel); (b) correction factor  $\delta_2$  (closed tunnel); (c) correction factor  $\delta_3$  (open tunnel); (d) correction factor  $\delta_4$  (open tunnel).

The corrections are given by the formulæ:—

$$\Delta\alpha = \frac{\Delta k_p}{k_L} = \delta \frac{S}{C} k_L$$

where the values of  $\delta$  corresponding to the four cases shown in fig. 1 (see also list of symbols on p. 603) are

$$\delta_1 = \frac{ab}{c^2} \sum \frac{rq^r}{1+q^r} G_r^2,$$

$$\delta_2 = \frac{ab}{c^2} \sum \frac{rq^r}{1-q^r} g_r^2,$$

$$\delta_3 = -\frac{ab}{c^2} \sum \frac{rq^r}{1-q^r} G_r^2,$$

$$\delta_4 = -\frac{ab}{c^2} \sum \frac{rq^r}{1+q^r} g_r^2,$$

where the summations are over all *odd* integral positive values of  $r$ . Also, when  $s/c$  is very small

$$\begin{aligned}\delta_1 &= \alpha_1 - \beta_1 \left(\frac{s}{c}\right)^2, & \delta_2 &= \alpha_2 + \beta_2 \left(\frac{s}{c}\right)^2, \\ \delta_3 &= -\alpha_2 + \beta_2 \left(\frac{s}{c}\right)^2, & \delta_4 &= -\alpha_1 - \beta_1 \left(\frac{s}{c}\right)^2.\end{aligned}$$

Further, when  $s/c = 1$ ,

$$\delta_1 = \frac{b}{2(a+b)} \quad \text{and} \quad \delta_3 = -\frac{a}{2(a+b)}.$$

### 3. *The Potential Function for a Rectilinear Vortex Inside an Ellipse.*

The starting point of the present investigation is the complex potential corresponding to a rectilinear vortex inside an ellipse.\* The fluid is incompressible, and the motion outside the vortex is irrotational. The vortex is of strength  $\kappa$  and is situated inside the ellipse  $\frac{x^2}{a^2} + \frac{y^2}{b^2} = 1$  at the arbitrary point  $z_1 = (x_1 + iy_1)$ .

If the vortex is in the fluid outside the cylinder, the appropriate complex potential for the external motion is

$$w = -\frac{\kappa}{2\pi} \log \frac{(z + \sqrt{z^2 - c^2}) - (z_1 + \sqrt{z_1^2 - c^2})}{(z + \sqrt{z^2 - c^2}) - (z_2 + \sqrt{z_2^2 - c^2})}, \quad (1)$$

where if

$$z_1 = a_1 \cos \eta_1 + ib_1 \sin \eta_1,$$

and

$$z_2 = a_2 \cos \eta_2 + ib_2 \sin \eta_2,$$

then

$$\left. \begin{aligned} \eta_1 &= \eta_2 \\ a_2 &= \frac{1}{2} \left[ \frac{(a+b)^2}{a_1 + b_1} + \frac{(a-b)(a_1 + b_1)}{a+b} \right] \\ b_2 &= \frac{1}{2} \left[ \frac{(a+b)^2}{a_1 + b_1} - \frac{(a-b)(a_1 + b_1)}{a+b} \right] \end{aligned} \right\} \quad (2)$$

\* The complex potential function was obtained as a result of some very helpful suggestions made by Mr. D. E. Littlewood of University College, Swansea. When, however, a preliminary paper was submitted embodying the results of this section, it was pointed out by a referee that the problem of the vortex inside an ellipse had already been solved (Coates, 'Quart. J. Pure Appl. Maths.,' vol. 15, p. 356, and vol. 16, p. 81 (1878-79). The solution obtained by Coates is substantially the same as that given above, but the present treatment is more direct, and considerably simpler, than the original one.



These expressions assume very simple forms if we put  $a = c \cosh \xi_0$  and  $b = c \sinh \xi_0$ . The complex potential function used in (1) of this section may be expressed as

$$w = -\frac{\kappa}{2\pi} \log \frac{z - z_1}{z - z_2} + F(z),$$

where  $F(z)$  is a function of  $z$  regular in the domain outside the ellipse, except at infinity, the introduction of this function being necessary in order to make one of the stream lines of the system coincide with the trace of the ellipse.

From (1), it is easy to see that the only points at which the velocity components, given by

$$\frac{dw}{dz} = u - iv$$

become infinite are  $z = z_2, +c_1 - c_1$  neglecting, of course, the expected infinity at  $z_1$ . Since these three points are all in the interior of the ellipse, we can apply equation (1) to the fluid outside the elliptic cylinder.

If now the point  $z_1$  is inside the ellipse, and we wish to investigate the motion in the internal fluid, we cannot use the above equation. As noted before, this complex-potential function produces infinite velocities at  $z = z_2, +c_1 - c$ , and although it is true that here the point  $z_2$  lies outside the ellipse, it is equally true that the points  $\pm c$  now lie within the fluid whose motion we are to investigate, and as it is unlikely from physical principles that an isolated vortex of arbitrary strength at an arbitrary point would produce infinitely large velocities at the foci of the ellipse, we cannot use equation (3.1). Apart from this, there will be a discontinuity in the potential function across the cut in the Riemann surface joining the two points  $\pm c$ . We must, therefore, search for some other function—one which possesses the following properties:—

- (1) It must make the ellipse a streamline of the system.
- (2) In the neighbourhood of the point  $z_1$ , it must be of the form

$$-\frac{\kappa}{2\pi} \log (z - z_1) + \text{regular function of } z.$$

- (3) There must be no singularities within the ellipse at points other than  $z = z_1$ .

Let us introduce the auxiliary transformation

$$\zeta = \xi + i\eta = \cosh^{-1} \frac{z}{c} \quad (3)$$

giving

$$x = c \cosh \xi \cos \eta,$$

$$y = c \sinh \xi \sin \eta.$$

To every value of  $z$  there correspond two values of  $\zeta$

$$\begin{aligned}\zeta &= \log \frac{1}{c} (z \pm \sqrt{z^2 - c^2}) \\ &= (\xi + i\eta) \quad \text{and} \quad (2\pi i - \xi - i\eta).\end{aligned}$$

Hence, the whole of the  $z$  plane is represented twice over in the  $\zeta$  plane in the infinite strip  $2\pi > \eta \geq 0$ , or rather, the whole Riemann surface is represented once. One sheet of the Riemann surface is represented by the semi-infinite strip  $\xi > 0$ , and the other by the semi-infinite strip  $\xi < 0$ . The line  $\xi = 0$  represents the line joining the foci of the ellipse taken twice over. The Riemann surface has two winding points at the foci of the ellipse,  $z = \pm c$ . The two sheets connect across the cut joining the two winding points. The region of the Riemann surface contained between the ellipse  $\xi = p$  (say) and the corresponding ellipse in the other sheet corresponds to the space between the lines  $\xi = \pm p$ .

If the potential function is the same for any given value of  $z$  for both sheets of the Riemann surface, then the function will be continuous across the cut and, therefore, regular in the plane. If we arrange that the boundary conditions and the singularities are the same on both sheets of the Riemann surface, then from considerations of symmetry, the potential function will be the same in both sheets. Hence, we must find the stream function on the Riemann surface due to irrotational flow with the two lines  $\xi = \pm \xi_0$  as stream lines and at the two points corresponding to  $z = z_1$  (i.e.,  $\zeta = \zeta_1$  and  $\zeta = 2\pi i - \zeta_1$ ) two equal vortices of strength  $\kappa$ .

Since  $\eta$  may be increased by any integral multiple of  $2\pi$ , the strip between 0 and  $2\pi i$  may be repeated indefinitely, and the problem in the  $\zeta$  plane is—to find the complex potential function which makes the infinite lines  $\xi = \pm \xi_0$  stream lines of the system and which has vortices of strength  $\kappa$  at the points

$$(\xi_1 + i\eta_1 + i2m\pi) \quad \text{and} \quad (-\xi_1 - i\eta_1 + i2m\pi)$$

where  $m$  assumes all integral values from  $-\infty$  to  $+\infty$  including zero. By the introduction of image vortices, we see that we need a function  $-\frac{\kappa}{2\pi} \log f(\zeta)$ , where  $f(\zeta)$  has simple zeros at the points,

$$(\xi_1 + i\eta_1) + 4m\xi_0 + i2n\pi, \quad -(\xi_1 + i\eta_1) + 4m\xi_0 + i2n\pi$$

and simple poles at the points

$$-(\zeta_1 - \eta_1) + (4m + 2)\xi_0 + i2n\pi, \quad (\xi_1 - \eta_1) + (4m + 2)\xi_0 + i2n\pi,$$

where  $m$  and  $n$  assume all integral values from  $-\infty$  to  $+\infty$ , including zero.

If now we put  $\omega = \zeta/4\xi_0$ , we find that the required complex function is

$$w = -\frac{\kappa}{2\pi} \log \frac{\wp_1(\omega - \omega_1) \wp_1(\omega + \omega_1)}{\wp_2(\omega - \bar{\omega}_1) \wp_2(\omega + \bar{\omega}_1)}, \quad (4)$$

where

$$\omega = \frac{1}{4\xi_0} (\xi + i\eta) = \frac{1}{4\xi_0} \log \frac{1}{c} (z + \sqrt{z^2 - c^2}),$$

$$\omega_1 = \frac{1}{4\xi_0} (\xi_1 + i\eta_1),$$

$$\bar{\omega}_1 = \frac{1}{4\xi_0} (\xi_1 - i\eta_1),$$

$$\xi_0 = \frac{1}{2} \log \left( \frac{a+b}{a-b} \right),$$

and where the periods of the  $\wp$  functions are 1 and  $i(2\pi/4\xi_0)$ . Explicitly in terms of  $z$ , this expression is

$$\begin{aligned} w &= -\frac{\kappa}{2\pi} \log \frac{\wp_1 \left[ \frac{1}{4\xi_0} \log \frac{z + \sqrt{z^2 - c^2}}{z_1 + \sqrt{z_1^2 - c^2}} \right] \wp_1 \left[ \frac{1}{4\xi_0} \log \frac{z + \sqrt{z^2 - c^2}}{z_1 - \sqrt{z_1^2 - c^2}} \right]}{\wp_2 \left[ \frac{1}{4\xi_0} \log \frac{z + \sqrt{z^2 - c^2}}{z_1 + \sqrt{z_1^2 - c^2}} \right] \wp_2 \left[ \frac{1}{4\xi_0} \log \frac{z + \sqrt{z^2 - c^2}}{z_1 - \sqrt{z_1^2 - c^2}} \right]}, \\ &= -\frac{\kappa}{2\pi} \log H(z). \end{aligned} \quad (5)$$

The  $w$  function has positive vortices at the points

$$z = c \cosh [4m\xi_0 + \xi_1 + i\eta_1],$$

i.e.,

$$z = z_1 \cosh 4m\xi_0 + \sqrt{z_1^2 - c^2} \sinh 4m\xi_0, \quad (6)$$

and negative vortices at the points

$$z = c \cosh [(4m + 2)\xi_0 - \xi_1 + i\eta_1],$$

i.e.,

$$z = \bar{z}_1 \cosh (4m + 2)\xi_0 + \sqrt{\bar{z}_1^2 - c^2} \sinh (4m + 2)\xi_0, \quad (7)$$

and in the neighbourhood of these positive and negative vortices, the function tends to the forms

$$\mp \frac{\kappa}{2\pi} \log (z - z_m)$$

respectively. Inside the ellipse the only singularity is at the point  $z_1$ .

On the ellipse  $|H(z)| = 1$ , so that the ellipse is a stream-line of the system. The velocity components are given by the equation

$$\begin{aligned} u - w &= \frac{dw}{dz} = \frac{d\omega}{dz} \frac{dw}{d\omega} \\ &= -\frac{\kappa}{8\pi\xi_0 c} \frac{1}{\sinh 4\xi_0 \omega} \left[ \frac{\vartheta'_1(\omega - \omega_1)}{\vartheta_1(\omega - \omega_1)} + \frac{\vartheta'_1(\omega + \omega_1)}{\vartheta_1(\omega + \omega_1)} \right. \\ &\quad \left. - \frac{\vartheta'_2(\omega - \bar{\omega}_1)}{\vartheta_2(\omega - \bar{\omega}_1)} - \frac{\vartheta'_2(\omega + \bar{\omega}_1)}{\vartheta_2(\omega + \bar{\omega}_1)} \right] \\ &= -\frac{\kappa}{8\pi\xi_0 c} \frac{1}{\sinh 4\xi_0 \omega} \left[ \frac{2\pi \sin 2\pi\omega}{\cos 2\pi\omega_1 - \cos 2\pi\omega} \right. \\ &\quad + 8\pi \sum_{r=1}^{\infty} \frac{q_1^{2r}}{1 - q_1^{2r}} \sin 2\pi r\omega \cos 2\pi r\omega_1 + \frac{2\pi \sin 2\pi\omega}{\cos 2\pi\bar{\omega}_1 + \cos 2\pi\omega} \\ &\quad \left. - 8\pi \sum_{r=1}^{\infty} \frac{(-)^r q_1^{2r}}{1 - q_1^{2r}} \sin 2\pi r\omega \cos 2\pi r\bar{\omega}_1 \right], \end{aligned} \quad (8)$$

where  $q_1 = e^{\pi\tau}$ .

This form shows that the velocity is finite at all points within the ellipse—except possibly at the foci. A closer examination shows that even at these points the velocity is finite. The foci  $z = \pm c$  are represented by the points  $s = 0, s = i\frac{\pi}{4\xi_0} = \frac{\tau}{2}$ , and at these points the expression  $u - w$  tends to finite limits. Further, the line joining the foci is not a stream line of the system, and the velocity is continuous across it.

By some manipulation it can be shown that the function given by (5) reduces to the usual formula for the circle as we make  $a \rightarrow b$ . This may be considered as a check on the work. We have that

$$\xi_0 = \frac{1}{2} \log \frac{a+b}{a-b} \rightarrow \infty,$$

$$\tau = i\frac{2\pi}{4\xi_0} \rightarrow 0, \quad q_1 = e^{\pi\tau} \rightarrow 1, \quad q = e^{\pi(-1/\tau)} \rightarrow 0.$$

Also

$$\begin{aligned} \frac{1}{4\xi_0} \log \frac{z + \sqrt{z^2 - c^2}}{z_1 - \sqrt{z_1^2 - c^2}} &= \frac{1}{4\xi_0} \log \frac{1}{c^2} (z + \sqrt{z^2 - c^2}) (z_1 + \sqrt{z_1^2 - c^2}) \\ &\rightarrow \frac{1}{4\xi_0} \log \frac{4zz_1}{c^2} = \frac{1}{4\xi_0} \log \frac{4zz_1}{(a+b)^2} \frac{a+b}{a-b} \\ &= \frac{1}{4\xi_0} \left[ \log \frac{4zz_1}{(a+b)^2} + 2\xi_0 \right] \rightarrow \frac{1}{2} + \log \frac{zz_1}{a^2}. \end{aligned}$$

Hence

$$w = -\frac{\kappa}{2\pi} \log \frac{\vartheta_1 \left[ \frac{1}{4\xi_0} \log \frac{z}{z_1} \right] \vartheta_2 \left[ \frac{1}{4\xi_0} \log \frac{zz_1}{a^2} \right]}{\vartheta_2 \left[ \frac{1}{4\xi_0} \log \frac{z}{z_1} \right] \vartheta_1 \left[ \frac{1}{4\xi_0} \log \frac{zz_1}{a^2} \right]},$$

and by transforming the  $\vartheta$  functions to those of periods  $(1, -1/\tau)$ , where  $q \rightarrow 0$ , we obtain

$$\begin{aligned} w &= -\frac{\kappa}{2\pi} \log \frac{\vartheta_1 \left[ -\frac{t}{2\pi} \log \frac{z}{z_1} \right] \vartheta_4 \left[ -\frac{t}{2\pi} \log \frac{zz_1}{a^2} \right]}{\vartheta_4 \left[ -\frac{t}{2\pi} \log \frac{z}{z_1} \right] \vartheta_1 \left[ -\frac{t}{2\pi} \log \frac{zz_1}{a^2} \right]} \\ &\rightarrow -\frac{\kappa}{2\pi} \log \frac{\sinh \left( \frac{1}{2} \log z/z_1 \right)}{\sinh \left( \frac{1}{2} \log zz_1/a^2 \right)} = -\frac{\kappa}{2\pi} \log \frac{(z - z_1)}{(z - a^2/z_1)}, \quad (9) \end{aligned}$$

where we have neglected the purely additive constants. This is the usual formula.

For purposes of convenience, we shall transform the  $\vartheta$  functions to those whose periods are  $(1, -1/\tau)$ , that is  $(1, i4\xi_0/2\pi)$  and the complex potential function is therefore

$$w = -\frac{\kappa}{2\pi} \log \frac{\vartheta_1(t - t_1) \vartheta_1(t + t_1)}{\vartheta_4(t - \bar{t}_1) \vartheta_4(t + \bar{t}_1)}, \quad (10)$$

where

$$\left. \begin{aligned} t &= \omega/\tau = -\frac{t}{2\pi} \log \frac{1}{c} (z + \sqrt{z^2 - c^2}), \\ t_1 &= -\frac{t}{2\pi} \log \frac{1}{c} (z_1 + \sqrt{z_1^2 - c^2}), \\ \bar{t}_1 &= \text{conjugate of } t_1, \\ q &= e^{-\pi/\tau} = e^{-2t} = \exp \left( -\log \frac{a+b}{a-b} \right) = \frac{a-b}{a+b}. \end{aligned} \right\} \quad (11)$$

In the following sections of this paper, we shall use the symbols given by equations (10) and (11).

#### 4. Aerofoil under Elliptic Loading in a Tunnel with Rigid Walls.

(a) *The Aerofoil along the Major Axis.*—Let us first consider the case of the aerofoil lying symmetrically along the major axis of the ellipse. In general, there is a circulation round the aerofoil, and we propose to discuss the elliptic distribution of circulation, that is, the one given by the law  $\kappa = \kappa_0 \sqrt{1 - \frac{x^2}{a^2}}$ ,

where  $2s$  is the span of the aerofoil. This is equivalent to a system of semi-infinite trailing vortices springing from each point of the trailing edge, the strength of the vortex starting from the point  $x_1$  being  $-\frac{d\kappa}{dx_1} dx_1$ . Under free air conditions the total lift  $L$  is given by the formula

$$L = k_L S \rho V^2$$

$$= \int_{-s}^s \rho V \kappa dx = \pi \kappa_0 \rho V s / 2, \quad (1)$$

where  $S$  is the area of the aerofoil,  $V$  its velocity, and  $\rho$  the density of the surrounding medium. The downward velocity at a point  $x_1$  of the aerofoil is given by the principal value of the integral

$$v = \int_0^s \frac{1}{4\pi} \frac{d\kappa}{dx} \left( \frac{1}{x - x_1} + \frac{1}{x + x_1} \right) dx = \frac{\kappa_0}{4s} = \frac{2k_L V}{\pi A}, \quad (2)$$

where  $A$  is the aspect ratio of the aerofoil, so that the induced velocity is constant along the aerofoil. The drag is therefore  $vL/V$ . The effect of the trailing vortex system is to reduce the lift at a given angle of incidence and to introduce a drag. When the aerofoil is inside the elliptic tunnel, the walls of the enclosure also induce an effect, so that measurements in the wind tunnel differ from those obtained in free air. We propose to determine these differences.

The complex function due to a semi-infinite vortex of strength  $\kappa$  at the point  $z_1$ , is

$$-\frac{\kappa}{4\pi} \log \frac{\vartheta_1(t - t_1) \vartheta_1(t + t_1)}{\vartheta_4(t - \bar{t}_1) \vartheta_4(t + \bar{t}_1)},$$

and that due to a vortex  $-\kappa$  at the point  $-z_1$ , is

$$\frac{\kappa}{4\pi} \log \frac{\vartheta_2(t - t_1) \vartheta_2(t + t_1)}{\vartheta_3(t - \bar{t}_1) \vartheta_3(t + \bar{t}_1)}.$$

Hence the function due to the vortex pair is

$$-\frac{\kappa}{4\pi} \log \frac{\vartheta_1(t - t_1) \vartheta_1(t + t_1) \vartheta_2(t - \bar{t}_1) \vartheta_2(t + \bar{t}_1)}{\vartheta_2(t - t_1) \vartheta_2(t + t_1) \vartheta_4(t - \bar{t}_1) \vartheta_4(t + \bar{t}_1)}. \quad (3)$$

The velocity distribution due to this system is

$$-\frac{\kappa}{4\pi} \frac{dt}{dz} F,$$

where

$$\begin{aligned} F &= \frac{\vartheta'_1(t-t_1)}{\vartheta_1(t-t_1)} + \frac{\vartheta'_1(t+t_1)}{\vartheta_1(t+t_1)} - \frac{\vartheta'_2(t-t_1)}{\vartheta_2(t-t_1)} - \frac{\vartheta'_2(t+t_1)}{\vartheta_2(t+t_1)} \\ &\quad + \frac{\vartheta'_3(t-t_1)}{\vartheta_3(t-t_1)} + \frac{\vartheta'_3(t+t_1)}{\vartheta_3(t+t_1)} - \frac{\vartheta'_4(t-t_1)}{\vartheta_4(t-t_1)} - \frac{\vartheta'_4(t+t_1)}{\vartheta_4(t+t_1)} \\ &= \pi [\cot \pi(t-t_1) + \cot \pi(t+t_1) + \tan \pi(t-t_1) + \tan \pi(t+t_1)] \\ &\quad + 16\pi \sum_{\text{odd}} \frac{q^r}{1-q^{2r}} \sin 2r\pi t \cos 2r\pi t_1 \\ &\quad - 16\pi \sum_{\text{odd}} \frac{q^r}{1-q^{2r}} \sin 2r\pi t \cos 2r\pi \bar{t}_1, \end{aligned}$$

where the summation is over all odd positive integral values of  $r$ . The contribution to the velocity due to the first part of  $F$  is

$$\begin{aligned} & - \frac{\kappa}{4\pi} \frac{dt}{dz} \pi [\cot \pi(t-t_1) + \cot \pi(t+t_1) + \tan \pi(t-t_1) + \tan \pi(t+t_1)] \\ &= - \frac{\kappa}{4\pi} \left( \frac{-1}{2\pi c \sin 2\pi t} \right) \pi \left[ \frac{2}{\sin 2\pi(t-t_1)} + \frac{2}{\sin 2\pi(t+t_1)} \right] \\ &= - \frac{\kappa}{4\pi} \frac{2c \cos 2\pi t_1}{c^2 \cos^2 2\pi t - c^2 \cos^2 2\pi \bar{t}_1} = - \frac{\kappa}{4\pi} \frac{2z_1}{z^2 - z_1^2} \\ &= - \frac{\kappa}{4\pi} \left( \frac{1}{z-z_1} - \frac{1}{z+z_1} \right), \end{aligned}$$

which is the velocity due to the vortex pair. Hence the interference velocity due to the walls is

$$- \frac{\kappa}{4\pi} \frac{dt}{dz} 16\pi \left[ \sum \frac{1}{1-q^{2r}} (q^{2r} \cos 2r\pi t_1 - q^r \cos 2r\pi \bar{t}_1) \sin 2r\pi t \right].$$

Two cases of importance present themselves (1) when the vortex pair lies along the major axis (fig. 1, *a*), and (2) when it lies along the minor axis (fig. 1, *b*). In the general case, when

$$z_1 = c \cosh \xi_1 \cos \eta_1 + ic \sinh \xi_1 \sin \eta_1,$$

then

$$2\pi t_1 = \eta_1 - i\xi_1,$$

and

$$2\pi \bar{t}_1 = \eta_1 + i\xi_1.$$

The interference velocity is therefore

$$- \frac{2\kappa}{\pi c} \sum_{\text{odd}} \frac{\sin 2r\pi t}{\sin 2\pi t} \left( \frac{q^r}{1-q^r} \sin r\eta_1 \sinh r\xi_1 + i \frac{q^r}{1+q^r} \cos r\eta_1 \cosh r\xi_1 \right) \quad (4)$$

We shall first investigate the case where the vortex pair is along the major axis—i.e.,  $z_1 \equiv x_1$ . When  $x_1 < c$  then  $\xi_1 = 0$ , and when  $x_1 > c$ ,  $\eta_1 = 0$ , so that when  $z_1 = x_1$ , the interference velocity may be written as

$$-i \frac{2\kappa}{\pi c} \sum \frac{q^r}{1+q^r} \cos 2r\pi t_1 \frac{\sin 2r\pi t}{\sin 2\pi t}. \quad (5)$$

In order to apply this result to the case of the aerofoil, we put  $-\frac{d\kappa}{dx_1} dx_1$  where previously we had  $\kappa$ , and then we integrate the result between the limits 0 and  $s$ . Thus the effect of the walls is to induce a velocity

$$\frac{i2}{\pi c} \int_0^s \frac{d\kappa}{dx_1} dx_1 \sum \frac{q^r}{1+q^r} \cos 2r\pi t_1 \frac{\sin 2r\pi t}{\sin 2\pi t}. \quad (6)$$

The part within the sign of integration is always real when  $t$  or  $t_1$  are purely real or purely imaginary quantities, and hence, on the major axis  $dw/dz$  is purely imaginary. In this line, therefore,

$$\begin{aligned} v &= -\frac{2}{\pi c} \int_0^s \frac{d\kappa}{dx_1} dx_1 \sum \frac{q^r}{1+q^r} \cos 2r\pi t_1 \frac{\sin 2r\pi t}{\sin 2\pi t} \\ &= \frac{\kappa_0}{2s} \sum \frac{q^r}{1+q^r} F_r \frac{\sin 2r\pi t}{\sin 2\pi t}, \end{aligned} \quad (7)$$

where

$$F_r = -\frac{4}{\kappa_0 \pi} \int_0^s \frac{1}{c} \cos 2r\pi t_1 \frac{d\kappa}{dx_1} dx_1.$$

If use be made of equation (1), equation (7) can be put into the form

$$\frac{v}{V} = \frac{k_L S}{\pi s^2} \sum \frac{q^r}{1+q^r} F_r \frac{\sin 2r\pi t}{\sin 2\pi t}. \quad (7A)$$

Since  $r$  is odd, however, and since  $\cos 2\pi t = x/c$ , we have

$$\begin{aligned} \frac{\sin 2r\pi t}{\sin 2\pi t} &= \left[ \left(\frac{2x}{c}\right)^{r-1} - r^{-2} C_1 \left(\frac{2x}{c}\right)^{r-3} + r^{-3} C_2 \left(\frac{2x}{c}\right)^{r-5} \dots + (-1)^{\frac{1}{2}(r-1)} \right] \\ &= (-1)^{\frac{1}{2}(r-1)} \sum (-1)^{n-1} \frac{1}{2}(r+2n-3) C_{2n-2} \left(\frac{2x}{c}\right)^{2n-2}. \end{aligned} \quad (8)$$

The effect of the upward induced velocity  $v$  is to incline the lift force forward by an angle  $v/V$ , and this angle,  $\Delta\alpha$ , must be added to the angle of attack as measured in the wind tunnel in order to obtain the free-air value of the angle. Hence, defining  $\eta$  by means of the following equation

$$\Delta\alpha = \eta \frac{S}{C} k_L,$$



where  $C (\equiv \pi ab)$  is the cross-sectional area of the wind tunnel, we have

$$\eta = \frac{ab}{s^2} \sum (-1)^{\frac{1}{2}(r-1)} \frac{q^r}{1+q^r} F_r \left[ 1 + \frac{1}{2}(r+1) C_2 \left( \frac{2x}{c} \right)^2 + \frac{1}{2}(r+3) C_4 \left( \frac{2x}{c} \right)^4 \dots + (-1)^{\frac{1}{2}(r-1)} \left( \frac{2x}{c} \right)^{r-1} \right].$$

This value of  $\eta$  varies across the span of the aerofoil and determines the twist which must be given to the aerofoil to maintain elliptic distribution of lift. Glauert has shown, however, that the mean effective value of the correction to the angle of incidence is given by the equation

$$\Delta\alpha = \delta \frac{S}{C} k_L, \quad (9)$$

where  $\delta$  is defined below by considering the induced drag.

As a consequence of the change in the direction of lift, the drag  $D$  is decreased by amount

$$\int_{-s}^s \frac{v}{V} \frac{dL}{dx} dx,$$

or, the drag coefficient is decreased by amount  $\Delta k_D$  where

$$\begin{aligned} \Delta k_D &= \frac{1}{\rho S V^2} \int_{-s}^s \frac{v}{V} \frac{dL}{dx} dx, \\ &= \frac{1}{\rho S V^2} \int_{-s}^s \frac{v}{V} \rho \kappa V dx, \\ &= \frac{\kappa_0}{S V^2} \int_{-s}^s v \sqrt{1 - \frac{x^2}{s^2}} dx. \end{aligned} \quad (10)$$

If now we define  $\delta$  by the equation

$$\Delta k_D = \delta k_L^2 \frac{S}{C},$$

we have

$$\delta = \frac{ab}{s^2} \sum \frac{q^r}{1+q^r} F_r G_r, \quad (11)$$

where

$$G_r = \frac{2}{\pi s} \int_{-s}^s \sqrt{1 - \frac{x^2}{s^2}} \frac{\sin 2r\pi t}{\sin 2\pi t} dx, \quad (12)$$

or

$$G_r = 2 \left[ \frac{|r-1|}{(r+1) \left(\frac{1}{2}(r-1)\right)^2} \left(\frac{s}{c}\right)^{r-1} - \frac{r-3}{(r-1) \left(\frac{1}{2}(r-3)\right)^2} \left(\frac{s}{c}\right)^{r-3} \right. \\ \left. + \frac{r-5}{(r-3) \left(\frac{1}{2}(r-5)\right)^2} \left(\frac{s}{c}\right)^{r-5} \dots + (-)^{\frac{1}{2}(r-1)} \frac{1}{2} \right]. \quad (12A)$$

We note, however, that

$$F_r = -\frac{2}{\kappa_0 \pi} \frac{s}{c} \int_{-s}^s \cos 2r\pi t_1 \frac{d\kappa}{dx_1} dx_1 \\ = -\frac{2}{\kappa_0 \pi} \frac{s}{c} \left[ \cos 2r\pi t_1 (\kappa) + \int 2r\pi \frac{dt_1}{dx_1} \sin 2r\pi t_1 dx_1 \right]_{-s}^s.$$

Since  $\kappa = \kappa_0 \left(1 - \frac{x^2}{s^2}\right)^{\frac{1}{2}}$ , we see that  $\left[\kappa \cos 2r\pi t_1\right]_{-s}^s = 0$  and hence

$$F_r = -\frac{2}{\kappa_0 \pi} \frac{s}{c} 2r\pi \int_{-s}^s \kappa \frac{dt_1}{dx_1} \sin 2r\pi t_1 dx_1.$$

But  $dt_1/dx_1 = -1/2\pi c \sin 2\pi t_1$ , and so

$$F_r = -\frac{4r}{\kappa_0} \frac{s}{c} \int_{-s}^s \kappa_0 \sqrt{1 - \frac{x_1^2}{s^2}} \left(\frac{-1}{2\pi c \sin 2\pi t_1}\right) \sin 2r\pi t_1 dx_1 \\ = \frac{2r}{\pi} \frac{s}{c^2} \int_{-s}^s \sqrt{1 - \frac{x^2}{s^2}} \frac{\sin 2r\pi t_1}{\sin 2\pi t_1} dx_1 \\ = r \frac{s^2}{c^2} G_r \quad (13)$$

by equation (12). Hence, defining  $\delta_1$ , as the value of  $\delta$  when the aerofoil is along the major axis, we have

$$\delta_1 = \frac{ab}{c^2} \sum_{\text{odd } r} \frac{rq^r}{1+q^r} G_r^2. \quad (14)$$

(b) *The Circular Tunnel* ( $a \rightarrow b$ ).—When  $a \rightarrow b$ , we find  $c \rightarrow 0$  and

$$\frac{q^r}{1+q^r} = \frac{c^{2r}}{(a+b)^{2r} + c^{2r}} \rightarrow \left(\frac{c}{2a}\right)^{2r},$$

$$G_r \rightarrow 2 \frac{|r-1|}{(r+1) \left(\frac{1}{2}(r-1)\right)^2} \left(\frac{s}{c}\right)^{r-1}.$$

Hence

$$\begin{aligned}\eta &\rightarrow \Sigma \frac{1}{2^{r+2}} \frac{\left| \frac{r+1}{\left(\frac{1}{2}(r+1)\right)^2} \frac{x^{r-1}s^{r-1}}{a^{2r-2}} \right|}{\left(\frac{1}{2}(r+1)\right)^2} \\ &= \frac{1}{4} \left[ 1 + \frac{3}{4} \left( \frac{xs}{a^2} \right)^2 + \frac{5}{8} \left( \frac{xs}{a^2} \right)^4 + \frac{35}{64} \left( \frac{xs}{a^2} \right)^6 \dots \right],\end{aligned}\quad (1)$$

and

$$\begin{aligned}\delta_1 &\rightarrow \Sigma r \left[ \frac{\left| \frac{r-1}{(r+1)\left(\frac{1}{2}(r-1)\right)^2} \right|^2 \left( \frac{s}{2a} \right)^{2r-2}}{\left(\frac{1}{2}(r-1)\right)^2} \right] \\ &\rightarrow \frac{1}{4} \left[ 1 + \frac{3}{16} \frac{s^4}{a^4} + \frac{5}{64} \frac{s^8}{a^8} + \frac{175}{4096} \frac{s^{12}}{a^{12}} \dots \right].\end{aligned}\quad (2)$$

These results have been obtained previously from a direct examination of the case of the circular tunnel.\*

In the case of the almost circular tunnel when  $a = b(1+h)$ ,  $h$  being a quantity of the first order, we get as an approximation

$$\begin{aligned}\delta_1 &= -\frac{h}{8} + \Sigma r \left[ \frac{\left| \frac{r-1}{(r+1)\left(\frac{1}{2}(r-1)\right)^2} \right|^2 \left( \frac{s}{2a} \right)^{2r-2} \left\{ 1 - (r+1)h \frac{a^2}{s^2} - (r-1)h \right\}}{\left(\frac{1}{2}(r-1)\right)^2} \right] \\ &= -\frac{h}{8} + \left( 1 - h \frac{a^2 - s^2}{s^2} \right) \left[ \frac{1}{4} + \frac{3}{64} \frac{s^4}{a^4} + \frac{5}{256} \frac{s^8}{a^8} + \frac{175}{16,384} \frac{s^{12}}{a^{12}} \dots \right] \\ &\quad - h \left( \frac{a^2 + s^2}{s^2} \right) \left[ \frac{1}{4} + \frac{9}{64} \frac{s^4}{a^4} + \frac{25}{256} \frac{s^8}{a^8} + \frac{1,225}{16,384} \frac{s^{12}}{a^{12}} \dots \right].\end{aligned}$$

(c) *Span equal to the Focal Distance* ( $2s = 2c$ ).—When  $s = c$  there is considerable simplification and we find, by putting  $2\pi t = \lambda$ , that

$$\begin{aligned}G_r &= \frac{4}{\pi} \int_0^\pi \sin \lambda \sin r\lambda \, d\lambda \\ &= \begin{cases} 0 & \text{if } r \text{ is odd and greater than 1,} \\ 1 & \text{if } r = 1. \end{cases}\end{aligned}$$

Hence

$$\eta = \frac{ab}{c^2} \frac{q}{1+q} = \frac{ab}{c^2} \frac{a-b}{2a} = \frac{b}{2(a+b)}.\quad (1)$$

This means that the interference velocity is constant along the span, and this represents the ideal case for experimental work. Also

$$\delta_1 = \frac{ab}{c^2} \frac{q}{1+q} = \frac{b}{2(a+b)}.\quad (2)$$

\* See Rosenhead, 'Proc. Roy. Soc.,' A, vol. 129, p. 140 (1930), equation (8).

(d) *Small Aerofoils* ( $s/c$  very small).—When  $s/c$  is very small

$$G_r = (-)^{\frac{1}{2}(r-1)} \left[ 1 - \frac{1}{8} (r^2 - 1^2) \frac{s^2}{c^2} \right] \quad (1)$$

so that as a first approximation

$$\delta_1 \rightarrow \frac{ab}{c^2} \sum \frac{rq^r}{1+q^r}. \quad (2)$$

If we put  $a = c \cosh \theta$ ,  $b = c \sinh \theta$ ,  $\delta$  assumes the form obtained by Glauert\*

$$\delta_1 = \sinh \theta \cosh \theta \sum_{\text{odd}} \frac{r}{1 + e^{2r\theta}}. \quad (2A)$$

A second approximation to  $\delta_1$  is

$$\delta_1 = \frac{ab}{c^2} \sum \frac{rq^r}{1+q^r} \left( 1 - \frac{1}{4} (r^2 - 1^2) \frac{s^2}{c^2} \right) = \alpha_1 - \beta_1 \frac{s^2}{c^2}, \quad (3)$$

where

$$\left. \begin{aligned} \alpha_1 &= \frac{ab}{c^2} \sum \frac{rq^r}{1+q^r}, \\ \beta_1 &= \frac{ab}{c^2} \sum \frac{1}{4} (r+1) r (r-1) \frac{q^r}{1+q^r}. \end{aligned} \right\} \quad (4)$$

and

(e) *Aerofoil along the Minor Axis*.—Reverting to equation (4.4), which gives the interference velocity due to a vortex pair in the general case, we see that when  $z_1$  lies on the minor axis,  $\eta_1 = \pi/2$ . We note also that  $\cos r\eta_1 = 0$  and  $\sin r\eta_1 = (-)^{\frac{1}{2}(r-1)}$  when  $r$  is odd, so that the interference velocity is

$$-\frac{2\kappa}{\pi c} \sum \frac{(-)^{\frac{1}{2}(r-1)} q^r}{1-q^r} \sinh r\xi_1 \frac{\sin 2r\pi t}{\sin 2\pi t}$$

or

$$\frac{2\kappa}{\pi c} i \sum \frac{q^r}{1-q^r} \cos 2r\pi t_1 \frac{\sin 2r\pi t}{\sin 2\pi t}, \quad (1)$$

since here

$$2\pi t_1 = \pi - 2\pi t.$$

Extending this result to the case of the aerofoil, the interference velocity at right angles to the oncoming stream of air is  $-u$  where

$$\begin{aligned} u &= \frac{2i}{\pi c} \int_0^s \frac{d\kappa}{dy_1} dy_1 \sum \frac{q^r}{1-q^r} \cos 2r\pi t_1 \frac{\sin 2r\pi t}{\sin 2\pi t} \\ &= \frac{\kappa_0}{2s} \sum \frac{q^r}{1-q^r} f_r \frac{\sin 2r\pi t}{\sin 2\pi t}, \end{aligned} \quad (2)$$

\* Glauert, 'Aero. Res. Ctte. Rep. and Mem.,' No. 1470, p. 7, equation (12).

where

$$f_r = \frac{4t}{\pi\kappa_0} \frac{s}{c} \int_0^s \cos 2r\pi t_1 \frac{d\kappa}{dy_1} dy_1. \quad (3)$$

The change in the drag coefficient is  $\Delta k_D$  where

$$\begin{aligned} \Delta k_D &= \frac{\kappa_0}{SV^2} \int_{-s}^s u \sqrt{1 - \frac{y^2}{s^2}} dy, \\ &= \delta_2 k_L^2 \frac{S}{C}, \end{aligned} \quad (4)$$

and where

$$\delta_2 = \frac{ab}{s^2} \Sigma \frac{q^r}{1 - q^r} f_r g_r,$$

the quantity  $g_r$  being defined by the equation

$$g_r = \frac{2}{\pi s} \int_{-s}^s \sqrt{1 - \frac{y^2}{s^2}} \frac{\sin 2r\pi t}{\sin 2\pi t} dy. \quad (5)$$

We note, however, that

$$\begin{aligned} f_r &= \frac{2t}{\pi\kappa_0} \frac{s}{c} \int_{-s}^s \cos 2r\pi t_1 \frac{d\kappa}{dy_1} dy_1 \\ &= \frac{2t}{\pi\kappa_0} \frac{s}{c} \left[ \cos 2r\pi t_1 (\kappa) + \int 2r\pi\kappa_0 \frac{dt_1}{dy_1} \sin 2r\pi t_1 \sqrt{1 - \frac{y^2}{s^2}} dy \right]_{-s}^s. \end{aligned}$$

Along our line of integration  $ty_1/c = \cos 2\pi t_1$ , so that

$$\begin{aligned} f_r &= r \frac{s^2}{c^2} \frac{2}{\pi s} \int_{-s}^s \sqrt{1 - \frac{y_1^2}{s^2}} \frac{\sin 2r\pi t_1}{\sin 2\pi t_1} dy_1, \\ &= r \frac{s^2}{c^2} g_r. \end{aligned}$$

Hence

$$\delta_2 = \frac{ab}{c^2} \Sigma \frac{rq^r}{1 - q^r} g_r^2, \quad (6)$$

where

$$\begin{aligned} g_r &= (-1)^{\frac{1}{2}(r-1)2} \left[ \frac{|r-1|}{(r+1) \left(\frac{1}{2}(r-1)\right)^2} \left(\frac{s}{c}\right)^{r-1} + \frac{{}^{r-2}C_1 |r-3|}{(r-1) \left(\frac{1}{2}(r-3)\right)^2} \left(\frac{s}{c}\right)^{r-3} \right. \\ &\quad \left. + \frac{{}^{r-3}C_2 |r-5|}{(r-3) \left(\frac{1}{2}(r-5)\right)^2} \left(\frac{s}{c}\right)^{r-5} \dots + \frac{1}{2} \right]. \end{aligned} \quad (7)$$

When  $s/c$  is very small, then

$$\delta_2 \rightarrow \alpha_2 + \beta_2 (s/c)^2, \quad (8)$$

where

$$\left. \begin{aligned} \alpha_2 &= \frac{ab}{c^2} \sum \frac{rq^r}{1-q^r}, \\ \beta_2 &= \frac{ab}{c^2} \sum \frac{1}{4} (r+1) r (r-1) \frac{q^r}{1-q^r}. \end{aligned} \right\} \quad (9)$$

Finally, in the case of the almost circular tunnel, when  $a = b(1+h)$ , we get

$$\delta_2 = -\frac{h}{8} + \Sigma r \left[ \frac{|r-1|}{(r+1)(\frac{1}{2}(r-1))^2} \right]^2 \left( \frac{s}{2a} \right)^{2r-2} \left\{ 1 + (r+1)h \frac{a^2}{s^2} - (r-1)h \right\}. \quad (10)$$

##### 5. Aerofoil under Elliptic Loading in an Open Tunnel.

Following the method laid down by Prandtl, we have now to search for a complex potential function whose real part is constant over the ellipse  $(x^2/a^2) + (y^2/b^2) = 1$  and which has logarithmic singularities at the vortices inside the ellipse.

Following the method indicated in Section 3, we see that if there is a vortex of strength  $\kappa$  at the point  $z_1$  and a vortex  $-\kappa$  at the point  $-z_1$ , the appropriate complex potential function is  $w$  where

$$w = -\frac{\kappa}{4\pi} \log \frac{\vartheta_1(t-t_1) \vartheta_1(t+t_1) \vartheta_4(t-\bar{t}_1) \vartheta_4(t+\bar{t}_1)}{\vartheta_2(t-t_1) \vartheta_2(t+t_1) \vartheta_3(t-\bar{t}_1) \vartheta_3(t+\bar{t}_1)}. \quad (1)$$

It can be shown, after some manipulation, that the value of the ellipse is purely imaginary, and varies from point to point. Hence the value of  $\phi$  on the ellipse is zero. The velocity distribution due to this vortex pair is

$$-\frac{\kappa}{4\pi} \frac{dt}{dz} F_1,$$

where

$$\begin{aligned} F_1 &= \frac{\vartheta'_1(t-t_1)}{\vartheta_1(t-t_1)} + \frac{\vartheta'_1(t+t_1)}{\vartheta_1(t+t_1)} - \frac{\vartheta'_2(t-t_1)}{\vartheta_2(t-t_1)} - \frac{\vartheta'_2(t+t_1)}{\vartheta_2(t+t_1)} \\ &\quad - \frac{\vartheta'_3(t-\bar{t}_1)}{\vartheta_3(t-\bar{t}_1)} - \frac{\vartheta'_3(t+\bar{t}_1)}{\vartheta_3(t+\bar{t}_1)} + \frac{\vartheta'_4(t-\bar{t}_1)}{\vartheta_4(t-\bar{t}_1)} + \frac{\vartheta'_4(t+\bar{t}_1)}{\vartheta_4(t+\bar{t}_1)}, \\ &= \pi [\cot \pi (t-t_1) + \cot \pi (t+t_1) + \tan \pi (t-t_1) + \tan \pi (t+t_1)] \\ &\quad + 16\pi \sum_{\text{odd}} \frac{q^{2r}}{1-q^{2r}} \sin 2\pi r t \cos 2\pi r t_1 \\ &\quad + 16\pi \sum_{\text{odd}} \frac{q^r}{1-q^r} \sin 2\pi r t \cos 2\pi r \bar{t}_1. \end{aligned} \quad (2)$$

In the general case, when

$$z_1 = c \cosh \xi_1 \cos \eta_1 + i c \sinh \xi_1 \sin \eta_1$$

the interference velocity is

$$\frac{2\kappa}{\pi c} \sum \frac{\sin 2r\pi t}{\sin 2\pi t} \left( \frac{q^r}{1+q^r} \sin r\eta_1 \sinh r\xi_1 + i \frac{q^r}{1-q^r} \cos r\eta_1 \cosh r\xi_1 \right). \quad (3)$$

When the vortex pair lies along the major axis, this can be written as

$$i \frac{2\kappa}{\pi c} \sum \frac{q^r}{1-q^r} \cos 2r\pi t_1 \frac{\sin 2r\pi t}{\sin 2\pi t}, \quad (4)$$

and when along the minor axis

$$i \frac{2\kappa}{\pi c} \sum \frac{q^r}{1+q^r} \cos 2r\pi t_1 \frac{\sin 2r\pi t}{\sin 2\pi t}. \quad (5)$$

Hence when the aerofoil lies along the major axis the value of  $\delta$  is given by

$$\delta_3 = -\frac{ab}{c^2} \sum \frac{rq^r}{1-q^r} G_r^2, \quad (6)$$

and when along the minor axis

$$\delta_4 = -\frac{ab}{c^2} \sum \frac{rq^r}{1+q^r} g_r^2. \quad (7)$$

In the particular case of an aerofoil of span  $2c$  lying along the major axis of the open ellipse, we see that

$$\begin{aligned} \delta_3 &= -\frac{ab}{c^2} \frac{q}{1-q} \\ &= -\frac{ab}{c^2} \frac{a-b}{2b} \\ &= -\frac{a}{2(a+b)}. \end{aligned} \quad (8)$$

In this case too the interference velocity is constant along the span and equal to

$$-\frac{a}{2(a+b)} k_L \frac{SV}{C},$$

which is a result previously obtained by Glauert.

## 6. Numerical Investigation.

Comparing the values of  $\delta_1$ ,  $\delta_2$ ,  $\delta_3$  and  $\delta_4$ , we notice that as a first approximation  $G_r^2 = g_r^2 = 1$ , and

$$\delta_1 = \alpha_1, \quad \delta_2 = \alpha_2, \quad \delta_3 = \alpha_3, \quad \delta_4 = \alpha_4,$$

where

$$\left. \begin{aligned} \alpha_1 = -\alpha_4 &= \frac{ab}{c^2} \sum \frac{rq^r}{1+q^r}, \\ \alpha_2 = -\alpha_3 &= \frac{ab}{c^2} \sum \frac{rq^r}{1-q^r}. \end{aligned} \right\} \quad (1)$$

This detailed investigation demonstrates, in a particular case, the validity of a general theorem recently proved by Glauert, namely, that "The interference on a very small aerofoil in an open tunnel of any shape is of the same magnitude, but opposite in sign, as that on the same aerofoil, rotated through a right angle, in a closed tunnel of the same shape." A second approximation shows that

$$\left. \begin{aligned} \delta_1 &= \alpha_1 - \beta_1 \left(\frac{s}{c}\right)^2, \\ \delta_2 &= \alpha_2 + \beta_2 \left(\frac{s}{c}\right)^2, \\ \delta_3 &= -\alpha_2 + \beta_2 \left(\frac{s}{c}\right)^2, \\ \delta_4 &= -\alpha_1 - \beta_1 \left(\frac{s}{c}\right)^2, \end{aligned} \right\} \quad (2)$$

where  $\alpha_1$  and  $\alpha_2$  are as above, but  $\beta_1$  and  $\beta_2$  are given by

$$\begin{aligned} \beta_1 &= \frac{ab}{c^2} \sum \frac{1}{4} (r+1) r (r-1) \frac{q^r}{1+q^r}, \\ \beta_2 &= \frac{ab}{c^2} \sum \frac{1}{4} (r+1) r (r-1) \frac{q^r}{1-q^r}. \end{aligned}$$

The range in which results are required for practical purposes is  $a/b \leq 3$ , while the span  $2s$  may have any value up to the greater of  $2c$  or three-quarters of the width in the direction of the span. In this section results are given for values of  $s/c$  ranging from 0 to 1, but larger values of  $s/c$  will be required when  $a/b < 1.512$ . The corrections for large values of  $s/c$  are not tabulated here, but they can be obtained directly from the first few terms of the various series involved. In order to avoid a considerable amount of additional calculation  $\delta$  has been tabulated against the ratio [span/focal distance] instead of against the more natural parameter [span/width], but in any particular case  $s/c$  can be obtained by a trifling calculation from the values of  $s/a$  and  $a/b$ .

In the formulæ for  $\delta_1$  and  $\delta_3$ , the maximum value of  $s/c$  is  $a/c$ , while in  $\delta_2$  and  $\delta_4$  the maximum value of  $s/c$  is  $b/c$ . If  $s < a$  it can be verified without much difficulty that all the series are convergent.



First, it was necessary to obtain the values of  $G_r$  and  $g_r$ , and below are given the series which were required for numerical purposes. Putting  $s/c = x$ , we have

$$G_1 = 1,$$

$$G_3 = x^2 - 1,$$

$$G_5 = 2x^4 - 3x^2 + 1,$$

$$G_7 = 5x^6 - 10x^4 + 6x^2 - 1,$$

$$G_9 = 14x^8 - 35x^6 + 30x^4 - 10x^2 + 1,$$

$$G_{11} = 42x^{10} - 126x^8 + 140x^6 - 70x^4 + 15x^2 - 1,$$

$$G_{13} = 132x^{12} - 462x^{10} + 630x^8 - 420x^6 + 140x^4 - 21x^2 + 1,$$

$$G_{15} = 429x^{14} - 1716x^{12} + 2772x^{10} - 2310x^8 + 1050x^6 - 252x^4 + 28x^2 - 1.$$

The series for  $g_r$  was obtained by putting positive signs before all the component terms of  $G_r$ , and multiplying the resulting expression by  $(-)^{1(r-1)}$ , thus

$$g_1 = (-)^0 1, \quad g_3 = (-)^1 (x^2 + 1),$$

$$g_5 = (-)^2 (2x^4 + 3x^2 + 1), \quad \text{etc.}$$

The values of  $G_r$  and  $g_r$  for various values of  $s/c$  are given in Table I.

By means of Table I, it is possible to calculate  $\delta_1$ ,  $\delta_2$ ,  $\delta_3$  and  $\delta_4$ .  $\delta_1$  and  $\delta_2$  refer to an elliptic tunnel with rigid walls and have therefore been combined in Table II.  $\delta_1$  is the value of the interference factor when the aerofoil is along the horizontal diameter of an oblate circle, whereas  $\delta_2$  refers to the corresponding case in a prolate circle. Hence  $\delta_1$  and  $\delta_2$  have been tabulated against

Table I.—1st Section.

$r$ .	$s/c = 0.0$ .				$s/c = 0.2$ .			
	$G_r$ .	$G_r^2$ .	$g_r$ .	$g_r^2$ .	$G_r$ .	$G_r^2$ .	$g_r$ .	$g_r^2$ .
1	1	1	1	1	1.0000	1.0000	1.0000	1.0000
3	-1	1	-1	1	-0.9800	0.9216	-1.0400	1.0816
5	1	1	1	1	0.8832	0.7800	1.1232	1.2616
7	-1	1	-1	1	-0.7757	0.6017	-1.2563	1.5763
9	1	1	1	1	0.6458	0.4171	1.4502	2.1031
11	-1	1	-1	1	-0.5031	0.2531	-1.7210	2.9618
13	1	1	1	1	0.3587	0.1287	2.0925	4.3786
15	-1	1	-1	1	-0.2216	0.0491	-2.5946	6.7319

Table I.—2nd Section.

$r.$	$s/c = 0.4.$				$s/c = 0.6.$			
	$G_r.$	$G_r^2.$	$g_r.$	$g_r^2.$	$G_r.$	$G_r^2.$	$g_r.$	$g_r^2.$
1	1.0000	1.0000	1.0000	1.0000	1.0000	1.0000	1.0000	1.0000
3	-0.8400	0.7056	-1.1800	1.3456	-0.6400	0.4096	-1.3600	1.8496
5	0.5712	0.3263	1.5312	2.3446	0.1792	0.0321	2.3392	5.4719
7	-0.2765	0.0765	-2.2365	5.0019	0.0973	0.0095	-4.6893	21.990
9	0.0338	0.0011	3.5205	12.3940	-0.1099	0.0121	10.3561	107.249
11	0.1032	0.0107	-5.8524	34.251	-0.0025	0.0000	-24.3741	594.10
13	-0.1296	0.0168	10.1278	102.572	0.0636	0.0040	59.9620	3,595.44
15	0.0788	0.0062	-18.0665	326.398	-0.0244	0.0005	-152.3630	23,214.48

Table I.—3rd Section.

$r.$	$s/c = 0.8.$				$s/c = 1.0.$			
	$G_r.$	$G_r^2.$	$g_r.$	$g_r^2.$	$G_r.$	$G_r^2.$	$g_r.$	$g_r^2.$
1	1.0000	1.0000	1.0000	1.0000	1	1	1	1
3	-0.3600	0.1296	-1.6400	2.6896	0	0	-2	4
5	-0.1008	0.0102	3.7392	13.9816	0	0	6	36
7	0.0547	0.0030	-10.2467	104.996	0	0	-22	484
9	0.0619	0.0038	31.2117	974.17	0	0	90	8,100
11	-0.0019	0.0000	-101.6201	10,326.6	0	0	-394	155,236
13	-0.0349	0.0012	346.2525	119,890.8	0	0	1,806	3,261,636
15	0.0093	0.0001	-1,219.414	1,486,970.5	0	0	-8,558	73,239,364

$\lambda$  where  $\lambda = [\text{width of tunnel/height of tunnel}]$ .  $\delta_1$  corresponds to that part of Table II given by  $\lambda > 1$ , and  $\delta_2$  corresponds to  $\lambda < 1$ .

Table II.—Tunnel with Rigid Walls.  $\delta$  has been tabulated for different values of  $s/c$  and  $\lambda$ , where  $s/c = [\text{span/focal distance}]$  and  $\lambda = [\text{width of tunnel/height of tunnel}]$ .  $\delta_1$  corresponds to  $\lambda > 1$ , and  $\delta_2$  to  $\lambda < 1$ .

$\lambda$ $c/s$	1:3.	2:5.	1:2.	2:3.	1:1.	3:2.	2:1.	5:2.	3:1.
0.00	0.630	0.526	0.4265	0.3311	0.2500	0.2306	0.2541	0.2925	0.3365
0.20	0.683	0.554	0.4379	0.3339	0.2500	0.2279	0.2445	0.2716	0.3001
0.40	—	0.718	0.4854	0.3442	0.2500	0.2208	0.2217	0.2281	0.2333
0.60	—	—	—	0.3673	0.2500	0.2118	0.1964	0.1867	0.1783
0.80	—	—	—	0.4272	0.2500	0.2037	0.1761	0.1567	0.1418
1.00	—	—	—	—	0.2500	0.2000	0.1667	0.1428	0.1250

For similar reasons  $\delta_3$  and  $\delta_4$  have been combined into one table.

Table III.—Jet of Elliptic Section.  $\delta$  has been tabulated for different values of  $s/c$  and  $\lambda$ , where  $s/c$  = [span/focal distance] and  $\lambda$  = [width of tunnel/height of tunnel].  $\delta_3$  corresponds to  $\lambda > 1$ , and  $\delta_4$  to  $\lambda < 1$ .

$\lambda \backslash s/c$	1:3.	2:5.	1:2.	2:3.	1:1.	3:2.	2:1.	5:2.	3:1.
0.00	-0.337	-0.293	-0.2541	-0.2306	-0.2500	-0.3311	-0.4265	-0.5256	-0.6300
0.20	-0.388	-0.319	-0.2653	-0.2335	-0.2500	-0.3283	-0.4184	-0.5082	-0.5860
0.40	—	-0.477	-0.3110	-0.2436	-0.2500	-0.3211	-0.3923	-0.4553	-0.5097
0.60	—	—	—	-0.2665	-0.2500	-0.3119	-0.3653	-0.4084	-0.4430
0.80	—	—	—	-0.3264	-0.2500	-0.3038	-0.3434	-0.3733	-0.3965
1.00	—	—	—	—	-0.2500	-0.3000	-0.3333	-0.3571	-0.3750

The results are given in diagrammatic form in figs. 2 and 3.

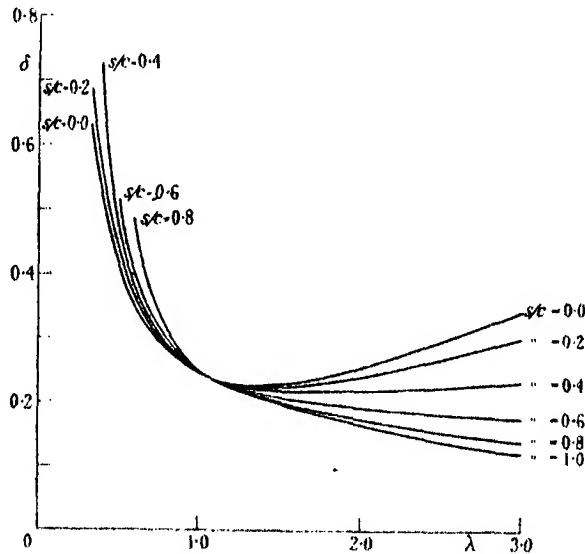


FIG. 2.—Elliptic Tunnel with Rigid Walls.

From the diagrams it is clear that if  $\lambda > 1$ , the absolute value of the correction factor decreases as the aerofoil becomes larger, whereas if  $\lambda < 1$  the reverse is the case.

Owing to the fact that the results have been tabulated for different values of  $s/c$ , the results for the circle do not emerge from the diagrams, for whatever the length of the aerofoil in the circular tunnel, we have  $s/c = \infty$ . The corrections for the case of the circular tunnel are, however, given below. The

results are taken from a table given by Glauert\* and are calculated from a formula which is identical with the limiting form mentioned in Section 4 (2).

Table IV gives the values of  $\delta$  for an aerofoil in a circular tunnel with rigid walls. If the sign of  $\delta$  is changed, we obtain the results for the circular jet.

$s/a$	0.0	0.2	0.4	0.6	0.8
$\delta$	0.250	0.250	0.251	0.256	0.273

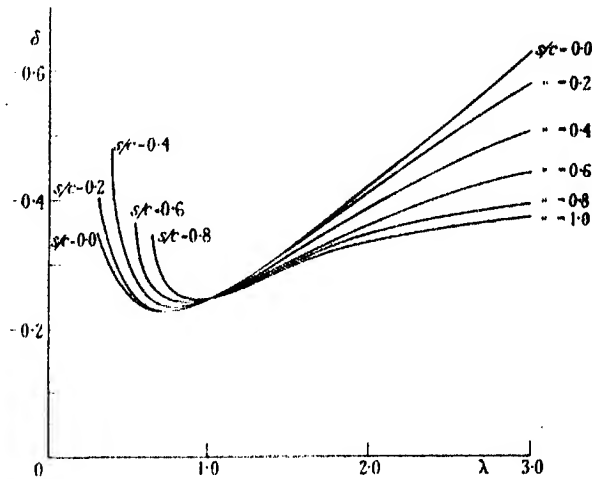


FIG. 3.—Jet of Elliptic Section.

The following is a list of symbols occurring in the paper :—

$2s$ ,  $S$  = span, area of the aerofoil.

$\alpha$ ,  $V$  = angle of incidence, velocity of aerofoil.

$A$  = aspect ratio (= span/chord).

$\rho$  = density of the medium.

$L$ ,  $D$  = lift, drag of the aerofoil.

$k_L$ ,  $k_D$  = lift coefficient, drag coefficient of the aerofoil ( $L/\rho SV^2$ ,  $D/\rho SV^2$ ).

$a$ ,  $b$  = major and minor semi-diameters of the ellipse.

$C$  = area of tunnel section (=  $\pi ab$ ).

$c$  =  $(a^2 - b^2)^{1/2}$ .

$\kappa$  = circulation.

\* 'Aero. Res. Ctte. Rep. and Mem.,' No. 1453, p. 4.

$\Delta\alpha$ ,  $\Delta k_D$  = corrections to angle of incidence and drag coefficients.

$\delta$  = numerical factor involved in the corrections, given by the equations

$$\Delta\alpha = \frac{\Delta k_D}{k_L} = \delta \frac{S}{C} k_L.$$

$$q = (a - b)/(a + b).$$

$$G_r = 2 \left[ \frac{|r-1|}{(r+1) \left(\frac{1}{2}(r-1)\right)^2} \left(\frac{s}{c}\right)^{r-1} - \frac{r^{-2}C_1 |r-3|}{(r-1) \left(\frac{1}{2}(r-3)\right)^2} \left(\frac{s}{c}\right)^{r-3} \right. \\ \left. + \frac{r^{-2}C_2 |r-5|}{(r-3) \left(\frac{1}{2}(r-3)\right)^2} \left(\frac{s}{c}\right)^{r-5} \dots (-1)^{\frac{1}{2}(r-1)} \frac{1}{2} \right].$$

$$g_r = (-1)^{\frac{1}{2}(r-1)} 2 \left[ \frac{|r-1|}{(r+1) \left(\frac{1}{2}(r-1)\right)^2} \left(\frac{s}{c}\right)^{r-1} + \frac{r^{-2}C_1 |r-3|}{(r-1) \left(\frac{1}{2}(r-3)\right)^2} \left(\frac{s}{c}\right)^{r-3} \right. \\ \left. + \frac{r^{-2}C_2 |r-5|}{(r-3) \left(\frac{1}{2}(r-3)\right)^2} \left(\frac{s}{c}\right)^{r-5} \dots + \frac{1}{2} \right].$$

$\delta_1$  = value of  $\delta$  when the aerofoil is along the major axis of a closed tunnel.

$\delta_2$  = value of  $\delta$  when the aerofoil is along the minor axis of a closed tunnel.

$\delta_3$  = value of  $\delta$  when the aerofoil is along the major axis of an open tunnel.

$\delta_4$  = value of  $\delta$  when the aerofoil is along the minor axis of an open tunnel.

$$\alpha_1 = \frac{ab}{c^2} \sum \frac{rq^r}{1+q^r}.$$

$$\alpha_2 = \frac{ab}{c^2} \sum \frac{rq^r}{1-q^r}.$$

$$\beta_1 = \frac{1}{2} \frac{ab}{c^2} \sum (r+1) r (r-1) \frac{q^r}{1+q^r}.$$

$$\beta_2 = \frac{1}{2} \frac{ab}{c^2} \sum (r+1) r (r-1) \frac{q^r}{1-q^r}.$$

The summations in the above series are taken over all *odd* positive integral values of  $r$ .

---

*Investigations in the Infra-red Region of the Spectrum. Part VIII.—  
The Application of the Grating Spectrometer to Certain Bands in  
the Spectra of Triatomic Molecules (Sulphur Dioxide, and Carbon  
Disulphide).*

By C. R. BAILEY and A. B. D. CASSIE, The Sir William Ramsay Laboratories  
of Inorganic and Physical Chemistry, University College, London.

(Communicated by F. G. Donnan, F.R.S.—Received December 14, 1932.)

In Part VI\* of the present series the spectroscopic similarity of the dioxides of sulphur and chlorine was demonstrated. The molecular structure of the two substances was left an open question, since the evidence then available gave contradictory results. The selection rules for the Raman spectrum demanded the obtuse-angled form, while, if complete resolution had been achieved in the infra-red bands, selection rules required the acute-angled modification. The present paper describes the reinvestigation of the bands in question using the grating spectrometer described in Part VII,† and the results show that both sulphur and chlorine dioxides are obtuse angled triangles with a vertical angle of approximately  $120^\circ$ .

*Experimental Results for Sulphur Dioxide.*

Bands E and F of  $\text{SO}_2$ .‡—The first of these bands at  $4.01 \mu$  was also investigated by Levin, Bronk, and Meyer with a grating of some 2880 lines per inch, and apparently consisted simply of a P and R branch doublet.§ Reference to Part VI will show that the structure of this band is critical, since the absence of a Q branch demands the acute-angled form; on the other hand, its presence denotes that the effective electric doublet vibrates parallel to the axis of least inertia, and the only possible solution is provided by the large vertical angle. The results for both bands are shown in figs. 1 and 2; the former and curve 2 (a) were obtained with slit widths of 50 A., or  $3.5 \text{ cm.}^{-1}$ , and curve 2 (b) with slits of 25 A., or rather less than  $2 \text{ cm.}^{-1}$ . Hence the available resolution was greater than that of the previous workers, whose slit widths were 86 A.;

\* 'Proc. Roy. Soc.,' A, vol. 137, p. 622 (1932).

† 'Proc. Roy. Soc.,' A, vol. 138, p. 531 (1932).

‡ Part II, 'Proc. Roy. Soc.,' A, vol. 130, p. 144 (1930).

§ 'J. Opt. Soc. Amer.,' vol. 15, p. 257 (1927).

thus band F at  $4.01\ \mu$  includes a well-defined Q branch, and band E at  $4.37\ \mu$  solely P and R branches. The two observations are consistent, and the only possible solution, giving a vertical angle of  $120^\circ$ , is obtained when a valence force system is applied to the fundamental frequencies allotted as in Table I, which incorporates the present results and those previously obtained with the prism instrument.

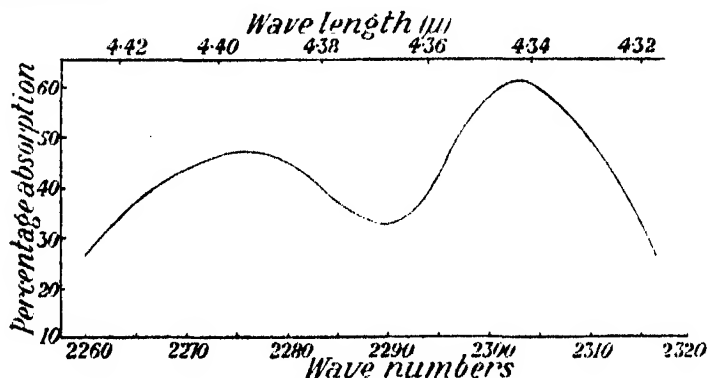


FIG. 1.

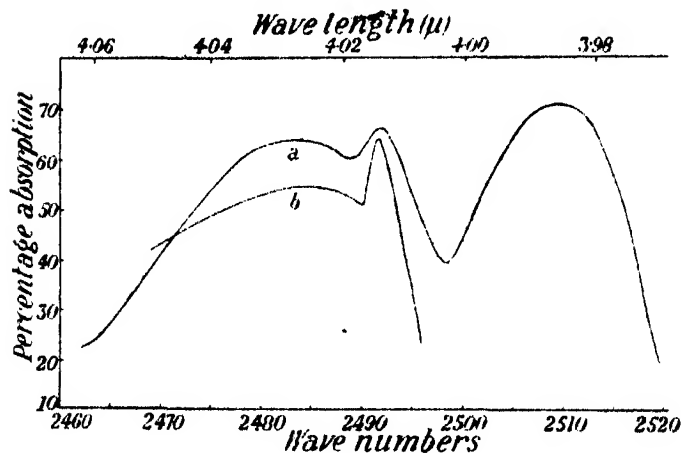


FIG. 2.

In Part II the centre of band F was given as  $2499\text{ cm.}^{-1}$ , being the minimum between the supposed P and R branches; the present value of  $2492\text{ cm.}^{-1}$ , or  $4.014\ \mu$ , is probably correct to within  $0.001\ \mu$ . For band E, the difference between the original determination of  $2305\text{ cm.}^{-1}$ , and that given above, is too large to be accounted for by ordinary experimental error; a disturbing fact is that an almost equal lack of agreement appears in the  $4.6\ \mu$  band for

CS<sub>2</sub>. It is possible that this may be caused by the fluorite prism, which contains a number of flaws, and the refractive index of the prism may not be that of another fluorite. This is to a certain extent confirmed by our observation in Part I\* that the resolving power of the given prism is only one-half that calculated.

Table II summarizes the most probable data for the two molecules, SO<sub>2</sub> and ClO<sub>2</sub>.

Table I.

Band.	Origin.	Band centre.		Maxima.	P - R separation (cm. <sup>-1</sup> ).	$\nu_0$ (calc.).	Difference $\nu_0 - \nu_g$ .
		$\lambda$ ( $\mu$ ).	$\nu_0$ (cm. <sup>-1</sup> ).				
B	$\nu_1$	8.680	1152	$\left\{ \begin{matrix} 1169 \\ 1138 \end{matrix} \right\}$	31	—	—
—	$\nu_2$	19.1	524	—	—	—	—
C	$\nu_3$	7.347	1361	$\left\{ \begin{matrix} 1377 \\ 1361 \\ 1348 \end{matrix} \right\}$	30	—	—
A	$\nu_1 - \nu_2$	16.494	606	$\left\{ \begin{matrix} 611 \\ 602 \end{matrix} \right\}$	9(?)	628	22
D	$\nu_2 + \nu_3$	5.345	1871	1871	—	1885	14
E	$2\nu_1$	4.369	2290	$\left\{ \begin{matrix} 2276 \\ 2303 \end{matrix} \right\}$	27	2304	14
F	$\nu_1 + \nu_3$	4.014	2492	$\left\{ \begin{matrix} 2510 \\ 2492 \\ 2485 \end{matrix} \right\}$	25	2513	21

Table II.

SO <sub>2</sub> .		ClO <sub>2</sub> .	
cm. <sup>-1</sup> .	$\times 10^8$ dynes per cm.	cm. <sup>-1</sup> .	$\times 10^8$ dynes per cm.
$a_1 = 1159, b_1 = -7$ $a_2 + b_2 = 524$ $a_3 + b_3 = 1361$ $c_2 = -21, c_3 = -14$	$K_1 = 9.6$ (S - O) $K_2 = 3.3$ (O - O)	$a_1 = 950, b_1 = -4$ $a_2 + b_2 = 527$ $a_3 + b_3 = 1109$ $c_2 = -21$	$K_1 = 6.7$ (Cl - O) $K_2 = 3.6$ (O - O)
$\angle \text{OSO} = 122^\circ$		$\angle \text{OClO} = 140^\circ$	

The observed combination and over-tones are not sufficient to determine the anharmonic constants completely. An estimate of the heat of dissociation corresponding to the symmetrical vibration  $\nu$ , fig. 3, can be made from the experimental value for  $b_1$ , and is found to be of the order of 134 k. cal. ; it is

\* 'Proc. Roy. Soc.,' A., vol. 130, p. 140 (1930).



interesting to see that this may reasonably correspond to dissociation according to the scheme  $(\text{SO}_2) \rightarrow (\text{S}) + (\text{O}_2)$ , since we have

$$\begin{array}{rcl}
 (\text{SO}_2) & = & [\text{S}]_{rh} + (\text{O}_2) - 69 \text{ k. cal.} \\
 [\text{S}]_{rh} & = & \frac{1}{2}(\text{S}_2) \quad \quad - 14 \text{ k. cal.} \\
 \frac{1}{2}(\text{S}_2) & = & (\text{S}) \quad \quad \quad - 51 \text{ k. cal.} \\
 \hline
 (\text{SO}_2) & = & (\text{S}) + (\text{O}_2) - 134 \text{ k. cal.}
 \end{array}$$

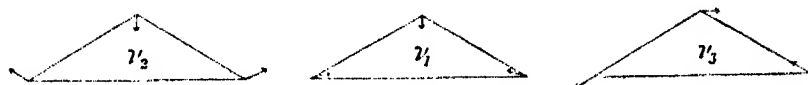
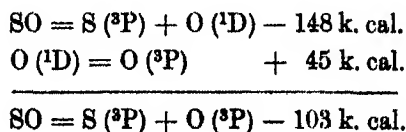


FIG. 3.

The close proportionality we have already observed to exist between the heats of dissociation and the force constants corresponding to the bonds in simple allied molecules is maintained. For  $\text{CO}_2$  and  $\text{SO}_2$ , the ratio of the heats of linking of the central atom to the external oxygen atom is  $182/126 = 1.44$ , and for the force constants is  $14.2/9.6 = 1.45$ . One would expect a similar relationship to hold for the monoxides, particularly as the ratio of the heats of dissociation of the carbon-oxygen bonds in  $\text{CO}$  and  $\text{CO}_2$  ( $237/182 = 1.31$ ) is again the ratio of the force constants for these bonds in the two substances ( $18.8/14.2 = 1.32$ ). One\* of us has pointed out that the value of the heat of dissociation of  $\text{SO}$  as determined by Henri from the band spectrum of this substance, namely, 148 k. cal.,† is greater than the heat of dissociation of the oxygen molecule, and is probably incorrect. At the same time it was shown that a relationship of an approximately linear nature existed between these heats of dissociation and the position of the element in the periodic series, and that whether  $\text{SO}$  was regarded as the oxide of sulphur or the sulphide of oxygen by interpolation on the curves, the value should lie in the neighbourhood of 100 k. cal. The calculated value from the heat of the  $\text{SO}$  link in  $\text{SO}_2$  and from the force constants for the mon- and di-oxides is  $126 \times 7.8/9.6 = 102 \text{ k. cal.}$ , and hence Henri's result represents dissociation into normal sulphur and excited oxygen atoms. We have accordingly



\* 'Nature,' vol. 130, p. 239 (1932).

† 'J. Phys. Rad.,' vol. 10, p. 81 (1929).

The three methods of arriving at the heat of dissociation of sulphur monoxide into normal atoms give concordant results.

*The Structure of the SO<sub>2</sub> Molecule.*

A rigorous application of the octet rule to sulphur dioxide would indicate that the two oxygen atoms were differently bound to the central sulphur atom by four and two electron links respectively. Although this assumption gives the correct interatomic angle, it seems to us from first principles untenable; the values of the force constants indicate equivalence of binding, and furthermore, if the molecule were unsymmetrical, the contours of the various bands would follow no definite scheme such as the inter-consistent appearance of P, Q, and R branches. Hund's suggestion\* of the presence of localized bonds accompanied by superimposed non-localized bonds, the former obtained from two *p* electrons providing directed valencies at 120°, seems more reasonable.

The interatomic dimensions can only be determined approximately from the data available; by analogy with carbon dioxide we are justified in assuming that the addition of another oxygen atom to the central atom will involve no considerable alteration in atomic distances. The rotational fine structure of the ultra-violet bands of sulphur monoxide as obtained by Henri (*loc. cit.*) gives the S-O distance as 1.34 Å.; the corresponding distance in the dioxide was found by Wierl,† using the electron diffraction method, to be 1.37 Å. The average value for the P-R separation in the doublets is 27 cm.<sup>-1</sup>, this should by substitution in the formula  $I = kT/c^2\pi^2\Delta\nu^2$  give an approximation to the largest moment of inertia, which is thus evaluated as  $5.1 \times 10^{-39}$  g. cm.<sup>2</sup>. The three moments  $A < B < C$  are given by  $A = (2ml^2 \cos^2 \alpha)M/(M + 2m)$ ,  $B = 2ml^2 \sin^2 \alpha$ , and  $C = A + B$ , where  $\alpha$  is the semi-vertical angle,  $l$  the S-O distance,  $M$  the mass of the central atom, and  $m$  of the external atoms. We can solve  $C = A + B$  for  $l$ , and the value so obtained is  $1.2 \times 10^{-8}$  cm., in reasonable agreement with Wierl's determination. The interatomic separations in the case of ClO<sub>2</sub> will probably be of the same order but somewhat larger. If it be assumed that the P-R separation observed corresponds to the smallest moment of inertia, then the interatomic distances become apparently too large, and are as given in Part VI, the S-O value rising to 2.3 Å.

Benzene offers another case where six electrons are available for every two chemical bonds, the angle between them being again 120°. The most intense

\* 'Z. Physik,' vol. 73, p. 1 and p. 565 (1931).

† 'Phys. Z.,' vol. 31, p. 1028 (1930).

Raman displacement is  $992\text{ cm.}^{-1}$ , and according to Placzek's rules must be identified with the symmetrical expansion and contraction of the ring. When this is done, the force constant between the CH groups appears as approximately  $7 \times 10^{-5}$  dynes/cm., representing single links between these groups. The stability of the benzene ring is thus similar to that of the sulphur dioxide molecule.

*Experimental Results for Carbon Disulphide.*

*Band C at  $4.6\text{ }\mu$ .*—Reasonable galvanometer deflections were obtained in this region, and the band was therefore reinvestigated. Its contour as determined with slit widths of  $50\text{ \AA}$ ., or  $3.5\text{ cm.}^{-1}$ , is shown in fig. 4; it has P and R branches, with a separation of slightly more than  $13\text{ cm.}^{-1}$ , whereas

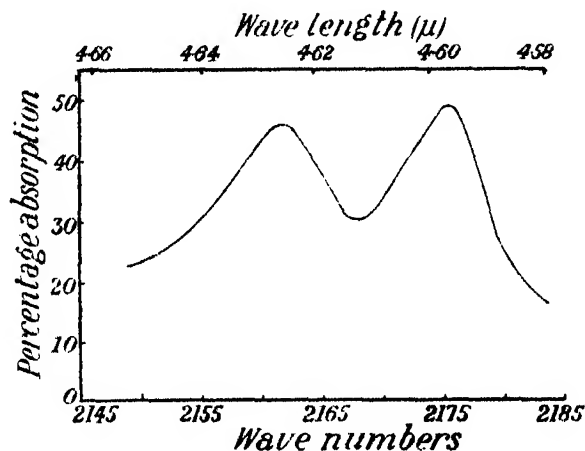


FIG. 4.

the values for the bands at  $11.4$  and  $6.57\text{ }\mu$  in Part III\* were  $13$  and  $12\text{ cm.}^{-1}$  respectively. Dennison and Wright† obtained the corresponding value for the band at  $25.2\text{ }\mu$  of  $16.4\text{ cm.}^{-1}$ ; our values are reproducible and easily determined, and, since both the grating and the prism give the same result, may be taken as definite. The discrepancy is too great either to arise from incomplete separation of the branches, or an increase in the effective moment of inertia owing to the vibrations of the constituent massive particles. The probable explanation is a coupling between oscillation and rotation such as Teller and Tisza‡ invoked to explain similar inconsistencies in the line separa-

\* 'Proc. Roy. Soc.,' A, vol. 132, p. 236 (1931).

† 'Phys. Rev.,' vol. 38, p. 2077 (1931).

‡ 'Z. Physik,' vol. 73, p. 791 (1932).

tions observed in certain bands of the methyl halides. Inconstancy in P and R branch separations is even more marked in the infra-red spectrum of  $\text{CO}_2$  and probably arises from the same cause.

The infra-red spectrum of  $\text{CS}_2$  is given in Table III.

Table III.

Band.	Origin.	Band centre.		Maxima.	P — R separation (cm. <sup>-1</sup> ).	$\nu_0$ (calc.).	Difference $\nu_e - \nu_0$ (cm. <sup>-1</sup> ).
		$\lambda(\mu)$ .	$\nu_0$ (cm. <sup>-1</sup> ).				
—	$\nu_2$	25.2	396.8	$\left\{ \begin{array}{l} 405.8 \\ 396.8 \\ 389.4 \end{array} \right\}$	16.4	—	—
Raman	$\nu_1$	15.3	655.5	—	—	—	—
A	$\nu_3 - \nu_1$	11.391	878	$\left\{ \begin{array}{l} 885 \\ 872 \end{array} \right\}$	13	867.5	—11
B	$\nu_3$	6.566	1523	$\left\{ \begin{array}{l} 1530 \\ 1518 \end{array} \right\}$	12	—	—
C	$\nu_3 + \nu_1$	4.613	2167	$\left\{ \begin{array}{l} 2175.3 \\ 2162.0 \end{array} \right\}$	13.3	2178	11
D	$\nu_3 + 2\nu_2$	4.292	2330	—	—	2318	—12

$\nu_1$  is the optically inactive frequency appearing in the Raman spectrum at 655.5 cm.<sup>-1</sup>, in conjunction with  $2\nu_2$  at 795.0. The allocation of frequencies in Table III is in accordance with Dennison's recent paper on the "Vibrational Levels of Linear Symmetrical Triatomic Molecules."\* In Part V we applied the resonance theory of Fermi† to the elucidation of the  $\text{CS}_2$  and  $\text{COS}$  spectra; it seems probable, especially in view of the failure of Fermi's theory to explain the constancy of the separations in the double doublets,‡ that Dennison's allocation is correct, a similar interpretation being possible for the  $\text{COS}$  spectrum as in Table IV.

Table IV.—The Infra-red and Raman Spectrum of  $\text{COS}$ .

Mode.	Frequency (cm. <sup>-1</sup> ).		Mode.	Frequency (cm. <sup>-1</sup> ).	
	Observed.	Calculated.		Observed.	Calculated.
$\nu_2$	527	—	$\nu_3$	2079	—
$\nu_1$	859	—	$\nu_3 + \nu_1$	2904	2938
$2\nu_2$	1051	1054	$\nu_3 + 2\nu_2$	3095	3133
$2\nu_1$	1718	1718	$\nu_3 + 2\nu_1$	3742	3797
$\nu_1 + 2\nu_2$	1898	1913	$2\nu_3$	4084	4158

\* 'Phys. Rev.', vol. 41, p. 304 (1932).

† 'Z. Physik,' vol. 71, p. 250 (1931).

‡ Cassie and Bailey, 'Z. Physik,' vol. 79, p. 35 (1932).

The band at  $1051\text{ cm.}^{-1}$  has a Q branch ; this is in accordance with Dennison's selection rules, since  $\nu_2$  is a symmetrical vibration, and the changes in electric moment have components along the axis of rotation. We have shown that failure to eliminate scattered radiation of shorter wave-length in the region of  $18\text{ }\mu$  results in poor resolution and a considerable diminution in the observed intensity of the band.\* Before this was realized, any interpretation of the strong band at  $1051\text{ cm.}^{-1}$  as the first harmonic of the weaker band at  $527\text{ cm.}^{-1}$  was ruled out. The contour of the latter band as given in Part V indicates the incomplete resolution achieved, and in analogy to the similar long wave bands of  $\text{CS}_2$  and  $\text{CO}_2$ , this band may be expected to contain a Q branch.

*Correction to Part V.†*

The values of the restoring couple per unit angular displacement are incorrectly given for the molecules  $\text{CO}_2$ ,  $\text{COS}$ , and  $\text{CS}_2$  on pp. 389 and 390. The three molecules are surprisingly similar, since in spite of the great polarizability of oxygen compared with sulphur, the restoring couple is the same in all three cases, and amounts to  $6 \times 10^{-12}$  dyne cm. The significance of this will be discussed in a future paper.

Our best thanks are due as always to Professor F. G. Donnan, F.R.S. One of us (A.B.D.C.) is indebted to the Department of Scientific and Industrial Research for a Senior Award.

*Summary.*

(1) The sulphur dioxide bands at  $4.01$  and  $4.37\text{ }\mu$  have been examined with a grating spectrometer, and the presence of a previously unrecognized Q branch in the former makes it certain that the molecule is triangular, with a vertical angle of  $120^\circ$ . Apparent contradictions between the selection rules for the Raman and infra-red spectra are thus removed.

(2) The carbon disulphide band at  $4.61\text{ }\mu$ , when explored with the grating instrument, confirms the previously determined separation for the P and R branches.

(3) The molecular structure of the above substances is discussed.

\* 'Proc. Roy. Soc.,' A, vol. 137, p. 623 (1932).

† 'Proc. Roy. Soc.,' A, vol. 135, p. 375 (1932).

---

*The Collision of Slow Electrons with Atoms. III.—The Excitation and Ionization of Helium by Electrons of Moderate Velocity.*

By H. S. W. MASSEY, Ph.D., Senior 1851 Exhibitioner, Trinity College, Cambridge, and C. B. O. MOHR, B.A., M.Sc., Trinity College, Cambridge, 1851 Exhibitioner, University of Melbourne.

(Communicated by R. H. Fowler, F.R.S.—Received December 17, 1932.)

It has been shown that quantum mechanical methods are capable of providing a general explanation of the phenomena observed in the excitation of helium by the impact of low velocity electrons. Thus a well-known feature of the observations is that the probability of excitation of a triplet state attains a maximum for electrons of much lower velocities of impact than in the case of the singlet state and falls off very much more rapidly as the velocity increases. By using Born's method of approximation and taking into account electron exchange the variation of excitation probability with velocity of impact has been calculated for various singlet and triplet levels of helium for energies between the resonance potential and 60 volts.† When one compares the observed and calculated curves it is found that qualitative but not quantitative agreement is obtained. It is therefore necessary to improve the methods of calculation and an attempt was made to do this by taking into account the distortion of the incident and outgoing electron waves by the fields of the normal and excited atom respectively.‡ As a result it was then found possible to explain the diffraction effects observed in the inelastic scattering of electrons at large angles but the calculated variation of cross-section with velocity is still not satisfactory.

In order to improve the theory it is important to determine the range of validity of the simple method of approximation by extending the calculations to higher velocities of impact (up to 400 volts) where the method should be more accurate. This is of special interest in view of the recent experimental measurements of Lees§ and of Thieme|| who have measured the excitation

† Massey and Mohr, 'Proc. Roy. Soc.,' A, vol. 132, p. 605 (1931); referred to subsequently as paper A.

‡ Massey and Mohr, 'Proc. Roy. Soc.,' A, vol. 139, p. 187 (1933); referred to subsequently as paper II.

§ 'Proc. Roy. Soc.,' A, vol. 137, p. 173 (1932).

|| 'Z. Physik,' vol. 78, p. 412 (1932).

functions of the various helium lines for electron energies up to, and in certain cases greater than 400 volts. In this paper we have extended the calculations in this way and have considered also ionizing collisions. Since the probability of ionization by electrons can be measured with considerable accuracy we can apply a very satisfactory test of the theory in this direction. In addition to the probabilities of ionization of hydrogen and helium the velocity and angular distributions of ejected and scattered electrons are also computed. The comparison of calculated and observed results is discussed in detail and it is found that Born's approximation is valid for electrons with energies greater than 200 volts.

### Section I. *Excitation of Helium.*

§ 1. *Method of Calculation.*—Employing throughout the same notation as that used in paper A we see that the differential cross-section  $I_n(\delta)d\omega$  corresponding to excitation of the state from the ground state by an electron which is scattered through an angle  $\delta$  into the solid angle  $d\omega$  is given by

$$\text{where} \quad I_n(\delta)d\omega = \frac{k'}{k} |f - g|^2 d\omega, \quad (1)$$

$$f = \frac{2\pi me^2}{h^2} \iiint \left( \frac{2}{r_3} - \frac{1}{r_{23}} - \frac{1}{r_{13}} \right) \Psi_0(r_2, r_1) \exp \{i(kn_0 - k'n_1) \cdot r_3\} \Psi_n(r_2, r_1) dv, \quad (2)$$

$$g = \frac{2\pi me^2}{h^2} \iiint \left( \frac{2}{r_3} - \frac{1}{r_{23}} - \frac{1}{r_{13}} \right) \Psi_0(r_2, r_1) \exp \{i(kn_0 \cdot r_3 - k'n_1 \cdot r_3)\} \Psi_n(r_1, r_2) dv \quad (3)$$

$\Psi_0$ ,  $\Psi_n$  are the wave functions for the initial and final states respectively,  $k/2\pi$  being the wave number of the electron incident in the direction of the unit vector  $\mathbf{n}_0$  and  $k'/2\pi$  that of the electron scattered in the direction of the unit vector  $\mathbf{n}_1$ .

We may use for the wave functions  $\Psi_0$ ,  $\Psi_n$  the same forms as those given in paper A for the P and D states. If we write

$$\psi_{nlm}(Z|r)$$

for the wave function of a single electron in the  $nlm$  state in the field of a charge  $Ze$ , the approximation used in paper A corresponds to a wave function for the  $nlm$  state of helium of the form†

$$\Psi_{nlm}(r_2, r_1) = 2^{-\frac{1}{2}} \{ \psi_0(2|r_1) \psi_{nlm}(1|r_2) \pm \psi_0(2|r_2) \psi_{nlm}(1|r_1) \}, \quad (4)$$

† Eckart, 'Phys. Rev.', vol. 36, p. 878 (1930).

while the wave function for the ground state takes the form

$$\Psi_0(r_2, r_1) = \psi_0(Z|r_1) \psi_0(Z|r_2), \quad (5)$$

where  $Z = 1.687$ .

Wave functions of this form are orthogonal to the ground state wave function except for S states, for which the choice of suitable wave functions is much more difficult. Those functions obtained by variation methods are not orthogonal to the ground state wave function, and errors due to this may be very great. Since paper A was written Vinti† has suggested a form

$$\Psi_{n00}(r_2, r_1) = 2^{-\frac{1}{2}} \{ \psi_0(\alpha|r_1) \psi_{n00}(\beta|r_2) + \psi_0(\alpha|r_2) \psi_{n00}(\beta|r_1) \} + \gamma \Psi_0(r_2, r_1), \quad (6)$$

where the constants  $\alpha$ ,  $\beta$  are adjusted by a variation method and  $\gamma$  is taken to be

$$\gamma = - \int \Psi_0(r_2, r_1) \psi_0(\alpha|r_1) \psi_{n00}(\beta|r_2) dv_1 dv_2 \quad (7)$$

so the function  $\Psi_{n00}$  is orthogonal to that of the ground state. Thus for the  $2^1S$  state we have

$$\alpha = 1.98 \quad \beta = 1.20,$$

and these values were adopted in the present calculations. For higher singlet S states this method may be extended in the manner suggested by Slater.‡ Thus for the  $3^1S$  state we choose an initial function obtained by the variation or other method, and then make up linear combinations of this function with the  $2^1S$  and  $1^1S$  functions so that the condition of orthogonality of  $3^1S$  to  $2^1S$  and  $1^1S$  is satisfied.

For triplet S states a similar method may be applied. The  $2^3S$  wave function must be chosen to be orthogonal to the  $1^3S$  function representing the excluded ground state of the triplet system. This function may be taken to be of the form§

$$\Psi_{10}^3 = N \{ e^{-ar_1-br_2} - e^{-ar_2-br_1} \}. \quad (8)$$

The use of these orthogonal wave functions certainly improves the results to a considerable extent, but it is still unlikely that they give results of as high an accuracy as is obtained for states with azimuthal quantum number greater than zero.

† 'Phys. Rev.', vol. 37, p. 448 (1931).

‡ 'Phys. Rev.', vol. 42, p. 33 (1932).

§ Hylleraas, 'Z. Physik,' vol. 54, p. 347 (1929).



Let us now consider, firstly, the excitation of singlet states. For the velocities of impact considered, we may neglect the exchange term  $g$  in comparison with  $f$ , and this introduces some simplification, for it enables one to choose the axis of the system for the calculations along the vector  $k\mathbf{n}_0 - k'\mathbf{n}_1$ , and so all transitions in which the magnetic quantum number changes are excluded. Following the method of paper A, we then find, using the wave function (4)

$$f = 2^{\frac{1}{2}(4l+18)} \pi^2 m \epsilon^2 \hbar^{-2} n^{l+1} (2l+1)^{\frac{1}{2}} Z^{3/2} K^{l-2} (l+1)! \\ \{(n-l-1)!\}^{\frac{1}{2}} \{(n+l)!\}^{-\frac{1}{2}} \frac{\{(nZ-1)^2 + 4\zeta^2\}^{\frac{n-l-3}{2}}}{\{(nZ+1)^2 + 4\zeta^2\}^{\frac{n+l+3}{2}}} [(nZ+1) \\ \{(nZ-1)^2 + 4\zeta^2\} C_{n-l-1}^{l+2}(x) - 2nZ \{(nZ-1)^2 + 4\zeta^2\}^{\frac{1}{2}} \{(nZ+1)^2 + 4\zeta^2\}^{\frac{1}{2}} \\ C_{n-l-2}^{l+2}(x) + (nZ-1) \{(nZ+1)^2 + 4\zeta^2\} C_{n-l-3}^{l+2}(x)]. \quad (9)$$

where

$$x = (n^2 Z^2 - 1 + 4\zeta^2) \{(nZ+1)^2 + 4\zeta^2\}^{-\frac{1}{2}} \{(nZ-1)^2 + 4\zeta^2\}^{-\frac{1}{2}} \\ \zeta = \frac{1}{2} \{k^2 + k'^2 - 2kk' \cos \delta\}^{\frac{1}{2}} na_0.$$

The coefficients  $C_s^v$  are defined in terms of the expansion

$$(1 - 2ut + u^2)^{-v} = \sum_{s=0}^{\infty} C_s^v(t) u^s,$$

and the expressions for the coefficients for  $S = 0, 1, 2, 3$  are

$$C_0^v(x) = 1, \quad C_1^v(x) = 2vx, \quad C_2^v = v\{(2v+1)x^2 - 1\}, \\ C_3^v(x) = 2v(v+1)\left\{\frac{2}{3}(v+2)x^3 - x\right\}.$$

For the  $S$  states it is not possible to give any general expressions, but the evaluation of  $f$  can be carried out in all cases without difficulty.

On substitution of the form (9) for  $f$  in (1), we obtain the angular distribution of the scattered electrons, and some of these are illustrated for various states in fig. 1, while numerical values are given in Table I. Integration over all angles of scattering gives the total cross-section corresponding to the excitation; the numerical values of the cross-sections for various excitations presented to electrons of 100-, 200- and 400-volts energy are also given in Table I.

Before discussing the experimental results, we will consider briefly the calculation of  $g$ . The labour of this calculation is very much greater than that for  $f$ , as it is only possible to evaluate  $g$  with any accuracy by expansion in a

series of spherical harmonics. For the velocities of impact considered, the zero term in this expression is small, and we may write, with the form (3) for  $g$ :

$$g = \sum_{\nu=-m}^{\infty} P_{\nu}^m(\cos \delta) i^{\nu} \Sigma'_{\nu} \Sigma''_{\nu} \int \gamma_{\nu} F_{\nu}(r_1) G_{\nu}(r_2) dr_2 \cdot (-)^{u-\nu+t} \\ \frac{(l+m+t)! (\nu+m)! s! (2u-2s)! u!}{(u-s)! (s-t)! t! (\nu-m)! (\nu-s+m+t)! (2u+1)! (l-m-t)! (u-l)! (u-\nu)!}, \\ F_{\nu}(r_1) G_{\nu}(r_2) = \frac{2^{\frac{1}{2}(2l+7)} Z^{3/2} \pi^3 m \epsilon^2}{a_0^{3+l} h^2 k^{\frac{1}{2}} k'^{-\frac{1}{2}}} \left[ \frac{(n-l-1)! (2l+1) (l-m)!}{n \{(n+l)!\}^3 (l+m)!} \right]^{\frac{1}{2}} \\ \times \exp - \frac{1}{a_0} \{nZr_1 + r_2\} \cdot r_1^{3/2} r_2^{l+3/2} J_{\nu+\frac{1}{2}}(kr_1) J_{s+\frac{1}{2}}(kr_2) L_{n+l}^{2l+1} \left( \frac{2r_2}{na_0} \right), \\ \gamma_{\nu} = r_1^{\nu} r_2^{-\nu-1} r_1 < r_2; = r_1^{-\nu-1} r_2^{\nu} \quad r_2 < r_1; \quad u = \frac{1}{2}(l + \nu + s). \quad (10)$$

The summation over  $t$  is carried up to such values that all factorial terms remain positive and the summation for  $s$  is over those values which do not violate the condition that  $l, \nu, s$  form the sides of a triangle of even perimeter.

For electron energies as great as 200 volts, at least six terms of this series are required, and although it is possible to evaluate each term by analytical methods using explicit expressions for the Bessel functions, the complications of algebra become so great that it is necessary to resort to numerical methods of integration. After carrying out calculations in this way for the P levels, it was found possible to develop a semi-empirical formula for the exchange integrals at the higher velocities of impact, and this was used to extend the calculations to the other levels.

The angular distributions of electrons which have excited various triplet levels are given in Table I, together with the corresponding total cross-sections.

2 §. *Comparison with Experiment.*—Let us first consider the angular dis-

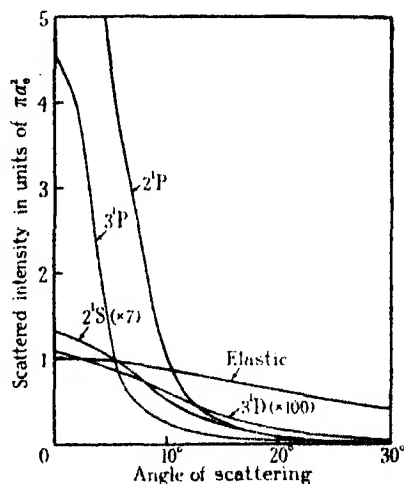


FIG. 1.—Angular distributions of electrons, of 200-volts incident energy, scattered after exciting various levels of helium.

Table I.—Calculated Angular Distributions (per unit solid angle), and Total Cross-Sections for Elastic and Inelastic Collisions of Electrons in Helium, in units of  $\pi a_0^2$ .

Level.	Volts.	0°.	5°.	10°.	20°.	30°.	40°.	Cross-section.
1 <sup>1</sup> S	100	0.99	0.98	0.92	0.79	0.61	0.45	0.375
	200	0.99	0.97	0.87	0.65	0.41	0.25	0.205
	400	0.99	0.95	0.77	0.45	0.22	0.10	0.107
2 <sup>1</sup> S	100	0.126	0.120	0.103	0.049	0.0200	0.0063	0.0087
	200	0.155	0.126	0.087	0.024	0.0039	0.0007	0.0049
	400	0.166	0.120	0.057	0.005	0.0004	0.0.3	0.0025
3 <sup>1</sup> S	100							0.0017
	200							0.0012
	400							0.0007
2 <sup>3</sup> S	100							0.0.27
	200							0.0.6
	400							0.0.2
2 <sup>1</sup> P	100	7.8	4.4	1.78	0.32	0.056	0.013	0.107
	200	17.7	4.5	0.99	0.068	0.0088	0.0007	0.069
	400	39	2.6	0.33	0.009	0.0003	0.0.2	0.047
3 <sup>1</sup> P	100	1.84	1.20	0.45	0.103	0.021	0.0043	0.031
	200	4.5	1.33	0.24	0.027	0.0025	0.0.28	0.021
	400	9.7	0.81	0.084	0.0035	0.0.14	0.0.8	0.013
4 <sup>1</sup> P	100	0.68	0.46	0.215	0.043	0.0092	0.0020	0.012
	200	1.71	0.52	0.131	0.011	0.0012	0.0.13	0.0086
	400	3.70	0.33	0.048	0.0015	0.0.6	0.0.4	0.0061
5 <sup>1</sup> P	100	0.36	0.245	0.115	0.0235	0.0050	0.0010	0.0063
	200	0.91	0.278	0.070	0.0059	0.0.57	0.0.62	0.0046
	400	2.06	0.177	0.026	0.0008	0.0.29	0.0.18	0.0034
2 <sup>3</sup> P	100	0.0026	0.0025	0.0023	0.0017	0.0.9	0.0.4	0.0.72
	200	0.0.63	0.0.59	0.0.49	0.0.23	0.0.7	0.0.1	0.0.69
	400							0.0.7
3 <sup>3</sup> P	100	0.0.40	0.0.38	0.0.34	0.0.24	0.0.14	0.0.7	0.0.12
	200	0.0.80	0.0.76	0.0.67	0.0.40	0.0.17	0.0.5	0.0.17
	400							0.0.2
4 <sup>3</sup> P	100	0.0.109	0.0.104	0.0.99	0.0.75	0.0.47	0.0.25	0.0.43
	200	0.0.20	0.0.19	0.0.17	0.0.11	0.0.5	0.0.2	0.0.52
	400							0.0.6
3 <sup>1</sup> D	100	0.0109	0.0098	0.0070	0.0028	0.0.7	0.0.14	0.0.50
	200	0.0132	0.0106	0.0052	0.0.86	0.0.8	0.0.7	0.0.28
	400	0.0142	0.0094	0.0023	0.0.11	0.0.3	0.0.1	0.0.15
4 <sup>1</sup> D	100	0.0055	0.0051	0.0039	0.0015	0.0.39	0.0.8	0.0.27
	200	0.0067	0.0055	0.0032	0.0.48	0.0.46	0.0.41	0.0.15
	400	0.0074	0.0049	0.0.16	0.0.63	0.0.18	0.0.8	0.0.79
5 <sup>1</sup> D	100	0.0031	0.0028	0.0021	0.0.87	0.0.23	0.0.49	0.0.153
	200	0.0037	0.0031	0.0018	0.0.28	0.0.27	0.0.24	0.0.85
	400	0.0040	0.0028	0.0.97	0.0.47	0.0.11	0.0.45	0.0.45

Table I.—(continued).

Level.	Volts.	0°.	5°.	10°.	20°.	30°.	40°.	Cross-section.
3 <sup>3</sup> D	100							0.0,32
	200							0.0,44
	400							0.0,6
4 <sup>1</sup> F	100	0.0,218	0.0,270	0.0,357	0.0,267	0.0,88	0.0,20	0.0,388
	200	0.0,130	0.0,288	0.0,396	0.0,108	0.0,102	0.0,74	0.0,204
	400	0.0,69	0.0,370	0.0,300	0.0,142	0.0,31	0.0,94	0.0,102
Total	100	12.2	8.0	3.6	1.32	0.75	0.47	0.546
	200	27.0	7.9	2.4	0.79	0.42	0.25	0.318
	400	57.8	5.1	1.3	0.46	0.22	0.10	0.180

tributions of the scattered electrons. Referring to Table I, we note that for the excitation of singlet states :—

- The angular distributions of electrons which have excited levels with the same azimuthal quantum number are very similar in form.
- The probability of excitation is large only of transitions which are also optically allowed, viz., the excited singlet P states. At small angles, the excitation of the 2 <sup>1</sup>P level takes place with greater probability than an elastic collision, but the reverse is the case at large angles.
- The limit of the probability for small angles of scattering increases as the velocity of the incident electron increases, although the total cross-section may be decreasing with increase of velocity in this range.

All these results are in agreement with experiment. Thus Whiddington and Roberts,† and Van Atta,‡ using different methods of velocity analysis of the scattered electrons, have measured the relative probabilities of excitation of helium and other atoms by undeviated electrons of various velocities. Whiddington and Roberts, using an incident electron beam of 400 volts in helium, were able to distinguish non-deviated electrons which had excited the 2 <sup>1</sup>P, 3 <sup>1</sup>P and 4 <sup>1</sup>P levels, but none which had excited other states. The relative intensities of these three groups of electrons is approximately in agreement with the values given in Table I. Again, Van Atta finds that the probability of excitation of the 2 <sup>1</sup>P level by non-deviated electrons increases with electron velocity from 100 to 300 volts. As the relative probabilities at

† 'Proc. Leeds Phil. Soc.,' vol. 2, p. 201 (1931).

‡ 'Phys. Rev.,' vol. 38, p. 876 (1931).

different voltages vary very rapidly with the angle of scattering, it is not possible to compare directly Van Atta's results with theory. However, as the angular range of collection used in his experiments was  $1^{\circ} 40'$ , and as he finds that the probabilities at 100, 200, and 300 volts are in the ratio  $1 : 1.55 : 1.61$ , it will be seen by reference to Table I that the angular distribution would indicate very much the same variation with velocity.

The experiments of Mohr and Nicoll† provide further evidence of agreement between theory and experiment. They find that the angular distributions of electrons of the same incident velocity which have excited the  $2^1P$  and  $3^1P$  levels of helium are almost superposable when fitted together at one angle, just as predicted by theory. The ratio of the probabilities of excitation of the two levels is measured as 2.7 in good agreement with the expected ratio. Finally, a detailed comparison of the theoretical and observed angular distributions shows that the agreement is quite satisfactory at angles less than  $50^{\circ}$  provided the incident electrons have energies greater than 80 volts. At large angles, deviations are apparent, the theory predicting too little scattering. Further experimental observations are required for other incident velocities.

We now consider the experimental evidence available as to the magnitude and form of variation with velocity of the cross-sections for excitation of the various levels. Such evidence is available from two sources, from the absolute measurements of the total cross-sections and ionization cross-sections for electrons of various velocities, and from the optical experiments in which the intensities of excitation of various spectral lines are observed.

The total cross-sections measured by Normand‡ include the elastic, discrete inelastic, and ionization cross-sections. Smith§ has measured the ionization cross-sections by a different method, so the difference of the total and ionization cross-sections can be compared with the calculated sum of the elastic and inelastic cross-sections given in Table I. The comparison is given in Table II, and it is seen that the agreement is reasonably good at 100, 200, and 300 volts, but at 400 volts the observed value is very small and is untrustworthy. Below 100 volts, there seems to be a definite disagreement between the theoretical and observed values.

Let us now turn to the evidence available from spectroscopic investigations. Measurements of the intensity of a given spectral line, say the  $2^1S-3^1P$  line, due to electronic excitation give the cross-section for excitation of the upper

† 'Proc. Roy. Soc.,' A, vol. 138, p. 229 (1932).

‡ 'Phys. Rev.,' vol. 35, p. 1217 (1930).

§ 'Phys. Rev.,' vol. 36, p. 1293 (1930).

Table II.—Comparison of Calculated and Observed Values for the Sum of the Elastic and Inelastic Cross-Sections (in units of  $\pi a_0^2$ ).

	60 volts.	100 volts.	200 volts.	400 volts.
Calculated .....	0.79	0.55	0.32	0.18
Observed .....	1.13	0.67	0.31	—

state from the ground state multiplied by the chance that the excited level will drop to the observed final state, instead of to other possible final states. As it has recently been found possible† to measure the relative magnitudes of the excitation probabilities of the different spectral lines, it is important to calculate the relative probabilities of the different optical transitions in order to reduce the observed values to represent relative cross-sections for excitation of the upper state. Thus if the measured cross-section for emission of a quantum of  $2^1\text{S}-3^1\text{P}$  radiation is  $Q(2^1\text{S}-3^1\text{P})$ , then the cross-section corresponding to the  $1^1\text{S}-3^1\text{P}$  excitation will be

$$Q(2^1\text{S}-3^1\text{P}) \frac{T_{3^1\text{S}}^{3^1\text{P}} + T_{2^1\text{S}}^{3^1\text{P}} + T_{1^1\text{S}}^{3^1\text{P}}}{T_{2^1\text{S}}^{3^1\text{P}}}$$

where  $T$  denotes the transition probability associated with the switch. The probability of transition between levels  $n$  and  $m$  is proportional to

$$\nu_{nm}^3 \left| \int \mathbf{r} \psi_n \psi_m^* dv \right|^2$$

where  $\nu_{nm}$  is the frequency associated with the transition. Knowing the wave functions of the various excited states, it is possible to calculate the  $T$ 's, but it was found unnecessary to recalculate the integrals for helium except for transitions to the deep S levels, the corresponding values calculated for hydrogen by Kupper‡ being sufficiently accurate. It also appears that the higher S wave functions described in the previous section are not very suitable for the calculation of optical transition probabilities, and considerable error is to be expected in the reduction of observed cross-sections for  $n^1\text{S}-2^1\text{P}$  and  $n^3\text{S}-2^3\text{P}$  transitions.

The two sets of measurements due to Lees and Thieme (*loc. cit.*) do not agree very well as to the absolute magnitudes of the cross-sections, but as this requires a knowledge of the actual number of quanta photographed, it is not

† Lees and Thieme, *loc. cit.*

‡ 'Ann. Physik,' vol. 86, p. 511 (1928).

surprising that this discrepancy exists. Because of this it was thought best to reduce all the observed values to compare with the value observed for the  $2^1S-3^1P$  line for 200-volt electrons (after reduction for optical transition probabilities). When this is done, we obtain the observed values, given in Table III, which are to be compared with the calculated values in the same table.

**Table III.**—Comparison of Observed and Calculated Excitation Cross-Sections for Electrons of various Incident Energies. (All values are adjusted to agree for the  $3^1P$  level and 200-volt electrons.)

Level.	60 volts.			100 volts.			200 volts.			400 volts.		
	Thieme.	Calc.	Lees.	Thieme.	Calc.	Lees.	Thieme.	Calc.	Lees.	Thieme.	Calc.	Lees.
$3^1P$	1.06	1.90	1.00	1.22	1.48	1.18	1.00	1.00	1.00	0.58	0.62	0.69
$4^1P$	0.46	0.74	0.45	0.54	0.57	0.50	0.43	0.41	0.41	0.23	0.29	0.29
$5^1P$		0.39	0.062		0.30	0.079		0.22	0.059		0.16	0.045
$3^3P$	0.35	0.03	0.016	0.116	0.0257	0.0268	0.032	0.028	0.027	0.014	0.021	0.0217
$2^1S$		0.67			0.41			0.23			0.12	
$3^1S$		0.15			0.09			0.06			0.03	
$4^1S$	0.012			0.0286			0.0256			0.0235		
$5^1S$	0.027		0.0282	0.020		0.0265	0.012		0.0246	0.0271		0.0227
$6^1S$	0.012		0.0244	0.0272		0.0235	0.0238		0.0218	0.0227		
$2^3S$		0.03			0.013			0.003			0.001	
$4^3S$	0.0265		0.0223	0.0225		0.0285	0.0247			0.0226		
$5^3S$			0.0229	0.0226		0.0295	0.0266			0.0233		
$6^3S$	0.0266			0.0222			0.0223					
$4^1D$	0.018	0.020	0.029	0.013	0.013	0.028	0.0273	0.0272	0.0256	0.0243	0.0237	0.0237
$5^1D$	0.011	0.011	0.0253	0.0285	0.0273	0.0254	0.0245	0.0240	0.0239	0.0226	0.0221	0.0225
$6^1D$	0.0261			0.0243			0.0226			0.0215		
$3^1D$	0.017	0.027		0.0287	0.0215		0.0245	0.0221		0.0233	0.0228	
$4^1D$	0.0281		0.0272	0.0245		0.0266	0.0222		0.0250	0.0213		0.0233

On comparing the two sets of observed results, we notice particularly the following discrepancies:—

- Thieme observes the  $1S-3^3P$  excitation to take place very much more strongly than Lees, and in Table II of his paper estimates that as much as 17 per cent. of the collisions made by 60-volt electrons actually result in radiation of the line  $2^3S-3^3P$ . As this refers to a total collision area  $\pi \times (9.6 \times 10^{-9})^2 \text{ cm.}^2$  and as the total cross section measured by Normand is only  $\pi \times (6.5 \times 10^{-9})^2 \text{ cm.}^2$ , this seems an inconceivably large value.
- For the  $1D$ ,  $1S$ , and  $3S$  levels, Lees obtains considerably smaller relative cross sections than Thieme. This is probably owing to overestimation

by Lees of the cross-sections for the excitation of  $^1P$  levels, as a result of broadening of the spectral lines by absorption of  $1S \rightarrow 3^1P$  radiation by neighbouring atoms, with consequent emission of  $2^1S \rightarrow 3^1P$  radiation. Thieme employs a very low gas pressure ( $5 \times 10^{-3}$  mm. Hg.) and such effects should be much smaller in his measurements.

Turning now to the agreement with experiment, we notice that for excitation to the levels  $3^1P$ ,  $4^1P$ ,  $4^1D$ , and  $5^1D$  there is very good agreement for voltages of 100 and upward. Comparison with observed values for  $S$  levels is difficult, as the reduced cross sections are very inaccurate (thus the reduction makes the probability of excitation to  $4^1S$  less than that to  $5^1S$ ), and it is not possible to calculate the excitation probabilities of the higher  $S$  levels with any accuracy. However, it does not appear that there is any marked discrepancy to be expected. It will be noticed that the calculated cross section for  $5^1P$  is between 3 and 4 times greater than that observed by Lees. It is unlikely that the calculations are incorrect for this level, as they agree with experiment for both the  $4^1P$  and  $3^1P$  levels, and also predict the correct ratio for the probabilities of excitation to  $2^1P$  and  $3^1P$ . As the ratio of the probabilities for levels differing by one in total azimuthal quantum number remains the same up to  $4^1P$ , it is very unlikely that there be any sudden jump between  $4^1P$  and  $5^1P$ .

For the triplet levels the position is not so clear. For  $3^3P$  the agreement with Lees' value at 100 volts is reasonable, but the observed values fall off much more slowly than the calculated values for higher velocities of impact. The observed values for  $^3D$  levels are not comparable with the calculated, as secondary processes are involved in the population of the higher  $D$  levels. Before discussing the triplets further, we will consider the comparison of observed and calculated cross section velocity curves.

In fig. 2 the observed† and calculated curves for  $^1P$ ,  $^1D$ ,  $^1S$ , and  $^3S$  levels are compared, the observed curves for  $^1S$  and  $^3S$  being fitted to the calculated curve at 200 volts, while the curves for  $^1P$  and  $^1D$  are obtained by merely fitting together the calculated and observed for  $3^1P$  at 200 volts. For the  $P$  levels we see that there is good agreement in the form of the curves above 100 volts, but below 100 volts the calculated values become much too great. For  $^1D$  levels the agreement between Thieme's observations and the calculations is very good down to voltages as low as 75 volts,‡ but below this voltage the

† The values given by Lees for the  $^1D$  levels do not agree so well as Thieme's, falling off much more slowly than the latter's as the velocity is increased beyond that corresponding to the maximum in the excitation curve.

‡ 'Phys. Rev.', vol. 39, p. 467 (1932).



calculations again give too big a cross section. But with the  $1S$  levels no exact comparison is possible, and it appears fairly certain that the cross-section-velocity curves for levels with the same azimuthal quantum number are of very much the same form, so the experimental points for  $4^1S$ ,  $5^1S$ , and  $6^1S$  are compared with the calculated  $3^1S$  curve, the relative magnitudes of all being adjusted to obtain agreement at 200 volts. In contrast to P and D levels no marked discrepancy between theory and experiment is apparent

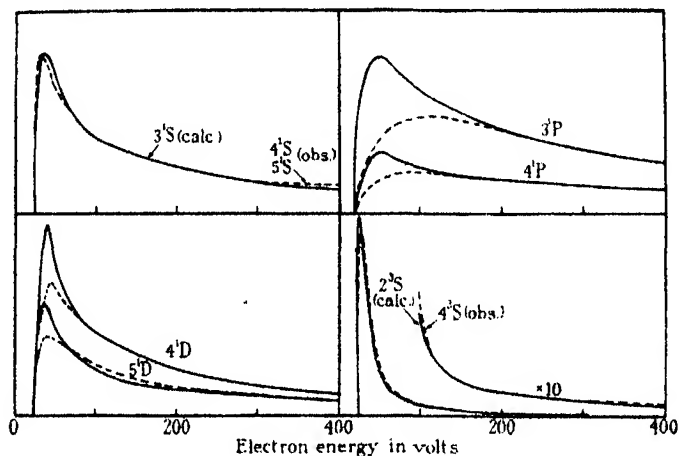


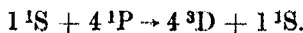
FIG. 2.—Comparison of observed and calculated excitation-cross-section-velocity curves.  
 ——— calculated; — — — — observed.

down to the lowest voltages. For  $3S$  levels the same procedure is followed and reasonable agreement is again obtained down to low voltages.

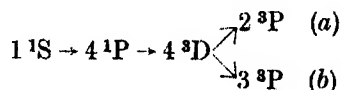
When we compare the experimental and theoretical variation with velocity of the excitation probabilities of  $3P$  and  $3D$  levels, we see that the observed values fall off only as  $v^{-2}$  for high velocities instead of  $v^{-6}$  as calculated. Such behaviour would be expected if spin-orbital interaction were appreciable, for in this case the  $2^3P_1$  level is not completely orbitally antisymmetric, and so may be excited without electron exchange. This has been illustrated by Penney† for the excitation of mercury, but for this atom intercombination lines appear quite strongly in the spectrum, whereas for helium only one such line has been observed. It is therefore inconceivable that spin-orbital interaction in helium is sufficient to explain the discrepancy. In view of the agreement obtained with  $3S$  levels, the disagreement is at first sight surprising, but it is very probable that cascade effects produce the observed intensity of the

† 'Proc. Roy. Soc.,' A, vol. 137, p. 186 (1932).

$2\ ^3\text{S}$ — $3\ ^3\text{P}$  lines at these velocities. Thus Lees and Skinner† have shown that the transition



may take place very readily on impact between helium atoms, and they showed that the peculiar form of their excitation curves for  $4\ ^3\text{D}$ — $2\ ^3\text{P}$  lines is due to this transition. If their interpretation of this is correct, then the cross section for the process (a) in the scheme



is  $5.4 \times 10^{-20}$  cm.<sup>2</sup> for electrons of 200 volts. Now the chance that an atom in the  $4\ ^3\text{D}$  state should radiate a quantum of  $4\ ^3\text{D}$ — $2\ ^3\text{P}$  radiation is only about three times greater than the chance of radiating a quantum of  $4\ ^3\text{D}$ — $3\ ^3\text{P}$  radiation. The cross-section for excitation of the  $3\ ^3\text{P}$  level by the cascade effect (b) is then about  $1.8 \times 10^{-20}$  cm.<sup>2</sup> and is comparable with the observed cross-section ( $4.7 \times 10^{-20}$  cm.<sup>2</sup>) for the  $3\ ^3\text{P}$ — $2\ ^3\text{S}$  transition at 200 volts. It therefore seems very probable that the apparent discrepancy between theory and experiment is not a real one. Further evidence in favour of this is afforded by the fact that no cascade process of the type above would result in the population of  $^3\text{S}$  levels to any appreciable extent, and so we expect the agreement between calculated and observed  $^3\text{S}$  cross-sections.

## Section II. Ionization.

§ 3. *Method of Calculation.*—We now consider inelastic collisions in which the atom is excited to a state which lies in the continuous spectrum. This state will be distinguished by the suffix  $\kappa$  where  $\kappa$  is related to the energy  $E_\kappa$  of the state by the expression

$$E_\kappa = \frac{\kappa^2 h^2}{8\pi^2 m}.$$

The problem of investigating the angular distributions of scattered and of ejected electrons is complicated by the fact that no experiment is capable of distinguishing between the two, and interference will take place between them just as for scattered and exchanged electrons in an elastic collision. This interference will not affect the calculation of the probability of ionization by

† The values given by Lees for the  $^1\text{D}$  levels do not agree so well as Thieme's, falling off much more slowly than the latter's as the velocity is increased beyond that corresponding to the maximum in the excitation curve.

electrons of definite energy, and under certain conditions it will appear that the interference of the two sets of electrons may be neglected. Thus we find, assuming no interference, that the velocity distribution of the ejected electrons indicates a marked concentration towards small velocities, and as a consequence that of the scattered electrons will have a strong concentration towards high velocities. Hence we expect little overlap of the two except at intermediate velocities, and the calculated angular distributions of the scattered electrons should represent the observations made on the faster electrons observed from ionizing collisions, whereas the observations made on the slow electrons should be comparable with the calculations for the ejected electrons. This is, in fact, the case, and we will therefore proceed on the assumption of distinguishability throughout the following calculation.

Owing to the large number of variables which must be taken into account, the problem of computing ionization probabilities is more complicated than that of the calculation for discrete levels. Within the range of validity of Born's formula, we see that the probability of ejection of an electron with momentum lying between  $\hbar\kappa/2\pi$  and  $\hbar(\kappa + d\kappa)/2\pi$  into the solid angle  $d\sigma$  in the direction  $(\chi, \Psi)$  by an electron which is scattered into the solid angle  $d\omega$  in the direction  $(\delta, 0)$  is given by

$$I_{\kappa} d\sigma d\omega d\kappa = \frac{4\pi^2 m^2}{\hbar^4} \frac{k'}{k} \left| \iint V \psi_0 \psi_{\kappa} e^{i(k\mathbf{n}_0 - k'\mathbf{n}_1) \cdot \mathbf{r}} dv dv_1 \right|^2 d\sigma d\omega d\kappa. \quad (11)$$

Using Bethe's formula†

$$\int \frac{e^{i\mathbf{k}\mathbf{n} \cdot \mathbf{r}}}{|\mathbf{r} - \mathbf{r}'|} dv' = \frac{4\pi}{k^2} e^{i\mathbf{k}\mathbf{n} \cdot \mathbf{r}}, \quad (12)$$

this reduces to

$$I_{\kappa} d\sigma d\omega d\kappa = \frac{64\pi^4 m^2}{\hbar^4} \frac{k'}{k} \frac{\varepsilon^4}{K^4} \left| \int \psi_0 \psi_{\kappa} e^{i(k\mathbf{n}_0 - k'\mathbf{n}_1) \cdot \mathbf{r}} dv \right|^2 d\sigma d\omega d\kappa, \quad (13)$$

where

$$K^2 = k^2 + k'^2 - 2kk' \cos \delta.$$

The wave function  $\psi_{\kappa}$  must be normalized so as to have the asymptotic form (apart from logarithmic phase factors):

$$\psi_{\kappa} \sim C \{ e^{-iK r \cos \Theta} + r^{-1} e^{iK r} f(\theta, \phi) \} \quad (14)$$

where

$$\cos \Theta = \cos \theta \cos \chi + \sin \theta \sin \chi \cos (\phi - \psi),$$

and the constant  $C$  is fixed by

$$\int \psi_{\kappa_1} \psi_{\kappa_2} dv = \delta(\kappa_1 - \kappa_2). \quad (15)$$

† 'Ann. Physik,' vol. 5, p. 325 (1930).

Sommerfeld† has obtained a convenient form for this wave function which, for an effective nuclear charge  $Z$  is given by

$$\psi_{\kappa}(r') = \kappa \left[ \frac{n'}{\pi(1 - e^{-2\pi n'})} \right]^{\frac{1}{2}} \frac{e^{i\kappa r'}}{\Gamma(1+n)} \int_0^{\infty} u^n e^{-u} I_0 \left\{ \frac{1}{2} (i\kappa \xi' u)^{\frac{1}{2}} \right\} du, \quad (16)$$

where

$$\xi = r'(1 + \cos \Theta) \\ n = Z/ia_0 \kappa, \quad n' = in.$$

This wave function is exactly correct for atomic hydrogen,‡ but for helium it is difficult to choose a satisfactory form for the aperiodic wave functions. As a sufficiently accurate approximation we take for this the wave function (16) with  $Z = 1.69$  (the effective nuclear charge for the ground state). This function has the advantage of being orthogonal to the ground state wave function, and in any case the error made will probably not be great for the high velocities of impact for which Born's formula is valid.

Substituting  $e^{-Zr/a_0}$  for  $\psi_0$  in (11), and (16) for  $\psi_{\kappa}$ , we see that we require

$$I = \iint \exp \{-Zr/a_0 + i(kn_0 - k'n_1) \cdot r + iKr'(1 - \cos \Theta) - u\} u^n I_0 \left\{ \frac{1}{2} (i\kappa \xi' u)^{\frac{1}{2}} \right\} du dv. \quad (17)$$

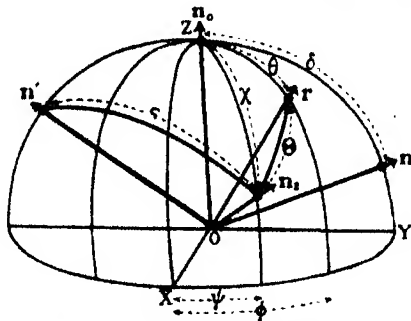


FIG. 3.— $n_0$  direction of incidence;  $n_1$  direction of scattering;  $n_2$  direction of ejection;  $n'$  direction of change of momentum of incident electron.

We choose our axis along the vector  $kn_0 - k'n_1$ , so that

$$(kn_0 - k'n_1) \cdot r = Kr \cos \theta$$

where

$$K^2 = k^2 + k'^2 - 2kk' \cos \delta. \quad (18)$$

† 'Ann. Physik,' vol. 9, p. 257 (1931).

‡ As the experiments refer to molecular hydrogen the calculations were carried out with a nuclear charge of 1.17 and allowance made for the two electrons present. In this way it is expected that all appreciable differences between the atom and molecule will be taken into account.

It is convenient to evaluate the integral (17) by using parabolic co-ordinates

$$\xi = r(1 + \cos \theta), \quad \eta = r(1 - \cos \theta), \quad \phi.$$

Writing  $Z/a_0 = \mu$  and using the formula (17) we find that

$$I = -\frac{1}{2} \frac{\partial}{\partial \mu} \iiint \exp \left\{ -\frac{\mu}{2} (\xi - \eta) + \frac{1}{2} iK (\xi - \eta) + \frac{1}{2} i\kappa (\xi + \eta) - u \right\} u^n I_0 \{z (i\kappa \xi' u)^{\frac{1}{2}}\} d\xi d\eta d\phi du, \quad (19)$$

where  $\xi', \eta'$  are parabolic co-ordinates referred to the direction of ejection ( $\chi, \psi$ ) as axis. If  $\vartheta$  is the angle which the direction of ejection makes with the vector  $kn_0 - k'n_1$ , then

$$\xi' = \xi \cos^2 \frac{1}{2} \vartheta + \eta \sin^2 \frac{1}{2} \vartheta + 2(\xi\eta)^{\frac{1}{2}} \cos \frac{1}{2} \vartheta \sin \frac{1}{2} \vartheta \cos \phi.$$

Using this expression we have†

$$I_0 \{2(i\kappa \xi' u)^{\frac{1}{2}}\} = \Sigma_m I_m \{2(i\kappa \eta \sin^2 \frac{1}{2} \vartheta)^{\frac{1}{2}}\} I_m \{2(i\kappa \xi \cos^2 \frac{1}{2} \vartheta)^{\frac{1}{2}}\} \cos m\phi. \quad (20)$$

Substituting in (19) and integrating over the  $\phi$  co-ordinates we see that

$$I = -\pi \frac{\partial}{\partial \mu} \iiint \exp \frac{1}{2} \{ \xi (-\mu + iK + i\kappa) + \eta (-\mu - iK + i\kappa) \} e^{-u} u^n I_0 \{2(i\kappa \eta u \sin^2 \frac{1}{2} \vartheta)^{\frac{1}{2}}\} I_0 \{2(i\kappa \xi u \cos^2 \frac{1}{2} \vartheta)^{\frac{1}{2}}\} d\xi d\eta du. \quad (21)$$

We now make use of the formula

$$\int_0^\infty e^{-\lambda t} I_0 \{2r\xi^{\frac{1}{2}}\} d\xi = \frac{1}{\lambda} e^{-r^2/\lambda}, \quad (22)$$

and obtain

$$\begin{aligned} I &= -\pi \frac{\partial}{\partial \mu} \{ \mu^2 - K^2 + \kappa^2 + 2i\kappa \}^{-1} \int_0^\infty \exp \{ -u(-\mu^2 + K^2 + \kappa^2 - 2\kappa K \cos \vartheta) \} u^n du, \\ &= -4\pi \Gamma(1+n) \frac{\partial}{\partial \mu} \frac{(\mu^2 - K^2 + \kappa^2 + 2i\kappa)^n}{(-\mu^2 - K^2 - \kappa^2 + 2\kappa K \cos \vartheta)^{n-1}}. \end{aligned}$$

Using now the fact that

$$n = -i\mu/\kappa,$$

we obtain

$$\begin{aligned} |I|^2 &= 16\pi^2 \mu^2 K^2 \frac{K^2 - 2K\kappa \cos \vartheta + (K^2 + \mu^2) \cos^2 \vartheta}{\{\mu^2 + (K + \kappa)^2\} \{\mu^2 + (K - \kappa)^2\} \{K^2 - 2K\kappa \cos \vartheta + \kappa^2 + \mu^2\}^4} \\ &\quad \exp \left\{ -\frac{2\mu}{\kappa} \arctan \frac{2\mu\kappa}{\kappa^2 - K^2 - \mu^2} \right\}. \quad (23) \end{aligned}$$

† 'Watson, "Theory of Bessel Functions," p. 361, Camb. Univ. Press (1922).

We note that the probability of ionization is a maximum when the conservation of momentum is satisfied in the electron-electron collision, for in this case  $\vartheta = 0$ .

To obtain the angular distribution of ejected electrons of a given energy, it is necessary to substitute in (13) and integrate over all angles of scattering of the incident electron.

Again, substituting (23) in (13) and integrating over all angles of ejection, we find that the angular distribution of the scattered electrons is given by

$$I(\delta) = \frac{2^{13} \pi^5 m^2 \epsilon^4 \mu^6 \kappa \kappa' \{K^2 + \frac{1}{2}(\mu^2 + \kappa^2)\}}{k K^2 \{\mu^2 + (K + \kappa)^2\}^3 \{\mu^2 + (K - \kappa)^2\}^3} \{1 - \exp(-2\pi\mu/\kappa)\} \\ \exp \left\{ \frac{-2\mu}{\kappa} \arctan \frac{2\mu\kappa}{K^2 - \kappa^2 + \mu^2} \right\}. \quad (24)$$

To obtain the probability of ionization, it is necessary to perform a second numerical integration over the wave number  $\kappa$  of the ejected electron.

§ 4. *Results of Calculation and Comparison with Experiment.* (a) *Ionization Probability.*—In figs. 4 and 5 the calculated probabilities of ionization of hydrogen and of helium are illustrated as functions of the energy of the incident

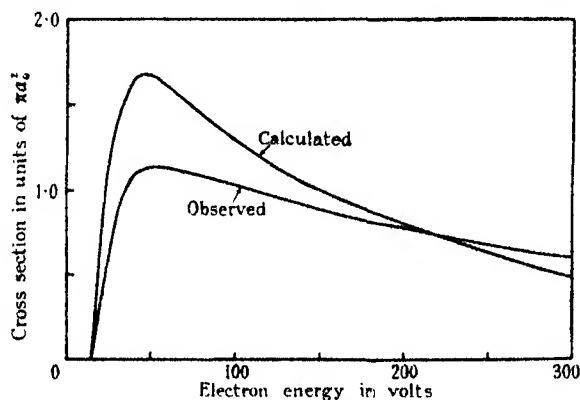


FIG. 4.—Ionization probabilities in hydrogen.

electron, and are compared with the experimental results obtained by Tate and Smith,<sup>†</sup> and Smith.<sup>‡</sup> For hydrogen the observed cross-section beyond 100 volts must be reduced by 8 per cent. to exclude the multiple ionization effects which are not allowed for in the calculation. No correction is necessary in helium owing to the small probability of such multiple excitations.

<sup>†</sup> 'Phys. Rev.,' vol. 39, p. 270 (1932).

<sup>‡</sup> 'Phys. Rev.,' vol. 36, p. 1293 (1930).

For electrons with energies greater than 100 volts in hydrogen and 150 volts in helium, the agreement is quantitatively exact to within 10 per cent. This is very satisfactory and confirms the conclusions arrived at from the study of the excitation of discrete levels. It is further of great interest to note that the calculated probability becomes greater than the observed in increasing ratio as the velocity of impact decreases, just as we remarked in discussing the excitation of P levels. Just the same feature has been noted<sup>†</sup> in the behaviour

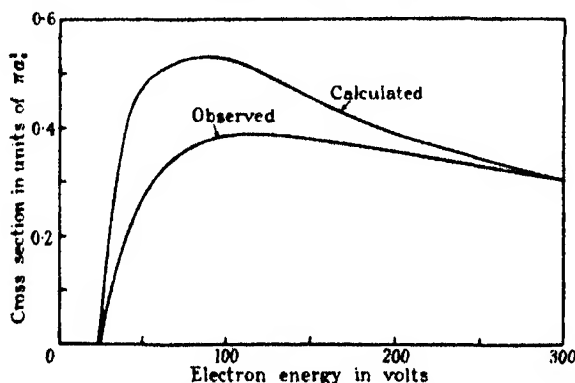


FIG. 5.—Ionization probabilities in helium.

of the calculated and observed probabilities of ionization of inner shells of heavy atoms by electron impact, and it appears to be undoubtedly due to a failure to Born's first approximation. However, this provides no ground for imagining a failure of the quantum theory of collisions, particularly as the agreement is so good at high velocities. In the concluding section we will discuss how the discrepancy might arise in the theory.

(b) *Velocity Distribution*.—Fig. 6 illustrates a number of calculated velocity distributions of ejected electrons, and the inset figure indicates the form of the velocity distributions of the ejected and scattered electrons combined, assuming no interference. The type of curve obtained is similar in form to that observed by Tate and Palmer<sup>‡</sup> for electrons resulting from ionizing collisions with mercury atoms. No observations are available for helium.

It is interesting to note that the energy of ejection of maximum probability remains unaltered as the incident energy increases beyond about 50 volts.

The form of the distribution curves indicates that there will be little interference between ejected and scattered electrons of the same energy except

<sup>†</sup> Webster, Clark and Hansen, 'Phys. Rev.', vol. 37, p. 115 (1931); Webster, Hansen and Duveneck, 'Phys. Rev.', vol. 42, p. 141 (1932).

<sup>‡</sup> 'Phys. Rev.', vol. 40, p. 731 (1932).

when this energy is nearly half the total available. The low velocity electrons can be taken as ejected, the higher as scattered, whereas the intermediate ones we cannot yet discuss. With this assumption we now proceed to the angular distributions.

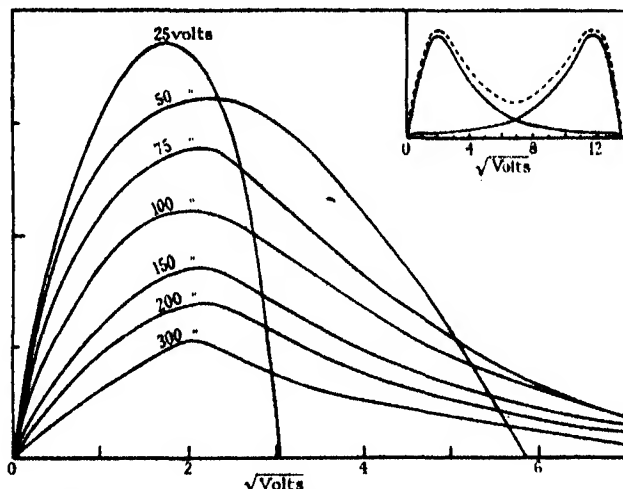


FIG. 6.—Velocity distributions of electrons of electrons ejected from hydrogen by electrons of various incident energies.

*Inset.*—Velocity distribution of ejected plus scattered electrons corresponding to electrons of 200 volts incident energy.

(c) *Angular Distributions.*—The calculated angular distributions of ejected and of scattered electrons under conditions suitable for observation are given in fig. 7. We notice that the scattered electrons are concentrated towards small angles, just as for excitation of P levels, whereas the ejected electron angular distribution has a maximum at the angle  $\chi$  given by

$$k^2 + \kappa^2 - 2k\kappa \cos \chi = k'^2. \quad (25)$$

The maximum corresponds to the conservation of momentum. Apart from this maximum, the distribution deviates comparatively slightly from uniformity. In particular, angular distributions of all ejected electrons with energies lying in a range of some volts would be monotonic with a slow fall in intensity with increase of angle.

These characteristics of the angular distributions of scattered and ejected electrons are in agreement with the observations of Tate and Palmer (*loc. cit.*) on the ionization of mercury vapour. Some of their curves are illustrated in fig. 7 (inset).



Hughes and McMillen have observed the angular distributions of slow electrons resulting from ionizing collisions in hydrogen<sup>†</sup> and argon,<sup>‡</sup> and these should be comparable with our calculations for ejected electrons. They find sharp maxima at certain angles, the distribution being otherwise fairly uniform. Although in certain cases these maxima might correspond to those arising from the formula (25), Hughes and McMillen find maxima at angles greater than  $90^\circ$  which could never be obtained from formula (25). It is possible that interference with scattered electrons is producing the effects, but it seems unlikely in view of the form of the velocity distributions in fig. 6. In a later paper we hope to discuss the interference effect in detail.

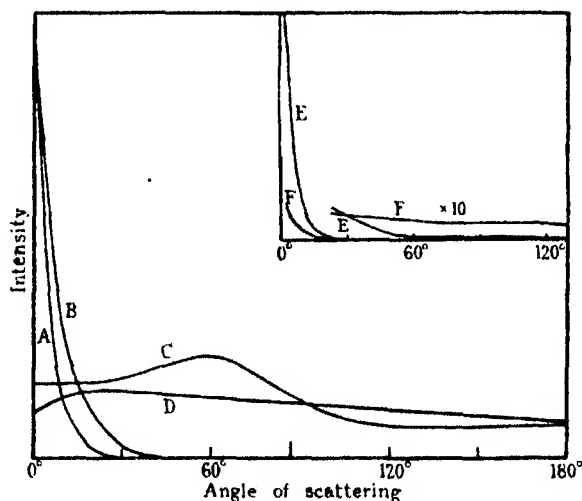


FIG. 7.—Angular distribution of scattered and ejected electrons corresponding to electrons of 200-volts incident energy. A, scattered electrons with 176-volts energy; B, scattered electrons with 163-volts energy; C, ejected electrons with 13.6-volts energy; D, ejected electrons with 0.85-volts energy.

*Inset.*—Observed angular distribution of electrons resulting from ionizing collisions of 80-volts electrons with mercury atoms. E, electrons with energies between 70 and 76 volts; F, electrons with energies between 0 and 35 volts.

### Section III. Discussion.

Throughout this discussion we will confine ourselves to the case of the excitation of singlet levels. In deriving formulæ for the excitation probabilities, the wave function  $\Psi$ , which is a solution of the wave equation for the complete

<sup>†</sup> 'Phys. Rev.', vol. 41, p. 39 (1932).

<sup>‡</sup> 'Phys. Rev.', vol. 39, p. 585 (1932).

system of atom plus incident electron, is expanded in a series of atomic wave functions

$$\Psi = (\Sigma_n + \int) \psi_n(r_a) F_n(r). \quad (26)$$

The suffix  $a$  denotes the aggregate of atomic electrons. It is shown that the functions  $F_n$  satisfy the infinite set of simultaneous equations

$$[\nabla^2 + k_n^2] F_n(r) = \frac{8\pi^2 m}{\hbar^2} \Sigma F_m V_{mn}, \quad n = 0, 1, 2, \dots, \quad (27)$$

where  $k_n/2\pi$  is the wave number of an electron which has excited the  $n$ th state of the atom, and  $V_{mn}$  is the matrix element of the interaction energy between the atom and incident electron with respect to the atomic wave functions  $\psi_n, \psi_m$ .

To obtain approximate formulæ for the asymptotic form of the functions, the assumption is first made of neglecting all scattered waves on the right side of relation (27), thus leaving only the incident plane wave  $e^{ik_0 \cdot r}$  and the equation

$$[\nabla^2 + k_n^2] F_n(r) = \frac{8\pi^2 m}{\hbar^2} e^{ik_0 \cdot r} V_{0n}. \quad (28)$$

This equation is immediately soluble and its solution leads to Born's formula which has been used throughout this paper. It is clear that it neglects all effects due to scattered waves. There seems no hope of including all such effects in the theory and so it is very important to determine which particular scattered waves are important at low velocities. The first thing to determine is whether it is necessary to consider any other states but the 0th and the  $n$ th in discussing the excitation of the  $n$ th state. If we make the assumption that this is not necessary, we obtain the simultaneous equations

$$\left. \begin{aligned} \left[ \nabla^2 + k_n^2 - \frac{8\pi^2 m}{\hbar^2} V_{nn} \right] F_n &= \frac{8\pi^2 m}{\hbar^2} F_0 V_{0n} \\ \left[ \nabla^2 + k^2 - \frac{8\pi^2 m}{\hbar^2} V_{00} \right] F_0 &= \frac{8\pi^2 m}{\hbar^2} F_n V_{n0} \end{aligned} \right\}. \quad (29)$$

In paper II we assumed that  $V_{0n}$  is sufficiently small to solve these equations by successive approximations, starting from

$$\left[ \nabla^2 + k^2 - \frac{8\pi^2 m}{\hbar^2} V_{00} \right] F_0 = 0. \quad (30)$$

The inclusion, in this way, of the effect of the interactions  $V_{00}, V_{nn}$  did not improve the agreement with experiment at low velocities, and it was clear

that the matrices  $V_{00}$ ,  $V_{nn}$  were not of great importance in determining the form of inelastic cross-section curves. The next stage, then, is to examine whether an exact solution of the equations (29) would be likely to improve the agreement with experiment. In short, is it only necessary to regard the  $0$ th and  $n$ th scattered waves as "closely" instead of "loosely" coupled? The experimental evidence does actually indicate that this may be so, for the important feature is that the calculated excitations for P levels become inaccurate at higher voltages than for D levels, and the D at higher than for S. Such an effect would seem to be connected with the matrices  $V_{0n}$  in particular, rather than the matrices associated with other states, and we would expect the deviations to appear first in the order given. This may be seen as follows.

For the special case of exact resonance where  $k^2 = k_n^2$ ,  $V_{00} = V_{nn}$ , the equations (29) have been solved by London.<sup>†</sup> He gives the cross-section for the  $0 - n$  transition in the form

$$Q = \frac{\pi}{k^2} \sum_s (2s + 1) \sin^2(\eta_s - \delta_s), \quad (31)$$

where the phases  $\eta_s$ ,  $\delta_s$  are determined by solving the equations

$$\left. \begin{aligned} \left[ \nabla^2 + k^2 - \frac{8\pi^2 m}{h^2} (V_{00} + V_{nn} + V_{0n}) \right] \mathfrak{F} &= 0 \\ \left[ \nabla^2 + k^2 - \frac{8\pi^2 m}{h^2} (V_{00} + V_{nn} - V_{0n}) \right] \mathfrak{F} &= 0 \end{aligned} \right\}. \quad (32)$$

In particular for small  $V_{0n}$ ,  $V_{nn}$  and  $V_{00}$

$$\eta_s - \delta_s = \frac{8\pi^2 m}{h^2} \int_0^\infty V_{0n} \{J_{s+\frac{1}{2}}(kr)\}^2 r dr, \quad (33)$$

and we obtain Born's approximation. From this special case we see that the potential  $V_{0n}$  acts as a scattering potential just as do  $V_{00}$  and  $V_{nn}$ , and the transition probability is measured by the phase shift which this field produces on an incident wave. If this phase shift is large, Born's formula fails and gives too large a result.

We now require to determine the conditions under which  $V_{0n}$  will have large scattering power and so produce large phase changes. It has been shown by Allis and Morse<sup>‡</sup> that the scattering power of a field may be taken as proportional to the integral

$$\int r^2 V_{0n} dr.$$

<sup>†</sup> 'Z. Physik,' vol. 74, p. 143 (1932).

<sup>‡</sup> 'Z. Physik,' vol. 70, p. 567 (1931).

If the  $0 - n$  transition is optically allowed, this integral is infinite, while for transitions associated with a quadrupole moment (D levels) it is much greater than for S — S transitions, as in the former case  $V_{0n} \sim Cr^{-4}$  for large  $r$  and for the latter it vanishes as  $e^{-Ar}$ . We therefore expect, if the neglect of this reaction between  $F_0$  and  $F_n$  is the cause of the discrepancy between theory and experiment, that the accuracy of Born's formula for calculating the probability of excitation of various levels from the ground state will increase as one proceeds from optically allowed transitions to those with higher moments only (i.e., in the order P, D, S excitation) by analogy with the case of exact resonance. It therefore seems reasonable to expect the deviations in the observed directions.

From the above point of view it is possible to form a physical picture of the collision processes which occur when the interaction is sufficiently strong to render Born's first approximation inadequate. When this is so, we may regard the incident electron as making multiple collisions in the field of the same atom. Owing to the long range of the field  $V_{0n}$  the electron may cause a transition in the atom and lose energy in the process without appreciable deviation from its course. The electron has still to traverse a powerful field due to the same atom and may produce a second transition in the atom in which it reverts to its normal state. This superelastic collision will also take place in all probability with little deviation. The result of these two collisions is to produce an electron which has lost no energy and is deviated only a little from its original course. Such electrons will have an angular distribution corresponding to inelastic scattering but a velocity corresponding to elastic scattering. Hence when such double collisions occur with sufficient frequency, the angular distribution of elastically scattered electrons will become much steeper at small angles than that given by Born's first approximation. This is just what has been observed at energies below 200 volts in helium.† Further, as the inelastic collisions can take place at greater distances than the elastic, we expect the effect of these double collisions to result in a decrease in inelastic scattering, accompanied by a corresponding increase of elastic scattering, a number of originally inelastically scattered electrons making superelastic collisions before leaving the atomic field. To a rough approximation, neglecting interference effects and jumps to intermediate levels, the total cross-section for all collisions should be unaltered. This is actually the case, for we found that below 100 volts in helium Born's formula predicts too large a probability of ionization (see figs. 4 and 5), but too small a probability of an elastic collision. Actually

† Hughes and McMillan, 'Phys. Rev.', vol. 41, p. 154 (1932).

in Table II we did not separate the elastic and discrete inelastic collisions, but we have evidence from two independent directions that the calculated elastic cross-section is too small, and all inelastic cross-sections too large. The first of these is derived from comparison of observed and calculated cross section velocity curves discussed above. Secondly, Hughes and McMillen (*loc. cit.*) have shown by relative measurement of the angular distributions of electrons scattered elastically in helium that the calculated curves predict too little scattering at both small and large angles.

Finally, we are able to see clearly what diffraction effects are to be expected in inelastically scattered electrons. On the above picture, the inelastic collisions which take place at large distances from the atom will result effectively in "beams" of electrons which have lost energy but which are otherwise incident in the atomic field just as the incident beam. These electron "beams" will then be diffracted by the field of the excited atom just as the incident beam is by the field of the normal atom. If the energy loss is small compared with the energy of incidence, the diffraction effects produced in the "inelastic" beams will closely resemble those produced by the incident beam and will be almost indistinguishable from those produced by the second double process in which the incident beam is diffracted by the field of the normal atom, and the diffracted beams make inelastic collisions without appreciable deviation. When the energy loss is comparable with the energy of incidence, the two sets of diffracted electrons which have lost energy will interfere strongly, and little resemblance between the angular distributions of the elastically and inelastically scattered electrons is to be expected. All these conclusions are in agreement with experiment. The above picture of the collision is admittedly incomplete, but seems to represent adequately the main phenomena occurring.

#### *Summary.*

In this paper, inelastic collisions of electrons with helium—including ionizing collisions—are investigated in considerable detail. A critical survey of the experimental material in the light of the calculations is given, and the range of Born's first approximation is fixed. All deviations from the formulæ derived from this approximation are explained, at least qualitatively, and it is found possible to develop a simple physical picture involving double collisions with the same atom which accounts for a number of observed collision phenomena. Among these are included the form of optical and X-ray excitation functions, and the diffraction of inelastically scattered electrons.

---

*Polish on Metals.*

By R. C. FRENCH.

(Communicated by G. P. Thomson, F.R.S.—Received December 21, 1932.)

[PLATES 7-9.]

The burnishing and rubbing of a metal surface to give it a smooth shiny finish is often used to give metal ware, jewellery and pieces of apparatus a better appearance. This is called polishing and is done by abrading and then finishing by rubbing with a soft, fine powder. Abrasion usually removes thin layers off the surface by taking out many small pieces of the metal. The sharp grains of the abrasive cut numerous small pieces out of the surfaces and work the surface down roughly to the desired level. The higher degree of polishing works the surface mechanically without removing much of the metal itself. When lastly a soft, fine powder is used, made into a very wet paste, this polishing material remains uncontaminated after having been rubbed on the metal continuously. A well-polished surface has the same colour as the rough metal had originally but the glassy finish reflects so highly that no structure is seen with the eye. It is difficult to describe the surface of a polished metal but Professor Flinders Petrie aptly describes it as having a "wet lustre." The microscope usually shows scratches left from the polishing which look like gently rounded furrows. Sir G. T. Beilby made a scientific study of polished surfaces with the use of a microscope and it is in supplement to his work that these experiments have been done. Beilby noticed in the final stages of polish that the surface appeared to flow and acted like a film to cover over scratches and pits and give a glassy finish.

This film is called the Beilby layer and has the appearance of a super-cooled liquid. During intermediate stages the parallel edges of a scratch in the surface could be seen to be drawing together and at points had come together and bridged over the furrow. Afterwards the film, which covered the scratch completely and hid it, could be removed by etching and the scratch would appear as it looked originally. The mechanical working of the metal to make it flow, moves the surface very much in relation to the greater portion of the metal underneath and is a kneading and twisting of the metal on the surface. In the following experiments pieces of copper, silver, gold, and chromium of  $1 \times 1.5 \times 0.5$  cm. size were used as different test metals. They were worked

on different grades of emery paper and with polishing powders, and electron diffraction pictures were taken at different stages of polish to notice changes in the crystal structure.

### *Apparatus.*

The electron camera\* is particularly useful for investigating these mechanically worked surfaces as the electrons have a small depth of penetration not more than  $10^{-6}$  cm. and so confine themselves to the topmost surface layer. A fine beam (0.23 mm. diameter) of electrons is selected from a cold cathode gas discharge tube of which the voltage depends on the "hardness" of the vacuum of the discharge tube. The electrons hit the surface of the specimen at a small angle and because of their wave-length  $\lambda = h/mv$  (De Broglie) and the crystal-line nature of the surface are diffracted along selected angles  $\theta$  given by  $n\lambda = 2d \sin \theta$  (Bragg). A photographic plate set at right angles to the incident beam is exposed to the beam of diffracted electrons. The spacings between crystal planes in the specimen are found by the use of the above formulæ and geometry of the camera.

$$d = \frac{L \sqrt{150}}{x \sqrt{V}} \times 10^{-8} \text{ cm.} \quad (1)$$

$d$ , spacing of planes ;  $L$ , distance from specimen to plate ;  $x$ , distance of point on plate from centre of undeviated beam ;  $V$ , voltage of discharge.

### *Theory.*

It was found that the sharp rings given by a polycrystalline surface became blurred if the surface were polished

I.—This could be explained by the breaking up of the large crystals into smaller crystals by the action of polishing. For X-rays Scherrer† deduced the formula  $B = \frac{K\lambda}{D (\cos \theta_0/2)}$  by which the width of the rings depends on the crystal size.  $B$ , half intensity breadth of ring.  $K = 2 \left( \log \frac{2}{\pi} \right)^{1/2}$ .  $D$  is the length of one edge of the crystal, assumed a cube.  $\theta_0$  = Bragg angle. As the wave-length for high speed electrons are comparable with that of X-rays, the above formula might be applied for electrons.

\* Thomson and Fraser, 'Proc. Roy. Soc.,' A, vol. 128 (1930).

† 'Nachr. ges. Wiss. Gött.,' p. 190 (1918).

II.—If the polishing were so severe as to reduce the crystals infinitely, the polished surface would be a mass of the atoms in no orderly arrangement. The atoms would not be evenly spaced as in a crystal lattice, but two atoms could only approach each other to a common distance of separation after which the two would "touch." This limiting distance of approach would predominate in large collections of these atoms displaced from their positions in the crystal lattice and so evince a degree of orderliness. Wierl\* gives a formula for such a semi-orderliness of gas molecules. For equal atoms this becomes  $I = 2\psi^2 \left(1 + \frac{\sin \chi}{\chi}\right)$ .  $I$ , intensity of diffracted electrons.  $\psi$  atom form factor.  $\chi = 4\pi s_0 \frac{\sin \theta}{\lambda}$ .  $s_0$  distance between two atoms. If  $\psi$  is constant maxima will occur for  $I = 7.725, 14.066$ , etc., which will show as rings on the photograph.

To allow for the variation of  $\psi$  with  $\sin \theta/\lambda$ ,  $I = 2\psi^2 \left(1 + \frac{\sin \chi}{\chi}\right)$  was plotted against  $\sin \theta/\lambda$ .  $\psi$  was obtained from the X-rays values of the atom form factor corrected to make it suitable for electrons.† In the formula for  $\chi$  the value of  $s_0$  was taken as the closest distance of approach of the atoms in the crystal according to X-rays. The percentage difference between the maxima on the graph and the maxima of the photographs for each metal was found and the chosen value  $s_0$  was changed by this amount to give  $s$  the closest distance of approach of the atoms in the polished layer as found by experiment.

### Refractive Index.

From Sommerfeld's theory, the inner potential of most metals is of the order of 15 volts. As the potential outside the metal from where the electrons are coming is zero, and the potential inside the metal is positive, there will be a refractive effect at the boundary of these two media. The electrons will be bent towards the normal to the surface where they are incident. The index of refraction  $\mu$  is equal to  $\sqrt{1 + \frac{\Phi}{P}}$ .  $\Phi$  = inner potential of the metal and  $P$  = the velocity of incident electrons in volts, so that  $\mu$  is slightly more than 1. When the electron beam is incident on an ordinary surface composed

\* 'Ann. Physik,' vol. 8, p. 521 (1931).

† G. P. Thomson, 'Wave Mechanics of Free Electrons,' p. 118 (1923).



of lumps as in fig. 1 the glancing angle is quite large and since  $\mu$  is little more than 1 the refractive effect will be negligible. For a very flat surface with no projections on the surface more than a few atoms high, the effect of the refractive index would appear.

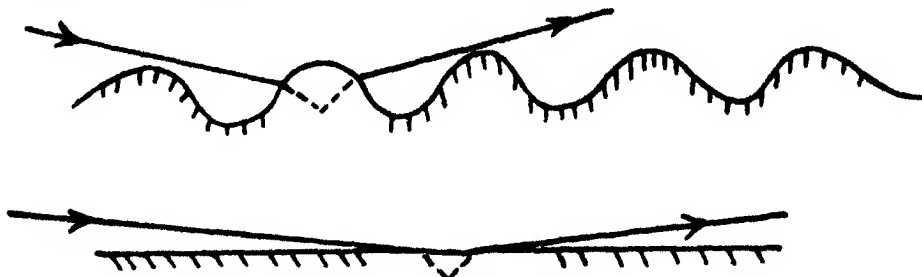


FIG. 1.

Because of the small angle which the electrons make with the surface, the refractive index would take more effect just as a refracted ray of light is bent more when the glancing angle is small (Snell's formula  $\frac{\sin i}{\sin r} = \mu$ ).

The diffracted electrons make a curve on the photographic plate. In the absence of the refractive effect the curve is a circle R as in fig. 2.

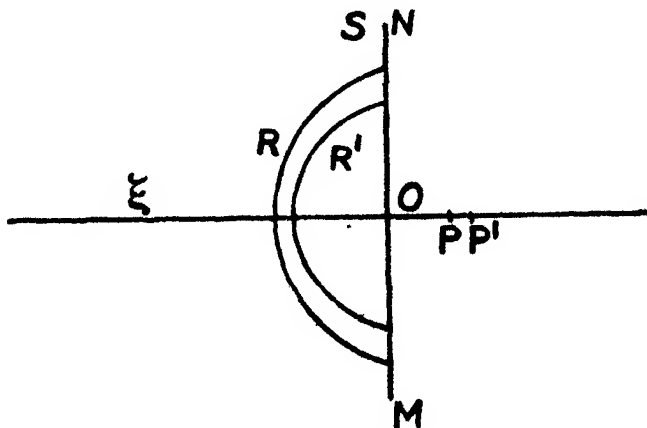


FIG. 2.

Its equation is  $\zeta^2 + (\xi + R \sin \alpha)^2 = R^2 \tan^2 2\theta$  the intersection of a cone by a plane.

$\zeta$  and  $\xi$  are the co-ordinates of the points on the plate in reference to the origin O.

MN is the line of the shadow made on the plate by the edge of the specimen, and

$R$  = length between the specimen and plate.

$\alpha$  = angle the incident ray makes with the crystal face.

$\theta$  = Bragg angle.

For the electrons undergoing refraction the curve on the plate would appear like  $R'$  with the equation  $\zeta^2 + (\sqrt{R^2\alpha + \xi^2} + R \sin \beta)^2 = R^2 \tan^2 2\theta$ .\*

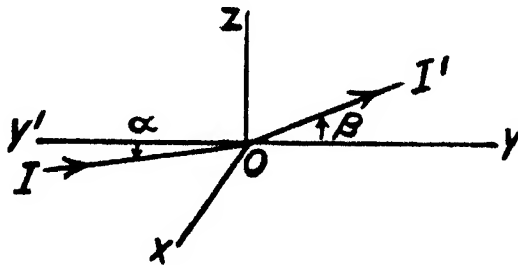


FIG. 3.

The plane OZY is the surface of the crystal upon which the ray of electrons OI is incident.

OI makes an angle  $\alpha$  with the axis OY in the plane XOY.

The refracted ray OI makes an angle  $\beta$ , where  $\mu \cos \beta = \cos \alpha$

$\mu$  = refractive index.

$a = \mu^2 - 1$ .

The centre of the ring would be displaced to  $p'$  by an amount  $= R \sin \beta - R \sin \alpha$ , and points on the ring would be displaced similarly. In addition all points are drawn towards MN, points towards the ends of the ring being affected more than the central points so that the rings would become U-shaped instead of arcs of circles. For single crystal patterns of spots the spots would be elongated.

#### Method and Results.

All emerying was done on blue-back emery paper held in a hand polishing board which has a plate glass top over which the paper is held tight by rollers at either end. During the rubbing the paper and specimen were kept wet by

\* G. P. Thomson, in course of publication.

a continuous dribble of benzene to keep the abrasive rolling freely and from sticking into the metal surface. The different grades of emery used started with the coarsest No. 1 then No. 0, No. 00, No. 000 to the finest No. 0000. In working the specimen from No. 0 grade emery to No. 00 for example, the block was rubbed on No. 0 in one direction until all pits were removed and the marks made by the emery were all running in one direction. The specimen was rotated  $90^\circ$  and rubbed in that direction until the marks of the No. 0 had been obliterated by the rubbing on No. 00 in the new direction. The same procedure was followed in bringing the specimen through No. 000 and No. 0000 grades. By rubbing new emery paper with a piece of the same grade emery paper, high points were worn down and the surface assumed more uniformity for abrasion. Scratching was the difficulty in bringing a specimen to a smooth finish and it was always better to return to a coarser abrasive to obliterate the scratch than to continue with too fine an abrasive. The sludge washed down by the benzene contained emery and bright specks of the metal and was formed for all grades of emery and all metals. Under the microscope the emery had caused many furrows, some running parallel and many running into each other at very small angles. There did not appear to be any points or pits where the emery had taken out small pieces, this suggests that small cuts of the metal had been shaved off or that any gouges of metal taken out were small and had more length than depth.

*Copper.*—A  $1 \times 1$  cm. section was cut with a hack-saw from a copper bar. The surface of the hack-saw cut was filed flat with a "dead smooth" file and washed in absolute alcohol. An electron diffraction picture was taken of this filed copper surface. The surface was irregular from the file marks and necessitated the specimen being set at a large angle so that it was impossible to obtain the first two rings of copper of the (111) and (200) planes. The picture taken showed clearly the (220) and (331) rings of copper. The specimen was etched in dilute nitric acid for a few seconds and a picture taken. The above two rings appeared and were more intense than the rings given by the original unetched copper surface. Both the unetched and etched surfaces gave pictures indicating the normal crystal structure of copper. The abrading of the surface of the unetched block had not broken all the copper crystals into pieces so small as to be unable to give the normal crystal structure of copper. The sharper rings given by the etched surface indicated there might be some crystals broken into very small pieces by the abrading action. These small pieces of crystal would tend to blur the rings given by larger crystals. Etching would remove the material causing this blurring and so sharpen the rings.

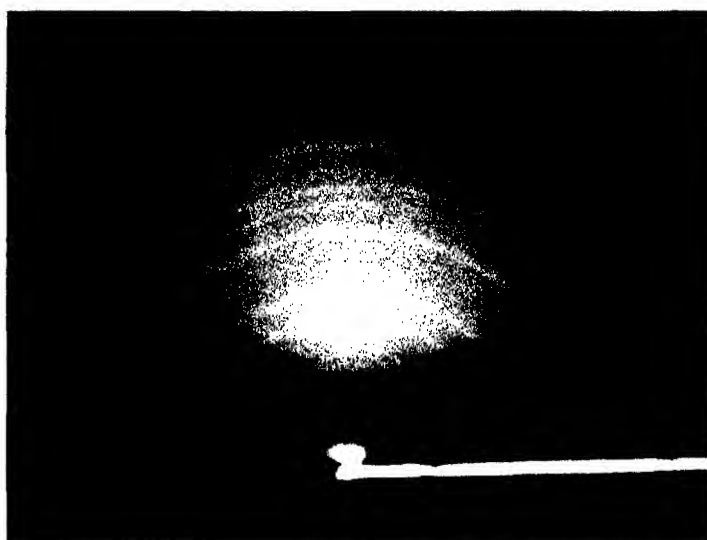


FIG. 4.  
Etched  
copper  
block.

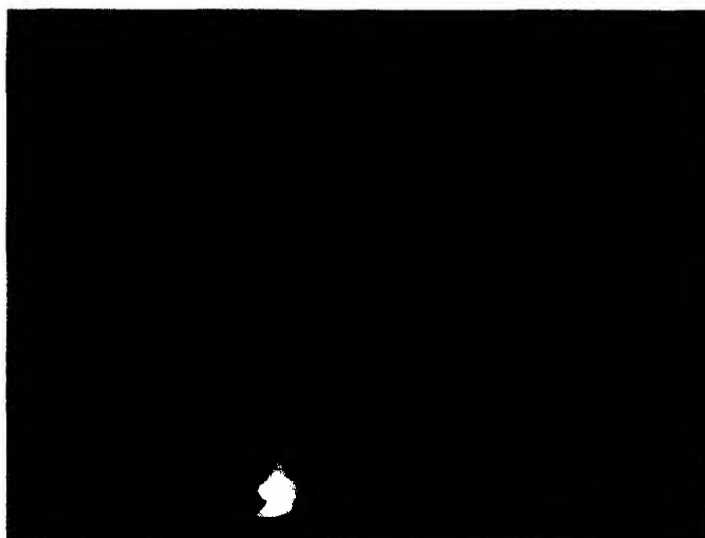


FIG. 5.  
Etched  
copper block  
rubbed on  
No. 0000  
emery and  
on Blue Bell  
polish.

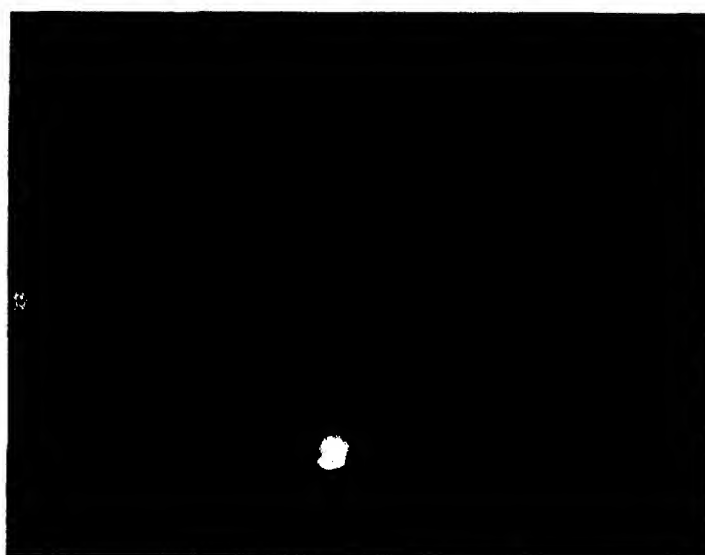


FIG. 6.  
Etched  
copper block  
rubbed on  
No. 0000  
emery, and  
wet rouge,  
and  
chamois.

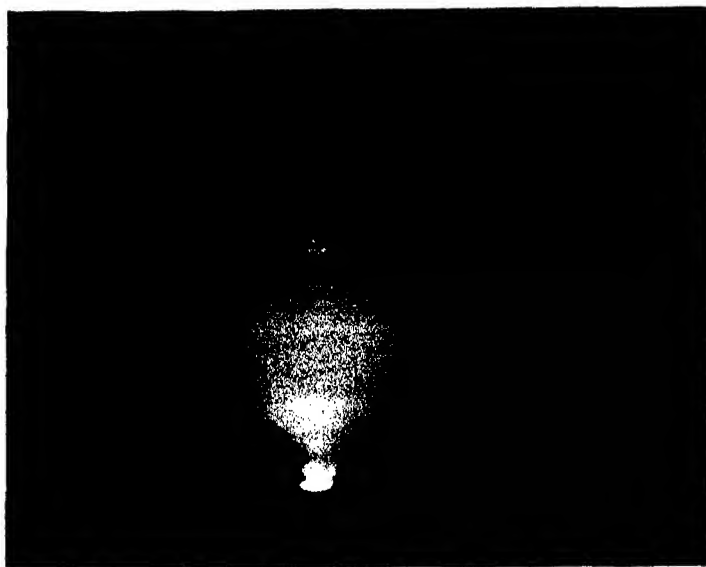


FIG. 7.—Copper block finished on prepared emery paper (line on plate was made for measurements).



FIG. 8.—Polished gold showing the two smudgy rings.

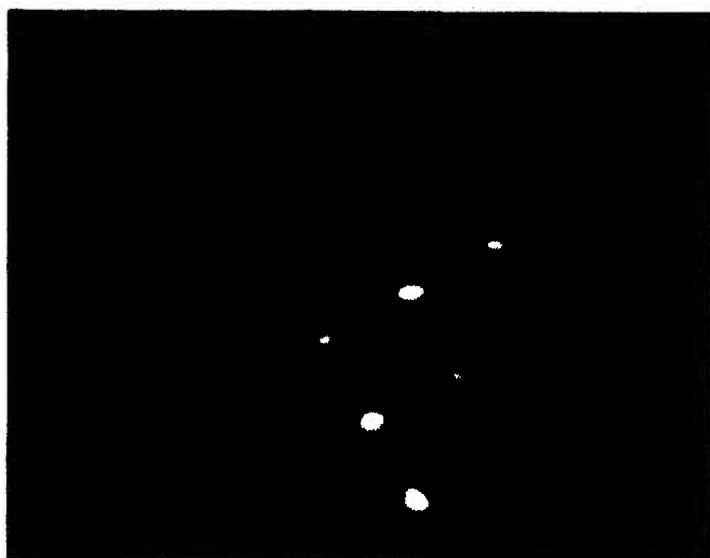


FIG. 9. — Etched chromium single crystal.



FIG. 10. — The same specimen as No. 9, rubbed lightly 2800 strokes on chamois, light magnesium powder and water.



The copper block was rubbed to a flat finish on No. 0000, etched in dilute hydrochloric acid, washed in absolute alcohol and an electron diffraction picture taken, fig. 4, Plate 7. The picture showed rings with parts of rings darker than others indicating the copper block to be polycrystalline but made up of large crystals. A perfect polycrystalline substance shows rings having uniform darkening throughout the ring while large single crystals show individual spots lying on rings. This copper block, a piece of commercial copper bar, had a crystalline structure between the two. Copper being a face centred cube the rings corresponded to reflections from the (111), (200), (220) and (311) planes with the rings appearing in that order from the central spot. These rings were the chief ones used to identify copper during experiments.

Taking the size of the unit cube as  $3.60 \times 10^{-8}$  cm. the spacings were calculated and compared with those observed by electron diffraction photographs. The spacings given by a specimen plate are shown in Table I.

Table I.

Plane of reflection.	Calculated.	Observed.
(111)	cm. $2.08 \times 10^{-8}$	cm. $2.12 \times 10^{-8}$
200	$1.81 \times 10^{-8}$	$1.81 \times 10^{-8}$
220	$1.28 \times 10^{-8}$	$1.30 \times 10^{-8}$
311	$1.08 \times 10^{-8}$	$1.09 \times 10^{-8}$

For all metals observed the spacings compared as well as the above with the accepted calculated spacings.

A voltage change occurring during the exposure was shown by a change in the spark gap reading taken before and after the exposure. Plates taken under these variable conditions were not used.

The same etched copper block was rubbed on No. 000 emery in one direction, turned through  $90^\circ$  and rubbed in the new direction until the markings of the first emery had been obliterated. The block was rubbed on chamois using a fluid commercial polish known as Blue Bell. The specimen was washed in alcohol and a picture taken, fig. 5, Plate 7. The rings of the (111), (200), (220) and (311) planes had broadened and lost their sharpness.

An etched copper block was rubbed on No. 0000 emery and rubbed in addition on wet rouge and chamois, giving a smoother appearance than the previous finish with Blue Bell. A picture was taken, fig. 6, Plate 7, showing



the (111) and (200) rings merging into one broad ring and the (220) and (311) rings merging into another similar broad ring.

Thirty minute decanted emery powder was washed in water several times, poured over duplicating paper and allowed to evaporate until just moist. A copper block finished on No. 0000 emery was rubbed on this moistened finer grained emery paper until the No. 0000 markings were obliterated. The specimen was washed in alcohol and a picture taken "A," fig. 7, Plate 8. Only two very broad rings appeared, the spacing of the inner ring was  $2.26 \times 10^{-8}$  cm., the outer  $1.22 \times 10^{-8}$  cm. Two additional pictures were taken "B" and "C," which were similar to "A." The radii of the broad rings of the three photographs were measured with dividers and by a recording microphotometer. The readings taken by both methods agreed closely so that measurements thereafter were only done by eye.

A copper block finished on No. 0000 emery was rubbed on chamois and rouge with a quantity of water. The No. 0000 markings were obliterated by this rubbing and a picture taken. Again only two very broad rings appeared with spacings  $2.33$  and  $1.30 \times 10^{-8}$  cm.

*Silver.*—A piece of pure silver was obtained and treated in the same three ways as the copper specimen above, except that after the rubbing with Blue Bell polish and chamois the specimen was rubbed in addition on chamois and magnesium oxide (a soft, light, powder) and water to give the surface a better degree of polish. In all cases the pictures of the polished silver gave two broad rings similar in appearance to the rings given by polished copper. The first ring of polished silver corresponded to a spacing lying between the (110) and (200) spacings of silver. The second broad ring was near the (331) spacing of silver. All polishing was done with the polishing media quite wet.

To obtain a picture of a specimen polished by another method the silver block was polished by a leading optical instrument company. A picture of the specimen showed the ordinary rings of the (111), (200), (220) and (311) planes of silver instead of the two smudgy rings given previously by polished specimens. But besides these rings there was an extra ring which fitted the spacing of iron oxide (rouge) with which the specimen had been polished. With the eye alone the surface seemed very highly and smoothly polished but under the microscope using a 1/12-inch immersion objective there appeared many dark patches probably of imbedded rouge. With the microscope showing a patchy and contaminated surface and the pictures showing a ring well resolved yet not due to silver the polished silver was rejected as not being a characteristic polished surface.

A copper specimen was similarly contaminated by allowing the rouge paste to become almost dry during polishing. The rouge particles not being free to float around during polishing were probably forced into the metal to become imbedded there. The block was swabbed with cotton lint and alcohol and a picture taken. An extra ring appeared lying between the (200) and (220) rings of copper.

*Chromium.*—Some pieces of chromium for alloying were chipped along the cleavage planes and ground to specimen size. The chromium was in large crystals. The metal was hard and brittle and took a high polish of a bluish tinge. It was not easily abraded on the emery paper but the markings from the coarse emery were shiny and had a flow appearance.

A block of chromium was rubbed on No. 0 and a picture taken which showed two smudgy rings. Another block of chromium was finished on No. 0000 and a picture taken which showed a similar pair of smudgy rings. The same specimen was rubbed on decanted emery and duplicating paper which reduced the sharpness of the No. 0000 markings into gentle waves. The block was again rubbed on No. 0000 and was harder than before. It was difficult for the No. 0000 to make any impression on the surface. As the finish became smoother from the mechanical working, the surface became harder. A picture was taken showing two smudgy rings. The block was etched in cold concentrated hydrochloric acid and a picture taken. The picture showed a number of single spots regularly placed indicating the chromium block to be a single crystal.

Also two photographs were taken of a polished stainless steel mirror classed in the tables as iron. This also gave two broad smudgy rings.

*Gold.*—A block of 24 carat gold was rubbed on No. 0000 emery. The gold was very soft and the emery made deep markings. The block was rubbed with light magnesium oxide on the forearm with water. This rounded the edges of the furrowed emery markings but was not enough to make them disappear entirely. A picture was taken showing only two broad rings, fig. 7, Plate 8.

The polished surface was etched in aqua regia for 20 seconds and under a magnifying glass did not appear to have been etched. A picture taken showed the two smudgy rings not so intense and other broad rings on the plate beyond these first two. The block was etched one minute in addition by holding the polished surface in contact with the surface of a pool of aqua regia. There was still no visible effect of having been etched but the picture taken showed the first broad ring faintly resolved into the (111) and (200) rings. The

second broad ring was replaced by the (220) and (311) rings fully resolved. The gold block was etched for an additional  $3\frac{1}{2}$  minutes and a picture taken showed the normal (111), (200), (220) and (311) rings clearly. The increase of the resolution of the rings increasing with the amount of etching shows that the crystals at an appreciable depth from the surface are reduced in size by the mechanical working of the surface during polishing.

Table II.

	Cu.	Ag.	Au.	Cr.	Fe.*
	cm.	cm.	cm.	cm.	cm.
Calculated values of $\frac{\sin \theta}{\lambda}$ — (Graph)					
1st maxima .....	$0.223 \times 10^{-8}$	$0.210 \times 10^{-8}$	$0.210 \times 10^{-8}$	$0.223 \times 10^{-8}$	$0.223 \times 10^{-8}$
2nd maxima .....	$0.420 \times 10^{-8}$	$0.380 \times 10^{-8}$	$0.380 \times 10^{-8}$	$0.420 \times 10^{-8}$	$0.420 \times 10^{-8}$
Observed values of $\frac{\sin \theta}{\lambda}$ — (Photographs)					
1st maxima .....	$0.222 \times 10^{-8}$	$0.221 \times 10^{-8}$	$0.214 \times 10^{-8}$	$0.212 \times 10^{-8}$	$0.201 \times 10^{-8}$
2nd maxima .....	$0.399 \times 10^{-8}$	$0.401 \times 10^{-8}$	$0.388 \times 10^{-8}$	$0.385 \times 10^{-8}$	$0.378 \times 10^{-8}$
Closest approach of atoms—					
For 1st maxima .....	$2.56 \times 10^{-8}$	$2.63 \times 10^{-8}$	$2.82 \times 10^{-8}$	$2.51 \times 10^{-8}$	$2.74 \times 10^{-8}$
For 2nd maxima .....	$2.66 \times 10^{-8}$	$2.72 \times 10^{-8}$	$2.82 \times 10^{-8}$	$2.63 \times 10^{-8}$	$2.78 \times 10^{-8}$
In crystal (by X-rays) .....	$2.54 \times 10^{-8}$	$2.87 \times 10^{-8}$	$2.88 \times 10^{-8}$	$2.50 \times 10^{-8}$	$2.48 \times 10^{-8}$

\* Stainless steel mirror.

### *Heating of Polished Layer.*

It was thought that the layer of polish might be a mixture of the metal and the different polishing media used. To test this the polished gold specimen, giving a picture of two broad rings, was annealed in an open-ended pyrex tube in an electric furnace. The heating in the furnace was a gradual increase in temperature from  $570^{\circ}$  to  $640^{\circ}$  for 40 minutes after which the specimen was plunged into a beaker of cold, distilled water. After the heating, the surface of the specimen was not so polished but still had a "mirrored" appearance. There were about twenty slightly flashing areas indicating the presence of large crystals. A picture was taken showing the two broad rings resolved into rings of the (111), (200), (220) and (311) spacings of gold and no extra rings other than gold appeared. In addition to the rings, and positioned on the rings, were elongated spots diffracted from the large crystals of gold made by the heating.

The gold specimen was repolished on chamois with light magnesium oxide and water and with decanted chromium oxide and water. The polishing brought into relief some of the twenty large crystals formed by the previous heating. Probably the surface flowed more rapidly from the crystals having the weak planes nearly parallel to the surface than from the crystals which had strong planes nearly parallel to the surface. Looking at the surface with a magnifying glass, after the polishing, there were certain areas slightly in relief but there was no appearance of crystalline structure only a shiny continuous surface. A picture was taken and showed two broad rings but in addition there were faint diffuse rings further out on the plate. The block was heated near the melting point  $1063^{\circ}$  to form single crystals in the block. It was kept between  $950^{\circ}$  and  $964^{\circ}$  for 64 minutes, then cooled from  $964^{\circ}$  to  $938^{\circ}$  in 20 minutes ( $-1.3^{\circ}$  per minute); cooled from  $938^{\circ}$  to  $900^{\circ}$  in 30 minutes ( $-1.27^{\circ}$  per minute); cooled from  $900^{\circ}$  to  $860^{\circ}$  in 20 minutes ( $-2^{\circ}$  per minute) after which the current was turned off and the furnace allowed to cool overnight.

The surface had kept the polished appearance to a marked extent and there were eleven flashing areas indicating the formation of crystals from the heating. A picture was taken and showed elongated spots lying on rings corresponding to the spacings for gold.

The polished silver specimen which gave a picture of two broad rings was similarly heated below its melting point of  $960^{\circ}$ . It was heated for 5 minutes at  $310^{\circ}$  and plunged into a beaker of cold distilled water. A picture of the specimen was taken and the rings of the (111), (200), (220) and (311) were faintly resolved. No single spots appeared but the (220) ring was orientated.

#### *Polishing of Single Crystals.*

*Copper.*—A piece of a single copper crystal rod was cut and mounted in a block of Wood's metal. It was abraded down to a flat surface and alternately abraded and etched until it gave a regular pattern of single spots characteristic of a single crystal. The copper piece was lightly pressed with the fingers on No. 0000 emery wet with benzene and rubbed in one direction for 200 strokes of about 10 cm. in length. The specimen was similarly rubbed in a direction at right angles to the previous rubbing.

A picture was taken showing the ordinary (110), (200), (220) and (311) rings sharply defined and no single spots were on the photograph. The single crystal surface had been broken up by the mechanical working on the emery into a polycrystalline mass.

The specimen was re-etched and rubbed on chamois, absolute alcohol and water in one direction. The surface had a flashing etched appearance but the edges were shiny and polished. A picture was taken which showed the (110), (200), (220) and (311) rings clearly, with the (311) ring orientated. The copper was re-etched and rubbed on the forearm with water for 200 strokes of 3 cm. length. A picture was taken showing the single spots in their original positions but part of an arc had formed going through two of the spots and a faint broad ring was appearing near the positions of (110) and (311) rings.

The copper appeared to be too soft for just small amounts of the single crystal to be moved during the polishing. Large pieces of the single crystal were twisted or broken from the single crystal mass so that the surface became polycrystalline before it gave pictures showing two broad rings.

*Chromium.*—The chromium block consisting of a single crystal was re-etched and the picture showed a pattern of regularly placed spots, fig. 9, Plate 9. Successive pictures were taken after successive stages of polishing done on chamois with decanted light magnesium oxide and water. After the first light polishing each spot showed a faint elongated shadow beginning from the spot and lying inwards towards the edge of the plate and two faint broad rings become visible near the positions where the (110) and (220) rings should lie, fig. 10, Plate 9. As the polishing progressed two additional spots appeared and increased in intensity. Three spots of the original pattern remained of good intensity during the polishing while others of the original pattern became fainter and disappeared. After 3800 strokes all the spots disappeared and were replaced by two broad rings given by the polished metal. The shadows or elongations of the spots never extended above the spot, only below it, the dark centre of the spot remaining in the same position. The two broad rings became more intense at the expense of the fading of the greater number of spots.

The two spots given in addition to the regular pattern after polishing must have been reflected from a new set of planes brought into being by the polishing. The force of the rubbing must have twisted some of the standing pyramids of the single crystal surface so that there was a slip along a selected plane to cause twinning. As the amount of polish increased more twinning occurred and the new spot from the increased number of twinned crystals became stronger.

#### *Conclusion and Discussion.*

The rings given by etched metals were sharp and showed the ordinary spacings of the planes in the crystals. The broadening of these rings as the

polishing was increased and their final replacement by two broad rings was considered to be a strong indication of the formation on the surface of an amorphous or Beilby layer resulting from the polishing action. The polishing was thought to reduce the size of the crystals and finally displace the atoms from their arrangement in the crystal lattice to a new spacing corresponding to the separation of the atoms by a common distance determined by the size of the atoms.

The broadening of the rings was probably owing to the reduction in size of the crystals caused by the polishing, so decreasing the resolving power of the crystals as to broaden the rings. Randall and Rooksby\* show a series of X-ray photographs beginning with graphite and extending through amorphous carbons. The photographs show a transition beginning with well defined lines for the (001) and (002) spacings, and at the end these lines are broad and diffuse with the (002) spacing increased by a greater amount than the amount of decrease in the (001) spacing. However, they believe the most amorphous carbon to be really crystalline and they consider the surfaces of the polished metals in these experiments similarly to be crystalline.

The spacings of the two broad rings of a well polished surface usually differed from the spacings of the crystal structure and were not equal to a mean spacing given by the blurring together of two rings given by the crystal structure. The spacing of the first broad ring of the polished surfaces of copper and chromium was larger than the spacing of the first ring given by the crystal structure. A new arrangement of the atoms would be necessary for this as just a broadening of the (111) and (200) rings for copper to give a single smudgy ring would give a ring with a spacing between the (111) and (200) spacings. Similarly the spacing of the first broad ring for polished chromium is larger than the mean spacing of the (110) and (200) rings. For copper and chromium using the formula for a random arrangement of the atoms as in a gas the spacing between the two atoms is found to be larger than their spacing in the unit crystal cell. The broadening of the (111) and (200) rings of gold would not give the large spacing of the first broad ring of polished gold. The spacing of the first broad ring of silver lies between the (111) and (200) spacings of the crystal structure. Perhaps in this case small crystal aggregates persist in spite of the polishing, and the spacing of the broad ring is an average of the (111) and (200) rings blurring together. However, the atoms of silver (when in the liquid state) might have this mean spacing of the (111) and (200) rings.

\* *Nature*, vol. 129, p. 281 (1932).

Randall and Rooksby,\* in another paper, by the use of X-rays find maxima for liquid metals of low melting points. The first maxima for liquid potassium, rubidium, and caesium are larger than the first maxima in the ordinary crystal structure, while for liquid sodium the spacing is slightly smaller than the first maxima of the crystal structure.

Stewart and Morrow† using X-rays find the first maximum of liquid lauryl alcohol to be larger than that for the solid. Stewart suggests that the atoms in the liquid state assume positions approximating as closely as possible to the arrangement of the atoms in the crystal structure. This predicts that the first maxima for the liquid will lie close to the first maxima for the solid.

The polished surface was considered to be uncontaminated as the finished surface was photographed after being washed in different liquids such as benzene, absolute alcohol, and water with the two broad rings remaining the same. Similarly there was no difference in the spacings or character of the rings using different polishing materials such as rouge, magnesium oxide, decanted emery, and Blue Bell, a liquid commercial polish.

Boas and Schmidt‡ took some X-ray photographs of polished surfaces. They found that the single crystal surface was distorted into a polycrystalline surface from the action of polishing but did not find broad rings. Since X-rays have a great power of penetration the diffraction caused by the surface would be small in comparison with the diffraction caused by the underlying material. If the underlying material were not completely broken up, the diffraction from it would predominate over the diffraction from the surface layers.

The theory on p. 638 may be used to calculate from the width of the rings the number of unit cubes in an average crystal, while that on p. 639 gives the effective distance between scattering atoms. To compare the two theories it is interesting to calculate the number of unit cells which on the crystal theory§ would give the width predicted by Wierl's curve. It is found to be about two unit cells. The random distribution of Wierl's theory would thus account for the new spacings of the broad rings. But an aggregate of small crystals of a few unit cells in one dimension would also give rings of the same degree of broadness, and because of the smallness of the crystals there might be a difference in the spacings given by these crystals. This might account for the

\* 'Nature,' vol. 130, p. 473 (1932).

† 'Phy. Rev.,' vol. 29, p. 919 (1927).

‡ 'Naturwiss,' vol. 27, p. 416 (1932).

§ In calculating M from the width of the rings of the photographs, the geometrical width was neglected as it was small. This would cause a slightly larger value for M in the tables.

new spacings of the broad rings. The two theories rather supplement each other, and they both support the view that the material of the polished layer is in a finely divided state. If crystal structures are present they are in small aggregates of a few unit cells and there is the strong possibility of the presence of atoms arranged at random as in a liquid. Some of the preceding results are summarized in Table III.

Table III.

	Closest distance of approach of atoms.		M. length of side of average crystal from photographs.
	By experiment.	By X-rays in crystal.	
	cm.	cm.	
Cu .....	$2.56 \times 10^{-8}$	$2.54 \times 10^{-8}$	3.1
Cr .....	$2.56 \times 10^{-8}$	$2.50 \times 10^{-8}$	
Au .....	$2.83 \times 10^{-8}$	$2.88 \times 10^{-8}$	3.4
Ag .....	$2.73 \times 10^{-8}$	$2.87 \times 10^{-8}$	3.6
Fe* .....	$2.66 \times 10^{-8}$	$2.48 \times 10^{-8}$	3.9

\* Polished stainless steel mirror.

Professor Kirchner† suggests that the broadening of the rings can arise from the levelling of the surface, and is not dependent on the reduction in crystal size. An ordinary surface is usually uneven so that the electrons penetrate through the small lumps and are diffracted as shown by Thomson.‡ This is shown in fig. 1 where the lumps of crystal act as a diffraction grating, if the surface were levelled as in fig. 2 the penetration of the electrons into the surface would be smaller than before; and the electrons would be diffracted by a smaller number of series of planes corresponding to a smaller length of ruled lines of a diffraction grating. This would cause the electrons to be less precisely diffracted, because of lower resolving power, and so the rings would become diffuse.

But if the surface is to be considered so level it would seem as if the effect of the refractive index would appear. This would cause the ends of the rings to be drawn inward toward the central spot, making them U-shaped instead of arcs of circles. In fig. 3, which is to scale, R is a ring of 0.5 cm. radius and R' is the effect of the refractive index on the ring with  $\Phi = 15$  volts and  $P = 30,000$  volts. The broad rings given by the polished surfaces were found to

† 'Nature,' vol. 129, p. 545 (1932).

‡ 'Proc. Roy. Soc.,' A, vol. 128, p. 750 (1930).



be arcs of circles so far as they could be tested by comparison of radii taken at different points. It was found that the surface did not have to be very smooth to give the smudgy rings, as a specimen finished on No. 0000 emery gave the two broad rings.

Murison, Stuart and Thomson\* found both sharp and diffuse rings for mirrors formed by spluttering platinum films on glass. The surfaces were smooth for both kinds of rings, and the surface giving the sharp rings gave the better specular reflection. None of these rings showed any effect of the refractive index.

The elongation of the spots of the annealed polished gold block, and of the polished chromium single crystal must have been caused by the effect of the refractive index. The elongations were not sharp enough to measure and so compute the inner potential of the metal, but the direction inwards of the lengthening of the spots was the right way for a positive inner potential as for gold and chromium. Also the elongations were all parallel inwardly and not radially which would have been caused by a change in voltage during exposure.

I would like to express my appreciation to Professor Thomson who proposed the subject of the research, supervised the investigations and gave many valuable suggestions.

#### *Summary.*

The structures of polished surfaces of copper, silver, gold and chromium were investigated by electron diffraction using cathode rays.

The results show that highly polished surfaces are almost amorphous, in confirmation of the Beilby theory.

In some cases the distance apart of the atoms in the surface differed appreciably from that in normal crystals.

Reasons are given for concluding against Professor Kirchner's view that the polishing was only a levelling of the crystalline surface.

Single crystals of copper and chromium were also investigated and the breaking up of the structure under mechanical working was observed.

\* 'Nature,' vol. 129, p. 545 (1932).

---

*Phenomena Occurring in the Melting of Metals.*

By W. L. WEBSTER, Ph.D., Clerk Maxwell Scholar of Cambridge University.

(Communicated by P. Kapitza, F.R.S.—Received December 23, 1932.)

1. *Introduction.*

The problem of the melting and solidification of pure substances has, in the last few years, been given a considerable amount of attention, owing to the importance of the study of the physical properties of single crystals. Experimentally, great advances have been made in the development of methods of growth of single crystals and in our knowledge of their physical properties, and this work has yielded a considerable amount of information about the nature of the solid  $\longleftrightarrow$  liquid transition.

For metals, at least, there is ample evidence to show that this transition is not always a simple one occurring at a sharply defined temperature. In the solid state, the metal can show a gradual change of some of its properties as the temperature is raised towards its melting point where, without discontinuity, it acquires the characteristics of the molten metal. For example, Roberts,\* and Goetz and Hergenrother† have shown that the bulk linear coefficient of expansion of bismuth begins to decrease anomalously 20°–30° C. below the melting point. Carpenter and Harle‡ have found that in this same region the specific heat of bismuth increases anomalously. These results suggest that as bismuth is heated some fundamental characteristic of the solid state is disappearing, and latent heat of melting is absorbed long before the actual melting point is reached. Further, after the conventional melting point had been reached, Carpenter and Harle found that with further increase of temperature the specific heat decreased in contradiction to the normal behaviour of molten metals, suggesting that the process of melting did not finish at the melting point.

Soroos,§ who measured the variation of thermo-electric power with temperature in bismuth, also found that the transition between the solid and liquid states was spread over a considerable temperature range above and below the conventional melting point.

\* 'Proc. Roy. Soc.,' A, vol. 106, p. 385 (1924).

† 'Phys. Rev.,' vol. 40, p. 643 (1932).

‡ 'Proc. Roy. Soc.,' A, vol. 136, p. 243 (1932).

§ 'Phys. Rev.,' vol. 41, p. 516 (1932).

As the structure of bismuth is unusually complex, there is a possibility that the results described are due to this fact. The spread of the melting process to lower temperatures may well be associated with the existence of the secondary structure found by Goetz,\* and discussed theoretically by Zwicky; while the spread into the molten state is sometimes supposed to be owing to a rapid change in the degree of molecular aggregation in the melt. The experiments described below on the persistence of crystallization nuclei in the molten bismuth make this explanation rather inadequate so far as it refers to a normal dissociative equilibrium. These nuclei must presumably be associated with the molecular aggregates, the breaking down of which, when the molten metal is heated above the melting point, causes the specific heat anomaly in the liquid. Many experiments† on the supercooling of liquids, including those to be described below, show that these nuclei are not reformed on cooling to the melting point so that the process is not reversible, and it cannot therefore be described as ordinary dissociative equilibrium.‡

Further evidence as to the nature of these nuclei is given by the experiment of Goetz§ who found it possible on melting a single crystal of bismuth to recover from the persisting nuclei not only a single crystal, but, also, one with the identical orientation, a function which seems beyond the capacity of any simple molecular aggregation.

It is the purpose of this paper to describe some experiments on the history of these persisting nuclei in which the degree of subsequent undercooling has been used as a criterion of their behaviour. The experiments reveal the fact that undercooling phenomena may be as complicated with metals as they are in more complex organic substances, and there is, in fact, a very close qualitative agreement in the results for the two types of substances.

The importance of obtaining information about these persisting nuclei lies in the fact that they are products of the disintegration of the crystal occurring at melting, and that there is as yet no evidence to show whether they are a normal result of this disintegration or a fortuitous product due to a local impurity or imperfection in the parent crystal. If further research should show that the former is true, then in arriving at any detailed interpretation of the process of melting it will be necessary to provide a mechanism of disintegration not

\* 'Proc. Nat. Acad. Sci. Wash.,' vol. 16, p. 99 (1930).

† See also L. Graf, 'Z. Physik,' vol. 67, p. 388 (1931).

‡ The experiments quoted on the specific heat and thermo-electric power throw no light on this irreversibility, as they have only been carried out with increasing temperatures.

§ 'Phys. Rev.,' vol. 35, p. 193 (1930).

only into atoms and molecules, but also, perhaps entirely, into blocks of appreciable size. As a corollary there would be an inverse process in solidification in the building up of a single crystal from large blocks. There is as yet no information as to the relative importance of these two methods of breaking down, since we have no evidence as to the size and number of persisting nuclei present immediately after the melting of a crystal.

## 2. *Experimental Methods and Results.*

The experiments to be described were designed to investigate the factors affecting the disappearance of the nuclei when the melt was heated above the conventional melting point, and also the circumstances of their reappearance when the melt was subsequently undercooled below the melting point.

The metal (bismuth, cadmium, lead or tin) was placed in a quartz crucible open to the air in a heavy well-lagged copper furnace heated electrically. A copper-constantan thermo-couple in a thin quartz sheath was immersed in the metal, and the temperature measured by a calibrated potentiometer using a null method. The furnace temperature was first set at a point slightly above the melting point of the metal. Then, when the metal was completely molten, which could be determined from the temperature-time curve of the thermo-couple, the furnace temperature was raised a chosen amount above the melting point and held there for any desired time. The temperature was then lowered slowly through the melting point till solidification set in when there occurred the sudden rise in temperature associated with undercooling.

The two points investigated were the relation between the degree of superheating above the melting point and the degree of subsequent undercooling below the melting point, and the influence of time on this relation. It was not possible to go through the necessary temperature cycle very quickly on account of the long thermal period of the furnace, but the effect of maintaining any particular temperature for a number of hours could be ascertained.

The results are not completely consistent and it is not certain whether this is due to an inherent probability factor in the process of formation of nuclei, as is suggested by the experiments of Lange,\* who finds that the formation of nuclei in zinc, cadmium and lead for a given amount of preheating and undercooling is an exponential function of the time, or whether the control of conditions in these experiments is inadequate. Since the metal is open to the atmosphere there is considerable oxidation and there may be changes in the

\* 'Z. Metallkunde,' vol. 23, p. 165 (1931).

purity including gas content not under control, a factor which, by analogy with organic substances,\* may have some influence. Agitation by shaking or stirring seems to have no effect at all on the degree of undercooling.

Qualitatively, however, there seems to be no doubt about two fundamental points. First, there is definitely a correlation between the amount of preheating and subsequent undercooling such that a greater preheating produces a greater undercooling. A similar result is known to apply to sulphur and various organic substances.† Secondly, the influence of time seems to be unimportant compared with the effect of the actual temperature of preheating and undercooling.

In the figure the results are given for bismuth. The origin for both axes is the conventional melting point; the ordinates give the number of degrees above the melting point to which the molten metal was preheated, and the abscissæ gives the number of degrees to which the melt undercooled before solidification set in. A wide spread in the points is observed, but there seems to be no doubt that for the first 12 degrees of preheating there is a rapid increase in the amount of subsequent undercooling. Thereafter the results are more uncertain, but there is probably a gradual approach to a limit of undercooling of about 30°–35° C. as the amount of preheating is increased. The points marked in dots represent fairly rapid temperature cycles where the time between the end of melting and the beginning of solidification was about one half-hour. The points marked in crosses represent experiments when the melt has been kept constant at the maximum for from 1 to 5 hours; these show no consistently greater supercooling than the cases represented by the dots; but the points represented by triangles, which represent experiments in which the melt has been kept at its maximum temperature for about 15 hours, suggest a greater degree of undercooling than the other points; it is possible that they represent cases where the time of preheating is definitely sufficient to influence the disintegration of the persisting nuclei. If this is so, then the time of preheating only affects this disintegration when it is a matter of hours and it is doubtful, therefore, whether the explanation of Bloch, Brings and Kuhn,‡ who suggest that persisting nuclei are due to a natural decrease in the rate of solution of a crystal in its melt as the size of the remaining solid particles is diminished, is applicable.

\* Bigelow and Rykenboer, 'J. Phys. Chem.,' vol. 21, p. 474 (1917).

† Hinshelwood and Hartley, 'Phil. Mag.,' vol. 43, p. 78 (1922).

‡ 'Z. Phys. Chem.,' B, vol. 12, p. 415 (1931).

Nor does the time during which the melt is below the normal melting point seem to affect the degree of undercooling. For the single circle point the melt was heated  $34^{\circ}\text{C.}$  above the melting point, then cooled to  $4^{\circ}\text{C.}$  below the melting point and kept there for 12 hours. Solidification only set in with a further  $21^{\circ}\text{C.}$  undercooling. In the case of the point represented by a double circle,

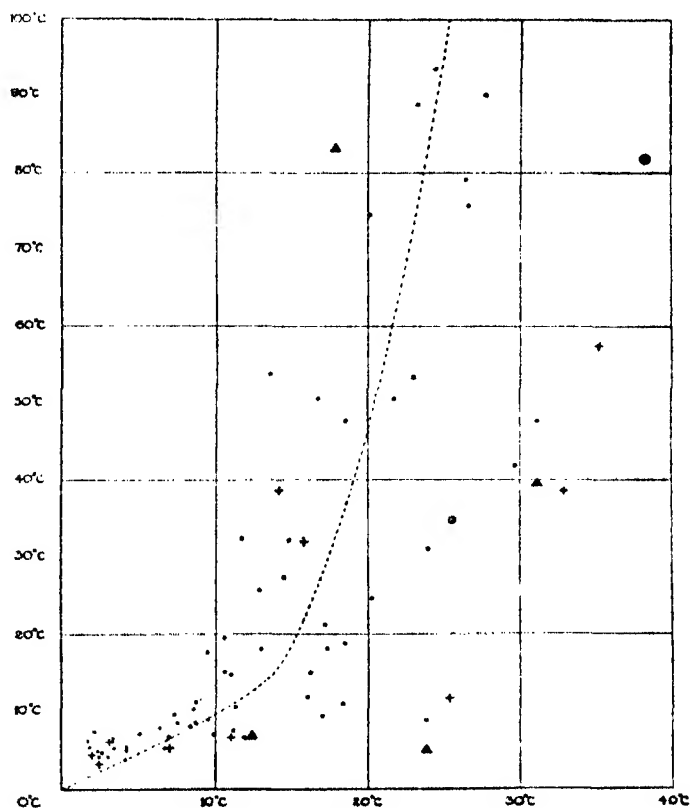


FIG. 1.

the bismuth was rapidly heated about  $82^{\circ}\text{C.}$  above the melting point, then cooled down to about  $8^{\circ}\text{C.}$  below the melting point where it was left for 15 hours. Then it had not solidified and with further cooling it undercooled  $38^{\circ}\text{C.}$

For lead there is much the same scattering of the points, but it is probable that the undercooling increases gradually to about  $3^{\circ}\text{C.}$  as the superheating increases to  $15^{\circ}\text{C.}$ , and is then little affected by a further  $150^{\circ}\text{C.}$  of superheating.

For tin, the undercooling was generally the same,  $20^{\circ}$ – $25^{\circ}$  C., for superheating ranging from  $2^{\circ}$ – $210^{\circ}$  C. But four points were obtained with superheating of  $2^{\circ}$ – $3^{\circ}$  C. which only undercooled  $3^{\circ}$ – $4^{\circ}$  C.; while between these two groups only one point occurred with  $2^{\circ}$  C. superheating and  $15^{\circ}$  C. undercooling. This division of the points for tin into two groups—those which undercooled the full amount and those which barely undercooled at all—is interesting in that on any ordinary view of the phenomenon it is what one would expect to happen; that is, the persisting nucleus would either be present with its full powers of acting as a centre of crystallization or would disappear entirely. There is a definite distinction between this behaviour and that of bismuth in which the nucleus seems to have the power of being partially destroyed so that solidification can set in at some intermediate temperature.

For cadmium no undercooling at all was found, even with superheating of  $165^{\circ}$  C., so that presumably no nucleus is required for crystallization.

These four metals thus give quite different results quantitatively, but with the exception of cadmium, all show undercooling. Whether in lead the small degree of undercooling observed is genuine, or whether it is due to impurities, is not certain; but it is interesting to note that lead, like cadmium, has a simple crystallographic structure.

To sum up, in bismuth, lead and tin, there is evidence that persisting nuclei remain when the solid is melted. For tin these are destroyed very easily if the melt is superheated and are usually not reformed till a definite degree of undercooling has followed. In bismuth and lead the nuclei are apparently only slowly destroyed as the melt is superheated, and to each stage of destruction there is a characteristic degree of undercooling at which what remains of the nuclei recovers the power to act as a centre of crystallization. The nuclei exhibit what may be termed a temperature hysteresis which is certainly not the behaviour associated with a simple molecular reaction.

These experiments throw little light on the critical problem of the number of nuclei left in the melt by a single crystal. Starting with a polycrystalline aggregate the repeated recrystallizations have usually left one or two large crystals in the crucible, but this is not satisfactory evidence that only one or two nuclei were left in the last melt. It is possible that the rise in temperature which occurs when crystallization commences on one nucleus prevents the further development of others, so that they are rendered sterile and are absorbed into the crystal lattice produced by the first. Such evidence as is obtainable from measurements on the viscosity of molten metals is rather indefinite.

Plüss\* finds that the viscosity of bismuth decreases about 10 per cent. between about 280° and 360° C., suggesting a gradual molecular dissociation, but there is no clear anomaly near the melting point that could be associated with the existence of many large aggregates. The experiments, however, are not very adequate for the critical range of 10° C. above the melting point.

### *3. The Melting Points of Bismuth in Capillary Tubes.*

Another phenomenon which has been observed in the course of the author's experiments on bismuth is an apparent lowering of the temperature of solidification in capillary tubes. This was reported in the paper dealing with the discontinuity in the magnetic susceptibility at solidification.† At that time it was thought to be an experimental error due to the position of the thermo-couple which was outside the bulb containing the bismuth, but similar effects have since been observed with the same furnace arrangement and a thermo-couple protected by a quartz sheath actually immersed in the bismuth, so that this explanation cannot hold.

With the arrangement used, when the thermo-couple sheath rested on the bottom of the bulb and partially blocked the opening of the capillary appendix tube into the bulb, there was always undercooling of about 0.8° C. whatever the rate of cooling; that is, it was not an effect due to thermal lag.

This makes it fairly certain that in a constricted space the temperature of solidification of bismuth is subnormal. Such a result has been reported for ice by Bigelow and Rykenboer.‡ Whether the effect is due to surface phenomena or to the restriction in volume is not known, but for ice the amount of undercooling is independent of the nature of the surface of the capillary.

If it is a volume effect, it becomes necessary to look for a factor governing the rate of advance of a crystal surface other than the simple thermal equilibrium providing for the escape of the latent heat of crystallization. For example, if one assumes that a bismuth crystal grows from blocks, then it might be that, when the area of the solid-liquid boundary is limited, the orientation of these blocks to the direction of the crystal axes becomes difficult, either on account of viscosity effects or because of a weakening of the orientating power of a small surface.

\* 'Z. anorg. Chem.,' vol. 93, p. 1 (1915).

† 'Proc. Roy. Soc.,' A, vol. 133, p. 162 (1931).

‡ 'J. Phys. Chem.,' vol. 21, p. 474 (1917).



It is not likely that the effect is due to the impurities rejected by the growing crystal. These might accumulate at a constriction, so lowering the temperature of crystallization, but the amount would vary with the rate of cooling which does not happen in the special case described.

In conclusion, I should particularly like to thank Dr. J. K. Roberts for many discussions and criticisms of this work, and for undertaking the proof-reading of this paper; and also Professor Kapitza for his interest and encouragement throughout.

### *Dissociation of Excited Diatomic Molecules by External Perturbations.*

By CLARENCE ZENER, H. H. Wills Physics Laboratory, Bristol.

(Communicated by R. H. Fowler, F.R.S.—Received December 27, 1932.)

1. *Introduction.*—An excited attractive state of a diatomic molecule, in the absence of an external field, is not affected by the crossing of a repulsive state with different symmetry.\* An appropriate external field will, however, induce perturbations between the two states.

It is generally recognized that the probability of transition from an attractive

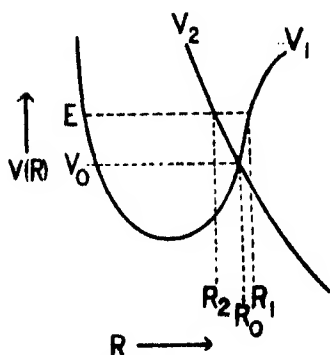


FIG. 1.—Potential energy curves of attractive and repulsive states.  $E > V_0$ .

to a repulsive state, during one oscillation, will be very small, except when the molecule is in an energy level,  $E$ , which is very close to the value of the potential energy at the point of crossing,  $V_0$ . However, even a very small transition probability, per oscillation, may give a high probability that the molecule will dissociate before returning, by radiation, to the normal state. Hence the calculation of these small probabilities is of interest.

In section 2 these calculations are made for  $E > V_0$ , and in section 3 for  $E < V_0$ . The calculations are applied to electric and magnetic fields in section 4, and to collisions in section 5.

2. A simplification will be made by considering the internuclear separation  $R$  as the only nuclear variable. This neglect of the angular co-ordinates is

\* R. Kronig, 'Z. Physik,' vol. 50, p. 357 (1928).

justified since the transition occurs only in the immediate vicinity of the point of crossing,  $R_0$ , and because the rotation of the molecule, while  $R$  is in this vicinity, must be quite small. The effect of rotation will be taken into account sufficiently by considering the potential energy curves of the attractive and repulsive states,  $V_1(R)$  and  $V_2(R)$ , as functions of the rotational quantum numbers.

With this simplification, the standard perturbation theory gives the transition probability proportional to the square of the integral

$$J = \int U_1(R) (1|H_1|2) U_2(R) dR. \quad (1)$$

Here  $(1|H_1|2)$  is the matrix element of the perturbation  $H_1$ , introduced by the external field, with respect to the attractive and repulsive electronic states;  $U_1(R)$ ,  $U_2(R)$  are the vibrational wave functions, with energy  $E$ , which belong to the attractive and repulsive states, respectively. When  $E > V_0$ , the oscillatory portions of  $U_1$  and  $U_2$  overlap. The integrand of (1) is then an oscillating function, and a small error in the wave functions will thus introduce a large error in  $J$ .

Landau\* has shown how this difficulty may be avoided. His method consists essentially in using the Wentzel-Brillouin-Kramers approximate wave functions for  $U_1$  and  $U_2$ . The oscillatory factor in the integrand of (1) is then given by

$$\cos \left\{ \int_{R_1}^{R_2} p_1 dR - \frac{1}{4}\pi \right\} \cos \left\{ \int_{R_1}^{R_2} p_2 dR - \frac{1}{4}\pi \right\}.$$

Here  $R_1$ ,  $R_2$  are the points of intersection of  $V_1(R)$ ,  $V_2(R)$  with  $E$ ; and

$$p_k(R) = \frac{2\pi}{h} \sqrt{2m\{E - V_k(R)\}}. \quad (2)$$

Rewriting this factor in the form

$$\frac{1}{2} \cos \left\{ \int_{R_1}^{R_2} p_1 dR - \int_{R_1}^{R_2} p_2 dR \right\} + \frac{1}{2} \cos \left\{ \int_{R_1}^{R_2} p_2 dR + \int_{R_1}^{R_2} p_2 dR - \frac{1}{2}\pi \right\},$$

we see that by discarding the second term the rapid oscillations in the region of  $R_0$  may be eliminated. The argument of the first cosine has a minimum at  $R_0$ . Expanding this argument about its minimum, neglecting powers of  $(R - R_0)$  higher than the second, neglecting the variation of the other factors  $(1|H_1|2)$ ,  $p_1^{\frac{1}{2}}$ ,  $p_2^{\frac{1}{2}}$ , and extending the integral to  $\pm \infty$ , we obtain an approxi-

\* 'Phys. Z. Sowjetunion,' vol. 1, p. 88 (1932).

mate value to the integral. This approximation is better the higher  $E$  is above  $V_0$ .

Applied to our one dimensional problem, Landau's method gives

$$P_{12} = \frac{4\pi^2 \epsilon_{12}^2}{\hbar v |s_2 - s_1|} \quad (3)$$

as the probability that the change from attractive to repulsive state occurs when  $R$  passes once through  $R_0$ . Here  $\epsilon_{12}$  is the value of  $(1|H_1|2)$  at  $R = R_0$ ;

$$\left. \begin{aligned} v &= \sqrt{2(E - V_0)/m} \\ s_k &= \frac{dV_k(R_0)}{dR} \end{aligned} \right\} \quad (4)$$

Since this result has been obtained by a perturbation method, (3) is valid

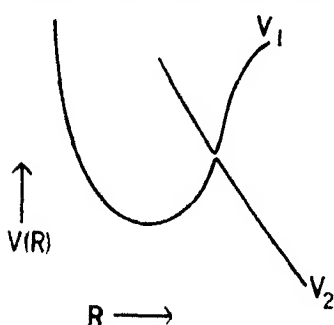


FIG. 2. — Adiabatic potential energy curves with external perturbation present.

only when  $P_{12} \ll 1$ . In the other extreme case, when  $P_{12}$  is nearly unity, the probability  $P = 1 - P_{12}$  may be calculated by a similar perturbation method, with  $U_1(R)$ ,  $U_2(R)$  being the wave functions associated with the adiabatic electronic states. Landau\* has carried out this calculation, finding

$$P = \exp \left\{ - \frac{4\pi^2 \epsilon_{12}^2}{\hbar v |s_1 - s_2|} \right\}. \quad (5)$$

The author has treated the same problem from another standpoint.† By introducing the same approximations, constant  $(1|H_1|2)$  and velocity in the vicinity of  $R_0$ , not at the end of the calculation, but at the beginning, I was able to reduce the problem to one for which the transition probabilities could be found exactly. I obtained

$$P_{12} = 1 - \exp \left\{ - \frac{4\pi^2 \epsilon_{12}^2}{\hbar v |s_1 - s_2|} \right\}, \quad (3')$$

while  $P$  proved to be identical with (5). The expression (3') is valid, subject to the approximations, for all values of  $P_{12}$ . It agrees with (3) in the range of validity of the latter.

\* 'Phys. Z. Sowjetunion,' vol. 2, p. 46 (1932).

† C. Zener, 'Proc. Roy. Soc.,' A, vol. 137, p. 696 (1932). The apparent discrepancy, mentioned in this reference, between the  $P$  derived by Landau and that derived by the author arose through confusing the ordinary  $\hbar$  with the Dirac  $\hbar$ , which was used by Landau.

The transition probability per oscillation,  $\gamma$ , is equal to twice  $P_{12}$ , provided  $P_{12} \ll 1$ . For then the two methods of dissociation indicated in fig. 3 are independent, and therefore their probabilities are cumulative.

Thus, for small  $\gamma$ ,

$$\gamma = \frac{8\pi^2 \epsilon_{12}^2}{\hbar v |s_1 - s_2|}. \quad (6)$$

3. When the vibrational energy of the molecule is less than  $V_0$ , the usual perturbation methods may be applied, since the integrand of (1) is not oscillatory, as when  $E > V_0$ , in the region between  $R_1$  and  $R_2$ .

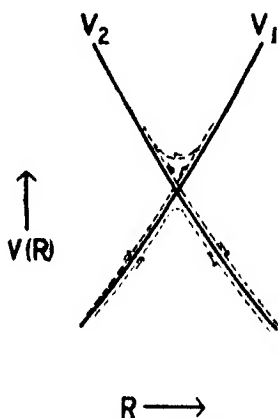


FIG. 3.—Two methods of dissociation. The broken lines indicate the two paths  $V(R)$  may follow in dissociation.

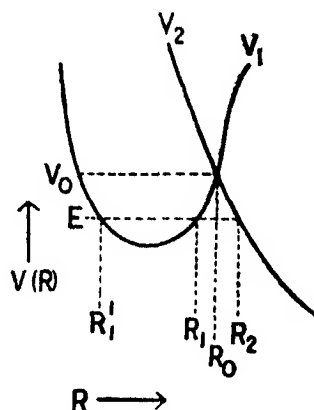


FIG. 4.—Potential energy curves of attractive and repulsive states.  $E < V_0$ .

The perturbation theory gives the probability of dissociation during one oscillation to be

$$\gamma' = \frac{1}{v} \left| \frac{4\pi}{\hbar} \int U_1(R) (1 | H_1 | 2) U_2(R) dR \right|^2. \quad (7)$$

Here  $v$  is the frequency of oscillation;  $U_1(R)$  is the normalized wave function of the attractive state, with eigenvalue  $E$ ; and  $U_2(R)$ , the wave function of the repulsive state, with energy  $E$ , is so normalized that

$$\lim_{R \rightarrow \infty} U_2(R) = \frac{\cos \left\{ \frac{2\pi}{\hbar} \sqrt{2m [E - V_2(\infty)]} + \delta \right\}}{\{2 [E - V_2(\infty)]/m\}^{\frac{1}{2}}}. \quad (8)$$

Except when  $E$  is nearly equal to  $V_0$ , the product  $U_1(R) U_2(R)$  is much smaller at  $R_1$  and  $R_2$  than at its maximum value between  $R_1$  and  $R_2$ . We

may thus, except when  $E \sim V_0$ , calculate  $\gamma'$  directly by means of the Wentzel-Brillouin-Kramers approximate wave functions. In the region between  $R'_1$  and  $R_1$ , exclusive of the immediate vicinity of  $R'_1$  and  $R_1$ , the appropriate approximate function for  $U_1(R)$  is

$$U_1(R) = \frac{2v^{\frac{1}{2}} \cos \left\{ \int_R^{R_1} p_1 dR - \frac{1}{4}\pi \right\}}{[2(E - V_1)/m]^{\frac{1}{2}}},$$

with  $p_1$  given by (2). Associated with this function is a flux of magnitude  $v$  in each direction. Hence it is properly normalized. To the right of  $R_1$ ,

$$U_1(R) \rightarrow \frac{v^{\frac{1}{2}} \exp \left\{ - \int_{R_1}^R |p_1| dR \right\}}{[2(V_1 - E)/m]^{\frac{1}{2}}}.$$

The approximation of  $U_2(R)$  which satisfies (8) becomes, to the left of  $R_2$ ,

$$U_2(R) \rightarrow \frac{\frac{1}{2} \exp \left\{ - \int_R^{R_2} |p_2| dR \right\}}{[2(V_2 - E)/m]^{\frac{1}{2}}}.$$

Substituting these approximate functions in (7), we observe that, in the region for which the functions are valid, the factor

$$Q(R) = \exp \left\{ - \int_{R_1}^R |p_2| dR - \int_R^{R_2} |p_1| dR \right\}$$

varies rapidly in comparison with the other factors. Slight error will thus be introduced by giving these other factors their values at the maximum of  $Q(R)$ , namely, at  $R_0$ . Since  $Q(R)$  has the general shape of a Gauss error curve, we shall expand the exponent of  $Q(R)$  about  $R_0$ , and neglect powers of  $(R - R_0)$  higher than the second.

The region of integration is then extended to  $\pm \infty$ . This procedure gives

$$\int_{R_1}^{R_2} Q(R) dR \sim \int_{-\infty}^{\infty} Q(R) dR \sim T^{\frac{1}{2}} \sqrt{\frac{hv}{|s_1 - s_2|}}$$

where

$$T^{\frac{1}{2}} = Q(R_0),$$

and  $v, s_k$  are defined by (4).

Substitution of this result in (7) gives finally

$$\gamma' = \frac{4\pi^2 e_1^2}{hv |s_1 - s_2|} T.$$

On comparing this probability with (3), we see that  $\gamma'$  is the product of two probabilities, an electronic transition probability and an atomic transmission probability. For the coefficient of  $T$  would be the probability, per crossing, of the electronic transition if  $E$  lay above  $V_0$  by the amount it lies below; while  $T$  would be the probability of dissociation per oscillation if the molecule had the potential energy

$$V(R) = \begin{cases} V_1(R), & R < R_0. \\ V_2(R), & R > R_0. \end{cases}$$

This well-known interpretation\* of  $T$  may be most readily derived from the relations given by Kramers and by Kramers and Ittman.† That particular solution of the wave equation which becomes approximately

$$(E - V)^{-1/2} \cos \left( \int_{R_2}^R p \, dR - \pi/4 \right)$$

to the right of  $R_2$  becomes

$$- \frac{1}{2} T^{1/2} (E - V)^{-1/2} \sin \left( \int_R^{R_1} p \, dR - \pi/4 \right)$$

to the left of  $R_1$ . Further, that particular solution which becomes approximately

$$(E - V)^{-1/2} \sin \left( \int_{R_1}^R p \, dR - \pi/4 \right)$$

to the right of  $R_2$  becomes

$$- 2T^{1/2} (E - V)^{-1/2} \cos \left( \int_{R_1}^R p \, dR - \pi/4 \right)$$

to the left of  $R_1$ . Hence corresponding to the approximate solution

$$(E - V)^{-1/2} \exp i \left( \int_{R_1}^R p \, dR - \pi/4 \right)$$

to the right  $R_0$ , we have a solution to the left of  $R_1$  whose dextro-flux is  $T^{-1}$  times as great.‡

\* G. Gamow, "Constitution of Atomic Nuclei and Radioactivity," Oxford University Press (1932), equation (26), p. 42. Here the factor 4 has arisen through an incorrect joining of the solutions at  $R_1$  and  $R_2$ .

† 'Z. Physik,' vol. 39, p. 828 (1926); vol. 58, p. 222 (1929). These relations have been written in detail by Rice, *ibid.*, vol. 35, p. 1542 (1930).

‡ [Note added in proof, February, 13, 1933.—The calculation of transition probabilities by the above approximate methods is not valid if  $|E - V_0|$  is too small. A calculation with exact wave functions shows the results of sections 2 and 3 to be valid provided  $2\pi m v |R_1 - R_2|/\hbar > 1$ . This condition is satisfied by the applications in the following sections.]

4. The above theoretical considerations will now be applied to various external perturbations. It is of particular interest to know the width,  $\Delta E$ , of the band of energy levels which are dissociated by a given perturbation.

With an external perturbation which is constant in time, dissociation is probable if the probability of dissociation per oscillation, as given by (6), multiplied by the number of oscillations in the left time of the excited state is comparable to unity.

Let  $\tau$  and  $\nu$  be the normal lifetime and the frequency of the excited molecule. We may then define  $\Delta E$  by the equation

$$\tau \nu \gamma(\Delta E) = 1,$$

where  $\gamma(\Delta E)$  is given by (6), with

$$\nu = \sqrt{2\Delta E/m},$$

$m$  being the reduced mass of the molecule. Solving for  $\Delta E$  gives

$$\Delta E = \frac{32\pi^4 \tau^2 \nu^2 m \epsilon_{12}^4}{h^2 (s_1 - s_2)^2}.$$

In order to see how large  $\epsilon_{12}$  must be for  $\Delta E$  to have the order of magnitude of 1 electron volt, put

$$(2\pi\nu)^2 m = \frac{d^2 V_1(R_m)}{dR^2}.$$

where  $R_m$  is that value of  $R$  which makes  $V_1(R)$  a minimum. We then see that  $(2\pi\nu)^2 m / (s_1 - s_2)^2$  has the magnitude of (electron volt) $^{-1}$ . If  $\tau = 10^{-8}$  seconds, we find that  $\epsilon_{12}$  must be about  $3.4 \times 10^{-16}$  ergs for  $\Delta E$  to be 1 electron volt.

An electric field will induce optically allowed transitions between two crossing states. If  $E$  is the magnitude of the electric field in volts cm. $^{-1}$ ,  $\epsilon_{12} \sim eAE/300$  ergs. Thus  $E$  must be about 20,000 if  $\Delta E \sim 1$  electron volt.

The component of a magnetic field parallel to the molecular axis will induce transitions between crossing  $O^+_{\text{u}}(O^+_{\text{g}})$  and  $O^-_{\text{u}}(O^-_{\text{g}})$  states. However, unless the lifetime of the excited state is much longer than  $10^{-8}$  seconds, or unless  $|s_1 - s_2| \ll$  electron volt/A, the strength of the magnetic field necessary to give appreciable effects will be larger than can be obtained experimentally with convenience. A magnetic field has been found to have a dissociative effect upon the excited  $O^+_{\text{u}}$  state of  $I_2^*$  which is probably crossed by a repulsive

\* Turner, 'Z. Physik,' vol. 65, p. 464 (1930).

$O_u^-$  state.\* It is thus likely that this crossing lies to the left of the minimum of the excited state, as such a crossing allows  $|s_1 - s_2|$  to be much smaller.

5. Transitions induced by collisions are forbidden by no general selection rule. All collisions may induce even  $\rightarrow$  odd transitions. Changes in multiplicity may occur by an exchange of electrons having opposite spins, provided the perturbing molecule is in a doublet state. Positive  $\rightarrow$  negative transitions may occur if the perturbing molecule undergoes a similar transition.

Since we cannot in general assume the collision to last for more than one vibration, we are here interested in the maximum value of  $E - V_0$ , say  $\Delta E$ , for which the transition probability per oscillation is large. Defining  $\Delta E$  by

$$\gamma(\Delta E) = 1,$$

with  $\gamma$  given by (6), we obtain

$$\Delta E = \frac{32\pi^4 m \epsilon_{12}^4}{\hbar^2 (s_1 - s_2)^2}.$$

Giving  $|s_1 - s_2|$  the reasonable value of 1 electron volt/Å, we finally get

$$\Delta E \sim 1.8 \frac{m}{m_H} \left( \frac{10\epsilon_{12}}{\text{electron volt}} \right)^4 \text{ electron volts.}$$

In a direct collision,  $\epsilon_{12}$  will be comparable to the relative kinetic energy of the two colliding molecules. Since this is about 0.1 electron volts in a discharge tube, every excited molecule with  $E > V_0$  is likely to be dissociated upon its first direct collision, provided it is crossed by an appropriate repulsive state.

Optically allowed transitions between crossing states will be induced by molecules having permanent dipoles. Taking the permanent dipole moment to be  $eA/5$  (as in HCl), in order that  $\Delta E > 0.1$  electron volt the radius of the collision must not be greater than  $5 \times 10^{-8}$  cm.

6. *Summary.*—The theory of inducing transitions by external perturbations between crossing attractive and repulsive states of different symmetry has been discussed. The theoretical results are of particular interest when the vibrational energy of the molecule is less than the potential energy at the

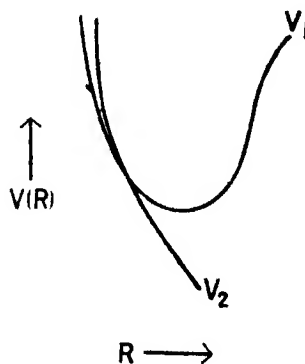


FIG. 5. — Potential energy curves of attractive and repulsive states. Point of crossing is to left of minimum.

\* Mulliken, 'Rev. Mod. Phys.', vol. 4, p. 17 (1932).



point of crossing. The transition probability is then equal to the product of an electronic transition probability and the probability that the nuclei pass through a potential barrier.

Applications have been discussed. It has been found that electric fields of 20,000 volts cm.<sup>-1</sup> have a marked dissociative effect upon excited states which are crossed by appropriate repulsive states. All types of transitions have been found to be readily induced by collisions.

### *A Contribution to the Theory of Film Lubrication.*

By A. M. ROBB.

(Communicated by J. Proudman, F.R.S.—Received January 13, 1932.)

The fundamental equation of the Reynolds' theory of film lubrication is

$$\frac{dp}{dx} = \lambda \frac{d^2w}{dy^2}, \quad (1)$$

where

$p$  is the pressure.

$\lambda$  is the coefficient of viscosity.

$w$  is the velocity of the lubricant at any point between the surfaces.

$x$  is measured in the direction of motion.

$y$  is measured perpendicular to the direction of motion.

This equation can be transformed into

$$\frac{dp}{dx} = 6\lambda u \frac{(h - h^1)}{h^3}, \quad (2)$$

where

$u$  is the velocity of the moving surface.

$h$  is the distance between the surfaces at any point other than that corresponding to

$h^1$ , which is the distance between the surfaces at the section where the pressure is maximum or minimum. The case of minimum pressure is, however, rejected from the immediate consideration.

For the particular case of the journal bearing, in which the distance between fixed and moving surfaces depends on the mean "play," or clearance, between

journal and bearing, and on the extent to which the journal is eccentric in the bearing, equation (2) becomes

$$\frac{dp}{d\theta} = 6\lambda u \frac{Re(\cos \theta - \cos \theta')}{r^3 (1 + e/r \cos \theta)^3}, \quad (3)$$

where

$R$  is the radius of the journal.

$(R + r)$  is the radius of the "brass."

$e$  is the distance between centres of journal and brass, so that  $e/r$  is the eccentricity ratio, referred to as the "eccentricity."

$\theta$  is measured in the direction of rotation of the journal.

$\theta'$  is the angular position of the section of maximum pressure.

Since Reynolds\* published his theory of lubrication in 1886 development has been concerned almost entirely with the method of solving equation (3) and, implicitly, equation (2). The solution which was generally accepted up to a very recent date was given by Sommerfeld† in 1904. That solution involved two assumptions: (a) that the extent of the lubricating film is determined by the extent of the brass; and (b) that the quantity  $h^1$  in (2), which is represented by the quantity  $r(1 + e/r \cos \theta')$  contained in (3), is a constant. Both assumptions are inaccurate. The effects of the inaccuracies are indicated in the following brief summary of results obtained.

The Sommerfeld solution shows that attitude and eccentricity are interdependent. Fig. 1 embodies experimental evidence on this point; it was obtained by correlating results from figs. 10, C and D, of a paper by Goodman,‡ and covers results for three oils at three different temperatures, in effect nine viscosities, at loads ranging from 500 to 4000 lb., at a constant speed of 300 revolutions per minute. Thus the Sommerfeld solution is sound as regards inter-relation of attitude and eccentricity; but it is necessary to examine the character of the relation.

Fig. 2 embodies the Sommerfeld relation between attitude and eccentricity for a "half" bearing. The important characteristic of this solution is that it indicates "seizure" occurring at the "off" side of a brass, whereas, in fact, it occurs at the "crown." Apart from this error in the solution there is another error underlying it. The other error is indicated by fig. 3, which indicates a form of pressure curve obtained from Sommerfeld's solution, showing that a

\* 'Phil. Trans.,' vol. 177, p. 157 (1886).

† Z. Phys. Math. J., p. 97.

‡ 'Proc. Inst. Civil Eng.,' vol. 226, p. 242 (1927-28).

lubricating film may have zero pressure at A, a region of negative pressure between A and B, and then terminate with zero pressure at B where the brass ends. The idea of a region of negative pressure towards the "off" side of the

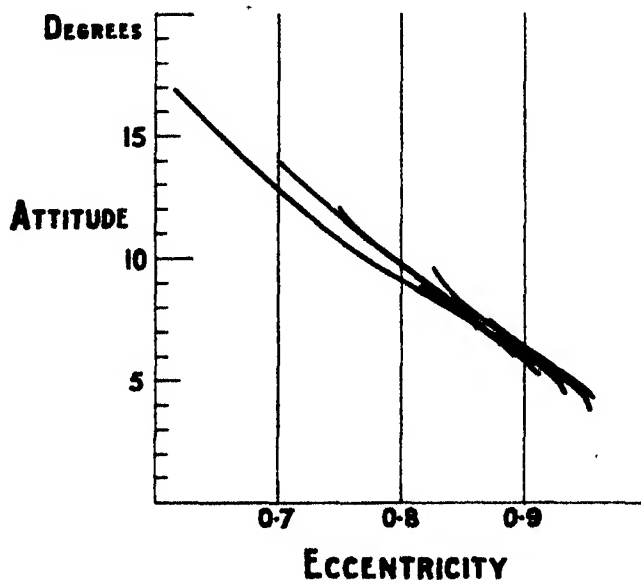


FIG. 1.

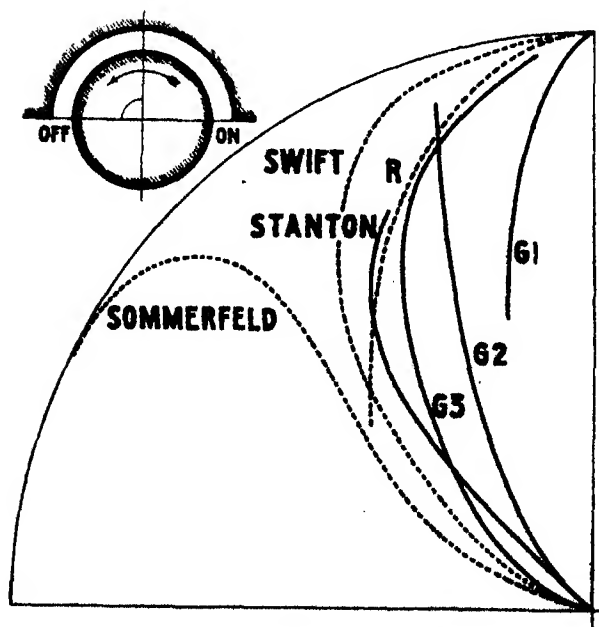


FIG. 2.—Solid line loci obtained by experiment; dotted line by calculation.

brass is consistent with the idea that seizure should occur at the "off" side of the brass; if the negative "loop" of the pressure curve is sufficiently large the journal and brass will be sucked together at the side.

Stanton has shown that pressure curves do not necessarily extend over the whole brass, and that they do usually terminate at a point such as A in fig. 3. Further, in his British Association paper of 1927 he gives the locus marked "Stanton" in fig. 2, and discusses the serious discrepancy between it and the Sommerfeld locus. Nevertheless, he does not reject the Sommerfeld solution.

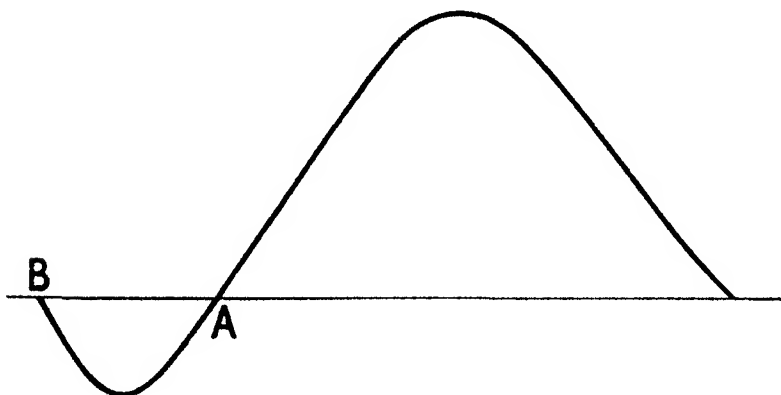


FIG. 3.

Goodman (*loc. cit.*) gives the locus marked G1 in fig. 2, this locus being an extension of the results plotted in fig. 1. Along with this locus he plotted the Sommerfeld locus, calling the whole a "Sommerfeld" diagram. On the other hand, in his 1932† paper he gives the loci marked G2 and G3 in fig. 2, these being obtained with smaller radial clearance than the locus G1. And he marks his rejection of the Sommerfeld solution by embodying the later loci in a "displacement" diagram.

The final stage in this consideration is the solution suggested by Swift‡ in a paper to the Institution of Civil Engineers in 1932. Swift rejects the Sommerfeld solution as regards the assumption that the film necessarily extends to the "off" side of the brass, but he retains the assumption that the film commences at the "on" side of the brass. In this way he avoids the "loop" of negative pressure and obtains an attitude-eccentricity locus which terminates at the crown of the brass, as shown in fig. 2. And he obtains different loci

\* "Engineering," September 2, 1927.

† Goodman, 'Proc. Inst. Civil Eng.,' vol. 233, pp. 244-322 (1931-32).

‡ 'Proc. Inst. Civil Eng.,' vol. 233, pp. 244-322 (1931-52).

for different angular positions of the "on" extremity of the brass. But not only is there an objection to Dr. Swift's solution on the ground that the shape of the attitude-eccentricity locus is appreciably different from the shape determined experimentally, there is an objection in principle to the idea that there are different loci depending upon the circumferential extents of the brass.

There is no basic consideration which justifies the rejection of the Sommerfeld, and incidentally Reynolds, assumption as regards the "outlet" extent of the film and the retention of it as regards the "inlet" extent. Indeed a consideration of the probable course of development of an oil film indicates that neither extremity should be determined by the extent of the brass. When the journal is at rest it makes contact with the crown of the brass. When the journal is set in motion it drags oil round with it and, in effect, "wedges" itself away from the brass. But gradual increase in speed must be associated with gradual increase in pressure, and accompanied by gradual extension of the film. Ultimately a stable condition will be reached; but the idea of gradual development of the oil film is alien to the idea that its boundaries, or either boundary, must be determined by the chance circumstance of the termination of the brass.

This brief summary of development of the Reynolds theory indicates lack of harmony between calculation and experiment. In itself it provides a justification for a reversion to the fundamental considerations of the theory, and a modified development on the basis that extent of brass is not a variable of prime importance.

If the trace of the fixed surface be a straight line it can be shown that the pressures are zero at the ends of the film if the inlet thickness,  $h_1$ , be  $\frac{1}{4}$ , and the outlet thickness,  $h_0$ , be  $\frac{3}{4}$ , the thickness at the section of maximum pressure,  $h^1$ , being taken as unity. We must now consider the character of the flow of the lubricant across sections whose heights are in that relation.

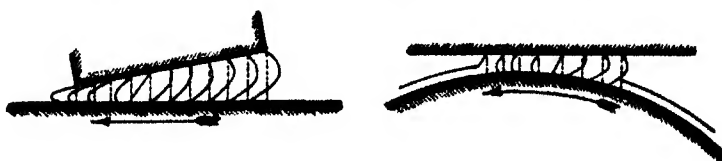


FIG. 4.

From equation (1) it follows that if the pressure does not vary across the film, from surface to surface, the cross curves of velocity are portions of parabolas. Parabolic cross curves of velocity are shown in both diagrams of fig. 4 which are reproduced from Reynolds' (*loc. cit.*) original paper; the left-hand

diagram represents the conditions which are now associated with a Michell pad, the right-hand diagram the conditions in a journal bearing. The flow across the end sections of the film demands consideration of the character of the parabolic cross curves.

An assumption underlying all but some specialized investigations of the theory of film lubrication is that the *width* of the surfaces, measured across the direction of motion, is infinite. This is tantamount to the rejection of any consideration of leakage of fluid at the sides of the surfaces. It entails the condition that the quantity of flow is constant across every section between the surfaces; and this can be expressed by the statement that the areas under the cross curves of velocity are constant. The basic assumption will have to be discarded at a subsequent stage; meantime the implications of the assumption will be examined.

Since  $dp/dx$  is zero at the section of maximum pressure the cross curve of velocity for that section is a straight line; this is the particular case of the parabolic cross curve of velocity having its vertex at infinite distance from the surfaces. This condition gives the assumed constant area under the cross curves, namely,  $\frac{1}{2} uh^1$ .

If  $h^1$  is unity and  $h_0$  is  $\frac{2}{3}$  the parabolic cross curve of velocity at  $h_0$  has its vertex on the moving surface. And if  $h_1$  is  $\frac{2}{3}$  the curve of velocity has its vertex on the fixed surface. These conditions are shown in fig. 5, where  $h_1 = 2h_0 = \frac{2}{3}h^1$  for both the Michell pad and the journal bearing.

If  $h_0$  be greater than  $\frac{2}{3}$  and  $h_1$  less than  $\frac{2}{3}$  the parabolic cross curves have their vertices respectively below the moving surface and above the fixed surface. Cross curves having these characteristics are shown in fig. 5, between the straight-line cross curve at the section of maximum pressure and the terminal cross curves.

The tangents to the cross curves at the surfaces indicate the magnitudes and directions of the frictional resistances between moving surface and lubricant and between lubricant and fixed surface.

Consider now in detail the "inlet" region, the region to the right of the sections of maximum pressure in fig. 5.

Between the section of maximum pressure and the section  $h_1 = \frac{2}{3}$  the cross curves of velocity are all completely to the left of their respective base lines, and the frictional resistance between lubricant and brass is everywhere in the direction of motion of the moving surface. Beyond the section  $h_1 = \frac{2}{3}$  the vertices of the cross curves lie between the surfaces, and the cross curves have portions on both sides of their respective base lines; thus there are regions

of negative velocity adjacent to the fixed surface. Cross curves showing this characteristic are indicated in fig. 4.

The supposition of a region of negative velocity adjoining the fixed surface, in association with the assumption of constancy of flow across the sections, implies the existence, first, of a line of zero velocity joining up the points at

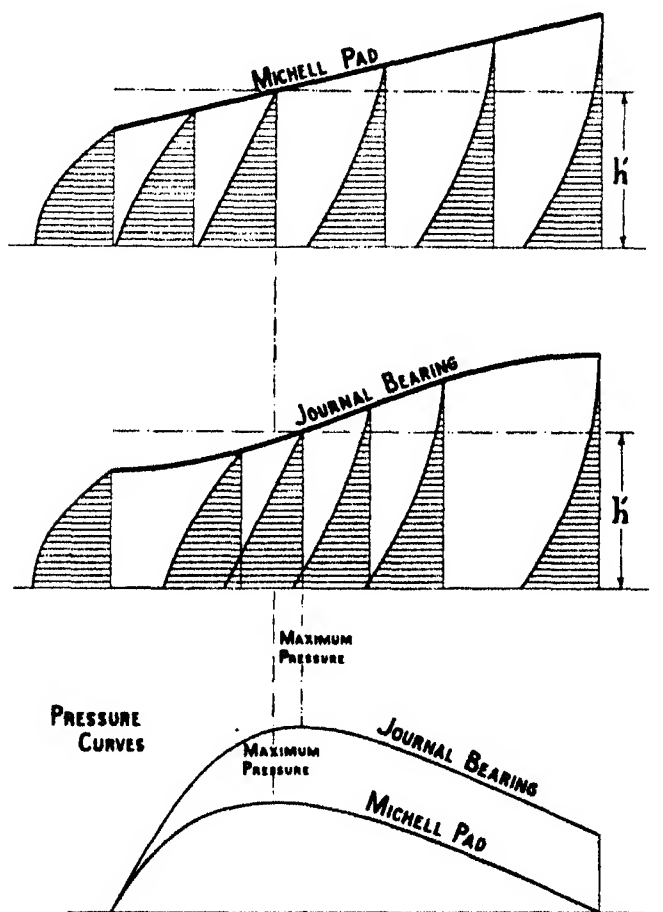


FIG. 5.

which successive cross curves cut their respective base lines, and, second, of a boundary line above which the "positive" flow exactly balances the "negative" flow represented by the "loops" of the cross curves, and below which is the quantity of lubricant which eventually fills the whole space between the surfaces. Hence arises the conception of a body of circulating lubricant in the region beyond the section  $h_1 = \frac{2}{3} h$ , as indicated in fig. 6.

Now it is possible to have a specious explanation of the existence of such a body of circulating lubricant in the particular case of a brass completely surrounding the journal. But for the half brass under immediate consideration, as indicated in fig. 6, it is impossible to justify the conception that in the approximately triangular region with the apex at A there is *part* of a body of circulating lubricant; to particularize—whence comes the lubricant at *a* and whither does it go at *b*? Hence either the film must extend from the beginning of the brass, and it has been indicated above that this is not a reasonable assumption, or else the *bearing* film must terminate at such a position as

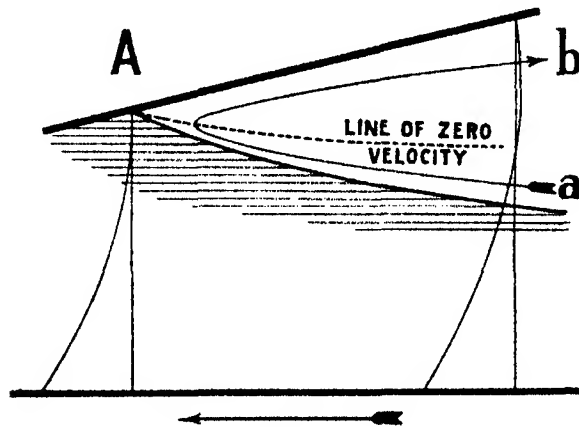


FIG. 6.

A, fig. 6, and the mathematical consideration may not be extended to the state of affairs beyond this point.

Incidentally, the assumption that the bearing film may commence at any position to the right of A involves the objectionable assumption that in the initial stages the film tends to drag the brass in a direction opposite to that of the moving surface; this follows from inspection of the tangents to the cross curves at the fixed surface.

Turning now to the "outlet" region it is clear that so long as  $h$  is greater than  $\frac{1}{2}$ ,  $h^1$  being unity as before, the tangents to the cross curves at the moving surface slope upwards towards the section of maximum pressure, and the moving surface exerts a drag on the lubricant. When  $h = \frac{1}{2}$ , as for the cross curves on the left-hand side of fig. 5, the tangent is vertical and the frictional resistance is zero. When  $h$  is less than  $\frac{1}{2}$  the vertices of the cross curves are between the surfaces, and the curves indicate the existence of velocity of lubricant greater than the velocity of the moving surface—a questionable supposition.



Further, the tangents at the moving surface slope upwards away from the section of maximum pressure, indicating that the lubricant is dragging the moving surface in the direction of motion. Now the idea of a lubricant assisting to rotate a journal, or a thrust collar, is as questionable as the idea of the extensive region of negative pressure discussed above. Hence it would seem that the outlet end of the bearing film, in other words the film which fills the space between the surfaces, should be found at the section where the cross curve of velocity has its vertex on the moving surface, and so the frictional resistance is zero.

Hence arises the conception of limiting thicknesses of bearing film, namely,  $h_0 = \frac{2}{3} h^1$ , and  $h_1 = \frac{1}{3} h^1$ , taking, for the present,  $h^1$  to be the height at the section of maximum pressure. This conception would seem to imply that the inlet thickness of the bearing film must be twice the outlet thickness; and if this relation holds good it follows that for each value of the eccentricity there is one, and only one, angular extent of film. Thus it would seem that the greater the eccentricity the smaller the extent of the film; and attitude, eccentricity, and extent of film become inter-dependent.

In order to explore the possibilities of this conception of limiting end thicknesses of bearing film an investigation was made of the properties of the film in a journal bearing at a range of eccentricities; and this investigation demands attention as a stage in the larger consideration. Superposed on the assumption that inlet thickness is twice outlet thickness was the further assumption that the outlet end coincides with the section of least clearance between journal and bearing. The mean clearance between journal and bearing,  $r$ , was taken to be unity, and values of  $h = r(1 + e/r \cos \theta)$ , were determined for a range of values of the eccentricity,  $e/r$ . Knowing the values of  $h$  for the outlet ends of the films at the different values of the eccentricity the associated values, and the positions, of  $h^1$  and  $h_1$  were determined.

For each eccentricity the values of  $\frac{dp}{dx} = \frac{h - h^1}{h^3}$ , were plotted, the terms in front of the bracket in equation (2) being left out of account. These curves of  $dp/dx$  were then integrated graphically, a typical pressure curve being given in fig. 5.

Fig. 5 shows also the pressure curve for a Michell pad, under which the end thicknesses of the film are the same as for the journal bearing. It is apparent that while the basic assumption as to end thicknesses of bearing film gives equality of pressure at the ends of a Michell pad it does not do so for a journal bearing. The explanation is that similar cross curves of velocity occur at

similar heights of section, but similar heights of section, and so similar values of  $dp/dx$ , occur at different positions; hence similar changes in character of flow, and so similar changes in  $dp/dx$ , are accomplished in different distances and so lead to differences in pressure.

For the series of pressure curves of the type shown in fig. 5 the magnitudes and positions of the resultant loads were determined by means of the polygon of forces, appropriate values of  $\lambda$  and  $u$  being inserted in the final stages of the calculation.

The calculated load curve, taking the value of  $\lambda$  to be  $7.73 \times 10^{-5}$ , the value appropriate to oil "A" at 60° F., and taking  $u$  to be the linear speed corresponding to 300 revolutions per minute, is shown in fig. 7. Along with it is plotted Goodman's experimental curve for oil "A" at 60° F., and 300 revolutions per minute. The lack of harmony is clear.

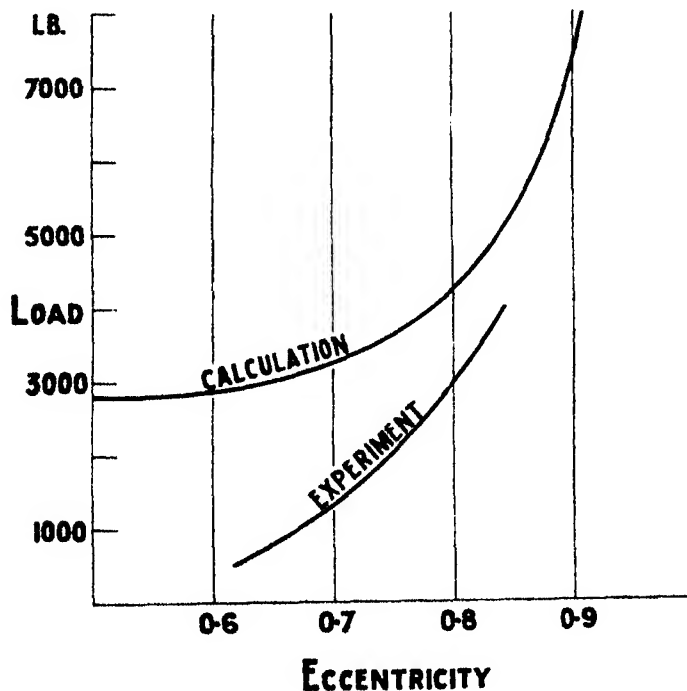


FIG. 7.

The attitude-eccentricity locus for this set of calculations is marked "R" in fig. 2. There seems to be fairly close agreement between this locus and the experimental curve G3 at the higher eccentricities, closer agreement than is

\* The oils used were well-known proprietary brands.

shown by the Swift locus. But this seeming agreement is actually misleading. The assumptions underlying curve R lead to completely inaccurate results for the lower eccentricities. For example, it can be shown that the locus terminates practically on the base-line at 0.3 eccentricity, and it is impossible to obtain results for eccentricities lower than this. On the other hand all the experimental loci are carried down to zero eccentricity, and in this respect the Swift locus is more satisfactory than locus R. In addition there is an objection to locus R, over and above the objection to the load curve associated with it, as indicated in the previous paragraph. This further objection is that the pressure curves from which locus R was derived all have appreciable ordinates at their inlet ends, of the character shown in fig. 5. Then both the Swift locus and locus R are open to criticism in that they are invariable whatever be the radial clearance, whereas it seems clear from comparison of Goodman's results in fig. 2 that radial clearance has a material effect upon attitude-eccentricity locus.

There is, however, an important general consideration indicated by both the Swift locus and locus R. It is that the rejection of the idea of negative pressure is involved in the obtaining of a locus which curves up towards the crown of the bearing, instead of tending towards the side as does the Sommerfeld locus. This feature of locus R seemed to justify some further general investigation.

Incidentally it was at about this stage in the series of calculations that Goodman's second paper became available; and in the further investigation to be discussed the author has had the benefit, not only of the paper, but of a complete set of all the experimental records kindly placed at his disposal by Professor Goodman.

The pressure equation is

$$\frac{dp}{dx} = 6\lambda u \frac{h - h^1}{h^3},$$

and the similar friction equation is

$$\frac{dF}{dx} = 4\lambda u \frac{\frac{3}{2}h^1 - \frac{1}{2}h}{h^2}.$$

If it be accepted, on the considerations outlined above, that there are definite limiting sections for the oil film independent of the extent of the brass, and so for any chosen eccentricity the inlet and outlet thicknesses of the film, and hence the angular extent, are determined, it follows that all the values of  $h$  and the value of  $h^1$  are fixed for each value of the eccentricity. Hence the integrations of  $(h - h^1)/h^3$  and  $(\frac{3}{2}h^1 - \frac{1}{2}h)/h^2$  are constant for each eccentricity

and therefore for any chosen value of the eccentricity both load and friction vary as  $\lambda u$ .

Evidence on this point is contained in fig. 8. Here are a wide range of values

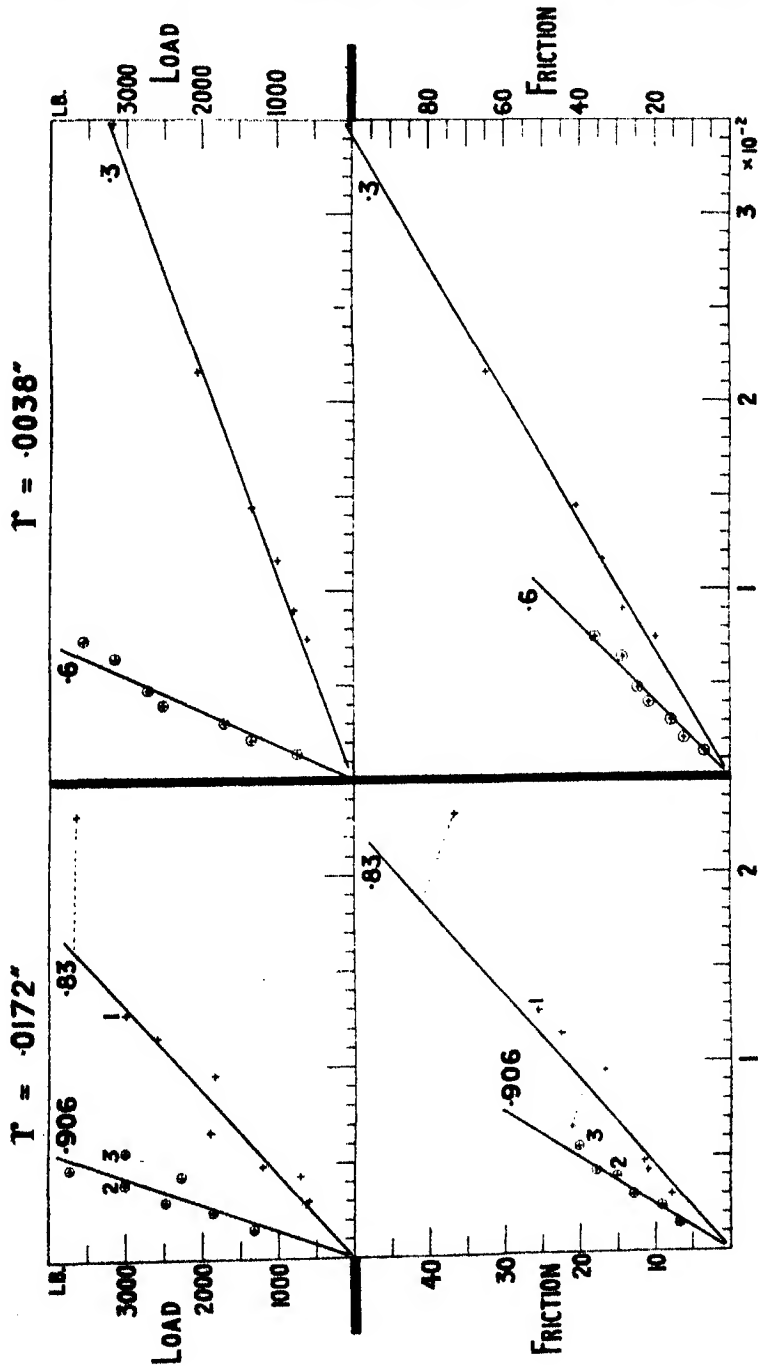


FIG. 8.

of load and friction for constant eccentricities from Goodman's experiments, plotted on a base of  $\lambda u$ . The values of  $\lambda$  were taken from fig. 18 of his 1928 paper; the values of  $u$  were taken to be the number of revolutions per minute since the diameter of the journal was the same throughout. For the first set of experiments, with radial clearance 0.0172 inch, the values of the load were read from fig. 10, C of Goodman's 1928 paper. But although the curves in the diagram range over loads from 500 to 4000 lb. and over nine viscosities, they are limited to one speed, namely, 300 revolutions per minute. The range was, however, extended by taking a series of readings from a number of unpublished diagrams, the readings actually being related values of friction, eccentricity and revolutions per minute for a constant load of 3000 lb.; there were four values of the speed, from 96 to 450 revolutions per minute. For example, with a load of 3000 lb., a speed of 330 revolutions per minute, using oil "F" at 60° F., the friction was 25.7 lb. at an eccentricity of 0.83. In order to get this spot on the diagram a series of values from Goodman's fig. 10, C was taken at 0.83 eccentricity. The extra spot for the 3000-lb. loading is marked "1" in fig. 8. The spots marked "2" and "3" are similar "extra" spots, "2" being for oil "F" at 80° F. and 250 revolutions, and "3" for oil "A" at 80° F. and 175 revolutions.

For the later experiments, with radial clearance 0.0038 inch, the load values were read from fig. 41 of Goodman's 1932 paper, and from a similar unpublished diagram giving the results for 96 and 150 revolutions per minute. The friction results were obtained from Goodman's fig. 46 and a series of unpublished diagrams carrying the loading down to 500 lb.; a certain amount of cross plotting, and some approximate but slight "fairing," was necessary.

From fig. 8 it is clear that there is experimental evidence to justify the idea that both load and friction vary as  $\lambda u$  at given eccentricity; this is emphasized by fig. 9. Here is a comprehensive picture of all Goodman's experimental results, those for the earlier bearing being brought to a common  $\lambda u$  value of  $2.319 \times 10^{-2}$ , corresponding to oil "A" at 60° F. and 300 revolutions per minute, and those for the later bearing brought to a common  $\lambda u$  value of  $1.546 \times 10^{-2}$ , corresponding to oil "A" at 60° F. and 200 revolutions per minute. In adopting this method of plotting the results the practical consideration that the journal might not actually run at high eccentricities with the high viscosity oil has properly been rejected; the diagram is concerned with the elucidation of principles governing the maintenance of the oil film and the conditions under which seizure occurs are not relevant. It should be noted that the load curves for the earlier bearing are those from Goodman's

fig. 10, C. The range of the consideration has, however, been widened by the addition of 24 isolated spots for constant loading and different speeds, these being obtained from other unpublished diagrams; the results were also plotted on the friction diagram. The results for the later bearing, with reduced radial

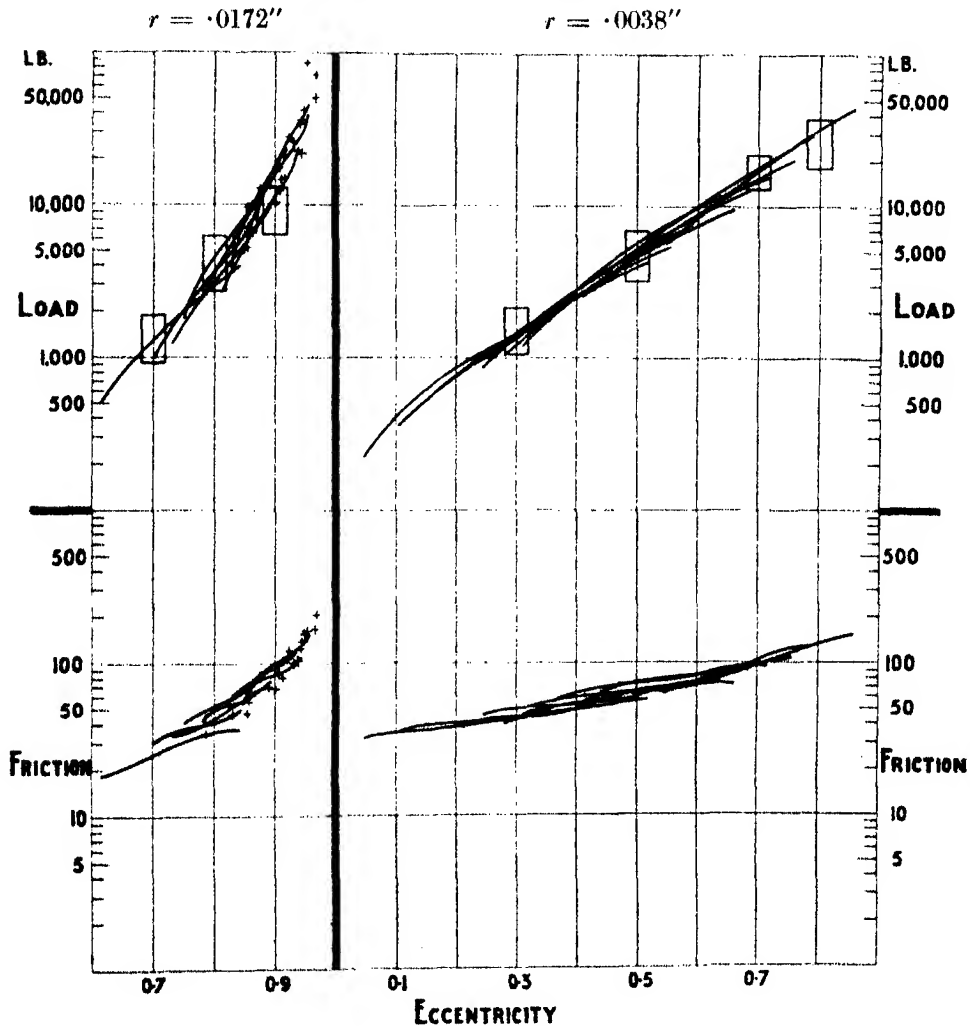


FIG. 9.

clearance, comprise 12 curves of load and of friction. The measured loads ranged from 500 to 4000 lb. There were four speeds, ranging from 96 to 450 revolutions per minute, and three viscosities, namely, those for oil "A" at 60°, 80°, and 100° F.

Fig. 9 was actually prepared in order to provide a background for a series of calculations subsequently to be discussed, and although it supports the thesis of load and friction varying as  $\lambda u$  for constant eccentricity, the logarithmic plotting adopted in order to obtain comprehensiveness tends to mask the "scattering" of the results. But the closer grouping of the later results in both figs. 8 and 9 is probably explained to some extent by the reference on the first page of Goodman's 1932 paper to the improvement in the measuring apparatus and the elimination of other sources of error.

Before discussing the further calculations it is necessary to consider the most important piece of evidence supporting the thesis that attitude, eccentricity and length of film are inter-dependent. From consideration of the pressure and friction equations it is clear that the quantities  $\lambda$  and  $u$  disappear from the coefficient of friction, and the coefficient is merely the quotient of the integrations of  $4 \frac{h^1 - \frac{1}{2}h}{h^2}$  and  $6 \frac{h - h^1}{h^2}$ . Hence if the values of  $h$  and  $h^1$  are determined only by the eccentricity, as will be the case on the thesis outlined above, there will be one, and only one, value of the coefficient of friction for each value of the eccentricity, whatever be the values of viscosity and speed.

This hypothesis was suggested to Goodman by the author in 1931 as the "acid test" of the thesis outlined above. Goodman applied the test and the result is shown in fig. 42 of his 1932 paper. Here again the spots for the later bearing are less "scattered" than those for the earlier bearing.

But there is a further point: from the pressure and friction equations it is clear that the coefficient of friction at any chosen eccentricity varies as  $h$ , and therefore as the radial clearance. The ratio of the radial clearances for the bearings of Goodman's experiments is 4.53. Hence it would seem that the ordinates of the curve of coefficient of friction for the earlier bearing, with the greater radial clearance, should be 4.53 times the ordinates of the curve for the earlier bearing.

Fig. 10 shows, in solid lines, the curves of coefficient of friction determined by Goodman. The dotted curve has ordinates obtained by multiplying the ordinates of the lower curve by 4.53; hence the relation indicated above does not hold good. Consideration of the discrepancy, between the upper solid curve and the dotted curve, led to the subsequent stage in the investigation and to the determination of a serious flaw in the accepted theory.

Fundamentally it would seem that with constancy in amount of lubricant supplied, a reasonable first approximation in view of the character of Goodman's experiments, a reduction in radial clearance should imply

the earlier filling-up of the space between journal and brass, and so an extension of the oil film. The idea of an extension of the oil film being associated with a

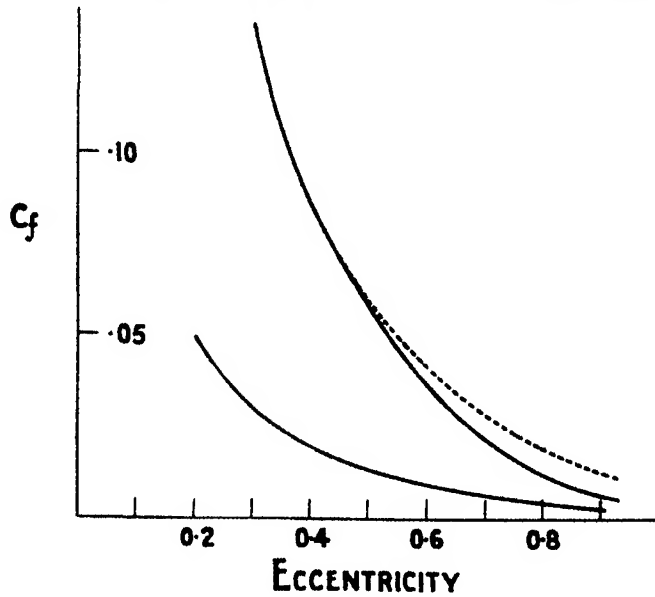


FIG. 10.

reduction in the radial clearance seemed to imply an increase in the amount of side leakage. Hence the next stage in the investigation, involving another reversion to the fundamental equation.

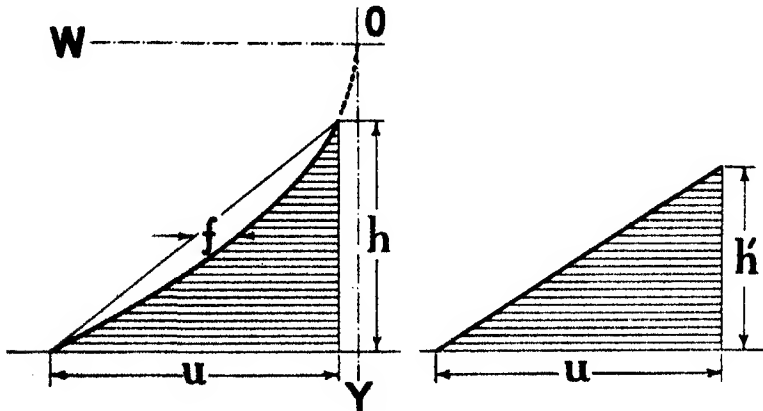


FIG. 11.

Fig. 11 shows a cross curve of velocity which forms part of the parabola  $w = \alpha y^2$ , so that  $\frac{d^2 w}{dy^2} = 2\alpha$ .



The area under the cross curve of velocity is given by  $\frac{1}{2}uh - \frac{2}{3}fh$ , where  $f$  is the horizontal intercept between the parabolic arc and its chord at half height. But it can be shown that  $f = \frac{1}{3}\alpha h^2$ . Hence the area under the cross curve  $= \frac{1}{2}uh - \frac{1}{6}\alpha h^3$ .

Let  $h^1$  be the height of a triangle whose base is  $u$  and whose area is equal to that under the cross curve. Then

$$\frac{1}{2}uh^1 = \frac{1}{2}uh - \frac{1}{6}\alpha h^3,$$

whence

$$2\alpha = 6u \frac{h - h^1}{h^3} = \frac{d^2w}{dy^2},$$

and

$$\begin{aligned} \frac{dp}{dx} &= \lambda \frac{d^2w}{dy^2} \\ &= 6\lambda u \frac{h - h^1}{h^3}. \end{aligned}$$

Hence a new definition of  $h^1$ , namely, that it is the height of a triangle which on the same base as the cross curve of velocity encloses the same area. Thus  $h^1$  is actually a measure of the quantity of flow across the section and there is no warrant for its assumed constancy.

Having determined that  $h^1$  is a variable it was necessary to investigate the character of the variation. For one value of the eccentricity a fairly extensive series of calculations was made on different assumptions as to the variation of  $h^1$ . The two basic assumptions were that the film terminates at the section of least clearance and that the value of  $h^1$  is a minimum at that section. All the results led, however, to the same difficulty, namely, that of obtaining small values of the attitude for other than very small loads, whereas from figs. 1 and 7 it is seen that a small attitude and a large load are quite compatible.

In order to surmount the difficulty of obtaining low attitudes with high loads it was necessary to re-examine the various essential conditions. In the first place it was clear that it must be possible to have the section of maximum pressure near to the section of closest approach. It was also clear that the inlet value of  $h^1$  must be two-thirds the inlet value of  $h$  in order to give zero frictional resistance at entry. Then the development of adequate load-carrying capacity at a high eccentricity demands a considerable length of film, on both sides of the section of maximum pressure. This consideration, in association with the requirement that the section of maximum pressure must have a possible position near the section of closest approach, in other words, in association with the condition that  $h^1$  may have a possible value

only slightly greater than the minimum value of  $h$ , led to the conception that  $h^1$  may have an increasing value in the outlet region. Here again is the basic condition that the outlet value of  $h^1$  is four-thirds the outlet value of  $h$ . It is fully realized that the argument for this limitation cannot be substantiated like the argument for the limitation at the fore end. The condition is, however, first suggested by analogy; the suggestion is then supported by the difficulty of conceiving a journal to be pulled round by its lubricant. Then if increase of  $h^1$  in the outlet region were to be ruled out as unjustifiable it would be impossible to obtain a reasonable pressure curve for the outlet region at low eccentricities.

Hence the introduction of a new conception, namely, increasing value of  $h^1$  in the outlet region, in other words, side "inflow" of the lubricant in that region.

When the logic of events imposed this conception of side inflow in the outlet region the author recalled a conversation he had, some three years ago, with

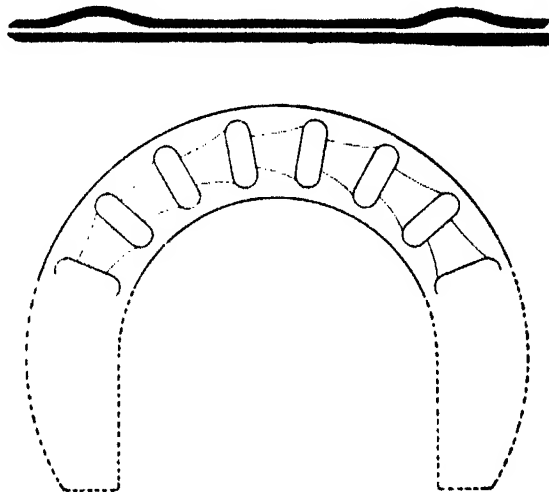


FIG. 12.

M. Henri Brillié, who has been responsible for a new arrangement of oil grooving in the "shoes" of thrust blocks on propeller shafting in ships of the Compagnie Générale Transatlantique. A typical thrust shoe is indicated in fig. 12. On the face of the shoe there is a number of "basins," or radial grooves with closed ends, and the lubricant is drawn up from a "sump" in the thrust-block by the collar on the shaft. When the shoes were examined it was found that there were clear indications of the path of the oil from groove to groove. The

approximate boundaries of the oil path are indicated in fig. 12. An enlarged section in way of two grooves, with the vertical scale considerably enlarged, is also shown in fig. 12. Consideration of this section leads to the thought that increasing pressure in the lubricant occurs in way of the "shoulder," or approximately wedge-shaped portion, of the groove and decreasing pressure over the long flat portion of the shoe where the space between shoe and collar is parallel. Thus there is here evidence, admittedly fragmentary, which suggests the actual occurrence of side inflow.

A final set of load calculations was developed taking account of the various factors that have been discussed above. An outline of the method of calculation is given in some following paragraphs, partly on the ground that the ultimate results are of such a character that the method of attaining them should be open to full scrutiny, and partly on the ground that the method seems to be of service in elucidating the results of further experiments.

For each value of the eccentricity a series of positions of the section of maximum pressure, in other words a series of values of  $\theta'$  measured from the section of closest approach, was chosen. Then for each value of  $\theta'$  a series of extents of film on each side was chosen. For example, referring to fig. 13, for 0.7 eccentricity, and  $\theta' = 19^\circ$ , the inlet extents of film, from  $\theta'$ , were  $20^\circ$ ,  $40^\circ$ ,  $60^\circ$  and  $80^\circ$ , and the outlet extents, also from  $\theta'$ , were  $10^\circ$ ,  $15^\circ$ ,  $20^\circ$  and  $25^\circ$ . For each partial film thus chosen the values of  $h$  were calculated from the expression  $h = r(1 + e/r \cos \theta)$ ,  $r$  being taken to be unity. The inlet and outlet values of  $h^1$  were taken at two-thirds and four-thirds, respectively, of the appropriate values of  $h$ , and the variation of  $h^1$  along the film was taken to be parabolic, with the vertex at the section of maximum pressure.

In this way there were obtained four sets of values of  $dp/dx$  for the inlet region and four for the outlet region. These were plotted on a common base-line as shown in fig. 13. As a matter of convenience the base-line was made 10 inches long, so that there was a different angular scale for each curve; also as a matter of convenience the scale for  $dp/dx$  was different for inlet and outlet regions.

The areas under the curves of  $dp/dx$  were measured by planimeter, corrections applied for the differences in scales, and the results plotted as shown in fig. 13.

Now the condition of equality of pressure at the ends of the film demands equality of area under associated curves of  $dp/dx$  for inlet and outlet regions. From the curves of area it is possible to determine a wide range of associated inlet and outlet curves which will give equality of end pressure, the equal pressures being taken to be zero. For example, from fig. 13 it is seen that inlet

extents of  $20^\circ$ ,  $41.2^\circ$  and  $66.15^\circ$  must be associated respectively with outlet extents of  $13.02^\circ$ ,  $20^\circ$  and  $25^\circ$  to give equality of end pressure. Transforming these values into angles measured from the section of closest approach the associated angles become :—

$$\theta_1 = +39^\circ \quad ; \quad \theta_0 = +5.98^\circ$$

$$\theta_1 = +60.20^\circ \quad ; \quad \theta_0 = -1^\circ$$

$$\theta_1 = +85.15^\circ \quad ; \quad \theta_0 = -6^\circ$$

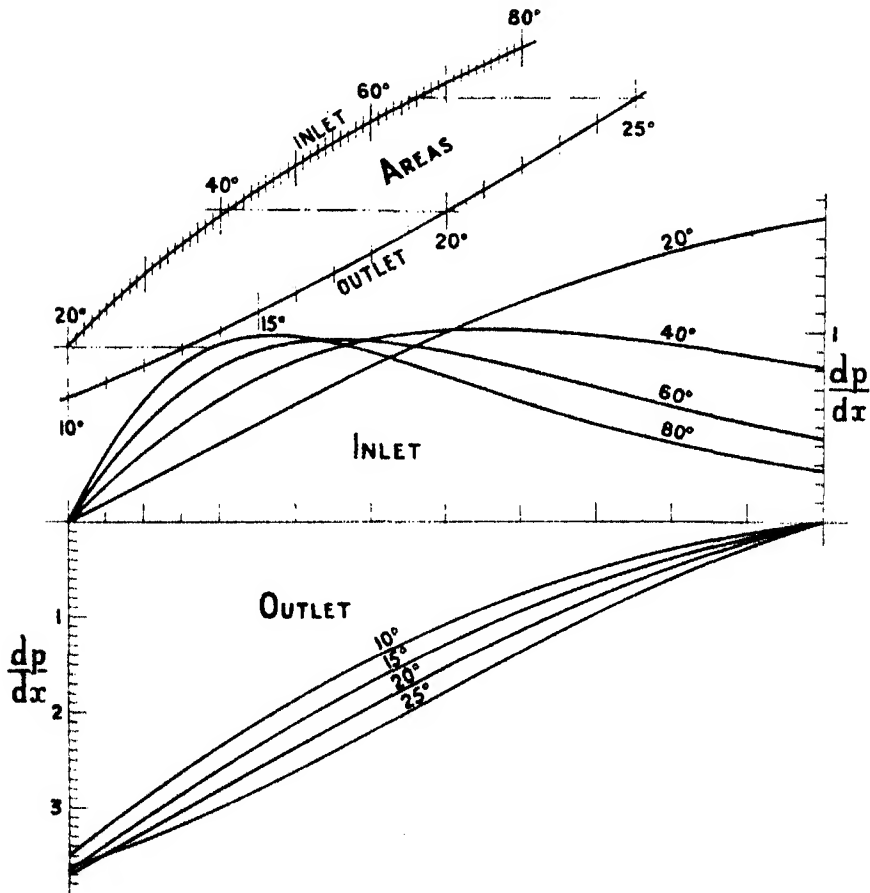


FIG. 13.

For each film whose angular extent is given above a fresh set of values of  $dp/dx$  was calculated and plotted as shown in fig. 14; the 10-inch base line was adopted throughout. Then from the curves of  $dp/dx$  the curves of pressure were determined by planimeter. The three pressure curves for 0.7 eccentricity

and  $\theta' = 19^\circ$  are also shown in fig. 14, the curves being denoted by the angular position of the inlet end of the film. The pressure curves are the actual areas in square inches under the curves of  $dp/dx$ . They represent the pressure along a central radial plane after account has been taken, in principle, of the effect of side flow in modifying the pressure.

Incidentally an advantage of this graphic method of treatment is that the calculations are practically "self-checking." An error in the calculation of

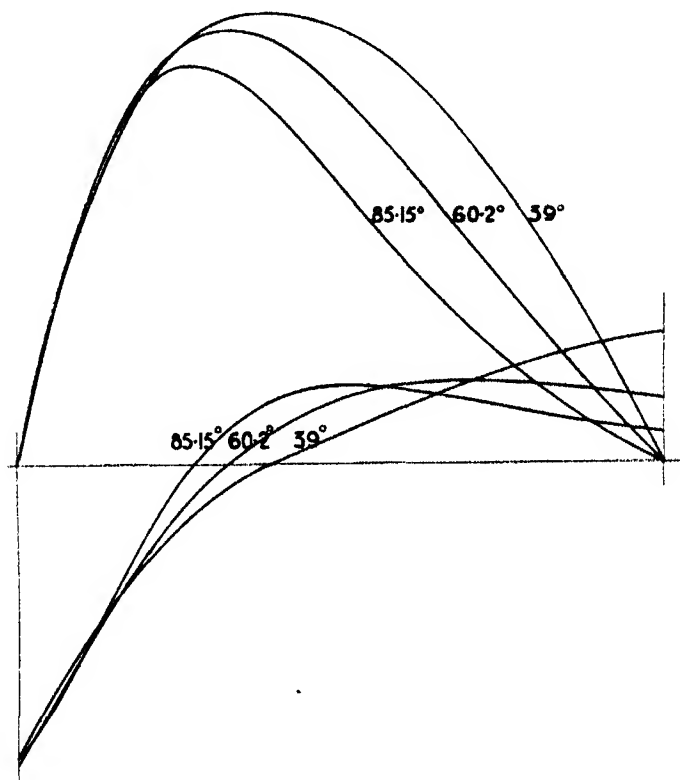


FIG. 14.

$dp/dx$  is at once disclosed as an "unfair" spot on the curve. And the requirement that the terminal spot in the pressure curve shall be zero is a severe test of the accuracy of the calculations and of the integration by planimeter. Taking the error to be measured by the relation between end and maximum ordinates the average amount for the 61 pressure curves actually plotted in this stage of the investigation was only slightly more than three-fourths of 1 per cent.

For each pressure curve the magnitude and direction of the resultant load

was determined by means of a polygon of forces. For this purpose the base-line was divided into 10 equal parts; each vector was the mean pressure over the section, and its angular position was readily calculated from the determined inlet and outlet angles. All the polygon resultants were measured in square inches of area under the curves of  $dp/dx$ .

The final stage was the translation of square inches of area into load.

The basic values are:—

$$\lambda = 7.73 \times 10^{-5} \text{ lb./in.}^2.$$

$$u = 300 \text{ revolutions per minute}$$

$$= 94.25 \text{ in./sec. for a 6-inch journal.}$$

$$r = 0.0172 \text{ inch.}$$

To convert  $\frac{h - h^1}{h^3}$  into inch units divide by  $1.72^2 \times 10^{-4}$ . Whence to convert nominal values of  $dp/dx$  into lb./inch units multiply by

$$6 \times (7.73 \times 10^{-5}) \times (94.25) \times \left(\frac{10^4}{2.96}\right) = 1.477 \times 10^2.$$

$$\text{Circumference of journal subtended by one degree} = 5.24 \times 10^{-2} \text{ inch.}$$

One square inch under curve of  $dp/dx$

$$= 1.477 \times 10^2 \times (\text{units of } dp/dx \text{ per inch}) \times (\text{degrees per inch} \times 5.24 \times 10^{-2})$$

$$= 7.74 \times (\text{units per inch}) \times (\text{degrees per inch}),$$

where the number of degrees is the total extent of the film. This enables the ordinates of the pressure curves to be measured in lb./in.<sup>2</sup>.

Each pressure vector operates over a length of 1 inch on the diagram, representing a length along the bearing of  $(1 \times \text{degrees per inch} \times 5.24 \times 10^{-2})$ . Whence the load per inch of axial length of bearing is given by

$$\begin{aligned} &\text{polygon resultant in square inches} \\ &\times 7.74 \times (\text{units per inch}) \\ &\times (\text{degrees per inch}) \\ &\times (\text{degrees per inch} \times 5.24 \times 10^{-2}). \end{aligned}$$

Finally, the bearing is 3 inches long, whence the load is given by

$$\begin{aligned} &\text{polygon resultant in square inches} \\ &\times 1.125 \times (\text{units per inch}) \times (\text{degrees per inch})^2. \end{aligned}$$

The values of load and attitude determined in the manner outlined above were plotted on a base of  $\theta_1$ , where  $\theta_1$  is the inlet angle, and zero angle is at the section of closest approach. The results for 0.7 eccentricity are shown in fig. 15; the actual calculation spots are marked in order to give a final indication of the accuracy of the method.

Now from fig. 1 it is seen that at 0.7 eccentricity the attitude is  $13/14^\circ$ . Two lines covering this range of attitude are plotted in fig. 15. Take first the

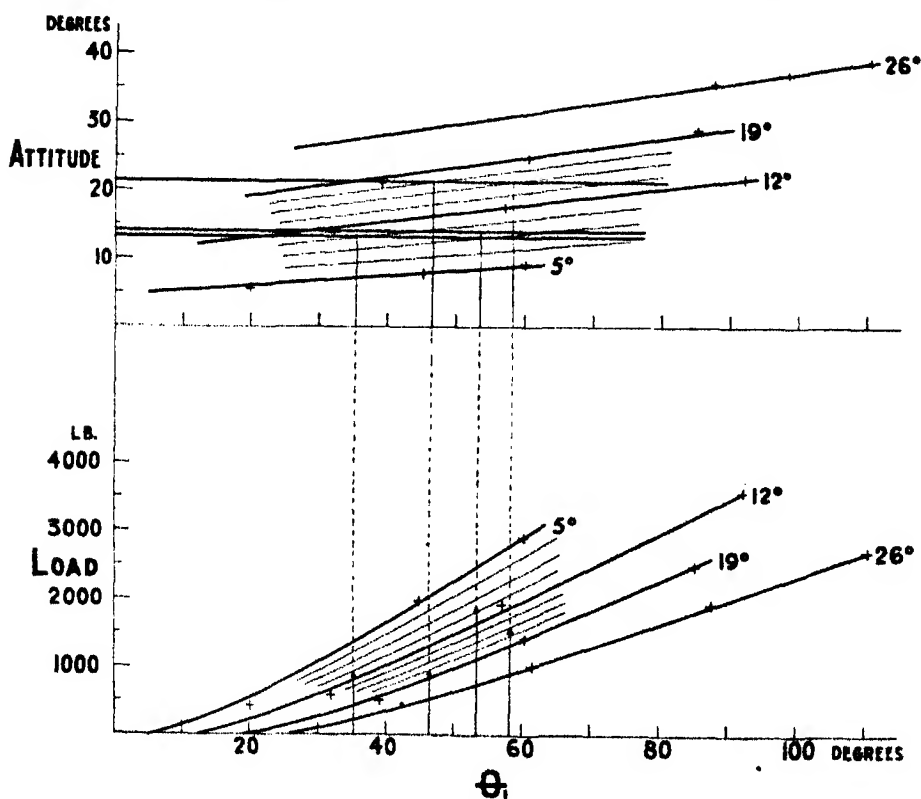


FIG. 15.

$13^\circ$ -line; from the diagram it is seen that at a  $\theta'$  value of about  $10.25^\circ$  the load is 930 lb.; similarly, for the  $14^\circ$ -line, with a  $\theta'$  value of about  $9.4^\circ$ , the load is 1900 lb. These values are plotted on the left-hand diagram of fig. 9, to form the horizontal sides of a rectangle, and they envelop all the experimental values.

From fig. 2 it is found that at 0.7 eccentricity the attitude given by curve G2 is  $21.25^\circ$ ; curve G3 can not be brought into the consideration because all the information as to load-carrying, etc., is not available. A  $21.25^\circ$ -line is

also drawn in fig. 15, and it is seen that with a  $\theta'$  value of  $17.25^\circ$  the load is 950 lb. But this value is for a radial clearance of 0.0172 inch and for 300 revolutions per minute, whereas the experimental records are for a clearance of 0.0038 inch and 200 revolutions per minute. Hence the calculated spot must be multiplied by  $\left(\frac{0.0172}{0.0038}\right)^2 \times \frac{200}{300}$  and becomes 13,020 lb. Similarly with a  $\theta'$  value of  $15.5^\circ$  the calculated load is 1570 lb., which, on correction for clearance and speed, becomes 21,500 lb.

These corrected values are plotted on the right-hand diagram of fig. 9 and envelop all the experimental values.

In the same way the experimental values have been enveloped over a range of eccentricities. The envelopment is incomplete only at 0.9 eccentricity; this lack of completeness demands a word of explanation. From fig. 15 it is seen that the higher loads are associated with the lower values of  $\theta'$ . For 0.9 eccentricity the obtaining of a load sufficiently high to envelop the experimental values requires a value of  $\theta'$  about, or less than,  $1^\circ$ . Unfortunately such a low value of  $\theta'$  with a high eccentricity results in the differences to be treated in the calculations being too small for correct handling with the means available. Thus the failure at 0.9 eccentricity is one of means and not of method.

When comparing the calculated and experimental results in fig. 9 it must be borne in mind that the calculated loads are based on the pressures in central radial planes, and do not take account of the axial reductions in pressure. In order to allow for the axial reduction the calculated loads should all be about 20 to 30 per cent. greater than the experimental loads. For illustrative purposes, however, it was considered desirable to seek for envelopment rather than for the more accurate result which does not actually present any difficulty in principle.

The final diagram, fig. 16, illustrates, in solid lines, three pressure curves determined experimentally. "A," with one point of inflexion, is from Goodman's 1928 paper, the questionable spots obtained by tilting the bearing being ignored. "B," without any point of inflexion, is from Goodman's 1932 paper; the actual spots taken from the published diagram are marked. "C," with two points of inflexion, was obtained by Stanton and is taken from fig. 35 of his book on "Friction." The three curves were chosen to illustrate three characteristics, and the dotted curves, obtained by calculation on the bases discussed above, reproduce the three characteristics. Moreover from the available evidence it is known that the experimental curve "A" is for high



eccentricity, and curve "B" is for low eccentricity; the calculated curves are for high and low eccentricities.

A point of importance in connection with curve "C" is that when analysing the results Stanton *assumed* that the point of inflexion on the outlet region of the curve corresponds to the section of nearest approach of journal and bearing. This assumption could, however, be justified only if the bearing were of infinite axial length and there were no axial flow of the lubricant. As a matter of

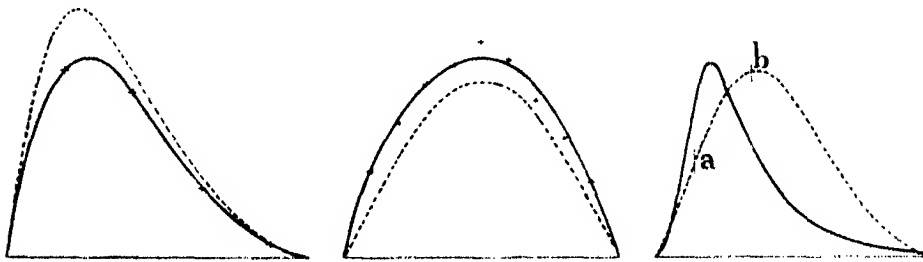


FIG. 16.

interest the point of inflexion on the calculated curve is at *a*, whereas the section of nearest approach corresponds to *b*.

It now seems desirable to summarize the arguments developed above.

In the first place it is clear that the existing theory is seriously at fault as regards the definition of  $h^1$  and the implied constancy of this quantity. In fact  $h^1$  can be constant only in the unreal case of a bearing of infinite axial length.

Then there is another flaw in existing theory in that it does not allow for the existence of limiting sections for the bearing film and so leads to the supposition of a completely unreal state of affairs in the region of the "on" extremity of the bearing.

When a reasonable assumption is made as to the variation of  $h^1$ , when a reasonable condition is taken to govern the state of affairs at the inlet end of the bearing film, and when a reasonable assumption is made as to the state of affairs at the outlet end, it is possible to obtain very full agreement between calculation and experimental results as regards attitude, eccentricity and load-carrying capacity. Possibly more important, however, than the agreement between calculation and experiment is a general consideration, namely, that the underlying thesis implies the inter-dependence of eccentricity, attitude, and extent of film, although the relation varies with the radial clearance; the experimental evidence in itself fully supports this implication.

The agreement between calculation and experiment may not, however, be stressed beyond the point that the thesis underlying the calculations is sound *in principle*. There is no reason why the variation of  $h^1$  should be exactly as assumed in the calculations; nor is there indeed any reason why the variation of  $h^1$  should follow the same law throughout the whole range of eccentricity values. Further, it would seem to be a reasonable generalization that for constant quantity of lubricant supplied the thickness of the bearing film at the inlet end should be the same, whatever be the radial clearance and the eccentricity; whence for constant eccentricity the bearing film should extend very much further with a radial clearance of 0.0038 inch than with a radial clearance of 0.0172 inch. This is not borne out by fig. 15. But the discrepancy here raises the question whether under the experimental conditions there was exact constancy in quantity of lubricant supplied. The determination of an exact theory, based on accurate knowledge of the manner of variation of  $h^1$ , demands further experiments in which the amount of lubricant supplied is accurately known.

To revert to generalization from the calculation results it would seem that a diagram such as fig. 15 embodies also all the information for bearings of varying axial lengths. For instance, if for a particular axial length the value of  $\theta_1$  were  $60^\circ$ , and the attitude  $12^\circ$ , an increased axial length would probably correspond to a reduced attitude, say  $5^\circ$ , with the load, *per unit length*, correspondingly increased.

Finally it seems desirable to give one figure illustrating the accuracy of workmanship and measurement necessary in experiments on film lubrication. With the bearing of small radial clearance the highest eccentricity value shown on Goodman's diagram of coefficient of friction is 0.86. Hence the least thickness of film was  $0.14 \times 0.0038$ , = 0.000532 inch, or about one-tenth of the thickness of a sheet of common foolscap.

#### *Summary.*

There is an assumption as the basis of nearly all the mathematical investigations based on Reynolds' original paper. It is that the length of the brass determines the length of the oil film which is under pressure. This assumption leads to an unreal conception of the velocity conditions at the inlet end of the film, it leads to unjustifiable curves of pressure along the film, and it does not give results which can be harmonized with the results of experiment.

When consideration is given to the character of the curves of velocity across the film, from fixed surface to moving surface, it is seen that extent of brass is

not a material factor in the problem and that the extent of the film is determined by other considerations.

Comparison of the experimental results recorded by Goodman in 1928 with those recorded by him in 1932 leads to the discovery of a serious flaw in the statement of the fundamental equation of Reynolds, namely,

$$\frac{dp}{dx} = 6\lambda u \frac{h - h^1}{h^3}.$$

Accepted theory, and all mathematical developments, take  $h^1$  to be the height at the section of maximum pressure and so to be a constant.  $h^1$  is, however, a variable, and is a measure of the quantity of flow at any section. From this fact springs the necessity for dealing with the matter of side outflow of lubricant; and this, in turn, introduces a new conception, namely, side inflow.

On these modified conceptions it is shown that for any radial clearance the coefficient of friction is dependent upon eccentricity alone; Goodman has tested this thesis and shown it to be true.

Further, on these modified conceptions it is possible to obtain agreement between experiment and calculation both as regards load-carrying capacity and attitude-eccentricity locus.

---

*The Principal Magnetic Susceptibilities of some Paramagnetic Crystals at Low Temperatures.*

By L. C. JACKSON, M.Sc., Ph.D.

(H. H. Wills' Physical Laboratory, University of Bristol.)

(Communicated by A. P. Chattock, F.R.S.—Received January 19, 1933.)

*Introduction.*

Our knowledge of the temperature variation of the principal susceptibilities of paramagnetic crystals is as yet fragmentary. The principal susceptibilities of a number of paramagnetic crystals have been determined by Finke\* and by Rabi† at room temperature but the first measurements on orientated crystals over any range of temperature were those of Foëx.‡ He has published the principal susceptibilities of siderose (a mineral which is mainly ferrous carbonate but which contains appreciable quantities of the carbonates of manganese and other metals) over the range 87° to 400° K. and some measurements but not actual principal susceptibilities for manganese sulphate,  $\text{MnSO}_4 \cdot 4\text{H}_2\text{O}$ . The writer§ measured the principal susceptibilities of cobalt ammonium sulphate and nickel sulphate,  $\text{NiSO}_4 \cdot 7\text{H}_2\text{O}$  over the temperature range 14°–290° K. and the writer and de Haas|| have published measurements on manganese ammonium sulphate crystals over the restricted range 14°–20° K. In addition Dupouy¶ has repeated Foëx's observations on siderose and has measured the principal susceptibilities of dialogite\*\* (a naturally occurring manganese carbonate) and oligist ( $\text{Fe}_2\text{O}_3$ ), all over a small range of temperature above 0° C.

\* 'Ann. Physik,' vol. 31, p. 149 (1910).

† 'Phys. Rev.,' vol. 30, p. 174 (1927).

‡ 'Dissertation,' Strasbourg, 1921, 'Ann. Physique,' vol. 16, p. 174 (1921).

§ 'Dissertation,' Leiden, 1923, 'Phil. Trans.,' A, vol. 224, p. 1 (1923).

|| 'Versl. gewone, Vergad. Akad. Amst.,' vol. 36, p. 1117 (1927); 'Commun. Phys. Lab. Univ. Leiden,' 187c.

¶ 'Ann. Physique,' vol. 15, p. 495 (1931).

\*\* Dupouy finds that the susceptibilities of dialogite in the different directions in the crystal are very nearly equal and that the  $1/\chi \cdot T$  curves are straight lines which are very nearly parallel. Both these results are to be expected with a manganous compound but the actual values of the susceptibilities are much smaller than would be expected, viz.,  $1.7 \times 10^{-6}$  instead of about  $120 \times 10^{-6}$ .

Quite recently Bartlett\* has employed Rabi's method to determine the principal susceptibilities of the following compounds,  $\text{CoSO}_4 \cdot 7\text{H}_2\text{O}$ ,  $\text{CoSO}_4 \cdot (\text{NH}_4)_2\text{SO}_4 \cdot 6\text{H}_2\text{O}$ ,  $\text{CoSO}_4 \cdot \text{K}_2\text{SO}_4 \cdot 6\text{H}_2\text{O}$ ,  $\text{CuSO}_4 \cdot (\text{NH}_4)_2\text{SO}_4 \cdot 6\text{H}_2\text{O}$ ,  $\text{CuSO}_4 \cdot \text{K}_2\text{SO}_4 \cdot 6\text{H}_2\text{O}$ ,  $\text{NiSO}_4 \cdot (\text{NH}_4)_2\text{SO}_4 \cdot 6\text{H}_2\text{O}$  over the temperature range  $-45^\circ$  to  $+55^\circ$  C. In the writer's opinion, however, Bartlett's procedure is liable to several objections.

On the theoretical side, considerable progress has been made within the last few months in the quantum mechanical treatment of the paramagnetic properties of crystals by Van Vleck† and his school. Following up the work of Bethe‡ and Kramers§ they have made a beginning with the calculation of the principal susceptibilities, allowing for the effect of the electrostatic field of the atoms or ions surrounding the magnetic ion.

Thus Kramers and Van Vleck have been able to show that the presence of these electrostatic fields is sufficient to explain the partial or complete suppression of the  $l$ -moment observed in the ions of the elements of the third row of the Periodic Table. Measurements of the susceptibilities of solutions or powdered salts have shown that for the ions  $\text{V}^{4+}$  to  $\text{Cr}^{2+}$  the  $s$ -moment only is effective, through the complete suppression of the  $l$ -moment. The ground state of the next ion,  $\text{Mn}^{2+}$  or  $\text{Fe}^{3+}$  is  ${}^6\text{S}$  and so for this also the  $s$ -moment only is present. With the ions  $\text{Fe}^{2+}$  to  $\text{Cu}^{2+}$  the electrostatic field causes an uncoupling of the  $l$  and  $s$  vectors and partially suppresses the  $l$ -moment. The theory further indicates that for those ions in which  $s$ -moment only is present or effective one must expect that crystals containing these ions will be nearly magnetically isotropic, independently of their crystallographic symmetry. On the other hand crystals containing  $\text{Co}^{2+}$  will show relatively large differences of susceptibility in the different directions because in this ion the  $l$ -moment is suppressed to the least extent among the elements under consideration.

Furthermore the theory shows that unless the crystalline electrostatic field possesses almost cubic symmetry one should obtain three different Curie constants and three different  $\Delta$ 's in the expression  $\chi(T + \Delta) = C$  for the principal magnetic axes of the crystal. Thus the  $1/\chi \cdot T$  curves of the principal susceptibilities of a crystal for not too low temperatures will generally be straight lines but these need not necessarily be all parallel.

\* 'Phys. Rev.,' vol. 41, p. 818 (1932).

† Van Vleck, "The Theory of Electric and Magnetic Susceptibilities," Oxford, 1932; 'Phys. Rev.,' vol. 37, p. 467 (A) (1931); vol. 41, p. 208 (1932); Penny and Schlapp, *ibid.*, vol. 41, p. 194 (1932).

‡ 'Ann. Physik,' vol. 3, p. 133 (1929).

§ 'Proc. Acad. Sci. Amst.,' vol. 32, p. 1176 (1929); vol. 33, p. 959 (1930).

## *Magnetic Susceptibilities of some Paramagnetic Crystals.* 697

The present paper deals with measurements over the temperature range 70° K to 300° K. of the principal susceptibilities of several crystals containing the ions  $\text{Mn}^{2+}$  and  $\text{Fe}^{3+}$  (and preliminary results for one containing  $\text{Cr}^{3+}$ ) as examples of  $s$ -moment ions and of  $\text{CoSO}_4 \cdot 7\text{H}_2\text{O}$  as an example of a cobalt salt. In addition the principal susceptibilities of potassium ferricyanide are given. This substance is an example of a co-ordination compound to which the above considerations do not apply immediately but for which theory suggests that the spin moment of one electron only contributes to the magnetic moment.

### *Apparatus and Experimental Procedure.*

The susceptibilities corresponding to various directions in the crystals were measured by the Faraday method in which the force exerted by the non-homogeneous magnetic field on a small specimen is determined and the susceptibility deduced from the expression

$$F = \chi_x m H \frac{dH}{dy}$$

in which  $F$  = force,  $\chi_x$  = specific susceptibility in direction of field,  $H$  =  $m$  mass of specimen, gradient of field in direction in which  $F$  is measured.

The apparatus employed was based on a design described by Sucksmith\* but adapted for use at low temperatures. In this method the force on the specimen is determined from the deformation of a ring of strip phosphor-bronze fixed at the top and subjected to the force at the bottom. Fig. 1 shows the essential parts of the arrangement. The crystal specimen  $C$  is attached with a minimum amount of "Durofix" diluted with amyl acetate to the table of the small quartz frame shown. The ground surface of the table was made accurately perpendicular to the quartz rod to which the frame is attached. A small brass fitting  $F$  allows the rod to be rotated, so that after the rod has been adjusted to be accurately vertical, the desired plane of the crystal can be set perpendicular to the direction of the magnetic field, by a method mentioned later.

The quartz rod and crystal carrier are attached to the circular ring  $R$  of strip phosphor-bronze by means of a thin brass rod and a screw-coupling not shown in the figure. (Diameter of ring = 6 cm., width of strip = 2.5 mm., thickness of strip = 0.075 mm.) The ring carries two small plane mirrors  $M_1$  and  $M_2$ . The position of the suspended system can be adjusted by means

\* 'Phil. Mag.', vol. 8, p. 158 (1929).

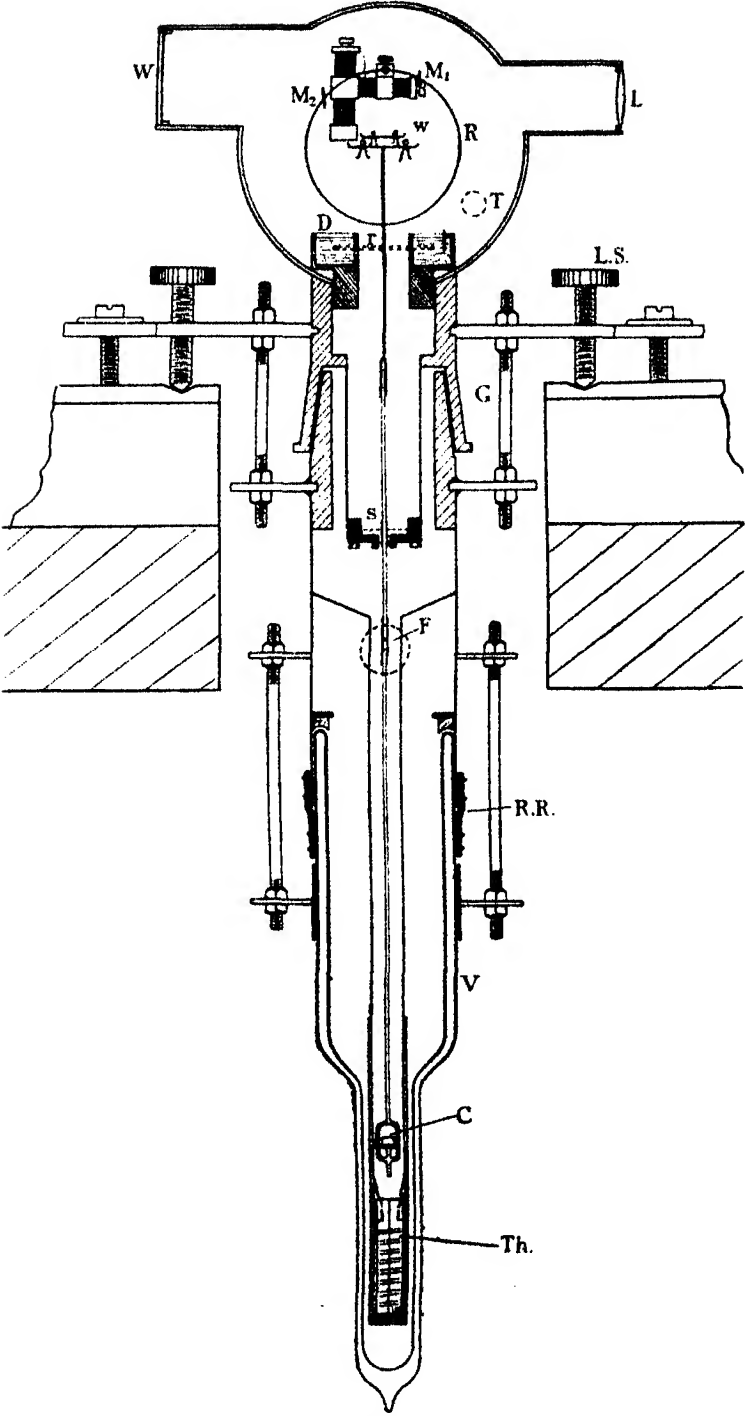


FIG. 1.

of the screw-slides shown and the final adjustment of the height of the crystal can be made by adding or removing the small weights  $w$ . These weights can be manipulated without opening the upper part of the apparatus by means of a hook provided with a handle which is attached by a short length of flexible rubber tube to the back of the cylindrical case housing the upper part of the apparatus.\* The front of the cylindrical case is closed and made airtight by means of a thick plate-glass window which permits a view of the phosphor-bronze ring and its subsidiary fittings.

A ring of wire  $r$  supported from the rod, which carries the quartz frame, etc., by a wire frame perpendicular to the plane of the ring  $R$ , is immersed in oil in the annular trough  $D$  and serves to damp the oscillations of the suspended system. A flat spiral spring of thin phosphor-bronze  $S$  serves to prevent the crystal being pulled sideways towards the pole-pieces. The movement of the crystal and frame under the influence of the magnetic field is thus accurately vertical.

The crystal and its carrier hang in a long tube the upper part of which is made of thin nickel-silver, and the lower of thicker copper to promote uniformity of temperature in the neighbourhood of the specimen. A platinum resistance thermometer, specially wound and calibrated for low temperatures, is placed at the end of the tube immediately below the crystal carrier. This tube is surrounded by a Dewar vessel, as shown, which is filled with the various liquefied gases, which serve to provide the constant low temperatures required. The Dewar vessel is supported by the bolts shown and the joint between it and the rest of the apparatus is made gastight by means of the wired-on rubber ring  $R.R.$  The liquefied gas is filled in through a small side-tube. The gas from the evaporating liquid leaves by the tube shown dotted and may pass either direct to a gas-holder or the atmosphere outside the building or through a vacuum pump by means of which the liquefied gas may be made to boil under known reduced pressures. By means of the ground-joint,  $G$ , the surrounding tube and Dewar vessel can be removed to allow of the crystal being changed. After a specimen has been mounted, the tube in which it hangs and the upper cylindrical case are evacuated through the tube  $T$  and then filled with hydrogen.

The electromagnet is mounted on a screw-actuated slide so that it can be withdrawn when the Dewar vessel, etc., have to be removed. Flat pole-pieces of 10 cm. diameter and a pole-gap of 3 cm. were used so that a constancy of

\* For a diagram of such an arrangement see 'Commun. Phys. Lab. Univ., Leiden,' No. 139, b.



$H dH/dy$  over the required volume could be obtained. The maximum field strength employed was about 10,000 gauss.

Light from a distant source passes through the lens L and after reflection at the mirrors  $M_1$  and  $M_2$  passes through the plane-glass window W and is observed with the aid of a travelling microscope placed somewhat more than a metre from the apparatus. A calculation\* shows that with the dimensions as given, the movement of the crystal is magnified about 100 times at the microscope. The zero of the system is extremely stable and the relation between force applied and deflection is accurately linear over the whole useful range.

The apparatus was calibrated by placing small cylindrical glass containers, of the same volume as the average crystal to be used (average mass of specimen = 150 mg.), and filled with a powdered salt of accurately known susceptibility such as ferrous ammonium sulphate, on the crystal carrier and measuring the deflections over a wide range of currents through the electromagnet. The results were checked against those obtained with other powders, allowance being made, of course, for the actual temperature at the time of the measurements and for the deflections due to the carrier and the empty container. The deflections due to the carrier were also measured over the whole range of temperature employed so that the necessary corrections could be applied to the observed deflections with the crystals.

Measurements were made on the various crystal specimens at room temperature, in a mixture of solid carbon dioxide and alcohol, in liquid ethylene, and in liquid oxygen† boiling under various pressures. With liquid oxygen as cooling agent the temperature was generally taken from the vapour pressure of the liquid but at higher temperatures the readings of the platinum thermometer were always taken. The closed form of the cooling system was chosen to make it possible to work with the liquefied gases under reduced pressures and also to allow of the extension of the measurements to lower temperatures later.

The orientation of the crystal specimens was carried out as follows. The specimen was attached to the table of the crystal holder in such a way that the face (natural or ground), which was to be arranged perpendicular to the lines

\* See Sucksmith, *loc. cit.*

† There is no objection to the use of liquid oxygen (which was readily obtainable in an adequately pure state) in the present experiment in spite of its very strong paramagnetism because the specimens are surrounded by an atmosphere of hydrogen and do not come into direct contact with the cooling bath. A calculation shows that the magnetic shielding due to the cylindrical layer of liquid oxygen is altogether negligible.

of force of the magnetic field, was vertical. A small plane-mirror was temporarily attached to the face in question, and the adjustment to perpendicularity with field made by an auto-collimation method similar to that employed by Foëx,\* the necessary rotation about a vertical axis being provided by the fitting F. The method used allowed one to adjust the crystal face to the required direction with an accuracy of a few minutes of arc which was ample for the present purpose.

*Experimental Results.*

*s-moment Ions.*—The principal susceptibilities of the following compounds have been measured,  $\text{MnSO}_4 \cdot (\text{NH}_4)_2\text{SO}_4 \cdot 6\text{H}_2\text{O}$ ,  $\text{MnSO}_4 \cdot 5\text{H}_2\text{O}$ ,  $\text{MnSO}_4 \cdot 4\text{H}_2\text{O}$ ,  $\text{Fe}(\text{CH}_3\text{COCH}(\text{COCH}_3)_2)_3$  (ferric acetylacetonate),  $\text{K}_3[\text{Fe}(\text{C}_2\text{O}_4)_3] \cdot 3\text{H}_2\text{O}$  (potassium ferrioxalate). Preliminary determinations have also been made with  $\text{K}_3[\text{Cr}(\text{C}_2\text{O}_4)_3] \cdot 3\text{H}_2\text{O}$  (potassium chromioxalate). Previous determinations by various workers of the susceptibilities of solutions or powdered specimens of the substances in the above list have shown that the magnetic moment is about 29.2 Weiss magnetons, in entire agreement with the theoretical value for a  $^6\text{S}_{5/2}$  ground state.

It would thus be expected that crystals of all these salts would be found to be magnetically isotropic and this is indeed so. At room temperature the measured susceptibilities in the different directions for no crystal differed by much more than 1 per cent. from the mean value for the three principal axes. This result thus confirms the previous determinations in which gadolinium ethylsulphate† (monoclinic) and manganese ammonium sulphate‡ (monoclinic) crystals were shown to be magnetically isotropic to within less than 1 per cent.; the ground state of the ion is in each case an S state.

The preliminary measurements on  $\text{K}_3[\text{Cr}(\text{C}_2\text{O}_4)_3] \cdot 3\text{H}_2\text{O}$  indicated that this crystal too is isotropic to within 1 per cent. in agreement with theory for an ion, the *l*-moment of which is completely suppressed by the crystalline field.

*Manganese Ammonium Sulphate.*—It is somewhat difficult to obtain this substance, which crystallizes in the monoclinic prismatic class, in large, well-formed, perfectly clear crystals. It shows a considerable tendency to produce cloudy crystals when grown by slow evaporation at room temperature. From several crops of crystals one can, however, pick out a number of perfectly transparent ones suitable for the magnetic measurements.

\* See 'Ann. Physique,' vol. 16, p. 174 (1921).

† Jackson and Kamerlingh Onnes, 'C. R. Acad. Sci. Paris,' vol. 177, p. 154 (1923).

‡ Rabi, 'Phys. Rev.,' vol. 30, p. 174 (1927).

The results given in Table I may be taken as typical of any direction in the crystal to an accuracy of about 1 per cent.\* No attempt has been made to calculate the position angle  $\psi$  (see later) for any of the  $s$ -moment crystals as the measured differences are too small to permit this being done with any accuracy.

Table I.— $\text{MnSO}_4 \cdot (\text{NH}_4)_2\text{SO}_4 \cdot 6\text{H}_2\text{O}$ .Crystal 5.  $\perp$  to (010)–(b).

T.	$\chi \times 10^6$ .	$\chi'_m$ .	$\chi'_m (T + 0.7)$ .
291.8	37.2	0.0147 <sub>3</sub>	4.31
199.1	54.6	0.0215 <sub>4</sub>	4.31
90.2	120.8	0.0474 <sub>3</sub>	4.31
86.1	126.0	0.0494 <sub>3</sub>	4.29
80.3	134.2	0.0526 <sub>4</sub>	4.27

$\chi'_m$  = molecular susceptibility corrected for diamagnetism of anion, water of crystallization, etc.

Manganese ammonium sulphate crystals thus obey the law  $\chi (T + \Delta) = \text{constant}$  with a very small value of  $\Delta$  ( $= 0.7$ ). The Weiss magneton number calculated from the above results is 29.2. These observations are thus in reasonable agreement with the measurements on powdered manganese ammonium sulphate between 290° K. and 14° 5 K.,† which gave  $\chi = 37.8 \times 10^{-6}$  at room temperature, with a magneton number of 29.2, the substance following Curie's law  $\chi T = \text{constant}$ .

Measurements made on cloudy specimens gave less concordant results in which values of  $\Delta$  of a few degrees were found. This observation probably furnishes the explanation for the larger differences of susceptibility in the different directions in the crystal found by the writer and de Haas‡ in their

\* Rabi ('Phys. Rev.,' vol. 30, p. 174 (1927)) using a method which gives  $\psi$  directly, has determined the principal susceptibilities of this crystal at room temperature. In agreement with the above, he finds that the principal susceptibilities are the same to within 1 per cent. but his actual values are as follows  $\chi_1 = 34.3 \times 10^{-6}$ ,  $\chi_2 = 34.2 \times 10^{-6}$ ,  $\chi_3 = 34.5 \times 10^{-6}$ ,  $\psi = 14^\circ$ , giving a Weiss magneton number of 28.1, assuming Curie's law. Several crystals were encountered in the present work which gave susceptibilities very nearly equal to  $34.3 \times 10^{-6}$ , and a Weiss magneton number of about 28.2 from the temperature variation of the susceptibility. All these crystals were, however, found to have cracked after the measurements, showing that originally they were strained, or in some other way imperfect.

† Jackson and Kamerlingh Onnes, 'Proc. Roy. Soc.,' A, vol. 104, p. 671 (1923).

‡ 'Verlag. gewone Vergad. Akad. Wet. Amsterdam,' vol. 36, p. 1117 (1927); 'Commun. Phys. Lab. Univ. Leiden,' No. 187 c.

measurements in the range of temperatures 20°–14° K. For this work larger crystals were necessary (about  $\frac{1}{2}$  gm. weight for the prepared section), and as it was found very difficult to grow perfectly clear crystals large enough to permit sections of this size being ground from them, somewhat cloudy specimens had to be used.\*

*Manganese Sulphate.*—A number of different hydrates can be obtained by the crystallization of manganese sulphate from aqueous solutions at different temperatures. Slow evaporation at room temperature leads to the formation of the triclinic pentahydrate  $\text{MnSO}_4 \cdot 5\text{H}_2\text{O}$ , while the monoclinic tetrahydrate,  $\text{MnSO}_4 \cdot 4\text{H}_2\text{O}$  crystallizes out between 30° and 40° C.

$\text{MnSO}_4 \cdot 5\text{H}_2\text{O}$ .—This substance tends to dehydrate when left in the air but with optically clear crystals the change is sufficiently slow for a set of observations of the susceptibility in any one direction to be determined over the range of temperature used. Observations with several crops of crystals showed that at room temperature they are magnetically isotropic to within 1 per cent. The results in Table II may be taken as typical of this substance.

Table II.— $\text{MnSO}_4 \cdot 5\text{H}_2\text{O}$ .

Crystal 1.  $\parallel c$  axis.

T.	$\chi \times 10^6$ .	$\chi'_m$ .	$\chi'_m (T + 3)$ .
293.2	60.8 <sub>2</sub>	0.0147 <sub>2</sub>	4.37 <sub>1</sub>
198.6	90.7 <sub>6</sub>	0.0219 <sub>6</sub>	4.43 <sub>1</sub>
197.8	91.5 <sub>6</sub>	0.0221 <sub>6</sub>	4.45 <sub>6</sub>
169.7	105.7 <sub>7</sub>	0.0255 <sub>7</sub>	4.41 <sub>6</sub>
147.8	119.8 <sub>8</sub>	0.0289 <sub>1</sub>	4.36 <sub>0</sub>
90.3	194.4 <sub>4</sub>	0.0469 <sub>9</sub>	4.38 <sub>3</sub>
90.2	194.8 <sub>8</sub>	0.0470 <sub>8</sub>	4.38 <sub>8</sub>
84.8	204.8 <sub>8</sub>	0.0494 <sub>8</sub>	4.34 <sub>4</sub>
78.8	220.8 <sub>8</sub>	0.0532 <sub>8</sub>	4.35 <sub>7</sub>

\* Krishnan ('Z. Physik,' vol. 71, p. 137 (1931)) has pointed out that an error was made in the calculation of  $\psi$  and hence in  $\chi_1$  and  $\chi_2$  in the paper referred to and has published the corrected values. Although it is more in accord with what may be expected *a priori* for a manganous salt to suppose that the  $1/\chi \cdot T$  lines for  $\chi_1$  and  $\chi_2$  are straight and parallel to that of  $\chi_2$  at the higher temperatures and curved at the lowest temperatures, the experimental results cannot themselves distinguish between this interpretation and that suggested by the writer and de Haas. This can readily be seen by plotting the corrected results; the points still lie within the experimental accuracy on three straight lines through the origin. Thus though it is agreed that the first interpretation is probably the correct one, the observations do not, as Krishnan states, lead quite definitely and exclusively to this interpretation. By examining the graphs and comparing them with the  $\Delta$ 's in Table II of Krishnan's paper, it will be seen that his calculations of the Curie constants for 17° K. and 15° K. have no meaning whatever.

The substance follows the law  $\chi(T + \Delta) = C$  with  $\Delta = +3$  and the Weiss magneton number is 29.4.

$\text{MnSO}_4 \cdot 4\text{H}_2\text{O}$ .—Crystallization was carried out at 35° C. and measurements were made on several crops of crystals. The greatest difference between a crystal susceptibility and the mean value at room temperature was rather more than 1 per cent. with this substance. These small differences were however, too small to make it worth while attempting to calculate the principal susceptibilities from the observed values. Table III may therefore be taken to represent the results for any direction in the crystal to within 1 to 2 per cent.

It is known that the susceptibility of powdered manganese sulphate\* obeys approximately Curie's law at high temperature but shows deviations from this law below 60° K. It will be of interest to measure the principal susceptibilities of the crystal down to liquid hydrogen temperatures, when this temperature range becomes available in this laboratory, and the more accurate determination of the principal susceptibilities at higher temperatures may profitably be left until this is attempted.

Table III.— $\text{MnSO}_4 \cdot 4\text{H}_2\text{O}$ .†  
Crystal 3.  $\perp$  to (010). (b).

T.	$\chi \times 10^6$ .	$\chi'_m$ .	$\chi'_m (T + 2)$ .
290.0	65.2 <sub>0</sub>	0.0146 <sub>3</sub>	4.27 <sub>3</sub>
197.5	95.6 <sub>3</sub>	0.0214 <sub>3</sub>	4.27 <sub>4</sub>
90.3	206. <sub>9</sub>	0.0462 <sub>4</sub>	4.26 <sub>9</sub>
84.7	218. <sub>7</sub>	0.0488 <sub>8</sub>	4.23 <sub>9</sub>
79.5	233. <sub>2</sub>	0.0521 <sub>1</sub>	4.24 <sub>7</sub>

The Weiss magneton number calculated from the observations in Table III is 29.0 and the crystal follows the law  $\chi(T + \Delta) = \text{constant}$  with  $\Delta = +2$ .

*Ferric Acetylacetonate*‡.—Measurements on this substance in powder form by Welo§ have shown that the magnetic moment of the Fe atom is the same as that of the  $\text{Fe}^{3+}$  ion in simple ferric salts. In agreement with this, measurements of the crystal susceptibilities of this substance (= orthorhombic) have

\* 'Commun. Phys. Lab. Univ. Leiden,' No. 132 c.

† These values are in general agreement with those published by Foëx, 'Ann. Physique,' vol. 16, p. 174 (1921), for the more limited temperature range 224° K. to 301° K.

‡ The writer is indebted to Dr. T. Malkin and to Dr. C. H. Johnson, of the Chemical Department of this University, for the material from which the crystals of ferric acetylacetonate and potassium ferrioxalate were prepared.

§ 'Phil. Mag.,' vol. 6, p. 481 (1928).

shown that it is magnetically isotropic to within less than 1 per cent. Typical results are given in Table IV.

Table IV.— $\text{Fe}(\text{CH}_3\text{COCH COCH}_3)_3$ .  
Crystal 2.  $\perp$  (001) (c).

T.	$\chi \times 10^6$ .	$\chi'_m$ .	$\chi'_m (T + 4)$ .
291.5	42.1 <sub>1</sub>	0.0150 <sub>3</sub>	4.43 <sub>3</sub>
198.4	62.3 <sub>0</sub>	0.0221 <sub>4</sub>	4.48 <sub>3</sub>
90.3	132.7	0.0470 <sub>0</sub>	4.43 <sub>1</sub>
90.2	132.8	0.0469 <sub>2</sub>	4.42 <sub>1</sub>
85.2	140.7	0.0498 <sub>0</sub>	4.44 <sub>2</sub>
79.0	151.1	0.0534 <sub>9</sub>	4.43 <sub>9</sub>

Ferric acetylacetonate obeys the law  $\chi (T + \Delta) = C$  with  $\Delta = +4^\circ$ . Weiss magneton number = 29.6.

*Potassium Ferrioxalate.*—This substance also possesses the same magnetic moment as a simple ferric salt, and again the crystals have been found to be magnetically isotropic to within 1 per cent. A typical set of results are given in Table V.

Table V.— $\text{K}_3[\text{Fe}(\text{C}_2\text{O}_4)_3] \cdot 3\text{H}_2\text{O}$ .  
Crystal 2.  $\parallel$  c axis.

T.	$\chi \times 10^6$ .	$\chi'_m$ .	$\chi'_m T$ .
289.4	30.5 <sub>1</sub>	0.0150 <sub>4</sub>	4.35 <sub>9</sub>
200.3	44.6 <sub>3</sub>	0.0220 <sub>4</sub>	4.41 <sub>4</sub>
169.6	52.1 <sub>4</sub>	0.0257 <sub>4</sub>	4.36 <sub>9</sub>
90.1	100.2	0.0493 <sub>2</sub>	4.44 <sub>3</sub>
90.0	99.1 <sub>7</sub>	0.0488 <sub>3</sub>	4.39 <sub>4</sub>
83.7	105.7	0.0520 <sub>3</sub>	4.35 <sub>4</sub>
79.8	110.6	0.0541 <sub>4</sub>	4.32 <sub>0</sub>
70.6	127.3	0.0626 <sub>3</sub>	4.42 <sub>2</sub>

$\Delta = 0$  and the Weiss magneton number is 29.4.

*Potassium Chromioxalate.*—Many attempts were made to grow crystals of this substance sufficiently large, and of good enough quality to enable them to be used to determine the crystal susceptibilities. The attempts have so far failed, only somewhat imperfect specimens having been obtained.

Preliminary observations with these crystals showed them to be magnetically isotropic to within 1 per cent. at room temperature. The actual values are not given here as they are regarded as provisional only, and it is hoped to secure better ones later.

*Cobalt Sulphate.*—Cobalt sulphate, when crystallized from aqueous solution at room temperature, deposits monoclinic crystals of the heptahydrate. A large number of crops of these crystals were grown and the best specimens used for the measurements.

On account of the difficulty of identifying the various faces of this crystal by visual inspection only, the specimens used were always mounted on a Tutton grinding goniometer, and a sufficient number of angles measured to make quite certain of the orientation of the crystal. A plane was then ground accurately parallel to the (010) plane, which never appeared as a prominently developed face. This then served as the reference plane for the orientation of the specimen on the crystal carrier of the magnetic apparatus.

To determine the magnetic properties of such a crystal completely the susceptibilities in four known directions have to be determined as functions of the temperature. It is known from symmetry considerations that the principal susceptibility  $\chi_3$  lies along the symmetry axis of the crystal, i.e., perpendicular to (010). A specimen was therefore mounted with the (natural) (001) face on the table of the holder and rotated until the vertical (010) face was perpendicular to the magnetic field, the accurate adjustment being carried out as previously described. This specimen then gave  $\chi_3$  directly from the observations. To determine  $\chi_1$  and  $\chi_2$  and the position angle  $\psi$ , it was necessary to measure the susceptibilities in three different directions (preferably) in the symmetry plane. Measurements were therefore made perpendicular to the natural faces (101), (001) and ( $\bar{1}$ 01) which were generally prominently developed. The specimen was therefore mounted with the (ground) (010) face on the table of the holder and so orientated that the required one of the above mentioned faces was perpendicular to the magnetic field.

It was intended, where possible, to carry out the whole four series of measurements on the same specimen selected so that it had roughly the same dimensions in all the required directions. After repeating the measurements with other specimens the consistency among the values of the principal susceptibilities so deduced may be examined. Unfortunately this is not possible with cobalt sulphate because the crystal shows a considerable tendency to dehydrate. A complete series of observations for one particular direction in the crystal only can be obtained before the specimen shows appreciable signs of dehydration. It was therefore necessary to measure each of the required susceptibilities on a fairly large number of specimens and, when a satisfactory agreement was found, to calculate the principal susceptibilities from the values which best represented the whole of the observational material.

# Magnetic Susceptibilities of some Paramagnetic Crystals. 707

These observed values were then plotted and the susceptibilities were read off for certain temperatures and used in the calculations as given below. The results so obtained are reproduced in Table VI.

Table VI.— $\text{CoSO}_4 \cdot 7\text{H}_2\text{O}$ .  
Observed Susceptibilities.

$\chi_I$ $\perp (010) (b)$ .		$\chi_{II}$ $\perp (001) (c)$ .	
T.	$\chi \times 10^6$ .	T.	$\chi \times 10^6$ .
290	34.8 <sub>0</sub>	290	33.7 <sub>4</sub>
200	49.8 <sub>1</sub>	200	46.7 <sub>1</sub>
150	65.4 <sub>4</sub>	150	59.1 <sub>8</sub>
90	104.8	90	86.6 <sub>1</sub>
82	113.8	82	92.2 <sub>8</sub>
75	122.9	75	97.8 <sub>0</sub>

$\chi_{III}$ $\perp (10\bar{1}) (\rho)$ .		$\chi_{IV}$ $\perp (101) (r)$ .	
T.	$\chi \times 10^6$ .	T.	$\chi \times 10^6$ .
290	39.8 <sub>4</sub>	290	33.0 <sub>8</sub>
200	58.2 <sub>7</sub>	200	45.7 <sub>1</sub>
150	78.6 <sub>9</sub>	150	57.9 <sub>0</sub>
90	134.4	90	85.2 <sub>7</sub>
82	146.8	82	90.1 <sub>4</sub>
75	162.1	75	96.1 <sub>8</sub>

The principal susceptibilities and the angle  $\psi$  were then calculated by the method given by Finke.\*

From the known crystallographic data† we then have  $\Phi_{II} = 58^\circ 2'$ ,  $\Phi_{III} = 14^\circ 40'$ ,  $\Phi_{IV} = 132^\circ 49'$ , the  $\Phi$ 's being the angles between the observed susceptibilities and the c-axis. The calculated values of the principal susceptibilities are given in Table VII.

The results in Table VII lead to the following values of  $\Delta$ :  $\Delta_1 = -4$ ,  $\Delta_2 = +54$ ,  $\Delta_3 = +12$ . The Weiss magneton numbers calculated in the conventional way for the three principal directions are then  $p_1 = 25.3$ ,  $p_2 = 25.0$ ,  $p_3 = 24.3$ .

\* 'Ann. Physik,' vol. 31, p. 149 (1910).

† Groth, "Chemische Krystallographie," vol. II, p. 528, Leipzig (1908).



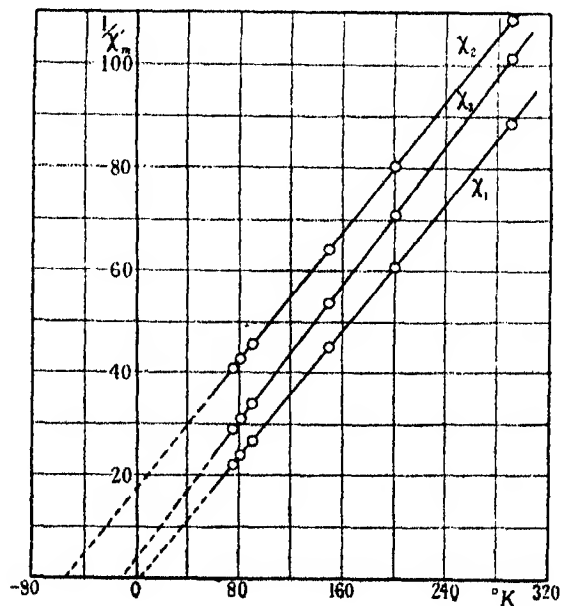
Table VII.— $\text{CoSO}_4 \cdot 7\text{H}_2\text{O}$ .

Principal Susceptibilities.

T.	$\chi_1 \times 10^6$ .	$\chi'_{1m}$ .	T.	$\chi_2 \times 10^6$ .	$\chi'_{2m}$ .
290	39.8 <sub>4</sub>	0.0113 <sub>1</sub>	290	32.3 <sub>4</sub>	0.0092 <sub>0</sub>
200	58.3 <sub>9</sub>	0.0165 <sub>4</sub>	200	44.2 <sub>3</sub>	0.0125 <sub>3</sub>
150	78.8 <sub>1</sub>	0.0222 <sub>3</sub>	150	55.2 <sub>9</sub>	0.0156 <sub>4</sub>
90	134.8	0.0380 <sub>0</sub>	90	78.1 <sub>9</sub>	0.0220 <sub>3</sub>
82	147.0	0.0414 <sub>2</sub>	82	82.3 <sub>5</sub>	0.0232 <sub>5</sub>
75	162.7	0.0458 <sub>1</sub>	75	86.4 <sub>5</sub>	0.0244 <sub>0</sub>

T.	$\chi_3 \times 10^6$ .	$\chi'_{3m}$ .	T.	$\psi$ .
290	34.8 <sub>0</sub>	0.0098 <sub>3</sub>	290	—49° 42'
200	49.8 <sub>1</sub>	0.0141 <sub>0</sub>	200	—50° 39'
150	65.4 <sub>4</sub>	0.0185 <sub>0</sub>	150	—51° 26'
90	104.8	0.0295 <sub>0</sub>	90	—52° 40'
82	113.8	0.0321 <sub>0</sub>	82	—52° 17'
75	122.8	0.0346 <sub>5</sub>	75	—52° 44'

FIG. 2.— $\text{CoSO}_4 \cdot 7\text{H}_2\text{O}$ .

The values of the reciprocals of the principal susceptibilities corrected for diamagnetism are plotted in fig. 2. It will be seen that the  $1/\chi \cdot T$  curves are straight lines, those of  $\chi_1$  and  $\chi_2$  being very nearly parallel. The third sus-

ceptibility  $\chi_3$ , however, gives a straight line which is definitely not parallel to the other two. This result is to be expected if the crystalline field does not possess approximately cubic symmetry.

A comparison of the above results with those of Bartlett shows that there is a qualitative agreement only, the observed susceptibilities being of the same order of magnitude and for each  $\chi_1 > \chi_3 > \chi_2$ . Finke's values for the measured susceptibilities perpendicular to (010), (001), (10 $\bar{1}$ ) and (101) at room temperature, viz.,  $34.9 \times 10^{-6}$ ,  $33.9 \times 10^{-6}$ ,  $36.1 \times 10^{-6}$ ,  $32.8 \times 10^{-6}$  are, with the exception of  $\chi_{111}$  ( $\perp$  10 $\bar{1}$ ), in excellent agreement with the present values.

In view of the complete disagreement with Bartlett's results and of the non-parallelism of all the  $1/\chi \cdot T$  lines, a check on the results by the following method was carried out. A parallel sided section was ground from a crystal in a definitely known direction. It was then finished to a cylindrical shape, leaving, however, a small strip about 1 mm. wide of a known face parallel to the axis of the cylinder. The cylindrical specimen was then mounted on the crystal-carrier in a known direction relative to the magnet, the unground strip serving as the reference plane. Then the axis of the specimen and that of the turn-table of the magnet having been carefully aligned, measurements were made of the susceptibility at regular intervals from the datum position by rotating the magnet. If now the axis of the cylindrical specimen was parallel to the  $b$  axis of the crystal (the section having been ground perpendicular to this) the observations gave directly the value of  $\chi_1$  and  $\chi_2$  and the angle  $\psi$ . Observations on another specimen could then give  $\chi_3$ . The method was very convenient as it enabled the necessary data to be obtained more directly and more rapidly than before.

The results so obtained checked well with those previously obtained. The higher value of  $\chi_{111}$  given in Table VI was definitely indicated rather than Finke's lower value. The later results have been taken into account in Table VI.

*Potassium Ferricyanide.*—Potassium ferricyanide crystallizes in the monoclinic prismatic class,  $\beta$  being, however, very nearly  $90^\circ$  ( $= 90^\circ 6'$ ). This substance is very difficult to obtain in sufficiently large perfect single crystals as it shows every grade of twinning from two individuals of approximately equal size to repeated twinning with microscopically thin lamellæ.

For the present work two twin crystals, which each consisted of two individuals of nearly equal size and showed no external signs (such as striated faces) of repeated twinning, were taken and one of the individuals ground away parallel to the twin plane (100). The individual so left was further ground so

as to be roughly of the same dimensions in all directions and to present the necessary faces for measurement.

Susceptibility measurements were made in the following directions  $\perp$  (100),  $\perp$  (010),  $\parallel$   $c$  axis and at an angle  $31^\circ 55'$  to the  $c$  axis in the  $ac$  plane. The observations were plotted and values of  $\chi$  read off for the temperatures given in Table VIII.

Table VIII.— $K_3$  [Fe (CN) $_6$ ].

XI $\perp$ (100).		XII $\Phi = 31^\circ 55'$ .	
T.	$\chi \times 10^6$ .	T.	$\chi \times 10^6$ .
290	7.43	290	6.57
273	7.84	273	6.98
200	10.4 <sub>4</sub>	200	8.86
170	12.0 <sub>6</sub>	170	9.73
150	13.4 <sub>4</sub>	150	10.5 <sub>1</sub>
90	20.1 <sub>6</sub>	90	13.6 <sub>3</sub>
82	21.6 <sub>6</sub>	82	14.1 <sub>6</sub>
75	23.1 <sub>6</sub>	75	14.7 <sub>4</sub>

XIII $\parallel$ $c$ axis.		XIV $\perp$ (010).	
T.	$\chi \times 10^6$ .	T.	$\chi \times 10^6$ .
290	6.25	290.6	6.99
273	6.62	197.4	10.1 <sub>1</sub>
200	8.20	90.3	19.0 <sub>7</sub>
170	8.87	90.3	18.9 <sub>3</sub>
150	9.42	84.9	19.9 <sub>6</sub>
90	11.3 <sub>6</sub>	80.6	20.9 <sub>3</sub>
82	11.6 <sub>6</sub>	75.7	22.2 <sub>0</sub>
75	11.9 <sub>7</sub>		

The principal susceptibilities were then calculated by Fincke's method using the following values of  $\Phi$ ,  $\Phi_I = 90^\circ$ ,  $\Phi_{II} = 31^\circ 55'$ ,  $\Phi_{III} = 0^\circ$ . The results are given in Table IX.

The figures in Table IX refer to the observations on crystal 1, our results obtained with crystal 2 gave a general confirmation of the data.

The order of the principal susceptibilities is in agreement with that found qualitatively by Grailich and von Lang,\* viz.,  $a > b > c$ .

The reciprocals of the corrected molecular susceptibilities are plotted in fig. 3. It will be seen that there is no trace of parallelism between the  $1/\chi \cdot T$

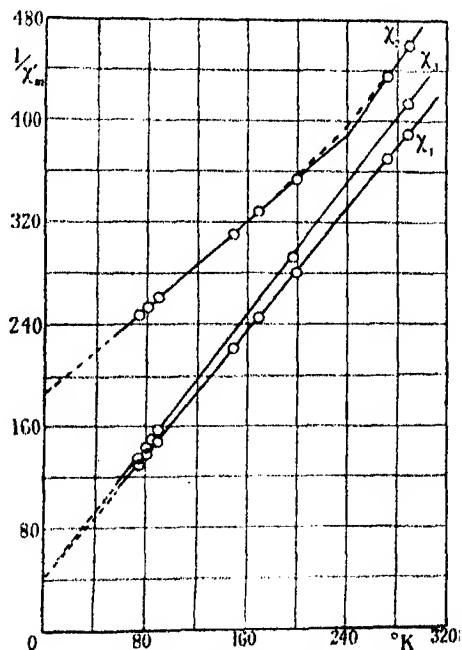
\* 'SitzBer. Akad. Wiss. Wien,' B, vol. 32, p. 43 (1858).

Table IX.— $K_3$   $[Fe(CN)_6]$ .

T.	$\chi_1 \times 10^6$ .	$\chi'_{1m}$ .	T.	$\chi_2 \times 10^6$ .	$\chi'_{2m}$ .
290	7.43	0.00256 <sub>6</sub>	290	6.25	0.00217 <sub>7</sub>
273	7.84	0.00270 <sub>1</sub>	273	6.62	0.00240 <sub>6</sub>
200	10.4 <sub>4</sub>	0.00355 <sub>7</sub>	200	8.20	0.00281 <sub>6</sub>
170	12.0 <sub>7</sub>	0.00409 <sub>8</sub>	170	8.87	0.00304 <sub>6</sub>
150	13.4 <sub>4</sub>	0.00454 <sub>8</sub>	150	9.42	0.00322 <sub>1</sub>
90	20.1 <sub>4</sub>	0.00675 <sub>0</sub>	90	11.3 <sub>0</sub>	0.00384 <sub>1</sub>
82	21.6 <sub>7</sub>	0.00725 <sub>8</sub>	82	11.6 <sub>8</sub>	0.00395 <sub>6</sub>
75	23.1 <sub>8</sub>	0.00775 <sub>8</sub>	75	11.9 <sub>6</sub>	0.00405 <sub>6</sub>

T.	$\chi_3 \times 10^6$ .	$\chi'_{3m}$ .	T.	$\psi$ .
290.6	6.99	0.00241 <sub>6</sub>	290	-89° 28'
197.4	10.1 <sub>1</sub>	0.00344 <sub>8</sub>	273	-91° 0'
90.3	19.0 <sub>7</sub>	0.00639 <sub>7</sub>	200	-90° 58'
90.3	18.9 <sub>8</sub>	0.00635 <sub>1</sub>	170	-89° 22'
84.9	19.9 <sub>6</sub>	0.00669 <sub>0</sub>	150	-89° 28'
80.6	20.9 <sub>8</sub>	0.00701 <sub>8</sub>	90	-88° 55'
75.7	22.2 <sub>0</sub>	0.00742 <sub>8</sub>	82	-88° 15'
			75	-87° 57'

FIG. 3.— $K_3$   $[Fe(CN)_6]$ .

curves. The experimental accuracy of the points at 200° K. and 273° K. (1-2 per cent.) is not sufficient to enable one to state definitely whether the

## 712 *Magnetic Susceptibilities of some Paramagnetic Crystals.*

curve for  $\chi_2$  should be drawn as two intersecting straight lines (full curve) or as a continuous curve (dotted). The departure from a single straight line is, however, quite definite as will be seen by plotting the observed susceptibilities  $\chi_I$ ,  $\chi_{II}$ ,  $\chi_{III}$ . The kink or sharp bend in the  $\chi_2$  curve at about  $240^\circ$  K. may be caused by some change in crystal structure which affects the crystalline field more strongly in one direction than in others.

Many instances are already known of kinks or sharp bends occurring in the  $1/\chi \cdot T$  curves for powdered paramagnetic substances. In particular Welo\* has found such a change of slope at  $340^\circ$  K. for powdered potassium ferricyanide and Ishiwara's† results for the temperature range  $155^\circ$  K. to  $260^\circ$  K. indicate that a second change of slope has probably occurred at about  $250^\circ$  K. The  $1/\chi \cdot T$  curve for the mean of the principal susceptibilities derived from the present results shows a small bend or kink near  $240^\circ$  and is not in disagreement with previous published work on the powdered material.

The anomaly in the behaviour of  $\chi_2$  may possibly be due to the specimen conceivably being a repeated twin with microscopically thin lamellæ, though the connection is not obvious. It was intended after the measurements to grind sections from the specimens perpendicular to the twin plane and examine the optical properties to test this point. Unfortunately crystal 1 broke in the grinding and crystal 2 was found to be cracked after the last series of observations. The question had therefore to remain unsettled. On account of the difficulty of producing specimens which were above all suspicion the measurements were not pursued further with other crystals.

A comparison of fig. 2 and 3 shows that the lack of parallelism of the curves is much greater with potassium ferricyanide than with cobalt sulphate and hence that the asymmetry of the crystalline field is presumably greater. The anisotropy of the potassium ferricyanide crystal at the lowest temperature measured will be seen to be very considerable, of the order 100 per cent. Microscopic lamellar twinning if present can only have had the effect of reducing, not increasing, the anisotropy in the magnetic properties. The results do not therefore agree with what would be expected if the magnetic moment in this substance were due to spin alone. The present theory of the magnetic properties of co-ordination compounds will need to be extended considerably before it can account for the present results.

I am indebted to Professor A. M. Tyndall for his continued interest in the above work.

\* 'Phil. Mag.,' vol. 6, p. 481 (1928).

† 'Sci. Rep. Tohoku Univ.,' vol. 3, p. 303 (1914).

*Summary.*

An apparatus is described for the rapid determination of the principal susceptibilities of crystals at low temperatures, with an accuracy of about  $\frac{1}{2}$  to 1 per cent. Results are given for the following crystals: manganese ammonium sulphate, manganese sulphate (penta- and tetra-hydrate), ferric acetylacetonate, potassium ferrioxalate, cobalt sulphate and potassium ferricyanide.

In agreement with recent theory the crystals containing ions with *s*-moment only present, or effective, are found to be magnetically isotropic to within about 1 per cent. Over the range of temperature employed, 290°–75° K., the  $1/\chi \cdot T$  curves for the principal susceptibilities of cobalt sulphate are straight lines but these are not all parallel. Potassium ferricyanide shows a rather complicated behaviour.

*The Photosynthesis of Hydrogen Chloride. III.—Mixtures Containing Oxygen.*

By RONALD G. W. NORRISH and MOWBRAY RITCHIE,  
Department of Physical Chemistry, Cambridge.

(Communicated by T. M. Lowry, F.R.S.—Received February 17, 1933.)

The inhibiting action of oxygen in hydrogen-chlorine mixtures was first observed by Bunsen and Roscoe,\* and has been generally confirmed by all later workers, but the exact part played by oxygen is still attended by some uncertainties. Chapman and MacMahon† found the sensitivity of stoichiometric mixtures of hydrogen and chlorine at atmospheric pressure to be inversely proportional to the oxygen content. In like manner, Bodenstein and Dux,‡ for stoichiometric mixtures and concentrations of oxygen up to 22.5 mm. Hg, state that the rate of formation of HCl under such conditions is given by

$$\frac{d[\text{HCl}]}{dt} = \frac{k[\text{Cl}_2]^2}{[\text{O}_2]}$$

for constant conditions of incident light intensity.

\* 'Pogg. Ann.,' vol. 100, p. 481 (1857).

† 'J. Chem. Soc.,' vol. 95, p. 959 (1909).

‡ 'Z. phys. Chem.,' vol. 85, p. 297 (1913).

The results of all workers are in agreement with the statement that in the presence of oxygen the rate of reaction is proportional to the first power of the light absorbed, and thus that the quantum efficiency is independent of variation of the intensity of light.

Further investigations of wider scope on the exact inhibiting action of oxygen have, however, extended the kinetic equation of Bodenstein and Dux, which is found to be only approximate. The results of M. C. C. Chapman\* for example, for light of constant intensity are expressed by means of an expression of the type

$$d[\text{HCl}] = \frac{k [\text{Cl}_2]^2 [\text{H}_2]}{[\text{Cl}_2] + k' [\text{H}_2]^{(2-y)} [\text{O}_2]},$$

while those of Cremer† conform to the formula

$$\frac{d[\text{HCl}]}{dt} = \frac{k [\text{Cl}_2]^2 [\text{H}_2]}{[\text{Cl}_2] + 0.02 [\text{H}_2] [\text{O}_2]}.$$

M. C. C. Chapman found that the rate of reaction is independent of the concentration of oxygen in mixtures in which the concentration of hydrogen is very small, and is inversely proportional to the concentration of oxygen in all other mixtures, and with this the formula of Cremer is in agreement. On the other hand the two expressions are in definite disagreement over the inhibiting effect of hydrogen, and in this respect crystallize a long standing difference of opinion between the Bodenstein and Chapman schools of workers. This inhibiting effect of hydrogen is marked by the fact that as the pressure of hydrogen is increased the velocity of formation of hydrogen chloride first increases to a maximum value and then decreases, and was first noticed by Chapman and Underhill‡ and confirmed later by M. C. C. Chapman (*loc. cit.*); it is expressed in their formula given above, by the index  $(2 - y)$  in which  $y$  is less than unity. It was, however, denied both by Bodenstein and Dux (*loc. cit.*) and by Thon§ that the velocity declines with increase of pressure of hydrogen and the results were attributed to the presence of oxygen as an impurity in the hydrogen used by Chapman. The question was thus left in a somewhat uncertain state, and it is satisfactory that the present investigation, while fully confirming the results of Chapman, also indicates in part a kinetic reason for the failure of the Bodenstein school to furnish confirmation.

\* 'J. Chem. Soc.,' vol. 123, p. 3062 (1923).

† 'Z. phys. Chem.,' vol. 128, p. 285 (1927).

‡ 'J. Chem. Soc.,' vol. 103, p. 496 (1913).

§ 'Fortschr. d. Chemie,' vol. 18, part 11 (1926).

The experiments of Cremer were carried out in the presence of phosphorus pentoxide and yielded results which varied according to the fillings of the latter substance in the reaction tube. It was therefore concluded that the reaction was sensitive to catalytic surface effects, and a similar possibility was also suggested by Thon (*loc. cit.*) to account for the diverse results of different observers. Further support for this hypothesis of surface action has been given by Chapman and Grigg\* as well as by Trifonoff† on the relative rates of reaction at low pressures in tubes of different diameters.

Certain results obtained by means of a new technique which we have described as the "photometric method" (in Part I‡) led us, however, to the conclusion that this discrepancy between the work of various authors is due rather to the neglect of an important factor in the reaction kinetics, and that the surface effect is really only marked at low pressures. It had previously escaped notice that hydrogen chloride itself is a strong inhibitor of the reaction, and as a result of our preliminary experiments (I, *loc. cit.*) we came to the conclusion that the problem merited a reinvestigation in the light of this new knowledge. It is believed that the results presented (in Part II§) for oxygen-free mixtures show that this expectation was not unjustified while for the results to be given now for mixtures containing oxygen, we would make the same claim. The results of Chapman and his co-workers, and especially of M. C. C. Chapman (*loc. cit.*) have received full confirmation by our work, and in the light of the new knowledge respecting the kinetic effect of hydrogen chloride, it has been found possible to propound a mechanism of reaction which explains in a remarkable manner the very varied observations of this latter worker, while at the same time rendering possible the calculation of quantum efficiencies over a wide range to a considerable degree of accuracy.

The experimental results now to be reported show that the effect of variation of oxygen on the quantum efficiency ( $\gamma$ ) can be expressed by means of a formula of the type

$$\gamma_{\text{HCl}} = \frac{k}{[\text{O}_2] + k'}$$

when *all* other factors, including the intensity of absorbed light ( $I_{\text{abs.}}$ ), are constant. It is certain, however, that the progressive addition of small amounts of oxygen to hydrogen-chlorine mixtures initially containing no

\* 'J. Chem. Soc.,' p. 3233 (1928).

† 'Z. phys. Chem.,' B, vol. 3, p. 195 (1929).

‡ 'Proc. Roy. Soc.,' A, vol. 140, p. 99 (1933), referred to later as I.

§ 'Proc. Roy. Soc.,' A, vol. 140, p. 112 (1933), referred to later as II.



oxygen involves the consideration of a gradual but complete change in reaction mechanism, one notable feature of which is the progressive change from  $I_{abs.}^{0.6}$  to  $I_{abs.}^{1.0}$  as a factor determining the rate of reaction. For this reason it has been found convenient to consider the experimental results in two main sections, one in which the rate of reaction is for all practical purposes inversely proportional to the oxygen concentration, and a second, a transition region, where such inverse proportionality does not exist. The experimental verification of such a distinction is now given. The apparatus and experimental procedure were as already described in I.

#### EXPERIMENTAL.

*Variation of Pressure of Oxygen.*—The experimental conditions, except for variation of the oxygen pressure, were kept constant, and the "method of averaging" (used in I) was employed. The following conditions were applied

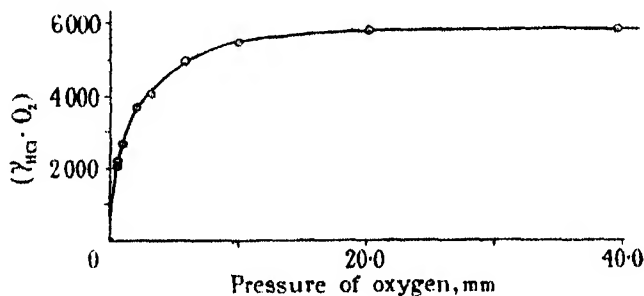


Fig. 1.

in all experiments; pressures of hydrogen and chlorine, 43–44 mm.; pressure of hydrogen chloride, 12–13 mm.; incident light intensity using violet light ( $\lambda = 406 \text{ m}\mu$ ), 15 cm., expressed as scale divisions of the galvanometer. Low pressures of oxygen were measured accurately by the calibrated Bourdon gauge-telescope system. Under these conditions, fig. 1 was obtained, in which the product of the quantum efficiency and the pressure of oxygen ( $\gamma[O_2]$ ) is plotted against the pressure of oxygen. If the quantum efficiency were everywhere inversely proportional to  $[O_2]$  then the graph would be a straight line, parallel to the abscissa; the actual curve obtained shows that such is only strictly true above about 10 mm. of oxygen, though as will appear later, the limit of pressure of oxygen above which the law of inverse proportionality holds is progressively lowered as the pressure of hydrogen is increased (*cf.* M. C. C. Chapman, *loc. cit.*). Before entering into any detail in this connection,

however, we shall give the experimental results according to the classification already mentioned.

*Experiments with Oxygen-Rich Mixtures.*

For these experiments, in view of the relative slowness of the reaction, it was convenient to apply the "graphical method," in which the actual concentration of chlorine was determined continuously throughout the exposure (see I). The light employed was of wave-length 365 m $\mu$ , the experimental details and procedure being as described in I.

(a) *Relation between Quantum Efficiency ( $\gamma$ ) and Light Absorbed ( $I_{\text{abs.}}$ ).—*Quantum efficiencies were here recorded for constant concentrations of hydrogen, chlorine, hydrogen chloride and oxygen, the range of light intensity being controlled by glass plates placed in the path of the beam. It was found that in accordance with the results of other workers for mixtures containing oxygen the rate of reaction was directly proportional to the light absorbed. Thus for  $[\text{Cl}_2] = 42.0$  mm.,  $[\text{H}_2] = 42.0$  mm.,  $[\text{HCl}] = 16.0$  mm., and  $[\text{O}_2] = 50.0$  mm., the values obtained for the quantum efficiency of hydrogen chloride formation were 117, 117 and 120 for values of  $I_{\text{abs.}}$  equal respectively to 14.6, 9.8 and 1.4 cm. The quantum efficiency was thus independent of the amount of absorbed light under the above conditions.

(b) *Relation between Quantum Efficiency ( $\gamma$ ) and Pressure of Hydrogen Chloride (HCl).—*Results are given in Table I. While the pressures of hydrogen and chlorine are constant throughout, in three experiments the concentration of oxygen was varied.

Table I.

$\lambda = 365 \text{ m}\mu$ ;  $[\text{Cl}_2] = 43.0$  mm.;  $[\text{H}_2] = 43.0$  mm.

$[\text{O}_2]$ .	$[\text{HCl}]$ .	$\gamma_{\text{expt.}}$	$\gamma_{\text{calc.}}$	$\gamma_{\text{calc.}}/\gamma_{\text{expt.}}$
mm.	mm.			
100.8	8.0	74.0	70.5	0.95
50.0	16.0	124.0	123.0	0.99
49.8	35.0	91.0	93.2	1.02
49.8	63.2	69.2	69.2	1.00
50.1	125.0	43.0	44.0	1.02
50.0	215	28.9	28.6	0.99
24.5	335	41.5	40.0	0.96
10.6	385	79.6	81.6	1.02

The values of  $\gamma_{\text{calc.}}$  are computed from the formula

$$\gamma_{\text{calc.}} = \frac{3.73 \times 10^5}{[\text{O}_2] (44.8 + [\text{HCl}])}$$

to which the general formula deduced later, p. 719, reduces under the present conditions, and the constancy of the ratio in the last column shows that the results are accurately represented by this simple expression. Thus it follows that hydrogen chloride has an inhibiting effect second only to that of oxygen; this is taken into account in the present experiments for the first time, and it will be seen in the sequel that when this is done, the quantum efficiency of the reaction may be calculated to a very considerable degree of accuracy.

(c) *Relation between Quantum Efficiency of Hydrogen Chloride Formation ( $\gamma$ ) and Pressure of Chlorine ( $[\text{Cl}_2]$ ).*—Results are given in Table II; the pressures of both oxygen and chlorine were varied, and for the range of pressures given ( $[\text{O}_2]$  from 10 mm. to 160 mm. and  $[\text{Cl}_2]$  from 10 mm. to 80 mm.) the quantum efficiency varies nearly linearly with pressure of chlorine and inversely as the pressure of oxygen.

The values for  $\gamma_{\text{calc.}}$  were calculated from the formula

$$\gamma_{\text{calc.}} = \frac{3.77 \times 10^4 [\text{Cl}_2]}{[\text{O}_2] (0.2 [\text{Cl}_2] + 256)},$$

which is obtained from the general expression deduced later by introducing the constant values of  $[\text{H}_2]$  and  $[\text{HCl}]$ .

Table II.

$\lambda = 365 \text{ m}\mu$ ;  $[\text{H}_2] = 47.0 \text{ mm.}$ ;  $[\text{HCl}] = 16.0 \text{ mm.}$

$[\text{Cl}_2]$ .	$[\text{O}_2]$ .	$\gamma_{\text{expt.}}$	$\gamma_{\text{calc.}}$	$\gamma_{\text{calc.}}/\gamma_{\text{expt.}}$
mm.	mm.			
9.9	10.0	143	144.5	1.01
16.5	40.7	54.3	58.5	1.07
22.0	30.7	93.5	103	1.10
23.1	49.9	65.5	66.8	1.02
28.2	39.8	94.0	102	1.08
32.7	51.5	91.2	91.2	1.00
42.0	50.1	117.0	120	1.02
49.0	100.1	66.0	69	1.04
56.8	146.3	53.3	54.0	1.02
66.7	163.9	59.2	57.0	0.97
72.0	51.2	190	194	1.02
73.0	160.4	63.5	63.7	1.00
77.5	143.5	72.5	74.8	1.03

There thus is no indication of inhibition by chlorine comparable with that produced by hydrogen chloride, and such as was observed for oxygen-free mixtures in II; the small term involving chlorine in the denominator of the expression for  $\gamma_{\text{calc.}}$  is obviously negligible except for high pressures of

chlorine, the departure from a strictly linear relationship between  $\gamma$  and  $[\text{Cl}_2]$  being no more than 7 per cent. over the range investigated.

(d) *Relation between Quantum Efficiency and Pressure of Hydrogen.*—Two series of experiments were carried out, one in which the pressure of hydrogen chloride was 15 mm., and the other in which it was 65 mm. The pressure of chlorine was in all experiments 43 mm. and of oxygen 50 mm. As the pressure of hydrogen was increased from a low value, the quantum efficiency first increased, and then passed through a maximum; at higher pressures a retarding effect was clearly indicated. This is seen in fig. 2, where curves 1 and 2 represent the results obtained in the above two series.

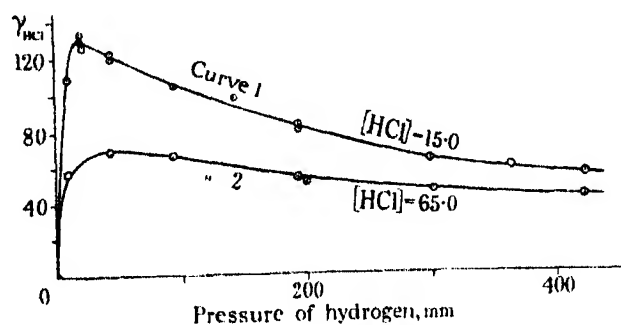


Fig. 2.

It is important to note that the hydrogen was prepared and purified in a manner exactly similar to that used in the oxygen-free mixtures of II, where quantum yields as high as  $10^5$  were observed, and therefore that the retarding influence exhibited here in oxygen-rich mixtures is a kinetic phenomenon dependent on the hydrogen itself, which must be accounted for in any scheme of reaction mechanism.

The results are accurately expressed by the two formulæ:—

$$\gamma_{\text{calc.}} = \frac{3.23 \times 10^4 [\text{H}_2]}{640 + ([\text{H}_2] + 200) [\text{H}_2]} \quad \text{for series (1)}$$

and

$$\gamma_{\text{calc.}} = \frac{3.23 \times 10^4 [\text{H}_2]}{1450 + ([\text{H}_2] + 400) [\text{H}_2]} \quad \text{for series (2).}$$

These both follow from the general expression on p. 718 referred to above, by putting in the appropriate values for  $[\text{HCl}]$ ,  $[\text{Cl}_2]$  and  $[\text{O}_2]$ .

In Table III values of  $\gamma_{\text{expt.}}$  have been read from the experimental curves and compared with the values of  $\gamma_{\text{calc.}}$  obtained from the above formulæ.

Table III.

 $\lambda = 365 \text{ m}\mu$ ;  $[\text{Cl}_2] = 43 \text{ mm.}$ ;  $[\text{O}_2] = 50 \text{ mm.}$ 

$[\text{H}_2]$ .	Series (i) $[\text{HCl}] = 15.0 \text{ mm.}$			Series (ii) $[\text{HCl}] = 65 \text{ mm.}$		
	$\gamma_{\text{expt.}}$	$\gamma_{\text{calc.}}$	$\gamma_{\text{calc.}}/\gamma_{\text{expt.}}$	$\gamma_{\text{expt.}}$	$\gamma_{\text{calc.}}$	$\gamma_{\text{calc.}}/\gamma_{\text{expt.}}$
mm						
10	115	118	1.03	57	58	1.02
20	131	129	0.99	64.5	66	1.04
40	122	126	1.03	69	68	0.99
70	114	116	1.02	67	66	0.99
100	104	105.5	1.02	64.5	63	0.99
200	79	80	1.01	53	53	1.00
300	63	64.5	1.02	45.5	45.5	1.00
400	55	53.5	0.97	41.5	40.3	0.97

*General Formula Tested by Continuous Runs.*—From the data of Tables I, II and III it will be seen that the experimental results are accurately expressed by the numerical formulæ employed. These formulæ are based on the following general expression for oxygen-rich mixtures:

$$\gamma_{\text{calc.}} = \frac{3.77 \times 10^4 [\text{H}_2] [\text{Cl}_2]}{9.25 [\text{O}_2] ([\text{Cl}_2] + 1.7 [\text{HCl}]) + [\text{O}_2] [\text{H}_2] ([\text{H}_2] + 4 [\text{HCl}] + 140)}, \quad (11)$$

the derivation of which is given below. This formula is thus valid over the whole range of pressures employed in Tables I to III. The results so far presented, however, deal with single determinations of the quantum efficiency for fixed values of the pressures of the various constituent gases. It was therefore of interest further to test the above formula by applying it to the data of any one experiment, in which no hydrogen chloride was initially present and of which the velocity of reaction was followed throughout by means of the graphical method illustrated in I. In such an extended run, the conditions of concentration of all reactants vary to an extent sufficient to test thoroughly the applicability of the formula. Tables IV to VIII give the results obtained with various initial pressures of the constituents. The values of  $\gamma_{\text{calc.}}$  were obtained by putting the measured values of  $[\text{Cl}_2]$ ,  $[\text{HCl}]$ ,  $[\text{H}_2]$ , and  $[\text{O}_2]$  in equation (11). Full details of a sample experiment are given in I.

It will be seen that good agreement is obtained throughout all the five runs over wide ranges of variation of pressure. For most practical purposes, however, a simplified form of equation (11), is nearly as accurate, since the first term in the denominator is generally small compared with the second.

Table IV.

(1) Initial  $[\text{Cl}_2] = 50.6$  mm. Initial  $[\text{H}_2] = 49.5$  mm.  $[\text{O}_2] = 50.0$  mm.

$t$ (secs.):	200.	400.	600.	800.	1000.	1200.	1400.
$[\text{Cl}_2]$ .....	42.6	38.4	35.0	32.2	30.0	28.3	26.7
$[\text{H}_2]$ .....	41.5	37.3	33.9	31.1	28.9	27.2	25.6
$[\text{HCl}]$ .....	16.0	24.4	31.1	36.7	41.2	44.6	47.8
$\gamma_{\text{expt.}}$ .....	124.5	95	83	72.6	61.4	53	52.1
$\gamma_{\text{calc.}}$ .....	122	97	81.5	74	61.6	55.4	51.6
$\gamma_{\text{calc.}}/\gamma_{\text{expt.}}$ .....	0.98	1.02	0.98	0.97	1.00	1.04	0.99

Table V.

(2) Initial  $[\text{Cl}_2] = 74.5$  mm. Initial  $[\text{H}_2] = 74.8$  mm.  $[\text{O}_2] = 100.6$  mm.

$t$ (secs.):	200.	400.	600.	1000.	1200.	1400.
$[\text{Cl}_2]$ .....	70.2	64.7	60.4	53.9	51.6	49.6
$[\text{H}_2]$ .....	68.1	62.6	59.3	51.8	49.5	47.5
$[\text{HCl}]$ .....	13.4	24.4	33.0	46.0	50.6	54.6
$\gamma_{\text{expt.}}$ .....	95.6	81	68	49.5	41.3	39
$\gamma_{\text{calc.}}$ .....	94.6	76.0	65.0	50.2	45.6	42.8
$\gamma_{\text{calc.}}/\gamma_{\text{expt.}}$ .....	1.00	0.94	0.96	1.02	1.10	1.09

Table VI.

Initial  $[\text{Cl}_2] = 80.2$  mm.; initial  $[\text{H}_2] = 249.4$  mm.;  $[\text{O}_2] = 60.1$  mm.

$t$ (secs.):	200.	400.	600.	800.	1200.	1400.	1600.
$[\text{Cl}_2]$ .....	73.2	66.8	63.4	59.7	53.7	51.1	48.8
$[\text{H}_2]$ .....	242.4	237.0	232.6	229	223	220.3	218.0
$[\text{HCl}]$ .....	14.0	24.8	33.6	41.0	53.0	58.2	62.8
$\gamma_{\text{expt.}}$ .....	93	81	70	63.2	51.5	49.5	45.8
$\gamma_{\text{calc.}}$ .....	103	88.5	77.0	69.0	57.7	53.5	49.5
$\gamma_{\text{calc.}}/\gamma_{\text{expt.}}$ .....	1.11	1.09	1.10	1.09	1.12	1.08	1.08

Table VII.

Initial  $[\text{Cl}_2] = 79.5$  mm.; initial  $[\text{H}_2] = 151.8$  mm.;  $[\text{O}_2] = 60.1$  mm.

$t$ (secs.):	200.	400.	600.	800.	1000.	1200.	1400.
$[\text{Cl}_2]$ .....	70.8	65.2	60.7	56.9	53.8	50.7	47.9
$[\text{H}_2]$ .....	143.1	137.5	133	129.2	126.1	123.2	120.2
$[\text{HCl}]$ .....	17.4	28.6	37.6	45.2	51.4	57.6	63.2
$\gamma_{\text{expt.}}$ .....	111	89.2	77.0	68.2	62.2	61.0	55.0
$\gamma_{\text{calc.}}$ .....	122	100	88	77.5	69.2	62.8	57.2
$\gamma_{\text{calc.}}/\gamma_{\text{expt.}}$ .....	1.10	1.12	1.14	1.13	1.11	1.03	1.04

Table VIII.

Initial  $[\text{Cl}_2] = 80.0$  mm. ; initial  $[\text{H}_2] = 91.9$  mm. ;  $[\text{O}_2] = 73.4$  mm.

$t$ (secs.) :	400.	600.	900.	1200.	1500.	1800.	2100.	2400.
$[\text{Cl}_2]$ .....	67.0	52.0	57.8	51.0	48.3	46.0	41.8	39.0
$[\text{H}_2]$ .....	78.9	73.9	69.7	62.9	60.2	57.9	53.7	50.9
$[\text{HCl}]$ .....	26.0	36.0	44.4	58.0	63.4	68.0	76.4	82.0
$\gamma_{\text{expt.}}$ .....	90	78.3	71.5	55.0	50.0	46.7	39.0	35.5
$\gamma_{\text{calc.}}$ .....	102	84.4	73.0	57.0	51.4	47.4	40.1	36.2
$\gamma_{\text{calc.}}/\gamma_{\text{expt.}}$ .....	1.13	1.08	1.02	1.04	1.03	1.01	1.03	1.02

The results of Tables IV to VIII are thus almost equally well represented by the approximate expression

$$\gamma_{\text{calc.}} = \frac{3.77 \times 10^4 [\text{Cl}_2]}{[\text{O}_2] ([\text{H}_2] + 4 [\text{HCl}] + 140)}, \quad (11A)$$

which yields values within 7 per cent. of those obtained by equation (11). The approximate expression does not, however, yield maxima in the  $[\text{H}_2]$ - $\gamma$  curves of fig. 2 and for this reason is inaccurate when the partial pressure of hydrogen is less than 40 mm., for in these circumstances the first term of the denominator is no longer negligible in comparison with the second.

*Dependence of Quantum Efficiency on Wave-length.*—The figures in Table IX show the relative quantum yields obtained respectively with light of 365 m $\mu$  and 406 m $\mu$  under equivalent conditions. From these figures it is apparent that the efficiency of the light of shorter wave-length under the given conditions is some 6 per cent. greater than for the light of longer wave-lengths. It is intended to carry out a more extended study of this aspect of the problem.

Table IX.

For  $\lambda = 406$  m $\mu$   $I_{\text{abs.}} \sim 1.60$  cm.For  $\lambda = 365$  m $\mu$   $I_{\text{abs.}} \sim 12$  cm. $[\text{Cl}_2] = 43$  mm.  $[\text{O}_2] = 50$  mm.

$[\text{H}_2]$ .	$[\text{HCl}]$ .	$\gamma_{365}$ .	$\gamma_{406}$ .	Ratio: $\gamma_{365}/\gamma_{406}$ .
mm.	mm.			
43	15	123	115	1.07
43	65	67.5	65	1.04
43	214	28.2	26.2	1.08
294	15	63.0	59.0	1.07
294	65	46.5	45.0	1.03

when a monochromator now under construction is available. In the meantime the difference between the efficiencies at the two wave-lengths is small enough to justify the use of the same numerical formula for both wave-lengths.

*Experiments with Mixtures containing small Pressures of Oxygen.*

The results of the previous section have been concerned with a region in which sufficient oxygen was present to render the rate of formation of hydrogen chloride inversely proportional to the concentration of oxygen, and directly proportional to the first power of the amount of light absorbed. On the other hand, the data given in II confirmed that in gas-mixtures rendered as free from oxygen as possible, the rate of reaction is proportional to a power of the absorbed light which is not far removed from 0.5. The question of the intervening region was therefore examined.

Because of the high velocities the experiments were carried out with light of wave-length 406 m $\mu$ . which is more feebly absorbed by the chlorine than the light of wave-length 365 m $\mu$ . used in the determinations recorded above for oxygen-rich mixtures. We have already seen (Table IX) that the quantum efficiencies with these two wave-lengths are nearly identical, other factors being equal, so that the data of the "oxygen-rich" region and "transition" region are directly comparable. The experimental results are given below in Tables X, XI and XII, where  $I_0$  expresses the total incident light flux after correction for reflection losses, etc., and  $I_{abs.}$  is the total light absorption calculated therefrom using the known extinction coefficient as described in I and II.

Table X.—Relation between Quantum Efficiency and Amount of Light Absorbed. (Transition Region.)

$\lambda = 406 \text{ m}\mu$ .  $[\text{Cl}_2] = 43 \text{ mm}$ .  $[\text{H}_2] = 43 \text{ mm}$ .  $[\text{HCl}] = 14 \text{ mm}$ .

$[\text{O}_2]$ .	$I_0$ .	$I_{abs.}$	$\gamma_{\text{expt.}}$	$\gamma (I_{abs.})^{0.12}$ .
mm.	cm.	cm.		
0.95	15.1	1.28	2880	2980
0.93	15.7	1.23	2800	2900
0.94	8.25	0.70	3100	2980
0.95	6.85	0.58	3080	2880

The variation of intensity was effected by blue glass plates placed in the path of the incident beam, and although the variation is not large, the value of  $I_{abs.}$  being limited by experimental convenience, and the fact that the concentration of chlorine must be kept constant, the results in Table X justify



the conclusion that the reaction is proportional neither to  $(I_{\text{abs.}})^{1.0}$  nor to  $(I_{\text{abs.}})^{0.6}$  as previously determined for oxygen-rich and oxygen-free mixtures respectively. The actual value calculated from the above figures is  $(I_{\text{abs.}})^{0.88}$ , that is, the product  $(I_{\text{abs.}})^{0.12}$  is constant (final column).

Table XI.—Relations between Quantum Efficiency and Pressure of Oxygen.  
(Transition region.)

$\lambda = 406 \text{ m}\mu$ .  $[\text{Cl}_2] = 43 \text{ mm}$ .  $[\text{H}_2] = 43 \text{ mm}$ .  $[\text{HCl}] = 14 \text{ mm}$ .

$[\text{O}_2]$ .	$I_0$ .	$I_{\text{abs.}}$	$\gamma_{\text{expt.}}$	$\gamma_{\text{calc.}}$
mm.	cm.	cm.		
0.0	20.2	1.71	6830*	6680*
0.53	15.3	1.30	3860	4480
0.55	17.7	1.50	3750	4270
0.93	15.7	1.33	2800	3550
2.0	15.3	1.30	1850	2355
3.2	15.2	1.29	1260	1700
5.8	17.7	1.50	863†	1010†
10.1	19.1	1.62	580	618
20.0	15.6	1.32	280	315
39.7	15.5	1.31	150	161
50	27.7	12.3	125‡	127.5
350	23.7	10.6	17.1‡	18.2

\*  $[\text{H}_2] = 44$ ,  $[\text{Cl}_2] = 44$ ,  $[\text{HCl}] = 12.5$ .

†  $[\text{H}_2] = 41.5$ ,  $[\text{Cl}_2] = 42.5$ ,  $[\text{HCl}] = 14.0$ .

‡  $\lambda = 385 \text{ m}\mu$ .

Table XII.—Relation between Quantum Efficiency  $\gamma$  and Pressure of chlorine. (Transition region.)

$[\text{H}_2] = 43 \text{ mm}$ .  $[\text{HCl}] = 14.0 \text{ mm}$ .  $\lambda = 406 \text{ m}\mu$ .

$[\text{O}_2]$ .	$[\text{Cl}_2]$ .	$I_0$ .	$I_{\text{abs.}}$	$\gamma_{\text{expt.}}$	$\gamma_{\text{calc.}}$
mm.	mm.	cm.	cm.		
0.94	20.0	6.85	0.285	1860	2350
0.95	43.0	15.1	1.28	2880	3500
0.93	43.0	15.7	1.33	2800	3550
0.94	60.5	7.05	0.83	3680	4800
0.98	75.5	7.90	1.15	3940	5000

For the transition region, the quantum efficiency takes probable values between those to be expected for the "oxygen-free" and "oxygen-rich" regions, as may be seen by comparing the first line with the last lines of Table XI. In the final columns of Tables XI and XII are shown the calculated values of  $\gamma$  obtained from a formula derived below on p. 736 from general theoretical considerations, which reduces under the appropriate conditions

to those already used in the representation of the data of the "oxygen-free" and "oxygen-rich" regions.

#### THEORETICAL DISCUSSION.

The results which we have given above, for oxygen-rich mixtures ( $[O_2] > 10$  mm.), and which are fully represented by the approximate formula

$$\gamma = \frac{3.77 \times 10^4 [H_2] [Cl_2]}{9.25 [O_2] ([Cl_2] + 1.7 [HCl]) + [O_2] [H_2] ([H_2] + 4 [HCl] + 140)} \quad (11)$$

differ from those obtained by Bodenstein and his co-workers, and there emerge two points of major importance for the establishment of an accurate kinetic mechanism. They are:—

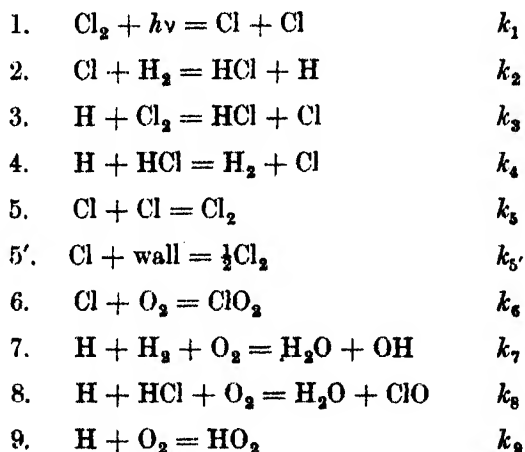
- (1) The confirmation of the inhibitory effect of hydrogen, first observed by Chapman and Underhill (*loc. cit.*), and later confirmed by M. C. C. Chapman (*loc. cit.*), but denied by other workers (*loc. cit.*).
- (2) The discovery of the inhibitory effect of hydrogen chloride, which with oxygen and hydrogen is now revealed as one of the factors controlling the length of chains.

The photometric method by which these results have been established, involving as it does no disturbance of the reacting system by addition of water or by "freezing out" is the most reproducible method of following the reaction yet devised, and this, coupled with the fact that by taking the inhibitive effects of hydrogen and hydrogen chloride into account we have obtained an expression for the quantum efficiency which describes our results over a wide range, leads us to enter into the following discussion with confidence in the experimental results upon which it is based.

In developing a mechanism of reaction, it is important to pay attention to the results obtained in II for mixtures containing no oxygen. Here it was proved that a modification of the Nernst Scheme (reactions 1-5 below) was capable of explaining the observed experimental facts.\*

\* In this mechanism the supposed catalytic action of water has been purposely neglected, since it is now known not to exist. Professor Bodenstein in a private communication informs us that he has recently been able to show that completely dried mixtures of hydrogen and chlorine react as readily as wet and that the supposed inhibition produced by drying according to the experiments of Coehn and Jung ('Z. phys. Chem.,' vol. 110, p. 705 (1924)) was really due to the introduction of impurities ( $HgCl_2$  and  $AuCl_3$ ). This is supported by later results of Rodebush and Klingenhofe ('Proc. Nat. Acad. Sci.,' vol. 18, p. 531 (1932)) and of Allmand and Craggs ('Nature,' vol. 130, p. 927 (1932)) and is in accord with our own results carried out in the presence of  $P_2O_5$ , as will be described in Part IV.

Now so far as the propagation of reaction chains is concerned, the same mechanism, to be consistent, must also apply to the results for mixtures containing oxygen. The difference between the two processes lies in a complete change of the reactions by which chains are terminated, as is clearly evidenced by the alteration in the power of the intensity of absorbed light governing the rate of reaction from *ca.* 0.5 to 1.0. This complete change has been brought about by the addition of oxygen, which must now therefore be held responsible for the rupture of the reaction chains. This has long been accepted as proven by the experimental establishment of the relationship of inverse proportionality between reaction velocity and pressure of oxygen. But in addition the reaction velocity and quantum efficiency have been shown above to be diminished as the pressure of hydrogen and hydrogen chloride is increased, and to take account of all these facts we shall extend the scheme proposed in II, to include the possible reactions by which the reaction chains may be ended through the medium of oxygen. The complete series of reactions is as follows:—



*Oxygen-Rich Mixtures.*—For oxygen-rich mixtures reactions (5) and (5') become insignificant in comparison with reactions (6) to (9). The concentration of reaction chains is therefore much lower in the presence of oxygen, and the quantum efficiency correspondingly smaller. This holds good as the pressure of oxygen is reduced until we reach the "transition region" where the relationship of inverse proportionality between the pressure of oxygen and the reaction velocity breaks down. In this region because of the lower pressure of oxygen the concentration of chains, and therefore of chlorine atoms is greater, and reactions (5) and (5') are no longer negligible in comparison with the

others. We shall see the importance which these reactions may assume when we discuss the kinetics of the transition region below. For the present, neglecting reactions (5) and (5') we may develop an expression for the quantum efficiency in oxygen-rich mixtures as follows.

Equating for the equilibrium of chlorine atoms we have

$$k_1 I_{\text{abs.}} + k_3 [\text{H}] [\text{Cl}_2] + k_4 [\text{H}] [\text{HCl}] = k_2 [\text{Cl}] [\text{H}_2] + k_6 [\text{Cl}] [\text{O}_2]. \quad (1)$$

For the equilibrium of hydrogen atoms, we have similarly

$$k_2 [\text{Cl}] [\text{H}_2] = k_3 [\text{H}] [\text{Cl}_2] + k_4 [\text{H}] [\text{HCl}] + k_7 [\text{H}] [\text{O}_2] [\text{H}_2] + k_8 [\text{H}] [\text{O}_2] [\text{HCl}] + k_9 [\text{H}] [\text{O}_2]. \quad (2)$$

From (1) and (2), we obtain

$$[\text{H}] = \frac{k_1 k_3 I_{\text{abs.}} [\text{H}_2]}{k_6 [\text{O}_2] (k_3 [\text{Cl}_2] + k_4 [\text{HCl}]) + [\text{O}_2] (k_2 [\text{H}_2] + k_6 [\text{O}_2]) (k_7 [\text{H}_2] + k_8 [\text{HCl}] + k_9)}. \quad (3)$$

The rate of formation of hydrogen chloride is given by

$$\frac{d[\text{HCl}]}{dt} = k_2 [\text{Cl}] [\text{H}_2] + k_3 [\text{H}] [\text{Cl}_2] - k_4 [\text{H}] [\text{HCl}]. \quad (4)$$

Substituting the value of  $[\text{Cl}]$  obtained from equation (1) we obtain

$$\frac{d[\text{HCl}]}{dt} = k_1 I_{\text{abs.}} \cdot \frac{k_3 [\text{H}_2]}{k_2 [\text{H}_2] + k_6 [\text{O}_2]} + [\text{H}] \left( \frac{2k_3 [\text{H}_2] + k_6 [\text{O}_2]}{k_2 [\text{H}_2] + k_6 [\text{O}_2]} \cdot k_3 [\text{Cl}_2] - \frac{k_4 k_6 [\text{HCl}]}{k_2 [\text{H}_2] + k_6 [\text{O}_2]} \right). \quad (5)$$

Substituting for  $[\text{H}]$  from equation (3) we obtain

$$\frac{d[\text{HCl}]}{dt} = \frac{k_1 k_3 I_{\text{abs.}} [\text{H}_2]}{k_2 [\text{H}_2] + k_6 [\text{O}_2]} + \frac{k_1 k_3 I_{\text{abs.}} [\text{H}_2] \left( k_3 [\text{Cl}_2] \cdot \frac{2k_2 [\text{H}_2] + k_6 [\text{O}_2]}{k_2 [\text{H}_2] + k_6 [\text{O}_2]} - k_4 [\text{HCl}] \cdot \frac{k_6 [\text{O}_2]}{k_2 [\text{H}_2] + k_6 [\text{O}_2]} \right)}{k_6 [\text{O}_2] (k_3 [\text{Cl}_2] + k_4 [\text{HCl}]) + [\text{O}_2] (k_2 [\text{H}_2] + k_6 [\text{O}_2]) (k_7 [\text{H}_2] + k_8 [\text{HCl}] + k_9)}. \quad (6)$$

By the application of but one simple condition, which will be subject to subsequent confirmation, this complicated expression reduces to a simple form which is capable of expressing all our results for oxygen-rich mixtures, and of being extended to include the "transition region" of low oxygen pressures. This condition is that

$$k_2 [\text{H}_2] \gg k_6 [\text{O}_2],$$

and has as a consequence the fact that practically all chains end through the medium of the reaction of hydrogen atoms with oxygen, rather than by the reaction of chlorine atoms with oxygen. In agreement with this it will be found below that  $k_2:k_6 \sim 10^3$ ; we thus have for comparable pressures of hydrogen and oxygen:

$$k_2 [\text{H}_2] + k_6 [\text{O}_2] \sim k_2 [\text{H}],$$

$$\frac{2k_2 [\text{H}_2] + k_6 [\text{O}_2]}{k_2 [\text{H}_2] + k_6 [\text{O}_2]} \sim 2,$$

and

$$\frac{k_6 [\text{O}_2]}{k_2 [\text{H}_2] + k_6 [\text{O}_2]} \sim 0.$$

Further, when the absorbed light flux is measured in quanta per second, and the concentrations of reactants in molecules per cubic centimetre,

$$\gamma = \frac{1}{I_{\text{abs.}}} \cdot \frac{d[\text{HCl}]}{dt} \quad (7)$$

gives the quantum yield for the synthesis of hydrogen chloride. It therefore follows, after simplifying equation (6) in accordance with the above principle, and combining with equation (7) that

$$\gamma = k_1 + \frac{2k_1 k_2 k_3 [\text{H}_2] [\text{Cl}_2]}{k_6 [\text{O}_2] (k_3 [\text{Cl}_2] + k_4 [\text{HCl}]) + k_2 [\text{H}_2] [\text{O}_2] (k_7 [\text{H}_2] + k_8 [\text{HCl}] + k_9)} \quad (8)$$

Now  $k_1 = 2$ , representing two atoms of chlorine per light quantum absorbed, and  $\gamma$  is of the order 40 to 150 for oxygen-rich mixtures. We shall therefore neglect  $k_1$  in comparison with  $\gamma$  and write

$$\gamma = \frac{\frac{2k_1 k_3}{k_7} [\text{H}_2] [\text{Cl}_2]}{\frac{k_6 k_3}{k_2 k_7} [\text{O}_2] ([\text{Cl}_2] + \frac{k_4}{k_3} [\text{HCl}]) + [\text{O}_2] [\text{H}_2] \left( [\text{H}_2] + \frac{k_8}{k_7} [\text{HCl}] + \frac{k_9}{k_7} \right)} \quad (9)$$

*Consideration of Equation (9) with reference to the experimental results for Oxygen-Rich Mixtures.*—(a) In the first place, it may be questioned whether the inhibiting effect of hydrogen chloride cannot be explained solely by reaction (4) and without recourse to reaction (8). We can test this by putting  $k_8 = 0$ .

The expression would then become

$$\gamma = \frac{\frac{2k_1 k_3}{k_7} [\text{H}_2] [\text{Cl}_2]}{[\text{O}_2] \left\{ \frac{k_6 k_3}{k_2 k_7} \left( [\text{Cl}_2] + \frac{k_4}{k_3} [\text{HCl}] \right) + [\text{H}_2]^2 + \frac{k_9}{k_7} [\text{H}_2] \right\}} \quad (10)$$

Now from the results of II,  $k_4/k_3 = 1.7$  and the above expression then involves nearly as big an inhibiting effect by chlorine as by hydrogen chloride, as is indeed observed in oxygen-free mixtures; but with oxygen-rich mixtures, this is not so, for the inhibition by chlorine is hardly detectable, while that by hydrogen chloride remains very strong, as is seen by referring back to Tables I and II. There is other evidence which points in the same direction: the first of the two terms in the denominator of equation (9) accounts for the maxima in the curves showing the variation of  $\gamma$  with  $[H_2]$ . In order to fit the expression to the experimental curve this term must be *small* compared with the second. If, however, we attempt to explain the inhibition by hydrogen chloride without the use of reaction (8), and by reaction (4) alone, this same term must be *large* in comparison with the second; the expression could therefore not be self-consistent. Nor is the position modified if we go back to the more complicated equation (6). The forms of the experimental curves can only be obtained if we admit that  $k_6 [O_2]$  is small compared to  $k_3 [H_2]$ , and that reaction (8) occurs. Thus, while reaction (4) accounts for the inhibition by hydrogen chloride in oxygen-free systems, it is reaction (8) which is practically the whole source of the inhibition in oxygen-rich systems.

(b) The calculated values for  $\gamma$  in Tables I to VIII are all obtained from the formula

$$\gamma = \frac{3.77 \times 10^4 [H_2] [Cl_2]}{9.25 [O_2] ([Cl_2] + 1.7 [HCl]) + [O_2] [H_2] ([H_2] + 4 [HCl] + 140)}, \quad (11)$$

which conforms to the theoretically derived expression given in equation (9). In all cases the agreement is so close as to leave little doubt of the general validity of this expression. It can, however, be still further simplified without much loss of accuracy over a very considerable range, for except where the concentration of hydrogen is relatively small, or that of the chlorine very high, the first term of the denominator is in general negligible as compared with the second. In these circumstances we obtain

$$\gamma = \frac{3.77 \times 10^4 [Cl_2]}{[O_2] ([H_2] + 4 [HCl] + 140)}. \quad (11A)$$

This may be compared with the approximate result of Bodenstein and Dux (*loc. cit.*)

$$\gamma = k \cdot \frac{[Cl_2]}{[O_2]}.$$

Although these two expressions are not fully consistent it may be noted that in our expression the two inhibiting effects are partially self-compensating

during the course of a continuous run, for as the hydrogen chloride is formed the concentration of hydrogen decreases. As an example the results of Thon for oxygen-rich mixtures, carried out by the Bodenstein technique, have been calculated in Table IX according to the expression

$$\frac{d[\text{HCl}]}{dt} = \frac{k[\text{H}_2][\text{Cl}_2]^2}{9.25[\text{O}_2](\text{Cl}_2 + 1.7[\text{HCl}]) + [\text{O}_2][\text{H}_2](\text{H}_2 + 4[\text{HCl}] + 140)},$$

which is derived from our equation (11) by putting

$$I_{\text{abs.}} \propto [\text{Cl}_2].$$

Table XIII.\*

$[\text{O}_2] = 11.7 \text{ mm.}$

Time.	$[\text{H}_2]$ .	$[\text{Cl}_2]$ .	$[\text{HCl}]$ .	$\frac{d(\text{HCl})}{dt}$ .	$k \times 10^3$ .
mins.	mm.	mm.	mm.	mm./min.	
0	183	528	0	3.46	65
15	157	502	52	3.00	79
35	127	472	112	2.55	116
57	99	444	168	2.08	131
82	73	418	220	1.72	140
110	49	394	268	1.27	134
140	30	375	306	0.86	106
175	15	360	336		

For about 80 per cent. of the total period of the reaction, approximate constancy is obtained for  $k$ ; and it is possible that better agreement especially in the early part of the experiment would be obtained if the actual values of  $I_{\text{abs.}}$  were available, since the approximation

$$I_{\text{abs.}} \propto [\text{Cl}_2]$$

becomes inaccurate at high pressures of chlorine. It must be admitted, however, that this partial cancellation of the two inhibiting effects of hydrogen chloride and hydrogen cannot entirely explain the failure of the workers of the Bodenstein school to recognize their existence. It is certainly a fact that they have recorded very few specific experiments to test the effect of hydrogen chloride

\* Thon, 'Z. phys. Chem.,' vol. 124, p. 341 (1926), Table (3), Versuch (16).

in large excess, under conditions where the effects of the other reactants remained constant. Had they done this and especially if they had used relatively lower partial pressures of hydrogen and chlorine as compared with hydrogen chloride they could not have failed to observe the inhibition.

On the other hand the question of inhibition by hydrogen chloride was never tested by the experiments of Chapman, who almost invariably used a water actinometer by which the pressure of hydrogen chloride was automatically kept exceedingly small. Putting  $[HCl] = 0$ , our expression (11A) reduces very simply to that of Mrs. Chapman, whose results, except when the pressure of hydrogen was very low ( $< 1.0$  mm.), can be expressed by the equation

$$\gamma = \frac{k [Cl_2]}{[O_2] [H_2]^{1-\nu}},$$

where  $\gamma$  is less than unity and lies between 1.0 and 0.5. We shall return to this point when dealing with the kinetics of the transition region, and it will be found that her formula and ours are still further in very close agreement.

*Evaluation of Reaction Probabilities.*—By comparing the experimental equation (11) with the theoretical expression (9) it will be seen that

$$\frac{2k_1k_2}{k_7} = 3.77 \times 10^4 \quad (12)$$

$$\frac{k_8k_3}{k_2k_7} = 9.25 \quad (13)$$

$$\frac{k_4}{k_3} = 1.7 \quad (14)$$

$$\frac{k_6}{k_7} = 4 \quad (15)$$

$$\frac{k_9}{k_7} = 140 \quad (16)$$

(a) From (12) since  $k_1 = 2$ , we obtain  $k_2/k_7 \sim 10^4$ . This gives a ratio of reactive binary collisions in reaction (3) to ternary collisions in reaction (7) of  $10^2$ , the partial pressures of hydrogen, chlorine, and oxygen, being taken as 100 mm. each. Taking Bodenstein's value for the collision efficiency of reaction (3) (see II, p. 122) as  $10^{-2}$  and assuming a unit probability for all ternary reactions, we obtain a ratio of total binary to ternary collisions of  $10^4$ , which is in agreement with the accepted figure in a gas at this pressure.

(b) From this value of  $k_2/k_7$  we can compute from (13) that  $k_8/k_3 \sim 10^{-3}$ . Now it has already been seen from the results of II that  $k_3/k_2$  is about  $10^2$



and this result was there shown to be in dimensional agreement with the independent deductions of Bodenstein and Kistiakowski. It now follows therefore that  $k_6/k_3 \sim 10^{-5}$  and taking the collision efficiency of reaction (3) as  $10^{-2}$  in accordance with the considerations there presented,  $10^{-7}$  gives the maximum probability of occurrence of reaction (6). This result is in accordance with the kinetic necessity referred to above that the probability of reaction (6) should be small as compared with that of reaction (2).

(c) From equation (14) it is seen that the probabilities of reactions (3) and (4) are about equal, in agreement with the results of II; while in (15) the ratio  $k_6/k_7$  compares the probabilities of two triple collisions, and is in reasonable accord with the probable space relationships of the two molecules concerned ( $H_2$  and  $HCl$ ).

(d) For reaction (9) which might conceivably take the forms



and

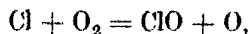


we may calculate from the ratios  $k_3/k_7 \sim 10^4$  and  $k_6/k_7 = 140$  that  $k_6/k_3 \sim 10^2$ . If the collision efficiency of reaction (3) be taken as  $10^{-2}$  (*vide supra*) this gives a corresponding value of  $10^{-4}$  for reaction (9). The maximum activation corresponding to this is 5.3 k. cals. and is insufficient for (9A) which is endothermic to the extent of 13 k. cals.\* Reaction (9B) on the other hand would be exothermic, the heat of reaction being of the order of 69 k. cal. (Frankenburger and Klinkhardt, *loc. cit.*) and we may therefore assume in view of its much greater probability that this is the course taken. Recently Bates and Lavint† have discussed this reaction and come to a similar conclusion. Their work indicates a maximum probability of  $10^{-3}$  which agrees satisfactorily with the value of  $10^{-4}$  calculated above. Considerations are given which indicate a life of  $10^{-8}$  seconds for the quasi (unstabilized)  $HO_2$  molecule, as against the usually accepted value of  $10^{-13}$  or  $10^{-14}$  second. Following Kassel they point out that in consequence of this the necessary stabilization of the quasi  $HO_2$  molecule will probably lose its ternary character and kinetically become a "straight bimolecular process." This is in accord with our own result that reaction (9) is unaffected by total pressure except in so far as ternary collisions with  $H_2$  and  $Cl_2$  give rise to reactions (7) and (8). Such an effect if it existed would have been easily detected in our results by the variation of  $k_p$ .

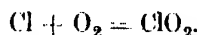
\* Frankenburger and Klinkhardt, 'Trans. Faraday Soc.,' vol. 27, p. 439 (1931).

† 'J. Amer. Chem. Soc.,' vol. 55, p. 81 (1933).

(e) Similar considerations apply to reaction (6). The process

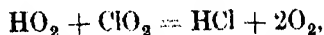


is endothermic to the extent of 70 k. cal., if we accept the value of 46 k. cal. given by Finkelnberg and Schumacher\* for the heat of binding of the ClO molecule. The value of  $10^{-7}$  for the collision efficiency obtained above (para. (b)), however, corresponds to a maximum of 10 k. cal., and even if we adopt the most favourable circumstances by accepting the view of Rollefson and Eyring† that the Cl atom of the chain may be energized to a maximum of about 23 k. cal.‡ there is not enough energy available. It cannot therefore be accepted as expressing the facts, and we shall adopt the alternative exothermic form



The question of the stabilization of the  $\text{ClO}_2$  molecule by a third body is left undecided by the present work, since reaction (6) enters so insignificantly into the kinetics ( $k_6$  very small) that it is impracticable to detect any dependence on total pressure.

With the subsequent history of the stabilized  $\text{ClO}_2$  and  $\text{HO}_2$  molecules we are not here concerned, since once formed they are removed from the sphere of active participation in the kinetics of the main hydrogen chloride reaction. Since they do not accumulate to a measurable extent, and do not disturb the kinetics of the system it may be assumed that they ultimately disappear by reactions of the type :



The above results may be combined with those of II and summarized in the Table XIV, which modifies some of the values already computed by Bodenstein (*loc. cit.*).

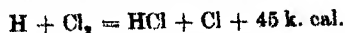
It is probable that in the next few years a check on the accuracy of these figures will be forthcoming as a result of direct quantitative experiments involving atoms. Already Rodebush and Klingenhofers have investigated the reaction



\* 'Z. phys. Chem. Bodenstein Band,' p. 709 (1931).

† 'J. Amer. Chem. Soc.,' vol. 54, p. 170 (1932).

‡ By virtue of the exothermic character of the reaction



§ 'J. Amer. Chem. Soc.,' vol. 55, p. 130 (1933); 'Proc. Nat. Acad. Sci.,' vol. 18, p. 531 (1932).

Table XIV.

Reaction.	Collision efficiency.	Activation.
		k. cal.
$\text{H} + \text{Cl}_2 = \text{HCl} + \text{Cl}$ .....	$10^{-2}$	$\sim 0$
$\text{H} + \text{HCl} = \text{H}_2 + \text{Cl}$ .....	$10^{-2}$	$\sim 0$
$\text{Cl} + \text{H}_2 = \text{HCl} + \text{H}$ .....	$10^{-4}$	$2.5-3.6^*$
$\text{H} + \text{O}_2 = \text{HO}_2$ .....	$10^{-4}$	?
$\text{Cl} + \text{O}_2 = \text{ClO}_2$ .....	$10^{-7}$	?
$\text{H} + \text{H}_2 + \text{O}_2 = \text{H}_2\text{O} + \text{OH}$ } .....	1.0	0
$\text{H} + \text{HCl} + \text{O}_2 = \text{H}_2\text{O} + \text{ClO}$ } .....	1.0	0

\* See II.

at low pressures, with the help of a new technique for preparing chlorine atoms; they report a collision efficiency of  $10^{-5}$  as a result of direct measurement and an activation of 5.5 k. cal. (from temperature coefficient). This compares favourably with our figures in Table XIV, especially when we take into account the considerations of Rollefson and Eyring in section (d) above.

*The Transition Region.*—When the pressure of oxygen falls below a limiting value, the quantum efficiency of the reaction no longer remains inversely proportional to the oxygen content. The departure is at first gradual but later becomes very marked (fig. 1); at the same time there is a departure (Table X) from the strict independence of quantum efficiency and light intensity which marked the kinetics of the oxygen-rich region. We are here witnessing a transition from the kinetics of the oxygen-rich region which are expressed by equation (9)

$$\gamma = \frac{\frac{2k_1k_2}{k_7} [\text{H}_2] [\text{Cl}_2]}{\frac{k_8k_9}{k_2k_7} [\text{O}_2] \left( [\text{Cl}_2] + \frac{k_3}{k_8} [\text{HCl}] \right) + [\text{O}_2] [\text{H}_2] \left( [\text{H}_2] + \frac{k_9}{k_7} [\text{HCl}] + \frac{k_8}{k_7} \right)} \quad (9)$$

to those of the oxygen-free region, which are expressed by a formula of the form deduced by Christiansen, Herzfeld and Polanyi for the hydrogen-bromine reaction

$$\gamma = \frac{2k_1k_2 [\text{H}_2] [\text{Cl}_2]}{\sqrt{k_1k_3} I_{\text{abs.}}^{\frac{1}{2}} \frac{k_2}{k_3} \left( [\text{Cl}_2] + \frac{k_4}{k_3} [\text{HCl}] \right)} \quad (17)$$

The quantum efficiencies measured take probable values between those to be expected on the basis of these two expressions. We can, however, proceed further, and (referring back to the scheme on p. 726) by taking account of reactions (5) and (5') which were negligible in the oxygen-rich region, can

derive a general expression which covers the whole range of the hydrogen chlorine reaction, and which gives results of the right order of magnitude for the transition region. Proceeding as already indicated in the derivation of equation (9) we obtain the expression

$$\gamma = \frac{\frac{2k_1k_2}{k_7} [\text{H}_2] [\text{Cl}_2]}{\frac{k_2}{k_2k_7} (k'_5 + k_5[\text{Cl}] + k_6[\text{O}_2]) \left( [\text{Cl}_2] + \frac{k_4}{k_3} [\text{HCl}] \right) + [\text{H}_2][\text{O}_2] \left( [\text{H}_2] + \frac{k_6}{k_7} [\text{HCl}] + \frac{k_2}{k_7} \right)} \quad (18)$$

This equation contains the term  $[\text{Cl}]$  which indicates the (unknown) concentration of chlorine atoms. It cannot therefore be used directly. In the absence of oxygen we may evaluate the concentration of chlorine atoms from the equation

$$k_1 I_{\text{abs.}} = k'_5 [\text{Cl}] + k_5 [\text{Cl}]^2 \quad (19)$$

and assuming  $k'_5 [\text{Cl}]$  is small compared with  $k_5 [\text{Cl}]^2$  (which will be true except at low pressures) we may write :

$$[\text{Cl}] \sim \sqrt{\frac{k_1}{k_5}} I_{\text{abs.}} \quad (19A)$$

On introducing this into equation (18) and writing  $[\text{O}_2] = 0$  we obtain

$$\gamma = \frac{2k_1k_2 [\text{H}_2] [\text{Cl}_2]}{(\sqrt{k_1k_5} I_{\text{abs.}} + k'_5) \frac{k_2}{k_2} \left( [\text{Cl}_2] + \frac{k_4}{k_3} [\text{HCl}] \right)}, \quad (20)$$

which is practically identical with (17) except for the term  $k'_5$ . This term represents the removal of Cl atoms by the wall, and has by hypothesis been considered small; since it measures the speed of diffusion of chlorine atoms to the surface it will assume values in inverse proportion to the total pressure. The assumption that its effect is small is in accord with the fact that except at low pressures (Trifonoff, *loc. cit.*) the rate of reaction is independent of the surface of the reaction vessel.\* A small finite value for  $k'_5$ , however, undoubtedly accounts for the slight deviation of the kinetics in oxygen-free systems from the  $I_{\text{abs.}}$  law, which was described in II.

On the other hand, in the presence of high concentrations of oxygen  $k'_5$  and  $k_5 [\text{Cl}]$  become negligible compared to  $k_6 [\text{O}_2]$  and the expression reduces to equation (9) already found valid for oxygen-rich mixtures.

\* Coehn and Heymer 'Ber. duets. chem. Ges.' vol. 59, p. 1794 (1926).

It is not, however, possible to evaluate the concentration of chlorine atoms in the presence of oxygen by a simple theoretical expression. Failing this we may construct an approximate working formula by using the semi-empirical expression

$$[\text{Cl}] = \sqrt{\frac{k_1}{k_5}} \cdot \frac{(I_{\text{abs.}})^{\frac{1}{2}}}{(1 + f[\text{O}_2])} \quad (19\text{B})$$

(where  $f[\text{O}_2]$  is positive and becomes zero when  $[\text{O}_2] = 0$ ) which takes account of the fact that  $[\text{Cl}]$  is reduced as  $[\text{O}_2]$  is increased, and at the same time reduces to (19A) when  $[\text{O}_2] = 0$ . By combining (18) and (19B) and giving to the coefficients their previous numerical values, we derive

$$\gamma = \frac{3 \cdot 77 \times 10^4 [\text{H}_2][\text{Cl}_2]}{\left(31 \cdot 4 + \frac{104}{(1 + f[\text{O}_2])} (I_{\text{abs.}})^{\frac{1}{2}} + 9 \cdot 25 [\text{O}_2]\right) ([\text{Cl}_2] + 1 \cdot 7 [\text{HCl}] + [\text{O}_2][\text{H}_2]([[\text{H}_2] + 4[\text{HCl}] + 140])} \quad (21)$$

For  $[\text{O}_2] = 0$  this reduces virtually to the original working formula for oxygen-free mixtures used in II, *i.e.*,

$$\gamma = \frac{2 \cdot 8 \cdot 10^2 [\text{H}_2][\text{Cl}_2]}{(0 \cdot 78 (I_{\text{abs.}})^{\frac{1}{2}} + 0 \cdot 235) ([\text{Cl}_2] + 1 \cdot 7 [\text{HCl}])} \quad (21\text{A})$$

with the modification that the original term  $(I_{\text{abs.}})^{0 \cdot 4}$  is now replaced by the term  $(0 \cdot 78 (I_{\text{abs.}})^{0 \cdot 5} + 0 \cdot 235)$ . The agreement between the observed and calculated data of II when this modified expression is used is without exception at least as good as with the original.

For the transition region the calculated values of  $\gamma$  depend partly on the form adopted for  $f[\text{O}_2]$ . If we write

$$f[\text{O}_2] = 0 \cdot 1 [\text{O}_2]^{\frac{1}{2}},$$

the results shown in Tables XI and XII are obtained, and although the agreement is not of the high order obtained in the oxygen-free and oxygen-rich regions, it is fairly satisfactory in view of the uncertainties of equation (19B). It may at any rate, be claimed, that in equation (21) we have a numerical formula with a satisfactory theoretical basis which reproduces a variation in quantum yield between limits as extreme as  $10^5$  and 10, with a high degree of accuracy over the major part of the range.

*Limit of the "Transition Region."*—The results of previous workers indicate that inverse proportionality of the reaction velocity, and therefore quantum efficiency, to the pressure of oxygen is maintained down to much lower values than we have found in this work. Thus, whereas our limit of strict adherence

to the law is set at about 10 mm. of oxygen, that of other workers is at a pressure about ten times lower. A simple explanation of this fact exists, however, since it will be seen by reference to equation (21) that the relative magnitudes of the terms in the denominator is dependent on the pressures of the other reactants as well as oxygen. An examination of the literature\* shows that the law of inverse proportionality has been in general established at total pressures of hydrogen and chlorine and hydrogen chloride which were about ten times those used by us, *i.e.*, generally at total pressures approaching one atmosphere. Inspection of equation (21) shows that if as in our case the terms in the denominator *not* involving oxygen are negligible compared with the others for pressures of oxygen exceeding 10 mm., then if the pressure of hydrogen, hydrogen chloride, and chlorine be increased some tenfold the corresponding limiting pressure of oxygen will be reduced to 1 mm., and marked deviations will not become apparent till somewhat below this.

The data of Bodenstein and Dux do not extend below 6 mm. of oxygen, and those of Chapman and MacMahon only contain one experiment in which the pressure of oxygen was less (and only slightly less) than 1 mm. Their results are thus in this connection fully in agreement with our numerical expression.

In further support of the above contention we may cite the recent work of Rodebush and Klingenhofner (*loc. cit.*) who report a value of  $\gamma$  of 10 at "low pressures" and an independence of the quantum yield on the pressure of oxygen under these conditions. If we assume values for the partial pressures of reactants of from 0.01 to 0.1 mm. this is exactly the result to be expected from equation (21) which yields values of from 5 to 50 for  $\gamma$  within the above limits, and which at these low pressures reduces to an expression in which the effect of oxygen is insignificant.

*Comparison with Work of M. C. C. Chapman.*—It has been mentioned above that for oxygen-rich mixtures, our formula is practically identical with that of M. C. C. Chapman (*loc. cit.*) when the pressure of hydrogen chloride is taken as zero. This is in accord with the use of the water actinometer in her experiments by which the partial pressure of hydrogen chloride is obviously kept extremely low. If now we apply to equation (21) the condition that  $[HCl] = 0$  and  $[O_2] < 2$ , it assumes the approximate form

$$\gamma = \frac{3.77 \times 10^4 [H_2] [Cl_2]}{(31.4 + 104 I_{abs.}) [Cl_2] + [O_2] ([H_2]^2 + 140 [H_2])}, \quad (22)$$

\* See particularly Chapman and MacMahon, 'J. Chem. Soc.', vol. 95 (1909); Bodenstein and Dux, *loc. cit.*, p. 320.

which is in general qualitative agreement with her expression (transformed to give quantum efficiency instead of reaction velocity), namely,

$$\gamma = \frac{k [\text{H}_2] [\text{Cl}_2]}{k' [\text{Cl}_2] + [\text{O}_2] [\text{H}_2]^{(2-x)}}, \quad (23)$$

$x$  being variable and less than unity. In these circumstances it will be seen that the rate of combination will be practically independent of the concentration of oxygen in mixtures in which the concentration of hydrogen is very small, as was definitely pointed out by Mrs. Chapman. In her experiments this was found to obtain when the pressure of hydrogen was between 1 and 5 mm., and that of the chlorine about 600 mm., and on testing by equation (22) this is readily seen to follow. In all other respects this expression is in agreement with the conclusions summarized in her paper, and in particular, with the inhibiting effect of hydrogen to which special attention was drawn.

*Inhibiting Effect of Hydrogen Chloride (Christiansen).*—Although no previous observation of the inhibiting effect of hydrogen chloride on the photosynthesis of hydrogen chloride is on record, our results fall strikingly into agreement with those of Christiansen\* obtained in Bodenstein's laboratory for the thermal union of hydrogen and chlorine. A marked inhibiting effect both by oxygen and by hydrogen chloride was observed, the magnitudes of which accord well with our own experimental results. If for example we assume a similar mechanism of chain propagation for the thermal as for the photochemical reaction and suppose with Christiansen that the chlorine atoms initiating the chains are generated on the wall of the vessel at a rate independent of the pressure of chlorine and given by  $k'_1$  we obtain (after neglecting  $k_6$ ) the result

$$v = \frac{d[\text{HCl}]}{dt} = \frac{2k'_1 k_2 [\text{Cl}_2]}{[\text{O}_2] (k_7 [\text{H}_2] + k_8 [\text{HCl}] + k_9)}. \quad (24)$$

This may be compared with our approximate expression, and so, introducing the numerical values previously found for the various constants we obtain

$$v = \frac{K [\text{Cl}_2]}{[\text{O}_2] ([\text{H}_2] + 4 [\text{HCl}] + 140)}, \quad (25)$$

the concentrations being expressed in *millimetres*. A recalculation of Christiansen's extensive results by this formula gives values of  $K$  which remain throughout of the same order of magnitude. In Table XV we give the calculation for his experiments (23) and (32) in which the inhibiting effect of hydrogen chloride was definitely established.

\* 'Z. phys. Chem.,' B, vol. 2, p. 143 (1929).

Table XV.\*

Serial No.	Time interval $\Delta t$ .	Average pressures in millimetres during interval.				v. 10 <sup>3</sup> .	K.
		[O <sub>2</sub> ].	[Cl <sub>2</sub> ].	[H <sub>2</sub> ].	$\frac{1}{2}$ [HCl].		
23	mins.						
	5	1.29	190.5	143.7	0.6	2.3	
	25	1.13	164.4	123.4	2.7	1.36	275
	30	0.98	139.7	104.2	5.3	0.97	196
	60	0.86	116.6	86.1	8.6	0.91	196
32 (HCl rich)	5	1.19					
	25	1.11	163.2	126	36.3	0.76	292
	61	0.97	138.6	105.6	34.3	0.64	235
	62	0.84	116.3	88.3	33.6	0.69	250
	161 (?)	0.73	96	71.7	33.7	0.40	(146 ?)†

† The mark of uncertainty in the last line is as indicated in the original table of Christiansen.

It will be seen from the last column that K remains reasonably constant: the relative inhibiting effects of O<sub>2</sub>, and HCl as measured by him are thus in agreement with our own data.

The authors are indebted to the Government Grant Committee of the Royal Society for a research grant which has been applied in part to this work, and to the Commissioners of the Exhibition of 1851 for a senior award to one of them (M. R.). They would also express their thanks to Dr. R. B. Mooney for useful criticism during the preparation of this paper.

### Summary.

The kinetics of the photochemical combination of hydrogen and chlorine in the presence of both large and small quantities of oxygen have been re-examined by the new technique (I).

It has been discovered that the hydrogen chloride produced by the reaction has a powerful inhibiting effect. This is in accord with a similar effect noticed by Christiansen in the thermal reaction of hydrogen and chlorine.

In agreement with the result of Chapman and Underhill, hydrogen also has an inhibiting effect and the quantum efficiency passes through a maximum as the pressure of hydrogen is increased. This effect of hydrogen is about four times smaller than the corresponding effect of hydrogen chloride.

\* Christiansen, 'Z. phys. Chem.,' B, vol. 2, p. 413 (1929), Table I.



In oxygen-rich mixtures the quantum efficiency is inversely proportional to the pressure of oxygen, and independent of the intensity of the absorbed light.

In mixtures containing small quantities of oxygen ("transition region") this inverse proportionality no longer holds, and the quantum efficiency becomes increasingly dependent on the light intensity as the pressure of oxygen is reduced.

The pressure of oxygen for the upper limit of the transition region is dependent on the total pressure of hydrogen, chlorine, and hydrogen chloride.

By an extension of the Nernst scheme of reactions already adopted for oxygen-free mixtures (II), to include ternary and binary reactions of hydrogen atoms with oxygen molecules, an expression is obtained which satisfactorily takes account of all the above facts, and from which the quantum efficiency of any mixture varying from oxygen-free to oxygen-rich may be calculated to a high degree of accuracy. The quantum efficiencies so calculated vary from  $10^5$  to 20. This formula, reduces to one similar to the "hydrogen-bromine" formula of Herzfeld, Christiansen, and Polanyi for oxygen-free mixtures, and virtually to the empirical formula of M. C. C. Chapman for mixtures containing oxygen.

The relative values of the velocity coefficients of the component reactions of the reaction scheme have been computed, in conjunction with the results of II, and they are found to be in general dimensional accord with each other and with the data of other workers where comparable.

#### *Correction.*

The figures given under  $I_0$  in Tables I-IV of Part II (*loc. cit.*) represent the actual recorded galvanometer deflection. They should have been multiplied by the correction factor to allow for the absorption and back reflection of the optical system. This factor for  $\lambda = 406 \text{ m}\mu$  is 1.50 for  $[\text{Cl}_2] = 44 \text{ mm.}$  and 1.49 for  $[\text{Cl}_2] = 67 \text{ mm.}$  The figures are then uniform with the other data tabulated under  $I_0$  in the present paper.

On p. 114 of Part II "*will be given in Part III*" should read "*have been given in Part I.*"

---

## INDEX TO VOL. CXL. (A.)

- Acid strength and nature of the solvent (Wynne-Jones), 440.  
Adam (N. K.) The Structure of Surface Films. XVII— $\gamma$  Hydroxy-Stearic Acid and its Lactone, 223.  
Adsorption upon electrically conducting films (Johnson and Starkey), 126.  
Aerofoil in a wind tunnel of elliptic section (Rosenhead), 579.  
Anthracene, crystalline structure (Robertson), 79.  
Arnot (F. L.) The Diffraction of Electrons in Mercury Vapour, II, 334.  
Aston (F. W.) The Isotopic Constitution and Atomic Weight of Lead from Different Sources, 535.  
Atomic volume in copper-zinc alloys (Owen and Pickup), 179.  
Atomic volume in silver-zinc alloys (Owen and Pickup), 344.  
Atomic volume variation with temperature (Owen and Pickup), 191.  
Badami (J. S.) and Rao (K. R.) Investigations on the Spectrum of Selenium, II, 387.  
Bailey (C. R.) and Cassie (A. B. D.) Investigations in the Infra-red Region of the Spectrum, VIII, 605.  
Bengough (G. D.) and Wornwell (F.) The Theory of Metallic Corrosion in the Light of Quantitative Measurements, VI, 399.  
Beryllium excitation potentials (Skinner), 277.  
Bloch (A. M.) *See* Newitt and Bloch.  
Brindley (G. W.) On the Reflection and Refraction of X-Rays by Perfect Crystals, 301.  
Calculating machine, electrical (Mallock), 457.  
Cassie (A. B. D.) *See* Bailey and Cassie.  
Chemical equilibrium in mixtures of hydrocarbons (Wilson), 1.  
Conductor, semi-, change of resistance in a magnetic field (Harding), 205.  
Conductors, semi-, theory of electronic (Fowler), 505.  
Cornish (R. J.) Flow of Water through Fine Clearances with Relative Motion of the Boundaries, 227.  
Corrosion distribution (Bengough and Wornwell), 399.  
Covalencies, determination of the angles between (Hampson and Sutton), 562.  
Crystals, magnetic susceptibilities of paramagnetic, at low temperatures (Jackson), 695.  
Davidson (P. M.) *See* Richardson and Davidson.  
Electrons, collision with atoms (Massey and Mohr), 613.  
Electrons, diffraction in mercury vapour (Arnot), 334.  
Electrons, scattering in thin films (Langstroth), 159.  
Emeléus (H. J.) and Riley (H. L.) The Luminous Reduction of Selenium Dioxide, 378.  
Energy absorbed in the cold working of metals (Rosenhain and Stott), 9.  
Errors, theory of (Jeffreys), 523.  
Ethane, slow combustion at high pressures (Newitt and Bloch), 426.  
Excitation potentials of light metals (Skinner), 277.  
Films, boundary potentials of adsorbed (Whalley, Rideal and Jacobs), 484, 489, 497.  
Films, gas adsorption upon electrically conducting (Johnson and Starkey), 126.

- Films, structure of surface (Adam), 223.
- Flow of water through fine clearances with relative motion of the boundaries (Cornish), 227.
- Fowler (R. H.) An Elementary Theory of Electronic Semi-Conductors, and Some of their Possible Properties, 505.
- French (R. C.) Polish on Metals, 637.
- Friction, skin, of flat plates to Oseen's approximation (Piercy and Winny), 543.
- Galvin (A. C.) *See* Nolan and Galvin.
- Goldsbrough (G. R.) The Tides in Oceans on a Rotating Globe, IV, 241.
- Hampson (G. C.) and Sutton (L. E.) The Determination of the Angles between Covalencies from Measurements of Electric Dipole Moment, 562.
- Harding (J. W.) The Change of Resistance of a Semi-Conductor in a Magnetic Field, 205.
- Hartley (G. S.) and Moilliet (J. L.) The Moving Boundary Method for the Determination of Transport Numbers, 141.
- Helium, excitation and ionization (Massey and Mohr), 613.
- Hughes (A. H.) and Rideal (E. K.) On the Rate of Oxidation of Monolayers of Unsaturated Fatty Acids, 253.
- Hydrogen chloride, photosynthesis (Ritchie and Norrish), 99, 112 and 713.
- Ions, diffusion coefficients in nitrogen and oxygen (Nolan and Galvin), 452.
- Jackson (L. C.) The Principal Magnetic Susceptibilities of Some Paramagnetic Crystals at Low Temperatures, 695.
- Jacobs (L.) *See* Whalley, Rideal and Jacobs.
- Jeffreys (H.) Probability, Statistics and the Theory of Errors, 523.
- Johnson (M. C.) and Starkey (T. V.) Gas Adsorption upon Electrically Conducting Films during their Condensation from Molecular Rays, 126.
- Langstroth (G. O.) The Scattering of Electrons in Thin Films, 150.
- Lead, isotopic constitution and atomic weight (Aston), 535.
- Lubrication, theory of (Robb), 668.
- Mallock (R. R. M.) An Electrical Calculating Machine, 457.
- Massey (H. S. W.) and Mohr (U. B. O.) The Collision of Slow Electrons with Atoms, III, 613.
- Metals, boundary potentials of adsorbed films on (Whalley, Rideal and Jacobs), 484, 489, 497.
- Metals, energy absorbed in cold working (Rosenhain and Stott), 9.
- Metals, phenomena occurring in melting (Webster), 653.
- Metals, polish on (French), 637.
- Mohr *see* Massey and Mohr.
- Moilliet *see* Hartley and Moilliet.
- Molecules, dissociation of excited diatomic, by external perturbation (Zener), 660.
- Newitt (D. M.) and Bloch (A. M.) The Slow Combustion of Ethane at High Pressures, 426.
- Nolan (J. J.) and Galvin (A. C.) The Effect of Water Vapour on the Diffusion Coefficients of Ions in Nitrogen and Oxygen, 452.
- Norrish (R. G. W.) *See* Ritchie and Norrish.

- Owen (E. A.) and Pickup (L.) The Relation between Mean Atomic Volume and Composition in Copper-Zinc Alloys, 179.
- Owen (E. A.) and Pickup (L.) The Relation between Mean Atomic Volume and Composition in Silver-Zinc Alloys, 344.
- Owen (E. A.) and Pickup (L.) Variation of Mean Atomic Volume with Temperature in Copper-Zinc Alloys, with Observations on the  $\beta$ -Transformation, 191.
- Oseen's approximation, skin friction of flat plates (Piercy and Winny), 543.
- Oxidation rate of monolayers of unsaturated fatty acids (Hughes and Rideal), 253.
- Pickup (L.) See Owen and Pickup.
- Piercy (N. A. V.) and Winny (H. F.) The Skin Friction of Flat Plates to Oseen's Approximation, 543.
- Radiation, penetrating from thunderclouds (Schonland and Viljoen), 314.
- Rao (K. R.) See Badami and Rao.
- Reaction velocity, effect of solvent (Williams and Soper and Roberts and Soper), 59, 71.
- Richardson (O. W.) and Davidson (P. M.) The Spectrum of  $H_2$ —The Bands Ending on  $2p^2\Pi$  Levels, II, 25.
- Rideal (E. K.) See Hughes and Rideal.
- Rideal (E. K.) See also Whalley, Rideal and Jacobs.
- Riley (H. L.) See Emeléus and Riley.
- Ritchie (M.) and Norrish (R. G. W.) The Photosynthesis of Hydrogen Chloride, I, II and III, 99, 112 and 713.
- Robb (A. M.) A Contribution to the Theory of Film Lubrication, 668.
- Roberts (R. E.) and Soper (F. G.) The Effect of the Solvent on Reaction Velocity, IV, 71.
- Robertson (J. M.) The Crystalline Structure of Anthracene. A Quantitative X-Ray Investigation, 79.
- Rosenhain (W.) and Stott (V. H.) The Energy Absorbed in the Cold Working of Metals, 9.
- Rosenhead (L.) The Aerofoil in a Wind Tunnel of Elliptic Section, 579.
- Schonland (B. F. J.) and Viljoen (J. P. T.) On a Penetrating Radiation from Thunderclouds, 314.
- Selenium dioxide, luminous reduction (Emeléus and Riley), 378.
- Selenium spectrum (Badami and Rao), 387.
- Sen (N. R.) On Eddington's Problem of the Expansion of the Universe by Condensation, 269.
- Skinner (H. W. B.) The Excitation Potentials of Light Metals, II, 277.
- Smith-Rose (R. L.) The Electrical Properties of Soil for Alternating Currents at Radio Frequencies, 359.
- Soil, electrical properties for alternating currents at radio frequencies (Smith-Rose), 359.
- Soper (F. G.) See Roberts and Soper.
- Soper (F. G.) and Williams (E.) The Effect of the Solvent on Reaction Velocity, III, 59.
- Spectra of triatomic molecules (Cassie and Bailey), 605.
- Spectrum of  $H_2$  (Richardson and Davidson), 25.
- Spectrum, investigations in infra-red region (Bailey and Cassie), 605.
- Spectrum of selenium (Badami and Rao), 387.
- Starkey (T. V.) See Johnson and Starkey.
- Stearic acid, structure of  $\gamma$ -hydroxy (Adam), 223.

Stott (V. H.) *See* Rosenhain and Stott.

Sutton (L. E.) *See* Hampson and Sutton.

Tides in oceans on a rotating globe (Goldsbrough), 241.

Transport numbers, determination by moving boundary method (Hartley and Moilliet), 141.

Universe expansion by condensation (Sen), 269.

Viljoen (J. P. T.) *See* Schonland and Viljoen.

Whalley (H. K.), Rideal (E. K.) and Jacobs (L.) Phase Boundary Potentials of Adsorbed Films on Metals, I, II and III, 484, 489, 497.

Webster (W. L.) Phenomena Occurring in the Melting of Metals, 653.

Williams (E.) *See* Soper and Williams.

Wilson (H. A.) Chemical Equilibrium in Vapour of a Mixture of Hydrocarbons, 1.

Winn *see* Piercy and Winn.

Wormwell (F.) *See* Bengough and Wormwell.

Wynne-Jones (W. F. K.) Acid Strength and its Dependence upon the Nature of the Solvent, 440.

X-rays, reflection and refraction by perfect crystals (Brindley), 301.

Zener (C.) Dissociation of Excited Diatomic Molecules by External Perturbations, 660.





**L. A. B. I. 75**

IMPERIAL AGRICULTURAL RESEARCH  
INSTITUTE LIBRARY  
NEW DELHI

[illegible]